

TRANSACTIONS
OF THE
AMERICAN SOCIETY
OF
CIVIL ENGINEERS

(INSTITUTED 1852)

VOLUME 124

1959

Edited by the Executive Secretary, under the direction of the Committee on Publications.

Reprints from this publication, which is copyrighted, may be made on condition that the full title of paper, name of author, and page reference (or paper number) are given.

NEW YORK
PUBLISHED BY THE SOCIETY

1959

Stand
TH
1
AS26
V.124

TRANSACTIONS
AMERICAN SOCIETY
CIVIL ENGINEERS

Copyright 1959 by the AMERICAN SOCIETY OF CIVIL ENGINEERS

NOTE.—The Society is not responsible for any statement made or opinion expressed
in its publications.

CONTENTS

No.		PAGE
2963	DESIGN OF FLEXIBLE STEEL ARCHES BY INTERACTION DIAGRAMS By HAAREN A. MIKLOFSKY AND OMAR J. SOTILLO.....	1
	DISCUSSION:	
	By Reinaldo Garcia-Iturbe.....	30
	Haaren A. Miklofsky and Omar J. Sotillo.....	30
2964	GENERATING STATION ON THE NIAGARA RIVER By FRANK DOBSON.....	32
2965	HURRICANE DESIGN-WAVE PRACTICES By CHARLES L. BRETSCHNEIDER.....	39
2966	STRENGTH OF VERY SLENDER BEAMS By ERNEST F. MASUR.....	63
2967	OCEAN WAVE FORCES ON CIRCULAR CYLINDRICAL PILES By ROBERT L. WIEGEL, KENNETH E. BEEBE, AND JAMES MOON.....	89
	DISCUSSION:	
	By Thomas E. Stelson.....	114
	Robert L. Wiegel, Kenneth E. Beebe, and James Moon.....	115
2968	PLATE BUCKLING IN THE STRAIN-HARDENING RANGE By GERRHARD HAAVER.....	117
2969	HIGHWAY PLANNING IN THE PAST, PRESENT, AND FUTURE By EDWARD H. HOLMES AND JOHN T. LYNCH.....	149
2970	ANALYSIS OF CONTINUOUS BEAMS BY FOURIER SERIES By SENG-LIP LEE.....	164
	DISCUSSION:	
	By Stefan J. Medwadowski.....	175
	Seng-Lip Lee.....	176
2971	CHARACTERISTICS OF NEW-TYPE CARGO SHIPS By DOUGLAS C. MACMILLAN.....	179
2972	ATTENUATION OF SOLITARY WAVES ON A SMOOTH BED By YOSHIKI IWASA.....	193
2973	EVOLUTION OF MISSISSIPPI VALLEY FLOOD-CONTROL PLAN By JOHN R. HARDIN.....	207
2974	SALT BALANCE IN GROUND-WATER RESERVOIRS By DAVID B. WILLETS AND CHARLES A. MCCULLOUGH.....	224
	DISCUSSION:	
	By Robert O. Thomas.....	232
	David B. Willets and Charles A. McCullough.....	235
2975	MODEL STUDIES OF REMEDIAL WORKS FOR NIAGARA FALLS By ANDREW P. ROLLINS, JR., AND GEORGE B. FENWICK.....	236

IV

No.		Page
2976	ELECTRONIC COMPUTERS IN SURVEYING	
	By ARTHUR J. McNAIR.....	252
2977	PREDICTING SURGE PRESSURES IN OIL PIPELINES	
	By ROBERT D. KERSTEN AND EDWIN J. WALLER.....	258
	DISCUSSION:	
	By Henry M. Paynter.....	273
	Robert D. Kersten and Edwin J. Waller.....	278
2978	WATER SUPPLY VERSUS IRRIGATION IN HUMID AREAS	
	By MARION C. BOYER.....	280
2979	VIBRATION OF SIMPLE-SPAN HIGHWAY BRIDGES	
	By JOHN M. BIGGS, HERBERT S. SUEB, AND JACOBUS M. LOUW.....	291
2980	ERRORS IN MEASUREMENT OF IRRIGATION WATER	
	By CHARLES W. THOMAS.....	319
	DISCUSSION:	
	By Odon Starosolszky.....	333
	Steponas Kolupaila.....	336
	Armando Ballofet.....	336
	Charles W. Thomas.....	338
2981	FLOW OF NATURAL GAS IN PIPELINES	
	By WILLIAM T. IVEY AND JAMES H. DOROUGH.....	341
2982	OFFSHORE BREAKWATERS	
	By RICHARD SILVESTER.....	356
2983	TECHNICAL PROBLEMS OF FLOOD INSURANCE	
	By H. ALDEN FOSTER.....	366
	DISCUSSION:	
	By Geoffrey N. Alexander.....	376
	Steponas Kolupaila.....	379
	H. Alden Foster.....	379
2984	OPERATION OF MISSOURI RIVER MAIN-STEM RESERVOIRS	
	By ROBERT J. PAFFORD.....	381
2985	INELASTIC BEHAVIOR OF IMPULSIVELY LOADED BEAMS	
	By MELVIN J. GREAVES AND FREDERIC T. MAVIS.....	395
2986	COMPACTING EARTH DAMS WITH HEAVY TAMPING ROLLERS	
	By JACK W. HILF.....	409
	DISCUSSION:	
	By Jack D. Hodgson.....	436
	C. Y. Li.....	438
	Jack W. Hilf.....	439
2987	THE WELLAND CANAL	
	By WILLIAM A. O'NEIL.....	443
2988	DESIGN OF MASONRY WALLS FOR BLAST LOADING	
	By KEITH E. MCKEE AND EUGENE SEVIN.....	457
2989	PRESTRESSED TRUSS-BEAMS	
	By RALPH L. BARNETT.....	472
2990	FIELD INVESTIGATIONS OF SPILLWAYS AND OUTLET WORKS	
	By BENSON GUYTON.....	491

No.		PAGE
2991	HYDRAULIC JUMP AT AN ABRUPT DROP By WALTER L. MOORE AND CARL W. MORGAN.....	507
	Discussion:	
	By Murray B. McPherson.....	517
	John W. Forster.....	519
	Walter L. Moore and Carl W. Morgan.....	521
2992	LITTORAL-DRIFT PROBLEM AT SHORE-LINE HARBORS By JOE W. JOHNSON.....	525
	Discussion:	
	By Richard Silvester.....	547
	Joe W. Johnson.....	551
2993	TESTS TO EVALUATE CONCRETE PAVEMENT SUBBASES By LAWRENCE D. CHILDS, BERT E. COLLEY, AND JOE W. KAPERNICK.....	556
2994	ADAPTABILITY OF INTERCHANGES TO INTERSTATE HIGHWAYS By JACK E. LEISCH.....	588
	Discussion:	
	By Gerald D. Love.....	614
	Jack E. Leisch.....	614
2995	DESIGN FEATURES OF THE DRESDEN NUCLEAR POWER STATION By JOSEPH E. LOVE, CHESTER S. DARROW, AND BURR H. RANDOLPH.....	617
2996	ENGINEERING GEOLOGY OF THE MISSISSIPPI VALLEY By CHARLES R. KOLB AND WOODLAND G. SHOCKLEY.....	633
	Discussion:	
	By Shu-T'ien Li.....	646
	Charles R. Kolb and Woodland G. Shockley.....	655
2997	GROUND TRANSPORTATION AT NEW YORK INTERNATIONAL AIRPORT By RICHARD I. STRICKLAND.....	657
2998	BEHAVIOR OF REINFORCED CONCRETE SHEAR WALLS By JACK R. BENJAMIN AND HARRY A. WILLIAMS.....	669
	Discussion:	
	By DeForest A. Matteson, Jr.....	703
	Jack R. Benjamin and Harry A. Williams.....	705
2999	REVIEW OF THE THEORIES FOR SAND DRAINS By F. E. RICHART, JR.....	709
	Discussion:	
	By Yoshichika Nishida.....	737
	S. J. Johnson.....	737
	F. E. Richart, Jr.....	738
3000	FIXED-WHEEL GATES FOR PENSTOCK INTAKES By SYLVAN J. SKINNER.....	740
	Discussion:	
	By Joseph R. Bowman.....	769
	Sylvan J. Skinner.....	771

VI

No.		Page
3001	DISCHARGE CHARACTERISTICS OF RECTANGULAR THIN-PLATE WEIRS	
	By CARL E. KINDSVATER AND ROLLAND W. CARTER.....	772
	DISCUSSION:	
	By Turgut Sarpkaya.....	802
	Steponas Kolupaila.....	808
	Ralph W. Powell.....	809
	John W. Paull.....	814
	Iwao Oki.....	814
	Marion R. Caretens.....	816
	Carl E. Kindsvater and Rolland W. Carter.....	818
3002	SEWAGE DISPOSAL IN SANTA MONICA BAY	
	By CHARLES G. GUNNERSON.....	823
	DISCUSSION:	
	By Charles H. Lawrance and David R. Miller.....	843
	David I. H. Barr.....	850
	Charles G. Gunnerson.....	850
3003	WAVE RUN-UP ON ROUGHENED AND PERMEABLE SLOPES	
	By RUDOLPH P. SAVAGE.....	852
3004	VORTEX FLOW THROUGH HORIZONTAL ORIFICES	
	By JOHN C. STEVENS AND RICHARD C. KOLF.....	871
	DISCUSSION:	
	By John W. Cunningham.....	884
	Chesley J. Posey.....	885
	John C. Stevens and Richard C. Kolf.....	888
3005	THIXOTROPIC CHARACTERISTICS OF COMPACTED CLAYS	
	By H. BOLTON SEED AND CLARENCE K. CHAN.....	894
	DISCUSSION:	
	By Edward S. Barber.....	917
	D. P. Krynine.....	917
	H. Bolton Seed and Clarence K. Chan.....	924
3006	TURBULENCE CHARACTERISTICS OF THE HYDRAULIC JUMP	
	By HUNTER ROUSE, TIEN TO SIAO, AND S. NAGARATNAM.....	926
	DISCUSSION:	
	By Edward Silberman.....	951
	A. J. Peterka and J. N. Bradley.....	952
	James M. Robertson.....	954
	Donald R. F. Harleman.....	959
	Philip G. Hubbard.....	962
	Hunter Rouse, Tien To Siao, and S. Nagaratnam.....	964
3007	PRESSURE LINES AND INELASTIC BUCKLING OF COLUMNS	
	By FRANK BARON AND HAROLD S. DAVIS.....	967
3008	HAAS HYDROELECTRIC POWER PROJECT	
	By J. BARRY COOKE.....	991
	DISCUSSION:	
	By F. L. Lawton.....	1024
	J. Barry Cooke.....	1025
3009	FLOW EQUATIONS FOR NATURAL GAS PIPELINES	
	By RICHARD F. BUKACEK.....	1027

VII

No.		Page
	Discussion:	
	By James H. Dorough.....	1035
	John F. Schomaker.....	1037
	William T. Ivey.....	1036
	Richard F. Bukacek.....	1037
3010	THE STATE OF THE CIVIL ENGINEERING PROFESSION	
	ANNUAL ADDRESS AT THE CONVENTION, CLEVELAND, OHIO, MAY 5, 1959	
	By FRANCIS S. FRIEL, President.....	1038
	MEMOIRS OF DECEASED MEMBERS: ABSTRACTS.....	1049
	SUBJECT INDEX.....	1084
	AUTHOR INDEX.....	1113

ERRATA

Transactions, Vol. 122, 1957

Page 1244, lines 6 and 7 should be changed to read: "He is survived by his widow; a son, James LaRoy; a sister; and a brother."

Transactions, Vol. 124, 1959

Page 262, in Eq. 11 the first term inside of the brackets should be changed from

$$\frac{4 (D_l)^2 - 2 (D_l)^2}{\pi}$$

to

$$\frac{4 (D_l)^2 - 2 d^2}{\pi}$$

NOTE

Membership designations used herein are those in effect prior to June 6, 1959.

국립중앙도서관

국립중앙도서관

국립중앙도서관은 1945년 8월 15일 광복을 맞이하여, 서울에 있는 일본제국도서관의 소장도서와, 1946년 10월 1일부터 1947년 12월 31일까지의 기간 동안, 국내외에서 수집한 도서, 그리고 1948년 1월 1일부터 1949년 12월 31일까지의 기간 동안, 국내외에서 수집한 도서를 포함하여, 총 1,000,000여 권의 도서를 소장하고 있다.

국립중앙도서관

국립중앙도서관은 1945년 8월 15일 광복을 맞이하여, 서울에 있는 일본제국도서관의 소장도서와, 1946년 10월 1일부터 1947년 12월 31일까지의 기간 동안, 국내외에서 수집한 도서, 그리고 1948년 1월 1일부터 1949년 12월 31일까지의 기간 동안, 국내외에서 수집한 도서를 포함하여, 총 1,000,000여 권의 도서를 소장하고 있다.

국립중앙도서관

국립중앙도서관

국립중앙도서관은 1945년 8월 15일 광복을 맞이하여, 서울에 있는 일본제국도서관의 소장도서와, 1946년 10월 1일부터 1947년 12월 31일까지의 기간 동안, 국내외에서 수집한 도서, 그리고 1948년 1월 1일부터 1949년 12월 31일까지의 기간 동안, 국내외에서 수집한 도서를 포함하여, 총 1,000,000여 권의 도서를 소장하고 있다.

AMERICAN SOCIETY OF CIVIL ENGINEERS

Founded November 5, 1852

TRANSACTIONS

Paper No. 2963

DESIGN OF FLEXIBLE STEEL ARCHES BY INTERACTION DIAGRAMS

BY HAAREN A. MIKLOFSKY,¹ A. M. ASCE, AND
OMAR J. SOTILLO,² J. M. ASCE

WITH DISCUSSION BY MESSRS. REINALDO GARCÍA-ITURBE;
AND HAAREN A. MIKLOFSKY AND OMAR J. SOTILLO

SYNOPSIS

The use of interaction diagrams in the structural design of all types of flexible steel arches is described. The interaction diagram developed gives the fiber stress and deflection of the arch cross section as a function of its dimensions. The diagram is analogous to a structural interaction diagram for the beam column, which is a statically determinate structure. The method is illustrated by the design of the quarter-point sections of several steel arch bridges.

INTRODUCTION

In any type of arch the rib or truss serves to (1) withstand direct compression and (2) furnish the flexural rigidity necessary to resist the bending moment created when the equilibrium polygon for the applied load system does not coincide with the position of the arch axis. The moment at any point of the arch axis, determined by the usual elastic-theory methods, is equal to the axial thrust at that point multiplied by the perpendicular distance from the funicular polygon for the applied load system to the unmoved arch axis. However, for long-span arches this method of analysis is deficient because the arch axis moves considerably and creates additional moments that, in turn, further increase the distance between the funicular polygon and the arch axis. This inevitable amplification of the moment merits careful consideration by the designer.

NOTE.—Published, essentially as printed here, in March, 1957, in the Journal of the Structural Division, as *Proceedings Paper 1190*. Positions and titles given are those in effect when the paper or discussion was approved for publication in *Transactions*.

¹ Associate Prof., Dept. of Civ. Eng., Rensselaer Polytechnic Inst., Troy, N. Y.

² Technical Director, Technical Office, OMIG, Caracas, Venezuela.

Several deflection theories³ are available to determine the additional stresses and deflections produced by the deflection of the arch axis under load. Either restrictive application or extensive computations, however, have prevented any of these methods from gaining universal acceptance. Of greater importance is the fact that these are methods of analysis and not methods of design.

The interaction diagram, which consists of a set of curves describing the structural behavior of a member as a function of its dimensions, will enable the designer to visualize the entire design range so that he can select a cross section that will result in a desired fiber stress and radial deflection without trial or error.

In order to clarify the structural behavior of the arch when the displacement of the arch axis is considered, a simple beam subjected to transverse bending and axial compression loads will be analyzed first. The bending interaction of this statically determinate structure will be proved to be analogous to that of the arch. The simple illustration for the beam will explain the nature of an interaction diagram and its function in design. Furthermore, such a study, based on the interpretation of the physical behavior of the beam (a statically determinate structure), aids in understanding the physical behavior of the arch (a stati-

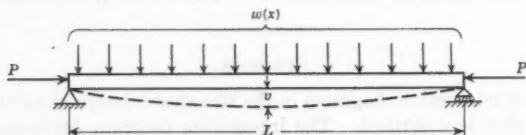


FIG. 1.—TRANSVERSE BENDING AND AXIAL COMPRESSION OF SIMPLY SUPPORTED BEAM

cally indeterminate structure). The bending interaction diagram for the stresses and deflections of the arch will be developed subsequently for its variable dimensions.

Notation.—The letter symbols adopted for use in this paper are defined where they first appear, in the illustrations or in the text, and are arranged alphabetically, for convenience of reference, in the Appendix.

INTERACTION DIAGRAM FOR A BEAM COLUMN

Fig. 1 shows a simply supported beam that is subjected to an axial compressive load, P , at its ends and the transverse load system, $w(x)$. The center deflection, v , becomes

$$v = \frac{k M L^2}{E I} \dots \dots \dots (1)$$

in which M is the bending moment at the center produced by the direct load, P , and the transverse load, $w(x)$; L represents the length of the beam; E is the modulus of elasticity; and I denotes the moment of inertia. The term k is a

³ "Design of Flexible Steel Arches by Interaction Diagrams," by O. J. Sotillo, thesis presented to Rensselaer Polytechnic Institute, Troy, N. Y., in 1956, in partial fulfillment of the requirements for the degree of Doctor of Philosophy, pp. 128-132.

constant depending on the distribution of the bending loads and the variation of I along the beam.

The maximum fiber stress, s_{\max} , occurs at the outside top fiber of the beam at midspan and is determined from

$$s_{\max} = \frac{P}{A} + \frac{M_t c}{I} + \frac{P v c}{I} \dots \dots \dots (2)$$

in which A represents the cross-sectional area; M_t denotes the bending moment at the center due to the transverse load only; and c is one-half the beam depth. Combining Eqs. 1 and 2 leads to

$$s_{\max} = \frac{P}{A} + \frac{M_t c}{I - \left(\frac{k P L^2}{E} \right)} \dots \dots \dots (3)$$

The term $k P L^2/E$ has the same units as I . The function of this term in Eq. 3 is to reduce the flexural rigidity of the beam. Therefore, it is termed the "reduction factor" and is represented by I_r . Hence, Eq. 3 can be written as

$$s_{\max} = \frac{P}{A} + \frac{M_t c}{I - I_r} \dots \dots \dots (4)$$

and because

$$M = M_t + P v \dots \dots \dots (5)$$

Eq. 1 becomes

$$v = \frac{k M_t L^2}{E (I - I_r)} \dots \dots \dots (6)$$

The second part of Eq. 4 is a bending expression for the interaction of (a) the bending stress $M_t c/I$ induced by $w(x)$, and (b) the bending stress $P v c/I$ induced by P acting on the sagged beam. The effect of each separate action on the structural behavior of the beam will be considered for varying beam depths and cross-sectional areas by first varying the depth, d , and maintaining the cross-sectional area, A , constant. The resulting curves will yield stress and deflection values for the various depths. By changing the cross-sectional area, a family of curves will result.

If only the transverse load, $w(x)$, acts, then $P = 0$ and $I_r = 0$, and the bending stress from Eq. 4 becomes

$$s' = \frac{M_t c}{I} = \frac{M_t d}{2 K A d^2} \propto \frac{1}{A d} \dots \dots \dots (7)$$

in which K is a constant that is dependent on the distribution of the cross-sectional area. For a given value of A , Eq. 7 plots as a hyperbola (Curve b) in Fig. 2 (b).

The effect of P only is given by the second part of Eq. 4. When $I = 0$,

$$s'' = \frac{M_t c}{I_r} = \frac{M_t d}{2 I_r} \propto d \dots \dots \dots (8)$$

which plots as a straight line (Curve c) in Fig. 2(b).

The reciprocal of the bending stress from Eq. 4 is equal to the reciprocal of Eq. 7 minus the reciprocal of Eq. 8:

$$\frac{1}{s_b} = \frac{1}{s'} - \frac{1}{s''} \dots \dots \dots (9)$$

Eqs. 6 and 9 can be simplified further—

$$v \propto \frac{1}{A d^2 - 1} \dots \dots \dots (10a)$$

and

$$s_b \propto \frac{d}{A d^2 - 1} \dots \dots \dots (10b)$$

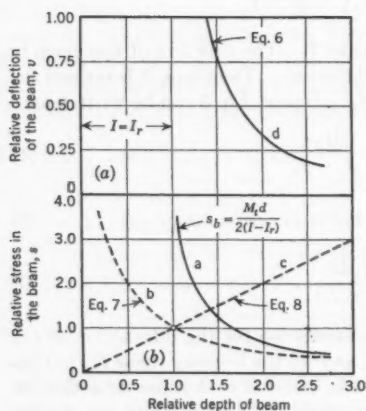


FIG. 2.—STRESS AND DEFLECTION OF BEAM FOR VARIABLE DEPTH AND FIXED CROSS-SECTIONAL AREA

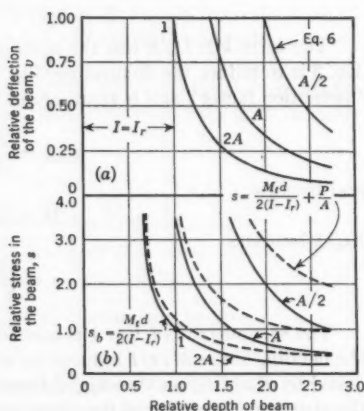


FIG. 3.—INTERACTION DIAGRAM FOR BEAM SUBJECTED TO TRANSVERSE BENDING AND AXIAL LOAD

The relative bending stress, s_b , is plotted as Curve a in Fig. 2(b), and the relative deflection, v , is plotted as Curve d in Fig. 2(a).

The curve for s' is asymptotic to both the d -abscissa and the s -ordinate, whereas the bending stress s'' is a linear function of d . The curve for the total bending stress, s_b , is asymptotic to the ordinate axis at $I = I_r$ and the d -axis. At the d -value in which $I = I_r$, the influence of P acting on the sagged beam has become so great that the moment of inertia available to resist the bending action has been neutralized by the reduction factor, I_r . When this occurs, the beam buckles in the vertical plane and $s_b \rightarrow \infty$. As the depth increases, the total bending stress, s_b , approaches the bending stress s' because the influence of the reduction factor, I_r , on the s_b -curve diminishes as the depth, d , increases. For this reason, as I becomes much greater than the reduction factor, I_r , the s_b -curve practically coincides with the s' -stress or bending stress due to simple beam action.

In the deflection diagram the same behavior is evident. Fig. 2(a) shows the deflection curve asymptotic both to the ordinate at $I = I_r$ and to the depth axis. As the depth decreases, the value of I decreases to the point where $I = I_r$, and the beam buckles in the vertical plane as $v \rightarrow \infty$. If the depth increases appreciably, the value of I will become greater, thus producing an extremely high flexural rigidity. The deflection then tends toward zero.

Fig. 3 (an extension of Fig. 2) includes the effect of various relative areas on the relative stress and deflection. The solid curves in Fig. 3(b) can be computed from the interaction expression for bending only. Once a scale for the relative unit coordinates for the graphs can be established for a given problem, the rest of the coordinates follow by proportion to Fig. 3.

However, an interaction diagram is not complete for this problem unless the effect of axial stress is included. Because the axial stress is dependent only on the area and not the depth, the stress merely raises each bending interaction stress curve by a quantity P/A . A sample set of final stress curves (dashed lines) is shown in Fig. 3(b). Relative values of P/A cannot be established for all problems on a proportional relative graph but must be computed individually for each problem.

As soon as scales have been established for the coordinates of the deflection and stress curves, and the effect of axial stress has been included at this scale, it is possible to determine directly the depth and area that will satisfy simultaneously a given stress and deflection. Only one solution using a minimum cross-sectional area is possible, as will be illustrated subsequently in the use of the arch interaction diagram for design.

INTERACTION DIAGRAM FOR ARCHES

The problem of the arch is similar to that of the beam subjected to transverse and axial compressive loads. The arch problem is the beam problem, with added consideration being given to horizontal displacement, settlement of supports, and axial distortion.

Because the elastic theory will be used for all derivations and solutions of the deflected arch, instead of referring to the usually accepted terms of "elastic theory" and "deflection theory," it would be more appropriate and descriptive to use the terms "rigid arch theory" and "flexible arch theory."

Two-Hinged Rib Arch.—For the two-hinged rib arch shown in Fig. 4, the application of $w(x)$, critical for a point a , produces the illustrated displacement of the arch axis. The moment at point a in the rigid arch is

$$M_{ra} = V x_a - W (x_a - x_b) - H y_a \dots \dots \dots (11)$$

in which W is the sum of all downward loads acting between A and a , and V is the vertical reaction.

As the arch axis deflects, it is assumed that the value of H remains unchanged and that point b , at which W is considered to act, does not move relative to the load points, which also experience a horizontal displacement. The moment at point a in the flexible arch is expressed by

$$M_{fa} = V (x_a + n) - W [(x_a - x_b) + (n - n_b)] - H (y_a - m) \dots (12)$$

which, when combined with Eq. 11, reduces to

$$M_{fa} = M_{ra} + Hm + Vn - W(n - n_b) \dots \dots \dots (13)$$

A two-hinged arch rib must satisfy the equilibrium dictated by Eq. 13. The values of M_{ra} , V , H , and W can be determined from the rigid-arch system, but m , n , and n_b are still unknown. Therefore, in order to solve Eq. 13, three more equations must be introduced.

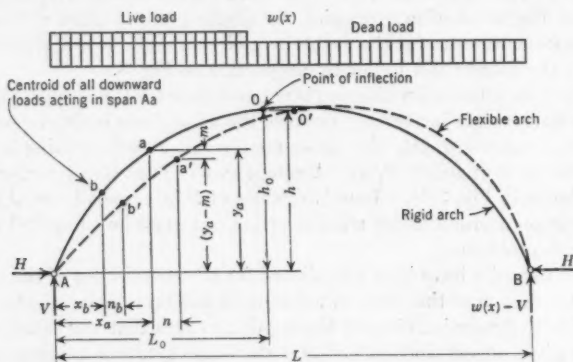


FIG. 4.—DEFLECTION OF THE TWO-HINGED ARCH RIB

Fig. 5 shows the moment diagram for both the rigid arch and the flexible arch for the loading under consideration. The ordinate, M_{fa} , is unknown. It

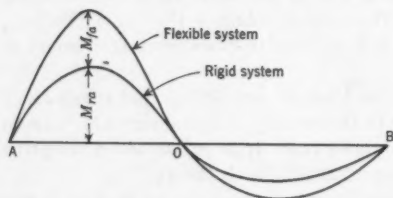


FIG. 5.—MOMENT DIAGRAMS FOR RIGID AND FLEXIBLE ARCHES

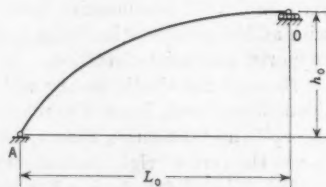


FIG. 6.—THE SHORT ARCH AND THE ROLLER SUPPORT

has been assumed that point O is the point of zero moment for both the rigid system and the flexible system. For convenience, it is assumed that at any point of the arch,

$$I = I_c \sec \theta \dots \dots \dots (14)$$

in which I_c is the moment of inertia at the crown and θ is the angle of inclination of the arch axis with the horizontal at that point. If the arch is cut at point O and a roller is inserted at the same point, an arch of span L_0 with a rise differential, h_0 , between supports will furnish two relationships as a function of M_{fa} . Such an arrangement is shown in Fig. 6.

The purpose of the roller is to permit horizontal, but not vertical, translation of point 0. From the shape of the moment diagram, it is evident that there is a relative displacement between points A and 0. Because point A is a hinged support with no displacement, point 0 must move horizontally to satisfy the flexural straining implied by the moment parabola with the ordinate, M_{fa} . When the horizontal displacement of point 0 has taken place, the span A0 acts as an arch.

If the conjugate-structure method⁴ is used, an equation for both m and n as a function of M_{fa} can be derived. Fig. 7 shows the conjugate structure loaded

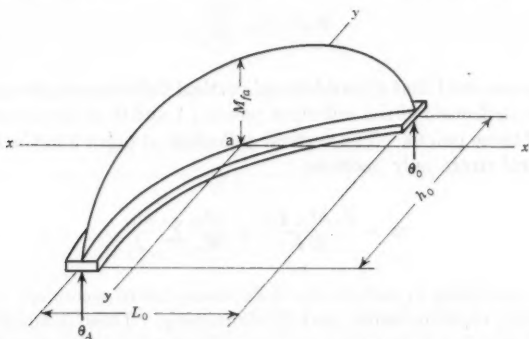


FIG. 7.—THE CONJUGATE STRUCTURE FOR THE SHORT ARCH

with the elastic loads $M_x ds/EI$, in which M_x is the moment at each ds -segment along the conjugate structure, and EI is the flexural rigidity of each increment.

Because of Eq. 14 and

$$ds = dx \sec \theta \dots \dots \dots (15)$$

the elastic-load term becomes $M_x dx/EI_c$. If point 0 undergoes no vertical deflection, the vertical deflection undergone by point a is equal to the bending moment at point a about the $(y-y)$ -axis. This is produced by the elastic loads, which act on the conjugate structure lying on a horizontal plane—that is,

$$m' = \frac{k_1 M L_0^2}{EI_c} \dots \dots \dots (16a)$$

Taking moments about the $(x-x)$ -axis at point a leads to

$$n' = \frac{k_2 M L_0 h_0}{EI_c} \dots \dots \dots (16b)$$

in which k_1 and k_2 are constants depending on the section considered, the loading system, and the distribution of I in the arch.

⁴ "Analysis of Multi-Span Rigid Frames," by J. S. Kinney, in "Steel Rigid Frames Manual, Design and Construction," by Martin P. Korn, J. W. Edwards, Inc., Ann Arbor, Mich., 1953, pp. 50-66.

The values of k_1 and k_2 can be assumed to be 5/48 and 1/6, respectively, without introducing a significant error. However, the computation of these values is simple, and it is preferable to compute them in order to improve the accuracy of the analysis.

The vertical deflection, m_0 , in the arch at point 0 is not equal to zero. By the conjugate-structure method, the initial deflection, m_{0r} , at point 0 can be determined. If it is assumed that this initial displacement, as a result of the change in configuration of the arch axis, is amplified by the same proportion as the moment at point a, then

$$m_0 = m_{0r} \frac{M_{fa}}{M_{ra}} \dots \dots \dots (17)$$

It can be assumed that the additional vertical deflection at the quarter point a, due to the deflection of the inflection points (A and O) is equal to the average deflection of these points. The vertical deflection at point a in the flexible arch due to flexural strain only becomes

$$m = \frac{k_1 M_{fa} L_0^2}{E I_c} + \frac{M_{fa}}{M_{ra}} \sum \frac{m_{0r}}{2} \dots \dots \dots (18)$$

It is also desirable to include the deflections due to secondary effects, such as temperature, erection errors, and rib shortening. These deflections increase the moment at point a, but they are not subject to amplification themselves. The total vertical deflection at point a becomes

$$m = \frac{k_1 M_{fa} L_0^2}{E I_c} + \frac{M_{fa}}{M_{ra}} \sum \frac{m_{0r}}{2} + m_2 \dots \dots \dots (19)$$

Similarly,

$$n = \frac{k_2 M_{fa} L_0 h_0}{E I_c} + n_2 \dots \dots \dots (20)$$

in which m_2 and n_2 are the vertical and horizontal deflections, respectively, at point a, as a result of axial distortion of the arch rib. Using the same amplification factor used in Eq. 17 leads to

$$n - n_b = \frac{M_{fa}}{M_{ra}} (n_r - n_{br}) + (n_2 - n_{b2}) \dots \dots \dots (21)$$

If Eqs. 19, 20, and 21 are substituted into Eq. 13, then

$$M_{fa} = \frac{M_{ra} + H m_2 + V n_2 - W (n_2 - n_{b2})}{1 - \frac{1}{E I_c} \left[k_1 H L_0^2 + k_2 V L_0 h_0 + \frac{H \sum E I_c m_{0r} - 2 W E I_c (n_r - n_{br})}{2 M_{ra}} \right]} \dots \dots \dots (22)$$

Because of Eq. 14 and

$$s = \frac{T}{A} + \frac{Mc}{I} \dots \dots \dots (23)$$

and if c is taken as one-half the depth, d , the total unit fiber stress at point a is

$$s = \frac{T}{A} + \frac{[M_{ra} + H m_2 + V n_2 - W (n_2 - n_{br})] \frac{d}{2}}{I - \frac{\sec \theta}{E} \left[k_1 H L_0^2 + k_2 V L_0 h_0 + \frac{H \sum E I_c m_{or} - 2 W E I_c (n_r - n_{br})}{2 M_{ra}} \right]} \quad (24)$$

The second part of the denominator in the bending expression has the same units as I . As in the case of the simple beam, this term is denoted as the reduction factor and is also represented by I_r .

Letting M_1 represent the multiplier of $d/2$ in Eq. 24 leads to

$$s = \frac{T}{A} + \frac{M_1 d}{2 (I - I_r)} \quad (25)$$

The deflection expressions in Eqs. 19 and 20 become

$$m = \frac{M_1 \sec \theta \left(k_1 L_0^2 + \frac{\sum E I_c m_{or}}{2 M_{ra}} \right)}{E (I - I_r)} + m_2 \quad (26a)$$

and

$$n = \frac{M_1 \sec \theta (k_2 L_0 h_0)}{E (I - I_r)} + n_2 \quad (26b)$$

The form of Eqs. 25 and 26 is adequate for analysis but not for design because neither the shape nor the distribution of area in the cross section is considered. Consequently, these three equations must be modified.

To effect such modification it is necessary to introduce the following symbols: d is the depth of the rib; t is the web thickness; I_W represents the moment of inertia of the web about the bending axis; I_F is the moment of inertia of the flange about the bending axis; $R_I = I_F/I_W$; and $N = d/t$. The expression for the total area is

$$A = d^2 \left(\frac{R_I + 3}{3 N} \right) \quad (27a)$$

and the expression for the total moment of inertia is

$$I = d^4 \left(\frac{R_I + 1}{12 N} \right) \quad (27b)$$

In order to account for bracing plates near the bending axis in box-type rib sections and for the reduction in the cross-sectional area due to rivet or template holes in plates, Eq. 27a should be modified to

$$A = j d^2 \left(\frac{R_I + 3}{3 N} \right) \quad (28)$$

in which j is a factor varying from 0.95 to 1.15 in design work. If the designer assumes that 5% of the cross-sectional area for a box-type rib section will be removed for the riveting or welding operation, and that a transversal stiffening

plate at the neutral axis will constitute 15% of the box-section area, then $j = 1.00 - 0.05 + 0.15 = 1.10$.

From Eqs. 27b and 28 the final expressions for s , m , and n become

$$s = \frac{T}{j d^2 \left(\frac{R_I + 3}{3 N} \right)} + \frac{M_1 \frac{d}{2}}{d^4 \left(\frac{R_I + 1}{12 N} \right) - I_r} \dots \dots \dots (29)$$

$$m = \frac{M_1 \frac{\sec \theta}{E} \left(k_1 L_0^2 + \frac{\sum E I_c m_{or}}{2 M_{ra}} \right)}{d^4 \left(\frac{R_I + 1}{12 N} \right) - I_r} + m_2 \dots \dots \dots (30)$$

and

$$n = \frac{M_1 \frac{\sec \theta}{E} (k_2 L_0 h_0)}{d^4 \left(\frac{R_I + 1}{12 N} \right) - I_r} + n_2 \dots \dots \dots (31)$$

To construct the interaction diagram for design, the following procedure would be used: The value of N is selected, using the specifications and past experience as guides. The maximum allowable N -value depends on the specifications and the type of steel used. However, this value is never greater than 170, so that the web is safe against buckling. The value of j is selected on the basis of experience and predesign computations. Thus, the equations for s , m , and n simplify to expressions involving d and R_I . Working with a value of R_I in Table 1 (in which $N = 100$), the designer selects the values of $\frac{d^2 (R_I + 3)}{3 N}$

and $\frac{d^2 (R_I + 1)}{12 N}$, for each d -value, respectively. These different values are substituted into Eqs. 29 through 31, thus obtaining values for s , m , and n , respectively. The m -deflections and n -deflections are combined to determine the radial deflection,

$$u = \sqrt{m^2 + n^2} \dots \dots \dots (32)$$

Although the process appears long, the diagram plots rapidly by the use of Table 1. The resulting interaction diagrams have s and u as the ordinate, d as the abscissa, and a family of R_I -curves. The interaction diagrams are analogous to those for the beam column, except that R_I and u replace A and v , respectively.

Two-Hinged Truss Arch.—The problem of the truss arch is solved by treating it as a rib arch. The dotted line in Fig. 8 represents the arch axis, which coincides with the desired force polygon.

The moment equation for point a in the arch axis for a specified loading condition, assuming Eq. 14 is applicable, is given by Eq. 22. The loading

TABLE 1.—AREA AND MOMENT OF INERTIA FOR RIB ARCH AS A FUNCTION OF THE SHAPE FACTOR AND DEPTH FOR $N = 100$

Depth, d , in inches	VALUE OF R_f									
	1	2	3	4	5	6	7	8	9	10
(a) CROSS-SECTIONAL AREA, IN SQUARE INCHES										
40	21	27	32	37	43	48	53	59	64	69
50	33	42	50	58	67	75	83	92	100	108
60	48	60	72	84	96	108	120	132	144	156
70	65	82	98	114	131	147	163	180	196	213
80	85	107	128	149	171	192	213	235	256	277
90	108	135	162	189	216	243	270	297	324	351
100	133	167	200	233	267	300	333	367	400	433
110	161	202	242	282	323	363	403	444	484	524
120	192	240	288	336	384	432	480	528	576	624
130	225	282	338	394	451	507	563	620	676	732
140	261	327	392	457	523	588	653	719	784	849
150	300	375	450	525	600	675	750	825	900	975
160	341	427	512	597	683	768	853	939	1,024	1,109
170	385	482	578	674	771	867	963	1,060	1,156	1,252
180	432	540	648	756	864	972	1,080	1,188	1,296	1,404
190	481	602	722	842	963	1,083	1,203	1,324	1,444	1,564
200	533	667	800	933	1,067	1,200	1,333	1,467	1,600	1,733
210	588	735	882	1,029	1,176	1,323	1,470	1,617	1,764	1,911
220	645	807	968	1,129	1,291	1,452	1,613	1,775	1,936	2,097
230	705	882	1,058	1,234	1,411	1,587	1,763	1,940	2,116	2,292
240	767	960	1,152	1,344	1,536	1,728	1,920	2,112	2,304	2,496
250	833	1,042	1,250	1,458	1,667	1,875	2,083	2,292	2,500	2,708
260	901	1,127	1,352	1,577	1,803	2,028	2,253	2,479	2,704	2,929
270	972	1,215	1,458	1,701	1,944	2,187	2,430	2,673	2,916	3,159
280	1,045	1,307	1,568	1,829	2,091	2,352	2,613	2,875	3,136	3,397
290	1,121	1,402	1,682	1,962	2,243	2,523	2,803	3,084	3,364	3,644
300	1,200	1,500	1,800	2,100	2,400	2,700	3,000	3,300	3,600	3,900
(b) MOMENT OF INERTIA, IN INCHES ⁴										
40	4,267	6,400	8,533	10,667	12,800	14,933	17,067	19,200	21,333	23,467
50	10,417	15,625	20,833	26,042	31,250	36,458	41,667	46,875	52,083	57,292
60	21,600	32,400	43,200	54,000	64,800	75,600	86,400	97,200	108,000	118,800
70	40,017	60,025	80,033	100,000	120,050	140,058	160,065	180,073	200,083	220,092
80	68,267	102,400	136,533	170,668	204,800	238,933	273,068	307,200	341,332	375,467
90	109,350	164,025	218,700	273,375	328,050	382,725	437,400	492,075	546,750	601,425
100	166,667	250,000	333,333	416,667	500,000	583,333	666,667	750,000	833,333	916,667
110	244,017	366,025	488,033	610,042	732,050	854,058	976,067	1,098,075	1,220,078	1,342,092
120	345,100	517,650	690,199	862,750	1,035,300	1,207,849	1,380,400	1,552,950	1,725,500	1,898,050
130	476,017	714,025	952,033	1,190,043	1,428,050	1,666,058	1,904,066	2,142,075	2,380,083	2,618,092
140	640,268	960,400	1,280,533	1,600,667	1,920,800	2,240,933	2,561,067	2,881,200	3,201,321	3,521,479
150	843,750	1,265,625	1,687,500	2,109,377	2,531,250	2,953,125	3,375,000	3,796,875	4,218,750	4,640,625
160	1,092,267	1,638,400	2,184,531	2,729,667	3,276,800	3,822,931	4,369,067	4,915,200	5,461,333	6,007,467
170	1,392,017	2,088,025	2,784,033	3,480,070	4,176,050	4,872,058	5,568,067	6,264,075	6,960,080	7,656,092
180	1,749,600	2,624,400	3,499,200	4,373,999	5,248,900	6,123,600	6,998,400	7,873,200	8,747,997	9,622,800
190	2,172,017	3,258,025	4,344,033	5,430,085	6,516,050	7,602,058	8,688,071	9,774,075	10,860,083	11,946,096
200	2,666,667	4,000,000	5,333,333	6,666,667	8,000,000	9,333,333	10,666,667	12,000,000	13,333,333	14,666,667
210	3,241,350	4,862,025	6,482,700	8,103,375	9,724,050	11,344,724	12,965,400	14,586,075	16,206,749	17,827,425
220	3,904,267	5,856,400	7,808,526	9,760,745	11,712,860	13,664,983	15,617,067	17,569,200	19,521,333	21,473,467
230	4,664,018	6,996,025	9,328,024	11,660,134	13,992,050	16,324,049	18,656,067	20,988,075	23,320,074	25,652,082
240	5,529,601	8,294,400	11,059,199	13,824,110	16,588,800	19,353,589	22,118,400	24,893,200	27,647,989	30,412,801
250	6,510,418	9,765,625	13,020,832	16,276,043	19,531,250	22,786,445	26,041,667	29,296,875	32,552,082	35,807,304
260	7,616,267	11,424,400	15,232,381	19,040,667	22,848,800	26,656,932	30,465,068	34,273,200	38,081,331	41,889,619
270	8,857,352	13,286,025	17,714,700	22,143,376	26,572,050	31,000,707	35,429,418	39,858,075	44,286,732	48,715,602
280	11,550,956	17,326,400	23,101,864	28,577,335	34,652,800	40,428,243	46,203,756	51,979,200	57,754,667	63,530,133
290	11,928,186	17,692,275	23,556,367	29,820,482	35,784,565	41,748,639	47,712,736	53,676,825	59,640,893	65,605,932
300	13,500,000	20,250,000	27,000,000	33,750,000	40,500,000	47,250,000	54,000,000	60,760,000	67,500,000	74,250,000

condition that is critical for member uc is shown in Fig. 8. Because S_{uc} (the stress at uc) is equal to the moment at point i divided by the radial depth, d , and because the moment at point i is equal to

$$M_i = M + H h \dots \dots \dots (33)$$

Then,

$$S_{uc} = \frac{\frac{M_1}{d}}{1 - \frac{\sec \theta}{EI} \left[k_1 H L \phi^3 + k_2 V L \phi h_0 + \frac{H \sum EI_e m_{or} - 2 W EI_e (n_r - n_{lr})}{2 M_{ra}} \right]} + \frac{H h}{d} \dots \dots (34)$$

The unit stress in member uc is S_{uc}/A_{uc} , in which A_{uc} is the cross-sectional area of member uc. If d_1 and d_2 are the distances from the arch axis to the upper and

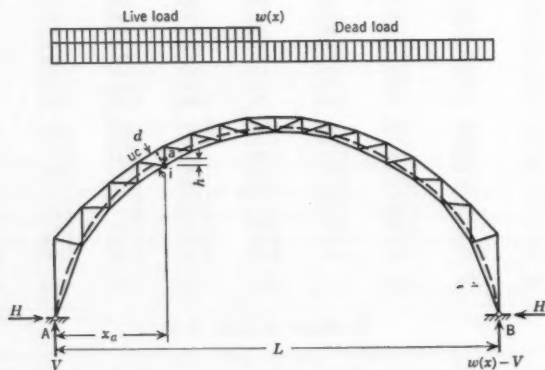


FIG. 8.—THE TWO-HINGED TRUSS ARCH

lower chord, respectively, and A_{lc} is the area of the lower chord, the total moment of inertia about the arch axis is

$$I = A_{uc} d_1^2 + A_{lc} d_2^2 \dots \dots \dots (35)$$

If it is assumed that the arch axis passes through the centroid of the chord areas ($A_{uc} d_1 = A_{lc} d_2$), the unit stress in the upper chord is

$$s = \frac{M_1 (d - d_2)}{A_{uc} d (d - d_2) - \frac{\sec \theta}{EI} \left[k_1 H L \phi^3 + k_2 V L \phi h_0 + \frac{H \sum EI_e m_{or} - 2 W EI_e (n_r - n_{lr})}{2 M_{ra}} \right]} + \frac{H h}{A_{uc} d} \dots \dots (36a)$$

Because the second part of the denominator is equal to I_r , Eq. 36a can be simplified to

$$s = \frac{M_1 (d - d_2)}{A_{uc} d (d - d_2) - I_r} + \frac{H h}{A_{uc} d} \dots \dots \dots (36b)$$

Using the same substitutions in Eqs. 26 results in

$$m = \frac{M_1 \frac{\sec \theta}{E} \left(k_1 L_0^2 + \frac{\sum E I_c m_{or}}{2 M_{ra}} \right)}{A_{uc} d (d - d_2) - I_r} + m_2 \dots \dots \dots (37a)$$

and

$$n = \frac{M_1 \frac{\sec \theta}{E} (k_2 L_0 h_0)}{A_{uc} d (d - d_2) - I_r} + n_2 \dots \dots \dots (37b)$$

Eqs. 36b and 37 provide an ample description of the structural behavior of the section as a function of A_{uc} , d , and d_2 . The value of d_2 is selected arbitrarily by the designer from architectural considerations. Therefore, the desired ($A_{uc} d$)-values are obtained for each value of A_{uc} in Table 2. Performing the

TABLE 2.—VALUES OF THE PRODUCT OF CHORD AREA AND RADIAL DEPTH FOR THE TRUSS ARCH

Depth, d , in inches	VALUE OF A , IN SQUARE INCHES										
	50	100	200	300	400	500	600	700	800	900	1,000
50	2,500	5,000	10,000	15,000	20,000	25,000	30,000	35,000	40,000	45,000	50,000
100	5,000	10,000	20,000	30,000	40,000	50,000	60,000	70,000	80,000	90,000	100,000
150	7,500	15,000	30,000	45,000	60,000	75,000	90,000	105,000	120,000	135,000	150,000
200	10,000	20,000	40,000	60,000	80,000	100,000	120,000	140,000	160,000	180,000	200,000
250	12,500	25,000	50,000	75,000	100,000	125,000	150,000	175,000	200,000	225,000	250,000
300	15,000	30,000	60,000	90,000	120,000	150,000	180,000	210,000	240,000	270,000	300,000
350	17,500	35,000	70,000	105,000	140,000	175,000	210,000	245,000	280,000	315,000	350,000
400	20,000	40,000	80,000	120,000	160,000	200,000	240,000	280,000	320,000	360,000	400,000
450	22,500	45,000	90,000	135,000	180,000	225,000	270,000	315,000	360,000	405,000	450,000
500	25,000	50,000	100,000	150,000	200,000	250,000	300,000	350,000	400,000	450,000	500,000
550	27,000	55,000	110,000	165,000	220,000	275,000	330,000	385,000	440,000	495,000	550,000
600	30,000	60,000	120,000	180,000	240,000	300,000	360,000	420,000	480,000	540,000	600,000
650	32,500	65,000	130,000	195,000	260,000	325,000	390,000	455,000	520,000	585,000	650,000
700	35,000	70,000	140,000	210,000	280,000	350,000	420,000	490,000	560,000	630,000	700,000
750	37,500	75,000	150,000	225,000	300,000	375,000	450,000	525,000	600,000	675,000	750,000
800	40,000	80,000	160,000	240,000	320,000	400,000	480,000	560,000	640,000	720,000	800,000
850	42,500	85,000	170,000	255,000	340,000	425,000	510,000	595,000	680,000	765,000	850,000
900	45,000	90,000	180,000	270,000	360,000	450,000	540,000	630,000	720,000	810,000	900,000
950	47,500	95,000	190,000	285,000	380,000	475,000	570,000	665,000	760,000	855,000	950,000
1,000	50,000	100,000	200,000	300,000	400,000	500,000	600,000	700,000	800,000	900,000	1,000,000

indicated operations and combining m and n into u results in the interaction diagrams having s and u as ordinates, d as the abscissa, and a family of A_{uc} -curves. For the design of the lower chord, Eqs. 36b and 37 are used, with A_k and d_1 replacing A_{uc} and d_2 , respectively. The loading condition is critical for the lower chord member.

Hingeless Rib Arch.—The hingeless rib arch is the same as the two-hinged rib arch, with the additional consideration of the fixed-end moments. In the subsequent derivation, two more terms are included: M_{rf} and M_{ff} , which represent the moment at the fixed end of the rigid arch and flexible arch, respectively.

Point a in Fig. 4, the critical point, is in equilibrium when the following equation is satisfied:

$$M + M_{ff} = V (x_a - n) - H (y_a - m) - W [(x_a - x_b) + (n - n_b)] \dots (38)$$

However, the increase in positive moment at point *a* that is introduced by the shifting of the arch axis is approximately equal to the increase in negative moment at the fixed end.⁵ Therefore, $M - M_{ra} = M_{ff} - M_{rf}$, and Eq. 38 becomes

$$M = \frac{M_{ra} + \frac{1}{2} [H m_2 + V n_2 - W (n_2 - n_{br})]}{1 - \frac{\sec \theta}{2 E I} \left[k_1 H L_0^2 + k_2 V L_0 h_0 + \frac{H \sum E I_e m_{or} - 2 W E I_e (n_r - n_{br})}{2 M_{ra}} \right]} \dots (39)$$

As a simplification,

$$M_1 = M_{ra} + \frac{1}{2} [H m_2 + V n_2 - W (n_2 - n_{br})] \dots (40)$$

and

$$I_r = \frac{\sec \theta}{2 E} \left[k_1 H L_0^2 + k_2 V L_0 h_0 + \frac{H \sum E I_e m_{or} - 2 W E I_e (n_r - n_{br})}{2 M_{ra}} \right] \dots (41)$$

Hereafter, the problem for analysis or design is identical to that of the two-hinged arch rib. Therefore, Eqs. 25 and 26 should be used for analysis, and Eqs. 29, 30, and 31 for design.

Hingeless Truss Arch.—The hingeless truss arch combines the flexural rigidities developed by the absence of hinges and also by the depth of the truss. The problem can be solved by combining the derivations for the hingeless rib arch and the two-hinged truss arch. The unit stress at the lower chord and the vertical and horizontal deflections are given by Eqs. 36*b* and 37, respectively, in which M_1 is given by Eq. 40 and I_r by Eq. 41.

Tied Arch.—The inward pull at each support of the tied arch is produced by the tie member connecting the hinges, and this internal pull enables the structure to be analyzed as an arch. This type of structure should be designed as a two-hinged arch, as considered previously.

DESIGN EXAMPLES

The design procedure proposed herewith is both accurate and simple for an experienced designer to apply. After the type, span, and rise of the arch have been selected, the floor deck has been designed, and the geometry of the arch axis has been established, the design of the arch rib or truss can be undertaken. Five definite design steps are necessary:

1. Assuming that Eq. 14 is applicable at any point of the arch rib, the influence line for the redundant horizontal reaction, H , at the supports must be computed. The assumption of Eq. 14 for direct design will involve only negligible errors and can be used safely in solving for external redundants. The external reactions in an indeterminate structure are influenced by the cross-sectional dimensions throughout the structure. However, another factor that exercises more influence on the magnitude of the external reactions is the location of the axis of the structure with respect to the force polygon. Therefore, if Eq. 14 is used and if the arch axis ordinates coincide with the desired force

⁵"Rainbow Arch Bridge over Niagara Gorge: A Symposium," *Transactions, ASCE*, Vol. 110, 1945, pp. 1-178.

polygon, hardly any accuracy is sacrificed in the procedure. Furthermore, Eq. 14 nearly approaches the variation in cross-sectional dimensions in most arches, whether they are two-hinged or hingeless.

2. Using the solved redundant information from step 1, the necessary influence lines for moment and axial thrust at the desired panel points must be computed. These influence lines must be used to determine the critical location of the live load in each case.

3. In the rigid-arch system, it is necessary to determine at each desired point the reactions due to dead load, critical live load, impact, wind, temperature, and errors of erection. For the critical loading for each point, values of H , V , W , L_0 , and h_0 must be determined.

4. For each critical loading condition, the values of k_1 and k_2 and the deflection values of n_r , m_{0r} , n_{0r} , m_2 , n_2 , and n_{b2} must be determined.

5. One must substitute the necessary values in the interaction expressions for every point considered. The resulting fiber stresses and deflections are then plotted. The interaction diagrams enable the designer to select an adequate cross section for each point in the arch system.

Design of the Two-Hinged Rainbow Bridge.—The two-hinged Rainbow Bridge, which had a span at 950 ft, never advanced beyond the preliminary design stage because it lacked flexural rigidity. Instead, the hingeless Rainbow Bridge was designed and built in 1941 at the Niagara gorge of the Niagara River (New York-Canada).

The design procedure will be demonstrated for the quarter point of the two-hinged Rainbow Bridge for the conditions of dead load, live load, and impact. Temperature and erection errors, which make the loading condition more critical, will be neglected in order that a comparison can be made with design information by the late Shortridge Hardesty,⁵ Hon. M. ASCE.

Step 1.—To compute the influence line for the redundant horizontal reaction, H , at the supports, the following expression for H for any load on the arch is used:

$$H = \frac{\sum M_s y \frac{ds}{EI}}{\sum y^2 \frac{ds}{EI}} \dots \dots \dots (42)$$

in which M_s is the simple beam moment at each segment due to the loading system. From Eqs. 14 and 15 (with dx being the panel length),

$$H = \frac{\sum M_s y}{\sum y^2} \dots \dots \dots (43)$$

Step 2.—Using the solved redundant information from step 1, the influence lines for the reactions at the quarter point, which is point 7, are computed. The influence line for the moment at point 7 and specifications⁵ of the American Association of State Highway Officials (AASHO) require that the uniform live load of 1.375 kips per ft be extended from the left support to $x = 400$ ft, and that the concentrated live load of 26.7 kips be placed at point 7 (Fig. 9).

Step 3.—For the loading shown, the rigid-arch analysis produces the following values: $M_{ra} = 24,877$ ft-kips; $T = 7,534$ kips; $H = 7,191$ kips; $V = 4,921$ kips; $W = 2,263$ kips; $L_0 = 438.2$ ft; and $h_0 = 149.8$ ft.

Step 4.—The values of k_1 and k_2 are determined by loading with elastic loads the conjugate structure of a short arch, the latter having a span of L_0 and a differential height of h_0 between supports, and by computing the quantities $m' E I_c$ and $n' E I_c$ at point 7 of the short arch. With these values,

$$k_1 = \frac{m' E I_c}{M_{rq} L_0^3} \dots \dots \dots (44)$$

and

$$k_2 = \frac{n' E I_c}{M_{rq} L_0 h_0} \dots \dots \dots (45)$$

in which M_{rq} is the moment at the quarter point of the rigid arch. Because the ordinates change as the arch deflects (the shape of the moment diagram does

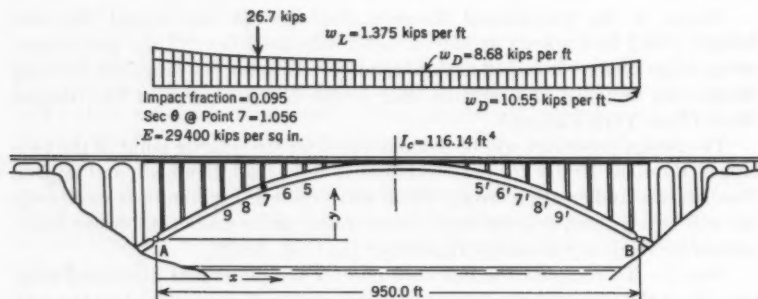


FIG. 9.—CRITICAL LOADING FOR QUARTER POINT OF TWO-HINGED RAINBOW BRIDGE (NEW YORK-CANADA)

not), the k -values are the same for the flexible-arch system as for the rigid-arch system. The elastic loads acting are $M_{ra} \frac{ds}{E I}$ or $M_{ra} \frac{dx}{E I_c}$, but because $\frac{dx}{E I_c}$ is a constant, the moment value, M_{ra} , at each segment can be used as the relative elastic load at the corresponding segment. Taking moments about an axis parallel to the y -axis and passing through point 0 (Fig. 6), the reaction θ_A is 94,149 ft-kips. Taking moments about the y -axis and x -axis at point a, the values of $m' E I_c$ and $n' E I_c$, respectively, are obtained and substituted in Eqs. 44 and 45:

$$k_1 = \frac{491,198,614}{(24,877) (438.10)^3} = 0.1029$$

and

$$k_2 = \frac{270,429,667}{(24,877) (438.10) (149.62)} = 0.1657$$

In the foregoing computations the numerator represents the statical moment of the elastic loads on a conjugate structure and includes the value of I_c as a component part. Hence, the absolute value of I_c is not needed in the computation. Because the deflections resulting from axis distortion are neglected, the terms m_2 , n_2 , and n_{b2} have a zero value. The terms n_r , m_{or} , and n_{br} can be determined by loading the conjugate structure of the 950-ft span and 150.75-ft rise with the moment values appearing in Table 3. Taking moments about the necessary axes leads to

$$\begin{aligned}\sum E I_c m_{or} &= 26,324,702 \text{ kip-ft}^3 \\ E I_c n_r &= 270,907,243 \text{ kip-ft}^3\end{aligned}$$

and

$$E I_c (n_r - n_{br}) = 75,585,940 \text{ kip-ft}^3$$

TABLE 3.—MOMENT VALUES FOR FIG. 9

Column point	x, in feet	y, in feet	M_{ra} , in foot-kips (12 to 1)	M_{rb} , in foot-kips (12' to 1')
12	19.6	12.546	6,238	-886
11	59.2	36.106	12,870	-6,280
10	98.8	57.302	18,221	-10,605
9	138.4	76.291	21,560	-14,584
8	178.0	92.972	24,011	-17,092
7	217.6	107.491	24,877	-18,825
6	257.2	119.863	23,251	-19,534
5	296.8	130.121	20,213	-19,296
4	336.4	138.294	15,907	-17,966
3	376.0	144.404	10,378	-15,502
2	415.0	148.468	3,534	-11,995
1	455.2	150.497	-2,597	-7,773
Crown	475.0	150.750

Step 5.—With the necessary values available, the following terms are computed:

$$I_r = 995,119 \text{ in.}^4$$

$$\frac{M_1 \sec \theta}{E} \left(k_1 L_0^2 + \frac{\sum E I_c m_{or}}{2 M_{ra}} \right) = 31,310,776 \text{ in.}^5$$

and

$$\frac{M_1 \sec \theta}{E} (k_2 L_0 h_0) = 16,807,649 \text{ in.}^5$$

Substituting these and previous values into Eqs. 29, 30, and 31 results in

$$s = \frac{7,534}{j d^2 \frac{R_I + 3}{3 N}} + \frac{298,524 \left(\frac{d}{2} \right)}{d^4 \frac{R_I + 1}{12 N} - 995,119}$$

$$m = \frac{31,310,776}{d^4 \frac{R_I + 1}{12 N} - 995,119}$$

and

$$n = \frac{16,807,649}{d^4 \frac{R_I + 1}{12 N} - 995,119}$$

In the actual two-hinged Rainbow Bridge, the value of N was $\frac{(14)}{(2)} \frac{(12)}{(5/16)} = 89.6$. The designer selects $N = 90$ for the quarter-point section. To account for a lateral bracing plate at the midheight of the section and also for area deductions due to rivet or template holes, the selected value of j is 1.10. This

INTERACTION DIAGRAMS

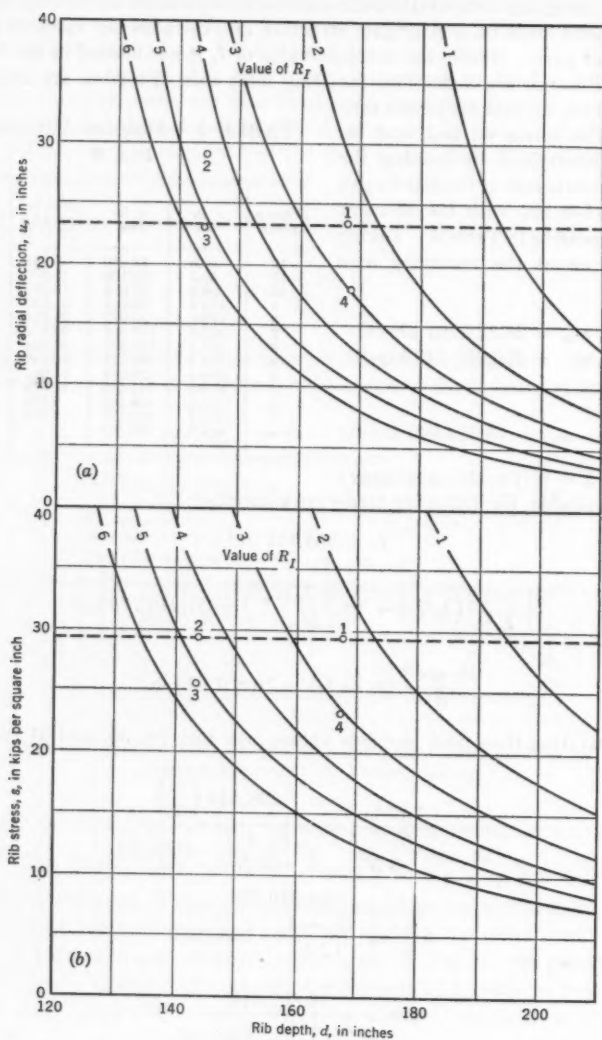


FIG. 10.—INTERACTION DIAGRAM FOR QUARTER POINT OF TWO-HINGED RAINBOW BRIDGE (NEW YORK-CANADA)

j -value usually varies from 0.95 to 1.15. Table 1 is for $N = 100$. Therefore, the values in that table should be multiplied by 100/90. However, for axial unit stress the values of Table 1(a) for $N = 100$ can be used, provided that the axial thrust is modified to $T = \frac{7,534 (1.00) (90)}{1.10 (100)} = 6,164$ kips. However, the moment-of-inertia values in Table 1(b) still must be multiplied individually by 100/ N , or 1.11 in this case. For example, for $R_I = 1$ and $d = 200$, from Table 1(a), $\frac{d^2 (R_I + 3)}{3 N} = 533$ sq in., and from Table 1(b), $\frac{d^4 (R_I + 1)}{12 N} = 2,666,667$ in.⁴ The values for s , m , n , and u are

$$s = \frac{6,146}{533} + \frac{298,524 \left(\frac{200}{2} \right)}{(1.11) (2,666,667) - 989,051} = 26.75 \text{ kips per sq in.}$$

$$m = \frac{31,310,776}{(1.11) (2,666,667) - 989,051} = 15.8 \text{ in.}$$

$$n = \frac{16,807,649}{(1.11) (2,666,667) - 989,051} = 8.5 \text{ in.}$$

and

$$u = \sqrt{(15.8)^2 + (8.5)^2} = 18.0 \text{ in.}$$

The foregoing computations are performed for the values of R_I and d and are plotted in Fig. 10.

The primary function of the interaction diagrams is to enable the designer to select a section that will be safe for the specified loading. If Hardesty's resulting values of $s = 29.22$ kips per sq in. and $u = 23.40$ in. are specified as allowable for the quarter point,⁵ any section that lies below these two values will satisfy the requirement. It is evident that the most economical section is that which meets both of these limiting conditions simultaneously. This can be accomplished by only one section because $29.22 = s_1 (R_I, d)$ and $23.40 = s_2 (R_I, d)$. These two equations involve two unknowns, R_I and d , which can describe only one section. This section can be located easily in the diagram—it is marked 1, $R_I = 2.30$, and $d = 168$ in. Therefore, the dimensions of the section are $d = 168$ in. = 14 ft, which agrees with Hardesty's value. Also,

$$A = j d^2 \frac{R_I + 3}{3 N} = 1.10 (168)^2 \frac{2.30 + 3}{270} = 609 \text{ sq in.}$$

which checks substantially with Hardesty's value of 614 sq in.;

$$I = d^4 \frac{R_I + 1}{12 N} = (168)^4 \frac{2.30 + 1}{12^4 (1,080)} = 118 \text{ ft}^4$$

which agrees closely with Hardesty's value of 120.24 ft⁴; and

$$t = \frac{d}{N} = \frac{168}{90} = 1.87 \text{ in.}$$

However, because a box-type section is used, each web plate must be 0.5 (1.87), or 0.93 in. thick. Hardesty's value was 15/16 in., or 0.94 in.

The area of the flange, including the area of the flange angles, is

$$A_f = \frac{R_f t d}{3} = \frac{2.30 (1.87) (1.68)}{3} = 241 \text{ sq in.}$$

If the arch is considered rigid, the reduction factor, I_r , equals 0 in the interaction expression, and the quarter-point unit stress in the rigid arch is

$$s = \frac{7,534}{609} + \frac{(24,877) (12) \left(\frac{168}{2}\right)}{(118) (12)^2 - 0} = 22.55 \text{ kips per sq in.}$$

Consequently, the increase in stress brought about by the change in the configuration of the arch axis is

$$s = \frac{29.22 - 22.55}{22.55} = 29.6\%$$

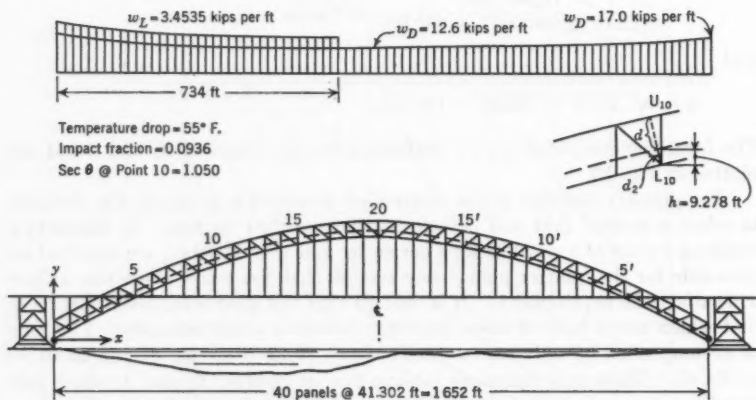


FIG. 11.—LOADING CONDITION FOR UPPER CHORD AT QUARTER POINT OF BAYONNE BRIDGE (NEW JERSEY)

However, architectural restrictions sometimes fix the depth, and it is impossible to satisfy exactly the s -, u -, and d -requirements simultaneously. If 29.22 kips per sq in. and 23.40 in. are retained, and if d is fixed at 144 in., point 3 with $R_f = 5.2$, $u = 23.4$ in., and $s = 25.8$ kips per sq in. would have to be selected. Point 2 with $R_f = 4.5$ satisfies the stress requirement at $s = 29.22$ kips per sq in., but it exceeds the allowable deflection with $u = 29$ in.

The two-hinged Rainbow Bridge was a preliminary design, and it was greatly overstressed as a result of the deflection stresses. Using the allowable unit stress for the silicon arch rib as 23.00 kips per sq in., the importance of the deflection of the arch axis will become more evident. If the designer had decided to keep the bridge as a two-hinged arch and desired to retain the depth of 168

in., point 4, at which $R_I = 3$, would satisfy the condition. However, the properties of the cross section would be

$$A = j d^2 \frac{R_I + 3}{3N} = (1.10) (168)^2 \frac{3 + 3}{270} = 687 \text{ sq in.}$$

and

$$I = d^4 \frac{R_I + 1}{12N} = \left(\frac{168}{12} \right)^4 \left(\frac{3 + 1}{1,080} \right) = 142.5 \text{ ft}^4$$

The radial deflection for this section would have been only 18.0 in., but the rib section is considerably heavier than that used in the hingeless bridge that was built eventually.

Design of Upper Chord at the Quarter Point of the Bayonne Bridge.—The Bayonne Bridge (Bayonne, N. J.) was designed and built as a 1,652-ft-long, two-hinged arch truss, so that the necessary flexural rigidity was obtained without design and construction problems.⁶ This examination is concerned with the design of the upper chord at the quarter point for the conditions of dead load, live load, impact, and temperature drop. This loading condition is the same as that used by Othmar H. Ammann,⁷ Hon. M. ASCE.

Assuming that the dead-load panel concentrations are known, the dead-load funicular polygon and arch axis are passed through the end pins and a crown point, 275.342 ft above them. This was the case in the actual design.

Step 1.—The influence line for the horizontal reaction is determined from Eqs. 42 and 43.

Step 2.—The influence line for the moment about the lower chord point, L_{10} , is then determined (Fig. 11 and Table 4). The lower chords of the arch truss, in order to satisfy the navigation-clearance requirements, lie on a parabola that passes through the pins and a midspan point 266.0 ft above the pins.

From the influence line for M_{L10} , the critical loading condition has a uniform live load of 3.4535 kips per ft of truss extending over 44.4% of the span, or from point 0 to $x = 734$ ft.

Step 3.—Using the standard procedure, $H = 18,216$ kips; $V = 13,141$ kips; $W = 6,845$ kips; $h = 9.278$ ft; $L_0 = 826$ ft; and $h_0 = 275$ ft.

TABLE 4.—MOMENT VALUES FOR
FIG. 11

Panel point	ORDINATES OF ARCH AXIS, IN FEET		MOMENTS, M_{cs} , IN ARCH AXIS, IN FOOT-KIPS	
	x	y	0 to 20	20' to 0'
0	0	0	0	0
1	41.302	27.849	35.456	-25.024
2	82.604	54.012	67.426	-47.069
3	123.906	78.625	95.172	-66.922
4	165.208	101.692	119.528	-83.723
5	206.510	123.210	140.132	-97.835
6	247.812	143.294	157.042	-109.200
7	289.114	161.905	169.877	-118.226
8	330.416	178.984	178.829	-124.668
9	371.718	194.562	184.568	-127.882
10	413.020	208.778	185.669	-129.292
11	454.322	221.568	183.658	-127.374
12	495.624	232.949	177.273	-123.389
13	536.926	242.960	166.882	-116.969
14	578.228	251.595	152.808	-107.790
15	619.530	258.871	135.055	-95.850
16	660.832	264.810	113.084	-81.778
17	702.134	269.422	87.219	-64.977
18	743.436	272.710	55.712	-45.751
19	784.738	274.682	26.620	-24.112
20	826.042	275.342	-50	-50

⁶ "Design of the 1,675-Ft. Kill van Kull Steel-Arch Bridge," *Engineering News-Record*, Vol. 101, No. 24, December 13, 1928, pp. 873-877.

⁷ "The Design, Materials and Erection of the Kill Van Kull (Bayonne) Arch," by L. S. Moisseiff, *Journal, Franklin Inst.*, Vol. 213, May, 1932.

Step 4.—Using the conjugate-structure method, $k_1 = 0.1038$; $k_2 = 0.1734$; $\sum E I_c m_{or} = -699,537,100 \text{ kip-ft}^3$; $E I_c n_r = 6,384,868,291 \text{ kip-ft}^3$; $E I_c n_{or} = 5,016,497,801 \text{ kip-ft}^3$; $E I_c (n_r - n_{or}) = 1,368,370,500 \text{ kip-ft}^3$; $m_2 = 0.566 \text{ ft} = 6.8 \text{ in.}$; $n_2 = 0.106 \text{ ft} = 1.3 \text{ in.}$; and $n_{o2} = -0.087 \text{ ft} = -1.0 \text{ in.}$

Step 5.—Using the foregoing values, $M_1 = 2,336,599 \text{ in.-kips}$, $I_r = 8,860,576 \text{ in.}^4$,

$$\frac{M_1 \sec \theta}{E} \left(k_1 L_o^2 + \frac{\sum E I_c m_{or}}{2 M_{ra}} \right) = 628,319,793 \text{ in.}^5$$

$$\frac{M_1 \sec \theta}{E} (k_2 L_o h_o) = 301,278,207 \text{ in.}^5$$

and

$$H h = 2,028,169 \text{ in.-kips}$$

The value of d_2 , the radial distance from L_{10} to the arch axis, is 8.85 ft, or 106 in. Substituting these values into Eqs. 36b and 37 leads to

$$s = \frac{2,336,599 (d - 106)}{A d (d - 106) - 8,860,576} + \frac{2,028,169}{A d}$$

$$m = \frac{828,319,793}{A d (d - 106) - 8,860,576} + 6.8$$

and

$$n = \frac{301,278,207}{A d (d - 106) - 8,860,576} - 1.3$$

Substituting the various values of chord area and radial depth that interest the designer, the necessary values for the interaction diagrams are computed and plotted as shown in Fig. 12.

The maximum compressive unit stress allowed in the silicon steel is 23.00 kips per sq in. Because there is no deflection specification, any point at or below the 23.00-kips-per-sq-in. line will satisfy all safety requirements. If a radial depth of 43 ft, or 516 in., is selected for this section, as in Ammann's design, the most economical upper-chord section is that indicated by point 1. This chord section has an approximate area of 390 sq in., which is in substantial agreement with the 385 sq in. of the member U_1, U_{10} in the actual design. Furthermore, the radial displacement undergone by the quarter point would be 18.0 in. for the present loading. Because all the upper-chord panel points must form a smooth curve, the radial depths cannot be varied. In fact, as soon as two or three upper chords have been designed, the radial-depth value is practically fixed for the remainder of the points. Consequently, the stress and deflection values become a function of A only and not of A and d . The use of a greater depth—for example, 975 in.—would have resulted in an upper-chord area of 200 sq in. However, this selection (indicated by point 2) would have involved much longer web members, further detracting from the esthetic element, and a radial displacement of approximately 12.0 in.

The truss provides a high degree of flexural stiffness. The radial displacement of 22.8 in. would have been far greater had a box-type rib been selected, as in the Rainbow Bridge. Furthermore, if the effect of deflections had been

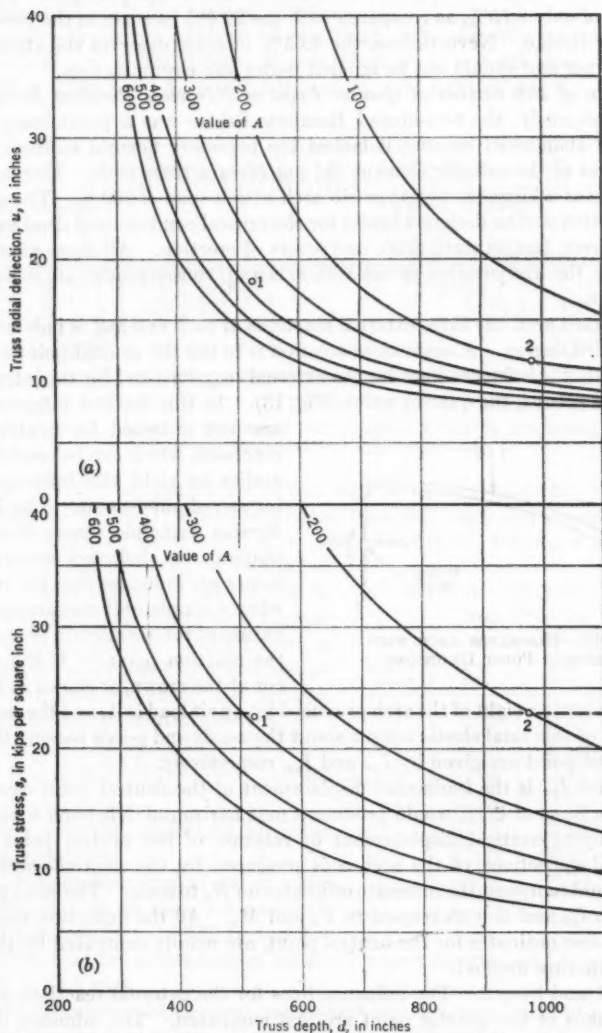


FIG. 12.—INTERACTION DIAGRAM FOR UPPER CHORD AT QUARTER POINT OF BAYONNE BRIDGE (NEW JERSEY)

neglected, then $M_1 = M_{ra}$ and $I_r = 0$, and $s = 21.15$ kips per sq in. This is an increase of only 8.75%, as compared with the 29.6% increase in the two-hinged Rainbow Bridge. Nevertheless, the 8.65% increase deserves the attention of the designer and should not be ignored under any circumstances.

Design of Rib Section at Quarter Point of Hingeless Rainbow Bridge.—As noted previously, the two-hinged Rainbow Bridge was a preliminary design that was abandoned because it lacked the necessary flexural stiffness. Considerations of the esthetic element did not favor a truss arch. Therefore, the solution was a hingeless box-type rib arch with a span of 950 ft. The quarter-point section will be designed herein for the critical conditions of dead load, live load, impact, temperature drop, and errors of erection. All these effects contribute to the disfiguration of the arch axis and, consequently, are included in the design.

The fixed arch has three external reactions at each end and is indeterminate to the third degree. A convenient solution is to use the neutral-point method⁸ to compute the influence lines for the external reactions and for the internal reactions at point f , the quarter point (Fig. 13). In this method influence lines

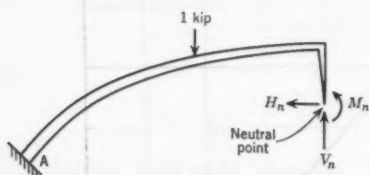


FIG. 13.—HINGELESS ARCH WITH NEUTRAL-POINT REACTIONS

are first obtained for neutral-point reactions, which can be combined by statics to yield the influence lines for any desired point. The Müller-Breslau principle states that "the shape of the deflected structure becomes an influence line for reaction when a simple unit movement in the nature of the reaction is produced at the reaction point." If the arch is cut at the crown, as shown in Fig. 13,

the total elastic weight of the arch produced by a unit load is A , and the moments of inertia of this total elastic weight about the x -axis and y -axis passing through the neutral point are given by I_{xx} and I_{yy} , respectively.

Because I_{xx} is the horizontal displacement of the neutral point caused by $H_n = 1$, a force of $1/I_{xx}$ would produce a unit horizontal deflection without an accompanying vertical displacement or rotation of the neutral point. The horizontal deflections of the arch axis produced by the neutral-point force, $1/I_{xx}$, would represent the influence ordinates for H_n to scale. The same pattern applies to I_{yy} and A with respect to V_n and M_n . All the deflection values, or influence-line ordinates for the neutral point, are readily computed by the conjugate-structure method.

Step 1 and Step 2.—The influence lines for the external reactions and for the reactions at the quarter point are first computed. The influence line for the moment at point f and AASHTO specifications require that the uniform live load of 1.375 kips per ft be extended from the left support to $x = 409$ ft, and that the concentrated load of 26.7 kips be placed at point f . As shown in Fig. 14, a temperature drop of 60° F. has been considered—the span is 1 in. too short,

⁸ "Statically Indeterminate Structures and Space Frames," in "Theory of Modern Steel Structures," by L. E. Grinter, The Macmillan Co., Inc., New York, N. Y., Vol. 2, 1949, Revised Ed., Chapter 8.

and point *f* has deviated from the computed position 1 in. in the horizontal direction and 1 in. in the vertical direction.

Step 3.—From the analysis of the rigid arch, the following values are obtained: $M_{ra} = 17,524$ ft-kips; $H = 6,186$ kips; $T = 6,404$ kips; $V = 4,513$ kips; $W = 2,958$ kips; $L_0 = 336.2$ ft; and $h_0 = 81.54$ ft (Table 5).

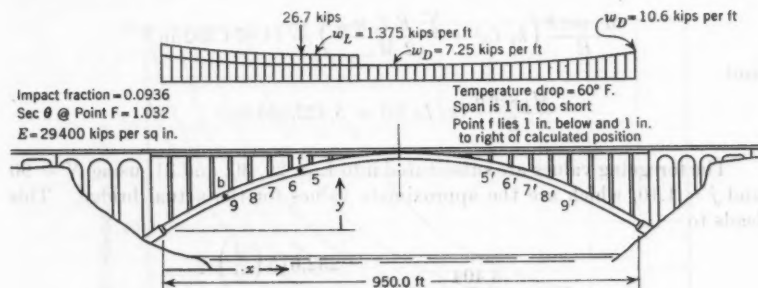


FIG. 14.—LOADING CONDITION FOR QUARTER POINT OF HINGELESS RAINBOW BRIDGE (NEW YORK-CANADA)

Step 4.—The conjugate structures determine the following values: $k_1 = 0.1032$; $k_2 = 0.1682$; and, due to dead load, live load, and impact, $\sum EI_c m_{0r} = -78,815,779$ kip-ft³; $E I_c n_r = 76,444,793$ kip-ft³; $E I_c n_{br} = 58,259,608$ kip-ft³; and $E I_c (n_r - n_{br}) = 18,185,185$ kip-ft³. Point *b* is located at $x = 135$ ft.

It was noted previously that I_{xx} was equal to the horizontal displacement of the neutral point caused by a unit load at that point. Consequently, the neutral-point thrust at the neutral point is

$$H = \frac{\alpha t L + \text{error}}{I_{xx}} \dots (46)$$

in which α is the coefficient of linear thermal expansion.

If a temperature drop of 60° F and a shortness of 1 in. in span are assumed, Eq. 46 becomes $H = 1.0287 I_c$, and if it is assumed that the crown section has already been designed and $I_c = 81.17$ ft⁴, then $H = 83.5$ kips.

From experience the designer must select a preliminary value of I_c that will approximate the final value. If these values are different the preliminary value is modified accordingly. This successive-correction procedure is used only for the design of the crown, which should be the first section to be designed.

Using the conjugate-structure method, the deflections at the desired points caused by the temperature drop of 60° F and the 1-in. span shortness are $n_2 = -0.7$ in., $m_2 = 6.3$ in., and $n_{b2} = -0.3$ in. However, considering the dis-

TABLE 5.—MOMENT VALUES FOR FIG. 14

Column point	<i>x</i> , in feet	<i>y</i> , in feet	<i>M_{rs}</i> , in foot-kips
12	22.307	14.394	-27.685
11	61.672	37.768	-15.940
10	101.036	58.698	-4.864
9	140.401	77.251	4.414
8	179.766	93.582	11.123
7	219.130	107.751	15.624
6	258.495	119.817	18.032
f	278.177	125.958	17.524
5	297.859	129.826	17.171
4	337.224	137.808	14.761
3	376.589	143.783	10.734
2	415.953	147.763	5.248
1	455.318	149.751	785
Crown	475.000	150.000	-2.324

placements of point *f* due to erection errors, $n_2 = -0.7 + 1.0 = 0.3$ in., and $m_2 = 6.3 + 1.0 = 7.3$ in., in which negative signs indicate that the deflection is either in an upward direction or to the left.

Step 5.—Because at point *f*, $M_{ra} = 17,524$ ft-kips, Eq. 40 becomes $M_1 = 232,615$ in.-kips, and Eq. 41 becomes $I_r = 192,052$ in.⁴ In addition,

$$\frac{M_1 \sec \theta}{E} \left(k_1 L_0^2 + \frac{\sum E I_c m_{or}}{2 M_{ra}} \right) = 11,074,392 \text{ in.}^5$$

and

$$\frac{M_1 \sec \theta}{E} (k_2 L_0 h_0) = 5,422,436 \text{ in.}^5$$

The foregoing values are substituted into Eqs. 29, 30, and 31, using $N = 90$ and $j = 1.10$, which are the approximate values for the actual bridge. This leads to

$$s = \frac{6,404}{j d^2 \frac{R_I + 3}{270}} + \frac{232,615 \left(\frac{d}{2} \right)}{d^4 \frac{R_I + 1}{1,080} - 192,052}$$

$$m = \frac{11,074,392}{d^4 \frac{R_I + 1}{1,080} - 192,052} + 7.3$$

and

$$n = \frac{5,422,536}{d^4 \frac{R_I + 1}{1,080} - 192,052} + 0.3$$

Varying d and R_I , with the aid of Table 1, the values of s , m , and n are computed and plotted to yield the interaction diagrams of Fig. 15. In the actual design the quarter-point section has a depth of 12 ft, a total moment of inertia of 88.2 ft⁴, and each web plate is 13/16 in. thick.⁵ The shape factor is $I_F/I_W = [(88.2)(12)^4 - 404,352]/404,352 = 3.52$. Point 1 represents this section, and from Fig. 15 the stress is approximately 22.00 kips per sq in. and the total displacement is 14.7 in. The section, stressed below the allowable 23.00 kips per sq in. for the silicon steel, is safe and fairly economical for the given depth. Point 2 indicates a somewhat more economical section with a shape factor of approximately 3.3 and the same depth. This section would be stressed to the allowable 23.00 kips per sq in., deflect 15.2 in. radially, and its dimensional properties would be

$$I = \left(\frac{144}{12} \right)^4 \left(\frac{3.3 + 1}{1,080} \right) = 82.5 \text{ ft}^4$$

and

$$A = 1.10 (144)^2 \left(\frac{3.3 + 3}{270} \right) = 556 \text{ sq in.}$$

The fact that the actual quarter-point section is slightly understressed is not surprising because the section was designed by the elastic theory, with 20.00 kips per sq in. as the allowable unit stress in the silicon steel rib. In the rigid

system, $M_1 = M_{ra} = 17,524$ ft-kips and $I_r = 0$. Then,

$$s = \frac{6,404 (270)}{1.10 (144)^2 (6.52)} + \frac{17,524 (12) (72)}{1,830,000} = 19.98 \text{ kips per sq in.}$$

The change in geometry of the arch axis produces a 10.01% increase in stress.

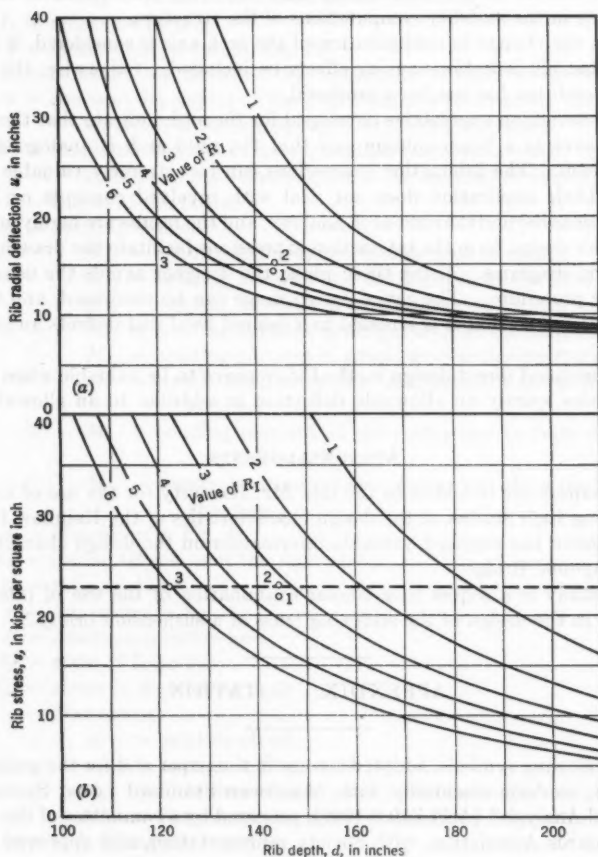


FIG. 15.—INTERACTION DIAGRAM FOR QUARTER POINT OF HINGELESS RAINBOW BRIDGE (NEW YORK-CANADA)

A section with a smaller depth could have been used without making the rib any heavier by increasing the shape factor. Point 3 has a fiber stress of 23.00 kips per sq in. and a radial displacement of 16.8 in. The R_1 -value is equal to 6. Therefore, the effective area is $A = 546$ sq in., whereas the actual section has a value of $A = 554$ sq in. Thus, the interaction diagram is useful

in design because it can yield the stress and deflection values for many combinations of dimensions of the cross section without extended, or sometimes prohibitive, computations.

CONCLUSIONS

In long-span flexible arches, the neglect of the deformed configuration of the arch axis caused by the load system may introduce an intolerable degree of inaccuracy in the stability computations of the structure.

When the change in configuration of the arch axis is considered, it is mandatory that all deflection-causing effects be included. Otherwise, the critical loading condition has not been produced.

The interaction expressions developed for the arch indicate that the flexible arch behaves as a beam column and that the rigid arch is analogous to the simple beam. The interaction expressions can be extremely valuable for analysis. Their application does not deal with involved concepts or lengthy computations beyond the rigid-arch analysis, and the results are highly accurate.

In their design form the interaction expressions facilitate the drawing of the interaction diagrams. Using these plots, the designer avoids the usual trial-and-error procedure. The entire design range can be visualized, and the section is selected so that it is stressed to a desired level and deflects an intended degree.

The proposed direct design method may prove to be valuable when bridge-design codes specify an allowable deflection in addition to an allowable unit stress.

ACKNOWLEDGMENTS

The writers are indebted to the late Mr. Hardesty for the use of his office data during their studies of the design characteristics of the Rainbow Bridges. Mr. Ammann has supplied valuable information on the design characteristics of the Bayonne Bridge.

This study is a sequel to a similar examination of the use of interaction diagrams in the design of the stiffening truss of a suspension bridge.*

APPENDIX. NOTATION

The following symbols, adopted for use in the paper and for the guidance of discussers, conform essentially with "American Standard Letter Symbols for Structural Analysis" (ASA Z10.8-1949), prepared by a committee of the American Standards Association, with Society representation, and approved by the Association in 1949:

- A = cross-sectional area;
- c = one-half the beam depth;
- d = beam depth;
- E = modulus of elasticity;
- H = horizontal reaction;

* "Bending Interaction in Suspension Bridges," by Haaren A. Miklofsky, *Proceedings-Separate No. 652*, ASCE, March, 1955.

h_0 = dimension in Fig. 7;

I = moment of inertia:

I_c = moment of inertia at the crown;

I_F = moment of inertia of the flange;

I_W = moment of inertia of the web;

I_{xx} = moment of inertia about the x -axis;

I_r = reduction factor;

j = factor used in design, Eq. 28;

K = constant dependent on the distribution of the cross-sectional area;

k = constant dependent on the distribution of the bending loads and the variation of the moment of inertia along the beam;

k_1, k_2 = constants dependent on the section being considered, the loading system, and the distribution of the moment of inertia;

L = length of the beam;

M = bending moment:

M_{fa} = bending moment in a flexible arch at point a ;

M_{ff} = bending moment in a flexible arch at the fixed end;

M_{ra} = bending moment in a rigid arch at point a ;

M_{rf} = bending moment in a rigid arch at the fixed end;

M_{rq} = bending moment in a rigid arch at the quarter point;

M_s = simple beam moment at each segment due to the loading system;

M_t = bending moment at the center due to transverse loads only;

M_x = bending moment at each ds -segment along the conjugate structure;

m = dimension in Fig. 4;

m_{or} = initial deflection of the rigid arch;

N = ratio of d to t ;

n = dimension in Fig. 4;

P = axial compression load;

R_I = ratio of I_F to I_W ;

S_{ue} = stress in member ue ;

s = fiber stress:

s_b = bending stress;

s_{max} = maximum fiber stress;

s' = fiber stress due to axial compressive load only;

s'' = fiber stress due to transverse load only;

t = web thickness;

u = radial deflection;

V = vertical reaction;

v = center deflection;

W = total of all downward loads;

$w(x)$ = transverse load system;

x = dimension in Fig. 4;

y = dimension in Fig. 4;

α = coefficient of linear thermal expansion; and

θ = angle of inclination of the arch axis with the horizontal.

DISCUSSION

REINALDO GARCÍA-ITURBE.¹⁰—A clear, comprehensive, and concise manner of developing an interaction diagram for any type of flexible steel arch has been presented. This concept has also been extended to actual design problems. The diagram will allow the designer to tell at a glance which dimensions of the arch rib or truss chord satisfy the requirements for stress and radial deflection, and which are the most economical. It can also be used to indicate the economic feasibility of the use of materials other than carbon or silicon steel for the arch rib or truss members.

The effectiveness and accuracy of such a tool are demonstrated in the design illustrations by comparing the results obtained by its use with those obtained by other forms of the deflection theory.

The main advantage of the interaction diagram is that once it has been drawn for a particular section of a particular structure, it can be used over and over again to check different combinations of sectional dimensions, without repetitious and extensive computations. As in the case of the interaction diagrams for suspension bridges,⁸ the use of the moment of inertia of the chord of the truss arch, whether two-hinged or hingeless, instead of the chord area, is permissible, although the latter is of more immediate importance to the designer.

The interaction diagram, as developed, is based on several assumptions, and the question arises as to how the present analysis would be altered by considering (a) the movement of the inflection point for the flexible system with respect to that for the rigid system; (b) the value of the horizontal reaction, H , not to remain constant as the arch axis deflects; and (c) the centroid of all downward forces acting to the right of the section under consideration to move relative to the load points.

HAAREN A. MIKLOFSKY,¹¹ A.M. ASCE, AND OMAR J. SOTILLO,¹² J. M. ASCE.—The three questions that Mr. García-Iturbe poses can be satisfactorily answered in a qualitative sense:

1. If the movement of the inflection point for the flexible system with respect to that for the rigid system is considered, the alterations are negligible. Computations on the two-hinged Rainbow Bridge indicate that L_0 increases about 3%, and in the case of the hingeless Rainbow Bridge, L_0 increases about 1%.⁸ Using these new values of L_0 in the interaction expressions may give a more accurate set of values for m , n , and M , but they are practically the same as the values obtained without considering the change in L_0 .

2. It is correct that the value of H changes as the arch axis deflects. This change in H is less than $\frac{1}{2}\%$. However, the error in assuming H constant becomes insignificant as soon as ΔH is multiplied by the value of m . For

¹⁰ Graduate Student, Dept. of Civ. Eng., Carnegie Inst. of Technology, Pittsburgh, Pa.

¹¹ Associate Prof., Dept. of Civ. Eng., Rensselaer Polytechnic Inst., Troy, N. Y.

¹² Technical Director, Technical Office, OMIG, Caracas, Venezuela.

example, if $H = 7,500$ kips, then $\Delta H = 38$ kips, and for a deflection of 1 ft, $\Delta M = \Delta H m = (38) (1) = 38$ ft-kips. This ΔM -value can be neglected in a long-span structure.

3. The centroid of all downward forces acting to the right of the section under consideration will move relative to the load points, as Mr. García-Iturbe implies. Consideration of this problem would involve determining the horizontal deflections of all the load points and the location of a new centroid for the downward forces. This would be long and cumbersome, and would not introduce any worthwhile accuracy. Furthermore, to the writers' knowledge, no deflection theory considers such refinements.

AMERICAN SOCIETY OF CIVIL ENGINEERS

Founded November 5, 1852

TRANSACTIONS

Paper No. 2964

GENERATING STATION ON THE NIAGARA RIVER

BY FRANK DOBSON¹

SYNOPSIS

The design, construction features, and associated works of a hydroelectric-power generating station on the Niagara River are described. The pump-storage-generating plan and remedial work to preserve the scenic spectacle of Niagara Falls are emphasized.

INTRODUCTION

Construction on the new Sir Adam Beck-Niagara Generating Station No. 2 began in the fall of 1950, immediately following the ratification of a treaty between the United States and Canada permitting additional diversion of water from the Niagara River for power purposes. This treaty stressed the preservation of the scenic spectacle of the falls by stipulating that during the daylight hours of the tourist season a minimum of 100,000 cu ft per sec of water must flow over the falls. At all other times a minimum of 50,000 cu ft per sec would flow over the falls. The remaining river flow in excess of these volumes could be divided equally between the United States and Canada for power.

General Scheme.—The Niagara River, in flowing between Lake Erie and Lake Ontario, drops 326 ft. Of this fall, 315 ft is concentrated on a 7-mile reach in the river between the villages of Chippawa and Queenston (Canada). Approximately 225 ft of the 315 ft is concentrated in the rapids above the falls and in the falls themselves, and an additional 90 ft occurs in the lower rapids below the falls. The Sir Adam Beck project is designed to utilize the full head concentration of this reach, together with the maximum permissible diversions within economic limits.

NOTE.—Published, essentially as printed here, in October, 1957, in the Journal of the Power Division, as *Proceedings Paper 1419*. Positions and titles given are those in effect when the paper was approved for publication in *Transactions*.

¹ Project Mgr., Sir Adam Beck Generating Station No. 2, Niagara Falls, Ontario, Canada.

The project consists of

a. Two submerged intakes of the Johnson-Wahlman type, constructed along the bank of the river approximately $\frac{1}{4}$ mile downstream from the village of Chippawa;

b. Twin tunnels driven at a diameter of 51 ft, lined with 3 ft of concrete for a finished diameter of 45 ft, and extending $5\frac{1}{4}$ miles beneath the city of Niagara Falls (Ontario);

c. An open-cut canal, approximately $2\frac{1}{4}$ miles long and 200 ft wide, leading to the forebay of the power plant located on the lower river near Queenston;

d. A pumping-generating station with an associated reservoir located adjacent to the power canal; and

e. Remedial works in the upper river—including a control structure below the intakes to regulate the level of the Grass Island pool.

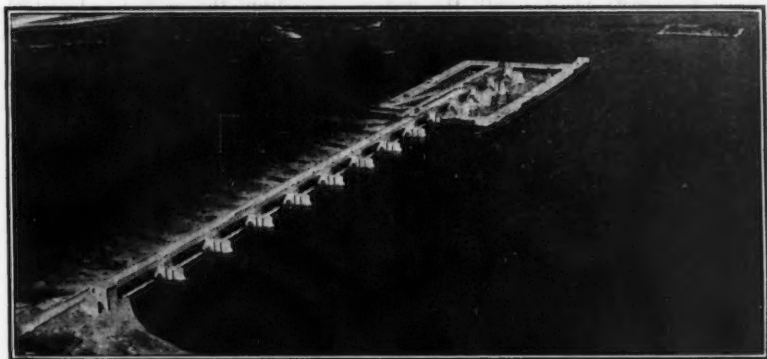


FIG. 1.—GRASS ISLAND DAM CONTROL STRUCTURE

Construction Progress.—In April, 1954, with construction completed on the intake structures, the tunnels, and the power canal, the first 105,000-hp unit went into operation at the new plant. Unit 12 went into service in August, 1955. Construction of the pump-generating plant was begun in 1955 and was completed in the summer of 1958. In January, 1956, authorization was received to proceed with the construction of four more units at the main generating plant to be used in conjunction with the pump-storage plant. Two of these units went into service in the latter part of 1957 and the remaining two, in the summer of 1958.

GRASS ISLAND DAM

The Grass Island control dam, completed as of 1957, was constructed in accordance with the 1950 treaty to control the water level of the Chippawa-Grass Island pool. It is in this reach of the river that the new intake structures for both the United States and the Canadian power diversions are located. Without this dam, the water in the pool would drop 4 ft with maximum diversion. This would virtually eliminate the flow of water over the American Falls and would also lower the level of Lake Erie. Furthermore, the dam

provides a means of regulating the flow over the falls within the minimum specified flows of 100,000 cu ft per sec and 50,000 cu ft per sec.

The completed control dam extends 1,550 ft into the river from the Canadian shore and contains thirteen 100-ft sluices (Fig. 1). The flow through these sluices is controlled by steel gates hinged at the sills, and opened or closed by hydraulically operated pistons in the piers at each end of the gate. These gates are among the largest submersible type in the world, each 100 ft wide and 10½ ft high above the sill elevation. Providing access to the piers is a 24-ft-wide service deck extending the entire length of the dam. This roadway is carried between the piers on prestressed-concrete girders.

The most unique construction feature of Grass Island Dam was the steel-crib type of cofferdam. This cofferdam is basically a series of steel cribs, 30 ft wide, 15 ft high, and 10 ft long, supported off the bottom of the river by 12-by-12 H-pilings fitted into slots in the steel frames, weighted down by precast-concrete blocks, with the water sealed from the enclosure by steel sheet piling.

The Grass Island control dam was part of the over-all plan of the Niagara River remedial works. Another phase of this plan included work at the Horseshoe Falls, where excavations were completed on both the American and Canadian flanks to distribute the flow more evenly over the full crest of the falls. The remedial works have been implemented and paid for jointly by Canadian and United States agencies.

PUMP-STORAGE RESERVOIR AND POWERHOUSE

The pump-storage plan is to store water at night, during the hours of low power demand and when surplus energy is available, by pumping water into a reservoir. This water is used during the daylight hours of high demand, being discharged back through the same pumps, which are reversed in direction to become turbines. After the stored water is discharged from the pump-storage plant, its major advantage lies in its re-use at either of the main generating stations where a high head is available.

The pump-storage canal is 1,450 ft long and 140 ft wide. The average rock cut was 58 ft, with a maximum of more than 80 ft at the powerhouse, and the depth of overburden averaged 20 ft.

The reservoir covers an area of 750 acres and will provide 15,500 acre-ft of live storage on the basis of a 25-ft drawdown. The reservoir is formed by an embankment approximately 5 miles long, varying in height from 15 ft to 65 ft. The embankment is essentially a rock mass made watertight by an impervious clay layer. Filters of crushed stone, both fine and coarse, were placed on either side of the clay blanket to retain the material in place, on top of which was laid down a heavy layer of riprap.

The rock fill was placed by end dumping from trucks and by sluicing with water (in the proportion of two of water to one of rock) with high-pressure hydraulic monitors to achieve compaction and stability in the fill. The sloping filters on the dike were placed in horizontal lifts by belly-dump trucks and compacted by controlling the movement of the hauling and spreading equipment.

Placing and compacting the impervious clay zone required close control of the materials and of the placing methods. Although some deposits of suitable silty clay were found within the reservoir, the bulk of the clay was obtained by stripping a quarry site approximately 6 miles from the reservoir. The clay was dumped on the dike from trucks and scrapers. Then bulldozers spread it in position in comparatively thin layers ranging from 6 in. to 9 in. When the surface of a previously placed layer became too dry or too smooth, it was scarified and sprinkled to promote a better bond with the succeeding layer. The clay was compacted to the proper density by the use of sheepfoot rollers.

Pump-Storage-Generating Plant.—Forming an integral part of the dike is the pump-storage-generating plant (Fig. 2) at the head of the canal. The



FIG. 2.—PUMP-GENERATING STATION DURING CONSTRUCTION

width of the structure between the headworks and the tailrace piers is approximately 200 ft, and the over-all length of the powerhouse is 570 ft, including an erection bay at one end for servicing the units. The six units in this plant are on 74-ft centers and are physically the largest in the system, with the exception of those at the St. Lawrence Seaway project, which are on 80-ft centers.

The pump-generating station has no superstructure. The roof deck of the powerhouse is immediately above the top of the generators, and access to the machines for major repairs is obtained through retractable hatches in the roof. The units are serviced by an outside gantry crane that traverses the full length of the powerhouse deck. This crane has a capacity of 175 tons and sufficient housing to enclose one unit fully.

The steel penstocks, which are approximately 60 ft long, vary in diameter from 19 ft at the scrollcase to 26 ft in the headworks transition.

At the pump-generating station six reversible feathering Francis-type pump turbines, each directly connected to a motor generator, are installed. As pumps, these units are rated at 55,000 hp, and when throughout the head range of from 60 ft to 85 ft, they will discharge between 5,000 cu ft per sec and 4,000 cu ft per sec. As turbines, the units are rated at 47,500 hp under a net head of 85 ft. Over the full head range the units will discharge between 5,600 cu ft per sec and 4,100 cu ft per sec, or they can be operated to give a continuous discharge of approximately 4,100 cu ft per sec. The speed of the

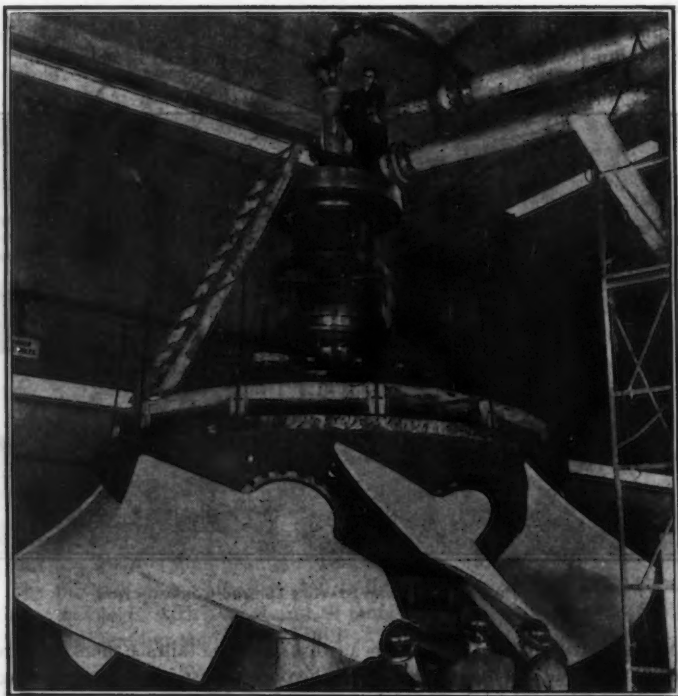


FIG. 3.—REVERSIBLE FEATHERING FRANCIS RUNNER IN ERECTION BAY

machines is 92.3 rpm. With this equipment it is estimated that the reservoir can be filled in about $7\frac{1}{2}$ hr.

Pump Turbine Units.—The pump turbine units (Fig. 3) have many differences in construction and in operation compared with the conventional units installed at the main plant. In the installation of the embedded parts the first unusual piece of equipment was the air-admission nozzle at the heel of the draft tube. This nozzle admits outside air to the draft tube as hydraulic conditions may require. Another unusual feature is the runner envelope,

which is a large saucer-shaped ring resting on top of the throat ring. This envelope has a 45° slope incorporating a spherical stainless-steel-clad surface that serves as clearance for the runner blades. The runner envelope must be set very carefully because of the small running clearance between it and the wheel. Following this the speed ring is installed. The ring differs from the conventional machine in that the water passages are at a 45° angle instead of being horizontal. The stay vanes are also at 45° as are the six movable diffuser flaps, which are extensions to the stationary vanes. These flaps are used at heads of less than 60 ft when generating, but at high heads and when pumping they are in line with the fixed vanes. There are no wicket gates in these machines, the water passages being controlled by the movement of the runner blades. Large steel columns are erected on top of the speed ring up to the generator bracket. The total weight of the generator and turbine moving parts is carried down through these columns to the stationary vanes and through the vanes to special footings in the concrete foundation below the speed ring.

The runner of these machines is known as a feathering-type Francis wheel, or as a Deriaz runner. Two models were built and were operated successfully both as turbines and pumps. The first full-scale machine built was the one assembled on the project. It was manufactured for the most part in Canada—the major exception being the blades, which were machined in Switzerland.

Due to the runner's size and weight it was necessary to ship the component parts to the site and assemble them in the erection bay. The runner hub weighs 44 tons and when assembled holds 11 tons of lubricating oil. After the hub was placed on a support stand in the erection bay, the blades, which operate at a 45° angle, were lined up with optical instruments on a launching ramp and drawn into position with a winch. Each blade weighs 4 tons and is bedded to close tolerances with the adjoining blades. The tips of the blades are stainless-steel clad to reduce wear. A large cylindrical servomotor to actuate the blades is installed inside the hub. The runner shaft weighs 27 tons and has an 8-ft, 8-in.-diameter flange at the connection to the runner hub.

After the assembly was completed the runner was tested under simulated operating conditions to check design figures. An actuator cabinet, a pressure tank, and a high-pressure compressor were installed and connected to the runner to yield a test pressure of 300 lb per sq in. of oil to actuate the blades. The arc movement of the blades, designed to close in 10 sec, is 28° . The tests verified these conditions.

A further test was made to simulate the condition of the centrifugal force of the lubricating oil when the runner rotates at its rated speed of 92.3 rpm. This force was computed as 60 lb per sq in. The test assured that there would be no leakage through the oil seals when the machine was in operation.

Governor System.—The governor system consists of a single cabinet-type actuator incorporating built-in pumps and a sump tank with one pressure tank and two air tanks.

There are two sets of pressure pipes from the governor. One small set leads to six servomotors mounted in the headcover to operate the diffuser flaps. The larger set is routed from the actuator to a runner head at the top of the generator shaft, and then down through the hollow generator and turbine

shafts to the runner servomotor. The servomotor actuates the movable blades, depending on the load on the machine and the head of water on the plant. In a closed position the blades act as wicket gates to close off the water passages.

To reduce the water leakage past the blades when the machine is shut down, the clearance between the runner blades and the runner envelope is decreased by admitting water pressure from the scrollcase into a chamber in the head-cover. This introduces an additional load on the generator thrust bearing, which is designed to depress slightly, thus allowing the turbine blades to seal more closely to the runner envelope.

The motor generators differ from those at the main plant in that they use separate motor-generator sets for excitation, specially designed transformer and motor windings for pump operation, and full-voltage starting as a motor. Ultimately, the pump-generating units will be operated from the control room in the Sir Adam Beck Generating Station No. 2.

Construction of the pumphouse, which began in the early part of 1955, has been completed. The first of the six pump turbines was in service in June, 1957, and the remaining units were in operation by the summer of 1958.

MAIN GENERATING STATION

The main generating station is 1,150 ft long with a generator hall 63 ft wide and 50 ft high. In this station are installed sixteen 60-cycle generators, each with a capacity of 80,500 kw, coupled directly to sixteen hydraulic turbines on 55-ft centers, each having a capacity of 105,000 hp at a rated head of 292 ft. The speed of these machines is 150 rpm.

A screenhouse at the top of the cliff controls the water entering the penstocks. In this structure are housed control gates, which may be operated by remote control from the control room, as well as trash racks to prevent the entrance of debris in the penstocks. The penstocks are 500 ft long, 19 ft in diameter, and vary in thickness from $\frac{5}{8}$ in. at the top of the cliff to $1\frac{1}{2}$ in. at the connection to the scrollcase.

At the rear of the station are single-phase transformers, which accelerate the generator voltage from 13,800 kw to 230,000 kw for transmission.

CONCLUSIONS

The Sir Adam Beck No. 2 Generating Station was designed for maximum utilization, within economic limits, of Ontario's share of the water available from the river for power purposes. The most interesting phase has been the pump-storage plant. This installation is a unique undertaking in Canada, allowing storage of the Niagara River flow where a conventional storage dam is not feasible.

AMERICAN SOCIETY OF CIVIL ENGINEERS

Founded November 5, 1852

TRANSACTIONS

Paper No. 2965

HURRICANE DESIGN-WAVE PRACTICES

BY CHARLES L. BRETSCHNEIDER,¹ A. M. ASCE

SYNOPSIS

Methods are presented that result in a better estimate than heretofore available for obtaining hurricane design waves for offshore structures and coastal structures. Two important concepts are introduced that allow the hurricane design wave and its recurrence interval to be obtained with fair reliability. First, the "energy index" concept, which was originally proposed by Robert O. Reid, is used to obtain the design hurricane for deepwater wave conditions. Second, techniques are used for computing wind waves over a shallow bottom, considering bottom friction as proposed by the writer. To illustrate these techniques, a hurricane is selected off the coast of North Carolina for which wave computations are made.

INTRODUCTION

The hurricane design-wave problem has become important during the past few years with reference to the design of both the offshore structures and the coastal structures. Unless one can predict accurately the design-hurricane wave and its recurrence interval, there is little assurance, if any, of absolute safety, or of a justified economic balance between cost and the safety of life and property. Computations of design-wave forces can be no more accurate than the selection of the design wave.

Originally, design-wave practices used wave-forecasting relationships based on constant wind speed and constant wind direction. This is not a correct procedure for hurricane design because the wind over the fetch varies in both direction and speed. In the case of bringing the waves across the continental shelf, original practices assumed that only refraction and shoaling changed the wave height. Later studies revealed that bottom friction has a considerable effect on modifying the wave height in shallow water prior to reaching the critical breaking depth of $1.28 H_B$, in which H_B denotes the breaker height. With

NORGE.—Published, essentially as printed here, in May, 1957, in the Journal of the Waterways and Harbors Division, as *Proceedings Paper 1253*. Positions and titles given are those in effect when the paper was approved for publication in *Transactions*.

¹ Hydr. Engr. (Research), Beach Erosion Board, Corps of Engrs., U. S. Dept. of the Army, Washington, D. C.

respect to earlier practices, once a design hurricane was selected, two main drawbacks existed. First, an average wind speed and fetch length were selected, from which the hurricane design wave was predicted. This prediction was purely subjective, and as many hurricane design waves could be obtained as there were forecasters. Second, no allowance was made in shallow water to account for wave-energy loss due to bottom friction, and the final selection of the hurricane design wave frequently had little meaning other than a good guess.

It was apparent that the foregoing practices were not satisfactory. Nevertheless, it was necessary to build structures using the best available information on hurricane waves, and it was hoped that either a hurricane would never be experienced, or that one would be experienced as a test before many structures were built.

Because earlier techniques were unsatisfactory, new approaches were made to the subject of hurricane-wave forecasting, and these approaches have been tested. The methods were improved and revised as time went on, and, as of 1959, the material presented herein illustrates the latest proposed method for obtaining the hurricane design wave. Further improvements are still in progress. Refinements can be made as more is learned about hurricanes and their behavior, and as more wave observations are obtained during hurricanes, both in deep water and shallow water.

GENERATION OF DEEPWATER WIND WAVES

Notation.—The letter symbols adopted for use in this paper are defined where they first appear and are arranged alphabetically, for convenience of reference, in the Appendix.

General.—Before examining the generation of deepwater waves during hurricane conditions, it is necessary first to review the deepwater wave-forecasting relationships developed for constant wind speed and constant wind direction. At present, there are two schools of thought in wave forecasting, the Sverdrup-Munk-Bretschneider^{2,3} method and the Pierson-Neumann-James⁴ method. The first method uses the term "significant wave," and the second method utilizes the term "the wave spectrum." The wave height-frequency distribution and the wave period-frequency distribution can be obtained from relationships given by Robert R. Putz,^{5,6} using the significant wave height and period, respectively. The wave-spectrum method uses the theoretical frequency distribution of wave heights stated by M. S. Longuet-Higgins.⁷ The results by the two methods for wind waves should give comparable results because the

²"Wind, Sea, and Swell: Theory of Relationships for Forecasting," by H. U. Sverdrup and W. H. Munk, *Hydrographic Office Publication No. 601*, U. S. Dept. of the Navy, Washington, D. C., March, 1947.

³"The Generation and Decay of Wind Waves in Deep Water," by C. L. Bretschneider, *Transactions, Am. Geophysical Union*, Vol. 33, No. 3, June, 1952, pp. 381-389.

⁴"Practical Methods for Observing and Forecasting Ocean Waves by Means of Wave Spectra and Statistics," by W. J. Pierson, Jr., Gerhard Neumann, and Richard W. James, *Hydrographic Office Publication No. 603*, U. S. Dept. of the Navy, Washington, D. C., 1955.

⁵"Statistical Distribution for Ocean Waves," by R. R. Putz, *Transactions, Am. Geophysical Union*, Vol. 33, No. 5, 1952, pp. 685-692.

⁶"Wave-Height Variability: Prediction of Distribution Function," by R. R. Putz, *Technical Report HE 116-518*, Univ. of California, Berkeley, 1950.

⁷"On the Statistical Distribution of the Heights of Sea Waves," by M. S. Longuet-Higgins, *Journal of Maritime Research*, Vol. 11, No. 3, 1952, pp. 345-366.

Longuet-Higgins theoretical distribution is almost identical to that of Putz,⁵ which is based on actual wave data. However, agreement is not always reached, and it is not possible herein to examine in detail all the reasons for disagreement, except that the major difficulty apparently arises primarily because the two methods do not use the same wave data to describe wave generation. Also, the data in each case have not been analyzed by the same techniques.

In so far as wind-wave generation is concerned, the most important wave data existing are given by Joe W. Johnson,³ M. ASCE, and were obtained from Abbotts Lagoon, near Point Reyes, Calif. With respect to these

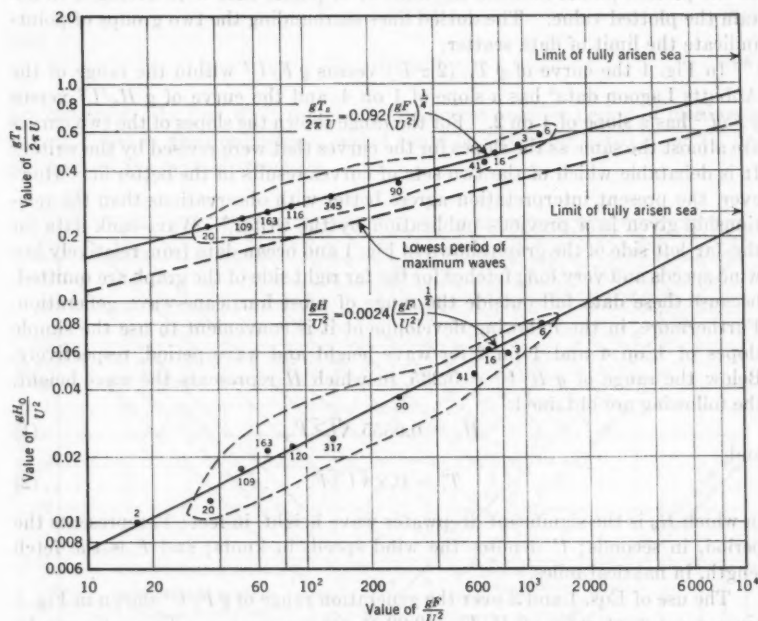


FIG. 1.—GENERATION OF DEEPWATER WIND WAVES FOR SHORT FETCHES AND HIGH WIND SPEEDS

data, waves were measured (not visually observed), wind instruments and wave instruments were calibrated carefully, and the records were analyzed carefully by reproducible techniques. The results are tied in with the Putz⁵ frequency distribution. Therefore, to the best of the writer's knowledge, they represent the best available data that can be used for predicting wind waves having similar dimensionless values of gF/U^2 , gH_s/U^2 , and $gT_s/(2\pi U)$. In the preceding values, g represents the acceleration of gravity; F denotes the fetch length; U designates the horizontal surface wind speed; H_s represents the

³"Relationships Between Wind and Waves, Abbotts Lagoon, California," by J. W. Johnson, *Transactions*, Am. Geophysical Union, Vol. 31, No. 3, 1950, pp. 386-392.

deepwater significant wave height; T_s designates the significant wave period; and π is a constant. The range in values of gF/U^2 for the Abbotts Lagoon data (Fig. 1) extends through the range of gF/U^2 for high wind speed and for short fetches to moderate fetches for ocean waves. There may be some argument as to a possible scale-factor effect involved in the use of these data. However, any error resulting from the use of the Abbotts Lagoon data must be less than that obtained from using actual ocean deepwater wave data, due to the difficulty in measuring the limits of fetch length, wind duration, and wind speed, and the purely subjective wave observations. In Fig. 1 the numerals adjacent to the plotted points indicate the number of points that were averaged to obtain the plotted value. The dotted lines surrounding the two groups of points indicate the limit of data scatter.

In Fig. 1 the curve of $gT_s/(2\pi U)$ versus gF/U^2 within the range of the Abbotts Lagoon data³ has a slope of 1 on 4, and the curve of gH_o/U^2 versus gF/U^2 has a slope of 1 on 2. For the range shown the slopes of the two curves are almost the same as the slopes for the curves that were revised by the writer.³ It is debatable which of the two sets of curves results in the better fit.¹ However, the present interpretation agrees better with observations than the relationship given in a previous publication by the writer.³ Wave-tank data for the far left side of the graph shown in Fig. 1 and ocean data from relatively low wind speeds and very long fetches for the far right side of the graph are omitted, because these data fall outside the range of most hurricane-wave generation. Furthermore, in the following development it is convenient to use the simple slopes of 1 on 4 and 1 on 2 for wave height and wave period, respectively. Below the range of $gH/U^2 = 0.235$, in which H represents the wave height, the following are obtained:

$$H_o = 0.0555 \sqrt{U^2 F} \dots \dots \dots (1)$$

and

$$T_s = 0.5 \sqrt[4]{U^2 F} \dots \dots \dots (2)$$

in which H_o is the significant deepwater wave height, in feet; T_s represents the period, in seconds; U denotes the wind speed, in knots; and F is the fetch length, in nautical miles.

The use of Eqs. 1 and 2 over the generation range of gF/U^2 shown in Fig. 1 gives a constant ratio of $H/T^2 = 0.22$ ft per sec per sec. This ratio can be interpreted as an apparent steepness of 1 to 23, which agrees closely with the steepness of 1 to 20 that has been used in design for many years. However, in so far as the maximum wave is concerned, a greater steepness would result.

The minimum duration, t_{\min} (in hours), to generate waves of H_o and T_s can be obtained from

$$t_{\min} = \int_0^{F_{\min}} \frac{1}{C_g} dx \dots \dots \dots (3)$$

In Eq. 3,

$$C_g = 1.515 T_s \dots \dots \dots (4)$$

and F_{\min} represents the minimum fetch length. Combining Eqs. 3 and 4 results in

$$\frac{F_{\min}}{t_{\min}} = 0.57 \sqrt[4]{U^2 F_{\min}} \dots \dots \dots (5a)$$

and

$$\frac{F_{\min}}{t_{\min}} = 1.14 T_s \dots \dots \dots (5b)$$

If one is interested in the maximum wave, which is higher than the significant wave, it is sometimes desirable to predict the lowest possible period of the maximum wave. In deep water the maximum probable wave height, H_{\max} , equals $1.87 H_s$,⁵ and the critical steepness from wave theory results in $H/T^2 = 0.877$ ft per sec per sec, from which

$$T' = 1.46 \sqrt{H_s} \dots \dots \dots (6a)$$

and

$$T' = 0.69 T_s \dots \dots \dots (6b)$$

are obtained. In Eqs. 6, T' represents the lowest possible period of maximum wave. That is, the design-wave period could be either (or both) T' or T_s , depending on the type of structure.

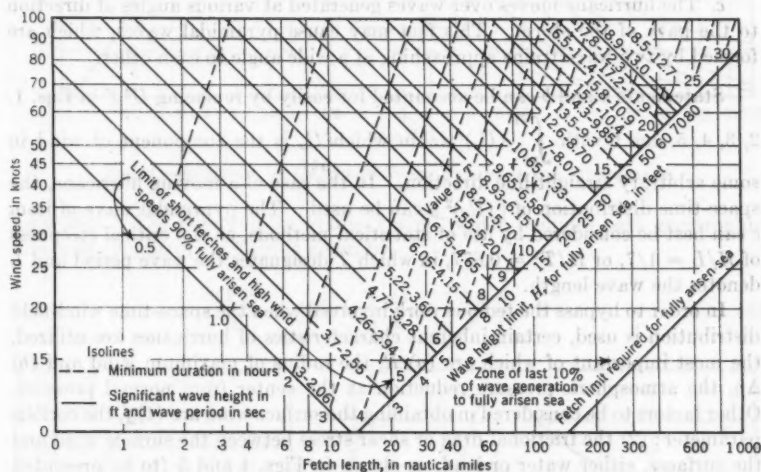


FIG. 2.—DEEPWATER WAVE-FORECASTING CURVES FOR SHORT FETCHES AND HIGH WIND SPEEDS

Fig. 2 represents forecasting relationships based on Eqs. 6 and is intended primarily for short fetches and high wind speeds (that is, for $gF/U^2 \approx 10^4$). In Fig. 2 the lower period is the lowest possible for maximum waves. The upper limit of Fig. 2 is equivalent to from approximately 85% to 90% of a fully arisen sea, defined as ($gH_s/U^2 = 0.26$), assuming unlimited fetch length and wind duration. Figs. 1 and 2 show that it takes a much longer time and a greater fetch length to reach 100% of a fully arisen sea than for the first 85%-to-90% range. This fact should be remembered when hurricane-wind wave generation is considered.

The preceding forecasting relationships can be used for hurricane-wave generation in a manner similar to the method used by Basil W. Wilson,⁹ A. M. ASCE, in which the space-time wind-field pattern was utilized. This would provide sufficient wave information for hurricane-wave generation for design purposes. Because the space-time wind-field distribution requires extensive work, a simple method is developed for obtaining directly the highest waves that can be generated by a hurricane. The results can be checked by another method.⁹

— GENERATION OF DEEPWATER WIND WAVES UNDER HURRICANE-WIND CONDITIONS

Three of the most important fundamental differences between the generation of wind waves under hurricane conditions and the generation of normal wind waves are:

- a. Winds within a hurricane are not constant in speed.
- b. The direction of winds within a hurricane is circular as opposed to a straight-line direction.
- c. The hurricane moves over waves generated at various angles of direction to the path of the storm. This fact may cause pyramidal waves, which are formed by two wave trains approaching at a wide angle to each other.

Statements *a* and *b* can be accounted for easily by replacing $U^2 F$ in Eqs. 1, 2, 3, 4, 5, and 6 with $\int_{x_1}^{x_2} (U_x)^2 dx$, in which U_x is the component of wind in some arbitrary straight-line direction. In the case of a moving hurricane, the space-time distribution of $[(U_x)^2]_t$ can be used. The pyramidal wave of item *c* can best be considered by use of statistical methods, or the critical steepness of $H/L = 1/7$, or $H/T^2 = 0.877$, in which T designates the wave period and L denotes the wave length.

In order to bypass the tedious work involved when the space-time wind-field distribution is used, certain inherent characteristics of hurricanes are utilized, the most important of which are (a) R , the radius of maximum wind and (b) Δp , the atmospheric-pressure reduction at the center from normal pressure. Other factors to be considered in obtaining the surface wind are (1) f , the coriolis parameter; (2) the frictional drag or shear stress between the surface wind and the surfaces, either water or land, as shown in Figs. 4 and 5 (to be presented subsequently); and (3) V_F , the forward speed of the storm. The preceding five factors are used to obtain the surface wind, a result of cyclostrophic flow and geostrophic flow, reduced in speed and deflected toward the center of the storm as a result of frictional drag. Cyclostrophic flow represents a balance between the centrifugal force and the pressure-gradient force. This is the primary balance near the center of the storm. Geostrophic flow represents a balance between the coriolis force and the pressure-gradient force. This is the primary balance near the outer periphery of the storm. Within the zone of maximum wave generation, both cyclostrophic and geostrophic flow are im-

⁹ "Graphical Approach to the Forecasting of Waves in Moving Fetches," by Basil W. Wilson, Technical Memorandum No. 73, Beach Erosion Board, Corps of Engrs., U. S. Dept. of the Army, Washington, D. C., April, 1955.

portant. The equation for cyclostrophic wind is

$$\frac{(V_c)^2}{r} = \frac{1}{\rho} \frac{dp}{dr} = \frac{1}{\rho} \frac{\Delta p}{r} \frac{R}{r} e^{-R/r} \dots \dots \dots (7)$$

In Eq. 7, V_c denotes the cyclostrophic wind speed; r designates the radial distance to V_c ; ρ represents the density of air; and e is the base of the natural

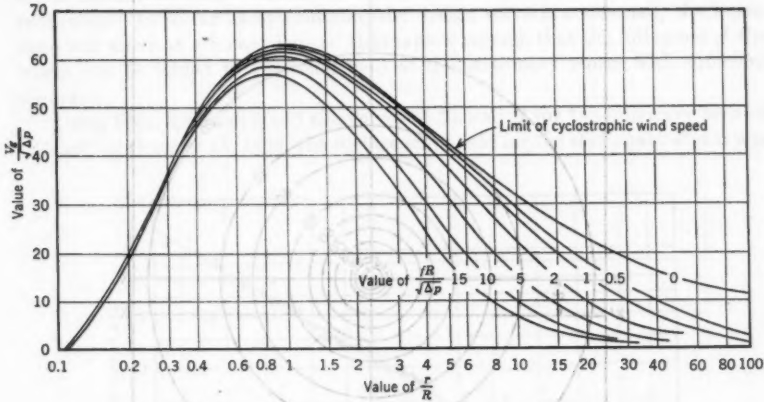


FIG. 3.—SOLUTION OF GRADIENT WIND EQUATION FOR HURRICANES

logarithm. The equation for gradient wind, which includes both geostrophic flow and cyclostrophic flow, is given by

$$\frac{(V_g)^2}{r} + f V_g = \frac{1}{\rho} \frac{dp}{dr} = \frac{1}{\rho} \frac{\Delta p}{r} \frac{R}{r} e^{-R/r} \dots \dots \dots (8)$$

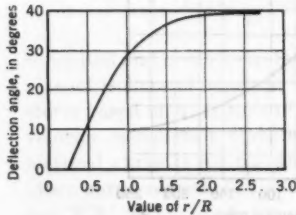


FIG. 4.—WIND DEFLECTION AS A FUNCTION OF r/R

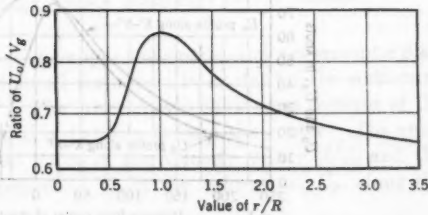


FIG. 5.—RATIO OF SURFACE WIND SPEED TO GRADIENT WIND SPEED AS A FUNCTION OF r/R

in which V_g represents the geostrophic wind speed and dp/dr denotes the pressure gradient. Fig. 3 is the solution of Eq. 8, for which the units are in nautical miles, knots, and hours, and in which the atmospheric-pressure anomaly, Δp , is in inches of mercury. The coriolis parameter, in radians per hour for various

latitudes, is given by

Latitude, in degrees	25	30	35	40
f , in radians per hour . . .	0.222	0.264	0.300	0.338

It is necessary to make three corrections to obtain the actual surface wind speeds. These corrections are (a) change in the direction of the velocity vector

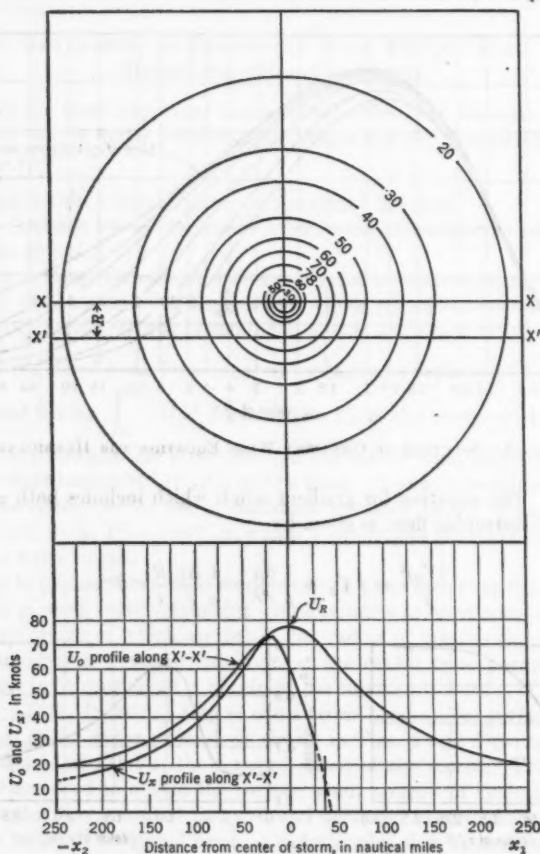


FIG. 6.—THEORETICAL SURFACE WIND-VELOCITY DISTRIBUTION FOR STATIONARY STORM—HURRICANE HAZEL, OCTOBER, 1954

due to surface drag, (b) change in the speed of the velocity vector due to surface drag, and (c) change in the speed of the velocity vector to take into account the effect of the forward speed of the storm. The foregoing items (a) and (b) may be obtained from empirical data. Based on a hurricane that was analyzed in

detail by the Weather Bureau (United States Department of Commerce) and Vance A. Myers,¹⁰ such relationships are developed and reproduced in dimensionless form in Figs. 4 and 5, respectively. With respect to item (b), the present practice is to superimpose the forward speed of the storm on the resulting surface wind field obtained by using Figs. 3, 4, and 5. The foregoing procedure is permissible for a slowly moving storm, but some error will result for rapidly moving storms. Some value of speed less than that of a quickly moving storm should be used. However, little data are available to justify such a reduction. In so far as determining the design wave is concerned, the hurricane will move at a forward speed that is slow enough that the full speed of the storm can be added to the wind field of the stationary storm with sufficient accuracy.

Using Figs. 3, 4, and 5 and the values of Δp and R for the hurricane termed "Hazel" of October 15, 1954, the surface wind field for the stationary storm was

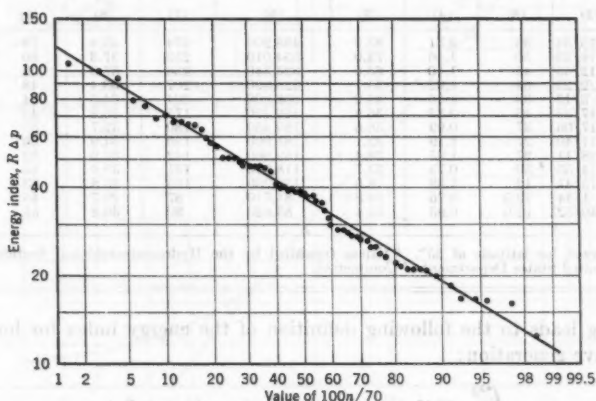


FIG. 7.—ENERGY INDEX ($R \Delta p$) VERSUS FREQUENCY OF OCCURRENCE

computed and is shown in Fig. 6. The upper concentric circles represent a plan view of isolines of constant wind speed (expressed in knots) for the stationary storm based on a latitude of 35° . The lower curves show cross sections of the velocity distribution along a line at a distance R from the center. The symmetrical curve is for the absolute value of the velocity vector $|U_o|$, and the other curve represents the component of U_o in the x -direction, U_x , along the line $X'X'$.

In terms of wave generation along line $X'X'$, the value of $\int_{x_1}^{x_2} (U_x)^2 dx$ must be used when the limits of x_1 and x_2 have been set arbitrarily at $U_x = 15$ knots.

¹⁰ "Characteristics of United States Hurricanes Pertinent to Levee Design for Lake Okeechobee, Florida," by V. A. Myers, Report No. 32, Hydrometeorological Section, Weather Bureau, U. S. Dept. of Commerce, Washington, D. C., March, 1954.

Because a model hurricane is defined readily by its parameters, R and Δp , the concept of the "energy index," proposed originally by Robert O. Reid,^{11,12} is used for classifying hurricanes and their frequency of occurrence. Fig. 7 shows the relationship $R \Delta p$ versus the frequency of occurrence of sixty-nine hurricanes in the United States (from 1900 to 1949). For design purposes the recurrence interval of storms for any particular section of coast is a separate study.

The kinetic energy of a hurricane is proportional to $R \Delta p$, and the wave energy is proportional to H^2 , which, from Eq. 1, is proportional to $U^2 F$. The

TABLE 1.—SUMMARY OF THIRTEEN SELECTED HURRICANES
OFF EASTERN COAST OF UNITED STATES*

No.	Date	R , in nautical miles ^b	Δp , in inches of mercury ^b	$R \Delta p$	$\int_{x_1}^{x_2} (U_x)^2 dx$	Δx , in nautical miles	U_r , in knots	U_x , in knots	V_F , in knots
(1)	(2)	(3)	(4)	(5)	(6)	(7)	(8)	(9)	(10)
1	10/15/54	36	2.31	83.2	488,200	274	43.4	78	26
2	9/19/55	50	1.46	73.0	354,010	253	37.3	60	8.5
3	8/12/55	45	1.40	63.0	323,340	236	37.3	59	7
4	12/2/55	54	1.02	55.1	225,920	207	33.4	48	14
5	9/3/13	39	1.16	45.2	238,300	204	34.5	54	16
6	8/17/55	45	0.82	36.9	160,220	175	30.8	45	15
7	9/17/06	37	0.99	36.6	189,460	180	32.7	50	17
8	8/11/40	27	1.19	32.1	181,960	150	34.9	56	14
9	8/28/11	27	1.05	28.4	159,060	142	32.9	52	9
10	8/14/53	30	0.79	23.7	118,940	131	30.6	45	13
11	10/15/47	12	1.38	16.6	136,250	105	35.8	63	17
12	8/1/44	19.5	0.76	14.8	84,710	87	29.7	45	20
13	8/30/52	12.0	0.95	11.4	85,620	80	30.8	51	12

* Analyzed for latitude of 35°. ^b Values furnished by the Hydrometeorological Section, Weather Bureau (United States Department of Commerce).

foregoing leads to the following definition of the energy index for hurricane-wind-wave generation:

$$\int_{x_1}^{x_2} (U_x)^2 dx = (U_r)^2 F = \text{function of } R \Delta p \dots \dots \dots (9)$$

in which U_r is the root-mean-square of the wind-speed component, U_x , obtained by the use of Eq. 12 (to be presented subsequently).

In order to establish a relationship between $\int_{x_1}^{x_2} (U_x)^2 dx$ and $R \Delta p$, it was necessary to analyze sufficient hurricanes covering the range of $R \Delta p$ shown in Fig. 7. This was done for thirteen east coast hurricanes (Table 1), information for which was furnished to the Beach Erosion Board, Corps of Engineers (United States Department of the Army), by the Weather Bureau.

Each hurricane summarized in Table 1 was analyzed for the wind-field pattern, based on a stationary storm for the latitude of 35°. The line of com-

¹¹ "On the Classification of Hurricanes by Storm Tide and Wave Energy Indices," by Robert O. Reid, *Meteorological Monographs*, Vol. 2, No. 10, June, 1957, pp. 58-66.

¹² "Surface Waves and Offshore Structures: The Design Wave in Deep or Shallow Water, Storm Tide, and Forces on Vertical Piling and Large Submerged Object," by R. O. Reid and C. L. Bretschneider, *Technical Report*, Research Foundation, The Agri. and Mech. College of Texas, College Station, October, 1953.

putation, $X'X'$, was selected at a radial distance equal to R . For the most severe storm (October 15, 1954) it was found that $\int_{x_1}^{x_2} (U_z)^2 dx$ was a maximum along this line. The limits of x_1 and x_2 were set arbitrarily at a distance at which $U_z = 15$ knots. If the storm moved, the maximum value of $\int_{x_1}^{x_2} (U_z)^2 dx$ would occur at a distance greater than R from the center. Fig. 8 shows the energy-index relationships based on the thirteen hurricanes in Table

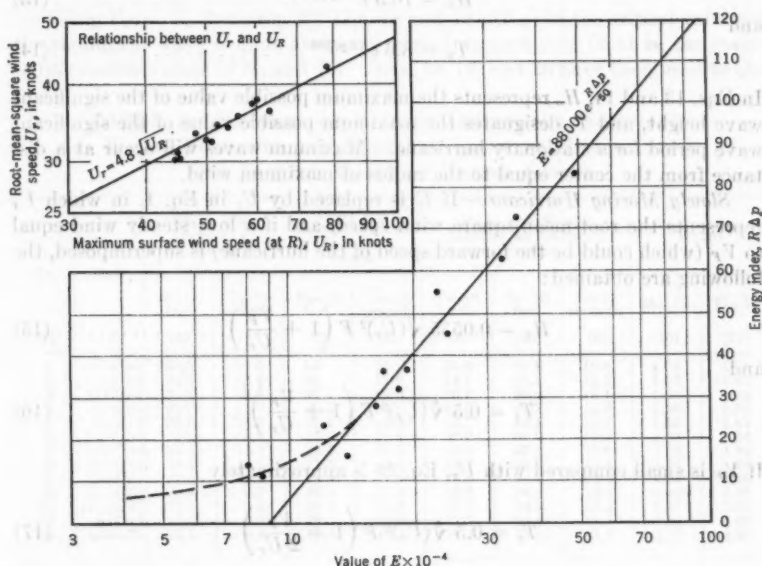


FIG. 8.—HURRICANE ENERGY-INDEX RELATIONSHIP

1. For all hurricanes, excluding weaker tropical storms, the following relationships for a latitude of 35° are useful:

$$\int_{x_1}^{x_2} (U_z)^2 dx = 88,000 e^{R \Delta p / 60} \quad (10)$$

and

$$(U_r)^2 = 23 U_R \quad (11)$$

in which U_R represents the sustained wind speed at R , and

$$(U_r)^2 = \frac{1}{\Delta x} \int_{x_1}^{x_2} (U_z)^2 dx \quad (12)$$

in which Δx represents an increment of horizontal distance. Subsequent illustrations (Figs. 12 and 13) are based on a latitude of 35° . Based on the analysis

of five of the thirteen storms for a latitude of 25° , it was found that the right side of Eqs. 10 and 11 should be multiplied by a factor of 1.1, which also is the ratio of $\cos 25^\circ$ to $\cos 35^\circ$. If the preceding and all following equations are applied at a latitude of 25° , a correction is required as follows: H must be multiplied by $\sqrt{1.1}$, and T must be multiplied by $\sqrt[4]{1.1}$. Four cases for hurricane-wave generation (latitude of 35°) will be cited subsequently.

Stationary Hurricane.—Using Eq. 10 with Eqs. 1 and 2, the following are obtained for a stationary hurricane:

$$H_o = 16.5 e^{R\Delta p/100} \dots \dots \dots (13)$$

and

$$T_s = 8.6 e^{R\Delta p/200} \dots \dots \dots (14)$$

In Eqs. 13 and 14, H_o represents the maximum possible value of the significant wave height, and T_s designates the maximum possible value of the significant wave period for a stationary hurricane. Maximum waves will occur at a distance from the center equal to the radius of maximum wind.

Slowly Moving Hurricane.—If U is replaced by U_r in Eq. 1, in which U_r represents the root-mean-square wind speed, and if a low, steady wind equal to V_F (which could be the forward speed of the hurricane) is superimposed, the following are obtained:

$$H_o = 0.0555 \sqrt{(U_r)^2 F} \left(1 + \frac{V_F}{U_r} \right) \dots \dots \dots (15)$$

and

$$T_s = 0.5 \sqrt[4]{(U_r)^2 F} \left(1 + \frac{V_F}{U_r} \right)^{1/4} \dots \dots \dots (16)$$

If V_F is small compared with U_r , Eq. 16 is approximately

$$T_s = 0.5 \sqrt[4]{(U_r)^2 F} \left(1 + \frac{V_F}{2U_r} \right) \dots \dots \dots (17)$$

Eqs. 15 and 16 are exact for a wind field of constant speed and direction. If it is assumed that V_F is equal to the forward speed of the storm and that αV_F is the effective increase in wind speed, use can be made of Eqs. 10 and 11 with Eqs. 15 and 17, and

$$H_o = 16.5 e^{R\Delta p/100} \left(1 + \frac{0.208 \alpha V_F}{\sqrt{U_r}} \right) \dots \dots \dots (18)$$

and

$$T_s = 8.6 e^{R\Delta p/200} \left(1 + \frac{0.104 \alpha V_F}{\sqrt{U_r}} \right) \dots \dots \dots (19)$$

can be obtained.

For a slowly moving storm, the value of α is approximately equal to unity, and Eqs. 18 and 19 will yield the maximum values of the significant wave height and wave period for a slowly moving hurricane. Using $\alpha = 1.0$ tends to compensate for a slight increase in the minimum fetch length for a moving storm.

Hurricane Moving Forward at Critical Speed.—There is a critical forward speed of any hurricane that will result in maximum wave generation. If this speed is exceeded waves will decrease in magnitude and period. The critical forward speed is obtained by equating $V_F = 1.52 T_s$. Substituting $T_{cr} = V_F / 1.52 = V_{cr} / 1.52$ into Eq. 19, the following approximation is obtained for the critical forward speed:

$$V_{cr} = 13.1 e^{R\Delta p/200} \left(1 - \frac{1.36 \alpha e^{R\Delta p/200}}{\sqrt{U_R}} \right)^{-1} \dots \dots \dots (20)$$

Using $V_F = V_{cr}$ from Eq. 20, Eqs. 18 and 19 will yield the critical values of the significant wave heights and wave period, respectively (that is, the maximum possible values of H_o and T_s). Eqs. 18, 19, and 20 have been used to ob-

TABLE 2.—SUMMARY OF HIGHEST DEEPWATER SIGNIFICANT WAVES PREDICTED FOR THIRTEEN SELECTED HURRICANES OFF EASTERN COAST OF UNITED STATES

No.	Date	DATA FOR STATIONARY STORM		DATA FOR STORM MOVING AT ACTUAL SPEED		DATA FOR STORM MOVING AT CRITICAL SPEED			RATIO	
		H_o , in feet	T_s , in seconds	H_{ac} , in feet	T_{ac} , in seconds	V_{cr} , in knots	H_{cr} , in feet	T_{cr} , in seconds	H_{cr}/H_o	V_{cr}/T_s
(1)	(2)	(3)	(4)	(5)	(6)	(7)	(8)	(9)	(10)	(11)
1	10/15/54	37.9	13.0	59	16	24.8	59.8	16.4	1.58	1.91
2	9/19/55	34.2	12.4	42	13.5	24.1	56.4	15.9	1.65	1.94
3	8/12/55	31.0	11.8	37	13.0	22.7	50.0	15.1	1.61	1.92
4	12/2/25	28.7	11.3	40.5	13.5	22.0	47.7	14.6	1.66	1.95
5	9/3/13	26.0	10.8	37.5	13.0	20.7	42.1	13.7	1.62	1.92
6	8/17/55	23.9	10.3	35.0	12.5	20.0	39.0	13.2	1.63	1.94
7	9/17/06	23.5	10.2	35.5	12.5	19.3	37.2	12.8	1.58	1.89
8	8/11/40	22.6	10.1	31.5	12.0	18.7	34.7	12.4	1.54	1.85
9	8/28/11	22.4	9.9	28.0	11.0	18.6	34.7	12.3	1.55	1.88
10	8/14/53	20.8	9.7	29.0	11.5	18.5	29.5	12.2	1.42	1.91
11	10/15/47	19.5	9.4	28.0	11.0	17.2	28.2	11.4	1.45	1.83
12	8/1/44	19.1	9.3	28.0	11.0	17.5	29.5	11.5	1.55	1.88
13	8/30/52	18.5	9.2	25.0	10.5	17.1	27.6	11.3	1.49	1.86
Average									1.56	1.90

tain wave heights and wave periods for the thirteen storms given in Table 1, for which α was assumed to be equal to 1.0. The results are summarized in Table 2 and in Figs. 9 and 10, respectively. Actual storm speeds are given in Table 1. From Figs. 9 and 10 the corresponding heights and periods can be determined. These results are given as H_{ac} and T_{ac} in Table 2. In general, actual heights and actual periods are less than the maximum possible values as given for the critical forward speed.

From the data in Table 2 the following deductions were made:

- The critical forward speed of the storm, in knots, is equal to approximately 1.9 times the value of the significant period for the stationary storm.
- The critical significant wave height is equal to approximately 1.56 times the value of the significant wave height for the stationary storm.

c. The critical significant wave period is equal to approximately 1.25 times the value of the significant wave period for the stationary storm.

From items *a*, *b*, and *c*,

$$V_{cr} = 16.3 e^{R\Delta p/200} \quad (21)$$

$$H_{cr} = 25.8 e^{R\Delta p/100} \quad (22)$$

and

$$T_{cr} = 10.7 e^{R\Delta p/200} \quad (23)$$

Eqs. 21, 22, and 23 are for a latitude of 35° . In Eq. 22, H_{cr} denotes the critical significant wave height, and in Eq. 23, T_{cr} represents the critical significant

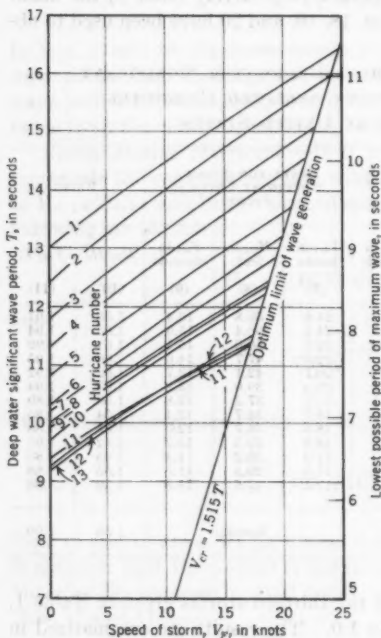


FIG. 9.—PREDICTED SIGNIFICANT HURRICANE-WAVE HEIGHT FOR THIRTEEN UNITED STATES EAST COAST HURRICANES

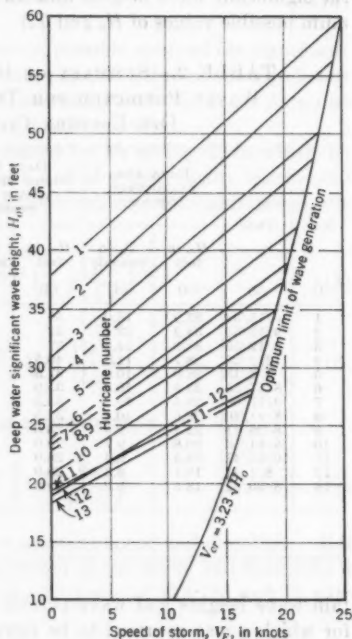


FIG. 10.—PREDICTED SIGNIFICANT HURRICANE-WAVE PERIOD FOR THIRTEEN UNITED STATES EAST COAST HURRICANES

wave period. If α were assumed to be equal to 0.75, the preceding equations would have to be multiplied by the factor 0.95 for V_{cr} and T_{cr} and by 0.91 for H_{cr} .

Eqs. 22 and 23 yield maximum possible values for the significant wave height and significant wave period, respectively, that can be generated in any hurricane passing critical conditions. These waves will occur in the right rear quadrant of the hurricane moving forward. Conditions for critical wave generation are

probably never attained fully because the duration required at critical speed is generally insufficient prior to the storm moving forward at a speed greater than critical speed, and because α is less than 1.0. Another factor is that the storm may change its course prior to critical conditions.

Hurricane Moving Forward at Speed Greater than Critical Speed.—Under these conditions the preceding development cannot continue. The assumption of $\alpha = 1.0$ can no longer be used to represent an added wind-speed effect. Furthermore, the storm will move ahead of the maximum waves, which would act as swell but would still be under the influence of relatively high winds. Only a rough rule of thumb is used—the highest significant waves for a storm speed of $V_{cr} + \Delta V$ will be of the same order of magnitude as those for $V_{cr} - \Delta V$, in which ΔV is the increase in storm speed beyond the critical value. In order to obtain a better answer, use could be made of the space-time wind-field

TABLE 3.—DATA FOR PACIFIC OCEAN TYPHOON OF SEPTEMBER 26, 1935

Name of ship	Time— 135th meridian, civil time	OBSERVED HIGHEST WAVES*				COMPUTED PERIOD	
		H, in feet	L, in feet	C, in feet per second	T, in seconds	$T = L/C$	$T = \sqrt{L/5.12}$
(1)	(2)	(3)	(4)	(5)	(6)	(7)	(8)
<i>Hocho</i>	1215	33
<i>Mikuma</i>	1250	26	590	47	13	12.5	10.70
<i>Hocho</i>	1400	46
<i>Hoguro</i>	1418	49	1,150*	15.0
<i>Hocho</i>	1420	58
<i>Mikuma</i>	1445	33	658	47	13.3	14.0	11.4
<i>Amogini</i>	1458	82	985
<i>Asakaze</i>	1500	49	650-1,000*
<i>Nachi</i>	1500	42-46	395	29.5	9.0	13.4	8.8
<i>Tsurumi</i>	1500	33	658	11.3
<i>Naka</i>	1522	46
<i>Susaki</i>	1540	65-98 ^b	490	9.8
<i>Nachi</i>	1550	42-46 ^b	395	26	9	15.2	8.8

* Summary of highest waves observed by the Imperial Japanese Navy (from *Monthly Weather Review*).
^b Pyramid waves. * Approximation. ^c Estimation.

technique and of the graphical method proposed by Wilson.⁹ A value of α would have to be assumed, or all available synoptic weather maps would have to be analyzed for a storm with characteristics similar to those of the design storm.

MAXIMUM DEEPWATER WAVES IN PACIFIC OCEAN TYPHOON OF SEPTEMBER 26, 1935

With respect to verifying the foregoing techniques, few data are available concerning deepwater wave heights in a hurricane. Perhaps the best available data for this type of storm are those taken by the Imperial Japanese Navy during the Pacific Ocean typhoon of September 26, 1935, a summary of which is given by H. Orakawa and K. Suda.¹³ The center of this typhoon passed over the main squadron, approximately 15 nautical miles to the left of the

¹³ "Analysis of Winds, Wind Waves, and Swell Over the Sea to the East of Japan during the Typhoon of September 26, 1935," by H. Orakawa and K. Suda, *Monthly Weather Review*, Weather Bureau, U. S. Dept. of Commerce, Washington, D. C., Vol. 81, No. 2, 1953, pp. 31-37.

squadron. Other ships encountered various sections of the typhoon, and complete wind data and wave data were taken. Nine different ships reported observations of the highest waves encountered. Thirteen of these observations have been published¹⁰ and are partly reproduced in Table 3.

For this storm the radius of maximum wind was equal to approximately 50 nautical miles, and the value of Δp was approximately 1.63 in. of mercury. By use of Fig. 3, the value of U_R is equal to 65 knots. During observation the forward speed of the storm was equal to or greater than 39 knots, and the maximum sustained wind speed at the radial distance, R , was greater than 40 m per sec (86 knots), but less than 45 m per sec (97 knots). By using the preceding

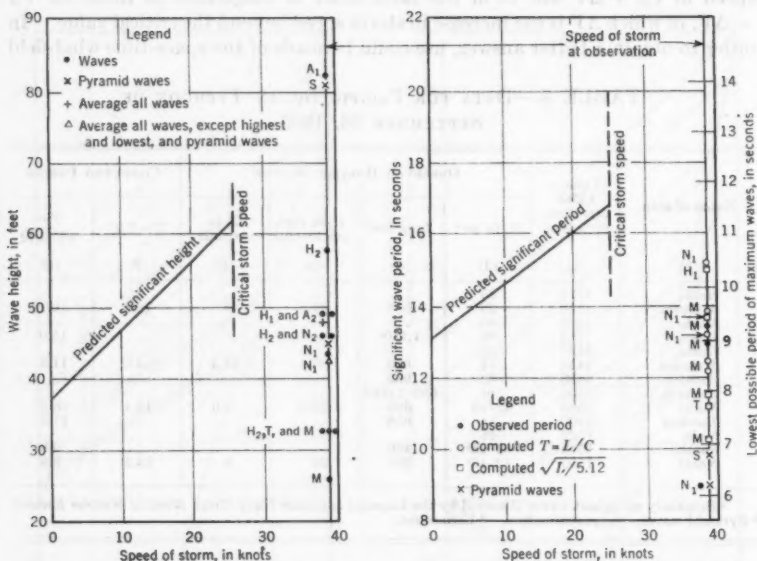


FIG. 11.—PREDICTED WAVES AND OBSERVED WAVES FOR PACIFIC TYPHOON OF SEPTEMBER 26, 1935 (THE LETTERS USED REFER TO DATA COLLECTED BY THE FOLLOWING SHIPS: Amogini—A₁; Asakaze—A₂; Hoguro—H₁; Hoshio—H₂; Mikuma—M; Nachi—N₁; Naka—N₂; Susaki—S; AND Taorumi—T)

values of R , Δp , and U_R , maximum values of the significant waves were predicted. The results are compared with the observations of highest waves in Fig. 11. The critical storm speed for maximum waves computed from Eq. 20 is approximately 25 knots, whereas the forward speed of the storm during observations was greater than 40 knots. For this reason it was expected that the observations would be less than the critical height. Estimated heights and periods are of the same order of magnitude as those given for $V_F = V_{cr} - (40 - V_{cr}) = 10$ knots. This would indicate excellent agreement between observations and forecasts, provided that the average of all observations (which is equal to 45.4 ft) is considered indicative of the significant wave. The maximum observed wave height was approximately 82 ft, from which $H_{max}/H_s = 82$

$/45.4 = 1.8$, which is also reasonable. In the preceding expression H_s represents the significant wave height in shallow water. The lowest possible period for the maximum wave is $T' = \sqrt{82/0.877} = 9.7$ sec. This would indicate that the wave was near breaking, and from $H/L = 1/7$, the lowest possible wave length is equal to $L = 82 \times 7 = 574$ ft. The preceding values of $T = 9.7$ sec and $L = 574$ ft are in fairly good agreement with data from the maximum wave given in Table 3, considering the difficulties in observing waves from aboard ship.

Unfortunately, there are no actual recorded wave data within a hurricane or typhoon, and the preceding verification, although it is the best available, must be considered tentative.

GENERATION OF WIND WAVES IN SHALLOW WATER

The foregoing procedures are used for deep water, whereas actual design conditions are more frequent for shallow water. However, it is necessary first to predict deepwater waves, which are then propagated across the continental shelf, with consideration being given to bottom friction and refraction. Hence, the accuracy of wave forecasts in shallow water can be no more accurate than the deepwater wave forecast.

Wave-forecasting techniques for shallow water are not as numerous as for deep water. Some of the earlier work was performed¹⁴ by J. Th. Thyse and J. B. Schijf, who presented dimensionless relationships for obtaining wave heights and wave velocities as functions of relative depth as well as relative fetch length. A similar set of relationships was obtained by the writer,¹⁵ using numerical methods to combine the relationships of wave generation³ with those of wave-energy dissipation due to bottom friction, as proposed by the writer and Reid.¹⁶ Observations obtained in the shallow water of the Gulf of Mexico¹⁷ and from Lake Okeechobee, Florida,¹⁸ show fairly good agreement with this technique, provided that a bottom friction factor of 0.01 is selected. The friction factor entails other considerations because the theory is based on the linear wave theory, which is not representative of high waves in a complex sea under high wind conditions. Probably it would be preferable to state that the bottom friction factor of 0.01 is actually an apparent factor or a calibration factor, which, when used with the equation for shallow-water wave computations, will result in verification with observed data.

The foregoing being the case for known conditions,^{17,18} techniques for forecasting waves in shallow water are extended to the continental shelf. Fairly reasonable results can be expected, provided that the slope of the continental shelf is not too great—that is, flatter than from 5 ft per mile to 10 ft per mile.

¹⁴ "Report on Waves," by J. Th. Thyse and J. B. Schijf, *Section II, Communication 4*, 17th International Navigation Cong., Lisbon, 1949.

¹⁵ "Generation of Wind Waves Over a Shallow Bottom," by C. L. Bretschneider, *Technical Memorandum No. 51*, Beach Erosion Board, Corps of Engrs., U. S. Dept. of the Army, Washington, D. C., October, 1954.

¹⁶ "Modification of Wave Height Due to Bottom Friction, Percolation, and Refraction," by C. L. Bretschneider and R. O. Reid, *Technical Memorandum No. 45*, Beach Erosion Board, Corps of Engrs., U. S. Dept. of the Army, Washington, D. C., October, 1954.

¹⁷ "Field Investigation of Wave Energy Loss in Shallow Water Ocean Waves," by C. L. Bretschneider, *Technical Memorandum No. 46*, Beach Erosion Board, Corps of Engrs., U. S. Dept. of the Army, Washington, D. C., September, 1954.

¹⁸ "Waves and Wind Tides in Shallow Lakes and Reservoirs," *Summary Report*, Project CW-167, Office of the Dist. Engr., Corps of Engrs., U. S. Dept. of the Army, Jacksonville, Fla., June, 1955.

The material presented previously^{15,16,17} will not be studied in detail. Instead, an actual example will be analyzed to obtain a hurricane design wave.

EXAMPLE FORECAST OF DESIGN WAVE

The following is based on hurricane Hazel, which occurred on October 15, 1954. As a hurricane moves over the continental shelf, two cases must be considered. First, the initial deepwater waves that are generated may be propagated shoreward as swell under the continued influence of hurricane winds. Second, regeneration of wind waves is constantly taking place as the hurricane

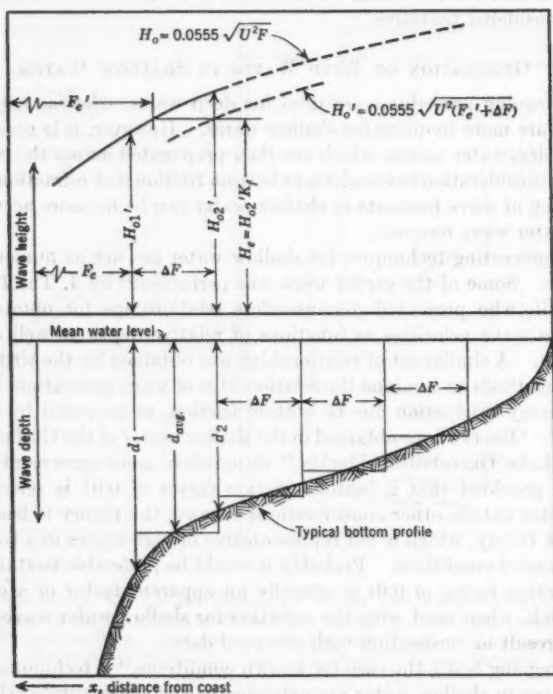


FIG. 12.—SCHEMATIC DIAGRAMS ILLUSTRATING PROCEDURE FOR COMPUTING WIND WAVES IN SHALLOW WATER

moves over the continental shelf. The swell will feel bottom far from shore and will commence losing energy at an early stage, whereas wind waves with shorter periods continue to grow and do not feel bottom until they are sufficiently large and near the coast. Therefore, it is necessary to determine whether the swell or the wind wave is more critical. Refraction may determine the final design wave.

As soon as the design hurricane is selected and maximum deepwater waves are computed, a path must be selected across the continental shelf, over which

shallow-water computations are made. A path perpendicular to the coast is usually critical. Storm-tide computations (wind set-up and pressure surge) are made, and refraction diagrams are constructed.

Shallow-water computations are made as follows:

- a. Maximum wind over shallow water is selected as equal to $U_R + V_F$.
- b. The equivalent deepwater fetch length, F_e , is obtained from Eq. 1 as follows:

$$F_e = \left[\frac{H_o}{0.0555 (U_R + V_F)} \right]^2 \dots \dots \dots (24)$$

In effect, Eq. 24 represents the fetch required under steady wind conditions,

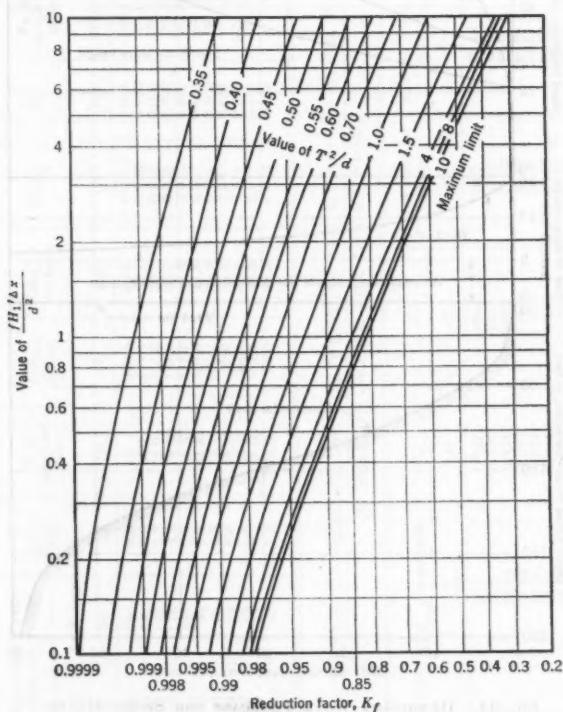


FIG. 13.—RELATIONSHIP FOR FRICTION LOSS OVER A BOTTOM OF CONSTANT DEPTH

which (the actual minimum fetch in shallow water always being equal to or less than F_e) results in the same wave energy as Eq. 18.

c. The traverse is segmented into equal increments, ΔF , usually from 5 miles to 10 miles long, depending on the bottom slope (Fig. 12).

d. An average depth, d_{ave} , is determined over each increment.

e. A deepwater wave height, H_o , is computed at the beginning of the first increment of ΔF .

f. The value of H_o in step e is assumed to travel over the increment, ΔF , as well, with consideration being given to bottom friction. Fig. 13, from which a reduction factor, K_f , is determined, is used to accomplish the foregoing. The actual significant wave height at the end of the increment becomes equal to

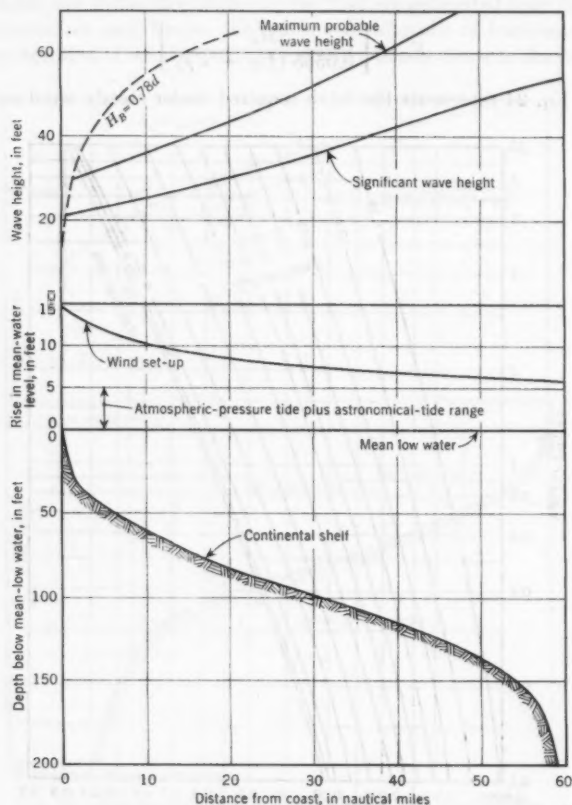


FIG. 14.—HURRICANE-WAVE FORECAST FOR STORM MOVING PERPENDICULAR TO COAST

$H_s = H_o K_f K_s K_r$, in which K_s is the shoaling factor and K_r is the refraction occurring over the fetch-length increment, ΔF .

g. An equivalent deepwater wave height, H_o' , is obtained from $H_o' = K_f H_o$.

h. An equivalent deepwater fetch length, F_e' , is obtained from

$$F_e' = \left[\frac{H_o'}{0.0555 (U_R + V_F)} \right]^2 \dots \dots \dots (25)$$

TABLE 4.—SUMMARY OF COMPUTATIONS FOR HURRICANE SWELL IN SHALLOW WATER UNDER INFLUENCE OF WIND FOR DESIGN STORM

X in nautical miles	X + Δx in nautical miles	MEAN-LOW-WATER LEVEL, IN FEET		S, in feet	F ₀ in nautical miles	(d) ₀ in feet	(H) ₀ in feet	(K) ₀ ave	K _f	P ₀ in nautical miles	H ₀ (at X + Δx) in feet	H _{max} /H ₀	H _{max} (at X + Δx) in feet
		At X	At X + Δx										
63	55	600	150	0.3	110	380.5	56.6	0.974	0.994	108.7	51.96	1.53	79.4
55	50	150	137	0.8	108.7	149.4	56.15	0.928	0.910	91.0	47.85	1.515	72.3
50	45	137	125	1.3	91.0	159.6	52.7	0.933	0.905	78.58	44.76	1.50	67.1
45	40	125	115	1.8	78.58	177.7	47.6	0.945	0.875	61.82	40.10	1.480	58.6
40	35	115	107	2.4	68.57	117.7	43.3	0.952	0.865	50.12	36.51	1.47	53.6
35	30	107	98	3.1	61.82	109.0	39.2	0.958	0.860	40.98	33.26	1.46	48.6
30	25	98	90	3.8	50.12	103.2	35.6	0.967	0.853	33.43	30.35	1.450	44.2
25	20	90	82	4.6	40.98	96.0	32.3	0.975	0.840	27.00	27.53	1.44	39.6
20	15	82	74	5.4	33.43	88.9	29.3	0.993	0.813	21.09	24.90	1.42	35.4
15	10	74	61	6.3	27.00	79.4	26.2	1.020	0.782	15.97	22.47	1.40	31.50
10	5	61	47	7.5	21.09	66.6							

TABLE 5.—SUMMARY OF COMPUTATIONS FOR HURRICANE-WIND WAVES IN SHALLOW WATER FOR DESIGN STORM

X in nautical miles	(H) ₀ in feet	(T) ₀ in seconds	(K) ₀ ave	K _f	P ₀ in nautical miles	H _{1/2} (at X + Δx) in feet	H _{max} /H _{1/2} in feet	H _{max} (at X + Δx) in feet
63	56.6	16.0	0.947	0.994	108.7	53.43	1.53	81.6
55	56.45	16.0	0.926	0.917	92.37	48.06	1.515	73.0
50	52.6	15.65	0.928	0.893	77.70	44.03	1.50	66.0
45	48.8	14.8	0.938	0.865	66.47	40.94	1.49	60.5
40	44.8	14.26	0.929	0.890	56.47	37.82	1.47	54.8
35	41.5	13.76	0.924	0.885	48.28	34.52	1.47	50.8
30	38.7	13.26	0.920	0.885	41.70	32.08	1.46	46.8
25	35.7	12.73	0.924	0.885	30.05	30.05	1.45	43.6
20	33.7	12.36	0.926	0.858	27.47	27.47	1.44	39.6
15	31.0	11.86	0.923	0.840	25.09	24.97	1.42	35.4
10	28.4	11.35	0.932	0.795	19.12	21.93	1.40	30.7

i. An equivalent deepwater wave height is computed at the end of the second increment, using $F = F_e' + \Delta F \approx F_s$ from Eq. 1. An average wave height over this increment is computed, using H_{e1}' and H_{e2}' , in which the first term is the equivalent deepwater height at the beginning of the increment, and the latter denotes the equivalent deepwater height at the end.

j. With the average wave height equal to $\frac{1}{2} (H_{e1}' + H_{e2}')$, steps *f*, *g*, *h*, and *i* are repeated for all except the last increment, or until the wave breaks, whichever occurs first. Usually the last increment cannot be treated by the preceding method because at this point the bottom slope increases too rapidly in a shoreward direction.

k. The maximum wave height for all except the last increment is computed from

$$H_{\max} = H_s \left(\frac{145 g d}{U^2} \right)^{0.1} \pm 10\% \approx 0.78 d \approx 1.87 H_s, \dots (26)$$

Maximum waves over the last increment and the location of breaking are obtained by plotting $H_b = 0.78 d$ seaward from the coast. The smooth curve of H_{\max} obtained in step *k* is continued until it intersects the curve of $H_b = 0.78 d$.

Results of computations for maximum swell for hurricane Hazel are presented in Fig. 14 and Table 4. Storm-tide computations were made.¹² Because of the work entailed, refraction was not considered in this example, and the actual wave height may be higher or lower than computed, depending on the degree of refraction.

A similar process is used to obtain the maximum wind wave that is regenerated over the continental shelf. In this case a constant period, T_s , is not used, but a new period over each increment is obtained by using Eq. 2 in a similar manner as Eq. 1. The results of these computations are presented in Table 5. Tables 4 and 5 indicate that the swell height and wind-wave height are almost the same, which demonstrates that the wave-energy loss for shallow-water wind waves is practically independent of the wave period. This is correct only in cases for which the bottom slope does not break off but becomes very steep at relatively shallow depths.

CONCLUSIONS

The latest proposed techniques for obtaining the hurricane design wave have been presented and are intended to supplement prior information.¹² The material is based on experience in using the information presented by Reid and the writer,¹² and is also based on additional research and supplemental data.

The concept of the energy index contributes greatly to classifying hurricanes. The history of a hurricane is confusing, but once formed, its characteristics are similar to those of its predecessors or its followers. In fact, for any particular latitude a hurricane can be characterized by the radius of maximum wind, R , the pressure anomaly at the center from normal pressure, Δp , and the forward speed, V_F . The kinetic energy of a hurricane is proportional to $R \Delta p$ and, therefore, can be used as an energy index. On the other hand, wave

energy is proportional to H^2 , and from Eq. 1, H^2 is proportional to $U^2 F$. This leads to the energy-index relationships, $H^2 \sim U^2 F = f(R \Delta p)$. In the final development for maximum deepwater waves, any hurricane has a critical speed that, if reached, will generate the largest waves, and, if exceeded, will result in waves smaller than those created by critical conditions.

The technique used for computing hurricane waves over the continental shelf, with consideration being given to bottom friction, represents an extension of a method used for computing hurricane-wind waves in shallow water of constant depth. This method has been calibrated, using hurricane-wave data recorded in Lake Okeechobee, and it is believed to be the best available method to date (1959). However, it is expected that improvement can be made as more information on wind and waves is obtained within a hurricane, both for deep and shallow water.

ACKNOWLEDGMENTS

The writer appreciates the help extended by Francis N. Kellum, Verner E. Dahlin, and Dolores Sutton (all of the Beach Erosion Board) in preparing the paper. Appreciation is also extended to Mr. Reid and to the Hydrometeorological Section of the Weather Bureau.

APPENDIX. NOTATION

The following symbols, adopted for use in the paper, conform essentially with "American Standard Letter Symbols for Hydraulics" (ASA Z10.2-1942), prepared by a committee of the American Standards Association, with Society representation, and approved by the Association in 1942:

C = wave speed;

C_g = group velocity;

d = depth of water;

e = base of natural logarithm = 2.7183;

F = fetch length:

F_e = equivalent deepwater fetch length for generation of hurricane deepwater waves;

F'_e = equivalent deepwater fetch length for generation of equivalent deepwater wave height, H'_e , in shallow water;

F_{\min} = minimum fetch length;

f = bottom friction factor and coriolis parameter;

g = acceleration of gravity;

H = wave height:

H_B = breaker height;

H_{cr} = critical value of significant wave height;

H_{\max} = maximum probable wave height;

H_e = deepwater significant wave height;

- H_o' = equivalent deepwater significant wave height;
 H_s = significant wave height in shallow water;
 K_f = coefficient for reduction in wave height for wave-energy loss due to bottom friction;
 K_r = refraction coefficient;
 K_s = shoaling factor;
 L = wave length;
 p = atmospheric pressure;
 R = radius of maximum wind;
 r = radial distance (in storm) to occurrence of gradient, or surface wind, or both together;
 S = storm tide;
 T = wave period:
 T_{cr} = critical value of significant wave period;
 T_s = significant wave period;
 T' = lowest possible period of maximum wave;
 t = duration of wind;
 t_{min} = minimum duration of wind;
 U = horizontal surface wind speed (constant):
 U_R = maximum sustained wind speed (at distance from center equal to R) for a stationary hurricane;
 U_r = root-mean-square wind speed over a fetch of variable wind speed;
 U_x = surface-wind-speed component in the x -direction;
 V = wind speed:
 V_c = cyclostrophic wind speed;
 V_{cr} = critical forward speed of hurricane;
 V_F = forward speed of hurricane;
 V_g = gradient wind speed;
 α = factor equal to or less than unity multiplied by V_F to obtain increase in wind speed due to forward speed of hurricane;
 ΔF = increment of fetch length;
 Δp = pressure anomaly at center of hurricane from normal pressure;
 Δx = increment of horizontal distance; and
 ρ = density of air.

AMERICAN SOCIETY OF CIVIL ENGINEERS

Founded November 5, 1852

TRANSACTIONS

Paper No. 2966

STRENGTH OF VERY SLENDER BEAMS

BY ERNEST F. MASUR,¹ A. M. ASCE

SYNOPSIS

The response of a slender beam to lateral loads and twisting couples is affected by the presence of bending moments in the plane of major stiffness in the same manner as the bending of beams may be influenced by the presence of axial forces. In addition, if the major bending moments are statically indeterminate and if the beam is sufficiently slender to admit relatively large lateral deformations, these deformations may, in turn, affect the distribution of the principal bending moments. The resulting nonlinear theory is the subject of the paper.

After establishing the basic equations, it is demonstrated that the inclusion of nonlinear terms in the strain-displacement relationships corresponds to a stiffening of the structure as compared with the familiar linear theory. The redistributed major bending moments and reactions satisfy a minimum principle that represents an extension of the classical Castigliano theorem. It is demonstrated further that for increasing lateral loads and torsional moments a limiting major bending-moment distribution is approached asymptotically. For certain singular cases the corresponding equilibrium configuration may not be unique. In this case, the possibility of a "snap-through" (Durchschlag) phenomenon arises.

The theory presented herein is corroborated experimentally with a fair degree of accuracy. Elastic behavior is assumed throughout.

INTRODUCTION AND ESTABLISHMENT OF BASIC EQUATIONS

Notation.—The letter symbols adopted for use in this paper are defined where they first appear, in the illustrations or in the text, and are arranged alphabetically, for convenience of reference, in Appendix II.

General.—As presented herein, a beam will be referred to as being "slender" when its moment of inertia, I_y , about the vertical y -axis is much smaller than the moment of inertia, I_x . In addition, the torsion constant of the beam, K ,

NOTE.—Published, essentially as printed here, in October, 1957, in the Journal of the Engineering Mechanics Division, as *Proceedings Paper 1413*. Positions and titles given are those in effect when the paper was approved for publication in *Transactions*.

¹ Prof., Dept. of Eng. Mechanics, Univ. of Michigan, Ann Arbor, Mich.

will be assumed to be small compared with I_x . An example of a slender beam is furnished by a rectangular beam whose thickness is small in comparison with its depth.

The response of such a beam to lateral loads and torsional couples in the presence of bending moments about the x -axis has been the subject of numerous investigations.^{2,3} These investigations have indicated the degree to which the bending moments influence and often aggravate the displacements of a slender beam. This is analogous to the behavior of beam-columns, whose response to loads in the presence of axial forces is well known.

In all the literature it has been assumed tacitly that the bending moments are either statically determinate or that they may be computed on the basis of the conventional linear theory in the event of statical indeterminacy in the major plane of stiffness. However, this may not actually be correct. In fact, if the lateral displacements, u , and the rotations, β , are sufficiently great, the introduction of nonlinear strain-displacement relationships may modify the predicted moments. This question will be explored in detail subsequently. It will be shown that a redistribution of bending moments takes place that serves to stiffen the structure relative to the stiffness predicted according to conventional theory. For example, if there are no vertical loads acting on the beam, the linear theory predicts vanishing bending moments everywhere in the absence of initial stresses. However, such moments arise when certain nonlinear terms are included in the analysis, and approach limiting values as the magnitude of the lateral loads and torques approaches infinity.

Before proceeding to the analysis, it may be well to point out the limitations of the proposed theory. Actually, the nonlinearity is partial only because the strain-displacement relationships contain terms up to the second order but ignore those of a higher order. This implies that the lateral displacements may be comparable physically to the thickness of the beam, but that they are still assumed to be small in relation to its length. Analogous theories are widely used in connection with the analysis of structural elements, in which at least one dimension is much smaller than the remaining dimensions. The best-known example is probably the plate theory of Theodore von Kármán, Hon. M. ASCE. Furthermore, because the effect of plasticity in this presentation is ignored, it follows that the beam must be very slender to lend physical significance to the proposed theory. In the subsequent numerical example, appreciable deviations occur from the linear theory at fiber stresses of approximately 30,000 lb per sq in. in a beam whose depth-to-thickness ratio is 16:1.

Analysis.—The beam in Fig. 1 is subjected to lateral loads, λq , and twisting couples, λt , in which q and t are given functions of z measured along the axis of the beam, and λ is a multiplier which is allowed to vary. If $\lambda u(z)$ and $\lambda \beta(z)$ are the horizontal displacement and the rotation, respectively, u and β are governed by the equilibrium equations,

$$(EI_y u'')'' + P u'' + [(M + P y_0) \beta]'' = q(z) \dots \dots \dots (1)$$

² "Strength of Slender Beams," by George Winter, *Transactions, ASCE*, Vol. 109, 1944, pp. 1321-1358.

³ "Torsion, Bending, and Lateral Buckling of I-Beams," by Henrik Nylander, *Bulletin No. 22*, Div. of Building Statics and Structural Eng., Royal Inst. of Technology, Stockholm, 1956.

and

$$(E \Gamma \beta'')'' - [(G K - P \rho^2 - 2 k M) \beta']' + (M + P y_0) u'' - p a \beta = t(z) \dots (2)$$

in which primes denote differentiation with respect to z . In Eqs. 1 and 2, P represents the axial force measured positive in compression, $M(z)$ is the bending moment about the centroidal x -axis, and $p(z)$ denotes the given vertical load applied at a distance a above the shear center S . The terms E and G are Young's modulus and the shear modulus, respectively; Γ is the warping constant; ρ represents the radius of gyration about S ; and y_0 designates the position of S . The assumption that S lies on the principal y -axis introduces no sig-

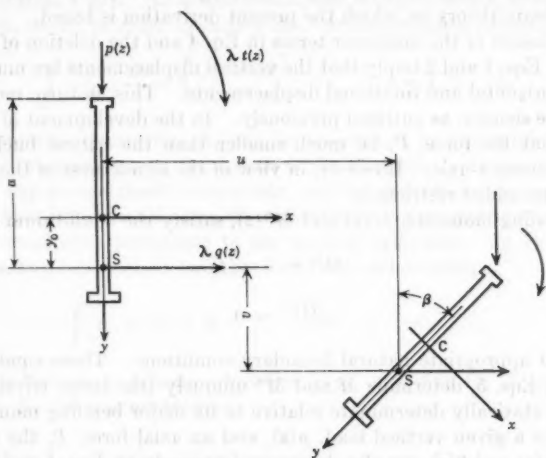


FIG. 1.—TYPICAL CROSS SECTION

nificant loss of generality. Finally, k is a cross-sectional constant and is defined by

$$k = y_0 - \frac{1}{2 I_x} \int_A y (x^2 + y^2) dA \dots (3)$$

which vanishes for sections symmetrical about the x -axis.

Eqs. 1, 2, and 3 are the familiar equations of lateral bending and torsion and are given by F. Bleich,⁴ although slight discrepancies are present, as noted by the writer and Kenneth P. Milbradt,⁵ A. M. ASCE. It can be shown further that the vertical displacement, $v(z)$, satisfies the relationship,

$$v'' = \frac{(M - M^*)}{E I_x} + \lambda^2 (u'' \beta - k \beta'^2) \dots (4)$$

⁴ "Buckling Strength of Metal Structures," by Friedrich Bleich, McGraw-Hill Book Co., Inc., New York, N. Y., 1952.

⁵ "Collapse Strength of Redundant Beams after Lateral Buckling," by E. F. Masur and K. P. Milbradt, *Transactions, Journal of Applied Mechanics*, A.S.M.E., Vol. 24, 1957, pp. 283-288.

in which the second term on the right side represents the effect of the nonlinearity in the strain-displacement relationships. The term $M^*(z)$ designates prestressing moments, if any, and has been incorporated for the sake of completeness.

An alternate derivation of these equations is from large deflection plate theory. This process can be performed for the technically most significant case of a thin rectangular beam, and, with the exception of the introduction of the term $(1 - \mu^2)^{-1}$, it leads to relationships that are identical to Eqs. 1 and 2 (properly simplified for this case). However, the form of Eq. 4 is modified slightly by this procedure. This discrepancy, which may affect the results somewhat in the presence of nonuniform bending, is due to a minor variation in the basic assumptions underlying plate theory as compared with the Euler-Bernoulli beam theory on which the present derivation is based.

The inclusion of the nonlinear terms in Eq. 4 and the deletion of analogous terms from Eqs. 1 and 2 imply that the vertical displacements are much smaller than the horizontal and rotational displacements. This, in turn, requires that the beam be slender, as outlined previously. In the development of Eq. 4 it is assumed that the force, P , be much smaller than the critical buckling force about the strong x -axis. However, in view of the slenderness of the beam this represents no added restriction.

The bending moments, M and $M^*(z)$, satisfy the equilibrium equations,

$$M'' = -p(z) \dots \dots \dots (5a)$$

and

$$M^{*''} = 0 \dots \dots \dots (5b)$$

and a set of appropriate natural boundary conditions. These conditions, together with Eqs. 5, determine M and M^* uniquely (the latter trivially) if the structure is statically determinate relative to its major bending moments. In that case for a given vertical load, $p(z)$, and an axial force, P , the calibrated functions, $u(z)$ and $\beta(z)$, are also determined uniquely by Eqs. 1 and 2 and the associated boundary conditions. Hence, the total response, λu and $\lambda \beta$, increases in proportion to the total lateral load and torque, λq and λt , respectively.

A different condition is presented by a structure in which the major bending moments are statically redundant. In that case the actual moment, $M(z)$, is distinguished, among all moments satisfying Eq. 5 and boundary conditions, by being associated with a geometrically compatible vertical deflection, $v(z)$. Because this deflection is related to M by Eq. 4, it becomes apparent that increasing lateral loads and torques, as expressed by increasing values of λ , are accompanied by a redistribution of the principal bending moments. The equations governing this redistribution will be developed subsequently.

In a structure of the n th degree of indeterminacy, the most general expressions for M and M^* are

$$M(z) = \lambda_a m_a(z) + m_0(z) \dots \dots \dots (6a)$$

and

$$M^*(z) = \lambda_a^* m_a^*(z) \dots \dots \dots (6b)$$

in which $m_0(z)$ is governed, but not uniquely determined, by

$$m_0'' = -p(z) \dots \dots \dots (7)$$

and the same boundary conditions that apply to M . The set of self-equilibrated moments, $m_r(z)$, in which $r = 1, 2 \dots n$, satisfies

$$m_r'' = 0 \quad (r = 1, 2 \dots n) \dots \dots \dots (8)$$

and equivalent homogeneous boundary conditions. The set of numbers, λ_r ($r = 1, 2 \dots n$), as yet unknown, will be referred to hereafter as "redundant parameters," whereas λ_r^* ($r = 1, 2 \dots n$) constitutes a set of "prestressing parameters." Repeated subscripts, as in Eqs. 6, represent summation over the range of from 1 to n . It is convenient, and always possible, to select the set of functions, $m_r(z)$, in order to satisfy the "orthonormality condition,"

$$\int \frac{m_r m_s dz}{E I_z} = \begin{cases} 1 & (r = s) \\ 0 & (r \neq s) \end{cases} \quad (r, s = 1, 2 \dots n) \dots \dots \dots (9)$$

The redundant parameters, λ_r , can be determined by multiplying Eq. 8 by $\bar{v}(z)$ and by integrating over the length of the structure. The expression $\bar{v}(z)$ represents any geometrically admissible, vertical deflection function—that is, a function that is sufficiently smooth and satisfies the geometric boundary and continuity conditions pertaining to the vertical deflection. In view of these restrictions, two integrations by parts lead to the relationships,

$$\int m_r \bar{v}'' dz = 0 \quad (r = 1, 2 \dots n) \dots \dots \dots (10)$$

If $\bar{v}(z)$ is the actual deflection function, $v(z)$, satisfying Eq. 4, then by Eqs. 4, 6, and 9, Eq. 10 is converted to

$$\lambda_r - \lambda_r^* = \lambda^2 \int m_r (u'' \beta - k \beta'^2) dz - \int \frac{m_0 m_r dz}{E I_z} \quad (r = 1, 2 \dots n) \dots \dots \dots (11)$$

There is no generality lost in letting $m_0(z)$ be the actual bending moment in the beam derived on the basis of linear theory, and in the absence of prestressing and of lateral loads and torques. That is, one can let the set of redundant parameters, λ_r , vanish when all prestressing parameters, λ_r^* , and the load parameter, λ , also vanish. When substituted into Eq. 11,

$$\int \frac{m_0 m_r dz}{E I_z} = 0 \quad (r = 1, 2 \dots n) \dots \dots \dots (12)$$

In view of Eq. 12, which is an expression of the principle of virtual work, the compatibility conditions expressed by Eq. 11 become

$$\lambda_r - \lambda_r^* = \lambda^2 \int m_r (u'' \beta - k \beta'^2) dz \quad (r = 1, 2 \dots n) \dots \dots \dots (13)$$

LARGE-DEFLECTION THEORY

For every redundant parameter there will be an Eq. 13. Because the bending moment, $M(z)$, is expressed in the form of Eq. 6a, it is apparent that the nonlinear range is governed by the solution of differential Eqs. 1 and 2, in which $M(z)$ satisfies, simultaneously, the compatibility equations derived previously. The complexity of the resulting system of equations is evident and, hence, the necessity of solving it by inverse or trial-and-error methods.

This is relatively easy for singly redundant beams. A value for λ_1 may be assumed arbitrarily at the beginning. With the bending moment, $M(z)$, chosen thus, Eqs. 1 and 2 are solved, and the solution (u, β) is inserted in the single Eq. 13, which, in turn, is solved for the load parameter, λ . If the value of λ obtained is real, and if the assumed moment, $M(z)$, is statically admissible in the sense defined subsequently, a point has been established in the load-response diagram because of the uniqueness of the solution (also proved subsequently). The diagram may be completed by repeating this process for different values of λ_1 .

For higher degrees of redundancy the process may become prohibitively difficult. However, some insight into the nonlinear behavior of the structure can be gained by several principles that will be developed subsequently. In addition, it is possible that these principles may be instrumental in the reduction of the numerical labor involved.

For this purpose a quadratic form, U , can be defined by

$$2 U(M; u, \beta) = \int (E I_y u''^2 + E \Gamma \beta''^2 + G K \beta'^2) dz - \int [P(u'^2 + \rho^2 \beta'^2) - 2(M + P y_0) u' \beta + 2k M \beta'^2 + p a \beta^2] dz. \quad (14)$$

In Eq. 14 the first integral represents the bending and torsional strain energy. The second integral can be shown to give the work performed by the vertical load, $p(z)$, and the axial force, P . Also, a bending moment, $M(z)$, will be referred to hereafter as being "statically admissible" if it satisfies the equilibrium equations (Eqs. 5) and the stability condition,

$$U(M; \bar{u}, \bar{\beta}) \geq 0. \quad (15)$$

for all nontrivial functions $(\bar{u}, \bar{\beta})$ that are geometrically admissible—that is, they are sufficiently smooth and satisfy the pertinent geometric boundary conditions.

If the potential energy, V , is defined by

$$V(M; u, \beta) = U(M; u, \beta) - \int (q u + t \beta) dz \\ = U(M; u, \beta) - W(u, \beta) \quad (16)$$

in which the integral expression, W , represents the work done by the lateral loads and the torsional moments, it can be shown readily that

$$V(M; \bar{u}, \bar{\beta}) \geq V(M; u, \beta) \quad (17)$$

if M is statically admissible and if (u, β) satisfies Eqs. 1 and 2. Because Eqs. 1 and 2 are the variational Euler equations of V , and as the actual natural boundary conditions are the variational boundary conditions of V , the correct solution (u, β) makes V stationary for all moments satisfying the equations of equilibrium. The additional minimum principle, expressed by Eq. 17, represents an extension to the restricted class of moments that satisfy also the stability condition of Eq. 15. The equality sign in Eq. 15 implies trivial equality between $(\bar{u}, \bar{\beta})$ and (u, β) , provided that only the inequality of Eq. 15 is admitted. Conversely, if $U = 0$ for (u, β) , then the equality of Eq. 17 applies also to

$$(\bar{u}, \bar{\beta}) = (u, \beta) + c(u, \beta) \dots \dots \dots (18)$$

in which c is an arbitrary number. The pair of functions (u, β) represents the fundamental buckling mode of the beam.

With these definitions one can let a bending moment,

$$\bar{M}(z) = m_0 + \lambda_a m_a \dots \dots \dots (19)$$

be statically admissible, relative to a given load, and the functions $(\bar{u}, \bar{\beta})$ can be associated with \bar{M} through solving Eqs. 1 and 2. Also, one can allow M and (u, β) to represent the correct bending moment and configuration for the same load, respectively. This implies that Eqs. 6a and 13 are satisfied also.

Because (u, β) are certainly geometrically admissible, it follows that

$$V(\bar{M}; u, \beta) \geq V(\bar{M}; \bar{u}, \bar{\beta}) \dots \dots \dots (20)$$

similarly to Eq. 17. However,

$$\begin{aligned} V(\bar{M}; u, \beta) &= V(M; u, \beta) + (\bar{\lambda}_a - \lambda_a) \int m_a (u'' \beta - k \beta'^2) dz \\ &= V(M; u, \beta) + \frac{1}{\lambda^2} (\lambda_a - \lambda_a) (\lambda_a - \lambda_a^*) \dots (21) \end{aligned}$$

in which the second equality is in consequence of Eq. 13.

Moreover, if Eq. 1 is multiplied by u and Eq. 2 is multiplied by β , and if several integrations by parts are performed, it is readily demonstrated that because of the boundary conditions,

$$W(u, \beta) = 2 U(M; u, \beta) \dots \dots \dots (22)$$

An identical relationship applies to the system, $(\bar{M}; \bar{u}, \bar{\beta})$. Thus, in view of the definition of V in Eq. 16, the inequality (Eq. 20) becomes

$$U(\bar{M}; \bar{u}, \bar{\beta}) \geq U(M; u, \beta) - \frac{1}{\lambda^2} (\bar{\lambda}_a - \lambda_a) (\lambda_a - \lambda_a^*) \dots (23a)$$

or

$$U(\bar{M}; \bar{u}, \bar{\beta}) + \frac{1}{2\lambda^2} (\lambda_\alpha - \lambda_{\alpha^*}) (\lambda_\alpha - \lambda_{\alpha^*}) \geq U(M; u, \beta) + \frac{1}{2\lambda^2} \\ \times (\lambda_\alpha - \lambda_{\alpha^*}) (\lambda_\alpha - \lambda_{\alpha^*}) + \frac{1}{2\lambda^2} (\lambda_\alpha - \lambda_\alpha) (\lambda_\alpha - \lambda_\alpha) \dots (23b)$$

The last term on the right side of Eq. 23b is positive definite. Hence, in the absence of initial bending moments ($\lambda_r^* = 0$), the following inequality is established:

$$U(M; u, \beta) + \frac{1}{\lambda^2} U_b(M) \leq U(\bar{M}; \bar{u}, \bar{\beta}) + \frac{1}{\lambda^2} U_b(\bar{M}) \dots (24a)$$

in which

$$U_b(M) = \frac{1}{2} \int \frac{M^2 dz}{E I_x} \dots (24b)$$

The term U_b represents the familiar expression for the strain energy in bending about the major axis. Eq. 24a follows from Eq. 23b through the application of Eqs. 6a, 9, and 12. An alternate statement of the inequality (Eq. 24a), which takes account of Eq. 22, is

$$W(u, \beta) + \frac{2}{\lambda^2} U_b(M) \leq W(\bar{u}, \bar{\beta}) + \frac{2}{\lambda^2} U_b(\bar{M}) \dots (25)$$

These last two inequalities may be expressed in the following principle: Of all statically admissible bending moments, the actual one corresponds to the smallest value of $\lambda^2 U + U_b$ (or, alternately, of $\lambda^2 W + 2 U_b$) if these values are determined on the basis of a deflected configuration that is related to the bending moments through solving Eqs. 1 and 2.

It should be emphasized that this minimum principle is related to the distribution of the redundant moments rather than to the deflection configuration itself. It is well known that the latter is itself governed by minimum principles, which were, in fact, utilized in the derivation of the present principle. It represents an extension of the classical Castigliano "theorem of least work" into the nonlinear range. Indeed, the Castigliano theorem represents a special case, which can be obtained from either Eq. 24a or Eq. 25 by letting λ approach zero. Actually, the customary statement of the Castigliano theorem does not imply a minimum, but only a stationary property of the strain energy in bending. The present principle can be broadened similarly. In fact, if M satisfies the equilibrium equations (Eqs. 5), but not necessarily the stability condition of Eq. 15, the quantities dealt with in Eq. 24a and in Eq. 25 can be shown to be stationary. That is, if (u, β) , as solved from Eqs. 1 and 2, are differentiable functions of λ_r , the satisfaction of Eq. 13 assures that the derivative of $(\lambda^2 U + U_b)$, or of $(\lambda^2 W + 2 U_b)$, with respect to λ_r , vanishes.

To clarify the foregoing further, one can let the inequality Eq. 20 be subtracted from Eq. 17. This results in

$$(\lambda_\alpha - \bar{\lambda}_\alpha) \int m_\alpha (\bar{u}'' \bar{\beta} - k \bar{\beta}^2) dz \geq (\lambda_\alpha - \bar{\lambda}_\alpha) \int m_\alpha (u'' \beta - k \beta^2) dz \dots (26)$$

If both $(M; u, \beta)$ and $(\bar{M}; \bar{u}, \bar{\beta})$ are assumed to satisfy the conditions of compatibility expressed by Eq. 13, it follows that

$$(\lambda_\alpha - \bar{\lambda}_\alpha) (\bar{\lambda}_\alpha - \lambda_\alpha^*) \geq (\lambda_\alpha - \lambda_\alpha) (\lambda_\alpha - \lambda_\alpha^*) \dots \dots \dots (27a)$$

or, after some rearrangement of terms,

$$0 \geq (\lambda_\alpha - \bar{\lambda}_\alpha) (\lambda_\alpha - \bar{\lambda}_\alpha) \dots \dots \dots (27b)$$

Obviously, the foregoing inequality is impossible for real values of the redundant parameters. On the other hand, the equality is possible only if $M(z)$ and $\bar{M}(z)$ are trivially identical. This, in turn, implies the following principle: If a statically admissible bending moment exists that satisfies the conditions of compatibility expressed by Eq. 13, relative to a configuration (u, β) that is a solution of Eqs. 1 and 2, it is the actual bending moment and is unique.

In general, it follows from the uniqueness of $M(z)$ that $u(z)$ and $\beta(z)$ are also unique. However, due to a condition of "neutral equilibrium," singular cases may occur in which two equilibrium configurations become possible. This was already suggested following the establishment of the inequality Eq. 17. A detailed consideration of this question is contained in Appendix I as well as in later sections in connection with the numerical example and in the report on the experiments.

With reference to the minimum principle established previously, it is clear that any statically admissible bending moment furnishes an upper bound to the two functions with which the principle deals. It will now be necessary to derive also a lower bound and to consider a possible application of these bounds toward the simplification of the computational labor.

A "kinematically admissible" bending moment, $\bar{M}(z)$, can be defined as one that satisfies the equilibrium equations (Eqs. 5); it can be expressed therefore also in terms of Eq. 6a subject to Eqs. 7, 8, and 9. It is compatible because it satisfies Eq. 13 for some geometrically consistent configuration $(\bar{u}, \bar{\beta})$. It finally does not violate the inequality,

$$U(\bar{M}; \bar{u}, \bar{\beta}) - \frac{1}{2} W(\bar{u}, \bar{\beta}) \leq 0 \dots \dots \dots (28)$$

The concept of kinematic admissibility follows from the fact that if the equality sign in Eq. 28 is satisfied, the external work equals the "internal work." However, it must be noted that the equilibrium equations, Eqs. 1 and 2, need not be satisfied. If Eq. 28 is subtracted from the inequality Eq. 17, in which the actual state $(M; u, \beta)$ is compared with the state $(\bar{M}; \bar{u}, \bar{\beta})$, then, in view of Eq. 22,

$$2(\lambda_\alpha - \bar{\lambda}_\alpha) \int m_\alpha (\bar{u}'' \beta - k \bar{\beta}^2) dz - W(\bar{u}, \bar{\beta}) \geq -W(u, \beta) \dots (29)$$

in which λ_α represents the set of redundant parameters designating $\bar{M}(z)$. The integrals in Eq. 29 may be replaced according to Eq. 13, and, after some rear-

rangement of terms, this becomes

$$W(u, \beta) + \frac{1}{\lambda^2} (\lambda_\alpha - \lambda_{\alpha^*}) (\lambda_\alpha - \lambda_{\alpha^*}) \geq W(\bar{u}, \bar{\beta}) + \frac{1}{\lambda^2} (\bar{\lambda}_\alpha - \lambda_{\alpha^*}) \\ \times (\bar{\lambda}_\alpha - \lambda_{\alpha^*}) + \frac{1}{\lambda^2} (\bar{\lambda}_\alpha - \lambda_\alpha) (\bar{\lambda}_\alpha - \lambda_\alpha) \dots (30)$$

in which the final term, as before, is positive definite. Hence, using the same argument,

$$W(\bar{u}, \bar{\beta}) + \frac{2}{\lambda^2} U_b(\bar{M}) \leq W(u, \beta) + \frac{2}{\lambda^2} U_b(M) \dots (31)$$

or, in view of Eqs. 22 and 28,

$$U(\bar{M}; \bar{u}, \bar{\beta}) + \frac{1}{\lambda^2} U_b(\bar{M}) \leq U(M; u, \beta) + \frac{1}{\lambda^2} U_b(M) \dots (32)$$

Because the actual bending moment, $M(z)$, is also kinematically admissible, it follows that of all kinematically admissible bending moments, the actual moment corresponds to the smallest possible value of the functions $\lambda^2 W + 2 U_b$ or $\lambda^2 U + U_b$.

It appears that this lower-bound principle may be useful in estimating the nonlinear response of the structure. In fact, if an upper bound and a lower bound are determined for a given value of the load parameter, λ , then an error estimate has been established. Because the bounds can be narrowed down arbitrarily, a correct solution can presumably be approached in this fashion.

ASYMPTOTIC BEHAVIOR

As the load parameter, λ , grows beyond bounds, the bending moment, $M(z)$, and with it the deflection mode, (u, β) , usually approaches a limiting condition. This asymptotic behavior is examined in this section with respect to both the governing equations and the appropriate energy principles.

For a given load, $p(z)$, it was shown by the writer and Milbradt⁵ that the stable domain (that is, the one in which the inequality Eq. 15 is satisfied) is generally a closed region in a space in which the coordinates of a point are given by the redundant parameters, λ_r , associated with $M(z)$ through Eq. 6. As the value of p approaches an ultimate value, p_u , this region shrinks to a point. For $p > p_u$, no statically admissible bending moments are available. The value of p is assumed herein to be fixed and less than p_u . Because of the boundedness of the associated stable domain, it follows that all the redundant parameters, λ_r , will remain finite as the load parameter, λ , attains infinity.

The foregoing determines the form of the governing equations of the limiting state. In fact, if λ approaches infinity in Eq. 13 while the left side remains bounded, the asymptotic deflection mode (u_l, β_l) satisfies

$$\int m_r (u_l'' \beta_l - k \beta_l'^2) dz = 0 \quad (r = 1, 2 \dots n) \dots (33)$$

together with the equilibrium equations (Eqs. 1 and 2). This system of equations does not contain the prestressing parameters, $\lambda,^*$. In other words, the "final" state is independent of whatever initial stresses are in the structure (due to settlement of support, temperature gradients, and similar phenomena), although the "history" of the structure does display such dependence.

By the same token, an asymptotic minimum principle can be derived. If λ is permitted to approach infinity in the inequality Eq. 24a, it follows (for $\lambda,^* = 0$) that

$$U(M_i; u_i, \beta_i) = U(m_0; u_i, \beta_i) \leq U(\bar{M}; \bar{u}, \bar{\beta}) \dots \dots \dots (34a)$$

or

$$W(u_i, \beta_i) \leq W(\bar{u}, \bar{\beta}) \dots \dots \dots (34b)$$

in which $(\bar{M}; \bar{u}, \bar{\beta})$ represents, as before, any statically admissible bending moment and associated deflection mode. The first equality in Eq. 34a follows from Eq. 33. Accordingly, the limiting bending moment makes U or W smaller than does any other statically admissible bending moment.

In general, this minimum is in the interior of the region of stability. It is approached asymptotically, and the corresponding configuration is unique. The existence of such an interior minimum is proved in Appendix I. Also, certain singular cases are explored in which U may assume a minimum on the boundary of the stable domain. In that case the limiting bending moment may be reached for a finite value of the load parameter, λ . Also, it is not necessary for the deflection mode to be unique in such a case, as appears reasonable in view of the limitations on the uniqueness principle that was established under the heading, "Large-Deflection Theory."

The upper-bound principle expressed by Eq. 34a has a counterpart in the form of a limiting lower-bound principle. This is derived readily by considering Eq. 31, with λ approaching infinity. If (u_c, β_c) represent any pair of functions that—in addition to being otherwise acceptable—satisfies Eq. 33, and, furthermore, if this collapse mode satisfies the condition,

$$2 U_*(m_0; u_c, \beta_c) - W(u_c, \beta_c) = 0 \dots \dots \dots (35)$$

then

$$U(m_0; u_c, \beta_c) \leq U(m_0; u_i, \beta_i) \dots \dots \dots (36a)$$

or

$$W(u_c, \beta_c) \leq W(u_i, \beta_i) \dots \dots \dots (36b)$$

Unless one of the terms in Eq. 35 vanishes, that equation can always be satisfied nontrivially by properly selecting the amplitude and sign of the assumed collapse mode. This follows from the fact that U is quadratic, but W is linear in u and β . Therefore, of all possible collapse modes, the actual mode corresponds to the largest value of U or W .

NUMERICAL EXAMPLE

In this section the principles and equations of the preceding sections will be applied to an illustrative example. For this purpose a beam is considered, having a length, L , which is of thin rectangular cross section ($\Gamma = 0$) and has a second degree of redundancy relative to bending in its major plane because of

being elastically restrained at both ends. However, only one degree of indeterminacy need be considered here because of the complete symmetry of the problem. Simple supports are provided at both ends in so far as lateral movement is concerned. A single lateral force of magnitude λ is applied halfway between supports and at an eccentricity, e , above the center line. As before, if the total response is denoted by $(\lambda u, \lambda \beta)$, and if m is the restraint moment, in the absence of the vertical load, $p(z)$, Eqs. 1 and 2 and the boundary conditions take the form,

$$\begin{cases} E I_y u^{iv} - m \beta'' = 0 \\ G K \beta'' + m u'' = 0 \end{cases} \quad \left(0 \leq z \leq \frac{L}{2}\right) \dots\dots\dots (37)$$

$$u(0) = u''(0) = \beta(0) = 0 \dots\dots\dots (38)$$

and

$$u' \left(\frac{L}{2} \right) = E I_y u''' \left(\frac{L}{2} \right) - m \beta' \left(\frac{L}{2} \right) + \frac{1}{2} = G K \beta' \left(\frac{L}{2} \right) - \frac{e}{2} = 0 \dots\dots (39)$$

Eq. 39 follows from the symmetry of the problem. Hence, the solution for (u, β) need be considered only for half the beam—that is, from the left support ($z = 0$) to the center ($z = L/2$).

For the present case, in the absence of prestressing, the compatibility Eq. 13 becomes

$$m = -2\lambda^2 \left(\frac{E I_z}{L} \right) \gamma \int_0^{L/2} u'' \beta \, dz \dots\dots\dots (40)$$

in which

$$\gamma = \frac{C}{C + 2 E I_z / L} \dots\dots\dots (41)$$

represents the degree of end restraint and varies from zero (no restraint) to unity (full fixity). The spring constant is denoted by C and is measured in inch-pounds per radian.

For the range between 0 and $L/2$, the solution of Eq. 37, subject to the boundary conditions Eqs. 38 and 39, is given by

$$u(z) = A (1 - \phi \alpha) \left(\frac{\sin \alpha z / L}{\cos \alpha / 2} - \frac{\alpha z}{L} \right) \dots\dots\dots (42)$$

and

$$e \beta(z) = A \phi \alpha \left[- (1 - \phi \alpha) \frac{\sin \alpha z / L}{\cos \alpha / 2} + \frac{\alpha z}{L} \right] \dots\dots\dots (43)$$

in which

$$A = \frac{L^3}{2 E I_y \alpha^3} \dots\dots\dots (44a)$$

$$\phi = \frac{e}{L} \sqrt{\frac{E I_y}{G K}} \dots\dots\dots (44b)$$

and

$$0 \leq \alpha^2 = \frac{m^2 L^2}{E I_y G K} = \pi^2 \left(\frac{m}{m_1} \right)^2 < \pi^2 \dots\dots\dots (44c)$$

in which m_1 identifies the moment associated with neutral equilibrium and ϕ is a dimensionless constant.

If Eqs. 42 and 43 are substituted into Eq. 40, this leads to the relationship,

$$\alpha^5 = \frac{I_x}{2 I_y} \frac{L^5}{E I_y G K} \gamma \lambda^2 F(\alpha) \quad (45)$$

in which

$$F(\alpha) = (1 - \phi \alpha) \left[\left(\tan \frac{\alpha}{2} - \frac{\alpha}{2} \right) + \frac{1}{2} (1 - \phi \alpha) \times \left(\tan \frac{\alpha}{2} - \frac{\alpha}{2} - \frac{\alpha}{2} \tan^2 \frac{\alpha}{2} \right) \right] \quad (46)$$

Eq. 45 can be made dimensionless. In fact, one can let the dimensionless ratio, ω , be defined by

$$\omega = \frac{s_y}{s_1} \quad (47)$$

in which

$$s_y = \frac{\lambda L/4}{S_y} \quad (48a)$$

and

$$s_1 = \frac{m_1}{S_x L} = \frac{\pi}{S_x L} \sqrt{E I_y G K} \quad (48b)$$

with S_y and S_x designating, respectively, the section moduli about the y -axis and the x -axis. It is apparent that s_y represents the maximum fiber stress in lateral bending, whereas s_1 is the maximum fiber stress associated with the buckling moment, m_1 . With these definitions and considering the relationship between the moments of inertia and section moduli for rectangular sections, Eq. 45 becomes

$$(8 \gamma \pi^2) \omega^2 = \frac{\alpha^5}{F(\alpha)} \quad (49)$$

As ω and, hence, the lateral load, λ , approach zero, both the numerator and the denominator on the right side of Eq. 49 also approach zero. For very small values of ω ,

$$(\gamma \phi \pi^2) \omega^2 = 3 \alpha \quad (\alpha \ll \pi) \quad (50)$$

Conversely, as the lateral load increases, it follows from Eq. 49 that

$$\lim_{\omega \rightarrow \infty} F(\alpha) = 0 \quad (51)$$

The best way to establish a functional relationship between α and ω is probably to assume a value for α and to solve for ω by use of Eq. 49. However, for small values of α the inverse procedure may be followed by using Eq. 50. The asymptotic magnitude of α for very large lateral loads can be obtained from Eq. 51. It can be verified that the smallest positive root of Eq. 51 is given by

$\alpha = 1/\phi$ for $\phi > \pi$, whereas for $\phi < \pi$, the smallest root must be computed through a trial-and-error process.

With the $(\omega - \alpha)$ -relationship thus established, the maximum lateral deflection occurring at the midpoint of the beam is

$$u_{\max} = A (1 - \phi \alpha) \left(\tan \frac{\alpha}{2} - \frac{\alpha}{2} \right) = \kappa_u \frac{L^3}{48 E I_y} \dots \dots \dots (52a)$$

in which

$$\kappa_u = \frac{24}{\alpha^3} (1 - \phi \alpha) \left(\tan \frac{\alpha}{2} - \frac{\alpha}{2} \right) \dots \dots \dots (52b)$$

In Eq. 52 the quantity A was defined in Eq. 44a, whereas κ_u represents the ratio between the computed maximum deflection and the equivalent value determined on the basis of the linear theory, which does not predict the development of restraining moments, m (that is, $\alpha = 0$). For very small values of α , Eq. 52b can be approximated by

$$\kappa_u = 1 - \phi \alpha = 1 - \left(\frac{\pi^2}{3} \right) \gamma \phi^2 \omega^2 \quad (\alpha \ll \pi) \dots \dots \dots (53)$$

in which the second equality follows from Eq. 50.

Similarly, the maximum rotation occurs also at the middle of the beam and is governed by

$$e \beta_{\max} = A \phi \alpha \left[\frac{\alpha}{2} - (1 - \phi \alpha) \tan \frac{\alpha}{2} \right] = \kappa_\beta \frac{e^2 L}{4 G K} \dots \dots \dots (54a)$$

in which

$$\kappa_\beta = \left(\frac{2}{\phi \alpha^2} \right) \left[\frac{\alpha}{2} - (1 - \phi \alpha) \tan \frac{\alpha}{2} \right] \dots \dots \dots (54b)$$

and in which, as in the preceding equation, κ_β is defined as the ratio between the computed maximum rotation and the corresponding rotation computed on the basis of the linear theory. For very small values of α , Eq. 54b can be approximated by

$$\kappa_\beta = 1 - \left(\frac{\alpha}{12 \phi} \right) = 1 - \left(\frac{\pi^2}{36} \right) \gamma \omega^2 \quad (\alpha \ll \pi) \dots \dots \dots (55)$$

The lateral deflection of the point of application of the force itself is found by adding Eqs. 52a and 54a, or

$$\begin{aligned} (u + e \beta)_{\max} &= A \left[(1 - \phi \alpha)^2 \tan \frac{\alpha}{2} - (1 - 2 \phi \alpha) \frac{\alpha}{2} \right] \\ &= \kappa \frac{L^3}{48 E I_y} (1 + 12 \phi^2) \dots (56a) \end{aligned}$$

in which

$$\kappa = \left(\frac{24}{\alpha^3} \right) (1 + 12 \phi^2)^{-1} \left[(1 - \phi \alpha)^2 \tan \frac{\alpha}{2} - (1 - 2 \phi \alpha) \frac{\alpha}{2} \right] \dots (56b)$$

and in which the definition of κ is analogous to that of κ_u and κ_β , and which, for small values of α , becomes

$$\kappa = 1 - (2\phi\alpha)(1 + 12\phi^2)^{-1} = 1 - \left(\frac{2}{3}\right)\pi^2\phi^2 \times (1 + 12\phi^2)^{-1}\gamma\omega^2 \quad (\alpha \ll \pi) \dots (57)$$

From Eq. 56b, $dk/d\alpha$ can be shown to be proportional to $F(\alpha)$. Hence, by Eq. 51, for very large values of ω , $dk/d\alpha$ vanishes. Furthermore, as the second derivative is positive, the limiting value of κ is an absolute minimum if only stable values of α (lying in the closed region between $-\pi$ and $+\pi$) are admitted in comparison. However, this is not surprising. Because κ is a measure of the total work performed by the external force—all other terms being independent of α —this property of κ is a natural concomitant of the minimum principle expressed in the inequality Eq. 34b.

Some of the preceding results become invalid for the singular case of $\phi = 1/\pi$. Physically, this means that the force is applied at a point that would not move if the beam were to buckle laterally under the critical end moment, m_1 , when $\alpha = \pi$. This special case, which was alluded to briefly under the heading, "Asymptotic Behavior," is treated in a general fashion in Appendix I. In its application to the present example it will be analyzed fully. A comparison with Appendix I shows that the general principles developed in it are confirmed for the case under consideration.

It can be verified easily that $F(\alpha)$, which is defined in Eq. 46, has no root in the range $0 < \alpha < \pi$ for the singular case of $\phi = 1/\pi$. The term $F(\pi)$ is indeterminate, but the customary limit procedure leads to a value of $1/\pi$. Hence, when Eq. 49 is used, the boundary of the stable range is reached when ω assumes the finite value governed by

$$\omega_0^2 = \frac{\pi^4}{8\gamma} \dots (58)$$

whereas, using Eqs. 52b, 54b, and 56b, and similar limit procedures,

$$\kappa_u(\pi) = \frac{48}{\pi^4} \dots (59a)$$

$$\kappa_\beta(\pi) = 1 - \frac{4}{\pi^2} \dots (59b)$$

and

$$\kappa(\pi) = \left(1 + \frac{\pi^2}{12}\right)^{-1} \dots (59c)$$

Similarly, the deflection mode approaches the limiting functions,

$$\left. \begin{aligned} u_0(z) &= \lim_{\alpha \rightarrow \pi} u(z) = \frac{L^3}{\pi^4 E I_y} \sin \frac{\pi z}{L} \\ e \beta_0(z) &= \lim_{\alpha \rightarrow \pi} e \beta(z) = \frac{L^3}{\pi^4 E I_y} \left(\frac{\pi^2 z}{2L} - \sin \frac{\pi z}{L} \right) \end{aligned} \right\} \left(0 \leq z \leq \frac{L}{2} \right) \dots (60)$$

For values of $\omega > \omega_0$, the restraint moment, m , retains its critical value, m_1 , or $\alpha \equiv \pi$, throughout. However, the solution of Eq. 37, as expressed by Eq. 60, is no longer unique. It can, in general, be expressed by

$$\left. \begin{aligned} u(z) &= u_0(z) + c \frac{L^{7/2}}{\pi^4 E I_y} u_1(z) \\ e \beta(z) &= e \beta_0(z) + c \frac{L^{7/2}}{\pi^4 E I_y} e \beta_1(z) \end{aligned} \right\} \dots \dots \dots (61)$$

in which c is as yet an arbitrary multiplier. The factor associated with c in Eq. 61 has been added for convenience, and (u_1, β_1) is the normalized buckling mode given by

$$u_1(z) = (L)^{-1} \sin \frac{\pi z}{L} = -e \beta_1(z) \dots \dots \dots (62)$$

The value of c is determined from the compatibility condition of Eq. 40, which, in view of Eqs. 60, 61, and 62 and of the definitions of α and ω , becomes

$$c^2 = 1 - \left(\frac{\pi^4}{8 \gamma \omega^2} \right) \dots \dots \dots (63)$$

If a factor of $\tau \leq 1$ is defined by

$$\tau = \frac{\omega_0}{\omega} \dots \dots \dots (64)$$

in which ω_0 is given in Eq. 58 and represents (in review) the value of ω as $\alpha = \pi$ is reached initially, then c is related to τ by the equation of the unit circle,

$$c^2 + \tau^2 = 1 \dots \dots \dots (65)$$

There are two possible values of c for $\tau < 1$ in conformity with Appendix I. In particular, for $\tau = 0$, as the force, λ , goes to infinity, $c = \pm 1$, or two distinct equilibrium configurations not adjacent to one another are possible. Therefore, a "snap-through" (Durchschlag) phenomenon can be expected.

The reduction factors, κ , are obtained by considering Eqs. 60, 61, 62, 64, and 65. This leads to the relationships,

$$\kappa_u = \left(\frac{48}{\pi^4} \right) (1 \pm \sqrt{1 - \tau^2}) \quad \lim_{\tau \rightarrow 0} \kappa_u = \left(\frac{96}{\pi^4} \right), \quad 0 \dots \dots (66a)$$

$$\kappa_\beta = 1 - \left(\frac{4}{\pi^2} \right) (1 \pm \sqrt{1 - \tau^2}) \quad \lim_{\tau \rightarrow 0} \kappa_\beta = 1 - \frac{8}{\pi^2}, \quad 1 \dots \dots (66b)$$

and

$$\kappa = \left(1 + \frac{\pi^2}{12} \right)^{-1} \dots \dots \dots (66c)$$

That is, the limiting configurations represent either predominant bending with little twisting, or else pure twist without any bending. However, only one value of κ appears, because the transition from one configuration to the other configuration constitutes a rotation about the point of application of the force. This value of κ remains constant as soon as the condition $\alpha = \pi$, or $\omega = \omega_0$, is reached. For $\omega > \omega_0$ ($\tau < 1$), the force-displacement relationship is linear,

but the apparent stiffness of the structure is almost double that predicted by the linear theory.

For sufficiently large values of the applied force, the response of the structure is a discontinuous function of the eccentricity, e , of the force. In fact, for "small" eccentricities ($\phi < 1/\pi$), the configuration approaches one of bending and little twisting—the ratio being nearly independent of ϕ . More surprisingly, the response for "large" eccentricities ($\phi > 1/\pi$) approaches one of pure twist without any bending—the reduction factors, κ_u and κ_β , being zero and unity irrespective of the value of ϕ . For the singular case of $\phi = 1/\pi$, the two possible configurations examined previously represent limiting cases as the value of ϕ approaches $1/\pi$ from below or from above, respectively.

This type of discontinuity seems to be one of the salient features that distinguishes the present theory from the conventional linear approach. Other examples have been investigated and have been found to lead to similar results. For example, if the same beam is subjected to two forces applied at equal distances from the ends and at equal—nonvanishing—eccentricities, but pulling in opposite directions, then the asymptotic response is found to be a discontinuous function of the ratio of the magnitudes of the forces. In fact, the greater of the two forces dominates the behavior entirely. Singularity, or snap-through, occurs when the forces are equal.

EXPERIMENTAL RESULTS

To check the results of the preceding section experimentally, a test arrangement similar to the one described by the writer and Milbradt⁴ was used. The beam specimen used was a strap 1 in. high and $\frac{1}{8}$ in. thick, made of heat-treated steel with a yield point of approximately 180,000 lb per sq in. Spanning a distance of 20 in., the beam was restrained elastically at both ends in the vertical plane with the degree of end fixity, γ (Eq. 41), computed to be 0.74. However, by loosening the clamps this end restraint could be removed entirely. In this fashion the beam was made statically determinate to provide a check for the linear theory. The values for Young's modulus, E , and Poisson's ratio, μ , were 30,000,000 lb per sq in. and 0.3, respectively. This establishes the relationship $\lambda = 1.48 \omega$, in which λ is the applied force measured in pounds and ω is defined in Eq. 47.

A relatively rigid vertical bar was attached to the beam at midspan. This bar was then subjected to a horizontal lateral force of increasing magnitude and varying eccentricity. The results corresponding to eccentricities, e , of 4 in., 8 in., and 12 in. will be considered subsequently. These eccentricities are associated with values of ϕ that very nearly equal $\frac{1}{2\pi}$, $1/\pi$, and $\frac{3}{2\pi}$, respectively, in which the second value represents the singular case. The lateral deflections, λu , and rotations, $\lambda \beta$, as well as the total displacement, $\lambda(u + e\beta)$, of the applied force, were measured in the usual manner by scales and mirrors.

A comparison between the predicted results and the measured results is given in Fig. 2 that corresponds to the three types of eccentricities—small, singular, and large—mentioned previously. In each case the curves show the computed values of the reduction ratios on the basis of Eqs. 52b, 54b, and 56b

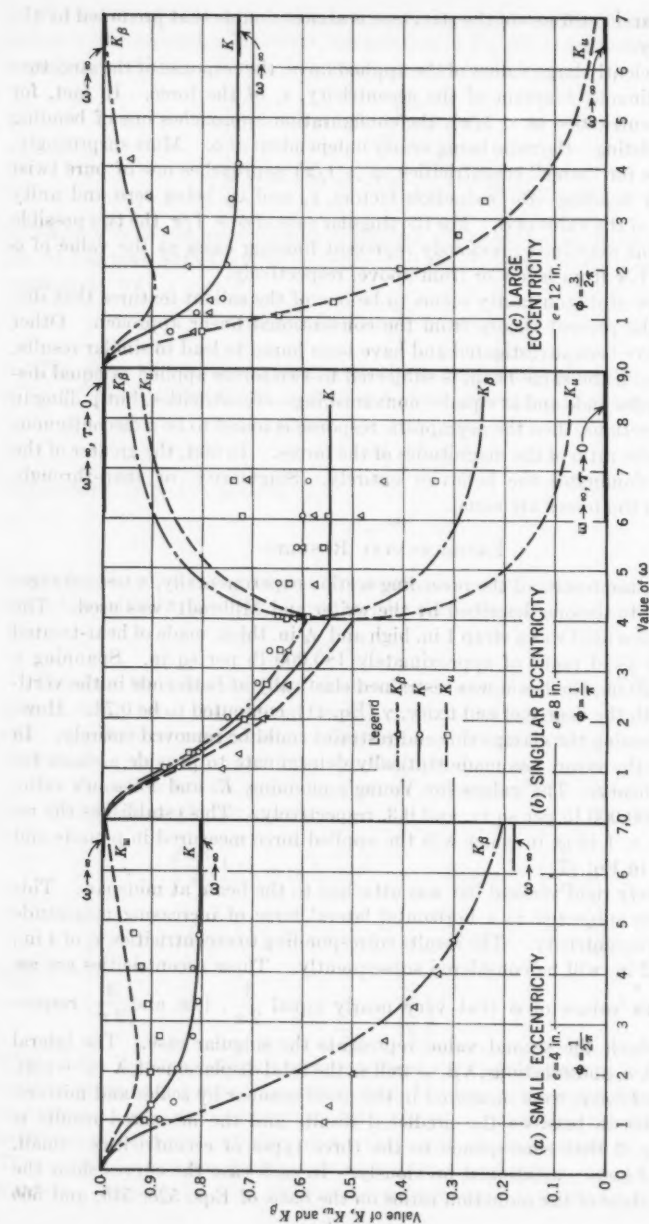


FIG. 2.—REDUCTION FACTORS

as functions of the dimensionless loading parameter, ω , defined in Eq. 47. For the singular case of $e = 8$ in., or $\phi = 1/\pi$, the boundary of the stable domain is reached for $\omega_0 = 4.06$, as given in Eq. 58, with the associated reduction coefficients computed in accordance with Eqs. 59. For values of ω in excess of ω_0 , these coefficients are governed by Eqs. 66.

The experimental points shown in the figures represent average values based on several test sequences. Reasonable agreement was obtained for small eccentricities and for large eccentricities. Such quantitative discrepancies that occur seem to be due to the effects of initial imperfections and of prestressing moments. For large values of ω , other nonlinear factors that were ignored in the present analysis cause further discrepancies. In fact, because both the measured deflections and rotations were somewhat in excess of the limitations cited under the heading, "Introduction," a more accurate analysis, which involves powers of u and β greater than the second power, yields more compatible results. Nevertheless, there is excellent qualitative agreement between the theory and experiment. In particular, the discontinuous character of the asymptotic solution is corroborated fully.

For the singular case ($e = 8$ in., $\phi = 1/\pi$), the agreement is confined to values of ω less than ω_0 . For larger values of ω , two possible solutions (Durchschlag) occurred, but the quantitative agreement between the theory and the experimental values is poor. A possible explanation can be found in the effect of initial imperfections. These imperfections, such as initial curvatures, become increasingly important as the boundary of the stable domain is approached—that is, as the value of α approaches π . In fact, if Eq. 37 is properly modified to include the effect of an initial deviation from perfect shape, it can be readily verified that, in the general case, the solution "blows up" as the support moments approach their critical values. In effect, the orthogonality condition of Eq. 74 (Appendix I) is violated, which means that neutral equilibrium is approached only as the load approaches infinity instead of the finite value of ω_0 predicted by the idealized theory. This may explain why the double-valued equilibrium configuration was "delayed" beyond its theoretical value.

CONCLUSIONS

The theory presented herein constitutes a third approximation to the problem of a beam subjected to a combination of bending and torsion. In the first approximation the strains are assumed to be linear functions of the displacements, whereas the equilibrium equations refer to the undistorted configuration. This leads to an entirely linear theory to which the principle of superposition applies. Such a theory, which is commonly used in ordinary design, is valid when the magnitude of the lateral stiffness of the beam is comparable to its major stiffness.

When this condition is violated there is a need for a second approximation. The presence of large lateral deflections and rotations makes it imperative that the equilibrium equations be referred to the distorted geometry. The resulting theory is linear with respect to the lateral loads and twisting couples. However, the effects of the vertical loads can no longer be added linearly.

The third approximation described herein abandons further the assumption of linear strain-displacement relationships. This arises as a natural result of

the large lateral displacements, and, consequently, the second approximation appears illogical. However, this is not quite the case. Actually, at least in so far as the lateral displacements and rotations are concerned, the results of the last two approximations are identical for beams that are statically determinate relative to moments in their major plane of stiffness. This may provide an explanation as to why this point has been ignored heretofore. It appears that, at least in the case of statically redundant structures, the introduction of nonlinear strain-displacement relationships leads to substantial modifications in their predicted behavior.

ACKNOWLEDGMENTS

The writer wishes to extend his appreciation to the Office of Ordnance Research, United States Department of the Army, under whose sponsorship this investigation was conducted.

APPENDIX I

It will be shown that, in general, the function $U(M; u, \beta) \equiv U(\lambda_r)$ —or, equivalently, $W(\lambda_r)$ —has an interior minimum that is approached asymptotically as the load parameter, λ , goes beyond bounds. In addition, the singular case, in which such an interior minimum may not exist, is explored further.

For this purpose the region of stability, which will be assumed to be bounded, is considered again. In the λ_r -space, this region, R , is enclosed by the boundary, B , on which the homogeneous Eqs. 1 and 2 admit a nontrivial solution (u_1, β_1) . On boundary B the equilibrium is therefore "neutral," with (u_1, β_1) representing the buckling mode. Moreover, in the general case the inhomogeneous Eqs. 1 and 2 admit no solution on boundary B , while U grows beyond bounds as the stress point, P (whose coordinates are the redundant parameters, λ_r), approaches B . If U can be shown to be convex, the existence of a unique interior minimum can be postulated.

To demonstrate the foregoing, it is assumed that λ_r and $\bar{\lambda}_r$ represent the coordinates of two arbitrary stress points. It is noted that the compatibility condition, Eq. 13, need not be satisfied for either point. For this general case the inequality Eq. 23a assumes the form,

$$U(\bar{\lambda}_r) \geq U(\lambda_r) - (\bar{\lambda}_\alpha - \lambda_\alpha) \int m_\alpha (u'' \beta - k \beta'^2) dz \dots \dots (67)$$

the proof of which proceeds along similar lines as does the proof of Eq. 23a.

If a plane is considered that is tangent to U at λ_r , its equation is given by

$$U_t(\lambda_r) = U(\lambda_r) + \frac{\partial U}{\partial \lambda_\alpha} (\lambda_\alpha - \lambda_\alpha) \dots \dots \dots (68)$$

The term $\partial U / \partial \lambda_r$, appearing in Eq. 68 is obtained from Eq. 14 by differentiation with respect to λ_r . If the same process is applied to Eqs. 1 and 2 and the results are utilized in the evaluation of the integral, then a series of integra-

tions by parts, together with the consideration of the boundary conditions, leads to

$$\frac{\partial U}{\partial \lambda_r} = - \int m_r (u'' \beta - k \beta'^2) dz \quad (r = 1, 2, \dots, n) \dots \dots (69)$$

When Eq. 69 is substituted in Eq. 68 and the result is compared with Eq. 67' it follows that

$$U(\bar{\lambda}_r) \geq U_t(\bar{\lambda}_r) \dots \dots \dots (70)$$

That is, the surface, U , does not cross any of its tangent planes. It is convex, and the existence of a unique interior minimum is proved, provided that all the other previous assumptions hold.

The exceptional (singular) case occurs when the inhomogeneous equations Eqs. 1 and 2 admit a finite solution. For simplicity, if Eqs. 1 and 2 are rewritten in the symbolic form,

$$L_u(M; u, \beta) = q \quad L_\beta(M; u, \beta) = t \quad (\text{in } R) \dots \dots \dots (71)$$

and if, in accordance with the previous consideration,

$$L_u(M_1; u_1, \beta_1) = L_\beta(M_1; u_1, \beta_1) = 0 \quad (\text{on } B) \dots \dots \dots (72)$$

then the system of equations,

$$\left. \begin{aligned} L_u(M_1; u, \beta) &= q \\ L_\beta(M_1; u, \beta) &= t \end{aligned} \right\} \quad (\text{on } B) \dots \dots \dots (73)$$

has a finite solution on that part, B' , of B on which the orthogonality condition,

$$\int (q u_1 + t \beta_1) dz = 0 \quad (\text{on } B') \dots \dots \dots (74)$$

holds. Moreover, because U is finite on B' the existence of an interior minimum can no longer be postulated.

For the purpose of studying singular behavior, if it is assumed that an interior minimum does not exist, this means, in turn, that U has an exterior minimum that lies on B' . In that case as the load factor, λ , increases, the stress point, P , reaches some point on B' from which it proceeds along B' toward the minimum. If B' is represented by a single point, as in the case of the present example, the stress point remains fixed after reaching B' and the structure exhibits the quasi-linear behavior examined previously.

After P has reached the boundary, B' , the most general solution of Eq. 73 subject to the conditions of Eq. 74 can be expressed as

$$(u, \beta) = (u_0, \beta_0) + c(u_1, \beta_1) \dots \dots \dots (75)$$

in which (u_0, β_0) represents some solution of Eq. 73, and (u_1, β_1) is governed, subject to an arbitrary multiplicative constant, by Eq. 72. It is convenient to identify these functions further by the orthonormality conditions,

$$\int (u_0 u_1 + b^2 \beta_0 \beta_1) dz = 0 \dots \dots \dots (76a)$$

and

$$\int [(u_1)^2 + b^2 (\beta_1)^2] dz = 1 \dots \dots \dots (76b)$$

in which b is an arbitrary number having the dimension of a length. Except for the sign of (u_1, β_1) , the conditions of Eqs. 76 determine all the functions uniquely for a given value of b .

If the point at which the stress path "first" reaches the boundary, B' , is designated by P' , and if P' is associated with a load parameter, λ' , and a parameter, $c = c'$ (Eq. 75), then the value of c' can be determined by the following limit process:

Even while the stress point, P , is still in the interior of the region of stability, the solution of Eq. 71 can be represented by Eq. 75, subject to the orthonormality conditions of Eqs. 76, if (u_1, β_1) satisfies

$$L_u (M; u_1, \beta_1) = \mu u_1 \dots \dots \dots (77a)$$

and

$$L_\beta = (M; u_1, \beta_1) = \mu b^2 \beta_1 \dots \dots \dots (77b)$$

in which μ is the eigenvalue of Eqs. 77. This eigenvalue satisfies the relationship,

$$\int [u_1 L_u (M; u_1, \beta_1) + \beta_1 L_\beta (M; u_1, \beta_1)] dz = \mu \dots \dots \dots (78)$$

which is obtained by multiplying both sides of Eqs. 77 by u_1 and β_1 , respectively, by integrating, and by considering Eq. 76b. Similarly, the following condition is obtained:

$$\begin{aligned} \int [u_0 L_u (M; u_1, \beta_1) + \beta_0 L_\beta (M; u_1, \beta_1)] dz \\ = \int [u_1 L_u (M; u_0, \beta_0) + \beta_1 L_\beta (M; u_0, \beta_0)] dz = 0 \dots (79) \end{aligned}$$

In Eq. 79 the second integral follows from the first through integrations by parts. Finally, from Eqs. 71, 75, 78, and 79, and the linearity of the differential operators, the parameter, c , is given by

$$c = \left(\frac{1}{\mu} \right) \int (q u_1 + t \beta_1) dz \dots \dots \dots (80)$$

As the point, P , approaches the boundary, B , the eigenvalue, μ , approaches zero, and the factor, c , increases generally beyond bounds. However, on B' the numerator in Eq. 80 also vanishes, as postulated in Eq. 74. Hence, the fraction becomes indeterminate, and the following relationship is established by the usual limit considerations:

$$c' = \lim_{\mu \rightarrow 0} c = \frac{1}{\mu} \int (q u_1 + t \beta_1) dz \dots \dots \dots (81)$$

In Eq. 81 and subsequently, a dot (as in $\dot{\mu}$) signifies differentiation along the path—that is, $\partial/\partial\lambda_s$.

The denominator in Eq. 81 is obtained from Eq. 78 by differentiation. This leads to

$$\begin{aligned}\dot{\mu} = & \int [\dot{u}_1 L_u (M; u_1, \beta_1) + \beta_1 L_\beta (M; u_1, \beta_1)] dz \\ & + \int [u_1 L_u (M; \dot{u}_1, \beta_1) + \beta_1 L_\beta (M; \dot{u}_1, \beta_1)] dz \\ & + \int \{u_1 (m_s \beta_1)'' + \beta_1 [m_s u_1'' + 2 (k m_s \beta_1)']\} dz \dots (82)\end{aligned}$$

The last integral on the right side of Eq. 82 follows from the definitions of L_u and L_β and from the fact that $\dot{M} = m_s$ by Eq. 6a.

The first integral in Eq. 82 vanishes, which can be demonstrated by substituting Eq. 77 and by differentiating Eq. 76b with respect to λ_s . The second integral vanishes similarly because it can be converted into the first integral, and hence zero, through four integrations by parts and in view of the boundary conditions. Two more integrations by parts finally convert the third integral into

$$\dot{\mu} = 2 \int m_s (u_1'' \beta_1 - k \beta_1'^2) dz \dots (83)$$

The establishment of the numerator in Eq. 81 proceeds along analogous lines. In fact, because (u_0, β_0) satisfies Eq. 71 at P' (for $M = M_1$), the following holds:

$$\begin{aligned}\int (q \dot{u}_1 + t \beta_1) dz &= \int [\dot{u}_1 L_u (M; u_0, \beta_0) + \beta_1 L_\beta (M; u_0, \beta_0)] dz \\ &= \int [u_0 L_u (M; \dot{u}_1, \beta_1) + \beta_0 L_\beta (M; \dot{u}_1, \beta_1)] dz \dots (84)\end{aligned}$$

The second equality in Eq. 84 is the result of several integrations by parts. However, if Eq. 77 is differentiated with respect to λ_s , and if μ is set equal to zero, then on B' ,

$$\dot{L}_u (M; u_1, \beta_1) = L_u (M; \dot{u}_1, \beta_1) + (m_s \beta_1)'' = \dot{\mu} u_1 \dots (85)$$

and

$$\dot{L}_\beta (M; u_1, \beta_1) = L_\beta (M; \dot{u}_1, \beta_1) + m_s u_1'' + 2 (k m_s \beta_1)' = \dot{\mu} b^2 \beta_1 \dots (86)$$

When Eqs. 85 and 86 are substituted into the last integral and Eq. 76a is considered, after several more integrations by parts the following is established:

$$\int (q \dot{u}_1 + t \beta_1) dz = - \int m_s (u_0'' \beta_1 + u_1'' \beta_0 - 2 k \beta_0' \beta_1') dz \dots (87)$$

Hence, by Eq. 81, c' is expressed as the quotient of the two integrals appearing on the right side of Eqs. 83 and 87. This quotient would seem to depend on the direction of the approach path, but this is not the case as will be shown.

In the linear space in which the stress point, P , is defined, the moment component, m_n , can, in general, be expressed in the form, $m_n = \gamma_n m_a$, in which the set of γ_n represents the direction cosines of the approach path relative to the coordinate axes. Similarly, the integrals on the right side of Eqs. 83 and 87 represent linear combinations involving these direction cosines.

Both denominator and numerator components vanish for all directions that are tangent to the boundary surface, B' . Because μ vanishes identically throughout B , then $\dot{\mu} = 0$ for all directions other than the direction normal to B . Similarly, the numerator is different from zero only in the normal direction, which can be verified by considering that the orthogonality condition of Eq. 74 is satisfied identically on B' . Hence, the direction of the approach path is immaterial, and the limiting coefficient, c' , can finally be expressed by

$$c' = - \frac{\int m_n (u_0'' \beta_1 + u_1'' \beta_0 - 2 k \beta_0' \beta_1') dz}{2 \int m_n (u_1'' \beta_1 - k \beta_1'^2) dz} \dots \dots \dots (88)$$

in which m_n represents the moment component normal to B' .

After the bounding surface of instability, B' , has been reached (for $\lambda = \lambda'$), the stress point, P , travels on B' as the load parameter, λ , is increased further. The response, $\lambda(u, \beta)$, continues to satisfy Eq. 75, and when this is substituted in the compatibility conditions of Eq. 13,

$$\lambda_n - \lambda_n^* = \lambda^2 \int m_n (u_0'' \beta_0 - k \beta_0'^2) dz + c \lambda^2 \int m_n (u_0'' \beta_1 + u_1'' \beta_0 - 2 k \beta_0' \beta_1') dz + c^2 \lambda^2 \int m_n (u_1'' \beta_1 - k \beta_1'^2) dz \dots \dots \dots (89)$$

and

$$\lambda_t - \lambda_t^* = \lambda^2 \int m_t (u_0'' \beta_0 - k \beta_0'^2) dz \dots \dots \dots (90)$$

The subscript n denotes the direction of the outer normal to B' , whereas the subscript t designates the totality of all directions that are tangent to B' and for which the condition of Eq. 74 is identically satisfied. In the set of equations expressed by Eq. 90, only one integral appears on the right side. Two more integrals, which are similar to the second and third integrals in Eq. 89, can be shown to vanish.

In general, the stress point, P , moves on B' so that the value of $U + U_b/\lambda^2$ is minimized further. With λ passing all bounds, a limiting point, P_t , is approached that corresponds to the smallest value of U on B' . This point is found by setting the integrals appearing on the right side of Eq. 90 equal to zero. A limiting value of c is obtained then by substituting in Eq. 89 the func-

tions (u_0, β_0) as determined previously. It should be noted that there are two solutions.

In special cases the stress point, P , may remain at P' . This occurs either when P' is the only point on B' , as in the present example, or when P' happens to be the point associated with the lowest value of U on B' . This latter case occurs when the vector, $\overline{P^* P'}$, is normal to the instability surface. In either case the final state of stress designated by P' is generally reached when the load parameter is finite ($\lambda = \lambda'$). For $\lambda > \lambda'$, the response functions, $\lambda(u_0, \beta_0)$, increase linearly with λ similarly to a statically determinate structure. However, two solutions for c are possible according to Eq. 89. That is, two distinct equilibrium configurations are possible so that one may be reached from the other only through a snap-through (Durchschlag) process. As before, a limiting value of c is approached as the parameter, λ , grows beyond bounds.

In the $(\lambda, c\lambda)$ -plane, Eq. 89 defines a hyperbola. This becomes apparent from the fact that the right side, if multiplied by two, can be converted into the form, $-\lambda^2 W + c\lambda^2 B + c^2 \lambda^2 \dot{\mu}$, in which the dot represents differentiation in the n -direction. It is clear that $\dot{\mu}$ is negative because μ is positive inside the region of stability and negative outside of it. Similarly, W is negative. If it were positive then W would exhibit an interior minimum, in which case P would not reach (or remain) on the boundary. Finally, if W were zero, P' would be reached only in the limit. The quadratic form has therefore a negative discriminant, and hence it designates a hyperbola.

APPENDIX II. NOTATION

The following symbols, adopted for use in the paper, conform essentially with "American Standard Letter Symbols for Structural Analysis" (ASA Z10.8-1949), prepared by a committee of the American Standards Association with Society representation, and approved by the Association in 1949:

- a = distance to vertical load from shear center;
- B = boundary of a region;
- b = any number;
- C = end-restraint constant;
- c = multiplier;
- E = modulus of elasticity;
- e = eccentricity;
- G = shear modulus;
- h = depth of beam;
- I = moment of inertia;
- K = torsion constant;
- k = cross-sectional constant (Eq. 3);
- L = beam length;
- M, m = bending moment;
- M^* = prestressing moment;
- n = degree of static indeterminacy;

- P = axial force;
 p = vertical load (per unit length);
 q = horizontal load (per unit length);
 R = region;
 S = section modulus;
 s = stress;
 t = torsional couple (per unit length);
 U = quadratic form defined in Eq. 14;
 u = lateral displacement;
 V = potential energy defined in Eq. 16;
 v = vertical displacement;
 W = work performed by horizontal load and torsional couple in Eq. 16;
 x, y = rectangular coordinates;
 y_0 = distance to shear center from centroid;
 z = distance along beam length;
 β = rotational displacement;
 T = warping constant;
 γ = degree of end restraint defined in Eq. 41;
 κ = displacement reduction factor as defined in Eqs. 52b, 54b, and 56b;
 λ = load parameter;
 μ = eigenvalue of Eq. 77;
 ρ = radius of gyration about the shear center;
 r = load ratio defined in Eq. 64;
 ϕ = dimensionless ratio defined in Eq. 44b; and
 ω = dimensionless ratio defined in Eq. 47.

AMERICAN SOCIETY OF CIVIL ENGINEERS

Founded November 5, 1852

TRANSACTIONS

Paper No. 2967

OCEAN-WAVE FORCES ON CIRCULAR CYLINDRICAL PILES

BY ROBERT L. WIEGEL,¹ KENNETH E. BEEBE,² J. M. ASCE,
AND JAMES MOON³

WITH DISCUSSION BY MESSRS. THOMAS E. STELSON; AND ROBERT L. WIEGEL,
KENNETH E. BEEBE, AND JAMES MOON

SYNOPSIS

The forces exerted by ocean waves on circular cylindrical piles were studied at an exposed location near Davenport (Calif.) in water that was from 45 ft to 50 ft deep. The studies were made by the University of California (Berkeley) under contract to an oil and gas company. Measurements were made of forces resulting from waves that were as high as 20 ft by means of a strain-gage-type force meter. The measured forces are presented in graphical form. The pile test sections were 6½ in., 12½ in., 2 ft, and 5 ft in diameter. Coefficients of drag and mass were computed from the measured data using linear-wave theory to predict the water-particle velocities and water-particle accelerations. The coefficient of drag was found to have no well-defined relationship to R , the Reynolds number, in the test range of Reynolds numbers of from 3×10^4 to 9×10^5 . The average value of the coefficient of mass was 2.5 with a normal Gaussian distribution about this average value. Within the limits of accuracy of the tests, and within the range of conditions, there appeared to be no relationship between the coefficient of mass and the flow conditions as represented by the Reynolds number, with water-particle acceleration, or with wave period. Large lateral vibrations of the 2-ft pile were noted under the action of high waves, probably due to the alternate breaking off of the large vortices, which were noticeable. The period of these vibrations was approximately 2.5 sec and the wave period was approximately 13 sec. As a result of the effect of the

NOTE.—Published, essentially as printed here, in April, 1937, in the Journal of the Hydraulics Division, as *Proceedings Paper 1199*. Positions and titles given are those in effect when the paper or discussion was approved for publication in *Transactions*.

¹ Associate Research Engr., Inst. of Eng. Research, Univ. of California, Berkeley, Calif.

² Graduate Research Engr., Inst. of Eng. Research, Univ. of California, Berkeley, Calif.

³ Cons. Engr., Signal Oil & Gas Co., Los Angeles, Calif.

vibration force, combined with the effect of the continual alternating forces due to the drag force and the inertia force, the 6-in. central supporting pile broke in the middle seat of the threads at a point 3 ft below the bottom collar. An examination of the break indicated that it was a fatigue failure.

INTRODUCTION

Since 1949 the Wave Research Laboratory at the University of California (Berkeley) has engaged in research on the problem of forces exerted by water gravity waves on piles. A theory has been developed to account for both drag forces and inertia forces.^{4,5} The applicability of the theory has been tested in the laboratory, and a few tests have been performed in the field.^{6,7,8,9} In order for the theory to be useful to engineers in the design of offshore structures, it was necessary to undertake a comprehensive field test for the purpose of determining the coefficient of drag and the coefficient of mass which appear in the equations. In addition, it was necessary to obtain data at a series of submergence depths of the test sections in order to determine the distribution of forces with respect to distance below the surface. The study described herein was conducted near Davenport (Calif.) at a location exposed to large waves. Measurements were made of forces exerted by waves as high as 20 ft, whose depth varied between approximately 45 ft and 50 ft. The wave forces were measured by strain gages mounted on restraining bars—the outer ends were attached to the test section, and the inner ends were attached to a supporting central pile. Measurements were made of forces exerted on a 12½-in. and a 2-ft diameter test-pile section. The equipment was modified, and measurements were made of forces exerted on a 6½-in. test section. The equipment was modified again, and a few measurements were made of forces exerted on a 5-ft section. However, the supporting unit failed before adequate data could be obtained.

THEORETICAL CONSIDERATIONS

Notation.—The letter symbols used in this paper are defined where they first appear, in the illustrations or in the text, and are arranged alphabetically, for convenience of reference, in the Appendix.

General.—In the design of a pile structure exposed to waves of a given height and a given period, some of the factors involved are the size, shape, and spacing of the piles, and the distribution of moments on the various members. Theo-

⁴ "The Force Exerted by Surface Waves on Piles," by J. R. Morison, M. P. O'Brien, J. W. Johnson, and S. A. Schaaf, *Technical Publication No. 2848, Petroleum Transactions, A.I.M.E.*, Vol. 189, 1950, pp. 149-154.

⁵ "The Design of Piling," by J. R. Morison, *Proceedings, 1st Conference on Coastal Eng., Council on Wave Research, The Eng. Foundation, Berkeley, Calif.*, 1951, pp. 254-258.

⁶ "Wave Force Experiments at Atchafalaya Bay, Louisiana," *Technical Report No. 38-1, Dept. of Oceanography, The Agri. and Mech. College of Texas, College Station, February, 1954.*

⁷ "Experimental Studies of Forces on Piles," by J. R. Morison, J. W. Johnson, and M. P. O'Brien, *Proceedings, 4th Conference on Coastal Eng., Council on Wave Research, The Eng. Foundation, Berkeley, Calif.*, 1954, pp. 340-370.

⁸ "The Forces Exerted by Waves on Objects," by M. P. O'Brien and J. R. Morison, *Transactions, Am. Geophysical Union, Vol. 33, No. 1, February, 1952, pp. 32-38.*

⁹ "Analysis of Wave Force Experiments at Caplen, Texas," by R. O. Reid, *Technical Report No. 38-4, Final Report, Dept. of Oceanography, The Agri. and Mech. College of Texas, College Station, report to the Bureau of Yards and Docks, U. S. Dept. of the Navy, N0y-27474, January, 1956.*

retical investigations and experimental investigations have shown that the force exerted on the sections consists of two parts, a drag force and an inertia force. Two methods have been developed to handle the problem. Although the particle motion in waves is orbital, the methods are based on rectilinear flow. The first method, described by Jack R. Morison, Morrrough P. O'Brien, M. ASCE, Joe W. Johnson, M. ASCE, and Samuel A. Schaaf,⁴ is based on the assumption that the drag force and the inertia force can be treated separately, and that the total force can be obtained by adding the solutions linearly. The writers believe that this assumption is open to question. However, until a greater insight can be obtained of the flow phenomenon, the method is a useful tool for the design engineer. The equation contains two coefficients that must be determined empirically.

In steady rectilinear flow, the drag force has a magnitude that depends on the Reynolds number. At a very low Reynolds number, the drag force consists predominantly of shearing forces above the surface of the pile. However, when the turbulence of the fluid and the geometry of the system are such that a turbulent boundary layer exists and separation occurs, the drag force is proportional to the fluid density, the projected area, and the square of the fluid particle velocity, and is usually represented by

$$F_D = C_D \rho A u^2 \dots \dots \dots (1)$$

In Eq. 1, F_D denotes the drag force on the pile, in pounds; C_D designates the coefficient of drag; ρ represents the mass density of sea water, in pound-seconds² per foot⁴; A designates the projected area perpendicular to the particle motion, in square feet; and u denotes the horizontal component of water-particle velocity, in feet per second.

The inertia force is proportional to the fluid density, the volume of the object, and the fluid-particle acceleration. The inertia force can be represented by

$$F_M = (M_o + M_s) \frac{\partial u}{\partial t} \dots \dots \dots (2a)$$

in which F_M represents the inertia force on the pile, in pounds; M_o is the mass of the fluid displaced by the pile, in pound-seconds² per foot; M_s denotes the added mass, in pound-seconds² per foot; and $\partial u / \partial t$ designates the horizontal component of water-particle load acceleration, in feet per square second. Eq. 2a may be written as

$$F_M = C_M \rho V \frac{\partial u}{\partial t} \dots \dots \dots (2b)$$

in which C_M represents the coefficient of mass, and V denotes the volume of submerged piles, in cubic feet.

The total horizontal force⁴ exerted on a vertical differential section, dS , along the pile is

$$dF = \left[\frac{1}{2} C_D \rho D |u| u + C_M \rho \left(\frac{\pi D^2}{4} \right) \frac{\partial u}{\partial t} \right] dS \dots \dots \dots (3)$$

In Eq. 3, dF represents the increment of force on the pile, in pounds; dS represents the increment of pile length, in feet; D denotes the pile diameter, in feet; and $|u|$ has been introduced in place of u^2 to maintain correct sign convention.

The equations¹⁰ for the undisturbed horizontal components of water-particle velocity and water-particle acceleration, as obtained from the linear theory of water gravity waves, are

$$u = \frac{\pi H}{T} \frac{\cosh(2\pi S/L)}{\sinh(2\pi d/L)} \cos \frac{2\pi t}{T} \dots \dots \dots (4)$$

and

$$\frac{\partial u}{\partial t} = \frac{2\pi^2 H}{T^2} \frac{\cosh(2\pi S/L)}{\sinh(2\pi d/L)} \sin \frac{2\pi t}{T} \dots \dots \dots (5)$$

In Eqs. 4 and 5, H represents the wave height, in feet; T denotes the wave period, in seconds; S designates the elevation of water particle above the ocean bottom, in feet; d represents the still-water depth, in feet; and L denotes the wave length, in feet.

Eqs. 4 and 5 are good first approximations only for low values of H/L and for values of d/L greater than approximately 0.2.^{10,11} There are more complex solutions that have a greater number of terms, but laboratory studies indicate that they do not predict the velocities or accelerations with a greater degree of accuracy than the use of Eqs. 4 and 5.¹⁰ It is believed that the engineer is served best by using the simpler formulas and thereafter using an adequate safety factor in his design. The hyperbolic functions used in these equations may be obtained from published tables.¹²

In the linear theory, the maximum drag forces and the maximum inertia forces are 90° out of phase, and the resultant maximum force on the pile leads the crest of the wave (or the trough, when the force is in the opposite direction). The relative importance of the inertia force increases with the ratio of pile diameter to wave height. The limiting effect occurs when the diameter is so great that the structure begins to act as a section of a sea wall. Theoretically, the equation is valid only for infinitesimal values of D/L . Details on obtaining the total force on a pile have been presented previously.⁴

The second method, described by Robert Curtis Crooke,¹³ is based on the study by Harold W. Iversen and R. Balent¹⁴ of the forces exerted on a body in accelerated motion through a fluid. This method assumed that there was a linear dependence of velocity on acceleration so that the force could be expressed as the product of one coefficient, the fluid density, the projected area of the body, and the square of the particle velocity.

¹⁰ "The Mechanics of Deep Water, Shallow Water and Breaking Waves," by J. R. Morison and R. C. Crooke, *Technical Memorandum No. 40*, Beach Erosion Board, Corps of Engrs., U. S. Dept. of the Army, Washington, D. C., March, 1953.

¹¹ "Prediction of Linear Effects from Instrument Records of Wave Motion," by R. A. Fuchs, *IER Series S, Issue 337*, Univ. of California, Berkeley, June, 1952 (unpublished).

¹² "Gravity Waves; Tables of Functions," by R. L. Wiegel, Council on Wave Research, The Eng. Foundation, Berkeley, Calif., February, 1954.

¹³ "Re-Analysis of Existing Wave Force Data on Model Piles," by R. Curtis Crooke, *Technical Memorandum No. 71*, Beach Erosion Board, Corps of Engrs., U. S. Dept. of the Army, Washington, D. C., April, 1955.

¹⁴ "A Correlating Modulus for Fluid Resistance in Accelerated Motion," by H. W. Iversen and R. Balent, *Journal of Applied Physics*, Vol. 22, March, 1951, pp. 324-328.

The equation for the wave force on a pile segment is

$$dF = \frac{1}{2} C \rho D |u| u dS \quad (6)$$

in which C is the coefficient of resistance and u is given by Eq. 4. In the work of Iversen and Balent,¹⁴ it was found that the total resistance coefficient, C , was related primarily to Iversen's modulus, which expresses the product of the acceleration and the body diameter divided by the square of the velocity. The total resistance coefficient, C , is related also to the Reynolds number.

For the case of wave action on piles, it is evident that, in addition to the factors that have been mentioned, the past history of the water particles plays an important part in the explanation of the action by either of the methods described previously.

EXPERIMENTAL EQUIPMENT

Preliminary field studies of wave forces on piles were made by measuring the force necessary to restrain a pile suspended by a hinge, using strain gages mounted on restraining bars as the transducer. This system permitted the measurement of the total movement about the hinge. However, it did not permit the direct determination of force distribution. Furthermore, the dynamics of the system was such that the entire pile vibrated with a period that was nearly that of the locally generated wind waves, and this action served to invalidate much of the data. Because of this, a force meter¹⁵ was developed to allow for the measurement of the force exerted by waves over a small section of pile, and to decrease the effect of vibrations.

Force Meters.—The system consisted of a 1-ft section of the particular diameter pile that was to be tested, mounted around a 6-in. (6½-in. O.D. pipe) central support pile. Mounting shoes were fastened on the inside of the test section, and restraining bar clamps were fastened on the outside of the central pile. The test section was connected to the central support pile by bolting the restraining bars to the mounting shoes and to ears on the restraining bar clamps, as shown in Fig. 1. One bar was mounted on each side of the pile. Thus, even though the central support pile was subject to forced vibrations, the force being measured was due to the relative motion between the test section and the central support pile. Hence, only a relatively small vibration would appear on the force record except during extreme conditions. The actual test section was designed so that its natural frequency was very high (the order of magnitude ranging from 15 cycles per sec to 50 cycles per sec, depending on the restraining bar) compared with the wave period. Complete design details have been described by Kenneth E. Beebe, J. M. ASCE, and Morison.¹⁵

The preceding condition applied provided that the amplitude of pile vibration was small enough that the forces induced by the movement of the test pile back and forth through the water were negligible. In practice, this was found to be the case for small submergence depths of the test section. For

¹⁵ "An Ocean Wave Force Meter," by K. E. Beebe and J. R. Morison, *Proceedings, 1st Conference on Coastal Eng. Instruments, Council on Wave Research, The Eng. Foundation, Berkeley, Calif., 1956*, pp. 173-183.

greater submergence depths it became necessary to guy the bottom of the central support pile to prevent excessive motion.

In order to have natural flow conditions surrounding the test section, a shroud of the same diameter as the test section was mounted above and below this section. The two shrouds were each 5 ft long, as shown in Fig. 2.

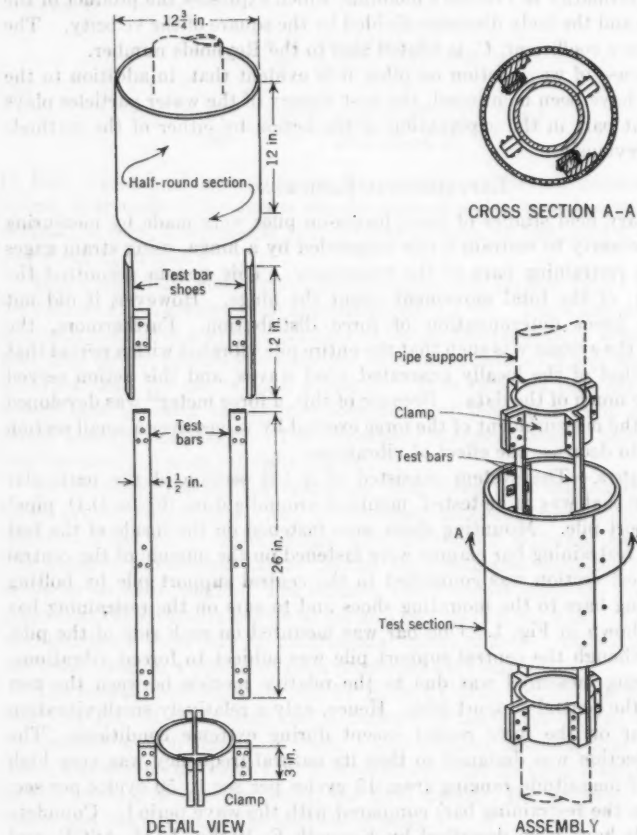


FIG. 1.—12 1/2-IN.-DIAMETER FORCE METER

The transducer consisted of two SR-4 paper-backed strain gages mounted on each of the two restraining bars between the center and the top of the bar. The strain gages were mounted to the points of maximum test-bar moment as closely as possible for maximum sensitivity. The strain gages were glued to the flat side of the restraining bar by a special glue and then waterproofed by means of synthetic tape, a primer, and neoprene. The waterproofing was

excellent, although considerable care had to be taken during the many steps to avoid the development of pinholes in the neoprene. Bars that were submerged at sea for several months remained in a satisfactory condition. Several sets of strain bars were manufactured, with different sensitivities, so that measurements could be made for a wide range of forces.

Waterproof cable was used to connect the strain gages to the bridge of an oscillograph. The connections were waterproofed with synthetic cement and tape.

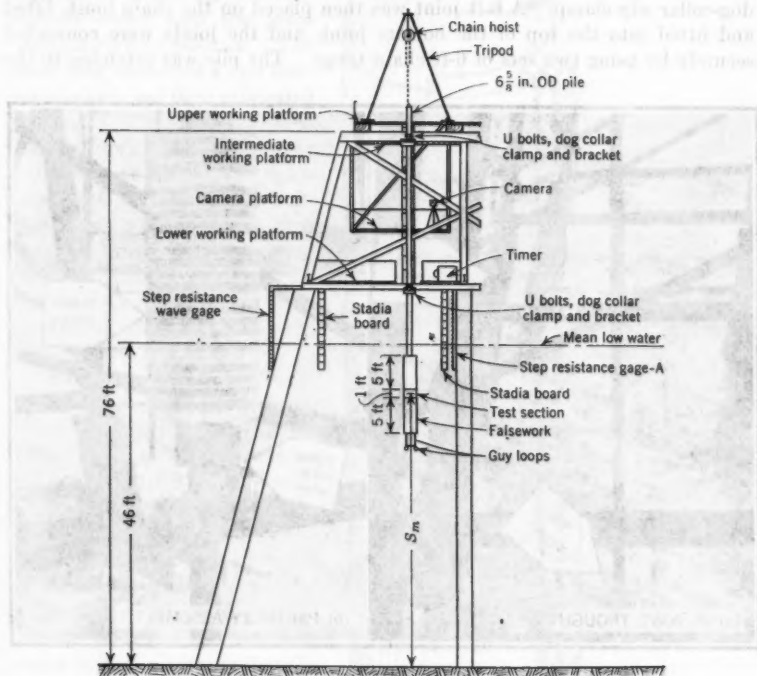


FIG. 2.—SCHEMATIC DIAGRAM OF TEST EQUIPMENT

Although the test-pile system was subject to large bending moments, computations showed that the error induced in the force-measuring system by pile deflection due to such moments did not exceed 0.4%, and that for approximately 95% of the data, the induced error did not exceed 0.1%. A comparison of the moments of inertia of the test bar with that of the drill casing indicated that the drill-casing second moment was approximately 10,000 times that of the test bars. Because the moment taken by each component of a system in bending was proportional to the moment of inertia of the component in question, it was realized that only a small error would be induced into the strain measured by the strain gages.

Pile Installation.—The sections of the pile were installed, using a 15-ft-high tripod derrick made of 2½-in. standard-pipe legs, which were approximately 6 ft apart at the base. The pipe legs were made rigid by the use of turnbuckles, which were mounted midway up the legs, with a 2-ton chain hoist suspended from the crown (Fig. 2).

For the case of the 12½-in.-diameter test pile and the 2-ft-diameter test pile, the bottom joint, which was 12 ft long, was installed and lowered until the top was just above the upper pile bracket, at which stage it was secured by a dog-collar slip clamp. A 6-ft joint was then placed on the chain hoist, lifted and fitted into the top of the bottom joint, and the joints were connected securely by using two sets of 6-ft chain tongs. The pile was extended to the

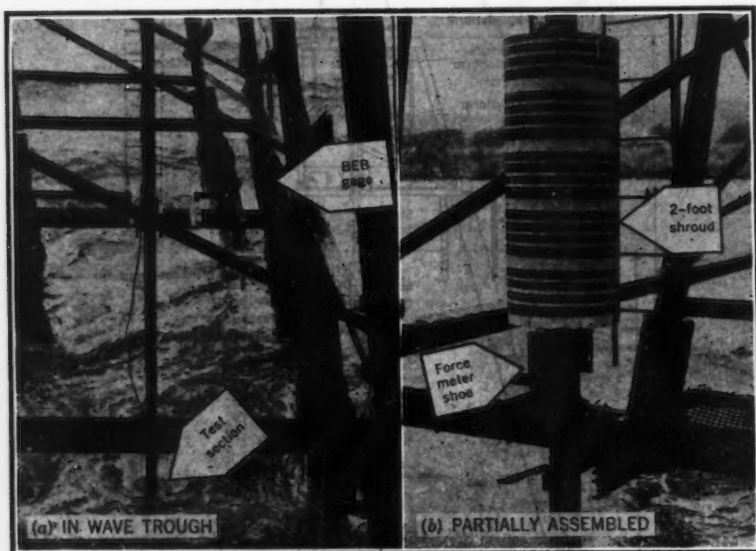


FIG. 3.—2-Ft TEST PILE

desired length by using a series of 6-ft joints. When the bottom joint had reached the lower work platform, the pile was secured by U-bolts at the lower pile bracket. The test section and the shrouds were mounted, and the test section (force meter) was calibrated. The test section and the shrouds were painted with anti-fouling paint, and the pile was lowered to the desired depth of submergence, oriented so that the restraining bars were facing the waves and the top and bottom were clamped in position (Fig. 3).

Minor modifications were made in installing the 6½-in.-diameter test pile and the 5-ft-diameter test pile.

Calibration of Force Meter.—The wave force meter was calibrated, using a device built around a 4-in. channel, which was approximately 4 ft long, and the

ends were fastened to the shrouds above and below the test section by metal straps and U-bolts. A hole was drilled in the center of the channel, and the channel was mounted so that this hole lay opposite the center of the test section. Through this hole a link was placed—one end was connected to a strap and a U-bolt around the test section (Fig. 4), and the other end was connected to one end of a proof ring. The other end of the proof ring was fastened by a small J-bolt to a support which held the proof ring in a vertical position. The proof ring contained a dial indicator, which had been calibrated prior to the field installation. The calibration of the force meter was performed by tightening the nut on the J-bolt, which pulled on the proof ring, which, in turn, pulled on the test section. The dial readings were noted on the record on the oscillograph, which recorded the strain-gage deformations.

Wave Recorders and Stadia

Boards.—Two Beach Erosion Board, Corps of Engineers, United States Department of the Army (BEB), step-resistance gages of the parallel type were used to measure the wave heights.¹⁶ They were mounted on each side of the test pile, at a distance of approximately 20 ft from the piles, and were oriented in such a manner that the line formed by the gages and the test pile faced directly into the prevailing swell (Figs. 3 and 5). The recorders were calibrated by

separately immersing in the water each of the four 5-ft sections, which made up the gages, and by noting the results of the recorder. It was found that the calibration was approximately linear. The outputs from the wave gages were recorded on potentiometer-type recorders. In addition, the seaward gage was wired in parallel to one channel of the oscillograph so that the waves were recorded on the same chart as were the force records. Thus, there was no problem

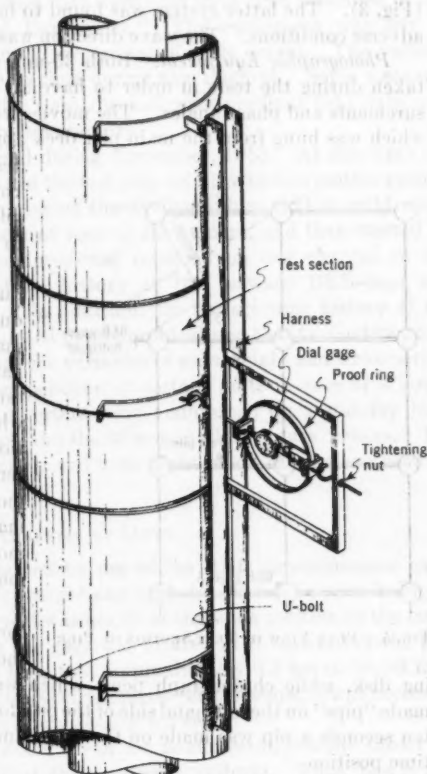


FIG. 4.—CALIBRATION OF FORCE METER

¹⁶ "The Step-Resistance Wave Gage," by Joseph M. Caldwell, *Proceedings, 1st Conference on Coastal Eng. Instruments*, Council on Wave Research, The Eng. Foundation, Berkeley, Calif., 1956, pp. 44-60.

of matching records from two charts. Constant voltage transformers were used with the wave recorders.

In addition to using the wave recorders, a record of the waves was obtained from the motion pictures taken during the tests by the installation of two stadia boards in the field of view of the camera (Fig. 2), or by painting the test pile in alternately light and dark bands and using it in place of stadia boards (Fig. 3). The latter system was found to be satisfactory even under the most adverse conditions. The wave direction was determined by direct observation.

Photographic Equipment.—Both 35-mm and 16-mm motion pictures were taken during the tests in order to have an independent source of wave measurements and phase angles. The movies were taken from a camera platform, which was hung from the main pier deck approximately 20 ft landward of the

test pile. The data on the film were correlated with the data on the oscillograph by locating a special timer in the field of view of the camera.

Timing Equipment.—A special duodecimal timing unit was used during the tests. The system was made visual by means of lights (the pattern showing the time to the nearest second) and a rotating black and white disk (which showed the fraction of the second to the nearest one-tenth second), and from which even more refined time estimates could be made. In addition, a camera-penmotor synchronization light remained on during each test run.

The timing unit gave a time history of the test. The flashing lights showed on the film, as did the rotat-

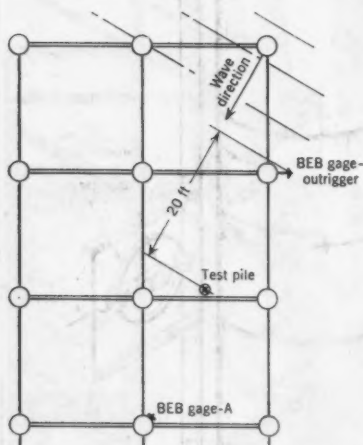


FIG. 5.—PLAN VIEW OF TEST SECTION OF PIER

ing disk, while chronograph pens, which were synchronized with the lights, made "pips" on the left-hand side of the oscillograph chart every second. Every ten seconds a pip was made on the righthand side for ease in determining the time position.

The timer lights had relays which would arc when actuated. The arcing was broadcast and the signals were picked up by the oscillograph, making pips every second on the strain-gage side (right-hand side) of the penmotor. Initially, these interfered with the wave force trace, but the trouble was eliminated by installing an isolation transformer between the timer and the oscillograph.

Power.—Because all the equipment was installed at the sea end of the pier (approximately 2,200 ft from the shore), the problem of getting adequate power to the end of the pier was critical. It was found after the first tests that the voltage dropped to as low as 90 volts, and the oscillograph would not work properly at this low voltage. Consequently, 440-volt transformers were

installed at the shore end and at the sea end to decrease the power loss. No trouble was encountered thereafter.

EXPERIMENTAL PROCEDURE

After the pile had been installed at the desired depth of submergence, the equipment was checked by a complete test run. The several imperfections that were detected and the remedies that were used have been described in the section entitled, "Experimental Equipment." The equipment was left in proper operating condition pending the arrival of large waves. The various units were calibrated from time to time during this interval. Some measurements were made and the results were checked with previous field data and model data and were found to be satisfactory.

The first major storm occurred during November, 1953. At this time the field crew checked the orientation of the test pile, set up a 35-mm motion picture camera on the camera platform, started the oscillograph so that it could warm up, installed the timer in the field of view of the camera, and then started all the recording equipment. The force was recorded on one channel of the oscillograph, and the surface-time history at the seaward BEB-gage was recorded on the other channel. In addition, the surface-time history of the water surface at the pile was recorded photographically so that two independent sources were available to measure the variables of wave height and wave period.

In order to prevent the nonoperation of certain units in case of a power overload, truck batteries and inverters were maintained on a standby basis to be used to run the oscillograph and the 35-mm motion picture camera. The system was found to be satisfactory and with slight modifications was used for the remainder of the tests.

ANALYSIS OF DATA

Wave Data.—The data obtained by use of the BEB step-resistance gages were analyzed wave by wave for height and period. As can be seen in Fig. 6, for the 1-ft test pile, the wave crest was nearly at the same position as the maximum force. This was because the gage was located 21 ft seaward of the pile, and the waves present at that time took approximately 0.5 sec to travel from the gage to the pile. Hence, for measuring phase relationships, it was necessary to shift the wave record by the equivalent of 0.5 sec.

The gravity water waves of the ocean are nonuniform, yet the theory for wave forces on piles assumes that the waves are uniform. Thus, one is presented with the problem of how to apply the theory for uniform waves to the case of nonuniform waves. It is possible, provided that the linear theory is valid, to utilize a Fourier integral and the appropriate kernel, in a manner similar to that used by Robert A. Fuchs,¹¹ to predict certain linear effects from instrument records of wave motion, or to make a Fourier analysis of the wave system and utilize the individual components. These methods are tedious to apply, and, unless their use leads to remarkable improvements from a design standpoint as compared with the more simple method, they probably will not find general application.

The simple method that was used for the data presented herein was to assume each wave to be approximated by a train of waves of the same amplitude and period as the measured wave. Because only the more distinct series of waves were used, this method is reliable. The period was measured directly on the chart and was considered to be one-half the time interval for two successive waves to pass the gage. The period of wave 6 was considered to be one-half the time interval necessary for the crest of waves 5 and 7 to pass ($\frac{1}{2} \times 28.2 = 14.1$ sec), as shown in Fig. 6(a). The vertical distance between the crest and the preceding trough was used as the wave height. The values read from the oscillograph were transformed from chart divisions to feet by the proper calibration graph. For wave 6 (Fig. 6(a)) the wave height was found to be 13.5 ft.

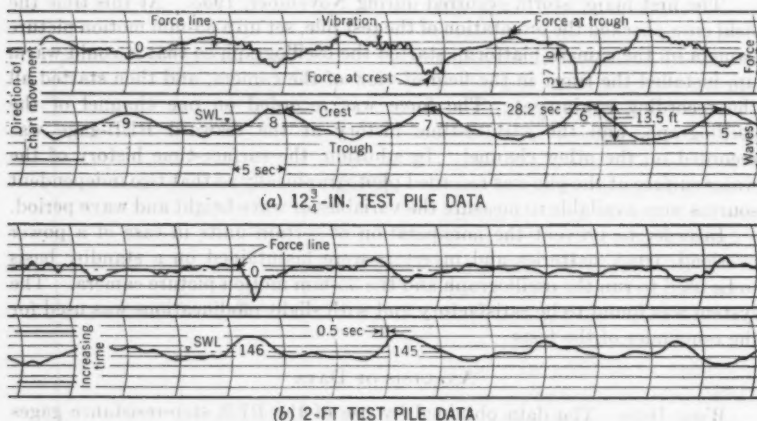


FIG. 6.—TYPICAL STRAIN-ANALYZER RECORDING

Force Data.—A sample of the forces exerted on the force meter, as recorded on the oscillograph, is shown in Fig. 6(a). The maximum force was considered to be represented by the vertical displacement of the crest or trough on the force record from the line of zero force. The reading of the chart was transformed into pounds of force by use of the appropriate calibration curve. For example, the maximum force in the direction of wave advance was 37 lb for wave 6.

It is readily apparent that the force was not symmetrical about the line of zero force because the data were obtained in relatively shallow water. The waves were not symmetrical, and the horizontal components of velocity and acceleration in the direction of movement of the wave crest were greater than the components in the opposite direction. As a result, the maximum horizontal component of force acting in the direction of wave motion was greater than the maximum horizontal component of force acting in the opposite direction. Vibration-type force traces (Fig. 6(a)) were noticeable when a series of

nearly periodic uniform waves passed the test pile. During the parts of the records for which the waves were irregular, the vibration-type traces were practically nonexistent.

Coefficients of Drag and Mass.—For the case of a force exerted on a section of pile, the vertical dimension of which is small compared with water depth and wave length, it can be shown that the force equation can be approximated rather accurately by

$$F = \frac{dF}{dS} \Delta S \quad (7a)$$

or

$$F = \frac{dF}{dS} = \frac{F}{\Delta S} \quad (7b)$$

In Eqs. 7,

$$\frac{dF}{dS} = \frac{1}{2} C_D \rho D |u_m| u_m + \frac{\pi}{4} C_M \rho D^2 \left(\frac{\partial u}{\partial t} \right)_m \quad (8)$$

$$u_m = \frac{\pi H}{T} \frac{\cosh(2\pi S_m/L)}{\sinh(2\pi d/L)} \cos \frac{2\pi t}{T} \quad (9)$$

and

$$\left(\frac{\partial u}{\partial t} \right)_m = \frac{2\pi^2 H}{T^2} \frac{\cosh(2\pi S_m/L)}{\sinh(2\pi d/L)} \sin \frac{2\pi t}{T} \quad (10)$$

in which the subscript m refers to conditions at the center of the pile test section.

The values of ΔS , d , and S_m were known for each test, and the values of F , H , and T were measured on the oscillograph. Thus, it was possible to solve for (a) C_D when $\cos 2\pi t/T = \pm 1$ (when the crest or trough of the wave passed the pile); (b) C_M by measuring the force record when $\sin 2\pi t/T = \pm 1$ (when the crest or trough of the wave passed the pile); and (c) C_M by measuring the force record when $\sin 2\pi t/T = \pm 1$ (when the wave passed through the still-water level for linear-wave theory).

In addition, the Reynolds number was computed, using the pile diameter and the maximum horizontal particle velocity at the test section.

Resistance Coefficient.—The resistance coefficient in Eq. 6 was determined for values of the Iversen modulus,

$$\frac{\partial u / \partial t}{|u| u} D \quad (11)$$

for various values of $2\pi t/T$. Because of time limitations on the contract this method was used for only a few waves.

RESULTS

Force on Pile Sections.—Samples of the basic data obtained during the tests are illustrated in Fig. 7. The figure shows the maximum force exerted on the 2-ft test section when $S = 33$ ft and $T_{avg} = 13$ sec, and similar data were ob-

tained for the 1-ft test section. The scatter of data is not excessive when one considers the variation of periods, the large difference in wave shape from the theoretical, the varying degree of turbulence in the flow (especially the eddies), and the roughness of the piles.

Distribution of Force with Distance Below Still-Water Level.—In Fig. 8 data are presented illustrating the distribution of force with distance below the still-water surface. These data were obtained using the 2-ft test section, locating it at different submergence depths, and measuring waves for a long period of time at each submergence. The water depth was 51 ft for all cases, and the average wave period was approximately 13 sec. The data were plotted as wave height versus force for each submergence, and then the average values for heights of 4 ft, 5 ft, 6 ft, 7 ft, 8 ft, and 9 ft were picked from the graphs and plotted.

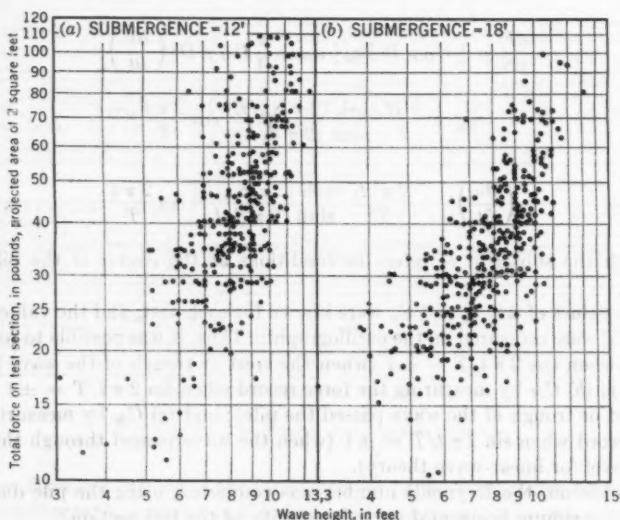


FIG. 7.—WAVE FORCE AS A FUNCTION OF WAVE HEIGHT

Impact Forces.—From a design standpoint, one of the most interesting features of the curves, as shown in Fig. 8, is the data which were taken at a point 2 ft below the still-water level. Because all the waves were 4 ft or higher, the test section was almost always exposed in the wave trough. Therefore, as the crests of the waves approached, the test section was resubmerged but without noticeable impact.

Although impact is of considerable importance, the lack of it is not surprising when one considers the studies of R. A. Bagnold¹⁷ and D. F. Denny.¹⁸

¹⁷ "Interim Report on Wave-Pressure Research," by R. A. Bagnold, *Journal, Inst. C. E.*, London, Vol. 7, June, 1939, pp. 202-226.

¹⁸ "Further Experiments on Wave Pressures," by D. F. Denny, *ibid.*, Vol. 4, February, 1951, pp. 330-345.

They found that, even in the laboratory, conditions had to be controlled very carefully to obtain impact because it was necessary for the waves to curl over in such a manner as to trap a certain-shaped volume of air between the wave front and the face of the structure. They found that impact did not occur if there were even slight variations in conditions. Thus, it is necessary for a wave to be in the process of curling over in breaking in order to have impact on a cylindrical pile. This is a rare phenomenon except in the breaker zone.

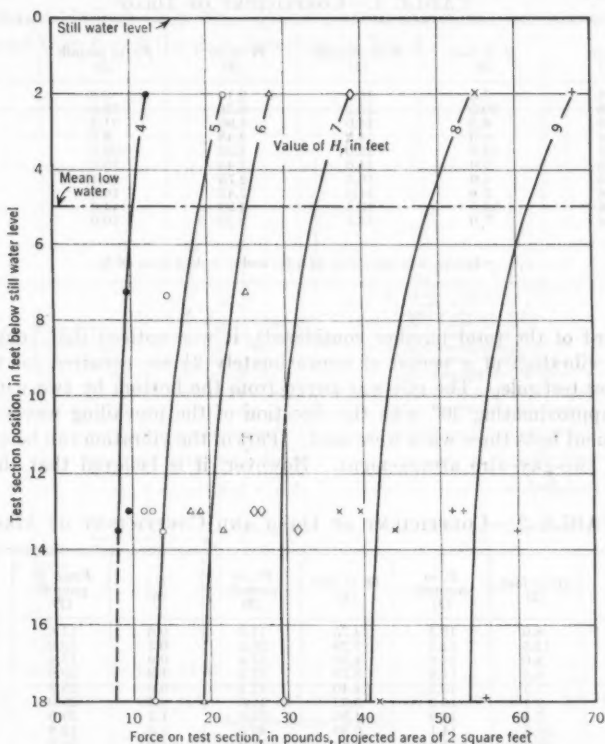


FIG. 8.—DISTRIBUTION OF FORCE WITH RESPECT TO DEPTH

In deeper water the breaking encountered is usually that of the wind blowing the top off a wave and causing a "whitecap."

Both Bagnold and Denny commented that the occurrence of impact force was accompanied by a rather loud sharp noise. This was noticed at Davenport during the presence of large waves. The cross bracings of the pier consisted of H-beams and L-beams, with the lowest horizontal members being H-beams with a horizontal web. When the large waves traveled the length of the pier, a booming noise was heard as the crest passed each horizontal

member. It is believed that as the crest passed and completely submerged the lowest bracings, the vertical component of water motion trapped air in the bottom half of the H-beams, and the dimensions and dynamics caused impact to occur.

Lateral Vibration of Test Section.—When subjected to large waves, approximately 12 ft high and having a 13-sec period (obtained by averaging the highest

TABLE 1.—COEFFICIENT OF DRAG^a

Wave (1)	H, in feet (2)	T, in seconds (3)	$R \times 10^{-5}$ (4)	F_c , in pounds (5)	C_D (6)
228	7.0	16.5	2.14	6.8	0.8
238	20.5	15.2	6.30	58.0	0.8
248	6.3	14.0	1.96	21.2	3.0
258	8.0	14.8	2.48	8.6	0.7
268	13.6	15.0	4.22	36.0	1.1
278	7.9	14.6	2.44	10.0	0.9
288	9.0	16.3	2.75	13.4	1.0
298	7.8	14.0	2.42	16.0	1.5
308	13.0	13.5	4.09	44.0	1.4
318	7.0	14.7	2.23	10.0	1.1

^a 12½-in. test pile; $S = 42.5$ ft; and $d = 49.3$ ft to 46 ft.

one-third of the total number considered), it was noticed that considerable lateral vibration of a period of approximately $2\frac{1}{2}$ sec occurred for the 2-ft-diameter test pile. The pile was guyed from the bottom by two wires at an angle approximating 30° with the direction of the prevailing waves. In all subsequent tests three wires were used. Part of the vibration can be explained by the two-guy-wire arrangement. However, it is believed that the major

TABLE 2.—COEFFICIENT OF DRAG AND COEFFICIENT OF MASS^a

Wave (1)	H, in feet (2)	T, in seconds (3)	$R \times 10^{-5}$ (4)	F_c , in pounds (5)	C_D (6)	F_{SWL} , in pounds (7)	C_M (8)
47	8.0	13.2	4.75	11.6	0.6	11.6	1.2
57	12.5	14.3	7.29	23.2	0.5	52.2	3.7
67	8.0	11.0	4.52	17.4	0.9	17.4	1.5
77	6.6	11.9	3.79	17.4	1.2	29.0	3.3
87	7.5	13.5	4.40	17.4	0.9	23.2	2.5
97	9.1	15.2	5.32	11.6	0.4	29.0	3.0
107	7.5	14.2	4.36	23.6	1.2	29.0	3.4
117	10.8	14.1	6.30	40.6	1.0	12.8	1.0
127	10.0	15.3	5.89	31.9	1.0	36.0	3.4

^a 24-in. test pile; $S = 33$ ft; and $d = 48$ ft to 46 ft.

contribution came from the periodic peeling off of noticeably large vortices. This problem is of considerable importance in regard to large stacks, cables, and bridges.

After nearly a week of continual storm conditions, the 2-ft pile broke in the middle seat of a joint approximately 3 ft below the lower clamp. An examination of the break indicated a fatigue failure.

Coefficient of Drag.—Examples are given in Tables 1 and 2 of the measured force as the wave crests passed the test piles, together with wave heights, wave periods, computed coefficients of drag, and Reynolds number. In Fig. 9 the values of C_D are plotted with respect to the Reynolds number. The data from experiments conducted⁹ are also plotted in Fig. 9 for comparison.

Because the engineer is interested in the effect of the larger waves, a graph of C_D versus R was prepared, using the data obtained from waves that were greater than 10 ft high (Fig. 10). It can be seen that these data show no different trend than for all the data presented in Fig. 9.

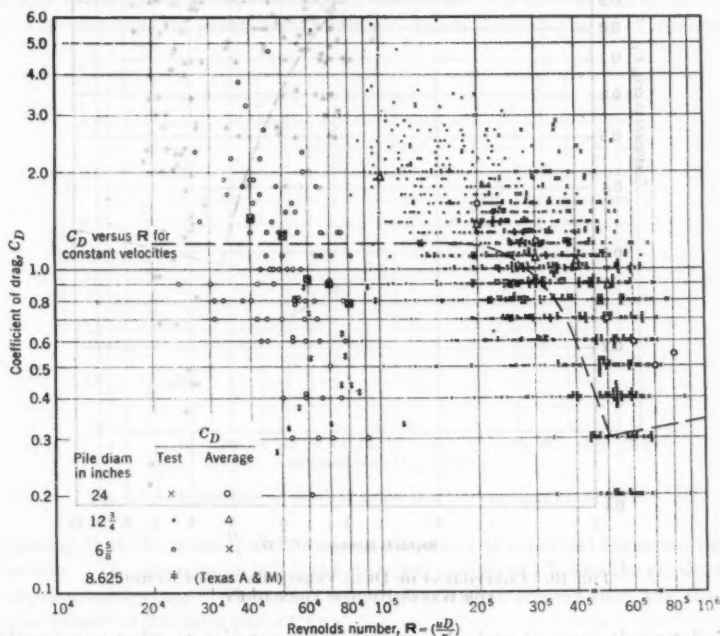


FIG. 9.—COEFFICIENT OF DRAG VERSUS REYNOLDS NUMBER

There is considerable scatter in the data shown in Figs. 9 and 10, but this is to be expected considering the variation in degree of turbulence that exists in the vicinity of a pier, the variation of the waves from those described by theory, and the fact that locally generated wind waves often existed in addition to the large storm waves. When considering the scatter, one should keep in mind the difficulty encountered in correlating aerodynamic data from several

⁹ "The Design of Low-Turbulence Wind Tunnels," by H. L. Dryden and I. H. Abbott, *Technical Note No. 1765*, National Advisory Committee for Aeronautics, Washington, D. C., November, 1948.

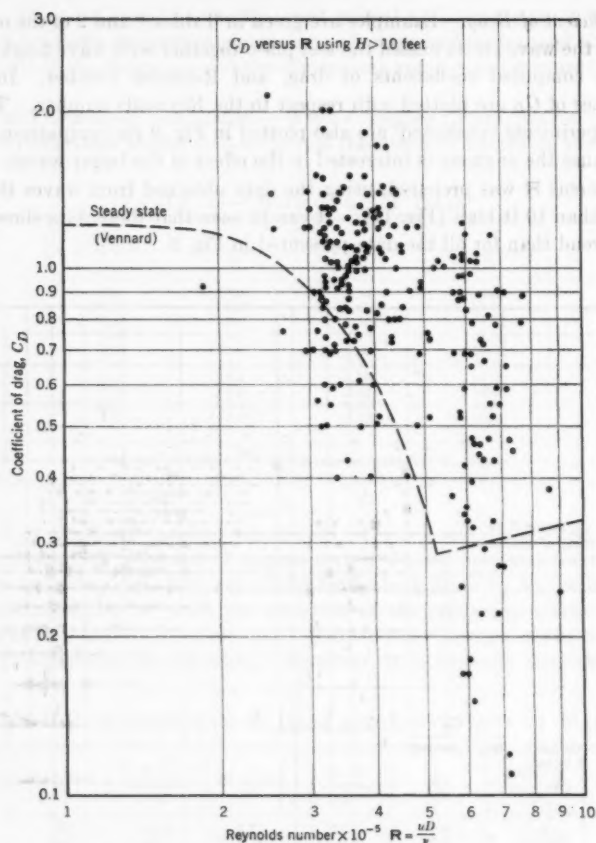


FIG. 10.—COEFFICIENT OF DRAG VERSUS REYNOLDS NUMBER FOR WAVES HIGHER THAN 10 FT

wind tunnels, even though the control is far superior to what can possibly be obtained in nature. H. L. Dryden and I. H. Abbott state¹⁹:

"The use of wind-tunnel data for predicting the flight performance of aircraft has always been hampered by the presence of turbulence in the air stream. Comparison of results obtained on spheres in the wind tunnels of Prandtl and Eiffel in 1912 showed that turbulence could have gross effects on aerodynamic measurements comparable with the effects of Reynolds number. Such results led to the establishment of international programs of tests of standard airfoil and airship models and to numerous comparative tests of spheres in wind tunnels of different turbulence. It is now known that the drag of a sphere may vary by a factor as large as 4, the minimum drag of an airship airfoil model by a factor of at least 2, and the maximum lift of an airfoil by a factor of as much as 1.3 in air streams of different wind tunnels at the same Reynolds and Mach numbers."

A word of caution should be made in regard to the trend of the coefficient of drag versus the Reynolds number. A. Fage and J. H. Warsap²⁰ have shown that the effect in surface roughness is to cause the coefficient of drag to remain much higher at Reynolds numbers in the critical and supercritical region ($R > 2 \times 10^5$). N. K. Delany and N. E. Sorensen²¹ found in wind-tunnel tests on circular cylinders that the coefficient of drag increased with the increasing Reynolds number for $R > 4 \times 10^5$.

Coefficient of Mass.—Examples are given in Table 2 of the measured force as the still-water level (leading the crest) of the waves passed the test pile, together with wave heights, wave periods, and computed coefficients of mass.

In Fig. 11, values of C_M have been plotted on statistical graph paper as a function of the cumulative percentage of values less than the value in question. It can be seen that the points form a straight line in the major range of interest,

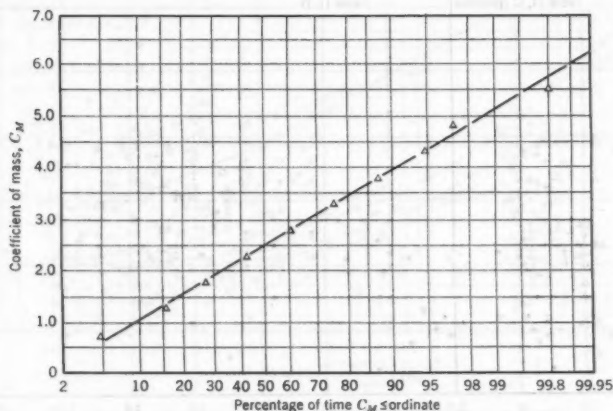


FIG. 11.—DISTRIBUTION OF VALUES OF THE COEFFICIENT OF MASS

indicating that the scatter of data about the mean is a normal Gaussian distribution. The mean value is 2.5, the standard deviation 1.2, and the skewness is approximately zero. The mean value is somewhat greater than the theoretical value²² of 2.0 for a perfect fluid.

The coefficient of mass was plotted as a function of the Reynolds number, which was computed using the maximum horizontal component of velocity for the particular wave for which the value of C_M was obtained. It was considered that the coefficient of mass should exhibit some relationship with the flow conditions, as represented by Reynolds number. However, this was not the case, at least within the limits of experimental error and the range of experimental conditions. In addition, for the same waves, values of the co-

²⁰ "The Effects of Turbulence and Surface Roughness on the Drag of a Circular Cylinder," by A. Fage and J. H. Warsap, *R & M No. 1283*, Aeronautical Research Committee, England, October, 1929.

²¹ "Low Speed Drag of Cylinders of Various Shapes," by N. K. Delany and N. E. Sorensen, *Technical Note 3038*, National Advisory Committee for Aeronautics, Washington, D. C. November, 1953.

²² "Hydrodynamics," by Sir Horace Lamb, Dover Publications, New York, N. Y., 6th Ed., 1945, p. 93.

efficient of mass were plotted as a function of the values of the coefficient of drag—again no apparent relationship was noticed.

After the original analyses had been made, it was suggested that a relationship might exist between C_M and $\partial u/\partial t$. Fig. 12(a)²³ disproves this relationship, at least within the range of experimental conditions. The same data that showed a relationship between C_M and $\partial u/\partial t$ also showed a definite relationship between C_M and the wave period. As can be seen in Fig. 12(b), this did not apply to the Davenport data. However, the two sets of C_M -values were determined in a different manner, and it is not surprising that the same relationships were not found.

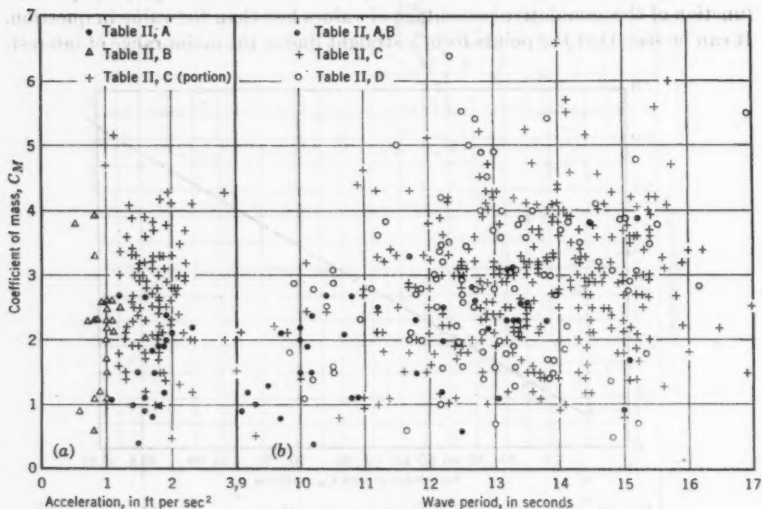


FIG. 12.—COEFFICIENT OF MASS VERSUS (a) HORIZONTAL COMPONENT OF WATER-PARTICLE ACCELERATION AND (b) WAVE PERIOD

Resistance Coefficient.—A few wave records and force records were analyzed in a manner similar to that used by Crooke,¹² and the results have been plotted in Fig. 13. The average curve of Crooke's data is shown also. Crooke's curve forms an upper limit to the few Davenport data. In addition, the curves obtained by Seward R. Keim,²⁴ J. M. ASCE, for vertically accelerated cylinders are given for comparison purposes.

General.—As was mentioned briefly, the Morison, O'Brien, Johnson, and Schaaf theory⁴ for forces exerted by water gravity waves on piles involves several rather severe assumptions. They are: (1) The linear theory for waves correctly predicts wave behavior; (2) the equation for fluid drag and inertia

²³ "Ocean Wave Forces on Piles," by R. L. Wiegel, K. E. Beebe, and R. W. Barrey, *Technical Report Series 35, Issue 9*, Inst. of Eng. Research, Univ. of California, Berkeley, September, 1954.

²⁴ "Fluid Resistance to Cylinders in Accelerated Motion," by Seward Russell Keim, *Proceedings Paper 1113*, ASCE, December, 1956.

forces on a pile in rectilinear flow are valid for oscillatory flow; and (3) the equations for drag forces and inertia forces may be added linearly to obtain the total force.

The work of Morison and Crooke¹⁰ shows that the linear theory predicts the characteristics of wave shape, particle paths, particle velocities, and particle accelerations for uniform waves in the laboratory fairly accurately in water that is deeper than $d/L = 0.2$. An examination of the data of Morison and Crooke indicates that the linear-theory equation for particle velocity is no less reliable than the more complex equations of George Stokes. These equations show that the horizontal component of particle velocity is greater under the crest than under the trough. However, the simple equation predicts the horizontal component of particle velocity under the crest more reliably on

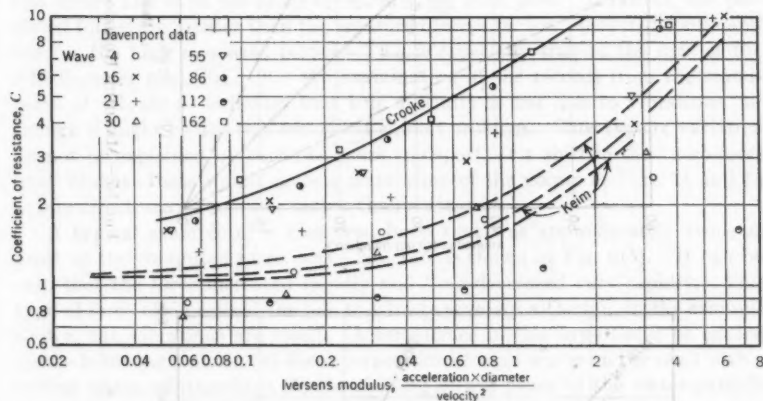


FIG. 13.—COMPARISON OF RESISTANCE COEFFICIENTS FOR RIGHT CIRCULAR CYLINDERS

the whole than do the more complex equations. In addition, if the surface-time history of the wave is known, the theory can be used in the manner presented herein (Eq. 4) to predict a greater velocity at the crest than at the trough. It is the force exerted by the wave in the direction of wave travel that is of more interest to the engineer because it is greater than the force exerted on the pile when the pile is in the wave trough. The data in Fig. 6 show a higher force leading the crest than leading the trough of the waves. In addition, the more complex equations of Stokes are not valid for shallow water because the series which they approximate "blows up."

The main disadvantage of the linear-wave theory is in regard to the prediction of the water-particle acceleration. In addition to the change in magnitude the phase angle at which the maximum acceleration occurs shifts toward the crest. The data collected by John G. Elliott²⁵ indicate that the actual shift

²⁵ "Interim Report," by John G. Elliott, Hydrodynamics Lab., California Inst. of Technology, Pasadena, N.Oy-12561, July, 1953 (unpublished).

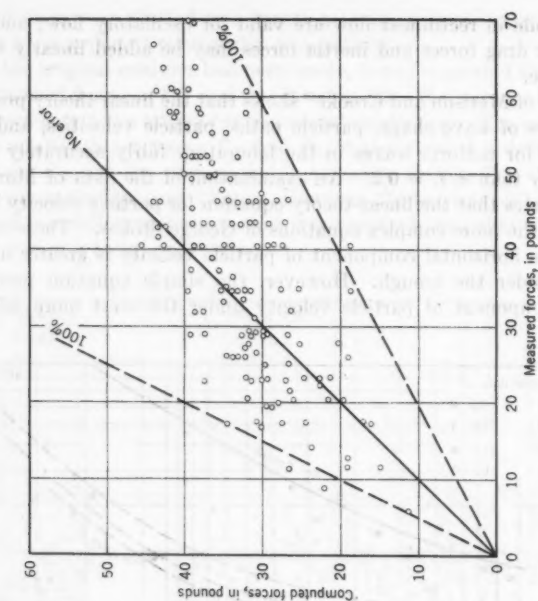


FIG. 15.—MAXIMUM HORIZONTAL FORCES ON A 2-FT-DIAMETER PILE

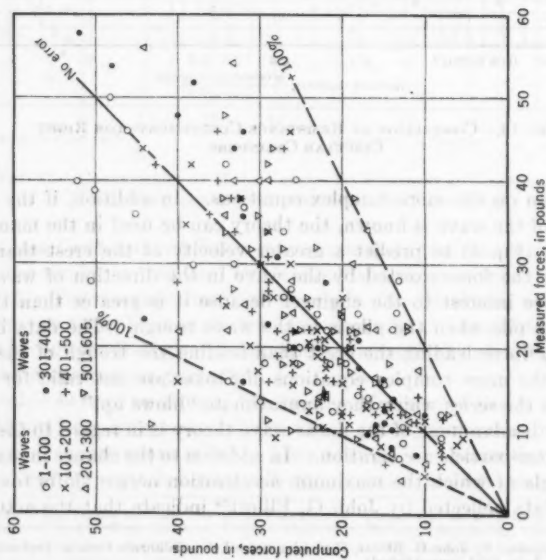


FIG. 14.—MAXIMUM HORIZONTAL FORCES ON A 12 1/4-IN.-DIAMETER PILE

is greater than the theory predicts. This would not introduce much error in the determination of the coefficient of mass because the actual still-water level was used as the reference in obtaining the data. However, this shift would introduce an error in predicting the maximum total force that would occur in cases for which the inertia force is a significant part of the maximum total force, and it apparently would result in an underprediction of the maximum total force.

In order to check partly the validity of some of the assumptions made in the wave-force theory and the analysis of the data, the average values of C_D versus Reynolds number and the average value of $C_M = 2.5$ were used to predict the maximum wave force on the 12½-in.-diameter pile and the 2-ft-diameter pile. These values were compared with the maximum measured forces (Figs. 14 and 15). The scatter of the predictions with respect to the "no error" line is on the order of $\pm 100\%$ for both piles. However, the predicted forces are greater than the measured forces for low measured forces and less for the high measured forces. This is especially true in the case of the 2-ft-diameter pile (Fig. 15). An examination of the records from the standpoint of vibrations indicates that this difficulty is not due to vibrations, although it might be due to a somewhat similar problem. This type of variation cannot be explained by currents, mass transport, or a shift in the "zero-force line" because these would cause a translation of the points in Figs. 14 and 15 in one direction or the other rather than a rotation.

A typical example of a measured force that was approximately twice as great as the computed force, wave No. 146, is shown in Fig. 6(b). It can be seen that the force increased rapidly and then decreased very rapidly. This type of force often caused the pile to vibrate severely although, in the example shown, the vibrations are small. A force trace of this type could be caused by the following factors: (a) the superposition of wind waves on the swell with a critical phase relationship; (b) the shifting of the phase of the water-particle accelerations with respect to wave period; (c) a transient phenomenon due to the higher harmonics which are apparent in the wave records; (d) an eddy hitting the pile in such a manner that the eddy and stream velocities were additive; and (e) a combination of any or all of the previously mentioned phenomena.

The writers believe that the modified linear theory for predicting wave forces, as presented herein, is only an approximation, and serious questions arise in regard to the results. A comparison of predicted maximum wave forces and measured maximum wave forces (including some too great to be included in Figs. 14 and 15) indicates that within the range tested a safety factor of from 2 to 2.5 should be used if average values of C_D and C_M are used in the computations. However, it is believed desirable to use values greater than the average for C_D and C_M and to adjust the safety factor accordingly.

Although considerable scatter was observed in the comparison of predicted maximum forces and measured maximum forces, and a trend for underprediction was observed for the greater measured forces, the results are rather re-

markable if the differences between the actual conditions and the conditions expressed in the equations are considered.

CONCLUSIONS

1. The force meter and test-pile setup performed as expected and were satisfactory. Vibration pickup on the force records were considerably less than in the case of the hinged pile. When the motion of the pile through the water became so great as to create a secondary force, the bottom of the test pile was guyed and the problem of motion was largely overcome.

2. The distribution of force with distance below the still-water surface was approximately as predicted by the simple theory. As was expected from a study of the work of Morison and Crooke, the difference between predicted and measured values was greatest in the range between the trough and the crest of the wave.

3. Tests performed in a manner whereby the test section was exposed in the trough and then submerged by the crest gave no evidence of impact force.

4. The coefficients of drag, determined for the range of Reynolds numbers between 3×10^4 and 9×10^5 , were of the same order of magnitude as for the curve for steady-state rectilinear flow. The scatter was not extreme when one considers the great variation in the turbulence of the flow, the pile roughness, eddies from other piles, and the fact that the pile is subject to its own eddies at the leading edge as the flow reverses. A comparison of C_D for the several pile sizes indicates that there is a secondary effect of pile diameter.

5. The coefficient of mass compared favorably with the theoretical value for a perfect fluid (2.0), and the median value was 2.5. No relationship was found between the coefficient of mass and the coefficient of drag, the Reynolds number, the horizontal component of local water-particle acceleration, or the wave period.

6. A comparison of predicted maximum forces and measured maximum forces, using the average values of C_D versus Reynolds number and the average value of C_M in the modified linear theory for predicting wave forces, showed serious discrepancies. However, for the range of conditions tested, a safety factor of from 2 to 2.5 should be sufficient.

7. After many days of continual action by large waves on the 2-ft test section, the 6-in. central pile broke in the middle seat of the thread at a point approximately 3 ft below the bottom clamp. An examination of the break indicated a fatigue failure.

ACKNOWLEDGMENTS

The work described herein was performed under contract to the Signal Oil and Gas Company of Los Angeles (Calif.). The writers wish to express their appreciation to Garth L. Young, Robert A. Kinzie, Mr. Johnson, Allan D. K. Laird, Richard W. Barry, Orville O. Goodwin, Philip H. Dirks, Michael A. Hall, Ernest R. Settles, and Margaret M. Lincoln for their invaluable contributions to the program.

APPENDIX. NOTATION

The following symbols, adopted for use in this paper and for the guidance of discussers, conform essentially with "American Standard Letter Symbols for Hydraulics" (ASA Z10.2—1942) prepared by a committee of the American Standards Association with Society representation, and were approved by the Association in 1942:

- A = projected area perpendicular to particle motion;
 C = coefficient of resistance;
 C_D = coefficient of drag;
 C_M = coefficient of mass;
 D = pile diameter;
 d = still-water depth;
 F = total force exerted by wave on pile;
 F_D = drag force on pile;
 F_M = inertia force on pile;
 g = acceleration of gravity;
 H = wave height;
 L = wave length;
 M_o = mass of the fluid displaced by the pile;
 M_a = added mass;
 R = Reynolds number, $D u / \nu$;
 S = elevation of water particle above the ocean bottom;
 S_m = elevation above the ocean bottom of the center of the pile test sections;
 T = wave period;
 t = time;
 u = horizontal component of water-particle velocity, in feet per second;
 V = volume of submerged pile;
 ΔS = vertical dimension of test section of pile;
 dF = increment of force on pile;
 dS = increment of pile length;
 $\partial u / \partial t$ = horizontal component of water-particle local acceleration;
 ν = kinematic viscosity of sea water; and
 ρ = mass density of sea water.

DISCUSSION

THOMAS E. STELSON,²⁶ A. M. ASCE.—Large-scale model tests, such as those described in the paper, are of great value in obtaining immediate design data as well as providing a basis for evaluating both theoretical relationships and the results of smaller-scale model studies. When so much time, money, and skill result in data that show such great variation, nonuniformity, and scatter, something is lacking either in experimental method or theoretical understanding. Measured values for apparently identical experimental conditions vary by factors of more than 10, as shown in Figs. 9, 10, and 11. The paper provides the stimulus to evaluate present knowledge in the field, considering both basic theory and supporting experimental data.

One example of such an area of deficient understanding is that of inertia drag. The coefficient of mass, C_M , as defined in Eq. 3 would have a theoretical value of 1 for a circular cylinder of infinite length at rest in an ideal fluid of infinite extent accelerated uniformly in irrotational motion at infinity.²⁷ This theoretical coefficient was erroneously given as 2 in the paper.

The experimental data summarized in Fig. 11 would therefore show that 91% of the measured values for the mass coefficients were in excess of the theoretical value. The mean experimental value of 2.5 is 150% in excess of the theoretical value. Furthermore, the data presented in Table 2 show the maximum coefficient to be more than seven times the minimum coefficient.

Some deviations from the theoretical value would be expected because of divergence in physical conditions, such as (1) limited length of the test cylinder; (2) wake formation behind the pile; (3) nonuniform movement within the wave and incorrect determination of acceleration; and (4) presence of the free surface as well as the variation in turbulence as mentioned by the authors. However, none of these items offer any reasonable explanation for such great diversity and scatter of data unless item (3) applies.

The coefficient of drag as shown in Fig. 9 also indicated tremendous variation—the larger values being more than twenty times the smaller values for the same pile and Reynolds number.

When mean values of the drag coefficient and the mass coefficient (plotted in Figs. 14 and 15) are used, the computed forces show considerable scatter, indicating that (a) measured forces are incorrect; (b) mean coefficients are incorrect; or (c) understanding of the phenomena is inadequate. The tendency for computed forces to be greater than measured forces when forces are low, and for computed forces to be less than measured forces when forces are high (a dangerous tendency), may point to the cause of some of the irregularity. The force due to fluid inertia varies as the height of the waves, whereas the force due to drag varies as the square of the height of the waves. Thus, acceleration-dependent forces seem to be too large, and velocity-dependent forces appear to be too small because the larger forces are associated with the higher waves.

²⁶ Associate Prof. of Civ. Eng. and Acting Dept. Head, Carnegie Inst. of Technology, Pittsburgh, Pa.

²⁷ "Theoretical Hydrodynamics," by L. M. Milne-Thomson, The Macmillan Co., New York, N. Y., 3d Ed., 1955, p. 233.

Again, this would indicate that mean coefficients of mass are too large and that mean coefficients of drag are too small. Lower values for the mass coefficients would make them more consistent with theory, and the possibility of greater drag forces has been stated by the author.

A possible conclusion from the paper is that if the experimental measurements are correct, a re-evaluation of all concepts of wave movement, fluid inertia, and viscous drag should be made. They do not seem to provide an adequate basis for reasonable correlation for the reported data. So much divergence cannot be tolerated in most engineering situations unless large safety factors are used consistently. Thus, designs tend to be conservative and expensive, and fewer projects are economically feasible.

ROBERT L. WIEGEL,²⁸ KENNETH E. BEEBE,²⁹ J. M. ASCE, AND JAMES MOON.³⁰—Considerable scatter is usually present in measurements of phenomena associated with large ocean waves. No two ocean waves are identical. They only appear so because of the rather crude methods used to describe wave characteristics, considering that they are nonuniform in three dimensions. This is especially true when both swell and locally generated wind waves are present.

Mr. Stelson states that there was an area of deficient understanding regarding inertia drag. Little is known of inertia drag, especially when it is associated with large velocities and the resulting phenomena. The writers feel that the definition of the term, C_M , has been misunderstood. Mr. Stelson has defined it as the added mass constant. However, the problem concerns a fluid accelerating about a cylinder at rest, not a cylinder accelerating through a fluid at rest. The force necessary to accelerate a mass through a fluid is associated with the mass itself and is termed the added mass (the added mass constant being unity for a right circular cylinder). The inertia force exerted by a fluid accelerating about a submerged body is associated with the mass of the displaced fluid and the added mass. The coefficient of mass as given by Lamb²² for this case is $C_M = 1 + 1 = 2$ for a right circular cylinder. This development of the coefficient of mass was used because of the ease in understanding the physical phenomenon. Using the linear theory for waves in shallow water Richard C. MacCamy and Fuchs³¹ have solved the diffraction problem for a right circular cylinder with a diameter that is small compared with the wave length. When the resulting equation is put in the writers' terms, it is

$$F_M = 2 \rho V \frac{\partial u}{\partial t} \dots \dots \dots (12)$$

which shows a value of 2 for what has been termed the coefficient of mass.

The scatter cannot be accounted for any of the reasons stated by the writers. However, each reason accounts for some of the scatter, and, undoubtedly, there are other causes.

²⁸ Associate Research Engr., Inst. of Eng. Research, Univ. of California, Berkeley, Calif.

²⁹ Graduate Research Engr., Inst. of Eng. Research, Univ. of California, Berkeley, Calif.

³⁰ Cons. Engr., Signal Oil & Gas Co., Los Angeles, Calif.

³¹ "Wave Forces on Piles: A Diffraction Theory," by R. C. MacCamy and R. A. Fuchs, *Technical Memorandum No. 69*, U. S. Beach Erosion Board, Corps of Engrs., U. S. Dept. of the Army, Washington, D. C., December, 1954.

Some advances are being made in understanding the basic phenomenon. For example, data by John McNown, M. ASCE, and Garbis H. Keulegan²² showed a strong dependency of the coefficients of mass on the wake for a right circular cylinder in standing-water gravity waves. Tests made by Laird at the University of California, using a right circular cylinder pair extending through an air-water free surface, as the mass of a long pendulum oscillating in a direction that is approximately parallel to the free surface, showed that variations in forces as great as from 50% to 100% could occur when large eddies in the wake of one cylinder hit the other cylinder in a certain manner.

²² "Vortex Shedding and Resistance in Unsteady Flow," by John McNown and G. H. Keulegan, paper presented at a meeting of the ASCE, New York, N. Y., October, 1957.

AMERICAN SOCIETY OF CIVIL ENGINEERS

Founded November 5, 1852

TRANSACTIONS

Paper No. 2968

PLATE BUCKLING IN THE STRAIN-HARDENING RANGE

BY GEERHARD HAAIJER,¹ A. M. ASCE

SYNOPSIS

The application of plastic design to continuous frames constructed of wide-flange shapes imposes more severe limitations on the geometry of these shapes than does conventional elastic design. In regions in which yielding begins first, the flanges must be able to sustain strains considerably larger than the yield strain without the occurrence of local (plate) buckling.

With this practical application in mind, the problem of buckling of steel plates compressed beyond the yield strain is treated herein. In the strains hardening range the material is considered to be homogeneous. However, because of the yielding process, the material cannot be expected to remain isotropic. Therefore, general expressions for the buckling strength are derived, assuming that the material has become orthogonally anisotropic.

Orthogonal anisotropy in the case of plane stress is expressed mathematically by stress-strain relationships involving five moduli. Numerical values of the moduli are estimated from the incremental theory of plasticity, using the second invariant of the deviatoric stress tensor as the loading function. The influence of initial imperfections is taken into account through proper adjustment of the values of the moduli. For the selection of these values, due consideration is given to the results of buckling tests.

In the yielding range, the average strain in the direction of loading is between the strain at which yielding begins and the strain at which strain hardening commences. For this case the material is considered to be partly elastic and partly strained up to the strain-hardening range.

Finally, theoretical estimates are compared with test results. It is considered that the theory adequately describes the behavior.

NOTE.—Published, essentially as printed here, in April, 1957, in the Journal of the Engineering Mechanics Division, as *Proceedings Paper 1212*. Positions and titles given are those in effect when the paper was approved for publication in *Transactions*.

¹ Research Engr., Applied Research Lab., U. S. Steel Corp., Monroeville, Pa.; formerly Research Associate, Fritz Eng. Lab., Dept. of Civ. Eng., Lehigh Univ., Bethlehem, Pa.

INTRODUCTION

Presently (1959) used steel wide-flange shapes are proportioned so that no local buckling occurs within the elastic range. Consequently, such shapes can be used safely for structures in which the design is based on theoretical first yield as the limiting condition (conventional design). However, design based on ultimate strength (plastic design) imposes more severe requirements on the sections with respect to local buckling. The structure will reach its full ultimate load only if those parts in which yielding begins first can undergo sufficiently large deformations. For framed structures constructed of wide-flange shapes, the flanges at the locations previously mentioned must be able to sustain considerably greater strains than the yield strain. Consequently, the flanges should be proportioned such that local (plate) buckling does not occur under this condition.

To solve problems of plate buckling, the relationships between the increments of stresses and strains due to the deflection of the plate out of its plane must be known. Within the elastic range the assumption that the material is isotropic and homogeneous leads to predictions that are in good agreement with test results.² A satisfactory transition curve for the range from the elastic-limit stress to the yield stress can be obtained easily by applying F. Bleich's semirational theory to an effective stress-strain curve.³

During the yielding process the material is heterogeneous. Yielding takes place in so-called slip bands, and the strain jumps from its value at the elastic limit to that at the beginning of strain hardening.⁴ When all the material has been strained to the strain-hardening range, the material again becomes homogeneous. In the strain-hardening range stress-strain relationships of different theories of plasticity could be applied. Such theories can be divided into two groups: Deformation, or total stress-strain relationships and incremental stress-strain relationships.

Paulus P. Bijlaard,⁵ M. ASCE, was first to apply deformation stress-strain relationships to the plate-buckling problem. The theory was developed further by A. A. Ilyushin⁶ and modified by Elbridge Z. Stowell.⁷ Incremental stress-strain relationships were applied by George H. Handelman and William Prager,⁸ M. ASCE, and an extensive survey of stress-strain relationships in the plastic range has been made by Daniel C. Drucker,⁹ M. ASCE. Although the necessity for an incremental type of mathematical theory of plasticity has been

² "Theory of Elastic Stability," by S. Timoshenko, McGraw-Hill Book Co., Inc., New York, N. Y., 1936.

³ "Buckling Strength of Metal Structures," by F. Bleich, McGraw-Hill Book Co., Inc., New York, N. Y., 1952.

⁴ "Theory of Flow and Fracture of Solids," by A. Nadai, McGraw-Hill Book Co., Inc., New York, N. Y., 1950.

⁵ "Some Contributions to the Theory of Elastic and Plastic Stability," by P. P. Bijlaard, *Publications International Assn. for Bridge and Structural Eng.*, Zurich, Vol. VIII, 1947.

⁶ "Stability of Plates and Shells Beyond the Proportional Limit," by A. A. Ilyushin, *NACA TM-116*, National Advisory Committee for Aeronautics, Washington, D. C., October, 1947 (translated from the Russian).

⁷ "A Unified Theory of Plastic Buckling of Columns and Plates," by E. Z. Stowell, *Report No. 598*, National Advisory Committee for Aeronautics, Washington, D. C., 1948.

⁸ "Plastic Buckling of a Rectangular Plate Under Edge Thrusts," by G. H. Handelman and W. Prager, *Technical Note No. 1530*, National Advisory Committee for Aeronautics, Washington, D. C., August, 1948.

⁹ "Stress-Strain Relations in the Plastic Range—A Survey of Theory and Experiment," by D. C. Drucker, *Report A11 S1*, Graduate Div. of Applied Mathematics, Brown Univ., Providence, R. I., December, 1950.

shown, the results of plastic-buckling tests on aluminum plates are correlated well by a deformation theory and do not resemble predictions of incremental theory. E. T. Onat and Drucker¹⁰ investigated the influence of initial imperfections on torsional buckling for a simplified model of a cruciform section. For this case the paradox appears at its worst. It was shown that incremental plasticity leads to proper results when unavoidable initial imperfections are taken into account.

All theories of plate buckling in the plastic range imply orthotropic behavior of the material, which seems to be a reasonable assumption. Therefore, under the heading, "Buckling of Rectangular Orthotropic Plates: General," expressions for the buckling strength of orthotropic plates are derived from general stress-strain relationships involving five moduli. Tests of steel tubes under combined compression and torsion showed that the behavior of the material is described well by the incremental theory, with the second invariant of the deviatoric stress tensor as the loading function.¹¹ Consequently, this theory is used in order to obtain values of the moduli of the general stress-strain relationships.

Generalities on stress and strain and incremental stress-strain relationships are summarized under the heading, "Incremental Stress-Strain Relationships," in which the influence of initial imperfections is illustrated. From the results of coupon tests, numerical values of the moduli are shown under the heading, "Stress-Strain Relationships for the Strain-Hardening Range of Steel." A combination of the results yields numerical solutions of the plate-buckling problem that are compared with test results.

The objective of the paper is to predict the strain at which buckling occurs in steel-plate elements in cases for which the strain has exceeded the elastic limit.

BUCKLING OF RECTANGULAR ORTHOTROPIC PLATES

Notation.—The letter symbols adopted for use in this paper are defined where they first appear, in the illustrations or in the text, and are arranged alphabetically, for convenience of reference, in the Appendix.

General.—A rectangular steel plate is considered, with the center plane of the plate as the (xy) -coordinate plane. Compressing the plate in the x -direction into the strain-hardening range may affect all deformation properties of the material. Hence, the tangent moduli, E_x and E_y , in the x -direction and y -direction, respectively, are probably different. The coefficients of dilatation, ν_x and ν_y , in the x -direction and y -direction and the shear modulus, G , also may be affected.

Thus,

$$\frac{\partial \epsilon_x}{\partial \sigma_x} = \frac{1}{E_x} \dots \dots \dots (1a)$$

$$\frac{\partial \epsilon_y}{\partial \sigma_y} = \frac{1}{E_y} \dots \dots \dots (1b)$$

¹⁰ "Inelastic Instability and Incremental Theories of Plasticity," by E. T. Onat, and D. C. Drucker, *Journal of the Aeronautical Sciences*, Vol. 20, March, 1953.

¹¹ "Combined Compression and Torsion of Steel Tubes in the Strain-Hardening Range," by G. Haasler and B. Thürlimann, *Fritz Laboratory Report No. 241.2*, Lehigh Univ., Bethlehem, Pa.

$$\frac{\partial \epsilon_x}{\partial \sigma_y} = - \frac{\nu_y}{E_y} \dots \dots \dots (1c)$$

$$\frac{\partial \epsilon_y}{\partial \sigma_x} = - \frac{\nu_x}{E_x} \dots \dots \dots (1d)$$

and

$$\frac{\partial \gamma_{xy}}{\partial \tau_{xy}} = \frac{1}{G_t} \dots \dots \dots (1e)$$

in which ϵ is the normal strain; γ represents the shear strain; σ denotes the normal stress; and τ is the shear stress.

The relationships between the increments of strains and stresses can be written as follows:

$$d\epsilon_x = \frac{1}{E_x} d\sigma_x - \frac{\nu_y}{E_y} d\sigma_y \dots \dots \dots (2a)$$

$$d\epsilon_y = - \frac{\nu_x}{E_x} d\sigma_x + \frac{1}{E_y} d\sigma_y \dots \dots \dots (2b)$$

and

$$d\gamma_{xy} = \frac{1}{G_t} d\tau_{xy} \dots \dots \dots (2c)$$

If Eqs. 2 are valid for the entire cross section, the expressions for the bending moments and twisting moments in terms of the deflection, w , in the direction of the z -axis become

$$M_x = - \frac{E_x I}{1 - \nu_x \nu_y} \left(\frac{\partial^2 w}{\partial x^2} + \nu_y \frac{\partial^2 w}{\partial y^2} \right) \dots \dots \dots (3)$$

$$M_y = - \frac{E_y I}{1 - \nu_x \nu_y} \left(\frac{\partial^2 w}{\partial y^2} + \nu_x \frac{\partial^2 w}{\partial x^2} \right) \dots \dots \dots (4)$$

and

$$M_{xy} = - 2 G_t I \frac{\partial^2 w}{\partial x \partial y} \dots \dots \dots (5)$$

in which I is the moment of inertia per unit width of plate and is equal to $t^3/12$, and t denotes the thickness of the plate.

The condition that the bent position be in equilibrium can be expressed by

$$D_x \frac{\partial^4 w}{\partial x^4} + 2 H \frac{\partial^4 w}{\partial x^2 \partial y^2} + D_y \frac{\partial^4 w}{\partial y^4} = - \frac{t \sigma_x}{I} \frac{\partial^2 w}{\partial x^2} \dots \dots \dots (6)$$

in which $D_x = \frac{E_x}{1 - \nu_x \nu_y}$; $D_y = \frac{E_y}{1 - \nu_x \nu_y}$; $D_{xy} = \frac{\nu_y E_x}{1 - \nu_x \nu_y}$; $D_{yx} = \frac{\nu_x E_y}{1 - \nu_x \nu_y}$; and $2 H = D_{xy} + D_{yx} + 4 G_t$.

The derivation of these equations can be found elsewhere.¹² Only if $H^2 = D_x D_y$ (an assumption made by Bleich³) can solutions of Eq. 6 be obtained easily.

¹² "Flachentragwerke," by K. Girkmann, Springer Verlag, Vienna, 2d Ed., 1948.

If the plate initially is perfectly plane, the value of σ_x at which bifurcation of equilibrium occurs (the plane position and the bent position both being equilibrium positions) is determined by Eq. 6. The condition that both the plane position and the bent position are equilibrium positions can also be expressed in terms of work. The additional work performed by the external forces due to plate bending must equal the change in the internal energy of the plate.

The foregoing yields:

$$\frac{\sigma_x t}{I} \iint \left(\frac{\partial w}{\partial x} \right)^2 dx dy = \iint \left[D_x \left(\frac{\partial^2 w}{\partial x^2} \right)^2 + D_y \left(\frac{\partial^2 w}{\partial y^2} \right)^2 + (D_{xy} + D_{yx}) \times \left(\frac{\partial^2 w}{\partial x^2} \right) \left(\frac{\partial^2 w}{\partial y^2} \right) + 4 G_t \left(\frac{\partial^2 w}{\partial x \partial y} \right)^2 \right] dx dy \quad (7)$$

When the plate is provided with external restraints, the right-hand side of Eq. 7 must be supplemented by additional terms expressing the work of these restraints.

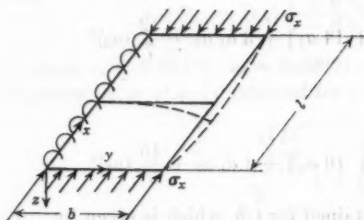


FIG. 1.—PLATE WITH ONE FREE EDGE

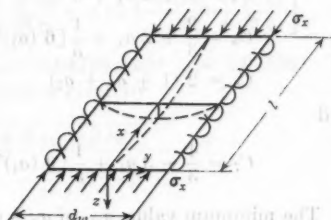


FIG. 2.—PLATE SUPPORTED AT ALL FOUR EDGES

When an appropriate deflection surface is assumed, Eq. 7 yields an approximate solution. The degree of approximation depends on the correctness of the assumed deflection surface. In any case the result will be conservative.

Plates with One Free Edge.—For a rectangular plate with the loaded edges $x = 0$ and $x = l$ hinged, with edge $y = 0$ restrained against rotation, and with edge $y = b$ as the free edge (Fig. 1), the following deflection surface is assumed:

$$w = \left\{ A \frac{y}{b} + B \left[\left(\frac{y}{b} \right)^2 + a_1 \left(\frac{y}{b} \right)^3 + a_2 \left(\frac{y}{b} \right)^4 \right] \right\} \sin \frac{\pi x}{l} \quad (8)$$

In Eq. 8, A and B are constants and b is the width of the plate.

The ratio B/A depends on the restraint. In the case of elastic restraint, in which ψ equals the moment per unit length required for a unit rotation,

$$\beta = \frac{B}{A} = \frac{\psi b}{2 D_y I} \quad (9)$$

The deflection surface (Eq. 8) is similar to the one used by Eugene E. Lundquist, M. ASCE, and Stowell.¹³ It can be shown¹⁴ that better results are ob-

¹³ "Critical Compressive Stress for Outstanding Flanges," by E. E. Lundquist and E. Z. Stowell, Report No. 734, National Advisory Committee for Aeronautics, Washington, D. C., 1942.

¹⁴ "Local Buckling of Wide Flange Shapes," by G. Haaijer, thesis presented to Lehigh University, in Bethlehem, Pa., in 1956, in partial fulfillment of the requirements for the degree of Doctor of Philosophy.

tained with Eq. 8 if the following values for a_1 and a_2 are used: For $0 < \beta < 0.1$, $a_1 = -0.7$ and $a_2 = 0.2$; and for $\beta = \infty$, $a_1 = -1.10$ and $a_2 = 0.54$.

Substituting w in Eq. 7 and integrating results in

$$\sigma_x = \frac{t^2}{12 b^2} \left[D_x \left(\frac{\pi b}{l} \right)^2 + D_y \left(\frac{l}{\pi b} \right)^2 \frac{2\beta + \beta^2 C_3}{\frac{1}{3} + \beta C_1 + \beta^2 C_2} - (D_{xy} + D_{yx}) \frac{\beta C_4 + \beta^2 C_5}{\frac{1}{3} + \beta C_1 + \beta^2 C_2} + 4 G_t \frac{1 + \beta C_6 + \beta^2 C_7}{\frac{1}{3} + \beta C_1 + \beta^2 C_2} \right] \quad (10)$$

in which

$$C_1 = \frac{1}{2} + \frac{2}{5} a_1 + \frac{1}{3} a_2$$

$$C_2 = \frac{1}{5} + \frac{1}{3} a_1 + \frac{1}{7} [(a_1)^2 + 2 a_2] + \frac{1}{4} a_1 a_2 + \frac{1}{9} (a_2)^2$$

$$C_3 = 4 + 12 (a_1)^2 + \frac{144}{5} (a_2)^2 + 12 a_1 + 16 a_2 + 36 a_1 a_2$$

$$C_4 = 1 + 2 a_1 + 3 a_2$$

$$C_5 = \frac{2}{3} + 2 a_1 + \frac{1}{5} [6 (a_1)^2 + 14 a_2] + 3 a_1 a_2 + \frac{12}{7} (a_2)^2$$

$$C_6 = 2 (1 + a_1 + a_2)$$

and

$$C_7 = \frac{4}{3} + 3 a_1 + \frac{1}{5} [9 (a_1)^2 + 16 a_2] + 4 a_1 a_2 + \frac{16}{7} (a_2)^2$$

The minimum value, σ_{cr} , of σ_x is obtained for l/b , which is given by

$$\frac{l}{b} = \pi \sqrt{\frac{\frac{1}{3} + \beta C_1 + \beta^2 C_2}{2\beta + \beta^2 C_3}} \sqrt{\frac{D_x}{D_y}} \quad (11)$$

In the limiting case in which edge $y = 0$ is hinged ($\beta = 0$) and $l = L$, Eq. 10 reduces to

$$\sigma_{cr} = \left(\frac{t}{b} \right)^2 \left[\frac{\pi D_x}{12} \left(\frac{b}{L} \right)^2 + G_t \right] \quad (12)$$

For a long plate the first term can be neglected and

$$\sigma_{cr} = \left(\frac{t}{b} \right)^2 G_t \quad (13)$$

In the limiting case in which edge $y = 0$ is completely fixed ($\beta = \infty$), the minimum value, σ_{cr} , of σ_x is obtained when the half-wave length, l , satisfies

$$\frac{l}{b} = 1.46 \sqrt{\frac{D_x}{D_y}} \quad (14)$$

and

$$\sigma_{cr} = \left(\frac{t}{b} \right)^2 [0.769 \sqrt{D_x D_y} - 0.270 (D_{xy} + D_{yx}) + 1.712 G_t] \quad (15)$$

Plates Supported Along All Four Edges.—The loaded edges, $x = 0$ and $x = l$, are hinged, and the edges $y = \pm d_w/2$ have equal restraint against rotation (Fig. 2). For this case the following deflection surface is used¹⁵:

$$w = \left[B \pi \left(\frac{y}{d_w} - \frac{1}{2} \right) + (A + B) \cos \frac{\pi y}{d_w} \right] \sin \frac{\pi x}{l} \dots (16)$$

The ratio B/A depends on the restraint. For elastic restraints, with ψ equaling the moment per unit length required for unit rotation,

$$\beta = \frac{B}{A} = \frac{\psi d_w}{2 D_y I} \dots (17)$$

Substituting w from Eq. 16 into Eq. 7 and integrating yields

$$\sigma_x = \frac{\pi^2 l^2}{12 d_w^2} \left[D_x \left(\frac{d_w}{l} \right)^2 + D_y \left(\frac{l}{d_w} \right)^2 \frac{\frac{1}{4} + \left(c_1 + \frac{2}{\pi^2} \right) \beta + \beta^2 c_3}{\frac{1}{4} + \beta c_1 + \beta^2 c_2} + (D_{xy} + D_{yz}) \frac{\frac{1}{4} + \beta c_1 + \beta^2 c_4}{\frac{1}{4} + \beta c_1 + \beta^2 c_2} + 4 G_t \frac{\frac{1}{4} + \beta c_1 + \beta^2 c_4}{\frac{1}{4} + \beta c_1 + \beta^2 c_2} \right] \dots (18)$$

in which $c_1 = 0.09472$; $c_2 = 0.00921$; $c_3 = 0.04736$; and $c_4 = 0.01139$. The minimum value of σ_x is obtained for l which is given by

$$\frac{l}{d_w} = \sqrt[4]{\frac{D_x}{D_y} \frac{\frac{1}{4} + \beta c_1 + \beta^2 c_2}{\frac{1}{4} + \left(c_1 + \frac{2}{\pi^2} \right) \beta + \beta^2 c_3}} \dots (19)$$

In the limiting cases when the unloaded edges $y = \pm d_w/2$ are hinged or completely fixed, the minimum values of σ_x are

(a) Edges $y = \pm d_w$ hinged ($\beta = 0$):

$$\sigma_{cr} = \frac{\pi^2}{12} \left(\frac{l}{d_w} \right)^2 (2 \sqrt{D_x D_y} + D_{xy} + D_{yz} + 4 G_t) \dots (20)$$

in cases for which

$$\frac{l}{d_w} = \sqrt[4]{\frac{D_x}{D_y}} \dots (21)$$

(b) Edges $y = \pm d_w/2$ completely fixed ($\beta = \infty$):

$$\sigma_{cr} = \frac{\pi^2}{12} \left(\frac{l}{d_w} \right)^2 [4.554 \sqrt{D_x D_y} + 1.237 (D_{xy} + D_{yz}) + 4.943 G_t] \dots (22)$$

in cases for which

$$\frac{l}{d_w} = 0.664 \sqrt[4]{\frac{D_x}{D_y}} \dots (23)$$

¹⁵ "Critical Compressive Stress for Flat Rectangular Plates Supported Along All Edges and Elastically Restrained Against Rotation Along the Unloaded Edges," by E. E. Lundquist and E. Z. Stowell, Report No. 735, National Advisory Committee for Aeronautics, Washington, D. C., 1942.

In subsequent sections, values of D_x , D_y , D_{xy} , D_{yz} , and G_i will be determined. On substituting these values into the preceding general expressions, numerical solutions to the local buckling problem will be obtained.

INCREMENTAL STRESS-STRAIN RELATIONSHIPS

General.—Tensor notation is used in referring to generalized stress and strain. Cartesian coordinates, x_1 , x_2 , and x_3 , corresponding to the x -, y -, and z -axes of engineering notation, are denoted by the subscripts i , j , k , and l , which take the values of 1, 2, and 3. Thus, the nine components of stress tensors and strain tensors are represented by the single symbols σ_{ij} and ϵ_{ij} , respectively. Repeated subscripts indicate summation.¹⁰

It is commonly assumed that yielding occurs whenever some function of stress, $f(\sigma_{ij})$, equals some number, k . If the material is originally isotropic this yield condition is independent of the orientation of the coordinate system. In this instance, the value of f must be a function of the stress invariants. An extension of the yield function is obtained by assuming the existence of a loading function, $f(\sigma_{ij})$, which depends on the state of stress and strain and the history of loading. For ideally plastic materials, plastic flow occurs whenever f equals some number, k . For materials exhibiting strain hardening, plastic deformations occur when the loading function exceeds k .

Prager¹¹ proved that (1) if a loading function exists and (2) if the relationship between infinitesimals of stress and strain is linear, the only permissible stress-strain relationship for strain-hardening material when loading is

$$d(\epsilon_{ij})^p = F \frac{\partial f}{\partial \sigma_{ij}} \frac{\partial f}{\partial \sigma_{kl}} d\sigma_{kl} \dots \dots \dots (24)$$

When unloading, the stress-strain relationship is

$$d(\epsilon_{ij})^p = 0 \dots \dots \dots (25)$$

in which $(\epsilon_{ij})^p$ is the plastic component of strain, ϵ_{ij} , and F and f are functions of stress and strain. Drucker also includes the geometric proof of Prager's stress-strain law (Eqs. 24 and 25) in his survey of stress-strain relationships in the plastic range.⁹

Because no information was available concerning the actual behavior of steel in the strain-hardening range, combined compression and torsion tests were conducted on steel tubes.¹¹ The tubes were compressed into the strain-hardening range and then subjected to torsion while the axial load was kept constant. It was found that for this particular loading path the behavior is described well by Prager's incremental stress-strain relationships, using $f = J_2$, in which J_2 is the second invariant of the deviatoric stress tensor. The state of stress, with the components σ_{ij} , can be split into two parts: (1) A uniform tension (or compression), s , and (2) another state of stress, with the components s_{ij} , having the same shear stress but with zero mean normal stress. The latter

¹⁰ "Mathematical Theory of Elasticity," by I. S. Sokolnikoff, McGraw-Hill Book Co., Inc., New York, N. Y., 1946.

¹¹ "Recent Developments in the Mathematical Theory of Plasticity," by W. Prager, *Journal of Applied Physics*, Vol. 20, No. 3, 1949.

is called the deviatoric stress tensor. Thus, $\sigma_{ij} = s_{ij} + s \delta_{ij}$, in which $s = \frac{1}{3} \sigma_{ii}$. The second invariant is given by $J_2 = \frac{1}{2} s_{ij} s_{ij}$.

Although these tests are not a general verification of the theory, they indicate its possible validity. In view of these results and because of the simplicity of the theory, the loading function, $f = J_2$, will be applied in the following derivations.

Loading Function, $f = J_2$.—Applying the loading function, $f = J_2$, to Eqs. 24 and 25 results in

$$d(\epsilon_{ij})^p = F s_{ij} dJ_2 \dots \dots \dots (26)$$

when $dJ_2 > 0$, and

$$d(\epsilon_{ij})^p = 0 \dots \dots \dots (27)$$

when $dJ_2 \leq 0$. The increments of the elastic components, $\epsilon_{(ij)}^e$, of the strains are given by Hooke's law,

$$d(\epsilon_{ij})^e = \frac{1+\nu}{E} d\sigma_{ij} - \frac{\nu}{E} d\sigma_{kk} \delta_{ij} \dots \dots \dots (28)$$

in which E is the modulus of elasticity, ν represents Poisson's ratio, and δ_{ij} denotes the Kronecker δ , defined as unity for $i = j$ and as 0 for $i \neq j$.

For the case of plane stress ($\sigma_z = \tau_{xz} = \tau_{yz} = 0$), the stress-strain relations, written in unabridged form, are

$$d\epsilon_x = \frac{1}{E} d\sigma_x - \frac{\nu}{E} d\sigma_y + \frac{1}{3} F (2\sigma_x - \sigma_y) dJ_2 \dots \dots \dots (29)$$

$$d\epsilon_y = -\frac{\nu}{E} d\sigma_x + \frac{1}{E} d\sigma_y + \frac{1}{3} F (2\sigma_y - \sigma_x) dJ_2 \dots \dots \dots (30)$$

$$d\epsilon_z = -\frac{\nu}{E} (d\sigma_x + d\sigma_y) - \frac{1}{3} F (\sigma_x + \sigma_y) dJ_2 \dots \dots \dots (31)$$

and

$$d\gamma = \frac{2(1+\nu)}{E} d\tau + 2F\tau dJ_2 \dots \dots \dots (32)$$

when

$$dJ_2 = \frac{1}{3} (2\sigma_x - \sigma_y) d\sigma_x + \frac{1}{3} (2\sigma_y - \sigma_x) d\sigma_y + 2\tau d\tau > 0 \dots \dots (33)$$

and

$$d\epsilon_x = \frac{1}{E} d\sigma_x - \frac{\nu}{E} d\sigma_y \dots \dots \dots (34)$$

$$d\epsilon_y = -\frac{\nu}{E} d\sigma_x + \frac{1}{E} d\sigma_y \dots \dots \dots (35)$$

$$d\epsilon_z = -\frac{\nu}{E} (d\sigma_x + d\sigma_y) \dots \dots \dots (36)$$

and

$$d\gamma = \frac{2(1+\nu)}{E} d\tau \dots \dots \dots (37)$$

when $dJ_2 \leq 0$.

The function, F , can be obtained from the results of a simple coupon test for which $\sigma_y = \tau = d\sigma_y = d\tau = 0$. Denoting

$$\frac{d\sigma_x}{d\epsilon_x} = E_t \dots \dots \dots (38)$$

the value of F is defined by Eq. 29 as

$$F = \frac{3}{4J_2} \left(\frac{1}{E_t} - \frac{1}{E} \right) \dots \dots \dots (39)$$

Because of unavoidable initial imperfections, the previously derived stress-strain relationships cannot be applied without modification to the local buckling problem. After the influence of initial imperfections on two simplified models has been investigated, effective stress-strain relationships for the strain-hardening range of steel will be derived.

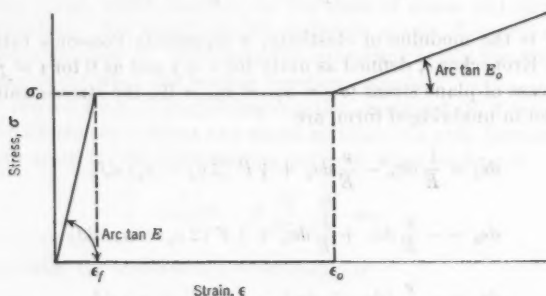


FIG. 3.—SIMPLIFIED STRESS-STRAIN CURVE

INFLUENCE OF INITIAL IMPERFECTIONS

General.—A perfectly plane plate will remain plane if it is subjected to loads acting in its center plane that do not exceed the corresponding buckling loads. In the case of longitudinal loading in the x -direction, producing a state of stress with σ_x as the only component, this stress will remain unchanged until buckling occurs. Consequently, the buckling stress can be obtained from stress-strain relationships in Eqs. 29, 30, 31, and 32 with $\sigma_y = \tau = 0$.

However, the buckling strength of actual plates with unavoidable imperfections does not agree with the predictions for perfectly plane plates. The main reason for the discrepancy is probably due to Eq. 32, which predicts elastic behavior with respect to the superimposed shear stresses.

Applying a simplified stress-strain diagram to a simplified model of a cruciform section, Onat and Drucker¹⁰ show that small unavoidable imperfections may account for the differences between predicted behavior and actual behavior. Apparently the influence of imperfections on sections failing by torsional buckling is completely different from those that fail in bending. The

latter case has been investigated by Thomas W. Wilder, William A. Brooks, Jr., and Eldon E. Mathauser.¹³

This difference in behavior will be demonstrated for simplified models that buckle in the strain-hardening range. The applied simplified stress-strain curve with $n = E/E_t = 40$ is shown in Fig. 3. The reasons why the compressive stresses can exceed the yield stress, σ_o , will be examined subsequently.

Simplified WF Column.—The simplified WF column consists of two thin flanges of equal area separated by a web of infinite shear stiffness and negligible area (Fig. 4). Instead of a true initial imperfection, the deflections at the beginning of strain hardening ($\sigma = \sigma_o$ and $\epsilon = \epsilon_o$) are used in the computations.

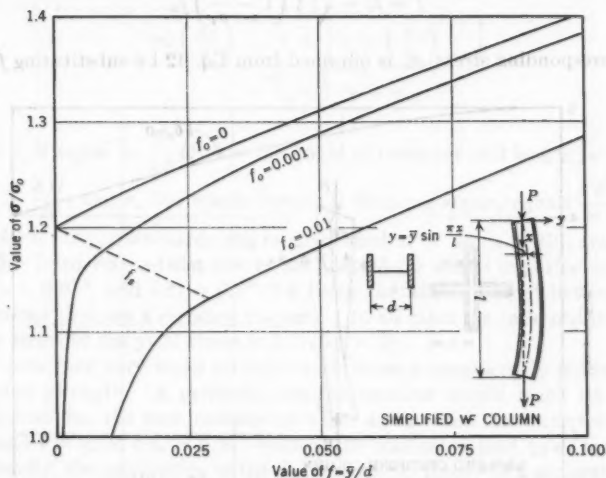


FIG. 4.—EFFECT OF INITIAL IMPERFECTIONS ON A SIMPLIFIED WF SECTION

Following the same approach as Wilder, Brooks, and Mathauser, the deflection curve is assumed to be

$$y = \bar{y} \sin \frac{\pi x}{l} \dots \dots \dots (40)$$

At the beginning of strain hardening,

$$y_o = \bar{y}_o \sin \frac{\pi x}{l} \dots \dots \dots (41)$$

The load-versus-deflection curve is found by considering the equilibrium of the center section of the column.

For the first part of the load-versus-deflection curve, the strain in both flanges increases and the relationship between average stress and deflection is

¹³ "The Effect of Initial Curvature on the Strength of an Inelastic Column," by T. W. Wilder, III, W. A. Brooks, Jr., and E. E. Mathauser, Technical Note 2875, National Advisory Committee for Aeronautics, Washington, D. C., January, 1953.

given by

$$\frac{\sigma}{\sigma_o} = \frac{\sigma_t}{\sigma_o} - \left(\frac{\sigma_t}{\sigma_o} - 1 \right) \frac{f_o}{f} \quad (42)$$

in which σ represents the average stress of both flanges; $\sigma_t = \frac{\pi^2 E_t}{(l/r)^2}$ (tangent modulus stress); f is the ratio of \bar{y}/d ; d denotes the depth of section; and f_o designates the value of f at the beginning of strain hardening.

Strain reversal occurs for

$$f = f_s = \sqrt{\frac{1}{2} \left(1 - \frac{\sigma_o}{\sigma_t} \right)} f_o \quad (43)$$

The corresponding stress, σ_s , is obtained from Eq. 42 by substituting $f = f_s$.

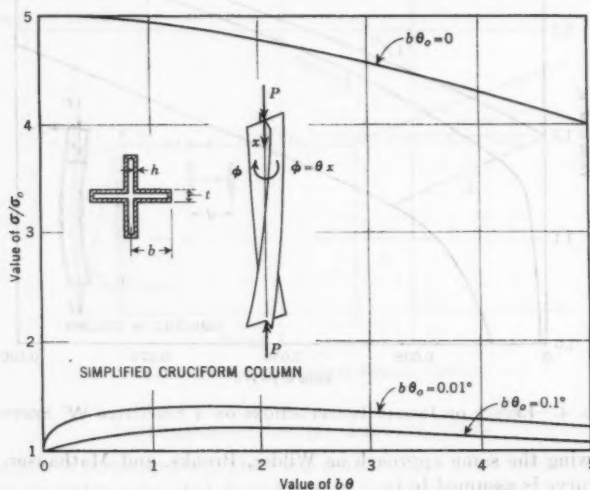


FIG. 5.—EFFECT OF INITIAL IMPERFECTIONS ON A SIMPLIFIED CRUCIFORM SECTION

After strain reversal has begun, the load-versus-deflection relationship is given by

$$\frac{\sigma}{\sigma_o} \left[\frac{n-1}{2(n+1)} + f \right] = \frac{\sigma_s}{\sigma_o} \left[\frac{n-1}{2(n+1)} + f_s \right] + \frac{\sigma_t}{\sigma_o} \frac{2n}{n+1} (f - f_s) \quad (44)$$

Fig. 4 shows curves of σ/σ_o versus f for $\sigma_t/\sigma_o = 1.2$ and different values of f_o . The figure illustrates the behavior of the column for loads corresponding to stresses $\sigma \cong \sigma_t$. Although the deflections begin increasing more rapidly, the load continues to increase. Therefore, it is safe to use the tangent modulus load, which corresponds to $\sigma = \sigma_t$, as the limit of usefulness of the column.

Simplified Cruciform Section.—In contrast to the preceding example, the influence of initial imperfections on the buckling strength of a column of simplified cruciform cross section will be illustrated subsequently. The solution of the problem as given by Onat and Drucker¹⁰ can be applied without modification to the simplified stress-strain curve of Fig. 3.

The cross section consists of a thin shell of constant thickness, h (Fig. 5). The column, which is loaded uniformly, is assumed to fail by twisting. The ends provide no restraint, which considerably simplifies the kinematics of the problem and makes the state of stress and strain the same at each cross section. An approximate solution for low values of χ is given as

$$\sigma = \frac{\sigma_o \left(\frac{\chi_o}{\chi} \right)^{1/2n'} + \sigma_e \left[1 - \left(\frac{\chi_o}{\chi} \right)^{1/2n'} \right]}{1 + \frac{n' - 1}{2n} (\chi - \chi_o)} \quad (45)$$

in which χ is equal to $\frac{b^4}{3I^2} \theta^2$; θ is the angle of twist per unit length; n' equals $\frac{3G}{E_t} + 1 - \frac{3G}{E}$; and σ_e , the elastic torsional buckling stress, equals $\frac{3I^2}{b^2} G$.

Results for the strain-hardening range of steel, $n' = 46$ ($n = 40$), are shown in Fig. 5. Load-versus-twist curves are plotted for initial imperfections, $b\theta_o = 0$, $b\theta_o = 0.01^\circ$, and $b\theta_o = 0.1^\circ$ ($b\theta_o$ being the angle of twist between two cross sections that are a distance b apart). In all cases the ratio of the elastic buckling stress to the yield stress is 5 ($\sigma_e/\sigma_o = 5$).

It is seen that very small imperfections cause a considerable reduction of the column strength. A perfectly straight member would reach its elastic buckling load for the case considered when $\sigma_e/\sigma_o = 5$. An imperfection at $\sigma = \sigma_o$ and $\epsilon = \epsilon_o$ of $b\theta_o = 0.01^\circ$ reduces the maximum load to $\sigma_m/\sigma_o = 1.4$. Consequently, the application of the J_T -incremental theory to a perfectly plane plate that fails primarily by twisting cannot be expected to predict correctly the buckling strength of actual plates.

Rather than attempt to solve the buckling problem of a plate with initial imperfections, effective stress-strain relationships will be determined in the section entitled, "Stress-Strain Relationships for the Strain-Hardening Range of Steel: The Tangent Modulus in Shear; Biaxial Normal Stresses." It will be necessary to modify the values of D_x , D_y , D_{xy} , D_{yz} , and G , so that the application to the general expressions stated under the headings, "Buckling of Rectangular Orthotropic Plates: Plates with One Free Edge; Plates Supported Along All Four Edges," will result in a correct description of the behavior of actual plates.

STRESS-STRAIN RELATIONSHIPS FOR THE STRAIN-HARDENING RANGE OF STEEL

Results of Coupon Tests.—A simplified stress-strain curve obtained from a simple coupon test is shown in Fig. 3. It must be remembered that the strain represents an average strain measured over a certain gage length. It would be

entirely erroneous to assume that the local strains within the plastic range from ϵ_f to ϵ_o are equal to the average strain. Yielding of mild steel occurs in small slip bands.⁴ Slip takes place in a "jump" in such a manner that the strain across such a narrow band jumps from ϵ_f to ϵ_o . The first slip band originates at a weak point in the specimen due to an inclusion, a stress concentration, or other defects. Subsequently, yielding will spread along the specimen.

This consideration leads to the conclusion that there is no material within the specimen at a strain between the yield strain, ϵ_f , and the strain-hardening strain, ϵ_o . Either the material has remained elastic, or it has reached the strain-hardening range.

TABLE 1.—RESULTS OF COMPRESSION COUPON TESTS

Coupon ^a	Fritz Engineering Laboratory number	Section	Yield stress, σ_s , in kips per square inch	Strain, ^b ϵ_o , in 10 ³ in. per in.	Strain-hardening modulus, E_s , in kips per square inch
(1)	(2)	(3)	(4)	(5)	(6)
1	220A-UF3	14WF30	39.7	13.0	730
2	220A-UF4	14WF30	41.5	14.6	690
3	220A-LF1	14WF30	42.5	14.6	650
4	220A-LF2	14WF30	39.0	12.5	790
5	220A-LF3	14WF30	39.7	12.5	730
6	220A-LF4	14WF30	42.0	13.0	670
7	220A-A	14WF30	40.8	15.0	640
8	220A-B	14WF30	40.8	12.5	675
9	220A-D	14WF30	40.3	15.5	650
10	220A-E	14WF30	39.6	14.5	650
11	220A-F	14WF30	35.3	(6.0) ^c	780
12	220A-G	14WF30	36.2	(6.5) ^c	700
13	220A-B2F3	8WF31	40.0	17.4	770
14	220A-B2F6	8WF31	38.8	11.5	810
15	220A-B2F7	8WF31	39.0	14.8	730
16	205E-C14	10WF33	40.0	14.5	855
17	205E-C15	10WF33	37.0	13.8	805
18	205E-C2	8WF40	38.4	12.8	1,060
19	205E-C9	L6 × 6 × 1	39.0	12.8	710
20	205E-C12	L6 × 6 × 1	37.6	14.3	906
21	205E-C13	L6 × 6 × 1	35.1	14.6	845
Average values ^a			39.2	13.9	755

^a All WF-section coupons taken from flanges. ^b Strain at initiation of strain hardening. ^c Numbers in parentheses not used for determining average value.

In the strain-hardening range, $\epsilon > \epsilon_o$, the material is again homogeneous, and in this range the J_2 -theory of plasticity will be applied. In the intermediate range, $\epsilon_f < \epsilon < \epsilon_o$, the specimen can be considered to consist of two materials.

The results of twenty-one compression coupon tests that were conducted at the Fritz Engineering Laboratory of Lehigh University, Bethlehem, Pa., are summarized in Table 1. The coupons were cut from the flanges of WF shapes and from angles. For the interpretation of the results of coupon tests the following must be taken into account. Coupons are tested continuously in a hydraulic testing machine. It has become customary in the Fritz Engineering Laboratory to test coupons with a valve opening of the machine corresponding to a strain rate of 1 μ in. per in. per sec in the elastic range. It has been shown

by Alfons W. Huber and Lynn S. Beedle,¹⁹ Associate Members, ASCE, that the ratio of the yield stress of a static test, during which the load settles down after each increment of strain, and the yield stress of a continuous coupon test is approximately 0.925. Consequently, a value of the yield stress, σ_o of 0.925 (39.2) = 36 kips per sq in. will be used in the following derivations.

Stress-strain curves for the strain-hardening range, as obtained from five selected coupon tests, have been replotted in Fig. 6. Coupons 9 and 18 represent the extreme cases, whereas coupons 5, 15, and 17 represent tests with average results.

The average stress-strain curve for the strain-hardening range can be expressed by the three parameters introduced by W. Ramberg and R. Osgood.²⁰

$$\epsilon - \epsilon_o = \frac{\sigma - \sigma_o}{E_o} + K \left(\frac{\sigma - \sigma_o}{E_o} \right)^m \dots \dots \dots (46)$$

in which σ_o = 36 kips per sq in.; ϵ_o = 14×10^{-3} in. per in.; E_o = 900 kips per sq in.; K = 21; and m = 2. Eq. 46 is also plotted in Fig. 6. The values of

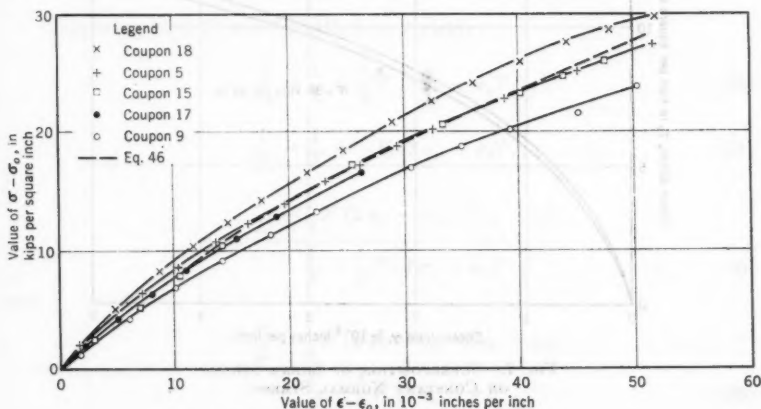


FIG. 6.—RESULTS OF COMPRESSION COUPON TESTS IN THE STRAIN-HARDENING RANGE

E_o in Table 1 are taken from Fritz Engineering Laboratory reports, in which they usually are not given as the slope of the stress-strain curve at the initiation of strain hardening, but as the slope at a strain somewhat greater than ϵ_o . Consequently, E_o as used in Eq. 46, is greater than the average value given in Table 1.

The available information is sufficient to determine $F(J_2)$ defined by Eq. 39. From Eqs. 39 and 46, it follows that

$$F = \left(67.357 \frac{1}{\sqrt{J_2}} - 591.667 \frac{1}{J_2} \right) \times 10^{-6} \frac{\text{in.}^6}{\text{kips}^2} \dots \dots \dots (47)$$

for $J_2 > \frac{1}{3} \sigma_o^2 = 432 \text{ kips}^2 \text{ per in.}^4$

¹⁹ "Residual Stress and the Compressive Strength of Steel," by A. W. Huber and L. S. Beedle, *Welding Journal*, Vol. 33, December, 1954.

²⁰ "Description of Stress-Strain Curves by Three Parameters," by W. Ramberg and R. Osgood, *Technical Note 902*, National Advisory Committee for Aeronautics, Washington, D. C., 1943.

The Tangent Modulus in Shear.—Considering the case in which shear stresses, τ , are superimposed on a constant normal stress, σ_x , taking $\sigma_y = 0$ and $d\sigma_x = d\sigma_y = 0$, the relationships between the increments of stress and strain given by Eqs. 29 and 32 reduce to

$$d\epsilon_x = \frac{4}{3} F \sigma_x \tau d\tau \dots \dots \dots (48)$$

and

$$d\gamma = \frac{2(1+\nu)}{E} d\tau + 4 F \tau^2 d\tau \dots \dots \dots (49)$$

Integrating Eq. 49 gives the relationship between τ and γ , as shown in Fig.

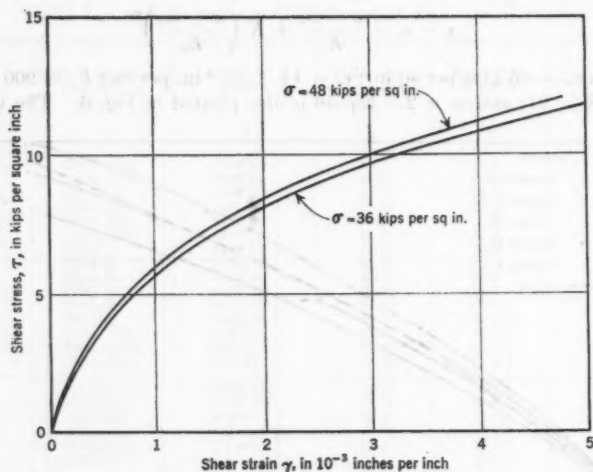


FIG. 7.—SUPERPOSITION OF SHEAR STRESS ON CONSTANT NORMAL STRESS

7, for $\sigma_x = 36$ kips per sq in. and $\sigma_x = 48$ kips per sq in. The corresponding slope,

$$G_t = \frac{d\tau}{d\gamma} \dots \dots \dots (50)$$

is plotted in Fig. 8.

It is seen from Fig. 8 that the value of G_t drops rapidly for small values of γ . However, in the region of 2,000 kips per sq in. $< G_t < 3000$ kips per sq in., the decrease becomes slower. Consequently, any value in this region could be selected as a useful value of G_t for the strain-hardening range of steel. Because of the results of torsional buckling tests on angle specimens presented subsequently, the value of $G_t = 2,400$ kips per sq in. is selected as being applicable to the strain-hardening range. From Fig. 7 it follows that the influence of the magnitude of the normal stress can be neglected for that part of the strain-hardening range under consideration.

Biaxial Normal Stresses.—For regions of a plate in which cross bending is important, the shear stresses are zero or very small—that is, the center of plates supported along all four edges or the fixed edge of a clamped outstanding flange.

In this case Eqs. 29 and 30 reduce to

$$d\epsilon_x = \left[\frac{1}{E} + \frac{1}{9} F (2\sigma_x - \sigma_y)^2 \right] d\sigma_x - \left[\frac{\nu}{E} - \frac{1}{9} F (2\sigma_x - \sigma_y) (2\sigma_y - \sigma_x) \right] d\sigma_y \quad (51)$$

and

$$d\epsilon_y = \left[\frac{1}{E} + \frac{1}{9} F (2\sigma_y - \sigma_x)^2 \right] d\sigma_y - \left[\frac{\nu}{E} - \frac{1}{9} F (2\sigma_x - \sigma_y) (2\sigma_y - \sigma_x) \right] d\sigma_x \quad (52)$$

Comparing Eqs. 51 and 52 with Eqs. 2 yields

$$\frac{1}{E_x} = \frac{1}{E} + \frac{1}{9} F (2\sigma_x - \sigma_y)^2 \quad (53)$$

$$\frac{1}{E_y} = \frac{1}{E} + \frac{1}{9} F (2\sigma_y - \sigma_x)^2 \quad (54)$$

$$\nu_x = \frac{\frac{\nu}{E} - \frac{1}{9} F (2\sigma_x - \sigma_y) (2\sigma_y - \sigma_x)}{\frac{1}{E} + \frac{1}{9} F (2\sigma_x - \sigma_y)^2} \quad (55)$$

and

$$\nu_y = \frac{\frac{\nu}{E} - \frac{1}{9} F (2\sigma_x - \sigma_y) (2\sigma_y - \sigma_x)}{\frac{1}{E} + \frac{1}{9} F (2\sigma_y - \sigma_x)^2} \quad (56)$$

For a perfectly plane plate ($\sigma_y = 0$), Eqs. 53 to 56 reduce to

$$E_x = E_t \quad (57)$$

$$E_y = \frac{4 E E_t}{E + 3 E_t} \quad (58)$$

$$\nu_x = \frac{E - (1 - 2\nu) E_t}{2 E} \quad (59)$$

and

$$\nu_y = \frac{2 E - (1 - 2\nu) E_t}{E + 3 E_t} \quad (60)$$

Eqs. 57 to 60 have been applied with different notation by Handelman and Prager.⁸

Eqs. 54 to 56 are valid only if

$$dJ_2 > 0 \dots\dots\dots (61)$$

or rewritten as

$$2 d\sigma_x - d\sigma_y > 0 \dots\dots\dots (62)$$

Eqs. 51 and 52 are valid provided that

$$(2 - \nu) d\epsilon_x - (1 - 2\nu) d\epsilon_y > 0 \dots\dots\dots (63)$$

Fig. 9 shows the assumed linear strain distribution due to curvatures dK_x

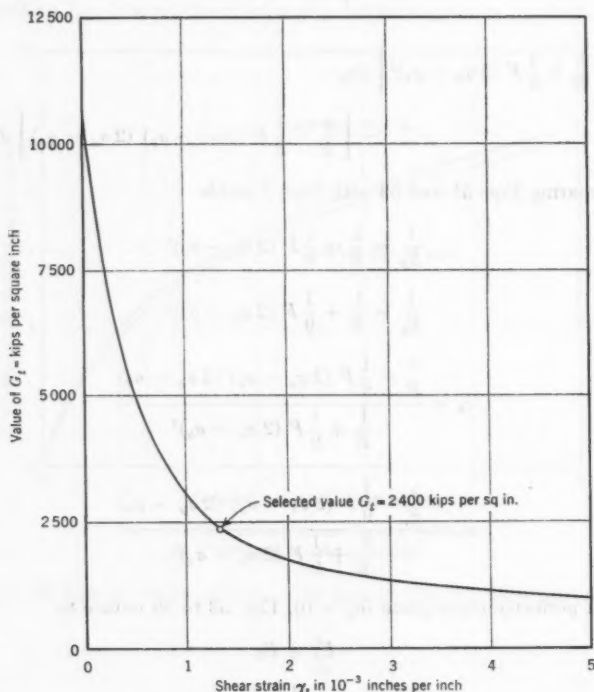


FIG. 8.—THE TANGENT SHEAR MODULUS

and dK_y in the x -direction and y -direction,

$$d\epsilon_x = d\epsilon_1 + z dK_x \dots\dots\dots (64)$$

and

$$d\epsilon_y = d\epsilon_2 + z dK_y \dots\dots\dots (65)$$

in which $d\epsilon_1$ and $d\epsilon_2$ are strain increments of the central plane in the x -direction and y -direction, and z is the distance to the central plane.

The condition that the entire section is deformed plastically is obtained by substituting Eqs. 64 and 65 into Eq. 63 as follows:

$$(2 - \nu) (d\epsilon_1 + z dK_x) - (1 - 2\nu) (d\epsilon_2 + z dK_y) > 0 \dots \dots (66)$$

for $-t/2 \leq z \leq t/2$.

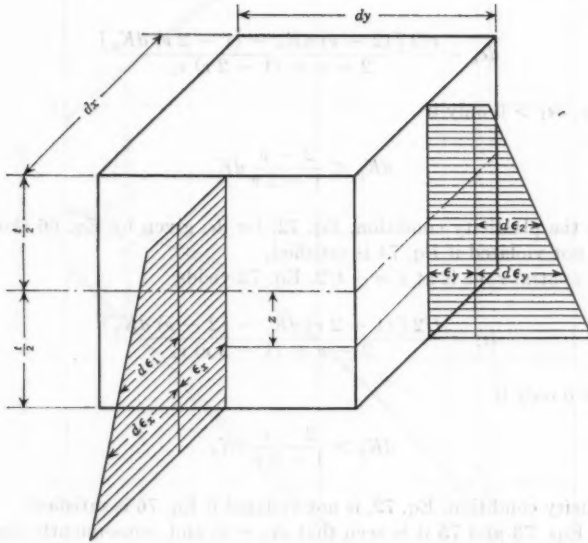


FIG. 9.—ASSUMED LINEAR STRAIN DISTRIBUTION

The increase of the force per unit width in the x -direction, N_x , is found by rearranging Eqs. 2 and integrating over the thickness of the plate—

$$dN_x = \int_{-t/2}^{t/2} (d\sigma_x) dz = D_x t (d\epsilon_1 + \nu_y d\epsilon_2) \dots \dots \dots (67)$$

The increase of the force per unit width in the y -direction is

$$dN_y = \int_{-t/2}^{t/2} (d\sigma_y) dz = D_y t (d\epsilon_2 + \nu_x d\epsilon_1) \dots \dots \dots (68)$$

However, no external forces are applied in the y -direction. Thus,

$$dN_y = 0 \dots \dots \dots (69)$$

or

$$d\epsilon_2 = -\nu_x d\epsilon_1 \dots \dots \dots (70)$$

Substituting Eq. 70 into Eq. 67 results in

$$dN_x = E_x t d\epsilon_1 \dots \dots \dots (71)$$

The plasticity condition, Eq. 66, becomes

$$[2 - \nu + (1 - 2\nu)\nu_x]d\epsilon_1 + (2 - \nu)z dK_x - (1 - 2\nu)z dK_y > 0 \quad (72)$$

for $-t/2 \leq z \leq t/2$.

If the neutral zone between loading and unloading zones is at $z = t/2$, Eq. 72 yields

$$d\epsilon_1 = \frac{t/2 [(2 - \nu) dK_x - (1 - 2\nu) dK_y]}{2 - \nu + (1 - 2\nu)\nu_x} \quad (73)$$

Obviously, $d\epsilon_1 > 0$ only if

$$dK_y < \frac{2 - \nu}{1 - 2\nu} dK_x \quad (74)$$

Checking the plasticity condition, Eq. 72, for $d\epsilon_1$ given by Eq. 66 shows that Eq. 72 is not violated if Eq. 74 is satisfied.

If the neutral zone is at $z = -t/2$, Eq. 72 yields

$$d\epsilon_1 = \frac{t/2 [(1 - 2\nu) dK_y - (2 - \nu) dK_x]}{2 - \nu + (1 - 2\nu)\nu_x} \quad (75)$$

and $d\epsilon_1 > 0$ only if

$$dK_y > \frac{2 - \nu}{1 - 2\nu} dK_x \quad (76)$$

The plasticity condition, Eq. 72, is not violated if Eq. 76 is satisfied.

From Eqs. 73 and 75 it is seen that $d\epsilon_1 = 0$, and, consequently, according to Eq. 71, $dN_x = 0$ for

$$dK_y = \frac{2 - \nu}{1 - 2\nu} dK_x \quad (77)$$

Furthermore, $dJ_2 = 0$ for the entire cross section. Thus,

$$d\sigma_x = \frac{1}{2} d\sigma_y \quad (78)$$

for an initially plane plate with $\sigma_y = 0$.

Because in the preceding case bending is not accompanied by an increase in the axial load, the influence of initial imperfections will be the greatest. Assuming that biaxial loading begins at $\sigma_x = \sigma_x^*$, $\sigma_y = 0$, $\epsilon_x = \epsilon_x^*$, $\epsilon_y = \epsilon_y^*$, it follows from Eq. 33 with Eq. 78 that initially,

$$dJ_2 = \frac{1}{2} \sigma_y d\sigma_y \quad (79)$$

If the ratio of $d\sigma_x$ and $d\sigma_y$ is taken according to Eq. 78 during biaxial loading, integrating Eq. 79 results in

$$J_2 = J_2^* + \sigma_y^2 = \frac{1}{2} \sigma_x^{*2} + \sigma_y^2 \quad (80)$$

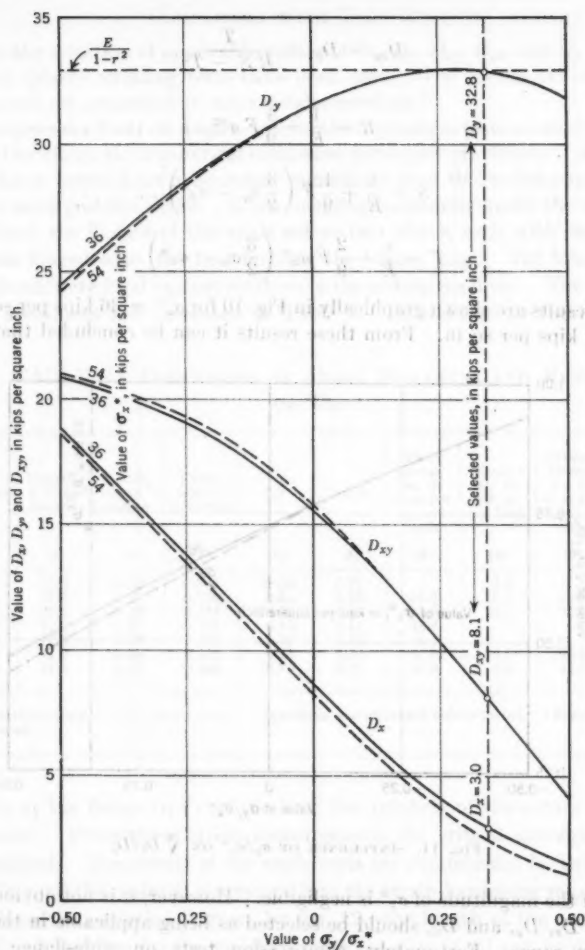


FIG. 10.—INFLUENCE OF σ_y/σ_x ON D_x , D_y , AND D_{xy}

Applying Eqs. 53, 54, 55, and 56 to the computation of the moduli, D_x , D_y , and D_{xy} , as defined by Eq. 6, yields

$$D_x = \frac{R S^2}{R S - T^2} \quad (81)$$

$$D_y = \frac{R}{R S - T^2} \quad (82)$$

and

$$D_{xy} = D_{yz} = \frac{T}{RS - T^2} \dots \dots \dots (83)$$

in which

$$R = \frac{1}{E} + \frac{4}{9} F \sigma_x^{*2} \dots \dots \dots (84)$$

$$S = \frac{1}{E} + \frac{1}{9} F \left(\frac{3}{2} \sigma_y - \sigma_x^* \right)^2 \dots \dots \dots (85)$$

$$T = \frac{\nu}{E} - \frac{2}{9} F \sigma_x^* \left(\frac{3}{2} \sigma_y - \sigma_x^* \right) \dots \dots \dots (86)$$

The results are shown graphically in Fig. 10 for $\sigma_x^* = 36$ kips per sq in. and $\sigma_x^* = 54$ kips per sq in. From these results it can be concluded that the in-

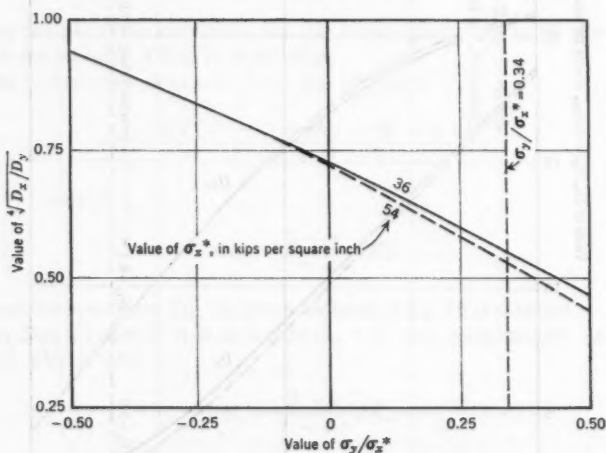


FIG. 11.—INFLUENCE OF σ_y/σ_x^* ON $\sqrt[4]{D_x/D_y}$

fluence of the magnitude of σ_x^* is negligible. However, it is not obvious which values of D_x , D_y , and D_{xy} should be selected as being applicable in the strain-hardening range. Fortunately, compression tests on wide-flange sections presented under the heading, "Comparison with Test Results: Tests on Wide-Flange Shapes," reveal that the ratios of the half-wave length of the buckled shape over the depth of the section for web-buckling cases are 0.55 and 0.54 (tests D4 and D6, respectively). According to Eq. 21 this ratio is equal to $\sqrt[4]{D_x/D_y}$ if the small restraining effects of the flanges are neglected. Fig. 11 shows the influence of σ_y/σ_x^* on $\sqrt[4]{D_x/D_y}$. Because of the results of the web-buckling tests, the values of D_x , D_y , and D_{xy} corresponding to $\sigma_y/\sigma_x^* = 0.34$ have been selected as applicable to the strain-hardening range. Thus, $D_x = 3,000$ kips per sq in.; $D_y = 32,800$ kips per sq in.; and $D_{xy} = D_{yz} = 8,100$ kips per sq in.

COMPARISON WITH TEST RESULTS

For the selection of applicable values of D_x , D_y , D_{xy} , D_{yz} , and G_t , the results of local (plate) buckling tests have been used. The results are summarized herein and are presented in more detail elsewhere.²¹

Compression Tests on Angles.—Several compression tests on angles were performed to check the theoretical estimates developed previously. Angle specimens have better-known boundary conditions than WF sections and therefore yield a more positive check. When buckling torsionally under the action of an axial load, the flanges of the angle act as two plates, each with one free edge and one hinged edge, the heel forming the hinged edge. The loaded ends of the column were fixed against rotation in the testing machine. The dimensions of all specimens are presented in Table 2. In addition to the longitudinal

TABLE 2.—DIMENSIONS OF ANGLE SPECIMENS AND RESULTS OF TESTS

Specimen	Length, 2 L, in inches	Width, b, in inches	Thick- ness, t, in inches	b/t	2 L/b	Yield stress, σ_y , in kips per square inch	Strain,* ϵ_{cr} , in 10 ³ in. per inch	Critical stress, σ_{cr} , in kips per square inch	Type of buckling
(1)	(2)	(3)	(4)	(5)	(6)	(7)	(8)	(9)	(10)
A-22 ^b	25.0	4.79	0.381	12.60	5.21	...	3.0	32.2	torsional
A-31 ^b	17.9	3.27	0.370	8.85	5.48	34.9	16.5	35.8	torsional
A-32 ^b	17.9	3.28	0.374	8.79	5.46	34.6	16.5	35.6	torsional
A-41 ^b	12.5	2.31	0.377	6.13	5.41	35.3	bending
A-42 ^b	12.5	2.34	0.371	6.36	5.35	34.1	bending
A-33 ^a	17.5	3.30	0.378	8.73	5.30	41.3	16.0	46.4	torsional
A-51 ^a	21.2	4.07	0.380	10.70	5.21	41.0	6.0	41.2	torsional

* Critical strain corresponding to σ_{cr} . ^b Specimen was annealed before tested. ^a Specimen was tested as delivered.

strains at the flange tips and the heel, the rotation of the center section was measured. From the rotation measurements the critical average strain was determined. The results of the angle tests are summarized in Table 2.

When all the material is strained into the strain-hardening range ($\epsilon_{cr} \geq \epsilon_o$), the theoretical solution is given by Eq. 12—the length of the angle specimen is 2 L. A solution for the yielding range ($\epsilon_f < \epsilon_{cr} < \epsilon_o$) can be derived if the following assumptions are made:

1. The material is elastic up to the yield stress.
2. In the yield range the specimen is partly elastic and partly strain hardened.
3. The strain-hardening zones initiate at both ends and move toward the middle.

²¹ "On Inelastic Local Buckling in Steel, A Theoretical and Experimental Study with Recommendations for the Geometry of Wide-Flange Shapes in Plastic Design," by G. Haaijer and B. Thürlimann, Fritz Laboratory Report No. 205E.3, Lehigh Univ., Bethlehem, Pa., August, 1956.

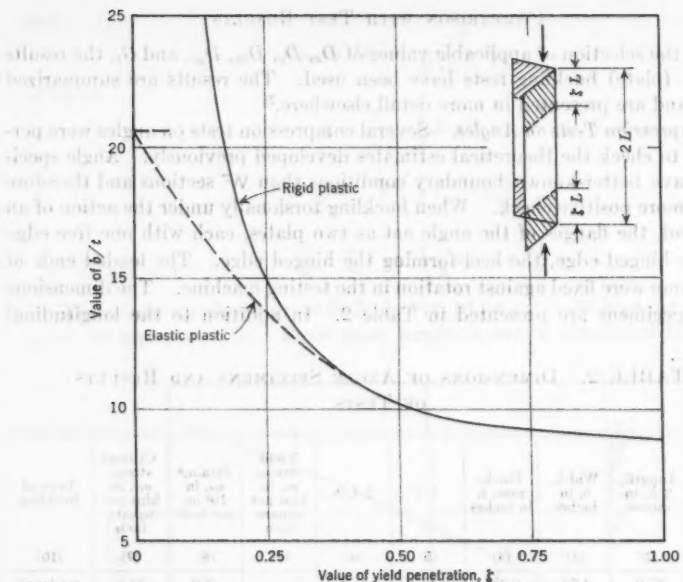
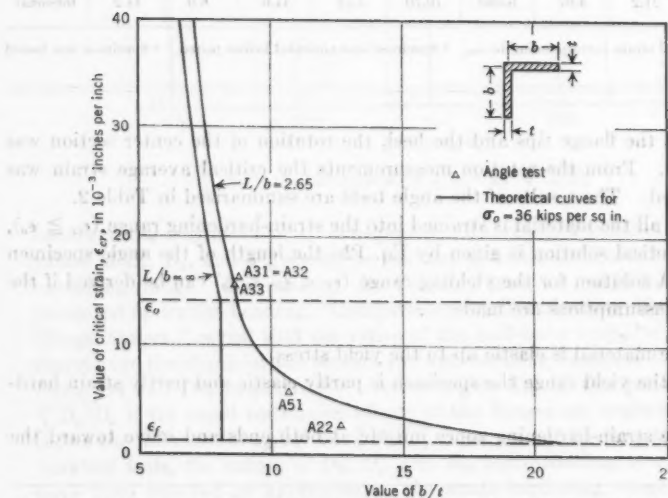
FIG. 12.—YIELD PENETRATION, ζ , AS A FUNCTION OF b/t FOR $L/b = 2.65$ 

FIG. 13.—TEST RESULTS AND THEORETICAL CURVES FOR TORSIONAL BUCKLING TESTS ON ANGLES

From the first assumption it follows that if $\sigma_{cr} \leq \sigma_o$, the critical stress is given by

$$\sigma_{cr} = \left(\frac{t}{b}\right)^2 \left[\frac{\pi^2 E}{12(1-\nu^2)} \left(\frac{b}{L}\right)^2 + G \right] \quad (87)$$

When σ_{cr} obtained from Eq. 87 exceeds σ_o , yielding will have begun. From the second assumption it follows that the middle section, being still elastic, is practically rigid compared with the yielded zones. Assuming that only the latter will deform results in the following expression for the buckling stress:

$$\sigma_{cr} = \sigma_o = \left(\frac{t}{b}\right)^2 \left[\frac{\pi^2 D_x}{12} \left(\frac{b}{\xi L}\right)^2 + G_t \right] \quad (88)$$

in which ξL is the length of each yielded zone.

TABLE 3.—DIMENSIONS OF WF SPECIMENS

Specimen	Shape	Flange width, 2 b, in inches	Flange thickness, t _f , in inches	Distance, d, in inches ^a	Web thickness, t _w , in inches	LENGTH		b/t _f	d/t _w
						L ^b in inches	L _t ^c in inches		
(1)	(2)	(3)	(4)	(5)	(6)	(7)	(8)	(9)	(10)
B1, D1	10WF33	7.85	0.429	9.37	0.294	32	32	9.2	31.9
B2, D2	8WF24	6.55	0.383	7.63	0.236	26	26	8.6	32.3
B3, D3	10WF39	8.02	0.512	9.37	0.328	32	32	7.8	28.6
B4, D4	12WF50	8.18	0.620	11.57	0.351	32	32	6.6	33.0
B5, D5	8WF35	8.08	0.476	7.65	0.308	32	32	8.5	24.8
B6, D6	10WF21	5.77	0.318	9.56	0.232	23	26	9.1	40.9

^a Distance between center planes of flanges. ^b Length of compression specimen. ^c Length of part of bending specimen subjected to pure bending.

The corresponding critical strain is

$$\epsilon_{cr} = (1 - \xi) \epsilon_f + \xi \epsilon_o \quad (89)$$

Substituting the values of D_x and G_t into Eq. 88 determines the relationship between b/t and ξ . For $L/b = 2.65$ (the average value of the tested sections), the (b/t versus ξ)-curve has been plotted in Fig. 12 as a solid line. Because elastic deformations have been neglected in Eq. 88, $b/t = \infty$ for $\xi = 0$. For this case, $b/t = 20.7$, which is found from Eq. 87 by taking $\sigma = 36$ kips per sq in. and $L/b = 2.65$. Knowing the rigid-plastic solution and the point for $\xi = 0$ of the elastic-plastic solution, the latter has been sketched in Fig. 12 as a dotted line. The elastic-plastic solution of b/t versus ξ with Eq. 89 yields ϵ_{cr} as a function of b/t for the range $\epsilon_f < \epsilon_{cr} < \epsilon_o$. The complete theoretical curves are shown in Fig. 13 for $L/b = \infty$ and $L/b = 2.65$, and are compared with the test results. The theoretical curves give a good description of the buckling strength.

Tests on Wide-Flange Shapes.—In order to investigate the actual behavior of WF shapes with regard to local buckling, six different shapes were tested

under two loading conditions: (a) Axial compression (test D1, D2, D3, D4, D5, and D6), and (b) pure bending (test B1, B2, B3, B4, B5, and B6). The dimensions of all *W*F specimens are given in Table 3, and the test results are summarized in Table 4.

TABLE 4.—RESULTS OF *W*F TESTS

Test	Yield stress, σ_e , in kips per square inch	CRITICAL STRAIN, ϵ_{cr} , IN INCHES PER INCH		CRITICAL STRESS, σ_{cr} , IN KIIPS PER SQUARE INCH		Flange l/b	Web l/d	Type of buckling
		Flange	Web	Flange	Web			
(1)	(2)	(3)	(4)	(5)	(6)	(7)	(8)	(9)
D1	34.4	8.5	8.5	34.2	34.2	1.8	0.56	flange
D2	34.0	13.5	12.7	34.0	34.0	1.5	0.50	flange and web
D3	35.2	19.0	19.0	39.0	39.0	1.5	0.46	flange
D4	35.0	18.5	5.0	36.8	35.4	1.5	0.55	web
D5	36.6	17.0	17.0	38.0	38.0	2.1	0.56	flange
D6	38.0	4.3	1.6	33.8	37.2	...	0.54	flange
B1	...	7.0	2.4	...	web
B2	...	23.0	2.0	...	flange and lateral
B3	...	22.5	2.2	...	flange and lateral
B4	...	29.0	lateral
B5	...	22.0	2.0	...	flange and lateral
B6	...	14.0	2.4	...	flange and lateral

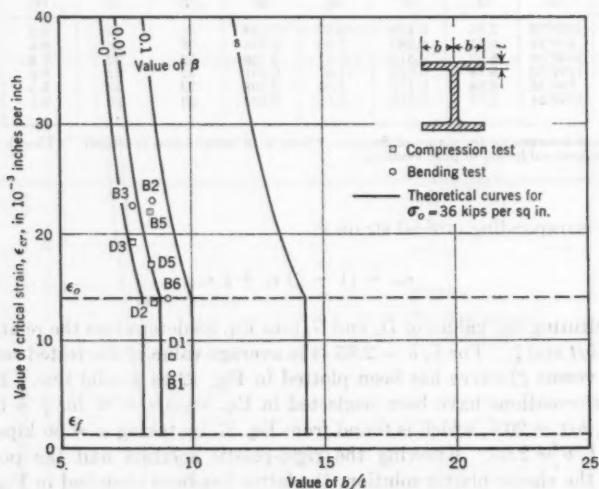


FIG. 14.—TEST RESULTS AND THEORETICAL CURVES FOR BUCKLING OF WIDE-FLANGE SHAPES

For the cases in which flange buckling was predominant, the critical strains of the flanges versus the (b/t) -ratios and the theoretical curves are plotted in Fig. 14. The theoretical solution is given by Eq. 10. The results of tests D4 and D6 are omitted because web buckling occurred first and obviously caused

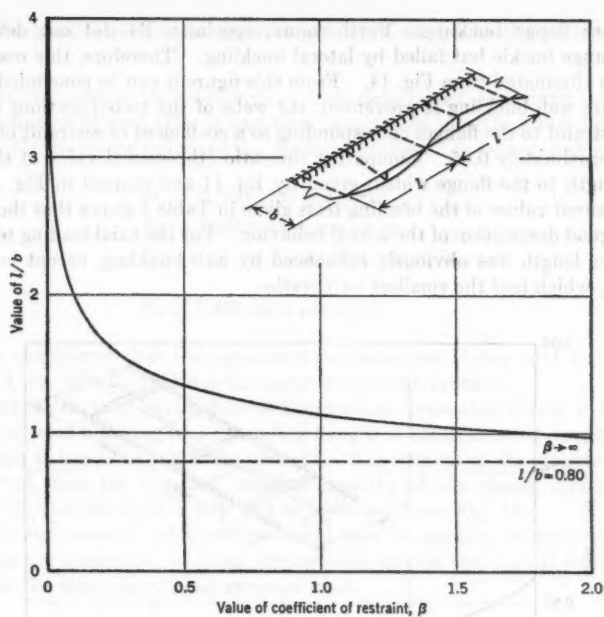


FIG. 15.—HALF-WAVE LENGTH OF OUTSTANDING FLANGES

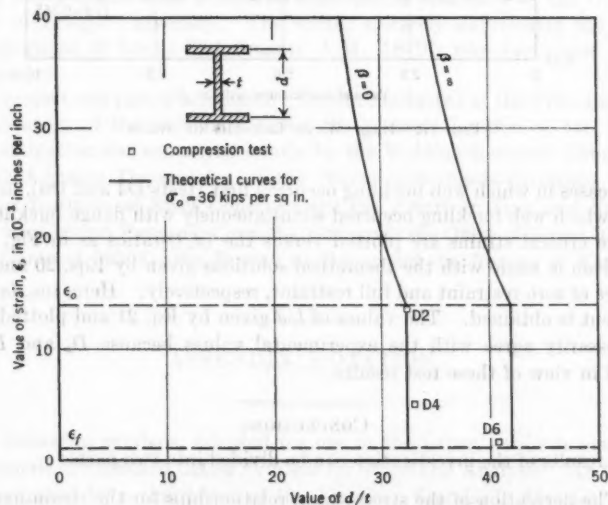


FIG. 16.—UNIFORM COMPRESSION TEST RESULTS AND THEORETICAL CURVES FOR BUCKLING OF WEBS OF WIDE-FLANGE SHAPES

premature flange buckling. Furthermore, specimen B4 did not develop a major flange buckle but failed by lateral buckling. Therefore, this result also has been eliminated from Fig. 14. From this figure it can be concluded that if premature web buckling is prevented, the webs of the tested sections provide some restraint to the flanges corresponding to a coefficient of restraint of β from 0 to approximately 0.05. Comparing the ratio (theoretical value of the half-wave length to the flange width) given by Eq. 11 and plotted in Fig. 15 with the measured values of the bending tests given in Table 4 shows that the theory gives a good description of the actual behavior. For the axial loading tests, the half-wave length was obviously influenced by web buckling, except for specimen D5, which had the smallest (d/t)-ratio.

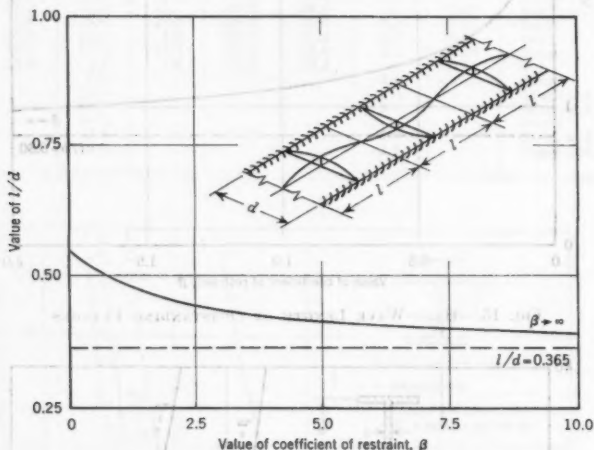


FIG. 17.—HALF-WAVE LENGTHS OF WEBS

For cases in which web buckling occurred first (tests D4 and D6), or for the case in which web buckling occurred simultaneously with flange buckling (test D2), the critical strains are plotted versus the (d/t)-ratios as in Fig. 16. A comparison is made with the theoretical solutions given by Eqs. 20 and 22 for the cases of zero restraint and full restraint, respectively. Here, too, favorable agreement is obtained. The values of l/d given by Eq. 21 and plotted in Fig. 17 necessarily agree with the experimental values because D_x and D_y were selected in view of these test results.

CONCLUSIONS

The results of the investigation can be divided into two parts:

- a. The derivation of the stress-strain relationships for the strain-hardening range of structural steel; and

b. The application of the stress-strain relationships to the plate-buckling problem.

Effective stress-strain relationships were determined describing the orthotropic behavior of steel after it had been compressed into the strain-hardening range. The following values of the moduli were found to be applicable:

$$D_x = 3,000 \text{ kips per sq in.}$$

$$D_y = 32,800 \text{ kips per sq in.}$$

$$D_{xy} = D_{yz} = 8,100 \text{ kips per sq in.}$$

and

$$G_t = 2,400 \text{ kips per sq in.}$$

It is considered that the agreement between the theory and test results (Figs. 13, 14, and 16) justifies this approach to the problem.

A direct practical application of the findings presented herein is the prevention of local buckling of outstanding flanges in continuous frames, in which the design is based on ultimate strength. The strains of the flanges can be determined from the required rotation capacity of the plastic hinges. The required (b/t) -ratio for $\beta = 0.01$ can be obtained from Fig. 14.

These stress-strain relationships could also be applied to other problems involving the occurrence of shear stresses and strains and biaxial stresses and strains in the strain-hardening range of steel.

ACKNOWLEDGMENTS

This paper is based on a doctoral dissertation presented to the Graduate Faculty of Lehigh University. The writer sincerely appreciates the advice and suggestions of Bruno Thürlimann, A.M. ASCE, who supervised the research project.

The project was part of a research program conducted at the Fritz Engineering Laboratory of the university under the general direction of Mr. Beedle. The investigation was sponsored jointly by the Welding Research Council and the United States Department of the Navy, with funds furnished by the American Institute of Steel Construction; the American Iron and Steel Institute; the Column Research Council (Advisory); the Office of Naval Research (under Contract 39303); the Bureau of Ships; and the Bureau of Yards and Docks.

APPENDIX. NOTATION

The following symbols, adopted for use in the paper, conform essentially with "American Standard Letter Symbols for Structural Analysis" (ASA Z10.8-1949), prepared by a committee of the American Standards Association with Society representation, and approved by the Association in 1949:

Tensor Notation.—

F = function defined by Eq. 24;

f = yield and loading function;

i, j, k, l, m = letter subscripts taking the values 1, 2, and 3;

J_2 = second invariant of deviatoric stress tensor;

k = constant;

s = mean normal stress;

s_{ij} = components of deviatoric stress tensor;

x_i = coordinate axis;

δ_{ij} = Kronecker δ ;

ϵ = strain:

ϵ_{ij} = components of strain tensor;

$(\epsilon_{ij})^e$ = elastic strain component;

$(\epsilon_{ij})^p$ = plastic strain component; and

σ_{ij} = components of stress tensor.

Engineering Notation.—

A, a_1, a_2 = constants;

B = constant;

b = width of plate with one free edge;

$C_1, C_2, C_3, C_4, C_5, C_6, C_7$ = constants;

c_1, c_2, c_3, c_4 = constants;

$$D_x = \frac{E_x}{1 - \nu_x \nu_y};$$

$$D_y = \frac{E_y}{1 - \nu_x \nu_y};$$

$$D_{xy} = \nu_y D_x;$$

$$D_{yx} = \nu_x D_y;$$

d = depth of section;

d_w = width of plate supported along all four edges;

E = modulus of elasticity:

E_t = tangent modulus;

E_x = tangent modulus in the x -direction;

E_y = tangent modulus in the y -direction;

E_o = strain-hardening modulus;

f = ratio of \bar{y} to depth of simplified column;

f_o = value of f at initiation of strain hardening;

f_s = value of f at which strain reversal takes place;

G = modulus of elasticity in shear:

G_t = tangent modulus in shear;

H = function defined in Eq. 6;

h = thickness of sheet forming simplified cruciform section;

I = moment of inertia per unit width of plate;

K = constant:

- K_x = curvature of plate in the x -direction;
 K_y = curvature of plate in the y -direction;
 K_{xy} = twist of plate;
 L = length of angle specimen;
 l = half-wave length of buckled shape;
 M = bending moment:
 M_x = bending moment per unit width of plate in the x -direction;
 M_y = bending moment per unit width of plate in the y -direction;
 M_{xy} = torsional moment per unit width of plate;
 N_x = axial force per unit width of plate in the x -direction;
 N_y = axial force per unit width of plate in the y -direction;
 m = exponent in Eq. 46;
 n = ratio of modulus of elasticity to tangent modulus;
 n' = ratio defined by Eq. 45;
 R = function defined by Eq. 84;
 S = function defined by Eq. 85;
 T = function defined by Eq. 86;
 t = thickness of plate;
 w = deflection of plate;
 y = deflection of simplified column;
 \bar{y} = maximum value of y ;
 $\beta = B/A$ = coefficient of restraint;
 γ = shear strain;
 γ_{xy} = angular strain in (xy) -plane;
 ϵ = strain:
 ϵ_{cr} = critical strain corresponding to σ_{cr} ;
 ϵ_f = yield strain;
 ϵ_o = strain at initiation of strain hardening;
 ϵ_x = normal strain in the x -direction;
 ϵ_x^* = value of ϵ_x at which biaxial loading begins;
 ϵ_y = normal strain in the y -direction;
 ϵ_y^* = value of ϵ_y at which biaxial loading begins;
 ζ = coefficient determining length of yielded zone;
 θ = angle of twist per unit length;
 ν = Poisson's ratio:
 ν_x = coefficient of dilatation for stress increment in the x -direction;
 ν_y = coefficient of dilatation for stress increment in the y -direction;
 σ = stress:
 σ_{cr} = critical (buckling) stress;
 σ_e = elastic buckling stress;

σ_o = yield stress;

σ_s = value of σ at which strain reversal takes place;

σ_t = tangent modulus stress = $\frac{\pi^2 E_t}{(l/r)^2}$;

σ_x = normal stress in the x -direction;

σ_x^* = value of σ_x at which biaxial loading begins;

σ_y = normal stress in the y -direction;

τ_{xy} = shear stress;

χ = function defined by Eq. 45; and

ψ = edge moment per unit length to produce unit rotation of edge.

AMERICAN SOCIETY OF CIVIL ENGINEERS

Founded November 5, 1852

TRANSACTIONS

Paper No. 2969

HIGHWAY PLANNING IN THE PAST, PRESENT, AND FUTURE

BY EDWARD H. HOLMES¹ AND JOHN T. LYNCH,² A. M. ASCE

SYNOPSIS

Highway planning on a comprehensive scale has been conducted jointly by the Bureau of Public Roads, United States Department of Commerce (BPR), and the state highway departments since 1935. Facts have been assembled and highway needs determined that have greatly affected state and federal legislation. Methods must be perfected in order to keep the studies of the needs up to date and to project them into the future.

INTRODUCTION

Highway planning on a national scale has evolved largely from several important acts of the United States Congress over a forty-year period. The 1956 Federal-Aid Highway Act,³ providing for the present program, was signed just forty years after the signing of the Federal-Aid Road Act of 1916,⁴ which marked the beginning of the state and federal partnership in road building.

SELECTION OF FEDERAL-AID SYSTEM

The state and federal partnership consists of the Bureau of Public Roads, United States Department of Commerce (BPR), and the highway department of each state. The first extensive joint planning undertaking was the selection of the federal-aid system of highways provided for in the Federal Highway Act of 1921.⁵ In the earlier years of road building, the automobile had been regarded as a pleasure vehicle rather than as an important means of transportation. Consequently, comparatively short sections of roads were built out from

NOTE.—Published, essentially as printed here, in July, 1957, in the Journal of the Highway Division, as *Proceedings Paper 1298*. Positions and titles given are those in effect when the paper was approved for publication in *Transactions*.

¹ Asst. Commr. for Research, Bureau of Public Roads, U. S. Dept. of Commerce, Washington, D. C.

² Chief, Highway Planning Branch, Bureau of Public Roads, U. S. Dept. of Commerce, Washington, D. C.

³ *Federal-Aid Highway Act*, approved June 29, 1956, 84th Cong., 2d Session, 70 Stat., 374.

⁴ *Federal-Aid Road Act*, approved July 11, 1916, 64th Cong., 1st Session, 39 Stat., 355.

⁵ *The Federal Highway Act*, approved November 9, 1921, 64th Cong., 1st Session, 42 Stat., 212.

cities into the country with little regard to transportation needs. As the automobile was improved and ownership became more widespread, the idea of a highway transportation network became established.

The laying out of the federal-aid system, which was limited by law to 7% of the rural road mileage existing in each state, was not difficult. It consisted mainly of selecting routes that would connect all important population centers, disregarding the state lines.

The idea of a continuous, nationwide system of roads was advanced still further by the adoption of a United States numbered system in 1925, composed of important through routes extending entirely across the United States. It was not an administrative system but simply a basis for route marking as a guide for motorists.

CLOSING THE GAPS

With the adoption of a federal-aid system and the marking of through routes, the demand of the public was to "close the gaps." With state highway-user tax and other funds, supplemented in some cases by bond issues and federal-aid funds, this task was largely completed by the early 1930's. At that time, it was possible to travel from almost any point in the United States to almost any other point on smooth all-weather roads except for a few miles at either end of the journey.

The problem facing road builders during this period of completing the through routes was fairly definite and simple. The system on which funds were to be expended was set forth, and the work of constructing the system progressed as rapidly as funds became available. Considerable research was undertaken by the various states and the federal government to aid in the establishment of specifications and standards of construction. However, road types and standards were governed by definite cost limitations to permit the construction of the greatest possible mileage in the shortest possible time.

PROBLEMS ARISE

In the early 1930's different and far more complex problems were faced due largely to the rapid change in the character of highway transportation. Increases in automobile ownership, traffic volumes, vehicle speeds, and in the number and weight of trucks were far greater than could be anticipated by the engineers of the early road-building days. If they had been anticipated they could not have been provided for because of the popular demand to use every available dollar to build all-weather surfaces on the through routes. Hence, early highways were entirely inadequate for the increased service demanded of them—that is, as to surface thickness, width, grade, and alinement.

Because the gaps in the important through routes were generally closed, there was an increasing public demand to extend the state system mileage to include roads of lesser importance, transfer parts of the state highway-user taxes to local agencies for the improvement of local roads, and divert other parts to nonhighway purposes. Thus, highway departments were faced with increasing responsibilities without correspondingly increased revenues. The public did not realize the extent of the modernization and replacement problem,

and there was a need to collect, analyze, and publicize the facts if public support was to be gained for an adequate highway program.

Other important problems required the collection and analysis of facts. One problem was the selection of the secondary or feeder roads on which federal funds might be expended, as provided for in the Federal-Aid Highway Act of 1936⁶ and subsequent legislation. Another problem dealt with trucks, which were rapidly increasing in numbers, size, weights transmitted to the pavement, and range of operation. It was necessary to know the changes in design needed to accommodate these vehicles, the damage they were doing to the highways, the limitations that should be imposed on them, and how and to what degree they should be taxed. It became clear to those who had devoted much thought to highway problems that there was an urgent need for the collection and analysis of facts concerning highways (and the vehicles that use them) on a much more comprehensive scale than had ever before been attempted.

HIGHWAY PLANNING SURVEY INITIATED

Beginning with the Federal-Aid Highway Act of 1934,⁷ Congress provided that 1½% of the federal-aid funds apportioned for any year to any state could be used for surveys, plans, and engineering and economic investigations of projects for future construction. Beginning in the autumn of 1935, the states, one by one, took advantage of this provision in the federal law and entered into an agreement with the BPR relative to conducting a comprehensive highway planning survey. Full state participation began in 1940 and is still continuing.

In the initiation of this cooperative undertaking, the BPR proposed studies, developed procedures, rendered technical assistance, and consolidated data for use in the study of national problems. The states proposed additional studies, set up work programs, made field surveys, and summarized and analyzed the results. The programs and reports have been subject to approval by the BPR in the discharge of its responsibilities with respect to the expenditure of federal funds.

FUNDS AVAILABLE

The funds available under the foregoing program have been reasonably adequate for the needed investigations, although not sufficient in relation to the magnitude of the problem. In the period from 1936 to 1939, unemployment relief funds, which were still available for highway work, were sufficient to permit the initial collection of information on a comprehensive scale. In 1940 federal 1½% funds were approximately \$2,000,000, and state matching funds almost equaled this sum. In 1955 federal funds were approximately \$8,000,000. Under the presently enlarged federal program the sums will be much greater, but the state funds will be considerably less than the federal funds because of the 90:10 matching ratio for the interstate system. Then, too, the need for information will be greater.

⁶ Federal-Aid Highway Act, approved June 16, 1936, 74th Cong., 2d Session, 49 Stat., 1519.

⁷ The Hayden-Carterwright Act, approved June 18, 1934, 73d Cong., 2d Session, Section 11, 48 Stat., 993.

The studies made by the states in the cooperative program have been supplemented by research projects conducted by the BPR with administrative funds. This research has resulted in improved procedures, better interpretation of survey results, and improvements in design, thus enhancing the usefulness of the data at both state and federal levels. The states have applied the results of the studies to their problems, and the BPR has applied them to federal problems and to problems common to all or many of the states.

The surveys have been conducted differently regarding various particulars in some states, but on the whole they have followed a practically uniform pattern, which will be described briefly.

ROAD INVENTORY

Initially, a complete inventory was made of all rural roads that were open to travel by the public in order to determine in detail the existing road facilities. Observers drove over every mile of road and recorded the width, type, and condition of all roadway surfaces; the type, dimensions, and condition of all structures; the location of all dwellings and other cultural features that are sources of traffic; and the physical characteristics of all railroad grade crossings. On the important routes they measured the location and degree of curvature of all sharp curves, the location and rate of all steep grades, and the location and nature of all restrictions to road visibility that might present a traffic hazard.

The inventory data were summarized by states³ and, in addition, a series of county maps was prepared in accordance with standards agreed on by all states, showing all public roads and their surface type in relation to the adjacent dwellings and other improvements. State maps, indicating the principal highways but not the cultural features, were also prepared. The maps are an extremely valuable tool for the use of the state highway organizations in their regular work, and, in addition, supply valuable information to other state, federal, and private agencies as well as individuals. They are generally sold at a price approximating their reproduction cost, and the demand for them has been great and continuous.

Most states have provided for the periodic reinventory and revision of county maps at varying intervals (generally five years). State maps are generally revised annually.

RURAL TRAFFIC SURVEY

A traffic survey was made consisting of several distinct phases. The two most important phases initially were the determination of the volumes of traffic by vehicles of different types on all rural roads, and the acquiring of information concerning weights and dimensions.

A sampling method was used to determine traffic volumes. Automatic traffic-recorder and control-station counts were used to establish factors to translate short counts, taken over the entire road network, into average daily traffic volumes. This procedure has been greatly refined over the years and is now placed on a firm statistical basis. Following the original survey, traffic

³ "State of Improvement of Rural Roads in Relation to Traffic and Dwelling Units Served," by John T. Lynch and Thomas B. Dimmick, *Public Roads*, Vol. 21, No. 8, October, 1940.

trends have been determined by the operation of continuous-count machines at selected points, and extensive traffic counts have been made periodically by sampling procedures.⁹ State traffic-flow maps have been prepared and, in general, are revised annually, whereas county traffic maps are revised at less frequent intervals.

Trucks were weighed and measured at a large number of stations located on important highways. The information obtained included (a) the type and some measure of the capacity of the vehicle; (b) the total weight and the load on each axle; (c) the width, height, length, and axle spacing; (d) the commodity carried and, when possible, the weight of the carried load; (e) the origin and the destination of the vehicle; and (f) other pertinent facts.¹⁰

The weight information has been kept current by trends established through annual weighings at selected points during comparable periods.^{11,12} In addition, most states have occasionally made more extensive weight surveys to determine variations in different hours and in different seasons, and on different classes of roads.

FINANCIAL AND MOTOR-VEHICLE-USE STUDIES

A group of financial studies was undertaken^{13,14} to determine the present relationship of street and highway finances to the finances of all other governmental operations within each state; to determine the ability of the state to finance the necessary highway maintenance, replacements, and improvements; and to indicate an equitable base for the assessment of highway-user taxes.

One of these studies was the road-use survey,¹⁵ in which a representative sample of motor-vehicle owners were interviewed to determine their annual travel and the class of roads and streets used for that travel. The data obtained made it possible to determine the proportional amount of travel on each of the road systems of the state, originating in the respective governmental jurisdictions. This information, correlated with that of the foregoing studies, indicated the relationship between the contributions to highways and the benefits obtained from their use. Most of the states made this study in the early period of the planning surveys, and twenty-three of them repeated it recently under somewhat modified procedures, known as the motor-vehicle-use study.¹⁶

⁹ "Applications of Automatic Traffic Recorder Data in Highway Planning," by L. E. Peabody and O. K. Normann, *Public Roads*, Vol. 21, No. 11, January, 1941.

¹⁰ "Amount and Characteristics of Trucking on Rural Roads," by John T. Lynch and Thomas B. Dimmick, *ibid.*, Vol. 23, No. 9, July-August-September, 1943.

¹¹ "Axle-Load and Gross-Load Trends," by John T. Lynch and Thomas B. Dimmick, *ibid.*, Vol. 25, No. 12, February, 1950.

¹² "Traffic and Travel Trends, 1956," by Thomas B. Dimmick, *ibid.*, Vol. 29, No. 11, December, 1957.

¹³ "Financial-Road Use Survey," *Legislative Document (1936)*, State of New York, Report prepared by Div. of Highway Transport, Bureau of Public Roads, U. S. Dept. of Commerce, Washington, D. C., Vol. 1, No. 115, 1936.

¹⁴ "Highway Planning Survey Data as a Basis for Highway Finance Policy," by Murray D. Van Wagoner, *Proceedings*, Highway Research Board, National Research Council, Washington, D. C., Vol. 20, 1940, pp. 141-157.

¹⁵ "Preliminary Results of Road-Use Studies," by Robert H. Paddock and Roe P. Rodgers, *Public Roads*, Vol. 20, No. 3, May, 1939.

¹⁶ "Motor-Vehicle-Use Studies in Six States," by Thurley A. Bostick, Roy T. Messer, and Clarence A. Steele, *ibid.*, Vol. 28, No. 5, December, 1954.

A fiscal study¹⁷ comprised an analysis of the financial reports of the state and its political subdivisions for one year. This analysis indicated the source of all revenues and classified expenditures as to whether they were used for highways (or streets), education, public welfare and services, or for government in general. The highway finance data are kept up to date from year to year.

The road-cost (or road-life) study^{18,19,20,21,22} involves research on highway investment, service lives, and depreciation of various road types on the state highway system. Since about 1938, most states have kept a continuing record of the mileages constructed and retired. Several states have also recorded their construction cost and have analyzed salvage values, thus permitting determinations to be made of the highway investment in terms of grading, surfacing, and structures.

Thus, with the acquired information it is possible for highway departments to estimate the rate at which highways wear out and to judge the cost of making needed replacements. Such information is extremely useful in scheduling long-range highway construction programs and in determining the rate at which highway needs will be met under various highway financing alternatives.

URBAN TRAVEL STUDIES

Another important group of studies included in the highway planning survey program are the urban-area travel studies.²³ These studies were not begun until 1944, at which time appreciable federal funds were made available for expenditure on federal-aid projects in urban areas as a result of the passage of the 1944 Federal-Aid Highway Act.²⁴

At that time, there was a lack of information on travel in urban areas that could be used as a basis for the planning of highway facilities that would best serve the public. In fact, no comprehensive survey methods had been developed that would give the necessary information. Because of the complex nature of the city street network and the shifting of travel from route to route in search of the most favorable one (or the least unfavorable), traffic volumes on existing streets are not a satisfactory guide to improvement. A study of the origin and destination of trips and the basic factors affecting travel was necessary.

Before the passage of the 1944 Federal-Aid Highway Act,²⁴ the BPR developed a method for studying urban travel that would give information in

¹⁷ "Highway Finance," *Bulletin No. 12*, Highway Research Board, National Research Council, Washington, D. C., 1948.

¹⁸ "Life Characteristics of Surfaces Constructed on Primary Rural Highways," by Robley Winfrey and Fred B. Farrell, *Proceedings*, Highway Research Board, National Research Council, Washington, D. C., Vol. 20, 1940, pp. 165-199.

¹⁹ "Life Characteristics of Highway Surfaces," by Fred B. Farrell and Henry R. Paterick, *ibid.*, Vol. 28, 1948, pp. 40-52.

²⁰ "A Procedure for Determining the Annual Cost of a Section of Rural Highway," by Harold W. Hansen, *Public Roads*, Vol. 26, No. 7, April, 1951.

²¹ "Lives of Highway Surfaces—Half Century Trends," by Gordon D. Gronberg and Nellie B. Blosser, *Proceedings*, Highway Research Board, National Research Council, Washington, D. C., Vol. 35, 1956, pp. 89-101.

²² "The Investment Analysis Approach to Estimating Highway Needs," by Fred B. Farrell, *ibid.*, pp. 9-13.

²³ "Origin-Destination Surveys and Traffic Volume Studies," by Robert E. Barkley, *Bibliography No. 11*, Highway Research Board, National Research Council, Washington, D. C., 1951.

²⁴ *Federal-Aid Highway Act*, approved December 20, 1944, 78th Cong., 2d Session, 58 Stat., 838.

anticipation of the provisions of the act with respect to urban funds.^{25,26} The method involved interviewing residents of a representative sample of dwelling units concerning their travel on a specified day. This was supplemented with information obtained at roadside interviews on all important routes entering the city, so that the travel by nonresidents of the area could be included in the study. Information was obtained on the origin and destination of trips, mode of travel, and trip purpose. Surveys based on these procedures have been or are being made in 139 urban areas, and are being completely repeated in twelve of these areas to provide current data. In 167 additional urban locations, traffic surveys have been made that are somewhat less comprehensive because they give information on automobile travel only.^{27,28}

These urban travel studies have been used in the planning of highway facilities, particularly expressway systems, and in determining the design features for these facilities.^{29,30,31} In order to be of maximum use for these purposes, the travel data must not only be brought up to date, but must be projected into the future. Much research is being performed by the BPR and other agencies in order to perfect the methods.^{32,33,34,35,36,37,38} The availability of electronic computers has made it possible to analyze large masses of data obtained in these surveys in order to establish relationships between travel and land use and other factors, so that future highway needs can be related to anticipated urban development.

SPECIAL RESEARCH STUDIES

In addition to the regular highway planning activities, there have been a number of special research studies associated with planning, paid for in part with highway planning survey funds and in part with other funds, including BPR administrative funds. One group of these studies deals with traffic

²⁵ "Traffic Planning Studies in American Cities," by John T. Lynch, *Public Roads*, Vol. 24, No. 6, October-November-December, 1945.

²⁶ "Conducting a Home Interview Origin-Destination Survey," *Procedure Manual 2B*, National Committee on Urban Transportation, Public Administration Service, Chicago, Ill., 1958.

²⁷ "Traffic Surveys by Post Cards," *Bulletin No. 41*, Highway Research Board, National Research Council, Washington, D. C., 1951.

²⁸ "Simplified Methods for Travel Studies in Smaller Cities," by Daniel O'Flaherty, *Proceedings*, Highway Research Board, National Research Council, Washington, D. C., Vol. 27, 1947, pp. 297-311.

²⁹ "Thoroughfares—Dallas Metropolitan Area, A Report on Existing and Proposed Traffic Facilities," Dept. of City Planning, Dallas, Tex., 1957.

³⁰ "Metropolitan Tulsa Expressways," prepared by the Tulsa Metropolitan Area Planning Comm., in cooperation with the Oklahoma State Dept. of Highways and the Bureau of Public Roads, U. S. Dept. of Commerce, 1957.

³¹ "Traffic Assignment," *Bulletin 61*, Highway Research Board, National Research Council, Washington, D. C., 1952.

³² "Highway Traffic Estimation," by Robert E. Schmidt and M. Earl Campbell, Eno Foundation for Highway Traffic Control, Saugatuck, Conn., 1956.

³³ "Traffic Forecast Based on Anticipated Land Use and Current Travel Habits," by Ramiro Ramirez Carril (Puerto Rico), *Proceedings*, Highway Research Board, National Research Council, Washington, D. C., Vol. 31, 1952, pp. 386-410.

³⁴ "Shopping Habits and Travel Patterns," by Alan M. Voorhees, Gordon B. Sharpe, and J. T. Stegmaier, *Special Report 11-B*, Highway Research Board, National Research Council, Washington, D. C., 1955.

³⁵ "Travel to Commercial Centers of the Washington Metropolitan Area," by Gordon B. Sharpe, *Bulletin 79*, Highway Research Board, National Research Council, Washington, D. C., 1953.

³⁶ "Forecasting Distribution of Interzonal Vehicular Trips by Successive Approximations," by Thomas J. Fratar, *Proceedings*, Highway Research Board, National Research Council, Washington, D. C., Vol. 33, 1954, pp. 376-384.

³⁷ "A General Theory of Traffic Movement," by Alan M. Voorhees, *The 1955 Past Presidents' Award Paper*, Inst. of Traffic Engrs., New Haven, Conn.

³⁸ "Factors Influencing Travel Patterns," *Bulletin 119*, Highway Research Board, National Research Council, Washington, D. C., 1956.

operations and with subjects such as driver behavior, highway accidents, and highway capacity.^{39, 40, 41, 42, 43, 44, 45, 46, 47, 48, 49, 50, 51} Another group consists of studies and tests relating axle-load frequencies to pavement damage and construction and maintenance costs.^{52, 53, 54}

TABLE 1.—HIGHWAY PLANNING SURVEY
FOR 1955

Item	Percent- age	Total percent- age
Traffic studies		
Traffic counting	20	46
Urban origin and destination	16	
Weight studies	3	
Special traffic studies	7	
Inventory and mapping		22
Financial studies		
Finance and statistics	5	11
Motor-vehicle use	2	
Highway cost and road life	4	
Special studies		18
Physical research		3
Total		100

tures on many subjects, such as the need for funds, the allocation of funds to different systems, the extent of the systems, and the size and weight limita-

PROGRAM COST BREAKDOWN

The relative sums spent for the various phases of the highway planning survey have varied from year to year. A breakdown of the program for 1955—typical of recent years—is shown in Table 1.

STATE USES OF THE DATA

The states began putting the survey results to use as soon as they could be analyzed by setting up road programs, determining priorities, designing individual projects, and in many other ways. The results have been used in reports to legisla-

³⁹ "Highway Capacity Manual," prepared by the Committee on Highway Capacity, Dept. of Traffic and Operations, Highway Research Board, published by Bureau of Public Roads, U. S. Dept. of Commerce, Washington, D. C., 1950.

⁴⁰ "The Influence of Alinement on Operating Characteristics," by O. K. Normann, *Proceedings*, Highway Research Board, National Research Council, Washington, D. C., Vol. 23, 1943, pp. 329-342.

⁴¹ "The Efficiency of Public Transit Operations in the Utilization of City Streets," by William P. Walker, and Roy A. Flynt, *Public Roads*, Vol. 29, No. 10, October, 1957.

⁴² "New Methods for Determining Capacity of Rural Roads in Mountainous Terrain," by O. K. Normann, James O. Granum, and Harry C. Schwender, *ibid.*, Vol. 30, No. 2, June, 1958.

⁴³ "How Access Control Affects Accident Experience," by Charles W. Priek, *ibid.*, Vol. 29, No. 11, December, 1957.

⁴⁴ "Effect of Roadway Width on Traffic Operation—Two-Lane Concrete Roads," by A. Taragin, *Proceedings*, Highway Research Board, National Research Council, Washington, D. C., Vol. 24, 1944, pp. 292-317.

⁴⁵ "Influence of Driver Characteristics on Passenger Car Operation," by O. K. Normann, *ibid.*, pp. 318-331.

⁴⁶ "Driver Performance on Horizontal Curves," by Asriel Taragin, *Public Roads*, Vol. 28, No. 2, June, 1954.

⁴⁷ "Lateral Placements of Trucks on Two-Lane Highways and Four-Lane Divided Highways," by Asriel Taragin, *ibid.*, Vol. 30, No. 3, August, 1958.

⁴⁸ "Stopping Ability of Motor Vehicles Selected from the General Traffic," by F. William Petring, *ibid.*, Vol. 29, No. 8, June, 1957.

⁴⁹ "Hill-Climbing Ability of Motor Trucks," by Carl C. Saal, *ibid.*, Vol. 23, No. 3, May, 1942.

⁵⁰ "Operating Characteristics of a Passenger Car on Selected Routes," by Carl C. Saal, *Bulletin* 107, Highway Research Board, National Research Council, Washington, D. C., 1955.

⁵¹ "Time and Gasoline Consumption in Motor Truck Operation as Affected by the Weight and Power of Vehicles and the Rise and Fall in Highways," *Research Report No. 9-A*, Highway Research Board, National Research Council, Washington, D. C., 1950.

⁵² "Road Test One-MD," *Special Report 4*, Highway Research Board, National Research Council, Washington, D. C., 1952.

⁵³ "The WASHO Road Test, Part 1: Design, Construction, and Testing Procedures," *Special Report 18*, Highway Research Board, National Research Council, Washington, D. C., 1954.

⁵⁴ "The WASHO Road Test, Part 2: Test Data, Analyses, Findings," *Special Report 22*, Highway Research Board, National Research Council, Washington, D. C., 1955.

tions of vehicles and road-user fees, especially license fees for trucks of different sizes.

Prior to World War II, some of the states prepared reports on highway needs, confined mainly to the state highway system. This was a good beginning, but it was not until after the war that really comprehensive studies of highway needs were made and reported. California was the first to issue a report⁵⁵ covering the total needs of all systems, in compliance with a legislative request. The report was under the general guidance of the Automotive Safety Foundation with headquarters in Washington, D. C. Extensive use was made of available highway planning survey data, supplemented with data from other sources, especially cities. More than one-half of the states have now made comprehensive highway-needs studies of this type.⁵⁶

FEDERAL USES

The BPR has correlated the data collected by the states and analyzed them to develop information of nationwide significance.

During the war the planning survey data were of special importance in such matters as the allocation of strategic materials, gasoline rationing, and the relaxation of weight restrictions for trucks. From an annually revised bridge record, the continuing needs of the armed services for helpful information in the routing of vehicles of unusual weights and dimensions are met.

Since the beginning of the war, traffic volume trends, vehicle miles of travel, ton-mileages hauled by trucks, and frequency of gross weights and axle loads of various magnitudes have been computed and published regularly. One of the important trends emphasized in these publications was the alarming increase in frequency of heavy axle loads that took place between 1936 and 1948.⁵⁷ Partly as a result of these findings, stricter enforcement and other measures taken by the states and truck operators have resulted in reducing the frequency of heavy axle loads considerably below the 1948 peak. However, there was a tendency during the period from 1954 to 1956 for the frequency of heavy axle loads to increase again.⁵⁸

The survey information has been used by the BPR in testimony before Congressional committees and in reports to Congress that have had an important effect on legislation. For example, a report⁵⁷ submitted to Congress in 1939 showed the impracticability of a nationwide system of toll roads and laid the groundwork for consideration of an interregional system of free roads. Other reports to Congress^{58,59} resulted in the setting up of what is presently known as the interstate system. This 40,000-mile system (before the adding of 1,000 miles in the 1956 act⁶⁰) constituted only about 1% of the road and

⁵⁵ "Engineering Facts and a Future Program, A Study for the California Legislature," by the Joint Fact-Finding Committee on Highways, Streets, and Bridges, 1946.

⁵⁶ "Objectives and Findings of Highway Needs Studies," by J. P. Buckley and Carl E. Fritts, *Proceedings, Highway Research Board, National Research Council, Washington, D. C.*, Vol. 28, 1948, pp. 1-13.

⁵⁷ "Toll Roads and Free Roads," *House Document No. 272*, 76th Cong., 1st Session, 1939, U. S. Govt. Printing Office, Washington, D. C.

⁵⁸ "Highways for the National Defense," *Senate Committee Print*, 77th Cong., 1st Session, 1941, U. S. Govt. Printing Office, Washington, D. C.

⁵⁹ "Interregional Highways," *House Document No. 379*, 78th Cong., 2d Session, 1944, U. S. Govt. Printing Office, Washington, D. C.

street mileage, but, when completed, it will carry approximately 20% of the total traffic.

Other reports to Congress^{60, 61, 62, 63} by the BPR have had important effects on federal legislation. One report⁶² laid the groundwork for the greatly expanded highway program provided for in the 1956 Federal-Aid Highway Act. None of these reports could have been compiled without the benefit of the comprehensive data collected in the highway planning surveys.

REQUIREMENTS OF THE 1956 ACT

The 1956 act calls for five major studies and reports. These will require an extensive analysis of planning survey data currently available and will necessitate the collection of additional data of a type not previously obtained.

The first study will deal with the determination of the cost of completing the interstate system in each state to standards adequate for anticipated 1975 traffic.⁶⁴ The study assumes special importance because the results will be used as a basis for apportioning funds among the states.

The principal role of the highway planning divisions in this undertaking is the forecasting of the 1975 design hourly volumes of traffic for each road section. This involves a study of traffic diversion, generation, and growth under anticipated conditions. These determinations are especially difficult because of the lack of experience with an extensive network of freeways proposed as a result of the Federal-Aid Highway Act of 1956.⁶⁵

The second study is to determine the maximum desirable dimensions and weights of vehicles operated on the federal-aid highway systems. The needed data are currently (1959) being obtained largely through a series of road tests and studies of vehicle operating costs conducted by the Highway Research Board (National Research Council) in cooperation with the BPR and other agencies. Also, a study is being made of road costs in relation to the actual frequency of weights on selected road sections as a part of the highway planning survey operation.

The third study is to provide Congress with information that will aid in making a determination with respect to reimbursement for highways on the interstate system (both free and toll) that were constructed approximately to interstate standards between 1947 and 1957.⁶⁶

The fourth study is to determine what steps can be taken by the federal government to promote highway safety. Some of the subjects to be explored

⁶⁰ "The Local Rural Road Problem," a report by the Bureau of Public Roads, U. S. Dept. of Commerce, to the Senate Subcommittee on Roads of the Committee on Public Works, January, 1950.

⁶¹ "A Factual Discussion of Motortruck Operation, Regulation, and Taxation," Statement submitted by Thomas H. MacDonald, Commr., Bureau of Public Roads, U. S. Dept. of Commerce, to the Senate Subcommittee on Domestic Land and Water Transportation of the Committee on Interstate and Foreign Commerce, June, 1950.

⁶² "Progress and Feasibility of Toll Roads and Their Relation to the Federal-Aid Program," *House Document No. 159*, 84th Cong., 1st Session, 1955, U. S. Govt. Printing Office, Washington, D. C.

⁶³ "Needs of the Highway Systems, 1955-84," *House Document No. 130*, 84th Cong., 1st Session, 1955, U. S. Govt. Printing Office, Washington, D. C.

⁶⁴ "A Report of Factors for Use in Apportioning Funds for the National System of Interstate and Defense Highways," *House Document No. 300*, 85th Cong., 2d Session, 1958, U. S. Govt. Printing Office, Washington, D. C.

⁶⁵ "Consideration for Reimbursement for Certain Highways on the Interstate System," *House Document No. 301*, 85th Cong., 2d Session, 1958, U. S. Govt. Printing Office, Washington, D. C.

are federal assistance to state and local governments in the adoption of uniform highway safety and speed laws, the promotion of highway safety in the manufacture of vehicles, safety educational programs, and design and physical characteristics of highways.

The fifth study is to aid Congress in determining what federal taxes should be imposed to insure, in so far as is practicable, an equitable distribution of tax burden among the various classes of persons using the federal-aid highways or those otherwise deriving benefits from them.^{66, 67, 68, 69, 70, 71, 72} It involves the determination of the extent to which vehicles of different classes use the highways of the different systems (urban as well as rural), the loads which they impose, and the cost of constructing and maintaining roads with design features adequate to accommodate these vehicles. It also involves a determination of operating savings because of superior design features, and an appraisal of indirect benefits. Much of the information needed in this study is not available at present (1959) and must be obtained. For example, weight surveys have previously been confined to rural roads and do not provide information as to weight frequencies on city streets.

The completion of these studies will tax the ingenuities and resources of the highway planning survey personnel at both the state and federal levels. The results will undoubtedly greatly influence federal legislation and will be far-reaching regarding the future of the highways.

HIGHWAY PLANNING BECOMES ESTABLISHED

In the late 1930's the idea of highway planning resulted in mixed reactions. Prior to that time there had been limited activity that might be termed planning, and it was only then that the idea of a comprehensive integrated effort to do a complete planning job was advanced. Some considered the new idea with enthusiasm; others were mildly skeptical yet were willing to wait and see what developed; others looked on the idea with considerable doubt or trepidation; and still others with a certain disdain or amusement. Today highway planning is a solidly established function in all state highway departments. Perhaps the hopes of the more enthusiastic have not been fully realized, but the skeptics have generally been convinced, the fears of others that some ritual of planning might supersede sound judgment has been proved unfounded, and, at present, no one is amused. This change represents no insignificant accomplishment because highway planning, like other new ideas in history, had to prove itself under trying and often adverse conditions.

⁶⁶ "First Progress Report of the Highway Cost Allocation Study," *House Document No. 106*, 85th Cong., 1st Session, 1957, U. S. Govt. Printing Office, Washington, D. C.

⁶⁷ "Second Progress Report of the Highway Cost Allocation Study," *House Document No. 344*, 85th Cong., 2d Session, 1958, U. S. Govt. Printing Office, Washington, D. C.

⁶⁸ "The Federal-Aid Highway Act of 1956—Its Implications, Benefits and the Problem of Highway Cost Allocation," by A. K. Branham, *Proceedings, A.A.S.H.O.*, 1957, pp. 12-25.

⁶⁹ "Highway Benefits and the Cost Allocation Problem," by R. M. Zettel, *ibid.*, pp. 25-38.

⁷⁰ "Estimate of User Taxes Paid by Vehicles in Different Type and Weight Groups," by Edwin M. Cope, John T. Lynch, and Clarence A. Steele, *Public Roads*, Vol. 28, No. 2, June, 1954.

⁷¹ "Road-User and Property Taxes on Selected Motor Vehicles, 1956," by Edwin M. Cope and Laurence L. Liston, *ibid.*, Vol. 29, No. 3, August, 1956.

⁷² "State Highway-User Taxes Paid in 1954 and 1955 on Vehicles of Various Type and Weight Groups," by Elizabeth Samson, *ibid.*, Vol. 29, No. 12, February, 1958.

However, planning is still far from the goal originally set. In general, the fundamental purpose of the activity was to place highway financing on a sound, continuing basis so that the cost of supporting the systems might be distributed as equitably as possible among the users and other beneficiaries. Additionally, facts should be provided on which the administrative and engineering officials can plan, construct, and operate the highway systems efficiently and in the best public interest. That this goal has not yet been reached is shown by the direction of the Congress in the 1956 act to study the costs and benefits of the federal-aid highway systems, and the actions now pending in many state legislatures that are working toward additional needed highway revenues. In effect, highway planners are being directed by legislative bodies to accomplish what they have been trying to do for twenty years. That the ultimate goal has not been reached is not necessarily grounds for criticism, despite the fact that progress should have been greater.

Highway planning is entering its third decade. In retrospect it can be seen that the first half of the first decade was spent largely in assembling basic facts and laying the groundwork for keeping them up to date. However, when the first turning point had been reached, World War II virtually put a stop to efforts to plan ahead. Nevertheless, the war served to focus attention on the importance of what had been accomplished previously. The important uses made of traffic and other data already available, or quickly supplied by the highway planning divisions, can be recalled during that period. The necessity of highway projects was demonstrated so that the slim supplies of critical material that could be spared were made available to the highway departments. The planning divisions aided in the routing of military convoys and war material shipments, and supported the need of gasoline and rubber to keep highway transportation alive. The war compelled highway planning to operate on a hand-to-mouth basis, as it did other highway functions. The war also brought to the attention of highway administrators the idea that facts that would convince rationing officials could be equally useful in developing the continuing peacetime programs. The planning function became established.

EMPHASIS ON HIGHWAY NEEDS

The second decade of highway planning began as the United States emerged from the war. Its highways had been regarded as expendable, and their condition was poor. With the resurgence of highway travel and the increasingly evident highway inadequacies, many states undertook the highway-needs studies described previously. During this decade greater attention was given to analysis and interpretation of the assembled facts as well as their use in forecasting future needs. Paralleling this activity as the decade continued was the growing interest in financial surveys and the development of long-range financing programs to meet the anticipated needs. Even considering this shifting of emphasis, collection of data was not forgotten. Great strides were made in improving methods and developing new techniques to improve the accuracy, extend the scope, and reduce the cost of the data needed for planning the expanding highway programs.

As highway planning enters its third decade it is solidly established under competent leadership in the states, adequately financed, yet handicapped, as

are all other highway functions, by staffs of insufficient size. In this situation several problems must be faced.

A current and more accurate appraisal of highway needs is necessary. Three of the five studies demanded by the 1956 act require a state-by-state and system-by-system reappraisal of the status of the highways and of the cost of putting them into condition to accommodate present and future traffic. Although this is a requirement of federal legislation, it is just as real a need in most of the states. Although over half the states have made detailed needs studies since the end of World War II, many of these studies are out of date or show that estimates of future needs were based on unrealistic forecasts of traffic volume increases. Assembling information, in response to the direction of Congress to aid in future national policy decisions, will absorb a major share of the efforts of the state highway planning divisions during the next few years, but the data obtained will be valuable to the states in providing the basic facts on which policies can be determined.

However, much more must be accomplished in order to take full advantage of this reinventory of needs that will soon be available. Perhaps the most obvious solution is to develop a means of keeping the needs surveys current. It will be only two years until the estimate of the cost of completing the interstate system must be revised under the terms of the 1956 act. The state legislatures should be equally interested in periodic appraisals of state highway needs. The groundwork should be laid for continuing inventories.

NEED FOR STUDYING HIGHWAY BENEFITS

Beyond this step several important areas require much attention. First is the development of a more accurate and refined method of determining the benefits resulting from the existence and use of the highway systems. With the increasing demands for funds for all governmental purposes in the years ahead, means must be developed not only to estimate highway costs, but also to appraise their benefits if the public is expected to support its highway systems to a justifiable degree. Therefore, questions such as the following must be answered:

- a. What actual savings in vehicle operating costs result from highway improvement?
- b. What is the actual value of time saved by passenger or commercial vehicles?
- c. What are the actual benefits to property newly served by new or improved highways?

Satisfactory answers to these questions will be forthcoming only with far more comprehensive and precise data than are available (as of 1957).

LONG-RANGE PROGRAMING DESIRABLE

It is necessary to develop practicable means of carrying the findings of the statewide and systemwide needs studies to the next logical step—the preparation of long-range construction programs that will give first priority to the most urgent projects. Many devices have been used, one being the sufficiency rating scheme, which is, perhaps, the most widely accepted. This device has

advantages not possessed by others. Nevertheless, it is still far from the scientific approach that could be developed with skill and imagination. The sufficiency rating has been compared to a sieve test for aggregates to be used in construction. It is a useful and essential test, but by no means an exclusive basis for decision. Although projects in an annual program cannot be selected with the same objectivity as aggregates for paving mixtures, there is a great need for the development of a sounder basis for orderly long-range programming.

COORDINATION WITH PLANNING AGENCIES

Another major effort would be the coordination of highway planning with city and regional planning in and around urban areas.⁷³ Within the immediate future, highway construction under the interstate program alone will have a profound effect on the growth and development of urban areas for many years to come. If properly located and designed, the new planned-access highways can stimulate desirable growth. If they are executed improperly they can retard or even prevent the development best suited for the area. Little that will be accomplished in public or private works will be of more permanent character than the highways that soon will be seen in every metropolitan area.

The problem of urban highway development probably receives more widespread attention than any other phase of the highway program. The National Committee on Urban Transportation, the joint committee of the American Municipal Association, the American Association of State Highway Officials, and the Committee on Urban Research of the Highway Research Board are actively attacking this problem from different directions.

Research and planning must actively cooperate if there is to be assurance that the funds entrusted to the highway departments are being wisely spent. Highway engineers have never before been in the position in which correct decisions can accomplish so much good and where wrong decisions can be so costly. They should not be required to make such decisions alone, nor should they be faced with the necessity of projecting highways into an area uncertain of its own plans for the future. The engineers should be supported and counseled by the city and regional authorities, who should be ready with sound plans for over-all development and plans that not only have the assured support of all area officials, but of the public as well. Certainly, nothing that has been undertaken in highway planning demands more patient, skillful, objective analysis than the problem of coordination of planning in urban areas, nor does any effort promise more fruitful results. The tremendous population growth forecast for the two decades ahead will take place largely in the areas surrounding the present cities. They are areas of mutual interest to federal, state, and local officials that cannot be allowed to become areas of disagreement.

Fortunately, the work of highway planning and traffic researchers in the past few years has opened up the prospects of relating travel to land use, and, consequently, of predetermination of highway needs in any area whose growth pattern can be forecast. Conversely, the growth pattern related to any pro-

⁷³ "Better Transportation for Your City, A Guide to the Factual Development of Urban Transportation Plans," prepared by the National Committee on Urban Transportation, published by the Public Administration Service, Chicago, Ill., 1958.

posed highway development can be forecast equally well. High-speed computers make relatively easy analyses that hitherto were virtually impossible, and once the basic facts of travel habits are recorded, the desired answers can be turned out with great rapidity. The facts that can be produced in this area should provide grounds for a meeting of the minds of state and local planners and other officials, an end often more difficult to achieve than provision for the physical meeting of the expressways that their plans envision.

OTHER AREAS TO BE EXPLORED

There are many other areas in which effort will be expended in the subsequent ten years. More precise means will be required to estimate future traffic growth and to coordinate better the results of physical research with structural design in order to produce highways consistent with future traffic. More uniformity in motor-vehicle registration practices and means of classifying vehicles in the registration records consistent with visual classification on the road are essential to studies of highway taxation. The road-life studies should be extended and expanded to include analyses of the life of the investment in the highway plant as well as its physical life expectancy. Improvement of the management of the highway departments and of the basic laws under which they operate are obviously needed and will be studied. Development and application of techniques to insure efficient operation of the costly high-volume expressways and to find the answers to the tragic loss of life and the staggering economic loss of traffic accidents are areas in which the need is great but in which insufficient progress has been made. Still others could be named, and areas not presently visible will become apparent in the future.

CONCLUSIONS

Those who have been associated in one way or another with highway planning since its inception can take pride in the accomplishments and remarkable progress over a period of two decades. They can anticipate a period in which they must carry forward routine planning activity as well as explore and exploit uncharted areas to assure that the inevitable expansion in transportation is orderly and beneficial. They can see the need to bring new skills and disciplines to bear on new problems as they become more complex and their solutions more difficult.

AMERICAN SOCIETY OF CIVIL ENGINEERS

Founded November 5, 1852

TRANSACTIONS

Paper No. 2970

ANALYSIS OF CONTINUOUS BEAMS BY FOURIER SERIES

BY SENG-LIP LEE,¹ A. M. ASCE

WITH DISCUSSION BY MESSRS. STEFAN J. MEDWADOWSKI,
AND SENG-LIP LEE

SYNOPSIS

The analysis of continuous beams by infinite trigonometric series is examined. The values of the redundant reactions corresponding to any load distribution are determined by the application of Castigliano's theorem. The same procedure is used to derive expressions for the influence lines for the reactions.

INTRODUCTION

Notation.—The letter symbols adopted for use in this paper are defined where they first appear, and are arranged alphabetically for convenience of reference in the Appendix.

General.—Continuous beams can be analyzed by expanding an arbitrary load function and the intermediate redundant reactions into infinite trigonometric series.² The differential equation of the deflection of a beam of constant cross section under an arbitrary transverse load, $p(x)$, is

$$EI \frac{d^4 y}{dx^4} = p(x) \dots \dots \dots (1)$$

in which E is the modulus of elasticity and I is the moment of inertia of the beam. The general solution of Eq. 1 is

$$y(x) = C_1 + C_2 x + C_3 x^2 + C_4 x^3 + y_p(x) \dots \dots \dots (2)$$

NOTE.—Published, essentially as printed here, in October, 1957, in the *Journal of the Engineering Mechanics Division*, as *Proceedings Paper 1369*. Positions and titles given are those in effect when the paper or discussion was approved for publication in *Transactions*.

¹ Associate Prof. of Civ. Eng., Northwestern Technological Inst., Northwestern Univ., Evanston, Ill.

² "Mathematical Methods in Engineering," by T. Von Kármán and M. A. Biot, McGraw-Hill Book Co., Inc., New York, N. Y., 1940, p. 323.

in which y_p is a particular solution of Eq. 1. For a simply supported beam of span l , the boundary conditions,

$$y(0) = y(l) = y''(0) = y''(l) = 0 \dots \dots \dots (3)$$

provide four equations for the determination of the constants of integration, C_1 , C_2 , C_3 , and C_4 .

ELASTIC CURVE

The continuous beam shown in Fig. 1 can be treated as a simply supported beam of span l , subjected to the action of a given load, $q(x)$, and the reactions

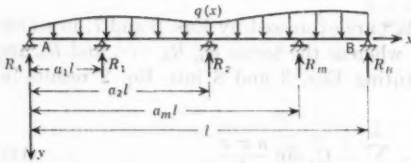


FIG. 1.—CONTINUOUS BEAM SUBJECTED TO A GIVEN LOAD

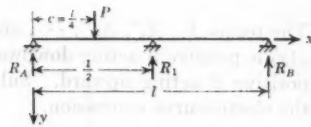


FIG. 2.—TWO EQUAL SPANS WITH A CONCENTRATED LOAD

of the intermediate supports, R_1, R_2, \dots , and R_m , which can be approximated by a Fourier series of the following type:

$$q(x) = \sum_{n=1}^{\infty} A_n \sin \frac{n \pi x}{l} \dots \dots \dots (4)$$

and

$$\left. \begin{aligned} R_1 &= \sum_{n=1}^{\infty} A_n' \sin \frac{n \pi x}{l} \\ R_2 &= \sum_{n=1}^{\infty} A_n'' \sin \frac{n \pi x}{l} \\ &\dots \\ R_m &= \sum_{n=1}^{\infty} A_n^m \sin \frac{n \pi x}{l} \end{aligned} \right\} \dots \dots \dots (5)$$

in which

$$A_n = \frac{2}{l} \int_0^l q(x) \sin \frac{n \pi x}{l} dx \dots \dots \dots (6)$$

and

$$\left. \begin{aligned} A_n' &= \frac{2}{l} \lim_{r \rightarrow 0} \int_{(a_1 l - r)}^{(a_1 l + r)} \frac{R_1}{2r} \sin \frac{n \pi x}{l} dx = \frac{2 R_1}{l} \sin n \pi a_1 \\ A_n'' &= \frac{2}{l} \lim_{r \rightarrow 0} \int_{(a_2 l - r)}^{(a_2 l + r)} \frac{R_2}{2r} \sin \frac{n \pi x}{l} dx = \frac{2 R_2}{l} \sin n \pi a_2 \\ &\dots \\ A_n^m &= \frac{2}{l} \lim_{r \rightarrow 0} \int_{(a_m l - r)}^{(a_m l + r)} \frac{R_m}{2r} \sin \frac{n \pi x}{l} dx = \frac{2 R_m}{l} \sin n \pi a_m \end{aligned} \right\} \dots \dots \dots (7)$$

If $y_p(x)$ is approximated by the series,

$$y_p(x) = \sum_{n=1}^{\infty} B_n \sin \frac{n\pi x}{l} \quad (8)$$

then substituting Eqs. 4, 5, and 8 into Eq. 1 leads to

$$B_n = \frac{l^4}{EI\pi^4} C_n \quad (9)$$

in which

$$C_n = A_n - A_n' - A_n'' \dots - A_n^m \quad (10)$$

The terms A_n, A_n', A_n'', \dots , and A_n^m are expressed by Eqs. 6 and 7, in which $q(x)$ is positive if acting downward, whereas the terms R_1, R_2, \dots , and R_m are positive if acting upward. Substituting Eqs. 3 and 8 into Eq. 2 results in the elastic-curve expression,

$$y(x) = \frac{l^4}{EI\pi^4} \sum_{n=1}^{\infty} \frac{1}{n^4} C_n \sin \frac{n\pi x}{l} \quad (11)$$

Eq. 11 is defined if the values of R_1, R_2, \dots, R_m in terms of $q(x)$ are known.

REDUNDANT REACTIONS

When Eq. 11 is differentiated twice with respect to x ,

$$y''(x) = -\frac{l^2}{EI\pi^2} \sum_{n=1}^{\infty} \frac{1}{n^2} C_n \sin \frac{n\pi x}{l} \quad (12)$$

The strain energy in the beam is expressed by

$$U = \frac{EI}{2} \int_0^l [y''(x)]^2 dx = \frac{l^3}{4EI\pi^4} \sum_{n=1}^{\infty} \frac{1}{n^4} (C_n)^2 \quad (13)$$

and applying Castigliano's theorem results in

$$\left. \begin{aligned} \frac{\partial U}{\partial R_1} &= d_1 \\ \frac{\partial U}{\partial R_2} &= d_2 \\ &\dots \\ \frac{\partial U}{\partial R_m} &= d_m \end{aligned} \right\} \quad (14)$$

in which d_1, d_2, \dots , and d_m are the relative vertical displacements of R_1, R_2, \dots , and R_m , respectively, with regard to the straight line passing through the points of end supports A and B , being positive if upward. The difference between the sign convention stated previously and that for the differential equation should be noted. Substituting Eq. 13 into Eq. 14 and considering Eqs. 6, 7, and

10 leads to

$$\left. \begin{aligned} R_1 D_{11} + R_2 D_{12} \cdots + R_m D_{1m} &= \frac{l}{2} D_1 + F d_1 \\ R_1 D_{12} + R_2 D_{22} \cdots + R_m D_{2m} &= \frac{l}{2} D_2 + F d_2 \\ \cdots \\ R_1 D_{1m} + R_2 D_{2m} \cdots + R_m D_{mm} &= \frac{l}{2} D_m + F d_m \end{aligned} \right\} \cdots \cdots (15)$$

in which

$$F = \frac{E I \pi^4}{2 l^3} \cdots \cdots \cdots (16)$$

and

$$\left. \begin{aligned} D_{11} &= \sum_{n=1}^{\infty} \frac{1}{n^4} \sin^2 n \pi a_1 \\ D_{12} &= \sum_{n=1}^{\infty} \frac{1}{n^4} \sin n \pi a_1 \sin n \pi a_2 \\ D_{1m} &= \sum_{n=1}^{\infty} \frac{1}{n^4} \sin n \pi a_1 \sin n \pi a_m \\ D_{22} &= \sum_{n=1}^{\infty} \frac{1}{n^4} \sin^2 n \pi a_2 \\ D_{2m} &= \sum_{n=1}^{\infty} \frac{1}{n^4} \sin n \pi a_2 \sin n \pi a_m \\ D_{mm} &= \sum_{n=1}^{\infty} \frac{1}{n^4} \sin^2 n \pi a_m \\ D_1 &= \sum_{n=1}^{\infty} \frac{1}{n^4} A_n \sin n \pi a_1 \\ D_2 &= \sum_{n=1}^{\infty} \frac{1}{n^4} A_n \sin n \pi a_2 \\ D_m &= \sum_{n=1}^{\infty} \frac{1}{n^4} A_n \sin n \pi a_m \end{aligned} \right\} \cdots \cdots (17)$$

Thus, R_1, R_2, \cdots , and R_m can be determined by solving Eq. 15 for any loading conditions, provided that the relative displacements of the supports are known. Substituting the values of these reactions into Eq. 11 yields the expression for the deflection of the beam. The series in Eq. 17 converges rapidly, as shown in the subsequent example.

EXAMPLE 1

Considering the two-span continuous beam shown in Fig. 2, and assuming that the center support does not yield under the load, $d_1 = 0$ and the first expression of Eq. 15 becomes

$$R_1 = \frac{l}{2} \frac{D_1}{D_{11}} \quad (18)$$

Substituting the known quantities into Eqs. 6 and 17 yields

$$A_n = \frac{2P}{l} \sin \frac{n\pi c}{l} = \frac{2P}{l} \sin \frac{n\pi}{4} \quad (19)$$

$$D_1 = \frac{2P}{l} \sum_{n=1}^{\infty} \frac{1}{n^4} \sin \frac{n\pi}{4} \sin \frac{n\pi}{2} \quad (20)$$

and

$$D_{11} = \sum_{n=1}^{\infty} \frac{1}{n^4} \sin^2 \frac{n\pi}{2} \quad (21)$$

and substituting these values into Eq. 18 leads to

$$R_1 = P \frac{\sum_{n=1}^{\infty} \frac{1}{n^4} \sin \frac{n\pi}{4} \sin \frac{n\pi}{2}}{\sum_{n=1}^{\infty} \frac{1}{n^4} \sin^2 \frac{n\pi}{2}} = P \frac{\frac{\sqrt{2}}{2} - \frac{1}{81} \frac{\sqrt{2}}{2} \dots}{1 + \frac{1}{81} \dots} \quad (22)$$

Taking only the first two terms of the expansion, Eq. 22 yields $R_1 = 0.690 P$. An exact solution yields $R_1 = 11/16 P = 0.6875 P$.

Substituting the value of R_1 into Eq. 11 leads to

$$y(x) = \frac{2Pl^3}{EI\pi^4} \sum_{n=1}^{\infty} \frac{1}{n^4} \left(\sin \frac{n\pi}{4} - 0.69 \sin \frac{n\pi}{2} \right) \sin \frac{n\pi x}{l} \quad (23)$$

which, when differentiated, results in

$$y'(x) = \frac{2Pl^3}{EI\pi^3} \sum_{n=1}^{\infty} \frac{1}{n^3} \left(\sin \frac{n\pi}{4} - 0.69 \sin \frac{n\pi}{2} \right) \cos \frac{n\pi x}{l} \quad (24)$$

Eqs. 23 and 24 are convenient to use in determining the deflection and slope of the elastic curve at any point along the continuous beam. Although $y(x)$ and $y'(x)$ converge rapidly, the convergence decreases with each differentiation. When the redundant reaction is known, the bending moment and shear can be determined easily by conventional methods.

The beam shown in Fig. 3 can be treated as the limiting case of the beam shown in Fig. 1 as $a_1 l$ approaches zero and R_1 approaches infinity, whereas the product, $R_1 a_1 l = M_1$, remains constant. For this case the first expression of Eq. 7 becomes

$$A_n' = \frac{2n\pi M_1}{l^2} \quad (25)$$

and Eq. 15 becomes

$$\left. \begin{aligned} M_1 \frac{\pi}{l} D_{12}' + R_2 D_{22} \cdots + R_m D_{2m} &= \frac{l}{2} D_2 + F d_2 \\ M_1 \frac{\pi}{l} D_{1m}' + R_2 D_{2m} \cdots + R_m D_{mm} &= \frac{l}{2} D_m + F d_m \end{aligned} \right\} \dots (26)$$

in which

$$D_{12}' = \sum_{n=1}^{\infty} \frac{1}{n^3} \sin n \pi a_2 \dots (27a)$$

and

$$D_{1m}' = \sum_{n=1}^{\infty} \frac{1}{n^3} \sin n \pi a_m \dots (27b)$$

The first expression of Eq. 15 drops out in this case because all the coefficients become zero.

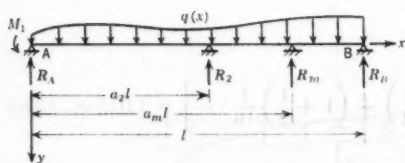


FIG. 3.—REDUNDANT MOMENT AT THE LEFT END

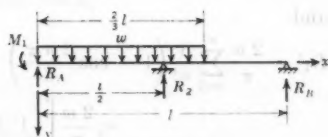


FIG. 4.—CONTINUOUS BEAM FIXED AT THE LEFT END WITH A PARTIAL UNIFORM LOAD

Differentiating Eq. 13 with respect to M_1 and considering Eq. 25, the following expression results:

$$\frac{\partial U}{\partial M_1} = \theta_a \dots (28)$$

or

$$M_1 \frac{\pi}{l} D_{11}' + R_2 D_{12}' \cdots + R_m D_{1m}' = \frac{l}{2} D_1' + F \frac{l}{\pi} \theta_a \dots (29)$$

in which

$$D_{11}' = \sum_{n=1}^{\infty} \frac{1}{n^3} = \frac{\pi^2}{6} = 1.645 \dots (30a)$$

and

$$D_1' = \sum_{n=1}^{\infty} \frac{1}{n^3} A_n \dots (30b)$$

and θ_a is the angular displacement of the tangent to the elastic curve at A, being positive if it is in the assumed direction of M_1 . Under any loading conditions, M_1 , R_2 , ..., and R_m can be determined by solving Eqs. 26 and 29 simultaneously.

EXAMPLE 2

For a beam loaded as shown in Fig. 4, $\theta_a = 0$, $d_2 = 0$, and Eqs. 26 and 29 become

$$M_1 \frac{\pi}{l} D_{11}' + R_2 D_{12}' = \frac{l}{2} D_1' \dots \dots \dots (31a)$$

and

$$M_1 \frac{\pi}{l} D_{12}' + R_2 D_{22} = \frac{l}{2} D_2 \dots \dots \dots (31b)$$

Substituting the known quantities into Eqs. 6, 17, 27, and 30 yields

$$A_n = \frac{2}{l} \int_0^l w \sin \frac{n\pi x}{l} dx = \frac{2w}{n\pi} \left(1 - \cos \frac{2n\pi}{3} \right) \dots \dots \dots (32)$$

$$D_{11}' = 1.645 \dots \dots \dots (33a)$$

$$D_{12}' = \sum_{n=1}^{\infty} \frac{1}{n^2} \sin \frac{n\pi}{2} = 1 - \frac{1}{27} \dots = 0.963 \dots \dots \dots (33b)$$

and

$$\begin{aligned} D_1' &= \frac{2w}{\pi} \sum_{n=1}^{\infty} \frac{1}{n^4} \left(1 - \cos \frac{2n\pi}{3} \right) \\ &= \frac{2w}{\pi} \left[\left(1 + \frac{1}{2} \right) + \left(1 + \frac{1}{2} \right) \frac{1}{16} \dots \right] = 1.015 w \dots (33c) \end{aligned}$$

and

$$D_{22} = \sum_{n=1}^{\infty} \frac{1}{n^4} \sin^2 \frac{n\pi}{2} = 1 + \frac{1}{81} \dots = 1.012 \dots \dots \dots (34a)$$

and

$$\begin{aligned} D_2 &= \frac{2w}{\pi} \sum_{n=1}^{\infty} \frac{1}{n^5} \left(1 - \cos \frac{2n\pi}{3} \right) \sin \frac{n\pi}{2} \\ &= \frac{2w}{\pi} \left[\left(1 + \frac{1}{2} \right) \dots \right] = 0.955 w \dots (34b) \end{aligned}$$

Substituting Eqs. 32, 33, and 34 into Eq. 31 leads to

$$5.17 \frac{M_1}{l} + 0.963 R_2 = 0.5075 w l \dots \dots \dots (35a)$$

and

$$3.025 \frac{M_1}{l} + 1.012 R_2 = 0.4775 w l \dots \dots \dots (35b)$$

and the solution of Eqs. 35 yields $M_1 = 0.0233 w l^2$ and $R_2 = 0.402 w l$.

INFLUENCE LINES FOR REACTIONS

The procedure cited under the headings, "Example 1" and "Example 2," can be used to derive expressions for the influence lines for the reactions as a unit load passes from one end of the beam to the other. In deriving an expression for the influence line for R_1 in the beam shown in Fig. 5(a), the force system

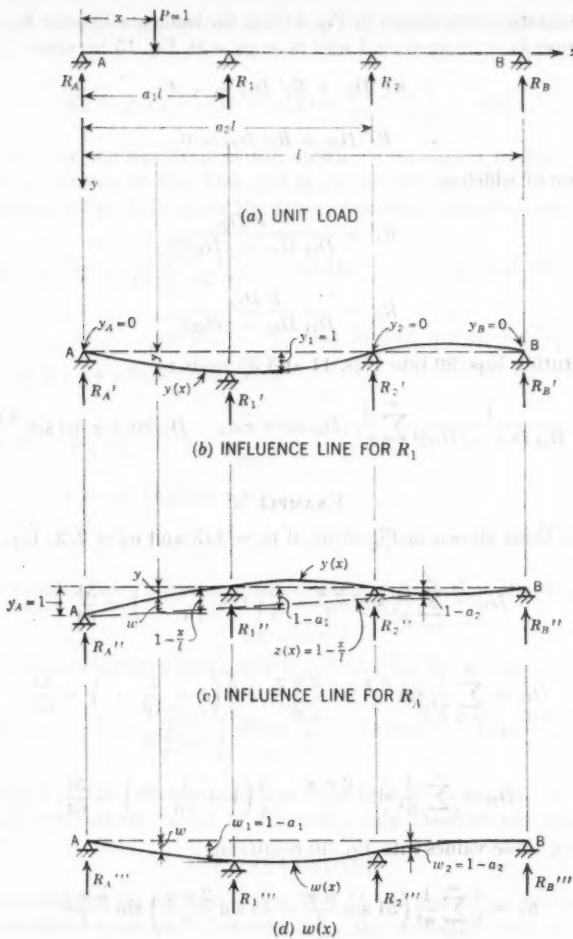


FIG. 5.—INFLUENCE LINES FOR REACTIONS

shown in Fig. 5(b) is considered first. Displacing the point of support at R_1' a unit distance, keeping $y_2 = 0$, and applying the reciprocal theorem to the two force systems result in

$$P y - R_1 y_1 = 0 \dots \dots \dots (36)$$

or

$$R_1 = P \left(\frac{y}{y_1} \right) = y \dots \dots \dots (37)$$

Thus, the elastic curve shown in Fig. 5(b) is the influence line for R_1 . For this case, because $d_1 = -y_1 = -1$ and $d_2 = y_2 = 0$, Eq. 15 becomes

$$R_1' D_{11} + R_2' D_{12} = -F \dots \dots \dots (38a)$$

and

$$R_1' D_{12} + R_2' D_{22} = 0 \dots \dots \dots (38b)$$

the solution of which is

$$R_1' = \frac{-F D_{22}}{D_{11} D_{22} - (D_{12})^2} \dots \dots \dots (39a)$$

and

$$R_2' = \frac{F D_{12}}{D_{11} D_{22} - (D_{12})^2} \dots \dots \dots (39b)$$

Substituting Eqs. 39 into Eqs. 11 and 37 leads to

$$R_1 = y = \frac{1}{D_{11} D_{22} - (D_{12})^2} \sum_{n=1}^{\infty} \frac{1}{n^4} (D_{22} \sin n \pi a_1 - D_{12} \sin n \pi a_2) \sin \frac{n \pi x}{l} \dots (40)$$

EXAMPLE 3

For the beam shown in Fig. 5(a), if $a_1 = 1/3$ and $a_2 = 2/3$, Eq. 17 yields

$$D_{11} = \sum_{n=1}^{\infty} \frac{1}{n^4} \sin^2 \frac{n \pi}{3} = \frac{3}{4} \left(1 + \frac{1}{16} \dots \right) = \frac{51}{64} \dots \dots \dots (41a)$$

$$D_{12} = \sum_{n=1}^{\infty} \frac{1}{n^4} \sin \frac{n \pi}{3} \sin \frac{2 n \pi}{3} = \frac{3}{4} \left(1 - \frac{1}{16} \dots \right) = \frac{45}{64} \dots \dots \dots (41b)$$

and

$$D_{22} = \sum_{n=1}^{\infty} \frac{1}{n^4} \sin^2 \frac{2 n \pi}{3} = \frac{3}{4} \left(1 + \frac{1}{16} \dots \right) = \frac{51}{64} \dots \dots \dots (41c)$$

Substituting these values into Eq. 40 results in

$$R_1 = \frac{1}{9} \sum_{n=1}^{\infty} \frac{1}{n^4} \left(51 \sin \frac{n \pi}{3} - 45 \sin \frac{2 n \pi}{3} \right) \sin \frac{n \pi x}{l} \dots \dots \dots (42)$$

The ordinates of the influence diagram for R_1 , as given by Eq. 42, are given in Table 1 for various values of x/l , using only the first two terms of the expansion.

TABLE 1.—ORDINATES OF INFLUENCE
DIAGRAMS FOR R_1 AND R_A

x/l	0	1/6	1/3	1/2	2/3	5/6	1
(1)	(2)	(3)	(4)	(5)	(6)	(7)	(8)
R_1	0	0.789	1.000	0.577	0	-0.211	0
R_A	1.000	0.378	0	-0.077	0	0.0448	0

By referring again to the beam shown in Fig. 5(a), an expression for the influence line for R_A shown in Fig. 5(c) can be derived similarly with slight modifications. The relative displacements of the points of supports at R_1'' and R_2'' , as shown in Fig. 5(c), with respect to the straight

line passing through A and B are $(1 - a_1)$ and $(1 - a_2)$, respectively. Therefore,

$$R_A = y(x) = z(x) - w(x) = \left(1 - \frac{x}{l}\right) - w(x) \dots (43)$$

in which $w(x)$ is the equation of the elastic curve shown in Fig. 5(d), $z(x) = 1 - x/l$, as shown in Fig. 5(c), and R_A is the left reaction. For the force system shown in Fig. 5(d), using the same procedure cited previously results in

$$w(x) = \frac{1}{D_{11} D_{22} - (D_{12})^2} \sum_{n=1}^{\infty} \frac{1}{n^4} \{ [(1 - a_1) D_{22} - (1 - a_2) D_{12}] \sin n \pi a_1 \\ + [(1 - a_2) D_{11} - (1 - a_1) D_{12}] \sin n \pi a_2 \} \sin \frac{n \pi x}{l} \dots (44)$$

Substituting Eq. 44 into Eq. 43 yields

$$R_A = 1 - \frac{x}{l} - \frac{1}{D_{11} D_{22} - (D_{12})^2} \sum_{n=1}^{\infty} \frac{1}{n^4} \{ [(1 - a_1) D_{22} \\ - (1 - a_2) D_{12}] \sin n \pi a_1 \\ + [(1 - a_2) D_{11} - (1 - a_1) D_{12}] \sin n \pi a_2 \} \sin \frac{n \pi x}{l} \dots (45)$$

Eq. 45 is simpler than it appears, as demonstrated by the following example.

EXAMPLE 4

For the beam examined in example 3, substituting Eq. 41 into Eq. 45 leads to

$$R_A = 1 - \frac{x}{l} - \frac{1}{9} \sum_{n=1}^{\infty} \frac{1}{n^4} \left(19 \sin \frac{n \pi}{3} - 13 \sin \frac{2 n \pi}{3} \right) \sin \frac{n \pi x}{l} \dots (46)$$

The ordinates of the influence diagram for R_A , as given by Eq. 46, are shown in Table 1 for various values of x/l , using only the first two terms of the expansion.

CONCLUSIONS

An advantage of the solution is that Eqs. 11, 40, and 45 are continuous over the intermediate supports. Consequently, the deflection and slope of the elastic curve, as well as the influence lines for the redundant reactions, are each given by one expression that takes all the spans into account. The rapid convergence of the series used in the solutions minimizes the numerical work.

APPENDIX. NOTATION

The following symbols, adopted for use in this paper and for the guidance of discussers, conform essentially with "American Standard Letter Symbols for Structural Analysis" (ASA Z10.8—1949), prepared by a committee of

the American Standards Association with Society representation, and approved by the Association in 1949:

A_n, A_n', A_n'', A_n^m = Fourier coefficients for loads and reactions;

a_1, a_2, a_m = span ratio;

B_n = Fourier coefficient for deflection;

C_n = term defined by Eq. 10;

C_1, C_2, C_3, C_4 = constants of integration;

c = distance of concentrated load from left end;

$D_{11}, D_{12}, D_{1m} \dots$ = series defined by Eqs. 17, 27, and 30;

d_1, d_2, d_m = displacements of intermediate supports;

E = modulus of elasticity;

F = term defined by Eq. 16;

I = moment of inertia;

l = span length;

M_1 = redundant moment on left end;

m = redundancy;

P = concentrated load;

$p(x)$ = arbitrary load function;

$q(x)$ = given load;

R_A = left reaction;

R_1, R_2, R_m = intermediate, or redundant reactions;

r = infinitely small length increment;

U = strain energy;

$w(x)$ = deflection;

x = independent variable, distance from left end;

$y(x)$ = deflection;

$y_p(x)$ = particular solution for y ;

$z(x) = 1 - x/l$, as shown in Fig. 5(c); and

θ_a = angular displacement of the tangent to the elastic curve at left end.

DISCUSSION

STEFAN J. MEDWADOWSKI,³ A.M. ASCE.—Two principal advantages, achieved at a presumably slight loss of accuracy, have been claimed by the author for the use of the Fourier series technique in the analysis of problems of continuous beams of constant bending rigidity:

1. The possibility of representing deflection, and related quantities, by a single expression that is valid for $0 \leq x \leq l$.
2. The reduction of the numerical work to a minimum.

The first of these advantages results also by using classical methods if use is made of the Heaviside unit function.⁴ The closed-form solution yields exact results, within the assumptions of the theory. In addition, it possesses the advantage of yielding directly closed-form expressions for bending moments and shears, as well as slope. Because of the poor convergence of the series involved, these expressions have to be found by a separate, indirect procedure if the Fourier series representation is used, as was indicated under the heading, "Example 1," of the paper.

Any reduction in the numerical evaluation of the unknown reactions, R_i , must occur in the computation of the coefficients of Eqs. 15, and in particular in the computation of the coefficients D_{ij} , defined in Eqs. 17. Written in a more compact notation, the definition is

$$D_{ij} = \sum_{n=1}^{\infty} \frac{1}{n^4} \sin(n\pi a_i) \sin(n\pi a_j) \dots \dots \dots (47)$$

The closed-form solution leads to the following, essentially equivalent definition:

$$D_{ij}' = a_j (1 - a_i) [a_i (2 - a_i) - a_j^2] \quad (i \geq j) \dots \dots \dots (48)$$

In both cases $D_{ij} = D_{ji}$. It is seen that the numerical computation of D_{ij} from Eq. 47 involves eleven operations (if only two terms of the series are retained), whereas the use of Eq. 48 results in six operations only and yields the exact value of the coefficients.

Thus, it would appear that the advantages claimed for the Fourier series representation are, in fact, illusory.

The system of Eqs. 15 is usually derived directly from Eq. 11 by substituting into it the prescribed deflections, $y(a_i l) = -d_i$. The use of Castigliano's theorem leads to a somewhat lengthier procedure.

It is well known that a formal application of the Fourier series expansion technique often yields solution of a physical problem, even though some of the series involved may be divergent. Bending of continuous beams is such a problem since the series that occur in Eqs. 5 are divergent. Therefore, the

³ Cons. Engr., Berkeley, Calif.

⁴ "The Application of Heaviside's Step-Function to Beam Problems," by John E. Goldberg, *Proceedings-Separate No. 202*, ASCE, July, 1953.

writer feels that the statement under the heading, "Elastic Curve," that a concentrated load function can be "approximated" by a Fourier series is incorrect.

The application of the Fourier series representation to problems of static bending of continuous beams may be considered a particular case of the problem of dynamic bending, which has been examined by Edward Saibel and Elio D'Appolonia,⁵ A.M. ASCE. It is regretted that a more complete list of references was not provided by Mr. Lee.

SENG-LIP LEE,⁶ A.M. ASCE.—According to Mr. Medwadowski, the Heaviside step function can be used (as in the paper) to obtain the deflection function and its derivatives, which are continuous in the range $0 \leq x \leq l$. That this statement is not quite correct can be illustrated by the following:

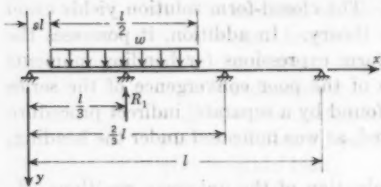


FIG. 6.—CONTINUOUS BEAM UNDER MOVING UNIFORM LOAD

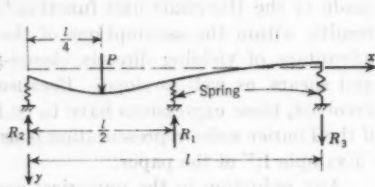


FIG. 7.—CONTINUOUS BEAM ON SPRING SUPPORTS UNDER CONCENTRATED LOAD

In order to determine the maximum value of R_1 produced by a moving, uniformly distributed load extending over a distance of $l/2$ in Fig. 6, Eq. 42 yields

$$R_1 = \frac{wl}{9} \sum_{n=1}^{\infty} \frac{1}{n^4} \left(51 \sin \frac{n\pi}{3} - 45 \sin \frac{2n\pi}{3} \right) \int_{s-l}^{s+l} \sin \frac{n\pi x}{l} dx \dots (49a)$$

or

$$R_1 = \frac{wl}{9\pi} \sum_{n=1}^{\infty} \frac{1}{n^5} \left(51 \sin \frac{n\pi}{3} - 45 \sin \frac{2n\pi}{3} \right) [\cos n\pi s - \cos n\pi (s + \frac{1}{2})] \dots (49b)$$

The location of the load corresponding to the maximum value of R_1 is given by

$$\frac{dR_1}{ds} = 0 \dots (50a)$$

or

$$\sum_{n=1}^{\infty} \frac{1}{n^4} \left(51 \sin \frac{n\pi}{3} - 45 \sin \frac{2n\pi}{3} \right) [\sin n\pi (s + \frac{1}{2}) - \sin n\pi s] = 0 \dots (50b)$$

Taking only the first two terms of the series yields

$$1 - 4 \sin \pi s - \tan \pi s = 0 \dots (51)$$

⁵ "Forced Vibrations of Continuous Beams," by Edward Saibel and Elio D'Appolonia, *Transactions, ASCE*, Vol. 117, 1952.

⁶ Associate Prof. of Civ. Eng., Northwestern Technological Inst., Northwestern Univ., Evanston, Ill.

the solution of which yields $s = 0.0639$. The corresponding value of R_1 is

$$(R_1)_{\max} = \frac{w l}{9 \pi} \sum_{n=1}^{\infty} \frac{1}{n^3} \left(51 \sin \frac{n \pi}{3} - 45 \sin \frac{2 n \pi}{3} \right) \\ \times (\cos 0.0639 n \pi - \cos 0.5639 n \pi) = 0.386 w l \dots (52)$$

If Heaviside's step function were used in this case, Eq. 49a would be replaced by

$$R_1 = \frac{27 w}{5 l^3} \int_{s,l}^{(s+\frac{1}{2})l} \left\{ 8 \left[-\frac{2}{3} x^3 + H_1 \left(x - \frac{l}{3} \right)^3 + \frac{10}{27} l^2 x \right] \right. \\ \left. - 7 \left[-\frac{1}{3} x^3 + H_2 \left(x - \frac{2}{3} l \right)^3 + \frac{8}{27} l^2 x \right] \right\} dx \dots (53)$$

in which

$$H_1 = \begin{cases} 0 & 0 \leq x \leq \frac{1}{3} l \\ 1 & \frac{1}{3} l \leq x \leq l \end{cases}$$

and

$$H_2 = \begin{cases} 0 & 0 \leq x \leq \frac{2}{3} l \\ 1 & \frac{2}{3} l \leq x \leq l \end{cases}$$

Although Eq. 53 gives R_1 in a single expression, the integrand is actually discontinuous at $x = \frac{1}{3} l$ and $x = \frac{2}{3} l$. In this problem it is obvious that $s + \frac{1}{2} < \frac{2}{3}$, for which Eq. 53 takes the form,

$$R_1 = \frac{27 w}{5 l^3} \left[8 \int_{s,l}^{(s+\frac{1}{2})l} \left(-\frac{2}{3} x^3 + \frac{10}{27} l^2 x \right) dx + 8 \int_{\frac{1}{3}l}^{(s+\frac{1}{2})l} \left(x - \frac{l}{3} \right)^3 dx \right. \\ \left. - 7 \int_{s,l}^{(s+\frac{1}{2})l} \left(-\frac{1}{3} x^3 + \frac{8}{27} l^2 x \right) dx \right] \dots (54)$$

For $s + \frac{1}{2} > \frac{2}{3}$, Eq. 53 yields a longer expression for R_1 with additional integrals. In problems in which the limits of integration are not obvious, the choice of one or the other must be made before differentiating in order to determine the value of s corresponding to $(R_1)_{\max}$. If the wrong choice is made the procedure must be repeated. This difficulty is avoided by the use of Eq. 49a, in which the integral is truly continuous between $s l \leq x \leq (s + \frac{1}{2}) l$. It is obvious that the numerical work involved in solving the present problem by Eq. 49a is less than if Eq. 53 were used. Furthermore, in problems in which the limits of integration extend over several supports, Eq. 53 yields additional integrals, whereas the integrand of Eq. 49a remains unchanged.

It is agreed that Eqs. 15 can be derived from Eq. 11 by directly substituting the prescribed deflections of the intermediate supports. The example shown in Fig. 7 explains the reason for using Eq. 13 with the aid of Castigliano's theorem.

To determine the reactions of the springs on the beams loaded as shown in Fig. 7, the center reaction, R_1 , is taken as the redundant quantity. For this

case Eq. 13 takes the form,

$$U = \frac{l^5}{4\pi^4 EI} \sum_{n=1}^{\infty} \frac{1}{n^4} (C_n)^2 + \frac{1}{2} \sum_{r=1}^3 \frac{(R_r)^2}{K_r} \\ = \frac{l^3}{\pi^4 EI} \sum_{n=1}^{\infty} \frac{1}{n^4} \left(P \sin \frac{n\pi}{4} - R_1 \sin \frac{n\pi}{2} \right)^2 + \frac{1}{2K} \sum_{n=1}^3 (R_r)^2 \dots (55)$$

in which $K = kEI/l^3$ is the spring constant, and the values of R_r , the spring reactions, are

$$R_2 = \frac{3}{4}P - \frac{1}{2}R_1 \dots (56a)$$

and

$$R_3 = \frac{1}{2}R_1 - \frac{1}{4}P \dots (56b)$$

The application of the theory of minimum energy leads to

$$\frac{dU}{dR_1} = 0 \dots (57a)$$

or

$$- \sum_{n=1}^{\infty} \frac{1}{n^4} \sin \frac{n\pi}{2} \left(P \sin \frac{n\pi}{4} - R_1 \sin \frac{n\pi}{2} \right) + \frac{1}{2k} \left(\frac{3}{2}R_1 - \frac{1}{2}P \right) = 0 \dots (57b)$$

which yields

$$R_1 = \frac{0.688 + 24.0/k}{1 + 72.0/k} P \dots (58)$$

For infinitely stiff springs, $k \rightarrow \infty$, for which $R_1 = 0.688P$, whereas for very flexible springs, $k \rightarrow 0$, for which $R_1 = P/3$.

In this case the energy method makes it unnecessary to consider the deflections at the spring supports. This method also lends itself to a simpler solution, whereas the other approach involves a somewhat lengthier procedure.

Mr. Medwadowski questions the statement that a given load and the reactions of the intermediate supports can be approximated by Fourier series of the type given by Eq. 4. It is of interest to note, however, that this technique of representing load functions by Fourier series has been used elsewhere.⁷ The laborious part of the analysis of continuous beams is the determination of the deflection and slope functions, including the influence lines for reactions. For such determinations, among others, it has been demonstrated that the Fourier series analysis yields simple solutions that converge rapidly. As soon as the redundant reactions are known, the shearing force and bending-moment functions are derived best by the classical procedure of integrating the load functions.

⁷ "Theorie und Berechnung der Eisernen Brucken," by F. Bleich, Julius Springer, Berlin, 1924, p. 51.

AMERICAN SOCIETY OF CIVIL ENGINEERS

Founded November 5, 1852

TRANSACTIONS

Paper No. 2971

CHARACTERISTICS OF NEW-TYPE CARGO SHIPS

BY DOUGLAS C. MACMILLAN¹

SYNOPSIS

The design characteristics and the functional problems of roll-on roll-off ships and certain lift-on lift-off types having similar basic features are described.

INTRODUCTION

The object of the new designs is to reduce port time and to revise cargo-handling methods in order to reduce radically or eliminate manual labor by stevedores in terminals and ships. Prepacked cargo in freight cars, trailers, van bodies, containers, or pallets may be moved on or off specially designed

TABLE 1.—LOADING RATES

Type	Cargo-handling rate, in measurement—tons per hour
Single-deck train ferry	4,000
Seatrains	1,700
Two-deck trainship	4,000
Trailership	6,000
Containership (lift-on lift-off)	1,200 to 3,000
Pallet (sideport—fork truck)	350 to 700
Conventional ship	20 to 40 ^a
Vehicle ship	150 to 500 ^b
Self-unloading bulk carrier	2,000 ^c
	4,000 to 8,000

^a Per gang. ^b Total. ^c Approximate measurement.

ships rapidly and with a minimum of manpower. The use of prepacked containers drastically reduces terminal and ship cargo-handling time and costs by eliminating the unpacking of the shoreside vehicle, restowing of the cargo aboard ship, and repeating this process at the delivery point.

¹ Pres., George G. Sharp, Inc., New York, N. Y.

NOTE.—Published, essentially as printed here, in May, 1957, in the Journal of the Waterways and Harbors Division, as *Proceedings Paper 1237*. Positions and titles given are those in effect when the paper was approved for publication in *Transactions*.

The roll-on roll-off type of vessels, which include train ferries, trainships, containerships, and certain lift-on lift-off vessels that handle prepacked cargo containers, are characterized basically by a rapid rate of cargo handling. Various designs that are either in use or being developed have rates as indicated in Table 1. The terminal facilities must provide for cargo receipt and cargo

TABLE 2.—GENERAL-CARGO SHIPS

Type	Speed, in knots	Total dead weight, in tons	Cargo dead weight, in tons ^a	Bale capacity, in cubic feet	STOWAGE FACTOR	
					Per cubic foot ^a	Per ton ^b
(1)	(2)	(3)	(4)	(5)	(6)	(7)
SHIPS PRESENTLY IN USE						
Liberty	10.0	10,800	9,900	500,000	50.5	52.8
ClB	14.0	9,120	8,150	437,000	53.6	64.3
C2-S-B1	15.5	9,280	8,050	546,000	67.8	77.3
C3-S-A2	16.5	12,100	10,500	658,000	62.6	68.3
Victory AP3	16.5	10,700	9,430	453,000	48.0	60.8
Mariner	20.0	13,400	11,640	737,000	63.3	75.0
Navy Stores Issue	18.5	7,220	5,440	358,000	65.7	75.7
PROPOSED NEW MARITIME DESIGNS						
Freedom	16.0	8,800	7,840	497,000	65.8	75.0
Clipper	18.0	10,900	9,730	600,000	61.2	74.4
Seafarer	18.0	14,940	13,550	744,500	56.0	72.3

^a Cargo dead weights based on 6,000-mile range.

^b At designed range.

TABLE 3.—ROLL-ON ROLL-OFF SHIPS AND CONTAINERSHIPS

Type	Speed, in knots	Total dead weight, in tons	Cargo dead weight, in tons ^a		Cargo capacity inside container, in cubic feet		Bale ca- pacity inside ship, in cubic feet	Cargo space molded volume, in cubic feet	Ratio ^d
(1)	(2)	(3)	(4)	(5)	(6)	(7)	(8)	(9)	
Single-deck train ferry.....	17.5	3,850	2,350 ^a	1,440 ^a	160,000 ^a	160,000 ^a	495,000	582,000	0.275
Two-deck trainship.....	18.0	8,540	8,000 ^a	4,560 ^a	576,000 ^a	480,000 ^a	1,314,000	1,546,000	0.372
Trailership.....	18.0	8,710	7,225 ^a	5,075 ^a	600,000 ^a	483,000 ^a	1,453,000	1,710,000	0.350
Containership.....	15.5	5,640	4,930 ^a	3,730 ^a	503,000 ^a	415,000 ^a	678,000	798,000	0.63
Vehicle ship—design vehicle load.....	18.0	6,500	5,950 ^a	...	548,000 ^a	...	766,500 ^a	900,000	0.61

^a Based on 2,000-mile range. ^b Including weight of container. ^c Excluding weight of container. ^d Including open-deck cargo. ^e Approximate capacity for vehicles. ^f Excluding open-deck cargo. ^g Roll-on roll-off holds = 630,000 cu ft; general-cargo holds = 136,500 cu ft; and total bale = 766,500 cu ft. ^h Ratio of cargo capacity (inside containers) to molded volume of cargo space.

dispatch from the ship's side at these rates. The high loading rates are associated with low costs. An analysis of the roll-on roll-off type of train ferries indicates that costs of from 2¢ to 6¢ per measurement-ton are incurred, as compared with from \$6.00 to \$12.00 per measurement-ton for conventional break-bulk methods.

SHIP CHARACTERISTICS

The present (1959) general-cargo ship could be classed as an all-purpose tool and is usually designed to handle a wide variety of miscellaneous items, including bulk cargoes, such as ores, grain, coal, or special oils, and general freight, such as manufactured goods exported from the United States. The exports that are carried by one line include hundreds of commodities in quantities of from one ton to thousands of tons. The dead weights and bale capacity of general-cargo ships are indicated in Table 2.

TABLE 4.—SUMMARY OF STUDIES OF A C-3 VESSEL ON A
2,000-MILE ROUND-TRIP COASTAL ROUTE

	Conventional ship		Trailership		Containership	
Volumes						
Molded cargo space, in cubic feet.....	770,000		770,000		770,000	
Usable cargo space, in cubic feet.....	578,000		260,000		420,000	
Percentage used.....	75		34		55	
Measurement-tons used.....	14,450		6,500		10,500	
Round-trip port time, in days						
Loaded both ways.....	20		2		3	
Loaded only one way.....	10		2		3	
Round trips per year						
Loaded both ways.....	13.9		46.5		40.2	
Loaded only one way.....	23.0		46.5		40.2	
Measurement-tons of cargo per year						
Loaded both ways.....	402,000		605,000		844,000	
Loaded only one way.....	332,000		303,000		422,000	
	Dollars	Percent-	Dollars	Percent-	Dollars	Percent-
	per ton	age	per ton	age	per ton	age
Cargo transportation costs*						
Loaded both ways						
Ship operating and fixed.....	3.85	18.5	2.60	71.5	1.98	32.1
Trailer, container, and tractor.....			0.91	25.2	0.23	3.7
Cargo handling.....	17.00	81.5	0.12	3.3	3.96	64.2
Total.....	20.85	100.0	3.63	100.0	6.17	100.0
Loaded only one way						
Ship operating and fixed.....	4.67	21.5	3.20	71.7	3.96	46.1
Trailer, container, and tractor.....			1.31	25.0	0.46	5.4
Cargo handling.....	17.00	78.5	0.24	3.3	4.16	48.5
Total.....	21.67	100.0	7.25	100.0	8.58	100.0

* Terminal to terminal.

The bale capacity of the general-cargo ships varies from 85% to 90% of the molded volume of the cargo spaces. In actual practice, approximately 85% of the bale is used for cargo, the difference being due to broken stowage and dunnage. Thus, approximately 75% of the original molded volume is occupied by cargo. Roll-on roll-off ships and some lift-on lift-off types cannot make effective use of as large a percentage of the molded cargo-hold volume, and representative data on these types are presented in Table 3.

For two ships of identical dimensions and form (although the most efficient designs of each type would not be the same), the general-cargo ship will carry approximately twice the volume of cargo per voyage as the roll-on roll-off type

of ship. However, the substantial reduction in port time for the latter tends to cancel this deficiency in cargo capacity. Two ships of the C3-size would transport nearly equal measurement-tons of cargo per year on a 7,000-mile round-trip route, and as the length of the trip decreases, the roll-on, roll-off ship becomes more advantageous. For a 2,000-mile-trip coastal run, the roll-on roll-off trailership can carry approximately 50% more cargo annually, and a containership can carry about 100% more cargo annually than the conventional ship. Table 4 presents a comparative estimate for such a case.

SHIP SIZE AND FORM

The economics of ship operation results in roll-on roll-off ships and containerships having optimum characteristics that are somewhat different from the conventional general-cargo ships. Table 5 presents the dimensions, coefficients, and capacities of representative ships of each type.

The roll-on roll-off type of ship, as compared with the general-cargo type, has larger cubic capacity, smaller dead weight, finer form, greater beam and depth, and less draft. The finer form and lesser port time justify higher speeds than are economically justified for general-cargo ships. The speed for the new type of general-cargo ship is rather high because of defense requirements.

STRUCTURAL DESIGN

The requirement for (a) clear decks without interruption by transverse bulkheads and (b) large 'tween-deck heights to accommodate vehicles makes it necessary that the design of the roll-on roll-off ship differ significantly from that of the standard transversely framed cargo ship. In the case of the roll-on roll-off ship, the transverse bulkheads, which rise above the freeboard deck to the uppermost through-running deck in a standard design in order to provide transverse strength, must be replaced by deep web frames in conjunction with closely spaced deep beams. The spacing of such webs varies between 8 ft and 12 ft, depending on the size of the vessel. Because the web frames are mandatory, the spaces between the webs at the decks and side should be carried by longitudinal framing. The deck thicknesses, which are required to accommodate the panel load of concentrated wheel loads of heavy vehicles such as trailer trucks, are considerably greater than in the standard ship. In order to keep the increased deck thicknesses to a minimum, the spacing of the longitudinal deck beams (from 20 in. to 21 in.) is reduced from the spacing that is usually applied to a standard type of vessel of the same size (with a frame spacing of from 30 in. to 36 in.).

Because of the great deck thicknesses in conjunction with longitudinal beams and the substantial ship depth caused by the deep 'tween decks, the roll-on roll-off vessel has greater longitudinal strength characteristics than those for a standard-type vessel that is as long and has the same number of decks.

An exception to the foregoing would be one of the oldest types of roll-on roll-off vessels—the single-deck ferry—in which transverse strength is provided by box columns or vertical girders that are arranged on the port side and starboard side, or on the center line. The columns or webs usually are continuous

TABLE 5.—COMPARATIVE CHARACTERISTICS

	NEW-TYPE CARGO SHIPS					GENERAL-CARGO SHIPS			
	Con- tainer- ship	Trailer- ship	Roll-on roll-off pallet	Train- ship	Vehicle ship	Private design	Clipper	Sea- farer	Mari- ner
	(1)	(2)	(3)	(4)	(5)	(6)	(7)	(8)	(9)
Dimensions, in feet									
Over-all length....	508.7	637.5	320.0	579.0	499.0	499.0	496.0	530.3	563.6
Length between perpendiculars...	485.0	591.0	296.0	541.0	462.0	460.0	460.0	494.0	528.0
Length on load water line.....	...	619.0	304.0	565.0	479.0	474.0	465.0	...	535.5
Beam at load water line.....	72.0	83.2	50.0	86.5	78.0	70.0	73.0	74.5	76.0
Maximum beam....	72.0	87.0	50.0	86.5	78.0	70.0	73.0	74.5	76.0
Depth to upper deck.....	...	62.0	...	67.8	48.8
Depth to main deck.....	40.5	46.0	30.5	49.1	34.3	42.5	41.3	44.5	44.5
Depth to second deck.....	...	30.0	16.75	30.5	22.3	34.0	32.6	35.5	35.5
Design full-load draft.....	21.8	22.5	14.0	20.0	22.0	29.0	28.0	31.5	29.75
Maximum draft...	24.0	23.0	14.0	22.3	27.0	29.5	30.0	...	31.5
Coefficients based on load water line and max- imum draft									
Block.....	0.608	0.573	0.509	0.59	0.60	0.685	0.619	0.685	0.624
Prismatic.....	0.684	0.632	0.567	0.64	0.62	0.698	0.630	0.697	0.635
Midship section...	0.889	0.922	0.897	0.92	0.969	0.982	0.983	0.983	0.983
Waterplane.....	0.712	0.792	0.754	0.79	0.737	0.785	0.731	0.770	0.745
Speed-length ratio.	0.705	0.733	0.930	0.743	0.838	0.77	0.838	0.809	0.870
Beam-draft ratio...	3.30	3.69	3.57	3.93	3.55	2.41	2.61	2.36	2.55
Displacement and tonnage in tons									
Designed full-load displacement....	13,216	18,560	3,050	15,300	14,100	18,190	16,900	21,800	21,100
Total dead weight...	8,021	8,710	1,650	6,630	6,500	12,500	10,900	14,940	13,410
Gross tonnage....	...	14,600	700	9,500	...	10,400	10,350	11,500	9,215
Capacity, in cubic feet									
Bale.....	678,000	1,453,000	150,000	1,314,000	766,500*	662,000	601,000	744,500	637,000
Cargo.....	503,000*	600,000*	135,000	576,000*	...	563,000*	511,000*	631,000*	726,000*
Speed and power									
Design sea speed, in knots.....	15.5	18.25	16	18	18	16.5	18	18	20
Normal shaft horsepower.....	6,000	13,600	3,300	11,500	12,000	8,500	11,000	12,500	17,500
Number of propellers.....	1	2	2	2	2	2	1	1	1
Normal cruising range, in miles...	3,900	3,900	2,000	2,500	13,000	21,500	15,000	16,000	19,000
Subdivision and stability									
Standard of sub- division*.....	1	1	1	2	2	1	1	1	1
Metacentric height in full load, departure condition, in feet	3.6	4.5	3.7	3.3	4.1	2.6	3.4	4.7	4.5

* Number of adjacent compartments that can be flooded without loss of ship. * Inside containers.
 * Capacity of 630,000 for roll-on roll-off loading. * Assuming 15% loss for dunnage and broken stowage.

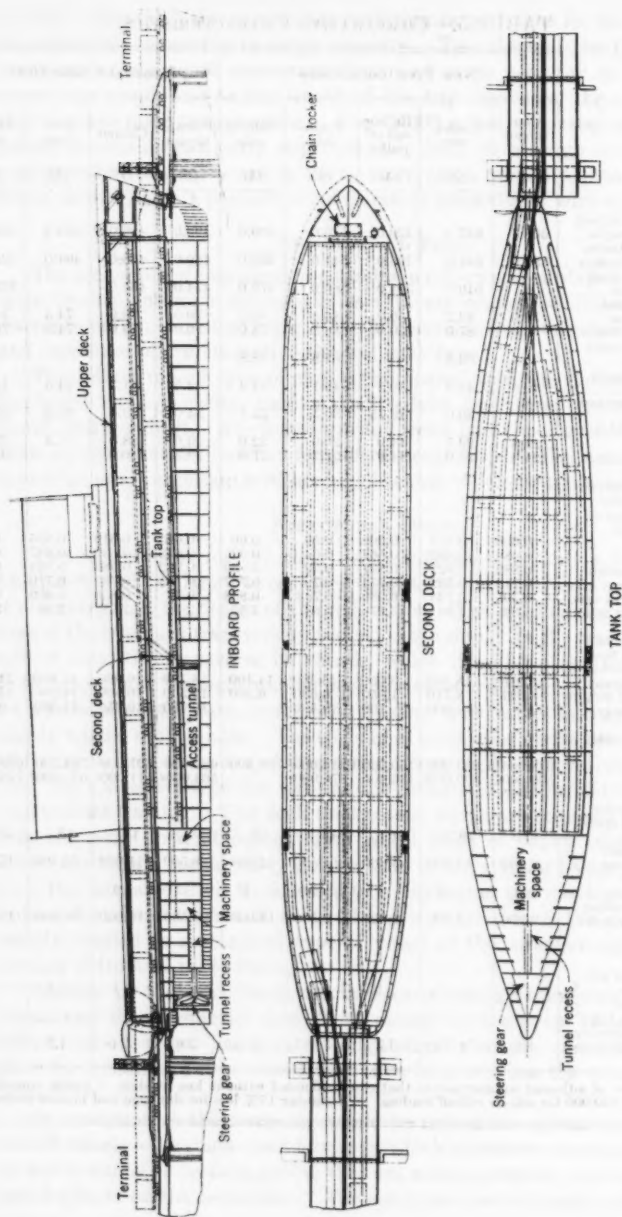


Fig. 1.—Roll-On Roll-Off Trainship with Sloped Decks for End Loading

and are held at the bottom shell girders and at the main deck. The columns or webs transversely carry, as a cantilever, the promenade deck, which forms the cover over the vehicles. For the single-deck ferry a transverse-framing system is advantageous.

One of the first roll-on roll-off vessels for unlimited ocean-going service is the Military Sea Transportation Service vehicle ship *Comet*, which was also designed to carry general cargo. The dual requirement, in addition to the requirement to keep deck heights low, made it necessary to depart from the previously described general concept of structure for the roll-on roll-off vessel and to revert to the transverse-framing system. Deck beams were located transversely to accommodate the distributed loading of very heavy vehicles such as tracked tanks. The beams are in line with the frames (30-in. spacing). Therefore, the plating was made rather heavy in conjunction with fore-and-aft panel breakers. The excessive deck thickness has contributed also to the improved longitudinal strength of the vessel as compared with the standard-vessel requirements.

SHIP TYPES

Ships that are presently (1959) used and that attain the desired high loading rate are single-deck rail-car ferries, seatrains, and containerships. The single-deck car ferries are loaded by the roll-on roll-off principle, the freight cars are

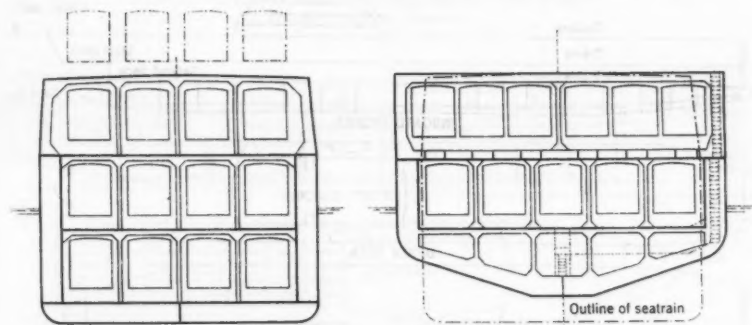


FIG. 2.—COMPARISON OF MIDSHIP SECTIONS OF SEATRIN AND ROLL-ON ROLL-OFF TRAINSHIP

lifted on and off the seatrains by a shore crane installation in each port of call, and the containers are lifted off containerships by gantry-type cranes mounted on the ship. A description follows of some of the newer types of ships that are being considered.

Roll-On Roll-Off Sloped-Deck Trainship.—A trainship design, as shown in Fig. 1, has been developed in order to produce a vessel having approximately the same dimensions and capacity as the seatrains, but requiring no special facilities on ship or shore for loading and unloading the freight cars. The trainship can dock at the usual car-float terminals that are found in harbors in the United States, and loading and discharging the freight cars via these terminals is accomplished as in car-float operation. The cars roll off and on

the ship at normal float-bridge level or pier level. The capacity of the trainship is 100 freight cars (45 ft long), or 180 trailers.

It was found that two car decks could be arranged within the ship so that from the lower deck, freight cars could be loaded or discharged at pier level through the vessel's bow, and from the upper deck, freight cars could be handled similarly through the stern. Such a procedure involved decks having a slope to the horizontal, which did not present any difficulties because the required slopes or gradients were those acceptable in normal railroad practice. The trainship can be designed with decks that are essentially flush, so that it can also carry trailers.

The preceding principle resulted in a design of a two-deck trainship that has the same capacity and approximately the same length as the four-deck seatrain, but it has less depth and larger beam (Fig. 2).

Dimension	Seatrain	Trainship
Length.....	468 ft	420 ft
Depth.....	55 ft 3 in.	50 ft 9 in.
Beam.....	63 ft 6 in.	76 ft

The total inside volume of the trainship is slightly less than that of the seatrain. The underwater part of the trainship that is not utilized for cargo or machinery

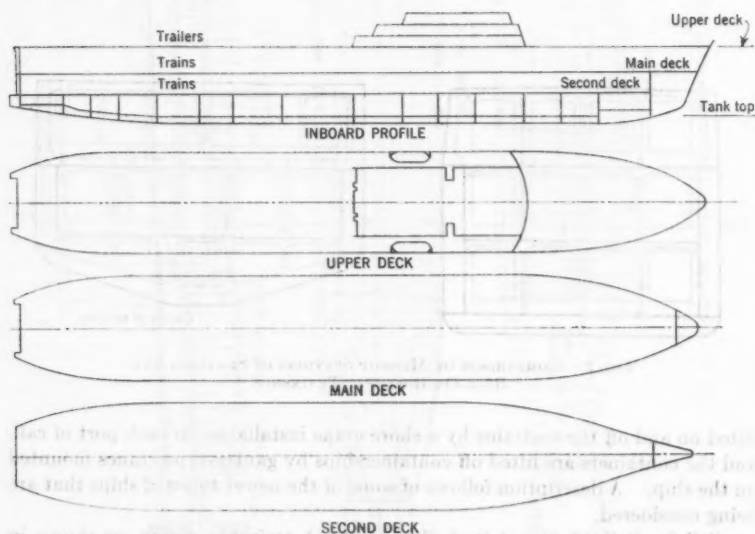


FIG. 3.—TRAINSHIP

is small, the vessel being of fairly shallow draft and fine form. At the midship section the seatrain and trainship use about the same percentage of their cross-sectional areas for cargo, but nearer the ends the trainship utilizes a progressively greater percentage of the cross-sectional area than the seatrain.

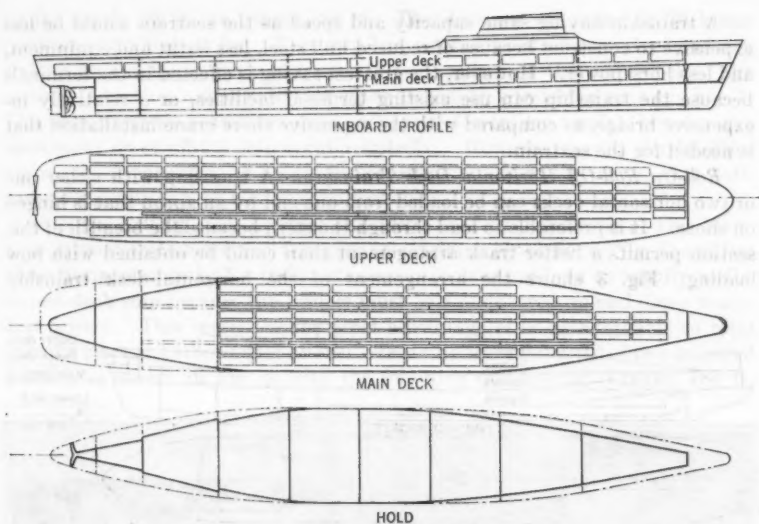


FIG. 4.—ROLL-ON ROLL-OFF TRAILERSHIP WITH SLOPED DECKS FOR END LOADING

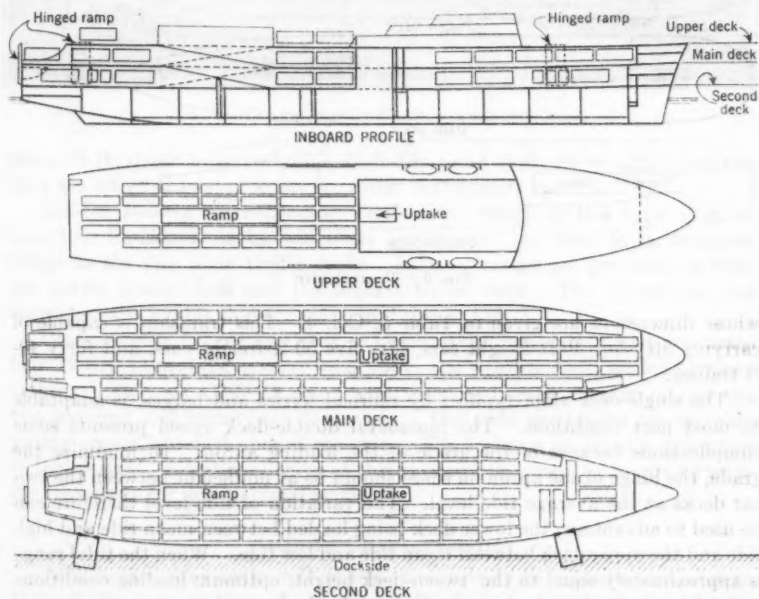


FIG. 5.—ROLL-ON ROLL-OFF TRAILERSHIP FOR SIDE LOADING AND STERN LOADING

A trainship having same capacity and speed as the seatrain would be less expensive to construct because of reduced hull steel, less outfit and equipment, and less horsepower. However, the greatest saving is effected in the terminals because the trainship can use existing terminal facilities, or a relatively inexpensive bridge, as compared with the expensive shore crane installation that is needed for the seatrain.

Roll-On Roll-Off Horizontal-Deck Trainship.—A trainship with either one or two horizontal decks can be loaded from one end by an apron that is hinged on shore. It is preferable to load through the stern because the breadth of this section permits a better track arrangement than could be obtained with bow loading. Fig. 3 shows the arrangement of the horizontal-deck trainship

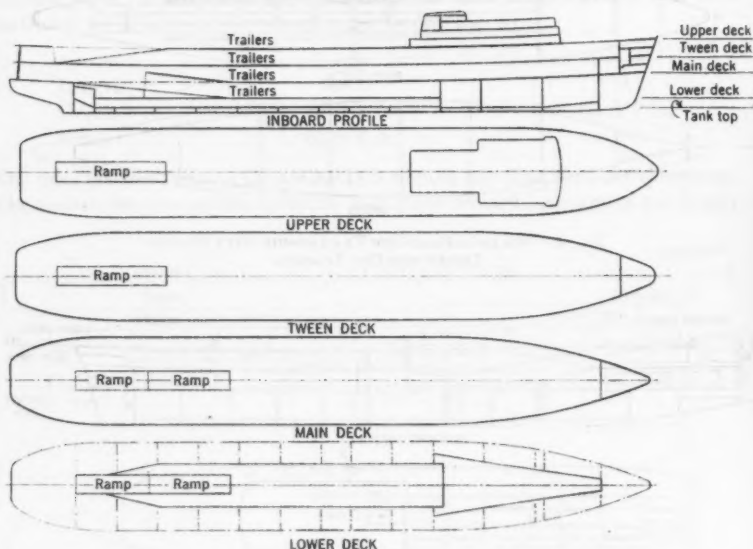


FIG. 6.—TRAILERSHIP

whose dimensions are given in Table 5, Col. 4. This trainship is capable of carrying fifty-five 40-ft freight cars, fifty-five 50-ft freight cars, and forty 40-ft trailers.

The single-deck ship, typified by railroad ferries and barges, is adaptable to most port conditions. The horizontal double-deck vessel presents some complications because of the grade of the loading apron. To minimize the grade, the hinge of the apron on shore should be at midheight between the two car decks at the average tide level. The variation of tide level therefore can be used to advantage, the lower deck being loaded between mean tide and high tide and the upper deck between mean tide and low tide. When the tidal range is approximately equal to the 'tween-deck height, optimum loading conditions and minimum bridge requirements are attained.

Roll-On Roll-Off End-Loading Sloped-Deck Trailership.—This type of ship is shown in Fig. 4 and has the following dimensions: Length, 555 ft; beam,

76 ft; depth, 34 ft; and draft, 20 ft. The designed sea speed is 20 knots requiring 12,500 shaft hp. This ship has a capacity of one hundred and ten trailers on the upper deck and seventy-two trailers on the main deck. The method of loading is similar to that of the sloped-deck trainship shown in Fig. 1. The ship provides maximum ease and speed for trailer loading because the vans move on or off the ship uninterrupted. However, special pier facilities are required, consisting of an apron projecting out from the pier so that both ends of the ship can be loaded simultaneously.

Roll-On Roll-Off Side-Loading and Stern-Loading Trailership.—The Maritime Administration design "Turnpike" class ship is of this type (Fig. 5) and has three horizontal decks for trailer stowage. It does not load as rapidly as the sloped-deck ship because the trailers must be maneuvered up and down ramps and turned. This vessel has the great advantage of being adaptable to most existing piers or harbor installations. This ship has a capacity of two hundred trailers, as shown in Fig. 5, with the following dimensions: Length, 480 ft;

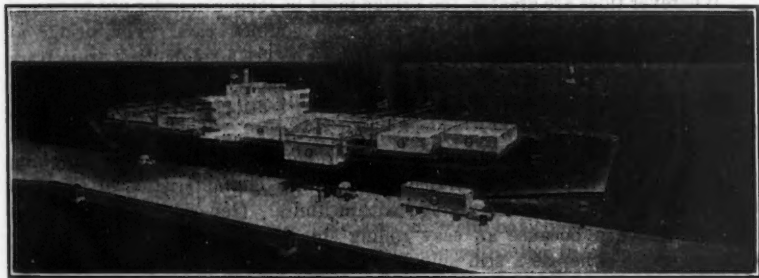


FIG. 7.—CONTAINERSHIP BEING LOADED BY CRANE

beam, 78 ft; depth to second deck, 26 ft 6 in.; and draft, 19 ft. It is designed for a sea speed of twenty knots requiring 15,000 shaft hp.

Roll-On Roll-Off Stern-Loading Trailership.—Ships of this type (Fig. 6) have four horizontal decks, which are loaded over the stern by a two-level bridge to the two main trailer decks. Internal ramps are provided to both the lowest trailer deck and the highest trailer deck. The dimensions and characteristics of this ship are given in Table 5, Col. 2.

Containership Loaded by Crane.—A steamship corporation first converted four T2-SE-A1 tankers to carry vans above the weather deck, loaded by shore cranes. Later, six C2-S-E1 ships were converted, each capable of carrying two hundred and twenty-six 35-ft vans. The vans are loaded by traveling gantry cranes installed aboard the ship. Fig. 7 shows an artist's conception of this design. Additional ships of this type are proposed by another steamship company for international service.

LOADING CHARACTERISTICS

As indicated previously, roll-on roll-off ships may be loaded over the stern, through the bow, or through sideports. Of the ship designs that are in use, the single-deck train ferries load over the stern via a transfer bridge, the trailers load through the stern, and the container or van ships are loaded by over-

head cranes. The Military Sea Transportation Service vehicle ship *Comet* uses stern-loading ramps and sideport-loading ramps as well as internal ones.

BRIDGE REQUIREMENTS

The transfer bridges for single-deck train ferries in ports with moderate tides (such as those on the east coast of the United States and in the Great Lakes area) use a gantry-supported bridge of from 70 ft to 100 ft long, which is hinged at the shore end and supported by the gantry and ship's stern at the outboard end. The dead load is supported by the shore pivot and the gantry via counterweights, and the live load by the shore pivot and the ship. The transfer bridge is designed so that it will twist, thus permitting the outboard end to follow the ship as it lists when strings of cars are pushed on or pulled off the ship. The design conditions of the transfer bridges generally provide for a list of 10° to either side and a maximum grade difference of 5% between adjacent cars, or, generally, maximum grades of $\pm 5\%$.

Wherever tides are greater, the bridge must be longer in order not to exceed the 5% grade-difference limitation between coupled cars. The bridge at Vancouver, British Columbia (Canada), which serves a single-deck train ferry and where maximum tides reach 16 ft, is approximately 200 ft long and is composed of a 110-ft-long inner section and an outer section that is approximately 90 ft long.

It is necessary to design the ship and bridge so that they have matching loading characteristics. The transverse stability characteristics of the ship can be adjusted in the design stage within limits. Generally, a compromise must be reached because an easy rolling ship is desired for good seagoing characteristics, whereas a stiff ship is advantageous for loading. The design shown by Fig. 3 attains reasonably good sea characteristics and, at the same time, restricts the angle of list to 10° when a full string of heavy cars is on the outboard track. In some designs the outboard rows must be removed in half strings in order not to exceed the 10° limitation dictated by bridge design and freight-car coupler characteristics.

As strings of cars are moved on and off the ship, the grade of the bridge changes, which is produced by the change in ship trim as a result of shifting weight. There is also a change in grade due to list. The changes may be on the order of 2% and must be considered in the design of the facilities and also when loading.

For loading trailerships the ramp requirements are considerably less exacting because of greater permissible grades, substantially less change in list, and generally lower unit loads. It is also possible to stabilize the ship effectively during loading by shifting water ballast, restricting the trim to $\pm 1\%$, and restricting the list to $\pm 1^\circ$. Although stabilizing a trainship is possible, the ultimate cost is considered to be more than just designing the bridge to match the ship.

BRIDGE DESIGN

The bridge that was designed for a steamship company at Whittier, Alaska, where the maximum tide is 19 ft and where 50% of the time the tidal range is

only 9 ft, is a 135-ft-long movable bridge that can be elevated or lowered at the shore end to connect with either of two track levels. Either level will serve any track on the ship by use of switches on the bridge and ship. The upper train level on the ship (main deck) will be loaded with the bridge at the upper shore level, and the lower train level (second deck) will be loaded with the bridge at the lower shore level. The bridge can serve both decks within the grade limits of 5% for the maximum combinations of tide, ship draft, list, and trim during any tidal cycle. The bridge will be used also to load and trim during any tidal cycle. The bridge will be used also to load and unload trailers on the upper deck of the ship, from the upper shore level, with an upward grade limit of 15%.

Because it is less expensive and lighter in weight, the movable bridge design was chosen instead of a two-section pivoted bridge approximately 250 ft long and equivalent in performance. In effect, a movable bridge span is replaced by fixed shore ramps. A description of the general characteristics and operation of the proposed transfer bridge follows.

The bridge is designed as a Pratt truss consisting of twelve panels with a depth of 1/10 of the span. The outboard end panel has been specially designed for support by the ship. The top chords of the truss have been extended over the inboard end panel and are slotted to pass a bar hanger, thus stabilizing the top chord at the inboard end. The outboard end of the top chord of the truss will be stabilized by a rigid leg, which is pinned through the top chord. Floor beams are pinned under the center of the bottom chord to allow for a list of 10°. The inboard hinge at the bottom of the truss is formed by a large pin, which is extended into a boxlike section. The box contains a buffer spring on either end for shock loading and will be constructed to slide vertically in guides at the inboard gantry tower. Both sides of the slide are connected by a rigid box-section beam. The bar hanger passing through the slotted top chord is pinned at its upper end to an overhead cross beam, the ends of which are constructed also to form a slide running in the same guides as for the lower section.

The ship end of the bridge is guided onto the vessel by a locating casting on the center line of the bridge. This casting fits over a horn fastened to the stern of the vessel and is seated on bearing plates on both sides of the vessel at the stern. The bridge is also guided at the outboard gantry by an overhead cross beam to which the rigid leg is pinned. The beam is extended, forming a slide which runs between guides fastened to the gantry tower. The ends of the slides are curved to allow the beam to remain guided while the vessel lists.

The gantry towers are bolted to the foundations, with the inner end post of the inboard gantry also rigidly bolted to the abutment, which has been carried beyond the upper level to absorb the bridge end reaction and shock loading via the tower structure.

The top of the foundation for the inboard gantry tower has been constructed to a level in order to clear the lower slide. The top of the foundation for the outboard gantry has been carried sufficiently high to form a positive step for

the vessel in light condition at high tide in conjunction with a buffer arrangement that is connected to the face of the ship end of the foundation.

The dead load of the bridge is counterbalanced at the inboard gantry by weights running inside the tower. The weights are connected to four cables, which run over large sheaves, with the other end of the cables connected to equalizer beams. The live load, plus the remainder of dead load, is carried at this stage by a screw arrangement, which is supported by girders at the top of the towers. The screw raises and lowers the bridge between the two levels.

At the outboard gantry the dead load of the bridge is also counterbalanced by a weight running inside the towers. The bridge then is raised and lowered by an auxiliary counterweight, which is lowered onto the main counterweights when the bridge is raised and lifted when the bridge is supported at the ship's stern.

Internal bracing for wind loads will be provided under the bridge, either as tension struts or in the form of a wide face plate on one chord of the trusses.

The gap between the bridge-floor system and the ship's deck will be covered by an auxiliary-hinged bridge plate, which will automatically position itself as the bridge rests on the deck. The ship must be moved forward to clear the outboard end of the bridge when the bridge is moved up or down.

CRANES

New designs of container ships, with many large containers stowed below the weather deck, will require shipboard-mounted traveling gantry cranes for loading. Synchronized independent suspension of the ends of long containers is essential for the rapid and accurate placement of the containers. New designs for shipboard application are required. The cranes should have a lifting capacity of approximately 25 long tons; a hoisting rate of approximately 75 ft per min; and a traversing rate of 125 ft per min. They should be capable of moving fore and aft with light load, and should be powered from 440-volt, 3-phase, 60-cycle AC current. It is necessary for the traversing track, which extends over the ship's side, to be retractable in order not to interfere with ship maneuvering and docking.

TRENDS

Although the roll-on roll-off type of ship has made considerable progress in the past and some new services are being initiated, the trend is to large-capacity, heavy-lift ships of the lift-on lift-off type. These designs are being considered for both domestic and overseas services and will be featured by high loading rates and quick turnarounds.

CONCLUSIONS

New-type cargo ships are designed to reduce pierside costs by increasing the rate of cargo handling and by reducing port time. Specifically, they are designed to carry prepacked containers and self-loading vehicles. In some cases special terminal facilities, such as bridges and cranes, must be provided to effect rapid loading. In all cases large areas adjacent to the dock or on the dock must be provided to handle containers or vehicles to be discharged and loaded in a short period.

AMERICAN SOCIETY OF CIVIL ENGINEERS

Founded November 5, 1852

TRANSACTIONS

Paper No. 2972

ATTENUATION OF SOLITARY WAVES ON A SMOOTH BED

BY YOSHIKI IWASA¹

SYNOPSIS

The hydraulic characteristics of solitary waves are examined. Special consideration is given to the mathematical analysis of the attenuation process of solitary waves. Then the theoretical results are compared with experimental data. It is found that the total kinetic energy minus the potential energy is twice the kinetic energy of the vertical motion.

INTRODUCTION

The theoretical and experimental research concerning the solitary wave (a single elevation of water above the still-water level moving with constant celerity without change of form) may be found in many references.^{2,3} Although this study was originally undertaken as the result of mathematical interest, regardless of the actual existence of the phenomenon, it is well known that a close analogy exists between the hydraulic characteristics of a solitary wave and those of an incoming water wave in surfs near coasts. Therefore, it is important to obtain the complete characteristics of solitary waves in order to apply them to the problems of coastal engineering.^{3,4}

Previous studies^{5,6} have been concerned with the hydraulic configuration of open-channel flows with appreciable vertical acceleration. The solution of a second-order approximation of transitory wave flow was expressed in terms of Jacobi's elliptic function, with the solitary wave as one of the limiting cases.

NOTE.—Published, essentially as printed here, in June, 1957, in the Journal of the Hydraulics Division, as *Proceedings Paper 1862*. Positions and titles given are those in effect when the paper was approved for publication in *Transactions*.

¹ Asst. Prof. of Hydraulics, Dept. of Civ. Eng., Faculty of Eng., Kyoto Univ., Kyoto, Japan.

² "Hydrodynamics," by H. Lamb, Dover Publications, New York, N. Y., 1932.

³ "The Solitary Wave," by J. W. Dally and S. C. Stephan, *Proceedings*, 3d Cong. on Coastal Eng., Cambridge, Mass., 1953.

⁴ "The Solitary Wave Theory and its Application to Surf Problem," by W. H. Munk, *Annals of the New York Academy of Science*, Vol. 51, 1949, Article 3.

⁵ "Analytical Considerations on Cnoidal and Solitary Waves," by Y. Iwasa, *Memoirs of the Faculty of Engineering*, Kyoto Univ., Kyoto, Japan, Vol. XVII, No. IV, October, 1955.

⁶ "Hydraulic Characteristics of Solitary Waves," by Y. Iwasa, paper presented at the Annual Convention of the Japan Soc. of Civ. Eng., Tokyo, May, 1956.

Use of this function revealed some fundamental hydraulic characteristics of the solitary wave.

The study of solitary waves is extended herein. Of special importance is the attenuation of solitary waves by viscous shear within the laminar boundary layer between the main potential flow under a passing solitary wave and a smooth horizontal channel bed. The mathematics of the attenuation problem was first treated⁷ by Garbis H. Keulegan in 1948, based on the small-amplitude theory of wave motion. In 1953 James W. Daily, A.M. ASCE, and Samuel C. Stephan published⁸ an empirical formula for the attenuation (a result of much experimental data), and in 1955 and 1956, Arthur I. Ippen,⁹ M. ASCE, and Gershon Kulin,⁹ J.M. ASCE, published results of additional experiments and presented a new approximate attenuation formula (which was experimentally verified by their work) based on the Blasius formula for the coefficient of friction.

The finite-amplitude theory of solitary waves is considered herein in the treatment of viscous damping in the laminar boundary layer. Therefore, it should be noted that the total kinetic energy is greater than the potential energy by twice the kinetic energy of the vertical motion, as Victor P. Starr¹⁰ originally verified in 1947. Assuming that the flow within the laminar boundary layer under a solitary wave is also translatory, as is the main flow outside the boundary layer, and the velocity distribution is given by some suitable formulas, the viscous damping of a solitary wave may be evaluated by using the usual concept that the rate of energy loss of the wave is equivalent to the rate of dissipation of energy in the laminar boundary layer.

Notation.—The letter symbols adopted for use in this paper are defined where they first appear, in the illustrations or in the text, and are arranged alphabetically, for convenience of reference, in the Appendix.

HYDRAULIC CHARACTERISTICS OF SOLITARY WAVES

Some hydraulic characteristics of solitary waves will now be derived, considering translatory wave flow with an appreciable acceleration in the vertical motion, and are presented for subsequent use. In the theory the velocity distribution in the horizontal direction is assumed to be truly translatory.

The solitary wave profile is given as being of the Rayleigh type—

$$\eta = a_o \operatorname{sech}^2 \left[\frac{1}{2} \frac{a_o}{y_o} \sqrt{\frac{3 a_o}{y_o + a_o}} (x - ct) \right] \dots \dots \dots (1)$$

in which η is the elevation of wave profile above still-water level; a_o denotes amplitude; y_o is the still-water depth; x represents the horizontal distance

⁷ "Gradual Damping of Solitary Waves," by G. H. Keulegan, *Journal of Research* RP 1895, Bureau of Standards, U. S. Dept. of Commerce, Washington, D. C., Vol. 40, 1948.

⁸ "Damping Characteristics of the Solitary Wave," by A. T. Ippen, G. Kulin, and M. A. Raza, *Technical Report No. 16*, Hydrodynamics Lab., Massachusetts Inst. of Technology, Cambridge, Mass., April, 1955.

⁹ "The Effect of Boundary Resistance on Solitary Waves," by A. T. Ippen and G. Kulin, *La Houille Blanche*, July-August, 1957.

¹⁰ "Momentum and Energy Integrals for Gravity Waves of Finite Height," by V. P. Starr, *Journal of Marine Research*, Bingham Oceanography, Yale Univ., New Haven, Conn., Vol. 6, No. 3, 1947.

along the wave measured from the wave crest; t is time; and c denotes the wave celerity expressed by $\sqrt{g(y_0 + a_0)}$ from a consideration of the law of continuity.

After transforming the coordinate system into the moving one,

$$x - ct \rightarrow x$$

Letting $y_0 \gg a_0$, the expression of J. Boussinesq¹¹ and of Keulegan for solitary waves is obtained.

The horizontal velocity in the main flow is given by considering the law of continuity, so that

$$u_0 = c \frac{\eta}{y_0 + \eta} \dots \dots \dots (2)$$

and the vertical velocity is given by using the usual hydrodynamic concept of the streamline,⁵

$$v_0 = \sqrt{3} c \left(\frac{a_0}{y_0} \right)^{\frac{1}{2}} \left(1 + \frac{a_0}{y_0} \right)^{\frac{1}{2}} \left[\left(\frac{\eta}{y_0} \right) \left(1 + \frac{\eta}{y_0} \right)^{-2} \left(1 - \frac{\eta}{y_0} \right)^{\frac{1}{2}} \left(\frac{y}{y_0} \right) \right] \dots (3)$$

in which y is the vertical distance from the channel bottom.

The volume of the solitary wave per unit width is obtained by integrating η from negative infinity to positive infinity:

$$V = \frac{4}{\sqrt{3}} y_0^2 \left(\frac{a_0}{y_0} \right)^{\frac{1}{2}} \left(1 + \frac{a_0}{y_0} \right)^{\frac{1}{2}} \dots \dots \dots (4)$$

In the small-amplitude theory of wave motion, the energy is half potential and half kinetic. This forms the basic idea of the study of attenuation of Keulegan⁷ as well as that by Ippen.⁸ In 1947, Starr¹⁰ first integrated the energy integral for the periodic gravity wave and applied it to the problem of solitary waves. Starr's results explain that the kinetic energy is greater than the potential energy by twice the kinetic energy of the vertical motion. However, it is rather difficult to examine quantitatively the hydraulic characteristics of solitary waves in Starr's derivation. The same conclusions as those of Starr have been obtained by using theoretical results⁶ and are as follows:

The potential energy, E_P , is given by

$$E_P = \frac{1}{2} \rho g \int_{-\infty}^{+\infty} \eta^2 dx \dots \dots \dots (5)$$

in which ρ is the density of fluid and g denotes the acceleration of gravity. Substituting η , expressed by Eq. 1, and integrating results in

$$E_P = \frac{4}{3\sqrt{3}} \rho g y_0^3 \left(\frac{a_0}{y_0} \right)^{\frac{1}{2}} \left(1 + \frac{a_0}{y_0} \right)^{\frac{1}{2}} \dots \dots \dots (6)$$

¹¹ "Théorie des ondes et des remous qui se propagent le long d'un canal rectangulaire horizontal, en communiquant au liquide contenu dans ce canal des vitesses sensiblement parallèles de la surface au fond," by J. Boussinesq, *Journal of Mathematics*, Liouville, France, Vol. 17, 1872.

The kinetic energy of the horizontal motion is

$$E_{KH} = \frac{1}{2} \rho \int_{-\infty}^{+\infty} u_o^2 (y_o + \eta) dx \dots \dots \dots (7)$$

and integration yields

$$E_{KH} = \frac{2}{\sqrt{3}} \rho g y_o^3 \left[\left(\frac{a_o}{y_o} \right)^{\frac{1}{2}} \left(1 + \frac{a_o}{y_o} \right)^{\frac{1}{2}} - \frac{1}{2} \left(1 + \frac{a_o}{y_o} \right) \log_e \left| \frac{1 + \sqrt{\frac{\frac{a_o}{y_o}}{1 + \frac{a_o}{y_o}}}}{1 - \sqrt{\frac{\frac{a_o}{y_o}}{1 + \frac{a_o}{y_o}}}} \right| \right] \dots (8)$$

The kinetic energy of the vertical motion is given by

$$E_{KV} = \frac{1}{2} \rho \int_{-\infty}^{+\infty} v_o^2 (y_o + \eta) dx \dots \dots \dots (9)$$

and integration yields

$$E_{KV} = \frac{2}{\sqrt{3}} \rho g y_o^3 \left[\frac{1}{3} \left(\frac{a_o}{y_o} \right)^{\frac{1}{2}} \left(1 + \frac{a_o}{y_o} \right)^{\frac{1}{2}} \left(3 + \frac{a_o}{y_o} \right) - \frac{1}{2} \left(1 + \frac{a_o}{y_o} \right) \log_e \left| \frac{1 + \sqrt{\frac{\frac{a_o}{y_o}}{1 + \frac{a_o}{y_o}}}}{1 - \sqrt{\frac{\frac{a_o}{y_o}}{1 + \frac{a_o}{y_o}}}} \right| \right] \dots (10)$$

The total energy of a solitary wave per unit width is expressed by the sum of Eqs. 6, 8, and 10:

$$E = \frac{4}{\sqrt{3}} \rho g y_o^3 \left[\left(\frac{a_o}{y_o} \right)^{\frac{1}{2}} \left(1 + \frac{a_o}{y_o} \right)^{\frac{1}{2}} - \frac{1}{2} \left(1 + \frac{a_o}{y_o} \right) \log_e \left| \frac{1 + \sqrt{\frac{\frac{a_o}{y_o}}{1 + \frac{a_o}{y_o}}}}{1 - \sqrt{\frac{\frac{a_o}{y_o}}{1 + \frac{a_o}{y_o}}}} \right| \right] \quad (11)$$

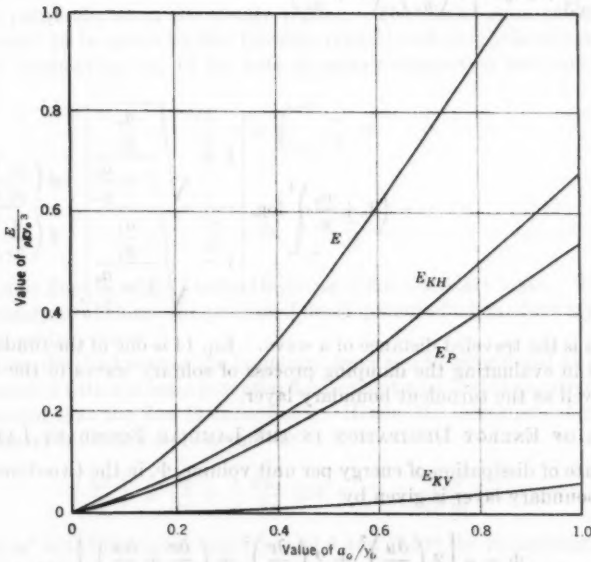


FIG. 1.—RELATIONSHIP BETWEEN ENERGY AND RELATIVE AMPLITUDE

Eq. 11 is the total energy of the finite-amplitude wave. When the wave amplitude is very small compared with the original water depth, $y_o \gg a_o$, Eq. 11 becomes

$$E = \frac{8}{3\sqrt{3}} \rho g y_o^{\frac{1}{2}} a_o^{\frac{3}{2}} \quad (12)$$

Eq. 12 is the same as Keulegan's expression, and it follows that the potential energy is equal to the kinetic energy in the small-amplitude theory. Denoting E_K as the total kinetic energy, the relationship between the kinetic and potential energies is

$$E_K - E_P = 2 E_{KH} \dots \dots \dots (13)$$

Eq. 13 shows that the kinetic energy in the finite-amplitude theory is greater than the potential energy, and the difference between them is twice the kinetic energy of the vertical motion, as Starr first derived by use of the gravitational wave theory. Fig. 1 shows the relationship between the dimensionless energy, expressed as $E' = \frac{E}{\rho g y_o^3}$, and the relative amplitude, a_o/y_o .

The rate of energy dissipation when the solitary wave passes through the channel is given by differentiating Eq. 11 with respect to time. That is,

$$\frac{dE}{dt} = -\frac{2}{\sqrt{3}} \rho g^{\frac{1}{2}} y_o^{\frac{1}{2}} \left[4 \left(\frac{a_o}{y_o} \right)^{\frac{1}{2}} \left(1 + \frac{a_o}{y_o} \right) - \left(1 + \frac{a_o}{y_o} \right)^{\frac{1}{2}} \log_e \left| \frac{1 + \sqrt{\frac{a_o}{y_o} + 1 + \frac{a_o}{y_o}}}{1 - \sqrt{\frac{a_o}{y_o} - 1 - \frac{a_o}{y_o}}} \right| \frac{d \left(\frac{a_o}{y_o} \right)}{d \left(\frac{s}{y_o} \right)} \right] \dots (14)$$

in which s is the traveled distance of a wave. Eq. 14 is one of the fundamental equations in evaluating the damping process of solitary waves in the laminar layer as well as the turbulent boundary layer.

RATE OF ENERGY DISSIPATION IN THE LAMINAR BOUNDARY LAYER

The rate of dissipation of energy per unit volume, Φ , in the two-dimensional laminar boundary layer is given by

$$\Phi = \mu \left[2 \left(\frac{\partial u}{\partial x} \right)^2 + 2 \left(\frac{\partial v}{\partial y} \right)^2 + \left(\frac{\partial v}{\partial x} + \frac{\partial u}{\partial y} \right)^2 \right] \dots \dots \dots (15)$$

in which u and v are the horizontal and vertical velocities in the boundary layer, and μ denotes the dynamic viscosity of the fluid. It is sufficient to consider that the gradient of horizontal velocity in the y -direction is very large compared with other terms, with the result that the principal part of Eq. 15

becomes

$$\Phi = \mu \left(\frac{\partial u}{\partial y} \right)^2 \dots \dots \dots (16)$$

Damping of a solitary wave on a smooth channel bed is usually considered to be due to the viscous shear expressed by Eq. 16. If the velocity distribution in the laminar boundary layer is determined from the original Navier-Stokes equations of motion,² the rate of energy dissipation can be obtained by integrating from the channel bottom to the thickness of the boundary layer, and from negative infinity to positive infinity. However, it is difficult to integrate the original hydrodynamic equations. Although Keulegan did this, his theory implies that the thickness of the boundary layer extends to infinity, whereas the flow is actually confined. Under some appropriate conditions, the original dynamic equations become linear, and a rigorous solution is obtained. However, the expression is so complicated, being composed of a Fourier series, that it is impractical. This difficulty is mainly a result of the finite thickness of the boundary layer.

Ippen, Kulin, and Raza⁵ first measured the velocity distribution in the laminar boundary layer by an electrical differential gage, and their results show that the velocity distribution in the boundary layer can be assumed to be linear or parabolic, as in the steady regime. The distribution of velocity is also assumed to be given by the Couette (linear) and parabolic types of flow. Thus, by integrating Eq. 16 the rate of energy dissipation per unit width is given by

$$\frac{dE}{dt} = \mu \int_{-\infty}^{+\infty} \frac{u_o^2}{\delta} dx \dots \dots \dots (17)$$

for Couette flow, and

$$\frac{dE}{dt} = 2\mu \int_{-\infty}^{+\infty} \frac{u_o^2}{\delta} dx \dots \dots \dots (18)$$

for parabolic flow, in which δ is the thickness of the boundary layer. Therefore, it is necessary to evaluate the process of development of a boundary layer under a passing solitary wave.

Because the thickness of the boundary layer can be considered to be rather thin compared with the main potential flow, except near and at negative infinity, it is assumed that the flow is unconfined. Hence, the development process of the boundary layer is simply given¹² by

$$\left(\frac{u^*}{u_o} \right)^2 = \frac{\partial \theta}{\partial x} + \frac{1}{u_o} \frac{\partial u_o}{\partial x} (2\theta + \delta^*) + \frac{1}{u_o^2} \frac{\partial}{\partial t} (u_o \delta^*) \dots \dots \dots (19)$$

in which u^* is the frictional velocity, and θ and δ^* are the momentum and displacement thicknesses defined by

$$\theta = \int_0^{\delta} \left(\frac{u}{u_o} - \frac{u^2}{u_o^2} \right) dy \dots \dots \dots (20)$$

¹² "Modern Developments in Fluid Dynamics," by S. Goldstein, Clarendon Press, Oxford, England, 1938.

and

$$\delta^* = \int_0^{\delta} \left(1 - \frac{u}{u_o}\right) dy \dots \dots \dots (21)$$

Transforming the coordinate system into the moving system with constant celerity leads to

$$\left(\frac{u^*}{u_o}\right)^2 = \frac{d\theta}{dx} - \frac{c}{u_o} \frac{d\delta^*}{dx} + \frac{1}{u_o} \frac{du_o}{dx} \left(2\theta + \delta^* - \frac{c}{u_o} \delta^*\right) \dots \dots \dots (22)$$

Assuming that the velocity distribution in the boundary layer is given by the Couette and parabolic types of flow, the momentum and displacement thick- nesses become, respectively,

$$\theta = \frac{\delta}{6} \dots \dots \dots (23)$$

and

$$\delta^* = \frac{\delta}{2} \dots \dots \dots (24)$$

for Couette flow, and

$$\theta = \frac{2\delta}{15} \dots \dots \dots (25)$$

and

$$\delta^* = \frac{\delta}{3} \dots \dots \dots (26)$$

for parabolic flow. Hence, substituting the foregoing values into Eq. 22, the following boundary layer equations are obtained, respectively:

$$\frac{d\delta^2}{dx} + \frac{2}{u_o} \frac{3c - 5u_o}{3c - u_o} \frac{du_o}{dx} \delta^2 = - \frac{12\nu}{3c - u_o} \dots \dots \dots (27a)$$

and

$$\frac{d\delta^2}{dx} + \frac{2}{u_o} \frac{5c - 9u_o}{5c - 2u_o} \frac{du_o}{dx} \delta^2 = - \frac{60\nu}{5c - 2u_o} \dots \dots \dots (27b)$$

in which ν is the kinematic viscosity. In transforming the independent variable from x to η and introducing the dimensionless parameters $\eta = a_o\sigma$, $\delta = a_o i$, and $a_o = y_o \lambda_o$, Eqs. 27 become

$$\frac{di^2}{d\sigma} + \frac{2}{\sigma} \frac{3 - 2\lambda_o\sigma}{(1 + \lambda_o\sigma)(3 + 2\lambda_o\sigma)} i^2 = \pm \frac{12}{\sqrt{3} R_e} \lambda_o^{-1} \frac{1 + \lambda_o\sigma}{\sigma \sqrt{1 - \sigma} (3 + 2\lambda_o\sigma)} \dots (28a)$$

and

$$\frac{di^2}{d\sigma} + \frac{2}{\sigma} \frac{5 - 4\lambda_o\sigma}{(1 + \lambda_o\sigma)(5 + 3\lambda_o\sigma)} i^2 = \pm \frac{60}{\sqrt{3} R_e} \lambda_o^{-1} \frac{1 + \lambda_o\sigma}{\sigma \sqrt{1 - \sigma} (5 + 3\lambda_o\sigma)} \dots (28b)$$

in which R_c is the Reynolds number of celerity, determined by the given flow condition expressed by $g^{\frac{1}{2}} y_o^{\frac{1}{2}} / \nu$, the positive sign indicating the equation for the positive direction from the origin to the infinity, and the negative sign, the equation for the negative direction. As it is still difficult to solve Eqs. 28, the following equation, as the first approximation for small values of λ_o , can be assumed for parabolic flow:

$$\frac{d\bar{i}^2}{d\sigma} + \frac{2}{\sigma} \bar{i}^2 = \pm \frac{12}{\sqrt{3} R_c} \lambda_o^{-\frac{1}{2}} \frac{1}{\sigma \sqrt{1-\sigma}} \dots \dots \dots (29)$$

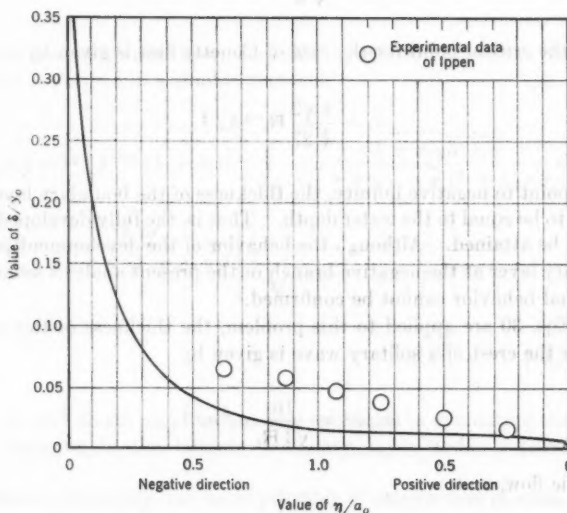


FIG. 2.—DEVELOPMENT OF THE BOUNDARY LAYER

Although Eqs. 28 have a singular point at $\sigma = 0$, the solution for the approximate equation under the boundary conditions, ($\bar{i}_1 = 0$ at $\sigma = 0$ for the positive direction and $\bar{i}_2 = \bar{i}_1$ at $\sigma = 1$ for the negative direction) becomes

$$\sigma^2 (\bar{i}_1)^2 = \frac{16}{\sqrt{3} R_c} \lambda_o^{-\frac{1}{2}} \left[1 - \left(1 + \frac{\sigma}{2} \right) \sqrt{1-\sigma} \right] \dots \dots \dots (30a)$$

and

$$\sigma^2 (\bar{i}_2)^2 = \frac{16}{\sqrt{3} R_c} \lambda_o^{-\frac{1}{2}} \left[1 + \left(1 + \frac{\sigma}{2} \right) \sqrt{1-\sigma} \right] \dots \dots \dots (30b)$$

in which subscripts 1 and 2 show the values in the positive and negative directions, respectively. Eqs. 30 are the approximations for the development of

the laminar boundary layer under a passing solitary wave. Fig. 2 shows an example of the development process of the boundary layer. Eqs. 30 imply that at negative infinity the thickness of the boundary layer becomes infinite although the actual flow is confined. Hence, Eqs. 30 may be applied to the present problem from positive infinity to the point at which the thickness of the boundary layer is equal to the water depth. For parabolic flow this point is computed with sufficient accuracy by the following relationship:

$$\sigma_c \approx \frac{4\sqrt{2}}{\sqrt[3]{3}} R_c^{-1} \lambda_o^{-1} \dots \dots \dots (31)$$

Similarly, the critical point for the case of Couette flow is given by

$$\sigma_c \approx \frac{4\sqrt{2}}{\sqrt[3]{27}} R_c^{-1} \lambda_o^{-1} \dots \dots \dots (32)$$

From this point to negative infinity, the thickness of the boundary layer can be considered to be equal to the water depth. That is, the fully developed laminar regime will be attained. Although the behavior of the development process in the boundary layer at the negative branch in the present analysis seems doubtful, its actual behavior cannot be confirmed.

When Eqs. 30 are applied to this problem, the thickness of the boundary layer under the crest of a solitary wave is given by

$$(\delta_{x=0})^2 = \frac{16}{\sqrt{3} R_c} y_o^{\frac{1}{2}} a_o^{-\frac{1}{2}} \dots \dots \dots (33a)$$

for parabolic flow, and

$$(\delta_{x=0})^2 = \frac{16}{3\sqrt{3} R_c} y_o^{\frac{1}{2}} a_o^{-\frac{1}{2}} \dots \dots \dots (33b)$$

for Couette flow. The theoretical thicknesses of Eqs. 33 are small and are approximately 20% of the experimental results presented by Ippen, Kulin, and Raza. More detailed experiments will be needed to clarify the development process of the laminar boundary layer.

Therefore, the expression of the rate of energy dissipation in the laminar boundary layer for parabolic flow from Eqs. 2, 18, and 30 is

$$\begin{aligned} \frac{dE}{dt} &= 2\mu \int_{-\infty}^{-|x|\sigma-\sigma_c} \frac{u_o^2}{y_o + \eta} dx + 2\mu \int_{-|x|\sigma-\sigma_c}^0 \frac{u_o^2}{\delta_2} dx + 2\mu \int_0^{+\infty} \frac{u_o^2}{\delta_1} dx \\ &= 2\mu \left(\int_{-\infty}^0 \frac{u_o^2}{\delta_2} dx + \int_0^{+\infty} \frac{u_o^2}{\delta_1} dx \right) - 2\mu \int_{-\infty}^{-|x|\sigma-\sigma_c} u_o^2 \left(\frac{1}{\delta_2} - \frac{1}{y_o + \eta} \right) dx \end{aligned}$$

$$= \frac{1}{3^{\frac{1}{2}}} \mu g y_0 R_c^{\frac{1}{2}} \lambda_0^{7/4} (1 + \lambda_0)^{\frac{1}{2}} \left\{ \int_0^1 \frac{\sigma \sqrt{2 + \sigma \sqrt{3 + \sigma}}}{\sqrt{3 + \sigma} \sqrt{1 - \sigma} (1 + \lambda_0 \sigma)^2} d\sigma \right. \\ \left. - \int_0^{\sigma_0} \frac{\sigma d\sigma}{\sqrt{1 - \sigma} (1 + \lambda_0 \sigma)^2} \left[\frac{1}{2} \frac{\sigma}{1 + \sqrt{\left(1 + \frac{\sigma}{2}\right) \sqrt{1 - \sigma}}} \right. \right. \\ \left. \left. - \frac{2}{3^{\frac{1}{2}} R_c^{\frac{1}{2}} \lambda_0^{\frac{1}{2}} (1 + \lambda_0 \sigma)} \right] \right\} \dots (34)$$

For the case of Couette flow, the following relationship of the rate of energy dissipation is derived in a similar manner:

$$\frac{dE}{dt} = \frac{3^{\frac{1}{2}}}{2} \mu g y_0 R_c^{\frac{1}{2}} \lambda_0^{7/4} (1 + \lambda_0)^{\frac{1}{2}} \left\{ \int_0^1 \frac{\sigma \sqrt{2 + \sigma \sqrt{3 + \sigma}}}{\sqrt{3 + \sigma} \sqrt{1 - \sigma} (1 + \lambda_0 \sigma)^2} d\sigma \right. \\ \left. - \int_0^{\sigma_0} \frac{\sigma d\sigma}{\sqrt{1 - \sigma} (1 + \lambda_0 \sigma)^2} \left[\frac{1}{2} \frac{\sigma}{\sqrt{1 + \left(1 + \frac{\sigma}{2}\right) \sqrt{1 - \sigma}}} \right. \right. \\ \left. \left. - \frac{2}{3^{\frac{1}{2}} R_c^{\frac{1}{2}} \lambda_0^{\frac{1}{2}} (1 + \lambda_0 \sigma)} \right] \right\} \dots (35)$$

Eqs. 34 and 35 are also fundamental equations in evaluating the process of viscous damping in the laminar boundary layer under a passing solitary wave.

As shown previously, the basic principle of attenuation of solitary waves is that the rate of energy dissipation in the laminar boundary layer under a passing solitary wave must be equal to the rate of energy loss manifested in the amplitude decrease of the wave. For the present case of parabolic flow, the following relationship is obtained from Eqs. 14 and 34:

$$\lambda_0^{-5/4} (1 + \lambda_0)^{-3/2} (1 + 1.6667 \lambda_0 + 0.1333 \lambda_0^2 - \dots) d\lambda_0 \\ + \left\{ \int_0^1 \frac{\sigma \sqrt{2 + \sigma \sqrt{3 + \sigma}}}{\sqrt{3 + \sigma} \sqrt{1 - \sigma} (1 + \lambda_0 \sigma)^2} d\sigma - \int_0^{\sigma_0} \frac{1}{2} \frac{\sigma^2 d\sigma}{\sqrt{1 - \sigma} (1 + \lambda_0 \sigma)^2} \right. \\ \left. \times \left[\frac{1}{\sqrt{1 + \left(1 + \frac{\sigma}{2}\right) \sqrt{1 - \sigma}}} - \frac{4}{3^{\frac{1}{2}} R_c^{\frac{1}{2}} \lambda_0^{\frac{1}{2}} \sigma (1 + \lambda_0 \sigma)} \right] \right\} \\ \times \frac{3^{\frac{1}{2}}}{4} R_c^{-1} d\left(\frac{s}{y_0}\right) = 0 \dots (36)$$

Integrating Eq. 36 under the boundary condition of $a_0/y_0 = a_i/y_0$ at $s = 0$ yields

$$\lambda_0^{-1} (1 - 0.8062 \lambda_0 - 1.6348 \lambda_0^2 - \dots) - \lambda_i^{-1} (1 - 0.8062 \lambda_i - 1.6348 \lambda_i^2 - \dots) = 0.10602 R_c^{-1} \left(\frac{s}{y_0} \right) \dots (37)$$

in which $\lambda_i = a_i/y_0$. Eq. 36 is the two-dimensional attenuation formula based on the distance traveled. However, if the channel is of limited width (B), some factor must be added to include the frictional effect along the side walls.

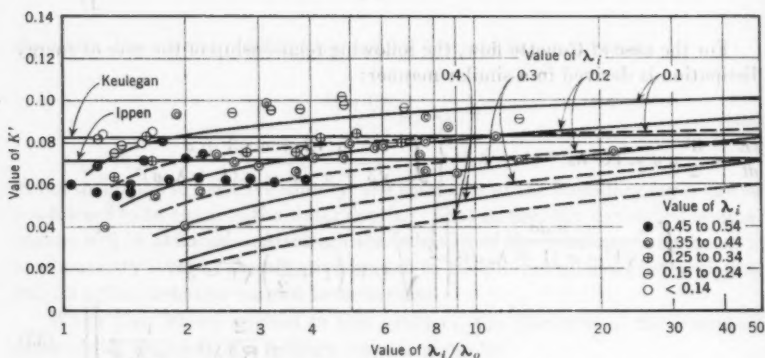


FIG. 3.—RELATIONSHIP BETWEEN K' AND λ_i/λ_0

If $1 + 2 y_0/B$ is used as a first approximation, which is correct only for very low waves, the following relationship for the rectangular channels is obtained:

$$\lambda_0^{-1} (1 - 0.8062 \lambda_0 - 1.6348 \lambda_0^2 - 5.0970 \lambda_0^3 - \dots) - \lambda_i^{-1} (1 - 0.8062 \lambda_i - 1.6348 \lambda_i^2 - 5.0970 \lambda_i^3 - \dots) = 0.10602 R_c^{-1} \left(1 + \frac{2 y_0}{B} \right) \left(\frac{s}{y_0} \right) \dots (38)$$

Similarly, for the case of Couette flow, the attenuation equation is

$$\lambda_0^{-1} (1 - 0.8062 \lambda_0 - 1.6348 \lambda_0^2 - \dots) - \lambda_i^{-1} (1 - 0.8062 \lambda_i - 1.6348 \lambda_i^2 - \dots) = 0.0918 R_c^{-1} \left(1 + \frac{2 y_0}{B} \right) \left(\frac{s}{y_0} \right) \dots (39)$$

ANALYTICAL RESULTS

To verify the foregoing theoretical approach, classical experimental data of J. Scott Russell,¹³ as well as data of Ippen, will be considered. In Fig. 3 these experimental data are plotted with the parametric notation, λ_i . In Russell's data the temperature is assumed (according to Keulegan) to be 15.8°C. In Ippen's data the kinematic viscosity is assumed to be 1×10^{-6} sq ft per sec.

¹³ "Report of the Committee on Waves," by J. Scott Russell, meeting of the British Assn. for the Advancement of Science, London, 1838.

Although the experimental data are scattered, the value of K' from

$$K' = \frac{\lambda_i^{-1} - \lambda_o^{-1}}{R_c^{-1} \left(1 + \frac{2y_o}{B} \right) \left(\frac{s}{y_o} \right)} \quad (40)$$

seems to increase as the ratio of λ_i to λ_o increases. The value of K' is not constant, but it is a variable of the amplitude as well as, in rigorous terms, the Reynolds number of celerity in this theory. It is constant for the small-amplitude theory (that is, 1/12 for Keulegan's expression, and 1/14 for Ippen's expression). Curves of K' versus λ_i/λ_o , expressed by parametric values of λ_i , are also shown in Fig. 3. The dotted lines show the relationship of the attenuation equation when Couette flow is assumed. When these curves are compared, Eq. 38, which represents the attenuation equation of a solitary wave in the laminar boundary layer by assuming a parabolic distribution of velocity, is a reasonably good expression. More approximately, Ippen's expression based on the Blasius formula of the coefficient of friction seems preferable to Keulegan's equation.

CONCLUSIONS

Although the foregoing approach to attenuation implies some physical assumptions that will influence considerably the development process of the boundary layer, it cannot be ascertained whether these assumptions are correct or not. The experimental technique is still too primitive to obtain detailed behavior in the boundary layer. After further progress is made in experimental technique, an examination of these assumptions will become helpful.

ACKNOWLEDGMENTS

The writer wishes to thank Tojiro Ishihara, director of the Hydraulics Laboratory of Kyoto University, Japan, for his considerable instruction; Mr. Ippen, for his cordial guidance and suggestions; and John C. Housley for his help in preparing the paper.

APPENDIX. NOTATION

The following symbols, adopted for use in the paper, conform essentially with "American Standard Letter Symbols for Hydraulics" (ASA Z10.2-1942) prepared by a committee of the American Standards Association with Society representation, and approved by the Association in 1942:

- a = amplitude above still-water level;
- B = channel width;
- c = wave celerity;
- E = energy:
 - E_K = kinetic energy;
 - E_{KH} = kinetic energy in the horizontal direction;

E_{KV} = kinetic energy in the vertical direction;

E_P = potential energy;

g = acceleration due to gravity;

i = dimensionless thickness = δ/a_0 ;

R = Reynolds number;

s = traveled distance;

t = time;

u = horizontal velocity;

u^* = frictional velocity;

V = volume of the solitary wave per unit width;

v = vertical velocity;

x = horizontal distance along the wave;

y = vertical distance from the channel bottom;

δ = thickness of the boundary layer;

δ^* = displacement thickness;

η = elevation of wave profile above still-water level;

θ = momentum thickness;

λ = dimensionless wave height = a_0/y_0 ;

μ = dynamic viscosity;

ν = kinematic viscosity;

ρ = density of the fluid;

σ = dimensionless surface elevation = η/a_0 ; and

Φ = rate of dissipation of energy per unit volume.

AMERICAN SOCIETY OF CIVIL ENGINEERS

Founded November 5, 1852

TRANSACTIONS

Paper No. 2973

EVOLUTION OF MISSISSIPPI VALLEY FLOOD- CONTROL PLAN

BY JOHN R. HARDIN,¹ M. ASCE

SYNOPSIS

The development of the lower Mississippi Valley flood-control plan is traced from its beginning with local levee construction at New Orleans, La., to the comprehensive plan presently (1958) being undertaken by the Corps of Engineers (United States Department of the Army). Flood-control methods for controlling the Mississippi River are analyzed.

INTRODUCTION

The control of floodwaters is complex. It is a problem that is not always susceptible to a precise engineering solution, and yet requires a high degree of professional skill and ingenuity. Although it is a problem that has existed or presently is being faced in almost every river valley in the United States, it is different in each location because of the volume of flow, the degree of settlement of the flood plain, and the topography of the basin. In addition, any single factor, or a combination of many, can strongly influence the method used to solve this problem, which is more complex in the lower Mississippi River Valley than in any other river valley.

THE LOWER MISSISSIPPI RIVER

The lower Mississippi River drains an area of 1,245,000 sq miles, including all or parts of thirty-one states and two Canadian provinces (Fig. 1). Fig. 1 also shows the major subdivisions of the drainage basin.

The average annual mean discharge at Vicksburg, Miss., is 595,000 cu ft per sec. The maximum discharge that has been measured in the Mississippi River itself was 2,159,000 cu ft per sec at Arkansas City, Ark., in 1937. However, if the 1927 floodwaters had been confined by levees at this site, it is estimated that the discharge would have been 2,472,000 cu ft per sec.

NOTE.—Published, essentially as presented here, in May, 1957, in the Journal of the Waterways and Harbors Division, as *Proceedings Paper 1261*. Positions and titles given are those in effect when the paper was approved for publication in *Transactions*.

¹ Maj. Gen. (retired); Pres., Engrs. of Central America, Inc., Washington, D. C.



FIG. 1.—THE DRAINAGE BASIN OF THE MISSISSIPPI RIVER

MISSISSIPPI RIVER FLOWS

Flow in the lower Mississippi River is derived in large part from its tributaries. Fig. 2 shows the contribution of each major subdivision to the entire drainage basin in terms of percentage of drainage area, percentage of total rainfall, and percentage of runoff.

The Ohio River Basin, which comprises only 16% of the total drainage area and receives only one-quarter of the rainfall, contributes 40% of the average

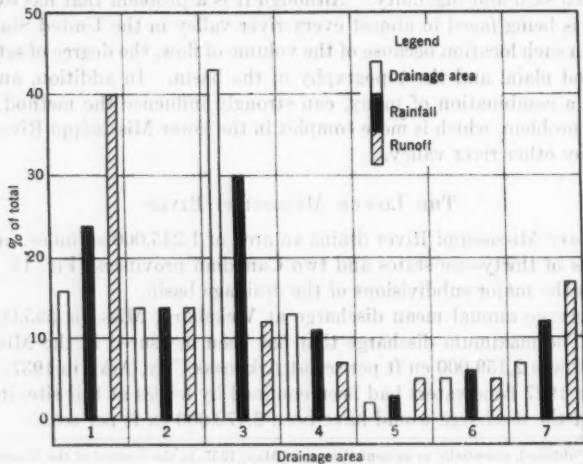


FIG. 2.—A COMPARISON OF DRAINAGE-AREA SIZE, AMOUNT OF RAINFALL, AND CONTRIBUTION TO TOTAL RUNOFF

annual runoff north of the latitude of Red River Landing, La. The Missouri River Basin forms 43% of the drainage area and receives 30% of the basin's annual rainfall, but it contributes only 12% of the runoff north of the latitude of Red River Landing. The area designated as No. 7 (approximately the lower Mississippi River Valley) is 7% of the total drainage area and receives 12% of the basin's rainfall. However, its contribution to runoff is extensive—it comprises 17% of the total runoff. It is necessary to understand this fact before a thorough analysis can be made of the flood problem in the lower Mississippi River Valley.

The unusually large drainage area, with its wide variations in climatic, topographic, and cultural conditions, makes it extremely difficult to arrive at a satisfactory solution to the control of floodwaters in the alluvial valley of the Mississippi River.

THE ALLUVIAL VALLEY OF THE LOWER MISSISSIPPI RIVER

The alluvial valley of the lower Mississippi River is a broad, gently sloping lowland which begins at Cape Girardeau, Mo., and extends to the Gulf of Mexico, a distance of more than 600 miles. This lowland is bordered by abrupt escarpments, the width varying from 30 miles to 125 miles. Tributary flow joins the main river at various locations, and the lowland extends upstream along the tributaries for many miles in addition to forming broad, flat basins in the vicinity of the junction. In recent geologic times the tributary basins and the lowlands along the main river have been subject to flooding as the river stages exceeded bankfull conditions.

The area, historically subject to overflow from Mississippi River floods and tributary floods, is the one to which authorizing legislation refers in defining the scope of the "Mississippi River and Tributaries Project."

The valley is truly alluvial from a geological standpoint and is considered to have been formed during the final cycle of glaciation sequences. During the last glacial stage, when the sea level was much lower than at present, the lower Mississippi River Valley became deeply eroded and entrenched between the walls of the valley. As the glacial ice mass melted and the sea level was raised, the valley filled, gravels and coarse sands being found generally in the lowest horizons. The present alluvial plain consists primarily of sands and silt, which become very fine sands and silt in the southern section of the plain. As is typical of rivers carrying a large quantity of alluvium, the lower Mississippi River developed a highly sinuous course, creating meander loops and bends and shifting its channel from time to time so that the alluvial plain has been worked and reworked by the river many times. Therefore, there is a complex soil structure in the valley. The materials are eroded easily by the river in its present pattern, and the improvement and control of the river for navigation or flood control is influenced greatly by the nature of the alluvial plain.

As is characteristic of alluvial streams, during floods the river deposits sediment in the overbank areas, dropping the greater part of its load adjacent to the stream. For this reason, the banks are generally from 10 ft to 15 ft higher than the lowlands within the tributary basins. Thus, drainage is directed away from the Mississippi River and enters the river through tributary

mouths. The drainage pattern is complicated further by the similar behavior of alluvial tributary streams. This basic complication must be remembered when developing a flood-control plan for the basin.

DEVELOPMENT OF PLANS OF CONTROL

The present flood-control plan began in 1928, following the flood of 1927, being restudied.

A careful and logical analysis, using known engineering methods and techniques, must be made when developing a plan for controlling floods. It is necessary to proceed logically, determining first what forces are being dealt with. Following this, it is possible to determine the magnitude and combination of the required engineering works. For that reason, it is not possible to begin with the hypothesis that only levees, only reservoirs, or only floodways, or even combinations of these elements, will control floods. One must first determine where and in what quantity the floodwaters will occur. Then it is possible to examine the elements of flood control to determine which structures can be used, and in what combinations, in order to control the determined flows most effectively.

DETERMINATION OF DESIGN-FLOOD FLOWS

To produce a major flood on the lower Mississippi River, a sequence of major storms is required, usually extending over a period of from one month to two months, or longer. Because of the large drainage area involved and the relatively short period of record, it is reasonable to assume that all critical combinations of storms and runoff have not been observed. This assumption was the basic approach to a study² of design-flood flows recently made by engineers of the Mississippi River Commission in re-examining the flood-control plan.

Approximately thirty-five storm combinations, selected by the Weather Bureau (United States Department of Commerce), were studied, including recorded storms that had occurred since the last review of the project. These combinations had extreme variations in rainfall and runoff characteristics and in contributions from major tributaries. Of the thirty-five storm combinations, four were selected for detailed study to be used as bases for determining the magnitudes of the lower Mississippi River project design flood. These four combinations represent the maximum contributions that would be expected from the major tributaries. Storm combinations and the critical arrangements of the four hypothetical floods are as follows:

1. Hypo-Flood 52A (late spring season) combines one transposed storm and two storms that actually occurred in the area.
2. Hypo-Flood 56 (early spring season) combines two actual storms.
3. Hypo-Flood 58A (winter season) combines one storm that actually occurred in the area, one storm that actually occurred and increased 10%, and one transposed storm.

² "Project Design Flood Study," Annex A to *Interim Review Report, Mississippi River and Tributaries*, Office of the Pres., Mississippi River Comm., Vicksburg, Miss., June, 1937.

4. Hypo-Flood 63 (early spring season) consists of two storms that actually occurred in the area and one transposed storm.

The four hypo-flood hydrographs were developed from combinations of events that are considered plausible from a meteorological standpoint and that are reasonably certain to occur, judging from past flood and storm sequences. It is probable that unusual combinations of meteorological and hydrological events could occur to produce a much greater flood than any of the four selected hypo-floods. However, such a sequence would be rare. The four hypo-floods are believed to represent the maximum flows that reasonably could be expected to occur. This is the basic concept of planning for the flood-control features of the project.

In general, Hypo-Flood 52A assumes the maximum component that could be expected from the upper Mississippi River Basin and the Missouri River Basin. Hypo-Flood 58A represents the maximum from the Ohio River Basin. Hypo-Flood 63 assumes the maximum from the Arkansas-White River Basin. In general, Hypo-Flood 58A has characteristics similar to those of the more frequent floods of record in which the maximum contribution has been from the Ohio River Basin, with moderate contributions from the upper Mississippi River Basin and the Missouri River Basin and relatively large ones from the other major tributaries.

Following the determination of the four hypo-floods, each was routed down the Mississippi River by a detailed method of flood routing to determine the resulting daily flows at St. Louis, Mo.; Cairo, Ill.; Memphis, Tenn.; Helena, Ark.; Vicksburg and Natchez, Miss.; and at the latitude of Red River Landing.

Modified hydrographs were obtained for the hypo-floods for two sets of conditions—with Group E reservoirs operating (reservoirs built and being constructed), and with Group EN reservoirs operating (Group E reservoirs, plus reservoirs scheduled for future construction).

Thus, hydrographs were determined for key stations within the alluvial valley for floods without reservoirs operating and for those with two different combinations of operating reservoirs. Using basic data, it is possible to make a sound reappraisal of the flood-control plan.

The foregoing method was used recently in reviewing the design-flood flows for this project. Similar methods have been used in the past. Development of the 1928 flood-control plan^a and the 1941 revision was, in fact, based on such a study. Following this, it was necessary to determine the flow lines for such a design flood and to select available engineering methods for containing it. In addition to the analytical procedures for flow-line determination, hydraulic-model techniques were used to verify the results.

ORIGINAL STUDY OF FLOOD-CONTROL PLANS

Before the 1928 flood-control plan was authorized by the United States Congress, hearings were held by the Flood Control Committee of the United States House of Representatives. Voluminous testimony was presented, advocating various plans of improvement, or combinations of such plans. At

^a House Document 90, 70th Cong., 1st Session, 1928.

the same time, earlier proposals were reviewed in an effort to arrive at the best possible plan.

For many years the efforts to control floods on the Mississippi River have been thoroughly studied and analyzed. The first important study resulted in the report of Andrew A. Humphreys and H. L. Abbot⁴ in 1861. Since that time, many other engineers have analyzed flood-control techniques. In 1917, C. McD. Townsend grouped⁵ flood-control methods into six major categories:

1. Methods of reducing extreme variations in runoff by increasing the soil absorption of rainwater, including reforestation, soil drainage, variations in methods of plowing, and the construction of small dikes in agricultural areas, so that a large part of the rainfall is retained in the soil until there is time to absorb it;
2. Reservoirs and detention basins that will retain the crests of the runoff and discharge them at lower stages;
3. Barriers thrown across mountain streams to prevent erosion and the transportation of debris;
4. Channel improvement, cutoffs, and the construction of auxiliary channels;
5. Levees to confine the floodwaters to the channel; and
6. Improved or new outlets to facilitate stream discharge.

Each measure has had staunch advocates as well as opponents. A brief mention of the measures is essential to an understanding of the final plan of improvement adopted.

The effects of forest growth in assisting to hold back runoff are well known. However, there is no evidence to support the use of reforestation as a primary means of flood prevention to the exclusion of any other measure. It should be remembered that in 1541, when Hernando DeSoto first viewed the Mississippi River, the river was in extreme flood. At that time, heavy forests existed throughout the entire Mississippi River drainage basin.

Soil drainage, contour plowing, and the construction of small dikes on agricultural lands assist in controlling floods to the extent that they hold back floodwaters in the immediate area. Advocates of these measures have contended strongly that they be adopted as the primary means for controlling floods. Yet, it was apparent in 1927 that the problem of Mississippi River flood control was far too complex to be solved by any single measure, and that upstream preventive measures, although desirable for control, would have only a minor influence on the over-all solution.

Townsend perceived the limited contribution to flood control by upstream improvements. In considering reservoirs and detention basins, he concluded⁵:

"At the headwaters of streams storage reservoirs and detention basins can be successfully employed to reduce flood heights. Which method is preferable is dependent upon local conditions. Their efficiency, however, rapidly diminishes as the distance from them increases."

⁴ "Report Upon the Physics and Hydraulics of the Mississippi River," by Andrew A. Humphreys and H. L. Abbot (1861); U. S. Govt. Printing Office, Washington, D. C., 1876.

⁵ "Final Report of the Special Committee on Floods and Flood Prevention," by C. McD. Townsend, Chairman, *Transactions, ASCE*, Vol. LXXXI, 1917.

In 1898, after a study of various flood-control measures and the value of reservoirs for full control of floods, a report⁶ of the Senate Committee on Commerce concluded that

"* * * the scheme (of reservoirs) is regarded by nearly all engineers and other experts as wholly impracticable; in short, your committee can discover no sure or adequate relief in reservoirs."

This theory was supported earlier by Humphreys and Abbot,⁷ who found that

"the impracticability of the scheme requires no further demonstration. * * * The idea that the Mississippi delta may be economically secured against inundation by such dams has been conclusively proved by the operations of this Survey to be in the highest degree chimerical."

The subject of cutoffs caused almost as much concern and difference of opinion. For example, Humphreys and Abbot⁸ concluded that

"the country above the cut is therefore relieved from the floods only at the expense of the country below. Moreover, if a series of cutoffs were to be made extending to the mouth of the river, the principles educed show that the height of the floods would be regularly decreased from a point near midway of the series to the upper end, and regularly increased from the same point to the lower end. The system, therefore, is entirely inapplicable to the Mississippi River, in whole or in part."

In 1912 Townsend summarized⁹ the various methods of flood control that had been proposed and concluded that cutoffs afford relief at one site at the expense of another locality. This was in general agreement with the earlier findings of Humphreys and Abbot.

Subsequent developments have proved that the conclusions regarding the downstream effect of cutoffs were incorrect. Generally, the views of Townsend and Humphreys and Abbot concerning the limited usefulness of upstream reservoirs to provide flood control in the lower valley have proved sound. Nevertheless, it has been found that there is a substantial benefit and reduction of flood crests resulting from reservoirs that are built and planned on tributaries primarily to benefit the tributary area.

With respect to outlets for the floodwaters, Humphreys and Abbot¹⁰ recognized the desirability of having a secondary outlet for floodwaters, but they found that:

"Unfortunately, however, the relief of the river itself is only half of the difficulty. The water taken from it still remains to be disposed of. * * * A channel to conduct the water must then be prepared. Here lies the great practical difficulty which renders the system of comparatively little avail for protecting Louisiana against overflow. * * *"

⁶ "Report on Mississippi River Floods," *Senate Report No. 1433*, U. S. Senate Committee on Commerce, 55th Cong., 3d Session, 1898.

⁷ "Report Upon the Physics and Hydraulics of the Mississippi River," by Andrew A. Humphreys and H. L. Abbot (1861); U. S. Govt. Printing Office, Washington, D. C., 1876, p. 387.

⁸ *Ibid.*, p. 373.

⁹ "Flood Control of the Mississippi River," by C. McD. Townsend, paper presented at Memphis, Tenn., September 26, 1912; *Senate Document 1094*, 62d Cong., 3d Session.

¹⁰ "Report Upon the Physics and Hydraulics of the Mississippi River," by Andrew A. Humphreys and H. L. Abbot (1861); U. S. Govt. Printing Office, Washington, D. C., 1876, p. 420.

At the time such a conclusion was undoubtedly warranted. The Atchafalaya River, presently (1958) the largest and most useful outlet of the Mississippi River, had not then developed to the extent that it could be considered seriously as an outlet for floodwaters of large magnitude.

Charles Ellet¹¹ also was interested in the many plans for controlling Mississippi River floods. In summarizing his findings, he recommended a comprehensive plan, which included, in addition to levees and reservoirs and the prevention of cutoffs, a recommendation for the

"* * * formation of an outlet of the greatest attainable capacity, from the Mississippi to the head of Lake Borgne at New Orleans, with a view, if possible, to convert it ultimately into the main channel of the river."

With respect to outlets, Townsend believed that they are not as effective in reducing flood heights as popularly supposed.⁹ He based his questioning of the practicability of an outlet on the fact that it must be controlled to be effective, and on the difficulty in regulating the velocity with which the water will flow through the outlet at varying heights of the main stream. He concluded:

"If it is so constructed that it will discharge at a greater velocity than the river itself, there is a danger of its enlargement to such an extent as to divert the greater part of the flow down it and transfer the main stream itself into an outlet; and, if, on the other hand, it discharges at a lower velocity, it will tend to fill with sediment."

This was the basic problem which concerned the Mississippi River Commission as a result of the indicated diversionary forces, so active in recent years at the Old River, which led to the current (1958) construction of control structures and the closure of this natural distributary into the Atchafalaya River Basin.

Many engineers and laymen supported strongly, and often to the exclusion of all other means, a great levee system designed to confine the floodwaters and prevent their overflowing the valley lands. Generally, it was agreed that levees must play a predominant role regardless of other features that would be worthy of incorporation in the over-all plan.

Townsend wrote of levees that "on the lower alluvial reaches of long rivers, such as the Mississippi and Colorado, they afford the only sure means of flood control."⁵

It is evident that, in the seventy-five years preceding the adoption of the present plan, the problem of controlling Mississippi River floods received most careful study and much thought. Not only engineers or local interests to whom the problem was personal took an interest, but there were many others who advanced solutions, some having doubtful application.

In 1925 Charles L. Potter stated¹² that

"there is more wasted ingenuity, unsupported by technical knowledge, applied to the control of floods in the Mississippi River than to any other problem in the United States. The public thinks it an unsolved problem,

¹¹ "The Mississippi and Ohio Rivers: Containing Plans for the Protection of the Delta from Inundation," by Charles Ellet, *Senate Document 20*, 32d Cong., 1st Session, 1853.

¹² "How the Mississippi River is Regulated," by Charles L. Potter, *Engineering News-Record*, April 2, 1925.

and expects that Yankee ingenuity, rather than deep study along the lines of hydraulic engineering, is going to hit upon a solution."

Potter cited briefly some of the theories to which his attention has been directed:

"One individual offered to carry a depth of 100 feet from the Gulf to St. Louis by directing the strong surface current to the bottom and flushing out all sediment. How the inversion of the river was to be accomplished has never been developed.

"Another suggests that the bottom current, which contains the greater part of the sediment, be conducted away in pipes.

"Just now a gentleman in Michigan has a scheme whereby floods may be reduced 'any amount desired'. When approached as to the nature of his plan, he declines to divulge it."

The engineers who grappled with the complex and perplexing flood-control problem were not without suggestions as to how the job might be accomplished. Nor were they without recommendations regarding the practicability of the various flood-control features.

After the flood of 1927, it was evident that effective national action was necessary. After exhaustive study, the plan (known as the Jadwin Plan) of the Chief of Engineers, Corps of Engineers (United States Department of the Army), was adopted by Congress in 1928.¹³

DEVELOPMENT OF THE 1928 PLAN

The Jadwin Plan was truly comprehensive. It provided for the control of the maximum flood that meteorologists considered plausible and has a reasonable probability of occurrence, judging from past flood and storm sequences, and it provided for future expansion to meet changing conditions. It included a spillway upstream from New Orleans, La., diversion floodways in the Atchafalaya River Basin and Tensas River Basin, a riverbank floodway from Cairo to New Madrid, Mo., together with the strengthening and moderate raising of existing levees. It was designed to prevent any material increase in flood stages. Channel stabilization and navigation improvements were also included.

The 1928 act was basically a plan for the control of main-stem flood flows of the Mississippi River in the alluvial valley. It was emphasized in the Jadwin Plan that recommendations for the tributary basins could not be prepared in the limited time available for the formulation of the main-stem plan, and plans for improvements in the tributary basins would be submitted separately. Subsequent legislation has incorporated tributary features into the project, thereby extending the benefits from flood control and making the development of the valley comprehensive.

Thus, the basis for the present flood-control plan was created in 1928 and was promptly subjected to analysis. An exhaustive report¹⁴ was prepared in 1931 as a result of a resolution adopted by the Flood Control Committee of the

¹³ *Flood Control Act*, approved May 15, 1928, 70th Cong., 1st Session.

¹⁴ "Flood Control Works in the Alluvial Valley of the Mississippi River," *Committee Document No. 1*, House Committee on Flood Control, 74th Cong., 1st Session.

House of Representatives. This report examined several suggested improvement plans, each of which was more expensive or less effective than the plan adopted by the Act of 1928. The Board of Engineers for Rivers and Harbors and the Chief of Engineers, reporting on the various plans considered, recommended that no modification of the adopted project be made. Again, after thorough study, it was concluded that the complete control of floods in the lower Mississippi River by reservoirs only was impracticable.

The Board of Engineers for Rivers and Harbors recommended that experimental work be undertaken to ascertain the feasibility of increasing the capacity of the main river channel by a well-coordinated plan, including channel rectification and stabilization, dredging, and bank protection, beginning at the mouth of the Red River and working gradually upstream. Thus, the foundation was laid for the program of cutoffs which was begun in 1932.

Progress was rapid on the construction of the features outlined in the 1928 act. Main river levees were closed and strengthened in time to withstand the high water of 1929, and other works were undertaken and proceeded rapidly. It soon became apparent that the plan of control was sound. However, technical sufficiency is not the only evaluation of a great project in which the holdings and livelihood of many people are involved. The justification for subjecting certain floodway areas to the degree of servitudes resulting from the basic law was questioned as the economy of the lower valley began to recover. This subject was also treated in the report¹⁴ of the Chief of Engineers to the Committee on Flood Control of the House of Representatives. A bill incorporating the recommendations of this report was enacted¹⁵ and approved by the President of the United States in 1936. This act amended the 1928 act to provide for modifying the project in so far as floodways were concerned; improving the Atchafalaya River and its outlets; partial protection in the White River backwater area; and headwater flood control in the Yazoo River tributary basin and the St. Francis River tributary basin. It also provided for elevated crossings of highways and railroads over floodways, drainage works made necessary by levee construction, and levee access roads.

Meanwhile, active construction continued on the various features of the plan. Levees were raised and strengthened. Work progressed on the floodways and outlets in the Atchafalaya River Basin. A program of cutoffs was initiated and completed. Sixteen cutoffs were made under the direction of the Mississippi River Commission. These cutoffs reduced the river distance between Memphis and Baton Rouge, La., by approximately 170 miles. All the construction had a marked influence on the effectiveness of the flood-control plan.

During the 1937 flood the completed works were put to another severe test and proved the soundness of the plan. The success of the cutoff was demonstrated effectively, even with flows upstream from Arkansas City greater than they were in 1927. Flood stages were lowered by from 8 ft to 10 ft at Greenville, Miss., and from 12 ft to 14 ft at Arkansas City without adverse effects on stages downstream from the cutoffs.

¹⁵ Public Number 678, approved June 15, 1936, 74th Cong., 1st Session.

In 1939 and in 1940, resolutions were adopted by committees of the House of Representatives and of the United States Senate requesting the Chief of Engineers to review the entire project again and to submit recommendations for any desirable modifications.

In 1941 the Chief of Engineers submitted a report¹⁶ setting forth several engineering plans both with and without floodways in the middle section. However, no specific plan was recommended. After extended hearings, Congress enacted the Flood Control Act of August 18, 1941. This act called for the abandonment of floodways in the middle section primarily because of the demonstrated effectiveness of the cutoffs; provided for raising main river levees to confine the project flood; added improvement of the Yazoo River backwater area and the Red River backwater area; and made other minor modifications to the plan.

Since 1941 numerous other additions and modifications have been made to the 1928 plan. Among these are extensions of works in the tributary areas, the provision of drainage works, and the addition of local protection projects. In 1954 the project was amended further to provide for the control of flow at the Old River and the Atchafalaya River to prevent the diversion of the Mississippi River through the Atchafalaya River Basin.¹⁷

DESCRIPTION OF PRESENT PLAN

It is apparent that the present plan for flood control and navigation improvements in the lower alluvial valley of the Mississippi River has gradually evolved, as a result of amendments and modifications, from the basic plan approved by the authorizing legislation in 1928. Although it is still the same plan, it has been modified to meet changing economic, physical, and engineering conditions. There is no doubt that the plan will be modified still further as conditions change. This is one of its outstanding characteristics and certainly one of its most admirable features.

The plan is designed to control a flood even greater than that of 1927. The design, or project, flood is the greatest flood that meteorologists believe can reasonably be expected to occur. It assumes a flow at Cairo of 2,450,000 cu ft per sec. (Without reduction by the headwater reservoirs on the upper Mississippi River, the Missouri River, and the Ohio River and their tributaries, the flood flow at Cairo would be 2,600,000 cu ft per sec.) Downstream from the mouth of the Arkansas River, the project flood is from 17% to 27% greater than the 1927 flood, being 3,000,000 cu ft per sec at the latitude of the Old River, just downstream from Natchez.

The flood-control plan blends carefully selected quantities of several proven features, each of which performs a contributing function and all of which, when completed, will protect the alluvial valley from the project flood.

The plan's major features are:

1. Reservoirs on the tributary streams, both within and outside the alluvial valley, to hold back flood flow in so far as is practicable;

¹⁶ "Flood Control on the Lower Mississippi River," *House Document No. 359*, 77th Cong., 1st Session, April 2, 1941.

¹⁷ "The General Problem," by John R. Hardin, in "Old River Diversion Control: A Symposium," *Transactions, ASCE*, Vol. 123, 1958.

2. Levees on the tributaries and on the Mississippi River to confine the flow to a carefully designed leveed channel and backwater areas;
3. Cutoffs on the Mississippi River to speed flow down the river and lower flood stages;
4. Revetment to protect flood-control structures and to assist in stabilizing the channel; and
5. Overbank floodways, which divert flow from the river.

The plan provides for dikes, pumping plants, floodgates, floodwalls, and other features contributing to the proper functioning of the comprehensive improvement plan.

Each feature has been subjected in the past to both praise and criticism, advocated to the exclusion of all other features, or condemned. This comprehensive plan supports the statement¹⁸ made in 1917 by Kenneth C. Grant, M. ASCE, that

"* * * in many cases no one method may provide an adequate solution to the flood problem, but the best plan will consist of a combination of two or more methods. It may be found unfeasible or uneconomical to reduce flood flow to existing channel capacities by reservoir or detention-basin control. It may be found equally unfeasible or uneconomical to provide an adequate channel to accommodate maximum floods. Protection by one method is best carried out up to the point where the remaining necessary protection is cheaper by some other method."

Protection against overflow by the main Mississippi River is accomplished by constructing levees and appurtenant flood outlet structures and floodgates (Fig. 3). The levees extend from high ground at the head of the several basins, into which the valley naturally divides, to the major tributaries that normally form the lower boundaries of the side basins. There are 1,599 miles of main-line levees and 1,955 miles of smaller embankments on the tributaries and floodways and in backwater areas.

The levee line on the west bank begins just south of Cape Girardeau, and except where the waters of the St. Francis River, the Arkansas-White River, and the Red River join the Mississippi River, it extends unbroken to the Gulf of Mexico. The east bank of the river is protected by levees alternating with high bluffs.

From Commerce, Mo., south, the west-bank levee line is continuous to the mouth of the St. Francis River, just north of Helena. Another levee line begins at Helena and protects the front of the White River Basin. The longest continuous levee line in the project, and probably in the world, begins at high ground near Pine Bluff, Ark., follows the south bank of the Arkansas River to its mouth, and then continues down the Mississippi River to the Old River, a distance of 380 miles. The levee line begins again at high ground on the south bank of Red River, a few miles upstream from Alexandria, La. Except for a gap at the head of the leveed Atchafalaya River and a stretch of approximately 11 miles, where the Mansura Ridge along the lower Red River is above over-

¹⁸ Discussion by Kenneth C. Grant of "Floods and Flood Prevention," *Transactions, ASCE*, Vol. LXXXI, 1917, p. 1253.

flow, the levee line extends continuously for 358 miles to its terminus at Venice, La.

On the east bank a short, 22-mile-long levee line begins at Hickman, Ky., and extends into northwestern Tennessee. Beginning just downstream from Memphis, at the head of the Yazoo Basin, there is a continuous 270-mile levee

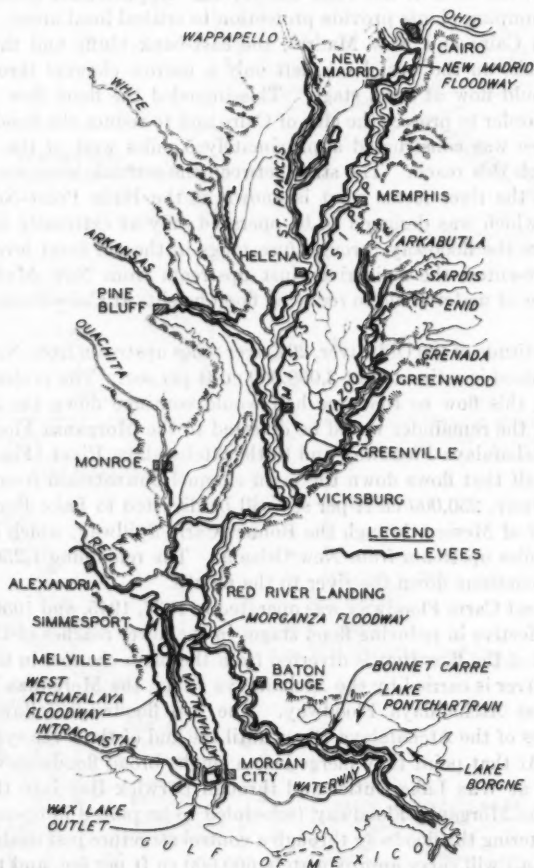


FIG. 3.—THE LOWER MISSISSIPPI RIVER VALLEY FLOOD-CONTROL PLAN

line to just north of Vicksburg. The east bank is largely hilly from Vicksburg to Baton Rouge, where the levee line begins again and extends continuously for 172 miles past New Orleans to Bohemia, La.

Near the mouths of the major tributaries, main-line levees are built to project grade and are fixed generally to correspond to the assumed peak dis-

charges of the project flood. The project also calls for levees extending upstream on lower sections of the basins of the St. Francis River, the White River, the Arkansas River, the Yazoo River, and the Red River at reduced grade. Thus, protection would be given against ordinary floods to lands that would otherwise be covered whenever overbank stages permitted water to back around the ends of the main-line levees. Appurtenant drainage works and some pumping plants provide protection to critical local areas.

Between Cairo and New Madrid, the east-bank bluffs and the levee, as originally built on the west bank, left only a narrow channel through which the river could flow at flood stage. This impeded the flood flow and raised stages. In order to protect the city of Cairo and to reduce the flood heights, a setback levee was constructed approximately 5 miles west of the river-front levee through this reach. The strip between the setback levee and the levee adjacent to the river forms what is known as the Birds Point-New Madrid Floodway, which was designed to be operated only at extremely high stages. Water enters the floodway through fuse plugs in the old front levee opposite Cairo and re-enters the main river just upstream from New Madrid. This floodway was of material aid in reducing flood heights at Cairo during the flood of 1937.

At the latitude of the Old River, 207 river miles upstream from New Orleans, the project flood is estimated at 3,000,000 cu ft per sec. The project provides for dividing this flow so that one half would continue down the main river channel and the remainder would be diverted to the Morganza Floodway and the West Atchafalaya Floodway and to the Atchafalaya River (Fig. 4).

Of the half that flows down the main channel downstream from the Morganza Floodway, 250,000 cu ft per sec will be diverted to Lake Pontchartrain and the Gulf of Mexico through the Bonnet Carre Spillway, which is approximately 25 miles upstream from New Orleans. The remaining 1,250,000 cu ft per sec will continue down the river to the mouth.

The Bonnet Carre Floodway was operated in 1937, 1945, and 1950. It was extremely effective in reducing flood stages in the lower reaches of the river.

The part of the flow that is diverted from the main channel in the vicinity of the Old River is carried by the Atchafalaya River, the Morganza Floodway, and the West Atchafalaya Floodway. The two floodways follow down on opposite sides of the Atchafalaya River until the end of the levee system along the river. At that point they merge into a single, broad floodway whose flow is drawn off at Wax Lake Outlet and through Berwick Bay into the Gulf of Mexico. The Morganza Floodway (scheduled to be placed in operation first, the water entering the floodway through a control structure just upstream from Morganza, La.) will carry approximately 600,000 cu ft per sec, and the Atchafalaya River will carry approximately 650,000 cu ft per sec. The remainder of the diverted flow (approximately 250,000 cu ft per sec) will be carried by the West Atchafalaya Floodway, entering through a fuse-plug levee at the head of the floodway.

The program for stabilization of the river banks is a vital part of the present plan and is accomplished by revetment, dikes, and dredging. The work is not continuous but is constructed at critical locations at which excessive bank caving

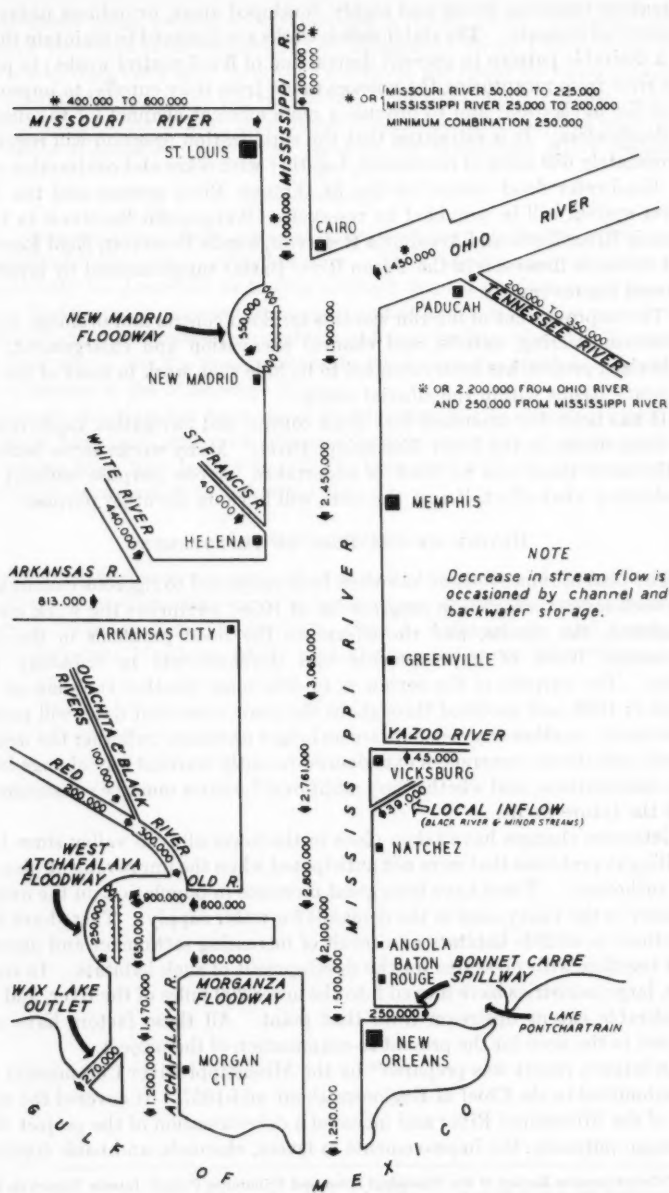


FIG. 4.—DISTRIBUTION OF THE PROJECT FLOOD

threatens main-line levees and highly developed areas, or induces unfavorable channel alinements. The stabilization works are designed to maintain the river in a desirable pattern to prevent destruction of flood-control works; to prevent the river from recapturing the mileage taken from it by cutoffs; to improve the river for navigation; and to provide a more efficient channel for the discharge of floodwaters. It is estimated that the stabilization program will require approximately 689 miles of revetment, together with dikes and contraction works.

Headwater flood control on the St. Francis River system and the Yazoo River system will be provided by reservoirs (Wappapello Reservoir in the St. Francis River Basin and Arkabutla Reservoir, Sardis Reservoir, Enid Reservoir, and Grenada Reservoir in the Yazoo River Basin) supplemented by levees and channel improvements.

The improvement of interior streams for flood control and drainage consists of stream clearing, cutoffs, and channel excavation and enlargement. The authorized project has been extended to include such work in most of the large tributary basins within the alluvial valley.

It has been demonstrated that flood control and navigation improvements are inseparable on the lower Mississippi River. Many works serve both ends at the same time, and no work is undertaken for one purpose without fully considering what effect, if any, the work will have on the other purpose.

REVIEW OF THE PLAN OF IMPROVEMENT

The plan of improvement has often been subjected to rigorous examination. One such review, which is in progress (as of 1958), comprises the work already completed, the results, and the effects on the flood problems in the lower Mississippi River of improvements and developments in tributary river basins. The purpose of the review is to determine whether the plan as conceived in 1928, and modified throughout the years since that date, will perform as intended; whether any elements are no longer necessary; whether the weather records and storm occurrences experienced recently warrant any change in the basic assumptions; and whether any additional features must be constructed to meet the future needs.

Extensive changes have taken place in the lower alluvial valley since 1928, resulting in problems that were not anticipated when the improvement plan was first authorized. There have been great increases in population, in the over-all economy in the valley, and in the demands for water supply. There have been reductions in wildlife habitats as a result of increasing settlement and development together with pressures for the development of such habitats. In recent years, large industries have moved into the lower 200 miles of the river, and to a considerable extent upstream from that point. All these factors have contributed to the need for the present re-examination of the project.

An interim report was prepared¹⁰ by the Mississippi River Commission and was submitted to the Chief of Engineers about mid-1957. It covered the main stem of the Mississippi River and included a determination of the project flood for design purposes; the improvements in levees, channels, and bank stabiliza-

¹⁰ "Comprehensive Review of the Mississippi River and Tributaries Project, Interim Report on Main Stem Features," Mississippi River Comm., Vicksburg, Miss., June, 1957.

tion warranted under present conditions; and a review of the economic justification of the main-stem features. The Mississippi River Commission will submit a final report at a later date that will cover the needs for improvements in the tributary basins of the alluvial valley. The final report will also include a study of the benefits of headwater reservoirs, including authorized reservoirs on all major tributaries covering all parts of the Mississippi River drainage basin.

CONCLUSIONS

No engineering undertaking probably has ever been studied so extensively and examined by so many qualified persons. The present plan of improvement can truthfully be described as having evolved from a gradual development, with the best features proposed being used and after the most thorough study. Each feature has been tested thoroughly and has proved successful. However, the present plan is not the final unalterable solution to the problem of controlling floodwaters of the Mississippi River.

Although the plan has been developed through sound thinking based on established hydraulic principles, changes in treatment and even in concept are necessary from time to time in order to keep pace with the great economic development occurring in the alluvial valley.

ACKNOWLEDGMENTS

Invaluable assistance was received from various members of the staff of the Mississippi River Commission. The writer appreciates the contributions of Rodney A. Latimer, John C. Goodrum, Elias J. Williams, Jr., and James E. Sanders, Associate Members, ASCE, and Eugene A. Graves, M. ASCE.

AMERICAN SOCIETY OF CIVIL ENGINEERS

Founded November 5, 1852

TRANSACTIONS

Paper No. 2974

SALT BALANCE IN GROUND-WATER RESERVOIRS

BY DAVID B. WILLETS¹ AND CHARLES A. MCCULLOUGH,²
ASSOCIATE MEMBERS, ASCE

WITH DISCUSSION BY MESSRS. ROBERT O. THOMAS; AND DAVID
B. WILLETS AND CHARLES A. MCCULLOUGH

SYNOPSIS

The development of water resources in California to meet ultimate water requirements has necessitated planned operation of ground-water reservoirs for seasonal and cyclic storage of water. A problem that must be solved in such operations is the maintenance of suitable mineral quality of the ground water. This paper examines the sources and disposal of salts in ground-water reservoirs and illustrates relationships and requirements for water to maintain salt balance in a hypothetical ground-water reservoir. Deficiencies in present knowledge and in data-collection programs for the evaluation of salt-balance problems are considered.

INTRODUCTION

The development of water resources in California to meet ultimate water requirements will necessitate the use of all economically feasible surface reservoirs. In addition, planned utilization of the immense storage capacity of the state's many ground-water reservoirs will be necessary. The gross usable storage capacity of the more important basins is estimated to exceed 130,000,000 acre-ft. This capacity is usually estimated for the interval of from 20 ft to 200 ft below ground surface, although in some basins dependent largely or entirely on ground water, pumping from considerably greater depths has been found to be economical. Utilization of this storage capacity requires planned

NOTE.—Published, essentially as printed here, in the Journal of the Irrigation and Drainage Division in September, 1957, as *Proceedings Paper 1559*. Positions and titles given are those in effect when the paper or discussion was approved for publication in *Transactions*.

¹Superv. Hydr. Engr., California State Dept. of Water Resources, Los Angeles, Calif.

²Superv. Hydr. Engr., California State Dept. of Water Resources, Sacramento, Calif.

operation of the basins^{3,4,5} under which the water level is drawn down during dry periods. Thus, during wet years storage capacity is made available for retention of part of the local runoff, imported water, or both.

One of the important problems that must be considered in the effective utilization of ground-water storage is the maintenance of a favorable salt balance. Salt balance has been defined as " * * the relationship of salt input to salt output."⁶ This has been amplified as follows:

"If the mass of the salt input exceeds the mass of the salt output the salt balance is regarded as adverse, because this trend is in the direction of the accumulation of salt in the area and such a trend is manifestly undesirable."⁶

Considerable attention has been given to salt balance in river systems in which diversion and irrigation with surface water are practiced, and to salt balance as it affects the accumulation of salts within the root zone of plants. Much less attention has been directed to the equally important problem of maintaining a favorable salt balance in areas in which a ground-water reservoir is the primary source of supply, as well as the facility for seasonal and cyclic storage of water. Primary consideration is given herein to the economic significance of salt balance, which is studied in regard to basins used to store and regulate imported water as well as basins in which the entire water supply is derived from precipitation within the boundaries of the tributary watershed. The scope of the paper does not permit consideration of the many complex legal considerations or of physical problems other than withdrawal of water, which must also be solved to accomplish effective planned utilization of the storage capacities of these ground-water basins.

SALT SOURCES

The major quantities of salts are usually water-borne, but the quantities imported to an area in other forms by man cannot be ignored.

The natural sources of salt are as follows:

1. Salt content of local surface streams tributary to the ground-water basin;
2. Salt contained in subsurface inflow to the basin;
3. Salt leached from the soil above the water table by deep percolation of water; and
4. Salts leached from aquifers below the water table.

Sources of salt resulting from human activities include

- a. The salt load of imported water;
- b. Salt leached from surface soil during each cycle of use and return percolation of ground water;

³ "Utilization of Underground Storage Reservoirs," by Harvey O. Banks, *Transactions, ASCE*, Vol. 118, 1953.

⁴ "Problems Involved in the Utilization of Ground Water Basins as Storage Reservoirs," by Harvey O. Banks, *Proceedings, 26th Annual Convention, Assn. of Western State Engrs.*, Reno, Nev., August 17-20, 1953, p. 91.

⁵ "Planned Utilization," by Robert O. Thomas, in "Ground-Water Development: A Symposium," *Transactions*, Vol. 122, 1957.

⁶ "Salt Balance in Irrigated Areas," by C. S. Scofield, *Journal of Agricultural Research*, Vol. 61, 1940, p. 17.

- c. Soluble minerals derived from fertilizers, soil conditioners, insecticides, and other agricultural chemicals, and transported by percolating water; and
- d. The increment, estimated to range from 100 ppm, to 300 ppm total dissolved solids,⁷ added by various domestic and industrial wastes.

Sea-water intrusion in coastal ground-water basins is usually attributable to human activities. It is not considered herein because it overshadows all other effects so much that it must be treated as a distinct problem. The same consideration applies to those basins in which connate brines underlie fresh water at shallow depths. When such brines are disturbed by heavy pumping draft, they mix with the fresh water.

SALT CONCENTRATION

Repeated cycles of water use for most purposes result in evaporation of part of the water without a corresponding reduction in the total quantity of salt. This concentration, whether due to irrigation, domestic and municipal uses, or industrial uses, can result in a salt content greater than is desirable. Evapotranspiration in high ground-water areas may result in a substantial increase in the salt concentration.

The salt concentration resulting from cycles of use and re-use can be illustrated readily with data obtained for several western streams. For example, Paul D. Haney, M. ASCE, and Thomas W. Bendixen used data⁸ from the Bureau of Reclamation (United States Department of the Interior) for the Arkansas River in the period from 1940 to 1941. This data showed an increase in concentration of salts from 346 ppm to 2,034 ppm in a 176-mile reach of the stream. In the same reach, 334,200 acre-ft of water plus all tributary inflow were used consumptively.

There is evidence of a similar concentration of salts in ground-water basins, but because of the slow movement of the water and the great storage capacity, it is much more difficult to illustrate.

In the upper Santa Ana Valley of Southern California, surface inflows, which largely replenish the ground-water basins, average from 100 ppm to 150 ppm in dissolved salts. Rising water outflow from the series of basins in this valley had an average salt concentration ranging from 450 ppm to 500 ppm in the period from 1907 to 1908 before there was any appreciable effect of man's occupation of the land. By 1955 the salt concentration in the rising water outflow had increased to values ranging from 600 ppm to 650 ppm.

SALT DISPOSAL

It follows from the definition of salt balance that the salt removed from a ground-water basin must equal that which enters from all sources if the basin is to be in balance. If an adverse condition of more salt entering than leaving the basin exists, the salt concentration in the ground water and in the outflow will increase until a balance is achieved. The basic problem is to provide

⁷ "Studies of Waste Water Reclamation and Utilization," Publication No. 9.1964, California State Water Pollution Control Board, Calif.

⁸ "Effect of Irrigation Run-off on Surface Water Supplies," by P. D. Haney and T. W. Bendixen, *Journal, A.W.W.A.*, Vol. 45, No. 11, November, 1953, p. 1159.

sufficient water to bring the basin into balance before the ground water becomes too saline for use. The principal means of disposal of salt are in surface and subsurface outflow, in exported water, and in exported sewage and industrial wastes. The quantity of salts contained in agricultural and manufactured products shipped out of the area is usually negligible in comparison with the quantity in other categories.

There are some ground-water reservoirs in which there is no subsurface outflow and from which export of water or wastes may not occur. Periodic maintenance of ground-water levels high enough to obtain the effluent seepage required for salt balance may result in extensive sections of the overlying land becoming waterlogged. The only apparent alternative would be to pump sufficient water from the lower section of the reservoir. Unless a substantial part of the cost of such pumping can be justified for drainage, it may not be economical to operate a reservoir under the foregoing circumstances.

ALLOWABLE SALT CONCENTRATIONS

An additional consideration is the degree of salt concentration that can be tolerated without undue impairment of the beneficial uses of the water.

Domestic and Municipal Supplies.—The United States Public Health Service standards⁹ are applied in many areas as the criteria of suitability of water for domestic and municipal purposes. Specific allowable concentrations of dissolved minerals are given in Table 1.

TABLE 1.—ALLOWABLE CONCENTRATIONS OF DISSOLVED MINERALS^a

Mandatory constituents	Concentration, in parts per million	Permissive constituents	Concentration, in parts per million
(1)	(2)	(3)	(4)
Lead (Pb)	0.1	Copper (Cu)	3.0
Fluoride (F)	1.5	Iron (Fe) and manganese (Mn)	0.3 total
		Magnesium (Mg)	125
Arsenic (As)	0.05	Zinc (Zn)	15
Selenium (Se)	0.05	Chloride (Cl)	250
		Sulfate (SO ₄)	250
Chromium hexavalent	0.05	Phenolic compounds	0.001

^a Total solids preferred = 500 ppm; limit of allowable total solids = 1,000 ppm.

Irrigation Supplies.—Quality requirements for irrigated crops are in some respects more severe than those for drinking water. Quality criteria used widely in California for irrigation water¹⁰ were formulated by Lloyd D. Doneen. This approach recognizes three broad classes of water as defined by four parameters shown in Table 2.

The classifications in Table 2 are necessarily arbitrary. Suitability of water for irrigation is also dependent on such factors as type of crop, soil type and structure, climate, and rainfall distribution. Doneen developed a newer

⁹ "Drinking Water Standards," U. S. Public Health Service, Washington, D. C., 1946.

¹⁰ "Water Resources of California," *Bulletin No. 1*, California State Water Resources Board, Calif., 1951.

approach to the evaluation of the suitability of irrigation water, which he termed "effective salinity."¹¹ This method considers the proportion of the salt in the water that can be expected to precipitate from the soil solution. The effective salinity then is the measure of soluble salts that will tend to increase in concentration in the soil solution. This criterion is gaining increasing acceptance in California and is worthy of consideration in water-quality studies.

Industrial Water Uses.—Quality requirements for industrial purposes vary widely according to the type of industry and the diverse uses within a particular industry. For some purposes, such as once-through cooling or log ponding and booming, water of inferior properties might be acceptable. On the other hand, the quality requirements for laundering, ice manufacture, boiler feed, food processing, and beverage industries are stringent. In general, highly

TABLE 2.—QUALITATIVE CLASSIFICATION OF IRRIGATION WATER

Factor	CLASS		
	1	2	3
	DESCRIPTION		
	Excellent to good	Good to injurious	Injurious to unsatisfactory
Conductance, K , in micromhos at 25°C.....	<1,000	1,000 to 3,000	>3,000
Boron, in parts per million.....	< 0.5	0.5 to 2.0	> 2.0
Sodium, in percentage.....	< 60	60 to 75	> 75
Chloride, in parts per million.....	< 178	178 to 355	> 355

mineralized waters would be unsatisfactory without elaborate treatment for any but rough industrial uses.

TYPICAL SALT-BALANCE STUDIES

Salt-balance studies heretofore published fall into two categories. The first involves river basins in which the quantity of salt that enters an irrigated valley situated on a major river is compared with the quantity of salt transported in the river water. In these studies irrigation is accomplished mainly by diversion from the streams without much utilization of ground-water storage. The second category involves salt balance in the root zone of crops. These studies are designed primarily to determine the irrigation and drainage practices necessary to prevent undesirable buildup of salts in the top few feet of soil. Again, ground water either is not used, or little consideration has been given to the effect on its quality when salts are carried downward into underlying aquifers. Detailed water-quality studies of ground-water basins have dealt largely with sea-water intrusion, lateral or upward diffusion of connate brines, or uncontrolled industrial-waste discharges. It is doubtful whether sufficient careful measurement and inventory of the salts entering and leaving

¹¹ "Salination of Soil by Salt in Irrigation Water," by L. D. Doneen, Pt. I, *Transactions, Am. Geophysical Union*, Vol. 35, No. 6, December, 1954, p. 943.

any basin have been made to permit an accurate evaluation of the slower and less spectacular but important trends toward adverse salt balance. The following examples serve to illustrate this type of problem.

SALT-BALANCE REQUIREMENTS

Operation of a Reservoir with Local Water Supplies.—Only salts derived from surface and subsurface inflow are considered herein. It is assumed that all salts leaving the reservoir, whether in effluent seepage or in pumping extractions at the lower end of the reservoir, enter a surface channel, in which the quantity of water can be measured and the salt content determined.

The ground-water reservoir is assumed to have an area of 75,000 acres, an average depth of alluvium of 320 ft, a specific yield of 8%, a saturated depth of 300 ft, and water in storage containing an average of 500-ppm total dissolved salts. It is also assumed that there is no subsurface outflow, and effluent seepage can be regulated by drawing down the water level in the reservoir.

TABLE 3.—SUPPLY AND DISPOSAL FOR GROUND-WATER RESERVOIR

Source	Average annual supply, in acre-feet	Concentration of total salts, in parts per million	Average annual surface disposal, in acre-feet	Net recharge of reservoir, in acre-feet, Col. 2—Col. 4	Average annual quantity of salt entering reservoir, in tons, Col. 2 \times Col. 3 \div 0.00136
(1)	(2)	(3)	(4)	(5)	(6)
Surface inflow	80,000	400	75,000	5,000	43,500
Precipitation	100,000	negligible	40,000	60,000	
Subsurface inflow	10,000	500	0	10,000	6,800
Total	190,000	...	115,000	75,000	50,300

Also, there is sufficient surface storage to prevent uncontrolled outflow of flood flows.

With the ground-water reservoir being operated with local water supply only, the average annual supply and disposal of water are shown in Table 3.

It is assumed that re-use of ground water can be controlled to permit outflow at concentrations of either 1,000 ppm or 1,500 ppm. To prevent excessive salt build-up in the reservoir, there must be an average annual outflow of 37,000 acre-ft at 1,000 ppm, leaving a net usable supply of 38,000 acre-ft of ground water. With a concentration of 1,500 ppm the required average annual outflow is 24,700 acre-ft and the net usable ground-water supply is 50,300 acre-ft. A net annual increase in the ground-water supply of 12,300 acre-ft is realized when the concentration of the outflow is raised from 1,000 ppm to 1,500 ppm. For simplicity and because of the lack of information, certain important sources of salt have not been considered in this example.

The importance of the yield of the ground-water reservoir can be illustrated in terms of land supplied with water and value of water. If the gross consumptive use of water in the area is 3 acre-ft per acre, of which 1 acre-ft is supplied by rainfall, the reservoir yield will supply 19,000 acres or 25,150 acres, depending on the concentration of the outflow and on the corresponding volume of water used to maintain the salt balance. The cost of water in

California ranges from less than \$1.00 to more than \$40.00 per acre-ft. If a cost of \$10.00 per acre-ft is assumed in this case, the value of the water obtained from the reservoir will be either \$380,000 or \$503,000 annually, depending on salt-balance requirements.

Operation of a Reservoir with Local and Imported Supplies.—The same hypothetical ground-water reservoir is used to demonstrate the effect of salt-balance requirements on the importing of supplemental water. The local supply is sufficient to furnish water for 39,000 acres plus an average depth of 1 ft of water from precipitation for the remaining area, when the concentration of salt in the surface outflow is 1,000 ppm. If 90% of the area is furnished its total water requirement each year, an additional 57,000 acre-ft annually will be required to meet the consumptive-use requirements. However, if this supplemental water contains 400-ppm total dissolved solids, it will be necessary to import an additional 38,000 acre-ft of water to remove the salt from the basin at a 1,000-ppm concentration. The additional water required for salt balance would cost \$380,000 annually at \$10.00 per acre-ft, or the net cost of the imported water used consumptively would be increased from \$10.00 per acre-ft to \$16.67 per acre-ft. As in the example of operation with local water supply, if a salt concentration of 1,500 ppm could be tolerated, 44,700 acre-ft of supplemental water would be required for consumptive use. The additional water required to remove the salt would be reduced to 16,250 acre-ft annually, and the net cost of the imported water used consumptively would be decreased to \$13.64 per acre-ft.

Use of Ground Water from the Reservoir During a Drought.—The effect of drought on the average quality of water in the ground-water reservoir, assuming complete mixing in the reservoir, can be computed. A period of four dry years is used for illustrative purposes. It is also assumed that precipitation was sufficient to supply 1 ft of consumptive-use requirements annually with no excess available for recharge. No ground-water inflow occurred, surface inflow and importation were reduced to 20,000 acre-ft per yr and 28,500 acre-ft per yr, respectively, and effluent seepage was prevented by the lowering of the water table. With the area, depth, and specific yield cited previously, the reservoir would have a storage capacity of 1,800,000 acre-ft.

If the average concentration were 500 ppm, total salt in storage at the beginning of the four-year period would be 1,224,000 tons, and salt added during the period would be 106,000 tons, or a total content at the end of the period of 1,330,000 tons. Withdrawal from storage for consumptive use of 346,000 acre-ft of water would result in a concentration of

$$\frac{1,330,000}{(1,800,000 - 346,000)(0.00136)} = 673 \text{ ppm.}$$

The foregoing implies that substantial use can be made of storage capacity in a large reservoir without unreasonable deterioration in the quality of the water.

DEFICIENCIES IN PRESENT KNOWLEDGE OF SALT-BALANCE FACTORS

The necessity of creating the foregoing hypothetical example of salt-balance computations rather than using an actual basin demonstrates the limited accomplishments in operating ground-water reservoirs, as well as the

many limitations in the knowledge of the quantitative values of the factors of salt balance involved. There are few reservoirs in which both the areal and vertical ground-water quality are sufficiently well known to permit the computation of average quality. There are even fewer cases in which such data have been collected for a sufficiently long period to permit an accurate correlation of the change in quality with related hydrologic data. Much more precise information must be obtained for the quality of water entering and leaving the reservoir than is generally available.

However, perhaps the greatest deficiency is in the knowledge of the quantities of salts added to a basin in the form of fertilizers, soil conditioners, weed killers and insecticides, and by other activities. Little is known about salts leached by the percolation of water downward from the surface. Evaluation of available data has demonstrated also that there are appreciable time lags between inflow and outflow of salt and proportionate changes in salt concentration in stored ground water. The reasons for such time lags are not yet apparent.

Salt-Balance Problems in California.—Studies of water requirements for California show that 25,800,000 acre-ft of supplemental water will be required to meet ultimate consumptive requirements south of the latitude of Sacramento. Most of this water will be obtained from the watersheds to the north. The additional water required to maintain a favorable salt balance will be a major consideration determining the size of the facilities required to regulate and transport the supplemental water, because much of the water will be used on lands overlying ground-water reservoirs, and the storage capacity in the reservoirs must be utilized for seasonal and cyclic regulation. If 10% of gross deliveries at a cost of \$10.00 per acre-ft is required to maintain the salt balance, the value of the water will be on the order of \$25,000,000 annually, which justifies the studies that are necessary to achieve reasonable economy in its use.

CONCLUSIONS

1. Maintenance of a favorable salt balance is essential for the planned operation of ground-water reservoirs and is of sufficient economic importance to justify the necessary expenditures for the collection and evaluation of data.
2. The physical and economic problems involved in the removal of sufficient water to maintain the salt balance from some ground-water reservoirs may preclude their planned operation.
3. Insufficient data have been collected to evaluate the discernible trends in water quality in many ground-water reservoirs, and far more information will be required to predict and evaluate salt-balance requirements for the reservoirs under planned operation.

DISCUSSION

ROBERT O. THOMAS,¹² M. ASCE.—The paper has focused attention on a problem of immediate concern to engineers engaged in the planning of irrigation developments for lands in which the use of ground-water storage is essential to successful project operation. The writer has previously called attention to the salt-balance problem in connection with the planned utilization of ground-water storage capacity.¹³

Generally, both surface waters and ground waters available contain mineral salts of calcium, magnesium, potassium, and sodium in varying quantities. These minerals are present in the water in the form of carbonates, sulfates, and chlorides. The salts are derived from the passage of water over and through rock formations and result from solution and weathering action. After application of water on the land, that part which is not used consumptively or which does not drain off on the surface will percolate to lower depths. This percolation may or may not join the main underlying ground-water body, depending on the geologic structure of the area. As a result of use, some salt compounds will be given up in promoting plant growth or in combining with soil elements. Conversely, percolating water will absorb other salt compounds in passing through the soil.

The chemical composition of ground water is often found to be quite different from that which would result from the free mixing of waters accumulating from various known sources. Movement of water into and through alluvial deposits creates favorable conditions for the occurrence of the phenomenon known as base exchange. Such action depends on the presence of base-exchange material in the soil structure penetrated by the downward percolating water.

Valley ground-water reservoirs, particularly in the western United States, are usually bordered on two sides, and sometimes completely enclosed, by mountain ranges from which both the water and the water-bearing materials of the valley fill are derived. A common form of progressive deterioration in water quality occurs in valley reservoirs that are replenished in large part from water that has already been subjected to use and has absorbed soluble minerals.

Most irrigation developments have made use of such valley lands because they generally have a fairly constant slope to some central point, thus facilitating the distribution of water. The use of surface waters for irrigation has frequently been accompanied by a rise of the water table due to percolation of unused water. In some areas, also, the water table has risen under much of the lowland area due to lateral movement of ground water from higher irrigated lands.

Pumping from many such reservoirs is a contributing factor to deterioration of water quality to the extent that the available storage capacity is emptied sufficiently to induce replenishment by contaminating waters. The problem

¹² Hydr. Engr., Sacramento, Calif.

¹³ "Ground-Water Development: A Symposium," *Transactions, ASCE*, Vol. 122, 1957, p. 441.

of increase in salinity is not solved by limiting the application of irrigation water to the required consumptive use, even if practical means could be developed to provide only such quantities of water as are required by growing crops. Adequate solutions will probably involve the provision of drainage facilities operated in order to intercept as great a quantity of saline percolating waters as possible, prior to the time the waters reach the main body of ground water.

Such drains will pose problems in effecting recharge of the ground-water reservoir for cyclic storage. However, these problems are not insurmountable. It may be necessary to plan recharge and extraction operations in order to create artificial mounds, or troughs, separating various parts of the basin. Also, certain lands can be set aside for use solely as percolation areas to ensure the good quality of recharge waters. It is possible to construct drainage facilities in such a manner that they may be closed during periods when recharge operations occur.

In many irrigated areas it will be found that without adequate drainage and due to salinization of the underlying soils the lands will fail to support intensive irrigated agriculture. Such salinization may occur as a result of the accumulation of salts from applied irrigation water, through the rise of the water table, or by the combination of both causes. Water used for irrigation, particularly in the western United States, may contain from 0.1 ton to 5 tons of mineral salts per acre-foot. With applied water generally from 3 acre-ft per acre to 5 acre-ft per acre, it is obvious that a large quantity of salt can be deposited on and in the soil in a short time.

The quantity of salt actually absorbed and used by the growing plant is minor. Consequently, the entire soluble salt load is concentrated in approximately one-third of the applied water remaining after the consumptive-use demand has been satisfied. This concentration of the soil solution is much greater than that of the applied irrigation water. As subsequent water is applied to the land the concentrated solution is forced downward, and, unless drainage is provided, it eventually mixes with the water in storage. In many cases rising water tables envelop this soil solution, causing swamp areas and high water-table lands. Evaporation of ground water is increased, leaving salt residues on the surface and in the upper soil layers.

Drainage of the accumulated concentrate will result not only in a major contribution to basin salt balance and assist in maintaining soil productivity, but will also preclude to a great extent deterioration of good-quality ground water by dilution. The quantity of water to be drained or leached from the soil complex may be estimated by reference to Fig. 1. This diagram has been prepared from data published by the United States Department of Agriculture.¹⁴ It has been found that the electrical conductivity of the soil solution in the vicinity of the root zone should be no greater than 4,000 micromhos at 25° C if salinization of the soil is to be prevented.

Soluble salts found in irrigation waters tend to create saline or alkaline conditions in the soil if concentrations are permitted to increase abnormally.

¹⁴ "Diagnosis and Improvement of Saline and Alkali Soils," *Agricultural Handbook No. 60*, U. S. Dept. of Agriculture, Washington, D. C., February, 1954.

At such times the constituents of soil solutions may cause base-exchange reactions that will result in altering the physical properties of the soil. Generally, calcium and magnesium compounds tend to improve the permeability and friability of the soil. Sodium and potassium compounds, particularly the carbonates, chlorides, and sulfates, tend to inhibit plant growth and cause sealing, cracking, and gelatinization of the soil particles.

Thus, it is apparent that effort should be made to intercept and dispose of unconsumed irrigation water applied during the growing season. However, it is not necessary to waste all such water because some drainage may be collected in strategically located sumps, diluted with other water of suitable quality, and again re-used in downstream areas. The economic limit to such re-use is the point at which excessive quantities of diluting water are required.

The writer believes that saline connate waters trapped in sedimentary formations of marine origin and magmatic and other juvenile waters rising

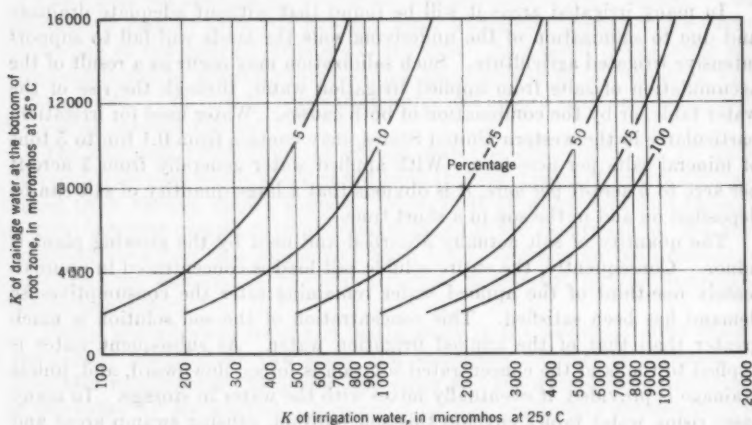


FIG. 1.—LEACHING REQUIREMENT AS A PERCENTAGE OF APPLIED IRRIGATION WATER

along fault planes or through fractures should be classified as natural sources of often serious problems of quality deterioration. Connate waters, particularly, have caused extensive damage in California's interior valleys.

Although the authors believe that substantial use can be made of the ground-water storage capacity without unreasonable short-time deterioration of the stored water, it is also true that it is much easier to increase the salinity than to decrease it. In the example given under the heading, "Use of Ground Water from the Reservoir During a Drought," it would subsequently require 350,000 acre-ft of imported water at 400 ppm and export of the same quantity at 1,000 ppm, in addition to the normal import of 95,000 acre-ft and export of 38,000 acre-ft, to reduce the average salinity to the value prevailing prior to the drought. Thus, the cost of quality deterioration is apparent. In this case, it would be approximately \$50 per irrigated acre.

Provision of adequate drainage facilities would prove to be a more economical and satisfactory means of achieving a measure of salt balance than that gained by permitting deterioration of the quality of ground water to the extent used in the illustrative example presented in the paper.

DAVID B. WILLETS¹⁵ AND CHARLES A. MCCULLOUGH,¹⁶ ASSOCIATE MEMBERS, ASCE.—The contributions Mr. Thomas has made to the work of the writers have amplified the need for maintaining a favorable salt balance in ground-water basins.

Fig. 1 is useful in planning for the successful long-term operation of an irrigation project when ground water is a factor in the water-supply system. Mr. Thomas has also introduced the problem of drainage, which is related closely to salt balance.

The writers fully understand the need for, and value of, adequate drainage. However, it must be emphasized that advance planning for an irrigation project should include an adequate supply of water to maintain the salt balance. When initial plans provide for such a supply to maintain a favorable salt balance, the engineer can evaluate better the possible drainage problems. More dependable data can also be derived for planning drainage facilities in those instances in which drainage problems may develop.

¹⁵ Superv. Hydr. Engr., California State Dept. of Water Resources, Los Angeles, Calif.

¹⁶ Superv. Hydr. Engr., California State Dept. of Water Resources, Sacramento, Calif.

AMERICAN SOCIETY OF CIVIL ENGINEERS

Founded November 5, 1852

TRANSACTIONS

Paper No. 2975

MODEL STUDIES OF REMEDIAL WORKS FOR NIAGARA FALLS

BY ANDREW P. ROLLINS, JR.,¹ AND GEORGE B. FENWICK,²
MEMBERS, ASCE

SYNOPSIS

Model studies of the Niagara River and of Niagara Falls were conducted in the period from 1950 to 1953 to determine how the scenic beauty of the falls would be affected by the additional diversions of the Niagara waters for power authorized under the United States-Canadian Treaty of 1950. The locations and designs of the remedial works required to compensate for these effects and to preserve and enhance the beauty of the Niagara River and Niagara Falls were also determined.

Results of the model tests indicated that three separate remedial works would be required. These consist of a Chippawa-Grass Island gated control structure extending out from the Canadian shore; an excavation at the Canadian flank of the Horseshoe Falls, with a 100-ft crest fill; and an excavation at the Goat Island flank of the Horseshoe Falls, with a 300-ft crest fill.

INTRODUCTION

The Niagara River carries the outflow of the four upper lakes of the Great Lakes system from Lake Erie to Lake Ontario. The vast storage capacity of the upper lakes results in a remarkably steady river discharge averaging about 200,000 cu ft per sec, although this discharge varies daily, seasonally, and annually.

The river is 36 miles long, in which the total drop from the mean level of Lake Erie to that of Lake Ontario is 326 ft. At Niagara Falls the river has a vertical drop of approximately 160 ft. An additional drop of approximately 140 ft occurs in the 8 miles of cascades and rapids immediately above and

NOTE.—Published, essentially as printed here, in September, 1957, in the *Journal of the Waterways and Harbors Division*, as *Proceedings Paper 1367*. Positions and titles given are those in effect when the paper was approved for publication in *Transactions*.

¹ Col., Corps of Engrs., U. S. Army, Student Detachment, U. S. Army War College, Carlisle Barracks, Pa.

² Chief, Rivers and Harbors Branch, U. S. Army Engr. Waterways Experiment Station, Vicksburg, Miss.

below the falls. The plan and profile of the river and falls are shown in Fig. 1.

This concentration of fall within a relatively short distance, together with the large and steady discharge of the river, makes possible the economical development of hydroelectric power. Furthermore, the falls of the Niagara River and its natural surroundings constitute one of the most spectacular scenic wonders of the world. Boundary-water treaty agreements between

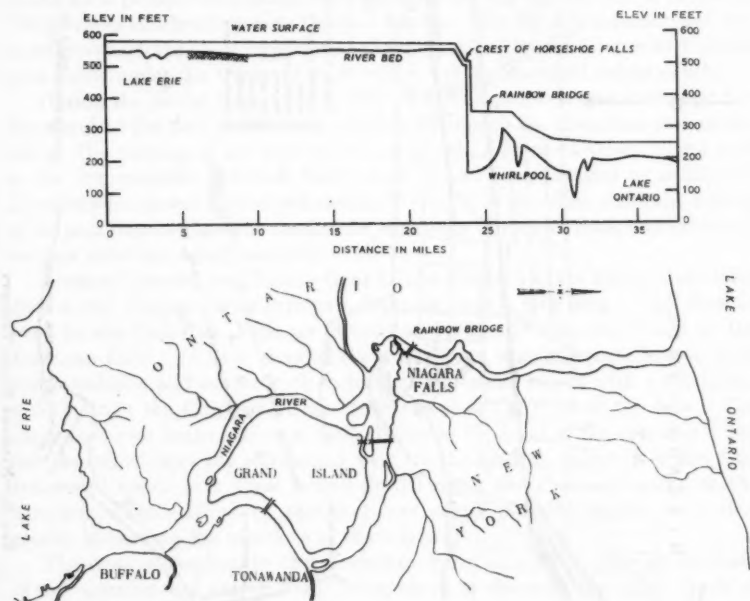


FIG. 1.—NIAGARA RIVER PLAN AND PROFILE

the United States and Canada regulate diversions of water from the river for power and reserve sufficient quantities in the river for scenic purposes.

THE PROTOTYPE

Upper Niagara River.—The Niagara River flows northward from Lake Erie near Buffalo (N. Y.) Harbor through a funnel-shaped entrance greatly obstructed by shoals. For the first 2 miles the river is little more than 1,500 ft wide, with a maximum depth of 20 ft and velocities of as much as 8 miles per hr. The river here is paralleled on the New York side by the Black Rock Canal, with a lift of about 5 ft that permits the passage of vessels between Buffalo Harbor and the Niagara River just below Squaw Island. Below this point the river is navigable through both channels around Grand Island, and a 21-ft channel has been dredged in the river from the Black Rock Canal to Tonawanda, N. Y. A 12-ft channel has been dredged from Tonawanda to the docks at Conners Island, Niagara Falls, N. Y.

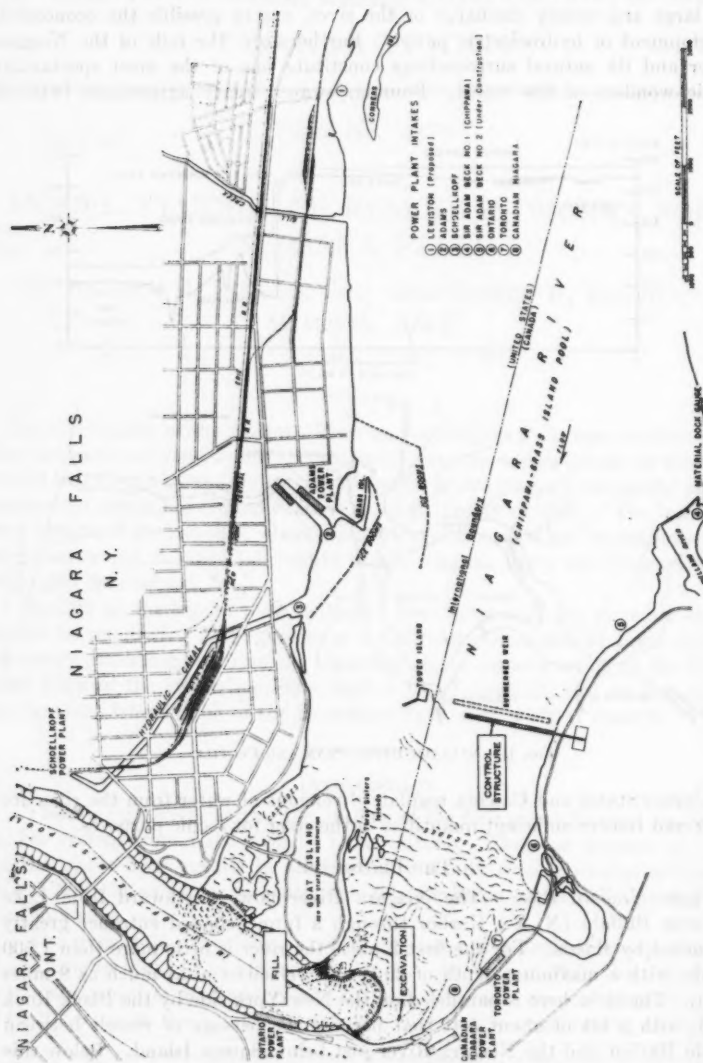


FIG. 2.—NIAGARA FALLS VICINITY

The 4-mile reach between the lower end of Grand Island and the head of the cascades immediately above the falls is known as the Chippawa-Grass Island pool (Fig. 2). At present (1959) four intakes divert water from the pool for power purposes—two intakes near Grass Island on the United States side of the river, and the intakes for the Sir Adam Beck No. 1 and No. 2 plants, the latter constructed in 1957, on the Canadian side near Chippawa, Ontario. The intake for a projected plant on the United States side of the river is presently (1959) under construction near Conners Island. The Sir Adam Beck plant No. 2 and the projected plant are planned to utilize the increased diversions of water permissible under the treaty of 1950, which will be examined subsequently.

During the period from 1942 to 1947, a submerged weir was built near the lower end of the pool in the main channel leading to the Canadian side of the falls. The purpose of the weir was to restore the Chippawa-Grass Island pool to the approximate elevation from which it had been lowered by additional diversions for power authorized during World War II. The resultant raising of the pool improved intake conditions, especially during ice runs, and increased the flow over the American Falls.

Niagara Cascades and Falls.—Goat Island, situated at the brink of the falls, divides the Niagara River into two channels, each $\frac{1}{2}$ mile long. One channel leads to the Canadian Falls, or Horseshoe Falls, and the other leads to the American Falls. In each channel the water flows over limestone ledges, scattered boulders, and broken rock to form cascades and rapids with a total drop of 50 ft from the Chippawa-Grass Island pool to the crest of the falls. The uppermost rock ledge acts as a natural weir at the head of the cascades. Before construction of the submerged weir (in the 1940's), only 5% of the total volume of water over these ledges flowed down the channel leading to the American Falls. However, this flow was nearly doubled by the weir, thus greatly improving the spectacle of these falls.

The channel leading to the Horseshoe Falls is 3,200 ft wide at the head of the cascades and only 1,200 ft wide, shore to shore, at the falls. Parts of the cascades are from 6 ft to 12 ft deep, but several small islands and numerous shoals have been formed by the irregular distribution of ledges and boulders. A large central shoal divides the flow in the Horseshoe Falls channel into two main channels, one near each shore, which converge toward the center part of the horseshoe. The intakes of several Canadian plants are situated along the Canadian shore of the cascades.

At the Horseshoe Falls there is a straight drop of 160 ft. Although the shore-to-shore width is only 1,200 ft, the total length of the crest measured around the horseshoe is 2,500 ft. Near both flanks, where the depth of water flowing over the crest was less than 1 ft before the recent improvement of the falls, the normal color of the falling sheet of water was white and the sheet was broken at times because of its thinness. Toward the center of the horseshoe, the depth increases to a maximum of 12 ft. As the depth at the crest increases to 4 ft or 5 ft, a greenish color mingles with the white and greatly enhances the appearance of the falls.

History of Power Development.—Efforts to harness the Niagara waters for power development began in 1725, when an uneconomical attempt was made

in the cascades above the falls. Successful exploitation of the river for power was initiated in 1877, followed by spasmodic and ever-increasing growth of power developments. However, at the present time diversions of water for power are limited by boundary-water treaty agreements between the United States and Canada. The first such treaty, made in 1909 and 1910, permitted a permanent daily diversion from the Niagara River above the falls for power of 20,000 cu ft per sec by the United States and 36,000 cu ft per sec by Canada. Because of the increased power need for defense activities, the two countries concluded agreements in 1940 and 1941 to utilize, on a temporary basis, an additional diversion of 26,500 cu ft per sec at Niagara Falls. In 1944 and in 1948 the earlier agreements were modified to provide for small additional temporary diversions, and proceedings that led to the treaty of 1950 were begun.

THE PROBLEM AND PURPOSE OF MODEL STUDIES

Treaty Provisions.—On February 27, 1950, a new treaty was made between the United States and Canada concerning water uses of the Niagara River. This treaty provides for remedial works to enhance the beauty of Niagara Falls, and reserves sufficient water in the Niagara River for scenic purposes. A falls flow of no less than 100,000 cu ft per sec must be maintained during daylight hours throughout the tourist season, and at no other time should the flow over the falls be less than 50,000 cu ft per sec. All water over and above these requirements and those for domestic, sanitary, and navigation uses is made available for power, and is to be divided equally between the United States and Canada.

The treaty specifies that the two governments recognize "their primary obligation to preserve and enhance the scenic beauty of the Niagara Falls and River." It states further that the two countries agree to complete remedial works necessary to increase the beauty of the falls by distributing the waters in order to produce an unbroken crest line around the falls for all flows.

Investigation Procedure.—The International Joint Commission, United States and Canada, was requested by the two governments to investigate and submit recommendations concerning the necessary remedial works. The commission then created the International Niagara Falls Engineering Board, drawn from the technical agencies of the two countries. This board was directed to make the necessary investigation of Niagara Falls and the Niagara River and to report its findings and recommendations. The board appointed a working committee consisting of representatives of agencies normally responsible for the types of work involved. The regular field organizations of the appropriate agencies were asked to perform the various surveys and studies, ensuring that the services of specialists available in both countries were utilized.

Flow conditions in the cascades and at the brink of the falls were so complex that the design of remedial works to redistribute the flow over the crest of the falls was not feasible by analytical procedures. This fact is noted in the 1931 report³ of the Special International Niagara Board. This report recommended a step-by-step procedure of constructing a combination of submerged weirs

³ "Preservation and Improvement of the Scenic Beauty of the Niagara Falls and Rapids," U. S. Govt. Printing Office, Washington, D. C., 1931, paragraphs 177-191.

and excavations, with observation of the results of each step to guide the design of the next step.

However, in recent times the hydraulic model has gained wide recognition as an invaluable tool for engineering design. Successful methods and techniques have been developed, and an impressive record of accomplishment has proved the reliability of conclusions drawn from model studies. Wherever applicable, such studies constitute a dependable method of solving complex hydraulic problems with a minimum expenditure of time and money.

The advantage of using hydraulic models in the investigation of the Niagara remedial works was evident. Any given river flow—past, present, or future—could be simulated at will. Remedial works in miniature could be inserted in the model and their performance studied under the full range of river conditions. It was necessary to determine future conditions in the river if no remedial works were to be constructed, and to develop the locations and designs of such works to correct these conditions in order to preserve the beauty of the falls. The International Niagara Falls Engineering Board believed that only by model tests could such reliable information be obtained.

Accordingly, the major phase of the engineering studies necessary for designing the remedial works was accomplished by two hydraulic model studies. One model study was conducted by the Hydro-Electric Power Commission of Ontario (a government agency) at Islington near Toronto, Canada, and the other was conducted by the United States Army Engineer Waterways Experiment Station at Vicksburg, Miss.

There were several reasons for utilizing two model studies. The preservation of Niagara Falls being an international question, it was necessary that both countries be satisfied as to the proposed solution. Also, in view of the far-reaching importance of the issues and the complexity of the problem, it was considered desirable to utilize fully the available technical forces of both countries. The use of two models, similar but not exactly the same in scale and complementary in coverage, would make possible a constant check on test findings and lend assurance to the reliability and accuracy of the results.

Purpose of the Model Studies.—The general purpose of the model studies was to work out the detailed procedures for implementing the provisions of the 1950 treaty. The achievement of this broad purpose involved establishing conditions that would exist in the Niagara River and in Niagara Falls under the future increased diversions for power permitted under the treaty of 1950 if no remedial works were constructed. Also, the locations and designs of the remedial works required to correct these conditions and to preserve and enhance the beauty of the falls would be determined.

THE MODELS

Canadian Model.—The Islington model reproduced the Niagara River from the lower end of Grand Island to the Rainbow Bridge below the falls. This model, constructed to linear scale ratios (model to prototype) of 1:250 horizontally and 1:50 vertically, was 95 ft long and 37 ft wide. A general view is shown in Fig. 3.

United States Model.—The Niagara River and Niagara Falls model constructed by the Waterways Experiment Station reproduced approximately 26 miles of the Niagara River, extending from 11,500 ft above the Peace Bridge at Buffalo to the Rainbow Bridge, which is approximately 5,000 ft below the falls (Fig. 4). The upper limit of the model extended far enough into Lake Erie to provide an accurate reproduction of flow entering Niagara River from the lake, and the lower limit included the gorge below the falls for pictorial purposes. The falls and cascades, the existing and proposed power intakes, Goat Island, Grand Island, and other significant topographical features were reproduced between these extremities. Extending the model to include a section of Lake Erie permitted studies of the extent and timing of the effects in the upper river and lake of remedial and regulating works in the vicinity of the cascades and falls.

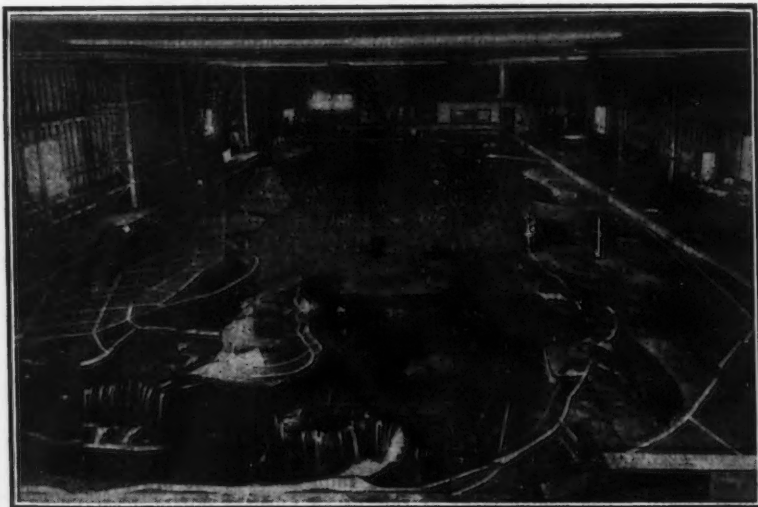


FIG. 3.—NIAGARA RIVER AND NIAGARA FALLS MODEL (ISLINGTON, CANADA)

The Niagara River and Niagara Falls model was constructed to linear scale ratios of 1:360 horizontally and 1:60 vertically, resulting in a model 260 ft long with a maximum width of 125 ft. Selection of these scale ratios was based on the following considerations:

a. Linear scale distortion (use of different scales for horizontal and vertical dimensions) was necessary because the extremely shallow depths in the most critical section of the prototype required a vertical scale large enough that its application to the great horizontal dimensions of the prototype would have produced a model of impractical size and cost.

b. Known physical and hydraulic characteristics of the Niagara River indicated that these linear scales would permit reproduction of the proper

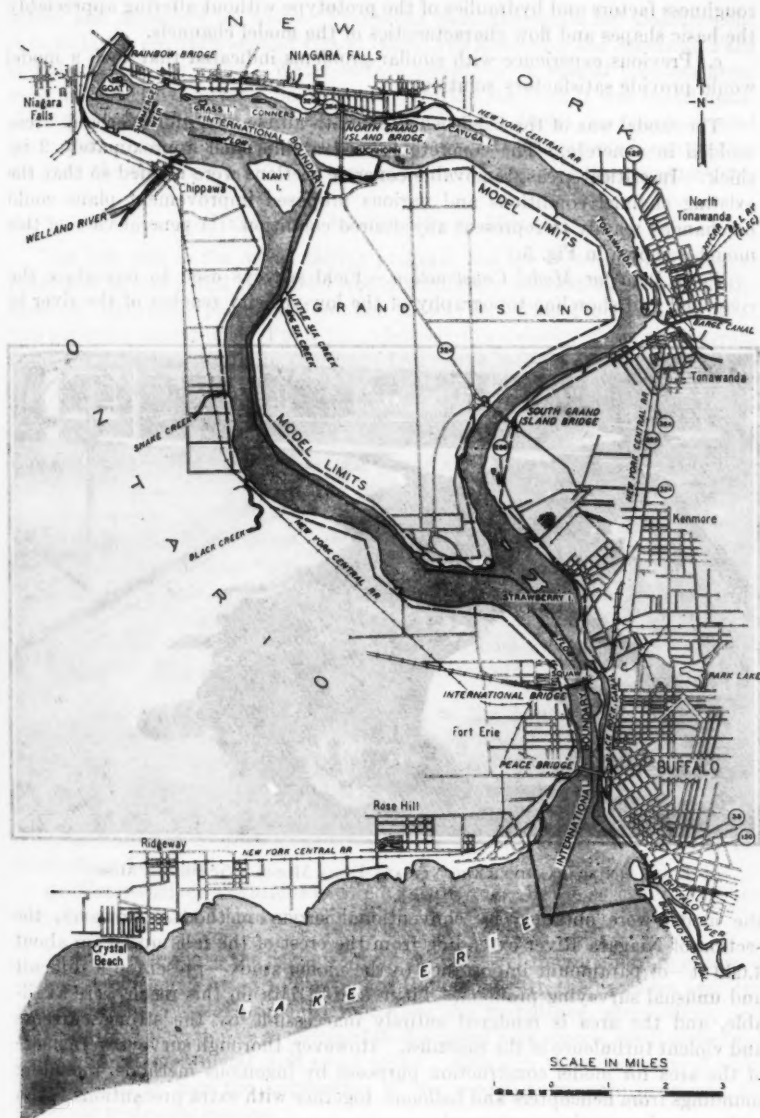


FIG. 4.—LOCATION MAP OF THE VICKSBURG (MISS.) MODEL

roughness factors and hydraulics of the prototype without altering appreciably the basic shapes and flow characteristics of the model channels.

c. Previous experience with similar problems indicated that such a model would provide satisfactory solutions.

The model was of the fixed-bed type, with all channel and overbank areas molded in concrete. The concrete formed a thin shell approximately 2 in. thick. In critical areas, removable concrete sections were molded so that the existing channel conditions and various proposed improvement plans could be changed readily to represent any desired condition. A general view of this model is shown in Fig. 5.

Field Data for Model Construction.—Field surveys used to reproduce the river bed and shoreline topography of the low-velocity reaches of the river in



FIG. 5.—NIAGARA RIVER AND NIAGARA FALLS MODEL (VICKSBURG, MISS.)

the model were obtained by conventional survey methods. However, the section of Niagara River extending from the crest of the falls upstream about 4,000 ft—of paramount importance to the model study—presented a difficult and unusual surveying problem. Little usable data on this reach were available, and the area is rendered entirely inaccessible by the strong currents and violent turbulence of the cascades. However, thorough surveys were made of the area for model construction purposes by ingenious methods, including soundings from helicopters and balloons, together with extra precautions taken with normal surveying equipment.

Model Appurtenances.—The bridges and the existing and proposed power intakes along the river were precisely reproduced in the model. The intakes were constructed of wood, and the bridges were built with wood piers and sheet-metal trusses. Flow into the intakes was regulated by standard gate

valves and measured by weirs. Provisions were also made for measurement of flows in the channels around Grand Island and flows over the American Falls and the Horseshoe Falls. Water-surface elevations in special problem areas were measured by portable point gages. During the tests it was found desirable to measure the flow over the Horseshoe Falls in 100-ft increments around the crest. This was accomplished by a specially constructed scoop that diverted the flow over any 100-ft section to one of the weirs for measurement.

HYDRAULIC ADJUSTMENT OF MODEL

The first step in the model testing program was the adjustment of channel roughness in order that the model would accurately reproduce in detail all the observed hydraulic phenomena of the prototype. This procedure involved two separate operations. First, the relatively low-velocity channel upstream from the cascades was adjusted, including obtaining the proper distribution of flow around Grand Island and Goat Island. Second, the high-velocity, turbulent cascades and falls section was adjusted.

The section of river from Lake Erie to the cascades was adjusted until the water-surface elevations at eighteen gages agreed with corresponding gage readings obtained in the river, at a discharge of 223,488 cu ft per sec, for this special purpose. Water-surface elevations in the model at all standard gages were checked further against prototype elevations computed from a gage-relationships formula for flows ranging from 150,000 cu ft per sec to 240,000 cu ft per sec. This ensured that the model was accurately adjusted for the entire range of discharges that would be used later in the testing program.

Adjustment of the cascades section of the model was a tedious "cut-and-try" process. The prototype data used consisted of:

- a. A water-surface contour map, known as the "searchlight survey," that was obtained by determining locations and elevations using a reflected beam of light moved at random over the cascades at night;
- b. A vertical, aerial photograph of the cascades and falls taken during a large ice flow and depicting general streamlines through the cascades area;
- c. A float survey indicating the general distribution of flow around the crest of the falls; and
- d. Water-surface elevations at twenty-three gages in the cascades along the Canadian and Goat Island shorelines.

In the reach above the cascades, proper degrees of roughness were obtained with wire screening fitted to the bed of the model. In the cascades area the roughness that was required to reproduce the turbulence, streamlines, and water-surface elevations was obtained in the model with stucco, small embedded rectangles of sheet metal, and small rocks. Although these mechanical additions tended to mar the appearance of the model, they were necessary for technical hydraulic reasons.

MODEL TESTS WITHOUT REMEDIAL WORKS

After adjustment of the model the first series of tests was made to determine the conditions that would be caused in the Niagara River and Niagara Falls

by the future increased diversions for power permitted under the treaty of 1950 with no compensating remedial works provided. The total diversion permitted by the treaty includes all flows in excess of those required to maintain total flows over the falls of 100,000 cu ft per sec during daylight hours in the tourist season, and 50,000 cu ft per sec at all other times. The model tests of these conditions indicated that without construction of additional remedial works the following would result from the increased permissible diversions:

a. The Chippawa-Grass Island pool level would be drawn down as much as 4 ft below its normal level, thereby exposing considerable areas of the river bed covered previously, particularly in the vicinity of the head of Goat Island. The drop would vary from 0 ft to 3 ft during daylight hours in the tourist season, and from 2 ft to 4 ft at other times, depending on river discharge. Lowering the pool would result in some lowering of the Lake Erie levels.

b. Because of the lowering of the pool level, flow over the American Falls would drop well below that required for a satisfactory scenic spectacle. The formerly satisfactory American Falls flow of 11,500 cu ft per sec for an average river discharge of 200,000 cu ft per sec would be reduced by the maximum permissible diversion to only 4,600 cu ft per sec during the tourist season and 2,500 cu ft per sec at other times.

c. Under maximum permissible diversion for average river discharge, the Horseshoe Falls would have a flow of only 95,000 cu ft per sec during the tourist season, producing unsatisfactory flows at the flanks. During other times the Horseshoe Falls flow would be only 47,000 cu ft per sec, which would leave both flanks dry. Even under conditions existing before the authorized increase in diversions, with an average flow of 105,000 cu ft per sec over the Horseshoe Falls, the flanks were covered inadequately.

d. Approximately 12 hr would be required to change the total falls flow from 50,000 cu ft per sec to 100,000 cu ft per sec, or conversely, because of the slow response of the Chippawa-Grass Island pool level to changes in diversions. Therefore, only a small part of the extra diversion authorized at night during the tourist season could be used, as it would be necessary to begin reducing diversions far in advance in order to build up the pool to the level required for a flow of 100,000 cu ft per sec over the falls by 8:00 A.M. Furthermore, the resulting pool lowering would adversely affect the output of power plants drawing water from it.

PERFORMANCE CRITERIA FOR REMEDIAL WORKS

In view of the intolerable conditions that would result from the authorized increased diversions if no remedial works were constructed, it was considered imperative that such works be provided to improve the flow distribution over the crest of the Horseshoe Falls, to maintain the satisfactory flow conditions at the American Falls, and to control the levels of the Chippawa-Grass Island pool. The maintenance of the existing relationship between river flow and pool level was considered essential to preserve the existing conditions and appearance of the Niagara River upstream from the pool and to ensure that Lake Erie levels and corresponding outflows would remain unaffected. Thus,

interests upstream would be protected that otherwise might be affected adversely by the general lowering or rapid fluctuation of the pool level.

Accordingly, the International Niagara Falls Engineering Board requested that model tests be performed to determine the locations and designs of remedial works that would ensure meeting the following criteria:

- a. A dependable flow over the American Falls and rapids, approximating the satisfactory intensity experienced under existing conditions;
- b. A dependable and ample flow over both flanks of the Horseshoe Falls to provide an unbroken crestline, the intensity of flank flows to be such that the following requirements are satisfied: (1) For a total volume over the falls of 100,000 cu ft per sec, a flow per foot of crest length of from 6 cu ft per sec to 8 cu ft per sec over the Goat Island flank, and from 10 cu ft per sec to 12 cu ft per sec over the Canadian flank; and (2) for a total volume over the falls of 50,000 cu ft per sec, an unbroken curtain of flow from shore to shore;
- c. Maintenance of the existing relationship between the total river flow and the level of the Chippawa-Grass Island pool; and
- d. Capacity to meet promptly the changes in permissible power diversions, at the same time assuring flows of either 50,000 cu ft per sec or 100,000 cu ft per sec over the falls.

The remedial works for meeting the foregoing criteria fall naturally into two categories: First, installations to preserve the existing range of levels in the Chippawa-Grass Island pool, and to maintain an adequate flow over the American Falls; and second, works to improve flow distribution along the crest of the Horseshoe Falls. Works in the first category would be in the pool just upstream from the head of the cascades. Those of the second category would be in the cascades at the crest of the Horseshoe Falls. In the model tests of such installations, the general procedure was to study first the control structure in the Chippawa-Grass Island pool and then examine the remedial works above the Horseshoe Falls because the design and location of the upper structures would have some effect on those downstream.

MODEL TESTS OF CONTROL STRUCTURE IN POOL

Tests performed with a gated-dam control structure at several sites at and downstream from the existing submerged weir near the head of the cascades indicated that the performance at all these locations was essentially the same. From the standpoint of feasibility and economical construction, it was decided that the dam should be parallel to and approximately 250 ft downstream from the submerged weir, as shown in Fig. 2. The tests indicated that the structure should begin from the Canadian shore because the deep channel, which must be intercepted to provide efficient control, lies near this shore. This deeper channel also offers less likelihood of ice grounding in the channel in the vicinity of the dam.

Extensive tests were conducted to determine the optimum length of the control structure. Installations extending various lengths from the Canadian shore were tested, including one across the entire river. In all these tests the control structure consisted entirely of piers with 100-ft gated openings between

them. In order to minimize interference with the free passage of ice, the gate sills were placed at an elevation not exceeding that of the river bed, or that of the submerged weir for the section of the dam opposite the weir. Also, in some of the tests in which the dam extended only partly across the river, experiments were made with an additional short structure from the United States shore into the channel leading to the American Falls.

In general, the results of these tests were as follows:

a. For the main gated control structure to be constructed from the Canadian shore, a minimum length of 1,705 ft would be necessary to regulate the pool under future diversion conditions to the same levels that existed previously for the same river flows. This structure would also maintain satisfactory flow over the American Falls, and would permit changing the total flow over the falls from 100,000 cu ft per sec to 50,000 cu ft per sec, and conversely, without a change in pool level. Thus, the 1,705-ft structure satisfied all the established performance criteria.

b. A 450-ft-long gated structure near the United States shore, although not necessary for pool control, was of some value in controlling flow into the channel leading to the American Falls, especially at high river flows. However, this feature was not considered further because its cost would be out of proportion to the resulting benefits.

As stated in the foregoing, the model tests indicated that the strict maintenance of the existing relationship between river discharge and pool level, allowing for no tolerance at any discharge, would require a minimum control-structure length of 1,705 ft. From a practical standpoint, however, the plan of operation of the control structure would logically allow a reasonable tolerance in the daily and monthly average deviation of the pool from its normal level. Furthermore, some small deficiency in pool level at high discharges would probably be beneficial in reducing flood damages upstream. Accordingly, on the basis of a balancing of all considerations, it was decided by the International Niagara Falls Engineering Board that the control structure would be constructed to a length of 1,550 ft.

MODEL TESTS OF REMEDIAL WORKS IN CASCADES

In the process of developing successful remedial works for improving flow conditions at both flanks of the Horseshoe Falls, many different schemes were tested in the model cascades above the falls. Some plans involved weirs in the deeper channels to intercept and divert flow to the flanks of the falls. Other schemes involved excavations on the flanks extending far enough upstream to divert flow to the flanks, and some consisted of both weirs and excavations. Consideration was given also to moderate shortening of both flanks by fills, not only to help intensify flow at the flanks and to reduce excavation, but also to provide excellent vantage points from which the falls and cascades could be viewed at close range.

Tests of flank excavations were begun with small quantities of excavation, which were progressively increased and tested until the criteria for flow over



FIG. 6.—HORSESHOE FALLS (MODEL)

the flanks were met. Each excavation scheme was tested both with and without the viewing fills at both ends of the crest. These tests culminated in the development of a satisfactory plan as follows (Fig. 2):

a. Excavations of an estimated 64,000 cu yd of rock on the Canadian flank and 24,000 cu yd on the Goat Island flank were accomplished to deepen these

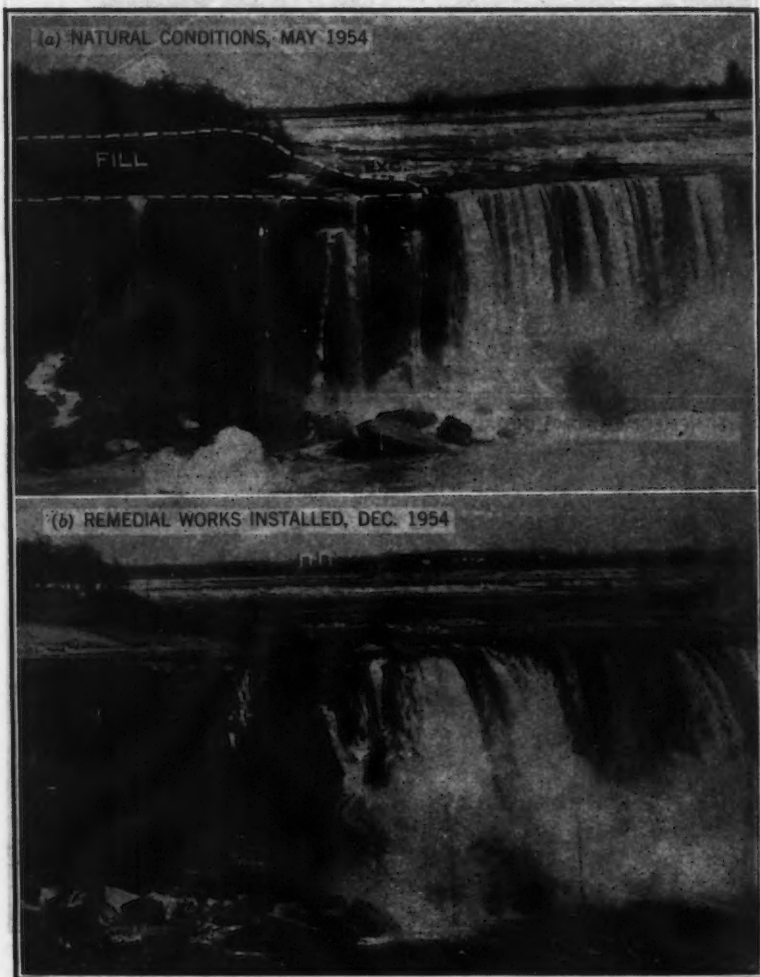


FIG. 7.—GOAT ISLAND FLANK OF THE HORSESHOE FALLS

areas and to tap the deeper waters upstream, thus diverting sufficient water to provide satisfactory flows over both flanks.

b. A 100-ft-wide crest fill, extending approximately 100 ft upstream, was constructed on the Canadian flank. On the Goat Island flank a crest fill approximately 300 ft wide and extending approximately 300 ft upstream was provided. Both fills would be surrounded by concrete retaining walls faced with stone to blend into the natural surroundings. Both would also be placed to the grades of the adjacent improved park areas and properly landscaped, thus providing excellent vantage points for viewing the cascades and falls.

With this scheme installed in the model, the minimum flow criteria for a total falls flow of 100,000 cu ft per sec were exceeded on both flanks. Also, there was a complete curtain of flow over the falls from shore to shore during a total flow of 50,000 cu ft per sec. Fig. 6 shows a comparison of flow conditions over the model Horseshoe Falls under natural unimproved conditions and with the remedial works installed.

Alternate schemes involving weirs, with and without flank excavations, were also developed, which gave the required crest flows. However, the required weirs were so high that the cascades would have an artificial appearance. Furthermore, their construction and maintenance would be difficult and hazardous, and their cost no less than that of the excavation plans. Consequently, the plans involving weirs were rejected.

CONCLUSIONS

The proposed plan of remedial works developed by the model tests consists of three separate installations, considered necessary to ensure that the provisions of the 1950 treaty will be met fully. These works are a Chippawa-Grass Island pool gated control structure extending 1,550 ft out from the Canadian shore; an excavation at the Canadian flank of the Horseshoe Falls, including a 100-ft crest fill at that flank; and an excavation at the Goat Island flank of the Horseshoe Falls, including a 300-ft crest fill at that flank.

The Chippawa-Grass Island pool control structure and the two excavations and fills at the flanks of the Horseshoe Falls have presently (1959) been completed, and the resulting flows confirm the model predictions. Fig. 7 shows a comparison of flow conditions over the Goat Island flank of the Horseshoe Falls before and after the installation of the remedial works.

ACKNOWLEDGMENTS

The 1953 report⁴ of the International Joint Commission of the United States and Canada, which contains results of both the Islington and Vicksburg model studies, formed the basis of much of the material presented. Acknowledgment is also made of the data furnished by Ernest B. Lipscomb, M. ASCE, of the Waterways Experiment Station, who directly supervised the Vicksburg model study. Stanley B. Hunt and Joseph G. Weinrub of the Buffalo District of the Corps of Engineers helped obtain and furnish the required field data and in developing the model testing program.

⁴ "Report of the International Joint Commission, United States and Canada, on the Preservation and Enhancement of Niagara Falls," U. S. Govt. Printing Office, Washington, D. C., 1953.

AMERICAN SOCIETY OF CIVIL ENGINEERS

Founded November 5, 1852

TRANSACTIONS

Paper No. 2976

ELECTRONIC COMPUTERS IN SURVEYING

BY ARTHUR J. MCNAIR,¹ M. ASCE

SYNOPSIS

Electronic digital computers provide civil engineers with the means to solve problems that are (a) routine, repetitious, and time consuming, or (b) new, elaborate, and so staggering in magnitude that heretofore they have been beyond consideration. Opportunities for new concepts in the teaching of surveying through the use of an electronic computer are described.

INTRODUCTION

Since approximately 1900 the process of performing mathematical computations advanced from longhand and logarithms to slide rule, desk calculator, and, presently, to electronic computers. The step having the most radical impact on the work of civil engineers is the present (1959) transition being made from desk calculators to the electronic computer. Although it is commonly believed that engineers are among the principal users of mathematics, they have been slow to use electronic computers. In general, accountants, statisticians, and research scientists have been the first to develop and use computing equipment. With the rapid development of electronic computers and the fact that they are becoming readily accessible in the United States, engineers are becoming more familiar with this method of computation.

TWO TYPES OF COMPUTERS

Most engineers are familiar with digital computers and analog computers. The pencil and paper of longhand arithmetic as well as desk calculators are types of digital computers. The slide rule, the deformatore, and the multiplex stereo-projector are typical analog computers. These devices provide an analogy to represent the quantities to be computed in a given problem. There are also electrical and electronic analog computers. An electrical analog computer used in surveying to represent the quantities that are to be adjusted in level

NOTE.—Published, essentially as printed here, in November, 1957, in the Journal of the Surveying and Mapping Division, as *Proceedings Paper 1444*. Positions and titles given are those in effect when the paper was approved for publication in *Transactions*.

¹ Prof. of Civ. Eng., Head of Surveying Dept., Cornell Univ., Ithaca, N. Y.

nets is the electrical survey net adjuster developed by Julius Speert, M. ASCE, and others, in the Geological Survey, United States Department of the Interior. The McIlroy pipeline net analyzer is an electronic analog computer familiar to hydraulic engineers. However, the analog computers, including the slide rule, have one common shortcoming. They usually provide only the first two or three significant figures in a result, whereas surveying usually requires accuracy much better than 1%. Because of the effect of cumulative errors, accuracies of at least 1 in 5,000 are quite common, and accuracies of 1 in 1,000,000, especially in geodetic work, are not uncommon.

ELECTRONIC DIGITAL COMPUTERS

Any subsequent reference to electronic computers pertains solely to digital electronic computers. The manufacture of electronic computers is experiencing a period somewhat similar to that of the automobile in the early 1900's. Several special-purpose computers have been designed and built. Some of them have been abandoned, whereas patent rights to others have been bought by major companies. Several computer manufacturers are better known for aircraft and aviation instruments. Many electronic computers are designed for special purposes and are not particularly adapted to the problems of civil engineering.

It is necessary to make a further distinction between electronic computers that affects the ease with which an engineer can program his problems and the speed at which the computing can be performed. This distinction pertains to the two types of programming, referred to as the interpretive language and the machine, or basic, language.

A general-purpose computer is designed to accept instructions so as to obtain maximum efficiency and generality consistent with keeping the machine itself as simple as possible. The result is a language of instructions to the machine that is difficult to use. This has been a deterrent to using the machine for relatively short-run problems. However, most computers have been programmed to simulate more specialized equipment, having instruction languages that make it easier to code a restricted range of problems such as those encountered in engineering computations. Thus, it is possible for the originator to solve his own problem with a minimum of assistance from specialists, but at the expense of machine efficiency. This may result in a decrease of machine running speed by factors of as much as 20. However, for relatively short problems (those representing less than a man-week of computation) the net effect is usually a more efficient operation. Most electronic computers operate in what is known as fixed-decimal form, with the decimal point at a predetermined position in the number of significant places available. However, in engineering it is usually necessary to operate with a specified number of significant figures, with the total frequently ranging beyond the number of places available. Thus, careful scaling of a problem is required. Greater flexibility is obtained using floating-decimal notation, in which the machine is programmed to carry a specified number of significant digits, together with a tens exponent to indicate the order of magnitude of the quantity. A typical interpretive language code for an electronic computer might be: 1—add; 2—subtract;

3—multiply; 4—divide; 5—negative multiply; 300—extract square root; 303—compute sine of an angle; and 304—compute cosine of an angle. In a typical system approximately fifty such codes include most ordinary mathematical operations and elementary functions. Of course, others can be added to the repertoire in the "memory" as desired.

SURVEY PROBLEMS

It is only possible to indicate a few of the various problems encountered in surveying that can be solved profitably through the use of electronic computers. It is certain that these computers are one more step in the trend to mechanization of human effort and relieving man of laborious and time-consuming operations. In general, there are two types of surveying problems. One would be classified as the routine problems commonly occurring. The other would be classified as imaginative, being complex and challenging. That is, the first and immediate use for an electronic computer is to relieve the burden of routine day-to-day computations. These are performed at the rate of from 5,000 to 500,000 mathematical operations per hr, depending on the type of computer. The second category of computations are those that have been so overwhelming in magnitude that it has been impossible even to consider computing them until the development of electronic computers. Many of these problems have occurred in geodetic surveying. Frequently they require the solution of hundreds of simultaneous equations using at least ten significant figures. An example of each of the foregoing problems may suffice to indicate the scope of possibilities.

A routine problem that contains many repetitious operations is computing latitudes and departures of traverse lines and thereafter computing the coordinates of traverse points. The foregoing consists of converting the azimuths from degrees and minutes to radian measure, computing the sines and cosines of the angles by expansion of the power series, and multiplying these values by the lengths of the lines to obtain latitudes and departures, which are added consecutively to the coordinates of an initial point. If the traverse closes within the required limit—for example, a ratio of 1 to 5,000—the machine will proceed to make an adjustment according to any prescribed rule, such as the transit rule or the compass rule. Adjusted coordinates are computed and the machine then computes the reverse problem, providing adjusted azimuths and lengths for each line in the traverse. The computer requires approximately 3 sec to compute and adjust each traverse line so that, for example, if ten parties were to arrive at a computing center, each party with a fifty-course traverse, all five hundred of the traverse lines would be computed, and the adjusted coordinates, azimuths, and lengths would be tabulated in approximately one-half hour. These quantities would all be carried out to eight significant figures. This volume of work would keep a computist with a desk calculator busy for nearly a month, and there would still be the possibility of some mistakes in the results.

One example of problems that are so overwhelming that they are rarely undertaken occurs in photogrammetry. When an aerial photograph contains the images of at least three known ground-control points, it is possible to

recapture the position in space and the pointing of the camera at the instant of exposure. One method of doing this is using the Church space resection and orientation problem.² In this case a problem requiring 10 hr on a desk calculator is solved in less than 3 min.

Another example is the study of the errors introduced into the computed position and orientation of a camera-exposure station by differential film shrinkage. This study of the effect of errors in film shrinkage would have taken 400 hr on a desk calculator, compared with little more than 1 hr on the type of electronic computer available. Using machine language the computing time could have been reduced to about 10 min.

ELECTRONIC COMPUTERS IN TEACHING SURVEYING

One of the primary goals of engineering education is to teach a man to think. Therefore, the training of technicians is not one of the goals. In teaching surveying no attempt is made to train slide-rule operators, transitmen, handbook engineers, multiplex operators, or programmers for electronic computers. Formal courses in the use of the slide rule, desk calculators, or electronic computers are not required in a civil engineering curriculum. However, the opportunity is provided for an engineering student to learn the use of these tools. At present (1959), courses in surveying and in statistics offer the best introduction to electronic computers. It is probable that in the near future structural courses will make greater use of the classical structural design methods and electronic computers, as contrasted with the use of relaxation methods typified by moment distribution.

More than fifty universities throughout the United States have electronic computers on the campus, and most have an established computing center. Time is available for both regular student use at little or no charge and for commercial computing at established rates. At these institutions many graduate students as well as undergraduate students attend the instructional periods that are offered, gaining sufficient information so they can program any of the simpler problems using the interpretive routine. Staff members at these computing centers are available to supervise programming and to assist with the more complicated programs. Of course, there are also expert programmers to assist with any complicated problems, particularly those in which it is more desirable to perform the computation in machine language.

The subject of electronic computers is exciting because new developments and uses appear continually. However, this device should be studied as a new and powerful tool that must be handled wisely so that it will perform economically. Surveying and the teaching of surveying are at least as challenging as the subject of new computers. This is especially true since the advent of electro-optical distance measurements, automation in photogrammetry, guided missiles, and similar developments. In another thirty years new tools for computing may be developed that will be as advanced over electronic computers as electronic computers presently are in advance of desk calculators. The same will probably be true of theodolites and distance-measuring devices. Nevertheless, surveying (which is basically the process of making measurements

² "Theory of Photogrammetry," by Earl Church, *Bulletin 19*, Syracuse Univ. Press, N. Y., 1948.

on or near the earth's surface) will be at least as interesting at that time as it is at present. It may be that surveying will be (a) a study of physical quantities at the bottom of the ocean or miles under the surface of the earth; (b) a measurement of the moon or some planet; (c) an attempt by topographic engineers to obtain the first complete topographic map of the United States; (d) settling disputes between two neighbors over a property boundary; and (e) rectifying the poorly made land surveys of the nineteenth century and of the first half of the twentieth century. The fundamentals of surveying—that is, the problems of engineering measurement, including geodesy and the shape of the earth—will be unchanged even though the techniques and instruments may be so different as to be unrecognizable to engineers of the present era.

Therefore, the problem is to make the best use of electronic computers in teaching surveying. One extremely important concept is the requirement that computations be organized thoroughly. Programming concepts are fundamental to all types of computers. With pencil and paper a student frequently is careless in selecting numbers somewhat at random and operating on them. He neglects to analyze his problem completely and to organize his computations in an orderly manner. He may think only in terms of the particular problem at hand without considering the limiting values of his parameters. Programming for electronic computers requires complete planning of the quantities and operations in the entire problem to take maximum advantage of the repetitious occurrence of these operations. The programmer must also consider the size and range of the quantities, the significant figures required, and positive and negative limits. This is excellent discipline for engineering students, instructors, and practicing engineers. Whether a student actually uses a computer after graduation or not, the discipline of programming is valuable. It emphasizes the importance of analyzing and organizing computations before becoming too involved in arithmetic.

An interesting use of the electronic computer in teaching surveying is the flexibility it provides the professor in assigning problems to his classes. For example, he can assign different values for a problem to each student in the class, program the problem once himself, and compute the twenty or more individual solutions in 5 min. An example of this type of problem—which is good for instruction, although generally shunned by engineers in practice—is the three-point resection problem. In hydrographic surveys, resection is commonly solved by using a three-armed protractor, or some other mechanical or graphical method. Analytical computation is somewhat tedious, although it is used by the Coast and Geodetic Survey, United States Department of Commerce, for locating horizontal control. The average student takes at least 2 hr to compute the coordinates of the unknown point. It requires a little more than 1 hr to program this problem and test it for an electronic computer. From that time forward, any number of three-point problems can be solved at any time, using the same program. For instance, an instructor assigned every student in an advanced surveying course different values for a resection problem. It required $5\frac{1}{2}$ min for the computer to solve seventy-five of these problems and an additional 3 min to print the results so that they could be distributed to the students after their own work had been corrected. It is not

difficult for an instructor to visualize that an opportunity is provided to make many interesting correlations with student work.

CONCLUSIONS

Presently constructed electronic computers, or the improved versions that are larger and faster, have become a permanent tool of the profession. They are an engineering triumph that can ease the tedious burden of engineering computations. Those engineers involved in surveying operations have an opportunity to make immediate use of electronic computers. Any problem that currently is being solved by digital operations should be examined carefully to determine the economics of electronic computing as compared with conventional computing. Small problems that are performed occasionally are best solved by conventional methods. However, repetitive problems, such as traverse computations, cut-and-fill computations on highways, or geometric highway design, can probably be performed less expensively and more accurately by electronic computers, thereby freeing personnel for other important jobs. Computing centers, especially those at universities, are usually more than willing to assist engineers with an educational program suitable to their own office operations.

The horizons have widened tremendously and civil engineers should use the opportunity to plan more extensive and more specialized jobs requiring more intricate computations. For example, the combination of automatic photogrammetry and electronic computers is in its early stage of development and offers many opportunities. Many networks and adjustment of errors involving the use of least squares and the solution of 5, 10, 40, or even 400 simultaneous equations can be computed rapidly. Heretofore, such problems have not been attempted by hand methods. Engineers should use their imaginations freely to make optimum use of this new tool.

AMERICAN SOCIETY OF CIVIL ENGINEERS

Founded November 5, 1852

TRANSACTIONS

Paper No. 2977

PREDICTING SURGE PRESSURES IN OIL PIPELINES

BY ROBERT D. KERSTEN¹ AND EDWIN J. WALLER,² ASSOCIATE
MEMBERS, ASCE

WITH DISCUSSION BY MESSRS. HENRY M. PAYNTER; AND ROBERT
D. KERSTEN AND EDWIN J. WALLER

SYNOPSIS

A method is presented for the analysis of surge problems based on a fundamental mathematical approach, and its validity is demonstrated through application to a full-scale pipeline system. The results of this work are sufficiently general in nature to permit the designer to apply them to a variety of piping configurations.

INTRODUCTION

Pressure-surge problems have remained unsolved notwithstanding the significant advances made in the technology and equipment of the pipeline industry. The various water-hammer theories have not been fundamental enough in their approach to permit widespread application to a variety of pumping situations. Commercial desurgers or pulsation dampeners, although helpful in some cases, are frequently detrimental in others. The result is that the pipeline engineer is still concerned with:

1. The inability to predict the points of extreme fluctuating pressure in a pumping system, which results in the overdesign of the entire system;
2. Breakdowns of the pumping system from elastic failure of the pipes and pumps as a result of extreme fluctuating pressure; and
3. Loss of revenue because "surges" necessitate the establishment of a line limit below the normal rating of the equipment.

NOTE.—Published, essentially as printed here, in March, 1957, in the Journal of the Pipeline Division, as *Proceedings Paper 1195*. Positions and titles given are those in effect when the paper or discussion was approved for publication in *Transactions*.

¹ Asst. Prof., Dept. of Civ. Eng., Arizona State College, Tempe, Ariz.

² Associate Prof., Dept. of Civ. Eng., College of Eng., Oklahoma State Univ., Stillwater, Okla.

It is the purpose of the paper to outline a method of analysis based on a fundamental mathematical approach. The validity of this method is demonstrated through application to an actual full-scale pipeline system, and its application will aid the designer in predicting points of extreme fluctuating pressure.

DEVELOPMENT OF A METHOD OF ANALYSIS

Notation.—The letter symbols adopted for use in this paper are defined where they first appear, in the illustrations or in the text, and are arranged alphabetically, for convenience of reference, in the Appendix.

Previous Investigations.—Early contributions to the water-hammer or pressure-surge theory were made by Lorenzo Allievi³ and N. Joukowski.⁴ The latter postulated the classic water-hammer formula for the increase in pressure due to the extinguishing of a given velocity of flow, whereas the work of Allievi represented the first fundamental mathematical approach to variable flow. Although the basic differential equations of variable flow were not solved for the steady-state case until 1951,^{5,6} the importance of the studies of Allievi should not be overlooked.

Water-hammer and pressure-surge studies draw heavily from the work of Allievi and Joukowski. The most significant contributions in this field have been summarized by the American Society of Mechanical Engineers⁷ and by Harry M. Wyatt.⁸ It is important to note that the methods of analysis outlined in these papers were essentially of a semiempirical nature, and some were dependent on graphical techniques.

Results of Recent Research.—Edwin J. Waller^{5,6} proposed a solution to the fundamental equations of variable flow postulated by Allievi,³ Lord Rayleigh,⁹ and Horace Lamb.¹⁰ The basic differential equations in this analysis were of the same form as those in the transmission of energy by heat, sound, and electricity. Therefore, the mathematical tools of wave analysis should be used. In the solution of the differential equations, it was assumed that the principle of superposition was valid for this case. The resulting solution consisted of a transient term and of a steady-state term.

The transient term was found to be the water-hammer solution, which will damp out after a period of time. Analyzing the steady-state term independently, the following result was obtained for the fluctuating pressure, P , and for the alternating volumetric flow rate or volume current, Q , at any point a distance x from the receiving end—

$$P_x = P_r \cosh \gamma x + Q_r Z_c \sinh \gamma x \dots \dots \dots (1)$$

³ "Teoria Generale del moto perturbato dell'acqua nei tubi in pressione," by Lorenzo Allievi, *Annali della Società degli Ingegneri ed Architetti Italiani*, Milan, 1903; "General Theory of Perturbed Flow of Water in Conduits," by E. E. Halmos, *Typography Riccardi Garreth*, Rome, 1925 (translation).

⁴ "Water Hammer," by N. Joukowski, *Proceedings, A.W.W.A.*, 1904, p. 341.

⁵ "A Theoretical Study of Impedance Matching as Applied to Surge Suppression Instruments in Hydraulic Systems," by E. J. Waller, thesis presented to Oklahoma State University, at Stillwater, in 1951, in partial fulfillment of the requirements for the degree of Master of Science.

⁶ "Fundamental Analysis of Unsteady Pressure Variations in Pipeline Systems," by E. J. Waller, *Publication No. 93*, Eng. Experiment Station, Oklahoma State Univ., Stillwater, May, 1954.

⁷ "Symposium on Water Hammer," A.S.M.E., 1933, presentation at Century of Progress Exposition, Chicago, Ill., sponsored by Hydraulics Div., A.S.M.E., and Power Div., ASCE.

⁸ "Pulsation Absorbers—Their Design and Application," by Harry M. Wyatt, *Paper No. 56Pet31*, A.S.M.E., September, 1956.

⁹ "Theory of Sound," by Lord Rayleigh, Macmillan & Co., Ltd., London, 1937.

¹⁰ "Hydrodynamics," by Horace Lamb, Dover Publications, New York, N. Y., 1945.

and

$$Q_x = Q_r \cosh \gamma x + \frac{P_r}{Z_c} \sinh \gamma x \dots \dots \dots (2)$$

in which Z_c and γ are constants defined as

$$Z_c = \frac{\rho a}{A} \dots \dots \dots (3)$$

and

$$\gamma = \alpha + j\beta \dots \dots \dots (4)$$

in which α is the attenuation coefficient and β is the phase constant. The reduction in magnitude of the wave as it travels down the pipeline may be determined from

$$\alpha = \frac{p n}{2 l \bar{U} a \rho} \dots \dots \dots (5)$$

The term β determines the change in phase between the pressure and volume current as the pressure wave travels in the pipeline, and is defined as

$$\beta = \frac{\omega}{a} \dots \dots \dots (6)$$

The primary interest herein is the application of this method of analysis to a full-scale field installation.

Eqs. 1 and 2 will be recognized as being of the same form as the classical wave equations of acoustics and electrical engineering, and an electrical-hydraulic analogy becomes evident. Therefore, it can be assumed that

$$P_x = Q_x Z_x \dots \dots \dots (7)$$

For example, Ohm's law for the hydraulic circuit becomes the defining equation of the impedance, Z , to the alternating flow. Eqs. 1 through 7 form the basis of the analysis for a pumping system. The recognition of the electrical analogy permits the formulation of a method for hydraulic-circuit analysis similar in many respects to the analysis of electric circuits.

The Pump Equation.—Eq. 7 reveals that if any two of the three quantities are known at a particular point in the pipeline system, the third quantity can be determined. Then, by application of Eqs. 1 and 2, the fluctuating pressure and the alternating volume current can be computed at other points in the system. Pressure is a measurable quantity, but volume, current, and impedance are not.

The use of a reciprocating pump in a pipeline system causes an alternating periodic volume current or volumetric flow rate. As the flow is periodic, it may be analyzed by Fourier-series methods and expressed in terms of a trigonometric series involving harmonics of a basic frequency. The response of the system to the various harmonics may then be determined, and, using superposition, the effects of all the harmonics may be found.

When the connecting-rod length, l , is not relatively long compared with the crank arm, r , the piston motion is not simple harmonic, and the piston velocity

for the constant, ω , is determined from

$$v_p = \frac{ds}{dt} = r\omega \left(\sin \omega t + \frac{r}{2} \sin 2\omega t \right) \dots \dots \dots (8)$$

Then the variable flow rate is

$$Q = A_c v_p \dots \dots \dots (9a)$$

in which A_c is the area of the cylinder. For a double-acting cylinder,

$$A_c = \frac{\pi (D_l)^2}{4} \dots \dots \dots (9b)$$

for $0 < \omega t < 180^\circ$, and

$$A_c = \frac{\pi [(D_l)^2 - d^2]}{4} \dots \dots \dots (9c)$$

for $180^\circ < \omega t < 360^\circ$, in which D_l is the liner diameter (which may be different from the pipeline diameter, D_p) and d denotes the diameter of the piston rod. Fig. 1 shows a plot of the discharge from one double-acting cylinder.

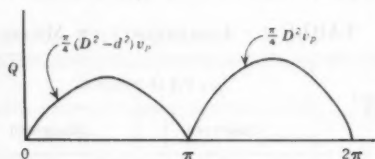


FIG. 1.—DISCHARGE FROM ONE DOUBLE-ACTING CYLINDER

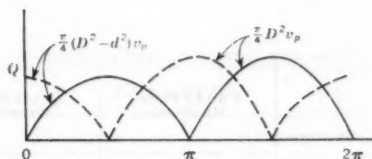


FIG. 2.—DISCHARGE FROM DOUBLE-ACTING DUPLEX PUMP

Referred to head-end dead center, the Fourier-series solution for this case is

$$Q = \frac{\pi r \omega}{4} \left[\frac{2 (D_l)^2 - d^2}{\pi} - d^2 \left(\frac{2r}{3\pi l} \cos \omega t + \frac{1}{2} \sin \omega t \right) \right. \\ + \frac{2 (D_l)^2 - d^2}{\pi} \left(\frac{\pi r}{4l} \sin 2\omega t - \frac{2}{3} \cos 2\omega t \right) \\ + \frac{r d^2}{2\pi l} \sum_{m=3,5,7,9\dots} \frac{4}{m^2 - 4} \cos m\omega t \\ \left. - \frac{2 (D_l)^2 - d^2}{\pi} \sum_{m=4,6,8\dots} \frac{2}{m^2 - 1} \cos m\omega t \right] \dots (10)$$

Referring Eq. 10 to crank-end dead center reverses the algebraic sign of the odd harmonics.

For two double-acting cylinders (for example, a double-acting duplex pump with one cylinder 90° ahead of the other, as shown in Fig. 2, and with the first

cylinder referred to head-end dead center), the Fourier-series analysis yields

$$Q = \frac{\pi r \omega}{4} \left\{ \frac{4 (D_1)^2 - 2 (D_2)^2}{\pi} - d^2 \left[\frac{r \sqrt{2}}{3 \pi l} \sin (\omega t + 135^\circ) \right. \right. \\ \left. \left. + \frac{\sqrt{2}}{4} \sin (\omega t + 45^\circ) \right] + \frac{r d^2}{2 \pi l} \left[\sum_{m=3,7,11 \dots} \frac{4 \sqrt{2}}{m^2 - 4} \cos (m \omega t + 45^\circ) \right. \right. \\ \left. \left. + \sum_{m=5,9,13 \dots} \frac{4 \sqrt{2}}{m^2 - 4} \cos (m \omega t + 135^\circ) \right] \right. \\ \left. - \frac{2 (D_1)^2 - d^2}{\pi} \left[\sum_{m=4,8,12 \dots} \frac{4}{m^2 - 1} \cos m \omega t \right] \right\} \dots (11)$$

Similar equations may be developed for any multicylinder double-acting pump referred to head-end dead center or crank-end dead center by superimposing the effects of the required, properly phased, double-acting single cylinders (Eq. 10).

The first term in Eqs. 10 and 11 is the mean flow component, q , whereas all the other terms are the variable flow components. The magnitude of all odd harmonics above the third harmonic and of all even harmonics above the eighth

TABLE 1.—COMPARISON OF MEASURED

Harmonic (1)	P 4 (AT PUMP) MEASURED		Q ₄ (AT PUMP) COMPUTED		P 3 (z = 32 Ft)			
	Lb Per Sq In.	φ Deg	Cu Ft Per Sec	φ Deg	COMPUTED		MEASURED	
					Lb Per Sq In.	φ Deg	Lb Per Sq In.	φ Deg
	(2)	(3)	(4)	(5)	(6)	(7)	(8)	(9)
(a) TEST NUMBER 1.								
1	12.62	-90.0	0.0980	-85.8	12.77	-96.2	12.50	-100.5
3	6.46	145.8	0.0481	133.5	6.23	127.1	5.11	122.2
4	16.46	-90.0	0.1187	-105.4	16.72	-113.6	15.33	-118.6
8	5.18	-104.1	0.0304	-130.5	4.26	-148.2	5.17	-150.4
PRMS	15.79				15.80		14.90	
(b) TEST NUMBER 2.								
1	12.73	-94.7	0.0988	-99.1	12.67	-101.4	12.39	-98.8
3	7.17	140.4	0.0529	127.5	6.70	125.2	6.55	117.2
4	15.86	-84.3	0.1129	-101.0	14.82	-110.2	15.17	-118.6
8	5.15	-103.4	0.0293	-130.5	4.15	-153.4	5.72	-155.7
PRMS	15.68				14.87		15.15	
(c) TEST NUMBER 3.								
1	12.22	-115.9	0.0950	-119.8	12.17	-121.4	13.05	-118.8
3	5.95	153.5	0.0448	142.8	5.80	137.2	5.50	143.6
4	13.13	-83.4	0.0963	-97.4	12.52	-104.7	13.55	-106.2
8	4.95	-79.1	0.0310	-103.2	4.23	-118.6	4.50	-120.4
PRMS	13.82				13.35		14.22	

harmonic is normally small in comparison with the predominant fourth harmonic. Neglecting these terms, Eq. 11 may be reduced to

$$Q = \frac{\pi r \omega}{4} \left\{ \frac{4 (D_1)^2 - 2 d^2}{\pi} - d^2 \left[\frac{r \sqrt{2}}{3 \pi l} \sin (\omega t + 135^\circ) + \frac{\sqrt{2}}{4} \sin (\omega t + 45^\circ) \right] + \frac{r d^2 4 \sqrt{2}}{2 \pi l 5} \cos (3 \omega t + 45^\circ) - \frac{2 (D_1)^2 - d^2}{\pi} \left[\frac{4}{15} \cos 4 \omega t + \frac{4}{63} \cos 8 \omega t \right] \right\} \dots (12a)$$

The following quantities are applicable to the pumps at the test station: $D_1 = 5\frac{1}{2}$ in. = 0.458 ft; $d = 2$ in. = 0.167 ft; $r = 6$ in. = 0.5 ft; $\omega = 2\pi/60$ (rpm) = 0.105 (rpm); and $l = 33\frac{1}{2}$ in. = 2.742 ft. Eq. 12a then reduces to

$$Q = 0.0103 \text{ (rpm)} + 0.000816 \text{ (rpm)} \sin (\omega t - 128.9^\circ) + 0.000221 \text{ (rpm)} \sin (3 \omega t + 135^\circ) + 0.00137 \text{ (rpm)} \sin (4 \omega t - 90^\circ) + 0.000325 \text{ (rpm)} \sin (8 \omega t - 90^\circ) \dots (12b)$$

Eq. 12b is used throughout the subsequent analyses as the value of the variable volume current, Q_s , generated by the pump.

AND COMPUTED PRESSURE VALUES

P2 (x = 111 Ft)				P5 (x = 554 Ft)			
COMPUTED		MEASURED		COMPUTED		MEASURED	
Lb Per Sq In.	φ Deg	Lb Per Sq In.	φ Deg	Lb Per Sq In.	φ Deg	Lb Per Sq In.	φ Deg
(10)	(11)	(12)	(13)	(14)	(15)	(16)	(17)
PUMP NUMBER 4 AT 77.4 RPM							
12.76	-105.2	11.44	-106.4	12.60	-159.7	9.89	-161.1
6.23	99.8	4.97	90.0	6.23	-115.6	4.95	-92.6
16.25	-148.2	15.61	-156.8	15.57	-8.4	12.27	-27.6
4.40	138.0	4.80	143.8	4.25	2.6	4.12	33.7
15.58		14.54		15.13		12.04	
PUMP NUMBER 4 AT 82.2 RPM							
12.68	-111.1	12.66	-108.7	12.67	-169.2	10.97	-169.9
6.70	96.2	6.82	91.3	6.70	-78.2	5.94	-102.8
14.82	-148.9	13.12	-151.6	14.67	-21.4	14.46	-42.9
4.15	129.2	5.09	128.6	4.15	24.2	3.71	-7.4
14.87		14.23		14.79		13.76	
PUMP NUMBER 4 AT 66.7 RPM							
12.17	-129.2	13.76	-124.2	12.17	-176.4	12.17	-151.2
5.80	113.7	5.84	111.5	5.80	-27.8	5.71	-50.5
12.53	-136.1	15.32	-136.7	12.52	35.3	12.40	24.8
4.23	178.6	4.39	169.7	4.23	161.4	4.00	133.5
13.35		15.45		13.35		13.24	

TABLE 2.—COMPARISON OF MEASURED

Harmonic	P ₁ (AT PUMP) MEASURED		Q ₁ (AT PUMP) COMPUTED		P ₂ (x = 32 Ft)			
					COMPUTED		MEASURED	
	Lb Per Sq In.	φ Deg	Cu Ft Per Sec	φ Deg	Lb Per Sq In.	φ Deg	Lb Per Sq In.	φ Deg
(1)	(2)	(3)	(4)	(5)	(6)	(7)	(8)	(9)
(a) TEST NUMBER 4,								
1	8.70	-90.0	0.0687	-90.0	8.72	-94.9	8.61	91.4
3	4.18	117.5	0.0378	-126.6	5.28	123.4	4.30	99.6
4	8.54	-106.5	0.0920	-95.6	9.94	-129.5	10.23	-130.6
8	1.40	-56.3	0.0312	-98.9	2.03	-160.9	1.79	-166.9
PRMS	9.16				10.17		9.99	
(b) TEST NUMBER 5,								
1	11.92	-131.2	0.0962	-126.2	12.09	-137.6	12.48	-141.0
3	3.77	136.2	0.0395	146.6	4.32	114.1	4.39	74.8
4	7.21	-108.4	0.0969	-100.2	9.27	-143.7	12.83	-161.3
8	4.10	-21.4	0.0472	-106.0	1.59	176.3	1.14	146.0
PRMS	10.60				11.26		13.05	
(c) TEST NUMBER 6,								
1	7.87	-114.9	0.0639	-109.4	8.01	-122.0	8.21	-125.9
3	3.88	115.7	0.0437	126.3	4.62	90.2	5.90	97.2
4	7.59	-104.3	0.1159	-99.8	10.59	-146.4	12.14	-142.7
8	7.82	-42.6	0.0629	-131.6	0.83	146.4	0.23	-135.0
PRMS	9.89				9.96		11.20	

For a pump with no return rod in the cylinder, in which $d = 0$, Eq. 10 for one double-acting cylinder becomes

$$Q = \frac{\pi r \omega}{4} \left[\frac{2 (D_1)^2}{\pi} + \frac{2 (D_1)^2}{\pi} \left(\frac{\pi r}{4 l} \sin 2 \omega t - \frac{2}{3} \cos 2 \omega t \right) - \frac{2 (D_1)^2}{\pi} \sum_{m=4,6,8,\dots} \frac{2}{m^2 - 1} \cos m \omega t \right] \dots (13)$$

For two double-acting cylinders 90° apart, Eq. 11 reduces to

$$Q = \frac{\pi r \omega}{4} \left(\frac{4 (D_1)^2}{\pi} - \frac{2 (D_1)^2}{\pi} \sum_{m=4,8,12,\dots} \frac{4}{m^2 - 1} \cos m \omega t \right) \dots (14)$$

Equations may be developed for any multicylinder double-acting pump by superimposing the effects of the required, properly phased, double-acting cylinders (Eq. 13).

FIELD TESTS

The test station was equipped with four double-acting duplex pumps with V-belt drive. Crude oil was pumped from storage tanks through approximately

AND COMPUTED PRESSURE VALUES

P3 (x = 111 Ft)				P5 (x = 507 Ft)			
COMPUTED		MEASURED		COMPUTED		MEASURED	
Lb Per Sq In.	φ Deg	Lb Per Sq In.	φ Deg	Lb Per Sq In.	φ Deg	Lb Per Sq In.	φ Deg
(10)	(11)	(12)	(13)	(14)	(15)	(16)	(17)
PUMP NUMBER 1 AT 59.4 RPM							
8.80	-94.4	8.94	-95.2	8.68	-136.4	7.89	-140.4
5.70	123.4	4.62	101.8	5.30	-2.6	3.19	-49.4
11.41	-129.8	12.17	-128.7	9.94	62.2	8.86	54.5
3.90	-160.4	3.72	-159.9	2.07	-184.8	1.86	-162.1
11.30		11.47		10.16		8.78	
PUMP NUMBER 1 AT 76.4 RPM							
12.25	-137.6	13.72	-133.5	12.09	-191.6	12.74	-174.2
4.91	114.1	5.28	87.2	4.32	-47.9	3.77	-101.6
11.73	-143.7	16.67	-148.6	9.27	0.2	9.77	-24.5
6.48	176.3	6.28	163.3	1.59	104.1	5.09	85.5
13.30		16.33		11.25		11.97	
PUMP NUMBER 1 AT 84.5 RPM							
8.15	-122.0	9.61	-131.7	8.01	-181.2	10.40	-178.1
5.40	90.2	6.78	94.8	4.61	-89.5	4.69	-99.9
14.18	-146.4	15.39	-146.2	10.59	-25.4	9.94	-20.4
7.38	146.4	7.94	152.9	0.83	28.4	0.51	-35.5
13.25		14.80		9.96		10.71	

45 miles of 8-in. line into additional storage tanks. There were several diameter changes and short stub lines involved in the test.

Instrumentation.—Fluctuating pressures were measured and recorded with pressure cells. The output of the cells was fed into a recording oscillograph. The measured values of pressure recorded in Tables 1 and 2 were obtained from the analysis of the oscillograph traces, and recording pressure gages were used to measure the mean discharge pressures at the sending and receiving ends.

Crude Oil Data.—Samples of crude oil were taken before, during, and after the test runs. Analysis of the samples gave the following data: Density—40.7° API¹¹ at 54° F, or 1.59 slugs per cu ft; and viscosity—51.5 SUS,¹² or 13.45×10^6 lb-sec per sq ft.

Velocity of Propagation.—The velocity of propagation of the pressure waves in the system was determined by measuring the time required for a downsurge to travel from the sending-end pumps to the receiving end. An average travel time of 59.3 sec was used, yielding a velocity of propagation of 4,029 ft per sec.

Determination of the Attenuation Coefficient.—The attenuation coefficient may be determined readily from Eq. 5. Data for determining n and α are shown

¹¹ "Fluid Mechanics," by R. C. Binder, Prentice-Hall Co., New York, N. Y., 1955.

¹² "Elementary Mechanics of Fluids," by Hunter Rouse, John Wiley & Sons, Inc., New York, N. Y., 1937.

in Table 3. The mean pressure drop was plotted against the mean velocity, and a value of 1.75 was determined for n . The resulting values of the attenuation coefficient were small enough to be ignored in the analysis of the test-station piping.

Analysis.—With the distance, x , measured from the receiving end, the pressure and volume current for any end termination, Z_r , are given by Eqs. 1 and 2.

With a small value of αx ($\cosh \alpha x \doteq 1$ and $\sinh \alpha x \doteq 0$), Eqs. 1 and 2 reduce to

$$P_x = P_r \cos \beta x + j Q_r Z_c \sin \beta x \dots\dots\dots (15)$$

and

$$Q_x = Z_r \cos \beta x + j \frac{P_r}{Z_c} \sin \beta x \dots\dots\dots (16)$$

TABLE 3.—DATA FOR DETERMINATION OF n AND α

Test no.	\bar{q} , in cubic feet per second	\bar{U} , in feet per second	PS , in pounds per square inch ^a	PR , in pounds per square inch ^b	$PS - PR$, in pounds per square inch	\bar{p} , in pounds per square inch ^a	$\alpha \times 10^{-4}$ numeric per foot	$R \times 10^{-4}$
(1)	(2)	(3)	(4)	(5)	(6)	(7)	(8)	(9)
1	0.797	2.29	111.0	9.339	1.800
2	0.847	2.44	138.0	8.3	129.7	289.5	9.945	1.920
3	0.687	1.98	67.0	7.5	59.5	219.3	8.309	1.558
4	0.612	1.76	60.0	7.3	52.7	212.5	7.712	1.383
5	0.787	2.27	90.0	7.5	82.5	242.3	9.241	1.785
6	0.870	2.50	148.0	8.5	139.5	299.3	10.036	1.965

^a Mean pressure as shown by recorder at the sending end. ^b Mean pressure as shown by recorder at the receiving end. ^c $PS - PR$ plus effects of elevation change between stations.

At the receiving end

$$P_r = Q_r Z_r \dots\dots\dots (17)$$

Letting $x = l$, the sending-end impedance becomes

$$Z_s = Z_c \frac{Z_r + j Z_c \tan \beta l}{Z_c + j Z_r \tan \beta l} = \frac{P_s}{Q_s} \dots\dots\dots (18)$$

By measuring the distance, x , from the sending end, the pressure and volume current for any end termination, Z_s , can be given as

$$P_x = P_s \cosh \gamma x - Q_s Z_c \sinh \gamma x \dots\dots\dots (19)$$

and

$$Q_x = Q_s \cosh \gamma x - \frac{P_s}{Z_c} \sinh \gamma x \dots\dots\dots (20)$$

When the value of αx is small ($\cosh \alpha x \doteq 1$ and $\sinh \alpha x \doteq 0$), Eqs. 19 and 20 can be reduced to

$$P_x = P_s \cos \beta x - j Q_s Z_c \sin \beta x \dots\dots\dots (21)$$

and

$$Q_x = Q_s \cos \beta x - j \frac{P_s}{Z_c} \sin \beta x \dots \dots \dots (22)$$

Letting $x = l$ and

$$P_s = Z_s Q_s \dots \dots \dots (23)$$

the receiving-end impedance, Z_r , becomes

$$Z_r = Z_c \frac{Z_s - j Z_c \tan \beta l}{Z_c - j Z_s \tan \beta l} \dots \dots \dots (24)$$

The field-test pipeline system in Fig. 3(a) was composed of pumps, pipeline, and receiving-end tank. This system may be diagrammed electrically as shown in Fig. 3(b). An analysis of the system based on this arrangement

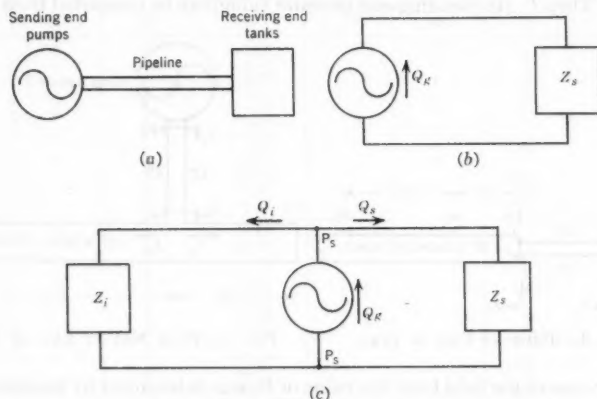


FIG. 3.—ELECTRICAL-ANALYSIS SKETCHES

yielded pressure magnitudes that were in agreement with measured values. However, the resulting phase angles generally were not in agreement with the measured values.

The concept of treating the pump as a constant current generator (in electrical terms) was introduced. The pump was considered as having an internal impedance, Z_i , in parallel and generating a volume current, Q_s . The current Q_s divides into Q_i , which circulates through the internal impedance, and the remainder, Q_r , which flows out into the pipeline system proper (Fig. 3(c)).

Then

$$P_s = Z_s Q_s = Z_i Q_i = Z_p Q_s \dots \dots \dots (25)$$

and

$$Q_s = Q_i + Q_r \dots \dots \dots (26)$$

From Eqs. 25 and 26

$$Z_p = \frac{Z_i Q_i}{Q_s} = \frac{Z_i Q_i}{Q_i + Q_r} = \frac{Z_i Z_s}{Z_i + Z_s} \dots \dots \dots (27)$$

or

$$Z_i = \frac{Z_p Z_s}{Z_s - Z_p} \dots \dots \dots (28)$$

The sending-end impedance, Z_s , may be computed from Eq. 18. The measurement of P_s permits the computation of Q_s from Eq. 25. Knowing the values of Q_s and Q_o (Eq. 12b), the value of Q_i may be determined from Eq. 26. With the values of Q_i and Q_o known, the values of Z_i and Z_p may be established from Eq. 25 or from Eqs. 27 and 28.

If the values of P_s and Z_s are known, the value of Q_s can be computed. It is not necessary to determine the value of Z_i in order to proceed with the analysis. However, if P_s is not known it becomes necessary to evaluate Z_i . In turn, this permits the evaluation of Z_p (impedance at the pump) by use of Eq. 27. Then P_s (the sending-end pressure value) can be computed from Eq. 25.

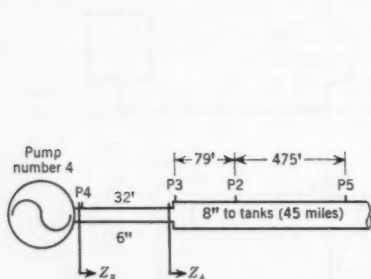


FIG. 4.—PUMP AT END OF LINE

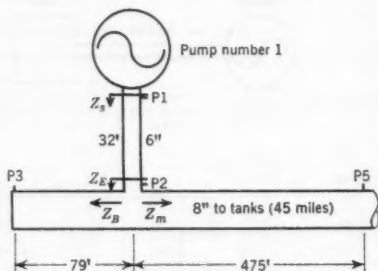


FIG. 5.—PUMP NOT AT END OF LINE

In the case of the field tests the value of P_s was determined by measurement. It was possible to compute Q_s and, therefore, the values of pressure and of volume current at the other points in the system.

One-Pump Tests with Pump at End of Line.—The physical arrangement of the equipment is shown in Fig. 4. Points P2, P3, P4, and P5 denote pressure pickups. Tests 1, 2, and 3 were run at 66.7 rpm, 77.4 rpm, and 82.2 rpm using the arrangement in Fig. 4. The circuit then can be visualized electrically as shown in Fig. 3.

The pressures at the various pickup points were determined by applying the equations and techniques outlined previously. Measured values and computed values are compared in Table 2.

One-Pump Tests with Pump Not at End of Line.—The physical arrangement of the equipment is shown in Fig. 5. Tests 4, 5, and 6 were run at 59.4 rpm, 76.4 rpm, and 84.5 rpm, using the arrangement in Fig. 5. The circuit can be visualized electrically as shown in Fig. 3. In this case the term Z_s is the parallel combination of the long line and of the short stub in series with the short 6-in. line.

The pressures at the various pickup points were computed again by applying the equations and techniques outlined previously, and measured pressure values and computed pressure values are compared in Table 2.

Analysis of Test Results.—The field test was composed of 6 one-pump tests. Oscillograph traces were analyzed for the first harmonic, third harmonic, fourth harmonic, and eighth harmonic at three different points in the pipeline. For the theory to predict the experimental pressure accurately, the difference, Y , between the observed pressure and theoretical pressure must have reasonable values when compared with the precision of measurement. The differences ($Y = P_{th} - P_{exp}$) are recorded in Table 4.

TABLE 4.—DIFFERENCE BETWEEN MEASURED AND COMPUTED PRESSURE VALUES FOR EACH HARMONIC

Test (1)	Pickup (2)	Harmonic (3)	Y-difference,* in pounds per square inch (4)	Test (5)	Pickup (6)	Harmonic (7)	Y-difference,* in pounds per square inch (8)
1	3	1	+0.27	2	3	1	+0.29
		3	+1.12			3	+0.15
		4	+1.39			4	-0.35
		8	-0.91			8	-1.57
	2	1	+1.32		2	1	+0.02
		3	-1.26			3	-0.12
		4	+0.64			4	+1.70
		8	-0.40			8	-0.94
	5	1	+2.71		5	1	+1.70
		3	+1.28			3	+0.76
		4	+3.30			4	+0.21
		8	+0.13			8	+0.44
3	3	1	-0.88	4	2	1	+0.11
		3	+0.30			3	+1.08
		4	-1.03			4	-0.29
		8	-0.27			8	+0.24
	2	1	-1.59		3	1	-0.14
		3	-0.04			3	+1.08
		4	-2.79			4	-0.76
		8	-0.16			8	+0.18
	5	1	...		5	1	+0.79
		3	+0.09			3	+2.11
		4	+0.12			4	+1.08
		8	+0.23			8	+0.21
5	2	1	-0.39	6	2	1	+0.20
		3	-0.07			3	-1.28
		4	-3.56			4	-1.55
		8	+0.45			8	+0.60
	3	1	-1.47		3	1	-1.46
		3	-0.31			3	-1.38
		4	-4.94			4	-1.21
		8	+0.20			8	-0.56
	5	1	-0.65		5	1	-2.39
		3	+0.55			3	-0.08
		4	-0.50			4	+0.65
		8	-3.50			8	+0.32

* Plus sign indicates the computed value is greatest.

When analyzing the seventy-two values in Table 4, it is found¹³ that

a. The value of Y is distributed normally with mean $\bar{Y} = -0.15$ lb per sq in. ≈ 0 .

b. The standard deviation is $\left[\frac{(Y_i - \bar{Y})^2}{72} \right]^{1/2} = 1.33$ lb per sq in.

c. Therefore, with 95% confidence the experimental pressure amplitudes are predicted by the theory within 2.66 lb per sq in. (two standard deviations)

¹³ "Introduction to Mathematical Statistics," by Paul G. Hoel, John Wiley & Sons, Inc., New York, N. Y., 1954.

of the theoretical pressure, without regard to the precision of measurement. Only one measurement differed by more than ± 4 lb per sq in., and only eight measurements differed by more than ± 2 lb per sq in. (Table 4).

Because the factors that comprise the error of measurement could be as much as ± 4.32 lb per sq in., it can be concluded that the fundamental principles and the theory predict satisfactorily the measured pressures within the limits of the instrumentation.

When the root-mean-square pressure values (prms) were compared, it was found that none of the eighteen values exceeded the probable error of ± 4.32 lb per sq in. (Table 5).

TABLE 5.—COMPARISON OF MEASURED AND COMPUTED
ROOT-MEAN-SQUARE PRESSURE VALUES

Test no.	Pickup no.	Computed prms, in pounds per square inch	Measured prms, in pounds per square inch	Difference,* in pounds per square inch
(1)	(2)	(3)	(4)	(5)
1	3	15.80	14.90	+0.90
1	2	15.58	14.54	+1.04
1	5	15.13	12.04	+3.09
2	3	14.87	15.15	-0.28
2	2	14.87	14.23	+0.64
2	5	14.79	13.76	+1.03
3	3	13.35	14.22	-0.87
3	2	13.35	15.45	-2.10
3	5	13.35	13.24	+0.11
4	2	10.17	9.99	+0.18
4	3	11.30	11.47	-0.17
4	5	10.16	8.78	+1.38
5	2	11.26	13.05	-1.79
5	3	13.30	16.33	-3.03
5	5	11.25	11.97	-0.72
6	2	9.96	11.20	-1.24
6	3	13.25	14.80	-1.55
6	5	9.96	10.71	-0.75

* Plus sign indicates the computed value is greater.

CONCLUSIONS

The results of the tests presented herein account for the pressure fluctuations in a reciprocating pump system. First, the validity of the basic underlying derivations was established, and the fundamental principles and equations formulated in the basic theoretical analysis were verified. In this case the principle of superposition is applicable, and simplification of the general mathematical expressions is valid.

Second, the applicability of the fundamental principles to a field-scale system was demonstrated, and the techniques of analysis were successfully applied to an actual field installation. The results of this work are sufficiently general to permit the designer to apply them to a variety of piping configurations.

The parameters based on the concepts of the hydraulic-electric analogy have been established. The study of these basic parameters should be continued and directed toward the further development of analytical techniques for more complex pipeline systems.

The basis of this research activity is the hydraulic-electric analogy. Thus, electronic-computer techniques could be applied and would facilitate the preparation of the material in chart and graph form. Such procedures will lessen the computational effort required in the analysis of pressure-surge problems.

ACKNOWLEDGMENTS

The tests were performed by the Division of Engineering Research of the College of Engineering, Oklahoma State University, at Stillwater. The study was under the administrative direction of Clark A. Dunn. Harold T. Fristoe, Roger L. Flanders, M. ASCE, and Joseph R. Norton rendered valuable consulting assistance.

APPENDIX. NOTATION

The following symbols, adopted for use in the paper and for the guidance of discussers, conform essentially with "American Standard Letter Symbols for Hydraulics" (ASA Z10.2—1942), prepared by a committee of the American Standards Association with Society representation and approved by the Association in 1942.

All capital P 's, Q 's, and Z 's in equations refer to vector quantities. A single subscript refers to a particular position. When two subscripts are used the first refers to position and the second to the particular harmonic in question:

A = area, in square feet; subscript referring to a particular point in the pipeline system;

a = velocity of propagation of the pressure wave, in feet per second;

B = subscript referring to stub or branch in the pipeline system;

D_1 = liner diameter for the pump analysis, in feet;

D_p = pipe diameter for the pipeline analysis, in feet;

d = piston-rod diameter, in feet;

E = subscript referring to equivalent parallel combination of branch and main-line impedances;

f = frequency, in cycles per second;

g = gravitation constant;

i = subscript referring to internal mechanism of pump;

$j^2 = -1$ (that is, j is complex operator $= \sqrt{-1}$);

l = length, in feet;

m = integer; subscript referring to main line;

n = exponent of U for mean flow;

P_{sub} = vectorial representation of standing wave-pressure amplitude, in pounds per square foot;

p = subscript referring to the equivalent impedance at the pump;

- \bar{p} = mean pressure causing mean flow in a finite length of line, in pounds per square foot;
 Q_o = volume current generated by the oscillating piston of the reciprocating pump, in cubic feet per second;
 Q_{sub} = vectorial representation of volume current or harmonic flow rate, in cubic feet per second;
 \bar{q} = mean rate of flow, in cubic feet per second;
 R = Reynolds number;
 r = subscript referring to the receiving end of the pipeline; radius of crank arm or eccentric of the crankshaft, in feet, or one-half of stroke;
 s = subscript referring to the sending end of the pipeline (usually at pump end); piston stroke ($2r$), in feet;
 t = time, in seconds;
 \bar{U} = mean velocity of fluid in the pipeline, in feet per second;
 v_p = piston velocity in a reciprocating pump, in feet per second;
 x = distance from receiving end or sending end, in feet; second subscript to denote existence of several harmonics;
 Y = statistical parameter, $P_{th} - P_{exp}$, theoretical or computed pressure minus experimental or measured pressure;
 Z_c = characteristic impedance of the pipeline, in pound-seconds per foot⁵;
 Z_{sub} = complex quotient of hydromotive pressure, P , and hydraulic volume current, Q , at any point in the system denoted by the subscript, in pound-seconds per foot⁵;
 α = attenuation constant, numeric per foot;
 β = phase constant, in radians per foot, or degrees per foot;
 γ = propagation constant, $\alpha + j\beta$;
 ρ = fluid density, in slugs per cubic foot;
 ϕ = phase angle of polar form of vectors (degrees); and
 ω = circular speed of rotating vectors; the angular velocity of the crankshaft, in radians per second.

DISCUSSION

HENRY M. PAYNTER,¹⁴ A.M. ASCE.—The paper shows vividly how far electrical-circuit concepts have penetrated into the field of pipeline engineering. The writer feels that he can lend considerable support to the authors' prognoses as he has been concerned with the application of mathematical models and

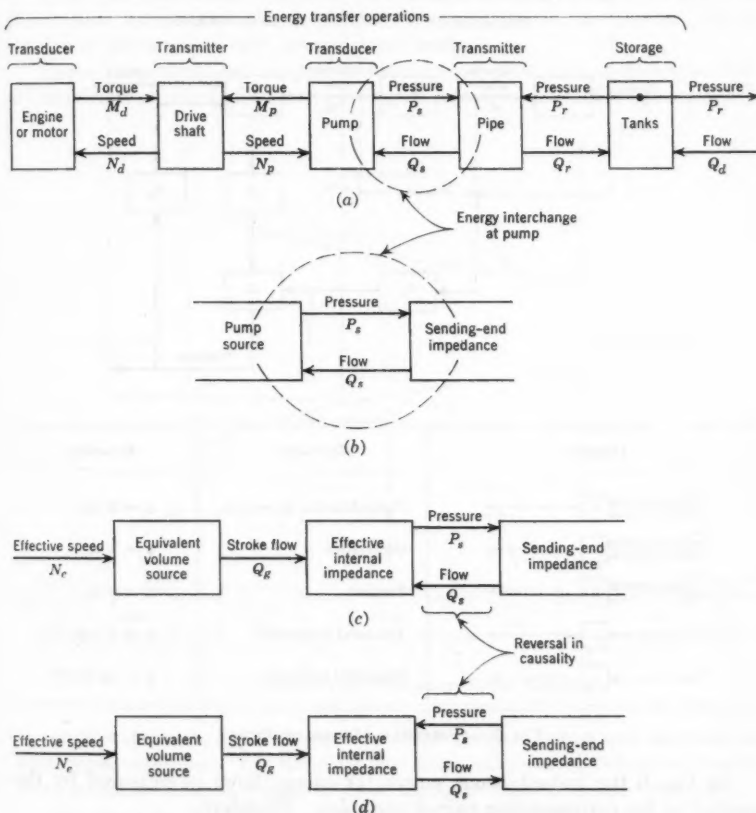


FIG. 6.—PUMPING-SYSTEM BLOCK DIAGRAMS

electronic computers to the rational analysis of complex engineering systems. This endeavor has embraced fluid systems encountered in pumping stations, pipelines, chemical processes, and hydroelectric plants.

In order to expedite the application of computing machinery to pipeline problems, it is advantageous to examine the paper in view of simplifications in

¹⁴ Asst. Prof. of Mech. Eng., Massachusetts Inst. of Technology, Cambridge, Mass.; Director, Am. Center for Analog Computing, Boston, Mass.

analysis and possible computer representations. Several publications that would be of help in this connection are available.^{15,16,17}

With respect to the schematic and circuit diagrams in Fig. 3, one may consider the block diagrams in Fig. 6. There is no longer a restriction to linearity in the analysis, and the same diagram can serve both for transient and steady-state behavior.

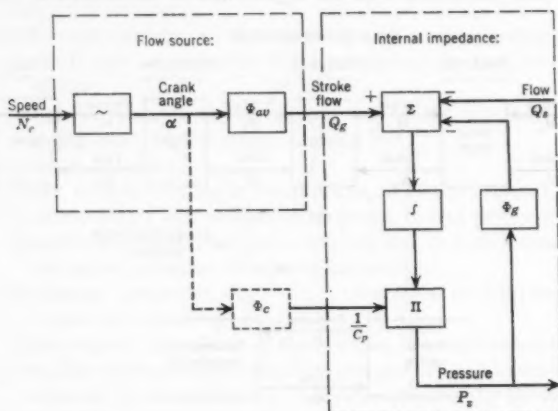


Diagram	Operation	Equation
x_h x_h x_h x_h x x	Static function generation Summation Product Temporal integration Sinusoidal oscillation	$y = \Phi(x_h)$ $y = \sum_k x_k$ $y = \prod_k x_k$ $y = \int x \, dt$ $y = \sin(2\pi x t)$

FIG. 7.—COMPUTER MODEL OF PUMP

In Fig. 6 the instantaneous power (or energy flow) is measured by the product of the corresponding pair of variables. Therefore,

Mechanical power input—

$$P_m = M(t) N(t) \dots \dots \dots (28)$$

¹⁵ "Surge and Water Hammer Problems," by H. M. Paynter, in "Electrical Analogies and Electronic Computers: A Symposium," *Transactions, ASCE*, Vol. 118, 1953, p. 962.

¹⁶ "A Palimpsest on the Electronic Analog Art," Ed. by H. M. Paynter, G. A. Philbrick Researches, Inc., Boston, Mass., 1955.

¹⁷ "Computer Representations of Engineering Systems Involving Fluid Transients," by F. D. Ezekiel and H. M. Paynter, *Transactions, A.S.M.E.*, November, 1957, pp. 1840-1850.

Sending-end fluid power—

$$P_s = P_s(t) Q_s(t) \dots \dots \dots (29)$$

Receiving-end fluid power—

$$P_r = P_r(t) Q_r(t) \dots \dots \dots (30)$$

Thus, the basic fluid transportation problem can be conceived in terms of three basic energy transfer operations—transduction in the pumps, transmission in the pipeline, and storage in the tanks.

These components can be represented for analysis and computation so that all significant physical phenomena are taken into account. It is not necessary

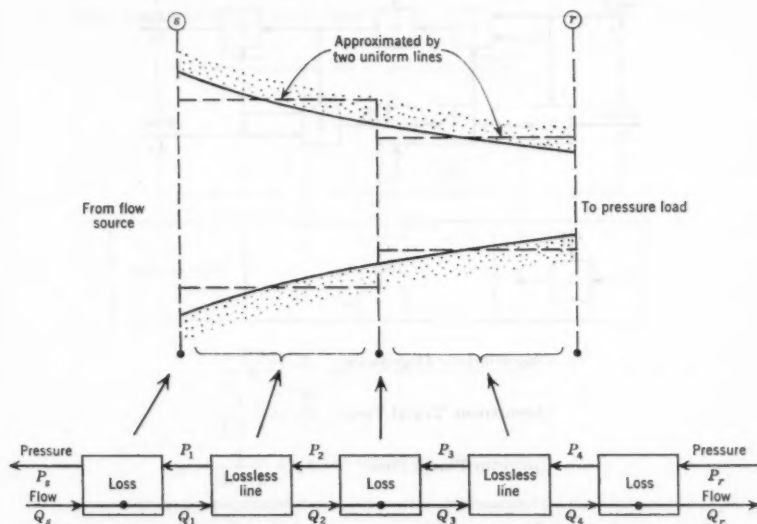


FIG. 8.—PIPELINE OF VARIABLE CROSS SECTION

to conduct elaborate experiments to establish the parameters and constants for such representations. For the most part these values can be obtained directly from mechanical fundamentals or from manufacturers' test and rating data.

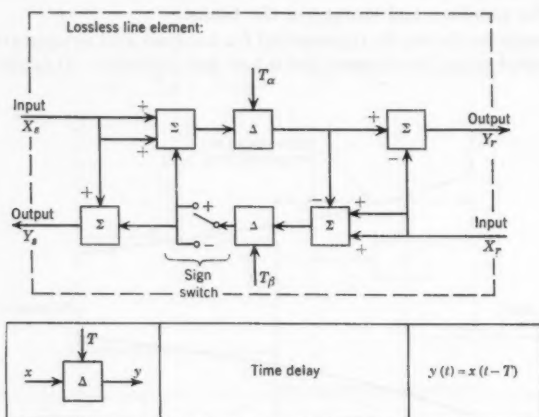
For example, in choosing to represent the reciprocating positive-displacement pumps as volumetric sources, as in Figs. 3(b), 3(c), 6(c), and 6(d), several physical facts must be considered:

1. The actual pump output cannot be independent of the connected prime-mover characteristics. Thus, for any given instantaneous flow, Q_s , as the pressure, P_s , changes, the torque, M_p , and the speed, N , must also change.
2. In the equivalent representation of the reciprocating pumps as volumetric sources delivering a nominal value of $Q_s(t)$ corresponding to a nominal constant

effective speed, $N_e(t)$, allowance must be made for the following known effects in the representation of the effective internal impedance, Z_i :

(a) Static operating characteristics—prime-mover torque versus speed relationship and pump pressure versus flow versus speed and torque versus flow versus speed relationships; and

(b) Dynamic impedances—drive-shaft elasticity, rotary mechanical inertia, fluid compressibility, and fluid inertia in pump passages.



$$\text{Characteristic Impedance: } Z_c = \frac{\rho a}{A}$$

$$\text{Downstream Travel Time: } T_\alpha = \frac{l}{a + \bar{U}}$$

$$\text{Upstream Travel Time: } T_\beta = \frac{l}{a - \bar{U}}$$

	CONFIGURATION		Sign switch	VARIABLES			
	Sending end	Receiving end		Inputs		Outputs	
				X_s	X_r	Y_s	Y_r
I	Admittance	Admittance	—	P_s	P_r	$Z_c Q_s$	$Z_c Q_r$
II	Admittance	Impedance	+	P_s	$Z_c Q_r$	$Z_c Q_s$	P_r
III	Impedance	Admittance	+	$Z_c Q_s$	P_r	P_s	$Z_c Q_r$
IV	Impedance	Impedance	—	$Z_c Q_s$	$Z_c Q_r$	P_s	P_r

FIG. 9.—COMPUTER MODEL OF LINE

3. Using straightforward mathematical, circuit, or block-diagram techniques, all these effects can be reduced and transferred to the fluid side and into an effective source internal impedance, Z_i , but only for the case of sufficiently small changes in variables that linearity in all elements can be assumed.

4. In the more general, and frequently more important, case of large non-linear changes, only a diagram such as Fig. 6(a) can predict results with any reliability.

The foregoing factors are important to avoid disappointments in future work and to correct the possible impression that experiments are mandatory before proceeding with computer studies for engineering design and operation.

Consider a possible computer representation corresponding to a block diagram such as that given in Fig. 6(c). This is indicated in Fig. 7, taking into account the following factors:

- a. Constant effective speed of the pump, N_e ;
- b. Nominal crank-angle-volume characteristic of pump, Φ_{av} ;
- c. Pump-leakage conductance characteristic, Φ_g ; and
- d. Pump mean effective capacitance, C_p .

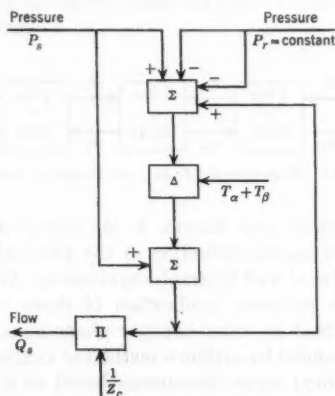


FIG. 10.—SENDING-END IMPEDANCE

In item *d* it may be desired to account for changes in the capacitance, C_p , as indicated. Definitions of the basic computing operations and more details are contained elsewhere.¹⁷ It is not necessary to compute the harmonics because they are generated automatically through Φ_{av} .

The second principal problem concerns the representation of the pipeline transmission elements. A practical solution for computing purposes has been presented.^{17,18} This solution is based on the assumption that any general variable section pipeline can be represented by a finite set of differing but uniform, nondissipating transmitters, each separated by grouped linear or nonlinear resistances in the form of friction joints. In practical instances only a few such sections are required for each pipe of the system, as indicated in Fig. 8. The full justification for such approximations has been presented.¹⁹

¹⁷ "Circuits and Block Diagrams: Dissipationless Transmission System," by F. D. Ezekiel and H. M. Paynter, *The Lightning Empiricist*, G. A. Philbrick Researches, Inc., Boston, Mass., October, 1956.

¹⁸ "Water Hammer in Nonuniform Pipes as an Example of Wave Propagation in Gradually Varying Media," by H. M. Paynter and F. D. Ezekiel, *Transactions, A.S.M.E.*, October, 1958, pp. 1585-1595.

The problem of representing a single length of frictionless pipe has been treated¹⁷ and is summarized in the universal block diagram of Fig. 9. For the flow of liquids, the travel times, T_a and T_b , for elastic waves upstream and downstream are essentially identical (that is, $T_a \cong T_b$). It should be noted that this is not generally true for gas flow in long pipelines.

In the special case of a single frictionless pipe terminating in a large tank or reservoir at constant pressure ($P_r = 0$), where the downstream flow, Q_r , is not required, the simplified diagram of Fig. 10 is applicable.

The pipeline design problem of interest to the authors can be studied on a computer representation of the type indicated in Fig. 11. This permits the determination of pressures and flows at two intermediate points in a pipeline. Design and operational problems can be studied on the same model because static and dynamic behavior are represented at the same time. The general philosophy underlying such approaches applied to all branches of engineering has been presented.²⁰

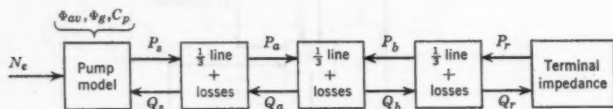


FIG. 11.—COMPUTER MODEL OF PUMPING SYSTEM

ROBERT D. KERSTEN²¹ AND EDWIN J. WALLER,²² ASSOCIATE MEMBERS, ASCE.—The lucid and logical deduction of the physical concepts of the dynamic analogy of electrical and hydraulic systems by Mr. Paynter¹⁵ has long been recognized. The principal application of these concepts has been to transient phenomena (that is, water-hammer phenomena).

However, it was intended to outline a method of analysis of the steady-state (periodic forced vibratory) surge phenomena based on a fundamental mathematical approach. The results of this analysis were recognized as being mathematically identical with the electric-wave equations for the alternating current transmission line. Thus, the circuit-analysis techniques, already well developed by electrical engineers, could be applied directly to pipeline-engineering problems. A mathematical proof supports the prior logical reasoning regarding the hydraulic-electrical analogy.

The details of the mathematical derivation have been presented elsewhere.^{23,24} The purpose of the paper was to demonstrate the validity of the theoretical solution through application to an actual field-scale pumping pipeline system. The experiments cited by the writers were designed to evaluate quantitatively the response of the pipeline system rather than leave this response as a symbol in a casual block diagram such as in Figs. 6 to 11. Such diagrams

²⁰ "Generalizing the Concepts of Power Transport and Energy Ports for Systems Engineering," by H. M. Paynter, *Paper No. 58-A-296*, A.S.M.E., December, 1958.

²¹ Asst. Prof., Dept. of Civ. Eng., Arizona State College, Tempe, Ariz.

²² Associate Prof., Dept. of Civ. Eng., College of Eng., Oklahoma State Univ., Stillwater, Okla.

²³ "Fundamental Analysis of Unsteady Pressure Variations in Pipeline Systems," by Edwin J. Waller, *Publication No. 52*, Oklahoma Eng. Experiment Station, Oklahoma State Univ., Stillwater, May, 1954.

²⁴ "Pressure Surges in Pipelines," by Edwin J. Waller, *Paper No. 57-Pet16*, A.S.M.E., September, 1957.

are quite informative, and the operations indicated by them can be performed only when the correct electrical impedances are placed in the analog computer. This can only be done after certain quantitative experiments are conducted on models or prototypes. Prior work included model studies. The results of experiments for the response of the prototype were listed in the paper. As a result of these experiments, the simplifying assumptions made in the solution of the differential equations have been verified. In addition, the applicability of the fundamental principles to a field-scale reciprocating pump has been shown.

Electronic-computer techniques can be applied with confidence. It is recognized that experimental work is not a prerequisite to computer studies. However, as in any realistic research and development program, prototype verification as opposed to model studies (including analogs) must be undertaken. That this has been done at this stage of the program indicates that the value of any analog or digital computer studies, past, present, or future, has been greatly enhanced.

AMERICAN SOCIETY OF CIVIL ENGINEERS

Founded November 5, 1852

TRANSACTIONS

Paper No. 2978

WATER SUPPLY VERSUS IRRIGATION IN HUMID AREAS

BY MARION C. BOYER,¹ M. ASCE

SYNOPSIS

Water is required for urban waste removal, fire protection, industrial processes, and agriculture (for which natural precipitation is un dependable). For maximum beneficial use, watershed inventories are necessary, so that present and future needs can be determined and such use can be recommended. An inventory of the White River Basin, Indiana, is described herein.

INTRODUCTION

Without abundant quantities of water, modern civilization could not exist for long. Water removes the waste from households, provides fire protection, is required in volume in many industrial processes, and compensates for the moisture deficiencies for growing crops in regions in which natural precipitation does not sustain plant growth.

The installation of sewer systems for the removal of household wastes probably received its greatest impetus with the advent of the water closet, once described as the most useful invention of western civilization. Since that time household use of water has increased rapidly. In recent years it has augmented as modern bathing facilities, automatic washers for clothes and dishes, and grinders for the disposal of garbage through the sewer system have been installed.

For many years water has been used to extinguish fires. Prior to the end of the nineteenth century, the quantity that could be utilized was dependent on the efficiency of bucket brigades or on the gravity pressure in supply mains. During the first part of the twentieth century efficient, mobile pumping apparatus has been developed. This equipment is capable of drawing much greater quantities from the water mains than the mains could deliver under their own normal pressure. Also, the water can be ejected much farther from

NOTE.—Published, essentially as printed here, in January, 1958, in the *Journal of the Irrigation and Drainage Division*, as *Proceedings Paper 1500*. Positions and titles given are those in effect when the paper was approved for publication in *Transactions*.

¹ Hydr. Engr., Indiana Flood Control and Water Resources Comm., Indianapolis, Ind.

the nozzles. Such apparatus, when converging on a major fire in quantity, places extensive demands on the water supply.

Many industrial processes require huge volumes of water for the cooling, washing, and treatment of products. In general, little of this water is consumed. Most of it is returned to stream or lakes at a higher temperature or containing contaminants.

The production of crops through irrigation is one of the early uses for water. In India canals built before the Christian era still convey water to arid regions of the Punjab. Many years before Christopher Columbus, highly civilized inhabitants of the Andes Mountains in South America transformed barren areas into crop-producing fields by terracing, fertilizing, and irrigating. Many of these all but imperishable hanging gardens are cultivated presently by descendants of the ancient Incas. Irrigation began nearly as early in the southwestern United States and still is an essential part of American life in the west.

With the advent of lightweight pipe and small, efficient engine-driven pumps, the use of water for irrigation has increased rapidly in humid regions. In these areas crops will grow unwatered during most years, but will produce much more bountifully when watered artificially during droughts. The use of water for irrigation during dry spells and its effect on the supplies for other needs must be evaluated and regulated in order to obtain the greatest benefit from the basin supplies.

CURRENT WATER USE

Municipal Water Supply.—Cities and towns require enough potable water to meet the needs of domestic uses, waste disposal, fire protection, and urban industries. Heavy demands are placed on national water resources. In 1953 there were approximately 16,000 public water-supply systems in the United States, serving 106,000,000 people.² Of these systems, 552 served cities with a population of 25,000, or more, and supplied the needs of nearly 80,000,000. The average output of the 16,000 systems was 11,800,000,000 gal per day. This volume is equivalent to an average use of 148 gal per person per day, as compared with from 140 gal per person per day to 150 gal per person per day in 1945 for cities with a population of 10,000 and more.³

Municipal Waste Disposal.—A considerable part of the water that a city receives in its supply mains is discharged as waste through the sewer system. In fact, in many cities infiltration and the intrusion of storm water, accidental or otherwise, produce a sewer outflow greater than the intake of potable water. This sewage is treated for the removal of solids and the reduction of the biochemical oxygen demand. Then it is released to a lake, watercourse, or the ocean, to be removed from the vicinity and rendered innocuous by the action of dissolved oxygen and sunlight.

In spite of the deleterious effects of wastes discharging into natural waters, not all cities and industries provide adequate treatment and several provide

² *Statistical Abstract of the United States*, 77th Annual Edition, Bureau of the Census, U. S. Dept. of Commerce, Washington, D. C., 1956, p. 163.

³ "A Water Policy for the American People," *Report of the President's Water Policy Commission*, U. S. Govt. Printing Office, Washington, D. C., 1950, p. 177.

none. Of 11,130 municipal sewer systems in operation in 1958 (compared with approximately 16,000 waterworks), only 8,000 discharge through a treatment plant. Nearly two-thirds of the population is served with public water supplies. One-half is served with sewage-collection facilities, but only one-third is served with sewage-treatment plants.⁴

Steam-Electric Power Generation.—Steam-electric power generation is one of the greatest industrial users of water. As designed at present (1959) plants remove by condenser cooling 5,000 Btu of heat from spent steam for each kilowatt-hour of electric generation. The quantity of cooling water required depends on the efficiency of the condensers and on the permissible increase in cooling-water temperatures. The volume varies but averages approximately 1,000 sec-ft for a plant having a rated capacity of 1,000,000 kw and operating at normal load.

In 1955 the total capacity of all electric generating stations operated for public use in the United States was approximately 114,000,000 kw. The stations produced 546,000,000,000 kw-hr during the same year.⁵ In 1945 by contrast the installed capacity was 50,000,000 kw and the production, 222,000,000,000 kw-hr.

Other Industries.—There are many diverse industries dependent on the water resources of the United States. Their needs are varied, but their consumptive uses are generally low. Nearly all the water is discharged to the ocean, lakes, or streams, except that ground water pumped for cooling is returned to the ground in some instances. Almost all industrial wastes are polluted to a certain degree or warmed. Additional water must be provided to remove the wastes in the same manner as sewage is removed. Although accurate data on industrial water needs are lacking, it is estimated that industries other than electric generation require approximately 10,000,000,000 gal per day.

Agriculture.—Water for crop irrigation is used primarily in the west, where few crops could be produced without it. Irrigation in the humid regions is not essential. However, because of its decidedly beneficial effects, primarily during periods of deficient rainfall, irrigation is being practiced more widely in these areas each year. In 1954 the estimated total acreage under irrigation in the United States was 29,500,000 acres, of which 20,500,000 acres were in the west. The remaining 9,000,000 acres were in the humid eastern regions.⁶ In 1939 the land being irrigated in the humid regions was 2,300,000 acres. The increase from 1939 to 1954 was 450,000 acres per yr, indicating the importance of irrigation in those regions in which natural precipitation suffices to produce a crop.

The regional growth rate of irrigation in humid areas is amply demonstrated by studies⁷ made at Purdue University at Lafayette, Ind., which show that:

⁴ "A Water Policy for the American People," *Report of the President's Water Policy Commission*, U. S. Govt. Printing Office, Washington, D. C., 1950, p. 189.

⁵ *Statistical Abstract of the United States*, 77th Annual Edition, Bureau of the Census, U. S. Dept. of Commerce, Washington, D. C., 1956, p. 528.

⁶ *Ibid.*, p. 605.

⁷ "Water Demand Potential of Irrigation in Humid Areas," by John R. Davis, *Report to Indiana Water Resources Study Committee*, Purdue Univ., Lafayette, Ind., 1956.

"From 1940 to 1950, the number of irrigated farms in humid areas increased 75 per cent, and the number of acres irrigated increased about 283 per cent—most of this increase occurring from 1946 to 1950. A survey in Virginia indicated that irrigated farmland increased 700 per cent from 1949 to 1954. Data from Tennessee indicated an increase of at least 2100 per cent from 1949 to 1954. Even in Iowa, which is usually confronted with drainage problems, the number of farmers using irrigation increased from 76 to 136 from 1949 to 1954. Farmers irrigating in Illinois increased from 139 to 266 from 1951 to 1954. In all humid states, irrigation on farms has increased about 70 per cent between 1949 and 1954. Sprinkler irrigation is well established also in Canada, where some 3,500 systems were installed up to 1951.

"Thus, even though irrigation is an infant farming practice, and the percent of lands irrigated is quite small; its growth has been phenomenal. It is this growth, and its potential use of water, that is disturbing to other water users."

FUTURE WATER USE

Trends in Population Growth.—A rising birth rate and the continuing elevation of the average age of death are reasons for the rapid growth of the population of the United States. Most of this increasing population is settling in urban areas and in contiguous suburban developments. In 1956 there were approximately 168,000,000 people in the United States. It is estimated⁸ that in 1975 there will be 210,000,000 and at the end of the century, 275,000,000.

Trends in Industrial Growth.—The growth in population, coupled with rapidly rising general prosperity, is triggering an immense expansion in the industrial complex. People must be clothed, fed, housed, transported, and amused. A principal water-using industry keeping pace with this growth is that for producing electric power. Three methods of power generation are available—falling water, the burning of fossil fuels, and the release of atomic energy. Great quantities of water are required no matter what method is used. Through using fossil fuels, atomic fission, or atomic fusion, power generation differs only in the nature of the fuel. The energy still is released to a conveying medium, such as steam, gaseous sodium, mercury vapor, or similar elements, which is used to whirl turbine rotors. The exhausted vapors are cooled to liquids, which will be used again. Such conversion requires great quantities of water to remove the residual heat.

Based on data from several sources, studies by the Indiana Flood Control and Water Resources Commission⁸ indicate that by 1980 the capacity of all utility systems in the United States will be 380,000,000 kw and that by 2000 their capacity will be 675,000,000 kw, as compared with 114,000,000 kw in 1955. Fig. 1 shows the energy production and capacity of electric-utility systems in the United States from 1920 to 1955 as well as estimated values to the year 2000.

Other industries will expand in a similar manner. An upsurge of chemical plants requiring large quantities of water is expected. Wood-pulp producing and processing industries already utilize the hardwoods of the central states

⁸ "Report of Investigation, Monroe Reservoir," Indiana Flood Control and Water Resources Comm., Indianapolis, Ind., 1956, p. 47

and produce wastes that add tastes and odors to the streams into which they are discharged. Steel mills use great quantities of water in cooling and washing their products. The foregoing serves to emphasize the enormous future increase in water requirements throughout the industrial regions of the country.

Trends in Irrigation in Humid Regions.—Irrigation procedures in humid regions differ markedly from those in arid regions. In the latter areas summer precipitation is never sufficient for crop growth, and the farmers must depend on water taken from streams, whose sources are the melting snows, ground-water outflows of distant mountain watersheds, or stored ground waters in the earth beneath the farms. Irrigation water requirements remain almost con-

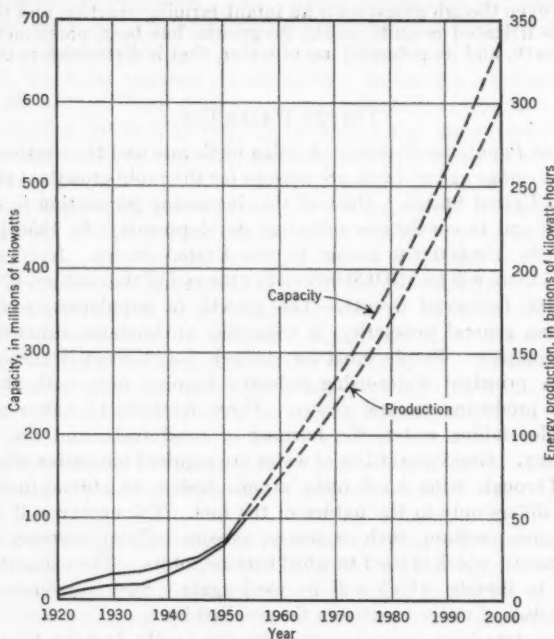


FIG. 1.—CAPACITY AND PRODUCTION OF ELECTRIC-UTILITY SYSTEMS IN THE UNITED STATES

stant from year to year. Therefore, projects can schedule water use on a rotation basis, so that diversions to many farms can be held practically constant throughout the season.

During nearly every summer the rainfall in humid regions is sufficient to produce crops. In some years, because of deficient or improperly distributed precipitation, crops suffer from lack of moisture and partial failures result. It is the humid-region irrigator's intent to add water during protracted dry spells so that the crops can be carried over from one period of rainfall to the next. Such a procedure not only insures that a crop will mature, but by main-

taining the moisture content in the soil at an optimum level a much greater yield can be extracted from the fields than if only nature were depended on to supply the soil moisture.

Because droughts usually occur at the same time over extensive regions, many farmers may decide to irrigate their crops simultaneously. The outcome can only mean that the streams and possibly the ground waters from which the irrigation supplies are taken will be seriously depleted, to the detriment of other users, such as municipalities and industries, who depend on them. For this reason serious consideration must be given to making hydrologic and water-resources analyses of humid-region watersheds, in order that the water they yield is put to the most beneficial use.

NEED FOR WATER-RESOURCES INVENTORY

With reference to irrigation in humid areas, the following question inevitably arises: Will there be enough water to go around? The answer can only be determined by a careful water-resources inventory of each watershed within which there is a possibility of inadequate supply.

A water-resources inventory of a basin should determine the following factors regarding supply: (1) The magnitude and distribution of runoff at critical sections (at the water-supply intakes to, and points of return of, sewage effluent from municipalities and industries within the basin area); (2) the manner in which the runoff distribution could be modified by the development of water-storage sites; and (3) an evaluation of the potentialities of ground-water reservoirs as alternates or supplements to surface water-supply sources.

The following facts concerning water demand should be included in the inventory: (a) Present and estimated future water-supply needs and sewage-disposal needs of municipalities and industries using the waters of the basin, and (b) the acreage of lands within the watershed that might be irrigated economically by the withdrawal of water from surface or underground sources and water required.

Finally, the supply should be compared with the demand and recommendations made as to obtaining the most efficient and beneficial use of the waters in the basin.

Water-supply inventories of different basins will produce different results. Some watersheds have large, shallow, ground-water storage reservoirs that feed to the streams during droughts and maintain substantial low flows. Other basins have highly favorable reservoir sites, permitting the retention of flood flows for release during periods of drought. Some watersheds lack one or both these advantages and may be difficult or impossible to develop as water-supply sources. Each basin needs to be developed on its own merits.

AN INVENTORY OF THE UPPER WHITE RIVER BASIN, INDIANA

Description.—Indiana is typical of the humid-region states with respect to both location and water needs. The upper White River watershed, northeast of Martinsville in the east-central section of the state, is a typical basin for which a water-resources inventory is essential. Within this basin area are

Indianapolis, the largest city in the state (population, 460,000), and two important industrial centers, Muncie (population, 60,000) and Anderson (population, 47,000). There are four steam-electric generating stations that depend on the river for cooling water. These stations are in Noblesville (100,000 kw), in Indianapolis (46,000 kw), at the south edge of Indianapolis (160,000 kw), and in Centerton, thirty miles downstream from Indianapolis (376,000 kw).

As far as future water requirements are concerned, the most critical section of the river is at Indianapolis. An adequate water supply for the city is available from the White River. The low flow of this river is bolstered by storage releases from two reservoirs constructed by a municipal water company on tributaries a short distance upstream. However, the supply of dilution

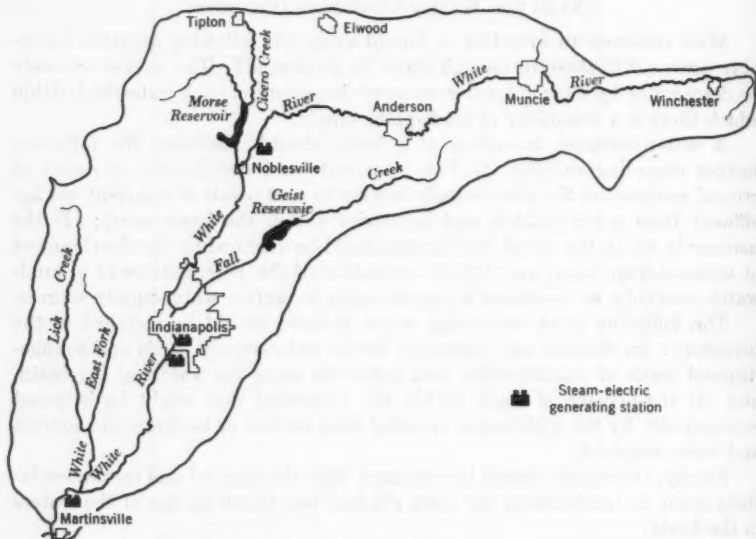


FIG. 2.—UPPER WHITE RIVER BASIN, INDIANA

water for the treated sewage effluent is not dependable and is inadequate at times. If the city continues to grow at its present rate, this will be the major water-supply problem. Lack of cooling water will also inhibit the expansion of the steam-electric generating stations, which have extensive cooling-tower installations to provide for condenser cooling during low river flows.

The upper White River watershed (Fig. 2), which drains a 1,200-sq-mile area northeast of the Indianapolis water-supply intake and a 2,485-sq-mile area northeast of Martinsville, is a region of low rolling hills, consisting principally of the debris deposited by the Illinois and Wisconsin glaciers. The topography of the basin is such that only a few low-capacity storage sites are available.

Modification of Runoff by Surface Storage.—The runoff from the White River watershed northeast of Indianapolis can be modified only slightly by the construction of storage reservoirs. Only a few small sites are available. Two have been developed, with a combined equivalent capacity of 0.52 in. of runoff from 1,200 sq miles. Further development of reservoir sites may increase the storage capacity to 1 in., but more than that volume appears unlikely.

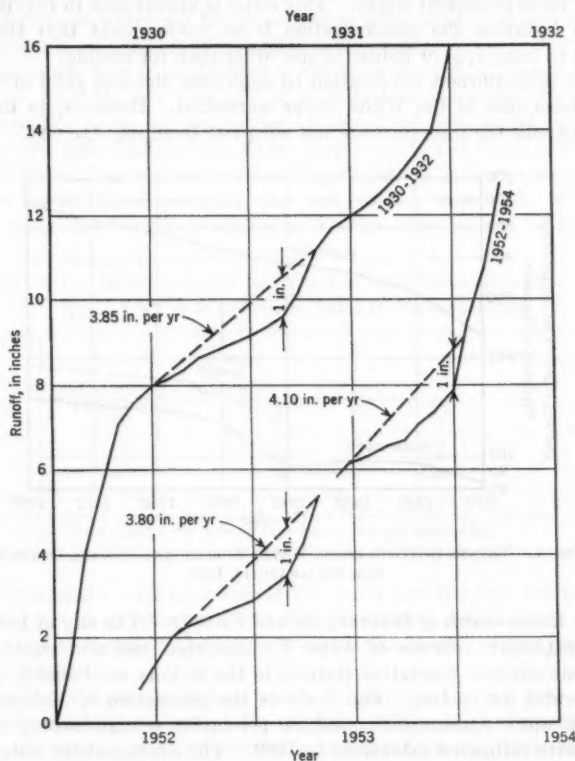


FIG. 3.—RUNOFF AND YIELD FOR 1-IN. STORAGE, WHITE RIVER AT INDIANAPOLIS, IND.

Fig. 3 shows the cumulative runoff, in inches, from the watershed during two dry periods, from 1930 to 1932 and from 1952 to 1954. Assuming an available storage of 1 in., the sustained yield from the watershed north of Indianapolis would be at the rate of approximately 3.9 in. per yr, or 350 sec-ft. Under the existing conditions of developed storage of 0.52 in., the rate would be 3.1 in. per yr, or 280 sec-ft.

Ground-Water Potentialities.—Sizable quantities of ground water are contained in the glacial debris left as a thin mantle over the basin. This water is found at shallow depths and is recovered easily by pumping. It is replenished to a large extent from the streams during high water and is discharged into them during droughts. The removal of the water would have some effect on streamflow.

Large quantities of ground water are also found in the underlying sedimentary rocks of ancient origin. This water is mineralized to varying degrees. In some instances the mineralization is so predominant that the water is unsuited to municipal or industrial use other than for cooling.

There is insufficient information to determine the safe yield of the underground reservoirs of the White River watershed. However, in the vicinity of Indianapolis the reservoirs are not adequate to supply the city.

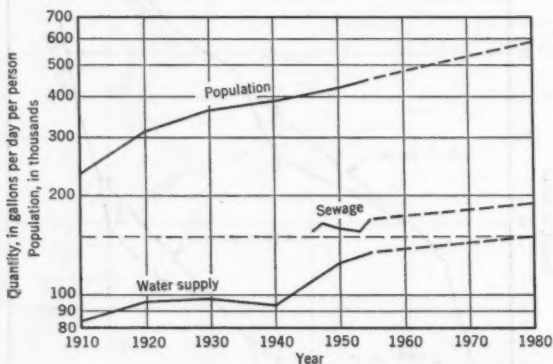


FIG. 4.—TRENDS IN POPULATION, WATER SUPPLY, AND SEWAGE OUTFLOW FOR INDIANAPOLIS, IND.

Water Requirements of Indianapolis and Vicinity.—The city of Indianapolis requires extensive volumes of water for municipal use and waste disposal. Three steam-electric generating stations in the vicinity need sizable quantities of river water for cooling. Fig. 4 shows the population of Indianapolis, its per-capita water consumption, and its per-capita sewage outflow from 1920 to 1955, with estimated extensions to 1980. The average daily water requirement for 1958 was 63,000,000 gal. The estimated requirement for 1980 is 89,000,000 gal. In addition to supplying the city, the municipal water company provides raw water through a diversion canal for certain industries within the city. The minimum measured flow is 83.7 sec-ft, approximately 54,000,000 gal per day. This volume is returned to the river upstream from the point of discharge of the city's sewage effluent.

The sewer system of Indianapolis collects a flow that is approximately 25% greater than the water supply. In 1958 the sewage passing through the treatment plant averaged 96,000,000 gal per day. The estimated flow for 1980 is 112,000,000 gal per day. The minimum flow available in the White River

upstream from the point of discharge of sewage effluent from the city should not be less than the sewage-outflow rate. This degree of dilution presupposes a highly efficient treatment of the sewage before it is released to the stream.

Relationship of Water Supply to Demand.—An interesting problem arises when relating water supply to demand at Indianapolis. Two privately owned reservoirs upstream from the city are operated primarily to provide adequate flow for the city water supply. Although these installations are capable of bolstering natural flow to a minimum of 280 sec-ft at the diversion works, it is unlikely that more water will be released than is required to supply city needs plus whatever is sold to industries utilizing raw water.

If a minimum flow is established in the river through Indianapolis that is sufficient to meet the requirements of an industrial raw-water diversion and to maintain the river, approximately 137 sec-ft of flow would be required. Table 1 shows 1958 Indianapolis water-supply needs and those of the future.

Future Water Use in Basin.—The foregoing study indicates that although the water supply to Indianapolis may not become inadequate within forty years or more, the supply available for sewage disposal will be insufficient.

TABLE 1.—RELATIONSHIP BETWEEN WATER REQUIREMENTS AND SUPPLY AT INDIANAPOLIS, IND., IN SECOND-FEET

Year (1)	WATER SUPPLY		SEWAGE DISPOSAL	
	Requirement (2)	Safe yield ^a (3)	Outflow (4)	River flow (5)
1958	98	143	150	137
1980	134	213	168	137
2000	180 ^b	213	226 ^b	137

^a Safe yield by operation of two reservoirs, less 137-sec-ft flow through city, with third reservoir before 1980. ^b Estimated by exponential extension of time-versus-demand relationship.

Even maintaining a minimum flow of 137 sec-ft past the city will not provide sufficient water at all times to dilute the effluent on a 1-to-1 basis. Any consumptive use of water in the upper White River Basin would aggravate this condition further.

Downstream from Centerton, where industry makes the final use of the river, water could be removed for irrigation without affecting users of the stream. However, any consumptive use of water from the White River would reduce the flow in the Ohio River below its mouth and in the Mississippi River below the Ohio River. Even though the volume is small, if there is widespread irrigation throughout the region both the Ohio River and the Mississippi River could be affected materially. Thus, the pollution problem would be aggravated in the former river, and the cost of low-water navigation would be increased in the latter.

CONCLUSIONS

Civilization places such demands on the waters of the United States that careful water-resources inventories become essential. In many watersheds

municipal and industrial needs are rapidly approaching the available supply. In such areas consumptive use by irrigation could seriously curtail municipal and industrial growth. For example, the foregoing applies to the upper White River Basin in east-central Indiana. By careful planning and by constructing two water-supply reservoirs, adequate water for Indianapolis is assured for several decades. However, inadequate streamflow at the point of discharge of sewage effluent promises to create a biologic desert in the river for a considerable distance south of Indianapolis. The flow is insufficient to provide satisfactory condenser cooling at the three power stations at and south of the city, and expensive cooling towers must be used.

AMERICAN SOCIETY OF CIVIL ENGINEERS

Founded November 5, 1852

TRANSACTIONS

Paper No. 2979

VIBRATION OF SIMPLE-SPAN HIGHWAY BRIDGES

BY JOHN M. BIGGS,¹ A. M. ASCE, HERBERT S. SUER,²
J. M. ASCE, AND JACOBUS M. LOUW³

SYNOPSIS

An analytical method is developed for predicting the magnitude and character of highway-bridge vibration due to the passage of heavy vehicles. The accuracy of the method of analysis and the validity of the assumptions presented are investigated by comparison with laboratory tests on model bridges. Tests of actual structures are used to prove the applicability of the method to field conditions and to indicate those conditions that should be assumed for design. Theoretical results obtained by both analog computers and digital computers show the effects of the various parameters. Finally, the problem is reduced to its simplest form, and charts are provided to predict maximum dynamic deflections. Only simple-span girder bridges and stringer bridges loaded by single two-axle vehicles are studied.

INTRODUCTION

There is little available information on highway-bridge vibration. Previous theoretical developments^{4,5} either were directed toward railway-bridge vibration or did not consider the actual field conditions. An attempt is made herein to bridge the gap between theory and field-test results. The latter are useful as check points for the theory, but by themselves cannot provide a solution to the problem.

NOTE.—Published, essentially as printed here, in March, 1957, in the Journal of the Structural Division, as *Proceedings Paper 1186*. Positions and titles given are those in effect when the paper was approved for publication in *Transactions*.

¹ Associate Prof. of Structural Eng., Massachusetts Inst. of Technology, Cambridge, Mass.

² Senior Structural Research Engr., North American Aviation, Inc., Downey, Calif.; formerly Research Asst., Massachusetts Inst. of Technology, Cambridge, Mass.

³ Research Asst., Massachusetts Inst. of Technology, Cambridge, Mass.

⁴ "A Mathematical Treatise on Vibration in Railway Bridges," by C. E. Inglis, Cambridge Univ. Press, London, 1934.

⁵ "Dynamic Influences of Smoothly Running Loads on Simply Supported Girders," by A. Hillerborg, Inst. of Structural Eng. and Bridge Building, Royal Inst. of Technology, Stockholm, 1951.

Earlier field tests by the writers⁶ lead to certain conclusions, the most important of which was that the major factor influencing the amplitude of vibration is the vertical oscillation of the vehicle on its own springs as it approaches the span. Although the magnitude of this oscillation depends on the roughness of the approach roadway, this factor is of primary importance even on surfaces normally considered "smooth." Except in extreme cases the condition of the surface on the bridge itself is less important and merely augments the initial oscillation of the vehicle.

This conclusion indicates that the dynamic behavior of the vehicle is a primary consideration in the study of bridge vibration. Therefore, the laboratory and field tests reported herein involve dynamic measurements on both bridge and vehicle. The subsequent theoretical development takes into account the dynamic characteristics of the vehicle as well as those of the bridge.

THEORETICAL ANALYSIS

Notation.—The letter symbols adopted for use in this paper are defined where they first appear, in the illustrations or in the text, and are arranged alphabetically, for convenience of reference, in the Appendix.

General.—The analysis is not a new theoretical development but a simplification of previously derived theory. The manner in which it is presented is intended to convey a clear physical concept of the behavior. The basic equations derived are essentially a simplified form of those used by C. E. Inglis, A. Hillerborg, and other investigators.⁷

It is believed that the form of the equations given permits solution by the simplest possible computational methods. The equations are not theoretically exact but are sufficiently accurate to predict bridge vibrations for practical purposes. This is particularly true because the dynamic loading conditions for an actual structure can never be predicted accurately.

The method of analysis is based on the following simplifications and assumptions:

1. Only the first mode of vibration is considered, and the bridge is represented as a simple beam. Thus, the bridge can be replaced by a single-degree-of-freedom system. The error resulting from this simplification is not serious if only the dynamic deflection at midspan is considered.
2. The vehicle is assumed to have only one degree of freedom. Actually, a two-axle vehicle has many degrees of freedom because the mass is usually supported on four springs and on four or more flexible tires. However, it is believed that the important vehicle motion with respect to bridge vibration occurs when all these elements act in phase.
3. The entire weight of the vehicle is assumed to be at the center of gravity of the vehicle mass. The effect of the two axles could be considered in the subsequent procedure, but this appears unnecessary.
4. Viscous damping is assumed in both bridge and vehicle.

⁶ "Vibration Measurements on Five Simple Span Bridges," by J. M. Biggs and H. S. Suer, *Bulletin No. 124*, Highway Research Board, National Research Council, Washington, D. C., 1956.

⁷ "Highway-Bridge Impact Problems," by T. P. Tung, L. E. Goodman, T. Y. Chen, and N. M. Newmark, *ibid.*

Based on these assumptions the system is simplified to that shown in Fig. 1, in which V is the velocity of the vehicle; L represents the span of the bridge; y_c denotes the midspan deflection at any time; x signifies the distance of the vehicle from the end of the span; and ω is the crossing frequency ($\pi V/L$). At time $t = 0$, the center of gravity of the vehicle is at the end of the span. Because it is assumed that the deflected shape is sinusoidal at all times, the bridge deflection beneath the vehicle is $y_c \sin(\omega t)$.

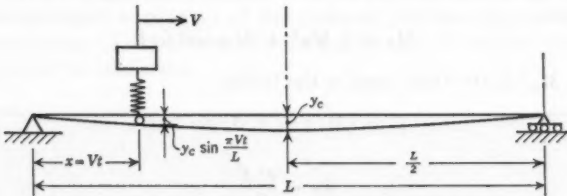


FIG. 1.—IDEALIZED DYNAMIC SYSTEM

The vehicle is represented by the single-degree system shown in Fig. 2, in which M_{vs} is the sprung mass of the vehicle; M_{vu} represents the unsprung mass of the vehicle; k_v denotes the spring constant of the vehicle suspension system;

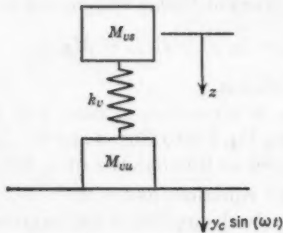


FIG. 2.—IDEALIZED VEHICLE

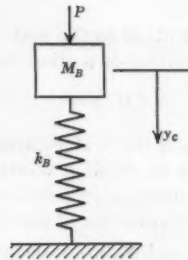


FIG. 3.—IDEALIZED BRIDGE

and z signifies the absolute deflection of the sprung vehicle mass measured from the neutral position. The distortion of the vehicle spring is given by

$$z - y_c \sin(\omega t) = \Delta \dots \dots \dots (1)$$

The force, F , in the spring is

$$F = k_v \Delta + M_{vs} g \dots \dots \dots (2)$$

Thus, the equation of motion for the sprung mass is

$$-k_v \Delta - c_v \dot{\Delta} = M_{vs} \ddot{z} \dots \dots \dots (3)$$

in which c_v is the damping coefficient. A single dot over any symbol indicates the first derivative with respect to t , and two dots indicate the second derivative with respect to t .

A typical vehicle actually has no unsprung mass because the tires behave as springs. The term is included in order to compare the theory with the model results.

The bridge can be represented by the single-degree system shown in Fig. 3, in which P , M_B , and k_B are the load, mass, and spring stiffness, respectively, of the equivalent system. The deflection of the equivalent mass is taken to be the same as the actual midspan deflection of the bridge. Considering only the first mode of vibration, it can be shown that the parameters of the equivalent system are

$$M_B = \frac{1}{2} M_B^T + M_{\text{rw}} \sin^2(\omega t) \dots \dots \dots (4)$$

in which M_B^T is the total mass of the bridge,

$$P = (M_v g + k_v \Delta) \sin(\omega t) \dots \dots \dots (5)$$

and

$$k_B = \frac{\pi^4 E I}{2 L^3} \dots \dots \dots (6)$$

in which $E I$ is the rigidity of the actual bridge. The fundamental natural frequency, p_B , of the equivalent system when the vehicle is not on the span is

$$p_B = \sqrt{\frac{k_B}{M_B}} = \sqrt{\frac{\pi^4 E I}{M_B^T L^3}} \dots \dots \dots (7)$$

which is identical to the first mode of the actual structure.

The equation of motion for the equivalent bridge system can be written as

$$(M_v g + k_v \Delta) \sin(\omega t) - k_B y_c - c_B \dot{y}_c = M_B \ddot{y}_c \dots \dots \dots (8)$$

in which c_B is the bridge-damping coefficient.

In order to obtain a solution for y_c as a function of time, Eqs. 3 and 8 are solved simultaneously after substituting Eq. 1 into Eqs. 3 and 8. To take into account the vibration of the vehicle itself as it enters the span, the initial conditions, Δ_0 and $\dot{\Delta}_0$, are inserted into the equations at $t = 0$.

Because Eqs. 3 and 8 cannot be solved directly in any convenient form, approximate methods of solution must be used. One such method, numerical integration, is a common device in solving dynamic problems and produces a continuous deflection record during the entire crossing. If hand computation is used, numerical integration is laborious and impractical unless a limited quantity of solutions is desired. However, it is easily handled by a digital computer, and the final theoretical results were obtained in that manner.

Solutions can also be obtained by an analog computer. This device is not as accurate as numerical integration, but it is more convenient for qualitative investigations of the effect of parameter variation. This procedure was used to obtain some of the results presented subsequently.

MODEL STUDIES

General.—Before attempting to confirm the theoretical analysis by field tests on actual structures, small-scale laboratory tests were conducted to check

the accuracy of the theoretical solution under carefully controlled conditions.⁸ The basic mathematical assumptions of the method were investigated without the uncertain conditions always present in actual field tests.

Tests were made on a single bridge model consisting of a simple beam with weights hung uniformly to provide mass. The model was designed to represent a typical two-lane girder bridge with a span of approximately 90 ft. The natural frequency and the static deflection of the model are the same as for the prototype. The vehicle model simulated a 20-ton, two-axle truck. Simultaneous measurements were taken of the midspan deflection and of the force in the vehicle spring. Tests were made, varying the vehicle velocity, frequency, damping, and initial oscillation.

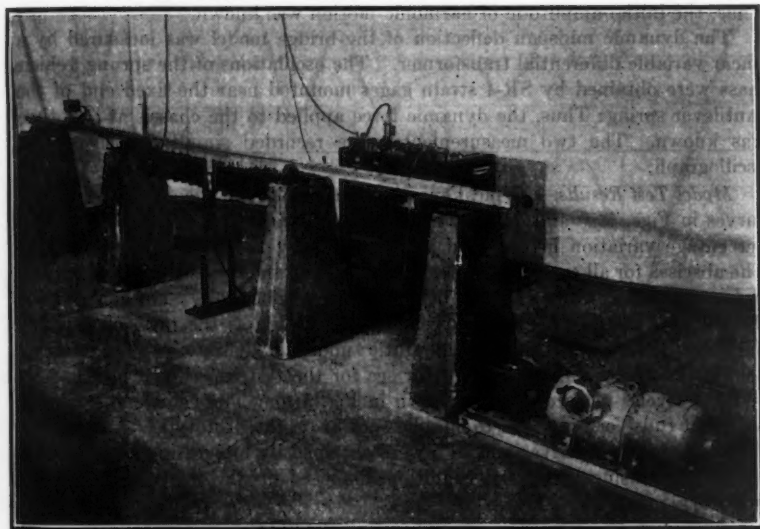


Fig. 4.—MODEL TEST APPARATUS

Test Apparatus.—The testing apparatus is shown in Fig. 4. The model beam consisted of two pieces of steel stock fastened together by screws in such a manner as to introduce a camber equal to the total dead-load deflection. The required mass of the model was obtained by hanging weights uniformly along the span. The fundamental natural frequency of the weighted beam was 4.05 cycles per sec. Two approach sections were provided for accelerating and decelerating the vehicle.

The model vehicle consisted of an aluminum chassis on two axles, which supported a cantilever beam of spring steel to which a steel mass was attached. The sprung mass was 85% of the total weight, of which 20% was on the front

⁸ "Model Investigation of Effects of Vehicular Vibrations on Simple Span Bridges," by R. M. Connell and R. J. Lamp, thesis presented to the Massachusetts Institute of Technology, at Cambridge, in 1955, in partial fulfillment of the requirements for the degree of Master of Science.

axle. Damping in the vehicle was provided by a friction device on the suspended mass. Three springs were used in the model, which provided natural vehicle frequencies of 2.27 cycles per sec, 3.07 cycles per sec, and 3.87 cycles per sec. The vehicle was pulled across the beam at constant speed by a synchronous motor with a master speed control. Tests were run at velocities corresponding to vehicle speeds on the prototype of 30 miles per hr, 40 miles per hr, and 50 miles per hr.

It was desired to reproduce in the model the condition that is the major cause of actual bridge vibration—that is, an initial oscillation of the vehicle as it enters the span. This oscillation was accomplished by a removable hold-down arm, which introduced a known deflection of the sprung mass. As the vehicle entered the span this arm was removed suddenly by a mechanical device. Thus, the initial amplitude of harmonic motion was known.

The dynamic midspan deflection of the bridge model was measured by a linear variable differential transformer. The oscillations of the sprung vehicle mass were obtained by SR-4 strain gages mounted near the fixed end of the cantilever spring. Thus, the dynamic force applied to the chassis at any time was known. The two measurements were recorded simultaneously by an oscillograph.

Model Test Results.—Typical experimental results are shown by the dashed curves in Figs. 5(a) and 5(b). The upper section of each figure indicates the percentage variation in the total force applied by the vehicle to the bridge. The abscissa for all curves indicates the position of the vehicle center of gravity in terms of span, which can also be considered a time scale. For convenience the ordinate of the deflection curves has been taken as the ratio of dynamic midspan deflection to maximum static midspan deflection. The natural vehicle frequency was 3.87 cycles per sec for the test run shown in Fig. 5(a) and 3.07 cycles per sec for that shown in Fig. 5(b). The vehicle velocity for both test runs corresponded to 30 miles per hr on the prototype.

The theoretical curves of Fig. 5 were obtained by integrating Eqs. 3 and 8 numerically, using the initial conditions imposed on the model. The upper curve is given by

$$\frac{100 \times k_v \Delta}{M_v g} \dots \dots \dots (9)$$

The ordinate of the lower curve is y_c/δ_{st} , or $\frac{y_c k_B}{M_v g}$, in which δ_{st} is the maximum static deflection at midspan.

As indicated by the typical model results, there is good agreement between analysis and experiment for both bridge and vehicle behavior. The most obvious discrepancies in bridge deflection occur when the amplitude of vibration is small. However, the magnitude of these smaller amplitudes is not significant. It is believed that the basic method of analysis is satisfactory. More specifically, the following conclusions can be made:

1. For computing midspan deflection, the bridge can be represented by a single-degree-of-freedom system without error.

2. For the type of bridge and vehicle represented by the model, the separate axle loads can be replaced by a single concentrated load.

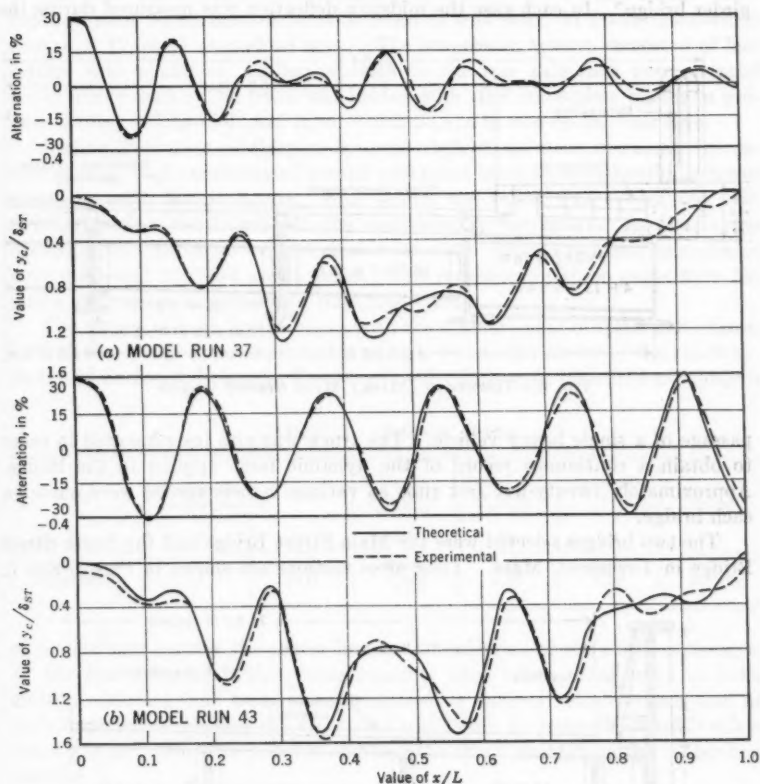


FIG. 5.—THEORETICAL AND EXPERIMENTAL COMPARISON OF MIDSPAN DEFLECTIONS

The bridge-deflection records obtained from the model are remarkably similar to those observed in actual field tests. This similarity indicates that the conditions imposed on the model represent the major cause of actual bridge vibration.

FIELD TESTS

After it was concluded that the theoretical analysis yields satisfactory results for the idealized system represented by the model, it was necessary to determine whether this system truly represents an actual bridge. More specifically, it was necessary to prove that (a) an actual bridge could be idealized as a simple beam; (b) an actual vehicle could be idealized as a single-

degree-of-freedom system; and (c) the surface roughness on the bridge was of secondary importance and could be ignored.

Two bridges were tested, one a stringer type and the other a typical through-girder bridge.⁹ In each case the midspan deflection was measured during the

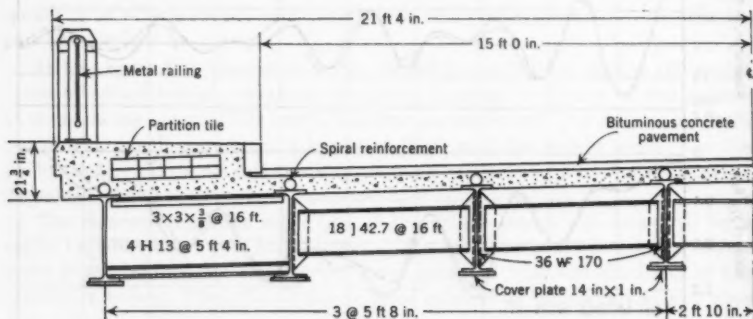


FIG. 6.—TOWNSEND (MASS.) MAIN STREET BRIDGE

passage of a single heavy vehicle. The truck was also instrumented in order to obtain a continuous record of the dynamic force applied to the bridge. Approximately twenty-five test runs at various vehicle speeds were made on each bridge.

The two bridges selected were the Main Street Bridge and the South Street Bridge in Townsend, Mass. Their cross sections are shown in Figs. 6 and 7,

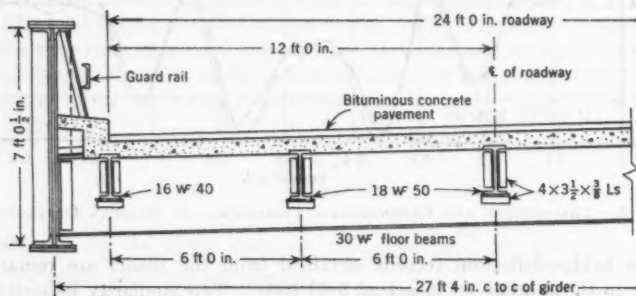


FIG. 7.—TOWNSEND (MASS.) SOUTH STREET BRIDGE

and some pertinent data are given in Table 1. In Fig. 7 the plate girder is composed of an 84-in.-by- $\frac{1}{2}$ -in. web plate, with flanges consisting of four angles 7 in. by 4 in. by $\frac{1}{2}$ in.; one cover plate 16 in. by $\frac{3}{4}$ in. by 54 ft; two cover plates 16 in. by $\frac{3}{4}$ in. by 38 ft; and one cover plate 16 in. by $\frac{3}{4}$ in. full length.

⁹ "Dynamic Response of Simple Span Highway Bridges to Moving Vehicle Loads," by H. S. Suer, thesis presented to the Massachusetts Institute of Technology, at Cambridge, in 1955, in partial fulfillment of the requirements for the degree of Doctor of Science.

The bridges were selected because they were typical medium-span structures and presented relatively few testing difficulties.

The test vehicle was a 1952 two-axle (six-wheel), 10-ton dump truck. This vehicle had a wheel base of 13 ft, a tread of 6 ft 6 in., 11:00-24 front-wheel tires, and 12:00-24 rear-wheel tires. The suspension system consisted of leaf springs with a pair of auxiliary springs on the rear axle that were engaged under heavy load. The truck was loaded with steel snow-plow blades to produce a total weight of 41,625 lb, of which 33,875 lb was on the rear axle.

Testing Procedure.—Midspan dynamic deflections were measured by deflectometers, each consisting of a small calibrated beam mounted within a tower placed beneath the structure. Also within the tower was a long rod held tightly between the beam and the underside of the bridge. As the bridge deflected, the calibrated beam was also forced to deflect, and resulting strains were measured by SR-4 strain gages. The responses of these gages were fed into a strain-gage amplifier and recording system.

The testing of each bridge began with the measurement of static deflections. In both static and dynamic tests the vehicle was in the center of the roadway. At the Main Street Bridge in Townsend, deflections were measured at midspan

TABLE 1.—BRIDGE DATA

Bridge	Skew angle, in degrees	Span	Weight, in pounds per foot	Design $E I$, in lb-in. ² $\times 10^{12}$	Composite $E I$, in lb-in. ² $\times 10^{12}$	δ_{st} , in inches
(1)	(2)	(3)	(4)	(5)	(6)	(7)
Main Street	21½	88 ft 8 in.	7,830	7.44	9.12	0.162
South Street	17	86 ft	5,120	6.27	7.20	0.125

of the stringer nearest the center line and at midspan of the exterior stringer. At the South Street Bridge, measurements were taken at midspan of both girders. Moving-load tests were conducted at various vehicle speeds and in both directions. During the tests care was taken to assure that the vehicle speed was as constant as possible and that the truck maintained the center-line position.

Instrumentation of the truck consisted of strain gages to measure the bending strains in the rear axle, and, in addition, an accelerometer was mounted at the center of the same axle. The responses of both the strain gages and the accelerometer were recorded by a portable recording system placed in the bed of the truck. This procedure was based on the assumption that the variations in the front-wheel loads were negligible compared with the total vehicle weight. This approximation was possible because only 19% of the total weight was on the front axle.

Four strain gages were mounted on the axle and calibrated under static loading in order to provide values of the total axle load. The individual wheel reactions were weighed as the truck was loaded. However, under dynamic conditions, corrections must be made for the inertia forces on the axle. For this purpose it was assumed that the entire mass of the axle assembly is

concentrated at the center of the wheels. The error is not appreciable because 90% of the total weight is concentrated at these points.

With these assumptions the sum of the two dynamic wheel loads is equal to that indicated by the strain gages minus the inertia force on the axle assembly. The latter is equal to the measured acceleration times the total mass of the assembly. This measurement was taken at the center of the axle. Although the acceleration is approximate for the individual wheels, it is essentially correct for the total axle load. The bending vibration of the axle itself is neglected. However, the natural frequency of this vibration is much greater than that of the rigid-body motion of the axle and has a negligible effect on the wheel loads.

A more serious error results from the fact that the resultant wheel load may not act at the same point along the axle as it did during the static calibration. This would occur if the roadway surface at each wheel were not parallel to the axle. Investigation reveals that the possible error involved is not too great to be tolerated.

It is difficult to achieve a completely satisfactory vehicle instrumentation. Nevertheless, in this study it was not necessary to obtain an exact measurement of the dynamic wheel loads but only an indication of the vehicle behavior. For this purpose the instrumentation was satisfactory.

The average velocity and position of the test vehicle were determined by the use of two simple switching devices placed in the roadway at both ends of the structure. Each device consisted of a vertical strip of spring steel mounted so as to close a microswitch when bent by the passing vehicle. The closed circuit caused a "pip" on the paper recording the bridge deflection. A similar device was mounted on the vehicle to provide a signal for the recording apparatus in the truck.

Test Results.—The dynamic properties of the test vehicle were determined independently of the test runs on the bridges. The truck was run slowly over a large obstruction, and the resulting free vibration was recorded. The variation in the rear axle load showed a consistent natural frequency of approximately 2.3 cycles per sec. The same frequency predominated in all test runs although the motion was never purely harmonic. Additional records obtained prior to and after the bridges were crossed indicated that the truck normally vibrates at essentially this frequency as it moves along the highway. However, this is not a practical method to determine the natural frequency because local surface conditions introduce forcing functions that prevent a truly free vibration.

An attempt was made to compute the natural truck frequency from statically measured spring and tire stiffnesses. This computed frequency was considerably lower than that actually measured. The difference is believed to be due to greater interleaf spring friction during short-term load variations. To verify this conclusion, vertical acceleration measurements were taken simultaneously on the axle and body of the vehicle as it moved along the roadway. With moderate roadway-surface conditions the two accelerations were almost identical in amplitude, frequency, and phase. The foregoing indicated that the leaf springs were almost entirely inactive and that the tires

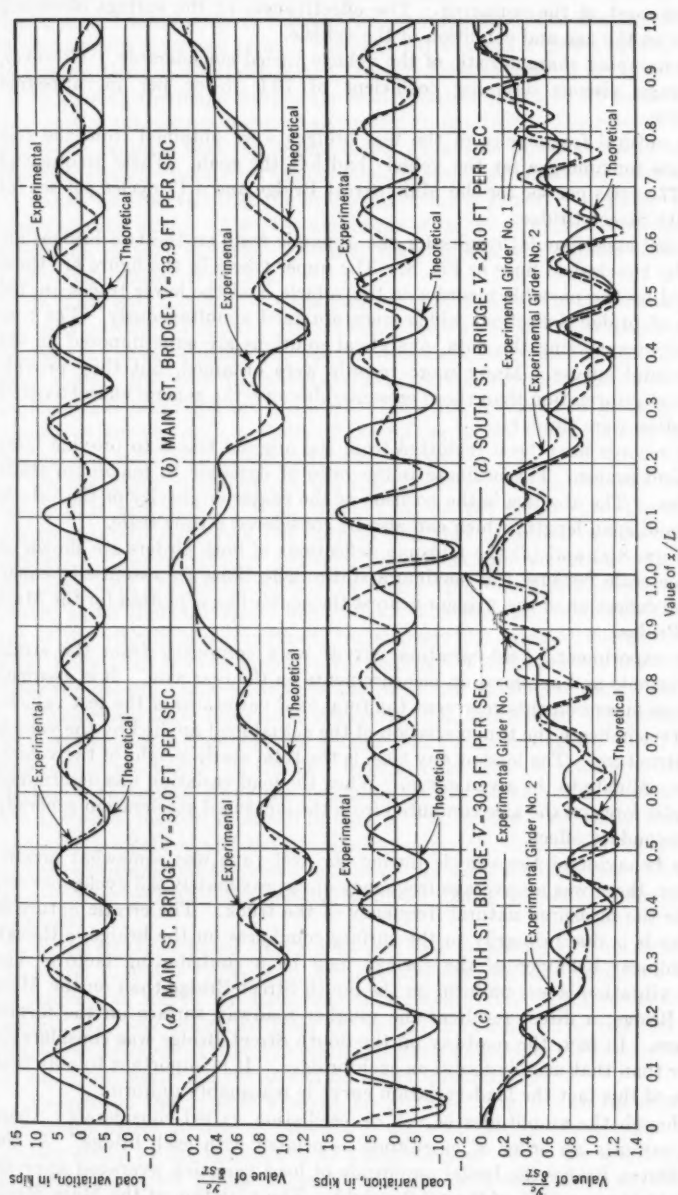


FIG. 8.—COMPARISON OF MIDSPAN DEFLECTIONS

provided most of the springing. The effectiveness of the springs obviously depends on the age and condition of the vehicle.

The damping characteristic of the vehicle varied considerably. However, an average viscous damping coefficient of 70.0 lb-sec per in. appeared reasonable.

The natural frequencies of the test bridges were obtained from the free vibrations remaining after the vehicle had left the span. These frequencies were 3.77 cycles per sec for the Main Street Bridge and 4.17 cycles per sec for the South Street Bridge.

Typical experimental results for the dynamic tests on the two bridges are shown by the dashed lines in Fig. 8. The upper traces in the figure are those produced by the portable recorder in the vehicle, and the lower traces are the records of bridge deflection, which were obtained simultaneously. For convenience in analyzing the data, analytical solutions are superimposed on the experimental curves. Many more records were obtained, but they provide little more information than those presented because the general characteristics of vibration were similar.

The records have been replotted from the original traces to provide more convenient scales. The ordinate is the ratio of dynamic to maximum static deflection. The abscissa is the position of the center of gravity of the vehicle in terms of span length, which can also be considered a time scale.

In Figs. 8(c) and (d) the midspan deflections of both girders are shown on the same scale because the maximum static deflections are essentially equal. Only the deflection of the stringer nearest the center line is plotted for the Main Street Bridge.

The experimental-load-variation curves were computed from the strain measurements and acceleration measurements on the rear axle. It is assumed that these measurements represent the total load variations of the test vehicle. The curves indicate the time variation of the actual load applied by the vehicle to the structure. The load at any time is the total static weight of the vehicle plus the ordinate to the given curve. When the load variation was determined the inertia force on the axle computed from the measured acceleration generally had a secondary effect.

The behavior of the vehicle during the test runs was somewhat erratic. However, there was an average frequency of approximately 2.3 cycles per sec, which is the measured natural frequency of the truck. The erratic nature of the records is due primarily to the surface roughness on the bridge, although the nonlinear behavior of the springs may be a contributing factor. The vehicle vibration is less uniform on the South Street Bridge than on the Main Street Bridge, a direct result of the rougher roadway surface on the former structure. In fact, the roadway on the South Street Bridge was considerably rougher than that usually found on such bridges. It is important to note that in spite of this fact the load-variation curve is reasonably uniform.

Although the amplitudes of vehicle oscillation varied considerably, there was apparently an order of magnitude associated with each bridge. At the South Street Bridge the initial amplitude of load variation averaged approximately 15 kips, or 35% of the total weight. The variation at the Main Street

Bridge was from 5 kips to 10 kips, or an average of 17.5% of the total weight. There was a critical range of vehicle speed at which sizable oscillations occurred. Obviously, for a certain type of roadway surface and a given natural vehicle frequency, there is a critical velocity that induces maximum load variation.

In general, the major part of the load variation is caused by surface roughness on the approaches rather than on the bridge itself. The records for both structures indicate that the nature of the expansion joints at the entrance to the span strongly influences the subsequent amplitude of vehicle oscillation.

It can be observed that the bridge vibration is generally in phase with the load-variation curve. Also, the amplitude of bridge vibration is related to the amplitude of load variation. Sizable deviations in the applied load always cause large bridge vibrations.

In Figs. 8(c) and 8(d) for the South Street Bridge, the deflection records for both girders are shown. In all cases the two records are displaced horizontally in the same manner as the crawl or static deflection curves, due to the skew angle. However, the phase and amplitude of the vibration superimposed on the crawl deflection are essentially the same for the two girders. Minor variations are probably a result of the rolling of the vehicle about its longitudinal axis induced by local surface conditions.

On the Main Street Bridge the exterior-stringer deflection was measured also but is not shown. With the vehicle on the center line the observed maximum static deflection was only 36% of that measured on the center-line stringer. However, under dynamic conditions the vibrations of the two stringers were almost completely in phase, and the amplitudes were more nearly equal than the static deflections. The foregoing indicates that in so far as the vibration is concerned, transversely the bridge behaves more as a rigid body than it does under static loading. Records of the free vibration after the vehicle has crossed show identical amplitudes for the two stringers.

Comparison with Theoretical Analysis.—The theoretical solutions, shown by the solid lines in Figs. 8 and 9, are based on Eqs. 1 through 8. Two different approaches are used. In the first intermediate step the dynamic bridge deflection is computed, using the measured load variation. The applicability of the analytical method to actual bridges is thus verified. Secondly, the vehicle behavior is idealized and the solution is completely theoretical, except for the initial conditions and the values of bridge and vehicle stiffnesses. The second approach investigates the feasibility of idealizing the vehicle for practical purposes.

In the solutions based on the measured load variation, only Eq. 8 was used. The term $k_v \Delta$ was replaced by the actual measured load variation, and the equation was solved by numerical integration. The effective mass of the bridge, M_B , was computed from the design drawings. The rigidity, EI , in Eq. 6 was determined from the measured static deflection. The damping term in Eq. 8 was neglected because of its minor importance.

Samples of this type of analysis are shown in Fig. 9. In the solution for the South Street Bridge no attempt is made to distinguish between the two girders as the bridge is idealized as a single beam. Only the interior stringer of the Main Street Bridge is considered. In both cases there is satisfactory

agreement between theory and experiment. The maximum dynamic deflections are almost identical, although there is less agreement when the amplitude of vibration is small. There are no more discrepancies than those normally expected in any comparison of theory with actual field tests. Thus, it is concluded that the basic method of analysis is satisfactory for field conditions. It is only necessary to idealize the vehicle behavior satisfactorily in order to obtain a completely theoretical solution.

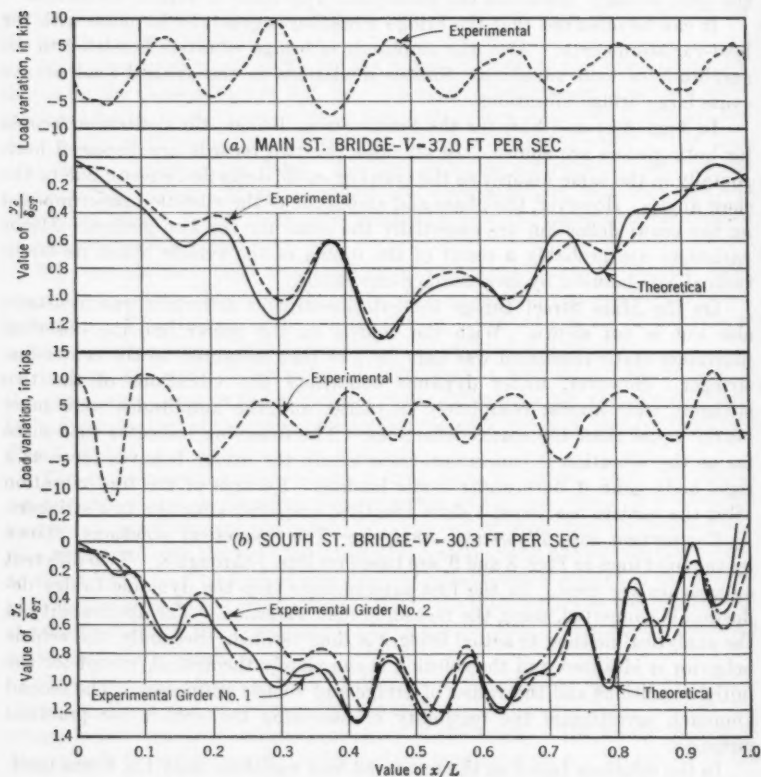


FIG. 9.—COMPARISON OF MIDSPAN DEFLECTIONS (MEASURED LOAD-VARIATION BASIS)

The theoretical results shown in Fig. 8 were obtained, using the complete analytical method without modification. The experimental values were used for the vehicle stiffness, k_v , and the damping coefficient, c_v . The oscillation of the vehicle at $t = 0$ was defined by the initial conditions, Δ_0 and $\dot{\Delta}_0$. These conditions were assumed rather arbitrarily in order to match as much of the experimental-load-variation curve as possible. The upper theoretical curves in the figures are plots of $k_v \Delta$ obtained from the analysis.

As expected, the agreement between the completely theoretical approach and the experimental results is generally not as good as for the solution based on the measured load variation. However, the comparison is still satisfactory. The agreement between theory and experiment is remarkable for the Main Street Bridge. Better agreement on the South Street Bridge probably could not be expected because of the extremely rough roadway on the structure and because of the obvious effect of the skew angle on the behavior of girder bridges. Most of the discrepancies in the bridge-deflection records involve a phase shift rather than a difference in amplitude. For practical purposes these phase shifts are of little importance. It is also significant that the greater the vibration the more accurate the theoretical analysis.

The differences between the theoretical bridge-deflection curves and the experimental bridge-deflection curves are primarily a result of the difference between the actual load variation and the idealized load variation. The latter difference is due largely to surface roughness on the bridge deck. This is much more pronounced on the South Street Bridge, which had the rougher roadway. Although the effect of the surface condition is quite obvious, it does not change significantly the maximum amplitude or the general character of the bridge vibration.

It is possible to include the effect of surface roughness in the analytical method by modifying the value of Δ according to the profile of the roadway surface. By this device the comparison between theory and experiment probably could be improved. However, this appears unwarranted for design.

It is concluded that the analytical method presented is satisfactory. The agreement between theory and actual field experiment is as good as can be expected for any general method of analysis. It possibly could be improved by including the effect of surface roughness and by other refinements in the analysis. However, experimental errors and the inherent difficulty of idealizing the dynamic properties of an actual bridge make significantly closer agreement improbable. For bridges with reasonable surface roughness, an adequate solution can be obtained by considering only an initial oscillation of the vehicle.

THEORETICAL RESULTS

The investigation of the theoretical results obtained by the analytical method is divided into parts: First, the general effects of parameter variations are studied. Second, maximum dynamic bridge deflections are determined for various practical combinations of bridge and vehicle parameters.

The first part of the investigation was accomplished by use of an analog computer. This computer is the best device for studying the effect of parameter variation, but it does not provide sufficient accuracy for final results. For this reason a digital computer was used in the second part of the investigation. It is believed that the final results are in a practical form for use in bridge design.

Basic Assumptions.—The assumptions on which the results are based include the theoretical approximations used in deriving the equations. It is believed that none of these approximations introduce serious errors. The most important assumption is that the effect of roadway roughness on the bridge can

be disregarded. The analysis includes only the effect of an initial oscillation of the vehicle, which is presumed to be induced by surface roughness on the approaches.

Severe pavement roughness or large obstructions on the bridge deck obviously would cause serious bridge vibrations. However, the magnitude and character of such vibration would differ little from that induced by an initial vehicle oscillation. Furthermore, it is questionable that extreme surface conditions or actual obstructions should be considered in design at normal working stresses. An allowance for surface roughness on the structure could be made in selecting the amplitude of initial oscillation. For design it appears that the assumption of an initial vehicle oscillation is adequate for predicting dynamic bridge behavior.

In these theoretical computations damping in both the bridge and the vehicle have been neglected. The damping coefficients of typical highway bridges are generally small and have little effect on the vibration during the crossing of a vehicle. Vehicle damping is ignored because it can be counteracted by the surface roughness, which may continuously excite the vehicle oscillation. If this is correct the inclusion of a vehicle damping coefficient appears unnecessary. Even if it were included it would be important only for the longer spans.

It is postulated further that the distinction between sprung vehicle masses and unsprung vehicle masses can be ignored and that the entire mass is spring supported. This is probably correct because the vehicle experiments indicated that much of the springing was in the tires rather than in the leaf springs. In any case the effect of the unsprung mass is secondary because it is a small part of the total mass.

Parameters.—A more convenient form of the theoretical equations is obtained by introducing the relationships,

$$(p_v)^2 = \frac{k_v}{M_v} \dots \dots \dots (10a)$$

and

$$(p_B)^2 = \frac{k_B}{M_B} = \frac{M_v g}{M_B \delta_{st}} \dots \dots \dots (10b)$$

in which p_v is the natural vehicle frequency and p_B is the natural bridge frequency. By substituting Eq. 1 into Eqs. 3 and 8, eliminating the damping terms, replacing M_{v1} by M_v , and introducing Eqs. 10a and 10b, the following result:

$$\frac{\ddot{y}_c}{\delta_{st}} = (p_B)^2 \left(\sin \omega t - \frac{y_c}{\delta_{st}} \right) + (p_v)^2 \frac{M_v}{M_B} \left(\frac{z}{\delta_{st}} - \frac{y_c}{\delta_{st}} \sin \omega t \right) \sin \omega t \dots (11a)$$

and

$$\frac{\ddot{z}}{\delta_{st}} = - (p_v)^2 \left(\frac{z}{\delta_{st}} - \frac{y_c}{\delta_{st}} \sin \omega t \right) \dots \dots \dots (11b)$$

All displacements are divided by the maximum static bridge deflection, δ_{st} , which is equal to $\frac{M_v g}{(p_B)^2 M_B}$. The parameters on which the dynamic deflection and amplitude of vibration depend are ω , M_v/M_B , p_v , and p_B/p_v . In addition, there are the initial conditions, z_0 , \dot{z}_0 , y_{c0} , and \dot{y}_{c0} . The initial bridge conditions, y_{c0} and \dot{y}_{c0} , are always taken as zero. The initial vehicle conditions, z_0 and \dot{z}_0 , depend on the maximum initial amplitude of vehicle oscillation, z_m , and the phase angle, ϕ . For convenience, z_m is replaced by

$$\beta = \frac{k_v z_m}{M_v g} = \left(\frac{p_v}{p_B} \right)^2 \frac{M_v z_m}{M_B \delta_{st}} \quad (12)$$

In Eq. 12, β is the maximum fractional variation in the applied load before entering the span. The phase angle is defined as the angular distance in terms of vehicle vibration from the end of the span to the point at which the vehicle mass has zero displacement and maximum downward velocity. Therefore,

$$z_0 = z_m \sin \phi \quad (13)$$

and

$$\dot{z}_0 = z_m p_v \cos \phi \quad (14)$$

Parameter Ranges.—In the subsequent results, each parameter is varied through a range of values that includes those encountered in most simple-span highway bridges.

The initial oscillation of the vehicle, which is defined by the parameter β , is the most important factor determining the magnitude of vibration. Unfortunately, it is also the most uncertain factor in a particular case. The magnitude of β depends entirely on the severity and the character of the surface roughness on the approach to the bridge. In the field tests described previously, the maximum observed value was approximately 0.4, which indicates that the maximum dynamic variation in total load was approximately 40% of the static vehicle weight. The probable occurrence of greater values of β could be determined only by a statistical study of surfaces and vehicles. For the purposes of this investigation, the value of β is varied from 0.1 to 0.6.

The mass ratio, M_v/M_B , is varied from 0.05 to 0.5. It should be noted that M_B is one-half the total mass of the bridge. Therefore, the two limiting values of the mass ratio represent cases in which the vehicle weighs 2.5% and 25% of the total weight of the bridge.

The natural vehicle frequencies (p_v) vary from 2π radians per sec to 6π radians per sec, or from 1 cycle per sec to 3 cycles per sec. No general vehicle study has been made, but it is believed that most heavy vehicles are included within this range.

A variation in natural bridge frequency (p_B) of between 4π radians per sec and 16π radians per sec, or 2 cycles per sec and 8 cycles per sec, is considered. In general, the lower values correspond to long-span structures and the higher values to short-span bridges. The range of frequency ratio, p_B/p_v , for which results are given, is from 0.67 to 7.0.

For each combination of the other parameters the crossing frequency, ω , is varied in order to determine the maximum possible dynamic deflection and amplitude of vibration. In order to keep the results within a practical range, limitations were placed on the variation of this parameter. These limits were derived as follows:

The range of vehicle velocities is taken as from 20 miles per hr to 50 miles per hr. Lower speeds would probably not involve appreciable vehicle oscillations, and higher speeds probably do not need to be considered. It was assumed that the natural bridge frequency is related to the length of the span, according to the approximate empirical formula, $p_B = 2,200/L$. In using this expression and the assumed range of vehicle speeds in the equation $\omega = \pi V/L$, the crossing-frequency range is from $0.04 p_B$ to $0.10 p_B$. The approximate and

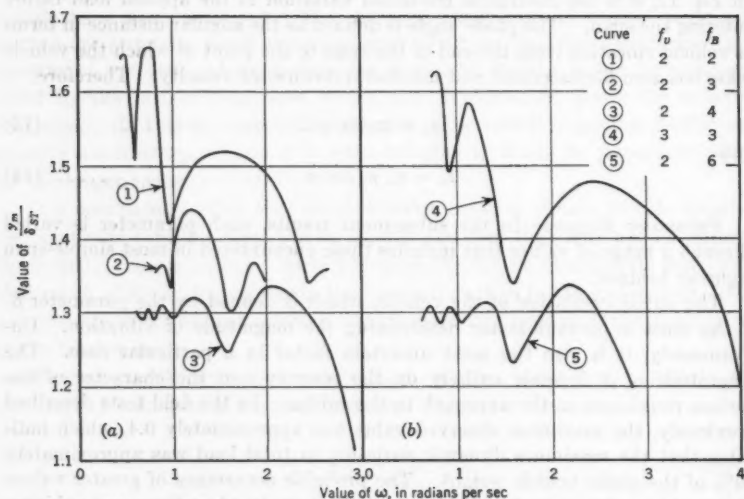


FIG. 10.—EFFECT OF ω ON MAXIMUM DEFLECTION

rather arbitrary nature of these limits is justified by the results, which indicate that the range of ω is not of primary importance.

Variations in the phase angle, ϕ , are also considered. No limitations are imposed because any value could occur under field conditions.

Effect of Parameter Variations.—The effect of vehicle velocity on maximum dynamic deflection was investigated, using the analog computer. The results for various combinations of p_v and p_B are shown in Fig. 10, in which $\beta = 0.30$, $M_v/M_B = 0.20$, and $\phi = 3\pi/2$. In all cases the curves have a wave form, and there are critical values of ω at which maximum deflections occur. When the frequency ratio is unity, the highest peaks, and hence the largest bridge deflections, occur at slow vehicle speeds. However, for frequency ratios of 2 or greater, the peak values increase with increasing velocity. For frequency ratios of between unity and 2, maximum deflection occurs at velocities between

these two extremes. In terms of the limitations imposed on values of ω , maximum deflection occurs near $\omega = 0.04 p_B$ for frequency ratios of unity, near $\omega = 0.10 p_B$ for ratios greater than 2, and at intermediate values for frequency ratios of between 1 and 2. For the higher frequency ratios the peaks occur when the velocity is such that the vehicle mass has a maximum downward displacement at midspan.

Field tests of actual structures cannot be expected to produce maximum deflection-velocity curves identical to those in Fig. 10. Those theoretical curves were obtained for a constant value of β . In field tests the value of β would probably vary unpredictably with vehicle speed.

The effect of the vehicle phase angle on maximum deflection was also investigated by an analog computer. Some results are shown in Fig. 11. The phase angle obviously has a definite effect and should be considered when determining maximum possible deflections.

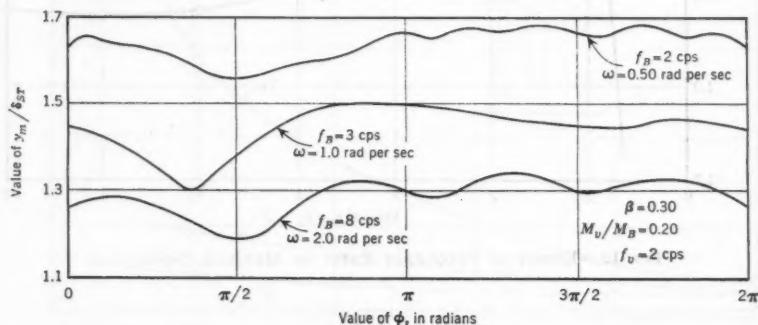


FIG. 11.—EFFECT OF ϕ ON MAXIMUM DEFLECTION

The results shown by Figs. 12, 13, and 14 are maximum dynamic deflections for combinations of parameters defining a particular bridge and vehicle. Each value is intended to be the maximum possible deflection for those parameters. The selection of the most critical values of ω and ϕ is involved in each case. The problem is difficult because there are infinite combinations of the two parameters. The critical values were estimated by analog studies and by certain theoretical considerations. The final results were obtained by digital computer. In an attempt to assure that the deflections were truly maximum ones, digital-computer solutions were obtained for several combinations of ω and ϕ in each case.

For high frequency ratios the critical condition is not difficult to determine because the bridge and vehicle are essentially two independent dynamic systems. In this case the bridge vibration can be considered approximately as the addition of two parts: (a) The vibration due to a constant force crossing the span, and (b) a vibration in phase with the vehicle oscillation. The critical values of ω and ϕ are those for which these two parts have maximum downward amplitudes at the same point near midspan.

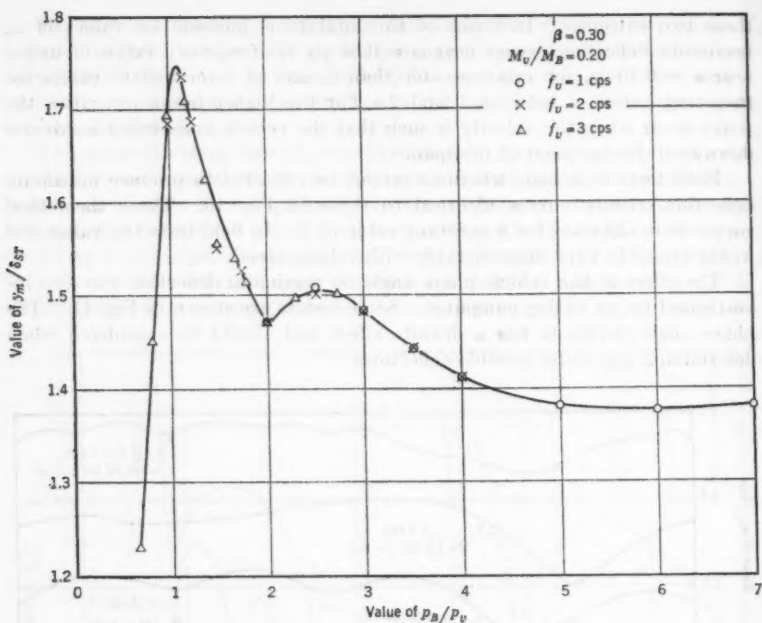
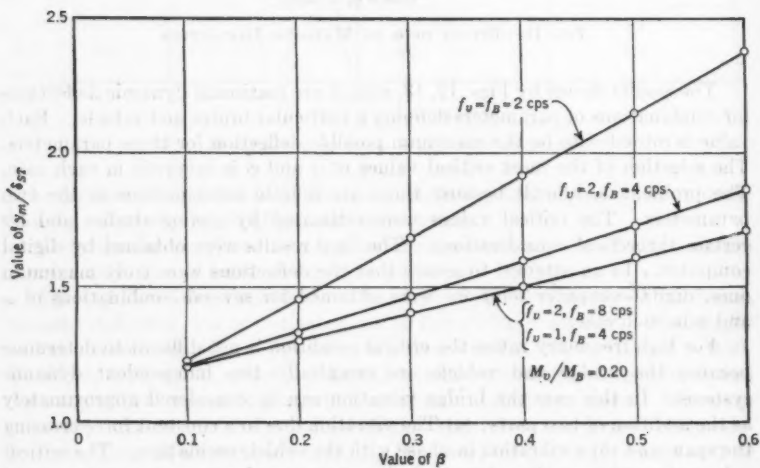


FIG. 12.—EFFECT OF FREQUENCY RATIO ON MAXIMUM DEFLECTION

FIG. 13.—EFFECT OF β ON MAXIMUM DYNAMIC DEFLECTION

When the frequency ratio is less than approximately 2.5, the two systems cannot be considered independently, and the theoretical determination of the critical condition becomes more difficult. The behavior of the bridge is somewhat analogous to the familiar "beat" of a linear two-degree system. However, the variable coefficients of the equations for the bridge problem make it difficult to interpret this analogy.

It is believed that the values plotted in Figs. 12, 13, and 14 are near the absolute maximum deflections. However, it is probable that for frequency ratios of less than 2.5, the points should be slightly higher.

The effect of the frequency ratio is shown in Fig. 12, in which results are given for constant values of β and M_v/M_B . For ratios greater than 2.5 the curve is smooth, and the dynamic deflection varies from approximately 1.375

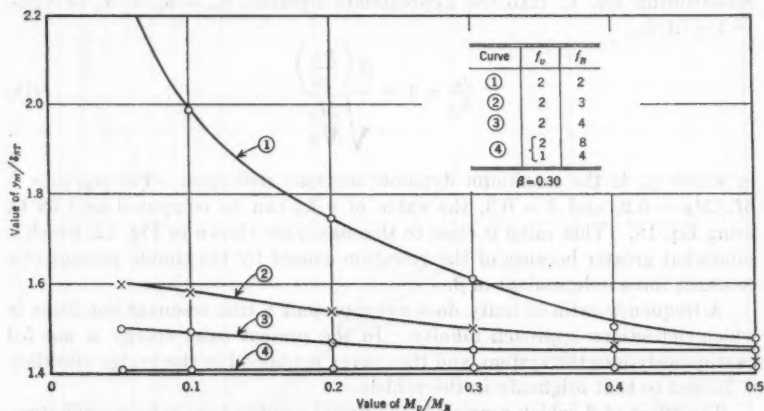


FIG. 14.—EFFECT OF MASS RATIO ON MAXIMUM DEFLECTION

to 1.50 of the static deflection. For ratios of less than 2.5 the curve is more irregular but generally increases to a maximum of approximately 1.74 at a frequency ratio slightly more than unity. Below this point the dynamic deflection decreases rapidly. It is significant that the curve is independent of the actual values of p_v and p_B and that only the frequency ratio is important.

The reason for the peak near $p_B/p_v = 1$ is apparent when the behavior of bridge and vehicle in this region is considered. Because of the beat effect, which occurs only at low frequency ratios, the oscillation of the vehicle almost disappears at one or more points along the bridge. At these points the bridge vibration greatly increases because most of the energy originally contained in the vehicle oscillation is transferred to the bridge. This effect is apparent in the model run shown in Fig. 5(a).

The validity of the foregoing statements can be demonstrated theoretically as follows: The total initial energy in the vehicle oscillation is

$$U_v = \frac{1}{2} k_v (z_m)^2 = \frac{1}{2} \frac{M_v \beta^2 g^2}{(p_v)^2} \dots \dots \dots (15)$$

The energy in bridge vibration is

$$U_B = \frac{1}{2} k_B A^2 = \frac{1}{2} M_B (p_B)^2 A^2 \dots \dots \dots (16)$$

in which A is the amplitude of bridge vibration.

Assuming a complete energy transfer, equating Eqs. 15 and 16, applying Eq. 10b, and rearranging yields

$$\frac{A}{\delta_{st}} = \frac{\beta \left(\frac{p_B}{p_v} \right)}{\sqrt{\frac{M_v}{M_B}}} \dots \dots \dots (17)$$

Substituting Eq. 17 into the approximate equation $y_m = \delta_{st} + A$, or $y_m/\delta_{st} = 1 + A/\delta_{st}$,

$$\frac{y_m}{\delta_{st}} = 1 + \frac{\beta \left(\frac{p_B}{p_v} \right)}{\sqrt{\frac{M_v}{M_B}}} \dots \dots \dots (18)$$

in which y_m is the maximum dynamic midspan deflection. For $p_B/p_v = 1$, $M_v/M_B = 0.2$, and $\beta = 0.3$, the value of y/δ_{st} can be computed as 1.68 by using Eq. 18. This value is close to the maximum shown in Fig. 12, which is somewhat greater because of the vibration caused by the simple passage of a constant force independent of β .

A frequency ratio of unity does not represent a true resonant condition in which deflections approach infinity. In the present case, energy is not fed continuously into the system, and the energy contained in the bridge vibration is limited to that originally in the vehicle.

The effect of β , which represents the initial amplitude of vehicle oscillation, is shown in Fig. 13, in which curves are plotted for three different combinations of p_v and p_B . It is apparent that in all cases the effect of β is linear. The curves indicate that this effect becomes slightly greater as the frequency ratio approaches unity. For the higher frequency ratios, y_m/δ_{st} is essentially equal to $1.1 + \beta$.

The effect of the mass ratio, M_v/M_B , is shown in Fig. 14. For high frequency ratios the value of the mass ratio has no effect on the maximum deflection. Nevertheless, the effect becomes apparent as the frequency ratio decreases and becomes quite significant for a frequency ratio of unity. It is important to note that for high mass ratios the maximum deflection ratio does not vary appreciably with that of the frequency. If the curve of Fig. 12 had been computed for a higher mass ratio, the peak near $p_B/p_v = 1$ would not have appeared. The reason for this effect can be deduced from Eq. 18, which indicates that as the mass ratio increases the maximum dynamic deflection decreases. Even if the complete energy transfer takes place, the deflection is no larger than would be expected with a high frequency ratio.

All results are given in terms of the deflection ratio, y_m/δ_{st} . A high value of this ratio may not be significant if δ_{st} is small, as might apply to the curve in

Fig. 14 for $p_B/p_v = 1$. The large deflection ratios may not be significant because the small mass ratio for which they were obtained may indicate small static deflections.

Application.—In Fig. 15 the curves presented previously have been redrawn for convenience in actual design. Fig. 15(a) is a direct reproduction of Fig. 12 and is completely independent of the actual values of p_v and p_B . In Fig. 15(b), which has been taken from Fig. 13, the values on each curve have been divided by the value at $\beta = 0.3$. Thus, Fig. 15(b) provides correction factors to be applied to results taken from Fig. 15(a). Fig. 15(c) also gives correction factors because the values of Fig. 14 have been divided by the deflection for $M_v/M_B = 0.2$.

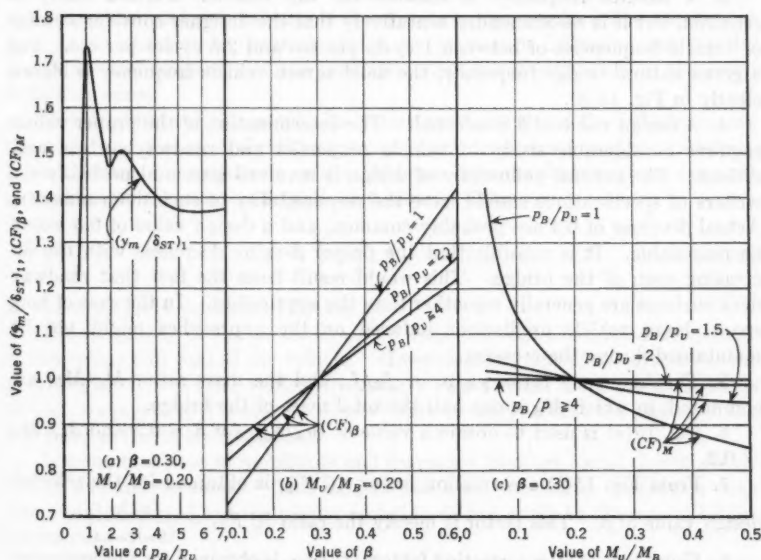


FIG. 15.—DESIGN CURVES FOR MAXIMUM DYNAMIC DEFLECTION

A detailed outline of the proposed procedure for predicting the maximum dynamic deflection for an actual bridge and a single two-axle vehicle is presented:

1. The maximum static deflection for a single design vehicle on the center line of the roadway (δ_{st}) is computed. Conventional methods are used, except that the moment of inertia should be taken as the composite value, including all secondary elements of steel or concrete that could conceivably contribute to the stiffness.⁶ However, in the case of a wide stringer bridge the contribution of the exterior stringers is questionable. The foregoing recommendation is based on the belief that composite action occurs in deck stringer bridges

even though shear connectors are not provided. It must be recognized that this may only be partly true of older bridges.

2. Computation is made of the natural frequency of the structure, which can be approximated by

$$f_B = \frac{1.2 \pi}{2 L^2} \sqrt{\frac{E I g}{W}} \text{ cycles per sec.} \quad (19)$$

in which I represents the composite moment of inertia, W denotes the weight per foot of bridge, and 1.2 is an approximate factor based on test results.⁶ The term I should be computed for the complete cross section even in the case of wide stringer bridges.

3. A natural frequency is selected for the vehicle. Further study is required, but it is recommended tentatively that the designer consider a range of vehicle frequencies of between 1 cycle per sec and 2.5 cycles per sec. For a given natural bridge frequency, the most severe vehicle frequency is shown clearly in Fig. 15(a).

4. A design value of β is selected. The determination of the proper values requires considerable study of vehicle properties and roadway-surface conditions. The general philosophy of design is involved also, and probably the writers of specifications should have the responsibility of such determination. Actual β -values of 0.4 are probably common, and a design value of 0.5 would be reasonable. It is possible that the proper β -value decreases with the increasing span of the bridge. This would result from the fact that roadway deck surfaces are generally smoother than the approaches. In the case of long spans, large vehicle oscillations induced on the approaches might not be maintained during the crossing.

5. The frequency ratio, p_B/p_v or f_B/f_v , and the mass ratio, M_v/M_B , are computed, in which M_B is one-half the total mass of the bridge.

6. Fig. 15(a) is used to obtain a value of $(y_m/\delta_{st})_1$ for $\beta = 0.3$ and $M_v/M_B = 0.2$.

7. From Fig. 15(b) a correction factor, $(CF)_\beta$, is obtained for the selected design value of β . This factor is merely the ratio $(CF)_\beta = \frac{(y_m)_\beta}{(y_m)_{\beta=0.3}}$.

8. Using Fig. 15(c) a correction factor, $(CF)_M$, is obtained for the computed mass ratio. This factor is the ratio $(CF)_M = \frac{(y_m)_{M_v/M_B}}{(y_m)_{(M_v/M_B)=0.2}}$.

9. The final deflection ratio is computed by

$$\frac{y_m}{\delta_{st}} = \left(\frac{y_m}{\delta_{st}} \right)_1 (CF)_\beta (CF)_M \quad (20)$$

10. The maximum dynamic midspan deflection is computed by

$$y_m = \left(\frac{y_m}{\delta_{st}} \right) \delta_{st} \quad (21)$$

Step 9 is not exact as it is assumed that the two correction factors are independent of each other. Although not proven, this is believed to be essentially correct.

Computed as outlined in the foregoing, the dynamic deflection ratio is for a single two-axle vehicle on the roadway center line. The deflection ratio for more than one vehicle, or for a single vehicle off the center line, would be somewhat less. Vehicles having more than two axles must be considered in future studies.

The results presented herein, together with other similar and related investigations, will eventually lead to specification criteria to guard against excessive vibration. In the meantime the foregoing procedure is believed to be a practical means for investigating the susceptibility of a particular bridge design to vibration.

Maximum Amplitude of Vibration.—One of the reasons for bridge-vibration studies is the possible effect of excessive vibration on pedestrians. Public complaint and perhaps distrust of the structure may result. The reaction of persons to vibration is determined not by maximum deflection but by the amplitude and frequency of the oscillation that is superimposed on the crawl deflection curve.

The amplitude of this oscillation varies continuously as the vehicle crosses the span, and the most significant value is not determined easily. However, it can be taken conservatively as the difference between the maximum dynamic deflection and the maximum static deflection. Thus,

$$A = \left[\left(\frac{y_m}{\delta_{st}} \right) - 1 \right] \delta_{st} \dots \dots \dots (22)$$

in which y_m/δ_{st} is determined by Eq. 20.

The frequency of the oscillation may vary between the natural frequency of the bridge and that of the vehicle. However, the greatest amplitudes occur generally at the natural vehicle frequency. As persons are more susceptible to high frequencies, it would be conservative to assume that the higher of the two natural frequencies applies.

The combinations of amplitude and frequency that are found objectionable are as yet undetermined. This subject has been studied in connection with automobile design,¹⁰ but the results probably do not apply to the case of bridge vibration.

Maximum Dynamic Stress.—Although dynamic stresses were not determined, it is possible to draw some general conclusions from the results obtained. The maximum static bending moment due to the vehicle represented by a single concentrated load can be expressed as

$$M_{st}' = \frac{12 EI}{L^2} \delta_{st} \dots \dots \dots (23)$$

Considering the sinusoidal shape of the fundamental mode of vibration, the midspan bending moment due to the dynamic increment of deflection is

$$M' = EI A \frac{\pi^2}{L^2} \dots \dots \dots (24)$$

¹⁰ "Vehicle Vibration Limits to Fit the Passenger," by R. N. Janeway, SAE Special Publication, Soc. of Automotive Engrs., New York, N. Y., March, 1948.

in which A is the dynamic increase in midspan deflection. Combining Eqs. 22, 23, and 24,

$$\frac{M_m'}{M_{st}} = 1 + 0.82 \left(\frac{y_m}{\delta_{st}} - 1 \right) \dots \dots \dots (25)$$

in which M_m' is the maximum dynamic bending moment at midspan. Eq. 25 is approximate because only the first mode of vibration is included. In general, the higher modes contribute more to the bending moment than to the deflection.

In most cases Eq. 25 should not be used to predict maximum dynamic bending stresses without modifying the value of y_m/δ_{st} given by Eq. 20. The latter equation gives deflection ratios for a single vehicle, which is not the design condition for most bridge elements. Numerical addition of the dynamic effects of two or more vehicles requires the improbable condition that the oscillation of all are in exact phase. In addition, only the case of a single two-axle vehicle traveling on the center line of the roadway has been considered. If the vehicle is not so positioned it is probable that the dynamic increase in the most heavily loaded girder is less than that indicated previously. For these reasons Eq. 25 yields a conservative moment ratio for most design cases.

CONCLUSIONS

1. The proposed simplified method of analysis is sufficiently accurate for engineering purposes. Reasonable agreement was obtained with both laboratory and field tests. The method may be used for both stringer bridges and girder bridges.

2. From the field tests it is concluded that the major cause of vibration is the initial oscillation of the vehicle on its own springs, and that for design purposes the effect of surface roughness on the bridge can be neglected.

3. Theoretical results based on conclusion 2 indicate that the initial amplitude of vehicle oscillation is by far the most important factor influencing the magnitude of bridge vibration.

4. However, in addition large vibrations occur generally when the natural frequency of the vehicle is close to that of the bridge.

5. The only other factor influencing the deflection ratio, y_m/δ_{st} , is the mass ratio, M_v/M_B , which is important only when the frequency ratio is near unity.

6. All results are in terms of the deflection ratio, y_m/δ_{st} . A bridge designed with a large static deflection can be expected to experience large amplitudes of vibration.

7. The tendency toward long-span bridges and slender bridges should be regarded with caution. For such structures the combination of low natural frequency approaching that of heavy vehicles and roadway roughness on the approaches can result in excessive vibration. However, the verifying laboratory and field tests cited herein were all for medium-span bridges. Additional verification is needed for extremely long spans.

ACKNOWLEDGMENTS

The studies cited herein were based on research by the Joint Highway Research Project established at the Massachusetts Institute of Technology

(Cambridge) by a grant from the Massachusetts Department of Public Works. The cooperation of the department staff is appreciated. Special help was rendered by Saul Namyet, A.M. ASCE, and Ralph G. Gray of the Institute.

APPENDIX. NOTATION

The following symbols, adopted for use in the paper, conform essentially with "American Standard Letter Symbols for Structural Analysis" (ASA Z10.8—1949), prepared by a committee of the American Standards Association with Society representation, and approved by the Association in 1949:

- A = amplitude of bridge vibration;
- c_B = bridge damping coefficient;
- c_v = vehicle damping coefficient;
- E = modulus of elasticity;
- F = spring force;
- f_B = fundamental natural bridge frequency, in cycles per second;
- f_v = fundamental natural vehicle frequency, in cycles per second;
- g = acceleration due to gravity (32.2 ft per sec²);
- I = composite moment of inertia of the bridge;
- k_B = spring constant of bridge;
- k_v = spring constant of vehicle;
- L = span of bridge;
- M = mass:
 - M_B = effective mass of bridge;
 - M_B^T = total mass of bridge;
 - M_v = mass of vehicle;
 - M_{vs} = sprung mass of vehicle;
 - M_{vu} = unsprung mass of vehicle;
- M_v/M_B = mass ratio;
- M' = dynamic increment in midspan bending moment;
- M_m' = maximum dynamic midspan bending moment;
- M_{st}' = maximum static bending moment;
- P = load on bridge;
- p = frequency:
 - p_B = fundamental natural frequency of bridge, in radians per second;
 - p_v = fundamental natural frequency of vehicle, in radians per second;
 - p_B/p_v = frequency ratio;
- t = time;
- U_B = energy in bridge oscillation;
- U_v = energy in vehicle oscillation;
- V = vehicle velocity;

W = weight per foot of bridge;

x = distance of vehicle from end of span;

y = deflection:

y_c = dynamic midspan bridge deflection;

y_m = maximum dynamic midspan deflection;

y_m/δ_{st} = deflection ratio;

z = deflection of sprung vehicle mass:

z_m = maximum deflection of sprung vehicle mass;

z_0 = initial vehicle-mass deflection;

β = initial load-variation parameter;

Δ = vehicle-mass deflection relative to bridge;

δ_{st} = maximum static midspan bridge deflection;

ϕ = phase angle; and

ω = crossing frequency, $\pi V/L$.

AMERICAN SOCIETY OF CIVIL ENGINEERS

Founded November 5, 1852

TRANSACTIONS

Paper No. 2980

ERRORS IN MEASUREMENT OF IRRIGATION WATER

BY CHARLES W. THOMAS,¹ M. ASCE

WITH DISCUSSION BY MESSRS. ÖDÖN STAROSOLSZKY; STEPONAS KOLUPAILA;
ARMANDO BALLOFFET; AND CHARLES W. THOMAS

SYNOPSIS

Devices and structures for measuring irrigation water are subjected to changes in water levels upstream and downstream from the point of measurement. The generally accepted approach to meet this problem is standardization and calibration of the measuring equipment. The use of tables, graphs, or charts developed (from the calibrations) for determining discharge in the field is based on the criteria that the field structure is a replica of the device from which the data were derived and that the flow conditions are identical. Deviations from these standards will result in errors. The magnitude of errors resulting from changes in certain dimensions, incorrect settings, changes in flow patterns, and other deviations is evaluated for some of the commonly used measuring devices. Measurements obtained from equipment capable of operating with a high degree of accuracy may be subjected to errors unless care is exercised in fabrication, installation, operation, and maintenance.

INTRODUCTION

The device or structure used in measuring flow in irrigation systems may not yield results as accurate as might be expected. In all probability, the order of accuracy of the flow measurements derived from the various devices will show variations. This deviation will be evident between the different types of structures and methods used. When units of the same type are compared, the deviation may be apparent.

Some of the reasons for the variations in accuracy are:

NOTE.—Published, essentially as printed here, in September, 1957, in the Journal of the Irrigation and Drainage Division, as *Proceedings Paper 1362*. Positions and titles given are those in effect when the paper or discussion was approved for publication in *Transactions*.

¹ Hydr. Engr., Bureau of Reclamation, U. S. Dept. of the Interior, Denver, Colo.

1. The principle of operation (volumetric or velocity);
2. The degree of exactness to which the flow coefficients have been established;
3. The workmanship and the care that are exercised in fabrication, construction, and installation;
4. The adaptability of the particular device to the existing conditions;
5. The proper setting with respect to approach and exit flow conditions;
6. Proper maintenance;
7. The manner of obtaining the final result (that is, whether the rate of flow is determined directly from the device or method, or whether head is measured and the end result obtained by computation, tables, charts, or curves);
8. The means for obtaining the needed information (for example, the use of a staff gage in the flow, a gage in a stilling well, or a continuous recorder for obtaining heads);
9. The care in obtaining the data; and
10. Other factors, such as extraneous material in the water, the range of flows to be covered, and similar items.

Absolute accuracy will not be obtained in all instances. The reduction of errors to a minimum may be possible, however, if all factors are considered.

In general, there are two classes of errors: (a) Avoidable errors, which result from carelessness and can be eliminated by thorough supervision and attention to detail, and (b) unavoidable errors of degree. Although the latter cannot be eliminated completely, they may be alleviated and satisfactory overall results can be obtained by using extreme care and by a knowledge of their nature and magnitude.

In the United States many devices and structures have been developed for measuring flow in irrigation systems. Nearly all these developments are designed to operate in conjunction with separate equipment to control the flows. A few serve the dual purpose of control and measurement. Except in rare cases, the control is operated manually.

The design of most open-channel irrigation systems is such that fluctuations of the water levels both upstream and downstream of the measuring device are tolerated. The measuring devices have been developed to accommodate this design procedure. In effect, any change in the upstream water level and, generally, in the downstream water level is reflected as a change in discharge through the measuring device.

The accepted approach to the solution of the problem of fluctuating water levels is the standardization and calibration of the measuring equipment. The result is a device that, when built and installed in accordance with established standards, will pass a range of known discharges for a range of upstream and downstream water levels. The exact instantaneous discharge can be determined by observing the upstream and downstream heads, by use of correctly referenced gages, and by entering charts, graphs, or tables that have been developed by prior calibration of the device under carefully controlled conditions.

Such a procedure assumes that the field installation is a suitable replica of the installation that was calibrated, usually in a hydraulic laboratory. Further assumptions are that conditions of flow, especially in regard to velocity-

distribution patterns, are similar and that the heads and other necessary measurements can be determined with comparable accuracy.

Because discharge tables, charts, or graphs are the results of calibration, they are based on empirical relationships and not on a rational analysis in all instances. Therefore, they are not necessarily susceptible to accurate extrapolation beyond the range of observations from which they were developed.

In order to obtain accurate flow measurements in an irrigation system, it is necessary to know the standards developed and the conditions of calibration. Emphasis will be given herein to some of the possible measurement errors that result from disregarding the adherence to close tolerances in the developed standards, from failure to make accurate observations, and from other deficiencies. The cited examples are of devices used in open-channel irrigation systems. Similar arguments can be applied to equipment and structures used in closed-conduit systems.

The devices are not necessarily those most susceptible to errors, nor are all the cited cases those that may cause measurement errors. Weirs are used widely in the United States for measuring irrigation and drainage water. Therefore, more attention has been given to possible errors in this type of structure. Sharp-crested weirs will be examined because broad-crested weirs are not generally used in irrigation measurements.

The usual practice in irrigation systems is to read the head gages on measuring devices at daily intervals as it is not practicable to obtain numerous readings every day at each point of measurement. Because an irrigation system rarely reaches steady flow conditions the foregoing practice may result in major errors. However, until a continuous recorder is developed that will be economically feasible for installation this practice will be followed.

SOURCES OF ERROR

Faulty Fabrication or Construction.—It is possible for errors to be introduced in flow measurements as a result of the faulty construction of measuring devices. Incorrect dimensioning of the structure is evaluated readily and can be used as an example of the error.

Table 1 shows the discharge error for rectangular weirs or Cipolletti weirs for an incorrect weir-crest length measurement of only 0.01 ft as compared with the calibrated standard from which the flow formula was derived. Because discharge is related directly to length in the flow equation, an error in length of 0.05 ft would cause the discharge to be in error by five times the values shown in Table 1 for any observed head. Eqs. 1 through 4 are used to determine the percentage error as shown in Table 1:

TABLE 1.—DISCHARGE ERROR FOR WEIRS

Weir length, l , in feet	Percentage error $(Q' - Q/Q) \times 100$
1.0	1.0
2.0	0.5
3.0	0.33
4.0	0.25

$$Q = C L H^{3/2} \dots \dots \dots (1)$$

$$Q' = C (L + \Delta L) H^{3/2} \dots \dots \dots (2)$$

$$\frac{Q'}{Q} = \frac{L + \Delta L}{L} \dots \dots \dots (3)$$

and

$$Q' = \left(\frac{L + \Delta L}{L} \right) Q \dots \dots \dots (4)$$

Table 2 shows the discharge error caused by a 0.01-ft incorrect measurement of the throat width for Parshall flumes having standard widths of from 1 ft to 4 ft. A constant head of 0.2 ft has been assumed. The error introduced by faulty measurements of 0.02 ft and 0.03 ft is also shown in Table 2. This error is essentially constant for different values of measured head. The flow equation (Eq. 5) used in developing Table 2 was derived empirically from calibrations²:

$$Q = 4 W H_s^{1.522} W^{0.026} \dots \dots \dots (5)$$

Similarly, an error in the measurement of width or breadth of a rectangular submerged orifice will cause a considerable error in discharge. Because the

TABLE 2.—DISCHARGE ERROR FOR PARSHALL FLUME

W, in feet (1)	H _s , in feet (2)	Q, in cubic feet per second (3)	Q', in cubic feet per second (4)	Percentage error (Q' - Q/Q) × 100 (5)
Error in width measurement of 0.01 ft				
1.0	0.2	0.348	0.351	0.86
2.0	0.2	0.656	0.659	0.45
3.0	0.2	0.972	0.975	0.30
4.0	0.2	1.264	1.267	0.23
Error in width measurement of 0.02 ft				
1.0	0.2	0.348	0.355	2.0
Error in width measurement of 0.03 ft				
1.0	0.2	0.348	0.359	3.1

discharge is related directly to the area of the orifice, the magnitude of error is similar to that for the weir, and an error in either the length or breadth measurement will be constant for various heads on the orifice or gate.

Error in Discharge Measurements Due to Transverse Slope of Weir Crest.—When installing Cipolletti weirs and rectangular weirs in the field, it is necessary to set the crest exactly horizontal. If it is known that the crest is not level, it is common practice to consider the effective head to be the average head on the weir. The error caused by this practice is shown in Fig. 1. An inclination of approximately 6° will cause an error of on the order of 1%. An angle of this magnitude should be detected by eye and corrective measures taken.

² "Improving the Distribution of Water to Farmers by Use of the Parshall Measuring Flume," by Ralph L. Parshall, *Bulletin No. 488*, Colorado Agri. Experiment Station, Fort Collins, Colo., May, 1945.

Eq. 6 was used to determine the percentage discharge error shown in Fig. 1:

$$\text{Percentage of error} = \frac{100 S^2 L^2}{32 H^2} \dots \dots \dots (6)$$

in which S is the slope of the weir.

A more precise method would be to compute the discharge, using the head at the low and high ends and averaging the discharge derived from these two computations.³ Thus, the error is reduced.

If it is not known that the weir is inclined and the gage zero is referenced to either the high end or the low end, the resulting error is considerably greater. Measurement of the head in this manner applies the error in reading to the entire crest length, and there is no compensation for a part of the crest being

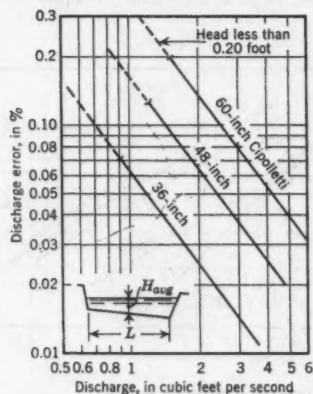


FIG. 1.—ERROR IN DISCHARGE DUE TO TRANSVERSE SLOPE OF CIPOLLETTI WEIR CREST WITH $S = 0.01$

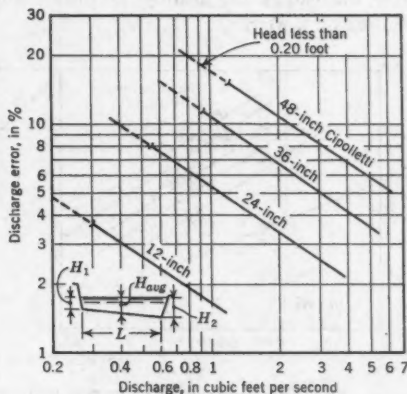


FIG. 2.—ERROR IN DISCHARGE FOR HEAD MEASURED AT END OF CIPOLLETTI WEIR WITH $S = 0.01$

above and a part being below the reference level. Fig. 2 shows the magnitude of the discharge error resulting from measuring the head at either end of 12-in., 24-in., 36-in., and 48-in. Cipolletti weirs having a transverse slope of 0.01 instead of using the average head over the weir.

Error in Discharge Due to Incorrect Head Reading.—In measuring irrigation water perhaps the most common error is to misread the head. This may result from (1) incorrect gage location, (2) dirty head gage, (3) failure to use a stilling well, (4) considerable fluctuation of the water surface, and (5) carelessness in not obtaining a correct average reading at the time the gage is observed.

Fig. 3(a) shows the error in discharge resulting from a 0.01-ft incorrect head reading on 12-in.-to-48-in. Cipolletti weirs and on a 90° V-notch weir. This figure demonstrates that an error of approximately 7½% in discharge results when the lower heads are measured. For greater heads the error is less.

³ "Error in Discharge Measurements Due to Transverse Slope of Weir Crest," by Warren E. Wilson, *Civil Engineering*, Vol. 9, No. 7, 1939, p. 429.

It can be noted as well that for the longer weirs this slight error in head reading results in significant errors in discharge measurements.

As in the case of weirs, the head at the throat of a Parshall flume is easily misread in the field. Parshall flumes with throat widths of from 6 in. to 36 in. are shown in Fig. 3(b). This figure shows the error in discharge measurements resulting from a 0.01-ft misreading of the gage. The error is approximately the same as for an equal misreading of the head when weirs are considered.

Fig. 4 shows the measurement error resulting from a 0.01-ft misreading of the head on 8-in., 12-in., and 18-in. metergates and on an 18-in. screw-lift gate. The metergate has a circular leaf, and the screw-lift gate has a rectangular leaf. Fig. 4 also shows the error caused by a 0.01-ft incorrect head reading for the constant-head orifice turnout.⁴ The percentage error in discharge resulting from misreading the head on an orifice is less, in general, than the same misreading on a weir.

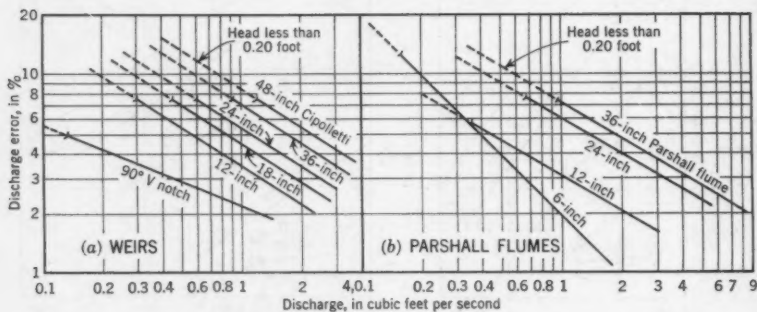


FIG. 3.—DISCHARGE ERROR FOR 0.01-FT INCORRECT HEAD READING

Error in Discharge Measurement Caused by Incorrect Zero Setting.—The error for incorrect zero setting of the head gage is of the same magnitude as for an equal misreading of the head. The improper positioning of the gage used to read the head is probably the most common error. In the field it is difficult to reference the exact zero of the gage to the crest of a weir, to a submerged orifice, or to a turnout gate. Extreme care should be exercised in setting the gages because incorrect settings cause errors at all flows (Figs. 3(a), 3(b), and 4).

Errors Resulting from Improper Gage Location.—Proper gage location to obtain head readings on measuring devices is important. In most instances flow relationships have been determined empirically, with a particular type of gaging device placed in a specific location. Hence, the over-all calibration includes a secondary calibration effect of the gaging system used to obtain head. Because of changes in the flow pattern of the stream as it passes through the measuring section, minor deviations from the standard used in gage design and location may appreciably affect the quality of the measurements.

⁴ "Water Measurement Manual," Bureau of Reclamation, U. S. Dept. of the Interior, Denver, Colo., 1st Ed., May, 1953, p. 77.

In the case of a weir, there is a downward curve of the water surface as the flow passes through the notch. This curved surface, or drawdown, extends a considerable distance upstream; the exact distance is dependent on local conditions. The head of the weir must be measured beyond the effect of the drawdown. In the development of the basic weir formulas, the head was observed at distances upstream from the weir notch varying from approximately four times to nine times the maximum head over the weir. Therefore, many authorities have accepted a minimum distance of four times the maximum head

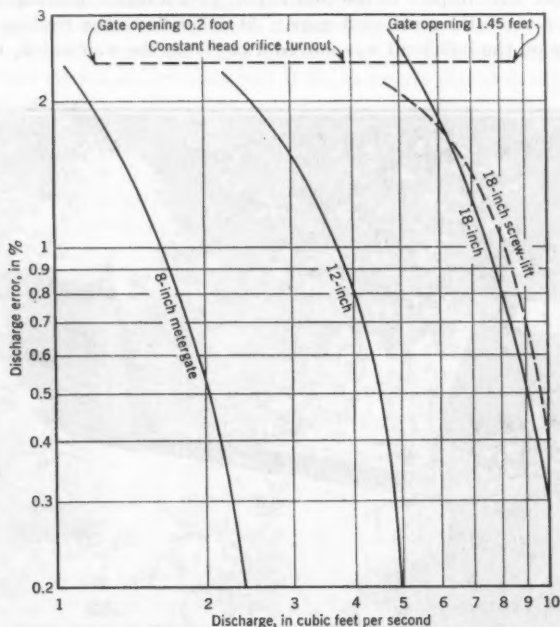


FIG. 4.—DISCHARGE ERROR FOR 0.01-Ft INCORRECT HEAD READING ON GATES (METERGATES AND SCREW-LIFT GATE FULLY OPEN)

to be measured. However, Horace W. King⁵ states that the distance should be at least two and one-half times the maximum head. Experiments have shown that there is some drawdown effect to a distance upstream of approximately six times the head on the weir.^{6,7} However, the influence at this distance is minor. Within the practical limits of the gages used at weir installations in irrigation systems, it appears that a distance upstream of four times

⁵ "Handbook of Hydraulics," by Horace W. King, McGraw-Hill Book Co., Inc., New York, N. Y., 3d Ed., 1939, p. 91.

⁶ "Description of Some Experiments on the Flow of Water Made During the Construction of Works for Conveying the Water of Sudbury River to Boston," by Alphonse Fteley and Frederic P. Stearns, *Transactions, ASCE*, Vol. XII, 1883, p. 1.

⁷ "Verification of the Bazin Weir Formula by Hydrochemical Gaugings," by Floyd A. Nagler, *ibid.*, Vol. 83, 1919, p. 105.

the maximum head is quite adequate, provided that other criteria are complied with.

Results of brief studies conducted in the hydraulic laboratory of the Bureau of Reclamation (United States Department of the Interior) show that it is extremely difficult to detect differences of head on enameled staff gages located at two, four, and ten times the head on the weir. These studies showed that positioning the enameled staff gage on the weir bulkhead, a practice sometimes followed in irrigation measurements, may result in errors. Some positions on the bulkhead, with respect to the weir notch, gave a higher reading for certain flows than a correctly positioned gage. At other flows the reading was less. As the gage on the bulkhead was moved away from the weir notch, more con-

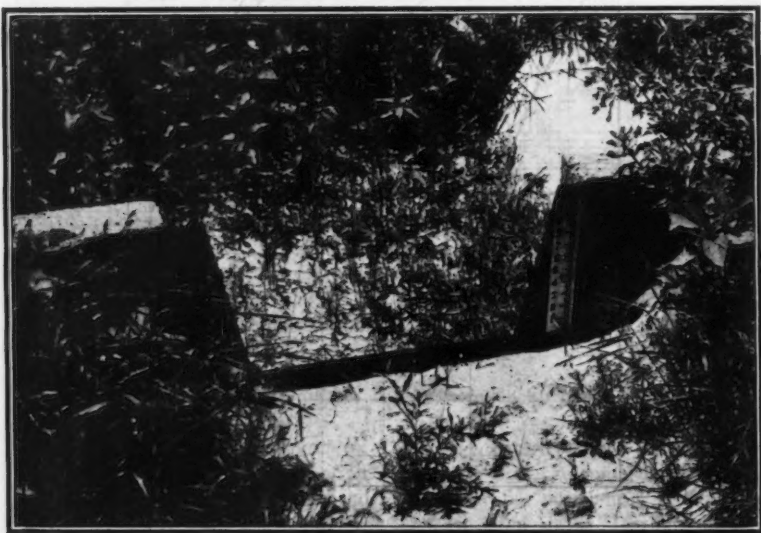


FIG. 5.—ENAMELED GAGE FASTENED TOO CLOSE TO WEIR NOTCH

sistent results were evident. For the flow conditions tested it was found that when the gage was placed on the weir bulkhead at a minimum distance of twice the maximum recommended head for the weir, the difference in the heads read on this gage and one correctly placed upstream was within the limits of visual observation. Fig. 5 shows an enameled gage for observing head fastened close to the weir notch.

When the velocity of approach is high and the irrigation channel has a high loss coefficient, there is a danger of placing the gage so far upstream from the weir crest that an error will prevail. Therefore, a correction must be made for the loss of head due to channel friction between the point of measurement and the weir.

Measurement errors can occur easily if the gages used in a Parshall flume are not placed in the manner and location developed in the standards. The ratings for this flume include a calibration of the gage positions. The gages are in drawdown areas. Under these conditions, movement of the gage upstream or downstream from the standardized location will change the head reading, and an error in discharge will result. For similar reasons if a stilling well is used the type and location of the entrance to the wells should be as specified. Substantial errors in field measurements have been traced to changes in location or design of the stilling-well entrances.

The foregoing statements apply to the location of the two gages used in the constant-head orifice turnout. The discharge tables developed from the calibration of this device are accurate only if the gages are placed as shown in the standard drawings.

Discharge Errors Due to Neglecting Velocity of Approach.—In practice the cross-sectional area of the approach channel can be made sufficiently large in

TABLE 3.—DISCHARGE ERROR (IN PERCENTAGE)
RESULTING FROM FAILURE TO CORRECT FOR
VELOCITY OF APPROACH

Velocity of approach, in feet per second	OBSERVED HEAD OVER WEIR, <i>H</i> , IN FEET				
	0.2	0.4	0.6	0.8	1.0
	DISCHARGE ERROR				
0.5	2.7	1.3	0.9	0.6	0.6
1.0	9.8	5.1	3.4	2.7	2.2
1.5	20.8	10.9	7.5	5.7	4.7
2.0	33.5	18.1	12.6	9.7	7.9
2.5	48.0	26.6	18.7	14.5	11.9
3.0	63.7	36.1	25.6	19.9	16.5

comparison with the weir notch to render the effect of the approach velocity negligible. However, if the approach velocity is not maintained at or less than 0.5 ft per sec, it must be taken into account and a correction must be applied. Thus, when discharge is obtained from measured head, an error will result if the equations, charts, or tables that are normally used are not corrected.

In irrigation practice the velocity of approach to a weir is usually increased to more than that for which it was originally designed by (a) a general restriction of the cross-sectional area of the weir pool as a result of vegetal-growth deposits, or (b) sediment or other accumulations at the bottom of the weir pool. Either item (a) or item (b) will change the standards to which the weir installation should conform.

A general reduction of the cross-sectional area of the weir pool will cause an increase in approach velocity that is related directly to the degree of restriction. The percentage error for a range of approach velocities and heads over weirs, except for the V-notch type, is given in Table 3. The error is such that the discharge is actually greater than that obtained from the discharge tables by the percentages shown in Table 3.

For accurate results the crest of the weir should be a distance that is not less than twice the depth of the water over the crest above the bottom of the approach channel. When practicable a greater weir-crest height is preferred. A weir installed in an irrigation channel in accordance with this standard may retain its accuracy for a short period only, because of the reduction of weir-pool depth by sediment deposits. The tables that are regularly used will no longer apply, but the error may be reduced or possibly eliminated by use of Rehbock's formula⁸ for computing discharge from the head observations on a rectangular sharp-crested weir:

$$Q = K L H^{3/2} = \frac{2}{3} \sqrt{2g} (L H^{3/2}) \left(0.605 + \frac{1}{320 H - 3} + 0.08 \frac{H}{P} \right) \dots (7a)$$

in which

$$K = 3.235 + \frac{1}{60 H - 0.56} + 0.428 \frac{H}{P} \dots \dots \dots (7b)$$

In Eq. 7b, H is the observed head over the weir, in feet, and P denotes the depth from the weir crest to the channel bottom.

TABLE 4.—ERROR IN DISCHARGE FOR CHANGES
IN HEIGHT OF WEIR

Weir height, P (1)	H/P (2)	Coefficient, K (3)	Percentage error ($K - K_{\infty}/K_{\infty}$) $\times 100$ (4)
Head = 0.2 ft			
0.5	0.4	3.49	5.1
1.0	0.2	3.41	2.7
2.0	0.1	3.37	1.5
3.0	0.07	3.35	0.9
∞	0	3.32	0
Head = 0.5 ft			
0.5	1.0	3.70	13.1
1.0	0.5	3.48	6.4
2.0	0.25	3.38	3.4
3.0	0.17	3.34	2.1
∞	0	3.27	0

Table 4 shows the percentage error in discharge that will occur if regular weir tables are used instead of correcting for the reduced height of weir by use of the Rehbock formula. The table is divided into two parts. The first section is computed for a constant head of 0.2 ft over a weir, and the second section is computed for a constant head of 0.5 ft. The value of the ratio of H to P is varied, and the error is shown. This percentage error is introduced in the field by the improper maintenance and cleaning of the weir pool. As the pool fills, both the ratio of H to P and the error increase.

In the field there have been instances in which weirs have been placed in channels having relatively high gradients. Under these conditions, it is diffi-

⁸ "Handbook of Hydraulics," by Horace W. King, McGraw-Hill Book Co., Inc., New York, N. Y., 3d Ed., 1939, p. 87.

cult to maintain a properly proportioned weir pool and to obtain smooth flow through the weir notch. The increased velocity of approach and turbulence will cause errors in measurement. Channel curvature and consequent, poor velocity distribution over the weir crest will also cause excessive errors that cannot be evaluated easily. Laboratory experiments^{*} have shown that the extreme difference in discharge over a weir for a constant head, but with varied upstream velocity distribution, was 26%. A weir with poor approach conditions is shown in Fig. 6.

Discharge Error Due to Turbulence and Surges.—Turbulence and surges occur in approach channels to weirs and other measuring devices. These dis-



FIG. 6.—WEIR WITH POOR APPROACH CONDITIONS

turbances are usually evidenced by erratic measurement results. Their cause is ordinarily a high approach velocity, but gates, valves, and sudden changes in section may yield the same results. Disturbances on the surface rarely follow a true sine-wave pattern. Therefore, an average reading of the head may cause appreciable error. Corrections are not applied readily to the computations as the pattern is complex. Corrective measures to quiet the flow provide the best solution, but such measures may not be easy to apply.

Weir Blade Sloping Upstream or Downstream.—It is necessary that the plane of the upstream face of the weir be vertical to obtain accurate measurements.

^{*} "Precise Weir Measurements," by Ernest W. Schoder and Kenneth B. Turner, *Transactions, ASCE*, Vol. 93, 1929, p. 999.

Experiments with sloping weirs show that the coefficient changes if the weir blade is tilted in an upstream direction or a downstream direction. The change is slight, and the weir face may be out of plumb a few degrees before the accuracy of the measurement is affected seriously.¹⁰

Roughness of Upstream Face of Weir and Bulkhead.—To obtain consistent and accurate flow measurements, the upstream face of the bulkhead and weir blade must be smooth. Offsets, protruding bolt heads, and surface roughness must be avoided on installation. Maintenance is necessary to retain a smooth surface. Sufficient work has not been performed to provide an exact evaluation of the errors resulting from the many possible roughnesses. It was found from one series of experiments⁹ that

"The percentage increase in discharge due to changing the roughness of the up-stream face of the weir bulkhead from that of a polished brass plate to that of a coarse file for a distance of 12 in. below the crest is shown to range from about 2% for 0.50-ft head to about 1% for 1.35-ft head."

The experiments of Floyd A. Nagler,¹¹ M. ASCE, showed that when the upstream face of the weir was roughened to the crest with coarse sand (retained on No. 8 standard sieve and passing No. 4 standard sieve), the increase in discharge ranged from 6.5% for a 0.2-ft head to 4.7% for a 0.5-ft head. The larger projections caused by the addition, in Nagler's experiment, of nuts and pieces of metal on the bulkhead below the crest caused a similar increase in discharge.

Rounding of Sharp Edge at Crest of Weir.—When weirs are constructed of wood the original sharp edge of the crest soon becomes rounded. Rust and corrosion also produce a rounding effect on metal weir blades. Rounding the edge causes an increase in the flow rate for a given head when compared with a sharp-crested weir. The results of experiments to evaluate the effect of the rounding of the crest show that the percentage increase in discharge due to the rounding decreases as the head increases. For a head of 0.5 ft increases of 2%, 3%, 5½%, 11%, and 13½% can be expected for roundings having radii of 1/24 in., ¼ in., ½ in., ¾ in., and 1 in., respectively. Data are lacking for the higher heads with larger radius roundings. However, with radii smaller than those described, the increases become consistently less as the head increases. For example, the 2% increase in discharge, given for the 1/24-in. rounding at a 0.5-ft head, becomes 0.7% at a 1.0-ft head and approximately 0.5% at a 1.35-ft head.

Submergence of Weirs.—When irrigation water is measured, weirs are usually not installed wherever submergence is anticipated. However, changes in the regimen of the channel downstream may cause a weir to operate under submerged conditions. Because submerged flow is relatively unstable, the results of the studies made of submerged weirs are not in agreement. It can be concluded that measurements made by use of a submerged weir should be considered as approximate.^{4,5} If practicable, the cause of submergence should be removed from the downstream channel.

¹⁰ Boulder Canyon Project Final Reports, Pt. VI, Hydraulic Investigations, Bulletin 3, Studies of Crest for Overflow Dams, Bureau of Reclamation, U. S. Dept. of the Interior, Denver, Colo., 1948.

¹¹ Discussion by Floyd A. Nagler of "Precise Weir Measurements," by Ernest W. Schoder and Kenneth B. Turner, Transactions, ASCE, Vol. 93, 1929, p. 1115.

Aeration of the Downstream Nappe of a Weir.—A general condition for accurate and consistent measurements by contracted weirs is that air circulates freely on all sides of the flow issuing from the weir notch. This condition ordinarily is not difficult to obtain. The weir bulkhead of irrigation structures in many instances is constructed of concrete. The use of metal weir blades that do not project sufficiently from the concrete, or an improper bevel of the concrete downstream from the blades, can easily restrict the desired air circulation. The effect of this restriction of air is to increase the flow rate for a given head. The increase in discharge can be appreciable and depends on the degree of air restriction.

The problem is more pronounced when suppressed weirs are used. For standard suppressed rectangular weirs used in irrigation, the side walls are generally carried straight through the structure. Thus, auxiliary means must be provided to supply air to the underside of the nappe. Unless adequate air is provided to this area to replace that removed by the jet, a partial vacuum will form. The result is a lowering of the nappe and an increase in discharge over that obtained with adequate aeration. A condition of instability may also exist, in which case erratic measurements would be obtained. Joe W. Johnson,¹² M. ASCE, found that the discharge would be increased approximately 3½% at a 0.5-ft head and approximately 2% at a 1.0-ft head when the pressure under the nappe was reduced to only 0.8 in. of water below atmospheric. When the pressure was reduced further to 1.2 in. of water below atmospheric, the increase in discharge was approximately 5% and 2½% for heads of 0.5 ft and 1.0 ft, respectively. The vent size adequate to relieve this negative pressure will depend on conditions at the weir. Both Johnson¹² and Joseph W. Howe,¹³ M. ASCE, have developed solutions for computing the size of vents. The important consideration is to design the vents of adequate proportions to relieve the low pressure in so far as possible.

Other Factors Affecting Discharge-Measurement Accuracy.—Other factors may cause errors in discharge measurements made with weirs, and many apply equally well to other types of structures and devices.

Obstructions in the measuring section cause errors that are proportionate to the magnitude of such obstructions. In irrigation systems, floating detritus, weeds, moss, and other vegetation may obstruct the water passage. Frequent and close inspection accompanied by remedial measures will relieve this condition.

Changes in the viscosity and surface tension of the fluid alter the flow coefficient. However, the effect of these factors is negligible in irrigation systems in which the flow media is water, and wide variations of temperature are not encountered. Furthermore, provided that the restrictions on high and low heads over the weir are complied with, such changes are of little importance.

At very low heads flow over a weir may become quite unstable, and errors and inconsistencies in the measurements will result. Heads of less than 0.2 ft will not produce reliable results when the usual discharge tables or formulas

¹² "The Aeration of Sharp Crested Weirs," by Joe W. Johnson, *Civil Engineering*, Vol. 5, No. 3, 1935, p. 177.

¹³ "Aeration Demand of a Weir Calculated," by Joseph W. Howe, Go Chean Shieh, and Arturo Obadia, *Civil Engineering*, May, 1955, p. 59.

are used, because of viscous drag and the tendency of the nappe to adhere to the weir crest.

The results of many experiments on weirs show that the formulas developed for rectangular weirs do not apply when the head exceeds approximately one-third the length. There are indications that the discharge formula for the Cipolletti weir, in lengths of more than 1 ft, is slightly in error at heads that are less than one-third the length.¹⁴ If errors are to be reduced to a minimum perhaps the rule should be that the head should not exceed one-fourth the length.

As stated previously, the flow formulas for weirs have been developed empirically and are not necessarily susceptible to extrapolation. Many of the data have been derived for heads as great as 2.0 ft. Although some data are available for higher heads, it is generally agreed that a 2.0-ft head should not be exceeded for a weir of any length if good results are desired.

It was noted previously that the percentage of error in discharge resulting from a given error in measuring the head will decrease as the head increases. Therefore, the minimum error and the greatest accuracy can be expected if the discharge occurs under the maximum head commensurate with the aforementioned limitations.

Careful visual inspections at regular intervals will remove many of the cited sources of error. These inspections should also disclose other sources, such as leaks around the measuring structure, through weir bulkheads, or from drains in the structure.

CONCLUSIONS

The charts, tables, and studies presented herein are not intended to indicate all the possible errors in the devices and structures used in measuring irrigation water. However, from the examples cited the following conclusions can be made:

To obtain accurate irrigation-water measurements it is necessary to study carefully the selection of a proper device to fit the conditions at the site. Even with careful planning and selection of an excellent primary measuring device, it is probable that errors may be introduced into the measurements unless care is exercised in fabrication, installation, operation, and proper maintenance of the devices or structures. The magnitude of these errors can be appreciable, and the value of a well-planned measuring program can be reduced considerably by not anticipating and removing the cause of the errors.

The possible errors are both negative and positive and may tend to cancel each other. However, especially in the case of weirs, more careful scrutiny shows that probably negative errors predominate. Indications are that usually more water is being delivered than is apparent from the measurements.

¹⁴ "The Discharge of Three Commercial Cipolletti Weirs," by Robert B. Van Horn, *Bulletin No. 85*, Eng. Experiment Station, Univ. of Washington, Seattle, Wash., November, 1935.

DISCUSSION

ÖDÖN STAROSOLSZKY¹⁵.—The accuracy of flow measurement is related closely to the metering equipment used. Economic aspects indicate the necessity for investigations into the degree of accuracy and into possible errors, especially if water rates are based on similar observations.

The deficiencies that Mr. Thomas cites and that are encountered in practice are not accidental and tend, in general, to result in regular errors. However, it should be noted that accidental errors also occur that cannot be eliminated and must be taken into account. Therefore, it is practicable to establish limits for the resultant of accidental errors and regular (systematic) errors—for example, to specify the permissible tolerance. The measuring device cannot be accepted unless the deviation of the value observed during calibration from the theoretical value accepted as correct remains within the specified tolerance—that is, the accuracy limit expressed in percentage.

Individual errors encountered in practice can be traced back to errors in factors in the characteristic hydraulic relationship. The probable discharge error can be computed from the error of individual factors in the discharge formula by use of the error theorem of Karl Friedrich Gauss.¹⁶ With the probable error, E , defined as the relative value,

$$E_Q = \sqrt{E_m^2 + E_b^2 + (a E_H)^2} \dots \dots \dots (8)$$

in which E_Q , E_m , E_b , and E_H denote the probable errors of discharge, flow coefficient, characteristic length (the length of the crest in the case of weirs), and stage observation, respectively. The characteristic constant, a , of the measuring device ($3/2$ for rectangular weirs) is the exponent of the head, H , in the discharge relationship. Summing up individual errors is thereby possible.

The relative probable error being inversely proportionate to the head, the poorest accuracies are obtained by the measuring device at low heads. The minimum head that can still be used for measuring should therefore be specified as a function of the permissible probable error (for example, of tolerance) for each measuring device. The lowest head suitable for measurement, considering accidental errors only, depends on the graduation of the gage, the tolerance of the discharge measurement and of the flow coefficient, and the constant, a . The minimum heads required for discharge measurement within accuracy limits (tolerance) of 3.5% and 10%, respectively, have been compiled in Table 5 for gage graduations of 8/10 in., 4/10 in., and 2/10 in., and for a 2% error in the flow coefficient. As revealed by Table 5, no reliable results can be obtained for low heads. However, it is equally correct that test results are valid up to a certain head limit only. These factors should be considered during design.

High heads involve extensive head losses. Consequently, for the conditions prevailing in the Hungarian plains area, in which gradients are as low as from

¹⁵ Research and Hydr. Engr., Research Inst. for Water Resources, Budapest, Hungary.

¹⁶ "Theoria motus corporum coelestium (Theorie der Bewegung der Himmelskörper—Methode der Kleinsten Quadrate)," by Karl Friedrich Gauss, Göttingen, 1809.

0.05 per 1,000 to 0.15 per 1,000, it was necessary to propose measuring devices involving low head losses at suitably high heads.¹⁷

Errors resulting from submergence are due partly to the inaccuracy introduced by the method of computation itself and partly to the unreliable determination of the limit of submergence. The influence of tailwater does not begin even in the case of sharp-crested weirs when the tailwater reaches the level of the crest, as shooting flow can still develop, but begins at a well-defined limit value of the tailwater-headwater ratio—for example, at the limit of submergence. However, the latter value depends on hydraulic conditions within

TABLE 5.—RELATIONSHIP BETWEEN ERROR IN MEASUREMENT AND MINIMUM HEAD FOR $F_m = 2\%$

Measuring device		VALUE OF E_Q								
		3			5			10		
		GAGE GRADUATIONS, IN INCHES								
		8/10	4/10	2/10	8/10	4/10	2/10	8/10	4/10	2/10
Rectangular weir, Venturi flume ($\alpha = 3/2$)	E_H	1.48			3.05			6.5		
	H_{min}	2.2	1.1	0.55	1.08	0.54	0.27	0.50	0.25	0.12
Thomson notch weir ($\alpha = 5/2$)	E_H	0.90			1.88			3.9		
	H_{min}	3.6	1.8	0.9	1.74	0.87	0.43	0.84	0.42	0.21
Linear weir and flume ($\alpha = 1$)	E_H	2.23			4.58			9.8		
	H_{min}	1.46	0.83	0.42	0.72	0.36	0.18	0.34	0.17	0.08
Venturi tube, submerged flow ($\alpha = 0.7$)	E_H	3.17			6.50			13.9		
	H_{min}	1.04	0.52	0.26	0.50	0.25	0.12	0.24	0.12	0.06

the approach channel and on the degree of contraction as well as on the measuring device itself. A mathematical analysis of this type of error is thus extremely difficult.

As indicated by Mr. Thomas, head observations at sufficiently close intervals or continuous records (obtained by a recording gage) are essential to any reliable measurement of conveyed quantities because even the most accurate device will fail to yield reliable results if the observed discharge is other than representative. The head varies during the period between successive observations. The error involved in the determination of flow quantities is depend-

¹⁷ "Virgázdálkodási Tudományos Kutató Intézet: Az öntözővíz mérése (Irrigation Water Measurement)," by Z. Károlyi and Ö. Starosolszky, *Proceedings of the Research Inst. for Water Resources*, No. 1, Budapest, 1957.

ent, therefore, on the daily stage readings. An additional error is introduced into the determination of flow quantities by computing for the period between observations, using a discharge that is not representative of the flow passing during the period. The error in flow quantities is shown in Fig. 7 for a meas-

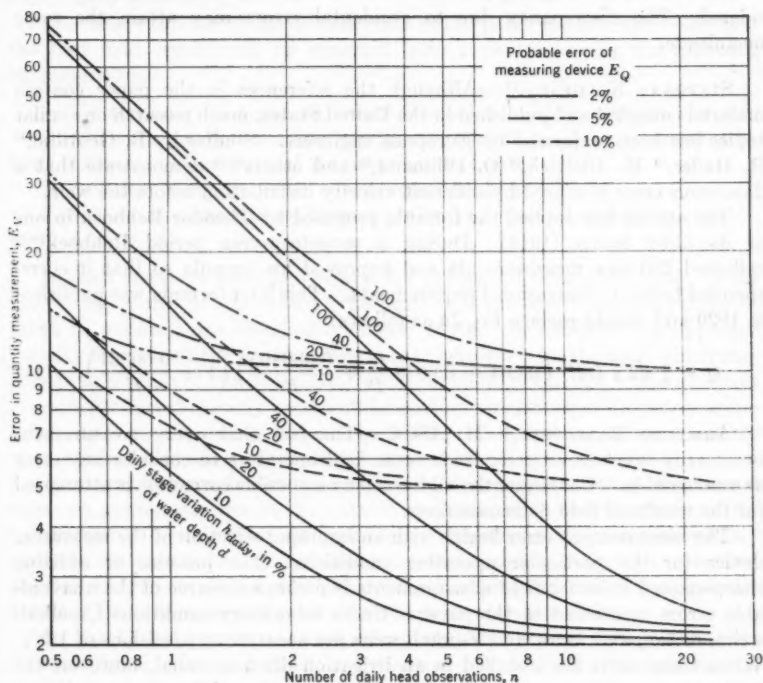


FIG. 7.—ERROR IN QUANTITY MEASUREMENT OF SUBMERGED FLOW

uring device operating on the staged difference principle (for example, a Venturi tube). The error in quantity measurement is determined as follows:

$$E_v = \sqrt{E_Q^2 + \left(\frac{1}{2} \frac{h_{\text{daily}}}{dn}\right)^2} \dots \dots \dots (9)$$

The depth of flow in the section under consideration is d , and the daily variation in stage is h_{daily} . Thus, the relative daily variation is

$$100 \frac{h_{\text{daily}}}{d} \dots \dots \dots (10)$$

Furthermore, the number of daily readings is n . The value of the increment error has been assumed to equal the variation in stage between observations. Curves have been drawn for errors of 25% and 10% in the discharge measure-

ment, E_Q . In general, readings taken once a day are unsatisfactory unless the stage fluctuation is small. Efforts to maintain a fairly constant water level in the system are, therefore, of great significance. The necessary daily gage readings can also be seen in Fig. 7.

In view of the foregoing a tolerance of from $\pm 10\%$ to 20% should be considered. The discrepancy due to accidental errors may attain the same magnitude.

STEPONAS KOLUPAILA¹⁸.—Although the references in the paper contain material compiled and published in the United States, much research on similar topics has been performed by European engineers. Studies by B. Gentilini,¹⁹ R. Hailer,²⁰ W. Dietrich,²¹ O. Dillmann,²² and others^{23,24} demonstrate that a dangerous error is caused by different velocity distribution before the weir.

The author has applied the formula proposed by Theodor Rehbock in one of its older forms (1912). During a seventeen-year period Rehbock^{25,26} collected 280 new measurements and improved his formula so that it corresponded better to dimensional requirements. This later formula was published in 1929 and should replace Eq. 7a as follows:

$$Q = \frac{2}{3} \sqrt{2g} L H^{\frac{3}{2}} \left(0.604 + 0.0813 \frac{H}{P} + \frac{0.000895}{P} \right) \left(1 + \frac{0.00361}{H} \right). \quad (11)$$

ARMANDO BALLOFFET,²⁷ M. ASCE.—The fact that every measurement necessarily involves an error leads some field operators to consider any error as unavoidable. Consequently, all too often no possible correction is attempted for the results of field determinations.

The measurement error begins with an improper selection of the measuring device for the particular operating conditions. The practice of utilizing sharp-crested weirs for field measurements is perhaps a source of the unavoidable errors mentioned in the paper. Under laboratory conditions Cipolletti weirs, rectangular weirs, and V-notch weirs are accurate to precisions of 1.0%. When these weirs are installed in an irrigation ditch or canal, however, the calibration conditions are irretrievably lost unless those laboratory conditions are reproduced carefully. Such a precaution usually is impossible because of either the cost of installation or maintenance.

¹⁸ Prof. of Civ. Eng., Univ. of Notre Dame, Notre Dame, Ind.

¹⁹ "Stramazzi in parete sottile liberi e rigurgitati," by B. Gentilini, *L'Energia Elettrica*, Vol. 13, Nos. 3, 5, and 10, 1936.

²⁰ "Fehlerquellen bei der Überfallmessung," by R. Hailer, *Mitteilungen des Hydraulischen Instituts der Technischen Hochschule München*, Munich, Vol. 3, 1929, pp. 1-21.

²¹ "Wassermessungen mit Ueberfall in der Zentrale Handeck der Kraftwerke Oberhasli," by W. Dietrich, *Schweizerische Bauzeitung*, Vol. 99, Nos. 1 and 2, 1932, pp. 1-4 and pp. 20-22.

²² "Untersuchungen an Überfällen," by O. Dillmann, *Mitteilungen des Hydraulischen Instituts der Technischen Hochschule München*, Munich, Vol. 7, 1933, pp. 26-52.

²³ "Der Einfluss der Geschwindigkeitsverteilung auf den Überfallbeiwert von Messwehren," by H. Gerber, *Wasserkraft und Wasserversorgung*, Vol. 32, Nos. 10-11, 1937, pp. 119-123.

²⁴ "Neue Untersuchungen an Überfällen mit Seiteneinschnürung," by E. Zschiech, *Mitteilungen aus dem Flussbaulaboratorium der Technischen Hochschule Dresden*, Leipzig, 1939.

²⁵ "Wassermessung mit scharfkantigen Überfallwehren," by Th. Rehbock, *Zeitschrift des Vereins Deutscher Ingenieure*, Vol. 73, No. 24, 1929, pp. 817-824.

²⁶ "Die Stetigkeit des Abflusses bei scharfkantigen Wehren," by Th. Rehbock, *Der Bauingenieur*, Vol. 11, No. 48, 1930, pp. 821-826.

²⁷ Prin. Design Engr., Tippetts-Abbott-McCarthy-Stratton, New York, N. Y.; Lecturer in Civ. Eng., Columbia Univ., New York, N. Y.

The calibration of measuring devices should not generally be extrapolated beyond the range of observations. Figs. 1, 2, 3, and 4 show that the most important errors are a result of not appraising the correct approach velocity either because the bottom upstream of a weir has silted or because the gage was located incorrectly.

The disadvantages of the devices cited in the paper leads to the belief that the best field results can be expected from a device having the following characteristics:

1. No tendency to cause sediment deposition in the upstream channel;
2. Ability to produce the flow conditions required for the measurement by itself (that is, independence of the upstream section);
3. Sufficient accuracy under adverse conditions; and
4. Safe extrapolation of calibration within the range of conditions encountered in practice.

In most instances weirs and orifices fail to meet all these conditions. They may cause a rise in the level of the bottom of the canal, and care must be taken to maintain the specified upstream depth. In addition, the approach velocity depends on the section of the canal upstream from the weir, which may change as a result of silt deposition, weeds, or sliding of banks. The accuracy of weirs is affected directly by the off-laboratory conditions of irrigation operation. As a result, unless rather expensive precautions are taken when the weirs are installed or operated, their apparent simplicity is deceptive.

However, Venturi flumes are installed in such a manner that they do not cause an appreciable rise in the bottom elevation, thus avoiding most of the inconvenience derived from silt deposition. The flumes may be prefabricated easily to contain all the required approach conditions in a single unit. Because the flow meter acts as a control section, the discharge determines the upstream depth in the same way as for a weir under laboratory conditions.

In the United States the most commonly used critical flow meter is the Parshall flume. It is an excellent measuring device when it is used strictly within the range of discharges, heads, and dimension ratios originally used when calibrated. Usually calibrations cannot be extrapolated because the critical section is in a convergent canal. The discharge coefficients must change substantially unless the angle of convergence and the remaining geometrical parameters are kept equal or proportional.

A review of several types of critical flow meters developed in several European countries, India, and Argentina²⁸ showed that, in general, care was taken to define precisely the control or critical section in a long reach of rectangular and horizontal canal. The experiments of Giulio De Marchi and Francesco Contessini,²⁹ as well as the calibration by the writer of several models,²⁸ demonstrated that if this simple precaution is taken, even with the use of fairly abrupt transition curves at the entrance of the measuring section, meter equation fulfils the theoretical discharge relationship with an error of approxi-

²⁸ "Critical Flow Meters (Venturi Flumes)," by Armando Balloffet, *Proceedings Paper No. 748*, ASCE, July, 1955.

²⁹ "Dispositivo per la misura della portata dei canali con minima perdita di quota," by Giulio De Marchi and Francesco Contessini, *L'Energia Elettrica*, January, 1936-March, 1937.

mately 5% or less. This degree of precision is satisfactory in many field installations. The discharge coefficient to correct the theoretical equation was determined with an error of about 1%. In the writer's experiments, several models showed a remarkable constancy of this empirical discharge coefficient with respect to discharge.

The theoretical equation is based on the critical flow on the control section of the meter. If this section is well defined, the Froude number upstream from the section is related to the discharge coefficient by a numerical constant. If the Froude analogy is accomplished when the calibration results are extrapolated to a different meter, the discharge coefficients should be equal. The results of field calibration of one such meter with a discharge that was thirty-nine times the maximum laboratory discharge and a ratio of upstream depth to approach width that was 60% greater showed no difference in discharge coefficients beyond the range of experimental errors (approximately 1.5%).²⁹

The independence of the discharge coefficient from the approach depth-to-width ratio has also been reported by H. R. Vallentine for sharp-edged contractions.³⁰ This property applies mostly to models with plane bottom between the gage section and the critical section.

Due to the relatively negligible difference between the theoretical equations and the actual equations when the critical section is well defined, Corrado Ruggiero and Piero Giudici³¹ designed meters to fulfil a prescribed error law for a wide range of discharges. This law caused the magnitude of the errors in discharge due to inaccurate gage readings to be an inverse function of the annual discharge frequency. The meters could give a weighted indication of the volumes measured throughout the year. Although the critical sections for those meters were not rectangular, laboratory tests showed a fairly satisfactory agreement between the predicted and the experimental rating curves.

Finally, because most of the accelerated and curvilinear flow is close to or within the narrowed section, the location of the measuring scale in this type of meter need not be as precise as for the Parshall flumes.

CHARLES W. THOMAS,³² M. ASCE.—The necessity for obtaining continuous records or representative head observations if accuracy is to be maintained has been emphasized further by Mr. Starosolszky. Presumably, each curve in the three families of curves shown in Fig. 7 represents a different daily percentage variation in differential head at the Venturi meter. However, the curves do not indicate what assumptions were made in computing each one.

In the case of a weir, the discharge varies more rapidly than the head. The relationship given by many weir formulas shows that the discharge varies as the $3/2$ power of the head. Therefore, the volume of discharge obtained by reading the gage at intervals and averaging the readings will yield a discharge that is somewhat less than that actually passing the weir.

²⁹ "L'écoulement dans des canaux rectangulaires présentant une section rétrécie," by H. R. Vallentine, *La Houille Blanche*, January-February, 1958.

³¹ "Sui misuratori di portata a grande campo di variabilità," by Corrado Ruggiero and Piero Giudici, *L'Energia Elettrica*, April, 1952.

³² Hydr. Engr., Bureau of Reclamation, U. S. Dept. of the Interior, Denver, Colo.

Assuming an initial head of zero (H_0) and a uniform rise to a depth H_2 at the end of the time interval, T , Robert E. Horton³³ showed that the ratio of discharge by integration is

$$\frac{\text{Volume by average head}}{\text{Actual volume}} = \frac{(\frac{1}{2})^{\frac{1}{2}}}{\frac{1}{2}} = 0.884$$

or the true discharge equals 1.13 times the discharge obtained by using the average head for the two readings taken at the beginning and end of the period.

This percentage of error will be the same regardless of maximum head (H_2) and for a rising stage or falling stage if the initial head (H_0) is zero. The error resulting from computing the discharge using the mean head will decrease as the ratio H_1/H_2 increases if there is an initial depth of flow, H_1 , over the weir. The percentage of error will decrease as the readings per time interval are increased and approach zero, as for continuous records.

Short period surface fluctuations approach wave conditions. Arnold H. Gibson³⁴ has shown that wave disturbance increases the discharge over a weir. When waves are present the discharge can be expressed as $(1 + K)$ times the discharge under the same observed head with undisturbed water in the approach channel. The values of K derived by Mr. Gibson are:

With waves of sinusoidal form, for a thin-crested rectangular weir,

$$K = 0.19 \left(\frac{a}{H} \right)^2 \dots \dots \dots (12)$$

and for a 90° V-notch weir,

$$K = 0.94 \left(\frac{a}{H} \right)^2 \dots \dots \dots (13)$$

In Eqs. 12 and 13, a is equal to one-half the wave length.

With waves of trochoidal form the effect is less than with sinusoidal waves. The value of K for rectangular weirs varies from $0.070 (a/H)^2$ to $0.182(a/H)^2$ for ratios of wave length over wave height varying from 3.14 (sharp-crested wave) to 15.0, respectively. For the same range of length-height ratios the value of K varies from $0.50 (a/H)^2$ to $0.92 (a/H)^2$, respectively, when applied to a 90° V-notch weir.

The error is negative as in many of the instances cited in the paper. Thus, when waves are present more water is delivered through the weir notch than the gage readings of the mean water level indicate.

With respect to the comments by Mr. Kolupaila, the purpose of the paper was to emphasize some of the reasons why measurements made in connection with the conveyance and delivery of irrigation water may not be as accurate as assumed. Also it was intended to indicate the order of magnitude of the error resulting from a few common deviations from accepted practice in the

³³ "Weir Experiments, Coefficients and Formulas," by Robert E. Horton, *Water Supply and Irrigation Paper No. 200*, Geological Survey, U. S. Dept. of the Interior, Washington, D. C., 1907.

³⁴ "The Effect of Surface Waves on the Discharge Over Weirs," by Arnold H. Gibson, *Selected Engineering Papers No. 99*, Inst. C. E., London, 1930.

general use of standard devices in the field. Much material has been and is being written on weirs. These devices have been subject to more hydraulic laboratory investigations than any others. Space limitations prohibit a complete list of references for weirs and other field measurement devices.

Engineers in the United States appreciate fully the value of writings done in other countries. Many articles by European engineers on weirs and other subjects have been studied and translated in full or abstracted, and the contents are well known. For example, the paper by Hailer²⁹ has been translated, and the work of Schoder and Turner⁹ can be considered an international symposium on sharp-crested weirs and a review of earlier European material.

The statement by Mr. Balloffet that "the measurement error begins with an improper selection of the measuring device" merits extensive consideration. The selection of the proper measurement device to best fit the physical conditions at the site would solve many operating problems. With respect to economics, the cost of a structure should be considered to include more than initial cost or first cost. To operate and maintain a weir installation in such condition that it will give reasonably accurate results is usually expensive.

A Venturi flume can measure a wide range of discharges accurately, and, for this reason, should be used more extensively. This type of device has been studied and is recognized on an international basis, as for example the interesting flow relationships in these devices established by Friedrich V. A. E. Engel.^{35,36}

²⁹ "Non-uniform Flow of Water," by Friedrich V. A. E. Engel, *The Engineer*, April 21 and 28, 1933; May 5, 1933.

³⁵ "The Venturi Flume," by Friedrich V. A. E. Engel, *ibid.*, August 3 and 10, 1934.

AMERICAN SOCIETY OF CIVIL ENGINEERS

Founded November 5, 1852

TRANSACTIONS

Paper No. 2981

FLOW OF NATURAL GAS IN PIPELINES

BY WILLIAM T. IVEY,¹ M. ASCE, AND JAMES H. DOROUGH²

SYNOPSIS

Test data derived from more than two hundred tests made on pipelines and conclusions resulting from examination of the data are presented.

Consideration is given to the various flow formulas in the design of natural-gas-transmission pipelines, and to the performance ratings of these lines. Generally, all formulas are derived from the general energy equation, the basic differences being found in the methods of considering the friction coefficient and in the adjustment for the deviation of gases for supercompressibility. After all adjustments are made, each formula assumes the incorporation of an "efficiency factor" to record the deviation of the formula from a selected norm, although no basic norm, or perfect operating condition, has been determined by the industry.

The need for a norm in the form of a standard formula based on maximum possible efficiency of operation, against which actual line performance may be compared, is emphasized. The merits of a proposed form for this standard equation are presented herein. Each of the basic differences is examined in order to attempt to simplify the mechanical application of the formula, and to permit its more rapid use by manual application and digital computers. Thus, the examination of the many problems presented by increasingly complicated pipeline networks will be more rapid and thorough.

HISTORY

The history of the development of formulas for flow of gas in pipelines began in approximately the early 1900's. The earlier applications did not consider deviation and generally applied a constant friction coefficient. Such formulas were proposed by William Cox (1902) and E. A. Rix (1904). Other early formulas, which expressed the friction coefficient as a function of the diameter, were proposed by F. H. Oliphant (1904), W. C. Unwin (1904),

NOTE.—Published, essentially as printed here, in March, 1957, in the Journal of the Pipeline Division, as *Proceedings Paper 1194*. Positions and titles given are those in effect when the paper was approved for publication in *Transactions*.

¹ Chf. Statistician and Planning Engr., Southern Natural Gas Co., Birmingham, Ala.

² Planning Engr., Southern Natural Gas Co., Birmingham, Ala.

T. R. Weymouth (1912), Pacific Coast Gas Association (1925), and J. M. Spitzglass (1926). A third group of formulas, which expressed the friction coefficient as a function of the Reynolds criterion (a factor considering diameter, velocity, density, and viscosity), was proposed by O. Fritzsche (1908), Charles H. Lees (1914), C. M. White (1929), and W. H. McAdams and T. K. Sherwood (1926). The Panhandle formulas fall into this category by making the friction coefficient a function of the Reynolds number with a constant viscosity factor.

The first attempt to produce a standard formula was made in 1935 by T. W. Johnson and W. B. Berwald.³ Numerous data on gas flow through commercial transmission lines were obtained and analyzed. This was probably the most thorough and comprehensive analysis of flow of gas in pipelines to that date. Johnson and Berwald concluded that for the larger diameter lines (free from condensates and other foreign materials) operating under steady flow conditions, the metered rates of delivery agreed more closely with the rates computed from Weymouth's formula than with those computed from any of the other formulas. In almost every test under these conditions, the volume computed from Weymouth's formula was within a small percentage of the metered delivery. Further experiments were recommended—these to be under actual conditions of natural gas transmission.

The work of Johnson and Berwald was extended in 1956 by R. V. Smith, J. S. Miller, and J. W. Ferguson.⁴ The intent was primarily to present the results of tests conducted on experimental pipelines, and to apply these data to a further improvement of the flow formula. Tests were made on experimental pipelines constructed of 2-in., 4-in., 6-in., and 8-in. seamless pipe, 8-in. welded pipe, and a specially prepared 3-in. superfinished pipe. The friction coefficient, f , was redefined as the "resistance coefficient," and a new factor ($\sqrt{1/f}$) termed the "transmission factor" was introduced.

Transmission factors for the various experimental pipelines were determined, and relationships were established between the transmission factors, the Reynolds numbers, the absolute roughness, and the internal radius of the pipe. Reynolds numbers for these determinations of transmission factors ranged from 49,900 to 36,000,000. At Reynolds numbers ranging from 250,000 to approximately 850,000, transmission factors for the 2-in. seamless pipe were found to be related to the Reynolds numbers, the internal radius of the pipe, and the absolute roughness of the internal surface of the pipe. At Reynolds numbers greater than 850,000, the transmission factors were constant and independent of the Reynolds number, being influenced only by the absolute roughness and the internal radius of the pipe. For larger diameters, extrapolated data indicated that the break between transition and fully rough flow moved to higher Reynolds numbers.

Field tests of pipeline flow efficiency conducted in 1952 and 1953 disclosed inconsistencies in the data resulting from differences in measuring technique. To satisfy the need for the proper evaluation of field measurement procedures

³ "Flow of Natural Gas through High-Pressure Transmission Lines," by T. W. Johnson and W. B. Berwald, *Monograph No. 6*, Bureau of Mines, U. S. Dept. of the Interior, Washington, D. C., February, 1935.

⁴ "Flow of Natural Gas through Experimental Pipelines and Transmission Lines," by R. V. Smith, J. S. Miller, and J. W. Ferguson, *Monograph No. 9*, Bureau of Mines, U. S. Dept. of the Interior, Washington, D. C., 1956.

and criteria for judging the validity of field data, a set of preliminary recommendations for efficiency testing was developed in 1954. In May, 1956, a formal procedure for pipeline efficiency testing was presented by Richard F. Bukacek and R. T. Ellington.⁵

In February, 1958, Ellington, Bukacek, and W. R. Staats,⁶ reported pipeline-flow-efficiency test data for sixteen natural-gas-transmission pipelines ranging from 12 in. to 36 in. in diameter. They concluded that, within experimental error, pipeline transmission factors are independent of flow rate for fully developed turbulent flow, which is represented by the operating conditions encountered normally.

THE BASIC FORMULA

Notation.—The letter symbols adopted for use in this paper are defined where they first appear, in the illustrations or in the text, and are arranged alphabetically, for convenience of reference, in Appendix II.

General.—Much information is available in the literature on flow of gas in pipelines. Numerous formulas are offered for practical solutions of the problem. They all originate from the basic flow equation as derived from the general energy equation. The basic derivation of the general flow formula appears in the work of Johnson and Berwald.³

The general flow formula is

$$Q = K \frac{T_0}{P_0} \left[\frac{(P_1)^2 - (P_2)^2}{G T L f} d^5 \right]^{\frac{1}{2}} \dots \dots \dots (1)$$

in which Q is the flow of gas, in cubic feet per hour at pressure base, P_0 , and temperature base, T_0 ; K represents the numerical constant, 1.6156; T_0 denotes the temperature base, in degrees Fahrenheit absolute, defining 1 cu ft of gas; P_0 indicates the pressure base, in pounds per square inch absolute, defining 1 cu ft of gas; P_1 signifies the inlet pressure, in pounds per square inch absolute; P_2 is the outlet pressure, in pounds per square inch absolute; d represents the internal pipe diameter, in inches; G denotes the specific gravity of the gas (air = 1.000); T indicates the temperature of the flowing gas, in degrees Fahrenheit absolute; L signifies the pipe length, in miles; and f is the coefficient of friction.

The foregoing gives no recognition to the deviation factor, which is recognized by Smith, Miller, and Ferguson⁴ as follows:

$$Q = K \frac{T_0}{P_0} \sqrt{1/f} \sqrt{1/Z} \left[\frac{(P_1)^2 - (P_2)^2}{G T L} d^5 \right]^{\frac{1}{2}} \dots \dots \dots (2)$$

in which f represents the dimensionless resistance coefficient; $\sqrt{1/f}$ denotes the dimensionless transmission factor; and Z is the dimensionless average effective compressibility factor of gas. In order to establish a clear and concise termi-

⁵ "Procedures for Pipeline Efficiency Testing," by Richard F. Bukacek and R. T. Ellington, Operating Section, Transmission Committee, Am. Gas Assn., Gas Supply, Transmission and Storage Conference, Chicago, Ill., May, 1956.

⁶ "Flow Phenomena in Large Diameter Natural Gas Transmission Lines," Project N.B.-13, Extension for the Pipeline Research Committee, Am. Gas Assn., New York, N. Y., February, 1958.

TABLE 1.—PIPELINE

Test no.	Volume	<i>d</i>	$(P_1)^2 - (P_2)^2$	<i>P</i>	Elevation factor	Specific gravity
	(1)	(2)	(3)	(4)	(5)	(6)
1	183,332*	23.500	19,934	717	-3.896	0.594
10	184,761	23.500	26,488	692	-1,392	0.594
20	178,631	23.500	15,373	516	619	0.594
30	167,563	21.375	34,378	321	-280	0.596
40	145,409	23.188	15,249	748	-2,414	0.608
50	185,681	21.375	17,615	333	-318	0.587
60	182,313	21.375	31,479	410	-606	0.588
70	229,176	17.375	105,234	878	-641	0.585
80	170,053*	17.375	79,992	1,148	-2,854	0.588
90	114,836	19.313	35,197	898	...	0.599
100	111,168	19.313	25,117	989	...	0.604
110	237,469	23.188	58,351	822	-9,951	0.596
120	131,623	19.313	24,602	943	...	0.581
130	108,542	13.375	154,849	905	1,201	0.615
140	102,460	15.438	52,494	801	-694	0.572
150	104,000	15.438	31,761	615	936	0.570
160	173,614	15.375	127,900	970	387	0.568
170	36,508	10.250	27,209	293	331	0.600
180	142,800	17.375	69,769	762	3,346	0.570
190	171,861	21.375	39,789	394	-1,472	0.578
200	125,476	17.375	33,367	452	...	0.583
210	255,524	17.375	141,968	1,135	-1,898	0.563
220	248,498	17.375	100,154	1,044	6,069	0.568
230	118,193	19.313	24,466	947	-1,251	0.594

* Measured by metered flow, all others measured by ammonia tracer.

nology, the definition of f was changed from coefficient of friction to resistance coefficient, and the new term, $\sqrt{1/f}$, was introduced.

Eq. 2 is the basic flow equation from which all other formulas are derived. At this stage, theory yields to the laboratory or field test in the evaluation of the f -term or the term that will bring the equation into balance. Three basic approaches have been used in the determination of the various proposed formulas: (1) The application of the friction factor or resistance coefficient as a constant, (2) its application as a function of the pipe diameter only, and (3) as a function of the Reynolds number.

REYNOLDS NUMBER

The Reynolds criterion, a dimensionless ratio used to characterize the conditions of fluid flow in circular pipes, is

$$R = \frac{d U \rho}{\nu} \dots \dots \dots (3)$$

in which R is the Reynolds number; d is the internal diameter of the pipe; U denotes the average linear velocity; ρ represents the density of fluid; and ν signifies the viscosity.

Osborne Reynolds⁷ observed that, at low velocities, flow proceeded in a steady straight line, in which it appeared that all the particles moved parallel to the walls of the tube. As velocities increased, the characteristics of the

⁷"An Experimental Investigation of the Circumstances which Determine Whether the Motion of Water Shall be Direct or Sinuous, and of the Law of Resistance in Parallel Channels," by Osborne Reynolds, *Philosophical Transactions*, Royal Soc. of London, Vol. 174, 1883, pp. 935-982.

TESTING PROGRAM

Absolute temperature	Deviation factor	Pipe length, in miles	Gas viscosity	Reynolds number	Resistance coefficient $\times 10^4$	Transmission factor
(7)	(8)	(9)	(10)	(11)	(12)	(13)
518	0.890	9.897	7.78	8,060,056	2.363	20.572
521	0.899	14.935	7.80	8,102,073	2.373	20.528
522	0.924	8.778	7.55	8,092,374	2.688	19.288
525	0.954	14.873	7.40	8,543,495	2.280	20.943
534	0.894	9.918	8.17	6,314,806	2.639	19.466
530	0.956	6.198	7.54	9,151,331	2.266	21.007
531	0.945	11.876	7.58	8,953,401	2.291	20.892
534	0.889	7.477	8.55	12,211,968	2.844	18.751
542	0.864	11.890	10.20	7,634,599	2.411	20.366
556	0.882	15.631	8.64	5,578,449	3.052	18.101
529	0.861	12.638	8.71	5,401,379	2.930	18.474
528	0.885	14.846	8.18	10,097,005	2.609	19.578
521	0.872	9.048	8.37	6,401,670	3.024	18.185
517	0.854	13.928	8.20	8,235,868	2.778	18.973
529	0.900	11.031	8.15	6,303,211	2.656	19.404
527	0.920	6.683	7.80	6,661,518	2.700	19.245
529	0.879	9.427	8.66	10,022,005	2.747	19.080
533	0.959	5.360	7.52	3,845,615	3.000	18.257
535	0.908	15.452	8.21	7,721,346	2.494	20.024
537	0.951	14.507	7.69	8,177,952	2.520	19.920
544	0.945	7.450	7.89	7,220,804	2.829	18.801
551	0.885	8.872	10.30	10,877,906	2.616	19.551
533	0.877	7.694	9.30	11,820,038	2.500	20.000
531	0.872	11.651	8.63	5,700,126	2.600	19.611

flow changed critically and a turbulence appeared. Smith, Miller, and Ferguson⁴ noted a change in the relationship between the transmission factor and the Reynolds number as this critical point was reached. They stated that the transmission-factor variation for the experimental data on a 2-in.-diameter pipe depended on Reynolds numbers only for ranges of from 49,900 to 250,000. At Reynolds numbers ranging from 250,000 to approximately 850,000, transmission factors were related to the Reynolds numbers, the internal pipe radius, and the absolute roughness of the internal pipe surface. At Reynolds numbers greater than 850,000 for the pipes considered, transmission factors were constant and independent of Reynolds numbers. They were influenced only by the absolute roughness and the internal diameter of the pipe. For larger diameters, extrapolated data indicated that the break between transition and fully rough flow moved to higher Reynolds numbers. Smith, Miller, and Ferguson⁴ interpreted the three areas of flow as smooth, transition, and fully rough, which compares with Reynolds observations of steady and turbulent areas of flow.

CONSIDERATION OF TEST DATA

During 1955 and 1956, careful tests have been conducted on pipelines whose sizes ranged from 10 in. to 24 in., inclusive. Flow was metered whenever possible and checked by an ammonia tracer. Because of the variable distances of orifice measurement from the point of test, the ammonia-tracer method was found to yield more consistent results. An abstract of these tests is given in Table 1. A complete set of data is available elsewhere.⁸ Table 1 shows

⁸ "Flow of Natural Gas in Pipelines," by William T. Ivey and James H. Dorrough, *Proceedings Paper 1194*, ASCE, March, 1957, pp. 14-24.

volumes of gas expressed in thousands of cubic feet per day at a pressure base of 14.73 lb per sq in. absolute, being measured by an ammonia tracer. When ammonia-tracer measurement was not available, metered flow was used, and the values so obtained are referenced in the table. Also indicated in Table 1 are the measured flow; the internal pipe diameter, d , in inches; the difference between the squares of the initial and terminal absolute pressures ($P_1^2 - P_2^2$); the average absolute pressure in the test section, P ; the specific gravity of the gas; the absolute temperature; the deviation factor; and the gas viscosity. An adjustment made for the elevation is cited in Table 1. Computations are made for the Reynolds number, the resistance coefficient, and the transmission factor.

Certain conclusions are immediately evident:

1. Two hundred and thirty-three tests were conducted in the actual operation of a large transmission system.³ Under varying ranges of normal operating conditions, results were obtained from varying lengths of pipe ranging in nominal size from 10 in. to 24 in. and under pressures ranging from a 300-lb-per-sq-in. gage to a 1,200-lb-per-sq-in. gage.

During the entire series, Reynolds numbers varied from 2,202,511 for one 12-in. pipe to 13,272,727 for one 18-in. pipe. That is, all the tests showed Reynolds numbers in ranges much higher than corresponding numbers in the smooth and transition ranges previously defined.⁴ They were also considerably greater than the Reynolds number that defines the limit above which transmission factors are influenced only by the absolute roughness and internal diameter.⁴ The conclusion that normal pipeline operation need not be concerned with the Reynolds criterion, but only with diameter and absolute roughness, was verified further by Ellington, Bukacek, and Staats.⁶

2. From the available test data, plots made of the transmission factor against the Reynolds number for 16-in., 18-in., and 24-in.-diameter pipes show a broad band of points at each Reynolds number. No clearly defined relationship is shown between the Reynolds number and the transmission factor within the range of the tests.

If the influence of the Reynolds number is not felt in rough, turbulent flow, but instead if the transmission factor is influenced only by the absolute roughness and internal diameter, the data should be examined by sizes of pipe, and roughness factors should be computed for each pipe size. The formula used by Smith, Miller, and Ferguson is the resistance equation,

$$\sqrt{\frac{1}{f}} = 4 \log \frac{7.4 r}{k} \dots \dots \dots (4)$$

in which r is the internal radius of the pipe, in inches, and k represents the absolute roughness coefficient. The results of this examination are shown in Table 2.

Each line in Table 2 represents a group of tests on a single pipeline of the same diameter and in the same continuing run of pipeline. For convenience the nominal pipe size is shown in Col. 3, but all computations are based on the internal diameter shown in Col. 4. The number of tests made and the maxi-

imum, minimum, and average transmission factors are shown for each group of tests. The absolute roughness factor is computed by Eq. 4, on the assumption that all Reynolds numbers exceed the critical criteria for rough, turbulent flow, and, therefore, that the transmission factor is a function of the diameter and the absolute roughness only.

Line 1 in Table 2 shows the results of twenty tests on a new, welded 24-in. pipeline operating in the range of from a 500-lb-per-sq-in. gage to a 750-lb-

TABLE 2.—COMPARISON OF TRANSMISSION FACTORS
AND ABSOLUTE ROUGHNESS COEFFICIENTS

Condition	Line	PIPE SIZE, IN INCHES		Number of tests	TRANSMISSION FACTOR			Absolute roughness coefficient $\times 10^6$
		Nominal outside diameter	Inside diameter		Minimum	Maximum	Average	
(1)	(2)	(3)	(4)	(5)	(6)	(7)	(8)	(9)
GOOD	1	24	23.500	20	19.741	20.933	20.195	0.777
	2	22	21.375	11	19.630	20.945	20.160	0.721
	5	22	21.375	18	19.245	21.320	20.413	0.624
	17	18	17.375	4	19.830	19.940	19.875	0.691
	23	16	15.438	5	18.945	19.745	19.432	0.792
	24	18	17.375	5	18.709	20.024	19.645	0.789
DIRTY	33	18	17.375	17	18.676	20.357	19.706	0.761
	3	20	19.313	8	16.265	18.818	17.591	2.596
	4	24	23.188	6	17.565	19.803	19.026	1.503
	7	12½	12.125	4	18.257	19.518	18.893	0.848
	8	20	19.313	16	17.678	19.952	18.921	1.329
	9	24	23.188	6	16.860	20.240	19.207	1.354
FIELD LINES	10	14	13.375	1	15.811	5.518
	11	16	15.375	1	18.257	1.552
	12	12½	12.125	1	16.514	3.372
OLD	25	20	19.250	2	17.140	17.321	17.230	3.509
	26	22	21.375	10	16.391	21.063	19.288	1.191
	27	18	17.600	2	18.098	18.257	18.178	1.848
	28	22	21.375	4	17.874	19.563	18.709	1.663
	29	18	17.375	4	18.411	19.121	18.768	1.307
	30	22	21.375	1	19.415	1.075
VARIES	6	18	17.375	22	18.315	20.528	19.350	0.935
	13	20	19.313	9	16.566	19.642	18.846	1.389
	14	20	19.313	2	18.474	20.228	19.351	1.038
	15	14	13.375	2	17.413	19.668	18.752	1.015
	16	16	15.438	13	17.413	19.668	18.752	1.015
	18	16	15.438	7	18.788	19.691	19.400	0.807
	19	16	15.438	1	19.245	0.882
	19	18	17.375	4	19.181	19.462	19.355	0.932
	20	16	15.375	9	18.380	20.000	19.211	0.950
	21	12½	12.250	3	18.898	20.000	19.503	0.603
	22	10½	10.250	4	18.257	20.000	18.896	0.716
	31	24	23.390	1	20.000	0.865
	32	24	23.500	4	18.452	18.966	18.688	1.850
	34	20	19.313	8	17.639	19.877	18.620	1.581

per-sq-in. gage. The transmission factor varies with the average value of 20.195 by less than $\pm 3\%$. This line was installed in 1953 and 1954 and has operated on clean gas for the entire period. Smith, Miller, and Ferguson reported absolute roughnesses of from 0.000553 to 0.00185, and used an absolute roughness factor of 0.0007 in computing the limits of the transition region. This compares favorably with the computed absolute roughness coefficient of 0.000777.

For the purpose of this analysis, it can be assumed that an absolute roughness of 0.000777 and a transmission factor of 20.000 for a 24-in. pipe indicates a line operating at high efficiency.

Lines 1, 2, 5, 17, 23, 24, and 33 indicate absolute roughness factors of between 0.000624 and 0.000792. All these tests may be interpreted as tests on pipes in good condition and operating efficiently.

Lines 3, 4, 7, 8, and 9 show absolute roughness factors of between 0.000848 and 0.002596. These lines are known to have contained foreign material, presumably liquids, at the time of the tests.

Lines 10, 11, and 12 were tests on field-gathering lines that had received liquids from time to time. These tests can be presumed to show results on lines that have operated at poor efficiency.

Lines 25 to 30, inclusive, record tests on the oldest section of the system, a great part of which consisted of coupled lines. These lines have operated for several years. Presumably, the results indicate greater roughness due to age and type of construction. Thus, a range of absolute roughness factors can be determined to show operating conditions from maximum efficiency to poor efficiency.

It is concluded that for the tests considered the condition of the pipeline, with respect to liquids or other foreign matter and with respect to the age of the pipeline and type of construction, inclusion of couplings, valves, and cross connections, has a much greater influence on the transmission factor than the pipe diameter or Reynolds criterion.

TABLE 3.—TRANSMISSION
FACTORS FOR ROUGH,
TURBULENT FLOW

Inside diameter, in inches	Transmission factor ^a
(1)	(2)
4.125	17.362
6.125	18.048
8.125	18.539
10.250	18.943
12.250	19.253
13.500	19.421
15.375	19.647
17.375	19.890
19.3125	20.043
21.250	20.209
23.1875	20.361
25.125	20.500
29.125	20.757

^a Transmission factor = $\sqrt{f}/f = 4 \log d + 14.9$, $k = 0.0007$.

THE DILEMMA OF THE GAS INDUSTRY

It is apparent from the foregoing that it is not possible to specifically express the percentage efficiency of a pipeline without a basic norm or standard base of reference. Each gas transmission company rates its pipelines according to its own formula (assuming friction coefficients based on either Reynolds numbers or pipe diameters), and on roughness coefficients related or unrelated to diameters. A line that may be rated at high efficiency by one formula will be rated

at a low efficiency by another. In fact, using some formulas, a line may be rated at more than 100% efficiency.

It is evident that line efficiency cannot be adequately determined by friction coefficients based on a constant without reference to line size. It also appears that in many actual operating conditions the friction coefficient or the transmission factor is independent of the Reynolds number. It could be assumed that a practical solution for commercial pipelines under normal operating conditions is in the area of high Reynolds numbers, with transmission factors based on diameters and absolute roughness only.

Smith, Miller, and Ferguson⁴ suggest a tentative average absolute roughness of 0.0007, and agree that for fully rough flow the transmission factor is not a function of the Reynolds number. On this basis, transmission factors are computed for varying pipe diameters in Table 3.

Such transmission factors are not presented as final, but are suggested as probably being representative of transmission factors for turbulent flow in areas of high Reynolds numbers. The acceptance of a basic absolute roughness coefficient for a pipe of maximum practical smoothness will permit the determination of transmission factors that might be used as standards of maximum line efficiency.

THE DEVIATION FACTOR

It has been shown that natural gas does not follow the ideal gas relationship. At high pressures, greater volumes of gas may be compressed into a given space than the ideal gas laws indicate. Failure to recognize this deviation in the past has not introduced a material error because of the low pressures at which earlier pipelines operated. However, with continuing increases in operating pressures, recognition of this deviation or supercompressibility characteristic of the gas becomes more and more important.

This subject has been examined thoroughly by George G. Brown,⁵ who explains that although numerous equations of state have been proposed, the most convenient method for computing the pressure-volume-temperature relationship of natural gas is by the use of the so-called compressibility factor, which represents the deviation of the gas in question from the ideal gas laws, as expressed by

$$P V = Z N R T \dots \dots \dots (5)$$

in which P is the pressure, in pounds per square inch absolute; V denotes the volume, in cubic feet; N represents the number of mol-pounds; and R is a constant value of 10.71 for all gases.

The compressibility factor, Z , is a dimensionless intensive factor independent of the extent or weight of the gas, and is determined by the characteristics of the gas, the temperature, and the pressure. Once Z is known or determined, the computation of the pressure-temperature-volume relationship can be made with as much ease at high pressure as at low pressure.

According to the theorem of corresponding states, the deviation of an actual gas from the ideal gas law is the same for different gases when at the same corresponding state. These conditions are found at the identical fraction of the absolute critical temperature and pressure, which are known, respectively, as

$$T_r = \frac{T}{T_c} \dots \dots \dots (6)$$

and

$$P_r = \frac{P}{P_c} \dots \dots \dots (7)$$

in which T_c is the absolute critical temperature; P_c represents the absolute critical pressure; T_r denotes the reduced temperature; and P_r signifies the reduced pressure.

⁵ "Natural Gas Under Pressure," by George G. Brown, *Proceedings, Natural Gasoline Assn. of America*, Tulsa, Okla., May, 1940.

Critical temperature is defined as the temperature above which a pure gas cannot be liquefied by pressure only. Critical pressure is defined as the pressure below which a pure gas can exist in a gaseous state in equilibrium with its liquid.

Therefore, if the theorem of corresponding states can be applied without appreciable error, all gases would have the same value of Z at equally reduced temperature and pressure. A plot of Z for methane, as a function of reduced temperature and pressure, can be applied to determine the unknown value of Z for some other gas if the critical temperature and pressure of the second gas are known or can be determined. Such a plot for methane and natural gas was presented by Brown⁹ and has been widely used in industry in the determination of compressibility factors.

Based on this chart, deviation factors are determined for each of the various gas mixtures found in the system on which gas tests were made. Characteristics of the gas considered are determined by laboratory analysis. Individual absolute critical temperatures and pressures of each constituent are determined, and the pseudoreduced temperature for the mol-fraction is computed. The arithmetic total of these fractions results in the absolute pseudocritical temperature and absolute pseudocritical pressure for the gas mixture. From these values the pseudoreduced temperatures and pseudoreduced pressures for varying actual temperatures and pressures are determined. The deviation factors can then be read from the chart. As noted by Brown,⁹ the value of Z depends on experimental data for its determination, as do all correction factors.

The standard apparatus used for determining supercompressibility experimentally is either one developed by E. S. Burnett or by H. S. Bean. The latter apparatus consists of a high-pressure gas bomb of known volume and a calibrated burette for measuring the volume of the gas at atmospheric pressure. It is simply an adaptation of the classic laboratory procedure of expanding an unknown quantity of gas in successive increments from a high-pressure bomb into a calibrated burette at essentially atmospheric pressure, and computing the total volume from a summation of these increments. The operation is tedious and undependable because one mistake can ruin the whole run. The Burnett apparatus consists of two adjacent high-pressure chambers of a known volume ratio, the gas being expanded from the first chamber into the evacuated second chamber, with successive expansions being made after re-evacuation of the second chamber. The deviation of the gas is computed from a comparison of the volume ratio of the chambers to the pressure ratio before and after the expansion. The operation is easy and not conducive to mistakes, and the methods are comparatively accurate, agreeing to within approximately 0.1%. Due to the ease of operation, the Burnett apparatus is preferred.

In 1955 data were prepared¹⁰ based on the specific gravity method of supercompressibility-factor determination. Tables were prepared for supercompressibility factors, F_{ps} , for natural gas considering (a) nominal temperatures of from 0°F to 180°F; (b) specific gravity from 0.554 to 0.750; and (c) pressures of from a 0-lb-per-sq-in. gage to a 3,000-lb-per-sq-in. gage. Separate

¹⁰ "Supercompressibility Factors for Natural Gas," A.G.A. Supv. Committee for PAR Project NX-7 and ASME Research Committee on Fluid Meters, *Promotion, Advertising and Research Project NX-7*, Am. Gas Assn., New York, N. Y., June, 1955.

tables were also included for determining supercompressibility factors for natural gas containing nitrogen and carbon dioxide.

A relationship between F_{pv} and Z may be derived as follows: By definition,

$$F_{pv} = \sqrt{\frac{NRT}{PV}} \dots \dots \dots (8)$$

Rearranging Eq. 5,

$$\sqrt{\frac{1}{Z}} = \sqrt{\frac{NRT}{PV}} \dots \dots \dots (9)$$

Therefore, combining Eqs. 8 and 9 results in

$$F_{pv} = \sqrt{\frac{1}{Z}} \dots \dots \dots (10)$$

TABLE 4.—COMPARISON OF DEVIATION FACTOR, Z ,
OF A SAMPLE GAS

Pressure, in pounds-per square-inch gage	Z , at 60°F	$1/Z$ at 60°F	$\sqrt{1/Z}$	F_{pv}
(1)	(2)	(3)	(4)	(5)
100	0.983	1.0173	1.0086	1.0083
200	0.967	1.0341	1.0169	1.0164
300	0.950	1.0526	1.0260	1.0246
400	0.934	1.0707	1.0347	1.0329
500	0.918	1.0893	1.0437	1.0416
600	0.903	1.1074	1.0523	1.0501
700	0.890	1.1236	1.0600	1.0589
800	0.876	1.1416	1.0685	1.0677
900	0.862	1.1601	1.0771	1.0763
1,000	0.848	1.1792	1.0859	1.0847
1,100	0.837	1.1947	1.0930	1.0933
1,200	0.825	1.2120	1.1009	1.1015

Table 4 compares Z -factors computed by the Brown method with (F_{pv})-factors. The differences are negligible, and it can be concluded that deviation factors can be determined by either method.

A PROPOSED FORMULA FOR FLOW OF NATURAL GAS

For a design formula applicable to the normal commercial use of pipelines in good condition, the following basic flow equation may be used:

$$Q = K \frac{T_0}{P_0} \sqrt{\frac{1}{f}} \sqrt{\frac{1}{Z}} \left[\frac{(P_1)^2 - (P_2)^2}{G T L} d^5 \right]^{1/2} \dots \dots \dots (11)$$

For normal use a constant, K_1 , may be determined in order to include all constant factors, including the diameter and the transmission factor, and a table prepared to give K_1 for each diameter. The equation then becomes

$$Q = K_1 \sqrt{\frac{1}{Z}} \left[\frac{(P_1)^2 - (P_2)^2}{L} \right]^{1/2} \dots \dots \dots (12)$$

In most applications, the factor $\sqrt{1/Z}$ is considered to be the deviation for the gas at the mean effective pressure between the initial and terminal pressure.

A compressibility factor can be determined, as fully outlined in Appendix I, which can be applied directly to the pressure. The modified flow formula becomes

$$Q = K_1 \left[\frac{(P_1 b_1)^2 - (P_2 b_2)^2}{L} \right]^{\frac{1}{2}} \dots \dots \dots (13)$$

A plot of deviation factors for a representative gas can be determined for varying pressures, and a tabulation can be prepared in order to adjust the actual pressure to an adjusted pressure, recognizing the deviation factor.

Thus, through the use of a table of constants taking into account the diameter and the transmission factor for each pipe size, as well as another table giving squares of absolute pressures adjusted for the deviation of a typical gas for varying gage pressures, the formula can be applied readily without graphs, charts, logarithms, or trial-and-error methods. It can be handled rapidly in manual operation with the use of a desk calculator, or it can be keyed into the operation of any of the basic digital computers.

In this manner and with digital computers, it is possible to examine more rapidly and thoroughly many complicated construction and operation problems.

CONCLUSIONS

Different formulas have been presented for determining the flow of gas in pipelines. All are derived from the basic flow equation. The chief difference is in the determination of the friction coefficient. Some formulas set a basic friction factor for all conditions, some relate the friction, or transmission, factor to diameter and absolute roughness, and others relate the transmission factor to the Reynolds number. Although early formulas did not make adjustments for deviation, it is generally accepted that such an adjustment is necessary.

For practical application, based on the tests presented herein, it is reasonable to conclude that the transmission factor is not a function of the Reynolds number for turbulent flow in the area of normal commercial operation, but is a function of the diameter and absolute roughness. It appears that variations of absolute roughness due to varying pipe conditions is of greater significance than the pipe diameter. It is urged that a basic absolute roughness factor, such as 0.0007, be agreed on as being the norm against which pipeline efficiency can be determined.

ACKNOWLEDGMENTS

The writers wish to express their thanks to the Operating Department of the Southern Natural Gas Company and to the American Gas Association for making much data available, as well as to Messrs. Smith, Miller, Ferguson, P. McDonald Biddison, and Bukacek for their criticism of the paper.

APPENDIX I

Correction for Elevation Change.—In areas in which there are material differences in elevation, it is necessary to make adjustments for these differences. Such adjustments have been made in the following analysis of test

data by applying an adjusting factor to the differences of the squares of the absolute pressure in Eq. 12 as follows:

$$Q = K_1 \left\{ \frac{[(P_1)^2 - (P_2)^2] - H_F}{L} \right\}^{\frac{1}{2}} \sqrt{\frac{1}{Z}} \dots \dots \dots (14a)$$

in which the elevation factor, H_F , is

$$H_F = \frac{0.0375 G (H_2 - H_1) (P_{avg})^2}{Z_{avg} T_{avg}} \dots \dots \dots (14b)$$

and H_1 and H_2 are the elevations of the inlet and outlet pipes, respectively, in feet.

*Computation for Reynolds Number*¹¹.—The Reynolds number equation (Eq. 3) has been expressed by Biddison¹² as

$$R = 0.011459 \frac{Q G P_b}{\nu d T_b} \dots \dots \dots (15)$$

in which Q is the flow, in cubic feet per hour, ν represents the viscosity, in pounds per second-foot, and the constant adjusts for the mixed units used. A simpler form can be obtained by making the following substitutions: $Q = (1,000/24) Q_1$; $P_b = 14.73$ lb per sq in. absolute; and $T_b = 60^\circ + 460 = 520^\circ$ absolute. The term Q_1 is the rate of flow, in thousands of cubic feet per day, at a pressure and temperature base of 14.73 lb per sq in. absolute and 60° F absolute, respectively. The resulting equation is

$$R = 0.0135321 \frac{Q_1 G}{\nu d} \dots \dots \dots (16)$$

in which ν is the viscosity times 10^6 , in pounds per second-foot.

Application of Deviation Factor.—The proposed formula in Eq. 12 expresses the deviation as a function of the mean effective pressure between the initial and terminal pressure of the span. This formula can also be expressed as

$$Q = K_1 \left\{ \frac{[(P_1)^2 - (P_2)^2] 1/Z}{L} \right\}^{\frac{1}{2}} \dots \dots \dots (17)$$

It has also been suggested that

$$\frac{1}{Z} = 1 + J P_M \dots \dots \dots (18)$$

in which J is the factor for supercompressibility, which is a constant for a given gas. The mean effective pressure, P_M , can be equated to P_1 and P_2 as follows:

$$P_M = \frac{2}{3} \left[\frac{(P_1)^3 - (P_2)^3}{(P_1)^2 - (P_2)^2} \right] \dots \dots \dots (19)$$

¹¹ "Flow of Natural Gas through Experimental Pipelines and Transmission Lines," by R. V. Smith, J. S. Miller, and J. W. Ferguson, *Monograph No. 9*, Bureau of Mines, U. S. Dept. of the Interior, Washington, D. C., 1956, p. 32.

¹² "Gas Flow Computations," by P. M. Biddison, *Proceedings, Natural Gas Dept., Am. Gas Assn.*, New York, N. Y., 1941, pp. 51-58.

Substituting Eq. 18 into Eq. 17 yields

$$Q = K_1 \left\{ \frac{[(P_1)^2 - (P_2)^2] + J P_M [(P_1)^2 - (P_2)^2]}{L} \right\}^{\frac{1}{2}} \dots \dots (20)$$

Substituting Eq. 19 for P_M in Eq. 20 results in

$$Q = K_1 \left\{ \frac{[(P_1)^2 - (P_2)^2] + J \frac{2}{3} \left[\frac{(P_1)^3 - (P_2)^3}{(P_1)^2 - (P_2)^2} \right] (P_1)^2 - (P_2)^2}{L} \right\}^{\frac{1}{2}} \dots (21)$$

which, when rearranged, is

$$Q = K_1 \left[\frac{(P_1)^2 (1 + J \frac{2}{3} P_1) - (P_2)^2 (1 + J \frac{2}{3} P_2)}{L} \right]^{\frac{1}{2}} \dots \dots (22)$$

Thus, expressing

$$1 + J \frac{2}{3} P_1 = (b_1)^2 \dots \dots \dots (23)$$

when b is a factor for the determination of the deviation of the gas at the particular pressure being considered, the formula becomes

$$Q = K_1 \left\{ \frac{[(P_1)^2 (b_1)^2] - [(P_2)^2 (b_2)^2]}{L} \right\}^{\frac{1}{2}} \dots \dots \dots (24)$$

as mentioned previously.

Therefore, a table can be prepared, making the appropriate adjustment for deviation of the gas considered and relating the square of the absolute pressure adjusted for deviation to the corresponding gage pressure. This table will yield factors that can be substituted into the proposed equation, which will adjust for deviation.

APPENDIX II. NOTATION

The following symbols, adopted for use in the paper, conform essentially with "American Standard Letter Symbols for Hydraulics" (ASA—Z10.2-1942), prepared by a committee of the American Standards Association with Society representation, and approved by the Association in 1942:

- b = deviation factor;
- d = internal pipe diameter, in inches;
- F_{pr} = supercompressibility factor;
- f = friction coefficient or resistance coefficient;
- $\sqrt{1/f}$ = transmission factor;
- G = specific gravity (air = 1.000);
- H_F = elevation factor (Eq. 14b);
- K = constant = 1.6156;

k = absolute roughness coefficient;

L = length, in miles;

N = mol-pounds;

P = pressure, in pounds per square inch absolute:

P_c = critical pressure, in pounds per square inch absolute;

P_m = mean effective pressure;

P_r = reduced pressure, in pounds per square inch absolute;

P_0 = pressure base, in pounds per square inch absolute;

P_1 = inlet pressure, in pounds per square inch absolute;

P_2 = outlet pressure, in pounds per square inch absolute;

Q = flow of gas, in cubic feet per hour;

R = Reynolds number;

R = constant = 10.71;

r = internal pipe radius, in inches;

S = fluid density;

T = temperature, in degrees Fahrenheit absolute:

T_c = critical temperature, in degrees Fahrenheit absolute;

T_r = reduced temperature, in degrees Fahrenheit absolute;

T_0 = temperature base, in degrees Fahrenheit absolute;

U = average linear velocity;

V = volume, in cubic feet;

Z = compressibility factor;

ν = dynamic viscosity; and

ρ = density.

AMERICAN SOCIETY OF CIVIL ENGINEERS

Founded November 5, 1852

TRANSACTIONS

Paper No. 2982

OFFSHORE BREAKWATERS

BY RICHARD SILVESTER¹

SYNOPSIS

The determination of height and pattern for waves that are diffracted by an infinitely long breakwater, or by a breakwater gap, has been based on the theoretical solution for optical diffraction. Correct results are obtainable at distances in the shadow zone many wave lengths from the breakwater, but within an area of three wave lengths the results are in error. Offshore breakwaters of limited length, although basically the same as the infinitely long breakwater, have peculiarities that must be studied if their operation, in preventing beach erosion for example, is to be successful. The main factor to be considered is the wave pattern close to the breakwater. Model tests for wave patterns with two different lengths of breakwater and waves of different steepnesses are described. Results are presented in a form suitable for application.

INTRODUCTION

Breakwaters constructed parallel to, and some distance from, the shore have not come into general use as a method of preventing beach erosion, even though their effectiveness in slowing down, if not completely stopping, littoral movement has been amply illustrated.² One reason for this lack of support for the offshore breakwaters is their greater cost over the shorebound structures, not only in money but possibly in human life. Their construction in the open sea is sometimes hazardous.

The lack of information on the action of offshore breakwaters is also a contributing factor. Unlike the land-based groin, which will sometimes effectively stop littoral drift immediately on installation, the offshore structure appears to be somewhat unpredictable. Even the cited work² can only advise the construction of a short breakwater initially and, after its action has been observed, adding to it until desired results are obtained. It is obvious that

NOTE.—Published, essentially as printed here, in September, 1957, in the *Journal of the Waterways and Harbors Division*, as *Proceedings Paper 1508*. Positions and titles given are those in effect when the paper was approved for publication in *Transactions*.

¹ Senior Lecturer in Civ. Eng. (Hydraulics), Univ. of Western Australia, Nedlands, Australia.

² "Cochin Harbour Works," by R. C. Bristow, *Minutes of Proceedings*, Inst. C. E., London, Vol. 230, No. 2, 1929-1930, p. 41.

such an empirical approach is not suitable to those responsible for preparing estimates and raising the necessary funds.

MATHEMATICAL SOLUTION

Although the mathematical solution for the height of diffracted waves behind an infinitely long breakwater has been applied from optical, sound, and electromagnetic wave diffraction,^{3,4,5,6,7} it has been realized that "only model tests will make it possible to state our assumptions will lead to errors too large for practice."⁵

Such experimental verification has not met with extraordinary success. For example, J. H. Carr and M. E. Stelzriede stated⁴: "The agreement between experiment and theory, while not exact, is reasonably close, and supports the important general conclusions of the theory." J. A. Putman and Robert S. Arthur⁷ noted that "although the accuracy with which the diffraction coefficients could be determined experimentally is not all that might be desired, it is possible to make the following conclusions * * *"

When seeking the reason for the apparent inaccuracy in the theoretical solution, it must be taken into account that the solution is founded on the sinusoidal wave form. Any deviation from this wave form must affect not only the distribution of wave height, but also the paths followed by the wave crests. Wave steepness may be the factor causing such deviation. In turn, this factor is dependent on wave height, wave period, and depth of water.

WAVE STEEPNESS

The waves used in the experimental studies cited previously were generally steep in nature. Putman and Arthur⁷ used deepwater waves whose steepness equaled 0.035. C. Carry and E. Chapus⁶ used waves in water whose depth was about one-eighth that of the wave length (wave heights not being included in the report). Carr and Stelzriede⁴ did not record data on their experimental waves, indicating that they were considered unimportant in the ultimate results.

When littoral drift is studied, average wave conditions are more important than maximum wave conditions or minimum wave conditions. Thus, average wave steepness should be used in tests rather than maximum values. In order to accomplish this, maximum steepness of ocean waves will be defined subsequently.

If the hindcasting method proposed by Jack Darbyshire is to be accepted,⁸ maximum values of $H_T/T = 0.44$ can be expected for the component waves in the wave spectrum. Although larger and smaller waves will occur due to the

³ "Shore Protection Planning and Design," by J. V. Hall et al, *Bulletin, Special Issue No. 2*, Beach Erosion Board, Corps of Engrs., U. S. Dept. of Army, Washington, D. C., 1953.

⁴ "Diffraction of Water Waves by Breakwaters," by J. H. Carr and M. E. Stelzriede, *Circular 521*, National Bureau of Standards, Washington, D. C., 1952, p. 109.

⁵ "The Diffraction of a Swell. A Practical Approximate Solution and its Justification," by H. Lacombe, *ibid.*, p. 129.

⁶ "Calculation of Diffracted Wave Height Behind a Semi Infinite Jetty," by C. Carry and E. Chapus, *La Houille Blanche*, January-February, 1951; translation in *Bulletin*, Beach Erosion Board, Corps of Engrs., U. S. Dept. of Army, Washington, D. C., Vol. 5, No. 3, July, 1951, p. 15.

⁷ "Diffraction of Water Waves by Breakwaters," by J. A. Putman and R. S. Arthur, *Transactions*, Am. Geophysical Union, Vol. 29, No. 4, 1948, p. 481.

⁸ "The Generation of Waves by Winds," by J. Darbyshire, *Proceedings*, Royal Soc. of London, Series A215, 1952, p. 299.

interference of wave groups, this value should be representative of average conditions. Wave steepness in deep water, H/L_o , becomes

$$\frac{H}{5.12 T^2} = \frac{0.44}{5.12 T} = \frac{0.086}{T} \dots \dots \dots (1)$$

in which H is the height of the wave, in feet, and T denotes the period of the wave, in seconds. Changes in wave height and wave length can be computed for waves traveling through shoaling water³ so that the steepness at various values of d/L_o or d/L can be determined (Fig. 1), in which d is equal to the still-water depth, in feet, and L_o represents the deepwater wave length, in feet. It can be seen that a steepness of 0.035 in deep water can only represent waves

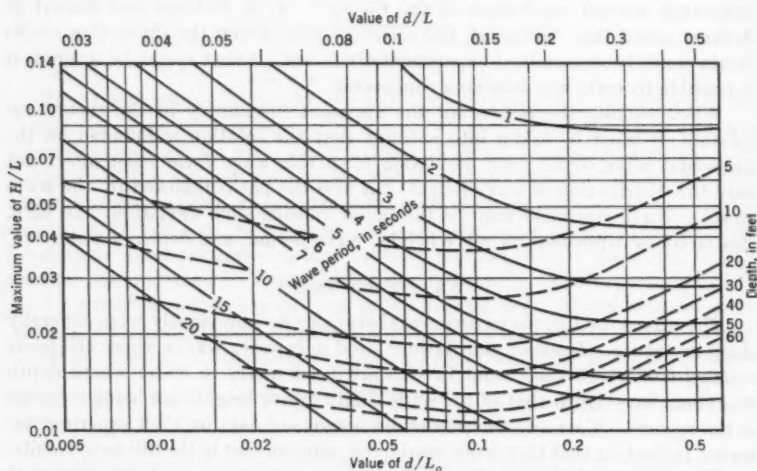


FIG. 1.—MAXIMUM EXPECTED OCEAN WAVE STEEPNESS FOR VARIOUS PERIODS AND DEPTHS OF WATER

of 2.5 sec or less, whereas for shallower conditions ($d/L_o = 0.01$) it could represent almost a 15-sec wave. The shape of the wave in each case would be quite different, the former being closer to the sinusoidal form.

WAVE PATTERN

Offshore breakwaters can be built to provide calm water for vessel anchorage. In that event the height of diffracted waves assumes importance. However, the usefulness of such breakwaters would be mainly in erosion mitigation. For this case the pattern of the waves behind the breakwater is paramount in the formation or nonformation of a tombolo or sand bar, especially within one or two wave lengths of the breakwater. It is generally accepted that within this region the theoretical solution is somewhat in error, mainly due to the fact that until attenuated by the diffraction the waves may not be in true sinusoidal

form. As the waves progress further into the shadow zone, they follow a pattern and a height distribution that are well represented by the mathematical solution of optical diffraction.

It was decided to check whether factors such as wave steepness, caused by differing the wave height, wave length, or water depth, had any effect on the wave pattern behind a short offshore breakwater. Measurements would be compared with the theoretical solution.

EXPERIMENTAL PROCEDURE

A model basin was available with a wave machine capable of producing waves of various heights and periods. Waves to a scale of $1/60$ of the prototype were produced to a natural scale by using the time scale of $1/\sqrt{60}$. Because the waves were generated in shallow water the blade of the machine not only rotated about an axis at the bottom of its face, but the base oscillated also.

TABLE 1.—WAVE CHARACTERISTICS^a

Still-water depth, in fathoms	Wave period, in seconds	Wave height, ^b in feet	Measured wave length, ^c in feet	Computed wave length, in feet	Ratio of height to length ^d	Ratio of depth to length ^d
(1)	(2)	(3)	(4)	(5)	(6)	(7)
3	7.2	5.64	155	162	0.036	0.116
	7.1	4.02	160	159	0.025	0.112
	7.1	3.18	165	159	0.019	0.109
	7.0	2.46	170	156	0.015	0.106
	9.2	8.70	205	212	0.042	0.088
	8.9	6.30	205	205	0.031	0.088
	8.5	4.80	210	194	0.023	0.085
5.75	7.2	5.58	230	207	0.025	0.150
	7.1	3.88	215	204	0.018	0.161
	7.1	2.76	210	204	0.013	0.164
	7.0	2.34	205	200	0.011	0.168
	9.2	7.62	285	281	0.027	0.121
	8.9	4.86	280	270	0.017	0.123
	8.5	3.12	265	256	0.012	0.130

^a All measurements in terms of prototype. ^b Measured in line with breakwater. ^c Measured in model. ^d Length as measured in model.

Two sections of the model were partitioned in front of the blade. One had a depth equivalent to 5.75 fathoms (0.575 ft) and the other a depth of 3 fathoms (0.30 ft). For the former section the concrete floor of the model was the base, whereas the latter section used $\frac{1}{8}$ -in. metal screenings to build up to the level. Frictional and percolation losses due to the screenings were negligible as judged by measured values of L and the theoretical values.

The equivalent lengths of the breakwaters tested were 240 ft and 360 ft, respectively. The characteristics of the waves used are presented in Table 1, in which the wave length was computed as outlined previously.³ It is seen that the two periods of 7 sec and 9 sec were reproduced fairly closely. The crest lag on the center line of the breakwater was traced by placing pegs along this line at 2-ft intervals (equivalent to 120 ft) and by locating others on a parallel line running through one end at the point of the crest when the same crest was at the center peg. The height of the diffracted waves was not measured.

EXPERIMENTAL RESULTS

In the 5.75-fathom depth it was difficult to trace wave crests for a great distance behind the breakwater due to wave interference from each side and reflections from the partitions. Only two traces of the crest were obtainable. With the 3-fathom depth the waves were steeper and could be traced more easily.

Although the crest lag differed somewhat for the various wave steepnesses, probably caused by the slightly varying periods, no trend was visible and the

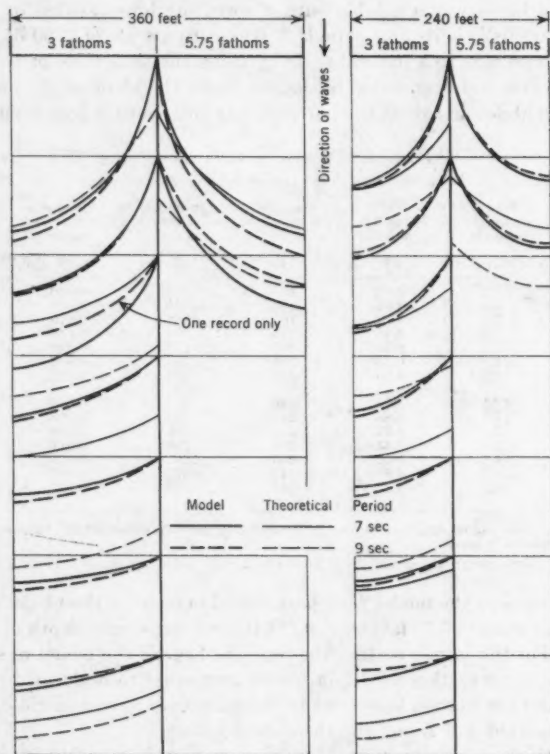


FIG. 2.—WAVE TRACES BEHIND BREAKWATERS FOR VARIOUS PERIODS, HEIGHTS, AND STILL-WATER DEPTHS

differences were attributed to experimental error. Therefore, where wave patterns are recorded (Fig. 2) each curve is representative of three or four waves of different steepness (Table 1). The theoretical solutions³ are also recorded in Fig. 2.

Crest lag is not affected by wave period as seen in Fig. 2, in which traces for 7-sec waves and 9-sec waves are almost identical, even within two wave

lengths of the breakwater. A comparison of wave patterns in the different depths of water shows that wave length does not affect the crest lag materially.

Crest lag is at a maximum when the diffracted wave reaches the center line of the breakwater. As soon as the waves from either side join forces, the crest at the center accelerates and decreases the lag to a point about 600 ft behind the breakwater, after which the decrease is slow.

Fig. 3 shows the ratio of the crest lag to the breakwater length versus the distance of the crest behind the breakwater (on center line) for both the model tests and the theoretical solution of the infinitely long breakwater. It can be seen how this solution yields the correct result beyond 600 ft from the breakwater. It would appear that the longer the offshore breakwater the more exact the mathematical solution. Whether model tests for an infinitely long breakwater would actually be predicted by it at points close to the breakwater requires further investigation.

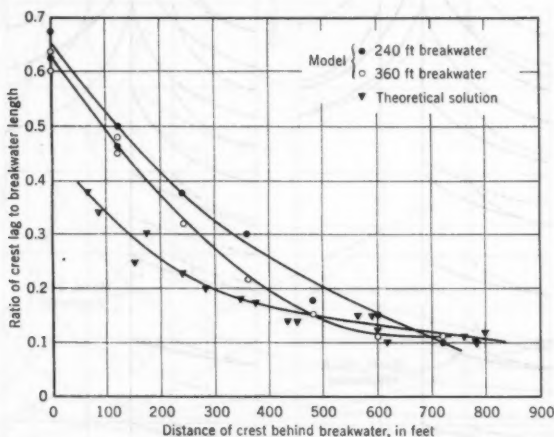


FIG. 3.—THE EFFECT OF DISTANCE BEHIND BREAKWATER ON THE RATIO OF CREST LAG TO BREAKWATER LENGTH

Comparison of the wave patterns for the two lengths of breakwater can be made from Fig. 4, in which the tips of the breakwaters have been made coincidental. As in Fig. 3, it can be seen that the wave pattern for the longer breakwater is nearer to the mathematical solution for the infinitely long breakwater. It can also be observed that until the diffracted waves meet at the center they follow a well-defined pattern for either length of breakwater.

PRACTICAL APPLICATIONS

Certain conditions are necessary in order for an offshore breakwater to form a tombolo and intercept littoral drift, or for it to cause a protuberance of the coast without completely blocking the passage between the structure and the shore. Assuming that the depth of the water is constant, these conditions

include (a) wave pattern because the equilibrium shape of the beach depends on it, and (b) wave height because it affects the steepness, which, in turn, affects the type of action the wave has on the beach. The contours of the ocean bed will affect materially the processes taking place. It is axiomatic that a breakwater can be constructed far enough offshore for the crest lag at the shore to be almost zero, thus leaving the shore line unchanged. However, a breakwater can be constructed at such a distance offshore as to produce a crest lag sufficient to cause a protuberance on the coast. A littoral current formed by the breaking of the waves at a slight angle to the shore causes such

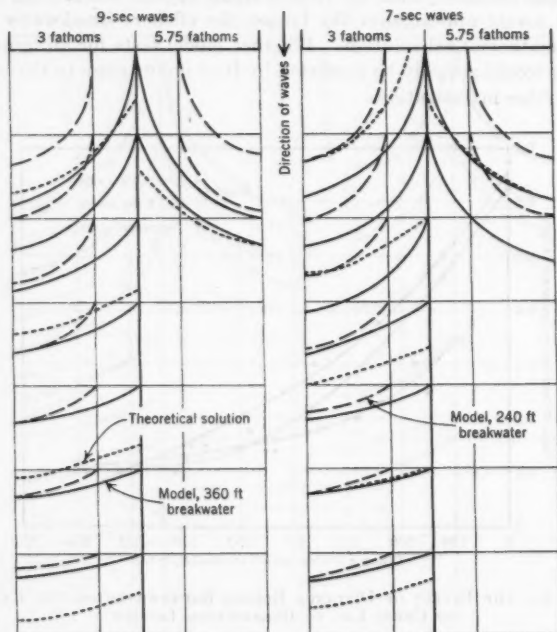


FIG. 4.—WAVE PATTERNS BEHIND BREAKWATERS OF DIFFERENT LENGTHS WITH COINCIDING ENDS

a protuberance. If the approaching waves are parallel to the breakwater and the shore when there is no other littoral current present, erosion will take place on either side of the center line of the structure in order to provide material at the center. In fact, the shore will tend to build further out than the wave pattern would indicate because the littoral currents transport sediment into the deep water not only in suspension but also by saltation action.

The importance of saltation in littoral drift has only recently been realized.⁹ When shallow-water waves causing oscillatory horizontal movement of water

⁹ "Movement of Sand Around Southern Californian Promontories," by P. D. Trask, *Technical Memorandum No. 76*, Beach Erosion Board, Corps of Engrs., U. S. Dept. of the Army, Washington, D. C., 1955.

particles near the ocean floor throw sediment into suspension momentarily, the sediment will move in any direction that a slight current may take it. Ripples form on the bed parallel to the crests of the waves and have dimensions dictated by several factors¹⁰—mainly the wave height and the wave period. In order to travel, the particles jump from ripple to ripple or along ripples, depending on the direction of the current, which does not have to be of great velocity to overshadow any mass transport effect.¹⁰ Because the wave height is greatest along the center line of the breakwater (by observation), greater saltation action occurs there, thus making it easier for the outmoving currents to transport sediment.

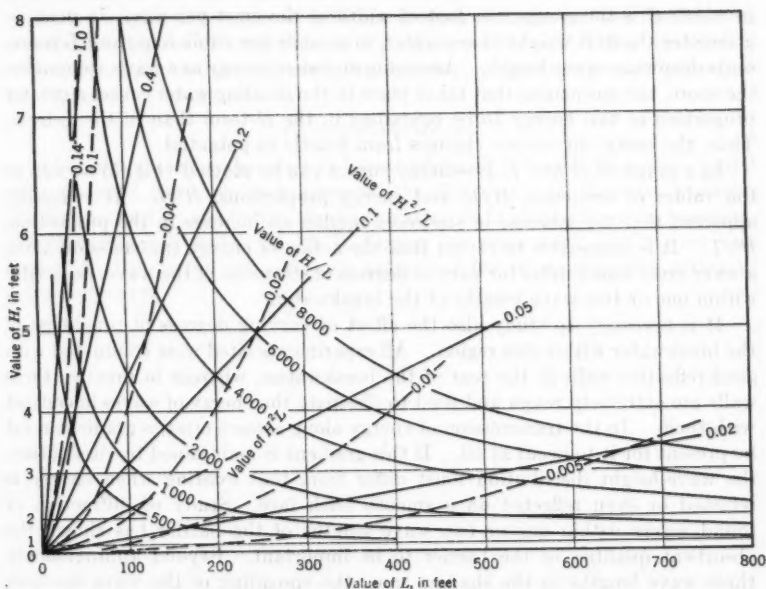


FIG. 5.—VARIATIONS OF H^2/L , H/L , AND H^2/L FOR VARIOUS VALUES OF H AND L

When there is already a littoral drift along the shore due to waves approaching at some angle to it, the presence of an offshore breakwater would cause greater erosion on the "leeward" side and silting on the "windward" side. The protrusion of the shore (if great enough) would cause a Venturi effect behind the breakwater and would expedite the passage of material through the gap.

It has been shown in the tests described herein that for constant depths the pattern of diffracted waves in the vicinity of offshore breakwaters is independent of period, height, steepness, or depth. However, such ideal conditions do not exist, and the slope of the ocean bed influences waves by the process of refraction.

¹⁰ "Mechanics of Bottom Sediment Movement Due to Wave Action," by Madhav Manohar, Technical Memorandum No. 75, Beach Erosion Board, Corps of Engrs., U. S. Dept. of the Army, Washington, D. C., 1955.

tion. Thus, waves will tend initially to straighten out more quickly than indicated in Fig. 3. As wave velocity influences wave refraction, wave period and water depth affect the wave pattern. As the protuberance on the coast forms, the contours will blend to the natural pattern of the waves.

WAVE ENERGY

Diffraction of ocean waves is defined as the phenomenon by which energy is transmitted laterally along a wave crest.³ Energy is expressed with reasonable accuracy by

$$E = \frac{1}{8} w L H^2 \dots \dots \dots (2)$$

in which E is the energy per foot of width of the crest per wave, in pounds; w denotes the unit weight of sea water, in pounds per cubic foot; and L represents deepwater wave length. Assuming no loss of energy as a wave approaches the shore, the steepening that takes place in the shoaling water causes a greater proportion of this energy to be contained in the H -term than in the L -term. Thus, the energy in essence changes from kinetic to potential.

In a graph of H and L , iso-energy curves can be plotted (Fig. 5) as well as the values of steepness, H/L , and energy proportions, H^2/L . It is readily apparent that the increase in steepness implies an increase in the proportion, H^2/L . It is reasonable to expect that the action of energy transmission along a wave crest would differ for various degrees of steepness of the wave, especially within one or two wave lengths of the breakwater.

It is necessary to study also the effect of varying degrees of roughness of the breakwater within this region. All experiments cited were conducted with good reflective walls at the rear of the breakwaters, whereas in practice these walls are extremely rough and tend to dissipate the energy of waves in contact with them. In the transmission of energy along a wave crest, a gradient must be present for it to occur at all. If this gradient is maintained by dissipation, the wave-height distribution must differ from that existing when energy is retained or even reflected on a smooth back face. Study of diffraction of sound waves within one or two wave lengths of the barrier has shown the absorbent qualities of the barrier to be important. Beyond approximately three wave lengths in the shadow zone, the spreading of the wave becomes paramount in energy distribution and end conditions are not effective.

Both these fields require continued study if useful information about offshore breakwaters is to be obtained.

CONCLUSIONS

From the limited tests on wave patterns described herein, the following conclusions can be drawn:

1. The pattern of waves behind an offshore breakwater in an area of ocean with a horizontal bed is not affected by wave steepness and, thus, is not affected by wave height, wave length, wave period, or still-water depth.
2. Crest lag behind an offshore breakwater is dependent on the length of the breakwater and decreases rapidly from a maximum of 65% of this length just behind the breakwater to 11% within 700 ft of the breakwater.

3. The mathematical solution for the crest lag behind an infinitely long breakwater yields correct results in the shadow zone beyond 600 ft of the breakwater, but yields values that are too small within 600 ft.

4. The mathematical solution for the crest lag is more correct for a longer offshore breakwater within the limitations of conclusion 2.

5. If the factor of sloping bottom can be accounted for, conclusion 1 leads to the result that the effect of offshore breakwaters on littoral drift can be studied in distorted models.

6. Examination of the nature of ocean wave diffraction and of past experimental verification leads to the following conclusion: There is a great need for model tests on the wave pattern and height distribution behind breakwaters of limited length with waves of different degrees of steepness, and breakwaters of different degrees of roughness on the shadow-zone face. The phenomena within the region of three wave lengths from the breakwater are most important for maritime structures.

ACKNOWLEDGMENTS

The work described herein has been performed in conjunction with model tests financed by a research grant of the University of Western Australia (Nedlands) and by the Public Works Department of Perth, Western Australia. The writer is indebted to Keith L. Cooper for supervision of the work and Robert B. Dingle for his advice on aspects of the mathematical solution of diffracted waves.

AMERICAN SOCIETY OF CIVIL ENGINEERS

Founded November 5, 1852

TRANSACTIONS

Paper No. 2983

TECHNICAL PROBLEMS OF FLOOD INSURANCE

BY H. ALDEN FOSTER,¹ M. ASCE

WITH DISCUSSION BY MESSRS. GEOFFREY N. ALEXANDER;
STEPONAS KOLUPAILA; AND H. ALDEN FOSTER

SYNOPSIS

Flood insurance is examined from an engineering standpoint with particular emphasis on the determination of flood probability from relatively short records, estimates of mean annual flood damage to particular properties for establishing self-supporting premium rates, spreading the risk of flood damage over many policies, and related technical problems involved in organizing any flood-insurance program.

INTRODUCTION

The problem of bringing financial relief to property owners from the effects of flood damage has received increasing attention. Private insurance companies, as well as the United States Congress, have studied the problem extensively. There has been considerable misunderstanding of the technical problems and difficulties that would have to be overcome in establishing any program of flood insurance or indemnity, either on a private basis or on a government-sponsored basis.

Therefore, the writer will examine the subject generally, emphasizing the basic problems, but without attempting to prove whether flood insurance is actually feasible.

BASIC PROBLEM OF FLOOD INSURANCE

When an insurance company issues a policy to indemnify the policyholder against a certain type of loss, such as fire, the policy provides that the owner pay a definite annual premium to the company as compensation for the risk

NOTE.—Published, essentially as printed here, in February, 1957, in the Journal of the Hydraulics Division, as *Proceedings Paper 1165*. Positions and titles given are those in effect when the paper or discussion was approved for publication in *Transactions*.

¹ Prin. Associate, Parsons, Brinckerhoff, Hall & Macdonald, New York, N. Y.

carried by the latter. This premium involves (1) the basic or "pure premium," which represents the average annual loss sustained by the company, and (2) a "loading charge" intended to cover the business costs of the firm.

Therefore, the basic problem in flood insurance is to determine the average annual damage that can be expected to occur to each insured property. The problem can be considered in three parts:

1. Estimating the average annual frequency or probability of occurrence of floods of a given magnitude at the locality under consideration;
2. Estimating the dollar value of damages caused to each property by a flood of any given intensity; and
3. Determining the average annual flood damage to the property by combining the results of the foregoing estimates.

FLOOD FREQUENCY

Statistical Methods.—Estimates of future flood occurrences must be based on past experience as modified by the anticipated changes in controlling conditions that may occur in the future. Although it is impossible to forecast the actual flood intensities that will be experienced in any year, it has been possible to estimate the probability of occurrence of floods of various intensities by the statistical analysis of past records.

Considerably refined statistical methods have been used in various fields, particularly in life insurance in which valuable technical procedures have been developed. Somewhat similar methods were introduced into the field of hydrology during 1914 and have been studied intensively by many engineers, particularly since 1940. However, there is a fundamental difference between the statistical methods used by engineers and those that have received general acceptance by statisticians.

In most statistical work the available data for analysis consist of many items or individual events, as in the case of life insurance. In hydrology, and particularly in the study of flood records in which the maximum yearly flood is considered, the items available in any record are limited, seldom extending to more than 50 yr and often limited to 20 yr or less.

At best, statistical methods must necessarily yield approximate results. As the available data become fewer, the degree of precision in the computed results will lessen progressively. This is an important consideration in evaluating any program of flood insurance.

Selecting the Curve of Best Fit.—Various methods have been advocated for plotting the flood-probability curve. The purpose of all the methods is to establish an approximate relationship between the magnitude of any particular flood and the probability of its future occurrence in any year. Some of the methods advocated for this purpose are adaptations of those used extensively in general statistical analysis. Others are based on formulas developed specifically for hydrological investigations. It is beyond the scope of the paper to make a detailed comparison of these methods.

When flood data are plotted on a diagram showing flood magnitude versus probability of occurrence, it is desirable to replace the individual items by a

smooth line termed the "curve of best fit." Although advocates of some plotting methods maintain that their curves have a reliable mathematical basis for the determination of this curve, it appears doubtful whether these claims can be substantiated fully. The writer believes that the best proof of a scientific basis for a given probability curve is that it gives a reasonably good fit to the recorded data. The practical tests of reliability are: (a) Which method represents best the actual data, and (b) which method is most convenient to use.

The various proposed methods of curve fitting generally produce reasonably accurate results with a given flood record when used to express probabilities or recurrence intervals within the length of the record. For example, a 20-yr record could be utilized to estimate reliably a 10-yr (10% probable) flood, regardless of which method is used to obtain the probability curve. When the flood-probability curve is extrapolated much beyond the recurrence interval covered by the record, considerable differences are revealed in the various methods. However, these differences are far outweighed in magnitude by the so-called errors of sampling.

Errors of Sampling.—A record of annual floods for several years at a particular site is termed a "sample" of all floods occurring at that location over a long period of time. The long-term record is known as the "population," and the individually recorded floods are termed the "items of the population." The items of the recorded sample can be analyzed by the various probability methods mentioned previously. A smooth probability curve can be established as representing the sample best. However, there is no assurance that a future sample record that covers the same length of time will produce the same probability curve. In a program of flood insurance it is important to determine the extent to which the future record may differ from the available sample.

Methods have been developed in the theory of statistics whereby the probable errors of future samples, or the spread of the items in the future sample as compared with the available record, can be estimated reasonably. Such methods show that the relative magnitude of the errors decreases rapidly as the items in the record increase. For records of less than 20 yr, the possible errors may be sufficiently large to affect appreciably any estimates of mean annual flood damages.

A conspicuous example of this problem is found in the hurricane floods of August, 1955, in the northeastern states. In many places these floods greatly exceeded any that had occurred within the previous century. A probability curve obtained from a flood record in such localities prior to 1955 would differ appreciably in shape from one based on a record including the 1955 floods.

Changes in River Conditions.—Wherever regulating works have been constructed on any river to reduce the peak discharge of floods, the probability of occurrence of floods on the river will be affected. Any studies of flood probability on such a river based on records prior to the construction of the regulating works would need to be revised before being useful in a subsequent flood-insurance program. Obviously, the detailed study required for preparing flood-probability estimates at a given site will be increased appreciably if the discharge of the river is affected by flood-control structures farther upstream. Similarly, past or anticipated changes in watershed conditions, which would

cause increased flood discharge, such as the removal of forests or the conversion of land to urban uses, must be considered in the determination of flood probabilities.

Methods of Curve Fitting.—After studying and comparing various methods of curve fitting proposed for hydrological studies, the writer was not able to determine conclusively which is best for use in flood-insurance studies. Within the time limits of the actual record, several methods seem to give substantially equivalent results. However, when the curves are extrapolated beyond the highest floods of record, there is considerable variation among the results.

Because a principal object in preparing a flood-probability curve for insurance purposes is to permit the extrapolation of flood frequencies beyond the time limits of the record, the question of the possible error in the sample for less frequent floods is of particular importance. Such errors can become relatively great, especially when the record covers only a few years. In fact, these errors of sampling far outweigh in magnitude any differences between the several types of theoretical probability curves that have been mentioned. Hence, the selection of the most suitable method becomes a question of convenience in application. Fortunately, a precise determination of the magnitude of floods with low probabilities (floods with long recurrence intervals) is not of great significance for computing insurance premiums because these rare floods have only a slight influence on the value of the average annual flood.

FLOOD DAMAGES

The second part of the problem of estimating average annual flood damages for a particular property is computing the probable damages that would be caused by a flood of a given intensity. The question can be considered in two parts: (1) The depth to which the property will be inundated by the flood, and (2) how much damage will be caused when the water reaches that depth.

The first part involves the relationship between flood stage, or flood elevation, and flood intensity. The second involves the relationship between flood stage and damages for the property in question.

Flood Stages as Related to Particular Properties.—The work required for the preparation of flood-stage diagrams at a particular property, as related to the intensity of the flood, involves:

1. Preparation of necessary topographic maps showing the location and elevation of all properties under consideration at a relatively large scale;
2. Preparation of river stage-discharge curves showing the elevation of the water surface at the gaging station for various intensities of discharge; and
3. Determination of the mean sea level elevation of each property under consideration. It is important to determine the "elevation of zero damage," or the flood stage at the property that must be reached before any material damage will occur.

Preparing the necessary maps and stage-discharge curves (mentioned in item 2) for a given locality may require much field surveying as well as office

preparation, involving considerable time and expense for preparation of the insurance program. This must be incurred regardless of the quantity of flood insurance issued subsequently in the area.

Classification of Flood Damages.—Damages to property are classified as follows:

a. Direct losses consist of physical damages to property and goods, measured by costs of repair or replacement in kind and by the cost of cleanup and moving goods. These losses can also be subdivided according to the type of use for the structures—such as residential, commercial, industrial, and other related items.

b. Indirect losses consist of the value of services, or uses lost or made necessary due to flood conditions and not chargeable to direct loss. These include losses of business and wages, and costs of relief and similar items (both within and outside the flood area) during the flood and the subsequent rehabilitation. It is doubtful whether the indirect losses mentioned should be included in a program of flood insurance, although indirect flood losses have commonly been included in determining the benefits produced by construction of flood-control projects.

c. Depreciation losses have been included occasionally as a credit for the economic justification of flood-protection works. The total depreciation of a property that has been flooded is equal to the value of the property before the flood minus its value after the flood. However, it is unlikely that such depreciation losses should be considered in connection with flood insurance if physical damage to the property has been compensated for under direct damages.

Estimates of Damages.—The determination of the damage that would be caused to the property by a particular flood stage is a question of appraisal. The most reliable damage estimates will be for floods of record from which the owner of the property has definite records of losses sustained. Generally, the appraiser must make his own estimate, which may involve a detailed examination of the property and the installed equipment, followed by estimates of the losses sustained by each piece of machinery or equipment and the cost of cleaning up. Damage to buildings generally will be less than the total replacement cost unless the construction is of a type resulting in total destruction, such as by undermining the foundation.

Dynamic Effects of Floods.—The stage-damage estimates described previously apply particularly to the inundation type of flood, in which the water surface gradually rises until the property is partly or fully submerged. This type of flooding will occur wherever the slope of the flood profile is moderate. However, wherever the surface profile of the river is relatively steep, or the flood waters are temporarily restrained by obstructions, the resulting high-velocity currents may cause serious damage. A simple inundation may cause only partial damage to a structure, whereas the dynamic effect of rapidly flowing water may cause its complete destruction. These effects are so difficult to estimate in advance that they can only be approximated by reference to past experiences in a given locality.

The type of flood damage on a particular stream may be greatly influenced by the character of the storm producing the flood, as was demonstrated clearly by the floods of August, 1955. On larger streams such as the Delaware River, the damage was caused largely by water transmitted from upstream at greater rates than could be handled by the natural river channel. Thus, the river banks were overflowed and the adjacent flood plains were inundated. On the smaller streams there was apparently extensive sheet runoff caused by unprecedentedly high rates of rainfall. The result was overland floods, with widespread damage and loss of life in sections that had never previously been subject to severe floods within the period of record.

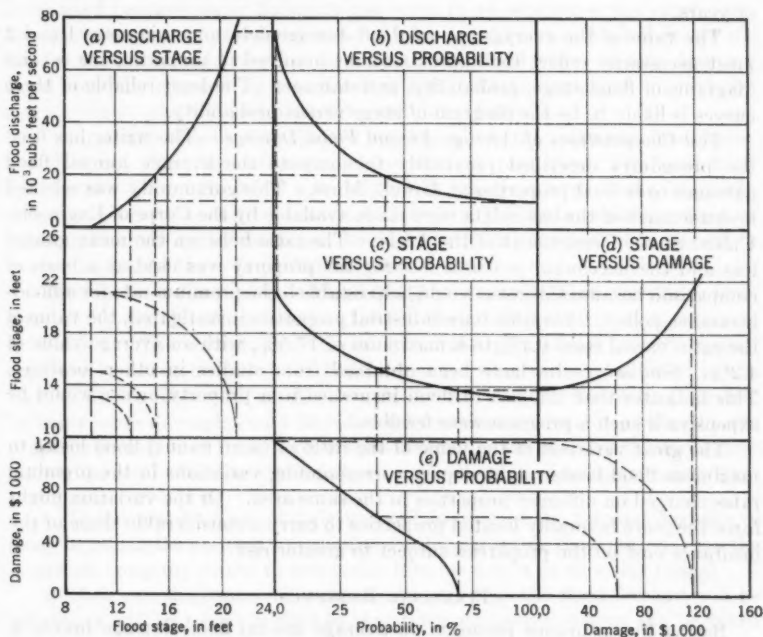


FIG. 1.—INTERRELATIONSHIP BETWEEN STAGE, DISCHARGE, PROBABILITY, AND DAMAGES

AVERAGE ANNUAL FLOOD DAMAGE

The average annual flood damage experienced by the owner of a particular property is the sum the insurer would have to collect each year merely to pay the losses occurring during a period of years. Assuming that the property is restored after each flood, the total losses for several years divided by the number of years would be considered the average annual damage. This quantity is computed as follows:

1. The diagram, in Fig. 1(a), of flood stage versus flood discharge (also termed the rating curve) at the gaging station corresponding to the property is

combined with the diagram, in Fig. 1(b), of flood discharge versus probability for the same gaging station in order to obtain, in Fig. 1(c), a curve of flood stage versus probability. This is applicable to all properties in the local area.

2. The curve of flood stage versus probability is combined with the diagram, in Fig. 1(d), of flood stage versus property damage described previously to obtain a curve, in Fig. 1(e), of flood damage versus probability for the property. The latter curve shows the probability of occurrence of flood damages equal to, or exceeding, various quantities. If the curve is plotted on a numerical scale the total area under the damage-probability curve is a measure of the average annual damage caused by all floods that can be anticipated for a long period of years.

The value of the average annual flood damage determined in steps 1 and 2 must necessarily reflect the approximations involved in preparing the several diagrams of flood stage, probability, and damage. The least reliable of these curves is likely to be the diagram of stage versus probability.

Test Computations of Average Annual Flood Damage.—The writer has used the procedures described previously to compute the average annual flood damages to several properties at Lowell, Mass. This community was selected because much of the basic data were made available by the Corps of Engineers, United States Department of the Army. The ratio between the mean annual loss and the maximum probable loss for the property was used as a basis of comparison because this ratio would help establish the premium rate for a flood-insurance policy. For fifty-four industrial properties investigated, the value of the ratio varied from 0.4% to a maximum of 17.5%, with an average value of 4.2%. Similar results have been obtained from studies in other localities. This indicates that the cost of flood insurance to a property owner would be expensive if such a program were feasible.

The great variation in the value of the ratio of mean annual flood losses to maximum flood losses might require corresponding variations in the premium rates charged on different properties in the same area. Or the variation might force the more favorably located properties to carry a considerable share of the insurance cost on the properties subject to greater risk.

FINANCIAL RESERVES

Basing the insurance premium on average annual flood damage makes it theoretically possible for the insurance company to reimburse itself for losses for an extensive period. However, this does not eliminate the possibility that the maximum probable flood may occur during any year. Unless the underwriter has provided for reserve funds sufficient to pay such maximum loss at any time on all insured properties subject to flooding by a particular river, the financial stability of the insurance program would be jeopardized. Consequently, the total reserves required to assure the solvency of the underwriter for any general area would be equal to the sum of the maximum insured losses of all the insured property in that area.

Spreading the Risk.—The total risk cannot be reduced by being spread over many properties situated in the same general flood area because a major flood will cause damage to all insured properties within the area affected by the river

in question. In this respect flood insurance differs materially from fire insurance. Under normal conditions only a small proportion of insured properties in a particular city suffer damage by fire in any single year. Therefore, the risk of loss can be spread over many policies. It is only in the case of a catastrophe, such as the Chicago (Ill.) fire of 1871, that numerous properties are damaged by fire at a single time. On the other hand, every major flood may be considered a catastrophe because it would result in damage claims from all insured owners within the affected area.

If the insurance program were placed in operation in widely separated sections of the United States, some beneficial effect of spreading the risk might be realized because major floods do not occur in all sections in the same year. An approximate study of flood-loss statistics for the entire United States indicates that the funds reserved to cover major flood losses in any drainage basin could be reduced by two-thirds if the insurance program covered the entire country and was not limited to individual basins.

The question of spreading the risk applies only to the maximum flood losses and does not affect the mean annual loss for any property. The total flood loss for the United States is not reduced in any year even if the insurance program covers the entire country. Therefore, the main practical effect of widespread coverage by insurance would be to reduce the reserves required to cover substantial losses in particular years.

Effect of Flood Forecasting.—Floods on the more important rivers have been forecast by the Weather Bureau, United States Department of Commerce, since 1900. The extent and reliability of the predictions have increased appreciably in recent years. If flood insurance were to be established in the United States, it would greatly benefit by an efficient forecasting service. In many cases damages could be reduced by emergency measures taken by the property owners and based on advanced warnings supplied by the flood-forecasting service. However, the following questions would require answering:

1. If the property owner fails to avail himself of the forecast because of delay in taking the necessary precautions or by neglecting them entirely, can the insurance company refuse to indemnify him for a part or all of his losses?
2. How can the insurance company be sure that the flood forecast will be reliable or will be issued in time so that precautionary measures can be taken by the covered property owner?

SPECIAL PROBLEMS

Numerous special problems need to be solved in organizing a program of flood insurance.

Types of Floods.—Floods have numerous causes and can be classified into various types. It is difficult to determine in some cases what damage to property has been caused by direct rainfall or by some type of flood. For example, certain areas that normally would not be considered as situated in a flood plain may be subject to damage from heavy rainfall flowing over steep ground slopes in the form of sheet runoff. There might be some doubt whether this condition should be properly classified as a flood, or as a case of direct

damage by rainfall. Similarly, the mudflows or discharges of large quantities of debris transported on the alluvial fans at the mouths of steep canyons, such as in the Los Angeles (Calif.) area, can cause widespread damage to structures, although the discharge of water might not be sufficient to cause great damage by itself.

Some floods are difficult or impossible to forecast from a probability standpoint. In a flood-insurance program it would be desirable to place certain limitations on the type of flood covered by the policy issued on any property, although practical considerations might make it difficult or impossible to impose such limitations.

Effect of Insurance on Land Use.—The owner of a property covered by flood insurance may be inclined to increase its use on the basis that if a flood comes he would be compensated for the additional loss. This condition might be taken care of by an annual inspection of the property and, if necessary, by increasing the premium charge to correspond with the increased risk.

The uneconomical development of land subject to periodic inundation may be controlled somewhat by the fact that insurance premiums on such properties necessarily would have to be relatively costly. Therefore, these properties would tend to be eliminated from the insurance program.

Effect of Protective Works.—The reduction of the risk of flood damage to properties on rivers where flood-protection works have been constructed will depend on how the works are operated during a flood. Although the design of the works may have been based on certain assumptions as to the manner of their operation, there is no guarantee that they always will be operated in that manner. If insurance is issued on the basis of those assumptions, an additional risk would have to be assumed because of possible changes in the operating program. There may be a similar additional risk in the case of lands protected by levees that are not properly maintained.

Property owners downstream from flood-control works may feel a false sense of security and assume that the degree of protection from which they benefit is greater than that provided in the design of the works. This may cause an increased use of land that is still unprotected and a greater risk of flood damage.

OTHER APPLICATIONS OF PROBABILITY METHODS

The general methods outlined herein for determining the average annual flood damage have been used extensively to determine the average annual benefits accruing to a flood-control project as a result of protection furnished to various properties in the flood basin. The purpose of these estimates is to justify construction of the project on an economic basis, estimating future benefits by reference to past flood experiences. If the indicated benefits exceed the annual cost of the project, the latter is considered to be justified in accordance with the law. In the future if greater floods occur than anticipated from past records, the project may still be justified because without the protective works the average annual damages would have been considerably greater. The government agency constructing the protection works is not held

liable for losses sustained by property owners if a flood occurs that exceeds in magnitude that for which the project was constructed.

On the other hand, with flood insurance the insuring agency agrees to reimburse the property owner for all future losses under the terms of the policy. If the resulting average annual loss exceeds that estimated from past flood records, the insurer necessarily takes a loss. Consequently, the reliability of probability estimates of future floods is more important in a program of flood insurance than in justifying a flood-protection project.

CONCLUSIONS

If a flood-insurance program were to be arranged the following factors would require careful consideration because of their influence on the premium charges required for protecting individual properties:

1. The average annual loss or damage is the sum that would have to be reserved from premium charges each year to cover losses chargeable to the policy. It equals the sum of all losses expected to occur during a period of years in the future divided by the number of years. It can be estimated by studying the probability of occurrence of floods of various magnitudes combined with estimates of the damage the various floods would cause to the property.
2. The errors of sampling measure the extent to which future flood records may vary from the sample record on which the estimate of the average annual flood damage is based. No precise estimate of future floods can be made in advance. Hence, the shorter the available record, the greater the possibility of future variation.
3. Sufficient financial reserves must be available to the insuring agency to equal the sum of all the maximum damage items on insured properties in the same general flood area. If the insurance program covers a sufficiently large section of the country so that maximum flood losses will not occur in all sections of the insured areas in the same year, the reserve funds can be reduced to some extent. However, such a reduction would not involve any change in the average annual flood losses, for which provision must be made in establishing the premium rates.

There is no constant ratio between the average annual flood loss and the insurance on a property, even for similar types of properties. This ratio is important in establishing the annual charge and will vary greatly with the location of the property with respect to the river channel. In general, premium charges must be determined individually for the various properties. Rates for flood insurance must be greater than for other types of insurance.

There are numerous other problems involved in a program of flood insurance, the effects of which are difficult to assess in advance because of the lack of actual experience in this field of insurance.

DISCUSSION

GEOFFREY N. ALEXANDER,² A. M. ASCE.—The two basic questions concerning flood probabilities are:

1. What is the best estimate of the probability or return period of a flood greater than a specified magnitude?
2. What is the precision or reliability of this estimate?

To answer the first question decisions are required on (a) the type of distribution and (b) the method of parameter estimation.

Earlier papers, such as those by Foster³ and Ralph D. Goodrich,⁴ M. ASCE, dealt only with part (a) of question 1—namely, the distribution type. Part (b) is seldom examined in engineering journals,⁵ but the subject is treated in statistical textbooks.⁶

The importance of question 2 was recognized by Arne Fisher⁷ when he stated:

"The paper deals only with the subject of graduation and leaves almost untouched the far more subtle and difficult aspects of the probable or presumptive values of future observations."

Because statistics are applied to flood data primarily to enable inferences to be made concerning the magnitude of future floods, the problem of the precision of the estimate is paramount. Precision is related closely to the sampling error, the effects of which, as the author states, are currently (1959) being recognized by engineering hydrologists, although no particular estimating procedures are generally accepted.

Given sufficient data and using recognized statistical techniques, questions 1 and 2 can be answered for recurrence intervals not exceeding greatly the length of record. As the author states, difficulties arise when extrapolation is necessary. For an assumed distribution the precision of an estimate decreases approximately as the logarithm of the recurrence interval and increases as the square root of the length of record. Consequently, extrapolation of short records may yield misleading results, but with long records some extrapolation is possible without undue loss of accuracy.

Failure to recognize the magnitude of the sampling errors invariably associated with short records was largely responsible for discrediting the use of probability methods in relation to floods. The writer believes that statistical techniques, properly applied, must ultimately form the basis of estimating

² Engr.-in-Charge, Water Resources Section, State Rivers and Water Supply Comm., Melbourne, Australia.

³ "Theoretical Frequency Curves and Their Application to Engineering Problems," by H. Alden Foster, *Transactions, ASCE*, Vol. 87, 1924, p. 142.

⁴ "Straight Line Plotting of Skew Frequency Data," by R. D. Goodrich, *ibid.*, Vol. 91, 1927, p. 1.

⁵ "Frequency Analysis of Hydrologic Data with Special Application to Rainfall Intensities," by Ven Te Chow, *Bulletin No. 414*, Univ. of Illinois, Urbana, Ill., 1953.

⁶ "Introduction to the Theory of Statistics," by A. A. Mood, McGraw-Hill Book Co., Inc., New York, N. Y., 1950.

⁷ Discussion by Arne Fisher of "Straight Line Plotting of Skew Frequency Data," by R. D. Goodrich, *Transactions, ASCE*, Vol. 91, 1927, p. 84.

flood probabilities, which are essential to actuarial estimates of flood-insurance premiums.

Methods of Curve Fitting.—The author states under the heading, "Flood Frequency: Selecting the Curve of Best Fit":

"The various proposed methods of curve fitting generally produce reasonably accurate results with a given flood record when used to express probabilities or recurrence intervals within the length of the record."

Step a. Type of Distribution.—Some attempts have been made to justify certain types of distribution for flood estimation by deductive reasoning. Thus, floods are regarded by E. J. Gumbel⁸ and others as "extreme values," and, hence, they favor the Fisher-Tippett type of distribution. Others⁹ contend that the log-normal distribution is basically more appropriate because floods can be regarded as the product of several independent causes. Such arguments are of limited value because they are seldom backed by a study of an appropriate model to define floods. The conventional use of the chi-squared test for satisfactory fit is of doubtful value in attempting to differentiate between types.

Ven Te Chow, A.M. ASCE, has shown⁹ that for one particular value of the variance, the asymptotic extreme value distribution and log-normal distribution, when standardized, are practically identical. For other values of the variance of the log-normal, a graph of Pearson's moment ratios, β_1 and β_2 , shows that there is an almost identical extreme value distribution derived from a normal parent having a certain finite size. This identity almost nullifies a priori or deductive arguments in favor of one particular distribution type. The statistical characteristics of the log-normal are becoming better known,¹⁰ and its conservatism in extrapolation renders it particularly suitable for estimating design floods for spillways.

Step b. Estimation of Parameters.—As long as there are insufficient grounds for differentiating between particular distributions and methods of parameter estimation, there is some justification for the time-saving process of fitting curves by eye. However, if mathematical methods are used it is desirable to specify the type of distribution and the method of fitting because different procedures yield different results. After the distribution is selected, the method of estimating parameters must be decided. Two methods are commonly used by statisticians—the method of moments and the method of maximum likelihood. The latter method is preferred by most statisticians for reasons that are no longer valid outside the range of observations. Hence, if curves must be extrapolated the method of moments, which weights the extreme values automatically, may be justified. When a log-normal distribution is fitted, estimates from extrapolated curves will differ considerably, depending on

⁸ "Statistical Theory of Extreme Values and Some Practical Applications," by E. J. Gumbel, *Applied Mathematics Series No. 33*, National Bureau of Standards, U. S. Dept. of Commerce, Washington, D. C., 1954.

⁹ "The Log-Probability Law and its Engineering Applications," by Ven Te Chow, *Proceedings-Separate No. 536*, ASCE, November, 1954.

¹⁰ "The Lognormal Distribution," by J. Aitchison and J. A. C. Brown, Cambridge Univ. Press, Cambridge, England, 1957.

whether the fit is to the original observations or, as appears more desirable, to their logarithms.¹¹

Precision of Estimates.—Under the heading, "Other Applications of Probability Methods," the author refers to the reliability or precision of estimates as follows: " * * the reliability of probability estimates of future floods is more important in a program of flood insurance than in justifying a flood-protection project." Any estimates, and flood estimates in particular, are of much greater value if some indication is given of their reliability.

The effect of sample size on the precision of estimates is a basic problem of statistical inference. W. S. Gossett, writing under the pseudonym of "Student," was one of the pioneers in studying this problem, his classical paper on the *t*-test being published in 1908. However, controversy still exists concerning the more technical problems of statistical inference, such as the relationship between the Neyman-Pearson concept of "confidence" limits⁶ and the "fiducial" limits of Ronald A. Fisher.¹² In addition to these two types of limits, "tolerance" limits may also be obtained within the range of observations. Hydrologists seeking to apply these procedures concerning what may be generally termed "probability" limits naturally have some doubt in trying to decide on their merits and their applicability.

Although the practical differences in the results obtained by using alternative methods may be small within the range of observations, the validity of inferences for the extrapolated estimates is questionable, particularly when the fitted curve depends on the distribution type assumed. For example, when the log-normal distribution and the Pearson Type III were both fitted to the annual maximum monthly discharges for a period of 50 yr for the Murray River at Jingellic, Australia,¹³ it was found that the log-normal estimate for a 100-yr return period was close to the upper 2½% risk curve (95% confidence limits) for the Pearson Type III. Although such differences are disturbing to those unfamiliar with the characteristics of statistical methods, they are believed to be no greater than differences associated with other more popular methods of flood estimation for long recurrence intervals, such as the "maximum possible precipitation" technique.

The rather misleading title to this technique implies that the flood determined thereby has zero probability of being exceeded. The method does show that, given certain meteorological conditions, floods can occur whose recurrence intervals are so great that probability methods that ignore the effect of sampling errors need reinterpretation. It is believed that current meteorological methods and those of statistical inference from flood data will be reconciled when the probabilities associated with steps in meteorological methods such as storm maximization and transposition are ascertained.

Conclusions.—It is clear that there is still much to be done both statistically and hydrologically before the estimation of future floods by statistical inference is placed on a firm foundation. With the recent enactment of flood-insurance

¹¹ "Flood Flow Estimation, Probability and the Return Period," by G. N. Alexander, *Journal of the Institution of Engineers, Australia*, Vol. 29, Nos. 10-11, 1957.

¹² "Statistical Methods and Scientific Inference," by R. A. Fisher, Oliver and Boyd, London, 1956.

¹³ "The Statistical Treatment of Flood Flows," by P. A. P. Moran, *Transactions, Am. Geophysical Union*, Vol. 38, No. 4, 1957.

legislation in the United States, and the consequent need for actuarial determination of premiums, studies of this type should be accelerated. Mr. Foster has made notable contributions in the field, and it is hoped that the paper will stimulate others to publish their findings.

STEPONAS KOLUPAILA¹⁴.—In his examination of the determination of flood probability, the author states under the heading, "Flood Frequency: Methods of Curve Fitting":

"After studying and comparing various methods of curve fitting proposed for hydrological studies, the writer was not able to determine conclusively which is best for use in flood-insurance studies."

Mr. Foster proposed his method in 1924³ and prepared tables based on two characteristic values—the coefficient of variation and the coefficient of skew. Mr. Foster's method was accepted and widely used in the United States and abroad. After some failures occurred in the extrapolation of the probability curve, the method was almost entirely eliminated.¹⁵ The writer feels that the cause of such a failure was improper application and lack of experience. The coefficient of variation can be established easily and checked, although it may be based on a short period of available data. The coefficient of skew is more intricate: The usual period of from 20 yr to 30 yr is definitely not sufficient for the establishment of any reasonable value. Sometimes the addition of just 1 yr causes a great change in the coefficient. Therefore, it is more accurate to presume a value by analogy with some more reliable long-range data.¹⁶ The adjustment suggested by Allen Hazen¹⁷ for inadequate length of records is not satisfactory. Different rules were offered for improving the coefficient of skew. Russian hydrologists¹⁸ made some significant progress by introducing different empirical relationships and an additional guarantee factor. The results obtained with these corrections are more satisfactory. The writer has been successful with Mr. Foster's method and hopes, therefore, that the method will be restored in the near future.

H. ALDEN FOSTER,¹⁹ M. ASCE.—Mr. Alexander emphasizes some of the difficulties encountered in preparing probability estimates for floods. From a practical viewpoint it is impossible to prepare an absolutely reliable probability curve from a limited flood record. The record itself may be represented by a standard flood-frequency curve, but the corresponding curve for any future sample of equal length may be appreciably different within so-called tolerance limits or confidence limits.

Numerous writers have indicated that the probability method is not suitable for determining the flood magnitude used in designing the spillway of an important dam. However, the writer has stated in the paper and else-

¹⁴ Prof. of Civ. Eng., Univ. of Notre Dame, Notre Dame, Ind.

¹⁵ "Elements of Applied Hydrology," by D. Johnstone and W. P. Cross, Ronald Press, New York, N. Y., 1949.

¹⁶ "Probability of Maximum Discharge," by S. Kolupaila, Žemėtvarka ir Melioracija, Kaunas, Vol. 10, No. 6, 1937 (in Lithuanian).

¹⁷ "Flood Flows," by A. Hazen, John Wiley & Sons, Inc., New York, N. Y., 1930.

¹⁸ "Practical Hydrology," by A. A. Luchaheva, Gidrometeoizdat, Leningrad, 1950 (in Russian).

¹⁹ Prin. Associate, Parsons, Brinckerhoff, Hall & Macdonald, New York, N. Y.

where²⁰ that probability methods have a proper and useful application in certain fields. They are particularly helpful in estimating average annual flood benefits for a flood-control project, or in the design of cofferdams for sites subject to floods, in which the precision of the estimate is not of primary importance. For satisfactory determination of flood-insurance rates, some kind of probability estimate is essential. However, in this case the possible range of the probability estimate between the confidence limits may add appreciably to the risk assumed by the insuring agency.

Mr. Alexander cites the differences of opinion among mathematicians as to the proper method of estimating the confidence limits for a particular record—essentially a statistical problem. P. A. P. Moran²¹ has examined methods for determining such confidence limits for the log-normal and Pearson Type III distributions.

The writer agrees with Mr. Alexander that the method of estimating floods by use of the maximum possible precipitation requires clarification, particularly its relationship to probability estimates.

Mr. Kolupaila's remarks about the writer's 1924 paper³ are greatly appreciated. The problem of sampling errors and confidence limits was not well understood by most engineers and hydrologists at that time. An appreciation of the importance of these problems would probably have prevented unsuitable application of the theoretical probability methods in hydrological studies.

²⁰ Discussion by H. Alden Foster of "Frequency Analyses of Streamflow Data," by David K. Todd, *Proceedings Paper 1166*, in *Proceedings Paper 1283*, June, 1957, p. 9.

²¹ "The Statistical Treatment of Flood Flows," by P.A.P. Moran, *Transactions, Am. Geophysical Union*, August, 1957, p. 519.

AMERICAN SOCIETY OF CIVIL ENGINEERS

Founded November 5, 1852

TRANSACTIONS

Paper No. 2984

OPERATION OF MISSOURI RIVER MAIN-STEM RESERVOIRS

BY ROBERT J. PAFFORD, JR.,¹ M. ASCE

SYNOPSIS

The six main-stem multiple-purpose reservoirs built under the "Pick-Sloan" program adopted in 1944 are described. The main operational features of these reservoirs concern flood control, irrigation, water supply and sanitation, power, navigation, recreation, and fish and wildlife. The writer outlines the development of the highly complex operating plans and criteria by the coordinating committee, with representation from nine states and seven federal agencies working with the Reservoir Control Center, in Omaha, Nebr.

INTRODUCTION

In the great plains area of the Missouri River Basin, in which some of the United States' first irrigation was nurtured and in which water rights have been defended at the point of a gun, reservoir-storage projects on a massive scale are removing some of the random variations from nature's pattern of water supply.

In no other place in the United States, with the possible exception of limited areas of the semiarid southwest, have water resources presented such a variety of problems to blunt economic progress and stability. These problems run the gamut of disastrous floods; severe drought cycles; limited water supply for municipal and industrial growth; alternate high streamflows and dry river beds; blanket wind erosion of farmlands; and erosion by water.

This vast section of the United States stretches 1,300 airline miles from Cut Bank, Mont., to St. Louis, Mo., a 600-mile-wide belt through which courses the unpredictable Missouri River. Three of the Missouri River's major tributaries each drain areas larger than the Tennessee Valley. Described by some geographers a century ago as the "Great American Desert," this region has

NOTE.—Published, essentially as printed here, in September, 1957, in the Journal of the Waterways and Harbors Division, as *Proceedings Paper 1370*. Positions and titles given are those in effect when the paper was approved for publication in *Transactions*.

¹ Head Hydr. Engr., Chief, Reservoir Control Center, Missouri River Div., Corps of Engrs., U. S. Dept. of the Army, Omaha, Nebr.

risen above many of its adversities to become one of the world's largest grain and cattle production areas. However, populationwise, it still lags far behind the national average. It still maintains the traditional status of an almost completely agricultural economy—hence, it is highly sensitive to the vagaries of annual precipitation.

A man-made system of river controls and water conservation projects of far-reaching significance has been superimposed in the last decade on this picture of a regional economy geared to nature's weather pattern. The Missouri River Basin has been the scene of tremendous construction in a large federal program of water-resources development for the past ten years, and is witnessing a transition of activity to the operating phase. At the end of

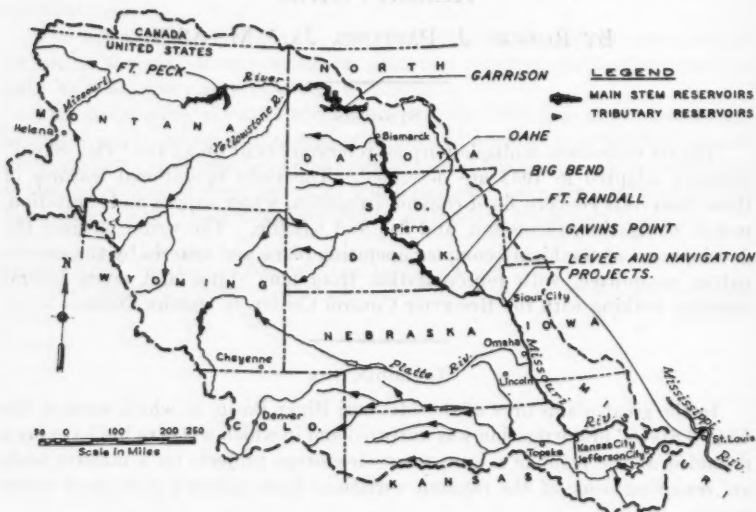


FIG. 1.—MAIN-STEM RESERVOIRS IN THE MISSOURI RIVER SYSTEM

1956 many of the projects had been completed or sufficiently advanced for initial operation, and the actual benefits for which they were authorized and constructed were beginning to be realized. Progress has been particularly outstanding on the main stem of the Missouri River, where the world's largest existing block of man-made reservoir-storage capacity is now well advanced into initial operation.

DESCRIPTION OF THE MAIN-STEM RESERVOIRS

The system of Missouri River main-stem reservoirs is a major component of the popularly termed "Pick-Sloan" water-resources development and control program for the Missouri River Basin. This program, which was authorized by the Flood Control Act of 1944,² includes widespread use of several scores

² Public Law 534, 78th Cong., approved December 22, 1944.

of multiple-purpose water-storage reservoirs, in combination with other works, to provide coordinated water service and control on the Missouri River and its tributaries. The Corps of Engineers, United States Department of the Army, and the Bureau of Reclamation, United States Department of the Interior (USBR), are the federal agencies assigned to the major construction works of this program. Companion programs by the United States Department of Agriculture and other agencies round out the basin resource program.

The Missouri River main-stem reservoir system consists of a series of six multiple-purpose projects, including four of the world's larger reservoirs, extending 1,100 miles along the main stem of the Missouri River in Montana, North Dakota, South Dakota, and Nebraska. Their location is shown in Fig. 1, which also indicates the geographic relationship with respect to the downstream navigation channel and flood-control levee projects and the tributary reservoirs that already are completed or nearing completion (as of 1959).

This six-reservoir main-stem system was planned as the backbone and foundation of the entire basin program. It is the key to successful reconciliation of intrabasin differences and to large-scale development of flood control, irrigation, navigation, and hydroelectric power in the basin. The primary purposes of this system are (a) to reduce flood flows on the Missouri River and Mississippi River; (b) to supply water for large-scale irrigation diversion projects in Montana and the Dakotas; (c) to regulate the remaining flow for water supply, stream sanitation, and open-channel navigation on the Missouri River; and (d) to provide for large-scale hydroelectric-power generation at the dams. Recreation, fish and wildlife, and other secondary purposes also are to be served. Gross storage capacity of the reservoir system will be as follows:

Reservoir	Gross storage, in 10 ⁶ acre-ft
Fort Peck (Missouri River, Mont.)	19.4
Garrison (Missouri River, N. Dak.)	24.5
Oahe (Missouri River, S. Dak.)	23.6
Big Bend (Missouri River, S. Dak.)	1.6
Fort Randall (Missouri River, S. Dak.)	6.3
Gavins Point (Missouri River, S. Dak. and Nebr.)	0.5
Total	75.9

The power plants, when completed, will have a total installed capacity of 1,800,000 kw, which, with interconnecting transmission lines, will constitute a coordinated central source of electrical generation for a large region in the Dakotas, Nebraska, eastern Montana, and western Minnesota and Iowa.

These main-stem reservoirs are being constructed by the Corps. Construction advanced sufficiently for Fort Randall Reservoir (Missouri River, S. Dak.) to be placed in initial operation in 1953, when it was teamed up with the earlier Fort Peck Reservoir (Missouri River, Mont.), which had been in operation since 1938. Garrison Reservoir (Missouri River, N. Dak.) came into initial operation in 1954, and Gavins Point Reservoir (Missouri River, S. Dak. and Nebr.), in 1955. Oahe Reservoir (Missouri River, S. Dak.) is currently

scheduled for initial storage impoundment in 1960, and Big Bend Reservoir (Missouri River, S. Dak.) is planned for initial operation early in the 1960's. By the end of 1956, the reservoir-storage capacity available for actual operation totaled approximately 50,000,000 acre-ft, and the name-plate rating of power units actually on the line totaled 712,000 kw. Electrical interconnection of the power plants was accomplished by USBR backbone transmission lines in June, 1956, as the final step permitting completely integrated main-stem system operation.

OPERATING PROCEDURES AND ARRANGEMENTS

Operation of the Missouri River main-stem reservoirs involves several elements that tend to make it a very complex problem and pose unusual requirements for coordination. Several special procedures and arrangements have had to be devised.

Complicating Factors.—The principal unusual complications that must be overcome in actual operations fall into six general categories.

The individual reservoirs on the main stem have interrelated effects on each other and must be coordinated into an integrated over-all system operation, while also serving individual requirements at each project site. The numerous tributary reservoirs also require consideration and must be properly accounted for in main-stem operations. Thus, there is a considerable requirement for coordination solely because of the number of reservoirs involved.

The problem is complicated further by the fact that the main-stem reservoirs were planned and designed for joint use of their storage capacity in order to serve five major primary functions and several other important secondary functions as well. There are no separate individual storage allocations, except for comparatively small exclusive allocations at the top of the reservoirs for use only in the very largest floods and the inactive storage in the minimum dead-storage pools. Instead, all five major functions with their diverse individual requirements, as well as the secondary functions with their own special needs, are to be served from joint use of common storage. As an example of some of the diversities that must be reconciled, downstream releases need to be substantially higher during the eight-month open-channel navigation season than is safe when the river is frozen in wintertime. Irrigation demands occur only in late spring, summer, and early autumn. The demands for power to be generated with the reservoir releases are high all year, with peaks in both midsummer and midwinter.

The sheer size of the main-stem reservoir system, with active storage capacity equal to twice the normal annual runoff, also poses somewhat of an unusual problem. The critical drawdown period for extreme low flows is a decade long instead of the one year or two years common at most reservoirs. Therefore, customary use of the usual annual rule-curve is precluded, and other media are needed as a long-range guide during drawdown periods.

The water supply available for regulation by the main-stem reservoirs varies widely within any year, from year to year, and even from decade to

decade. For example, the annual runoff from the Missouri River Basin above Sioux City, Iowa, during the 1898-1956 record period varied as follows:

Year	Annual runoff, in 10 ⁶ acre-ft
Median.....	25.0
Minimum.....	11.4
Maximum.....	36.7

Variations between the runoff in successive years are 5,000,000 acre-ft rather frequently and have exceeded 10,000,000 acre-ft. During one entire decade the water supply averaged only 60% of normal. Furthermore, the runoff is only partly predictable in any year, except on an extremely short-term basis of a few days or weeks. Because the main-stem system is intended to utilize almost all the flow of the river, except in the very wettest years, and is intended to control the runoff safely in even the wettest years, the vagaries of the water supply present some troublesome problems.

Geographically, the area from western Montana to St. Louis and down the Mississippi River is involved in operation of the Missouri River main-stem reservoirs. The hugeness of this area and the diversities of weather and climate encompassed present some serious operating problems.

As might be expected with the great geographic area and the different functions, there are numerous agencies and interests directly concerned with one aspect or another of main-stem reservoir operations. Even the single function of power is a divided responsibility—with the Corps operating the power plants to produce the hydroelectric power and the USBR operating the transmission lines and marketing the power. The recognition and reconciliation of the diverse viewpoints and rights of all these interests into coordinated operations for the mutual benefit of all poses a distinctly unique problem.

The foregoing, collectively, add up to a complex situation. However, actual experience demonstrates that, like any other complex problem, effective procedures can be evolved to reduce it to workable proportions.

Principal Media of Coordination.—Three principal media have been evolved for handling the Missouri River main-stem operating problem: (a) A special advance annual operating plan procedure; (b) a special coordinating committee of state and federal agency representatives; and (c) a special Reservoir Control Center establishment. Supplemented by additional arrangements for handling details between individual agencies—the most important of which are special arrangements for full continuous coordination between water and power operating organizations of the Corps and the USBR—these media are functioning effectively to overcome the basic complexities of the problem.

The present arrangements were evolved over a period of ten years beginning immediately after authorization of the Pick-Sloan plan in 1944. Background conditions were favorable. Effective leadership and guidance by the Missouri River States Committee and the Missouri Basin Inter-Agency Committee led to the establishment of procedures for cooperation and coordination of the many basin interests during the early years of project planning and design.

Many background planning studies for the operation of the completed main-stem reservoir system were made and generally agreed on during this period. Also, considerable experience on the Missouri River was accumulated from the Corps' actual operation of the Fort Peck Reservoir. With this background, a special work group of river control and power experts from the Corps and the USBR made an exhaustive study of the problem in 1951 and 1952 and came up with many of the fundamentals of the present arrangement. Considerable study was also given by basin interests and the states to the possible desirability of some type of special interstate or federal-state compact arrangement to handle the reservoir operation problems. This study clarified further some of the problems and thereby contributed considerably to the present arrangements.

Annual Operating Plans.—Annual operating plans, which are used as the basis for scheduling the actual operations of the main-stem reservoirs, are prepared well in advance. Each year's annual operating plan is presented in a report, which thoroughly covers (a) water supply; (b) special operational requirements and limitations; and (c) specific water demands and operational objectives for all functions all along the river. The report concludes with specific operating proposals that are "tailor made" for optimum coordination of the available water supply with water demands and operational requirements. These proposals are summarized into detailed month-by-month schedules of storage contents, releases, and power-generation rates for each main-stem reservoir and the system. In other words, they outline where the water will be kept in storage at any given time, what power plants will meet which parts of the system loads at any time, and how much water will be released from each reservoir at various times throughout the year. Each year's advance operating schedules are prepared for a wide range of possible water-supply conditions. Special five-year advance projections are also made for each year's annual operating plans to assure proper attention to the long-range requirements for main-stem operation.

The annual operating plans are prepared in August of each year and may be revised, if unforeseen conditions develop, prior to the next regular revision in the following August. The basic water schedules of the 1956-1957 annual operating plan are shown in Fig. 2. Fig. 2 shows actual operations through 1956 and indicates the operation schedules for a median-year water supply in 1957. Other complete schedules for 1957 also are available for the so-called "upper quartile," "lower quartile," and "adverse" year's water supply.

The water schedules, as shown in Fig. 2, and companion monthly power-generation schedules actually portray only the broad running-average situation at the reservoirs for the various conditions expected to be encountered. However, they are predicated on specific detailed objectives that will be met in actual daily operations. For example, the 1956-1957 winter releases from Fort Randall Reservoir and Gavins Point Reservoir represent the average of varying day-to-day releases necessary to maintain a current wintertime water supply and stream sanitation requirement of 9,600 cu ft per sec at Kansas City, Mo. The higher winter releases from the upstream reservoirs are phased to meet the system's firm power requirements without violation of minimum water

supply and sanitation requirements at any locality along the river between the reservoirs. Similarly, the 1957 spring and summer release schedules for Fort Randall Reservoir and Gavins Point Reservoir (Fig. 2) represent the average of varying day-to-day releases necessary to maintain flows of 28,000 cu ft per sec at Omaha, Nebr., and 35,000 cu ft per sec at Kansas City during the navigation season. The 1957 navigation season would begin in early April and extend through early November in the case of the normal water-supply situation on which this particular chart is predicated. The monthly storage and release schedules at all the reservoirs reflect, in this same general manner, the various specific operational requirements and objectives for all the various functions along the river.

The preparation of the annual operating plans is facilitated greatly by conformance with certain basic storage zoning provisions and basic operating

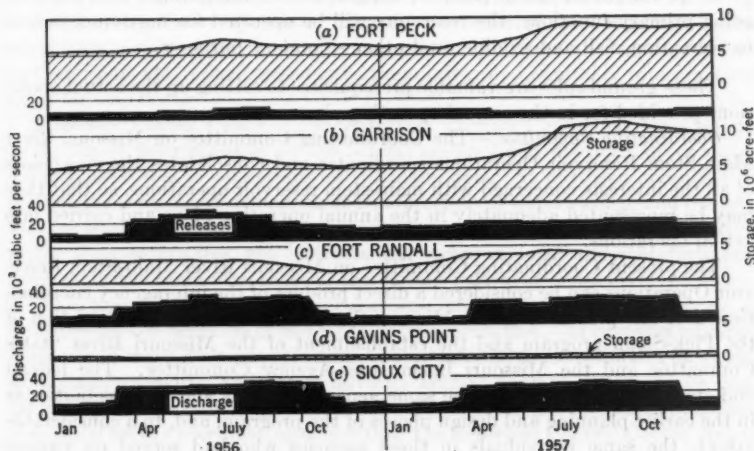


FIG. 2.—ANNUAL OPERATING PLAN WATER SCHEDULES FOR 1956-1957

"ground rules," which were set up for the main-stem reservoirs during their preconstruction planning and design. For example, the bottom inactive storage zones of the reservoirs, once filled, are to remain permanently filled with water. This is to assure the maintenance of minimum power heads, minimum irrigation diversion levels, and minimum pools for recreation and fish and wildlife purposes. Similarly, the top storage reservations for handling the largest floods are to be reserved exclusively for this purpose.

Also, the following general approach, which was developed and generally agreed on during planning and design of the reservoirs, is observed in setting up the annual operating plans:

1. Flood control will be provided for by observing the requirement that predetermined upper blocks of storage space in each reservoir will be vacant at the beginning of each year's flood season. This space is available for annual regulation of flood control and all conservation uses in every normal

and wet year, but must be vacant at the beginning of the next year's flood season.

2. Allowance will be made for all irrigation and other upstream tributary water uses during each year. This allowance also covers the effects of upstream tributary reservoir conservation operations, as anticipated from their advance operating plans.

3. Provision will be made for downstream urban water supply and stream sanitation requirements.

4. The remaining available water supply will be regulated so that the outflow from the lowermost reservoirs conforms to the seasonal requirements of navigation, with internal adjustments within the reservoir system and minor adjustments in over-all releases from the system to provide for the generation of the maximum usable power consistent with the foregoing uses.

5. To the fullest extent possible, without serious interference with the foregoing primary functions, the reservoirs will be operated for maximum benefit to recreation, fish and wildlife, and other secondary purposes.

These ground rules are valuable prerequisites to setting up the actual operations provided for in the annual operating plans.

Coordinating Committee.—The Coordinating Committee on Missouri River Main-Stem Reservoir Operations coordinates and consolidates the viewpoints of all the interests concerned with main-stem reservoir operations, so that they may be represented adequately in the annual operating plans and carried into actual operations.

The present Coordinating Committee on Missouri River Main-Stem Reservoir Operations can be considered a direct product of the interagency coordination that has prevailed in the Missouri River Basin since the formulation of the Pick-Sloan program and the establishment of the Missouri River States Committee and the Missouri Basin Inter-Agency Committee. The federal and state agencies still have the same general interests and responsibilities as in the earlier planning and design phases of the program, and, to a considerable extent, the same individuals in these agencies who had served on various earlier work groups and subcommittees logically continued as agency representatives in this new phase.

Since the inception of the coordinating committee in 1953, representatives of the states (Colorado, Iowa, Kansas, Missouri, Montana, Nebraska, North Dakota, South Dakota, and Wyoming) and federal agencies (Federal Power Commission; Corps of Engineers, United States Department of the Army; Weather Bureau, United States Department of Commerce; Public Health Service, United States Department of Health, Education, and Welfare; and Bureau of Reclamation, Fish and Wildlife Service, and Geological Survey, United States Department of the Interior) directly interested in main-stem operations have actively participated in its functions. The state representatives (governor-appointed) are generally the state water engineers.

The committee functions through general meetings, usually twice a year, and through interim contacts with and reports from the Reservoir Control Center. An annual meeting is held, usually in September, to review tentative annual operating plan schedules that have been prepared during August by

the Reservoir Control Center. At this meeting the views of all interests are given full consideration, and a specific set of advance operating plans is agreed on and made final by the committee as a basis for actual operations. A second committee meeting usually is held in April of each year to review actual operations subsequent to the preceding August meeting; discuss operations during the remainder of the year based on April 1 forecasts; revise the operating plan if necessary; and outline operational objectives to be considered by the Reservoir Control Center in setting up the tentative operating plans for consideration at the September meetings. In addition, special meetings are held to consider possible modifications of previously adopted annual operating plans should unforeseen conditions arise that might warrant important modifications. Such a special meeting was held on November 1, 1956, in connection with the Mississippi River low-water crisis which threatened St. Louis industry.

Each committee member is responsible for ascertaining and fully presenting and supporting the viewpoints of his agency or state at these meetings. The committee members are in an effective position to make the various desires and requirements known and to have them integrated equitably into practical plans for operations.

Reservoir Control Center.—The Reservoir Control Center has been set up as the action instrument of all the federal agencies and Missouri River states directly interested in operations on the main stem. It has been organized to provide the centralized management and direction of water storage and releases that are required for the main-stem reservoirs, but in a manner that coordinates, rather than subrogates, the interests and rights of local and state interests throughout the basin with those of the various federal agencies involved.

The Reservoir Control Center gathers information and is the base of activities for the members of the coordinating committee. It prepares advance estimates of main-stem water supply, consolidates advance estimates of water-supply requirements, and drafts advance annual operating plans to be considered by the coordinating committee. Then, after the operating plans are made final by the coordinating committee, the Reservoir Control Center directs actual execution of the details of operation by preparing and issuing daily schedules of water releases and power-generation rates for each of the reservoirs and power plants in the system. It is this latter activity that converts the broad monthly-average schedules of the annual operating plan into the actual day-to-day fulfilment of the various water and power requirements that will be met.

The Reservoir Control Center is manned 365 days per year to accomplish the job. Detailed records are kept of all activities, and the various interests throughout the basin are kept informed of actual current operations, and of new developments that may be pertinent to operation, or affected by it, as they arise.

The Reservoir Control Center is staffed with a group of expert hydraulic and hydroelectric engineers, specially equipped to meet the unique requirements of Missouri River reservoir operation. It is located in the Missouri River division office of the Corps in Omaha. The working staff is divided into two main groups—a reservoir regulation group and a power production group. The activities of these groups are fully self-coordinated within the Reservoir

Control Center. Each group maintains continuous working contact with related activities at the projects; at the district offices of the Corps; at the regional project and dispatching offices of the USBR; at the offices of the Weather Bureau and the Geological Survey; and at the offices of many other organizations. The completeness of coordination that is maintained through these working contacts is particularly outstanding.

A tremendous volume of weather, river, reservoir, and power data is communicated to the center, analyzed, and resolved into detailed operating schedules for the reservoirs and power plants. Reliable communications and special equipment for analyses are essential to its job. In addition to conventional engineering and computational equipment, the center is equipped with a special basin-wide situation-plotting map, special reservoir storage and river-discharge control charts, weather teletype and facsimile weather-map equipment, and special direct-wire teletype and radio communications with the various projects and the main-stem power plants.

One detail that is attracting considerable interest currently is the gradual conversion of analyses procedures for solutions using high-speed electronic computers. A practical automatic computer application has just been developed, as one item of the Corps' national Civil Works Investigations program, for preparation of the detailed schedules for the annual operating plans. In this application the basic inflow estimates, functional water-supply and power requirements, and other operational criteria and limits for each basic set of assumptions to be analyzed are fed into the computer. The computer then automatically develops schedules of storages, releases, and power-generation rates for each project in the system, which will fulfil the specified service requirements of all the other functions and maximize the generation of marketable power. Month-by-month solutions for an entire year can be obtained in a single automatic computation. This computer process is also adaptable and will be converted for use with shorter time periods, such as those required in actual day-to-day scheduling of operations. Automatic electronic computation processes are presently (1959) used by the Reservoir Control Center in seasonal water-supply forecasting and for probability analyses. They will be extended progressively to other major work items.

From the foregoing it can be seen that the Reservoir Control Center is the principal center of activity and "mainspring" of operation of the main-stem reservoirs.

Effectiveness of Arrangements.—The first four years of actual system operations have witnessed full conformance with the advance annual operating plan schedules and objectives that had been agreed on previously by the coordinating committee. Serious water-supply deficiencies in these years made it impossible to satisfy completely all the desires of all the different special interests involved. Some special problems were raised, and the new coordination processes were given a severe test. It was necessary to work out an operating program for equitable sharing of the water deficiencies—this was successful. Good service, although slightly limited, was given to all functions and interests. In actuality, the adversities of this period greatly strengthened the position and effec-

tiveness of the coordinating committee and demonstrated clearly the practicality of the annual operating plan procedure and the Reservoir Control Center arrangement.

SUMMARY OF ACTUAL MAIN-STEM OPERATIONS

Fort Peck Reservoir, the first of the main-stem reservoirs, was ready for initial operation in 1938. However, little water was accumulated the first four years because of seriously subnormal runoff in the river. After the subsequent return to normal runoff in 1942, filling proceeded steadily and the reservoir was filled to normal operating levels by 1945. The reservoir continued at normal operating levels through mid-1953. Throughout this period the project was operated primarily to stabilize the flows of the lower river during the open-water-navigation season and was also effective for flood control and power generation. The annual operation pattern was characterized by relatively low releases during the four-month winter ice period and the ensuing March-June high-water season, followed by higher releases in the summer and autumn periods as required to provide for navigation. Winter releases ordinarily averaged from 1,000 cu ft per sec to 5,000 cu ft per sec, and late summer releases usually peaked to an average of from 22,000 cu ft per sec to 25,000 cu ft per sec. Lower river navigation was sustained for the full eight-month open-water season except in the drier years.

The completion of Fort Randall Reservoir for initial operation in 1953, Garrison Reservoir in 1954, and Gavins Point Reservoir in 1955 brought an end to this single-project, limited-purpose operating pattern and marked the beginning of comprehensive multiple-purpose system operation on the Missouri River.

As at Fort Peck Reservoir fifteen years earlier, a subnormal flow period coincided with the time the new reservoirs were ready to be filled. As compared with the normal-year water yield of 25,000,000 acre-ft, the natural water yield from the basin above Sioux City decreased as follows:

Year	Yield, in 10 ⁶ acre-ft
1953.....	23
1954.....	19
1955.....	16
1956.....	19

During this same period the new Boysen Reservoir (Big Horn River, Wyo.), Canyon Ferry Reservoir (Missouri River, Mont.), and Tiber Reservoir (Marias River, Mont.), in upstream headwater areas, intercepted a total of 3,000,000 acre-ft for their initial filling.

Without the water previously accumulated in Fort Peck Reservoir, a really serious situation could have developed downstream on the Missouri River. Water supply, stream sanitation, and navigation requirements were needed to supply the lower river, and at the same time dead-storage pools totaling 6,500,000 acre-ft needed to be filled in order to bring power on the line by the required dates at the new projects. Fortunately, the water was available in Fort Peck Reservoir, and, as indicated in Fig. 3, it was possible to use some of

this previously accumulated storage water to augment the limited natural streamflow; fill the new reservoirs sufficiently for initial power generation by the time required; maintain adequate discharges for water supply and sanitation; and maintain navigation on the lower river with only moderate curtailment.

The unusually heavy demand on the Fort Peck Reservoir storage brought the level of that reservoir down from 13,100,000 acre-ft in December, 1952, to 5,300,000 acre-ft in December, 1955. This level was uncomfortably close to the minimum drawdown level (4,500,000 acre-ft). Although this drawdown was disturbing to local recreational and power interests, it has been agreed on by all the state and federal representatives, including state officials of Montana, as being fully justified by the circumstances. On the brighter side, the total water storage in the main-stem system in December, 1955, was 13,500,000 acre-ft, a gain of 500,000 acre-ft over the storage level in December,

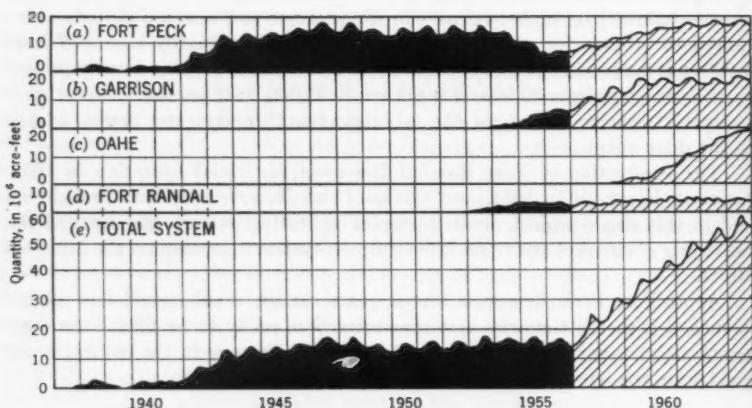


FIG. 3.—FILLING OF RESERVOIRS

1952. By the end of 1956 the storage contents of the system were increased to 14,000,000 acre-ft. This was a modest but important gain, which brought the usable active storage capacity in the four-reservoir system back to 3,000,000 acre-ft. It is important to note that the main-stem reservoirs came through this unusually adverse initial situation without any loss in total water storage, while maintaining good service, even if not ideal, to the various functions along the river.

The prospects are favorable for rapid completion of the initial filling of the main-stem reservoir system. In a recent study for the coordinating committee, the Reservoir Control Center found that the annual water demand from the main-stem supply from above Sioux City for the next few years will only need an average of approximately 18,700,000 acre-ft to meet all current basic annual requirements. This includes an average of approximately 800,000 acre-ft annually for new irrigation and reservoir filling on the upstream tributaries,

500,000 acre-ft for evaporation from the main-stem reservoirs, and 17,400,000 acre-ft to supply basic downstream requirements for water supply, stream sanitation, and navigation. A total of only 17,000,000 acre-ft per yr will be required in the next few years to meet tolerably restricted requirements in case of continued seriously subnormal water supply, whereas 22,000,000 acre-ft will provide the best service that could be desired to all functions. It is apparent that a substantial surplus will be available for rapid filling of these reservoirs as soon as the water supply returns to normal levels of 25,000,000 acre-ft per yr.

In later years when irrigation has fully developed, this currently surplus water for a normal water year will no longer be available, and future refilling of the main-stem reservoirs will have to be performed in wetter-than-average

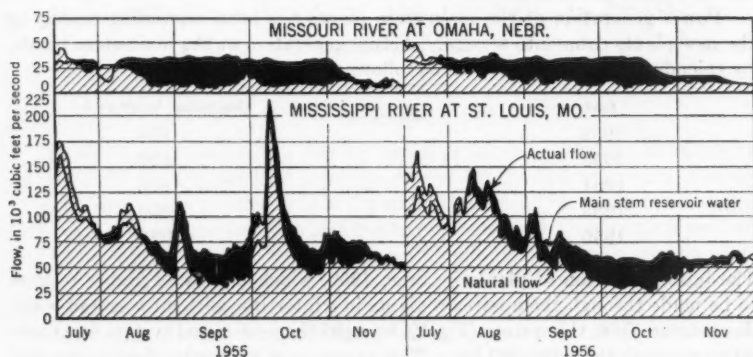


FIG. 4.—LOW-FLOW AUGMENTATION

years. However, the main-stem reservoirs will have completed their initial filling well in advance of the scheduled full-scale development of the irrigation.

The rate at which the main-stem reservoirs will be filled, assuming that 1957 and each subsequent year has a normal 25,000,000-acre-ft water supply, is also shown in Fig. 3. This forecast, based on the median-year expectancy, represents the most likely probabilities. Actual filling of these reservoirs may be advanced or retarded somewhat, depending on the actual magnitude and sequence of water supply during this filling period.

BENEFITS ALREADY BEING REALIZED

The transition into initial system operation of the Missouri River main-stem reservoirs has been accompanied by a rapid expansion in benefits.

Flood control on the Missouri River took its greatest single step forward with the bringing of Fort Randall Reservoir and Garrison Reservoir into operation in 1953 and 1954. Never again will a great flood from the area above these dams ravage the lower valley as occurred in 1952. The local protection works on the lower river and reservoirs on lower basin tributaries will have to

be completed before the Missouri River is free from floods, but the main-stem reservoirs are already handling one of the worst flood sources.

The initial operation of the main-stem reservoirs has been highly successful in maintaining satisfactory flows for water supply, stream sanitation, and navigation on the Missouri River. Also, the controlled flow on the Missouri River has contributed substantially toward maintaining adequate flows in the Mississippi River at St. Louis and below. The actual record of low-flow augmentation, as shown in Fig. 4, is a testimonial to the value of these reservoirs. Up to three-fourths of the necessary navigation-season flow at Omaha in the period from 1953 to 1956 was supplied from storage in the main-stem reservoirs. In October, 1956, 50% of the total flow in the Mississippi River at St. Louis came from these reservoirs, preventing what otherwise would have been a serious low-flow situation.

Power generation at the main-stem plants has been expanding rapidly as the new plants come into service. Actual generation at the main-stem plants, by calendar years, has increased as follows:

Year	Generation, in 10 ⁶ kw-hr
1952	610
1953	620
1954	820
1955	1,400
1956	2,280

The interconnection of plants in June, 1956, which permitted higher releases to be made through the upstream plants in wintertime without waste of water downstream from the system (Fig. 2), brought the year-round system firm capability to more than 400,000 kw. This power is of particular significance and value in the high fuel cost area in which it is marketed.

Actual use of main-stem water for large-scale irrigation awaits the completion of the actual irrigation project works. Meanwhile, expanding tributary water use is being fully allowed for, and the water bank is being filled for future large-scale irrigation directly from the Missouri River.

The initial filling of these "Great Lakes of the Missouri" is greatly expanding the recreational, fishing, and hunting opportunities in the region. The benefits that have been realized to date, although in themselves of great importance, are actually just a sample of the greater values to be realized when all the Missouri River main-stem reservoirs are completed and filled to normal operating levels.

CONCLUSIONS

Many complex problems and obstacles had to be solved to bring the Missouri River main-stem reservoirs into initial system operation. These problems are all being met and mastered by the procedures and arrangements that have been devised. Actual accomplishments of operation clearly attest to this success and indicate tangibly the ultimate value of the Missouri River main-stem reservoirs, when all are completed, to the region and to the United States.

AMERICAN SOCIETY OF CIVIL ENGINEERS

Founded November 5, 1852

TRANSACTIONS

Paper No. 2985

INELASTIC BEHAVIOR OF IMPULSIVELY LOADED BEAMS

BY MELVIN J. GREAVES¹ AND FREDERIC T. MAVIS,²

MEMBERS, ASCE

SYNOPSIS

Methods are presented for solving design problems involving a simple beam in which (a) the applied load is impulsive and (b) the distortions are inelastic. A similarity between deflections in the simple beam and moments in an analogous beam is demonstrated, in which the latter beam, with its length corresponding to time, is loaded with the unbalanced impulse applied to the simple beam. This analogy permits a designer who is familiar with the usual concepts of static design to cope with problems involving yield and motion.

A nondimensional characteristic number is proposed. This value varies directly as the product of the mass of a beam and the "braking" energy of inelastic bending distortion, and inversely as the square of the driving impulse. The number is the link between seemingly different forms of impact and impulsive loads and provides a new means of classifying all such loads on a single basis. The number facilitates the determination of the dynamic yield resistance of a beam from test data in which this resistance is often confused with inertial resistance.

THE PROBLEM

In engineering design emphasis is generally placed on solutions in which the materials behave elastically. This is natural because most engineering materials behave elastically when the stresses are within the customary working limits. However, there are certain situations in which it is necessary or desirable to consider inelastic behavior.

The problem is complicated further when the applied loads are functions of time. In general, solutions of problems involving the elastic behavior of

NOTE.—Published, essentially as printed here, in May, 1957, in the Journal of the Structural Division, as *Proceedings Paper 1252*. Positions and titles given are those in effect when the paper was approved for publication in *Transactions*.

¹ Asst. Chf. Engr., Arthur G. McKee and Co., Cleveland, Ohio.

² Dean, College of Eng., and Prof. of Civ. Eng., Univ. of Maryland, College Park, Md.; formerly Prof. and Head, Dept. of Civ. Eng., Carnegie Inst. of Technology, Pittsburgh, Pa.

impulsively loaded beams³ and the inelastic behavior of statically loaded beams⁴ cannot be combined by direct superposition.

DYNAMIC ANALOGY

Consider a mass, W/g , acted on by two opposed colinear forces, F_t and R_t , directed at the center of gravity of the mass and compatible with the following definitions: F_t and R_t are functions of time and are not equal for part of the time. At times t_1 and t_2 , the values of F_{t1} and F_{t2} are equal to F_y , which is a force required to yield the beam. The value of the integral $\int_{t_1}^{t_2} (F_t - F_y) dt$ is zero. When the value of t is less than t_1 or greater than t_2 , the value of R_t is equal to F_t . When the t -value is between t_1 and t_2 , the value of R_t is equal to F_y .

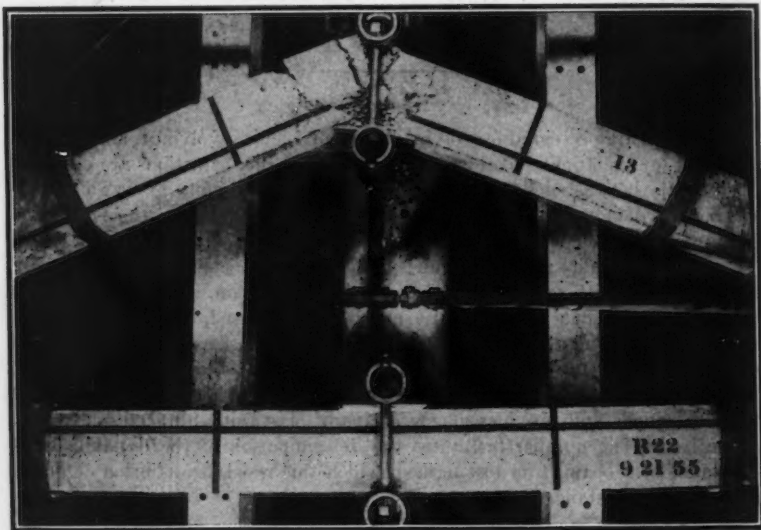


FIG. 1.—TYPICAL PLASTIC HINGE

The foregoing problem is encountered when a driving force, F_t , moves a heavy object in opposition to dry friction, uniform yield forces, or other steady (limited) resistance, R_t . The resistance can also be due to one or more plastic hinges in a beam in which the load, F_t , is applied transversely and W'/g is the effective mass of the beam. For a beam of uniform cross section, W'/g can be taken as one-third of the mass of the beam. Fig. 1 shows a well developed plastic hinge produced by an impulsive load of 8.5 kips.

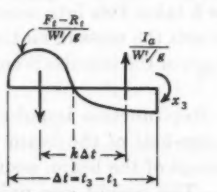

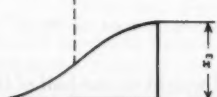
The motion of the object can be analyzed by Newton's laws and by simple calculus. The equations are analogous to those relating load, shear, and

³ "Application des potentiels," by J. Boussinesq, Gauthier-Villars, Paris, 1885, pp. 435-577.

⁴ "Theories of Strength," by A. Nadai, *Journal of Applied Mechanics, Transactions, A.S.M.E.*, Vol. 55, 1933, pp. 111-129.

moment for a prismatic beam in which (a) the time coordinate of the motion problem corresponds to the distance along the axis of the beam and (b) the quantity (ratio of the unbalanced force to the effective mass) corresponds to the

TABLE 1.—RELATIONSHIPS BETWEEN ANALOGOUS QUANTITIES

	Analogous beam	MOTION		
		Acceleration		
LOAD		$\frac{F}{W'/g}$	$\frac{dv}{dt}$	$\frac{d^2x}{dt^2}$
SHEAR		$\int \frac{F}{W'/g} dt$	Velocity	
			v	$\frac{dx}{dt}$
MOMENT		$\iint \frac{F}{W'/g} dt dt$	$\int v dt$	Displacement x

load on the beam. Table 1 illustrates the relationships that exist between analogous quantities.

IMPULSE CHARACTERISTIC NUMBER

From Table 1 it is found that

$$x_3 = \frac{1}{W'/g} I_a k \Delta t \dots \dots \dots (1)$$

and

$$F_y x_3 = \frac{1}{W'/g} I_a k (F_y \Delta t) \dots \dots \dots (2)$$

with

$$E_b = \frac{1}{W'/g} (I_a) k (I_b) \dots \dots \dots (3)$$

and

$$\frac{W'}{g} E_b = (k a b) I^2 \dots \dots \dots (4)$$

In Eqs. 1 through 4, E_b is the braking work, $x_3 F_y$; I_a denotes the accelerating impulse; I_b is the braking impulse, $F_y \Delta t$; W'/g represents the mass; W'/g

denotes the effective mass; $a = I_a/I$; $b = I_b/I$; $c = W/W'$; and I is the applied impulse, $\int F_t dt$.

The impulse characteristic number is defined as

$$N_I = k a b c = \frac{W E_b}{g I^2} \dots \dots \dots (5)$$

Only the part of the applied impulse that corresponds to the interval of time between t_1 and t_2 is effective. The factor b takes this into account. Furthermore, only the net or accelerating impulse sets the mass in motion. The factor a takes this into account. Finally, the shape of the impulse is considered by the factor k .

These methods can be adapted to a step-function impulse, $2 I_a = 2 F \delta t$, acting on a simple beam. In Fig. 2(a) one-half of the beam is a free body. The value of M_y is the dynamic yield moment of the beam, assumed to be constant and small compared with $F L/2$. The weight per unit length, w , is



FIG. 2.—STEP-FUNCTION IMPULSE ACTING ON BEAM

assumed to be constant, and W is the total weight of one-half of the beam. The polar moment of inertia is

$$J = \int_0^{L/2} \frac{w}{g} y^2 dy = \frac{1}{2} \frac{W}{g} \left(\frac{L}{2} \right)^2 \dots \dots \dots (6)$$

In Fig. 2(b) the driving impulse, I_a , is approximately equal to the applied impulse, I . The braking impulse, I_b , is due to the dynamic yield moment, which is effective only while the beam is actually yielding. The angular impulse as a function of time is

$$\left(\frac{L}{2} \right) I_t = \left(\frac{L}{2} \right) I_a \left(1 - \frac{t}{t_2} \right) \dots \dots \dots (7)$$

The corresponding change in the angular momentum is $J d\theta/dt$. Because the motion of the beam begins from rest, this angular impulse is equal to the angular momentum,

$$\left(\frac{L}{2} \right) I_a \left(1 - \frac{t}{t_2} \right) = J \frac{d\theta}{dt} \dots \dots \dots (8)$$

Multiplying by $(I_b/t_3) dt$ and integrating,

$$\frac{I_a I_b}{t_3} \left(\frac{L}{2} \right) \int_0^{t_3} \left(1 - \frac{t}{t_3} \right) dt = \frac{I_b}{t_3} J \int_0^{\theta_3} d\theta \dots \dots \dots (9)$$

from which

$$\frac{I_a I_b}{t_3} \left(\frac{1}{2} t_3 \right) = \frac{J}{L/2} \left(\frac{I_b}{t_3} \theta_3 \right) = \frac{1}{3} \left(\frac{W}{g} \right) \left[\left(\frac{L}{2} \right) \left(\frac{I_b}{t_3} \right) \theta_3 \right] \dots \dots \dots (10)$$

In Eq. 10

$$\frac{1}{2} I_a I_b = \frac{1}{3} \frac{W}{g} \text{ (braking work)} \dots \dots \dots (11)$$

Because $I \approx I_a = I_b$, the impulse characteristic number is

$$N_I = \frac{W E_b}{g I^2} = k a b c = 1.5$$

in which E_b is the braking work or energy absorbed in inelastic yielding; $k = 0.5$ because both accelerating and braking impulses are rectangular; $a \approx 1$, as the dynamic yield resistance is assumed to be small compared with the force of the impulse; $b = 1$ because all the applied impulse is effective; and $c = 3$ because the two halves of the beam rotate as rigid bodies about their reaction points.

DYNAMIC YIELD RESISTANCE

The concepts and methods behind the impulse characteristic number can be used to determine the dynamic yield resistance of any beam when sufficient data are available. The instantaneous resistance that a beam can offer to a transverse impulsive force is termed the dynamic strength of the beam. This strength is equal to the sum of the dynamic yield resistance and the inertial resistance of the beam.

The dynamic yield resistance of a beam involves bending stresses only. The dynamic yield stress of a material is greater generally than its static yield stress. Thus, the dynamic yield resistance of a beam is correspondingly greater than its static yield resistance.

The inertial resistance involves weights and accelerations only, and it is equal to $\Sigma \Delta W/g a$. In the foregoing expression ΔW is the weight of an element of the beam; a denotes the acceleration of that element; and g represents the acceleration of gravity.

A series of tests^{5,6} indicated that under the test conditions the load applied to the beam can be represented approximately by relationships taking the form,

$$F(t) = F_0 \exp - \frac{t}{\lambda e} \dots \dots \dots (12)$$

⁵ "Destructive Impulse Loading of Reinforced Concrete Beams," by F. T. Mavis and M. J. Greaves, *Journal, A. C. I.*, Vol. 54, 1957, pp. 233-252.

⁶ "Instrumentation and Method for Impulse Testing of Reinforced-Concrete Beams," by F. T. Mavis and M. J. Greaves, *Bulletin No. 26*, A. S. T. M., 1957, pp. 43-47.

For one group of tests this relationship is $F(t) = 8,500 \exp - t/0.0135$ e lb. Fig. 6(a), to be shown subsequently, indicates this function plotted with measured loads from one test of this series.

The "driving" impulse due to this load is

$$8,500 \int_{t=0}^{t_3} \left(\exp - \frac{t}{0.0135 e} \right) dt \dots (13)$$

The "resisting" impulse due to the yield resistance of the beam is

$$\int_{t=0}^{t_3} F_y dt \dots (14)$$

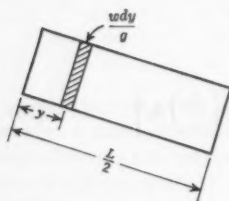


FIG. 3.—FREE BODY
DIAGRAM FOR ONE-
HALF OF BEAM

Assuming an average dynamic yield resistance, F_y , equal to 4,150 lb (15% greater than the ultimate strength of the control beams), t_3 is 0.061 sec from Eqs. 13 and 14.

Thus, if the elastic deflections are neglected (the maximum elastic deflection is approximately 5% of the maximum inelastic deflection), the beam that is at rest at time $t = 0$ is at rest again at time $t = 0.061$ sec.

As shown in Fig. 3, each half of the beam is considered a rigid free body. The polar moment of inertia is

$$J = 2 \int_0^{L/2} \frac{w}{g} y^2 dy = \frac{2}{3} \frac{w}{g} \left(\frac{L}{2} \right)^3 = \frac{w}{3g} \left(\frac{L}{2} \right)^2 \dots (15)$$

The angular momentum is $J d\theta/dt$. The angular impulse as a function of time is represented by

$$\begin{aligned} \frac{L}{2} \int_0^t \left(8,500 \exp - \frac{t}{0.0135 e} - 4,150 \right) dt &= \frac{L}{2} \left[8,500 \times 0.0135 e \right. \\ &\quad \times \left(1 - \exp - \frac{t}{0.0135 e} \right) - 4,150 t \left. \right] \dots (16) \end{aligned}$$

Equating the angular impulse to the change in the angular momentum and substituting dx/dt for $(L/2) (d\theta/dt)$ yields

$$\frac{L}{2} \left[312 \left(1 - \exp - \frac{t}{0.0135 e} \right) - 4,150 t \right] = \frac{L}{2} \frac{W}{3g} \frac{dx}{dt} \dots (17a)$$

$$312 \int dt - 312 \int \left(\exp - \frac{t}{0.0135 e} \right) dt - 4,150 \int t dt = \frac{W}{3g} \int dx \dots (17b)$$

$$312 t - 312 \times 0.0135 e \left(1 - \exp - \frac{t}{0.0135 e} \right) - \frac{4,150 t^2}{2} = \frac{W}{3g} x \dots (17c)$$

and

$$312t - 11.45 \left(1 - \exp - \frac{t}{0.0135e} \right) - 2,075t^2 = \frac{x}{8.05} \dots (17d)$$

For $t = 0.061$ sec, the final computed deflection, x_2 , equals 16 in. This agrees with the observed value.

Based on an assumed yield resistance of 4,150 lb, the computations predict the correct maximum deflection of 16 in. Hence, the value of 4,150 lb is the average dynamic yield resistance for the over-all dynamic test.

Similar computations, based on the same yield resistance, predict equally accurate deflections for other tests in which different loads were applied to similar beams.

The average dynamic yield resistance of a typical beam tested by Frederic T. Mavis, M. ASCE, and Fred A. Richards,⁷ J.M. ASCE, can be computed from observed quantities. The weight of this beam was 150 lb. No algebraic equations are available to characterize the loading function. However, from Fig. 4 the necessary data can be determined graphically. In Fig. 4(a) the accelerating

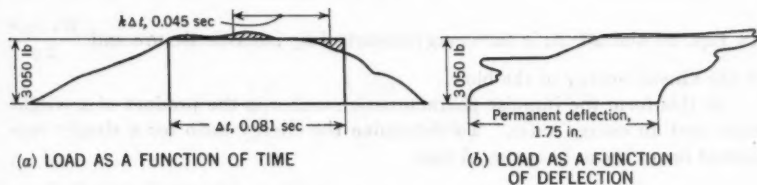


FIG. 4.—DYNAMIC BALANCE DIAGRAM FOR TYPICAL NEAR-BLAST TEST

impulse represented by the hatched area above the 3,050-lb level is 5.2 lb-sec. The decelerating impulse represented by the hatched area below the 3,050-lb level is also 5.2 lb-sec. The distance between centroids of the accelerating and decelerating impulses is 0.045 sec, the braking impulse is 247 lb-sec, and the total applied impulse is 396 lb-sec. In Fig. 4(b) the work performed on the beam is 5,470 in.-lb.

The impulse characteristic number from the preceding data is

$$N_I = \left(\frac{W}{g} \right) \left(\frac{E_b}{I^2} \right) = \frac{150 \times 5,470}{386 \times 396^2} = 0.014$$

Fig. 4 shows the measured load and deflection curves from which the values for E_b and I were derived. The yield resistance, F_y , was found by trial to be 3,050 lb, thus resulting in

$$N_I = k a b c = 0.56 \times 0.013 \times 0.62 \times 3 = 0.014$$

⁷ "Impulse Testing of Concrete Beams," by F. T. Mavis and F. A. Richards, *Journal, A. C. I.*, Vol. 27, 1955, pp. 93-102.

This value is correct and confirms the value of 3,050 lb as the average dynamic yield resistance of the beam. Similar control beams had an ultimate strength of 2,900 lb.

EQUIVALENT IMPACT

For the special case in which the impulse is produced by an inelastic collision the impulse characteristic number has an additional connotation. For example, if a hammer of weight W_1 and velocity v_a strikes a beam of weight W_2 , the impulse is

$$I = \frac{W_1 v_a}{g} \dots \dots \dots (18)$$

$$I^2 = 2 \frac{W_1}{g} \left(\frac{W_1 (v_a)^2}{2g} \right) \dots \dots \dots (19)$$

and

$$N_I = \frac{W_2 E_b}{g I^2} = \frac{1}{2} \left(\frac{W_2}{W_1} \right) \left(\frac{E_b}{\frac{W_1 (v_a)^2}{2g}} \right) \dots \dots \dots (20)$$

In Eqs. 19 and 20, E_b is the energy absorbed by inelastic flexure and $\frac{W_1 (v_a)^2}{2g}$ is the kinetic energy of the blow.

In this form the impulse characteristic number is the product of a weight ratio and an energy ratio. To determine the energy ratio for a simply supported beam it can be assumed that

1. The effective mass of the beam at the time of the initial impact is $\frac{17 W_2}{35 g}$.
2. The hammer and beam remain in contact after initial impact.
3. The energy remaining after initial impact is absorbed by the beam in inelastic flexure.

By the law of conservation of momentum the common velocity, which will be established at the first moment of impact, is

$$v_b = \left(\frac{W_1}{W_1 + \frac{17}{35} W_2} \right) v_a \dots \dots \dots (21)$$

The kinetic energy before impact is $\frac{W_1 (v_a)^2}{2g}$. The kinetic energy after impact, which must subsequently be absorbed by inelastic flexure, is represented by

$$\frac{\left(W_1 + \frac{17}{35} W_2 \right) (v_b)^2}{2g} \dots \dots \dots (22)$$

The energy ratio is the energy absorbed by inelastic flexure divided by the kinetic energy of the hammer:

$$\frac{W_1 + \frac{17}{35} W_2 \left(\frac{W_1}{W_1 + \frac{17}{35} W_2} \right)^2 (v_a)^2}{\frac{W_1 (v_a)^2}{2g}} = \frac{W_1}{W_1 + \frac{17}{35} W_2} \dots (23)$$

The impulse characteristic number is

$$N_I = \frac{1}{2} \left(\frac{W_2}{W_1} \right) \left(\frac{W_1}{W_1 + \frac{17}{35} W_2} \right) = \frac{1}{2} \left(\frac{W_2}{W_1 + \frac{17}{35} W_2} \right) \dots (24)$$

The impulse characteristic number permits many forms of destructive impulse tests to be compared on a single basis. For example, the tests of Mavis and Richards,⁷ L. G. Simms,⁸ and Thomas D. Mylrea,⁹ M. ASCE, can be ordered numerically with the tests of the writers:

1. Mylrea Series I Tests— $W_1 = 560$ lb and $W_2 = 1,280$ lb—

$$N_I = \frac{1}{2} \left(\frac{1,280}{560 + \frac{17}{35} \times 1,280} \right) = \dots 0.54$$

2. Simms Tests— $W_1 = W_2$ —

$$N_I = \frac{1}{2} \left(\frac{1}{1 + \frac{17}{35}} \right) = \dots 0.34$$

3. Mylrea Series II Tests— $W_1 = 2,040$ lb and $W_2 = 1,280$ lb—

$$N_I = \frac{1}{2} \left(\frac{1,280}{2,040 + \frac{17}{35} \times 1,280} \right) = \dots 0.24$$

4. Mavis and Greaves Series 50 Tests— $I = 311$ lb-sec, $W = 145$ lb, and $E_b = 38,000$ in.-lb—

$$N_I = \frac{W E_b}{g I^2} = \frac{145 \times 38,000}{386 \times 311^2} = \dots 0.15$$

⁷"Actual and Estimated Impact Resistance of Some Reinforced Concrete Units Failing in Bending," by L. G. Simms, *Journal, Inst. C. E.*, London, Vol. 23, 1945, pp. 163-179.

⁸"Effects of Impact on Reinforced Concrete Beams," by T. D. Mylrea, *Proceedings, Highway Research Board, National Research Council, Washington, D. C.*, Vol. 18, 1938, pp. 130-139; *Journal, A. C. I.*, Vol. 11, 1940, pp. 581-596.

5. Mavis and Richards Tests— $I = 396$ lb-sec, $W = 150$ lb, and $E_b = 5,470$ in.-lb—

$$N_I = \frac{W E_b}{g I^2} = \frac{150 \times 5,470}{386 \times 396^2} = \dots 0.014$$

A second comparison can also be made in which the ratio of the weight of an equivalent hammer to the weight of the beam is computed. This can be computed by means of the impulse characteristic number of the given tests as follows:

a. Mylrea Series I Tests— $W_1 = 560$ lb and $W_2 = 1,280$ lb—

$$\frac{W_1}{W_2} = \frac{560}{1,280} = 0.44$$

b. Simms Tests— $W_1 = W_2$ —

$$\frac{W_1}{W_2} = 1.0$$

c. Mylrea Series II Tests— $W_1 = 2,040$ lb and $W_2 = 1,280$ lb—

$$\frac{W_1}{W_2} = \frac{2,040}{1,280} = 1.6$$

d. Mavis and Greaves Series 50 Tests— $\frac{1}{2} \left(\frac{W_2}{W_1 + \frac{17}{35} W_2} \right) = 0.15$ and

$$W_2 = 0.30 W_1 + 0.15 W_2—$$

$$\frac{W_1}{W_2} = \frac{1 - 0.15}{0.30} = 2.8$$

e. Mavis and Richards Test— $\frac{1}{2} \left(\frac{W_2}{W_1 + \frac{17}{35} W_2} \right) = 0.014$

$$W_2 = 0.028 W_1 + 0.01 W_2—$$

$$\frac{W_1}{W_2} = \frac{1 - 0.01}{0.028} = 35$$

Fig. 5 shows the computed impulse characteristic number as a function of the weight ratio. The relative order of the foregoing series of tests is indicated on this curve.

Of significance is the fact that the impulse characteristic number is a measure of the quality of an impulse, thus causing some impulses to be more destructive than others, although the $(\int F dT)$ -value is the same. In the tests conducted by Mavis and Richards, 396 lb-sec were required to produce 1.75 in. of permanent deflection in a beam having a static load capacity of 2,900 lb. On the other hand, in the tests performed by the writers, beams of the same mass required only 311 lb-sec for complete destruction although the static load capacity was

3,600 lb. In the Mavis and Richards tests the impulse characteristic number was 0.014. The corresponding equivalent hammer would be a 5,300-lb weight moving horizontally with a velocity of 29 in. per sec. In the Mavis and Greaves tests the impulse characteristic number was 0.15. The corresponding equivalent hammer would be a 410-lb weight moving horizontally with a velocity of 290 in. per sec.

The equivalent of a conventional short-time test would be a heavy weight moving at a low velocity. The impulse characteristic number would be low. At the other extreme a small projectile hitting a massive target would correspond to a large impulse characteristic number.

RELATIVE IMPACT RESISTANCE

Destructive impulsive loads on a beam are resisted initially by the inertia (weight) of the member. The kinetic energy associated with this motion must

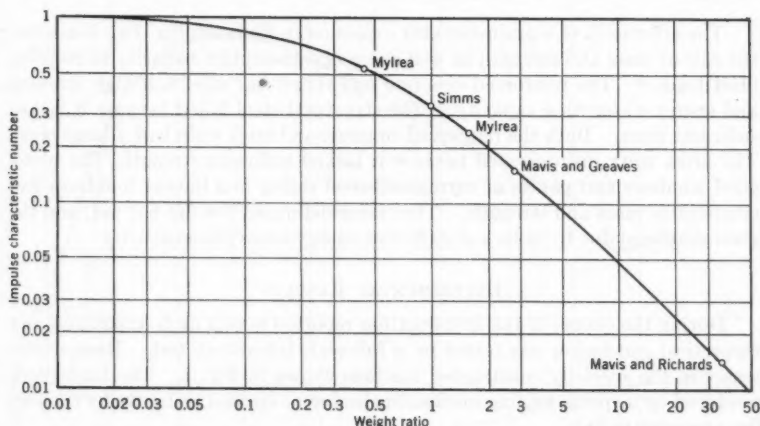


FIG. 5.—IMPULSE CHARACTERISTIC NUMBER FOR VARIOUS WEIGHT RATIOS

be absorbed to bring the member to rest. Similarly, the excess load impulse (that in excess of the flexural resistance of the beam) appears as momentum. It must be absorbed before the loaded system returns to rest. When the flexural resistance is high and the excess load impulse is low, a relatively large part of the load impulse itself is ineffective in causing damage. This case is especially true when the impulse is applied over a longer time interval than the natural period of vibration of the beam.

The impulse characteristic number facilitates an orderly arrangement of the factors influencing the capacity of a beam to resist an impulsive load. As shown in Eq. 5, $N_I = \frac{W E_b}{g I^2} = k a b c$. When solving for the square of the applied impulse, $I^2 = \left(\frac{1}{k c} \right) (W/g) E_b \left(\frac{1}{a b} \right)$. In the foregoing expression I

is the impulse applied to a beam of weight W , and E_a is the energy absorbed by the beam. An increase in yield resistance, F_y , will result in a decrease in a and b with a corresponding increase in the quantity, $\frac{1}{a b}$. Generally, the factor $\frac{1}{k c}$ is a constant, and its value usually falls between the limits of $\frac{1}{4}$ and $\frac{3}{4}$.

The impulse, I , that a given beam can resist depends on the weight, energy-absorbing capacity, and strength of the beam. Therefore,

1. If two beams of different weights are otherwise identical, the heavier beam can resist the larger impulse.
2. If two beams with different capacities of absorbing energy are otherwise identical, the beam with the greater energy-absorption capacity can resist the greater impulse.
3. If two beams have different strengths but are otherwise identical, the stronger beam can resist the larger impulse.

The aftermath of a grain-elevator explosion in Philadelphia, Pa., illustrates the role of mass and strength as well as energy-absorption capacity in resisting blast loads.¹⁰ The reinforced concrete and structural steel had high strength and energy-absorption capacity. The structural steel failed because it lacked sufficient mass. Both the reinforced concrete and brick walls had a large mass. The brick work disintegrated because it lacked sufficient strength. The plate-glass windows and panels of corrugated-steel siding in adjacent buildings had comparable mass and strength. The siding deformed but did not fail, and the glass shattered due to its lack of sufficient energy-absorption capacity.

EXPERIMENTAL RESULTS

During the course of the investigation reported herein each hypothesis and theoretical conclusion was tested by a full-scale laboratory test. Beams were tested in the specially constructed machine shown in Fig. 1. The loads were produced by a spring loading mechanism and were applied instantly by fracturing a temporary link.

Typical load-time records and reaction-time records for these tests are shown in Figs. 6(a) and 6(b). The measured loads and the reactions are represented by the dotted lines. They were measured by electrical resistance strain gages and recorded on film by a high-speed camera. The initial spring load for this test was 8.5 kips.

In Fig. 6(a)

$$P = 8,500 \exp - \frac{T}{0.0135 e} \dots \dots \dots (25)$$

and in Fig. 6(b)

$$R = 8,500 \frac{T}{0.0135} \exp \left(1 - \frac{T}{0.0135} \right) \dots \dots \dots (26)$$

¹⁰ "Philadelphia Explosion," by Charles F. Peck, Jr., *Engineering News-Record*, Vol. 156, No. 20, 1956, p. 8.

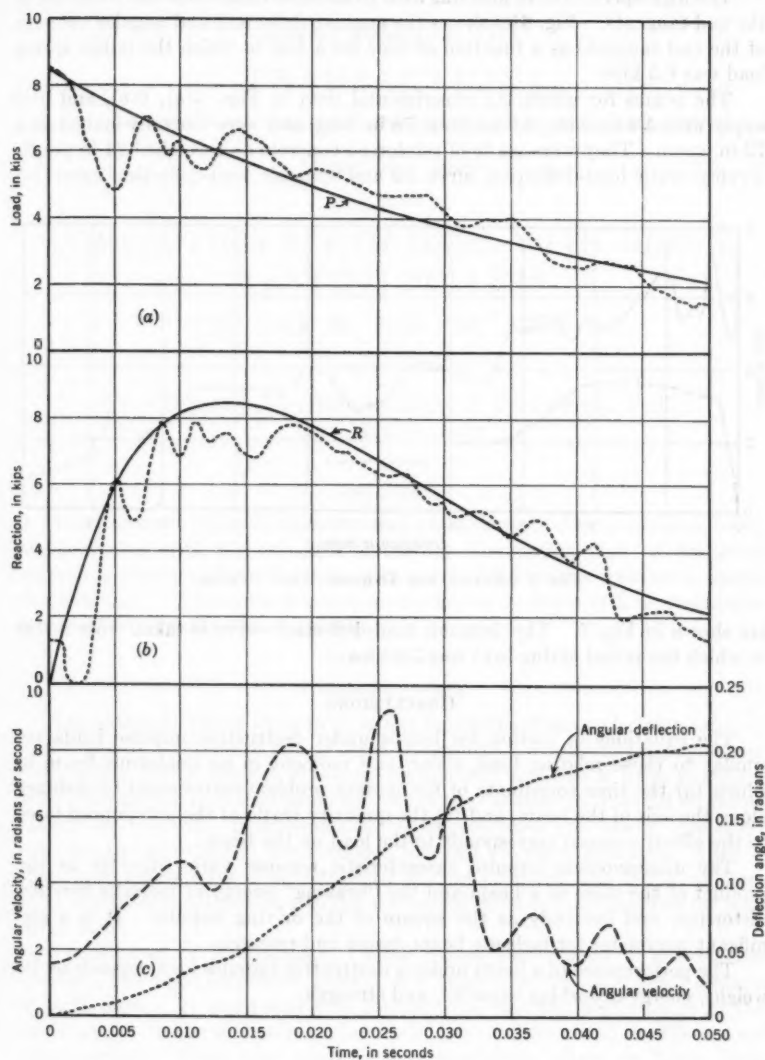


FIG. 6.—LABORATORY TEST CURVES

The high-speed camera also was used to measure deflections and rotations of the end tangents. Fig. 6(c) shows the angular deflection and angular velocity of the end tangents as a function of time for a test in which the initial spring load was 6.5 kips.

The beams for which the experimental data in Figs. 6(a), 6(b), and 6(c) apply were 4.2 in. wide, 5.9 in. deep, 78 in. long, and were centrally loaded on a 72-in. span. They were made of reinforced concrete and weighed 24 lb per ft. Typical static load-deflection curve I-2 and dynamic load-deflection curve I-5

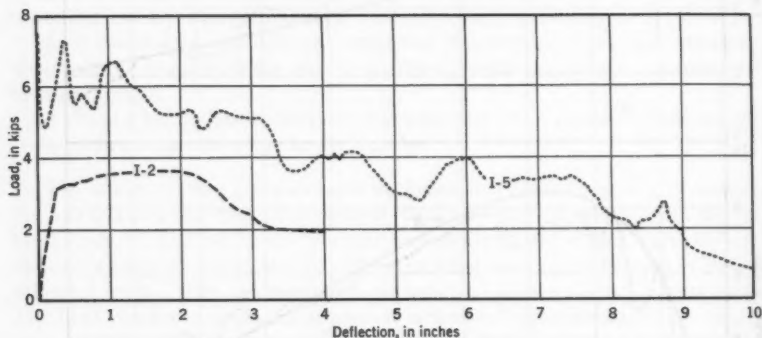


FIG. 7.—STATIC AND DYNAMIC TEST CURVES

are shown in Fig. 7. The dynamic load-deflection curve is taken from a test in which the initial spring load was 7.5 kips.

CONCLUSIONS

The equations of motion for beams under destructive impulse loads are similar to those relating load, shear, and moment in an analogous beam in which (a) the time coordinate of the motion problem corresponds to distance along the axis of the beam, and (b) the quantity (ratio of the unbalanced force to the effective mass) corresponds to the load on the beam.

The dimensionless impulse characteristic number varies directly as the product of the mass of a beam and the "braking" energy of inelastic bending distortion, and inversely as the square of the driving impulse. It is a significant parameter for inelastic beam design and research.

The performance of a beam under a destructive impulse load depends on its weight, energy-absorbing capacity, and strength.

AMERICAN SOCIETY OF CIVIL ENGINEERS

Founded November 5, 1852

TRANSACTIONS

Paper No. 2986

COMPACTING EARTH DAMS WITH HEAVY TAMPING ROLLERS

BY JACK W. HILF,¹ M. ASCE

WITH DISCUSSION BY MESSRS. JACK D. HODGSON; C. Y. LI;
AND JACK W. HILF

SYNOPSIS

The results of compacting thirty-nine earth dams by heavy tamping rollers are compared with the standard laboratory compaction test. A statistical method is presented for obtaining roller curves from control tests made during construction. The results of this type of analysis on dams with representative ranges of impervious soils are given.

INTRODUCTION

The extensive use of sheepfoot rollers for compacting earth dams has been challenged by a variety of new types of equipment. These include pneumatic-tired rollers, which differ in number, arrangement, and size of tires, in type of wheel suspension, in ballast capacity, and in the capacity to transmit vibratory energy to the soil. Nonpneumatic rollers comprise the heavy steel-mesh cylinder, the grooved roll, the scalloped roll, and the segmented roll. A few of these new rollers have demonstrated sufficient economy and technical merit to be included as alternatives to the sheepfoot roller in specifications for large earth dams.

The Bureau of Reclamation, United States Department of the Interior (USBR), has made large-scale tests of new types of rollers in selected sections of earth dams. It was possible to compare the cost and performance of this equipment with the sheepfoot roller under job conditions and in different soil classifications. Tests were made with rubber-tired rollers at Tiber Dam, Marias River, near Shelby, Mont. At Kirwin Dam, North Fork Solomon River, near Kirwin, Kans., and at Palisades Dam, South Fork Snake River, near

NOTE.—Published, essentially as printed here, in April, 1957, in the Journal of the Soil Mechanics and Foundations Division, as *Proceedings Paper 1205*. Positions and titles given are those in effect when the paper or discussion was approved for publication in *Transactions*.

¹ Superv. Civ. Engr., Bureau of Reclamation, U. S. Dept. of the Interior, Denver, Colo.

Idaho Falls, Idaho, compaction with rubber-tired rollers was permitted in sections of the dams outside of the water-barrier zone. However, specifications for compacting the impervious part of the USBR dams have retained the requirement for heavy tamping rollers.

When the technical effectiveness of different rollers is compared, the design objective of the fill must be considered carefully. Differences in function between embankments for dams and for roads and airfields can readily be seen. However, a valid comparison of rollers may require distinguishing between the earth dam built primarily for flood control and the dam used mainly for water conservation. Construction engineers are not in agreement on the subject of compacted cohesive soils. Thus, those who propose placing the soil with a water content that is wet of optimum and those favoring compacting the soil dry of optimum will probably use different criteria. The emphasis placed on the related concepts of pore-water pressure, overcompaction, and cracking in fills varies among soil-mechanics engineers. Any of these concepts may be decisive in evaluating rollers.

If compaction that is equal to or superior to that obtainable by the tamping roller can be achieved by new types of equipment traveling at much higher speeds over thicker layers, the sheepsfoot roller will become obsolete. However, in order for engineers to be satisfied that equivalence is actually obtained, the record of compaction by modern sheepsfoot rollers should be examined. The heavy tamping rollers used by the USBR during the construction of earth dams will be studied herein.

ORIGIN AND USE OF USBR ROLLER

The tamping feet of a flock of sheep crossing a scarified, oil-treated road in Southern California in 1906 (1)² provided the idea for the sheepsfoot roller. A patent on the "Petroolithic" roller was issued during that year. In 1912 rollers with feet 7 in. long, 4 sq in. in area, and exerting unit pressures of 75 lb per sq in. were used to compact earth storage reservoirs in California. This type of roller was reported to be "the only one which would compact a fill in layers without producing lamination, giving a uniform degree of compaction and density" (2).

Echo Dam, Weber River, near Coleville, Utah, constructed in 1928, was the first USBR dam to be compacted by a sheepsfoot roller. The equipment was a two-drum tamper with a 48-in.-diameter, 4-ft-long drum. The feet were 7½ in. long, were staggered on 8-in. centers, and had 3-in.-diameter, ball-shaped heads. The two-drum roller weighed 9,600 lb, or 1,200 lb per ft of drum length, and exerted a nominal unit pressure (the weight of the drum divided by the cross-sectional area of one row of feet) of 170 lb per sq in. From 1928 to 1938 fifteen USBR dams were compacted by sheepsfoot rollers. The rollers varied in weight per foot of drum length from 1,178 lb to 2,900 lb, and in unit pressures from 175 lb per sq in. to 434 lb per sq in. The weight of the rollers was increased gradually during this period. USBR specifications required competition between at least two available commercial rollers. The effectiveness of these

² Numerals in parentheses—thus, (1)—refer to corresponding references in the Bibliography (see Appendix).

rollers varied with the different soils. Hence, equipment and compaction procedures were modified during construction. For example, at Caballo Dam, Rio Grande River, near Truth or Consequences, N. Mex., constructed during the period from 1936 to 1938, it was found that unballasted sheepsfoot rollers could not adequately compact a silty, gravelly sand in 6-in. layers regardless of the passes used. By ballasting the roller drums with sand and water, thus increasing the nominal unit pressure from 250 lb per sq in. to 388 lb per sq in., twelve roller passes produced satisfactory densities.

The difficulties in obtaining satisfactory results with the available commercial rollers led USBR engineers to design a tamping roller that incorporated the best features of several existing rollers. Their experiences emphasized the importance of obtaining the maximum roller weight consistent with the pulling capacity of available tractors. The roller had to be rugged enough to meet the requirements of high construction rates and flexible in compactive effort to secure satisfactory compaction for a wide variety of soils. The size of the USBR roller was similar to that used to compact rocky materials at San Gabriel Dam No. 1, San Gabriel River, of the Los Angeles (Calif.) County flood-control district. The USBR design included rollers with demountable feet and swiveled drums, originally built for Bouquet Dam, Bouquet Canyon River, near Saugus, Calif., by a municipal power company.

The roller was first used in 1938 during construction of Deer Creek Dam, Provo River, near Provo, Utah. It consisted of a two-drum unit in hinged frames that permitted each drum to pivot about an axis parallel to the direction of travel. The drums were made of 1-in.-thick steel, and were 5 ft in diameter and 5 ft long. Cast-steel tamper shanks were welded to each drum in twenty curved rows, six to a row. Thus, each drum had one hundred and twenty equally spaced knobs $9\frac{1}{2}$ in. long, individually equipped with a removable 3-in.-diameter tamper head. When the two-drum unit was fully ballasted with sand and water, it weighed 41,500 lb and produced a unit pressure of 490 lb per sq in. Flexibility of compactive effort could be obtained by varying the number of passes and thickness of layer, changing the weight of the roller from 2,000 lb per ft of drum length, when empty, to twice that weight when fully loaded, and changing the shape or area of the removable tamper head. The latter feature was believed valuable for rapid replacement of heads worn by abrasive soils at the construction site.

From 1938 to 1947 this roller was used on all USBR earth dams, and was built and sold by several manufacturers. With an expanded reclamation program after World War II, the specifications were changed to permit the use of available commercial rollers that could be modified to meet the essential USBR requirements.

Current specifications (1959) are:

1. Tamping rollers must have drums not less than 5 ft in diameter and between 4 ft and 6 ft long, with the space between adjacent drums from 12 in. to 15 in.
2. Each drum must be free to pivot about an axis parallel to the direction of travel.

TABLE 1.—DAMS COMPACTED

Number	Dam	Location	AVERAGE SOIL CHARACTERISTICS							
			Unified Soil Classification symbols ^a	No. 4 sieve, + in %	No. 200 sieve, in %	Liquid limit, in %	Plasticity index, in %	Laboratory (— No. 4 Fraction)		
								Dry density, in pounds per cubic foot	Water content, W, in %	Proctor needle, in pounds per square inch
(1)	(2)	(3)	(4)	(5)	(6)	(7)	(8)	(9)	(10)	(11)
1	Deer Creek Zones 1 & 2	Provo River, Utah	GC	36	37	24.0	8.5	111.4	15.5	650
2	Green Mountain	Blue River, Colo.	SC	37	20	21.3	7.6	132.2	8.9	1,020
3	Shadow Mountain	Colorado River, Colo.	GC-SC	38	23	124.6	10.5	1,300
4	Deerfield	Castle Creek, S. Dak.	SC	19	48	119.2	13.1	890
5	Jackson Gulch Zone 1	W. Mancos River, Colo.	CL	6	75	40.3	21.3	100.4	21.4	380
6	Long Lake	Apple Creek, N. Dak.	SM	3	43	21.0	1.5	109.7	16.5	1,240
7	Angostura	Cheyenne River, S. Dak.	SC	20	40	122.2	11.7	650
8	Horsetooth	Cache La Poudre River, Colo.	CL	3	58	26.0	11.6	114.9	13.9	610
9	Soldier Canyon	Offstream, Fort Collins, Colo.	CL	3	64	27.0	12.8	113.6	14.1	590
10	Dixon Canyon	Offstream, Fort Collins, Colo.	CL	3	64	27.0	12.8	113.6	14.1	590
11	Spring Canyon	E. Muddy Creek, Colo.	CL	2	70	28.0	14.0	112.3	14.2	570
12	Heart Butte	Heart River, N. Dak.	CL	2	51	25.9	7.3	113.9	16.4	570
13	Olympus	Big Thompson River, Colo.	SM	2	31	17.6	0	120.1	11.6	1,300
14	O'Sullivan	Crab Creek, Wash.	ML	0	60	22.0	0	105.2	17.7	1,400
15	South Coulee	Offstream, Coulee City, Wash.	SM	7	38	105.2	19.1	1,440
16	Anderson Ranch	S.F. Boise River, Idaho	SC	11	33	28.5	13.5	119.2	13.0	740
17	Davis	Colorado River, Ariz.	SM-SC	14	44	25.0	5.1	117.8	13.1	770
18	Dickinson	Heart River, N. Dak.	SC	12	41	113.1	15.3	860
19	Enders	Frenchman Creek, Nebr.	ML	3	53	20.2	1.0	111.5	14.5	800
20	Granby	Colorado River, Colo.	SC	27	27	21.6	7.6	127.0	10.0	1,130
21	Medicine Creek	Medicine Creek, Nebr.	ML	0	93	19.5	1.0	107.7	17.3	550
22	Bonny (North Borrow)	S.F. Republican River, Colo.	ML	1	88	21.0	1.5	105.7	16.2	1,460
23	Bonny (South Borrow)	S.F. Republican River, Colo.	SM	1	35	21.0	1.5	112.2	13.9	1,390
24	Cedar Bluff	Smoky Hill River, Kans.	CL	1	64	29.0	13.0	111.0	14.8	700
25	North	Grand Coulee, Wash.	ML	0	87	21.6	1.4	103.0	18.2	1,350
26	Shadehill	Grand River, S. Dak.	SC	29	25	25.8	10.2	123.3	12.4	980
27	Big Sandy	Big Sandy Creek, Wyo.	SM	2	30	108.5	17.1	1,000
28	Boysen (Borrow K)	Big Horn River, Wyo.	SM-SC	28	16	21.1	4.5	120.0	11.8	650
29	Boysen (Borrow B)	Big Horn River, Wyo.	GM-SM	40	20	20.3	4.9	123.7	11.4	850
30	Boysen (Borrow B-1)	Big Horn River, Wyo.	GM	50	10	18.5	2.0	124.3	10.4	1,000
31	Carter Lake 1, 2, 3	Offstream, Berthoud, Colo.	CL	6	53	28.0	13.8	112.8	14.9	500

^a "Classification and Identifications of Soils," by Arthur Casagrande, *Transactions, ASCE*, 1948.

BY SHEEPSFOOT ROLLERS

COMPACTION RESULTS BASED ON - No. 4 FRACTION											
Specific gravity, <i>G</i>	Permeability, <i>K</i> , in feet per year	Volume rolled, in cubic yards $\times 10^3$	Number of tests	Water content, <i>W</i> , variation from laboratory optimum, in % dry weight		Dry Density, in Pounds per Cubic Foot				Average fill needle, in pounds per square inch	Roller walkout
						Variation from laboratory density at fill water con- tent, <i>W</i>		Variation from laboratory maximum density			
				Average, ^b \bar{X}	Standard deviation, σ	Average, ^b \bar{X}	Standard deviation, σ	Average, ^b \bar{X}	Standard deviation, σ		
(11)	(12)	(13)	(14)	(15)	(16)	(17)	(18)	(19)	(20)	(21)	(22)
2.67	0.1	2,580	628	-0.3 \pm 0.07	1.11	-0.1 \pm 0.19	2.86	-1.0 \pm 0.20	2.98	rocky	...
2.72	0.2	2,488	1,066	-0.4 \pm 0.03	0.63	0 \pm 0.17	3.30	-0.7 \pm 0.17	3.29	rocky	...
2.65	...	139	38	-0.7 \pm 0.26	0.94	-0.3 \pm 0.86	3.08	-1.9 \pm 1.02	3.65	1,890	some
2.65	0.1	511	60	0 \pm 0.31	1.44	-0.1 \pm 0.40	1.81	-1.1 \pm 0.46	2.12	950	...
2.72	0.05	1,215	203	-2.5 \pm 0.36	3.10	3.3 \pm 0.70	6.00	0.3 \pm 0.53	4.60	1,040	yes
2.70	3.0	405	396	-2.1 \pm 0.15	1.85	2.2 \pm 0.26	3.09	-0.2 \pm 0.28	3.35	1,780	some
2.64	0.3	291	117	-0.5 \pm 0.15	1.00	2.4 \pm 0.57	3.70	1.1 \pm 0.52	3.40	rocky	yes
2.67	0.1	1,443	288	-2.3 \pm 0.16	1.69	4.7 \pm 0.39	4.05	-2.4 \pm 0.45	4.67	1,530	yes
2.67	0.1	2,404	301	-2.5 \pm 0.17	1.84	4.0 \pm 0.37	3.84	-2.2 \pm 0.47	4.99	1,530	yes
2.67	0.1	1,986	240	-2.8 \pm 0.18	1.68	3.5 \pm 0.44	4.08	-1.7 \pm 0.47	4.40	1,370	yes
2.67	0.1	1,366	218	-3.0 \pm 0.17	1.55	4.7 \pm 0.49	4.37	-1.2 \pm 0.50	4.50	1,400	yes
2.67	0.4	898	365	-0.9 \pm 0.14	1.60	1.4 \pm 0.22	2.61	-0.1 \pm 0.27	3.08	930	some
2.65	0.2	238	79	-1.4 \pm 0.33	1.76	-1.0 \pm 1.12	5.93	-3.6 \pm 1.13	5.95	1,250	some
2.75	0.2	4,798	1,823	-1.4 \pm 0.07	1.91	2.3 \pm 0.12	3.10	0.7 \pm 0.13	3.40	1,390	no
2.63	0.6	530	410	-2.2 \pm 0.15	1.86	0.9 \pm 0.30	3.70	-1.7 \pm 0.36	4.35	2,230	yes
2.64	0.4	3,991	2,139	-0.5 \pm 0.04	0.97	2.5 \pm 0.09	2.52	1.4 \pm 0.09	2.40
2.66	0.02	986	492	-1.2 \pm 0.13	1.71	1.5 \pm 0.32	4.30	0 \pm 0.29	3.90	2,300	some
2.64	0.2	239	279	-1.6 \pm 0.16	1.59	1.2 \pm 0.25	2.50	-0.8 \pm 0.25	2.47	1,150	some
2.62	0.3	1,480	888	-1.3 \pm 0.09	1.68	2.2 \pm 0.17	3.17	0.1 \pm 0.19	3.41	1,070	no
2.63	0.4	1,705	550	-0.4 \pm 0.08	1.07	0.8 \pm 0.24	3.38	-0.2 \pm 0.22	3.15	rocky	yes
2.62	0.2	1,982	1,347	-1.0 \pm 0.06	1.33	-1.3 \pm 0.14	3.13	-2.7 \pm 0.16	3.46	1,360	some
2.62	0.4	4,618	1,069	-0.8 \pm 0.08	1.53	2.4 \pm 0.11	2.11	1.2 \pm 0.12	2.34	1,650	some
2.63	0.4	3,344	771	-1.2 \pm 0.10	1.74	3.3 \pm 0.16	2.75	1.3 \pm 0.20	3.38	1,670	some
2.61	0.08	7,135	2,692	-1.1 \pm 0.06	1.81	1.0 \pm 0.10	3.14	-0.9 \pm 0.11	3.54	1,070	yes
2.62	0.02	610	291	-2.5 \pm 0.21	2.21	0.7 \pm 0.28	2.84	-1.5 \pm 0.33	3.37	1,550	no
2.72	0.4	3,276	1,042	-1.2 \pm 0.07	1.36	0.4 \pm 0.20	3.85	-1.5 \pm 0.21	4.07	2,000	yes
2.69	0.2	474	262	-0.9 \pm 0.15	1.45	4.4 \pm 0.39	3.77	3.3 \pm 0.36	3.49	1,200	some
2.68	0.7	557	411	-0.5 \pm 0.12	1.50	1.9 \pm 0.46	5.69	0.5 \pm 0.41	5.08	rocky	some
2.68	2.0	323	265	-0.2 \pm 0.15	1.45	1.3 \pm 0.66	6.45	0.5 \pm 0.66	6.50	rocky	some
2.68	1.0	206	161	-0.1 \pm 0.22	1.65	-2.7 \pm 1.08	8.27	-5.2 \pm 1.00	7.65	rocky	some
2.67	0.09	2,086	839	-1.4 \pm 0.08	1.31	2.5 \pm 0.18	3.17	0.8 \pm 0.18	3.15	980	some

^aThe \pm entry indicates 90% confidence limits.

TABLE 1.—DAMS COMPACTED BY

Number	Dam	Location	AVERAGE SOIL CHARACTERISTICS							
			Unified Soil Classification symbol ^a	+ No. 4 sieve, in %	- No. 200 sieve, in %	Liquid limit, in %	Plasticity index, in %	Laboratory (- No. 4 Fraction)		
								Dry density, in, pounds per cubic foot	Water content, W, in %	Proctor needle, in pounds per square inch
(1)	(2)	(3)	(4)	(5)	(6)	(7)	(8)	(9)	(10)	
32	Keyhole	Belle Fourche River, Wyo.	CL	0	58	113.2	14.5	640
33	Lauro	Diablo Creek, Calif.	SC	16	25	116.0	13.3	880
34	Platoro	Conejos Creek, Colo.	GC-SC	39	21	30.0	12.7	123.3	12.2	910
35	Rattlesnake	Rattlesnake Creek, Colo.	SM	5	43	23.3	3.8	115.5	13.5	740
36	Cachuma	Santa Ynez River, Calif.	SC-SM	36	26	25.5	6.3	114.8	14.5	1,030
37	Flatiron	Chimney Hollow Creek, Colo.	SC-CL	4	50	26.8	8.4	115.5	13.7	560
38	Glen Anne Zone 1	Glen Anne Canyon River, Calif.	CL	2	68	31.0	16.0	115.3	13.7	1,050
39	Glen Anne Zone 2	Glen Anne Canyon River, Calif.	SM	0	13	22.0	0	109.1	15.8	1,240
40	Jamestown	James River, N. Dak.	CL	5	66	28.9	11.6	101.4	20.1	420
41	Willow Creek	Willow Creek, Colo.	SC	25	38	41.5	21.0	109.5	16.7	560
42	Trenton	Republican River, Nebr.	ML-CL	0	90	27.0	6.0	106.5	17.0	1,080
43	Trenton Foundation	Republican River, Nebr.	ML-CL	0	92	27.0	6.0	106.2	17.1	1,080
44	Vermejo 2, 3, & Stubblefield	Vermejo River, N. Mex.	CL	0	81	34.7	18.4	109.8	17.9	490

3. One tamping foot must be provided for each 100 sq in. of drum surface.
4. The space between the feet must be equal to or greater than 9 in.
5. The length of the feet must be maintained at a minimum of 9 in.
6. The cross section of the feet must be equal to or less than 10 sq in. at a distance of 6 in. from the surface of the drum. It must be equal to or greater than 7 sq in., but not greater than 10 sq in., at a distance of 8 in. from the surface.
7. The weight of the roller when fully loaded with sand and water must be not less than 4,000 lb per ft of drum length.
8. A pressure relief valve will be provided on each drum.
9. The loading and the operation of rollers are subject to approval by the United States Government, and the loading must obtain the desired compaction.
10. The contractor is required to keep the spaces between the tamping feet clear of material that would interfere with compaction.

Since the heavy tamping roller was introduced in 1938, 50,000,000 cu yd of impervious material used in the construction of thirty-nine USBR earth dams

SHEEPSFOOT ROLLERS—Continued

COMPACTION RESULTS BASED ON - No. 4 FRACTION											
Specific gravity, G	Permeability, K , in feet per year	Volume rolled, in cubic yards $\times 10^3$	Number of tests	Water content, W , variation from laboratory optimum, in % dry weight		Dry Density, in Pounds per Cubic Foot				Average fill needle, in pounds per square inch	Roller walkout
						Variation from laboratory density at fill water con- tent, W		Variation from laboratory maximum density			
				Average, ^b \bar{X}	Standard deviation, σ	Average, ^b \bar{X}	Standard deviation, σ	Average, ^b \bar{X}	Standard deviation, σ		
(11)	(12)	(13)	(14)	(15)	(16)	(17)	(18)	(19)	(20)	(21)	(22)
2.67	0.2	1,007	486	-0.7 \pm 0.11	1.43	0.6 \pm 0.21	2.80	-0.7 \pm 0.21	2.79	940	some
2.68	0.3	302	249	-1.9 \pm 0.14	1.36	5.2 \pm 0.39	3.69	2.2 \pm 0.37	3.53	rocky	...
2.74	0.4	299	304	-0.4 \pm 0.08	0.82	-3.7 \pm 0.43	4.50	-4.5 \pm 0.41	4.30	rocky	yes
2.67	0.1	192	157	-1.4 \pm 0.18	1.38	1.9 \pm 0.46	3.49	0.8 \pm 0.44	3.30	1,320	yes
2.66	1.0	3,000	1,324	-0.8 \pm 0.05	1.07	-1.5 \pm 0.16	3.52	-2.5 \pm 0.16	3.57	rocky	some
2.69	0.2	260	222	-0.7 \pm 0.13	1.19	1.9 \pm 0.32	2.85	0.9 \pm 0.29	2.61	980	some
2.68	0.4	166	76	-0.9 \pm 0.21	1.09	1.7 \pm 0.52	2.71	0.6 \pm 0.46	2.40	1,260	...
2.64	0.3	116	54	-3.2 \pm 0.37	1.62	4.9 \pm 0.74	3.20	2.3 \pm 0.88	3.83	1,520	...
2.66	0.1	606	381	-1.6 \pm 0.10	1.22	3.6 \pm 0.30	3.53	1.6 \pm 0.29	3.46	1,160	...
2.61	0.09	268	203	-1.0 \pm 0.13	1.10	2.3 \pm 0.38	3.29	0.8 \pm 0.35	2.97	1,050	...
2.63	0.3	1,791	1,448	-0.5 \pm 0.08	1.77	1.0 \pm 0.10	2.26	-0.4 \pm 0.11	2.58	1,010	some
2.65	0.2	4,756	3,185	-0.7 \pm 0.04	1.47	2.0 \pm 0.06	2.19	0.7 \pm 0.07	2.23	1,070	no
2.67	0.03	940	381	-0.6 \pm 0.10	1.13	1.3 \pm 0.42	4.37	0.2 \pm 0.34	3.60	720	...

have been compacted by essentially the same effort. The soils varied from mixtures of sand, gravel, and cobbles of as much as 5 in. in size to fine-grained, plastic clays. Approximately 28,000 field density control tests were made, or one test for every 1,800 cu yd of soil.

Table 1 shows all completed USBR earth dams (as of 1954). The water-barrier sections were compacted to 6-in. layers by twelve roller passes, following the foregoing specifications. Rollers built in accordance with USBR drawings have been used interchangeably with other rollers meeting the specifications. The control statistics in Table 1 are for all field density tests, including those made in areas that were compacted by small power tampers. Most of the tests were run in soils compacted by twelve passes of the heavy roller to 6-in. compacted layers. Because power-tamped fill must be equivalent to the rolled fill, Table 1 represents the degree of compaction that has been achieved by the roller for a variety of soils under construction conditions. In Cols. 3 through 12 the Unified Soil Classification symbols refer to the modification of the "Airfield Classification System" of Arthur Casagrande, M. ASCE, adopted by

the Corps of Engineers, United States Department of the Army (3), and the USBR in January, 1952 (4). The other data are equivalent to American Society for Testing Materials (ASTM) standards (5). The single exception is that the USBR compaction test is made in a 1/20-cu-ft cylinder in three 2-in. layers, with twenty-five blows per layer of a 5½-lb hammer dropped 18 in. The total effort is 12,375 ft-lb per cu ft of soil. This effort is the same numerically as the ASTM standard, although different results have been reported (6). The USBR obtains the Proctor penetration resistance of the compacted soil (7) and uses a permeability test of the constant-head type. Additional descriptive data and field compression characteristics of some of the soils listed in Table 1 are given elsewhere (8) (9).

Cols. 13 through 22 (samples passing a No. 4 sieve) list, in terms of differences or variations, the statistics for three comparisons of fill conditions with laboratory test results:

a. Variations in water content of fill from laboratory optimum water content;

b. Variations of fill dry density from laboratory dry density at the same water content (roller effort compared with laboratory effort); and

c. Variations of fill dry density from laboratory maximum dry density (fill related to the basic laboratory standard for strength, compression, and permeability tests).

F. J. Davis (10) has examined the statistical treatment of items *a* and *c*. Item *b* will be considered herein.

The field density tests, which furnished the results in Table 1, are performed as follows: All the uncompacted material is removed from the surface of the fill, and the soil is excavated to form a hole 8 in. in diameter and 12 in. deep. Proctor penetration resistance is measured at the surface and when the excavation is 6 in. deep. The volume of the hole is determined by being filled with loose, dry, uniform sand of known density. The excavated material is protected from loss of moisture and is taken to the field laboratory, where it is weighed and screened on the No. 4 United States standard sieve. The part retained on the sieve is dried and weighed, and its volume is determined. Specimens of the -No. 4 fraction are compacted by the standard laboratory procedure at four or more different water contents, including that of the fill. A dry density-water content curve is drawn and the peak is determined. The dry density of the fill on the -No. 4 basis is computed by deducting the volume of the +No. 4 fraction (samples retained on a No. 4 sieve) from the volume of the hole and by dividing the result into the computed dry weight of the -No. 4 fraction. This is compared with the laboratory dry density at the fill water content (item *b*) and with the laboratory maximum dry density (item *c*).

Qualitative data on whether the rollers "walked out" are shown in Col. 22 of Table 1 for dams for which such data were reported. On the average, if the roller feet penetrated the layer to at least 4 in. less at the twelfth pass than during the first pass, the roller was considered to walk out and was designated by the term "yes" in the table. However, if less than 2 in. of walkout was

reported, the notation "no" was made. Walkout of at least 2 in. but less than 4 in. was designated by "some." Col. 21 refers to penetration-resistance tests in the fill during the field density tests. This needle test was not made in soils containing appreciable quantities of gravel sizes. Those instances are designated as "rocky."

ANALYSIS OF FIELD RESULTS

Comparison of Roller and Laboratory Efforts.—Fig. 1 compares the roller and laboratory density results given in Table 1. It shows the influence of soil classification and of the excluded +No. 4 fraction (gravel percentage including cobbles of as much as 5 in.) on the apparent effectiveness of the roller. In Fig. 1 the numbers refer to the dams in Table 1, and density variation indicates the variation of fill dry density (—No. 4) from laboratory dry density at fill water content. For soils containing little or no gravel, there were only two instances of roller compaction averaging less than laboratory compaction at the same water content. These were the loess at Medicine Creek Dam, Medicine Creek, near Cambridge, Nebr. (21, ML), and the micaceous silty sand at Olympus Dam, Big Thompson River, near Estes Park, Colo. (13, SM). The fine-grained nonplastic soils similar to the silt at Medicine Creek Dam, such as those at Bonny Dam (North Borrow area), South Fork Republican River, near Hale, Colo. (22, ML), and North Dam, on the Grand Coulee, near Coulee City, Wash. (25, ML), and the coarse-grained silty sands similar to the sand at Olympus Dam, such as those at Bonny Dam (South Borrow area) (23, SM) and Rattlesnake Dam, Rattlesnake Creek, near Loveland, Colo. (35, SM), were compacted to densities greater than that obtained in the laboratory cylinder. Table 1 shows that the low densities for soils 13 and 21 cannot be attributed to significant differences in placement water content from comparable soils, nor to the roller failing to walk out. A combination of poor soils and excessively thick layers accounts for the results.

However, some of the high fill-density values shown in Fig. 1 may not represent true roller performance. The validity of the field-density-test procedure depends on no change in the gradation of the compacted soil after it is removed from the fill, reworked, and recompacted in the cylinder. For soils that were transported over great distances by wind or water, disintegration is usually minor. On the contrary, some residual soils continue to break down into finer gradations on repeated compaction. Finer gradation would tend to decrease the cylinder densities of such soils. This would account for an abnormally high difference of fill to cylinder density. Of the nine low-gravel-content soils with fill densities that are 3 lb per cu ft or more greater than laboratory density, six soils (Nos. 39, 11, 8, 9, 10, and 5) are residual.

The breakdown of the particles results in a higher optimum water content for the soil. This is reflected by an increase in the difference between the water content of the fill (which is independent of particle size) and the laboratory optimum determined in the field-density-test procedure. The average water content of the forty-four soils listed in Table 1 is 1.2% dry of the laboratory optimum. By contrast, the water contents of the six soils, whose high field densities may be a result of disintegration during recompaction, averaged 2.7% dry of optimum.

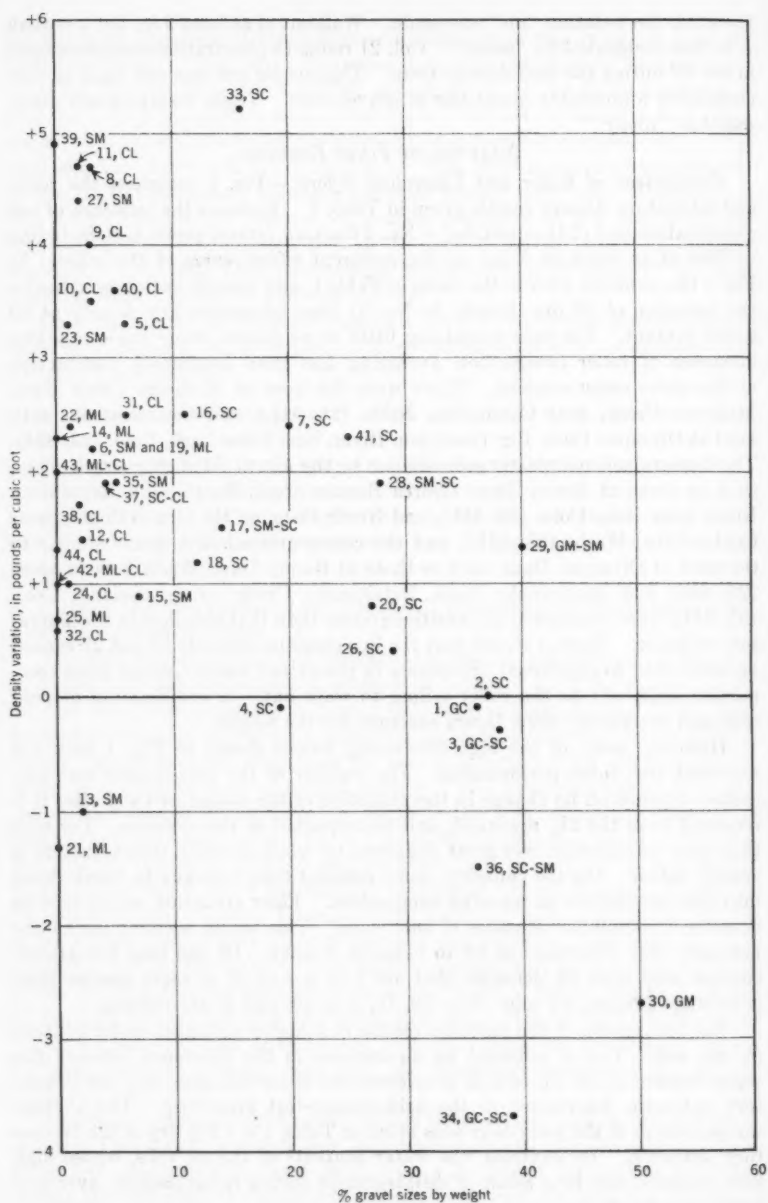


FIG. 1.—ROLLER VERSUS LABORATORY COMPACTION

The high value of the soil at Lauro Dam, Diablo Creek, near Santa Barbara, Calif. (33, SC), containing 16% gravel, tends to corroborate this hypothesis. Laboratory studies made during construction showed that a breakdown of friable-sandstone particles, retained on and passing a No. 4 sieve, in the old alluvial fan material caused the field-density-test results to indicate the following: The material was placed at a water content that was approximately 2% drier than desired, although water contents prior to compaction were satisfactory. The capacity of heavy tamping rollers to make significant changes in the gradation of rocky materials was reported by Paul Baumann, M. ASCE (11). The effects of these changes on the evaluation of field compaction results for soils susceptible to breakdown need further study on the basis of USBR experience.

With the exceptions cited in the foregoing, Fig. 1 indicates that a variety of gravel-free soils were compacted to densities averaging approximately 2 lb per cu ft greater than the laboratory standard by use of twelve passes of the USBR type of sheepfoot roller in 6-in. compacted layers. The fill density appears to exceed laboratory density for materials with gravel contents of as much as 25% when compared on the basis of the —No. 4 fraction. At greater than 25% gravel, it is evident that there is a generally decreasing trend in densities of the —No. 4 fraction with increasing gravel content. Such a trend must be expected because great quantities of hard gravel that cannot be broken down by the roller will tend to support the weight of the roller by arch action of the coarse particles, leaving part of the fines uncompacted. The significance of the low densities of the —No. 4 fraction of such soils will be examined subsequently.

Obtaining Roller Curves from Test Sections.—Under the heading, "Analysis of Field Results: Comparison of Roller and Laboratory Efforts," the densities obtained by roller compaction were compared with the laboratory density at the fill water content without considering the effect of varying the placement water content. If the result of roller compaction is a curve of fill dry density as the ordinate versus water content as the abscissa, similar to the laboratory compaction curve, the values plotted in Fig. 1 can be considered the average distances between the ordinates of the roller curve and the laboratory curve. Few comparisons of roller curves with laboratory compaction curves have been published. The available data were evaluated by a subcommittee of ASCE in 1950 (12). This report showed there was a tendency for the roller curves to approach the 100% saturation line when the soils were compacted wet of their optimums. In 1954 additional data were published by the Corps of Engineers (13). In the instances in which points determining the curves were shown, the scatter was characteristic of the roller curves.

A carefully controlled test fill of homogeneous material, in which all conditions are kept constant except the water content and the number of roller passes, should develop a series of roller curves. These curves can be related to the standard laboratory curve to determine the most desirable quantity of roller passes and placement water content for the soil. Test fills have been made on USBR earth dams as part of the contract work prior to large-scale embankment construction. These fills were valuable in training inspectors

and laboratory personnel in control procedures, but disappointing roller curves were obtained. The data showed that ten or twelve passes of the heavy roller were needed to compact a variety of soils to densities comparable to laboratory compaction.

The reasons for the failure of test sections to develop roller curves may be indicated by a review of the test undertaken at Cachuma Dam, Santa Ynez

TABLE 2.—LABORATORY PROPERTIES

	Average	90% confidence limits ^a	Standard deviation
	(1)	(2)	(3)
Maximum dry density, in pounds per cubic foot....	116.1	±0.2	1.34
Optimum water content, in %.....	14.0	±0.1	0.45
% +No. 4.....	27.1	±1.0	5.90

^a "Manual on Quality Control of Materials," A.S.T.M., January, 1951, p. 43.

River, near Santa Barbara, in 1951. A 310-ft-long, 70-ft-wide area was used for the test fill. It was divided longitudinally into six strips. Each strip was compacted by six, eight, ten, twelve, fourteen, and sixteen passes, respectively. The roller was ballasted to 47,000 lb, or 4,700 lb per ft of drum length. This corresponded to a nominal unit pressure of 553 lb per sq in. The test area was divided into four sections in the transverse direction. The object was to obtain water contents of 4% less than laboratory optimum, 2% less than laboratory optimum, laboratory optimum, and 2% greater than laboratory optimum. Six layers were placed, compacted to a thickness of 6 in. each.

TABLE 3.—CACHUMA DAM TEST SECTION COMPACTION RESULTS

Number of passes	Average gravel content, in percentage of dry weight	Average fill-water-content variation from optimum, in percentage of dry weight ^a	Average fill-dry-density variation from laboratory at fill water content, in pounds per cubic foot	Standard deviation
(1)	(2)	(3)	(4)	(5)
6	28.4	-1.91	-5.9 ± 2.46	5.43
8	27.4	-1.23	-5.5 ± 1.81	3.96
10	26.6	-1.43	-4.3 ± 1.76	3.89
12	27.4	-1.46	-3.2 ± 1.63	3.61
14	26.2	-1.55	-3.4 ± 2.13	4.70
16	26.8	-1.79	-2.0 ± 2.39	5.28

^a The ± entry indicates 90% confidence limits.

The material selected for the test fill was passed through a 3-in. screen at the separation plant to remove cobbles and boulders. Water was added at the plant. The soil was classified as a gravelly sand with a silt-clay binder (SC). Its gravel content averaged 27.1%, or 9% less than the average gravel content for the dam. The field density tests showed that the laboratory dry density

varied from 111.7 lb per cu ft to 119.3 lb per cu ft, despite efforts to obtain a homogenous soil. The laboratory optimum water content varied from 13.0% to 15.0%. The percentage of gravel varied from 17.1% to 40.2%. The corresponding laboratory properties are shown in Table 2.

Field density tests were made in accordance with the standard USBR procedure described previously. Four layers, each with a spread thickness of 8 in., were placed and rolled at the respective water content in each moisture area to provide a foundation. Then tests were made in the fourth, fifth, and sixth compacted layers. The fill was reported to be firm in all areas, except sponginess was noted in the area that was wet of optimum. Penetration of the roller feet varied from 5 in. in the driest material to 10 in. in the wettest material, and remained constant throughout the rolling of the layer.

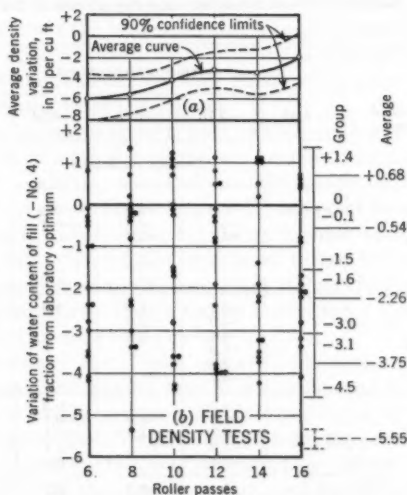
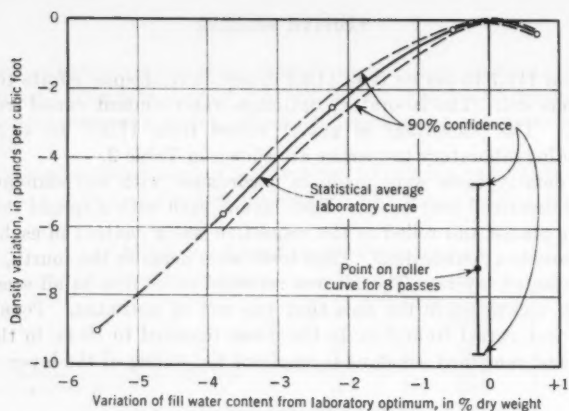


FIG. 2.—TEST SECTION, CACHUMA DAM

Table 3 and Fig. 2(a) show the effect of the number of roller passes on the difference between fill density (-No. 4 fraction) and laboratory density at the fill water content. The difference is the same compaction criterion used in Fig. 1. The average soil properties, other than the gravel contents in Table 3, were almost identical for all strips. The fill density progressively approaches laboratory density for each increase in roller passes except for the fourteen-pass trial. The distribution of the water-content variation from optimum in Fig. 2(b) shows that only two tests of the sixteen run in the fourteen-roller-pass strip were less than 1% from optimum as compared with eight tests for the twelve-pass strip. Because this moisture range would be expected to yield higher densities than wetter or drier ones, the results of the fourteen-pass strip should be expected. Similarly, the tests for six roller passes are unbal-



Number of passes	Average water content				
	-5.55	-3.75	-2.26	-0.54	0.68
	Density variations				
16	-9.9	-5.3	-3.2	-0.2	-0.1
	...	-5.0	-1.8	-0.4	-0.4
	...	-5.7	-3.7	...	-0.3
	-1.4	...	-0.2
	-2.1
14	-1.1
	...	-5.1	-1.6	-1.0	-0.6
	...	-4.9	-2.9	...	-0.6
	...	-6.6	-3.8	...	0.0
	...	-6.9	-0.1
12	...	-2.9	-1.1
	...	-3.7	-0.8
	...	-5.7	...	-0.3	-0.1
	...	-6.3	-3.0	-0.1	-0.1
	...	-6.7	-1.9	-0.1	-0.7
10	...	-5.2	...	-1.1	-0.5
	...	-5.3	...	-0.1	...
	...	-5.4	-2.8	-0.1	-0.2
	...	-8.0	-1.5	-0.8	-0.4
	...	-7.3	-0.9	0.0	-0.6
8	...	-4.4	-1.0
	...	-5.0	-0.1
	-8.1	-6.9	-5.7	-0.3	0.0
	...	-5.8	-3.0	-0.1	-0.2
	-1.9	0.0	-0.4
6	-0.1	-1.0
	-0.1	...
	-0.2	...
	...	-5.5	-3.2	-0.1	-0.2
	...	-2.5	-1.9	-0.2	...
Average	...	-6.1	-1.2	-0.1	...
	...	-7.5	-4.1	-0.1	...
	-2.7	-0.1	...
	-0.3	...

90% confidence	...	±0.46	±0.44	±0.08	±0.12
Standard deviation	...	1.31	1.17	0.22	0.32

FIG. 3.—DERIVATION OF AVERAGE COMPACTION CURVE AT CACHUMA DAM TEST SECTION

anced as to water content because only one test was run in material wet of optimum.

The 90% confidence limits shown in Fig. 2(a) are an expression used in quality control, which defines the values within which the true average curve lies with the probability of 0.90 of being correct. The magnitude of the confidence limits varies directly with the standard deviation of the data and inversely with the square root of the number of tests. The plot indicates generally increased density as the passes increased. It also shows that any attempt to draw conclusions as to the shape of the curve, which would be needed to determine the desirable number of passes, is not warranted because of the high values of the confidence limits. High standard deviations in field-density-test results must be expected even under carefully controlled field conditions because of the impracticability of avoiding soil variations. Only under research conditions can close control of materials be achieved. However, for a given standard deviation the confidence limits can be narrowed by increasing the tests. Thus, it appears that sixteen tests on each longitudinal strip were not sufficient to determine decisively how many roller passes were the most efficient for the Cachuma Dam test section.

Under these circumstances sixteen tests cannot yield a valid roller curve. However, in order to develop the procedure for obtaining such curves when sufficient tests are available, the analysis will continue. The laboratory optimum water content of a soil is used as a reference point for moisture control, although its magnitude varies somewhat for each cubic yard excavated from a borrow area. If the same concept is applied to the laboratory maximum dry density, thus using it as a reference point for all densities regardless of water content or compactive effort, a tool is available for developing average laboratory curves and average roller curves.

To obtain a laboratory curve from the available data the water contents of all ninety-six tests were divided into four groups, and the average water content of each group was determined (Fig. 2(b)). Then the variation of the laboratory dry density at the fill water content from the laboratory maximum dry density for each control test was tabulated, as shown in Fig. 3. Also shown are the average, the standard deviation, and the 90% confidence limits of these differences in laboratory densities for all tests in each moisture range. Fig. 3 contains a plot of the resulting curve. The 90% confidence limits are small enough to indicate the shape of the average laboratory curve.

If sufficient tests at various water contents were made in each of the rolled strips, composite roller curves could be constructed in a similar manner. This could be done either by plotting average differences of fill density from the fixed laboratory maximum-density point, or by plotting differences of fill density from laboratory density at fill water content along the average laboratory curve. To show that valid roller curves cannot be obtained from the sixteen tests made in each strip, one can select a group of the tests made in one strip at the same water-content variation from optimum. Then the statistics of the corresponding fill-density variation from laboratory density at the fill water content can be found. The greatest quantity of tests grouped closely about a single water-content variation. Hence, the most promising data for a

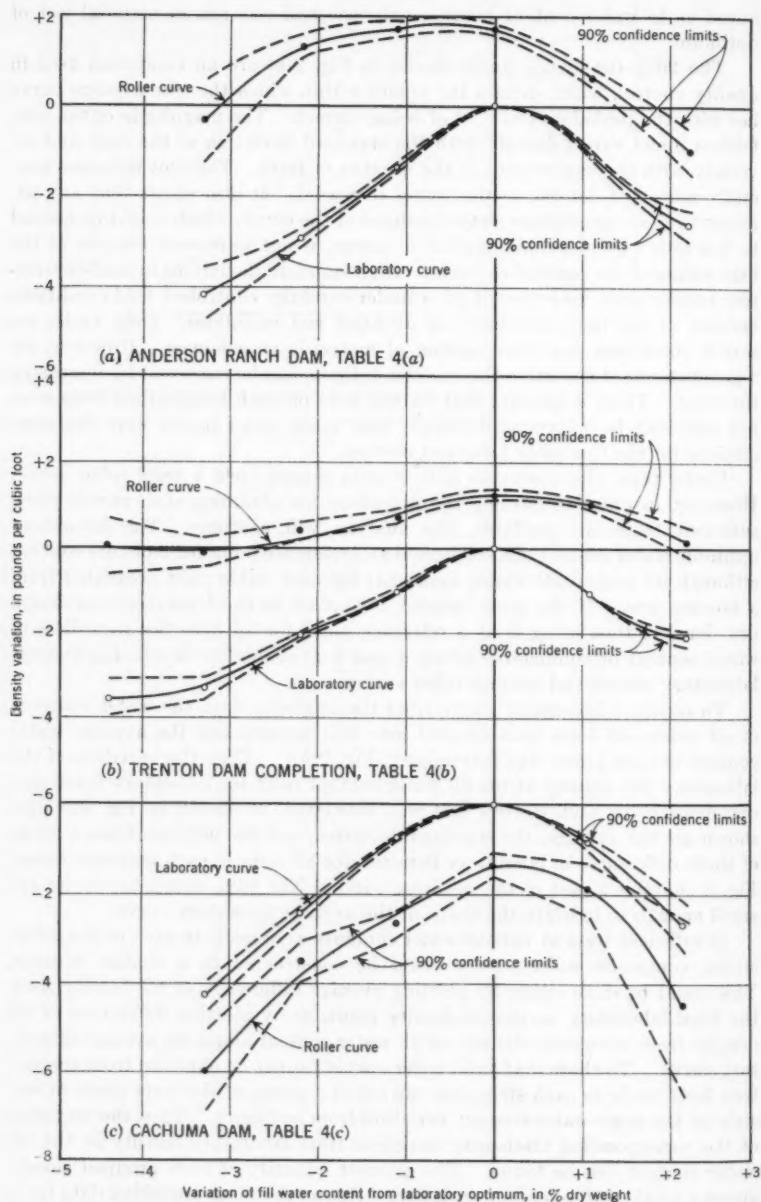


FIG. 4.—GRAPHICAL RELATIONSHIP BETWEEN ROLLER CURVE
AND LABORATORY COMPACTION CURVE

point on a roller curve are for eight roller passes, in which seven tests were made between 0.2% and -0.4% from optimum (Fig. 2). These data are:

Variation of the fill water content from optimum, in percentage	Variation of the fill dry density from laboratory dry density at fill water content, in pounds per cubic foot
-0.3.....	-11.8
-0.1.....	-5.0
-0.2.....	-8.2
0.....	-1.5
-0.2.....	-6.6
0.2.....	-6.6
-0.4.....	-9.9
Average.. -0.14	Average.. -7.1 ± 2.46
	Standard deviation = 3.1

The confidence limits show that the true mean roller curve for eight passes can lie between 4.6 lb per cu ft and 9.6 lb per cu ft from the average laboratory curve at a water content of -0.14 from laboratory optimum, as shown in Fig. 3. Comparing this extensive range with the average difference of 3.9 lb per cu ft between the results of sixteen roller passes and six roller passes makes it unnecessary to continue to derive roller curves from the Cachuma Dam test-section data.

Roller Curves from Control Tests.—Average laboratory curves and roller curves can be obtained by elementary statistical methods. This is possible if many tests are made at various water contents. The data that furnished the results reported in Table 1 are available for USBR dams, three of which were selected for analysis by this method. Fig. 4 and Table 4 show the results of the analyses (on the -No. 4 basis) for Anderson Ranch Dam, South Fork Boise River, near Mountainhome, Idaho (11% gravel); the Trenton Dam completion (Republican River, near McCook, Nebr.) (0% gravel); and Cachuma Dam (35.7% gravel). In Fig. 4 density variation indicates the variation of dry density from laboratory maximum dry density. These analyses provided sufficient tests run throughout wide moisture variations to allow the use of equal moisture groups for deriving both the laboratory curves and the roller curves. Therefore, the points are spaced equally along the abscissas. Only the tests on layers compacted by twelve roller passes were used. The optimum point for the roller curve of the material for Anderson Ranch Dam is slightly dry of laboratory optimum. For Trenton Dam the curve is at approximately the same optimum. For Cachuma Dam, where the roller curve is lower than the laboratory curve, it appears to be slightly wet of optimum. In all cases the shapes of the curves are well defined by the narrow confidence-limit lines.

The effect of the gravel content on the comparison of fill density to laboratory density at the fill water content was studied by Fred C. Walker and Wesley G. Holtz, Members, ASCE (14). The Cachuma Dam control-test results were analyzed separately to determine the effect of the gravel content on the position of the roller curve. The data in Table 5 and Fig. 5 were obtained from this analysis. The 90% confidence limits of these curves vary

considerably. This is the result of dividing the data into groups, thus decreasing the total tests available for deriving each curve. In Fig. 5 density variation indicates the variation of dry density from laboratory maximum dry density. The soils containing gravel have well-defined roller curves of total material, as shown in Fig. 5.

TABLE 4.—STATISTICAL RELATIONSHIP BETWEEN ROLLER CURVE AND LABORATORY COMPACTION CURVE

VARIATION OF FILL WATER CONTENT FROM LABORATORY OPTIMUM, IN % DRY WEIGHT		NUMBER OF TESTS	VARIATION OF LABORATORY DRY DENSITY AT FILL WATER CONTENT FROM MAXIMUM LABORATORY DRY DENSITY, IN POUNDS PER CUBIC FOOT			VARIATION OF LABORATORY DRY DENSITY AT FILL WATER CONTENT FROM FILL DRY DENSITY, IN POUNDS PER CUBIC FOOT		
Range	Mid-point	n	Average, ^a \bar{X}	Standard deviation, σ	Skewness, s_k	Average, ^a \bar{X}	Standard deviation, σ	Skewness, s_k
(1)	(2)	(3)	(4)	(5)	(6)	(7)	(8)	(9)
(a) ANDERSON RANCH DAM, FIG. 4(a)								
-3.8 to -2.8	-3.3	29	-4.21±0.57	1.78	0.75	-3.86±0.92	2.88	0.59
-2.7 to -1.7	-2.2	195	-2.96±0.20	1.63	-0.25	-4.25±0.29	2.44	-0.70
-1.6 to -0.6	-1.1	726	-1.40±0.06	0.99	-0.85	-3.03±0.15	2.51	-0.19
-0.5 to 0.5	0	990	0±0.00	0	0	-1.63±0.12	2.20	0.21
0.6 to 1.6	1.1	291	-1.15±0.08	0.75	-0.80	-1.72±0.20	2.09	-0.56
1.7 to 2.7	2.2	32	-2.68±0.36	1.18	-0.95	-1.68±0.53	1.69	-0.37
(b) TRENTON DAM COMPLETION, FIG. 4(b)								
-6.0 to -5.0	-5.5	10 ^a	-4.15±1.36	2.23	-0.27	-3.75±1.20	1.97	-0.10
-4.9 to -3.9	-4.4	44	-3.48±0.43	1.67	0.04	-3.57±0.65	2.52	-0.01
-3.8 to -2.8	-3.3	115	-3.31±0.24	1.53	-0.50	-3.22±0.34	2.22	0.15
-2.7 to -1.7	-2.2	388	-2.06±0.08	1.00	-0.51	-2.50±0.20	2.39	-0.40
-1.6 to -0.6	-1.1	726	-1.07±0.05	0.80	-0.66	-1.80±0.13	2.14	-0.12
-0.5 to 0.5	0	748	0±0.00	0	0	-1.22±0.12	1.96	-0.53
0.6 to 1.6	1.1	363	-1.12±0.05	0.86	-0.66	-2.11±0.10	1.84	-0.30
1.7 to 2.7	2.2	97	-2.14±0.20	1.18	-0.50	-2.28±0.33	1.95	0.14
2.8 to 3.8	3.3	19 ^b	-3.24±0.68	1.66	0.20	-2.92±0.74	1.82	-0.20
(c) CACHUMA DAM, FIG. 4(c)								
-4.9 to -3.9	-4.4	8 ^b	-6.05±0.65	0.90	0	0.41±1.50	2.10	0.20
-3.8 to -2.8	-3.3	48	-4.28±0.31	1.26	0.10	1.71±0.92	3.70	0.46
-2.7 to -1.7	-2.2	204	-2.45±0.14	1.17	-0.21	1.07±0.43	3.65	0.29
-1.6 to -0.6	-1.1	390	-0.71±0.06	0.68	0.57	1.94±0.29	3.41	0.24
-0.5 to 0.5	0	494	0±0.00	0	0	1.35±0.25	3.44	0.71
0.6 to 1.6	1.1	73	-0.86±0.16	0.78	0.31	1.03±0.58	2.97	0.75
1.7 to 2.7	2.2	9	-2.69±0.57	0.86	0.71	1.83±1.95	2.96	0.99
2.8 to 3.8	3.3	3 ^b

^a The ± entry indicates 90% confidence limits. ^b Not plotted.

Fig. 6 indicates how the compaction curves of the different soils used at Anderson Ranch Dam, Cachuma Dam, and the Trenton Dam completion compare with each other. The laboratory optimum reference point for each soil in Figs. 4 and 5 was plotted in Fig. 6 at the average laboratory dry density and water content of the soils. The 100% saturation curve for a specific gravity of 2.65, which is the average for the three soils, was also plotted. The

curve of total material for Anderson Ranch Dam was obtained from a statistical analysis similar to that for Cachuma Dam. Table 6 summarizes the data for Anderson Ranch Dam. Fig. 6 indicates that because of its greater gravel content the compacted total material of Cachuma Dam was more dense than both the soil for Anderson Ranch Dam and that for the Trenton Dam completion. This was the case notwithstanding the fact that the fill-density curve of its -No. 4 fraction was beneath the laboratory compaction curve.

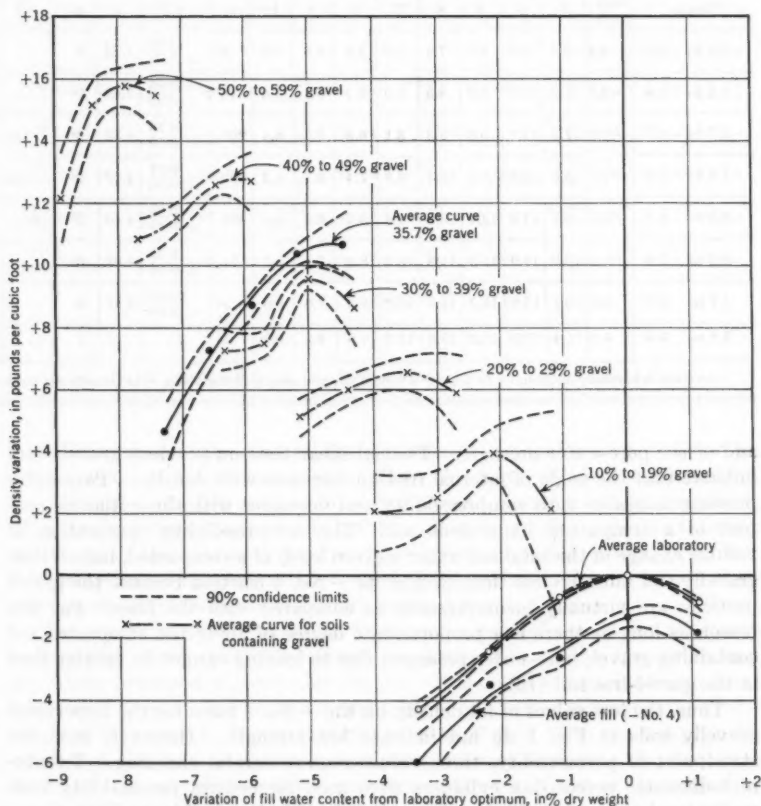


FIG. 5.—CACHUMA DAM ROLLER CURVES

In Figs. 5 and 6 the optimum points of the roller curves of materials containing gravel follow approximately the line of optimums of the laboratory curves. Therefore, the greater densities of the soils containing gravel should assure greater frictional strength than that found by tests of the -No. 4 specimens compacted to laboratory densities. This follows from the fact that frictional shearing strength is a function of the angle of internal friction

TABLE 5.—STATISTICAL DERIVATION OF

Variation of fill water content from laboratory optimum, in percentage		Water content* of total soil for gravel in Cols. 3 through 10, in percentage								VARIATION OF DRY					
										Average of all tests, 35.77% gravel			Soils with 0% to 9% gravel		
(1)		(2)								(3)			(4)		
Range	Mid-point	3	4	5	6	7	8	9	10	n	$\pm \bar{X}$	σ	n	$\pm \bar{X}$	σ
-4.9 to -3.9	-4.4	6.5	9.6	8.6	7.6	6.6	5.6	4.6	3.6	8*	11.00 ± 1.09	1.52	0
-3.8 to -2.8	-3.3	7.2	10.7	9.6	8.5	7.3	6.2	5.1	4.0	48	8.85 ± 0.90	3.68	0
-2.7 to -1.7	-2.2	7.9	11.7	10.5	9.3	8.1	6.8	5.6	4.4	204	9.79 ± 0.50	4.33	2*	5.00	...
-1.6 to -0.6	-1.1	8.6	12.8	11.5	10.1	8.8	7.4	6.1	4.8	390	9.37 ± 0.36	4.32	2*	6.60	...
-0.5 to 0.5	0.0	9.3	13.8	12.4	11.0	9.5	8.0	6.6	5.1	494	10.32 ± 0.33	4.40	2*	0	...
0.6 to 1.6	1.1	10.0	14.9	13.3	11.8	10.2	8.6	7.1	5.5	73	11.49 ± 0.95	4.87	0
1.7 to 2.7	2.2	10.7	15.9	14.3	12.6	10.9	9.3	7.6	5.9	9*	12.70 ± 2.28	3.47	0
2.8 to 3.8	3.3	11.4	17.0	15.2	13.4	11.6	9.9	8.1	6.3	3*	1

* Average laboratory optimum = 14.5%. * Average, \bar{X} , and standard deviation, σ , in pounds per cubic foot.

and of the pore-water pressure. Triaxial shear tests on pervious gravels (15) indicate that the angle of internal friction increases with density. Pore-water pressure increases with compressibility and decreases with the initial air content of a compacted impervious soil. The compressibility (percentage of volume change of the total soil under a given load) of a compacted, impervious, gravelly soil must be less than that of its -No. 4 fraction because the gravel particles are virtually incompressible as compared with the fines. For this reason as long as there is a proportionate degree of air in the compacted soil containing gravel, pore-water pressures due to loading cannot be greater than in the gravel-free soil (16).

Thus, the low values of fill density on the -No. 4 basis for the impervious gravelly soils in Fig. 1 do not indicate low strength. However, from the standpoint of permeability, these values require careful checking. Twenty-inch-diameter percolation cylinders were used for control permeability tests on the total material for Platoro Dam, Conejos Creek, near Monte Vista, Colo.; Boysen Dam, Big Horn River, near Thermopolis, Wyo.; Granby Dam, Colorado River, near Granby, Colo.; and Cachuma Dam. In some instances, in order to increase fill densities to assure adequate imperviousness, the placement water content of the fill, which was initially from 1% to 2% less than laboratory optimum, had to be increased to laboratory optimum.

Test Pits.—In addition to the field density test, there are other means for evaluating the effectiveness of compactive equipment. Whenever practicable,

ROLLER CURVES FOR CACHUMA DAM

DENSITY OF TOTAL SOIL FROM LABORATORY DRY DENSITY AT FILL WATER CONTENT^{a,c,d}

Soils with 10% to 19% gravel (5)			Soils with 20% to 29% gravel (6)			Soils with 30% to 39% gravel (7)			Soils with 40% to 49% gravel (8)			Soils with 50% to 59% gravel (9)			Soils with 60% to 69% gravel (10)		
n	$\pm \bar{X}$	σ	n	$\pm \bar{X}$	σ	n	$\pm \bar{X}$	σ	n	$\pm \bar{X}$	σ	n	$\pm \bar{X}$	σ	n	$\pm \bar{X}$	σ
0	1	6	1	0	0
4*	6.90 ± 1.17	0.86	22*	6.80 ± 0.89	2.38	12*	9.60 ± 1.40	2.60	4*	10.20 ± 1.56	1.15	5*	14.10 ± 2.60	2.44	1*	22.00	...
21	4.56 ± 1.27	3.28	62	7.58 ± 0.61	2.85	56	9.74 ± 0.62	2.73	44	13.27 ± 0.70	2.71	17	14.56 ± 1.46	3.34	2*	21.80	...
24	3.20 ± 0.83	2.32	89	6.68 ± 0.45	2.53	130	8.15 ± 0.40	2.73	114	12.20 ± 0.50	3.16	29	15.90 ± 0.87	2.70	3*	18.30	...
27	3.90 ± 0.80	2.38	92	6.54 ± 0.52	2.97	169	9.57 ± 0.37	2.93	145	12.62 ± 0.40	2.92	55	15.80 ± 0.64	2.78	5*	17.40	...
4	3.00 ± 3.18	2.34	10	6.72 ± 1.28	2.09	24	9.40 ± 1.11	3.10	18	13.57 ± 0.92	2.18	15	16.28 ± 1.11	2.36	2*	22.00	...
0	1	2	4	2	0
0	0	0	1	1	0

^aThe \pm entry indicates 90% confidence limits. ^bn signifies number of tests. ^cNot plotted in Fig. 5.

the field forces excavate a test pit in the compacted embankment to observe the over-all result of the fill operations. Thus, the degree of success in attaining homogeneity of the fill other than in density and moisture can be appraised. Of particular interest in these pits is the result of the tendency for the tamping feet to mask the boundary between successive compacted layers. The test pits have shown that compaction by sheepfoot rollers on the dry side of optimum results in the absence of smooth surfaces between layers.

The results of minor variations from proper control procedures are found occasionally. Such lapses in control are instructive to the inspection and laboratory personnel who examine the pit. It is found sometimes that a layer that was not rolled, due to an oversight, is not compacted subsequently by the weight of fill above it. Loose material beneath 27 ft of fill in one test pit indicated that the load probably arched over the soft material. Several local shear surfaces, or "slickensides," were encountered in a test pit excavated in the backfilled cutoff trench of the Trenton Dam foundation. This occurrence was reported by William P. Creager (17), who attributed it to excess rolling or to the passage of heavy equipment on material with a relatively high water content. In order to verify this conclusion, a representative sample of material from the pit was tested in the laboratory sheepfoot compaction machine (18), which was equipped with a 3-in.-diameter foot. While the unit pressures of 500 lb per sq in. were maintained, the water content and the coverages were varied to correspond approximately to twelve, twenty-four, and forty-eight

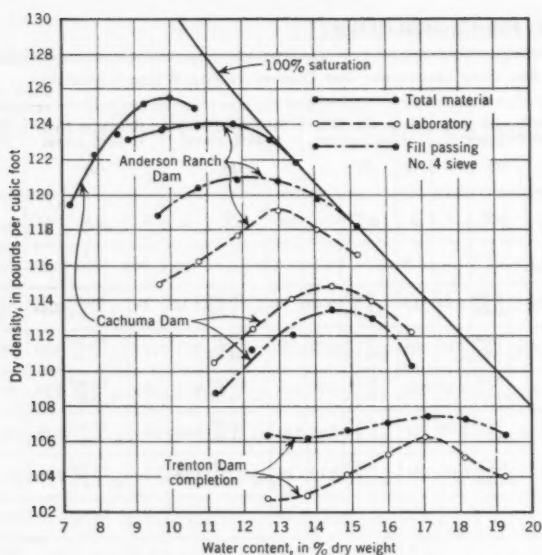


FIG. 6.—AVERAGE COMPACTION CURVES

TABLE 6.—ANDERSON RANCH DAM ROLLER CURVE DATA

VARIATION OF FILL WATER CONTENT (—No. 4) FROM LABORATORY OPTIMUM, IN PERCENTAGE OF DRY WEIGHT		Water con- tent of total material, in percentage of dry weight	Number of tests	VARIATION OF DRY DENSITY FROM LABORATORY DRY DENSITY AT FILL WATER CONTENT	
Range	Midpoint			Average,* in pounds per cubic foot	Standard de- viation, in pounds per cubic foot
(1)	(2)	(3)	(4)	(5)	(6)
-3.8 to -2.8	-3.3	8.9	29	8.07 ±1.07	3.33
-2.7 to -1.7	-2.2	9.8	195	7.45 ±0.32	2.69
-1.6 to -0.6	-1.1	10.8	726	6.04 ±0.17	2.75
-0.5 to 0.5	0.0	11.8	990	4.78 ±0.13	2.52
0.6 to 1.6	1.1	12.8	291	4.97 ±0.23	2.39
1.7 to 2.7	2.2	13.5	32	5.46 ±0.74	2.40

* The ± entry indicates 90% confidence limits.

passes of the USBR roller. After compaction each specimen was examined for localized shear failures. The sample tested was classified as a clayey loess (CL) having a liquid limit of 28%, a plasticity index of 10%, and a specific gravity of 2.67. It was determined that 95% of the grains passed the No. 200 sieve. The standard properties were: Maximum dry density—106.5 lb per cu ft; optimum water content—18.0%; and Proctor penetration resistance—700 lb per sq in. The laboratory tests were successful in producing localized shear surfaces similar to those observed in undisturbed samples obtained from the test pit. However, these surfaces were found only on samples compacted wet of optimum water content for the effort used, which, in every case, corresponded to an air content of less than 6%. Thus, the importance of maintaining close control for this material on the dry side of optimum was emphasized.

Instruments.—The performance of the embankment during the construction and operation periods reflects the effectiveness of the methods and equipment used to compact the soil. The USBR has installed internal settlement and pore-water-pressure measuring instruments in several earth dams. The results of the measurements show that during construction compacted soils exhibited a volume change under a load of superimposed fill that varied from 0.9% of the initial volume for the material (GM) at the Boysen Dam B-1 borrow pit to 4.0% for the soil (CL) at Carter Lake Dam, near Berthoud, Colo., under an effective load of 100 lb per sq in. (19). Measured pore-water pressures corresponded generally with the measured compression of the fill and the placement air content, in accordance with the USBR pore-water-pressure theory. Substantial construction pore-water pressures were observed in impervious materials placed wetter than an average of 0.6% below optimum. Localized high pore-water pressures coincided with substantial concentrations of lifts placed inadvertently in a wet condition. The analysis of the pore-water-pressure measurements indicates that the application of the principle of placing the soil on the dry side of optimum resulted in a noticeable reduction of the tendency to develop pressures in earth dams.

EVALUATION OF RESULTS

Relationship to Design Requirements.—The results of compacting the impervious sections of earth dams by heavy tamping rollers must be considered in relation to the criteria used in designing the structures:

1. The water-barrier zone must be constructed into a homogeneous mass that is free from potential paths of seepage and piping through the zone or along the foundation contacts.
2. The soil mass in this zone must be sufficiently impervious to prevent excessive water loss through the dam.
3. High compressibility of the impervious material is undesirable from the standpoint of pore-water-pressure development during construction and reservoir drawdown, in addition to the possible loss of freeboard during primary consolidation.
4. The maximum practicable shearing strength should be obtained from the available impervious materials.

5. The soil must not soften excessively on saturation. The foregoing objectives must be obtainable by simple, practicable construction equipment and operations, capable of high production rates.

From the standpoints of compressibility (item 3) and softening (item 5), higher densities are desired. Homogeneity (item 1) and impermeability (item 2) are satisfied only by both high density and lack of stratification. In order to meet the strength requirement, density must be accompanied by sufficient air in the impervious soil to preclude high pore-water pressures. This leads to the concept of placing material on the dry side and close to optimum for the compactive effort used.

On the basis of density only, some of the results obtained for the soils reported herein will not satisfy the Proctor density criterion of 300 lb per sq in. of indicated saturated penetration resistance (20). Table 1 shows that fifteen fill densities of soils containing less than 25% gravel were less than USBR laboratory maximum densities (on the -No. 4 basis), and the Proctor needle value for many of these soils at laboratory optimum is approximately 600 lb per sq in. However, all soils were compacted to densities (total material) that were equal to or exceeded 97.5% of laboratory maximum dry density. The average values were 99.8% for gravel-free soils and 103.1% for all soils. These densities assure that the internal-friction angle of the soil, the compressibility, and the permeability (the latter requiring additional checks for very gravelly soils) are comparable to the values used in design on the basis of laboratory tests. The relative positions of the roller curves of total material for the three soils and their laboratory curves, regardless of gravel content, indicate that twelve passes of the sheepfoot roller operating at 1% or 2% less than laboratory optimum on 6-in. compacted layers will avoid an appreciable reduction in the air content, which would affect shearing strength adversely.

In addition to the restriction of placing material too dry on the basis of density, the USBR considers carefully the possibility of softening or additional compression when a compacted material is saturated under load. Consolidation tests establish the lower moisture limit on major structures (21). Percolation-settlement control tests in the field laboratory on all earth-dam projects provide continual checks on the lower limit during construction. The effectiveness of lower-limit control is indicated by studies of the performance of completed dams. In not one case has seepage into the impervious zones of USBR dams been accompanied by an important increment of compression (22).

The capacity of heavy sheepfoot rollers to add appreciably to the mixing obtained by normal earthwork operations is an outstanding characteristic of this type of equipment. Using special equipment for thorough mixing of soil to obtain maximum homogeneity is usually expensive on a large earthwork project. Satisfactory construction requires that the excavation and placement methods obtain as much mixing as practicable. The problem of uniformity of water content when water is added on the spread lift is of special importance. Compaction by the sheepfoot roller contributes significantly to the uniformity of the soil and moisture, and, hence, to the homogeneity of the fill. This is due to the mixing action of the feet and the many passes used. The inability of a heavy tamping roller to walk out completely is a built-in safety feature

of such rollers. Satisfactory construction practice requires that hard, smooth surfaces left by rubber-tired hauling equipment should be reworked before the next loose lift is placed. It should be noted that penetration by the feet of heavy tamping rollers will diminish the hazard of such surfaces remaining in the fill.

Walkout.—The capacity to walk out has been used as a measure of roller efficiency, and tests to determine the proper size of feet have been reported (23). The available data on USBR earth dams (Table 1) show that on many of the dams the rollers walked out only partly, or not at all. In these qualitative data there is no apparent correlation of walkout with field penetration resistance, placement moisture, resulting density, or soil type. This is notwithstanding the fact that, with few exceptions, the foot area of all the rollers used was 7.07 sq in., and the nominal unit pressures were within the range of from 450 lb per sq in. to 600 lb per sq in. However, because different roller manufacturers use different numbers of feet per row and rows per drum for the same weight and total area of feet, the indeterminate actual unit pressures may be quite different from the nominal unit pressures (total weight divided by area of one row of feet). This may account in part for the lack of correlation.

Walkout by itself is not a measure of compaction efficiency. A very light roller will walk out of each layer but leave the entire embankment in a less dense condition than will a heavy roller that does not walk out. The use of heavy rollers, varying the size of feet so that the roller walks out, must be considered in the light of compactive results and economy. The advantages of walking out are: (1) The heavy roller can be pulled more easily, and (2) more effective construction control can be maintained because the field density tests can be made closer to the surface of the fill. These advantages must be weighed against the following: (a) There is no evidence that walking out will increase the over-all density of the fill; (b) determining the proper weight of the roller and the area of feet for each type of soil and moisture condition is likely to be time consuming; and (c) rollers with different sets of replaceable feet are costly. Experience with the heavy tamping roller indicates that, for the control concepts used, adequate compaction can be obtained in a variety of soils whether the rollers walk out or not.

CONCLUSIONS

The heavy tamping roller used slightly dry of the USBR standard laboratory optimum water content has compacted a variety of soils to satisfactory densities and air contents without any appreciable variation in the thickness of the layer or in the number of passes. USBR experience indicates that design criteria based on results of laboratory tests have been fulfilled or exceeded in the field. The mixing action of the roller and the resulting lack of stratification in the fill make this type of compaction equipment highly desirable for use on water-conservation dams.

From the construction standpoint the use of dry material facilitates the travel of equipment over the fill. However, the heavy sheepfoot roller with high unit pressures does not often walk out. Therefore, it is difficult to pull. In special cases the advantages of walking out may indicate the desirability

of providing rollers with demountable feet of various sizes. However, for most soils the additional engineering and equipment costs do not appear to be justified.

ACKNOWLEDGMENTS

The following assisted the writer in collecting and analyzing the data summarized herein: Richard W. Bock, Mr. Davis, Elbert E. Esmiol, A.M. ASCE, Romulo T. Garcia, Ricardo Y. Mayuga, Kenneth L. Muir, Alvaro B. Rocha, J.M. ASCE, Alexander Ziade, and Alexander Zlaten.

APPENDIX. BIBLIOGRAPHY

- (1) "Tamping Feet of a Flock of Sheep Gave Idea for Sheepfoot Roller," *Southwest Builder and Contractor*, Los Angeles, Calif., August 7, 1936, p. 13.
- (2) *Ibid.*, p. 14.
- (3) "The Unified Soil Classification System," *Technical Memorandum No. 3-357*, U. S. Army Engr. Waterways Experiment Station, Vicksburg, Miss., March, 1953.
- (4) "Unified Soil Classification System," Bureau of Reclamation, U. S. Dept. of the Interior, Denver, Colo., March, 1953.
- (5) "Procedures for Testing Soils," A.S.T.M., July, 1950.
- (6) Closure by F. C. Walker and W. G. Holtz to "Control of Embankment Material by Laboratory Testing," *Transactions, ASCE*, Vol. 118, 1953, p. 35.
- (7) "Earth Manual," Bureau of Reclamation, U. S. Dept. of the Interior, Denver, Colo., Tentative Ed., 1951, reprinted February, 1952, p. 165.
- (8) "Impervious Soils Used in Rolled Earth Dams," by E. E. Esmiol, *Technical Memorandum 649*, Bureau of Reclamation, U. S. Dept. of the Interior, Denver, Colo., August, 1954.
- (9) "Compression Characteristics of Rolled Fill Materials in Earth Dams," by J. P. Gould, *Technical Memorandum 648*, Bureau of Reclamation, U. S. Dept. of the Interior, Denver, Colo., March, 1954.
- (10) "Quality Control of Earth Embankment," by F. J. Davis, *Proceedings, 3d International Conference on Soil Mechanics and Foundation Eng.*, Zurich, Vol. 1, 1953, pp. 218-224.
- (11) "Design and Construction of San Gabriel Dam No. 1," by Paul Baumann, *Transactions, ASCE*, Vol. 107, 1942, p. 1607.
- (12) "Compaction of Cohesive Soils," Progress Report of the Subcommittee on Consolidation of Materials in Earth Dams and Their Foundations of the Committee on Earth Dams of the Soil Mechanics and Foundations Div., *Proceedings-Separate No. 48*, ASCE, December, 1950, pp. 1-9.
- (13) "Soil Compaction Investigations Report No. 6, Effect of Size of Feet on Sheepfoot Roller," *Technical Memorandum No. 3-271*, U. S. Army Engr. Waterways Experiment Station, Vicksburg, Miss., June, 1954, p. 15.

- (14) **"Control of Embankment Material by Laboratory Testing,"** by F. C. Walker and W. G. Holtz, *Transactions, ASCE*, Vol. 118, 1953, pp. 4-6 and pp. 36-37.
- (15) **"Triaxial Shear Tests on Pervious Gravelly Soils,"** by Wesley G. Holtz and Harold J. Gibbs, *Proceedings Paper 867*, ASCE, January, 1956.
- (16) **"Estimating Construction Pore Pressures in Rolled Earth Dams,"** by J. W. Hilf, *Proceedings, 2d International Conference on Soil Mechanics and Foundation Eng.*, Rotterdam, Vol. 3, 1948, p. 236.
- (17) **"Engineering for Dams,"** by William P. Creager, Joel D. Justin, and Julian Hinds, in *"Earth, Rock-fill, Steel, and Timber Dams,"* John Wiley & Sons, Inc., New York, N. Y., Vol. 3, 4th Ed., 1950, p. 755.
- (18) **"Control of Embankment Materials by Laboratory Testing,"** by F. C. Walker and W. G. Holtz, *Transactions, ASCE*, Vol. 118, 1953, p. 4.
- (19) **"Compression Characteristics of Rolled Fill Materials in Earth Dams,"** by J. P. Gould, *Technical Memorandum 648*, Bureau of Reclamation, U. S. Dept. of the Interior, Denver, Colo., March, 1954, Fig. 21.
- (20) **"The Design and Construction of Rolled Earth Dams,"** by R. R. Proctor, *Engineering News-Record*, September 7, 1933, p. 287.
- (21) **"The Determination of Limits for the Control of Placement Moisture in High Rolled Earth Dams,"** by W. G. Holtz, *Proceedings, A.S.T.M.*, Vol. 48, 1948, p. 1240.
- (22) **"The Compressibility of Rolled Fill Materials Determined from Field Observations,"** by J. P. Gould, *Proceedings, 3d International Conference on Soil Mechanics and Foundation Eng.*, Zurich, Vol. 2, 1953, p. 244.
- (23) **"Field Penetration Tests for Selection of Sheepsfoot Rollers,"** by S. J. Johnson and W. G. Shockley, *Proceedings-Separate No. 363*, ASCE, December, 1953.

DISCUSSION

JACK D. HODGSON².—It is felt that if the concept outlined by Chung Yuan Li,⁴ A. M. ASCE, were applied to the data in the paper, it would become obvious that quantities of energy were wasted by obtaining densities in excess of the design density. The writer believes that it is normal USBR practice to use shear-strength data obtained from samples prepared to optimum conditions for the design of embankments, and that during construction the aim is to place the soil well beneath the optimum moisture content. The average densities obtained seldom fall below the optimum, although, for the most part, the moisture contents are substantially lower than optimum. This indicates that the optimum moisture content for the rollers used is probably considerably lower than that obtained in the laboratory. The data given in the paper do not permit an estimate to be made of the occasions on which excessive foot pressures caused more passes to be used than required by properly adjusted rollers.

It is possible that other types of rollers would have permitted deeper layers to be used, with a consequent lessening of the energy per cubic foot applied to the soil. Variations in density of as much as 10% from the top of a layer to the bottom are of little significance when the possible variations resulting from improper rolling, soil variations, and other causes are considered. The over-all consolidation of the bank would compensate for such variations almost as soon as construction was completed, except in highly impermeable soils.

TABLE 7.—LIST OF VARIABLES

Heading	Variables
Roller.....	Type, size, weight, and bearing pressure
Product.....	Type, moisture content, thickness of layers, number of passes, strength, air voids, density, and shape of dam

The variables in compaction are shown in Table 7. Variations of any variable under one heading can affect one or more variables under the other heading. The differences are listed beginning with those that normally are fixed by nature or plant availability and ending with those that are controlled increasingly by the engineer.

One of the most important features of the various types of rollers is the different moisture contents at which a particular soil can be compacted satisfactorily. This characteristic is most useful in reducing earth-dam construction costs.

On small projects the most economical design will be that which uses available plant on the excavated soil to produce reasonable strength. In practice, water can be added and better types of material can be selected for use in certain zones without contributing greatly to the placement cost.

On projects where increases in strength may mean great savings in material, attention should be given to the selection of the roller in order that the maximum strength can be obtained with a minimum expenditure of energy in com-

²Superv. Engr., Soil Mechanics, Dept. of Public Works, New South Wales, Australia.

⁴"Basic Concepts on the Compaction of Soil," by C. Y. Li, *Proceedings Paper 862*, ASCE, January, 1956.

paction. A stage would be reached at which the saving in material caused by the increase in strength was balanced by the cost of the increased compaction energy. Increases in compaction and strength may not be obtainable at the natural moisture contents of the soil, and additional expense may be incurred in reducing or increasing the moisture content of the soil.

A greater use could be made of the compacting effort of traffic on fills if definite data were available on bonding layers. In the case of granular materials there is no reason to suppose that the bond of loose material on a hard, moist, smooth surface is any less effective in producing intergranular reaction than the loose-material bond on disturbed soil. The grain sizes are the same in each case. After compaction the contact area will be approximately the same as on any other plane taken through the compacted soil. Whether this also occurs for clay soils is doubtful.

TABLE 8.—PERCENTAGE AIR VOIDS

No.	Dam	% Air Voids		No.	Dam	% Air Voids	
		Fill	Optimum			Fill	Optimum
1	Deer Creek zones 1 and 2	6.9	5.7	24	Cedar Bluff	8.2	5.1
2	Green Mountain	4.4	3.9	25	North Coulee	12.5	7.0
3	Shadow Mountain	6.5	3.8	26	Shadelill	6.5	2.8
4	Deerfield	3.7	2.9	27	Big Sandy	4.8	5.6
5	Jackson Gulch zone 1	10.2	6.4		Boysen		
6	Long Lake	9.8	6.0	28	Borrow K	6.4	5.8
7	Angostura	3.3	3.1	29	Borrow B	3.6	3.7
8	Horsetooth	12.3	10.7	30	Borrow B-1	9.5	5.0
9	Soldier Canyon	12.6	6.4	31	Carter Lake 1, 2, and 3	7.5	6.7
10	Dixon Canyon	13.8	6.4	32	Keyhole	7.5	5.8
11	Spring Canyon	13.3	7.0	33	Lauro	7.6	6.0
12	Heart Butte	3.7	1.7	34	Platoro	8.0	3.3
13	Olympus	10.6	5.0	35	Rattlesnake	7.6	5.8
14	O'Sullivan	10.7	8.9	36	Cachuma	8.9	4.5
15	South Coulee	9.1	3.8	37	Flatiron	6.5	5.9
16	Anderson Ranch	2.9	2.9		Glen Anne		
17	Davis	6.6	4.3	38	Zone 1	7.4	5.9
18	Dickinson	7.4	3.3	39	Zone 2	10.0	6.1
19	Enders	7.2	5.3	40	Jamestown	7.5	6.5
20	Granby	8.3	4.3	41	Willow Creek	4.4	3.5
21	Medicine Creek	8.3	4.3		Trenton		
	Bonny			42	Foundation	7.7	6.0
22	North Borrow	8.3	9.1	43	Completion	8.8	6.5
23	South Borrow	7.9	6.5	44	Vermejo 2, 3, and Stubblefield	3.6	2.7

At Adamaby Dam (on the Encumhene River 40 miles west of Cooma, New South Wales, Australia) in the Snowy Mountains Hydro-Electric Scheme, excavations in the bank showed that each layer can be distinguished. The dividing line is straight and approximately parallel to the surface. Using the modified Casagrande classification system, the material varies from SC to SF clayey. The dam is being compacted by sheepfoot rollers, and all smooth surfaces are ripped before fresh material is placed. This procedure indicates that the sheepfoot rollers are causing stratification and that the ripping of compacted soil is wasting energy. If such is the case one of the reasons cited by the author for the use of sheepfoot rollers loses its validity.

The paper indicates that the dams have been compacted to a state in which a high strength has been obtained without causing high construction pore-water

pressures. Table 8 lists the air voids for "as constructed" conditions and optimum conditions for the dams listed in the paper. In most cases the air voids would ensure no serious rise in construction pore-water pressures. In nine cases—Green Mountain Dam, Deerfield Dam, Angostura Dam, Heart Butte Dam, Anderson Ranch Dam, Granby Dam, Boysen Dam, Willow Creek Dam, and Vermejo Dam—the writer feels that the materials were overcompacted for the moisture contents used. In only one of the cases was the average fill moisture content at or greater than the laboratory optimum. A more reliable method of field control might be the use of percentage air voids, which is independent of optimum but is influenced by dry density and moisture content. Data concerning whether or not abnormal construction pore-water pressures developed in the foregoing nine dams would be of interest.

It is felt that not enough attention was paid to the flexibility of the various compaction methods. Also, a more detailed examination could have been made of the economics that can be effected in dam construction by relating design requirements to the natural soil conditions and to the selection of rollers

C. Y. Li,⁵ A.M. ASCE.—The analysis of the extensive data on compacting earth dams is welcomed with interest. Valuable information on the subject has been presented. The examination of the results of the test section at Cachuma Dam is an excellent example of how not to draw unwarranted conclusions based on insufficient tests with large standard deviations. The statistical method of analysis is a logical interpretation of many control tests. However, it is hoped that the author is not entirely satisfied with the practice of the USBR on compacting earth dams.

The compaction of 50,000,000 cu yd of various soils by "essentially the same type and amount of compactive effort" is certainly wasteful. As shown in Table 1, the compacted materials for the thirty-nine dams vary from sand and gravel with fines to plastic clays. The laboratory—No. 4 densities vary from 100.4 lb per cu ft to 132.2 lb per cu ft, with optimum moisture contents of from 8.9% to 21.4%. It is reasonable to expect that the compactive effort necessary to obtain the required densities varies greatly for such a variety of soils with a wide range of moisture contents. For example, it appears that the material for Jackson Gulch Zone 1 Dam (West Mancos River, near Mancos, Colo.), North Coulee Dam, Jamestown Dam, and Vermejo 2, 3, and Stubblefield Dam could all be compacted to satisfactory densities with a lighter roller and fewer passes. It is often practical for small earth dams with limited design and few supervising personnel to generalize such specifications, as does the USBR in requiring twelve passes and 6-in. compacted layers with a heavy tamping roller. However, serious consideration should be given to the possible savings in time and expense with specifications designed for the particular material to be used on a large earth dam.

It would be interesting to know the experimental evidence of the current USBR specification for tamping rollers that would eliminate the use of some of the commercial rollers. The experience of the Corps of Engineers with soils

⁵ Civ. Engr., Gannett, Fleming, Corddry, and Carpenter, Inc., Harrisburg, Pa.

for Blakeley Mountain Dam,⁶ Ouachita River, near Hot Springs, Ark., indicated that the tamping roller with a 14-sq-in. foot size yields a better result than the one with a 7-sq-in. foot size. The roller weight used for a satisfactory result was only 2,800 lb per ft of drum. The experience the writer has had with material with a high moisture content at Quebradona Dam, Rio Grande, near Medellin, Colombia, showed that a tamping-foot area of as great as 21 sq in. yielded the most satisfactory result. Therefore, it would seem that the USBR specification of a maximum foot size of 10 sq in. is satisfactory only for certain types of soil. Also, the specification with a heavy tamping roller capable of exerting 4,000 lb per ft is not considered necessary when the field moisture content is relatively high, because the effort required for compacting a soil decreases rapidly with its moisture content.

It is correct that adequate compaction can be obtained in a variety of soils whether the rollers walk out or not. For the tamping roller that does not walk out, the underlying layer is compacted with reduced pressure as a result of the roller drum contacting the soil and the frictional resistance on the tamping feet by the surface soil layer. Therefore, to obtain the same density, more effort is needed to compact the underlying layer consistently than the surface layer. The soil may be compacted to the same density with a less heavy roller, which would result in walkout or partial walkout.

Under the heading, "Conclusions," the following statement appeared: "USBR experience indicates that design criteria based on results of laboratory tests have been fulfilled or exceeded in the field." The writer does not concur with the impression, as indicated by the conclusions, that the USBR practice of using heavy tamping rollers is a satisfactory answer or a logical approach to the method of compacting earth dams. Little of the compacting process may be learned from a unified method of compaction. It is felt that modern earth dams should be designed for a density that is not necessarily the practical maximum but the most economical. The cost of soil compaction and the improved means for reducing such cost should be a principal concern of earth-dam engineers, which can be achieved only through a better understanding of the fundamental relationships of the various compacting-process factors.

JACK W. HILF,⁷ M. ASCE.—It is interesting to note that both Messrs. Hodgson and Li conclude that too much energy must have been expended by using the same roller, thickness of lift, and number of passes on various soils.

Mr. Hodgson suggests that other types of rollers than the sheepfoot roller would have permitted deeper layers, thereby reducing the energy per cubic foot applied to the soil. He recognizes, but dismisses as being of little significance, "variations in density of as much as 10%" from the top of a layer to the bottom, which results from surface compaction of thick lifts by rollers other than the tamping roller. The writer believes that it is undesirable to accept as much as 10% density variation within a compacted layer of the water-barrier section of an earth dam. Density gradients within a layer are accompanied un-

⁶ "Review of Soil Design Construction and Prototype Analysis Blakeley Mountain Dam, Arkansas," Technical Report No. 3-439, U. S. Army Engr. Waterways Experiment Station, Vicksburg, Miss., October, 1956.

⁷ Superv. Civ. Engr., Bureau of Reclamation, U. S. Dept. of the Interior, Denver, Colo.

doubtedly by much greater permeability gradients. Flow-net analysis indicates that horizontal layers of different permeabilities within the embankment raise the phreatic line and reduce the stability of the dam for the steady-state condition.

Mr. Hodgson has observed correctly that the optimum water content for the rollers used was probably considerably lower than that obtained in the laboratory. The data also show that the peak density of the roller curve generally is several pounds per cubic foot greater than the peak density of the laboratory curve. For the design criteria used this condition is desirable and does not indicate wasted effort. For dams susceptible to pore-water pressure during construction, the objective in USBR procedure is to obtain fill densities that are comparable to the laboratory maximum density at a placement water content somewhat dry of the laboratory optimum. The only means to accomplish the foregoing is to specify a compactive effort greater than the laboratory effort.

The writer agrees with Mr. Hodgson that in granular materials (such as are commonly used in pervious sections of earth dams), efforts to improve the bond between layers by harrowing or similar methods generally are not warranted. Definite data on the bonding of fill layers can be obtained partly by examining the compaction studies made by the United States Army Engineer Waterways Experiment Station, Vicksburg, Miss.⁸ One of the reports⁹ states the following as one of the results of compacting a lean clay, CL (LL = 36% and PI = 15%) by use of a sheepfoot roller and a rubber-tired roller:

"For the material compacted by the rubber-tired roller, a poor bond between lifts was observed at all water contents, and laminations within the lifts or a flaky structure were observed for the material compacted on the wet side of optimum. For the material compacted with the sheepfoot roller, a good bond was obtained between lifts at all water contents; however, laminations were observed in the material compacted on the wet side of optimum but to a smaller degree than that observed for material compacted with the rubber-tired roller."

Similar results were obtained in the field and in the laboratory by the USBR.¹⁰ There is evidence that poor bond between layers is characteristic of the compaction of cohesive soils by pneumatic or other surface-type rollers.

The use of the sheepfoot roller is not in itself a guarantee that layers of compacted soil will be indistinguishable. Differences in soil type, color, or water content of the loose lifts will remain after compaction. Equipment cannot substitute for nonhomogeneity of material. However, it should assure that the layers are well bonded. The ripping of smooth surfaces caused by hauling equipment before fresh material is placed is a good method of facilitating bonding between lifts of cohesive soil. The writer believes that the energy used in achieving such a result is beneficial rather than wasteful in dam construction.

⁸ "Soil Compaction Investigation Reports Nos. 1-8," *Technical Memorandum No. 3-271*, U. S. Army Engr. Waterways Experiment Station, Vicksburg, Miss., 1949-1957.

⁹ "Soil Compaction Investigation Report No. 7," *ibid.*, June, 1956, p. 35.

¹⁰ Discussion by J. W. Hilf of "Effect of Tire Pressures and Lift Thicknesses on Compaction of Soil with Rubber-tired Rollers," by W. J. Turnbull and C. R. Foster, *Conference Papers*, Joint Meeting, A.S.T.M. Committee D-18 and Sociedad Mexicana de Mecanica de Suelos, A.S.T.M. *Special Technical Publication STP No. 232*, A.S.T.M., Philadelphia, Pa., December, 1957, pp. 444-445.

Data on construction pore-water pressures in nine of the dams reported is shown in Table 9. Quantitative material on some of these dams was given by Wilmar W. Daehn, A.M. ASCE.¹¹ The percentage of air voids in the soil mass is only one factor in the development of construction pore-water pressures. For example, the compressibility of the soil is even more important.

The idea proposed by Mr. Li of "stage" compaction by using first a light pressure roller followed by a heavy roller is believed to be theoretically sound. The variation of contact of sheepfoot rollers as well as the variation of weight for different soils, water contents, and layer thicknesses also appear to be conducive to efficient compaction.

The writer believes that the cost of requiring several rollers for stage compaction or several sets of tamper heads to meet varying soil conditions or moisture conditions of the borrow material will be appreciably greater than the expense of rolling with one heavy roller. In this connection, and to answer the question raised by Mr. Li on the cost of compacting various soils by the heavy

TABLE 9.—CONSTRUCTION PORE-WATER PRESSURE

Dam	Pressure
Green Mountain.....	Appreciable
Deerfield.....	No instruments installed
Angostura.....	No instruments installed
Heart Butte.....	Negligible
Anderson Ranch.....	Appreciable
Granby.....	Appreciable
Boysen.....	Appreciable
Willow Creek.....	No instruments installed
Vermejo.....	No instruments installed

tamping roller, the contract costs of the dams reported in the paper were reviewed in 1958.

For the dams in Table 1 the cost of earth fill in dam embankment, including spreading, moistening, harrowing (if necessary), and compacting each 6-in. (compacted thickness) layer of soil with twelve passes of the heavy tamping roller, varied from 8 cents per cu yd to 35 cents per cu yd, with a weighted average of 14.1 cents per cu yd. The actual cost per roller pass is estimated at 0.35 cent per cu yd, based on rental rates and average production output. The total cost of compacting 75,000,000 cu yd by this method was \$10,600,000, or 6.7% of the total cost of the dams in Table 1.

It is interesting to note that in the bid opening for Fort Cobb Dam, Pond Creek, near Fort Cobb, Okla., in January, 1958, the low bid for 3,300,000 cu yd of earth fill was 5 cents per cu yd, which constitutes only 5% of the total bid price. The average of the three low bids for this item was 8½ cents per cu yd. Few savings could have been accomplished on this project had special test sections been made to determine the optimum rolling area of tamping feet, number of passes, and layer thicknesses, and had the specifications been changed

¹¹ "Pore Pressure in Design," by W. W. Daehn, Pt. I, "Implications of Pore Pressure in Design and Construction of Rolled Earth Dams," *Transactions*, 4th Cong. on Large Dams, New Delhi, Vol. 1, 1951, pp. 259-270.

accordingly. There would have been no assurance that changing moisture conditions during construction would not require changes in the compaction method.

It is concluded that the actual cost of compacting dam embankments is low compared with its importance and with the total expense of the work. Until other methods for compacting cohesive soils are found that match the performance of the heavy tamping roller and permit more flexibility at no greater over-all cost, there is ample justification for continuing to use heavy sheepfoot rollers to compact the water-barrier section of earth dams.

AMERICAN SOCIETY OF CIVIL ENGINEERS

Founded November 5, 1852

TRANSACTIONS

Paper No. 2987

THE WELLAND CANAL

BY WILLIAM A. O'NEIL¹

SYNOPSIS

With the completion of the Welland Canal in 1932, the first major step toward the construction of a deep waterway from Lake Erie to Montreal, Canada, was realized. The canal connects Lake Erie to Lake Ontario, a difference in elevation of 326.5 ft. A 25-ft-deep channel and eight locks are provided to accommodate vessels to as much as 735 ft long so that navigation can bypass Niagara Falls.

The additional deepening of the Welland Ship Canal to the standards of the St. Lawrence Seaway Authority was undertaken under the jurisdiction of the Authority in 1955.

HISTORY

The present (1959) Welland Ship Canal is the latest in a series of four canals that have been built in the Niagara Peninsula of Canada to overcome the obstacles to navigation presented by the Niagara River and its rapids, and by Niagara Falls.

First Welland Canal.—The first Welland Canal, completed in 1829, was a private enterprise. The builders utilized natural watercourses as much as possible to save expense and labor. The route followed the Twelve Mile Creek from Port Dalhousie on Lake Ontario along its wavering course to the Niagara Escarpment. At this site a deep cut was made across the height of land to Chippawa Creek (also known as the Welland River) at Port Robinson, where ships descended the creek to the Niagara River and, from there, to Lake Erie. To obtain sufficient water to operate the canal, the summit level was connected by a feeder canal to the Grand River at Dunnville. To overcome the difference in elevation forty wooden locks were required, each 110 ft long and 22 ft wide, with an 8-ft water depth on the sills. The sailing vessels usually had to

NOTE.—Published, essentially as printed here, in March, 1958, in the Journal of the Waterways and Harbors Division, as *Proceedings Paper 1670*. Positions and titles given are those in effect when the paper was approved for publication in *Transactions*.

¹ Div. Engr., Welland Div., St. Lawrence Seaway Authority, St. Catharines, Ont., Canada.

be towed up the Niagara River against strong winds and currents. Ice jams in the early spring impeded navigation. To eliminate the bottleneck an extension of the canal from Port Robinson south to Port Colborne was constructed and opened to navigation in 1833. However, the canal was still fed from the Grand River.

Second Welland Canal.—In 1841 the legislature of the province of Upper Canada purchased the canal and decided to enlarge it to 9-ft navigation. The number of locks was reduced to twenty-seven by increasing the lift. These installations were redesigned and built of cut stone, and were 150 ft long, 26½ ft wide, and had a 9-ft water depth on the sills. The Port Maitland-Dunnville branch on the Grand River was built also. By 1853 it had become evident that the Grand River would not suffice as a feeder for a canal with much traffic. Plans were devised for an additional reconstruction, so that the canal could be fed directly from Lake Erie. It was not until 1881 that the reconstruction was finally completed, the water coming from the lake at Port Colborne.

Third Welland Canal.—The confederation of the provinces of Upper and Lower Canada in 1867 placed the inland waterways under federal jurisdiction. A uniform scale of navigation for the St. Lawrence River route and the Welland Canal was recommended, with locks that were 270 ft long, 45 ft wide, and had 12 ft of water on the sills (later changed to 14 ft). Enlarging the Welland Canal to these dimensions began in 1873 and ended in 1887.

The course of the third canal utilized much of the previous channel, but climbed the escarpment east of the second canal to Allanburg. Then it followed the previous route. Its twenty-six locks were built of cut stone, with lifts of from 12 ft to 14 ft. An aqueduct transported the canal over the Chipewawa Creek at Welland.

The improved and enlarged waterway, together with a similar canal system along the St. Lawrence River from Lake Ontario to deep water at Montreal, met the immediate demands of inland water commerce until the beginning of the twentieth century. However, it failed to keep pace with the ever-increasing size of the cargo carriers being built on the upper Great Lakes. Transshipment to small vessels at the Lake Erie entrance to the Welland Canal was costly, and caused traffic congestion on Lake Erie at the junction of 14-ft navigation with the greater draft accommodation of the upper Great Lakes. To remedy this situation the fourth waterway, the Welland Ship Canal, was planned and constructed by the Department of Transport and was completed in 1932. The St. Lawrence Seaway Authority was established in 1954 by the government of Canada to deepen and enlarge the fourth canal. The Authority maintains and operates all Canadian works in connection with a deep waterway between Montreal and Lake Erie.

THE WELLAND SHIP CANAL

At the Lake Ontario end of the ship canal its route was changed radically from the previous routes. The canal runs essentially in a straight line across the peninsula for nearly 28 miles, as seen in Fig. 1. The general dimensions

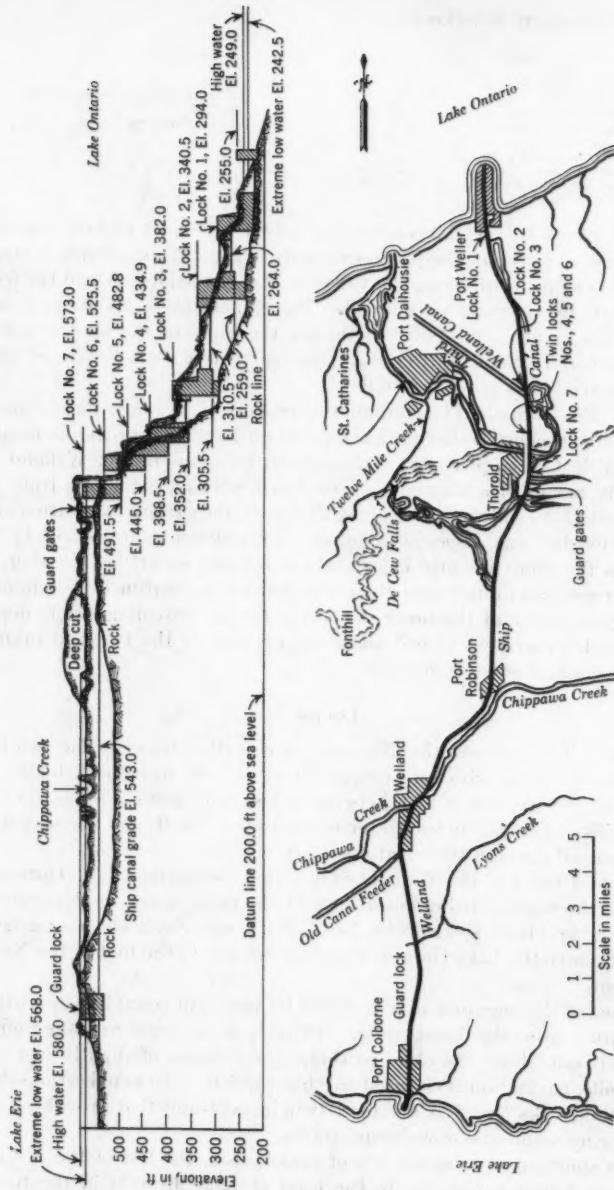


FIG. 1.—WELLAND SHIP CANAL

of the ship canal are as follows:

Length, lake to lake.....	25 miles
Bottom width.....	200 ft
Width of water line.....	310 ft
Depth of canal.....	27 ft to 30 ft (after deepening)
Depth on lock sills.....	30 ft
Lift of each lift lock.....	46.5 ft (approximately)
Number of lift locks.....	7
Number of guard locks.....	1
Number of guard gates.....	1
Usable length of locks.....	735 ft
Usable width of locks.....	75 ft

The canal leaves Lake Ontario approximately 4 miles east of Port Dalhousie, the northern terminus of the previous canals. Then, in practically a straight line, it follows due south along the valley of the Ten Mile Creek to the foot of the Niagara Escarpment at Thorold. The alinement is maintained in the ascent of the escarpment itself. Although the route of the former canals is followed generally from the top of the escarpment to Port Colborne, all the previous sharp bends are eliminated.

Port Weller Harbor.—The construction of Port Weller, an artificial harbor, was necessary because no harbor had existed on Lake Ontario at the mouth of the Ten Mile Creek, presently the northern terminus of the Welland Ship Canal. By means of a standard double-track railway, extending from Lake Ontario south for 7 miles or more along the canal, the surplus excavation of this northern division was disposed of by two embankments projecting $1\frac{1}{2}$ miles north from the shore line into Lake Ontario, forming an artificial harbor. At their outer ends and inner ends the embankments are outlined by reinforced-concrete cribs, those at the inner end of the harbor providing ample dockage space. Rock excavation placed along the exterior of the two embankments protects them against storm erosion.

LOCKS

General.—To overcome the difference in elevation between the two lakes, seven concrete locks, with an average lift of 46.5 ft, have been built. The locks are 80 ft wide, 859 ft long between gates, and have a 30-ft water depth over the sills. The usable length for navigation is 735 ft, and the widest ship that has passed through the canal was 75 ft.

The first 7 miles of the Welland Ship Canal south from Lake Ontario are banked by the slightly rising lower level of the peninsula. In this section of the canal the first three single locks, No. 1, No. 2, and No. 3, elevate navigation to 139.5 ft above the Lake Ontario level and bring it to the foot of the Niagara Escarpment.

The face of the escarpment is ascended by means of equal lifts and without any deviation from the direct route. Three locks in flight are superimposed immediately one above the other so that, in a distance of slightly more than one-half mile, navigation is elevated another 139.5 ft. To avoid serious delays to navigation, locks Nos. 4, 5, and 6 are twin installations that provide separate passage for upbound and downbound traffic.

With a short intervening stretch of canal prism, the last of the seven lift locks, which brings navigation to the level of Lake Erie, is in the town of Thorold. In this short reach there is sufficient distance for vessels to pass.

Because it is essential to control the summit level of the canal from Thorold to Port Colborne at a regulated level of El. 569.0, at Port Colborne there are a supply weir and a guard lock (lock No. 8), through which vessels are locked between the summit level and the fluctuating level of Lake Erie at Port Colborne. Lock No. 8 has a usable length of 1,148 ft. A guard gate and a safety weir are situated just above lock No. 7 to retain the summit level in case of accident to the lock.

Filling and Emptying.—In general the locks have been built with concrete entrance walls at both ends. The 46.5-ft lift permits the upper gate to be situated on a high concrete breast wall, thereby preventing it from being struck by a ship proceeding up the lock at the lower pool level. The pond for filling the lock is on the east side at its upper end, and the waste water passes over a weir provided with stoney valves, which are opened automatically if the water in the reach rises too high. The waste water flows down through an open raceway into the canal prism below the lock. A 14-ft-wide-by-16.5-ft-high water culvert with a semicircular top runs through each lock wall longitudinally at floor level. Both culverts lead to an intake in the east wall, and the inflow of water is controlled by four intake valves of the vertical-sector type. Each culvert discharges into the canal prism below the lower gates and the outflow is controlled by two discharge valves, also of the vertical-sector type. These culverts deliver or take the water to or from a lock chamber through laterals or ports. The latter are 3 ft wide by 4 ft high and are situated in the lock walls at floor level and spaced longitudinally at 30-ft intervals.

Flight locks Nos. 4, 5, and 6, the first two taking the water directly from the lock above them, are twinned in order that ships can pass simultaneously in opposite directions through the flight. The flow of the water is controlled in a manner similar to that of the other locks, except that the intakes for the culverts in the center wall are in its upper end. The water is taken directly from the entrances of the lock chambers, whereas the culverts in the east wall and west wall are fed from an intake in the east wall that takes the water from the pondage.

Approximately 70 acre-ft are required to fill a single lock with a lift of 46.5 ft. For that reason it is essential to provide a large pondage area above each lock to avoid the excessive lowering of the canal water level when filling a lock. In order to form the pondage for lock No. 6, an earth dam was built, 3,300 ft long with a maximum height of 75 ft.

Gates.—The operating gates used at all locks are of the mitring, horizontal-girder type, sheathed on both sides and built entirely of steel. All leaves are 48 ft long and have 5-ft-deep girders. The lower gates are 82 ft high, each leaf weighing almost 490 tons. The upper gates are 35 ft 6 in. high, each leaf weighing approximately 190 tons. The upper gates are 35 ft 6 in. high, each leaf weighing approximately 190 tons. The gates of lock No. 8 and the guard gate are 44 ft 6 in. high and weight 235 tons for each leaf.

Spare gates of each size have been provided. A pair of lower gate leaves are stored under water in a special dock below lock No. 1. The remainder of the leaves are stored under water in the pondage area east of the shipping channel above lock No. 1.

The leaves swing on a hemispherical, nickel-steel pintle anchored to the concrete, and are anchored at the top to two structural-steel anchorage frames embedded in the concrete.

The gates are opened and closed by 1½-in. wire ropes operated by double drum winches housed in buildings on the lock wall. Should the gates of locks Nos. 6, 7, and 8 be carried away, serious damage might be caused to the canal and navigation might be interrupted for a considerable time. Double gates have been provided at each end of the locks, thus giving extra protection. However, real protection is provided by the lock-gate fenders.

Safety Features.—Certain safeguards reduce the chance of damage to the canal from shipping mishaps. All service gates on the locks have rows of miter safety castings, staggered at their miter ends, which permit a gate leaf to be opened approximately 4 ft before the two leaves lose their miter contact with each other. The essential protection is provided by 3.5-in.-diameter, wire-rope fenders, situated about 70 ft away and transported across the lock chambers by booms. The fenders are designed so that if they are struck the boom will be smashed, but the wire rope will be carried along by the vessel. The rope pays out against a friction force on each side computed to be sufficient to bring a 25,000-ton vessel, traveling at the rate of 3.0 mph, to rest in a distance of approximately 46 ft. Since the canal was put into operation, the fenders have been struck thirteen times and have given the required protection for the gates. No gates have been damaged by ship movements in twenty-five years of operation.

Long-distance electric-light signals are placed above and below a lock. Regulations stipulate that a vessel shall not proceed past the "limit of approach" sign until the signal changes from red to green. The signals, fenders, bridges at locks, gates, valves, and other installations are electrically interlocked for a proper sequence of operation. This arrangement not only protects the equipment of the locks, but prevents any disaster resulting from the operation of lock gates or valves in other than the predetermined order. Similarly, limit switches on all lock and bridge machinery protects the equipment from careless operation.

Operation.—The gates, valves, and fenders of the locks are all operated electrically by remote control from two control houses placed one at each end of the lock. The control boards in the houses are interlocked electrically with each other, and the movement of the apparatus is indicated by signal lights.

Vessels pass through the canal, including the locks, under their own power. To control the lock requires a seven-man crew on duty twenty-four hours a day, seven days a week. The lockmaster is responsible for the complete operation. He supervises an operator in each control house and four linesmen who moor the vessel.

Electrically operated capstans with local controls handle the ships' lines over the lock walls.

Maintenance.—To assure a minimum of navigational delay, an extensive maintenance program is performed during the three-and-one-half-month winter season. In addition, routine greasing, cleaning, and inspections are undertaken during canal operation. As with all machinery, proper lubrication is

a chief factor in maintaining a long life and a low wear rate. There are several widely varying lubrication programs on the canal. The lock-gate operating ropes are removed each winter and are lubricated thoroughly in a pressure-vat system. They are treated in a cleaning oil, a core lubricant, and a cable dressing.

When the canal was built it was felt that water would provide sufficient lubrication for the gate pintles. However, shortly after operation one of the the pintles seized in its bushing, thus shearing the dowel pins holding the pintle casting. Jacking up the gates, cutting grease grooves in the pintles, and installing grease pipes up to the wall coping began in order to permit regular lubrication during the operating season. Since this system was provided, there have been no difficulties until recently. One of the gates seized, and, on being lifted, it was found that the grease grooves were full of bronze filings, which had been scraped off gradually over the years. This was a result of the grease pipe becoming plugged and of the pintle being scored because of inadequate lubrication. At present one or two gates each year are jacked up and new pintles and bushings are installed to forestall this condition.

The tainter valves, which control the filling and emptying of the locks, are difficult to lubricate owing to their position and construction. After the canal had been opened for several years, considerable wear was noticed at the yoke pins and main bearings of the valves. A program was instituted then of installing grease fittings and cutting grease grooves in the appropriate bushing points. As a result the rate of wear was lowered considerably. However, each winter some valve bushings and pins are replaced as found necessary upon inspection.

Protection against corrosion is a serious consideration on the canal, and there is continuous painting of the structures both above and below the water. A bituminous type of paint is used on underwater structures, such as gates and valves, which are painted during the winter months. Structural black and aluminum paints are used on steelwork not subject to immersion in water, such as bridges.

Each year the interiors and exteriors of from twelve to fourteen lock gates are painted, and thirty-five tainter valves are painted and reconditioned. The program continues at a rate sufficient to provide a new coat of paint for each structure from every five years to seven years.

Replacement of Worn Elements.—Replacing various worn or fatigued members is a continuous operation. In 1932 shortly after the canal opened, the anchorage I-bars holding the tops of the gates developed fatigue cracks at the shear necks, which had been provided in case a ship struck a lock gate, so that the I-bars would fail rather than pull and warp the A-frame embedded in the concrete. The I-bars were removed, and new stronger ones were installed without a shear neck. No further trouble has been encountered.

The anchorage jaw plates, which transport the load from the I-bars to the embedded A-frame, developed slight cracks. These jaw-plate assemblies are being replaced (as of 1959), and the plate thickness is being increased from $\frac{1}{2}$ in. to $1\frac{1}{4}$ in. Wherever the foregoing has been done, there has been no further cracking.

The stoney valves, which regulate the reach levels through the bypass weirs, consist of flat gate valves raised and lowered vertically by racks and pinions, the thrust against the face being taken by a roller train. The roller trains, which consisted of 4-in.-diameter, 8-in.-long steel rollers, with journals running in steel side plates, were reconditioned. Several methods were used. One method installed cast-iron rollers with mild-steel journals. Another used steel rollers with stainless-steel overlay, and a third method installed quality-controlled high-grade cast-iron rollers, with journals running in bearings pressed into the steel side plates.

During 1957 the replacement of the 3½-in. wire rope on the wire-rope fenders was begun as the rope had corroded badly wherever it passed around a fixed snubbing bollard in a semicircular groove. The cable is in good condition wherever it has been allowed to hang free in the air. On the other hand, wherever it has been clamped, or otherwise confined, it has rusted.

Cavitation and corrosion have caused some disintegration of concrete in the lock structure. The deteriorated sections are chipped out and the new concrete placed, as required, during the winter maintenance period.

The white-oak timbers, which form the miter sills, have deteriorated through time, and are replaced periodically.

Electrical maintenance is confined largely to routine, following corrective measures eliminating severe induction conditions in the original installation.

The various operations were interlocked originally at the main-circuit voltage of 550, causing considerable difficulty. The interlocking circuit was changed to 220 volts, which eliminated this condition.

Cables in ducts, galleries, and undercrossings have been subjected to surprisingly little corrosion or cold flow of the sheath. On the other hand, cables have had to be replaced in exposed positions where it was possible for water to accumulate in the conduit and freeze. The original tile shelves, installed through the cable galleries to hold the cables, pulled away from the wall due to the weight of their burden, and have been replaced with steel racks fastened to the wall.

Gate Lifter.—Should any of the gates be damaged or need removing for any purpose, a pontoon gate lifter, capable of hoisting the 490-ton gates, is kept moored below lock No. 1. The gate lifter is a self-contained unit except that it must be towed by tugs. The pontoon is trimmed by shifting water ballast, using pumps.

CANAL

Canal Prism.—The canal generally is 200 ft wide at the bottom and 310 ft wide at the water line, and the banks are sloped at 2 on 1. To prevent wave-action damage, the banks have been protected by a 12-in.-thick concrete wash wall, extending from 5 ft below the water line to 5 ft above it where excavation was done in the dry, and by a layer of broken-stone protection at all other sections.

The banks have proved to be unstable at various sites, and minor slides have occurred. The instability has been remedied by flattening the slope by dredging, by relieving the top of the bank, or by placing adequate drains in the banks to reduce moisture content. Bank protection and renovations have been major maintenance items.

Chippawa Creek.—As in the case of the previous canal, it has been necessary to provide a suitable structure to allow Chippawa Creek to cross under the Welland Ship Canal. Therefore, a concrete, inverted syphon culvert was constructed, consisting of six 22-ft-diameter tubes, which pass under the canal.

Port Colborne Harbor.—The outer harbor is formed by two breakwaters, approximately 7,200 ft long and placed approximately parallel to the shore, with a 500-ft opening through which navigation passes. A 2,000-ft spur extends outward from the westerly breakwater, giving protection against southwesterly gales.

Bridges.—Fourteen highway bridges and six railway bridges span the Welland Ship Canal. Eleven are of the vertical-lift type, with a 120-ft clearance from the surface of the water. They are counterbalanced by heavy concrete weights and chains. Other bridges are of the rolling-lift types. Large concrete weights counterbalance the weight of the moving span as the bridge rocks upward to an angle of 80°. Only two swing bridges are used on the canal for the railroads because they limit the width of the shipping lane.

All bridge machinery and wire ropes are lubricated regularly. The ropes that hold the counterweights on the vertical-lift bridges have been in continuous use since the canal opened. In the winter of 1957 the ropes at the eastern end of bridge No. 10, which is a railroad bridge, were changed as part of a replacement program. Under the clamps, which gather the cables together to line up for passage over the crown sheave, the wire ropes were corroded. The operating ropes, which move the bridge up and down, are replaced from time to time as they become worn. To replace one of these ropes usually takes from four hours to five hours. On some of the bridges the ropes lasted twenty years, with an average of from eight years to ten years for the others. The difference has been attributed to care in keeping the tension adjusted properly and in precautions taken to prevent the wind from slapping the ropes against the tower legs.

As originally installed, the counterweight guides were steel castings, which rubbed on angles back to back, keeping the counterweight in line as it traveled up and down the tower. Severe wear was noted on both the guide castings and on the guide rails. At each vertical-lift bridge the guide castings were machined out and replaceable bronze gibs installed, which has reduced the wear considerably.

The main power supply to the vertical-lift bridges is at 550 volts, and is transmitted to the span by trolley connectors running on three wires up the inner vertical face of one tower. The auxiliary control, at 110 volts for the traffic lights and roadway gates, and the telephone line are taken from the moving span by two flexible cables attached half way up each tower. The normal life span of ten years often is reduced because these cables catch on tower projections in a high wind, despite protective guide wires.

Electrical System.—All valves, gates, fenders, bridges, and similar structures are operated electrically. A transmission line extends from the mouth of the Port Weller harbor to the Port Colborne harbor. A powerhouse belonging to the canal is situated at the foot of lock No. 4. It contains three 5,000-hp, turbine-driven generators. The latter are actuated by a nominal 186-ft head

of water, conveyed through an 8-ft-6-in.-diameter penstock from above lock No. 7 to below lock No. 4, and connected to a 200,000 gal surge tank. Electric energy is transmitted at 22,000 volts with 550-volt, three-phase power being used for all main motors. Electric power at various voltages to suit requirements is used for lighting and heating.

Substations for transforming and switching the 22,000-volt power to the various stages are placed conveniently to the canal locks, bridges, and other structures.

The main hindrance to uninterrupted power is caused by tree branches blown into the line during summer storms. Since the beginning of operations a few transformers have failed in spite of a regular inspection and oil-testing program. These have had to be rewound, or emptied, dried, and reinsulated.

In general, the installed capacity of the powerhouse is more than required, and, hence, each generator is run only approximately one-third of the time. This allows ample opportunity for preventive maintenance.

The turbines are stripped down periodically, and the runners are built up by stainless-steel welding wherever cavitation has eroded them. In addition, the generators themselves have been torn down, the cooling ducts cleaned, and the winding revarnished. The lack of response with the hydraulic governors caused considerable difficulty in operating and changing machines. New governors having an electrical sensing circuit have been provided, and a more constant speed and steadier sixty-cycle frequency can be maintained than before.

Telephone System.—A complete self-contained automatic telephone system is used along the canal. It links the locks, bridges, substations, powerhouse, and executive buildings.

NAVIGATION

Canal Traffic.—A comparison of the traffic through the past and present canals is interesting. During 1831, which was the second year of operation of the first Welland Canal, 210,104 bu of wheat passed through the waterway. Presently there are several vessels in the "Upper Lake Class" that are capable of transporting in one trip approximately 600,000 bu, or nearly three times the total in 1831. In 1901 the total tonnage passing through the third canal was 620,200 tons, but by 1914 it had increased to 3,860,000 tons. In 1932 when the Welland Ship Canal was opened, the tonnage was 8,535,000 tons, and in 1958 it had increased almost threefold to 21,274,194. Fig. 2 shows the tonnage of freight that passed through the canal annually between 1872 and 1958. The ship canal was designed to allow vessels to make a complete through-passage in eight hours. With the present tonnage and vessel movements, the average time for an upbound vessel is eight hours and fifty-one minutes, and for a downbound vessel, ten hours and forty-three minutes. Ships longer than 640 ft require an average of nine hours and fourteen minutes for an upbound passage and eleven hours and forty-eight minutes for a downbound passage. The greater duration for the passage of the larger ships has been attributed to the difficulty in maneuvering them safely in the canal, particularly when approaching lift bridges and locks. The larger vessels do not respond as quickly

as the smaller ones. Consequently, their speed is reduced so that canalizing may be performed safely.

The cargoes are as varied as the vessels. However, the main items are grain, ore, coal, and petroleum products. Pulp, sulfur, limestone, and "package freight" are extensive secondary cargoes.

Tolls.—Prior to April, 1959, whatever the home port, no ship paid any toll for the privilege of using the canal. Nevertheless, captains had to have a "let pass," obtained either by agreement before the navigation season or at the canal office, to facilitate passage. Although tolls were abolished in 1905, a

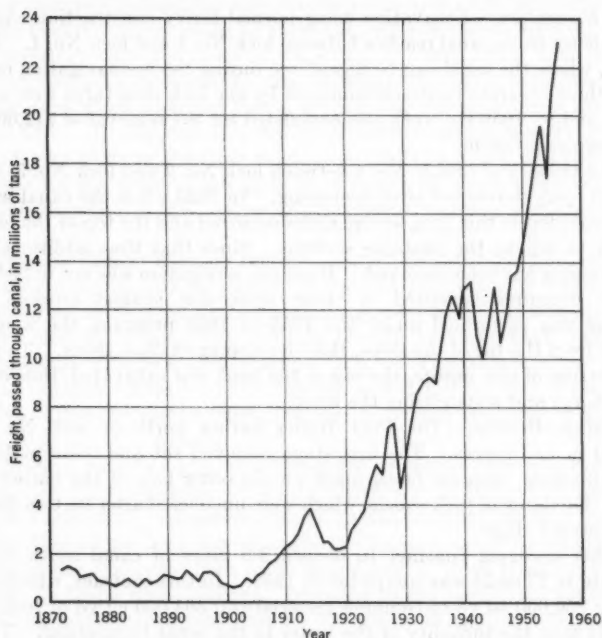


FIG. 2.—ANNUAL FREIGHT TONNAGE PASSING THROUGH CANAL

linesman's service fee was charged. Ships that were as long as 262 ft paid \$25.00, whereas larger vessels paid \$50.00. Prior to construction of the ship canal, casual labor was employed to moor and cast off the lines, the men following the tow paths. Because this system was impossible in the ship canal, men were engaged to do this work and the linesman's fee was established to pay for the service.

A complete revision of the toll structure commenced in April, 1959, and tolls are imposed as follows: For each passage through the Welland Canal only, a vessel will be assessed 2 cents per gross registered ton of the vessel, and, in addition, 2 cents per ton of bulk cargo and 5 cents per ton of general cargo

carried. In the Welland Canal a partial transit will be assessed 50% of the toll for complete passage irrespective of the number of locks used.

Deepening to Seaway Standards.—The deepening program undertaken by the St. Lawrence Seaway Authority is required to provide navigation facilities on the Welland Ship Canal that are equal to those that will be available upon completion of the construction project from Lake Ontario to Montreal. This will necessitate the removal of 1,541,000 cu yd of common excavation and 1,041,000 cu yd of rock in the canal reaches. Dredging or dry excavation will provide 27 ft of water where the bottom is of earth and 30 ft of water where the bottom is of rock.

Dry Excavation.—Excavation using normal heavy construction equipment is possible for three canal reaches between lock No. 1 and lock No. 4. In these sections, where the canal can be unwatered during the nonnavigation or winter season, three separate contracts bounded by the lock structures were awarded in 1955, and by 1959 the work was completed for the removal of 742,000 cu yd of common excavation.

In the vicinity of bridge No. 4 between lock No. 2 and lock No. 3, slides in the canal bank developed after deepening. In 1926 when the canal was originally excavated in this area, severe slides occurred and the top of the bank was cut back to relieve the unstable sections. Since that time additional minor bank slumping has been observed. However, navigation was not impeded, and remedial measures consisted of stone protection against erosion. When deepening was performed under the 1955-to-1959 program, the weight was removed from the toe of the slope, thus developing shallow slides. To prevent further action of this nature, the top of the bank was excavated, thus reducing the surcharge and restabilizing the bank.

Dredging—General.—The Port Weller harbor north of lock No. 1 was deepened in two stages. The first stage removed silt and loose material by suction dredging, disposal being made on the outer face of the harbor breakwaters. Dredging of rock shoals, which were uncovered after suction dredging, was the second stage.

Another dredging contract to deepen 3.9 miles of canal south from the guard gate at Thorold was completed in 1959. In this contract, which was for removing 250,000 cu yd of common material and 364,000 cu yd of rock, it was important that the turbidity of the water in the canal be minimal. This is a critical question for paper companies in the immediate vicinity who use unfiltered canal water in their process. Turbidity could also have presented a problem for municipalities if it had reached proportions beyond the capacity of their filters. To alleviate the condition all common material, including the silt overlying rock, was removed by a suction dredge. An area was cleared in this manner before drilling and blasting could begin.

The most extensive contract dredged 640,000 cu yd of shallow rock, providing a 4.2-mile-long deepened channel for the canal from north of lock No. 8 to Lake Erie.

Underwater Drilling and Blasting.—The rock was broken conventionally, using drill boats and regular underwater explosives or blasting agents. Each drill boat had four spuds and two or three pneumatic drills mounted on towers,

which traveled on rails along the same side of the boat, thus permitting the drilling of several holes in a row before the boat was moved.

The different methods of blasting used by the contractors are interesting. Although similar drill equipment was used, three contractors utilized the hole-at-a-time method of firing and two used millisecond delays. With the first method individual holes are drilled, loaded with from 8 lb to 14 lb of gelatin dynamite, and fired. The drill boat remained in place when the charge was exploded. When millisecond delays were used several holes in a row were drilled, loaded with a blasting agent, which consists largely of ammonium nitrate in waterproof containers, and fired without fear of propagation. Because of the load it was necessary to move the drill boat at each firing.

Some difficulty with the delay method was experienced in that misfires occurred. These were attributed to current leakage in the leg wires, and extra precautions were taken to assure that a ground was not made from the wires to the steel scow. In addition, the charges were fired using a generator rather than a condenser discharge blasting machine so that 120 volts could be applied to the circuit for the required length of time rather than 480 volts for an extremely short duration. This assured that sufficient heat was available to fire the caps.

Precautions to Prevent Blasting Damage.—Special precautions were required when blasting in the immediate vicinity of the lock structures, or near certain sections of the old third canal wall forming the present wall. At this site, close drilling was used to reduce the possibility of rock breaking back under the wall, thereby undermining it and causing a failure. To assure a proper line of breakage a contractor installed 3-in.-diameter sealed metal tubes in the close-drilled holes. Thus, an intermittent air space in the rock was created, through which the shock could not travel.

When blasting rock in water, shock-pressure waves are caused in the water and can damage nearby structures in contact with it. To obviate such damage a new method was used. An air-bubble screen was provided between the blast and the structure by placing a 3-in.-diameter, perforated pipe horizontally along the bottom of the canal and then by pumping into it 15 cu ft per min of air per linear foot of pipe while blasting. In rising to the surface the air bubbles formed the curtain that absorbs part of the energy of the blast transmitted through the water. Tests at other locations indicated a pressure reduction of at least 70 to 1.

To establish the maximum explosive that may be fired at any specific distance from the canal wall, the blasts were monitored seismically. When blasting at 25 ft from the wall in a 30-ft water depth, the data indicated that the charge at 50 ft should be 20 lb per delay and at 25 ft, 10 lb per delay. It is known that existing criteria for establishing a safe powder load are not reliable within 50 ft of a structure. Therefore, trial blasts with small charges at 5-ft intervals were monitored. From the data a drill pattern and maximum load per delay were established.

Underwater Television.—Before work was begun in the vicinity of the old third canal walls at Port Colborne, it was deemed advisable to make an underwater inspection of the timber cribs forming the wall to ascertain their condi-

tion. The survey was planned for a diver. However, an underwater television camera was available, and it was used to make the survey and, at the same time, appraise the television system for similar future operations. The camera in its watertight container presented too much resistance to the current to be handled satisfactorily by lines from the surface. For this reason it was necessary to utilize a diver to maneuver the camera into the proper position. A satisfactory picture was obtained, which was viewed by several engineers and photographed simultaneously, using a camera focused on the picture tube. A major disadvantage was the extremely restricted field of view possible with the camera. To obtain a comprehensive 4-ft-by-6-ft picture of a hole undermining a wall, it was necessary to prepare a mosaic of approximately twelve photographs. However, it was possible for a diver to see the hole and its relationship to the remainder of the structure from one position. In order for this procedure to be used extensively, it will be necessary to develop a camera that can provide a clear picture of 6 ft by 6 ft.

Underwater Excavation.—Using dipper and clam dredges with dump scows, standard mucking methods were used. In addition, in one instance the rock was moved to the shore in a unique fashion. Two flat 32-ft-by-170-ft scows, lashed together side by side, had standard land cranes mounted on one end. The cranes were equipped with rock grabs, which are a special type of clam-shell bucket and are operated conventionally. On the land side of the scows, which were placed parallel to the canal bank, a third flat scow equipped with a Bailey bridge was placed. This acted as a gangplank. The bridge was raised and lowered from the scow. Trucks traveled then from the shore over the bridge and onto the flat scows, where they were loaded directly by the cranes. The round-trip 38-mile tow to Lake Erie, which would be required using standard methods, was thereby eliminated.

During the winter, locations were dredged wherever interference with navigation during the shipping season would result. The standard method used was to dredge the rock after blasting with a dipper dredge and to scow it to a site for rehandling to shore disposal. The scows are dumped and the material then is removed from the water by clams or draglines and loaded into trucks. Ice caused difficulties during this operation. In addition to tripping the buckets on the dipper dredges, the ice filled the tunnels in one type of dump scow, making it impossible to open the doors and dump the rock. As a result, the scows had to be clammed out with a resulting loss in time.

Navigation During Dredging.—Navigation had to continue in the canal during dredging, and there had to be continual coordination between the contractors' operations and the vessel requirements. Accurate scheduling of the work along the face of the docks was very important because the normal operation of these facilities should be interfered with as little as possible. As mentioned previously, winter dredging was required wherever interference with navigation would have been hazardous. This was particularly necessary at lock entrances, where there would not have been space for a vessel to navigate past the dredging equipment.

AMERICAN SOCIETY OF CIVIL ENGINEERS

Founded November 5, 1852

TRANSACTIONS

Paper No. 2988

DESIGN OF MASONRY WALLS FOR BLAST LOADING

BY KEITH E. MCKEE,¹ A. M. ASCE, AND EUGENE SEVIN²

SYNOPSIS

The arching-action theory of masonry walls is applied herein to blast-resistant design. An equation of motion based on this theory is developed for a masonry beam of solid cross section restrained by essentially rigid supports. The equation is solved for a simplified, but realistic, form of blast loading. The results permit either the design of a wall for a given loading or the determination of the maximum loading a given wall can withstand. The theory is extended by an approximate method to wall panels supported on four sides. A comparison is made with test data for walls subjected to full-scale atomic blasts and to high-explosive blasts.

INTRODUCTION

In a previous paper³ a theory was developed to explain the increased resistance of certain unreinforced masonry-wall panels to statically applied lateral loadings. According to this theory, which is applicable to masonry panels constrained between essentially rigid supports, the resistance of the panel is due to forces developed in the plane of the panel as the masonry material tends to be crushed at midspan and at the end supports. The theory is applied herein to the problem of the response of a masonry wall to dynamic forces such as those that arise from an atomic blast. (The term "masonry" is used to include all unreinforced walls constructed of brick, concrete, stone, cinder block, or rubble.) The results are presented in a form suitable for designing masonry walls for given blast loads, and a comparison is made with available experimental data.

NOTE.—Published, essentially as printed here, in January, 1953, in the Journal of the Structural Division, as *Proceedings Paper 1611*. Positions and titles given are those in effect when the paper was approved for publication in *Transactions*.

¹Research Engr., Structural Analysis Section, Dept. of Mech. Eng. Research, Armour Research Foundation, Illinois Inst. of Technology, Chicago, Ill.

²Senior Research Engr., Structural Analysis Section, Dept. of Mech. Eng. Research, Armour Research Foundation, Illinois Inst. of Technology, Chicago, Ill.

³"Arching Action Theory of Masonry Walls," by E. L. McDowell, K. E. McKee, and E. Sevin, *Proceedings Paper 915*, ASCE, March, 1956.

MODE OF RESPONSE ACCORDING TO THE ARCHING THEORY

In Fig. 1 a masonry beam is constrained between nonyielding supports at its lateral edges. It is assumed that (a) the beam has a uniform, solid, rectangular cross section, with span L , depth d , and unit width; (b) the stress-strain curve of the material in compression is elastic up to a limiting (crushing) stress, s_c (and a corresponding strain, e_c); (c) for compressive strains greater than e_c , the stress remains constant at s_c , or, which is equivalent, the material crushes at a constant state of stress; (d) the material possesses zero tensile stress; and (e) the material exhibits no strength recovery beyond the elastic range. Fig. 2 shows a complete load-deflection cycle for masonry according to the foregoing assumptions of stress-strain behavior.

The assumed mode of response of the beam can be described as follows: Immediately on loading, cracks develop on the tension sides at the ends and center of the span. Initially, these cracks extend to the center line of the beam. During subsequent motion it is assumed that each half of the beam remains rigid and rotates about its end support and the center. The resistance to this rotation is developed by a force couple acting at the ends and center

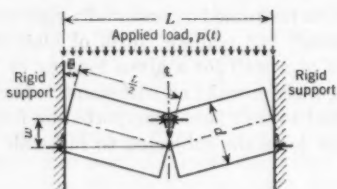


FIG. 1.—DEFLECTED POSITION OF IDEALIZED MASONRY BEAM

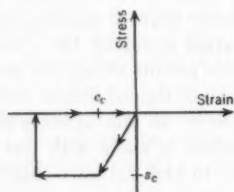


FIG. 2.—ASSUMED LOAD-DEFLECTION CYCLE FOR MASONRY

as a result of the crushing of the masonry at these locations (Fig. 1). The reference to "arching action" results from the resemblance of this configuration to that of a three-hinged arch.

EQUATION OF MOTION

In Fig. 1 a uniformly distributed, time-dependent pressure, $p(t)$, acts on the beam. According to the assumed mode of response, each half-span rotates as a rigid body about the point of contact at the support. By utilizing the D'Alembert approach,⁴ the equilibrium condition for the half-span (of unit width) can be written as

$$\frac{L^3 \gamma}{24 g} \ddot{\theta} + M(\theta) - \frac{L^2}{8} p(t) = 0 \dots \dots \dots (1)$$

in which γ is the weight of masonry beam per unit length per unit width; g represents the gravitational constant; θ is the angular displacement of the

⁴ "Analytical Mechanics for Engineers," by F. B. Seely and N. E. Ensinger, John Wiley & Sons, Inc., New York, N. Y., 1941, p. 233.

beam; $\ddot{\theta} = d^2\theta/dt^2$, which is the angular acceleration; $M(\theta)$ is the rotation-dependent moment resistance due to arching action; and t denotes time.

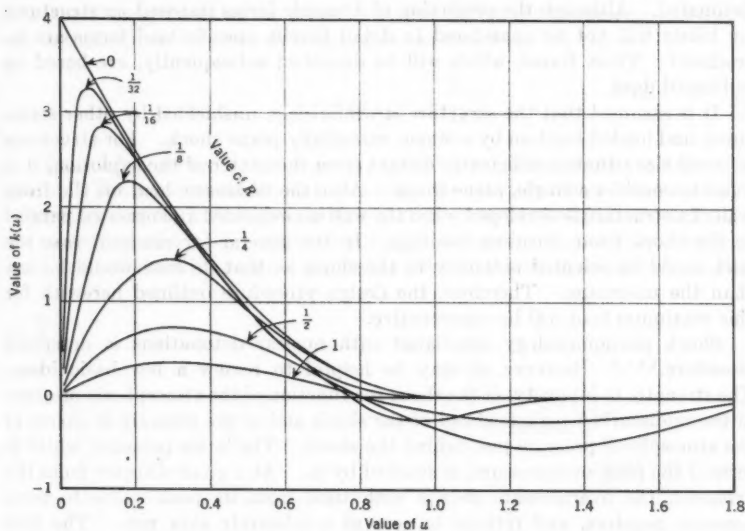


FIG. 3.—VARIATION OF ARCHING RESISTANCE WITH CENTER DEFLECTION

If the center deflection is represented by w , then for small displacements,

$$\theta = \frac{w}{L/2} \quad (2)$$

It is convenient to introduce a nondimensional center deflection, u , which is equal to w/d . Then Eq. 1 can be rewritten in the following nondimensional form:

$$m \ddot{u} + k(u) = f(t) \quad (3)$$

in which

$$m = \frac{4 L^2 \gamma}{3 g s_c d} \quad (4a)$$

$$k(u) = \frac{16 M(u)}{s_c d^2} \quad (4b)$$

and

$$f(t) = \frac{2 L^2}{s_c d^2} p(t) \quad (4c)$$

The analytical form for the moment resistance due to arching, $M(u)$, has been developed elsewhere.³ The nondimensional resistance, $k(u)$, is shown in Fig. 3 as a function of the parameter, R , in which

$$R = \frac{e_c L^2}{4 d^2} \quad (5)$$

BLAST LOADING

Complex patterns of shock waves are generated when atomic weapons are detonated. Although the prediction of dynamic forces imposed on structures by blasts will not be considered in detail herein, specific load forms are introduced. These forms, which will be described subsequently, are based on published data.

It is assumed that the structure is windowless, unshielded by other structures, and loaded head-on by a single, essentially plane shock. For structures of usual size situated sufficiently distant from the center of the explosion, it is valid to consider a single, plane shock. Also, the maximum load on the front wall of a structure is developed when the wall is unshielded and oriented parallel to the shock front (head-on loading). In the general (or random) case the wall would be oriented obliquely to the shock so that its load would be less than the maximum. Therefore, the design procedure outlined herewith for this maximum load will be conservative.

Shock phenomenology associated with nuclear detonations is described elsewhere.^{5,6,7,8} However, it may be helpful to review a few basic ideas. The strength, or intensity, of the shock is a function of the atmospheric pressure in the undisturbed regions ahead of the shock and of the pressure in excess of the atmospheric pressure just behind the shock. The latter pressure, which is termed the peak overpressure, is denoted by p_s . At a given distance from the explosion the overpressure decays with time from its peak value to zero, becomes negative, and returns to zero at a relatively slow rate. The first loading period is termed the positive phase, and its duration is denoted by t_s . The second period is termed the negative phase. In general, negative-phase loads are ignored in structural-response analyses because the forces are appreciably less than those developed during the positive phase.

Fig. 4 shows the variation in blast pressure on a front wall under the foregoing conditions. In Fig. 4 the pressure is reflected to the value p_r at the time at which the shock first strikes the wall. The pressure, p_r , depends on the peak overpressure, p_s , and on atmospheric conditions. For an atmospheric pressure of 14.7 lb per sq in.,

$$p_r = \left(\frac{206 + 8 p_s}{103 + p_s} \right) p_s \dots \dots \dots (6)$$

The reflected pressures decrease at a rate that generally is assumed to be constant to the clearing time, $3h/U$. The dimension h , termed the clearing distance, depends on the geometry of the structure. (It is assumed herein that at least one dimension of the wall panel is essentially the same as the structure, as would be the case for many single-story buildings.) The value

⁵ "The Effects of Atomic Weapons," Los Alamos Scientific Lab., Los Alamos, N. Mex., U. S. Govt. Printing Office, Washington, D. C., September, 1950.

⁶ "A Simple Method for Evaluating Blast Effects on Buildings," Armour Research Foundation, Illinois Inst. of Technology, Chicago, Ill., Revised Ed., July, 1954.

⁷ "Windowless Structures, A Study in Blast-Resistant Design," Technical Memorandum 5-4, Federal Civ. Defense Administration, U. S. Govt. Printing Office, Washington, D. C., June, 1952.

⁸ "An Engineering Approach to Blast-Resistant Design," by Nathan M. Newmark, *Transactions, ASCE*, Vol. 121, 1956, p. 45.

of h can be taken as either the height, H , or the one-half width, $W/2$, of the structure containing the wall, whichever is the smaller value. The quantity U is the average speed of the shock front and, based on one-dimensional shock-wave theory, can be given in terms of overpressure as

$$U = 425 \sqrt{7 + \frac{6 p_{\sigma}}{14.7}} \dots \dots \dots (7)$$

The loading period to the clearing time often is referred to as the diffraction phase. The subsequent loading period to the positive phase duration, t_o , is sometimes known as the pseudo-steady-state phase or drag phase, and takes its name from the analytical form normally associated with steady-state drag loadings. Generally accepted expressions⁶ for the overpressure-time variation,

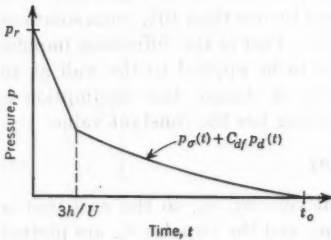


FIG. 4.—BLAST PRESSURE ON FRONT WALL

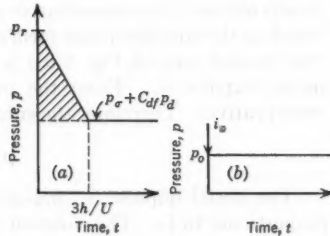


FIG. 5.—SIMPLIFIED BLAST PRESSURE ON FRONT WALL

$p_{\sigma}(t)$, the drag or dynamic pressure-time variation, $p_d(t)$, and the front-wall drag coefficient, C_{df} , are

$$p_{\sigma}(t) = p_{\sigma} e^{-t/t_o} \left(1 - \frac{t}{t_o} \right) \dots \dots \dots (8a)$$

$$p_d(t) = p_d e^{-2 t/t_o} \left(1 - \frac{t}{t_o} \right)^2 \dots \dots \dots (8b)$$

$$p_d = \frac{2.5 p_{\sigma}^2}{103 + p_{\sigma}} \dots \dots \dots (8c)$$

for an atmospheric pressure of 14.7 lb per sq in., and

$$C_{df} = 1.0 \dots \dots \dots (8d)$$

SIMPLIFIED FRONT-WALL LOADING

The loading shown in Fig. 4 is useful because it is a good measure of the correct value of the blast load. However, the analytical form in which this loading is expressed cannot be incorporated readily into the equation of motion, Eq. 3. To facilitate a solution of Eq. 3, the loading must be simplified further.

In order to justify the following simplification, it is helpful to consider the time scale indicated in Fig. 4. For a representative panel with a clearing distance of $h = 12$ ft and a shock speed of $U = 1,350$ ft per sec (corresponding to a shock of approximately 8 lb-per-sq-in. overpressure), the clearing time is $3h/U = 0.027$ sec. For a 20-kiloton bomb, $t_o = 0.6$ sec. Experience indicates that if a masonry panel were to fail structurally under the foregoing loading, it would fail in approximately 0.05 sec or less. From these values it can be concluded that the loading on the wall remains essentially constant between the clearing time and the failure or break time. At the latter time the values of $p_e(t)$ and $p_d(t)$ do not differ greatly from their initial values, p_e and p_d . Thus, the load form shown in Fig. 5(a) can be assumed to apply in those cases in which the loading is associated with wall-panel failure. Replacing the load form in Fig. 5(a) with the form in Fig. 5(b) is an additional simplification. (Eq. 3 was solved numerically for the load form shown in Fig. 5(a). The results obtained in representative cases differed by less than 10% from solutions based on the simplified load form of Fig. 5(b)). Part of the diffraction impulse (the shaded area in Fig. 5(a)) is considered to be applied to the wall as an initial impulse, i_o . From the point of view of design, this assumption is conservative. Therefore, the subsequent loading has the constant value

$$p_o = p_e + p_d \dots \dots \dots (9)$$

The initial impulse, i_o , imparts an initial velocity, \dot{u}_o , to the wall that is proportional to i_o . The constant pressure, p_o , and the impulse, i_o , are plotted against overpressure in Fig. 6. As will be shown subsequently, these load simplifications lead to a particularly convenient solution of the equation of motion.

SOLUTION OF THE EQUATION OF MOTION

Based on the simplified load form of Fig. 5(b), Eq. 3 can be written as

$$m \ddot{u} + k(u) = f \dots \dots \dots (10)$$

subject to the following modified initial conditions: At $t = 0$, $u = 0$, and $\dot{u} = \dot{u}_o = I/m$. In Eq. 10

$$f = \frac{2 L^2}{s_e d^2} p_o \dots \dots \dots (11a)$$

and

$$I = \frac{2 L^2}{s_e d^2} i_o \dots \dots \dots (11b)$$

and m is defined in Eq. 4(a). Using the identity

$$\ddot{u} = \dot{u} \frac{d\dot{u}}{du} = \frac{d}{du} \left(\frac{1}{2} \dot{u}^2 \right) \dots \dots \dots (12)$$

Eq. 10 can be integrated to yield

$$\frac{1}{2} m [\dot{u}(t)]^2 - \frac{1}{2} m \dot{u}_o^2 = \int_0^{u(t)} [f - k(u)] du \dots \dots \dots (13)$$

If the maximum displacement, u_c , occurs at time t_c —that is,

$$u(t_c) = u_c \dots \dots \dots (14a)$$

and

$$\dot{u}(t_c) = 0 \dots \dots \dots (14b)$$

then Eq. 13 yields

$$\frac{1}{2} m \dot{u}_o^2 = \int_0^{u_c} k(u) du - f u_c \dots \dots \dots (15)$$

The displacement, u_c , has been interpreted simply as a maximum displacement. It will be shown that Eq. 15 implies that for any given value of f , there is a \dot{u}_o -value that determines a critical maximum displacement. Conversely, for any \dot{u}_o -value there is a value of f that determines this displacement.

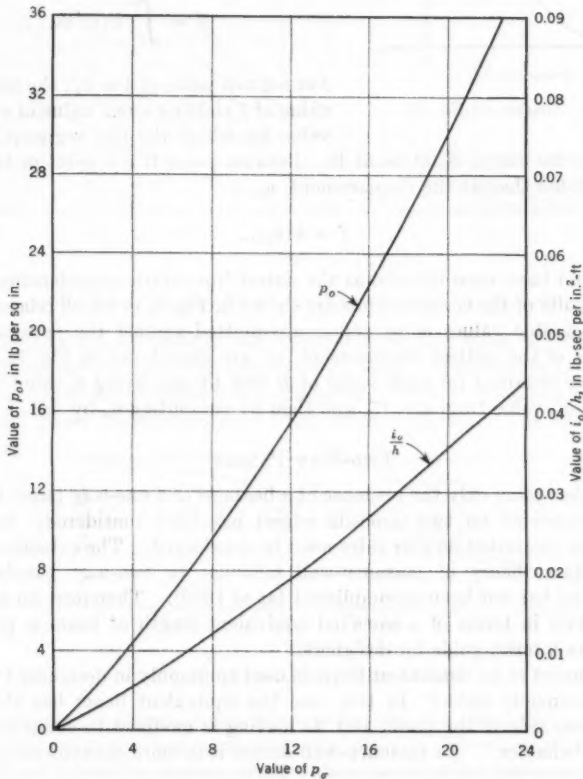


FIG. 6.—VARIATION OF p_o AND i_o WITH PEAK OVERPRESSURE

The displacement is termed "critical" because an infinitesimal increase in the value of f or of \dot{u}_0 produces a displacement that increases without bound. Thus, one can determine the related maximum values of f and \dot{u}_0 that a given wall can withstand safely.

The foregoing statements are established conveniently with reference to Fig. 7, in which the individual terms of Eq. 15, having units of work or energy,

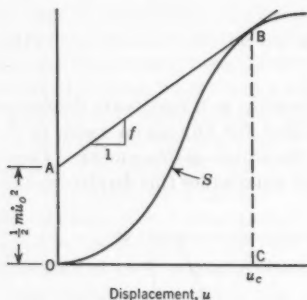


FIG. 7.—GRAPH OF EQ. 15

are plotted against the displacement, u . It should be noted that the initial kinetic energy, $\frac{1}{2} m \dot{u}_0^2$, is represented by the ordinate, OA ; that the straight-line segment, AB , has a slope equal to f ; and that the ordinate, BC , of the curve, S , is equal to the integral term of Eq. 15. The curve, S , is represented by

$$S = \int_0^u k(u) du \dots \dots (16)$$

For a given value of $\frac{1}{2} m \dot{u}_0^2$, the maximum value of f yielding a real value of u_c is that value for which the line segment, AB , is tangent to the curve, S , at point B . Because point B is a point of tangency it is concluded that at the displacement, u_c ,

$$f = k(u_c) \dots \dots \dots (17)$$

Eq. 17 could have been inferred at the outset from static considerations only.

The results of the computations are shown in Fig. 8, in which related maximum permissible values of p_0 and i_0 are plotted against the parameter, R . The values of the critical displacement, u_c , are also shown in Fig. 8. These results were obtained for each value of R first by specifying a value of f , by finding the u_c -value from Eq. 17, and then by computing \dot{u}_0 by use of Eq. 15.

TWO-WAY PANELS

In the foregoing only the response of a beam or of a one-way panel (that is, a panel supported on two opposite edges) has been considered. In many cases panels supported on four sides must be considered. The extension of the arching-action theory of masonry-wall behavior to two-way panels seems involved and has not been accomplished (as of 1959). Therefore, an approximate solution in terms of a so-called equivalent length of beam is proposed herein as an interim guide for designers.

The concept of an equivalent beam is used commonly in designing two-way reinforced-concrete slabs.⁹ In this case the equivalent beam has the same length as one side of the panel, but its loading is modified to compensate for "two-way behavior." In masonry-wall design it is more convenient to retain

⁹ "Building Code Requirements for Reinforced Concrete," A-318-56, Committee 318, A.C.I., May, 1956.

the loading and to determine an equivalent beam length. This length is determined so that a given uniform, static load will produce the same center (maximum) deflection in the beam as in the panel.

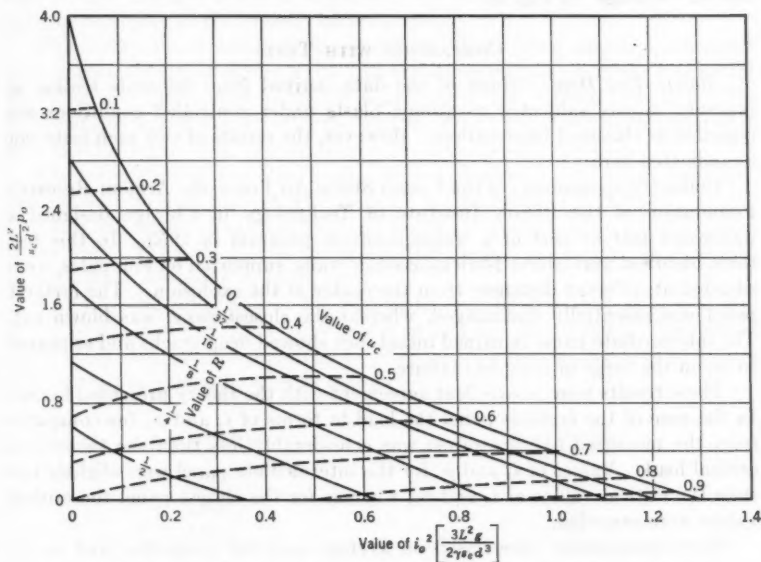


FIG. 8.—MAXIMUM LOADING THAT CAN BE SUSTAINED BY MASONRY PANELS

Equivalent beam lengths were computed on the basis of two separate assumptions for the action of the two-way panel. The results are shown in Fig. 9, in which the equivalent beam length, L , is plotted against the ratio of the actual panel dimensions, L_1/L_2 (in which $L_1 \leq L_2$). The curve labeled

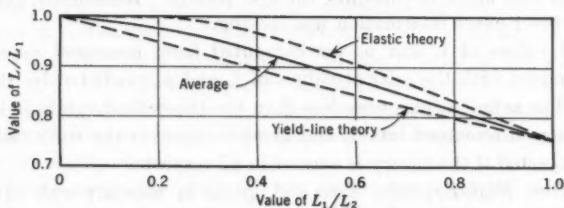


FIG. 9.—EQUIVALENT BEAM LENGTH

"elastic theory" is based on the assumption that the panel deflects similarly to a simply supported homogeneous elastic plate.¹⁰ The curve labeled "yield-line theory" is based on the assumption that the panel deflects according to the

¹⁰ "Theory of Plates and Shells," by S. Timoshenko, McGraw-Hill Book Co., Inc., New York, N. Y., 1940.

yield-line failure theory.¹¹ Because these curves agree fairly well it seems plausible to use an average of the curves for determining equivalent beam lengths. Accordingly, the recommended values are shown by the curve labeled "average" in Fig. 9.

COMPARISON WITH TESTS

Atomic Test Data.—Much of the data derived from full-scale testing of masonry panels subjected to atomic blasts under controlled conditions are regarded as classified information. However, the results of two such tests can be indicated here.

Under the sponsorship of the United States Air Force, the Armour Research Foundation of the Illinois Institute of Technology in Chicago designed a wall-panel test as part of a weapons-effects program in 1953. In this test three identical unreinforced-brick-masonry walls, supported on four sides, were situated at different distances from the center of the explosion. The farthest panel was essentially undamaged, whereas the closest panel was blown out. The intermediate panel remained intact, but showed deep cracks and appeared to be on the verge of complete failure.

These results were in excellent agreement with the theory presented herein. In the case of the farthest panel the load in terms of i_o and p_o (as computed from the measured overpressures) was considerably less than the theoretical critical load. Values of i_o and p_o for the intermediate panel were slightly less than the critical values of i_o and p_o , whereas for the closest panel the critical values were exceeded.

These predictions were based on average material properties and on an equivalent beam length. The panels were instrumented extensively to provide data on the forces transmitted to the supporting structure both in the plane of, and normal to, the panel. Again these data agreed with the arching theory.

Another extensive wall-panel test was sponsored by the Federal Civil Defense Administration, Washington, D. C., in this same program. Data describing the test structures completely were not available. Nevertheless, an attempt was made to interpret the test results. Reasonable guesses were made wherever exact information was lacking.

Actual values of i_o and p_o (as computed from measured overpressures) were compared with the critical values of i_o and p_o predicted by the arching theory. The actual values were less than the theoretical values in every case in which a wall remained intact, and greater wherever the walls failed, which is to be expected if the theory is correct in all respects.

Data from High-Explosive Tests.—A group of masonry-wall panels, both reinforced and unreinforced, was exposed to high-explosive detonations in an experimental program designed and conducted by the Armour Research Foundation. The objective of this program was to investigate the potentialities of structural clay-masonry walls for blast-resistant design.

¹¹ "Evaluation of Two-way Slabs by Yield Line Theory," by K. E. McKee, thesis presented to the Illinois Institute of Technology, at Chicago, in June, 1956, in partial fulfillment of the requirements for the degree of Master of Science in Civil Engineering.

In one phase of the program a rigid octagonal fixture was used that held eight wall panels of various types. A high-explosive charge was detonated in the center of the fixture, thereby loading each panel in identical fashion. Details of this test are available elsewhere.^{12,13} However, the behavior of one panel is pertinent to the present investigation.

This panel, which was built of unreinforced 8-in. brick masonry, measured 10 ft horizontally by 8 ft vertically and was designed to arch in the horizontal direction with essentially negligible restraints in the vertical direction. No deformations were observed after the wall received a measured impulse per unit area of 0.19 lb per sq in. per sec from a 45-lb charge of explosive.

Characteristically, the blast loading on a wall panel due to a high-explosive detonation is of extremely short duration—on the order of 3 millise. Therefore, it is reasonable to suppose that this loading imparts only an initial impulse to the wall. Thus, the results of the proposed theory, as given in Fig. 8, should be applicable, assuming p_0 to be zero.

The physical properties of the wall tested can be described as $e_s = 0.001$; $L = 120$ in.; $d = 8$ in.; $\gamma = 0.59$ lb per sq in.; and $R = 0.056$. The critical impulse, i_c (the impulse required to produce wall failure) for several values of the crushing strength, s_c , is as follows:

s_c , in pounds per square inch	i_c , in pound-seconds per square inch
1,000.....	0.20
2,000.....	0.29
3,000.....	0.35

It is seen that over a reasonable range of wall strength as characterized by s_c , the predicted impulse required for the wall to fail exceeds the measured impulse of 0.19 lb-sec per sq in. The present theory predicted correctly that the wall would withstand the impulse applied.

It is illuminating to compare this approach with results predicated on the elastic behavior of the wall. A critical impulse can be computed on the assumptions that only bending stresses are created in the wall, and that failure occurs when the ultimate tensile stress is exceeded at the center. For a beam with fixed ends the critical impulse found in this manner is less than 0.01 lb per sq in. per sec, even if the masonry material is assumed to have a tensile strength exceeding 200 lb per sq in. Because the applied impulse was nearly twenty times this value, the panel could not have derived its strength from the mechanism of simple bending.

It should be made clear that the test results are not proof of the arching theory. Nevertheless, these tests indicate that the effects of varying certain parameters can be predicted fairly satisfactorily, and on an over-all basis the theory seems to give rather accurate results. However, no definitive state-

¹² "Dynamic Characteristics of Structural Clay Masonry Walls," *Phase Report III*, Armour Research Foundation, "High-Explosive Test Program" for Structural Clay Products Research Foundation, Geneva, Ill., July, 1956.

¹³ "Destruction House," by K. E. McKee, *Frontier*, Armour Research Foundation, Illinois Inst. of Technology, Chicago, Ill., Winter, 1956.

ments can be made without additional testing, nor, especially, until more is known concerning the physical properties of masonry.

DESIGN DATA

From the point of view of blast-resistant design, two closely related problems must be considered, both of which can be solved by using arching theory. One problem is "investigation"—to determine the maximum overpressure a given wall can withstand. The other is "design"—to select a wall to resist a given overpressure. In general, with the results presented in the foregoing, both problems can be solved only by trial-and-error procedures. A procedure for the investigation problem is described in the following. The design procedure involves only an additional step.

Investigation Procedure.—The necessary information for investigation is contained in Figs. 6 and 8. Fig. 6 relates the pertinent load quantities, p_o and i_o , to p_o' . Fig. 8 shows the related maximum values of p_o and i_o a given wall can withstand. To determine the desired maximum or critical overpressure, a value of p_o' is assumed, the corresponding values of p_o and i_o are found, using Fig. 6, and then whether or not these values defined the proper point in Fig. 8 is verified. In general, the latter step will not check, indicating that the wrong overpressure has been assumed.

A systematic procedure would be to determine a value of p_o from Fig. 8 that corresponds both to the proper value of R and to the value of i_o associated with an assumed overpressure, p_o' . In turn, the value of p_o defines an overpressure, p_o'' , through Fig. 6. Thus, these overpressure values can be compared and the procedure repeated until $p_o' = p_o''$.

For example, let it be required to find the maximum overpressure that can be withstood by an 8-in. solid brick wall measuring 16 ft by 8 ft. It can be assumed that the wall acts as a two-way panel and that the following properties are given: $s_c = 1,200$ lb per sq in.; $e_c = 0.001$; $\gamma = 0.65$ lb per sq in.; $h = 8$ ft; $L_1 = 8$ ft; and $L_2 = 16$ ft. Thus, from Fig. 9 the equivalent beam length is

$$L = 0.91 \times 8 = 7.28 \text{ ft, or } 87.4 \text{ in.}$$

Then the parameter R is computed from Eq. 5 as 0.030. At this stage in the computation a value for the desired critical overpressure, p_o' , must be assumed. A value for p_o' of 4 lb per sq in. is chosen as a first guess. Using this value, i_o/h is read off from Fig. 6 as 0.005 lb-sec per sq in. per ft. Because $h = 8$ ft, the value of i_o becomes 0.04 lb-sec per sq in. Referring to Fig. 8, the abscissa is computed as 0.0176, and the ordinate corresponding to $R = 0.030$ is approximately 2.7. From this relationship, p_o is computed as 13.6 lb per sq in., which, from Fig. 6, corresponds to an overpressure, p_o'' , of approximately 10.5 lb per sq in. Because this value does not agree with the assumed overpressure of 4 lb per sq in., an incorrect value of p_o' has been selected. If this procedure is repeated for $p_o' = 10$ lb per sq in., for example, the computed overpressure, p_o'' , is about 8 lb per sq in. If a curve is plotted in this fashion of assumed values of overpressure (p_o') versus computed values of overpressure (p_o''), the two are equal at approximately 8.7 lb per sq in. The desired

maximum overpressure thus is represented for the panel, as can be verified by repeating the foregoing procedure beginning with the value of 8.7 lb per sq in.

An analogous procedure can be followed for the design problem. Computations of this type were performed for an 8-in. brick wall over a reasonable range of equivalent lengths, crushing strength, and crushing strain in order to determine the influence of the material properties on the critical overpressure. The results are presented in Fig. 10(a). For convenience the clearing distance, h , was taken as equal to the equivalent length, L . It is seen that the critical overpressure is relatively insensitive to values of e_c , but is quite dependent on crushing strength. Unless other information is available, it is recommended that values of $s_c = 1,000$ lb per sq in. and $e_c = 0.001$ be used.

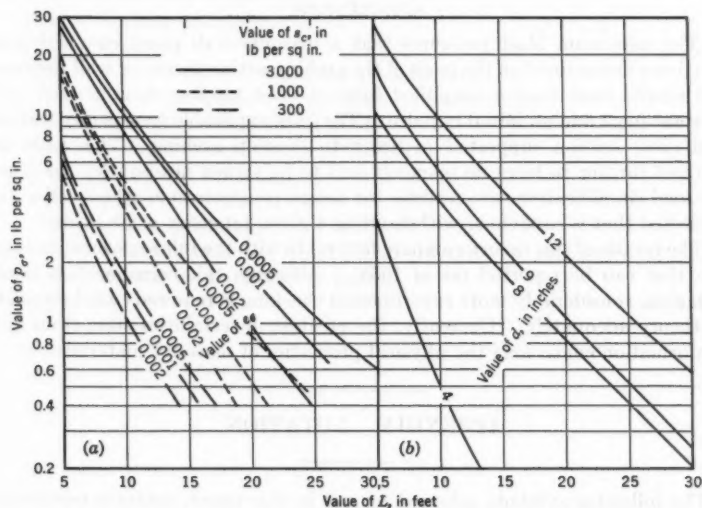


FIG. 10.—INFLUENCE OF PROPERTIES AND THICKNESS ON CRITICAL OVERPRESSURE FOR BRICK PANELS

In order to illustrate the influence of the thickness, d , on wall strength, computations were performed for various equivalent beam lengths and thicknesses of 4 in., 8 in., 9 in., and 12 in. All panels were assumed to have $s_c = 1,000$ lb per sq in., $e_c = 0.001$, and $h = 10$ ft. The results are shown in Fig. 10(b). From Fig. 10(b) it is seen that the wall thickness has an appreciable effect on the maximum overpressure the panel can withstand. For example, increasing the thickness from 8 in. to 12 in. increases the maximum overpressure by approximately 200% for the range shown.

The results shown in Fig. 10 provide design data for certain classes of walls. From the data presented herein, similar curves can be prepared for other conditions. Curves of this type provide the basis for a simplified and rapid method of design.

The theory in its present form is restricted to walls of solid cross section without door openings or window openings. However, the theory can be extended easily to walls of nonsolid cross section, provided that the cavities are situated symmetrically with respect to the center line of the cross section. In this case one can subtract from the resistance of the solid wall (at corresponding displacements) the resistance of another solid wall whose thickness is the same as the specified cavity in the first wall. The problem becomes increasingly complicated when the cavities are not located symmetrically.

The results obtained herein cannot be applied directly to walls having window openings or door openings. In such cases both the equivalent beam length and the form of the blast loading must be modified.

CONCLUSIONS

The maximum blast pressures that a masonry-wall panel can withstand have been determined on the basis of the arching-action theory of wall response. The results stem from a simplified form of blast loading characterized by a constant force and an initial impulse. They are applicable to masonry walls of solid cross section supported in order to develop arching. The walls are assumed further to have no openings and to be struck head-on by the blast. The load simplifications are realistic for design considerations whenever a wall is selected that is capable of withstanding a given intensity of blast load.

The results of this theory compare favorably with the full-scale experimental data that can be reported (as of 1959). Although this corroboration is encouraging, considerably more experimental checking is required to substantiate the theory adequately. Currently, the greatest uncertainties stem from lack of information concerning the physical properties of masonry materials.

APPENDIX. NOTATION

The following symbols, adopted for use in this paper, conform essentially with "American Standard Letter Symbols for Structural Analysis" (ASA Z-10.8—1949), prepared by a committee of the American Standards Association with Society representation, and approved by the Association in 1949:

- C_{df} = front-wall drag coefficient;
- d = depth;
- e_c = limiting or crushing strain;
- f = term defined in Eq. 11a;
- $f(t)$ = term defined by Eq. 4c;
- g = acceleration due to gravity;
- H = height of structure;
- h = clearing distance;
- I = term defined in Eq. 11b;
- i_o = initial impulse;
- $k(u)$ = nondimensional resistance term defined by Eq. 4b;
- L = length of span;

$M(u)$ = moment resistance due to arching;

$M(\theta)$ = rotation-dependent moment resistance due to arching action;

m = term defined by Eq. 4a;

p = pressure:

$p_d(t)$ = drag or dynamic pressure-time variation;

p_o = constant pressure;

p_r = reflected pressure;

p_σ = peak overpressure;

$p_\sigma(t)$ = overpressure-time variation;

$p(t)$ = applied time-dependent force per unit length on a unit width of beam;

R = parameter defined in Eq. 5;

s_c = limiting or crushing stress;

t = time:

t_c = time for maximum displacement;

t_o = duration of the positive-pressure phase;

U = average speed of shock front;

u = nondimensional center deflection;

u_c = maximum deflection;

W = width of structure;

w = center deflection;

γ = weight of masonry beam per unit length per unit width; and

θ = angular displacement of beam.

AMERICAN SOCIETY OF CIVIL ENGINEERS

Founded November 5, 1852

TRANSACTIONS

Paper No. 2989

PRESTRESSED TRUSS-BEAMS

BY RALPH L. BARNETT,¹ J. M. ASCE

SYNOPSIS

A procedure is presented for the design of simply supported beams, which makes possible the utilization of statically indeterminate composite action and favorable initial stress distribution to strengthen available beam sections. A variation of the Queen Post truss with a pretensioned tie rod is studied, with weight savings of more than 30% being realized. The techniques used are based entirely on elastic considerations.

INTRODUCTION

Notation.—The letter symbols adopted for use in this paper are defined where they first appear, in the illustrations or in the text, and are arranged alphabetically, for convenience of reference, in Appendix II.

Simple Design.—To illustrate the design procedure, one can consider a simply supported beam with a constant moment of inertia under an arbitrary, downward-acting load system. It can be assumed that the maximum moment, M_{\max} , governs the design of the beam. For example, if two negative end moments of magnitude, $M_{\max}/2$ were applied to this structure, the design moment clearly would be reduced to $|M_{\max}/2|$. Because the external shear distribution remains unchanged, the possible lighter design could be governed by shear, crippling of the web, deflection, or the moment $|M_{\max}/2|$. Under rather special loading conditions, continuous and overhanging beams may achieve a moment distribution similar to Fig. 1(b). However, in general a design based on these moments would be unrealistic. In an attempt to approach the condition illustrated in Fig. 1(a), one can examine the statically indeterminate structure formed by adding two similar rigid brackets and a tie rod.

The resulting moment diagram differs from that of a simple beam by the constant negative moment, He , throughout L , in which H is the tensile stress

NOTE.—Published, essentially as printed here, in March, 1957, in the Journal of the Structural Division, as *Proceedings Paper 1191*. Positions and titles given are those in effect when the paper was approved for publication in *Transactions*.

¹ Asst. Engr., Armour Research Foundation, Chicago, Ill.

induced in the tie rod by the loads, e is the eccentricity of H with respect to the centroid of the beam, and L is the beam length. The moment, He will not reduce the design moment to $|M_{\max}/2|$ unless e is large in comparison with the beam depth or unless the tie area assumes massive proportions.

The stress in the tie rod can be increased by pretensioning. To illustrate this procedure, one might imagine the tie rod with a turnbuckle in the center. By tightening the turnbuckle, a prestress force, F , can be added to H , which will produce a total negative moment in the loaded beam of $(F + H)e$, which is equal to $M_{\max}/2$. Then the beam design can be based on the bending moment, $|M_{\max}/2|$, and the axial load, $F + H$. With the e -value sufficiently great, this technique will increase the load capacity of a given simply supported beam designed for M_{\max} . Furthermore, if sufficient gradation exists in the available beams, a specified load may be carried on a lighter section than the corresponding simple beam.

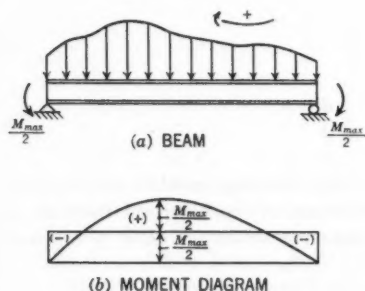


FIG. 1.—LOADED BEAM WITH TERMINAL COUPLES

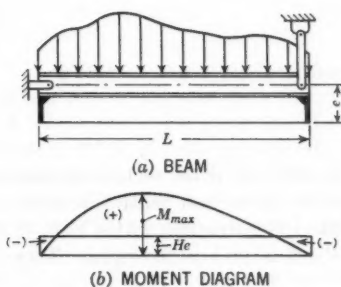


FIG. 2.—TRUSSED BEAM

A lower bound for e can be obtained by considering the states of stress in the beam shown in Fig. 2(a). Because the design of a combined stress member is sought, an interaction criterion must be assumed. Hence, it can be required that a beam be proportioned to satisfy the straight-line interaction formula:²

$$g \equiv \frac{f_a}{F_a} + \frac{f_b}{F_b} \leq 1 \quad (1)$$

in which f_a is the unit axial stress; F_a is the axial unit stress permitted if axial stress only existed; f_b is the bending unit stress; and F_b is the bending unit stress permitted if bending stress only existed.

The stresses resulting from the indeterminacy and the prestressing are

$$f = \frac{F + H}{A} - \frac{(F + H)e y}{I} \quad (2)$$

in which f is the unit stress; A is the area of the beam section; y is the distance from the neutral axis; and I denotes the moment of inertia. If an improvement

² Steel Construction Manual, A.I.S.C., 1954.

of the simple-beam design is to result from the addition of f to the simple beam stresses, then

$$\frac{F + H}{A F_a} - \frac{(F + H) e}{S_1 F_{b1}} < 0 \dots \dots \dots (3)$$

in which S is the section modulus and the subscript 1 refers to the top fibers. From Eq. 3

$$e > \frac{S_1 F_{b1}}{A F_a} \dots \dots \dots (4)$$

For an I-section or a wide-flange section, an upper bound can be obtained for the expression $(S/A)(F_{b1}/F_a)$ in Eq. 4. The maximum possible ratio of section modulus to section area is obtained from a symmetrical webless I-section with infinitely thin flanges. This ratio is

$$\frac{S_1'}{A} = \frac{d}{2} \dots \dots \dots (5)$$

and

$$\frac{S}{A} < \frac{S'}{A} = \frac{d}{2} \dots \dots \dots (6)$$

in which S' is the section modulus of the ideal bending member, and d represents the section depth. From the specifications² of the American Institute of Steel Construction (AISC), $F_a \geq 10.02$ kips per sq in. for $(L/r) \leq 120$ and $F_{b1} \leq 20.00$ kips per sq in. Then

$$\frac{S_1 F_{b1}}{A F_a} < \frac{d}{2} \frac{20.00}{10.02} < d \dots \dots \dots (7)$$

Hence, for any simply supported I-beam or wide-flange beam with $(L_u/r) \leq 120$, an e -value greater than d will always make possible an increase in the load capacity while satisfying the AISC requirements. In the foregoing, L_u is the distance between brackets and r is the least radius of gyration. To achieve a reduction in the total weight of a simply supported beam under a specified load, the e -value must provide a reduction in the section that exceeds the bracket and tie weight. As the value of e increases, the stresses in the beam and in the tie rod decrease linearly. The corresponding weights of these members are reduced accordingly. When the value of e becomes greater than $d/2$, a bracket is required to transmit the negative moment, $M_{\max}/2$. The weight of this bracket increases linearly with the eccentricity, and a value is reached after which the total weight economy diminishes.

Improved Design.—The simple prestress design presented previously can be refined substantially to permit greater savings in weight. In the subsequent material the following property of moment diagrams is assumed: Under a downward-acting load system the shape of a simple-beam moment diagram may never be convex with respect to an interior point. This fact is assured by

the fundamental relationship between the moment and the beam deflection, w ,

$$w = -\frac{d^2 M}{dx^2} \dots \dots \dots (8)$$

A unimodal shape is implied by this nonconvexity requirement.

Fig. 3 shows the typical moment diagram for a prestressed truss-beam whose maximum moment lies between the brackets and whose brackets lie within the span. The critical stress conditions are as follows:

$$g_{A1} = \frac{M_{\max} - e T}{S_1 F_{b1}} + \frac{T}{A F_a} \dots \dots \dots (9)$$

$$g_{B2} = \frac{e T - M_{w,e}}{S_2 F_{b2}} + \frac{T}{A F_a} \dots \dots \dots (10)$$

$$g_{C1,2} = \frac{M_{w,e}}{S_{1,2} F_{b1,2}} \dots \dots \dots (11)$$

and

$$g_{D2} = \frac{F e}{S_2 F_{b2}} + \frac{F}{A F_a} \dots \dots \dots (12)$$

in which g_A , g_B , g_C , and g_D refer to points A, B, C, and D, respectively, in Fig. 3; the subscripts w and e refer to the west end and east end of the beam, respectively; and the subscripts 1 and 2 refer to the top and bottom fibers, respectively. Therefore, the problem is to design a truss-beam that will render the values of Eqs. 9 through 12 less than or equal to unity.

For the typical prestressed truss-beam shown in Fig. 3(a), it can be assumed that the allowable moment resistance of the beam section is less than M_{\max} and that the loading is downward. The beam section outside the brackets must resist only the positive bending moment. The allowable moment on the section is given by $S F_b$. The abscissas associated with the ordinate $S F_b$ on the positive moment diagram are the optimum positions for the brackets, as will be noted subsequently. With the brackets so placed, Eq. 11 clearly is equal to unity. Because the moment M_{\max} is greater than that which the beam section can resist, a negative moment must be superimposed on the beam section between the brackets in order to reduce M_{\max} . The negative moment results from the induced force, H , and the prestress force, F , produced in the tie rod. Its magnitude is $(F + H) e$ and it is transferred to the beam through the brackets. The net or design moment is lowered, but an axial stress, $F + H$, is produced between the brackets. With a sufficient value of e , the combined effect of the axial stress and the negative moment reduces the stresses associated with M_{\max} (Eq. 4). The lowest permissible value, T , of $F + H$ is found by equating Eq. 9 with unity and solving for this quantity.

The moment $e T$ may be great enough to produce negative resultant bending moments near the brackets, as shown in Figs. 3(b) and 3(c). The maximum values of these moments would occur at the brackets, and the resulting stresses would add to the axial stresses also present. If the design is to satisfy Eq. 1,

then Eq. 10 must be verified as less than or equal to unity. If this condition can be met the possibility of producing a tie-rod stress, T , must be investigated.

The prestress force, F , will be sustained in the unloaded structure in contrast to the induced force, H . The unloaded beam is subjected to the negative moment, eF , and the axial force, F . By equating Eq. 12 with unity the

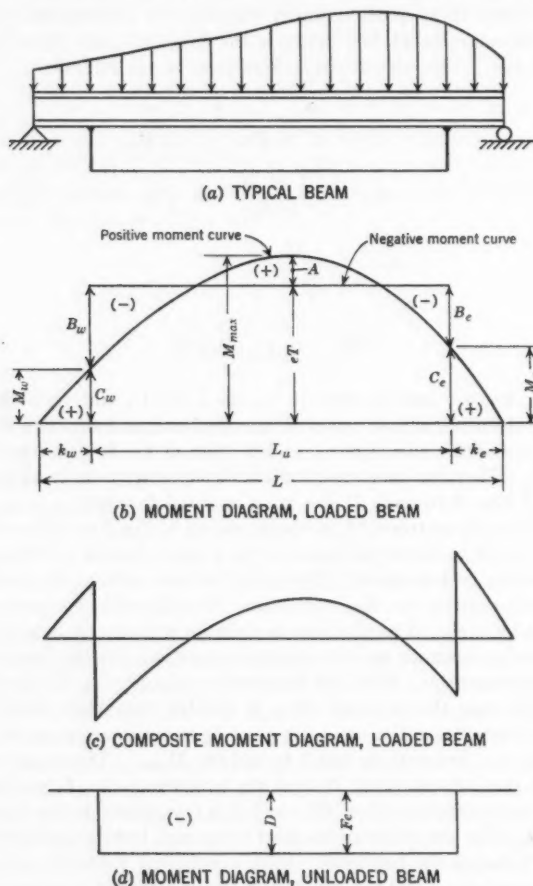


FIG. 3.—TYPICAL PRESTRESSED TRUSS-BEAM

maximum allowable value of this force, F_{\max} , is obtained. The induced force must be at least as great as the difference between T and F_{\max} if Eq. 9 is to be satisfied.

The minimum-size brackets and tie rod can be designed using the force, T . With the geometry and elastic properties of all structural elements known, the

indeterminate stress, H , can be computed by the use of standard procedures. If stress H is less than $T - F_{\max}$ it is possible to increase this quantity by increasing the stiffness of the tie rod. When the value of H is greater than $T - F_{\max}$ the required prestress force is equal to $T - H$.

DESIGN PROCEDURES

1. Select a lighter section than the corresponding simply supported beam without prestressing.

2. Compute the maximum value of $M_{w,e}$ by equating Eq. 11 to unity. The roots of the equation $M_x = S F_b$ represent the maximum values of k_w and k_e , in which the terms k_w and k_e are the distances from the left end and right end, respectively, of a beam to the nearest bracket, and M_x is the bending moment at any point. Using these values of k one can determine L_w . In these computations, S and F_b are the smaller of the possible values. As the L_w -value decreases, the values of F_a and H increase. Therefore, one should use the maximum values of k_w and k_e possible. If values of k_w and k_e are used that are less than the maximum allowable values, the associated moments, $M_{w,e}$, should be computed.

3. Method A—

a. Select a value for e .

b. Compute a minimum value for T by equating Eq. 9 with unity to result in

$$T = \frac{M_{\max} - S_1 F_{b1}}{e - \frac{S_1 F_{b1}}{A F_a}} \dots \dots \dots (13)$$

(1) If $e T > M_{w,e}$, then points $B_{w,e}$ must be checked (that is, Eq. 10 ≤ 1). If Eq. 10 > 1 , then one must try a stronger section, or increase e (using method B), or try a minimum L_w -value. If $S_1 = S_2$ and $F_{b1} = F_{b2}$, a necessary and sufficient condition for $B_{w,e}$ to satisfy Eq. 1 is that

$$M_{\max} - e T \geq e T - M_{w,e} \dots \dots \dots (14)$$

(2) If $e T \leq M_{w,e}$, the critical condition at $B_{w,e}$ does not exist.

Method B—

Compute the minimum e -value necessary for the stresses at A and $B_{w,e}$ to satisfy Eq. 1 and compute the associated value of T . The foregoing is accomplished by setting Eqs. 9 and 10 equal to unity and solving the equations simultaneously for e and T . That is,

$$e = \frac{M_{w,e} S_1 F_{b1} + M_{\max} S_2 F_{b2}}{A F_a (M_{w,e} - M_{\max} + S_1 F_{b1} + S_2 F_{b2})} \dots \dots \dots (15)$$

and

$$T = \frac{M_{w,e} S_1 F_{b1} + M_{\max} S_2 F_{b2}}{e (S_1 F_{b1} + S_2 F_{b2})} \dots \dots \dots (16)$$

in which the greater e -value should be used when $M_w \neq M_e$.

4. Compute the maximum allowable F -value by equating Eq. 12 with unity to result in

$$F_{\max} = \frac{S_2 F_{b2}}{e + \frac{S_2 F_{b2}}{A F_a}} \quad (17)$$

If part of the dead-load moment in the positive moment distribution acts on the beam without overstressing it before the pretensioning is applied, the prestress force, F , may be increased. The loads responsible for this dead-load moment may not be used in the computation of H . Then F_{\max} becomes

$$F_{\max} = \frac{S_2 F_{b2} + M_{dlx}|_{x=k}}{e + \frac{S_2 F_{b2}}{A F_a}} \quad (18)$$

in which k yields the lesser value of the dead-load bending moment, M_{dlx} . This can be derived by imposing a positive dead-load moment distribution on Fig. 3(d), with the smaller moment over either bracket equal to M_{dlx} .

5. Compute the H -value by using the principle of virtual work and design the brackets using the force, T . The necessary equations are

$$A_c = \frac{T}{f_{ca}} \quad (19)$$

and

$$H = \frac{\sum \int M m \frac{ds}{EI}}{\sum \int m^2 \frac{ds}{EI} + \sum \frac{u^2 L}{AE}} \quad (20)$$

in which A_c is the cable or tie-rod area; f_{ca} denotes the allowable cable stress; m is the virtual bending moment caused by a unit load; E represents the modulus of elasticity; s is the length of the increment; u denotes the virtual axial stress caused by a unit load; and M is produced by the loads not acting when the prestressing was applied.

a. If $H + F_{\max} \geq T$, the section is adequate.

b. If $H + F_{\max} < T$, then

(1) Increase A_c and, hence, H . Set $H = T - F_{\max}$ in Eq. 20 and solve for A_c .

(a) If $A_c > 0$, the section may be used with this value of A_c . However, the total weight may be excessive.

(b) If $A_c < 0$, the result is meaningless [see (2)].

(2) Increase e and return to step 3, method A. If e becomes too great one must select a stronger section.

6. Compute the prestressing force from

$$F = T - H \quad (21)$$

checking shear, deflection, and similar items.

COMMENTS ON THE DESIGN PROCEDURE

1. This procedure is intended to increase the strength of available beams at the expense of depth. If a girder or truss is to be designed with a given depth, only negligible weight savings result from this technique. The design of a prestressed girder has been considered² by Gustave Magnel.

2. The maximum values of k_u and k_e depend on the shape of the positive moment diagram. Therefore, the design may depend not only on the maximum moment but on the type of loading. A single concentrated load placed anywhere in the span produces the lowest L_u -value of all downward-acting load systems with equal maximum moments. The values of H given in Appendix I increase with diminishing values of L_u .

3. With respect to method A, a prestressed member having the prestressing element attached to it in such a way that the distance between their centroids remains fixed regardless of any configuration attained eliminates the possibility of axial buckling as a result of the prestressing force alone. If a hinged strut is subjected to an axial load and a lateral force or an initial crookedness provides some curvature in the strut, a moment is produced in the plane of the curvature that is proportional to the distance from the centroid of the strut to the line of action of the axial force. The moment causes more curvature and, hence, more moment, and so forth. When an axial force is produced by cables fixed to the edge of a strut, the line of action of the force remains at a fixed distance from the centroid, and no moment due to curvature is realized. If a wide-flange section has a hollow tube welded along the bottom flange through which a cable is passed and prestress is applied to the beam, then because the distance between the cable and the centroids of the bottom flange and the entire section cannot vary, no axial buckling in the weak direction or lateral buckling of the compression flange can occur without external loading. When the structure is loaded as a beam, lateral buckling is possible, although axial buckling remains unattainable. In the examples in which such a cable attachment was feasible, F_{b2} and F_a were valued at 20,000 lb per sq in. Fig. 4 indicates that an equivalent lateral load does not exist, and, hence, no second-order bending effects are produced when the cable is fixed to the section.

With respect to method B, by placing brackets at the intersection of the positive-moment curve and a horizontal line with ordinate $M_{\max}/3$, and then applying a negative moment of $2 M_{\max}/3$, the design moment assumes a value of $|M_{\max}/3|$. With the truss configuration used, this value is the smallest

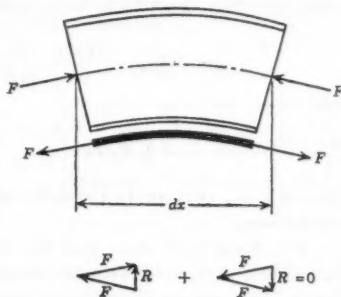


FIG. 4.—VANISHING RESULTANT LOAD

² "Structures in Precompressed Steel," by Gustave Magnel, *Ossature Metallique*, Brussels, Belgium, Vol. 15, No. 6, 1950, pp. 300-313 (in French).

possible one. When rolled beams are designed using method B, trial sections can be obtained by entering the $(L d/b t)$ -table⁴ of the AISC manual with $M_{\max}/3$ and L .

4. The high-strength steel used for prestressing may experience losses in stress due to creep or relaxation.⁵ The value of F_{\max} as computed in step 4 represents the maximum cable stress that can be applied to the unloaded section while satisfying the interaction formula, Eq. 1. If creep losses occur the remaining stress, F_{\max}' , can be used in step 5. It might be feasible to overstress (with respect to Eq. 1) the structure initially so that the final prestress is equal to F_{\max} .

5. The computation of the induced force, H , in the prestressed structure is equivalent to the determination of H in the single redundant structure without prestressing. This follows directly from the principle of superposition. The prestressed structure will have an upward deflection when unloaded and a downward deflection when loaded. The difference represents the total live-load deflection, Δ_{ll} , which can be computed by using the conjugate-beam theory:

$$\Delta_{ll} = \delta_{llx} - \frac{H e L_u (L_u/2 + k_e) x}{L E_b I_b} \quad 0 \leq x \leq k_w \dots \dots (22)$$

and

$$\Delta_{ll} = \delta_{llx} - \frac{H e L_u (L_u/2 + k_e) x}{L E_b I_b} + \frac{H e (x - k_w)^2}{2 E_b I_b} \quad k_w \leq x \leq L - k_e \dots (23)$$

in which δ_{llx} represents the deflection of the simply supported beam without prestressing.

The King Post truss and the conventional form of the Queen Post truss have been compared with the truss-beam studied herein. In general, these trusses were not as effective because of a lower induced moment—that is, the moment produced by the indeterminacy. Lower values of F_a in both trusses and the shape of the negative moment diagram for the King Post truss were contributing disadvantages.

6. The cost of prestressing will dictate the usefulness of the technique described herein. The techniques developed for prestressing high-strength bolts may conceivably be utilized for tie rods and high-strength cables.

NUMERICAL EXAMPLES

Example 1.—The beam in Fig. 5 will be designed to illustrate the suggested procedure. The conditions for design are:

1. The beam is laterally supported at the third points of both flanges.
2. Dead load is neglected.
3. A wide-flange section will be used.
4. The AISC specifications² for stresses will be followed.
5. The allowable cable stress, f_{ca} , is 100,000 lb per sq in.
6. The E -value for all members is 30,000,000 lb per sq in.

⁴ *Steel Construction Manual*, A.I.S.C., 1954, pp. 203-206.

⁵ "Method Presented for Computing Steel Prestress Losses," by H. K. Stephenson and T. R. Jones, Jr., *Civil Engineering*, August, 1955, p. 510.

Design Without Prestress.—From Fig. 5 it is seen that $M_{\max} = 210.0$ ft-kips. The unsupported length for lateral buckling is 10.0 ft. A 21WF62-section with $S = 126.4$ in.³ is selected because

$$S = \frac{M_{\max}}{F_b} = \frac{210 \times 12}{20} = 126.0 \text{ in.}^3$$

Design Using Prestressed Truss-Beam.—Using the method outlined under the heading, "Design Procedures," the following result:

1. A 16WF40-section is selected with $A = 11.77$ sq in., $S = 64.4$ in.³, $I = 515.5$ in.⁴, $r_{\min} = 1.50$ in., and $d/(b t) = 4.54$ in.⁻¹

2. From Fig. 5 it is seen that $M_{\max} = 210.0$ ft-kips, and because $F_b = 20$ kips per sq in., Eq. 11 yields

$$\frac{(20x - 0.4x^2) 12}{64.4 (20)} = 1 \dots \dots \dots (24)$$

from which $x = k_w = k_c = 6.11$ ft, $M = 107.33$ ft-kips, and $L_u = 17.78$ ft.

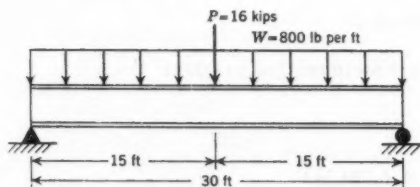


FIG. 5.—BEAM FOR EXAMPLE 1

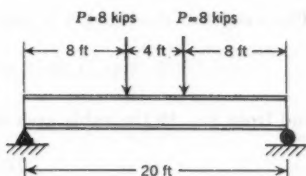


FIG. 6.—BEAM FOR EXAMPLE 2

3. Method A—An e -value of 24 in. is selected. Because $(L''/r) = 10 \times 12/1.5 = 80$, $F_c = 13.90$ kips per sq in., and from Eq. 13,

$$T = \frac{210.0 \times 12 - 64.4 \times 20}{24 - \frac{64.4 \times 20}{11.77 \times 13.90}} = 76.39 \text{ kips}$$

The term L'' denotes the unsupported length for axial buckling. Therefore, the value of $e T$ is 152.78 ft-kips. Because this value exceeds the M -value of 107.33 ft-kips, point B must be investigated. Because

$$M_{\max} - e T = 210.0 - 152.78 = 57.22 \text{ ft-kips}$$

is greater than

$$e T - M = 152.78 - 107.33 = 45.45 \text{ ft-kips}$$

point B is not overstressed.

4. From Eq. 17,

$$F_{\max} = \frac{64.4 \times 20}{24 + \frac{64.4 \times 20}{11.77 \times 13.90}} = 40.41 \text{ kips}$$

5. The truss brackets are designed as follows:

$$L_B = e - (d/2) = 24.0 - 8.0 = 16.0 \text{ in. or } 1.33 \text{ ft}$$

in which L_B is the length of the bracket. The latter is formed by placing two 3-in.-by-2½-in.-by-⅜-in. angles perpendicular to the 16W40-beam and bracing these with two 4-in.-by-3-in.-by-½-in. angles placed at a 45° angle. Because the bracket length is greater than 12 in., a bracket factor should be added to the denominator of Eq. 20. This bracket factor, B_f , is determined from

$$B_f = 2 E_b I_b \left(\sum \frac{u^2 L}{A_a E_a} + \int \frac{m^2 ds}{E_a I_a} \right) \dots \dots \dots (25)$$

and in this case it is found to be

$$B_f = \frac{2 (515.5)}{144} \left[\frac{1^2 (1.33)}{3.84} + \frac{(1.414)^2 (1.89)}{6.50} \right] = 6.64 \text{ kip-ft}^3$$

The weight of the bracket is determined as

$$2 (3.4) [1.33 (3.84) + 1.89 (6.50)] = 118.27 \text{ lb}$$

and from Eq. 19 the cable area is

$$\frac{76.39}{100} \doteq 0.764 \text{ in.}^2$$

The value of H is found by combining Eqs. 29a and 30 from Appendix I to yield

$$H = \frac{\frac{P e}{2} \left(\frac{L^2}{4} - k^2 \right) + \frac{w e}{12} (L^3 - 6 L k^2 + 4 k^3)}{L_u \left(\dot{e}^2 + \frac{I}{A} \right) + (L_u + 2 g) \frac{I}{A_c} + B_f} \dots \dots \dots (26)$$

from which

$$H = \frac{\frac{16 (2)}{2} \left(\frac{30^2}{4} - 6.11^2 \right) + \frac{0.8 (2)}{12} [30^3 - 6 (30) (6.11)^2 + 4 (6.11)^3]}{17.78 \left[2^2 + \frac{515.5}{144 (11.77)} \right] + (17.78 + 2.67) \frac{515.5}{144 (0.764)} + 6.64} = 32.56 \text{ kips}$$

The value

$$H + F_{\max} = 32.56 + 40.41 = 72.97 \text{ kips}$$

is less than T from step 3. Therefore, one must increase the value of A_c . From

$$H = T - F_{\max} = 76.39 - 40.41 = 35.98 \text{ kips}$$

one determines

$$H = \frac{5,828.40}{76.53 + \frac{20.45 (515.5)}{144 (A_c)} + 6.64} = 35.98 \text{ kips}$$

from which $A_c = 0.929 \text{ in.}^2$

6. From Eq. 21 the prestressing force is

$$76.39 - 35.98 = 40.41 \text{ kips}$$

7. The economy of using the prestressed truss-beam is found from

Weight of truss-beam

Cable	20.45 ft \times 0.929 in. ² \times 3.4 lb per ft-in. ² =	64.59 lb
Bracket		= 118.27 lb
Beam	30 ft \times 40 lb per ft	= 1,200.00 lb
Total		= 1,382.86 lb

Weight of unprestressed beam

$$21\text{WF}62 \quad 30 \text{ ft} \times 62 \text{ lb per ft} = 1,860.00 \text{ lb}$$

Saving of weight

$$\frac{1,860.00 - 1,382.86}{1,860.00} \times 100 = 25.7\%$$

Example 2.—The beam in Fig. 6 can be designed using the specifications for example 1 except that lateral support is at the center of both flanges.

Design Without Prestress.—Without prestressing, a 14WF30-beam is adequate for the loads and dimensions given in Fig. 6.

Design Using Prestressed Truss-Beam.—A step-by-step design of a prestressed truss-beam leads to the following:

1. A 8WF20-beam is selected with $A = 5.88 \text{ in.}^2$, $S = 17 \text{ in.}^3$, $I = 69.2 \text{ in.}^4$, $r_{\min} = 1.2 \text{ in.}$, and $d/(b t) = 4.08 \text{ in.}^{-1}$

2. With $M_{\max} = 64.0 \text{ ft-kips}$ and $F_b = 20 \text{ kips per sq in.}$, it is found that k_w and $k_s = 3.54 \text{ ft}$, $M = 28.33 \text{ ft-kips}$, and $L_u = 12.92 \text{ ft}$.

3. Method B—the value of L''/r is found to be $(12.92/2) (12) \div 1.2 = 65$ and $F_a = 14.95 \text{ kips per sq in.}$ The value of e is determined from Eq. 15 as

$$e = \frac{(M + M_{\max}) \frac{S F_b}{A F_a}}{2 S F_b + (M - M_{\max})} = \frac{(28.33 + 64.00) \frac{17 (20)}{5.88 (14.95)}}{\frac{2 (17) (20)}{12} + (28.33 - 64.00)} = 1.417 \text{ ft}$$

and

$$T = \frac{M + M_{\max}}{2 e} = \frac{(28.33 + 64.00) 12}{2 (17)} = 32.59 \text{ kips}$$

4. From Eq. 17, F_{\max} is found to equal 16.29 kips.

5. The cantilever bracket can be designed using a beam section. Hence,

$$S = \frac{M}{f_{ca}} = \frac{13 \times 32.59}{20} = 21.2 \text{ in.}^3$$

which is satisfied by a 12B19-section with an S -value of 21.4 in.³ The shear is

$$\frac{32.59}{12.16 \times 0.24} = 11.17 \text{ kips per sq in.}$$

which is acceptable because it is less than 13 kips per sq in. The bracket factor is determined as

$$B_f = 2 E_b I_b \int \frac{m^2 ds}{E_a I_a} = \left[\frac{2 x^3 I_b}{3 I_a} \right]_0^{1.08} = 0.667 (1.08)^3 \left(\frac{69.2}{130.1} \right) = 0.447$$

which is insignificant. In the foregoing, E_b is the modulus of elasticity of the beam; I_b denotes the I -value of the beam; E_a is the E -value for the bracket; and I_a represents the moment of inertia of the bracket. The weight of the two brackets is

$$\frac{2 \times 13 \times 19}{12} = 41.17 \text{ lb}$$

Also,

$$A_c = \frac{T}{f_{ca}} = \frac{32.59}{100} = 0.326 \text{ in.}^2$$

$$H = \frac{P e (a b - k^2)}{L_u (e^2 + I/A + I/A_c)}$$

$$= \frac{8 (1.417) [8 (12) - (3.54)^2]}{12.92 \left[(1.417)^2 + \frac{69.2}{144 (5.88)} + \frac{69.2}{144 (0.326)} \right]} = 20.55 \text{ kips}$$

and

$$H + F_{\max} = 20.55 + 16.29 = 36.84 \text{ kips}$$

which is greater than 32.59 kips and, therefore, is acceptable.

6. The prestressing force is

$$32.59 - 20.55 = 12.04 \text{ kips}$$

7. The economy of using the prestressed truss-beam is found from

Weight of truss-beam

Cable	14.92 ft \times 0.326 in. ² \times 3.4 lb per ft-in. ² =	16.54 lb
Bracket		= 41.17 lb
Beam	20 ft \times 20 lb per ft	= 400.00 lb
Total		= 457.71 lb

Weight of unstressed beam

$$14\text{WF}30 \quad 20 \text{ ft} \times 30 \text{ lb per ft} = 600.00 \text{ lb}$$

Saving of weight

$$\frac{600.00 - 457.71}{600.00} \times 100 = 23.7\%$$

Example 3.—The design conditions for the beam in Fig. 7 are:

1. The beam is supported laterally at the center of both flanges.
2. The cable is attached to the top of the lower flange.
3. The allowable cable stress is 100,000 lb per sq in.
4. The E -value for all members is 30,000,000 lb per sq in.
5. Both the value of k_w and the value of k_e equal zero.

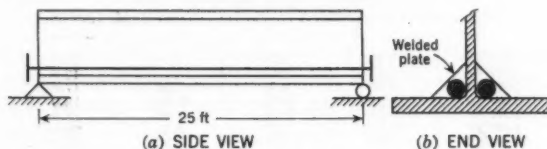


FIG. 7.—BEAM FOR EXAMPLE 3

Moment-Weight Ratio Without Prestressing.—For a 24WF76-section, $A = 22.37 \text{ in.}^2$, $S = 175.4 \text{ in.}^3$, and $d/(bt) = 3.90$. For an F_b -value of 20 kips per sq in., the moment-weight ratio, R , is

$$R = \frac{M_{\max}}{W} = \frac{S F_b}{W} = \frac{175.4 \times 20}{76} = 46.158 \text{ in.-kips per lb per ft}$$

Moment-Weight Ratio with Prestressing.—With the cable attached to the top of the lower flange of the 24WF76-beam, the e -value is

$$(23.91/2) - 0.682 - 0.500 = 10.773 \text{ in.}$$

From

$$\frac{f_a}{F_a} + \frac{f_b}{F_b} = \frac{M_{\max}}{2 e A F_a} + \frac{M_{\max}}{2 S F_b} = 1 \dots \dots \dots (27)$$

it is found that

$$M_{\max} = \frac{2 S F_b A F_a e}{e A F_a + S F_b} \dots \dots \dots (28)$$

which leads to

$$M_{\max} = \frac{2 (175.4) (20) (22.37) (20) (10.773)}{10.773 (22.37) (20) + 175.4 (20)} = 4,060.60 \text{ in.-kips}$$

Thus, the axial design load, P_d , is

$$P_d = \frac{M_d}{e} = \frac{M_{\max}}{2 e} = \frac{4,060.60}{2 (10.773)} = 188.46 \text{ kips}$$

The cable area is

$$A_c = \frac{P_d}{f_{ca}} = \frac{188.46}{100} = 1.885 \text{ in.}^2$$

The weight per foot of the beam and the cable is

$$76 + (3.4 \times 1.885) = 82.409 \text{ lb per ft}$$

TABLE 1.—TYPICAL DESIGNS OF PRESTRESSED TRUSS-BEAMS

Value of e , in inches	Beam section	Cable area, in square inches	Weight of equivalent cable, in pounds per foot	Weight of equivalent bracket, in pounds per foot	Total depth, $e+d/2$, in inches	Weight saved, in %
(1)	(2)	(3)	(4)	(5)	(6)	(7)
(a) Laterally Unsupported, Conventional Design Yields 12WF58						
8.0	14WF48	3.48	4.20	...	15.0	10.0
7.0	10WF49	1.73	1.60	...	12.0	12.8
12.0	10WF45	0.79	0.96	1.26	17.0	18.6
12.0	12WF45	1.22	1.67	1.00	18.0	17.8
18.0	10WF39	0.61	1.09	2.60	23.0	26.4
24.0	10WF39	0.42	0.75	3.30	29.0	25.8
33.05	8WF35	0.32	0.79	4.36	37.05	30.8
(b) Laterally Braced at Center, Conventional Design Yields 16WF50						
8.0	14WF38	4.81	4.45	...	15.05	15.1
9.0	16WF40	0.97	0.80	...	17.0	18.4
12.0	12WF40	0.76	0.80	1.00	18.0	16.4
12.0	14WF38	0.72	0.67	0.70	19.0	21.2
12.0	16WF36	4.15	6.11	0.51	20.0	14.8
12.0	12WF36	1.40	1.89	1.08	18.0	22.1
18.0	12WF31	0.59	0.95	2.40	24.0	31.3
24.0	12WF31	0.40	0.81	2.87	30.0	30.6
30.0	14WF30	0.47	1.14	3.69	37.0	30.4
(c) Laterally Braced for Entire Length Yields 16WF50						
8.5	16WF40	0.82	0.40	...	16.5	19.2
12.0	16WF36	0.61	0.52	0.37	20.0	26.2
12.0	14WF34	0.79	0.94	0.70	19.0	28.7
12.0	14WF30	2.20	3.30	0.73	19.0	31.9
18.14	12WF27	0.71	1.31	2.40	24.14	38.6
24.0	12WF27	0.43	0.97	4.58	30.0	34.9

Thus, the R -value becomes

$$\frac{4,060.60}{82.409 \times 12} = 49.274 \text{ in.-kips per lb per ft}$$

Therefore, the increase in the R -value due to prestressing is

$$\frac{49.274 - 46.158}{46.158} \times 100 = 6.75\%$$

With the cable attached to the bottom of the lower flange, $e = 12.455$ in., $M_{\max} = 4,305.22$ in.-kips, $P_d = 172.84$ kips, and $A_c = 1.728$ in.², and the weight per foot of the beam and cable is 81.875 lb per ft. It is found that the new R -value is 52.586 in.-kips per lb per ft. In this case, as a result of pre-

stressing, the increase in R is

$$\frac{52.586 - 46.158}{46.158} \times 100 = 13.93\%$$

Example 4.—Using the specifications of Example 1 and the method outlined under the heading, "Design Procedures," the beam shown in Fig. 8 is designed

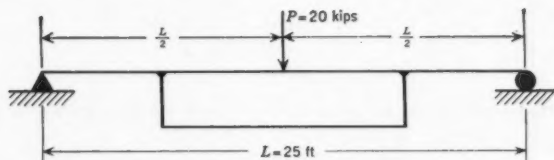


FIG. 8.—BEAM FOR EXAMPLE 4

for different eccentricities and different types of lateral bracing. Characteristics of the designs are shown in Table 1. In addition to demonstrating the possible weight savings, the results in Table 1 indicate the existence of an optimum eccentricity.

CONCLUSIONS

The major disadvantage of the prestressed truss-beam is the depth required for it to be effective. Eqs. 4 and 5 indicate that no improvement results from prestressing an ideal bending member without increasing its total depth. The technique described herein reinforces essentially a given beam. Therefore, an assortment of sections is required for design. A trial-and-error method is used to select a beam that produces the lightest structure. When rolled sections are used in design, substantial weight savings are gained by prestressing. This procedure is applicable wherever depth limitations are not severe, or when it is possible to utilize the space between the lower flange and the tie rod for pipes or ducts. Stresses produced by differential settlement and temperature changes in continuous beams are nonexistent in the truss-beam. The laborious problem of influence computations for continuous beams has a simple counterpart in the structure considered herein.

APPENDIX I. TIE-ROD STRESSES

For a truss-beam subjected to a concentrated load, such as shown in Fig. 9,

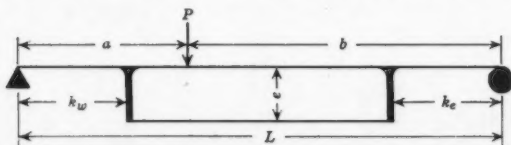


FIG. 9.

$$H = \frac{\frac{P e}{2 L} [a b L - b k_w^2 - a k_e^2]}{(L - k_w - k_e) \left[e^2 + \frac{I}{A} + \frac{I E_b}{A_c E_c} \right]} \quad k_w \leq a \leq L - k_e \dots (29a)$$

or

$$H = \frac{\frac{P a e}{2 L} [(L - k_w)^2 - k_e^2]}{(L - k_w - k_e) \left[e^2 + \frac{I}{A} + \frac{I E_b}{A_c E_c} \right]} \quad 0 \leq a \leq k_w \dots (29b)$$

For a truss-beam subjected to a uniform load, such as shown in Fig. 10,

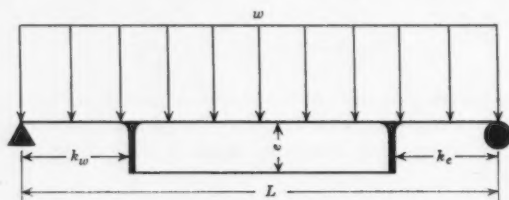


FIG. 10

$$H = \frac{\frac{w e}{12} [L^3 - 3 L k_w^2 - 3 L k_e^2 + 2 k_w^3 + 2 k_e^2]}{(L - k_w - k_e) \left[e^2 + \frac{I}{A} + \frac{I E_b}{A_c E_c} \right]} \dots (30)$$

For a truss-beam subjected to the loading shown in Fig. 11,

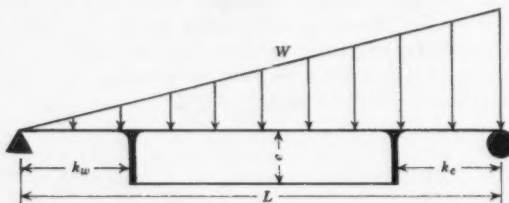


FIG. 11

$$H = \frac{\frac{W e}{12 L^2} [L^4 - 2 L^2 (k_w^2 + 2 k_e^2) + 4 L k_e^3 - k_e^4 + k_w^4]}{(L - k_w - k_e) \left[e^2 + \frac{I}{A} + \frac{I E_b}{A_c E_c} \right]} \dots (31)$$

in which W is the total load.

For a truss-beam subjected to the loading shown in Fig. 12,

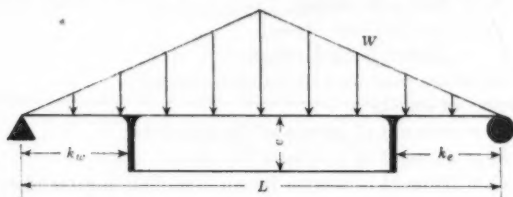


FIG. 12

$$H = \frac{W e}{12 L^2} \frac{[5 L^4 - 12 L^2 (k_w^2 + k_e^2) + 8 (k_w^4 k_e^4)]}{(L - k_w - k_e) \left[e^2 + \frac{I}{A} + \frac{I}{A_e} \frac{E_b}{E_c} \right]} \quad (32)$$

For brackets more than 12 in. long, a bracket factor given by Eq. 25 should be added to the denominators of Eqs. 29 through 32.

APPENDIX II. NOTATION

The following symbols, adopted for use in the paper, conform essentially with "American Standard Letter Symbols for Structural Analysis" (ASA Z10.8—1949), prepared by a committee of the American Standards Association with Society representation, and approved by the Association in 1949:

A = area of the beam section:

A_{ca} = area of the cable or tie rod;

B_f = bracket factor;

c = distance from centroid to extreme fibers;

d = depth of beam section;

E = modulus of elasticity:

E_a = modulus of elasticity of the brackets;

E_b = modulus of elasticity of the beam;

E_{ca} = modulus of elasticity of the cable;

e = eccentricity of cable with respect to centroid of beam;

F = force caused by prestress:

F_a = axial unit stress permitted if axial stress alone existed;

F_b = bending unit stress permitted if bending stress alone existed;

F_{max} = maximum allowable prestress force;

F_{max}' = remaining maximum allowable prestress after creep losses;

f = unit stress:

f_a = unit axial stress;

f_b = bending unit stress;

f_{ca} = allowable cable stress;

H = tie-rod stress produced by indeterminacy;

I = moment of inertia:

I_a = moment of inertia of the brackets;

I_b = moment of inertia of the beam;

I' = moment of inertia for an ideal bending member;

k_e = distance from right end of beam to the nearest bracket;

k_w = distance from left end of beam to the nearest bracket;

L = span length:

L_B = length of bracket;

L_u = distance between brackets or unsupported length for bending;

L'' = unsupported length for axial buckling;

M = bending moment:

M_d = design moment;

M_{dlx} = bending moment due to dead load;

M_e = bending moment at the right-hand bracket;

M_{\max} = maximum bending moment;

M_w = bending moment at the left-hand bracket;

M_x = bending moment at any point;

m = virtual bending moment;

P = axial load:

P_d = axial design load;

R = moment-weight ratios;

r = radius of gyration;

S = section modulus:

S' = section modulus of ideal bending member;

s = length of increment;

T = minimum permissible value of $F + H$;

u = virtual axial stress caused by a unit load;

W = total load;

w = load per unit length;

y = half depth of beam;

δ_{llx} = live-load deflection of a simple beam; and

Δ_{ll} = live-load deflection of a prestressed truss-beam.

AMERICAN SOCIETY OF CIVIL ENGINEERS

Founded November 5, 1852

TRANSACTIONS

Paper No. 2990

FIELD INVESTIGATIONS OF SPILLWAYS AND OUTLET WORKS

BY BENSON GUYTON,¹ A. M. ASCE

SYNOPSIS

Hydraulic field investigations of spillway and outlet works constructed and operated by the Corps of Engineers, United States Department of the Army, at the United States Army Engineer Waterways Experiment Station, Vicksburg, Miss., are presented. Test data examined include spillway, conduit-intake, and gate-leaf pressures as well as air demand and concrete conduit friction factors.

INTRODUCTION

The main purpose of field tests is to obtain data for more economical designs. The structure in which field tests are made is called the prototype, as opposed to a working model on which tests are made at a smaller scale. More variables are usually studied in the model tests than in field tests because of the ease in control and the lesser time and cost involved.

Data are sometimes needed for cases in which model studies are not applicable or in which the scale ratios are unknown. For example, it is difficult to simulate air-water mixtures in a model, and the scale ratios for cavitation and those involving high Reynolds numbers are not clearly understood. Another purpose of field tests is to investigate and evaluate the performance of the prototype for some phase of performance in which operating difficulties are occurring. Tests have been made to verify model indications and in some instances field tests have been necessary to obtain data for designing or operating the model.

The Corps of Engineers (United States Department of the Army) field tests are made either by the district operating the project or by the United States Army Engineer Waterways Experiment Station, Vicksburg, Miss., in conjunction with district personnel. District personnel make tests involving conventional equipment such as current meters and stage recorders, measure discharges

NOTE.—Published, essentially as printed here, in February, 1958, in the Journal of the Hydraulics Division, as *Proceedings Paper 1532*. Positions and titles given are those in effect when the paper was approved for publication in *Transactions*.

¹ Special Asst. to Chief, Eng. Branch, Industrial Div., Army Ballistic Missile Agency, Army Ordnance Missile Command, Redstone Arsenal, Ala.

for rating gates, and make river and harbor soundings. Some extensive tests involving pressure measurements, vibration, and hoist forces are also made. However, most of the extensive tests requiring the use of special equipment are made by the Waterways Experiment Station and cooperating districts.

The Experiment Station is the coordinating agency for hydraulic prototype testing by the Corps of Engineers. In this capacity recommendations are made to the districts concerned regarding collection of field data and the installation of testing facilities such as the embedment of piezometers or conduits for electric leads during construction. The Experiment Station is in a favorable position to accomplish this assignment because of its early association with new projects and through model tests during which the need for field tests may become apparent. In discharging its responsibility of disseminating hydraulic design criteria to the Corps of Engineers, the Station frequently sees the need of field tests. The presence of an Instrumentation Branch with electronic measuring equipment and instrumentation engineers adds much to the capabilities of the Experiment Station.

The scope of the Corps' hydraulic field-testing program includes flood-control and multipurpose projects, river and harbor works, and estuarial and wave-action problems. In recent years the program has been concentrated on multipurpose projects, particularly the spillways and outlet works of concrete and earth dams. The spillway tests have been primarily confined to the measurement of pressures and the collection of data for determining spillway discharge coefficients.

SPILLWAY TESTS

The problem of water availability for testing is more acute for spillways than for outlets. Obviously, spillways cannot be operated until the reservoir level rises above the spillway crest. In many cases this does not happen for years. Some uncontrolled spillways on projects more than fifteen years old have not yet gone into operation.

A severe limitation in testing controlled spillways is that large flows cannot always be tolerated downstream. This restriction hampered testing at Pine Flat Dam on the Kings River near Fresno, Calif., in 1956. Nevertheless, a limited number of spillway tests have been made. These include velocity measurements in the chute of Fort Peck Dam on the Missouri River near Nashua, Mont., in 1946. Ogee crest pressure measurements at 19% of the design head, and water-surface profiles were made at Arkabutla Dam on the Coldwater River near Coldwater, Miss., in 1953. Recording of crest and baffle pier pressures at 75% of the design head at McNary Dam² on the Columbia River near Plymouth, Ore.-Wash., were made in 1954. Recording of crest, tangent, and flip-bucket pressures at Pine Flat Dam at 57% of the design head for gate openings up to 8 ft were also made in 1956.

The most extensive tests made at a Corps of Engineers' spillway were at Chief Joseph Dam on the Columbia River near Bridgeport, Wash., during the summer of 1956. Chief Joseph Dam is a 235-ft-high, concrete-gravity structure on the Columbia River in eastern Washington approximately 50 miles down-

² "Model-Prototype Conformity, McNary Dam Spillway," Walla Walla Dist., Corps of Engrs., U. S. Dept. of the Army, Walla Walla, Wash., June, 1956.

stream from Grand Coulee Dam. Pressures both upstream and downstream from the tainter gate were measured with 23 piezometers, and pressure pulsations near the gate seat were measured with 3 electric pressure cells. At the time the field tests were made, only 4 power units were in operation. Therefore, most of the 300,000-cu-ft-per-sec discharge was passed over the 19-bay spillway. For test purposes, the reservoir pool elevation was altered by changes in discharge during the preceding night. Thus, testing at heads of 32.5 ft, 37.5 ft, 41.6 ft, and 46.5 ft, or 0.8, 0.9, 1.0, and 1.1 times the design head of 41.6 ft was possible. The piezometer lines were permanently installed in bay 9 during construction, as were inserts and conduits for the pressure cells. The cells themselves were installed just prior to testing. Piezometer pressures were observed from gages attached to a valve-bank manifold in the access gallery. Pressure-cell data were recorded on an oscillograph, also located in the gallery.

A section through bay 9 showing piezometers and pressure cells along the bay center line is shown in Fig. 1 for Chief Joseph Dam. The crest conforms to

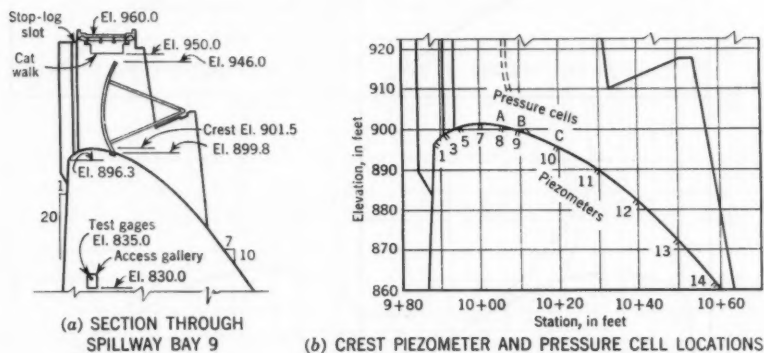


FIG. 1.—CHIEF JOSEPH DAM, SECTION THROUGH SPILLWAY BAY 9

the standard Corps of Engineers' shape for overfall spillways. The rising part of this shape is a compound curve with radii 0.2 and 0.5 times the design head. The falling part of the curve conforms to the equation

$$X^{1.85} = 2.0 H_d^{0.85} Y \quad (1)$$

in which H_d is the head for which the crest shape is designed. In the case of Chief Joseph Dam the crest shape is designed for a head of 41.6 ft, whereas the head at maximum pool would be 55.4 ft. The practice of designing the crest shape for a head as low as three-fourths of the maximum expected head was advocated after model tests indicated that discharge coefficients would be substantially increased and negative pressures would not be excessive.

Pressure profiles at the design head of 41.6 ft are shown in Fig. 2 for gate openings of 5 ft, 10 ft, 20 ft, and free overflow. Pressures on the area downstream from the gate are approximately the same regardless of gate opening,

being approximately -1 ft of water for the 10-ft opening and $+1$ ft for the 20-ft opening and for free overflow. These profiles were obtained with the adjacent gates closed. Tests were also made with the adjacent gates fully open and at openings equal to those in the test bay with resulting changes in pressures being less than 2 ft of water. There was little difference in pressures measured along the center line of the spillway bay and along a parallel line 1 ft from the pier. However, for the free overflow condition positive pressures on the rising part of the crest were considerably higher along the center line than near the pier.

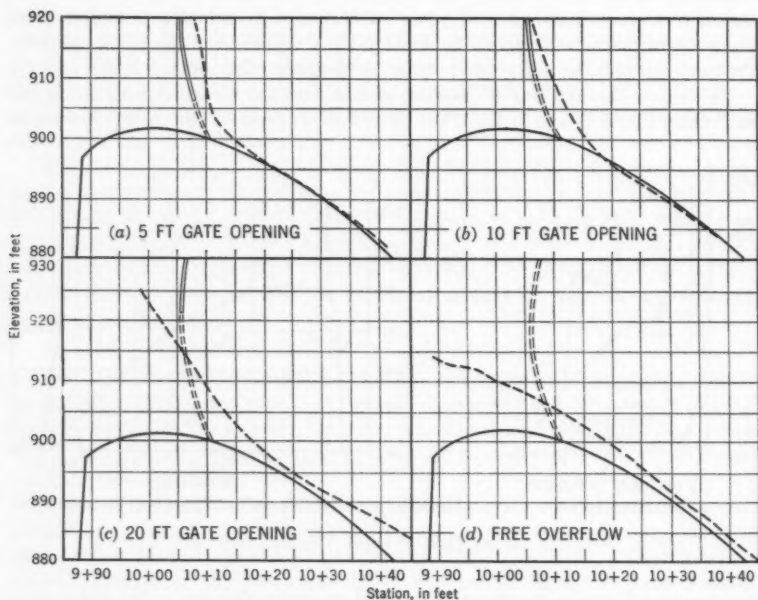


FIG. 2.—SPILLWAY PRESSURE PROFILES

Comparisons of pressure profiles from model tests of the Chief Joseph Dam and the prototype at 46.5-ft head, or 1.1 times the design head, are shown in Fig. 3 for 20-ft and 30-ft gate openings and for free overflow. Adjacent gates were opened equally, and negative pressures did not exceed -2 ft of water. Satisfactory correlation between model and prototype occurred for all comparable tests as would be expected from the Froude law.

The pressure cells measured the magnitude and frequency of the pulsations on the crest. Oscillograms of the tests for Chief Joseph Dam at design head are shown in Fig. 4. Cell A was flush with the concrete surface 5 ft upstream from the gate seat. Cell B was 1 ft upstream and cell C was 9 ft downstream from the gate. The pressure pulsations were of small magnitude and irregular

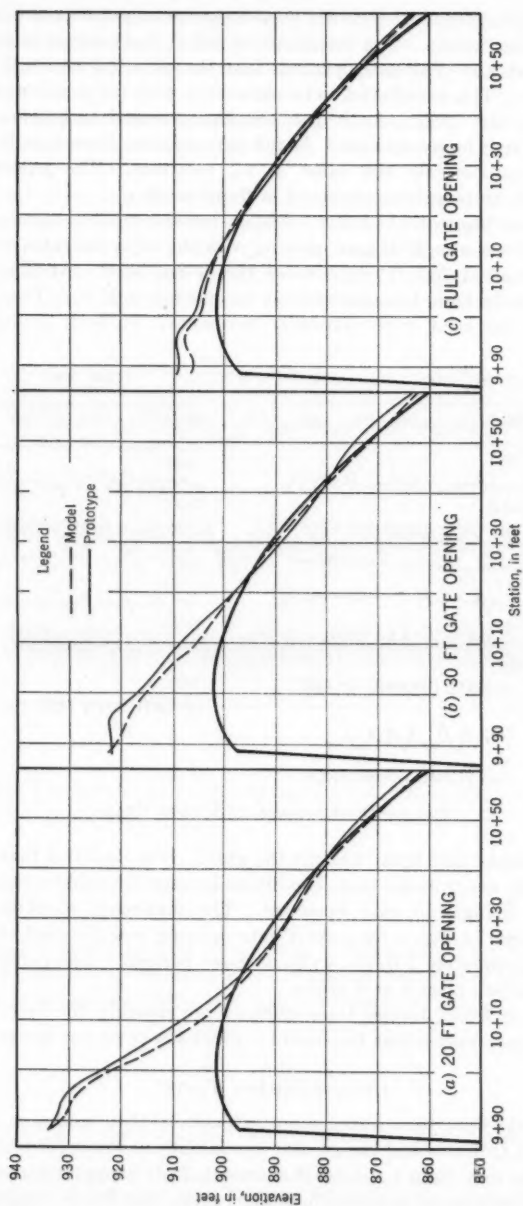


FIG. 3.—COMPARISON OF SPILLWAY PRESSURE PROFILES

frequency varying from 0.1 ft to 1.1 ft of water at frequencies of 0.1 cycle per sec to 100 cycles per sec. The turbulence at cell C, downstream from the gate, was much greater at small gate openings than that at cell A or cell B, upstream from the gate. This is believed to be associated with the development of the turbulent boundary layer. As the gate opening increased, turbulence upstream from the gate seat increased also. At full gate opening (free overflow) turbulence was approximately the same at all locations. The pattern closely resembles velocity pulsations observed in flume studies.

The only condition at which any tendency toward uniform, sinusoidal pulsations occurred was at a 20-ft gate opening with the adjacent gates closed while testing at a head of 32.5 ft or 0.8 times the design head. At this particular head the jet broke loose from the gate at an opening of 25 ft. Therefore, flow conditions at the crest were extremely turbulent. In fact, a violent roller

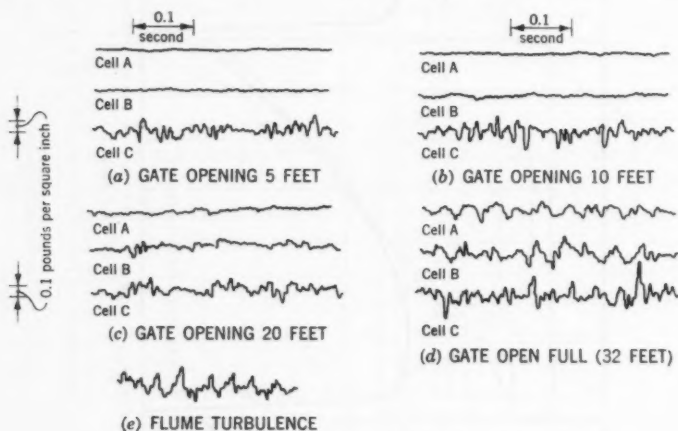


FIG. 4.—OSCILLOGRAMS AT DESIGN HEAD

alternately formed and broke against the gate. It is doubtful that operation would normally occur under these conditions because it could be eliminated by rather small changes in gate openings. The maximum magnitude of the pulsations shown in Fig. 5 for a 20-ft gate opening and the pool elevation at 943, was approximately $\frac{1}{4}$ lb per sq in. at 8-sec periods. The periodic oscillations were damped after 3 or 4 cycles.

The tests at Chief Joseph Dam spillway are possibly the first to be conducted at a head approaching the head for which the crest was designed.

OUTLET WORKS TESTS

Outlet works have been tested more extensively than spillways because of more installed facilities and the greater availability of water for test purposes. Tested outlets vary from 4-ft-by-6-ft sluices to 25-ft-diameter tunnels. Tests include measurements of pressures in intake curves, gate liners, conduits proper,

exit portals, buckets, and stilling basins. In addition, pressures and vibration have been measured on a variety of control gates, including hydraulically-operated slide gates, cable-operated tractor gates, and tainter gates. Extensive field tests were made on the Fort Peck Dam² cylinder gate and control shaft to investigate pressures, vibration, and air demand. The most extensive Corps of Engineers' installation for testing sluices at high heads is at Pine Flat Dam.

Pine Flat Dam is a 140-ft-high, concrete-gravity structure with an upper tier and a lower tier of 5 sluices each. A section through the spillway and sluices is shown in Fig. 6. Sixty-two piezometers have been installed in one of the 5-ft-wide by 9-ft-high lower sluices and 71 piezometers have been installed in an upper sluice. Fourteen series of pressure measurements have been

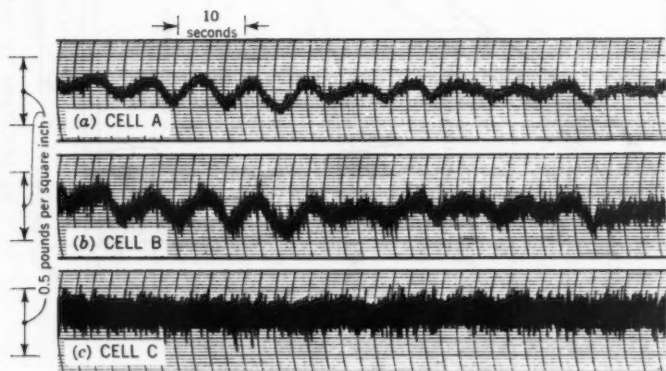


FIG. 5.—CREST PRESSURE PULSATIONS

made in the lower sluice at heads varying from 110 ft to 300 ft. In Fig. 7 the pressure drop coefficient, C , is determined by the equation

$$C = \frac{H_d}{\frac{V^2}{2g}} \dots \dots \dots (2)$$

Data from the closely spaced piezometers in the entrance curve have been reduced to pressure drop coefficients and compared with model data for similarly shaped elliptical intake curves based on the equation

$$\frac{X^2}{D^2} + \frac{Y^2}{\left(\frac{D}{3}\right)^2} = 1 \dots \dots \dots (3)$$

in which D is the dimension across the conduit in the direction concerned.

² "Hydraulic Prototype Tests, Control Shaft 4, Fort Peck Dam, Missouri River, Montana," *Technical Memorandum No. 2-402*, U. S. Army Engr. Waterways Experiment Station, Corps of Engrs., Vicksburg, Miss., April, 1955.

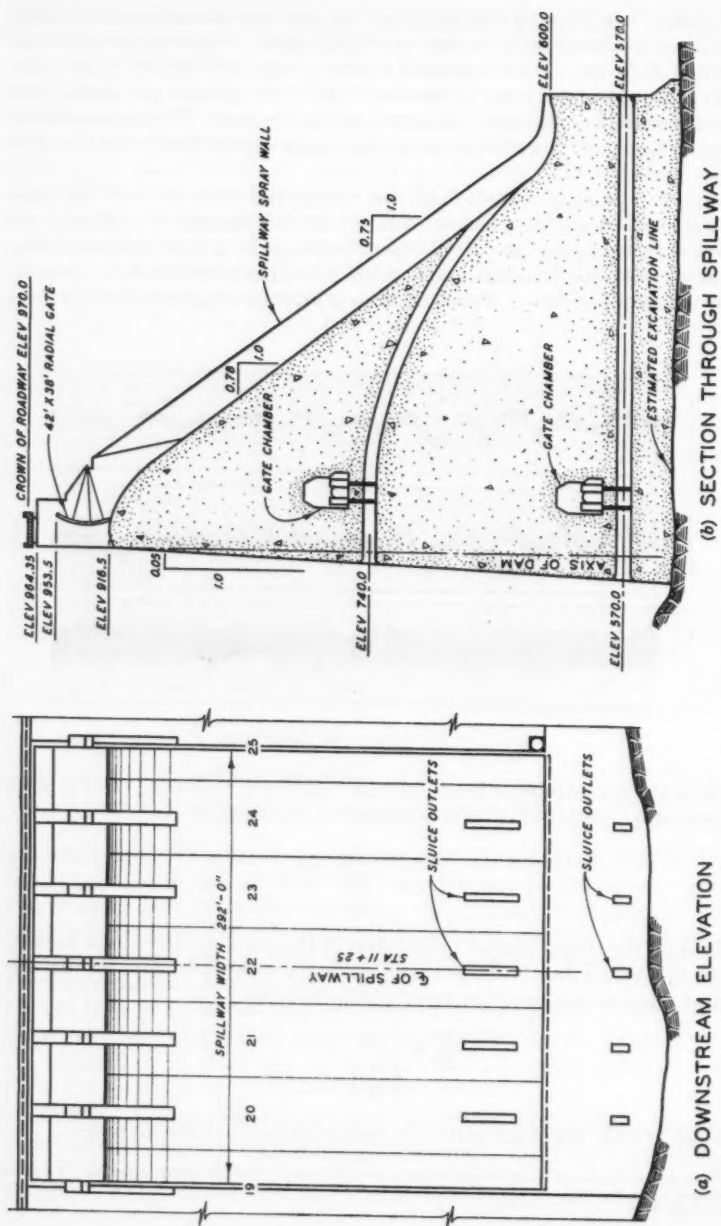


FIG. 6.—PINE FLAT DAM SPILLWAY AND SLUICES

Value of pressure drop coefficient, C

1.4

1.2

1.0

0.8

0.6

0.4

0.2

0

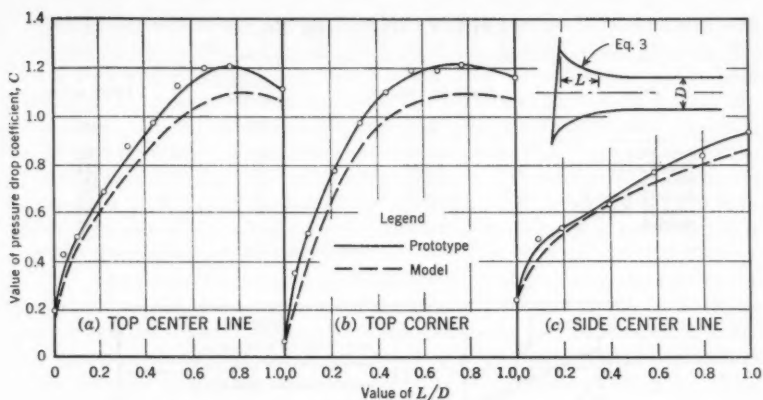


FIG. 7.—PINE FLAT DAM INTAKE PRESSURE DROP COEFFICIENTS

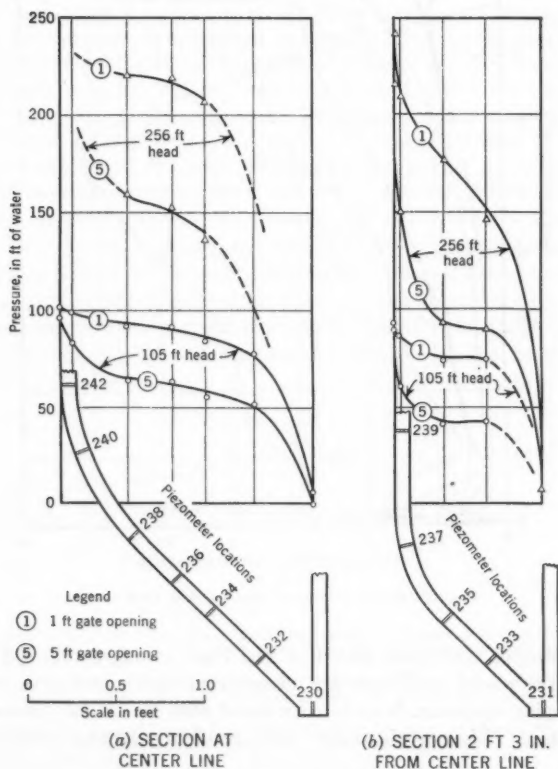


FIG. 8.—PINE FLAT DAM GATE LEAF PRESSURES

TABLE 1.—DATA FOR FIG. 9

Project	Sluice size, in feet	Vent diameter, in inches	Head, in feet
(1)	(2)	(3)	(4)
Pine Flat A	5 × 9	30	92
Pine Flat B	5 × 9	30	254
Pine Flat C	5 × 9	30	370
John H. Kerr A	5.7 × 10	30	73
John H. Kerr B	5.7 × 10	30	95
Norfolk	4 × 6	20	157

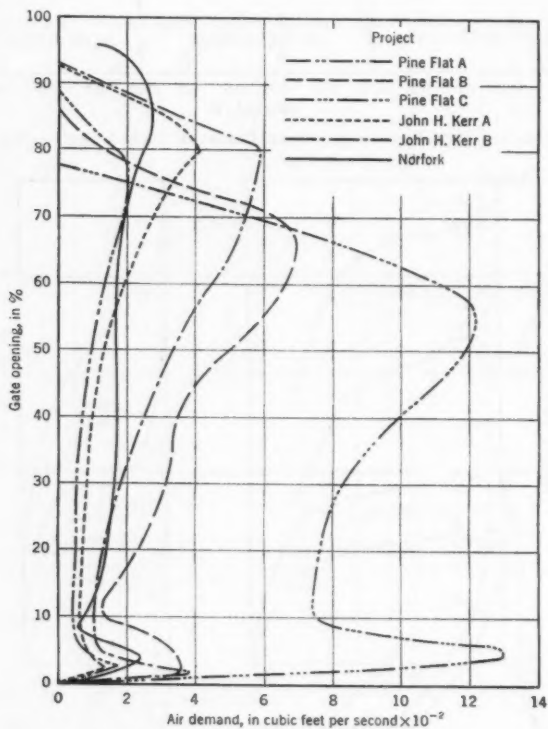


FIG. 9.—GATE OPENING VERSUS AIR DEMAND

The prototype coefficients shown in Fig. 7 are averages obtained from the 14 tests. The model coefficients are interpolated from model data on vertical and 10° sloping upstream faces to correspond with the $2^\circ 52'$ sloping face at Pine Flat Dam. The prototype data indicate slightly greater coefficients than the model.

The superiority of the 45° lip over the old flat bottom for slide gates was demonstrated in model and prototype tests of the Norfolk Dam⁴ gates on the North Fork of the White River near Norfolk, Ark. Tests were made at Pine Flat Dam⁵ to measure vertical and flexural vibration of the 5-ft-by-9-ft 45° lip slide gates. Acceleration measurements indicated stable vibration condition for all gate openings. These gates have been operated for long periods of time at partial gate openings with no apparent damage. Piezometric measurements of pressures on the gate leaf have been made for heads ranging from 100 ft to 256 ft. Pressures for gate openings of 1 ft and 5 ft observed at heads of 105 ft and 256 ft are shown in Fig. 8.

Air is admitted to the sluices through a vent pipe joining the roof of the gate chamber just downstream from the gate. Velocities in the 30-in.-diameter air vent have been measured for a range of heads varying from 92 ft to 370 ft. A plot of air demand versus gate opening in Fig. 9 shows peak demands at small openings and at approximately 60% to 80% opening (Table 1). This substantiates similar measurements at other projects including Norfolk Dam and John H. Kerr Dam on the Roanoke River near Boydton, Va.

One of the earlier installations of prototype testing facilities is in a 20-ft-diameter, cut-and-cover type conduit at Denison Dam⁶ on the Red River near Denison, Tex. Piezometric pressure measurements have been made using the 47 piezometers installed during construction. Piezometer locations and the results of piezometric measurements at a 98-ft head are shown in Fig. 10 for the Denison Dam flood-control conduit No. 6. The test conditions were (a) pool elevation, 621.25 ft; (b) discharge, 20,500 cu ft per sec; (c) water temperature, 68° F; and Reynolds number 1.20×10^8 . It is believed that the flat, uniform slope of the grade line in the downstream part of the conduit is the friction gradient. The Darcy-Weisbach friction coefficient computed from this slope is 0.00644 at a Reynolds number of 120,000,000. These values when plotted in Fig. 11 for friction factors in concrete conduits, fall approximately one-fourth of the distance between the smooth-pipe curves and the rough-pipe curves developed by Theodor Von Kármán and L. Prandtl. In Fig. 11 the equation for the friction factor is

$$f = \frac{h_f}{\left(\frac{L}{D}\right) \frac{V^2}{2g}} \dots \dots \dots (4)$$

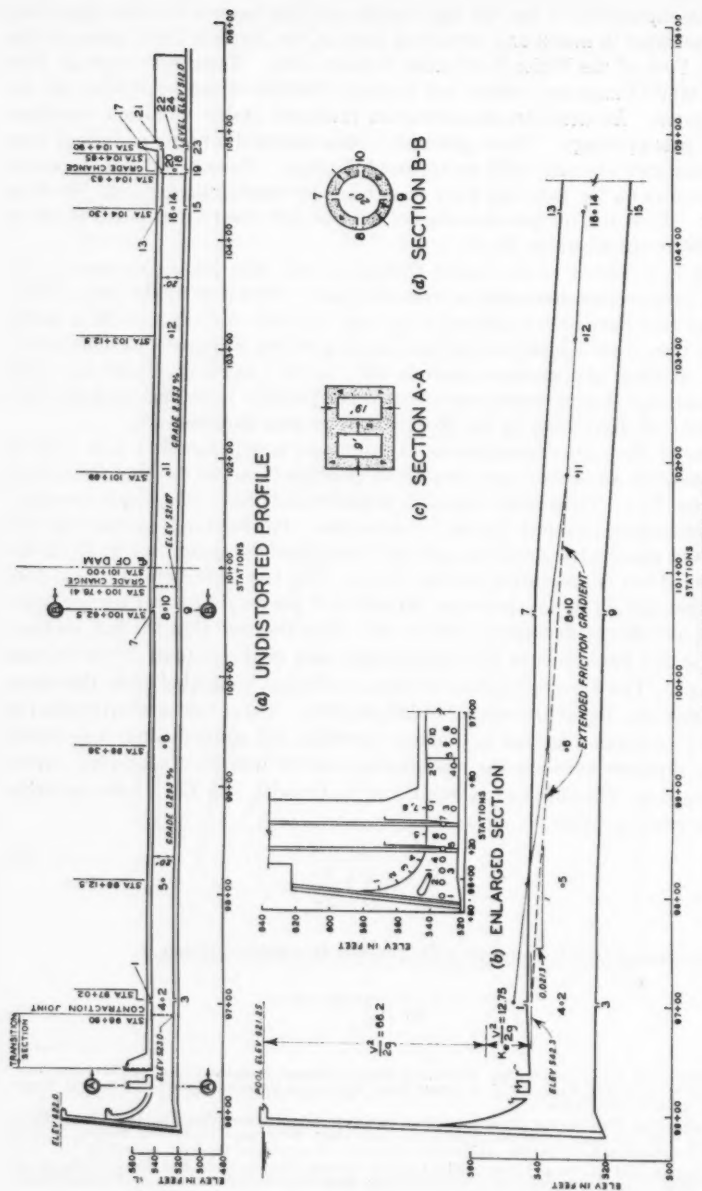
Relative roughness is equal to ϵ/D , and the Reynolds number is

$$R = \frac{VD}{\nu} \dots \dots \dots (5)$$

⁴ "Slide Gate Tests, Norfolk Dam, North Fork River, Arkansas; Model and Prototype Investigations," *Technical Memorandum No. 2-389*, U. S. Army Engr. Waterways Experiment Station, Corps of Engrs., Vicksburg, Miss., July, 1954.

⁵ "Vibration, Pressure and Air-demand Tests in Flood-control Sluice, Pine Flat Dam, Kings River, California," *Miscellaneous Paper No. 2-75*, U. S. Army Engr. Waterways Experiment Station, Corps of Engrs., Vicksburg, Miss., February, 1954.

⁶ "Pressure and Air-demand Tests in Flood-control Conduit, Denison Dam, Red River, Oklahoma and Texas," *Miscellaneous Paper No. 2-31*, U. S. Army Engr. Waterways Experiment Station, Corps of Engrs., Vicksburg, Miss., April, 1953.



The curves plotted are

$$\frac{1}{\sqrt{f}} = \frac{R}{200} \frac{\epsilon}{D} \dots \dots \dots (6)$$

$$\frac{1}{\sqrt{f}} = -2 \log \left(\frac{\epsilon}{3.7} + \frac{2.51}{R \sqrt{f}} \right) \dots \dots \dots (7)$$

and

$$\frac{1}{\sqrt{f}} = 2 \log R \sqrt{f} - 0.8 \dots \dots \dots (8)$$

The values of velocity of flow times the diameter of the conduit were for a water temperature of 60° F. Pressure-cell tests at the 24-ft-8-in.-diameter concrete

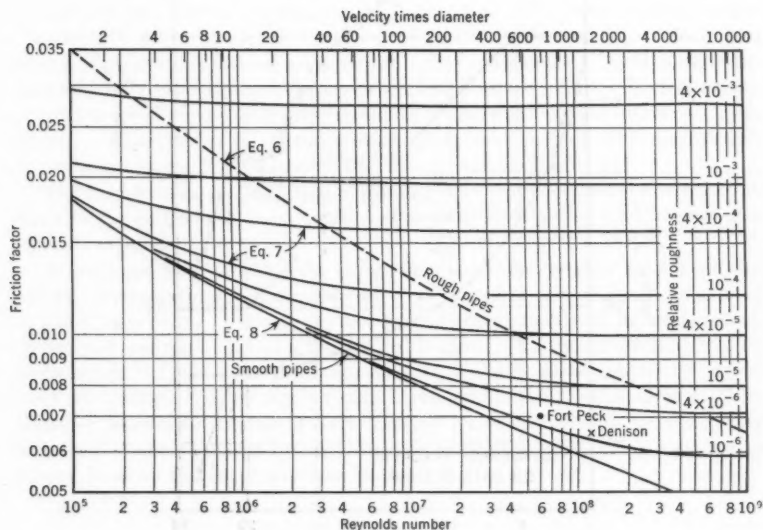


FIG. 11.—CONCRETE CONDUIT FRICTION FACTORS

conduit at Fort Peck Dam indicated an f -value of 0.0069 at a Reynolds number of 60,000,000.

Discharges through tunnels of earth dams are frequently controlled by cable-operated tractor gates. Usually 2, 3, or 4 gates separated by piers are used. Pressure and vibration measurements were made on the 45° lip, 11-ft-by-23-ft intake gates controlling flow into a 22-ft-diameter tunnel at Fort Randall Dam⁷ on the Missouri River near Pickstown, S. Dak. Vibration tests

⁷ "Vibration and Pressure-cell Tests, Flood-control Intake Gates, Fort Randall Dam, Missouri River, South Dakota," *Technical Report No. 2-435*, U. S. Army Engr. Waterways Experiment Station, Corps of Engrs., Miss., Vicksburg, June, 1956.

at heads of 79 ft, 97 ft, and 110 ft revealed no unstable oscillations that would indicate resonance with a forcing frequency. Pressures along the gate center line and near the side measured with 10 pressure cells were positive for heads of 97 ft and 110 ft. The dimensionless ratio of the average pressure on the gate bottom, P_{avg} , to the height of pool above the gate sill, H_{pg} , is shown in Fig. 12(b). The average pressures were determined for that part of the gate bottom within the conduit itself by integrating contoured plots of the measured pressures. The pressure-height ratios can be used to estimate pressures on the gate bottom for other pool elevations. Water-surface elevations in the gate

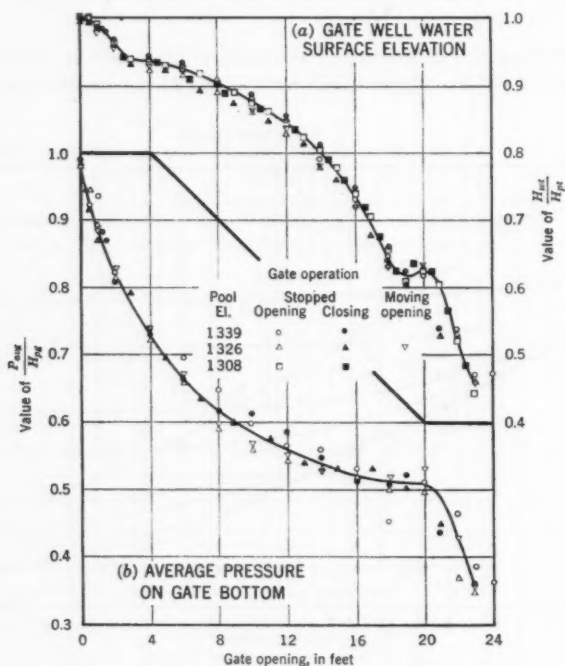


FIG. 12.—FORT RANDALL DAM GATE OPENING DATA

well were measured with an electrode sounding device simultaneously with the pressure-cell tests. The ratio of the height of the column of water in the gate well above the tunnel roof, H_{wt} , to the height of pool above the tunnel roof, H_{pt} , is shown in Fig. 12(a). The data in Fig. 12 are, of course, applicable only to the Fort Randall Dam project or to systems geometrically similar with respect to gate shape and gate-well clearances.

An examination of spillways and outlets would not be complete without considering stilling action. Pressures in spillway and outlet buckets have been measured for nominal flow conditions at several projects. Pressures

were measured at two points on a baffle block at McNary Dam. Prototype pressure-cell measurements on the elliptically shaped steps of the Bull Shoals Dam⁸ stilling basin on the White River near Mountain Home, Ark. revealed high-frequency pressures whose averages compared favorably with those obtained in the model. However, fast pressure drops to as low as -34 ft of water were indicated by the pressure cells. These low pressures occurred too fast to be indicated by model piezometric measurements. Considerable cavitation damage to the prototype concrete steps occurred. Perhaps the lesson to be learned is to be wary of piezometer indications in which high-frequency, pulsating pressures might be expected, as in gate slots, baffle piers, and in sudden changes in boundary shapes for high-velocity flows.

In field tests piezometer pressures are usually measured with a pressure gage or with a manometer filled with mercury or some other fluid. Pulsating pressures are measured with electric pressure cells and vibrations are measured with accelerometers. Direct writing recorders are used with pressure cells or accelerometers when frequencies are less than 100 cycles per sec. Recordors using a photographic process are used for higher frequencies. Air demands are measured with pitot tubes, velometers, and with orifice plates. Water-surface elevations are observed with the customary stage recorders and electrical probe devices. Adaptations of special testing equipment include deflection gages, electrical-resistance thermometers, and air-pressure cells.

The field-testing program is a continuing one. More tests will be made at many of the projects already mentioned as additional water for test purposes becomes available.

In addition to extending the range of measurements that have been described, investigations will be made of crest pressures and pressure pulsations on a low, ogee crest. Velocity profiles and air entrainment will be measured on chute-type spillways and at a high overfall dam. Pressure pulsations will be measured in the gate slots of a large tunnel. Velocity distribution and turbulence phenomena will be studied with a removable strut installed in a 22-ft-diameter, steel-lined tunnel at Fort Randall Dam. Provisions for measuring high-head sluice discharge by an ultrasonic method are also being installed at Sutton Dam on the Elk River near Sutton, W. Va.

CONCLUSIONS

The results of extensive field investigations of spillways and outlet works of hydraulic structures operated by the Corps of Engineers are presented. The data are indicated as applicable to the projects tested, although some data have been reduced to dimensionless parameters. Pressure measurements demonstrate close agreement with those obtained in models. This was verified for spillway crests, sluice intake curves, and large-diameter conduits, and for control gates. The soundness of basing spillway-crest design on heads exceeding the maximum expected head by as much as one-third was confirmed. The efficient operation of the 45° gate leaf was demonstrated. The field tests show that

⁸ "Pressure-cell Tests, Bull Shoals Dam Stilling Basin," *Miscellaneous Paper No. 2-77*, U. S. Army Engr. Waterways Experiment Station, Corps of Engrs., Vicksburg, Miss., February, 1954.

the concrete conduit friction factors commonly used in design practice are conservative.

ACKNOWLEDGMENTS

The tests described herein were conducted under the supervision of the Corps of Engineers' hydraulic prototype testing program. The writer wishes to express his appreciation to Jacob H. Douma, A. M. ASCE; Andrew P. Rollins, Jr., Joseph B. Tiffany, Eugene P. Fortson, Jr., Frank B. Campbell, Members, ASCE; and H. A. Bell, Jr. The writer is also indebted to the Corps of Engineers, particularly the Instrumentation Branch of the Waterways Experiment Station for their valuable assistance in obtaining field measurements.

AMERICAN SOCIETY OF CIVIL ENGINEERS

Founded November 5, 1852

TRANSACTIONS

Paper No. 2991

HYDRAULIC JUMP AT AN ABRUPT DROP

BY WALTER L. MOORE¹ AND CARL W. MORGAN,² ASSOCIATE
MEMBERS, ASCE

WITH DISCUSSION BY MESSRS. MURRAY B. MCPHERSON; JOHN W.
FORSTER; AND WALTER L. MOORE AND CARL W. MORGAN

SYNOPSIS

The hydraulic jump may form at various locations relative to a low abrupt drop in a rectangular channel. The role of the drop in determining the form of the jump and in stabilizing its position is clarified by analysis and experiment. The paper presents the application of the results to the analysis of a stilling basin.

INTRODUCTION

In many types of hydraulic structures a considerable portion of the kinetic energy of the flowing water must be dissipated to prevent erosion of the channel downstream from the structure. Various methods of energy dissipation have been used to achieve tranquil flow conditions as the flow enters the downstream channel. The primary purpose of all such methods is to convert as much as possible of the kinetic energy of flow into turbulent energy, and, ultimately into heat. One of the most effective means of accomplishing the required energy dissipation is a hydraulic jump. The hydraulic jump can assume several different forms depending on the geometry of the channel boundaries. An abrupt drop or rise in the channel bottom may be introduced in an effort to reduce the length of stilling basins, and to insure that the jump will not be swept from the stilling basin under varying flow conditions.

For economic reasons there has been a tendency in practical design to make the length of the stilling pool considerably less than the length of the jump. The paper presents information concerning the characteristics of the jump at an

NOTE.—Published, essentially as printed here, in December, 1958, in the Journal of the Hydraulics Division, as *Proceedings Paper 1449*. Positions and titles given are these in effect when the paper or discussion was approved for publication in *Transactions*.

¹ Prof., Dept. of Civ. Eng., Univ. of Texas, Austin, Tex.

² Asst. Prof., Dept. of Civ. Eng., Univ. of Texas, Austin, Tex.

abrupt drop in the channel bottom. Particular emphasis is placed on the characteristics of the jump when the drop is situated within the length of the jump.

ANALYSIS

The different forms of a hydraulic jump that will occur at an abrupt drop in a rectangular channel are shown in Fig. 1. In Fig. 1, Y_1 is equal to the depth of flow upstream from the drop; Y_2 is the depth of flow downstream from the drop; ΔZ_0 is the height of the drop; and h_D is the piezometric head on the drop. For convenience the different forms are identified as jump A, wave, jump B, and minimum jump B. The relative height of a stationary jump, Y_2/Y_1 , will be dependent on the dimensionless parameters, $\Delta Z_0/Y_1$ and h_D/Y_1 , and the Froude number, $\frac{V_1}{\sqrt{g Y_1}}$, of the entering flow. As the jump changes from one form to the other, the value of the hydrostatic head, h_D , will change, causing the

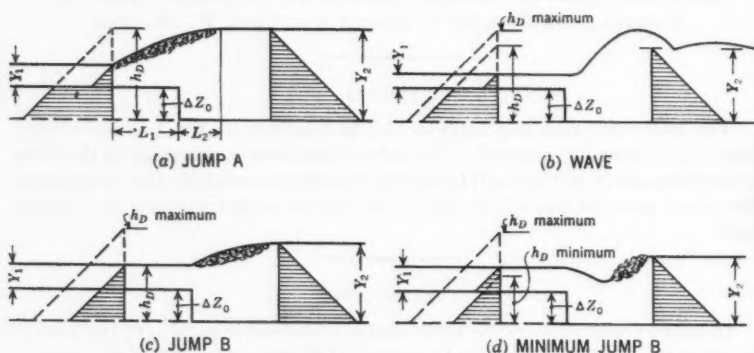


FIG. 1.—FORMS OF HYDRAULIC JUMP AT AN ABRUPT DROP

pressure on the face of the drop to change from a maximum value of $\gamma h_D = \gamma Y_2$ when the jump forms upstream from the drop, to a minimum value of $\gamma h_D < \gamma (\Delta Z_0 + Y_1)$, when the jump forms downstream from the drop.

Assuming that (a) the pressure distribution on the face of the drop is hydrostatic under a head of h_D ; (b) the shear stress along the solid boundaries between section 1 and section 2 is neglected; and (c) the momentum coefficients, β_1 and β_2 , are unity, the momentum equation for sections 1 and 2 is

$$\frac{\gamma Y_1^3}{2} + \gamma \left(h_D - \frac{\Delta Z_0}{2} \right) \Delta Z_0 - \frac{\gamma Y_2^3}{2} = \frac{\gamma}{g} q (V_2 - V_1) \dots \dots (1)$$

in which γ is the specific weight of the fluid and q is the discharge per unit width of the channel. If the continuity equation,

$$q = V_1 Y_1 = V_2 Y_2 \dots \dots \dots (2)$$

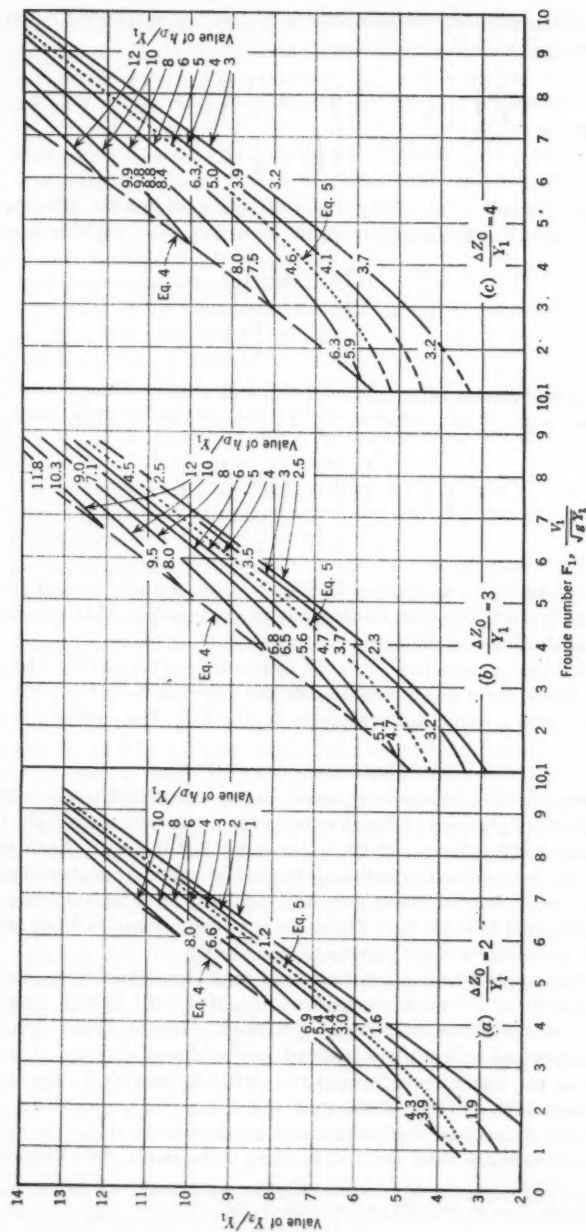


FIG. 2.—RELATIVE DOWNSTREAM DEPTH AS A FUNCTION OF FROUDE NUMBER AND THE PIEZOMETRIC HEAD AT THE DROP

and Eq. 1 are combined and reorganized, the following general equation relating the several variables is obtained:

$$F_1^2 = \frac{\left(\frac{Y_2}{Y_1}\right)^2 - \left(1 + \frac{\Delta Z_0}{Y_1}\right)^2 - 2 \frac{\Delta Z_0}{Y_1} \left(\frac{h_D}{Y_1} - \frac{\Delta Z_0}{Y_1} - 1\right)}{2 \left(1 - \frac{Y_1}{Y_2}\right)} \dots \dots \dots (3)$$

Fig. 2(a), (b), and (c) show Eq. 3 plotted as a solid line for different values of the variables. For the condition $h_D = Y_2$ in Fig. 1(a), Eq. 3 reduces to

$$F_1^2 = \frac{\left(\frac{Y_2}{Y_1} - \frac{\Delta Z_0}{Y_1}\right)^2 - 1}{2 \left(1 - \frac{Y_1}{Y_2}\right)} \dots \dots \dots (4)$$

Fig. 2 shows the upper limiting curve of Eq. 4 as a dashed line.

When $h_D = Y_1 + \Delta Z_0$ —that is, $h_D/Y_1 = 1 + \Delta Z_0/Y_1$ (Fig. 1(c)), Eq. 3 reduces to

$$F_1^2 = \frac{\left(\frac{Y_2}{Y_1}\right)^2 - \left(1 + \frac{\Delta Z_0}{Y_1}\right)^2}{2 \left(1 - \frac{Y_1}{Y_2}\right)} \dots \dots \dots (5)$$

Eq. 5 is plotted as a dotted line in Fig. 2. Eqs. 4 and 5 are equivalent to the equations given by En-Yun Hsu³ for the two values of h_D that were assumed to determine the characteristics analytically.

It is noted that a reduction of h_D/Y_1 causes the curves of Fig. 2 to shift to the right. Thus, for a given condition of the entering flow, the jump can be held in place with a reduced downstream depth, Y_2 . The converse is equally correct.

EXPERIMENTAL APPARATUS

Experimental observations were made on two drops that were constructed of $\frac{3}{4}$ -in. waterproof plywood and each mounted in a 1-ft-wide glass-walled flume. One drop was 0.400 ft deep and the other was 0.200 ft deep. Each was 3 ft long, with an elliptical section at the upstream end and a vertical section at the downstream end. A brass sluice gate adjustable by an attached screw device could be positioned to 0.001 ft. The sluice gate had a machined $\frac{1}{2}$ -in. rounded edge, which gave only a slight contraction in the jet.

Water was supplied from a constant head tank through an 8-in. pipe to the forebay of the flume. The discharge was regulated with an 8-in. gate valve, and the flow rate was measured by a $5\frac{1}{4}$ -by-8-in. Venturi-orifice meter with a $4\frac{3}{8}$ -in. sharp-edged orifice plate inserted in the throat section. The differential head on the meter could be read to ± 0.001 ft, making it possible to set the rate of flow with an error of less than 1%.

Surface elevations were determined with an electric point gage mounted on an instrument carriage that could slide along rails above the channel. The

³ Discussion by En-Yun Hsu of "Control of the Hydraulic Jump by Sills," by John W. Forster and Raymond A. Skrinde, *Transactions, ASCE*, Vol. 115, 1950, p. 990.

vertical position of the gage was read with a direct vernier reading to 0.001 ft. The depth of water in the downstream channel was controlled by a wicket-type gate, which caused a minimum disturbance to the flow pattern upstream. The gate was 17.5 ft downstream from the last section at which measurements were taken.

Velocities were measured with a standard Prandtl pitot-static tube that had a coefficient of 1.00. The pitot tube was fitted to the same instrument carriage that held the point gage and could be positioned to 0.001 ft. Velocities were measured near the bottom of the channel at several positions downstream from the drop. Distances were measured on a section of engineers' steel tape with an error of no more than ± 0.002 ft.

Values of h_D were measured by means of piezometers attached to piezometric holes drilled in a $\frac{1}{2}$ -in.-by-1-in. brass strip set into the face of the drop so as to be flush with the vertical surface. The openings were set at 0.073 ft, 0.200 ft, and 0.327 ft from the bottom of the 0.400-ft drop, and at 0.100 ft from the bottom of the 0.200-ft drop.

Table 1 lists the flow conditions that were chosen for observations. Values of the depth, Y_2 , the piezometric head at each piezometer, and velocity along the bottom were read for each of the flow conditions listed. The flow conditions chosen produced the three types of jumps shown in Figs. 1(a), 1(b) and 1(c).

RESULTS

It was found that the pressure on the face of the drop was hydrostatically distributed under a piezometric head, h_D , which varied with the position of the jump relative to the drop. The measured values of h_D/Y_1 are shown in Fig. 2 at the values of Y_2/Y_1 and F_1 at which they were observed. The decimal point indicates the plotted point. The observed values confirm the analytical computations within the limits of the accuracy of the observation and clearly indicate the variation of h_D with the change in the flow conditions.

The limiting values of Y_2/Y_1 , in which each type of jump would form at given entering flow conditions, are shown in Fig. 3. The conditions under which jump A will form are indicated as a very narrow band. Actually, jump A may form at values of Y_2/Y_1 greater than the upper bound, being limited only by the free distance upstream and the slope and resistance of the channels. The undular wave will form at values of the variables that fall within the middle band. The height of this wave may exceed the value of Y_2 by as much as 50% and might cause considerable damage unless adequate training walls were provided. Jump B will form when values of the variables are those within the lower band. The narrow gap between the intermediate and lower bands in Fig. 3 represents a transition zone in which there is uncertainty as to whether the wave or jump B will form. For values of Y_2/Y_1 and F_1 that would lie

TABLE 1.—FLOW CONDITIONS

Test no.	ΔZ_0	Y_1	$\Delta Z_0/Y_1$	F_1
(1)	(2)	(3)	(4)	(5)
1	0.400	0.100	4	2, 4, 6, 8
2	0.400	0.133	3	2, 4
3	0.200	0.067	3	6, 8
4	0.200	0.100	2	2, 4, 6

below the lower band, the jump would be swept downstream from the drop. Perhaps the most important characteristic presented is that the jumps can form over a wide range of Y_2/Y_1 for the entire range of entering Froude numbers covered by the experiments. This might be anticipated from the previous analysis because the hydrostatic head, h_D , should vary continuously between its limiting values. Visual observation of the gradual change in curvature of the main stream of the flow as it crossed the drop also indicated a continuous variation of h_D . As indicated by Eq. 3, a continuous variation of h_D implies a continuous variation of Y_2/Y_1 between its extreme values.

To demonstrate the effectiveness of the different types of jumps in reducing the velocity along the channel bottom, the velocity near the channel bottom is plotted against distance from the drop in Fig. 4. Of particular interest are the

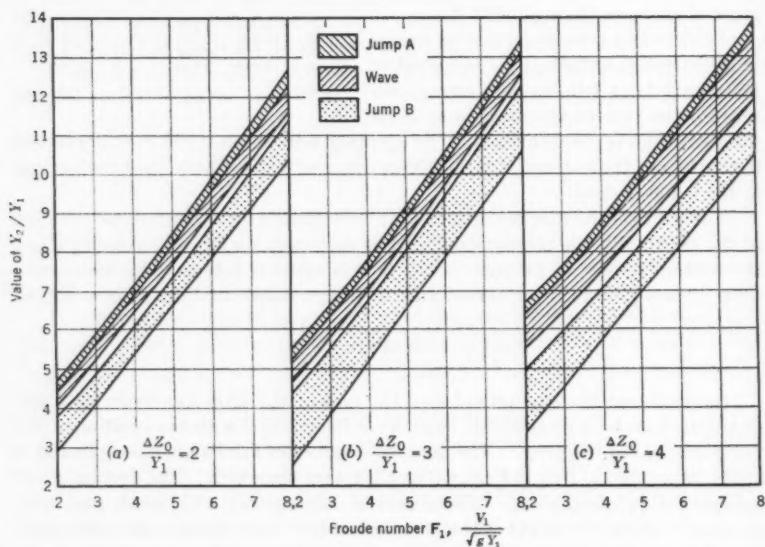


FIG. 3.—FORMS OF THE HYDRAULIC JUMP AS A FUNCTION OF FROUDE NUMBER AND RELATIVE DOWNSTREAM DEPTH

high velocities produced by jump B, which may yield ratios of V_b/V_2 of 5 or 6 at a value of L/Y_2 of approximately 2. The wave and jump A yield values of V_b/V_2 of from 2 to 3 in the upstream direction near the drop. The return flow results from the reverse roller produced by both the wave and jump A. The latter produces the lowest values of velocities along the bottom in the downstream direction. This condition would be expected because the greater pressure on the face of the drop causes the entering flow to be directed slightly upward and, therefore, the violent eddy motion occurs in the upper levels of the downstream channel.

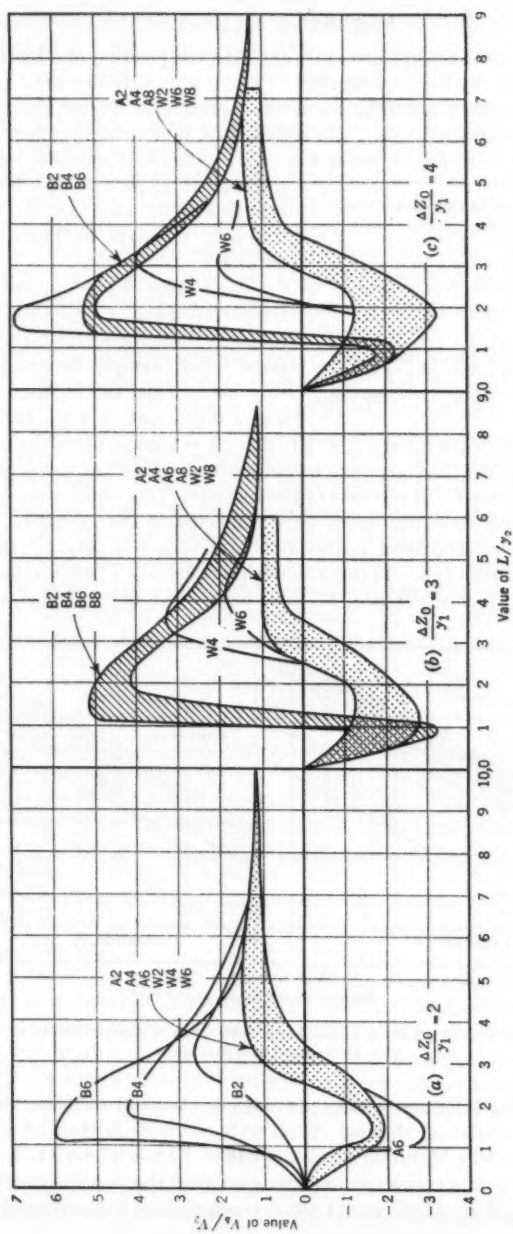


FIG. 4.—RELATIONSHIP BETWEEN VELOCITY ALONG THE CHANNEL BOTTOM AND THE DISTANCE FROM THE DROP

APPLICATION OF RESULTS

The action of an abrupt drop in stabilizing the position of a hydraulic jump has been clarified by the investigation. The results obtained are directly applicable to the design of a stilling basin incorporating an abrupt drop.

If the downstream depth, Y_2 , is required for given entering flow conditions, it can be read from Fig. 3, using the chart with the applicable relative drop height. If $Y_1 = 2$ ft, the Froude number equals 4, and $\Delta Z_0/Y_1 = 3$, from Fig. 3(b) the data in Table 2 could be obtained.

TABLE 2.—DATA OBTAINED FROM FIG. 3(b)

Type of jump	Range of Y_2/Y_1	Range of Y_2 , in feet
(1)	(2)	(3)
Jump B	5.1 to 6.8	10.2 to 13.6
Wave	7.0 to 7.6	14.0 to 15.2
Jump A	7.6 to 7.8	15.2 to 15.7

The results can be applied to analyze the performance of a stilling basin for a range of discharges and tailwater elevations. For example, assume that a spillway has a crest 100 ft long at El. 460 and a coefficient of 4.0. Let the apron be at El. 400, with a drop of 8 ft to El. 392. For a series of values for the head on the spillway, the discharge can be determined, as well as the depth, Y_1 , and the Froude number F_1 , at the base of the spillway. For convenience, the effects of resistance and air entrainment were neglected in the example. By use of Fig. 3, and by interpolating for intermediate values of $\Delta Z_0/Y_1$, the range of values of Y_2 for each type of jump can be determined. These results are shown in Fig. 5(a), in which the depths, Y_2 , have been converted into elevations. Also

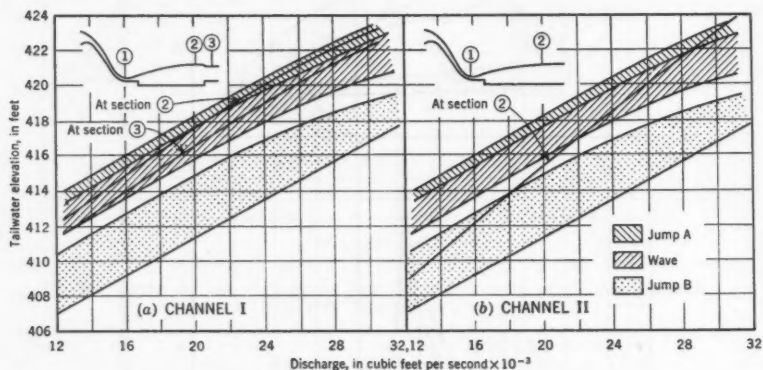


FIG. 5.—TAILWATER ELEVATIONS AND JUMP CHARACTERISTICS FOR DOWNSTREAM CHANNELS

shown in Fig. 5 are curves of the tailwater elevations at sections 2 and 3 for a rectangular downstream channel 100 ft wide, with its bottom at El. 398.5, a slope of 0.0016, and a Manning n -value of 0.03. This is referred to as channel I. In making the computations it was assumed that the depressed apron length (El. 392) was 125 ft, which would allow tranquil flow to develop at section 2.

If the depressed apron were shorter so that high-velocity flow would impinge on the step at the end of the apron, dynamic pressures would develop on the face of the step, thus adding an additional upstream force component tending to stabilize the jump. Because it is not yet possible to evaluate the effect of this force, it was eliminated from consideration by choosing a long apron.

From Fig. 5(a) it is apparent that the type A jump will occur at discharges of more than approximately 20,000 cu ft per sec, with the form changing to the wave at lower rates of discharge. There is no danger of the jump washing downstream for these conditions. From Fig. 4 it is apparent that the velocity near the bottom would be negligible while the type A jump forms—that is, $Q > 20,000$ cu ft per sec. When the wave forms at lower discharges, the velocity near the bottom at the end of the depressed apron would not exceed $3 V_2$, or approximately $3 \times 7 = 21$ ft per sec.

Fig. 5(b) indicates what would happen if the same spillway discharged into a channel 100 ft wide, with its bottom at the same elevation as the depressed apron (El. 392), and with a slope of 0.0010 and a Manning n of 0.035. This is referred to as channel II. From Fig. 5(b) it is apparent that the type A jump would form at the maximum discharge, with the form changing successively through the wave to type B as the discharge decreases. As the form of the jump changes, it would move progressively down over the drop, but even at the lowest tailwater it would remain close to the position of the drop.

The foregoing illustrates the type of analysis made possible by the results of these experiments. By making it possible to determine the jump characteristics for a wide range of Froude number and tailwater conditions, the effect of both upstream and downstream geometry on the jump characteristics can be determined.

CONCLUSIONS

1. An abrupt drop in the bottom of a rectangular channel is effective in stabilizing the hydraulic jump over a broad and continuous range of values of the relative downstream depth.
2. As the relative downstream depth is reduced from its upper limit, the jump shifts progressively downstream, resulting in a corresponding continuous decrease in the pressure on the face of the drop as the jump passes through three different forms.
3. A momentum analysis, which includes a term for the pressure force on the vertical face of the drop, yields results that are consistent with the experimental observations.
4. The maximum velocity attained near the channel bottom, which can be considered as an index of the scouring power of the flow leaving the jump, varies throughout a wide range and depends mainly on the form of the jump. For the type B jump (Fig. 1(c)) the velocity can attain a value several times greater than the downstream velocity, but for the type A jump, the maximum velocity near the bottom exceeds only slightly the average velocity in the downstream channel.

ACKNOWLEDGMENTS

The writers are grateful to the Bureau of Engineering Research of the University of Texas, Austin, for sponsoring the investigation and for aid in

preparing the manuscript and figures. Charles Schmidt made many of the experimental measurements, and Robert E. Pollak, J. M. ASCE, and John L. Phillips, J. M. ASCE, prepared the figures.

APPENDIX. HISTORICAL BACKGROUND

Edward A. Elevatorski,⁴ A. M. ASCE, has compiled a bibliography of published data concerning the hydraulic jump under various channel and flow conditions. The publication lists 504 references arranged chronologically from 1819 to 1954.

Data concerning flow problems allied closely with those presented in the paper have been published. The senior writer made an analytical and experimental study⁵ of a free overfall and determined the energy, velocity, and surface profiles for various conditions of flow. John W. Forster, M. ASCE, and Raymond A. Skrinde,⁶ A. M. ASCE, studied theoretically and experimentally the stabilizing effect of an abrupt rise at the end of a jump and developed a composite graphical summary of results by which the downstream depth could be computed after the rise. Hunter Rouse, M. ASCE, Baboobhai V. Bhoota, M. ASCE, and Hsu⁷ investigated the stabilizing characteristics of an abrupt drop in a channel bottom. It was found that two different types of flow may occur at a given drop, the transition from one to the other being characterized by an undular wave. The type of flow that will form is dependent on whether the downstream depth is above or below that which produces the undular standing wave. The conditions that produce the undular stage (critical transition zone) cannot be foretold by equations utilizing only the momentum and continuity relationships, but must be obtained by experimental measurements. Rouse, Bhoota, and Hsu presented such data, which verified their analysis, and indicated a systematic transition between the two regimes of flow, depending on the Froude number. To simplify the analysis for the two types of jumps, the pressure on the face of the drop was assumed to be distributed hydrostatically. Using this assumption, the jumps are dependent on (a) the downstream depth if the jump is upstream from the drop, and (b) on the upstream depth if the jump is downstream from the drop. Experimental data were not presented for the intermediate positions of the jump not subject to a simple analysis based on the two assumed hydrostatic-pressure distributions on the face of the drop.

⁴"The Hydraulic Jump—A Bibliography," by Edward A. Elevatorski, Albuquerque, N. Mex., 1st Ed., May, 1955.

⁵"Energy Loss at the Base of a Free Overfall," by Walter L. Moore, *Transactions, ASCE*, Vol. 108, 1943, p. 1343.

⁶"Control of the Hydraulic Jump by Sills," by John W. Forster and Raymond A. Skrinde, *ibid.*, Vol. 115, 1950, p. 973.

⁷"Design of Channel Expansions," by Hunter Rouse, B. V. Bhoota, and En-Yun Hsu, *ibid.*, Vol. 116, 1951, p. 360.

DISCUSSION

MURRAY B. MCPHERSON,⁸ A. M. ASCE.—The authors have made a valuable contribution in their presentation of pressure and velocity measurements. In addition, their studies have extended appreciably the range of performance reported previously. The objectives of this discussion are to compare and integrate their findings with other published results.^{9,10} Apparently the authors

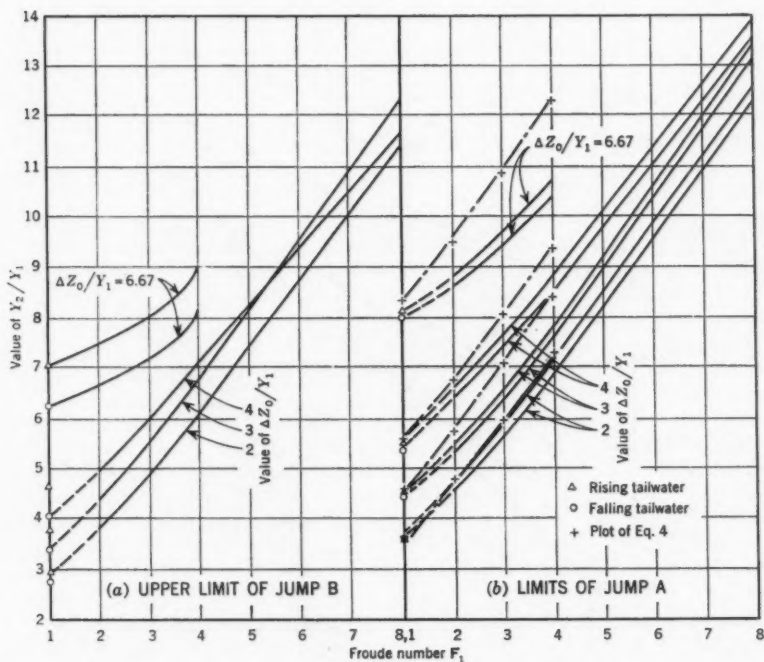


FIG. 6.—LIMITS OF THE HYDRAULIC JUMP

have overlooked the data published for a value of $\Delta Z_0/Y_1$ of 6.67 for F_1 from 1 to 4,⁹ and for a value of $F_1 = 1$ for $\Delta Z_0/Y_1$ from 2 to 6.67.¹⁰

The curves of Fig. 6(a) include the upper limit of jump B (or "plunging nappe") from Fig. 3. These curves as projected agree with the points for a

⁸ Research Engr., Philadelphia Water Dept., Philadelphia, Pa.

⁹ "Surface Profiles at a Submerged Overfall," by L. F. Ingram, R. E. Oltman, and N. J. Tracy, in "Seven Exploratory Studies in Hydraulics," by Hunter Rouse, *Proceedings Paper 1038*, ASCE, August, 1959, pp. 12-16.

¹⁰ Discussion by M. B. McPherson and R. G. Dittig of *Proceedings Paper 1038*, "Surface Profiles at a Submerged Overfall," by L. F. Ingram, R. E. Oltman, and N. J. Tracy, in "Seven Exploratory Studies in Hydraulics," by Hunter Rouse, *Proceedings Paper 1230*, ASCE, April, 1957, p. 41.

falling tailwater at $F_1 = 1$ (circled points).¹⁰ The statement by the authors under the heading, "Conclusions," "as the relative downstream depth is reduced from its upper limit, * * *" suggests that all their data may have been obtained only with a falling tailwater. However, if the lower limits of the wave regime were extended, they would practically intersect the rising tailwater points. According to the distribution of the points in Fig. 6(a), the effect of tailwater direction appears to become more pronounced as $\Delta Z_0/Y_1$ increases. The curve for $\Delta Z_0/Y_1 = 4$ does not appear consistent with the other curves for

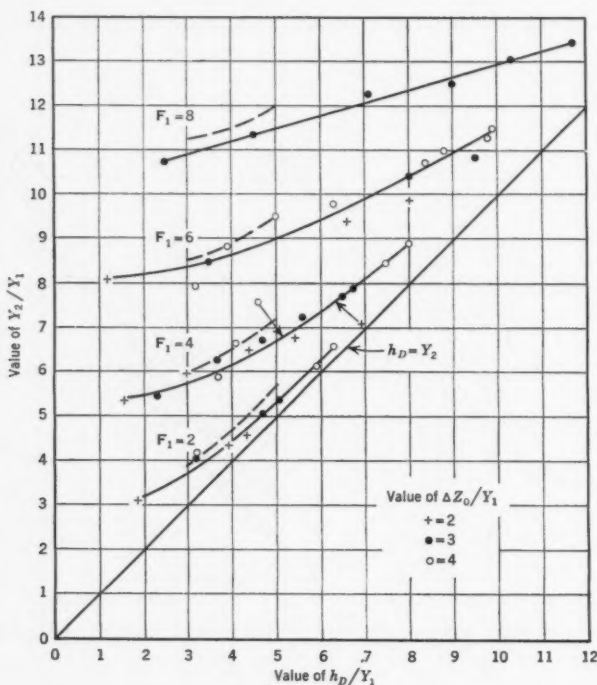


FIG. 7.—COMPARISON OF PIEZOMETRIC-HEAD MEASUREMENTS

values of 2 and 3 at the higher range of F_1 . The delineation of the upper limit of jump B is important because most of the high bottom velocities were observed for this case (Fig. 4).

The limits of jump A (a wave being termed a "riding nappe" and jump A being termed a "hydraulic jump" or a "small roller,"^{9,10}) reproduced in Fig. 6(b) are generally consistent. The reference data points for a value of $F_1 = 1$ indicate a small difference between a rising and a falling tailwater for this case. Is it possible that the pairs of curves for jump A are for these two tailwater conditions? Presumably equivalent data by Hsu^{3,7} differ from Fig. 6(b) in

that he noted a sudden drop in Y_2/Y_1 for

$\Delta Z_0/Y_1$	At F_1
1.....	4
2.....	5
3.....	6
4.....	8

from data points which closely satisfied Eq. 4 (up to the foregoing values of F_1). When the limits given by the authors and the plot of Eq. 4 in Fig. 6(b) are compared, there is evidently considerable disagreement between their data and the corresponding data given by Hsu. Beyond the values of F_1 given in the foregoing table, the lowered points satisfied Eq. 5. On the contrary, the authors' data and the data given by Rouse³ are in agreement with regard to trend.

All measurements of h_D/Y_1 plotted in Fig. 2 are shown in Fig. 7. Beyond the sudden drop in values described in the foregoing, the data by Hsu satisfied Eq. 5. It should be noted that the arbitrarily drawn curves of fit (solid lines) seem to approach $h_D = Y_2$ as a limit. Fig. 6(b) shows that Eq. 4 for $h_D = Y_2$ is most closely satisfied at $F_1 = 1$. The trend of the arbitrarily drawn F_1 -curves in Fig. 7 supports this idea. The dashed line is a plot of Eq. 5. Fig. 7 indicates a satisfactory correlation and consistency in the measurements reported by the authors.

The lower limits for jump B shown in Fig. 3 (sweepout condition) do not differ appreciably from the values of Y_2/Y_1 for a jump on a horizontal floor ($\Delta Z_0/Y_1 = 0$):

F_1	Y_2/Y_1
2.....	2.4
4.....	5.2
6.....	8.0
8.....	10.8

The erosive potential of jump B has been underscored very clearly by the authors through their presentation of measured velocities. The relationship between the curves of Figs. 4(a), 4(b), and 4(c) and the curves of Figs. 3(a), 3(b), and 3(c) in terms of Y_2/Y_1 are not stated. Only the jump type and F_1 are indicated in an abbreviated form in the foregoing figures.

JOHN W. FORSTER,¹¹ M. ASCE.—The authors have investigated systematically the effect of the hydraulic-jump position relative to an abrupt drop on the form of the jump and on the effectiveness of the stilling action. This comprises a valuable extension of the study presented by En-Yun Hsu³ and provides data useful for design purposes.

In a typical problem, the upstream depth and downstream depth for a given discharge, and, thus, F_1 and Y_2/Y_1 , are known. The size of the sill in the channel bottom required to stabilize a hydraulic jump is desired. When the downstream depth is greater than the sequent depth for a normal jump, there

¹¹ Civ. Engr., Hydroelectric Planners, Inc., Madison, Wis.

is no danger of the jump being swept downstream. Instead, it will tend to move upstream against the face of the spillway or sluice gate and be drowned. To prevent such drowning with associated high bottom velocities, a drop in the channel bottom is required. Data provided by the authors show how the form of the jump and its effectiveness in reducing bottom velocities vary with the size of drop for any given upstream and downstream flow conditions.

For example, with $F_1 = 4$ and $Y_2/Y_1 = 7$, and considering a point on the bottom corresponding to $L/Y_2 = 1.5$, Figs. 3(a) and 4(a) show that introducing a drop twice the upstream depth, Y_1 , will yield a type A jump with a downstream bottom velocity, $V_b = -1.5 V_2$, which is effective stilling. If the drop is increased to $3 Y_1$, Figs. 3(b) and 4(b) show that a wave type of jump will form, with $V_b = -2 V_2$, which is still effective stilling. If the drop is increased further to $4 Y_1$, Figs. 3(c) and 4(c) show that a type B jump will form, with V_b increased to $5 V_2$, which is comparatively ineffective stilling. An interesting question in the latter case is whether stilling would be as effective if no drop at all in the channel were introduced and if the jump were drowned.

An approximate answer to the question was given by Harold R. Henry,¹² J. M. ASCE. Henry investigated conditions within a drowned jump for a Froude number of 2.0 at the gate outlet (Fig. 33).¹² Assuming a coefficient of contraction of 0.8 for the rounded gate lip, this case would correspond to $F_1 = 2.8$ and $Y_2/Y_1 = 5$. The velocity-distribution measurements made by Henry indicate that at a distance below the vena contracta of $L = 1.5 Y_2$ the bottom velocity, $V_b = 6 V_2$.

As an alternative to this drowned jump, Fig. 3(a) shows that for the same upstream conditions ($F_1 = 2.8$ and $Y_2/Y_1 = 5$), by introducing a drop, $\Delta Z_o = 2 Y_1$, a wave type of jump can be produced. At $L = 1.5 Y_2$, Fig. 4(a) shows that $V_b = 1.7 V_2$. This is better stilling than in the case of the drowned jump.

If the depth of drop were increased to $\Delta Z_o = 3 Y_1$, Fig. 3(b) indicates that a type B jump would form, with the toe downstream of the drop. Fig. 4(b) shows that the downstream bottom velocity would reach a value of $V_b = 5 V_2$. The latter value is almost as great as the $(6 V_2)$ -value indicated by Henry's data for the case of a drowned jump with no drop.

Wherever the downstream depth is less than the sequent depth for a normal jump, a rise, rather than a drop, in the channel bottom is required to prevent the jump from being washed downstream. Whereas an overdimensioned rise will result in a drowned jump with any high-velocity bottom currents directed upward and away from the bottom by the sill, an overdimensioned drop will cause the jump to recede downstream with resulting high bottom velocities. Accordingly, to assure downstream protection it is safer for the designer to keep the size of a rise somewhat greater and the size of a drop less than the optimum dimension determined from the design charts.

In the case of the abrupt rise the force on the face of the sill and the effectiveness of the stilling vary with the position of the jump relative to the rise. This case was investigated by Forster and Skrinde⁶ for one relative position of

¹² Discussion by Harold R. Henry of "Diffusion of Submerged Jets," by M. L. Albertson, Y. B. Dai, R. A. Jensen, and Hunter Rouse, *Transactions, ASCE*, Vol. 115, 1950, p. 639.

the jump. Their investigation could be extended to include a range of relative jump positions in the same way as the authors have done in the case of the abrupt drop.

Because the authors were concerned only with the condition of jump formation, they did not investigate values of Y_2/Y_1 less than 1. This range, corresponding to supercritical flow shooting over an abrupt drop and continuing downstream, would comprise an extension, not only of the authors' study, but also of Moore's⁵ previous investigation of the free overfall. A theoretical plot based on an analysis¹³ by Merit P. White, M. ASCE, has been presented.¹⁴ An experimental investigation now appears to be a logical future step toward the completion of the over-all picture of flow over sills.

WALTER L. MOORE¹⁵ AND CARL W. MORGAN,¹⁶ ASSOCIATE MEMBERS, ASCE.—Mr. McPherson inquired about the influence of the direction of movement of the tailwater level on the limiting depths for various types of jumps. A brief investigation of the effect of rising and falling tailwater indicated a negligible effect of this variable, provided that sufficient time was allowed for equilibrium to be established. As a result of the comments by Mr. McPherson and the data he presented, additional experiments on this effect were made by the writers. These experiments indicated that if sufficient time is allowed, the effect of the direction of tailwater movement was of the same magnitude as the experimental error in determining the tailwater depth for Froude numbers of less than 6. In fact, for $\Delta Z_0/Y_1 = 3$ and $F_1 = 4$, and for $\Delta Z_0/Y_1 = 4$ and $F_1 = 6$, it was possible to set the tailwater so that the jump would alternate slowly between the jump B type and the wave type. In order to change from the jump B type to the wave type, or vice versa, in a moderate time it was necessary to set a higher value with rising tailwater than with falling tailwater, a result similar to those observed by others.^{9,10} However, those results were for a different range of F_1 and relative drop height, $\Delta Z_0/Y_1$, than used in the writers' experiments. The equilibrium condition that the writers obtained for $F_1 < 6$ could not be obtained at $F_1 = 8$. For $\Delta Z_0/Y_1 = 4.0$ and a rising tailwater, the change from the jump B type to the wave type required a value of $Y_2/Y_1 = 12.3$, whereas for a falling tailwater the change occurred at $Y_2/Y_1 = 11.4$. This may have been due to the fact that at this Froude number the top of the wave rose higher than the walls of the flume. On the other hand, it may be that at this high Froude number the flow pattern is such that the "hysteresis effect" mentioned by Mr. McPherson is present.

In the additional experiments by the writers previously mentioned, tailwater depths were ascertained by piezometers rather than with a point gage, as in the original experiments. The experiments with $\Delta Z_0/Y_1 = 3$ were made at a scale twice that used originally. These new tests indicated that the values shown in Fig. 3(b) for the maximum jump B are slightly high. Fig. 8 is presented to

¹³ Discussion by Merit P. White of "Energy Loss at the Base of a Free Overfall," by Walter L. Moore, *Transactions, ASCE*, Vol. 108, 1943, p. 1361.

¹⁴ "Control of the Hydraulic Jump by Sills," by John W. Forster and Raymond A. Skrinde, *ibid.*, Vol. 115, 1950, p. 1019, Fig. 23, Region VI(b).

¹⁵ Prof., Dept. of Civ. Eng., Univ. of Texas, Austin, Tex.

¹⁶ Asst. Prof., Dept. of Civ. Eng., Univ. of Texas, Austin, Tex.

define more clearly the several values required to insure that a jump B or a wave will form.

Mr. McPherson calls attention to the disagreement with data presented by Hsu,^{7,17} in which a systematic transition between the types of jumps (A, B, and wave) was found as a function of the Froude number, F_1 . The investigation reported by the writers was initiated to explore longitudinal characteristics of the jump at a drop, assuming the existence of the systematic transition reported by Hsu.^{7,19} It was soon found that type B jumps could be obtained at low

TABLE 3.—JUMP FORMS

Type of Jump	F_1	Fig. 4(a)	Fig. 4(b)	Fig. 4(c)
		(3)	(4)	(5)
		$\Delta Z_0/Y_1$		
		2	3	4
(1)	(2)	Y_2/Y_1		
B	2	3.1	4.1	4.2
W	2	4.3	5.1	6.3
A	2	4.6	5.4	6.5
B	4	5.4	6.3	5.9
W	4	6.8	7.2	8.5
A	4	7.1	7.8	8.9
B	6	8.1	8.4	8.8
W	6	9.4	10.4	10.7
A	6	9.9	10.6	11.4
B	8	...	11.4	10.5
W	8	...	12.4	11.8
A	8	...	13.5	...

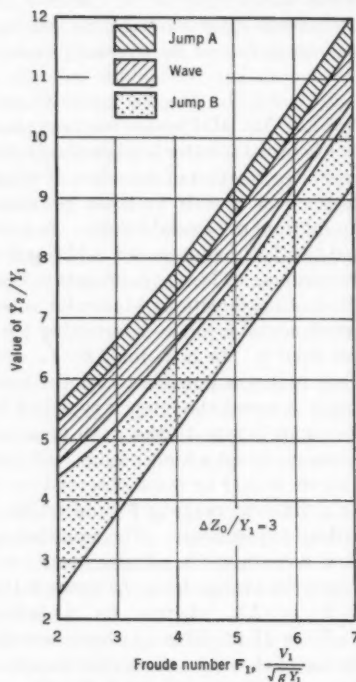


FIG. 8.—FORMS OF THE HYDRAULIC JUMP

values of F_1 when Hsu's curves indicated only jump A would form. Further investigation showed that the full range of jump types was possible at any value of F_1 (at least more than 2.0) controlled only by the tailwater elevation. The systematic transition as a function of the Froude number was not observed by the writers.

From considerations similar to those leading to Fig. 5(b), it is apparent that a tailwater control, which produced a relatively flat curve of tailwater elevation versus discharge, as opposed to the steep one shown in Fig. 5(b), would result

¹⁷ Discussion by En-Yun Hsu of "Control of the Hydraulic Jump by Sills," by John W. Forster and Raymond A. Skrinde, *Transactions, ASCE*, Vol. 115, 1950, p. 991, Fig. 10.

in a systematic transition from jump B through the wave to jump A as the discharge was decreased. With the depth Y_1 held constant, a reduction in discharge would correspond to a reduction in F_1 . This could explain a systematic change of jump type with a decreasing value of F_1 as reported by Hsu. However, it is not clear how the slope of the curve of tailwater depth Y_2/Y_1 versus the Froude number, F_1 , could be positive for the type A jump and type B jump and negative for the wave type of jump.

Fig. 6(b) emphasizes that the band shown for jump A in Figs. 3(a), 3(b), and 3(c) does not represent the maximum values of the tailwater. It is stated under the heading, "Results," that "the conditions under which jump A will form are indicated as a very narrow band. Actually jump A may form at values of Y_2/Y_1 greater than the upper bound* * *."

In response to Mr. McPherson's suggestion, values of Y_2/Y_1 are listed in Table 3 for the various forms of the jump for which relative bottom velocities are shown in Figs. 4(a), 4(b), and 4(c).

Mr. Forster emphasizes effectively the importance of the type of jump in determining the severity of attack on the channel bottom just downstream from the drop. His examples illustrate the effectiveness of jump A and the wave in protecting the bottom from high-velocity currents. However, the wave type can result in some fairly high bottom velocities for large drops, in which $\Delta Z_0/Y_1 = 3$ and $\Delta Z_0/Y_1 = 4$ (Figs. 4(b) and 4(c)). In Figs. 4(a), 4(b), and 4(c) the regions and curves are identified by a letter and a number, as shown in Table 3. It can be seen that with the wave type and a Froude number of 4 a downstream velocity of $3 V_2$ may be attained for $\Delta Z_0/Y_1 = 3.0$ and $4 V_2$ for $\Delta Z_0/Y_1 = 4.0$. It may appear unusual that a Froude number of 4 resulted in higher relative bottom velocities than Froude numbers of 2, 6, and 8. However, this does not seem unreasonable if the complex flow pattern below the drop is considered. With a large value of $\Delta Z_0/Y_1$ and a small Froude number, the momentum of the jet is not sufficient to penetrate to the bottom. At an intermediate Froude number the jet falling down from the wave still has sufficient momentum to penetrate to the bottom. At higher Froude numbers the rise in tailwater depth is sufficient to lift the jet off the bottom, thus preventing high velocities from developing on the bottom.

Mr. Forster demonstrates that an overdimensioned drop may be unconservative because jump B may be produced with associated high bottom velocities. This is correct when it is assumed that Y_2/Y_1 is constant. The latter is equivalent to assuming that the size of the drop is controlled by the elevation of the upstream channel, whereas the downstream-channel elevation and tailwater depth remain fixed. If the size of the drop were controlled by lowering the bottom elevation of the downstream channel for a suitable distance (while the tailwater elevation remains constant as controlled by conditions further downstream), an oversize drop will then be conservative. Using the same initial conditions as in Mr. Forster's example ($F_1 = 2.8$ and $Y_2/Y_1 = 5$) with a drop of $\Delta Z_0 = 2 Y_1$, Fig. 3(a) will yield a minimum wave type of jump, bordering on jump B. If by lowering a suitable length of the downstream-channel bottom the drop is increased to $\Delta Z_0 = 3 Y_1$, the values become $F_1 = 2.8$ and $Y_2/Y_1 = 6$. Fig. 8 yields a maximum wave type of jump bordering on

jump A. In this manner the low bottom velocities would be preserved even with an oversized drop.

Although Figs. 4(a), 4(b) and 4(c) produce valuable data indicating the range of velocities to be expected near the channel bottom, they are not intended to be used for precise estimates of velocities in particular instances. Due to the complex nature of the flow pattern there is necessarily considerable scatter in the data. In addition, the scour potential of the flow is certainly dependent on the turbulence characteristics of the flow as well as the mean velocity. Thus, the velocities should be considered merely as an index of the scour potential for making comparisons between the various types of jumps.

Mr. Forster indicates that jump B produces a bottom velocity of the same order of magnitude as a drowned jump on a flat apron. The peak values of the bottom velocities in Figs. 4(a), 4(b), and 4(c) are on the order of $6 V_2$, which is the same as that given by Henry¹⁸ for a moderately drowned jump. These relative high velocities are not necessarily harmful if a paved apron is provided downstream from the drop for a sufficient distance to protect the channel bottom. For a situation in which a rising discharge and a consequent rise in tailwater would cause increasing submergence of the jump as its size increases, the introduction of an abrupt drop would be beneficial by preventing severe drowning. Instead of drowning, the jump would shift toward the wave and jump A, with consequent reduction of attack on the channel bottom.

¹⁸ Discussion by Harold R. Henry of "Diffusion of Submerged Jets," by M. L. Albertson, Y. B. Dai, R. A. Jensen, and Hunter Rouse, *Transactions, ASCE*, Vol. 115, 1950, p. 690, Fig. 33.

AMERICAN SOCIETY OF CIVIL ENGINEERS

Founded November 5, 1852

TRANSACTIONS

Paper No. 2992

LITTORAL-DRIFT PROBLEM AT SHORE-LINE HARBORS

BY JOE W. JOHNSON,¹ M. ASCE

WITH DISCUSSION BY MESSRS. RICHARD SILVESTER;
AND JOE W. JOHNSON

SYNOPSIS

A harbor that fronts directly on an open shore line and has a relatively small flow into and out of it is defined as a shore-line harbor. Wherever there is a littoral drift along the shore line, certain design, construction, and maintenance problems are manifested. Some of these basic considerations are summarized, and a few case histories are cited.

INTRODUCTION

Harbors in which sedimentation is a serious maintenance problem have been classified by Joseph M. Caldwell,² M. ASCE, as (a) river-channel harbors, (b) off-river harbors, (c) fall-line harbors, (d) channel harbors in tidal estuaries, and (e) shore-line harbors. Sediment that is transported to a harbor entrance by littoral currents is a problem only in case (e) and possibly in case (d). In the latter instance, shoaling by littoral drift can occur at the entrance of the estuary, although the harbor proper might be at a remote site up the estuary and subject, therefore, only to sedimentation damage by material other than littoral drift. In the case of shore-line harbors the shoaling effects are generally in the immediate vicinity of the development. Only the shoaling conditions at harbors where man-made structures have been erected will be examined herein. The sedimentation problems at tidal inlets and the stabilization of such inlets for navigation have been examined by Earl I. Brown,³ Martin A. Mason,⁴ and Richard O. Eaton,⁵ Members, ASCE, (littoral processes

NOTE.—Published, essentially as printed here, in April, 1957, in the *Journal of the Waterways and Harbors Division*, as *Proceedings Paper 1211*. Positions and titles given are those in effect when the paper or discussion was approved for publication in *Transactions*.

¹ Prof. of Hydr. Eng., Univ. of California, Berkeley, Calif.

² "Sedimentation in Harbors," by Joseph M. Caldwell, in "Applied Sedimentation," John Wiley & Sons, Inc., New York, N. Y., 1950, pp. 291-299.

on sandy coasts); Morrough P. O'Brien,⁶ M. ASCE, and Thomas M. Robbins⁷ (the relationship between tidal entrance and entrance area); Robert E. Hickson, M. ASCE, and F. W. Rodolf⁸ (the design and construction of jetties); and Berkeley Blackman⁹ (the dredging of inlets on sandy coasts).

A shore-line harbor is defined as one fronting directly on the open shore of an ocean, a bay, or a large lake, and having a relatively small tidal flow or fresh-water flow from the tributary watershed. These harbors are protected generally from wave action by some natural feature or man-made structures. Sedimentation results primarily from the alongshore transport of sand due to wave action and littoral currents.

LITTORAL PROCESSES

Wave action is the primary source of energy available at a shore line for moving sediment. The result of waves breaking at an angle to the shore line is to generate an alongshore, or littoral, current. It is this current, combined with the agitating action of the breaking waves, that is the important factor in causing a movement of sand along a coast line. Perhaps the first comprehensive study of these processes and of shore-line development was made by Grove K. Gilbert.¹⁰ Douglas W. Johnson¹¹ later formulated the concepts and nomenclature that are generally accepted. The most comprehensive present-day viewpoints on the character and solution of shore-line problems confronting the engineer have been presented by Mason⁴ and Eaton.⁵ Some of the general principles of littoral processes are summarized herein.

From the geological point of view a particular segment of a coast can advance, retreat, or be in a state of approximate equilibrium. The status of such a shore segment depends on the material balance—that is, the rate at which the littoral material is delivered to the area as compared with the rate at which it is removed. Ordinarily, the changes resulting from natural geological processes are so slow that they are of minor importance to the engineer. More important is the effect of a man-made littoral barrier in altering the material balance by accelerating or retarding the littoral sediment transport. The functional planning of coastal works to provide an adequate solution of shore-control problems is contingent, therefore, on an accurate knowledge of the following factors:

1. The source and characteristics of the beach material for the "shore segment" or "physiographic unit" under study, which is understood to be so

³ "Inlets on Sandy Coasts," by E. I. Brown, *Proceedings, ASCE*, Vol. 54, 1928, pp. 505-553.

⁴ "Geology in Shore-Control Problems," by Martin A. Mason, in "Applied Sedimentation," John Wiley & Sons, Inc., New York, N. Y., 1950, pp. 276-290.

⁵ "Littoral Processes on Sandy Coasts," by Richard O. Eaton, *Proceedings, 1st Conference on Coastal Eng.*, Berkeley, Calif., 1951, pp. 140-154.

⁶ "Estuary Tidal Prisms, Related to Entrance Areas," by M. P. O'Brien, *Civil Engineering*, Vol. 1, No. 8, 1931, pp. 738-739.

⁷ "Maintenance and Improvement of Entrance Channels to the Pacific Coast Ports," by T. M. Robbins, *World Ports*, Vol. 21, No. 3, 1933, pp. 18-20.

⁸ "Design and Construction of Jetties," by R. E. Hickson and F. W. Rodolf, *Proceedings, 1st Conference on Coastal Eng.*, Berkeley, Calif., 1951, pp. 227-245.

⁹ "Dredging at Inlets on Sandy Coasts," by Berkeley Blackman, *ibid.*, pp. 169-174.

¹⁰ "Lake Bonneville," by G. K. Gilbert, *Monographs of the United States Geological Survey*, U. S. Dept. of the Interior, Washington, D. C., Vol. 1, 1890.

¹¹ "Shore Processes and Shoreline Development," by D. W. Johnson, John Wiley & Sons, Inc., New York, N. Y., 1919.

limited that the shore-line phenomena within the area are not affected by the physical conditions in adjacent areas;

2. The manner and direction of movement of material from the source to the shore segment under study, and from this segment to other areas; and

3. The rates of supply and loss of material to and from the problem segment.

The techniques and mechanical details of determining the first two factors are described elsewhere.¹² With respect to item 1, the definition of the limits of the shore segment and the determination of the source and characteristics



FIG. 1.—CHANGE IN ORIENTATION OF CALIFORNIA COAST LINE AT POINT CONCEPTION

of the littoral material can be supplied by studying the mechanical and mineral characteristics of the littoral materials and the general geological features of the area. In most instances it is necessary for a geologist trained in shore-line processes to determine the limits of the shore segment.

For example, Point Conception on the California coast was considered for many years to be a complete natural littoral barrier against southward drifting sand because of the rocky headland and the abrupt change in orientation of the shore line on the downdrift side of the point (Fig. 1). Extensive studies, in

¹² "Shore Protection Planning and Design," Technical Report No. 4, Beach Erosion Board, Corps of Engrs., U. S. Dept. of the Army, Washington, D. C., 1954.

TABLE 1.—SUMMARY OF MEASURED RATES OF LITTORAL DRIFT

Location (1)	Predominant direction of drift (2)	Rate of drift, in cubic yards per year (3)	Method of measurement of rate of drift (4)	Years of record (5)
ATLANTIC COAST				
Suffolk County, N. Y. ^a	West	200,000	Accretion	...
Sandy Hook, N. J. ^a	North	493,000	Accretion	1885-1933
Sandy Hook, N. J. ^a	North	436,000	Accretion	1933-1951
Asbury Park, N. J. ^a	North	200,000	Accretion	1822-1925
Shark River, N. J. ^a	North	300,000	Accretion	1947-1953
Manasquan, N. J. ^a	North	360,000	Accretion	1930-1931
Barneget Inlet, N. J. ^a	South	250,000	Accretion	1939-1941
Absecon Inlet, N. J. ^a	South	400,000	Erosion	1935-1946
Ocean City, N. J. ^a	South	400,000	Erosion	1935-1946
Cold Spring Inlet, N. J. ^a	South	200,000	Accretion	...
Ocean City, Md. ^a	South	150,000	Accretion	1934-1936
Atlantic Beach, N. C. ^a	East	29,500	Accretion	1850-1908
Hillsboro Inlet, Fla. ^a	South	75,000	Accretion	...
Palm Beach, Fla. ^a	South	150,000 to 225,000	Accretion	1925-1939
GULF OF MEXICO				
Pinellas County, Fla. ^f	South	50,000	Accretion	1922-1950
Perdido Pass, Ala. ^a	West	200,000	Accretion	1934-1953
Galveston, Tex. ^a	East	437,500	Accretion	1919-1934
PACIFIC COAST				
Santa Barbara, Calif. ^{h, i}	East	280,000	Accretion	1932-1951
Ornard Plainshore, Calif. ^j	South	1,000,000	Accretion	1938-1948
Port Hueneme, Calif. ^k	South	500,000	Accretion	1938-1948
Santa Monica, Calif. ^a	South	270,000	Accretion	1936-1940
El Segundo, Calif. ^a	South	162,000	Accretion	1936-1940
Redondo Beach, Calif. ^a	South	30,000	Accretion	...
Anaheim Bay, Calif. ^{a, l}	East	150,000	Erosion	1937-1948
Camp Pendleton, Calif. ^a	South	100,000	Accretion	1950-1952

^a From unpublished reports of the Corps of Engrs., U. S. Dept. of the Army.

^b "Ocean City, New Jersey," *House Document No. 184*, 83rd Cong., 1st Session, Beach Erosion Control Study, Corps of Engrs., U. S. Dept. of the Army, Washington, D. C., 1953, p. 23.

^c "Cold Spring Inlet (Cape May Harbor), N. J.," *House Document No. 206*, 83rd Cong., 1st Session, Beach Erosion Control Study, Corps of Engrs., U. S. Dept. of the Army, Washington, D. C., 1953, p. 30.

^d "North Carolina Shore Line," *House Document No. 763*, 80th Cong., 2d Session, Beach Erosion Control Study, Corps of Engrs., U. S. Dept. of the Army, Washington, D. C., 1948, p. 20.

^e "Sand By-Passing at Hillsboro Inlet, Florida," *The Bulletin*, Beach Erosion Board, Corps of Engrs., U. S. Dept. of the Army, Washington, D. C., Vol. 9, No. 2, 1955, pp. 1-6.

^f "Pinellas County, Florida," *House Document No. 380*, 83rd Cong., 2d Session, Beach Erosion Control Study, Corps of Engrs., U. S. Dept. of the Army, Washington, D. C., 1954, p. 27.

^g "Gulf Shore of Galveston Island, Texas," *House Document No. 218*, 83rd Cong., 1st Session, Beach Erosion Control Study, Corps of Engrs., U. S. Dept. of the Army, Washington, D. C., 1953, p. 19.

^h "Wave Action and Sand Movement near Anaheim Bay, California," by Joseph M. Caldwell, *Technical Memorandum No. 68*, Beach Erosion Board, Corps of Engrs., U. S. Dept. of the Army, Washington, D. C., February, 1956.

ⁱ "Sand By-Passing Plant at Salina Cruz, Mexico," by M. C. Rolland, *Proceedings*, 2d Conference on Coastal Eng., Berkeley, Calif., 1952, pp. 177-186.

^j "Appendix I, Coast of California Carpinteria to Point Mugu," *House Document No. 29*, 83rd Cong., 1st Session, Beach Erosion Control Study, Corps of Engrs., U. S. Dept. of the Army, Washington, D. C., 1953, p. 25.

^k "Port Hueneme, California," *House Document No. 362*, 83rd Cong., 2d Session, Beach Erosion Control Study, Corps of Engrs., U. S. Dept. of the Army, Washington, D. C., 1954, p. 25.

^l "Anaheim Bay Harbor, California," *House Document No. 349*, 83rd Cong., 2d Session, Beach Erosion Control Study, Corps of Engrs., U. S. Dept. of the Army, Washington, D. C., 1954, p. 37.

TABLE 1.—(Continued)

Location (1)	Predominant direction of drift (2)	Rate of drift, in cubic yards per year (3)	Method of measurement of rate of drift (4)	Years of record (5)
GREAT LAKES REGION				
Milwaukee County, Wis. ^m	South	8,000	Accretion	1894-1912
Racine County, Wis. ⁿ	South	40,000	Accretion	1912-1949
Kenosha, Wis. ^o	South	15,000	Accretion	1872-1909
Illinois state line to Waukegan, Ill. ^p	South	90,000	Accretion	...
Waukegan to Evanston, Ill. ^q	South	57,000	Accretion	...
South of Evanston, Ill. ^r	South	40,000	Accretion	...
OUTSIDE THE UNITED STATES				
Waikiki Beach, T. H. ^s	...	10,000	Suspended-load samples	...
Monrovia, Liberia ^t	North	550,000	Accretion	1946-1954
Port Said, Egypt ^u	East	910,000	Dredging	...
Port Elizabeth, South Africa ^v	North	600,000	Accretion	...
Durban, South Africa ^w	North	383,000	Dredging	1897-1904
Madras, India ^x	North	740,000	Accretion	1886-1919
Ponta de Mucuripe, Brazil ^y	North	427,000	Accretion	1946-1950

^m "Lake Michigan Shore Line of Milwaukee County, Wisconsin," *House Document No. 526*, 79th Cong., 2d Session, Beach Erosion Control Study, Corps of Engrs., U. S. Dept. of the Army, Washington, D. C., 1946, p. 16.

ⁿ "Racine County, Wis.," *House Document No. 28*, 83rd Cong., 1st Session, Beach Erosion Control Study, Corps of Engrs., U. S. Dept. of the Army, Washington, D. C., 1953, p. 10.

^o "Illinois Shore of Lake Michigan," *House Document No. 28*, 83rd Cong., 1st Session, Beach Erosion Control Study, Corps of Engrs., U. S. Dept. of the Army, Washington, D. C., 1953, p. 39.

^p "Waikiki Beach, Island of Oahu, T. H.," *House Document No. 227*, 83rd Cong., 1st Session, Beach Erosion Control Study, Corps of Engrs., U. S. Dept. of the Army, Washington, D. C., 1953, p. 23.

^q "Study of Monrovia Harbor, Liberia, and Adjoining Shore Line," Beach Erosion Board, Corps of Engrs., U. S. Dept. of the Army, Washington, D. C., 1955.

^r "A Short History of the Engineering Works of the Suez Canal," discussion by Sir John Wolfe Barry, *Minutes of Proceedings*, Inst. C. E., London, Vol. 141, 1899-1900, p. 197.

^s "The Harbours of South Africa," discussion by William Matthews, *ibid.*, Vol. 166, 1905-1906, p. 47.

^t "The Harbours of South Africa; With Special Reference to Causes and Treatment of Sand Bars," by C. W. Methven, *ibid.*, p. 40.

^u "Transport Littoral Formation de Fleches et de Tombolos," by Gaston Sauvage de Saint Marc and G. E. Vincent, *Proceedings*, 5th Conference on Coastal Eng., Berkeley, Calif., 1955, pp. 296-328.

^v "Harbours and Estuaries on Sandy Coasts," by L. F. Vernon-Harcourt, *Minutes of Proceedings*, Inst. C. E., London, Vol. 70, 1881-1882, pp. 1-32.

which the heavy minerals in the sands of the adjacent beaches and streams were used as "tracers," established that sand was moving around this promontory.¹³ Therefore, this finding fixed the northern limit of the shore segment downcoast from Point Conception at a more northerly site than had been considered previously to be possible.

The exact mechanism of the movement around rocky headlands has not been established completely, but it is probably a combination of (a) sand movement by the turbulent action of waves breaking at the base of the precipitous cliffs, and (b) the movement of sand by wave action in depths of as much as 80 ft.¹⁴ Underwater photographs of sand ripples on the ocean bottom at

¹³ "Source of Beach Sand at Santa Barbara, California, as Indicated by Mineral Grain Studies," by Parker D. Trask, *Technical Memorandum No. 28*, Beach Erosion Board, Corps of Engrs., U. S. Dept. of the Army, Washington, D. C., October, 1952.

¹⁴ "Mechanics of Bottom Sediment Movement Due to Wave Action," by M. Manohar, *Technical Memorandum No. 75*, Beach Erosion Board, Corps of Engrs., U. S. Dept. of the Army, Washington, D. C., 1955.

depths of from 60 ft to 80 ft indicate that appreciable sand movement caused by wave action definitely occurs at relatively great depths. The material moved in such depths is probably negligible compared with that moved in the vicinity of the shore, where the breaking of the waves creates a highly turbulent flow condition capable of placing large volumes of sediment into suspension. Both field and model measurements^{15,16} show that a large percentage of sediment occurs in suspension near the plunge point of a breaker as compared with the region on either side of this point.

As stated previously, the predominant direction of littoral drift is a necessary part of the factual data required in any shore-line study. This direction of drift often can be determined from an examination of all available information by noting:

- a. Accretion and erosion on either side of the jetties, groins, and other structures;
- b. Shore patterns in the vicinity of the headlands;
- c. The direction of trailing sand spits and trailing underwater bars;
- d. The migration of unimproved inlets;
- e. The movement of channels across outer bars;
- f. Characteristics of beach and bed materials; and
- g. Current measurements.

The classic work in using such evidence to establish the predominant direction of drift was that of F. P. Gulliver.¹⁷ Johnson¹¹ also examined these techniques, and the Beach Erosion Board,¹² Corps of Engineers (United States Department of the Army), presented the details of applying the procedures to engineering investigations.

The other factor for which information must be available for the proper solution of shore-line problems on sandy coasts is the rate of littoral transport. Unfortunately, no general relationship is available for computing this factor from easily determined variables, although Caldwell¹⁸ has attempted to do so. Observations have shown that the rate of transport is a function of the sediment characteristics and of the height, period, and direction of the waves. Using model studies under controlled conditions, it has been shown that for a given sand size and energy content of the waves the maximum rate of littoral transport occurs when the wave crests in deep water are at an angle of approximately 30° with the shore line, and the waves have a steepness¹⁹ (defined as the ratio of wave height to wave length) of about 0.025. Because of the lack of a general formula relating the rate of transport to the sediment and wave characteristics, present practice in shore-line problems must rely on rates of transport determined from measurements of the gradual accretion or scour

¹⁵ "Surface Water Wave Theories," by M. A. Mason, *Transactions, ASCE*, Vol. 118, 1953, p. 569.

¹⁶ "Model Study of Sand Transport Along an Infinitely Long, Straight Beach," by Thorndike Saville, Jr., *Transactions, Am. Geophysical Union*, Vol. 31, 1950, pp. 555-565.

¹⁷ "Shoreline Topography," by F. P. Gulliver, *Proceedings, Am. Academy of Arts and Sciences*, Vol. 34, 1899, pp. 151-258.

¹⁸ "Wave Action and Sand Movement near Anaheim Bay, California," by Joseph M. Caldwell, *Technical Memorandum No. 68*, Beach Erosion Board, Corps of Engrs., U. S. Dept. of the Army, Washington, D. C., February, 1956.

¹⁹ "Sand Transport by Littoral Currents," by J. W. Johnson, *Bulletin 34, Proceedings, 5th Hydraulics Conference*, Univ. of Iowa Studies in Eng., Iowa City, 1953, pp. 89-109.

at man-made littoral barriers. Table 1 summarizes all the known measured rates of drift. It also indicates the method of determining the rate (whether by accretion, scour, or dredging records) and the years of record for which the computations were made. The longer the record, the more reliable the average littoral-transport rate. For convenience the data in Table 1 are grouped by geographical areas: The Atlantic coast, the Pacific coast, the Gulf coast, and the Great Lakes region of the United States, and the few localities outside the United States for which there is available information.

The range of transport rates in Table 1 is considerable. The primary causes for this variation are the wide ranges in values of the wave characteristics and the shore-line orientation with respect to the prevailing wave direction occurring at the various sites. That is, the wave energy and the angle between the wave direction and the shore line vary greatly along the coast lines of the world. Unfortunately, no wave data were obtained simultaneously with the littoral-drift measurements at the various localities to permit the formulation of even an approximate relationship between the rate of littoral transport and the wave and sediment characteristics. Observations on measured drift rates, as given in Table 1, are the only reliable data available to those engaged in designing, constructing, and maintaining coastal works where the littoral movement of sediment is a problem. Table 1 also shows the predominant drift directions, but important reversals in drift do occur at many of the localities.

LITTORAL DRIFT AT SHORE-LINE HARBORS

There are three basic types of man-made works at shore-line harbors that function as littoral barriers: (a) A dredged channel, (b) a jetty or groin, and (c) an offshore or detached breakwater. The littoral processes in the vicinity of such coastal works are summarized briefly⁵ as follows:

Dredged Channels.—Harbors are often connected with deep water offshore by a dredged channel through the littoral zone (Fig. 2(a)). Such a channel creates greater-than-normal depths, with the result that littoral material accumulates in the channel. Sediment that is insignificant enough to be moved in the greater depths seaward from the end of the dredged channel would, of course, be unaffected. Both model and prototype measurements indicate that most alongshore transport of material occurs in the vicinity of the breakers, where the available wave energy is converted suddenly from an oscillatory motion into the form of turbulence. For that part of the wave crest that moves over a dredged channel, however, breaking does not occur because of the increased depth, and the wave energy passes the former breaking point to be spread by refraction and then dissipated farther inshore. The degree of turbulence is insufficient, therefore, to transport material across the channel, and the material accumulates. To maintain the channel in a navigable condition, this accumulation of littoral material must be dredged periodically. If it is removed and redeposited on the downcoast side of the channel, normal littoral transport will occur in that region, and the downcoast shore line will remain in equilibrium. However, if the channel deposits are placed elsewhere, the supply of material to the downcoast beach is reduced, and erosion and retreat of the shore line probably will result. In a harbor such as that

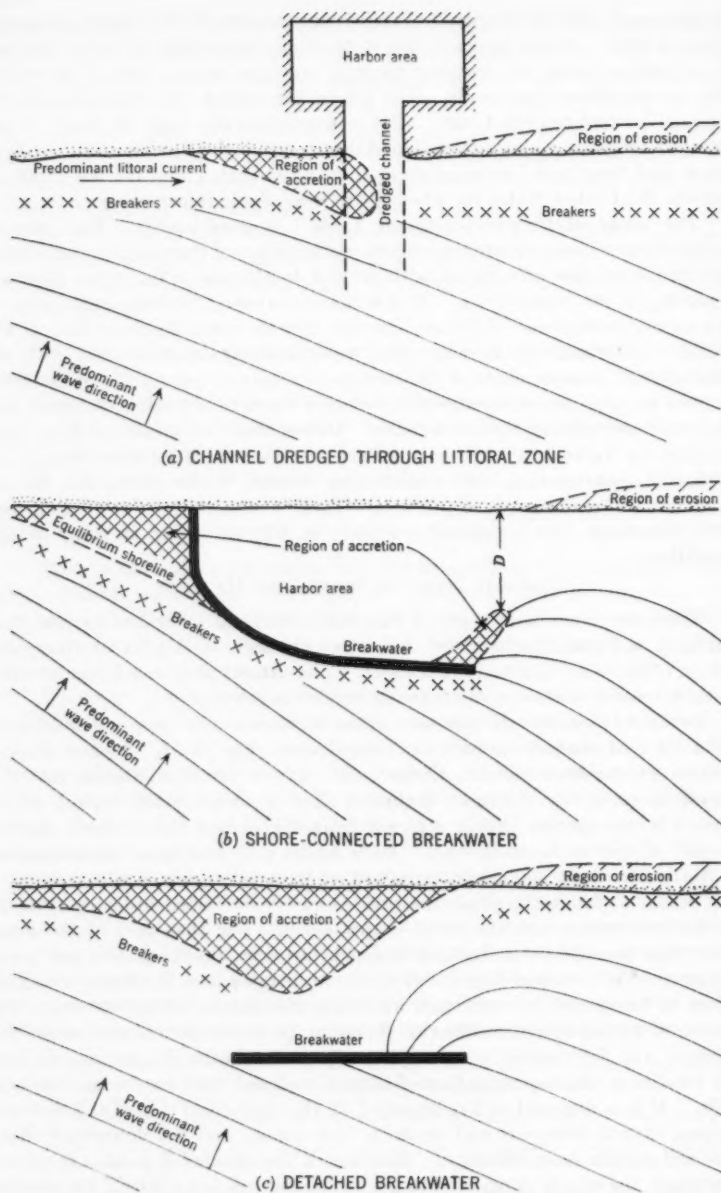


FIG. 2.—TRANSPORTATION, DEPOSITION, AND SCOUR OF LITTORAL SEDIMENTS

shown in Fig. 2(a), the wave action restores the natural littoral transport of material and thus reduces the entrance area to a size that is compatible with the tidal prism. The equilibrium size of entrance to be expected on the west coast of the United States could be estimated by the relationships between the entrance area and the tidal prism as given by O'Brien⁶ and Robbins.⁷

If the littoral-drift rate is relatively great, the type of harbor shown in Fig. 2(a) is seldom economically feasible. The dredged entrance is often further improved and stabilized by the construction of a shore-connected jetty or breakwater.

Harbors Created by Shore-Connected Breakwaters.—A structure that extends seaward from the shore and across the littoral zone acts as a dam and traps the littoral drift. The impounding capacity of such a barrier depends on the height of the structure, the bottom slope, and the equilibrium alinement of the shore in that region. The equilibrium alinement is normal to the resultant littoral forces. Thus, in Fig. 2(b), if the original shore line were stable with respect to the material balance and if a breakwater is constructed, accretion will occur first in the form of a fillet on the upcoast side with an alinement tending toward equilibrium. This will create a deficiency in material supplied to the downcoast shore line, where erosion probably will occur, with the shore line also tending toward equilibrium. As the upcoast fillet approaches equilibrium, littoral material will move along the outer face of the breakwater and be deposited in the relatively calm water in the lee of the structure. Thus, the turbulent characteristics of the wave action upcoast from the breakwater tip is sufficient to transport littoral material at a certain capacity. However, at the breakwater tip the waves are refracted and diffracted into the lee of the structure. Sufficient water turbulence is not available to transport material, and deposition occurs. This deposit grows progressively toward the downcoast shore line, and when it reaches the shore line the material balance will be re-established on each side of the barrier. The alinement of the harbor deposit depends primarily on the predominant wave direction. Typical examples of harbor deposits at Santa Barbara, Calif., and at Fortaleza, Brazil, will be cited subsequently.

The selection of the breakwater alinement at a proposed harbor depends on the functional aspects of the project. The termination of the outer tip of the breakwater is dictated primarily by the stipulation that the desired anchorage area is provided and that the littoral-drift deposit will not interfere with efficient harbor operation. A proper understanding of the littoral regimen of the area is the most important factor in the design procedure. Valuable experience is gained from observations of littoral processes at nearby littoral barriers. Such observations often permit determining whether or not important reversals in the direction of drift occur. A study of the filling pattern of deposits in the vicinity of barriers is also valuable in estimating what pattern could be expected at a proposed nearby barrier. Some typical examples of littoral-drift patterns at single-breakwater harbors will be presented subsequently. The model studies of Gaston Sauvage de Saint Marc and G. E. Vincent²⁰ on the accretion pattern at the tip of a breakwater are also interesting.

²⁰ "Transport Littoral Formation de Fleches et de Tombolos," by Gaston Sauvage de Saint Marc and G. E. Vincent, *Proceedings, 5th Conference on Coastal Eng., Berkeley, Calif., 1955*, pp. 296-328.

In order for a harbor to be maintained in an operating condition, the sand deposit at the breakwater must be removed periodically by dredging. This dredged material should be placed on the downcoast beach to maintain a material balance on it and to reduce the shore-line recession resulting from erosion. The material must be placed on the downcoast beach at a site that is fully exposed to littoral forces and in depths not exceeding the limiting effective depth of the barrier. The frequency of dredging depends on the impounding capacity of the barrier and on the rate of littoral drift. That is, for the typical condition shown in Fig. 2(b), the stockpiled material behind the breakwater must be removed by dredging when the width of the harbor entrance, D , has

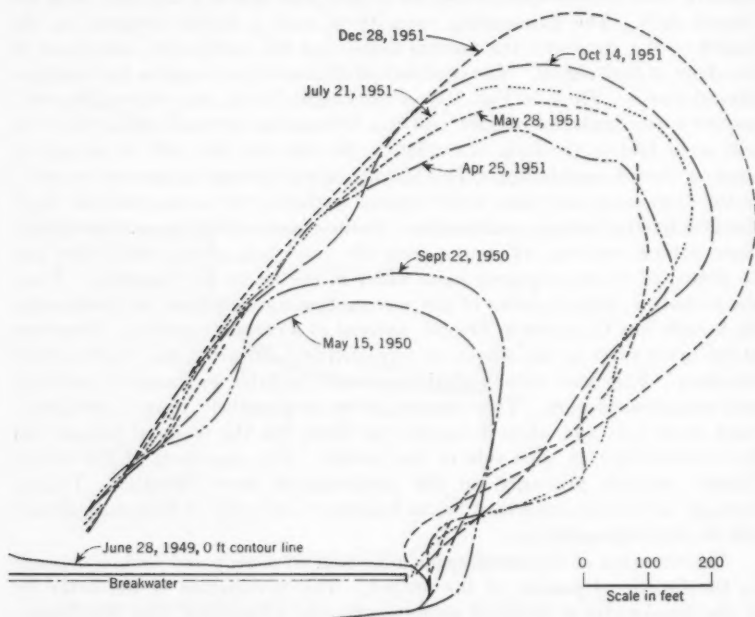


FIG. 3.—GROWTH OF SAND DEPOSIT IN SANTA BARBARA (CALIF.) HARBOR

decreased to the extent that ship operations into the harbor are seriously restricted. The frequency of dredging is approximately equal to the maximum allowable volume of stockpiled material divided by the average rate of littoral drift.

For example, at the Santa Barbara harbor, where the rate of drift as shown in Table 1 is approximately 280,000 cu yd per yr and the accretion pattern is as shown in Fig. 3, dredging must be practiced every 2 yr or 3 yr to prevent impairing the usefulness of the harbor.

Harbors of the type shown in Fig. 2(b), which consist of a single breakwater, are feasible when protection is required from storm waves arriving principally

from only one direction. In such cases littoral-drift reversals are nonexistent or unimportant. Littoral drift past the harbor entrance may be bypassed by (a) removing the material at the rate of accumulation, or (b) allowing the material to be "stockpiled" for periodic removal. The method that is used at a particular locality depends primarily on the type of dredge available locally. Removal at the rate of accumulation by a fixed pumping plant or by a hopper dredge could be used, whereas a large-capacity pipeline dredge has been the economical solution at some harbors for removing deposits occurring during periods of 2 yr or 3 yr.

A variation in the shape of a harbor formed by a shore-connected breakwater is a case in which two breakwaters must be provided to assure protection from storm waves that could approach the entrance from various directions. Pronounced reversals in the direction of littoral drift usually occur in such instances. The exclusion of both wave action and littoral drift from such harbors present considerations that are fundamentally opposed to each other. That is, a relatively narrow entrance between the breakwater tips is desirable to reduce wave action within the harbor. On the other hand, a wide entrance permits considerable flexibility in removing littoral-drift deposits once equilibrium has been reached at the adjacent shore lines. If the rate of littoral drift is relatively high and the entrance must be fairly narrow to provide adequate protection against wave action in the harbor, two solutions are possible. First, almost continuous bypassing of the sand by a fixed plant or hopper dredge must be practiced. Second, the littoral drift should be stockpiled by an auxiliary structure, as proposed for Port Hueneme, Calif.,²¹ and then pumped periodically to the downcoast side of the entrance. If there are any appreciable reversals in littoral drift, it may be necessary to bypass material in one direction at one season of the year and in the opposite direction during the remainder of the year. In a subsequent section typical examples of twin-breakwater harbors will be given for Salina Cruz, Mexico, Camp Pendleton, Calif., Port Hueneme, and Madras, India.

Detached Breakwater.—A detached breakwater intercepts the waves and creates a protected area of relatively calm water. The theory is that the littoral material will move along the coast uninterrupted by the presence of the structure, and, consequently, there will be no maintenance problems from the sediment deposition. However, this assumption is incorrect because the refraction and diffraction of the waves behind the breakwater reduce the energy available for littoral transport in the lee of the structure, as compared with the available energy on both the upcoast and downcoast shore lines (Fig. 2(c)). The result of the reduced energy is that littoral material accumulates in the protected area. If this material is not removed periodically by dredging, the accretion may eventually extend to the breakwater in the form of a tombolo, a phenomenon examined by Saint Marc and Vincent.²⁰

On the upcoast side of a detached breakwater, the accretion advances beyond the region of the direct effect of the structure itself, and a corresponding erosion occurs on the downcoast side. Typical harbors exist at Santa Monica,

²¹ "Port Hueneme, California," *House Document No. 392*, 83d Cong., 2d Session, Beach Erosion Control Study, Corps of Engrs., U. S. Dept. of the Army, Washington, D. C., 1954, p. 25.

Calif., and Ceara, Brazil, and the original harbor at Santa Barbara was of this type.

ACCRETION PATTERNS AT SHORE-LINE HARBORS

The following examples of filling patterns at typical shore-line harbors illustrate the previously cited littoral processes. The observed filling patterns give the design engineer a valuable concept of the expected conditions at a harbor site with a littoral-drift rate and a direction of wave attack similar to those presented thus far.

In this respect, attention should be directed to the harbors at Madras and Ceara, which were studied extensively in the nineteenth century following breakwater construction. The bitter lessons learned at these harbors are classic examples of the seriousness of littoral drift. Unfortunately, these

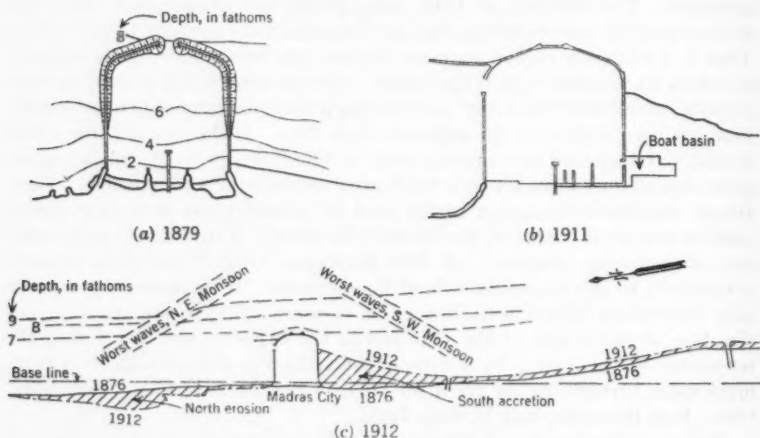


FIG. 4.—MADRAS HARBOR, INDIA

lessons were either overlooked or ignored as not being applicable to other coast lines when the harbors were constructed at Salina Cruz, Santa Barbara, Santa Monica, and other sites. Many past mistakes resulted apparently from confusion as to the relative strength of the littoral current and the general oceanic currents in the particular localities. Generally, only the littoral current generated by breaking waves is sufficiently strong to transport sediment of the sand sizes. Any reduction in the strength of this current, as a result of intercepting wave energy by breakwaters or of distributing wave energy by refraction because of increased depths, causes an accretion of littoral material. On the other hand, oceanic currents are relatively weak and cannot transport much littoral material. Many harbors throughout the world, which were filled with littoral material shortly after breakwater construction, were designed apparently on the erroneous assumption that the prevailing oceanic current would be sufficiently strong to transport all the material past the harbor entrance

and onto the downcoast shore line. In all instances this assumption has led invariably to disastrous results.

Madras Harbor.—Prior to 1875, there was only an open roadstead on the exposed sandy coast at Madras. The breakwaters shown in Fig. 4(a) were planned to provide protection from the violent storms sweeping this coast. The northern breakwater was begun in 1875 and the southern breakwater in 1877.²² Sand accumulated against the southern breakwater so rapidly that the foreshore almost kept pace with the end of the structure as construction progressed seaward. The accretion to the south of the harbor continued to enlarge after the breakwaters were completed. In 1910 it was necessary to close the original entrance, which was 550 ft wide, and provide a new entrance facing north (Fig. 4(b)). Simultaneously with the formation of the accretion to the south, there was a corresponding shore-line erosion to the north. The extent of the accretion and erosion by 1912 is shown²³ in Fig. 4(c). Surveys of the accretion to the south of Madras Harbor indicated that for 33 yr of record the littoral-drift rate was approximately 750,000 cu yd per yr.^{23,24,25} In considering this rate of drift and the narrow width of the original entrance (550 ft), it is obvious that the available stockpile area was fairly small and that frequent dredging was required to maintain navigable depths through the entrance. To provide additional stockpile area to the south of the harbor, an extension of the southern breakwater was constructed in 1929.

Ceara Harbor.—The harbor at Ceara and its rapid filling rate were examined extensively in engineering journals following breakwater construction in 1875.^{26,27,28} The breakwater was detached, approximately 1,400 ft long and more or less parallel to the shore, with a 750-ft-long iron viaduct designed to meet the eastern or upcoast end with the shore. The prevailing drift in this section of the Brazilian coast is from east to west, and it was expected that the littoral drift would pass through the open viaduct and out the other side of the harbor. Actually, as the construction of the viaduct progressed seaward, a tongue of sand also moved seaward, reached the detached breakwater, and completely closed the passage through the viaduct.²⁸ Sand eventually moved around the end of the breakwater and formed a bar, which joined the downcoast shore line. An enclosed pool of water was formed between this sand bar, the breakwater, and the accretion at the viaduct. Attempts to maintain Ceara Harbor in an operational condition by dredging apparently were made. By 1945, however, the harbor was practically useless except possibly for small craft. For the relatively high rate of littoral drift occurring along this coast, as computed for the nearby harbor at Ponta de Mucuripe, Brazil, and the somewhat negligible area within Ceara Harbor for stockpile purposes, this

²² "Harbours and Estuaries on Sandy Coasts," by L. F. Vernon-Harcourt, *Minutes of Proceedings, Inst. C. E.*, London, Vol. 70, 1881-1882, pp. 1-32.

²³ "Coastal Sand Travel Near Madras Harbour," by F. J. E. Spring, *Minutes of Proceedings, Inst. C. E.*, London, Vol. 194, 1912-1913, pp. 153-171.

²⁴ "Coastal Sand Travel Near Madras Harbour," by F. J. E. Spring, *ibid.*, Vol. 210, 1919-1920, pp. 27-28.

²⁵ "Coastal Sand Travel Near Madras Harbour," by F. J. E. Spring, *ibid.*, Vol. 194, 1912-1913, p. 162.

²⁶ "The Sanding-up of Tidal Harbours," by A. E. Carey, *ibid.*, Vol. 156, 1903-1904, p. 222.

²⁷ *Ibid.*, p. 268.

²⁸ "Harbour Engineering," by Brysson Cunningham, Charles Griffin & Co., Ltd., London, 1908, p. 25.

harbor can be maintained in a satisfactory navigational condition only by almost continuous dredging.

Henry Clay Ripley,²⁹ M. ASCE, stated that the filling of Ceara Harbor could have been prevented by the construction of an additional shore-connected breakwater to the west, leaving only a narrow harbor entrance. The fallacy of this design is that sand would not be moved by wave action in the great depths required for navigation at the harbor entrance.

La Guaira Harbor, Venezuela.—The central coast of Venezuela in the vicinity of Caracas is devoid of any natural protection for shipping operations. Consequently, in the years from 1885 to 1888 a breakwater was constructed

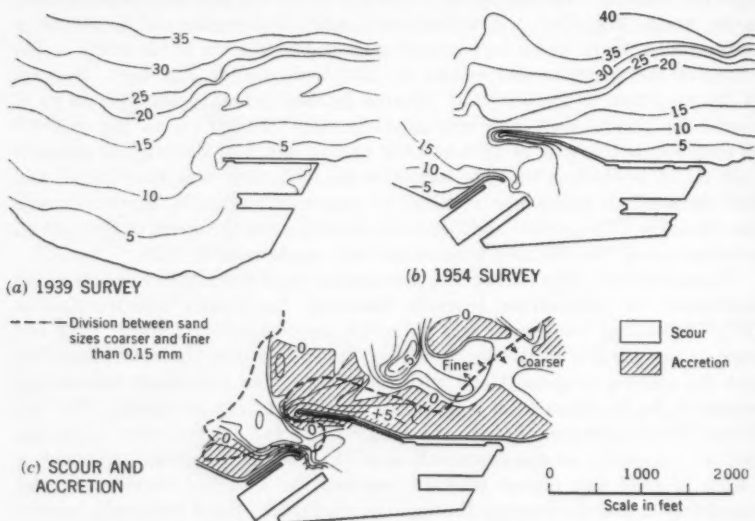


FIG. 5.—BOTTOM CHANGES (SOUNDINGS IN METERS) AT LA GUAIRA, VENEZUELA, FOLLOWING EXTENSION OF BREAKWATER

at La Guaira. The original breakwater was 2,050 ft long and protected a 90-acre water area having an average depth of 30 ft.³⁰ The trade winds in the Caribbean Sea blow from the east and thereby create a prevailing westward littoral drift along the Venezuelan coast. Because of the relatively great depths in the lee of the breakwater tip, an accretion occurred in the harbor and continued to increase for many years following completion of the breakwater. Dredging was required at intervals to maintain navigable depths in the harbor. The bottom configuration in the vicinity of the harbor in 1939 is shown in Fig. 5(a). In the period from 1949 to 1951 the breakwater was extended 1,900 ft, and the harbor dredged to an average depth of approximately 30 ft. The

²⁹ "Beach Erosion: Its Causes and Cure," by Henry Clay Ripley, *Transactions, ASCE*, Vol. 87, 1924, p. 594.

³⁰ "La Guaira Harbour Works," by W. C. Punchard and J. L. Houston, *Minutes of Proceedings, Inst. C. E.*, London, Vol. 115, 1893-1894, pp. 332-342.

result of a bottom survey made in 1954, several years after the breakwater extension was completed, is shown in Fig. 5(b). The maps presented in Figs. 5(a) and 5(b) were compared to determine areas in which accretion and scour occurred between 1939 and 1954. This comparison is shown in Fig. 5(c), in which the crosshatching indicates areas of accretion and the remaining area either is scoured or dredged. Fig. 5(c) demonstrates clearly that accretion occurred along the outer face of the breakwater and extended a considerable distance seaward of the breakwater tip. It is also evident that at the time of the 1954 survey, sand began moving around the breakwater tip and into the harbor. A sand deposit inside the harbor probably will eventually occur, with a configuration similar to that existing at the tip of the original breakwater shown in Fig. 5(a). Also of interest in Fig. 5(c) is the dotted line, which shows the division between bottom materials that are coarser and finer than 0.15 mm. As expected, the coarse materials are near the shore, whereas the fine materials are in deep water.

Salina Cruz, Harbor.—The shore line of the Pacific Ocean side of the isthmus of Tehuantepec consists of a series of "hooked bays," which face eastward. The port of Salina Cruz is one of these bays that have been improved by constructing two breakwaters: The east breakwater is 3,240 ft long and the west breakwater is 2,164 ft long.³¹ The first part of the west breakwater was constructed in 1890 and extended in an easterly direction from the headland. After approximately 850 ft of the breakwater was constructed, the harbor filled so rapidly³² that the alinement changed to a southerly direction and terminated opposite the tip of the east breakwater to leave an entrance approximately 600 ft wide. The maintenance of navigable depths in the harbor and in the entrance has been a continuous battle against the littoral drift since the breakwaters were completed. The harbor entrance is small and the rate of littoral drift is so high that stockpiling the material and dredging at infrequent intervals cannot be practiced. Almost continuous dredging, therefore, has been necessary. In approximately 1948, in order to bypass sand at the entrance a fixed dredge was constructed near the tip of the west breakwater. A complete description of this installation has appeared elsewhere.³³ The dredge has not been very successful in its purpose. The critical factor in designing a fixed dredge is that the pump intakes must be placed so that most of the littoral drift can be intercepted as it moves downcoast. Apparently, the Salina Cruz plant was too far inland from the normal shore line for effective pump intakes. In 1955 inspection of the installation showed that the fixed dredge was inoperative, and the harbor entrance was maintained at navigable depths by use of a hopper dredge working almost continuously.

Santa Barbara Harbor.—The original breakwater at Santa Barbara was detached. It consisted of a 1,425-ft-long outer arm that was nearly parallel to the shore, with a 400-ft-long short arm at the western end having a 600-ft

³¹ "The Harbor Improvements at Salina Cruz, Mexico," *Engineering Record*, Vol. 55, No. 13, 1907, pp. 400-402.

³² "The Sanding-up of Tidal Harbours," discussion by J. M. Dobson, *Minutes of Proceedings, Inst. C. E.*, London, Vol. 156, 1903, p. 252.

³³ "Sand By-Passing Plant at Salina Cruz, Mexico," by M. C. Rolland, *Proceedings, 2d Conference on Coastal Eng.*, Berkeley, Calif., 1952, pp. 177-186.

opening between the shore and the inner end (Fig. 6(a)).²⁴ The breakwater was completed early in 1929, but by the fall of that year shoaling had reached alarming proportions. This shoal consisted of a large sand accumulation along the shore line and extended seaward in the lee of the breakwater (Fig. 6(a)). The short arm of the breakwater was extended then to the shore, with closure being completed in the early part of 1930 (Fig. 6(b)). Sand immediately

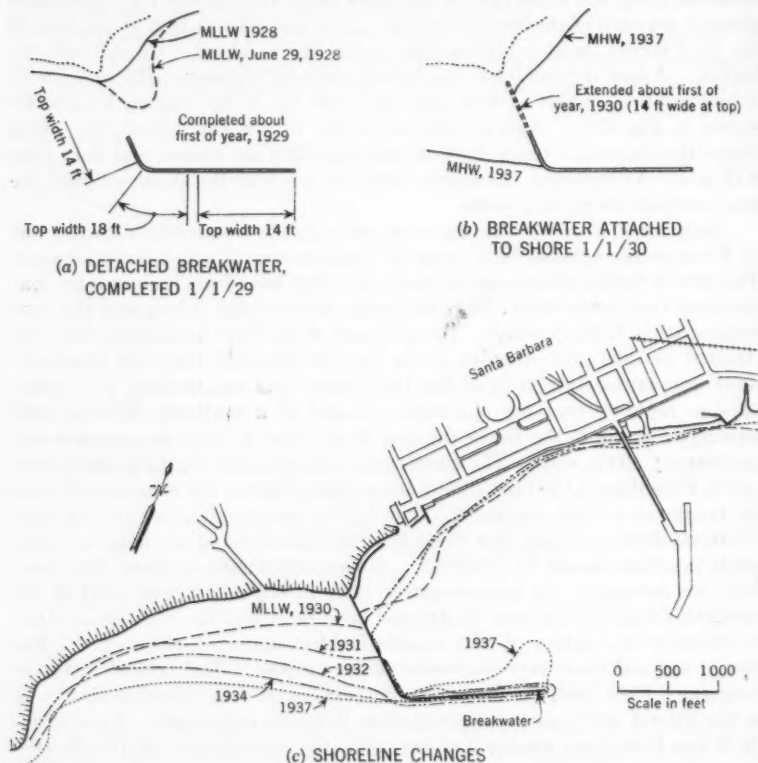


FIG. 6.—BREAKWATER AT SANTA BARBARA, CALIF.

accumulated west of the shore arm. By the fall of 1933 the accreting sand had extended almost the entire length of the shore arm (Fig. 6(c)). The updrift shore became stable, and all littoral material in transit shoreward of the limiting effective depth of the structure moved around it and deposited inside the harbor entrance. To maintain navigable depths in the harbor and to provide nourishment to the easterly beaches, it became evident that a program of sand bypassing was necessary. Beginning in 1935, the harbor

²⁴ "Beach Erosion at Santa Barbara, California," House Document No. 552, 75th Cong., 3d Session, 1938.

has been dredged every 2 yr or 3 yr, as shown in Fig. 7, which indicates the total accretion in the harbor since the completion of the breakwater. Average daily rates computed for the various periods between harbor surveys also are shown in Fig. 7.

To provide detailed information on both the rate of sand transport and the wave characteristics at Santa Barbara, a program of frequent harbor surveys and wave recording was instituted in 1950.¹⁹ A typical example of the growth of the sand deposit in the harbor is shown in Fig. 3. A critical examination of the data for Santa Barbara reveals that sufficient information is available to establish the average annual rates and maximum annual rates of sand movement along that section of the California coast. However, the data

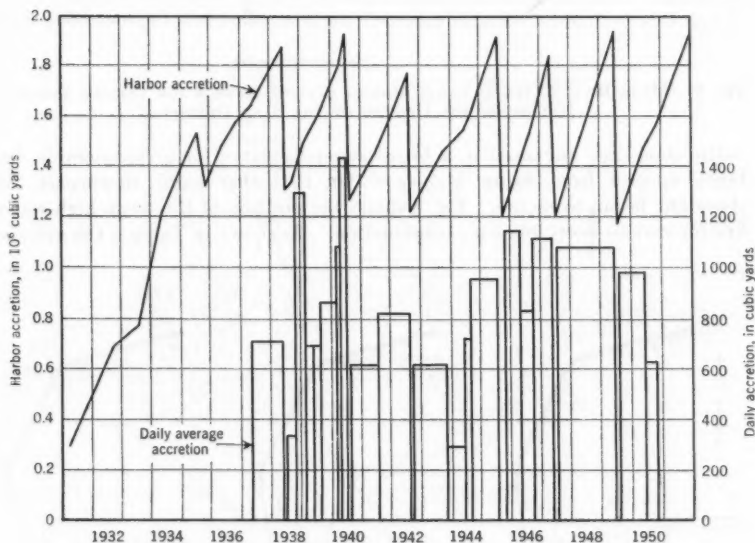


FIG. 7.—ACCRETION AT SANTA BARBARA, CALIF.

are insufficient to permit the formulation of a general relationship between the rate of transport and the wave characteristics. Although the determinations of harbor accretion were made more frequently than in previous years, observations at even more frequent intervals are necessary to determine accurately the actual rate of transport for a given wave condition. Harbor surveys should be made as often as the reliability of survey methods permits, but, in particular, they should be made when the wave characteristics are observed to change appreciably. Frequent observations of harbor accretion and wave conditions are not, however, the only factors to be considered. The effect of tide and the general variability of the height, period, and direction of the waves are added complications to the formulation of a general transport equation.

Santa Monica Harbor.—The harbor at Santa Monica was created in 1934 by the construction of a 2,000-ft-long, detached breakwater parallel to and about 2,000 ft distant from shore. Immediately following construction of this wave barrier, accretion formed on the beach in its lee. Within a few years, accretion extended in a seaward direction enough to act as a groin, and the

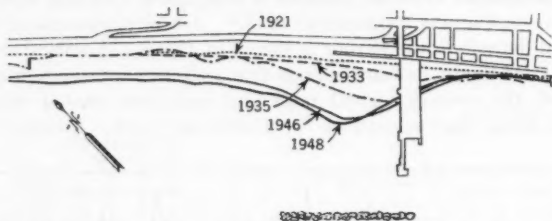


FIG. 8.—MEAN HIGH WATER AT SANTA MONICA (CALIF.) HARBOR FOR VARIOUS YEARS TO ILLUSTRATE THE GROWTH OF THE SAND DEPOSIT

entire shore line advanced in a broad sweeping curve for a considerable distance upcoast from Santa Monica.³⁵ On the other hand, downcoast the shore line began to recede. Fig. 8 shows the position of the mean high-water line for various years following construction. As shown in Table 1, the average

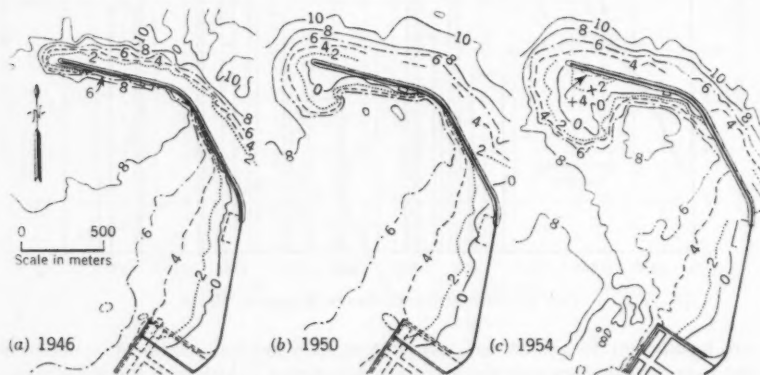


FIG. 9.—GROWTH OF SAND DEPOSIT AT FORTALEZA HARBOR, BRAZIL (SOUNDINGS IN METERS)

accretion rate upcoast from the breakwater for the period from 1936 to 1940 was 270,000 cu yd per yr.

Fortaleza Harbor.—Approximately 3 miles east along the coast from Ceara Harbor is the breakwater at Ponta de Mucuripe, on which construction began in 1940. Prevailing wave action and littoral drift is from the east, and a

³⁵ "Accretion of Beach Sand Behind a Detached Breakwater," by J. W. Handin and J. C. Ludwick, Technical Memorandum No. 16, Beach Erosion Board, Corps of Engrs., U. S. Dept. of the Army, Washington, D. C., 1950.

single shore-connected breakwater approximately 4,600 ft long has provided an adequate protected area for shipping. Yearly surveys of the accretion inside the breakwater have been made by the Brazilian government. A few of these surveys are shown in Fig. 9 to indicate the nature of this deposition. Computing the annual accretion for the period from 1946 to 1950, inclusive, yielded an average annual littoral-drift rate of 427,000 cu yd. As shown in Table 1, this rate is comparatively high. The advantage of this harbor has been that a relatively large area inside the breakwater tip is available for stockpiling, as compared with the small area at nearby Ceara Harbor. Therefore, the extensive stockpile area at Fortaleza permits dredging only at intervals of several years.

Port Hueneme Harbor.—This California harbor was constructed in the period from 1938 to 1940 and consists of an entrance channel 35 ft deep and 400 ft

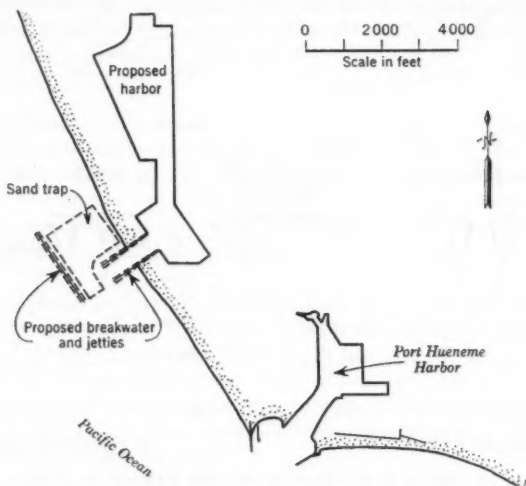


FIG. 10.—PRESENT AND PROPOSED HARBORS AT PORT HUENEME, CALIF.

wide, protected by two jetties 1,000 ft long and 1,100 ft long, respectively (Fig. 10). Since the jetties were constructed, accretion has occurred along the upcoast shore. Simultaneously with the upcoast accretion, the downcoast shore line receded, and in late 1948, this recession extended farther downcoast for 7 miles.²¹ Various attempts at shore protection have been made, including placing fill material and constructing a stone sea wall extending approximately 3,000 ft from the downcoast jetty. In 1954 material was dredged from the upcoast side of the jetties and deposited on the downcoast side to replenish the supply to that reach of the shore line. Shore-line records downcoast from Port Hueneme for the 82-yr period from 1856 to 1938 showed that the shore was exceptionally stable, indicating a close balance between supply and loss. The littoral supply passing Point Hueneme prior to the construction of the harbor

jetties probably was adequate for nourishing this section of the shore. To assure the future operational condition of Port Hueneme Harbor and to protect the downcoast shore line from serious erosion, as well as to provide a separate small-craft harbor, a sand-bypassing plan was developed.²¹ Fig. 10 shows that this plan provides for a 2,300-ft-long, detached breakwater and for two harbor-entrance jetties approximately 1,400 ft long each. A sand trap will be provided in the lee of the breakwater by dredging material to a depth of 30 ft. Dredging 1,000,000 cu yd of material from the stockpile area every 2 yr and depositing it downcoast of the Port Hueneme jetties to nourish the shore line is expected to solve the littoral-drift problems.

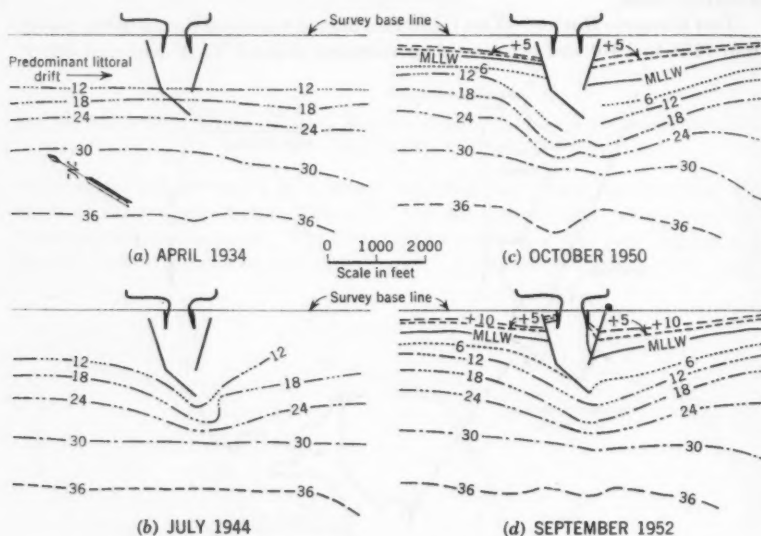


FIG. 11.—SHORE-LINE CHANGES AT CAMP PENDLETON (CALIF.) HARBOR (DEPTHS IN FEET)

Camp Pendleton, Calif.—To form a small boat harbor at Camp Pendleton, two shore-connected jetties were constructed in 1942 and 1943, and a boat basin was dredged as shown in Fig. 11(a). Since these structures were built, the shore line has changed progressively, as shown in Fig. 11(b).³⁶ Studies of the accretion and scour of the adjacent shore lines indicate that the direction of littoral drift is to the south during the winter and spring, and to the north during the summer and fall. The resulting littoral movement to the south predominates and is estimated at approximately 100,000 cu yd per yr. In 1955 the entrance to the harbor was almost completely closed because there had been no maintenance and dredging for the previous several years. Limited

³⁶ "Beach Erosion Control Report on Co-operative Study of Oceanside, Ocean Beach, Imperial Beach, and Coronado, San Diego County, California," Los Angeles Dist., Corps of Engrs., U. S. Dept. of the Army, Los Angeles, Calif., April, 1955 (unpublished).

littoral material presently (1959) passes around the end of the jetties. The stockpile area at this harbor entrance is so small that almost continuous dredging would be required to maintain navigable depths. The shore line at Ocean-side, Calif., downcoast of the harbor has eroded as a result of the accretion of the jetties.

CONCLUSIONS

When a shore-line harbor is created by the construction of an artificial littoral barrier, certain basic phenomena must be recognized. The greatest volume of littoral material is transported in the immediate vicinity of the breaker zone, where there is sufficient turbulence to maintain the sediment in motion. Along a particular shore line, but upcoast from the influence of the structures at a harbor entrance, the breaking waves transport littoral material at "capacity" in the relatively small depths of the surf zone. Because of the great depths seaward of the structure tips, the transporting capacity is less than along the beaches either upcoast or downcoast from the harbor entrance, and the littoral drift is deposited. The two following common conditions induce such deposition:

1. Littoral material is moved to the tip of a breakwater by wave-action turbulence along the outer face of the structure (Fig. 2(b)). Such turbulence is not present in the lee of the breakwater, and the littoral material deposits in the form of a spit in the protected area. The rate of transport in depths required for navigation is low compared with the surf-zone depths, and deposition occurs at the point of the change in the transporting capacity of the waves.

2. A detached breakwater intercepts part of the wave energy, with the result that the capacity of the waves to transport littoral material along the shore line in the lee of the structure is much less than in the upcoast section, and deposition occurs (Fig. 2(c)). The waves have the same capacity to transport sand downcoast from the structure as on the upcoast side. Because the sand supplied to the downcoast beach has been intercepted by the breakwater, the shore line has receded.

In planning either a new shore-line harbor or improvements to an existing one on a coast where there is littoral sand transport, the following statements are pertinent:

Alfred E. Carey²⁶ in 1904 stated that

"a harbor when built has to be defended; moreover, it has to be maintained by dredging, often at a cost relatively high compared with the direct return which it produces as a trade center."

In 1912 Francis J. E. Spring,²³ M. ASCE, cautioned that:

"The chief lesson to be learned from a study of the sand-travel at Madras appears to be that it is absolutely necessary, when an engineer is called on to advise about a work situated on a coast where there is any suspicion of travelling sand, mud, or shingle, that he should be allowed adequate time to make observations, conducted with due precautions, of the directions and causes of the travel; and that if he should arrive at the conclusion

that such travel is likely to affect the proposed works in the near or the distant future, he ought at least to acquaint his employers with what he conceives to be the broad general facts of the case and their probably financial effects, whether on the proposed works or on other works or interests."

Spring also asserted that sand movement on the eastern coast of India threatened to overwhelm Madras Harbor unless adequate precautions were taken against it. In discussing the foregoing, J. M. Dobson²⁷ stated:

"* * * it was an established fact that, wherever harbors were built on sandy coasts, such harbors must naturally be maintained either by dredging, or by other means adapted to counteract the sand-accretion; and it was almost impossible to imagine why it should ever have been assumed that Madras Harbor, on a coast where the sand was always on the move, should prove an exception to this rule."

In 1950 O'Brien cautioned²⁸ that the design of coastal works involves many criteria that are foreign to other phases of civil engineering and that

"along the coastlines of the world, numerous engineering works in various states of disintegration testify to the futility and wastefulness of disregarding the tremendous destructive forces of the sea. Far worse than the destruction of insubstantial coastal works has been the damage to adjacent shorelines caused by structures planned in ignorance of, and occasionally in disregard of, the shoreline processes operative in the area."

ACKNOWLEDGMENTS

Many of the data presented herein were assembled with the aid of a John Simon Guggenheim Fellowship.

²⁷ "Coastal Sand-Travel near Madras Harbour," discussion by J. M. Dobson, *Minutes of Proceedings*, Inst. C. E., London, Vol. 194, 1912-1913, p. 175.

²⁸ "Preface," *Proceedings*, 1st Conference on Coastal Eng., Berkeley, Calif., 1951.

DISCUSSION

RICHARD SILVESTER³².—The maintenance of harbor entrances is an expensive item in maritime administration. It would be helpful if some suggestions could be made on improving the design of the harbors cited or on possible lines of research.

The main conclusion of the paper is that the warnings of earlier engineers should be heeded. The writer feels that the greatest pitfall is to observe only half the picture. In a study of coastal sediment motion such factors as (a) the long-term and short-term meteorological effects, (b) the various means by which sediment is transported, and (c) the effect of wave spectra width on item (b) and its generation by item (a) should be included.

Meteorological Conditions.—Most waves of any consequence in littoral-drift studies are generated by winds in low-pressure centers or cyclones. Anticyclones may be more persistent, but the winds accompanying them are generally small in magnitude. Thus, if the location, duration, and intensity of low-pressure centers are studied, the direction and proximity of fetches (areas in which waves are generated) can be determined.

The foregoing information leads to the direction of wave approach toward a particular section of coast and to the expected types of waves from those directions. If such a study were taken over a year, the "balance of power" from upcoast and downcoast could be indicated, and if taken over several years a long-term trend may become apparent. Such a statistical analysis can assist in concurrent wave hindcasting or in littoral-drift observations.⁴⁰

The writer has found and believes it to be the rule rather than the exception that storm waves approach a coast from a different direction from the predominant swell. This results in a reversal of littoral drift, but the mode of movement is different in each direction. It is complementary in that the storm waves assist the predominant swell to move greater quantities of sediment than if the swell were working alone.

Mode of Movement.—There are three main methods by which sediment is moved alongshore: (a) Suspension in the surf zone; (b) rolling in the surf zone; and (c) saltation beyond the surf zone.

Under the heading, "Littoral Drift at Shore-Line Harbors: Dredged Channels," the author states:

"Both model and prototype measurements indicate that most alongshore transport of material occurs in the vicinity of the breakers, where the available wave energy is converted suddenly from oscillatory motion into the form of turbulence."

Of the references cited in this respect, that by Mason¹⁵ is an unqualified statement that 80% of the sediment movement takes place in the surf zone, whereas Saville¹⁶ describes model tests along a supposedly infinitely long beach in which only the surf zone is studied. With respect to measuring littoral drift

³² Senior Lecturer in Civ. Eng. (Hydraulics), Univ. of Western Australia, Nedlands, Western Australia.

⁴⁰ "The Use of Cyclonicity Charts in the Study of Littoral Drift," by R. Silvester, *Transactions, Am. Geophysical Union*, Vol. 37, No. 6, 1956, p. 694.

in nature, the writer believes that no instruments have been devised yet to cope adequately with this problem.

When a comparison is made between the relative volumes of material moved by suspension and rolling in the surf zone and by saltation beyond this zone, the apparent high velocities in the surf must be balanced against the extensive sea-bed area over which saltation actually occurs. Another factor to be remembered is that the finer sediment is sorted offshore and suffers saltation more easily than the coarser material near the beach. The term "saltation" was not used by the author, although some believe it to be the most important factor in littoral-drift processes.^{41,42,43}

Under the heading, "Littoral Processes," the author asserts that

"The exact mechanism of the movement around rocky headlands has not been established completely, but it is probably a combination of (a) sand movement by the turbulent action of waves breaking at the base of the precipitous cliffs, and (b) the movement of sand by wave action in depths of as much as 80 ft."

The type of action is not suggested, but it seems clear that the mode of movement is saltation together with a current near the ocean bed.

Saltation adjacent to a rocky headland is amplified by the standing waves or clapotis that are formed by the reflection of waves from the rock face. Experiments have been performed with clapotis,⁴⁴ and the excessive bed movement near vertical cliffs has been observed.⁴⁵

The current capable of transporting sediment continually thrown into suspension, across the ocean floor, can be due to (1) the littoral current in the surf zone; (2) ocean-wide phenomena, such as tides or wind drag; and (3) the mass transport of water due to the wave action. When considered in relation to the sediment cycle to be examined in the following section, the current (if it can be so termed) in item (3) may predominate.

The saltation mechanism has been studied both mathematically and in two-dimensional models,^{46,47,48,49,50,51} and the complicated particle motion makes it difficult to measure the net rate of movement. The writer feels that Table 1 is incomplete because the sand collected behind a breakwater, such as

⁴¹ "Introduction à l'étude de la saltation," by P. Danel, R. Durand, and E. Condolios, *La Houille Blanche*, Vol. 8, No. 2, 1953, p. 217.

⁴² "Quelques résultats à l'appui d'une hypothèse de Mm. Danel, Durand et Condolios sur le phénomène de la saltation," by L. Escande, *ibid.*, Vol. 9, No. 1, 1954.

⁴³ "Étude expérimentale de la formation des rides de sable sous l'action de la houle, saltation des grains, étude de l'effet Magnus," by A. Martinot-Lagarde and A. Fauquet, *Bulletin d'Information du Comité Central d'Océanographie et d'Étude des Côtes*, Vol. VII, No. 5, 1955, p. 215.

⁴⁴ "Contribution à l'étude des rides de sable, rides de clapotis," by A. Fauquet, *Bulletin d'Information du Comité d'Océanographie et d'Étude des Côtes*, Vol. III, No. 6, 1951, p. 206.

⁴⁵ "Breakers and Beach Erosion," by T. Hamada, *Report No. 1*, Transportation Technical Research Committee, Tokyo, Japan, 1951.

⁴⁶ "Motion of Waves in Shallow Water—Interaction Between Waves and Sand Bottoms," by R. A. Bagnold, *Proceedings, Royal Soc. of London, Series A*, Vol. 187, 1946, p. 1.

⁴⁷ "Sand Movement by Waves: Some Small Scale Experiments with Sand of Very Low Density," by R. A. Bagnold, *Journal, Inst. C.E.*, London, Vol. 27, 1947, p. 447.

⁴⁸ "The Final Equilibrium of Ridges of Material Thrown Down and Picked Up Again by Swell," by J. Larraz, *Le Génie Civil*, Vol. CXXX, 1953, p. 334.

⁴⁹ "Étude expérimentale de la formation des rides de sable sous l'action de la houle," by A. Fauquet, *Bulletin d'Information du Comité d'Océanographie et d'Étude des Côtes*, Vol. VI, No. 6, 1954, p. 245.

⁵⁰ *Ibid.*, No. 7, 1954, p. 291.

⁵¹ "Essais d'entraînement de matériaux solides sous l'effet de la houle et du clapotis," by A. Martinot-Lagarde and A. Fauquet, *Proceedings, 5th Conference on Coastal Eng., 1954-1955*, p. 383.

that at Santa Barbara, is not the total drift movement along the coast. Probably half as much again actually bypasses the harbor.

By observing sediment movement with the use of heavy mineral tracers,^{52, 53} it has been shown that sediment is not always deposited in quiescent water behind a breakwater or rocky headland, but is carried across the intervening bay by saltation and by a current near the ocean bed. In a recent investigation by the writer,⁵⁴ aerial photographs showed such a movement by a whitening of the water due to the "suspended" sand.

Wave Spectra.—As mentioned previously, two main types of wave can approach a coast—storm waves that are still being generated when they reach the coast (the fetch being adjacent to it), and swell that has been generated some distance from the coast and has traveled through an area of little or no wind (an area of decay).

Storm waves have certain characteristics: They are composed of waves of many periods—that is, the wave spectrum is wide⁵⁵ (the maximum period determined by the length of the fetch). The waves are multidirectional because a wind generates waves at angles of as much as 30° to its general direction. They are peculiarly shaped, being steep in front and mildly sloped at the back, and they are steeper than swell waves.

As a result of the water thrown toward a coast by storm waves, the shore erodes quickly, and material is moved from the beach to form a bar offshore, which, once established, prevents subsequent waves from attacking the beach, forcing them to break offshore. It is felt that the value of 0.025, cited by the author as the critical steepness in this respect, is of little practical significance when conditions in nature are considered.

The short period waves present, which are not refracted as much as the longer period waves, generally break at a greater angle to the beach and, hence, tend to generate a stronger littoral current. This is more than offset by the multidirectional nature of their approach, and the resultant motion is a slow current over a wide band of water (from the bar to the beach), in which large quantities of sand are suspended and rolled. Beyond the bar or breaker zone, saltation occurs, and again, due to the multidirectional characteristics of the wave movement, stable ripples are not formed and greater material than normal can be moved alongshore by the induced current from the surf zone.

Swell consists of waves that have emanated from a fetch and spread laterally as well as in the direction of propagation. Thus, at some distance from a fetch waves occur that are more unidirectional and have a small band of periods. The effect of this narrowing of the wave spectrum on the mass transport of water at the ocean bed has been studied mathematically.⁵⁶

⁵² "Sand Drift at Portland Victoria," by G. Baker, *Proceedings, Royal Soc. of Victoria, Australia*, Vol. 68, 1956, p. 151.

⁵³ "The Investigation and Design for Portland Harbour, Victoria," by E. P. C. Hughes, *Journal, Inst. of Eng. of Australia*, Vol. 29, 1957, p. 55.

⁵⁴ "A Model Study of Littoral Drift at Bunbury Harbour, W. A.," by R. Silvester, *ibid.*, Vol. 28, 1956, p. 219.

⁵⁵ "Analysis of Sea Waves," by G. E. R. Deacon, in "Symposium on Gravity Waves," *Circular 521*, National Bureau of Standards, U. S. Dept. of Commerce, Washington, D. C., 1952, p. 209.

⁵⁶ "Mass Transport in Water Waves," by M. S. Longuet-Higgins, *Philosophical Transactions, Royal Soc. of London, Series A*, Vol. 245, 1953, p. 535.

The saltation and mass-transport actions of the swell permit it to sweep sand toward the shore. The assistance of the infrequent storm waves can be observed as they move material offshore for the swell to operate on. In the process of moving shoreward, the sand is transported alongshore if the swell approaches the coast at an angle, which is generally the case.

Although the persistent swell determines the direction of the net littoral drift, the intermittent occurrence of storm waves, together with offshore saltation, permits groins and breakwaters to be bypassed by sand. The longer the waves, the wider the band of ocean affected by saltation. On the other hand, in the case of 7-sec waves or less, the bed outside the surf zone is hardly "touched." Thus, if models are to represent a prototype completely, storm cycles should be included in tests and sedimentary material should be used that can be self-sorted in a similar manner as in the prototype. These requirements present many difficulties.

In Fig. 2(a) accretion is shown to occur in the dredged channel above the general profile of the adjoining beach. Whether this is implied is not clear, but it is felt that nature will bridge the gap only as far as the level of the existing upshore beach, and the breaker line will not be deflected seaward as shown.

With respect to Fig. 2(b), there are few breakwaters at which waves are completely dissipated by breaking. The formation of a beach along the ocean side of such a breakwater will depend on (a) the reflective power of the breakwater; (b) the rate of sand supply from upcoast; and (c) the tidal range. Fig. 2(b) implies that where there is little or no breaking there is no sediment movement. On the contrary, there may even be more.

Although observations of the littoral processes at adjoining littoral barriers have been advised in order to determine the existence or nonexistence of drift reversals, no such probabilities have been included in Fig. 2(b). Reversal is so frequent that in a harbor such as the one in Fig. 2(b) accretion is likely to occur within the body of the harbor. Material will be moved from the downcoast area to sheltered regions within the harbor, thus aggravating the erosion problem. Again, the bidirectional wave approach will force the accretion at the tip of the breakwater along its inside face and render inoperative any wharves or jetties situated there. Fig. 9 should be compared in this respect.

When material is dredged behind a breakwater tip, where reversals of drift may occur, the time of the year must be chosen carefully to prevent material that was deposited downcoast from being forced into the harbor by the spasmodic storm waves. (For example, in the sand bypassing of Port Hueneme²⁷ weather conditions were ignored in dredging operations.) Bypassing material in both directions at different times of the year appears unnecessary because a drift in one direction will almost invariably predominate.

Fig. 2(c) shows an offshore breakwater and its effect on a coast line. Although the apex of the resulting accretion will vary with the direction of the predominant waves, it would seem that the one shown is somewhat too far upcoast, especially when compared with Fig. 8 and others cited by the author.²⁰

²⁷ "Sand By-passing at Port Hueneme, California," by R. P. Savage, *Technical Memorandum No. 92*, Beach Erosion Board, Corps of Engrs., U. S. Dept. of the Army, Washington, D. C., 1957.

The length and disposition of an offshore breakwater determines its effect on the adjacent shore line. It may be so short or so far from the shore that " * * the littoral material will move along the coast uninterrupted by the presence of the structure, and, consequently, there will be no maintenance problems from sediment deposition," as was stated under the heading, "Littoral Drift at Shore-Line Harbors: Detached Breakwater." Generally, the structure does not fulfil its purpose under these circumstances.

It would be interesting if mention could be made of the efficacy of several offshore breakwaters in line-spaced echelon fashion, as was practiced successfully at Cochin Harbor, India.⁵⁸ The diffraction of the waves through the gaps is sufficient to cause deposition with an accompanying saving in material.

In 1954 George E. R. Deacon made some statements pertinent to this study:⁵⁸

"The Chairman said that very little precise knowledge of wave characteristics was brought to bear on the design of ships, harbours and coast defences. Enormous sums of money were spent on engineering projects which might well be carried out more effectively if a fraction of the cost were devoted to increasing understanding of the underlying physical processes in the sea. It seemed to him that coastal engineering was a very vague subject, in which were any number of schools of thought."

JOE W. JOHNSON,⁵⁹ M. ASCE.—Wave action is the primary source of energy available at a shore line for moving sediment. Waves can be generated either by local winds or by storms relatively distant from the shore line under study. Locally generated waves usually are referred to as "seas," and waves generated by a distant storm are referred to as "swell." Those unfamiliar with the basic elements of wave generation and wave theory are referred to the work by Henry B. Bigelow and Walter T. Edmondson.⁶⁰ Workable relationships between the wave characteristics and a generating area are well established, and available graphical methods can estimate these wave characteristics (height, period, and direction) from known wind conditions. Most useful to the practicing engineer are the procedures outlined in other reports.^{61, 62, 63} By the use of these principles, "hindcasts" of wave characteristics have been made for many coastal regions, particularly in the United States. For example, wave statistics are available for the Pacific coast from Cape Blanco on the Oregon coast to the California-Mexico border,⁶⁴ the Gulf

⁵⁸ "Objects and Value of Oceanographic Research," by G. E. R. Deacon, *Proceedings, Commonwealth Oceanographic Conference, 1954, National Oceanographical Council, Cambridge Univ. Press, England, 1955*, p. 6.

⁵⁹ Prof. of Hydr. Eng., Univ. of California, Berkeley, Calif.

⁶⁰ "Wind Waves at Sea, Breakers and Surf," by Henry B. Bigelow and W. T. Edmondson, *H.O. Publication No. 602*, Hydrographic Office, U. S. Dept. of the Navy, Washington, D. C., 1947.

⁶¹ "Shore Protection Planning and Design," *Technical Report No. 4*, Beach Erosion Board, Corps of Engrs., U. S. Dept. of the Army, Washington, D. C., 1954, Chapter 1.

⁶² "Graphical Approach to the Forecasting of Waves in Moving Fetches," by B. W. Wilson, *Technical Memorandum No. 73*, Beach Erosion Board, Corps of Engrs., U. S. Dept. of the Army, Washington, D. C., 1955.

⁶³ "Revision in Wave Forecasting: Deep and Shallow Water," by C. L. Bretschneider, *Proceedings, 6th Conference on Coastal Eng., Berkeley, Calif., 1958*, Chapter 3.

⁶⁴ "A Statistical Study of Wave Conditions at Five Open Sea Localities along the California Coast," *Wave Report No. 63*, Scripps Institution of Oceanography, La Jolla, Calif., July 1, 1947.

of Mexico,^{65, 66, 67, 68, 69, 70} the Great Lakes region,^{71, 72, 73} and the North Atlantic seaboard.^{17, 74, 75, 76} Less accurate in detail, but of considerable value for preliminary analyses, is the frequency of wave conditions in the principal ocean areas of the world as presented by Bigelow and Edmondson.⁶⁰ The latter summaries present the distribution of high seas and high swells for the principal ocean areas of the world for various months. The characteristics of the winds producing these wave conditions also are examined.

An example of wind and wave conditions at a given site is shown in Fig. 4(c). The reversal of drift at Madras Harbor is shown to be the result of monsoons approaching the coast line from a southwest direction at one season of the year and from the northeast at another season. Madhav Manohar,⁷⁷ J. M. ASCE, studied the wind systems on the Indian coast and their effect on the littoral drift at Madras and other South Indian ports. In general, only a careful study of meteorological conditions for a particular site yields information on the wave conditions determining the littoral-drift movement. Walter H. Munk and Melvin A. Traylor⁷⁸ conducted a study of the typical meteorological occurrences in the widely separated areas of the Pacific Ocean that give rise to the characteristics of waves on the Pacific coast of the United States, with special reference to those at La Jolla, Calif. Along the Southern California coast, the predominant drift is in a southern direction and is caused by both seas and swell from the northwest. The reversal observed during the summer months is the result of the swell from the southern hemisphere. Mr. Silvester's statement that it is " * * the rule rather than the exception that storm waves approach a coast from a different direction from the predominant swell" is somewhat misleading, as a critical analysis of wave statistics will demonstrate.

⁶⁵ "Wave Statistics for the Gulf of Mexico off Brownsville, Texas," by C. L. Bretschneider and R. D. Gaul, *Technical Memorandum No. 55*, Beach Erosion Board, Corps of Engrs., U. S. Dept. of the Army, Washington, D. C., September, 1956.

⁶⁶ "Wave Statistics for the Gulf of Mexico off Caplen, Texas," by C. L. Bretschneider and R. D. Gaul, *Technical Memorandum No. 86*, Beach Erosion Board, Corps of Engrs., U. S. Dept. of the Army, Washington, D. C., September, 1956.

⁶⁷ "Wave Statistics for the Gulf of Mexico off Burrwood, Louisiana," by C. L. Bretschneider, and R. D. Gaul, *Technical Memorandum No. 87*, Beach Erosion Board, Corps of Engrs., U. S. Dept. of the Army, Washington, D. C., October, 1956.

⁶⁸ "Wave Statistics for the Gulf of Mexico off Apalachicola, Florida," by C. L. Bretschneider and R. D. Gaul, *Technical Memorandum No. 88*, Beach Erosion Board, Corps of Engrs., U. S. Dept. of the Army, Washington, D. C., October, 1956.

⁶⁹ "Wave Statistics for the Gulf of Mexico off Tampa Bay, Florida," by C. L. Bretschneider and R. D. Gaul, *Technical Memorandum No. 89*, Beach Erosion Board, Corps of Engrs., U. S. Dept. of the Army, Washington, D. C., October, 1956.

⁷⁰ "Hurricane Wave Statistics for the Gulf of Mexico," by B. W. Wilson, *Technical Memorandum No. 98*, Beach Erosion Board, Corps of Engrs., U. S. Dept. of the Army, Washington, D. C., June, 1957.

⁷¹ "Wave and Lake Level Statistics for Lake Michigan," by T. Saville, Jr., *Technical Memorandum No. 36*, Beach Erosion Board, Corps of Engrs., U. S. Dept. of the Army, Washington, D. C., 1953.

⁷² "Wave and Lake Level Statistics for Lake Erie," by T. Saville, Jr., *Technical Memorandum No. 37*, Beach Erosion Board, Corps of Engrs., U. S. Dept. of the Army, Washington, D. C., 1953.

⁷³ "Wave and Lake Level Statistics for Lake Ontario," by T. Saville, Jr., *Technical Memorandum No. 38*, Beach Erosion Board, Corps of Engrs., U. S. Dept. of the Army, Washington, D. C., 1953.

⁷⁴ "North Atlantic Coast Wave Statistics, Hindcast," by C. L. Bretschneider, *Technical Memorandum No. 66*, Beach Erosion Board, Corps of Engrs., U. S. Dept. of the Army, Washington, D. C., November, 1954.

⁷⁵ "Revised Sverdrup-Munk Method," by T. Saville, Jr., *ibid.*

⁷⁶ "North Atlantic Coast Wave Statistics by the Wave Spectrum Method," by G. Neumann and R. W. James, *Technical Memorandum No. 67*, Beach Erosion Board, Corps of Engrs., U. S. Dept. of the Army, Washington, D. C., 1955.

⁷⁷ "Sediment Movement at South Indian Ports," by Madhav Manohar, *Proceedings*, 6th Conference on Coastal Eng., Council on Wave Research, Berkeley, Calif., 1958, Chapter 22.

⁷⁸ "Refraction of Ocean Waves: A Process Linking Underwater Topography to Beach Erosion," by W. H. Munk and M. A. Traylor, *Journal of Geology*, Vol. 55, No. 1 1947, pp. 8-10.

Mr. Silvester questions the value of 0.025 for the critical steepness at which the characteristics of the bottom change near the shore. However, he does not state whether he believes that the value is too low, too high, or a variable. An examination of the observations on wave conditions and beach changes by Robert L. Wiegel, Donald A. Patrick, and Harold L. Kimberly⁷⁹ on a natural beach would indicate that the value of 0.025 obtained in laboratory studies may be higher than that occurring in nature. Nevertheless, additional field data are necessary to establish more accurately this critical value.

Nearshore sediment movement, which has been described elsewhere,⁸⁰ consists of movement by suspension and rolling in the turbulent region of the surf zone, and possibly by turbulent forces at fairly great depths seaward of the shore line. Apparently, the latter turbulent forces from wave action are great enough to cause a general alongshore sand movement to depths as great as 170 ft.⁸¹ Although some oceanic currents may be sufficiently strong to transport sand along the sea bottom, the primary sediment-transport mechanism in deep water appears to be the result of turbulence due to the oscillatory motion at the sea bed by surface waves. Sediment in temporary suspension as a result of such turbulence then may be transported along the sea bottom and possibly around headlands. The foregoing is due to either or both of the following forces: (a) An oceanic current, or (b) the forward velocity of the water under the wave crests, which exceeds the backward velocity under the trough, thus causing a net transport in the direction of the wave travel.⁸² Four rather comprehensive investigations of fundamental sand-movement mechanics by oscillatory waves have been made by Huon Li,⁸³ Manohar,⁸⁴ George Kalkanis,⁸⁴ and Vincent.⁸⁵ A summary of the results of these studies is beyond the scope of this discussion. However, it should be understood that because of the action of surface waves there are initial and general movements of sediment as well as the initiation, various developmental stages, and complete disappearance of bed undulations or ripples. Sediment movement takes place in a boundary layer that is developed at the sea bottom from the effects of the fluid viscosity. The initial and general motion of small sediment sizes is caused by laminar shear. Similar motions of large sediment sizes are caused by lift forces in a turbulent boundary layer. In general, ripples are not formed unless the flow is turbulent in the boundary layer. All motion in turbulent flow and the various stages of ripple development are functions of a dimensionless function representing the intensity of flow of the fluid near the bottom.⁸⁴

⁷⁹ "Wave, Longshore Current, and Beach Profile Records for Santa Margarita River Beach, Oceanside, California, 1949," by R. L. Wiegel, D. A. Patrick, and H. L. Kimberly, *Transactions, Am. Geophysical Union*, Vol. 35, December, 1954, pp. 887-896.

⁸⁰ "Dynamics of Nearshore Sediment Movement," by J. W. Johnson, *Bulletin, Am. Assn. of Petroleum Geologists*, Vol. 40, 1956, pp. 2211-2232.

⁸¹ "Wave Generated Ripples in Nearshore Sands," by D. L. Inman, *Technical Memorandum No. 100*, Beach Erosion Board, Corps of Engrs., U. S. Dept. of the Army, Washington, D. C., October, 1957.

⁸² "Shallow-Water Sediment Shifting Processes along the Southern California Coast," by U. S. Grant and F. P. Shepard, *Proceedings, 6th Pacific Science Cong. of Pacific Science Assn., Berkeley, Calif.*, Vol. 2, 1959, pp. 801-805.

⁸³ "Stability of Oscillatory Laminar Flow along a Wall," by H. Li, *Technical Memorandum No. 47*, Beach Erosion Board, Corps of Engrs., U. S. Dept. of the Army, Washington, D. C., 1954.

⁸⁴ "Turbulent Flow near an Oscillating Wall," by George Kalkanis, *Technical Memorandum No. 97*, Beach Erosion Board, Corps of Engrs., U. S. Dept. of the Army, Washington, D. C., July, 1957.

⁸⁵ "Contribution to the Study of Sediment Transport on a Horizontal Bed Due to Wave Action," by G. E. Vincent, *Proceedings, 6th Conference on Coastal Eng., Council on Wave Research, Berkeley, Calif.*, 1958, pp. 326-355.

Mr. Silvester states that the motion on the sea bottom beyond the surf zone is by saltation. If this term is used in the same sense that it has been used in sediment transport in streams since 1914,⁸⁶ the statement that this factor is "the most important factor in littoral-drift processes" is in error. The analysis by Anton A. Kalinske, M. ASCE, of a criterion for determining sand transport by surface creep and saltation⁸⁷ demonstrated conclusively that movement by saltation in flowing water is of minor importance. That is, "the height of grain-rise in the saltation-phenomena in water will be of the order of 1/1000 of that in air, or for most practical conditions, a few grain-

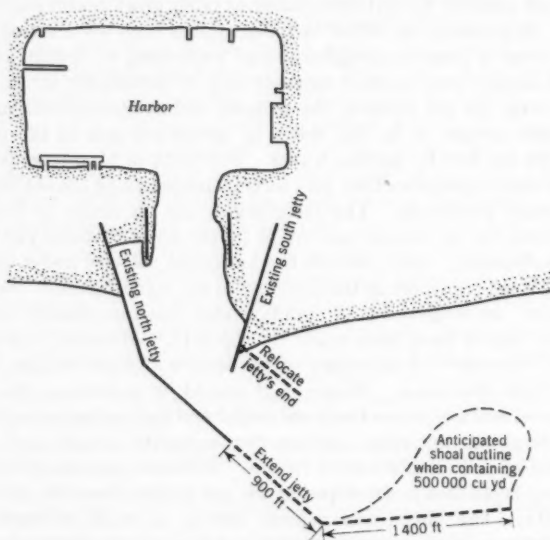


FIG. 12.—PROPOSED CHANGES TO CAMP PENDLETON HARBOR, CALIFORNIA, JETTIES TO PROVIDE A PROTECTED STOCKPILE AREA FOR SAND BYPASSING

diameters." The writer suggests therefore that the term saltation should not be used in connection with littoral-drift problems.

The movement of sand from offshore areas depends on the hydrography and predominant wave conditions. Attempts to nourish an eroded shore line by dumping material a short distance offshore by hopper dredge, on the assumption that the material would be moved onshore by wave action, has met with incomplete success.⁸⁸ For example, in such an operation at Long Branch,

⁸⁶ "Transportation of Debris by Running Water," by G. K. Gilbert, *Professional Paper No. 86*, Geological Survey, U. S. Dept. of the Interior, Washington, D. C., 1914.

⁸⁷ "Criteria for Determining Sand-Transport by Surface-Creep and Saltation," by A. A. Kalinske, Pt. II, *Transactions*, 23d Annual Meeting, Am. Geophysical Union, 1942, pp. 639-643.

⁸⁸ "Beach Rehabilitation by Fill and Nourishment," by Jay V. Hall, Jr., and George M. Watts, *Transactions*, ASCE, Vol. 122, 1957.

N. J., it was concluded that over a four-year period no material moved ashore from the stockpile nor did the shore benefit from the operation.⁵⁹

Mr. Silvester cites studies^{52, 53} at Portland Harbor, Australia, made to determine the path of sediment movement by tracer minerals. The sediments appeared to follow smooth paths somewhat identical to the orthogonals to the wave fronts. However, there is no evidence in these studies that sufficient samples were taken frequently enough to establish that the material moved around the harbor area in the indicated manner.

Mr. Silvester had difficulty in envisaging "the necessity of bypassing material in both directions at different times of the year." The writer believes that there are less expensive methods of keeping open a relatively narrow harbor entrance where important reversals in littoral drift occur. An excellent example of where the reversal in direction of bypassing sand could be practiced is the Camp Pendleton harbor shown in Fig. 12. The rate of drift, reversal of drift, width of opening, and tidal prism are such that navigable depths in the entrance channel cannot be maintained without continuous bypassing (in one direction or the other), or by continuous dredging in the channel itself. What appears to be a less expensive procedure for maintaining this harbor in an operational condition is realining the jetties, as proposed by the Corps.

In 1957 it was stated:

"Principal features of this plan would be to modify the jetties and develop a sand-bypassing operation that would be adequate to maintain navigable depths in the entrance to the harbor. The purpose of the jetty modification would be to cause deposit of littoral drift in a protected area behind the extended north jetty from which it could be readily removed by floating plant and deposited along the shore at Oceanside."⁶⁰

The predominant southerly drift is expected to accumulate as shown in Fig. 1. The northerly drift resulting from the southern swell will also deposit in a protected area, where it also can be removed periodically by a floating dredge.

⁵⁹ "Restudy of Test-Shore Nourishment by Offshore Deposition of Sand, Long Branch, New Jersey," by R. L. Harris, *Technical Memorandum No. 62*, Beach Erosion Board, Corps of Engrs., U. S. Dept. of the Army, Washington, D. C., November, 1954.

⁶⁰ "Oceanside, Ocean Beach, Imperial Beach, and Coronado, San Diego County, California," *House Document No. 399*, 84th Cong., 2d Session, Beach Erosion Control Study, Corps of Engrs., U. S. Dept. of the Army, Washington, D. C., 1957, p. 46.

AMERICAN SOCIETY OF CIVIL ENGINEERS

Founded November 5, 1852

TRANSACTIONS

Paper No. 2993

TESTS TO EVALUATE CONCRETE PAVEMENT SUBBASES

BY LAWRENCE D. CHILDS,¹ BERT E. COLLEY,² AND
JOE W. KAPERNICK,³ A. M. ASCE

SYNOPSIS

The contribution of subbases under concrete pavements to the strength of the roadway structure was evaluated by load-testing concrete panels built on five different foundations. Plain concrete slabs were cast and instrumented on the foundations to register the strains in the concrete, the panel deflections, and the vertical pressures at the slab-subbase interface and subbase-subgrade interface. Static loads were applied to the panels at the corners, edges, and interiors. The data obtained from tests made when the panels were fully in contact with the supporting soil showed the extent to which the granular subbases contributed to the strength of the pavement structure.

An analysis was made, based on measured load-strain relationships and load-deflection relationships under edge loadings and on close-fitting theoretical curves. Measured strains and deflections generally exhibited reasonable agreement with theoretical values that were computed using the Westergaard theory. However, in many cases, measured values were more sensitive to changes in subgrade support than is indicated by the theory.

INTRODUCTION

Since 1922 there have been many experimental and theoretical field studies of concrete pavement design. Among them were the "Bates Road Test," (1)⁴ the "Arlington" tests of the Bureau of Public Roads, United States Department of the Interior (2), the analyses of H. M. Westergaard (3), the "Lockbourne" tests of the Corps of Engineers, United States Department of the

NOTE.—Published, essentially as printed here, in July, 1957, in the Journal of the Highway Division, as *Proceedings Paper 1297*. Positions and titles given are those in effect when the paper was approved for publication in *Transactions*.

¹Senior Development Engr., Research and Development Laboratories, Portland Cement Assn., Skokie, Ill.

²Development Engr., Research and Development Laboratories, Portland Cement Assn., Skokie, Ill.

³Paving Engr., Chicago Dist. Office, Portland Cement Assn., Chicago, Ill.

⁴Numerals in parentheses—thus: (1)—refer to corresponding items in the Bibliography (see Appendix).

Army (4) (5), and "Road Test One-Md" (6). Important contributions also have been made by universities and highway departments.

Concrete pavements are designed primarily from the results of these studies. The Westergaard theory is the dominant influence in design. Ordinarily it is used with slight modifications because of the tendency for concrete panels to curl away from the foundation materials. Design methods based on the assumption of elastic layered systems have been considered seriously but have not been accepted readily because of their complexity and their lack of experimental confirmation.

A principal problem associated with the economical design of concrete pavements to withstand heavy axle loads is the effect of subbases on pavement performance. Subbases are required in areas in which the subgrade may be susceptible to pumping or weakened severely by melting frost. In pumping, fine-textured subgrade soils become suspended in water and are pumped from under the slab by the action of heavy traffic. Thus, subgrade support is reduced in local areas, and nonuniformity in bearing occurs. To correct this situation and, in some cases, to improve the load-carrying capacity of the foundation, subbases, usually of granular materials, are built on the subgrade. The subbase thickness varies from 3 in. to 12 in., or more. Experimental roads were built in Indiana (1949) and Ohio (1952) and tests have been made for the effect of thickness on highway performance, particularly from the standpoint of preventing pumping.

A layer of well-compacted granular material is inherently capable of supporting a load. Thus, a subbase built on a fine-grained subgrade primarily for pumping control also contributes directly to the pavement strength if the subbase is compacted properly to prevent further densification.

In this investigation performance criteria will be developed for evaluating the strength contributions made by subbases to the pavement structure. The data will aid in determining whether a subbase thicker than that required to prevent pumping is structurally economical. Ultimately, the tests will permit the development of concrete-slab-thickness relationships to subbase-thickness relationships that will enable the selection of the most economical and effective design for a particular traffic condition.

Scope of the Program.—The tests were made with 6-in.-deep, 10-ft-by-15-ft concrete panels built on dense-graded sand and gravel subbases. The data supplement available information on the Westergaard equations for computing strains and deflections in pavements.

It is recognized that an unrestrained, flat concrete panel is not equivalent to a highway slab that is restrained at both ends by dowels and possible end thrust and that is subject to vertical movement caused by curl. However, the results from the laboratory controlled tests are being correlated with field tests on highways in service to obtain supplementary material for evaluating subbases in actual use.

The foregoing report includes tests of one slab built on a dense sand and gravel subgrade and of another built on a clay subgrade. The two extreme conditions of subgrade support were selected to show the limiting values of deflections, pressures, and slab strains between which values for other slabs

constructed with subbases would probably lie. Data are also reported on slabs supported on 3-in., 6-in., and 12-in. sand and gravel materials placed on the clay subgrade.

Specific Objectives of the Program.—The investigation has the following specific objectives:

1. To determine the effect of subbase thickness on the load-carrying capacity of the slab;
2. To investigate the effect of subbases in distributing pressures to the subgrade;
3. To obtain data for establishing relationships between slab thickness and subbase thickness to effect pavement-design economy when strong foundations are specified; and

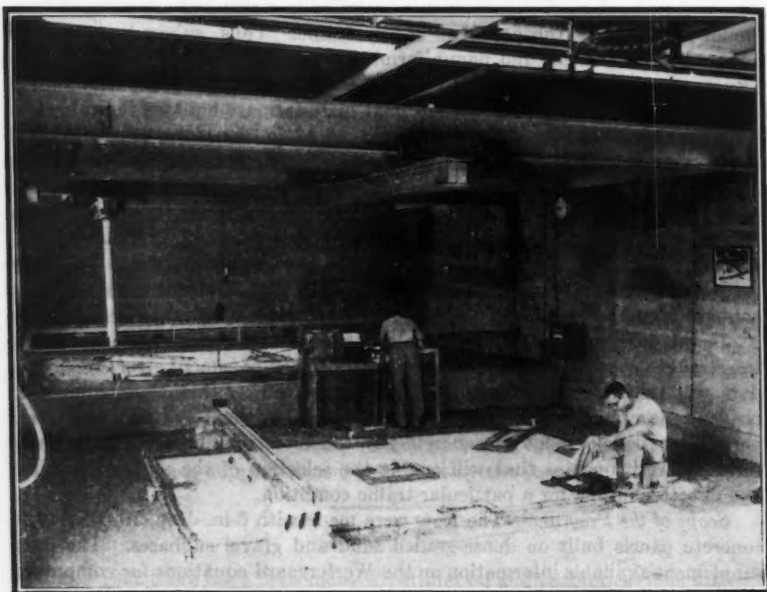


FIG. 1.—GENERAL VIEW OF TEST AREA

4. To compare experimental load-strain-deflection relationships with those computed in accordance with the theory that deflection is proportional everywhere to pressure.

TEST METHODS AND MATERIALS

Facilities.—The 24-ft-by-37-ft test area contained two concrete panels enclosed in a building equipped with thermostatically controlled heaters, providing a uniform temperature during the heating season. The area was

excavated 4 ft below grade to the bottom of the wall footings, and a 5-in. reinforced-concrete floor was cast. An expansion strip was installed to separate the floor from the walls, thus assuring that the floor would transmit stresses readily to the soil below. A shielded, membrane waterproofing treatment was applied to the floor and walls to protect the subgrade from moisture changes.

The area was separated into two 18-ft-by-24-ft test pits by a 6-in. wooden partition. The pits were filled then with subgrade soils to depths of 4 ft and 5 ft. Shoulders approximately 4 ft wide surrounded the 10-ft-by-15-ft test panels.

The subgrade depth was selected on the basis of studies by Gerald Pickett (7). The data obtained showed that a subgrade depth equal to twice the radius of the relative stiffness of the roadway structure would result in panel strains 95% as great as if the depth were five times this radius, and in deflections

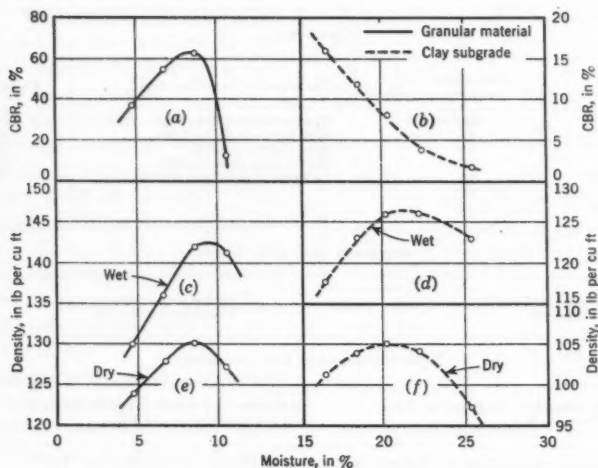


FIG. 2.—DENSITY AND CBR-VALUE VERSUS MOISTURE

80% as great. The radius of relative stiffness ranged from 24 in. to 30 in. Thus, a test pit from 4 ft deep to 5 ft deep was adequate.

The test area is shown in Fig. 1. The reaction beams are seen overhead with the loading column and the longitudinal trusses to support the deflection bridge in the background. The main girders were 14-in. WF beams, suspended below which were 8-in. transverse beams. Trolleys at each end of the latter beams permitted them to be placed above all parts of the working area. A third trolley traveled along the transverse beam, from which was suspended a pipe column to which a hydraulic jack was attached. The dikes on the panels retain water in order to maintain slabs in a flat condition.

Materials.—One test pit was filled to a depth of 4 ft with a high-bearing-value sand and gravel. The other pit was filled 5 ft deep with a low-bearing-

value clay. Some of the granular material used in the first pit was moved later to the second pit to form a subbase over the clay.

Granular Subgrade and Subbase Material.—The granular subgrade and the subbases were built with a bank-run sand and gravel that was modified at placement by the addition of stripping soil and a small quantity of coarse gravel. Gradation and subgrade soil constants of this material are shown in Table 1. Moisture-density relationships according to AASHO designation T99-57 and unsoaked CBR-values (8) are shown in Fig. 2. These tests indicate that the CBR-value was greater than 50 when the material was compacted near optimum moisture and maximum density.

TABLE 1.—GRADATION AND LIMITS OF SUBGRADE AND SUBBASE MATERIALS

Granular material		Clay material	
GRADATION			
Sieve	Percentage passing	Particle size, in millimeters	Percentage
$\frac{3}{4}$ in.	100	Coarse sand—2.0 to 0.42	4
$\frac{3}{8}$ in.	83	Fine sand—0.42 to 0.074	16
$\frac{1}{4}$ in.	79	Silt—0.074 to 0.005	40
No. 4	69	Clay—(less than 0.005)	40
No. 10	53	Colloids—(less than 0.001)	20
No. 40	30
No. 200	12
SUBGRADE SOIL CONSTANTS			
Liquid limit—23 Nonplastic ...		Liquid limit—48 Plasticity index—24	
MOISTURE-DENSITY RELATIONSHIPS*			
Maximum dry density, ^b 131 lb per cu ft Optimum moisture, ^b 8.5%		Maximum dry density, 105 lb per cu ft Optimum moisture, 20.4%	

* "Standard Specifications for Highway Materials and Method of Sampling and Testing," Part II, A.A.S.H.O., 7th Ed., 1958, Designation T99-57.

^b Includes from No. 4 to $\frac{1}{4}$ aggregate in the test specimen.

* "Standard Specifications for Highway Materials and Method of Sampling and Testing," Part III, A.A.S.H.O., 7th Ed., 1958, Designation T99-57.

^b Includes from No. 4 to $\frac{3}{4}$ aggregate in the test specimen.

The material for the deep granular subgrade was placed in 6-in. lifts and compacted at a moisture content slightly below optimum to approximately 96% maximum density by a combination of tamping and vibrating.

Control tests on each 1-ft sand and gravel layer included in-place density and moisture tests. The modulus of subgrade reaction, k , was determined by bearing plates. The tests were made with 12-in.-diameter plates, 24-in.-diameter plates, and 30-in.-diameter plates. The control data are cited in Table 2(a), and Fig. 3(a) shows plate-bearing values. In Fig. 3 the ratio of the plate perimeter to the area is P/A and the plate deflection is 0.05 in.

Clay Subgrade Soil.—Table 1 shows the gradation and plasticity characteristics of the clay soil. The associated moisture-density relationships and the CBR-values are exhibited in Fig. 2. The soil was prepared by spreading it on

a concrete apron, breaking it up with a rotary tiller, and mixing it with sufficient water to attain a moisture of approximately 23.5%. According to Fig. 2(b), the soil had a CBR-value of about 2.5 when it was tested at the foregoing moisture content. It was compacted then with the tamping rammer in lifts of from 4 in. to 6 in. and to a depth of 5 ft.

To assure reasonable uniformity, in-place density and moisture tests and plate-bearing tests were made on each 1-ft layer. The results of the control tests are shown in Table 2(b). Plate-bearing-value data are plotted in Fig. 3(c). Although the control value, k , on layer No. 5 was 65 lb per cu in., this value became 100 lb per cu in. at the outset of the routine tests. Some time elapsed between the completion of subgrade construction and the beginning of routine because of pilot studies for developing test techniques. The resulting moisture loss contributed to the increase in the k -value. Moisture barriers prevented further changes.

Subbases.—After the concrete-panel test was completed on the deep clay subgrade, sand and gravel subbases were built on the soil. They were placed in compacted thicknesses of 3 in., 6 in., and 12 in. Moisture, density, and plate-bearing tests results are given in Table 2(c), and plate-bearing-test data are plotted in Fig. 3(b).

Concrete Panels.—The dimensions of all slabs were 10 ft by 15 ft by 6 in. Natural sand and gravel aggregates from one source were used. The sieve analyses are shown in Table 3. The cement factor for the concrete was 6 sacks per cu yd, the water-cement ratio by weight was 0.48, air content was approximately 5%, and the slump was approximately 3 in. The concrete was placed in 6-cu-ft batches, carefully vibrated around the instrumentation, and surface compacted with a vibrating screen. Standard 6-in.-by-12-in. cylinders, 6-in.-by-6-in.-by-36-in. beams, and special 12-in.-by-6-in.-by-42-in. beams were cast during the placing of the mix. The concrete panel and the large beams, which were cast on the subgrade adjacent to the panel, were cured under wet burlap for fourteen days. The other test specimens were cured in steel molds overnight and placed in a fog room until tested.

The cylinders and the 6-in.-by-6-in. beams were tested by the sonic method at several ages to determine the elastic modulus, E . Then they were broken in compression and flexure. The 6-in.-thick-by-12-in.-wide beams were sub-

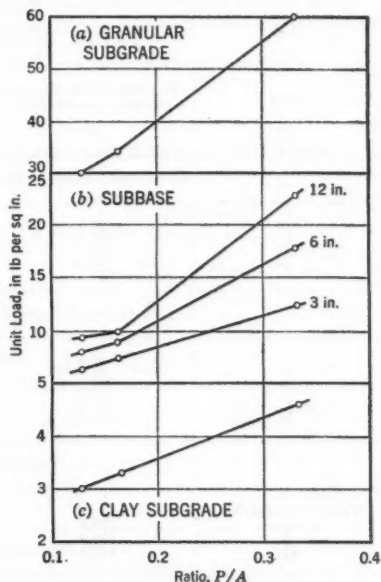


FIG. 3.—PLATE-BEARING TESTS

jected to the same curing as the slabs, and were tested in place with a device that applied loads at the third points. Table 4 records typical concrete test data.

Instrumentation and Equipment.—Instrumentation was provided to compare pressure, strain, and deflection relationships at various loads. The soil moisture, slab and soil temperatures, and curling deformation of the slabs were also measured.

Pressure-Cell Instrumentation.—Pressures directly under the slab and at the subbase-subgrade interface were determined with stress meters (9). The meters were installed with the sensing elements upward. To obtain uniform distribution of pressure on the meter, mortar was used to bed a $\frac{3}{4}$ -in.-thick,

TABLE 2.—CONTROL TESTS

Layer (1)	In-place dry density, in pounds per cubic foot (2)	Moisture content, in percentage (3)	K, in pounds per cubic inch ^a (4)
(a) CONTROL TESTS ON SAND AND GRAVEL SUBGRADE			
1	126.5	8.3	672
2	127.5	7.8	622
3	124.0	7.4	575
4	126.8	7.3	573
(b) CONTROL TESTS ON THE CLAY SUBGRADE			
1	100.8	23.3	...
2	102.1	23.0	54
3	103.0	23.8	54
4	101.7	23.9	60
5	101.5	24.1	65
(c) TESTS ON SUBBASES			
Thickness, in inches			
3	128.8	7.5	120
6	129.2	7.7	145
12	131.9	7.8	170

^a 30-in. plate, 0.05 in. deflection.

9-in.-diameter steel disk on the soil. A neat cement paste was placed between the disk and the stress-meter diaphragm. An improved stress meter was obtained for some of the later tests, and the auxiliary disk was not necessary. The $7\frac{1}{2}$ -in. diaphragm plate on these meters was bedded with a thin mortar layer directly onto the soil.

For pressure measurement between the subbase and subgrade, the stress meters were installed in a mortar bed with the stem downward, and all air was excluded under the meter. Sponge-rubber weatherstripping material was wrapped around the circumference of the diaphragm to assure unrestricted action. A small quantity of neat cement paste was placed in the center of the stress-meter diaphragm. A $\frac{3}{4}$ -in.-thick steel disk of the same diameter as the

cell plate was pressed in place over the cell until paste was extruded completely around the circumference and there was reasonable certainty that the paste layer was free from voids. A 10-lb weight was placed on the disk to assure continuous contact during setting of the cement. Instrument constants were furnished by the manufacturer, and the calibration curve was test-checked after the stress meter had been installed to assure the proper response.

Fig. 4 shows the arrangement of pressure cells under the panels. Slabs 1 and 2 had no subbase and, hence, no subbase pressure cells. Cells 2, 4, and 12 were omitted in slabs 3, 4, and 5. In Fig. 4(a), Nos. 1 to 8 indicate cells at the slab-subbase interface, and Nos. 11 to 18 denote cells at the subbase-subgrade interface.

Strain-Gage Instrumentation.—Surface strain measurements on top of the slab were satisfactory for determining critical stresses in concrete panels when

TABLE 3.—
CONCRETE
AGGREGATE
GRADATION

Sieve (1)	Percentage Passing (2)
(a) COARSE AGGREGATE	
1 in.	100
3/4 in.	89
3/8 in.	71
20 in.	48
(b) FINE AGGREGATE	
No. 4	98
No. 8	86
No. 16	68
No. 30	44
No. 50	21
No. 100	4

TABLE 4.—CONCRETE-PROPERTIES TEST DATA

Specimen (1)	Age, in days (2)	Strength, in Pounds Per Square Inch		E, in pounds per square inch × 10 ⁶ (5)
		Com- pression (3)	Flexure (4)	
6-in.-by-12-in. cylinders	{ 14	4,570	...	4.75
	{ 28	5,905	...	5.07
	{ 150	8,400	...	6.36
6-in.-by-6-in. beams	{ 14	...	610	5.12
	{ 28	...	680	5.75
	{ 150	...	1,030	7.85
6-in.-by-12-in. beams	{ 14	5.52*
	{ 28	6.57*
	{ 150	...	906	7.80*

* Indicates E by static deflection.

loads were applied at the corners. However, the measurements could not be used to determine critical tensile stress at other positions without assuming a uniform stress gradient and a constant neutral axis. Therefore, for this purpose a strain-measuring capsule (10) that was suitable for embedment in the panels was developed.

The housing for the strain capsule was steel tubing with a diameter of $\frac{1}{2}$ in. and a wall thickness of 0.05 in. An effective modulus was produced for the capsule that was less than twice that of the concrete. A 6-in. length yielded a length-to-radius ratio of 24. Two SR-4-type, A-12 gages were cemented longitudinally to the inner walls of the tube in diametrically opposed positions. The two gages were wired with a common ground, and the ground wire was soldered to a $\frac{3}{16}$ -in. copper tube, which housed the other two wires. The tube

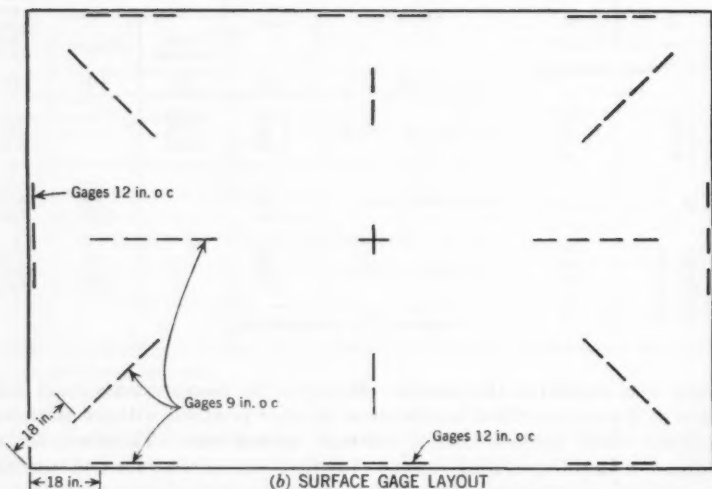
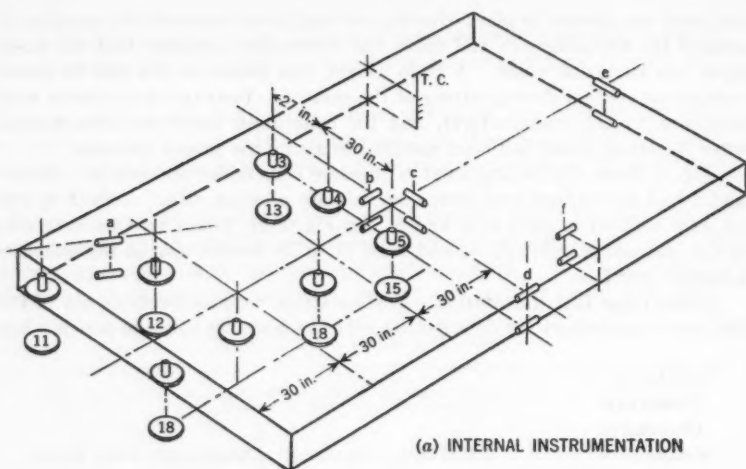


FIG. 4.—INSTRUMENTATION OF PANELS AND SUBBASES

was fastened to the capsule at the center of one of the turned steel plugs. After assembly, the unit was heat-cured, and the copper tube was plugged with a wax type of waterproofing compound. The strain capsules were supported above the subbase by wire frames to prevent the assembly from shifting while the concrete was being placed.

Surface strains were measured at several sites on the top surface of each panel. SR-4-type, A-9 gages were cemented to the concrete after the area had been prepared by grinding.

The sites of the embedded capsules and surface strain gages are shown in Fig. 4. The letters a to e indicate pairs of strain capsules near the slab surfaces, and the letter f represents the unbonded compensating strain capsules. The dimensions on the surface gage layout are representative and are not necessarily exact for all panels. During slab testing, satisfactory agreement was obtained between surface gage readings and the extrapolated values from the embedded capsules. Only in a few instances were the variations as great as 10%. Capsules in the bottom of the slab at the edge and interior yielded strain magnitudes averaging approximately 5% less than those in the top where a direct comparison was possible. Because the two methods of measuring strains agreed closely, only the data obtained with the SR-4 surface gages are reported.

The positions of the thermocouples, which were placed vertically throughout the slab to indicate temperature differences, are shown in Fig. 4(a), in which the term T.C. denotes a battery of four thermocouples.

Deflection Measuring Devices.—Deflections due to load were measured with 0.001-in. dial indicators supported by a wood bridge resting on longitudinal trusses fastened to the reinforced-concrete building walls. The stems of the dials contacted the slab surface on $\frac{3}{4}$ -in.-diameter, hardened-copper rivet heads embedded in a grid pattern in the concrete surface.

Loading Devices.—Loads were applied to the panels by 10-ton hydraulic jacks. The threaded top of the piston was fastened to a length of 3-in. pipe, which, in turn, was held in place by a flange fastened to the overhead trolley. A fitting adapted the bottom of the jack to a load cell (11), which was connected electrically to a strain indicator to show load intensity. A 70-sq-in. oval plate resting on a rubber pad was used to simulate a tire for wheel-load application.

TEST DETAILS AND RESULTS

Load-Deflection-Strain Relationships.—The data presented were obtained under "single-wheel" loading at four positions: (a) Interior loading at the center of each panel; (b) edge loading at the middle of a longitudinal, 15-ft-long edge; (c) corner loading; and (d) edge loading at the middle of a free transverse edge 10 ft long. In all cases, the long dimension of the loading area was parallel to the longitudinal center line of the panel. Two or three "seating" loads were applied before the deflections and strains were recorded. Repetitive loadings of as much as 100 cycles indicated that deflections were elastic and that replicate load tests checked closely within this range of repetitions. The test slabs are identified with the proper foundation *k*-values in Table 5(a).

Fig. 5 summarizes the maximum deflections and maximum strains measured under interior loads, longitudinal edge loads, and corner loads on flat slabs. The deflections caused by edge loads always lie between interior deflections and corner deflections. Strains due to edge loads are slightly greater than those due to corner loads except when small loads are applied.

The ratios of interior-to-edge deflections and strains and corner-to-edge deflections and strains were computed for 4-kip loads, 6-kip loads, and 8-kip

loads. Table 5(b) indicates the averages. The interior-to-edge deflection ratio remains constant at approximately 40% for all panels except slab 1. The corner-to-edge ratio decreases as the subbase thickness increases, indicating that in these tests corner deflections are affected more by subbases than interior deflections or edge deflections. The interior-to-edge strain ratio is slightly higher for slab 1 on the deep granular subgrade than for the other panels. However, at the corner the strain ratio is practically constant at 88% for all slabs.

Critical Load and Deflection.—A concrete pavement usually is designed so that the applied loads will produce stresses no greater than one-half the modulus of rupture of the concrete. A safe value for this design stress is 325 lb per sq in. This value is approximately equivalent to a strain of 54×10^{-6} in the concrete

TABLE 5.—SLAB AND FOUNDATION DATA

Slab number	(a) FOUNDATION DATA			(b) RELATIVE MAGNITUDES OF DEFLECTIONS AND STRAINS				(c) CRITICAL LOADS AND DEFLECTIONS			
	Depth of clay, in inches	Depth of gravel, in inches	k , in pounds per cubic inch ^a	Deflections, in % of Edge Value		Strains, in % of Edge Value		Critical Load, in Pounds		Critical Deflection, in Inches	
				Interior	Corner	Interior	Corner	Edge	Corner	Edge	Corner
(1)	(2)	(3)	(4)	(5)	(6)	(7)	(8)	(9)	(10)	(11)	(12)
1	0	48 ^b	600	35 ₁	160 ₁	60	88	7,000	8,300	0.011	0.021
2	60 ^b	0	100	41	240	47	85	4,500	5,300	0.014	0.042
3	60 ^b	3 ^c	120	40	246	51	91	4,700	5,400	0.014	0.040
4	60 ^b	6 ^c	145	41	190	46	86	5,000	5,800	0.013	0.030
5	60 ^b	12 ^c	170	41	190	53	88	5,800	6,700	0.013	0.030
Average	40	207	51	88

^a 30-in. plate, 0.05-in. deflection. ^b Subgrade. ^c Subbase.

panels. The deflections associated with strains of this critical magnitude may be termed critical deflections.

Loads that cause critical strains at the edges and corners of the test slabs and the critical deflections at these loads are listed in Table 5(c). As the subbase becomes thicker and as the value of k increases, the load that causes critical strain increases but the critical deflection decreases. For example, loads causing critical stress in slab 1 are more than 50% greater than those for slab 2, but the critical edge deflection for slab 2 is 27% higher than for slab 1, and the critical corner deflection is twice that of slab 1. Critical deflections in the corner region are more affected by the subbase thickness and corresponding changes in the value of k than are those at the edges.

Comparison of Experimental and Theoretical Values.—The prevailing theory for concrete pavement design was developed by Westergaard (3). His equa-

tions and modifications have been used to compute theoretical strains and deflections for comparison with the values measured in this investigation.

Development of Equations.—In 1926 Westergaard (3) developed equations for maximum stress and maximum deflection in concrete slabs, assuming that

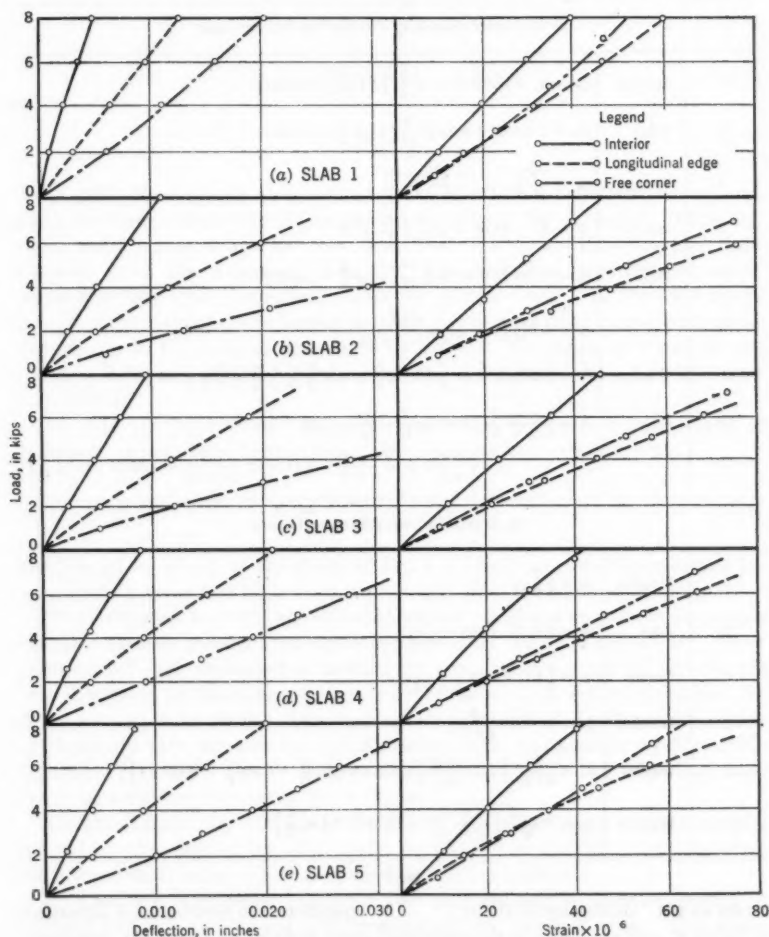


FIG. 5.—EXPERIMENTAL DEFLECTIONS AND STRAINS

reactive pressure under a slab is proportional everywhere to deflection. Westergaard postulated further that the proportionality factor was constant for a given subgrade. The foregoing assumptions are applicable if the soil behaves as a dense liquid. Accordingly, the Westergaard theory is referred to some-

TABLE 6.—DESIGN EQUATIONS

Number (1)	Location (2)	Equation (3)
(a) MAXIMUM STRESS, IN POUNDS PER SQUARE INCH		
1	Interior	$S_i = S_1 = 0.275 (1 + u) \frac{P}{h^3} \left(4 \log \frac{L}{B} + 1.069 \right)$
3	Edge	$S_e = 0.529 (1 + 0.54 u) \frac{P}{h^3} \left(4 \log \frac{L}{B} + 0.359 \right)$
5	Corner	$S_c = \frac{3P}{h^3} \left[1 + \left(\frac{r\sqrt{2}}{L} \right)^{0.4} \right]$
7	Interior	$S_i = S_1 - 15 (1 + u) \frac{P}{h^3} \left(\frac{L}{L_1} \right)^3 Z$
9	Edge	$S_e = 0.529 (1 + 0.54 u) \frac{P}{h^3} \left(4 \log \frac{L}{B} + \log B \right)$
10	Corner	$S_c = 4.2 \frac{P}{h^3} \left(1 - \frac{\sqrt{rL}}{0.925 L + 0.22 r} \right)$
11	Interior	$S_i = 0.275 (1 + u) \frac{P}{h^3} \left(4 \log \frac{L}{C} + 0.87 \frac{1-u}{1+u} \frac{a-b}{a+b} + 1.069 \right)$
13	Edge	$S_e = \frac{1+u}{3+u} \frac{P}{h^3} \left\{ 8.80 \log \frac{L}{C} - \frac{4u}{\pi} - 0.29 \right.$ $\left. + \frac{3}{\pi} \left[(1+u) \frac{a-b}{a+b} + 2 (1-u) \frac{ab}{(a+b)^2} + 1.18 (1+2u) \frac{b}{L} \right] \right\}$
(b) MAXIMUM DEFLECTION, IN INCHES		
2	Interior	$d_i = \frac{P}{8 k L^3}$
4	Edge	$d_e = 0.41 (1 + 0.4 u) \frac{P}{k L^3}$
6	Corner	$d_c = \left(1.1 - 1.24 \frac{r}{L} \right) \frac{P}{k L^3}$
8	Interior	$d_i = (1 - Z) \frac{P}{8 k L^3}$
12	Interior	$d_i = \frac{P}{8 k L^3} \left\{ 1 - \frac{0.183}{L^2} \left[(a^2 + b^2) \left(\log \frac{L}{C} + 0.159 \right) - 0.435 a b \right] \right\}$
14	Edge	$d_e = P \sqrt{\frac{2 + 1.2 u}{E h^3 k}} \left[1 - (0.76 + 0.4 u) \frac{b}{L} \right]$

times as the "dense liquid theory." The equations are numbered 1 through 6 in Table 6, and are listed in the simplified form derived by Royall D. Bradbury (12). In Table 6, the value of P is equal to the total load, in pounds; h represents the thickness, in inches; u denotes Poisson's ratio; r represents the radius of plate, with semiaxes a and b measured in inches; E is the elastic modulus of concrete, in pounds per square inch; Z denotes the deflection ratio; L_1 is a multiple of L ; and A is equal to the area of the soil supporting the load in square

inches. Using the data in Table 6,

$$L^4 = \frac{E h^3}{12 (1 - u^2) k} \dots \dots \dots (15)$$

$$k = \frac{P}{A d} \dots \dots \dots (16)$$

$$B = \sqrt{1.6 r^2 + h^2} - 0.675 h \dots \dots \dots (17)$$

and

$$C = \frac{a + b}{2} \dots \dots \dots (18)$$

In 1933 Westergaard (13) examined the effect of a redistribution of subgrade reactions under interior loads and developed Eqs. 7 and 8 (Table 6), which yield values somewhat less than Eqs. 1 and 2. Experimental data available from the Arlington tests (2), indicated that experimental stress values were less than theoretical values for interior loads. In the 1933 equations, Z is the ratio of the reduction in deflection as a result of the redistribution of pressures to the original deflections by Eq. 2. The limits of Z and L_1 are $0 < Z < 0.39$ and $L < L_1 < 5 L$. For the Arlington tests, $Z = 0.05$ and $L_1 = 1.75 L$.

In 1935 the interior-load equations were modified further in a study of stresses in airport pavements (14). The following term was derived:

$$S_2 = \frac{3 (1 - u) P}{64 h^2} \left(\frac{r}{L} \right)^2 \dots \dots \dots (19)$$

which must be added to the stress of Eq. 1. The correction is significant for large loading areas and high loads, but is negligible for highway loadings.

The Arlington tests (2) showed that strains measured at corners and edges indicated stresses greater than those computed by the 1926 equations. Then Westergaard (15) developed a method for computing stresses at corners not fully supported by the subgrade, but the method was not well received because of the estimates involved. An empirical modification of Eq. 5 was suggested by Bradbury (16), another by Earl F. Kelley (17), and another by Merlin G. Spangler, M. ASCE (18). Kelley also suggested that the edge equation, Eq. 3, be altered as shown in Eq. 9 (Table 6).

Gerald Pickett (19) compared the effects of the foregoing suggestions and derived another corner formula, shown in Table 6 as Eq. 10. This equation has a theoretical basis, but is simplified by approximation.

In 1943 the Westergaard analysis (20) was adapted to slabs supported in different fashions and loaded with areas other than circular ones. This study was the basis for new stress and deflection equations in airfield pavements (21), which appeared in 1947. Eqs. 11, 12, and 13 of Table 6 are the 1947 equations expressed in terms of L , and Eq. 14 in the table is reduced from the general form to yield the edge deflection.

Other methods for computing stresses based on the elastic theory were proposed by Pickett (7), A. H. A. Hogg (22), D. L. Holl (23), Donald M.

Burmister, M. ASCE (24), L. Fox (25), and R. J. Hank and Frank H. Scrivner, A. M. ASCE (26). These investigators assumed that the pavement structure was a multilayered, elastic solid. The equations are complex, and because they include soil "constants" not readily measured, they will not be considered herein.

Figs. 6, 7, 8, and 9 compare maximum strains and deflections of the five test panels with theoretical values computed using the Westergaard equations (or modifications). The numbers of the curves correspond to the equations in Table 6. Curves representing Eqs. 11 and 12 are not shown in Fig. 6 because,

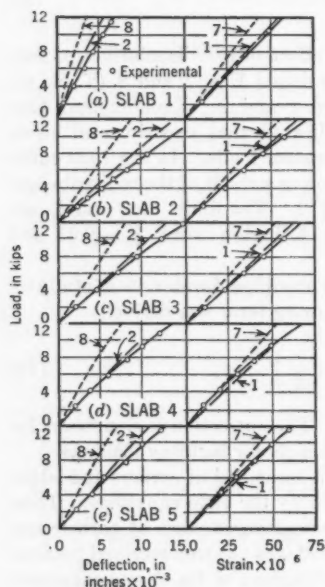


FIG. 6.—LOAD AT INTERIOR LOCATION

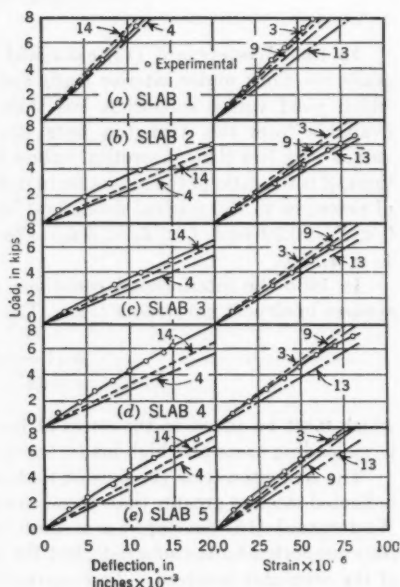


FIG. 7.—LOAD AT LONGITUDINAL EDGE

for the loadings being considered, the equations provide data essentially the same as do Eqs. 1 and 2.

Constants for the theoretical computations of strains and deflections were $h = 6$ in.; $a = 5.8$ in.; $b = 3.5$ in.; $r = 4.72$ in. (radius of a circle with area equal to that of the ellipse with semi-axes a and b); $u = 0.15$; and $E = 6,000,000$ lb per sq in. The elastic modulus selected was the interpolated value representing an average E -value for the concrete during the slab testing period of between 30 days and 60 days.

Conversion of Computed Stresses to Strain.—The equations of Table 6 yield stresses that were converted to strains in order to make the comparisons shown in Figs. 6, 7, 8, and 9. The conversion was performed as follows:

At interior locations the strains in the two principal directions were approximately equal. From the stress-strain relationship,

$$S_i = \frac{E}{1-u^2} (e_x + u e_y) \dots \dots \dots (20)$$

with $e_{\max} = e_x = e_y$, it can be shown that

$$e_{\max} = (1-u) \frac{S_i}{E} \dots \dots \dots (21)$$

At the edges it is assumed that stresses normal to the edge may be neglected, and the strain is the ratio of S_x to E . Along the corner diagonals the strain

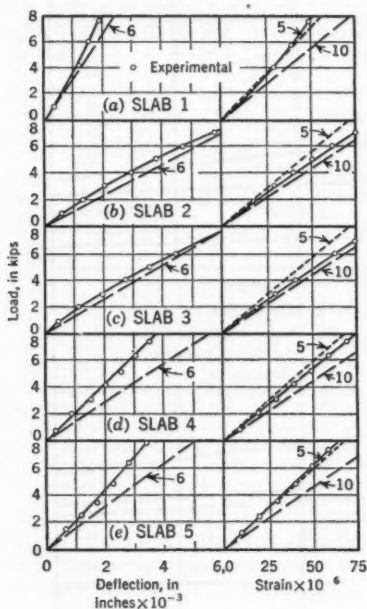


FIG. 8.—LOAD AT CORNER

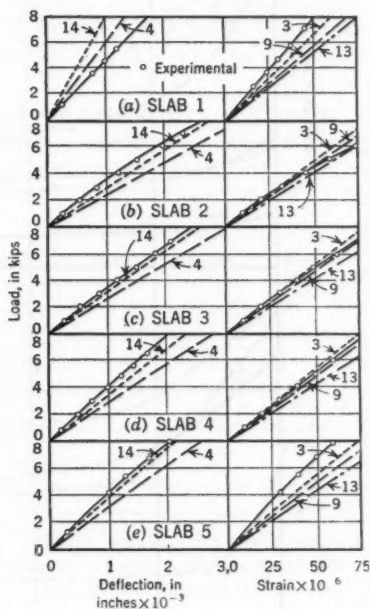


FIG. 9.—LOAD AT FREE TRANSVERSE EDGE

orthogonal to the maximum strain was found (18) to be approximately one-half the maximum strain but opposite in sign. The approximate maximum strain at the corner is

$$e_{\max} = \frac{2(1-u^2)}{2-u} \frac{S_c}{E} \dots \dots \dots (22)$$

which deviates from S_c/E by 6%.

Strain and Deflection Data.—Figs. 6, 7, 8, and 9 compare measured deflections and strains with computed values. In most cases the experimental curve approximates a line computed by one of the equations. However, a study of

the curves discloses that the equations do not reflect in all cases the variations in measured performance as the support conditions are altered.

Interior Loading.—The original 1926 equations of Westergaard (Eqs. 1 and 2) predict both deflections and strains accurately throughout the full range of subbase and subgrade conditions (from $k = 100$ to $k = 600$). The agreement in the measured strains and computed strains is excellent. In all cases com-

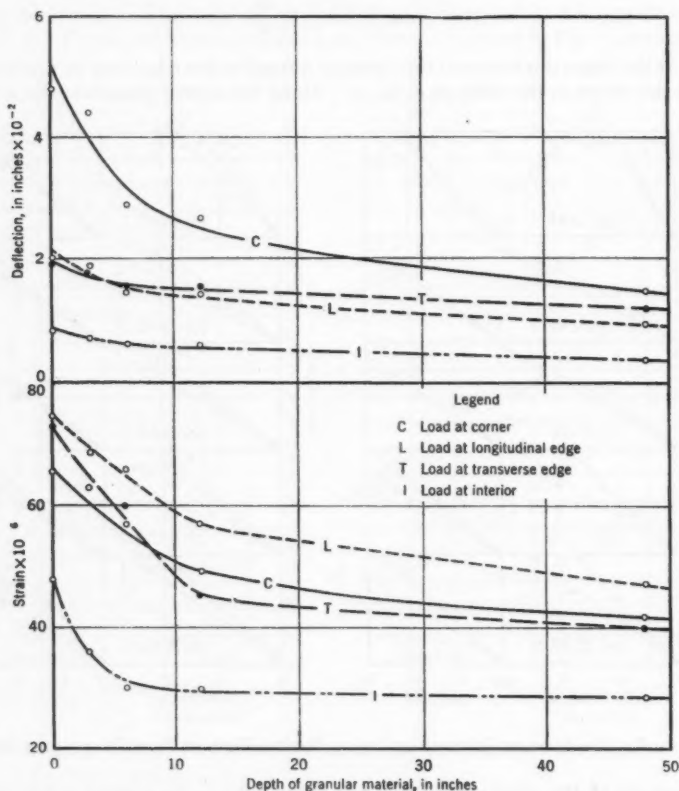


FIG. 10.—INFLUENCE OF GRANULAR-MATERIAL DEPTH ON PANEL DEFLECTIONS AND STRAINS

puted deflections are slightly less than measured deflections, but the measured effect of varying the foundation is represented accurately by the equations. The 1933 Westergaard strain equation (Eq. 7), in which $Z = 0.39$ and $L_1 = 5 L$, yields results that are less than the measured strains. The associated deflection equation (Eq. 8) yields theoretical deflections that also are less than measured values.

Edge Loading.—The equations considered for edge loading are derived for an infinitely long slab. The measured deflections for the 15-ft longitudinal transverse edges and the 10-ft transverse edges (Figs. 7, 8, and 9) agree except for the condition $k = 600$. At this value the deflection of the shorter edge is greater than that of the longer edge. The two edge lengths showed equal strains on the clay subgrade, but as the value of k was increased, the longer edge exhibited greater strains than the shorter edge.

The deflections at the longitudinal edge computed by use of Eq. 4 (the 1926 Westergaard equation) are greater in all cases than the measured deflections. The 1947 equation (Eq. 14) provides values that are slightly greater than those measured for the clay subgrade and for all subbase sections (from $k = 100$ to $k = 170$) and slightly less for the deep granular subgrade ($k = 600$). For strains the Westergaard 1947 equation (Eq. 13) agrees with the measurements for the lesser values of k , but the 1926 equation (Eq. 3) is in better agreement

TABLE 7.—REDUCTION IN DEFLECTIONS AND STRAINS DUE TO SUBBASES

Thick- ness of granular material, in inches	k , in pounds per cubic inch	REDUCTION IN PERCENTAGE OF VALUE ON CLAY ($k = 100$)											
		Deflection						Strain					
		Edge		Corner		Interior		Edge		Corner		Interior	
		W^a	X^b	W^a	X^b	W^a	X^b	W^a	X^b	W^a	X^b	W^a	X^b
(1)	(2)	(3)	(4)	(5)	(6)	(7)	(8)	(9)	(10)	(11)	(12)	(13)	(14)
48	600	59	56	64	71	59	57	20	37	19	37	17	20
12	170	24	33	26	52	24	30	6	25	5	26	5	19
6	145	17	27	18	38	17	27	4	13	3	17	4	17
3	120	9	14	10	25	8	15	2	8	2	9	2	11

^a Values computed from 1926 Westergaard equations.

^b Values computed from experimental results as plotted in Fig. 10.

for higher values of k . The 1933 Kelley equation (Eq. 9), which falls between the other two, represents closely the average condition. However, all three strain equations exhibit less response to changes in the value of k than do the measured strains.

Corner Loading.—The 1926 deflection equation (Eq. 6) agrees with the measurements for both the lesser k -values and the high values of k . However, the measured values are approximately 30% less for the intermediate k -values for 6-in. subbase sections and 12-in. subbase sections. The measured strains for corner loading, as shown also for edge loading, indicate greater response to variations in k than do the equations. Strains computed from the Westergaard 1926 stress equation (Eq. 5) agree satisfactorily for the higher values of k , but otherwise yield values that are lower than those measured. Eq. 10 was developed by Pickett for slabs having partial subgrade support. The equation provides values greater than those measured in all cases, and shows too little response to any variation in the k -value.

Effect of Subbase Thickness.—Data from Figs. 6, 7, 8, and 9 are plotted in Fig. 10 to indicate directly the effect of subbase thickness at the 6,000-lb load level. Although it is recognized that for other materials, even with the same k -values, the subbase-thickness effect might differ, significant indications are shown in Table 7 and are examined as follows:

1. Corner deflections are particularly sensitive to a subbase thickness of as much as 12 in. (or to variations in the k -value from 100 to 170). However, they are less sensitive to additional increases in subbase thickness or in the value of k . Within the test range the measured effect of subbase thickness from 0 in. to 12 in. on pavement corner deflections is significantly greater than

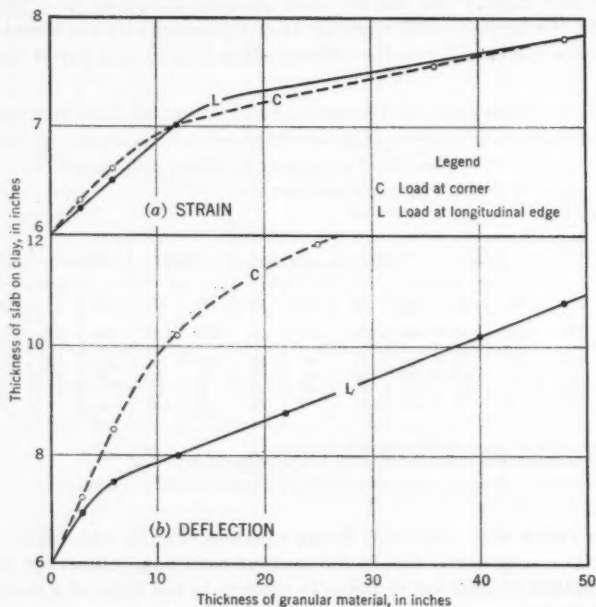


FIG. 11.—SLAB THICKNESS VERSUS DEPTH OF SUBBASE

the effect computed by the Westergaard equations. This is apparent from Fig. 8. According to the original Westergaard equations, a change in the k -value from 100 to 170 should reduce corner deflections by 26%. Fig. 10 indicates a reduction of approximately 50%.

2. Edge deflections and interior deflections are reduced approximately 55% by increasing the thickness of granular material to 48 in. (increasing the k -value from 100 to 600). About one-half of this beneficial effect is achieved with a subbase of 6 in. ($k = 145$). Some additional benefit is obtained with a subbase of 12 in. Such a reduction in deflection with a 6-in. subbase is more than that indicated by the Westergaard equations.

3. Maximum strains for edge and corner loading are reduced 37% by increasing the thickness of granular material to 48 in. Fig. 10 demonstrates that a subbase thickness of approximately 8 in. would develop about one-half of the maximum benefit possible. In terms of the k -value, an increase from 100 to approximately 150 was one-half as effective in reducing edge and corner strains as an increase from 100 to 600. For interior loading no significant strain reduction was shown for subbase thicknesses greater than 6 in.

Because deflections and strains can be reduced by thickening the concrete as well as by increasing subbase thickness, it is of economic importance to establish a relationship between slab thickness and depth of subbase to meet certain strain or deflection requirements. Curve B in Figs. 11(a) and 11(b) shows these relationships for 6-in. slabs supported by the materials used in the tests and loaded to 6 kips. Fig. 11(a) indicates the thickness of concrete on

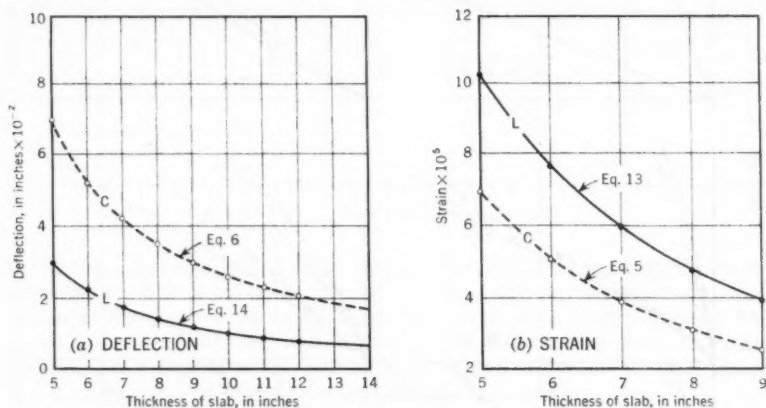


FIG. 12.—DEFLECTION VERSUS SLAB THICKNESS

clay that would deflect the same as a 6-in. slab on various subbase thicknesses. Fig. 11(b) shows the thickness of concrete on clay that produces the same strains as a 6-in. slab on various subbase thicknesses. The curves were derived as follows:

Curves in Figs. 12(a) and 12(b) express deflections and strains as functions of slab thickness on a clay subgrade at a 6-kip load. The curves were constructed from Eqs. 5, 6, 13, and 14 that previously agreed most satisfactorily with the test data. Experimental strains and deflections for 6-in. slabs as functions of subbase thickness, are shown in Fig. 10. For any subbase thickness in Fig. 10, a deflection or strain was selected, and adjusted by the difference between experimental and theoretical values for no subbase, to enter the curves in Figs. 12(a) and 12(b) to determine the thicknesses of a slab on clay at $k = 100$ in order to yield the particular deflection or strain. These relationships between subbase thickness and slab thickness furnished points for the curves in Figs. 11(a) and 11(b).

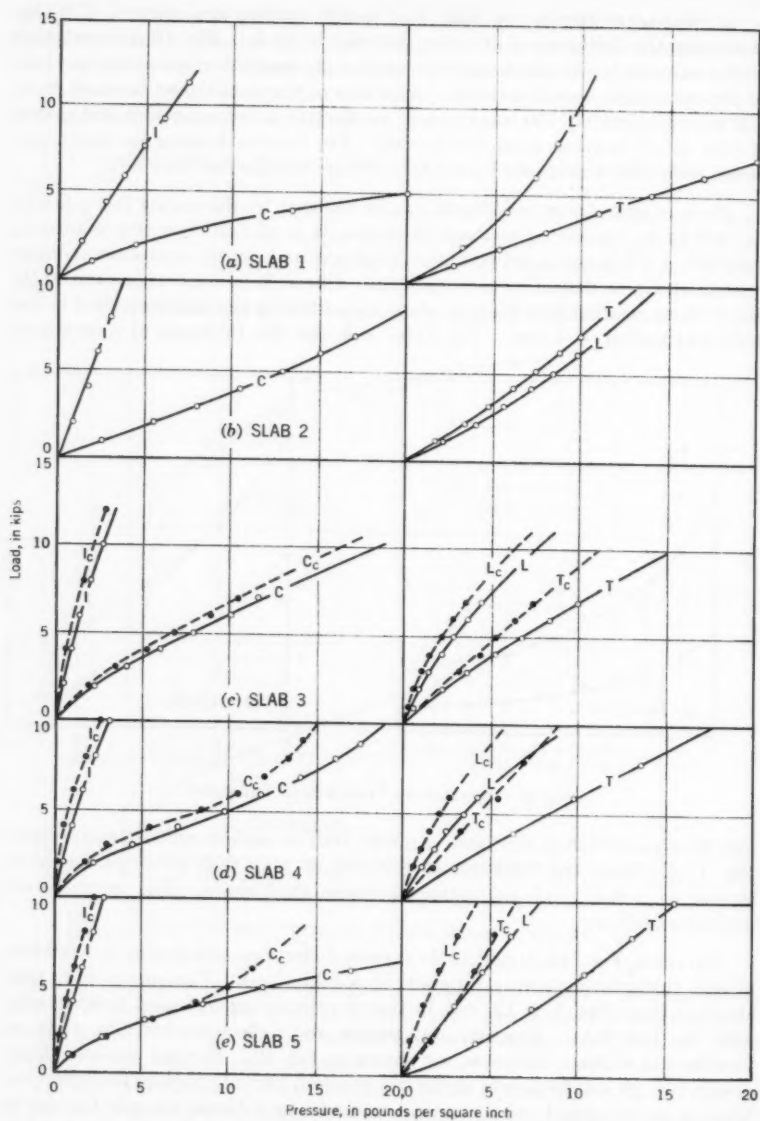


FIG. 13.—MAXIMUM PRESSURES BENEATH SLAB AND SUBBASE

Fig. 11(b) shows that clay requires a $7\frac{1}{2}$ -in. slab in order to yield the same edge deflections as a 6-in. slab on a 6-in. subbase. An 8-in. slab is required on clay in order to yield the same edge deflections as a 6-in. slab on a 12-in. subbase.

Fig. 11(a) indicates that equivalent stresses at both the corner and the edge can be controlled with less concrete thickness than is required for equivalent

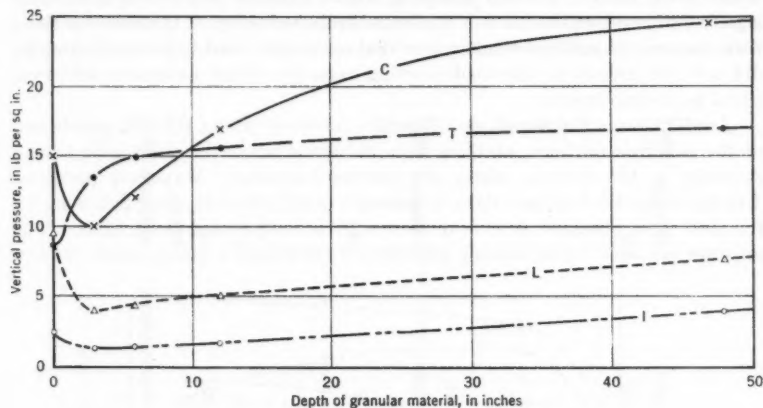


FIG. 14.—PRESSURE DIRECTLY UNDER LOAD

deflections. For example, a $6\frac{1}{2}$ -in. slab on clay yields the same strains as a 6-in. slab on a 6-in. subbase. Similarly, a 7-in. slab on clay maintains the strains at the same values as a 6-in. slab supported by a 12-in. subbase. At a free corner an $8\frac{1}{2}$ -in. slab is needed to control deflections in order to equal those of a 6-in. slab on a 6-in. subbase. To control deflections to equal those of a 6-in. slab on a 12-in. subbase, a 10-in. slab is necessary.

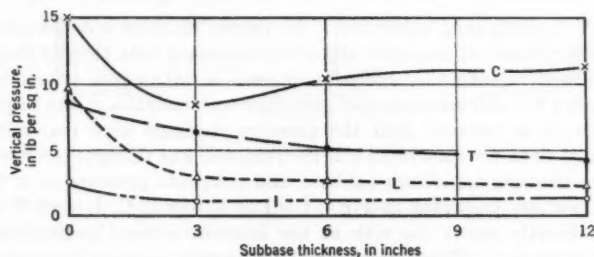


FIG. 15.—PRESSURE ON CLAY

These data, showing that the dense-graded subbase was much more effective in reducing deflections than in reducing strains, are of particular significance in designing concrete pavements on plastic subgrade soils susceptible to pumping. If the data represent average subbase performance, it is apparent

that one of the primary functions of a subbase is to reduce deflections, with an accompanying reduced tendency for pumping. Subbases are effective also in increasing pavement strength by reducing strains due to load. However, in most cases such an effect could be achieved more economically by thickening the slab. For the materials under study herein, it appears that a 6-in. subbase, which is sufficient to prevent pumping, will be effective in reducing deflections significantly and will result in a moderate strain reduction. However, in these tests the use of a subbase thicker than that commonly used to prevent pumping did not add greatly to the load-carrying capacity of the pavement and thus could be uneconomical.

Load-Pressure Relationships.—Reactive pressures under the test panels and at the subgrade-subbase interface were measured when the slabs were loaded statically at the corners, edges, and interior locations. Maximum pressures directly under the load and data on pressure distribution at other points under the slab were obtained in conjunction with accompanying deflections. The pressure cell used for measuring pressures is essentially a stress meter (9) and

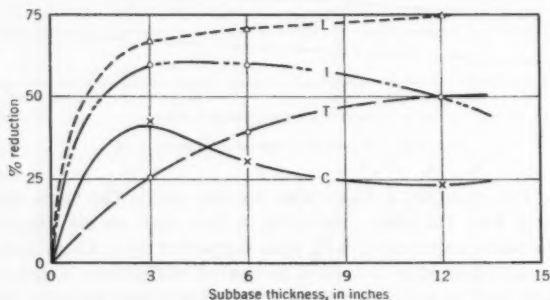


FIG. 16.—EFFECT OF SUBBASE IN REDUCING PRESSURE ON CLAY

is sensitive to small axial movement. Its proper function is dependent on the uniform distribution of material intimately in contact with the cell diaphragm. Particle intrusion into this critical area, soil shrinkage, or pavement-panel curl will alter the cell response and introduce uncertainties in the results. In most cases, it is believed that the pressure readings were reasonable, but occasionally, as in the case of slab 2, the response was thought erroneous.

Curves showing maximum subbase and subgrade pressure as a function of wheel load are presented in Fig. 13. The letters I, C, L, and T indicate pressures directly under the slab at the interior, corner, longitudinal edge, and transverse edge. The letters with the subscript *c* indicate pressures on the clay beneath the subbase. Pressures directly under the 6,000-lb loads, which apply 86 lb per sq in. to the slab, are shown in Fig. 14. The highest pressures, ranging from 10 lb per sq in. to 20 lb per sq in., or more, occurred at free corners. Pressures ranging from 2 lb per sq in. to 4 lb per sq in. occurred in the interior. Pressures under free longitudinal edges (15 ft long) ranged from 5 lb per sq in. to 10 lb per sq in. for a 6,000-lb load, and were less than one-half

those under transverse edges (10 ft long). The single exception was slab 2 on the clay subgrade, which showed approximately equal pressures for the two edge loadings. Of course, these pressures are for isolated slabs without load-transfer devices or end restraint.

Effect of Subbase in Reducing Pressures on the Subgrade Soil.—Fig. 15 shows pressures on the clay subgrade under 6,000-lb loads. The granular subbases reduce the pressures significantly. The reduction is most pronounced for the first 6 in. of subbase, although the pressures continue to decrease with a

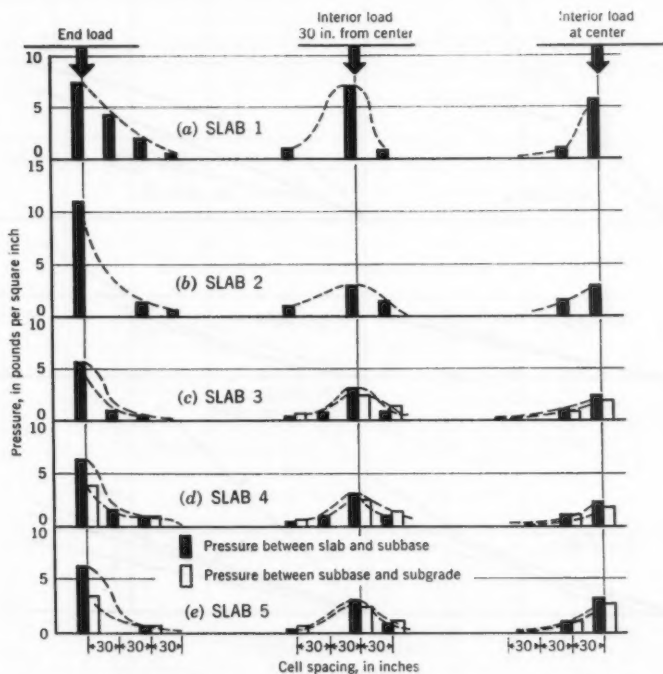


FIG. 17.—DISTRIBUTION OF REACTIVE PRESSURES ALONG CENTER LINE OF SLAB

further increase in subbase thickness. An unexplained variation in this trend can be noted at the free corner.

The capacity of a granular subbase to reduce pressures transmitted to the subgrade and greatly reduce slab deflections undoubtedly contributes to preventing pumping.

Fig. 16 shows the pressure-reduction data expressed on a percentage basis. The effect of subbases on pressures at the interior and the longitudinal edge is particularly significant. For a 3-in. subbase, reductions from 50% to 70% result, with only minor changes as the thickness is increased. The corner data

are inconsistent, showing a 40% reduction for the 3-in. subbase and somewhat less reduction for the thicker subbases.

Distribution of Pressures Along Slab Center Line.—Because pressures at the interface between a concrete slab and the subbase are not great compared with the applied load, the reactive pressures must be distributed over a large area. As indicated in Fig. 4, pressure cells were installed along the slab center lines to ascertain the nature of the pressure distribution.

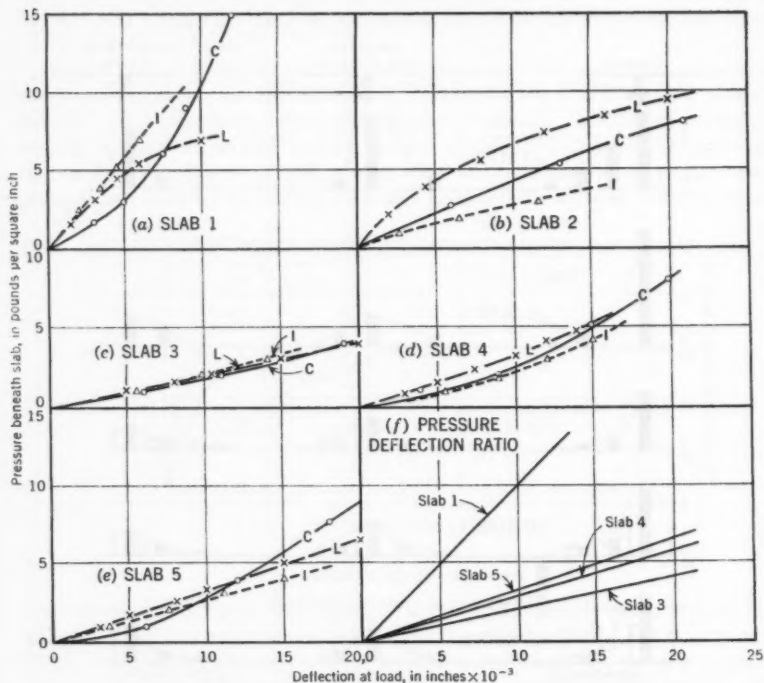


FIG. 18.—PRESSURE-DEFLECTION RELATIONSHIPS AT POINT OF LOADING

Fig. 17 indicates that an 8,000-lb load on the 6-in. slab produces reactive pressures for a considerable distance. When the load was applied at the end of the panel and at the center of the transverse edge, in three of the five slabs, pressures were indicated on the cell at the center, which was $7\frac{1}{2}$ ft from the load. Loads that were 5 ft from the end produced measurable pressures on the end cell in all five slabs, but loads at the slab center caused measurable pressure at the slab end in slab 3 only. Thus, an 8-kip load at the interior of a 6-in. slab caused reactive pressures of measurable magnitude throughout an area having a diameter greater than the panel width. This area is approximately 60% of the total panel.

Relationship Between Reactive Pressure and Deflection.—The theoretical equations of Table 6 are based on the assumption that the ratio of pressure to deflection is constant everywhere under a concrete slab. Observations of pressure-deflection relationships during the study confirmed this assumption as a reasonable approximation except for the case of slab 2, which was placed directly on the clay subgrade. In Fig. 18 the curves indicate the pressure-deflection relationship in the immediate vicinity of the load for all slabs. When measuring facilities were available, these trends were corroborated at points some distance from the load.

TABLE 8.—COMPARISON OF SLAB STRESSES AND DEFLECTIONS

Location	Equations and Experiments	SLAB NUMBER							
		1		3		4		5	
		p/d	k^*	p/d	k^*	p/d	k^*	p/d	k^*
		920	600	200	120	290	145	335	170

(a) MAXIMUM STRESS, IN POUNDS PER SQUARE INCH

Interior	Eq. 1	188	198	223	234	214	230	211	227
	Experiment	...	198	...	240	...	205	...	212
Edge	Eq. 3	272	290	335	257	320	349	314	343
	Eq. 9	299	318	363	385	347	378	342	371
	Experiment	...	282	...	415	...	402	...	343
Corner	Eq. 5	230	247	285	301	273	295	268	290
	Eq. 10	295	318	372	394	355	385	347	379
	Experiment	...	245	...	355	...	320	...	280

(b) MAXIMUM DEFLECTION, IN INCHES $\times 10^{-4}$

Interior	Eq. 2	23	29	50	66	42	59	39	55
	Experiment	...	33	...	72	...	60	...	59
Edge	Eq. 4	82	101	175	226	145	205	135	189
	Eq. 14	69	87	155	204	128	184	118	169
	Experiment	...	95	...	184	...	143	...	145
Corner	Eq. 6	148	191	357	475	289	429	267	391
	Eq. 15	136	168	290	371	240	343	226	315
	Experiment	...	160	...	450	...	290	...	270

* From slab tests and from 30-in. plate.

The curves for slabs 1, 3, 4, and 5 are grouped closely and demonstrate that it is reasonable to assume a constant pressure-deflection ratio for the slabs. Slab 2 shows a wide spread, and it is impossible at this time to ascertain whether the fault lies in the assumption or in some testing peculiarity. Fig. 18(f) indicates lines approximating the pressure-deflection ratio for each slab (except slab 2). The lines indicate ratios, or k -values, that are from 50% to 100% greater than those measured by the plate-bearing tests, as indicated

by the following:

Slab number	k -value from plate	(p/d) -value from slab
1.....	600	920
3.....	120	200
4.....	145	290
5.....	170	335

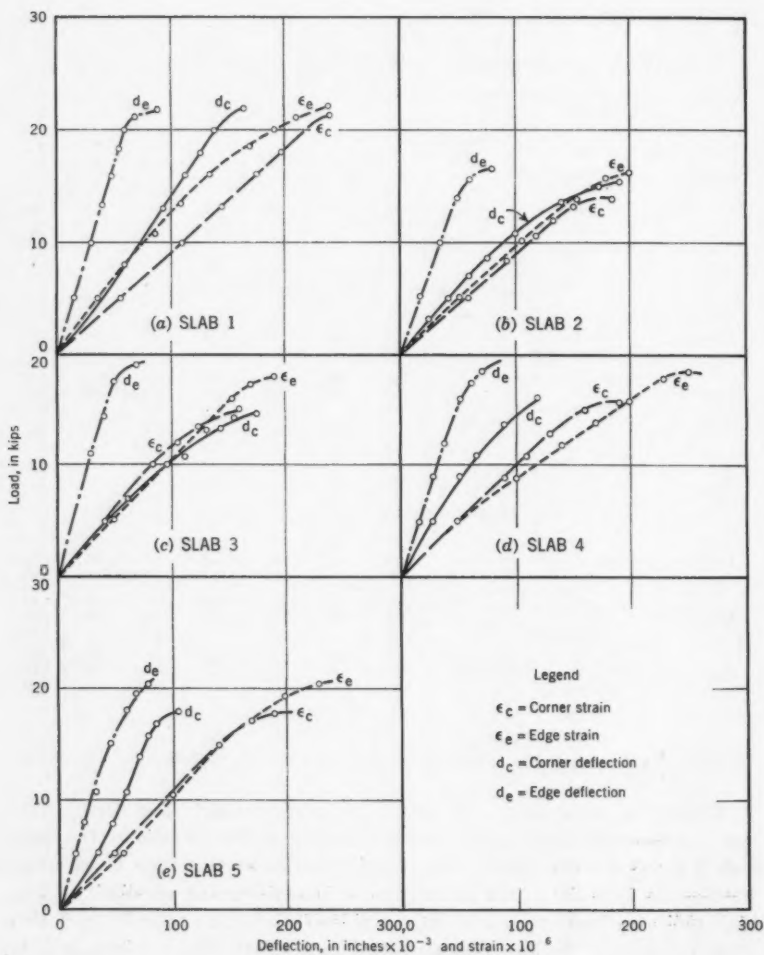


FIG. 19.—LOAD TEST TO FAILURE

Stresses and deflections were recomputed, using the (p/d) -value from the foregoing table. In Table 8 the results are compared with those using the k -value from plate tests.

Table 8 shows that stresses and deflections computed from theory are less when a value of p/d is used instead of a k -value. In general, this reduction does not cause the new theoretical value to approximate the experimental values more closely than before. However, significant improvement is obtained in the following:

1. Corner stresses for slabs 3 and 4, using Eq. 10;
2. Edge deflections for slabs 3, 4, and 5, using Eq. 4; and
3. Corner deflections for slabs 4 and 5, using Eq. 6.

It may be concluded that the use of the value of k in the theoretical equations, as determined from plate tests, produces stress and deflection values that agree reasonably well with experiments made in this test. This agreement occurs more often than when a value of p/d from slab tests is used.

TABLE 9.—LOADS, STRAINS, AND DEFLECTIONS AT FAILURE

Slab	k , in pounds per cubic inch	Corner Region			Longitudinal Edge		
		Load, in kips	Strain $\times 10^4$	Deflection, in inches	Load, in kips	Strain $\times 10^4$	Deflection, in inches
(1)	(2)	(3)	(4)	(5)	(6)	(7)	(8)
1	600	21.5	240	0.165	22.0	240	0.090
2	100	14.0	170	0.150	16.0	200	0.070
3	120	15.0	160	0.170	18.0	190	0.055
4	145	16.0	190	0.120	18.5	240	0.070
5	170	18.0	190	0.105	20.5	230	0.080

Computation of Pressures from Deflections.—Once the (p/d) -ratio has been established for a pavement slab by limited pressure and deflection measurements, the pressures under a slab at any point can be approximated by multiplying the deflection at that point by the ratio, p/d . Because deflections are measured easily, the foregoing relationship is valuable in studying pressure distribution.

Loads to Failure.—As a final evaluation of the contribution of subbases to roadway structural strength, the concrete slabs were loaded to failure. The loads were applied with the panels in a flat condition—that is, with no appreciable curl. A corner was broken first, and then the opposite longitudinal edge was loaded to failure. After these breaks occasionally a slab had sufficient integrity to justify a second corner break. No failure loads were attempted at interior positions.

Fig. 19 indicates the data from failure tests. Fig. 19 and Table 9 demonstrate that the ultimate load increases with an increase in subbase thickness for both edge and corner points, and that the failure load at the edge is slightly greater than that at the corner.

The corner-to-edge strain ratio of 88%, which was developed in Table 5(b), is not applicable in the data of Fig. 19. In slab 1, the corner strains exceeded

the edge strains for the entire load range but converged at failure. The load-strain curves for edge loads and corner loads were close together for slabs 2, 3, and 5 until the load approached that producing corner failure. In slab 4, edge strains exceeded corner strains in the middle load range.

In some cases at the "working-load" levels the strains and deflections in Fig. 19 are greater than those in Fig. 5. Small but unavoidable curling that developed prior to the failure tests was probably the cause. However, it is believed that this minor curling had little influence on the failure loads.

Flexure tests on control beams yielded modulus-of-rupture values (at an age of 10 weeks) approximating 800 lb per sq in. At $E = 6,000,000$ lb per sq in., an average strain at failure should be about 130×10^{-6} . This value is exceeded by the strains in Table 9. It is apparent that conventional elastic analysis is not applicable for computing the ultimate flexural failure in pavement slabs.

CONCLUSIONS

Static-load tests were made on isolated, rectangular, uncured concrete panels 6 in. thick. The panels were supported by dense-graded, well-compacted granular subbases of different thicknesses over a clay subgrade with a k -value of 100. The conclusions from the study apply to the materials and conditions described herein:

1. Slab deflections and stresses due to static load decreased as the subbase thickness was increased (Fig. 10). Failure loads increased as the subbase thickness increased (Table 9). The economic relationship between subbase depth and thickness of concrete slab may be estimated by the trend in the tests. An analysis based on measured load-strain relationships and load-deflection relationships and on the close-fitting theoretical curves of Figs. 10, 11, and 12 shows that:

- a. The stresses induced at the edge and at a free corner in a 6-in. slab on a 6-in., well-compacted, dense-graded subbase were the same as in a 6½-in. slab with no subbase. The stresses in a 6-in. slab on a 12-in. subbase were the same as in a 7-in. slab with no subbase.

- b. The deflections at the edge of a 6-in. slab on a 6-in. subbase were the same as with a 7½-in. slab with no subbase. The deflections of a 6-in. slab on a 12-in. subbase were the same as with an 8-in. slab with no subbase.

- c. The deflections at a free corner of a 6-in. slab on a 6-in. subbase were the same as with an 8½-in. slab with no subbase. The deflections of a 6-in. slab on a 12-in. subbase were the same as with a 10-in. slab with no subbase.

Thus, on low-bearing-value subgrades it appears that strains may be reduced effectively and economically by small increases in slab thickness. Deflections also may be reduced substantially by the use of a dense-graded, well-compacted subbase. The greatest effectiveness per inch of subbase in reducing deflections is obtained with subbases approximately 6 in. thick. Because experience indicates that 6-in.-thick subbases, or those even thinner, will prevent pumping, thicker subbases may not be structurally economical.

2. Pressures directly under the load at the top of the subbase increased as the thickness of granular material was increased (Fig. 14). At a load of 6,000

lb the pressures at the interior ranged from approximately 2 lb per sq in. to 4 lb per sq in.; those at the longitudinal edge, from 4 lb per sq in. to 8 lb per sq in.; and those at an isolated corner, from 10 lb per sq in. to 25 lb per sq in.

3. Pressures at the subbase-subgrade interface decreased with increases in subbase thickness except under slab corners. They were less by approximately 25% to 75% than those under the slab when the slab was built directly on the clay (Fig. 15).

4. The equations for computing deflections and strains provided reasonable agreement with measured values (Figs. 6, 7, 8, and 9), with the following qualifications:

a. For deflections and strains at the interior, the 1926 Westergaard formulas yielded computed values that were reasonably close to actual test results.

b. For deflections at the longitudinal edge, the 1947 Westergaard equation (Eq. 13) provided the best check. For strains at the edge, this equation agreed satisfactorily with measurements for the lower k -values, but the 1926 equation (Eq. 3) agreed better for higher values of k . Eq. 9 is a compromise, representing an average condition. For foundations including subbases with a k -value from 120 to 170, none of the theoretical equations were as responsive to changes in values of k as were measured strains and deflections.

c. When the load was at the corner the measured deflections at both high values of k and low k -values agreed with the 1926 Westergaard equation (Eq. 6). At intermediate k -values the measured quantities were approximately 30% less than computed values. In this area the Westergaard equation is less responsive to changes in the k -value than are the measured deflections. Measured strains were approximated by Eq. 5 for higher k -values, but were greater than values computed by this equation when the k -value was low. The Pickett equation (Eq. 10) yielded strains consistently greater than those measured.

5. For flat slabs, pavement-thickness design equations involving the subgrade reaction modulus, k , proved reasonably applicable to both the single subgrade and the layered system when the value of k was computed from 30-in. plate tests on the top surface of the composite system. However, in many cases, the theoretical equations were not as responsive to changes in subgrade support as were the measured values. The extent to which these formulas or their modifications agree with experimental results on curled panels must be ascertained fully by tests on slabs subjected to load cycling and restraints typifying highway conditions.

APPENDIX. BIBLIOGRAPHY

- (1) "Highway Research in Illinois," by C. Older, *Proceedings, ASCE*, Vol. 50, 1924
- (2) "The Structural Design of Concrete Pavements," by L. W. Teller and E. C. Sutherland, *Public Roads*, October-December, 1935; October, 1936; and April, 1943.

- (3) "Stresses in Concrete Pavements by Theoretical Analysis," by H. M. Westergaard, *Proceedings*, Highway Research Board, National Research Council, Washington, D. C., 1925; *Public Roads*, April, 1926.
- (4) "Lockbourne No. 1 Test Track," Ohio River Div. Labs., Corps of Engrs., U. S. Dept. of the Army, Mariemont, Ohio, March, 1946.
- (5) "Lockbourne No. 2 300,000 lb. Experimental Mat," Ohio River Div. Labs., Corps of Engrs., U. S. Dept. of the Army, Mariemont, Ohio, June, 1945.
- (6) "Road Test One-Md," by E. C. Sutherland and H. D. Cashell, *Special Report No. 4*, Bureau of Public Roads, U. S. Dept. of the Interior, Washington, D. C., 1953.
- (7) "Deflections, Moments and Reactive Pressures for Concrete Pavements," by G. Pickett, M. E. Raville, W. C. Janes, and F. J. McCormick, *Bulletin No. 65 and Supplement*, Engineering Experimental Station, Kansas State College, Manhattan, Kans., October 15, 1951.
- (8) "Suggested Method of Test for California Bearing Ratio of Soils," Corps of Engrs., U. S. Dept. of the Army, Eng. Div., *Procedures for Testing Soils*, A.S.T.M., July, 1950.
- (9) "Development of a Device for the Direct Measurement of Compressive Stress," by R. W. Carlson and D. G. Pirtz, *Proceedings*, A.C.I., Vol. 49, November, 1952.
- (10) "Development of a Cell for the Installation of Electrical Resistance Strain Gages in Concrete," by H. E. Worley and R. C. Meyer, *ibid.*, Vol. 50, October, 1953.
- (11) "Baldwin Type C Load Cell," *Bulletin No. 307*, Baldwin-Lima-Hamilton, Eddystone, Pa.
- (12) "Reinforced Concrete Pavements," by R. D. Bradbury, Wire Reinforcement Inst., Washington, D. C., 1938.
- (13) "Analytical Tools for Judging Results of Structural Tests of Concrete Pavements," by H. M. Westergaard, *Public Roads*, December, 1933.
- (14) "Stresses in Concrete Runways of Airports," by H. M. Westergaard, *Proceedings*, Highway Research Board, National Research Council, Washington, D. C., 1939.
- (15) "What is Known of Stresses," by H. M. Westergaard, *Engineering News-Record*, January 7, 1937.
- (16) Discussion by R. D. Bradbury of "Stresses in Concrete Pavement Slabs," by M. G. Spangler and F. E. Lightburn, *Proceedings*, Highway Research Board, National Research Council, Washington, D. C., 1937.
- (17) "Application of the Results of Research to the Structural Design of Concrete Pavement," by E. F. Kelley, *Public Roads*, July, 1939.
- (18) "Stresses in the Corner Region of Concrete Pavements," by M. G. Spangler, *Bulletin 157*, Iowa Eng. Experiment Station, Ames, 1942.
- (19) "A Study of Stresses in the Corner Region of Concrete Pavement Slabs under Large Corner Loads," by Gerald Pickett, *Concrete Pavement Design*, Portland Cement Assn., Chicago, Ill., 1946.
- (20) "Stress Concentrations in Plates Loaded Over Small Areas," by H. M. Westergaard, *Transactions*, ASCE, Vol. 108, 1943.

- (21) "New Formulas for Stresses in Concrete Pavements of Airfields," by H. M. Westergaard, *ibid.*, Vol. 113, 1948.
- (22) "Equilibrium of a Thin Plate, Symmetrically Loaded, Resting on an Elastic Foundation of Infinite Depth," by A. H. A. Hogg, *Philosophical Magazine*, Vol. 25, 1938.
- (23) "Thin Plates on Elastic Foundation," by D. L. Holl, *Proceedings*, 5th International Cong. for Applied Mechanics, Cambridge, Mass., Vol. 5, 1938.
- (24) "The Theory of Stresses and Displacements in Layered Systems and Applications to Design of Airport Runways," by D. M. Burmister, *Proceedings*, Highway Research Board, National Research Council, Washington, D. C., 1943.
- (25) "Computation of Traffic Stresses in a Sample Road Structure," by L. Fox, 2d International Conference on Soil Mechanics and Foundations, Rotterdam, Vol. 2, 1948.
- (26) "Some Numerical Solutions to Stresses in Two and Three-Layered Systems," by R. J. Hank and F. H. Scrivner, *Proceedings*, Highway Research Board, National Research Council, Washington, D. C., 1948.

AMERICAN SOCIETY OF CIVIL ENGINEERS

Founded November 5, 1852

TRANSACTIONS

Paper No. 2994

ADAPTABILITY OF INTERCHANGES TO INTERSTATE HIGHWAYS

BY JACK E. LEISCH,¹ A. M. ASCE

WITH DISCUSSION BY MESSRS. GERALD D. LOVE; AND JACK E. LEISCH

SYNOPSIS

Selecting the proper type of interchange for various crossroad conditions is the first and perhaps the most important step in design. The paper presents recommendations of interchange types based on analyses and comparisons of operational features and capacity potentials. A plan providing for operational uniformity in conjunction with exits on the interstate system of highways is also given.

INTRODUCTION

A novel interchange to handle traffic at the intersection of two highways was introduced in 1928 at Woodbridge, N. J. This first cloverleaf design permitted all traffic, including left-turning movements, to operate through the intersection without interruption. Since that time engineers have advanced the development of design techniques in order to cope with conflicting traffic movements. In recent years the art of interchange design has combined the talents of the highway engineer (geometric) and the traffic engineer. Thus, experience has resulted in the advancement of design techniques that are being used in the development of the vast network of interstate highways. The profession is still faced with traffic operation problems and is developing new design concepts for these interregional freeways.

The utility of this system of highways will be influenced by the location and design of interchanges—providing access to and from intersecting highways, as well as those interconnecting various parts of the system. Selecting the proper type of interchange for each location is the primary and most important step in design.

NOTE.—Published, essentially as printed here, in January, 1958, in the Journal of the Highway Division, as *Proceedings Paper 1525*. Positions and titles given are those in effect when the paper or discussion was approved for publication in *Transactions*.

¹ Chf. Highway Engr., De Leuw, Cather & Co., Chicago, Ill.

In urban areas the problem is primarily to provide adequate capacity and efficient operation. Wherever possible, the design should be sufficiently flexible to permit future adjustment and expansion. In rural areas the problem is generally to adopt interchange arrangements in keeping with the character of the intersecting highway. Of greater importance is that the layout be compatible with traffic operation at high sustained speeds of the magnitude experienced on turnpike facilities.

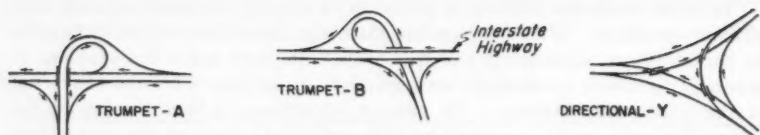
The paper examines the types of interchanges adaptable to various conditions found on the interstate system of highways. The approach taken is different in that the type and character of the intersecting street or highway is considered first, and then the forms of interchanges that apply are examined. This was done in preference to taking each type of interchange and showing under what variety of conditions it may be used. The adaptability of interchange types is considered with respect to minor crossroads (rural), major streets (urban), primary highways (rural and suburban), and expressways and freeways. In urban areas the capacity potentials of the cloverleaf, partial cloverleaf, and diamond interchanges are developed and compared. In rural areas the characteristics of interchanges and their suitability are presented primarily with regard to safety and operational features. The need for, and the means of, effecting uniformity in operational patterns of ramp exits through the use of collector-distributor roads are considered with respect to high standards and maximum safety.

General forms of interchanges and terminology are shown in Fig. 1. Several abbreviations and new terms are introduced for convenience of reference. A distinction is made between the two variations of trumpets. The one with the loop in advance of the intercepted road with respect to direction of travel is referred to as the "trumpet-A" (the letter A denoting the loop in advance). The one with the loop beyond the intercepted road is referred to as "trumpet-B." The same principle is applied to the partial cloverleaves, for which a new abbreviation, the "parclo," is introduced. Considering the direction of travel on the expressway as a base, the interchange with the loops in advance of the crossroad is referred to as "parclo-A," and the one with the loops beyond the crossroad as "parclo-B." Those with additional right-turn ramps in the other two quadrants are referred to as "parclo-A (4-quad)" and "parclo-B (4-quad)," respectively. Collector-distributor roads, which presently (1959) receive considerable attention, either as parts of individual interchanges or facilities between successive interchanges, are abbreviated herein as "C-D" roads.

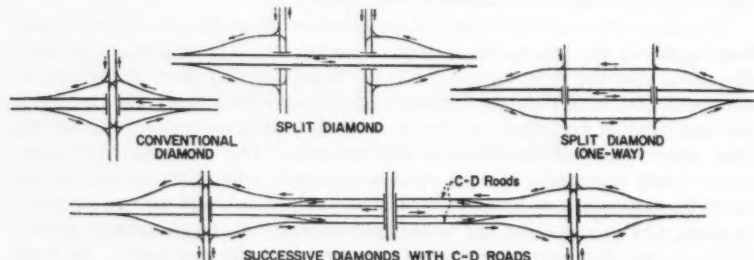
INTERCHANGES WITH MINOR CROSSROADS—RURAL

Interchanges on interstate highways are sometimes situated where the crossroad is minor or of local character. This avoids unduly long sections of interstate highway between points of egress and ingress, thus making the system more flexible and useful.

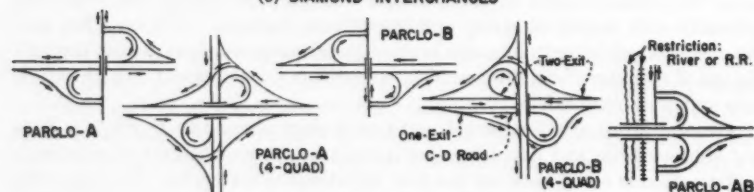
In the past, controlled-access highways of appreciable length have not been built in sparsely settled or undeveloped areas. Thus, engineers have gained little experience in the operation of interchanges at minor crossroads. Because the volume of traffic on such roads generally receives little or no consideration



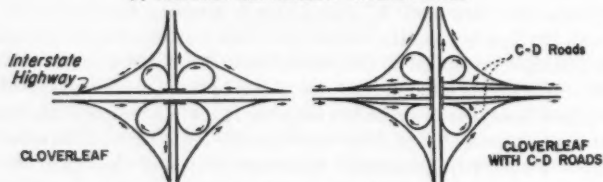
(a) T AND Y INTERCHANGES



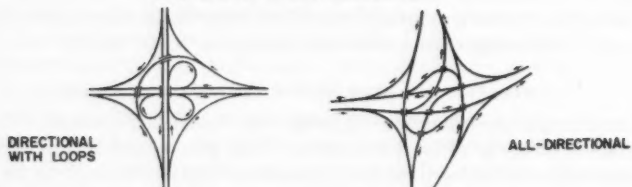
(b) DIAMOND INTERCHANGES



(c) PARTIAL CLOVERLEAF INTERCHANGES



(d) CLOVERLEAF INTERCHANGES



(e) DIRECTIONAL INTERCHANGES

FIG. 1.—INTERCHANGE TYPES AND TERMINOLOGY

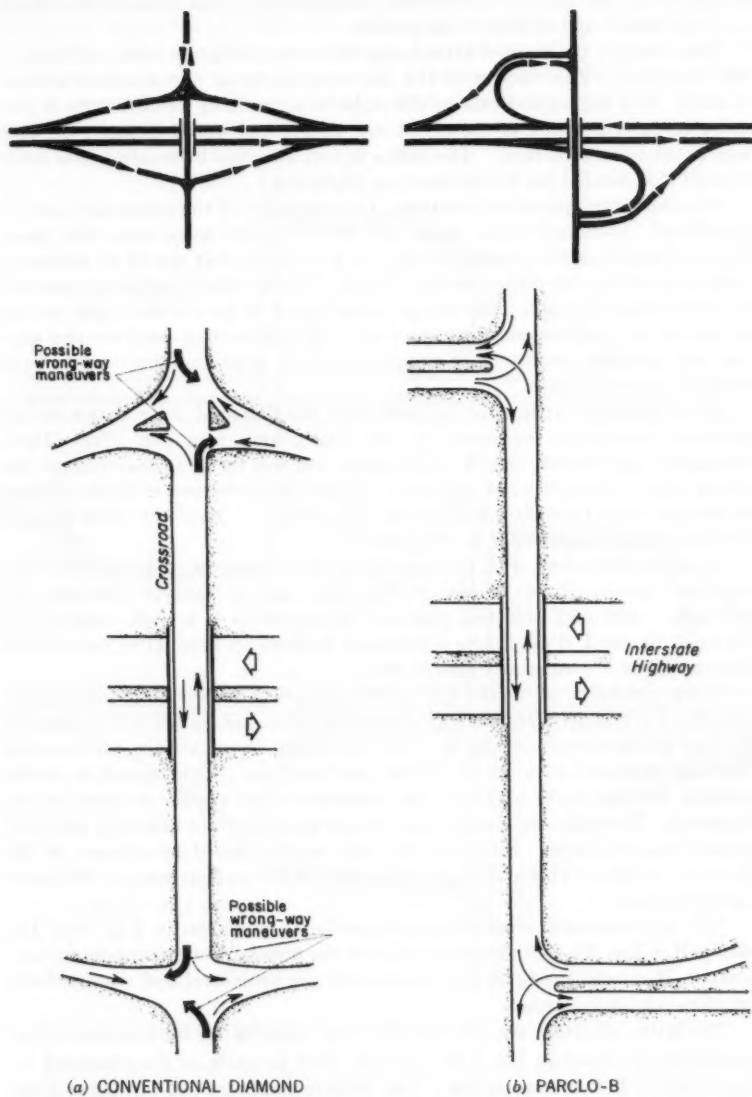


FIG. 2.—ADAPTABILITY OF PARCLO-B AND DIAMOND INTERCHANGES TO
MINOR RURAL CROSSROADS

in design, the tendency is to treat the problem lightly and consider the design as being simple and of little consequence.

Accordingly, the type of interchange which immediately comes to mind is the diamond. With respect to the interstate highway the diamond pattern is ideal. One high-speed exit on the right in advance of the structure is provided in each direction of travel, as well as one high-speed entrance on each side beyond the structure. The entire layout occupies little additional space beyond that needed for the intersecting highways.

In examining operational features, the character of the crossroad must be considered. Generally such roads will never require more than two lanes. In some instances the existing facility is a 16-ft or 18-ft gravel or macadam road, or possibly a 20-ft hard-surfaced road. Traffic is light and is not expected to increase appreciably. Drivers are accustomed to turn either right or left, as desired, at intersections along the road. All intersecting roads are two way, and any one-way operation or prohibited turns would not be expected and would be inappropriate.

In conjunction with a minor rural road the diamond interchange invites improper maneuvers, as shown by the heavy arrows in Fig. 2(a). These wrong-way movements can be made easily and will result in traveling on the wrong side of the interstate highway. Unless the crossroad is divided, channelization of the ramp terminals are of little help. A divided section through the interchange apparently is not justified.

A partial cloverleaf, with the loops along the expressway placed beyond the structure (parclo-B), as shown in Fig. 2(b), can be used to eliminate the difficulty. Although this two-quadrant arrangement is a little more costly than the diamond, it minimizes operational hazards by eliminating or reducing the possibility of wrong-way movements.

Using parclo-B, all traffic leaving the crossroad to reach the expressway operates in a manner identical with that on the diamond, as noted in comparing the two arrangements in Fig. 2. The two ramp terminals are conventional two-way junctions with which drivers are familiar. With respect to traffic entering the interstate highway, the connections are similar to those of the diamond. The exits are similar also, except that they are normally provided beyond the structure. However, the exit can be placed in advance of the structure, as shown in Fig. 2(b), in conjunction with the loop ramp in the lower-right quadrant.

The two-quadrant arrangement of parclo-A, as shown in Fig. 3(a), like parclo-B in Fig. 2(b), eliminates or reduces the possibility of wrong-way movements. However, the right-turn movements are unnatural and require direct left turns at the crossroad.

The latter objection is overcome when this interchange is expanded to four quadrants, as shown in Fig. 3(b). In this form no exits on the crossroad are made using left-turn maneuvers. This feature precludes left-turning vehicles from standing on the traveled way waiting for an opportunity to turn. It minimizes the hazard of rear-end collisions and increases capacity. In parclo-A (4-quad) the two added ramps (upper-left quadrant and lower-right quadrant)

do not invite wrong-way movements. However, for the type of crossroad considered herein, this variation of parclo-A is too elaborate and costly.

Another form of interchange, shown diagrammatically as parclo-AB in Fig. 1(c), can be used in special cases in which the crossroad closely parallels a river or a railroad. Crossroad realignment in order to permit the use of a parclo-B interchange generally would be preferred.

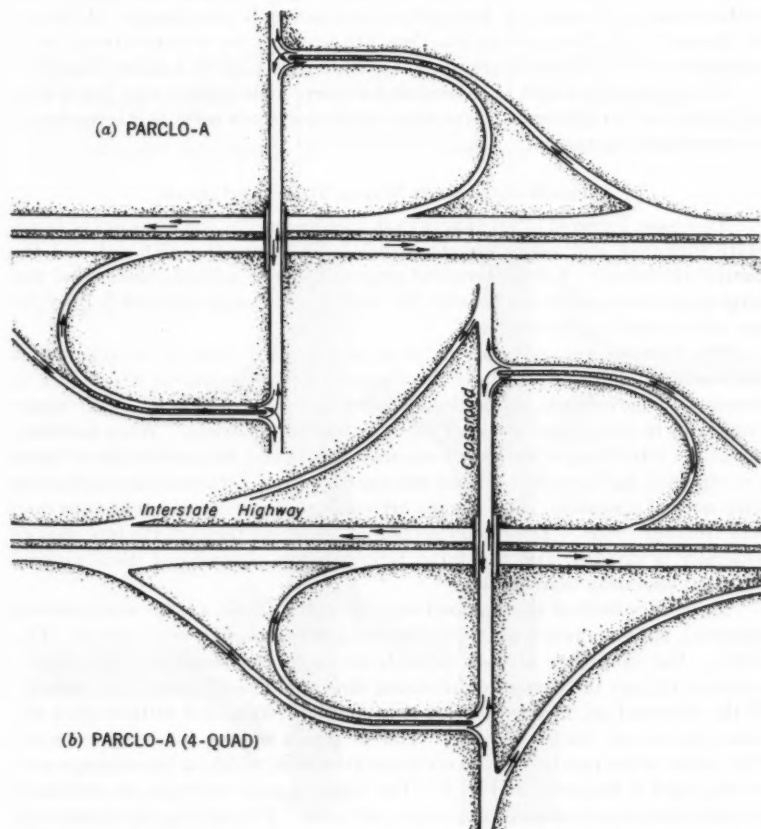


FIG. 3.—OPERATIONAL FEATURES OF PARCLO-A INTERCHANGES AT MINOR CROSSROADS

In summation, the parclo-B is the most suitable form of interchange in which the interstate highway crosses a minor rural road. It provides conventional and simple operation by use of two at-grade ramp terminals, compatible with the character of the minor crossroad. Parclo-B (4-quad), having the same form of interchange but with right-turning ramps added in the other two

quadrants, is inappropriate because these ramps invite wrong-way movements and the layout is too elaborate for the condition.

Parclo-A, like parclo-B, incorporates the design feature at ramp terminals to eliminate wrong-way operation. However, it involves unnatural turning maneuvers by requiring direct left turns on the crossroad for movements destined to the right on the expressway. Although parclo-A is less desirable, it may be used in place of parclo-B, in which physical features or right-of-way restrictions do not allow the development of a parclo-B interchange. A parclo-A (4-quad) interchange is an excellent arrangement for a major street, or, in some cases, for a primary highway, but it is overdesigned for a minor crossroad.

The diamond is simple in pattern and requires little right of way, but it is an inappropriate rural interchange at minor rural crossroads because it is conducive to wrong-way movements.

INTERCHANGES WITH MAJOR STREETS—URBAN

Two basic forms of interchanges that may be used at the crossings of interstate highways and major streets in urban areas are the diamond and the partial cloverleaf. A full cloverleaf generally is not suitable because of the large space it occupies, and because the continuous movements that it provides are not required on the street.

The simplest and perhaps the most widely used form of interchange at intersections of major streets is the diamond. The invitation it provides to wrong-way movements, as indicated previously in conjunction with minor crossroads in rural areas, does not apply in built-up districts. When considering urban interchanges the use of one-way streets and the prohibition of turns are expected and accepted so that the one-way ramp terminals are in keeping with normal operation. The ramps are connected usually to continuous one-way frontage roads. The rebuilt section of the street through the interchange generally is divided, and the ramp terminals are channelized, thus making intended operation more obvious.

Three variations of the diamond may be used. These are the conventional diamond, split diamond, and split diamond with one-way cross streets (Fig. 1(b)). The suitability of each depends on traffic requirements, right-of-way availability, and the pattern of adjoining streets. The efficiency and capacity of the diamond are increased when it is split, and increased further when the cross streets are made one way. This is shown by the following example. The traffic in conjunction with two major streets at which an interchange is to be provided is indicated in Fig. 4. The design hourly volumes are combined for both streets and are given in vehicles per hour. The existing streets are each 4 lanes wide, one or both of which are to be utilized for the interchange. The conditions represented are indicative of any large metropolitan area. With this basic information, the solutions using the three forms of diamond interchanges are demonstrated in Figs. 5, 6, and 7. As indicated in these figures, G/C is the proportional part of one hour devoted to the movement of traffic on a given intersection approach through a signalized intersection. Also, it is the ratio of the green signal time in seconds to the total length of signal cycle in seconds.

The conventional diamond, as shown in Fig. 5, requires the widening of one street to seven lanes through the interchange, or 88 ft between curbs, whereas the other street remains four lanes wide. Thus, a total of eleven lanes is used. One of the left-turn movements from the widened cross street must be accom-

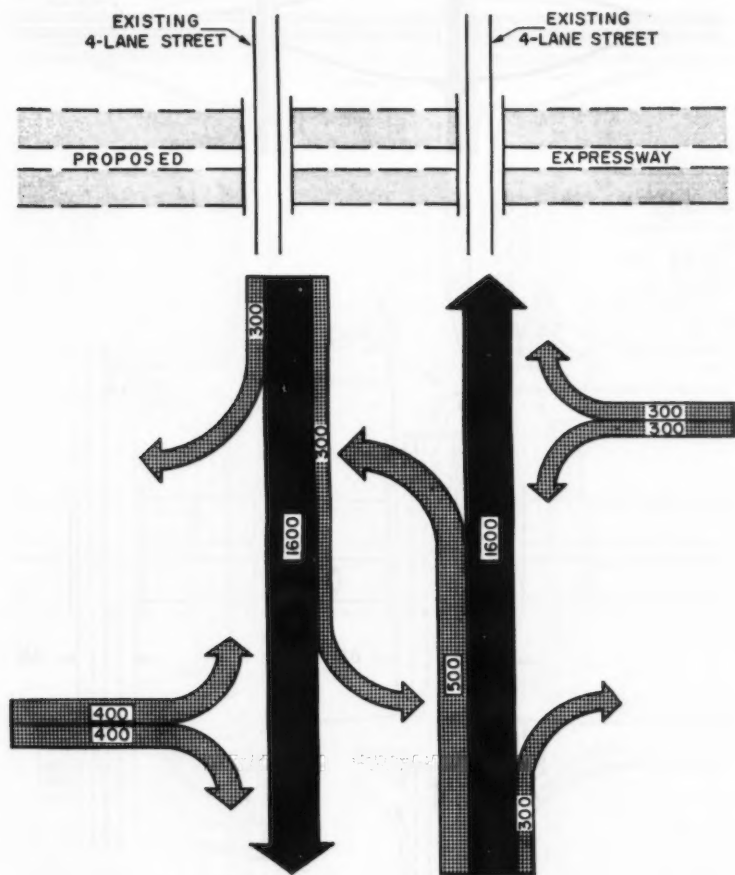


FIG. 4.—PROBLEM NO. 1 FOR DIAMOND INTERCHANGES

modated on 2 lanes. Three-phase control is necessary, utilizing a long cycle on the order of 80 sec. Thus, the signal waiting time is increased.

By using the split diamond (Fig. 6) each existing cross street is widened by one lane, resulting in curb-to-curb widths of 64 ft. A total of ten lanes is utilized, as compared with the eleven lanes used in Fig. 5. Although only one less lane is used as a total, each street is not unduly wide. The traffic conflicts

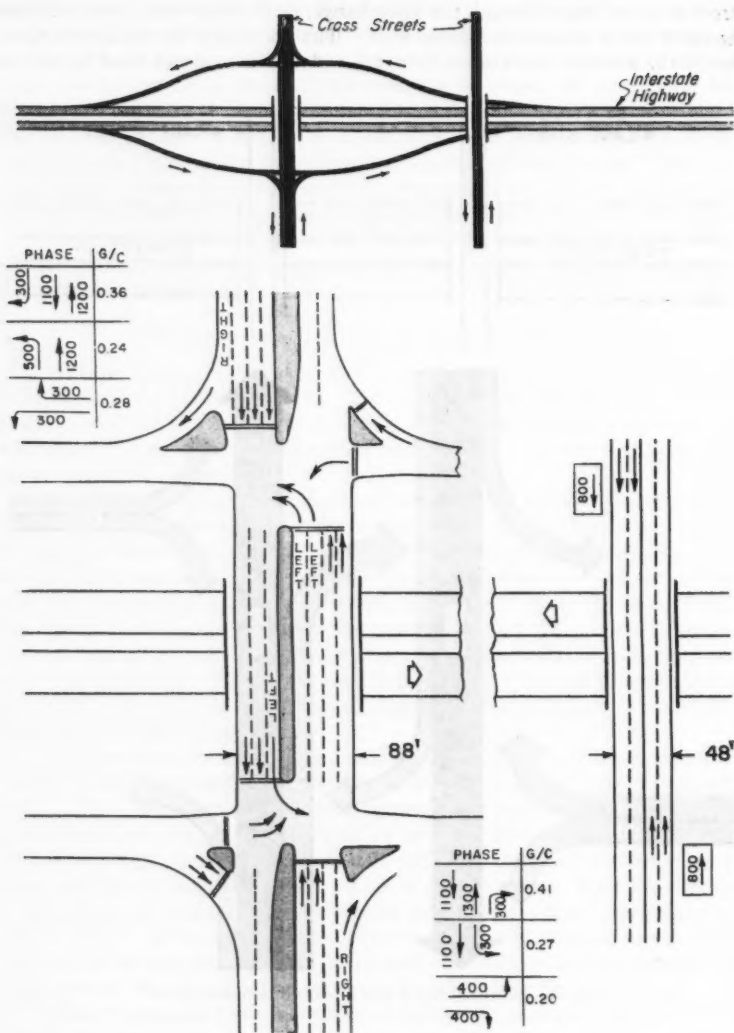


FIG. 5.—SOLUTION OF PROBLEM NO. 1 BY CONVENTIONAL DIAMOND

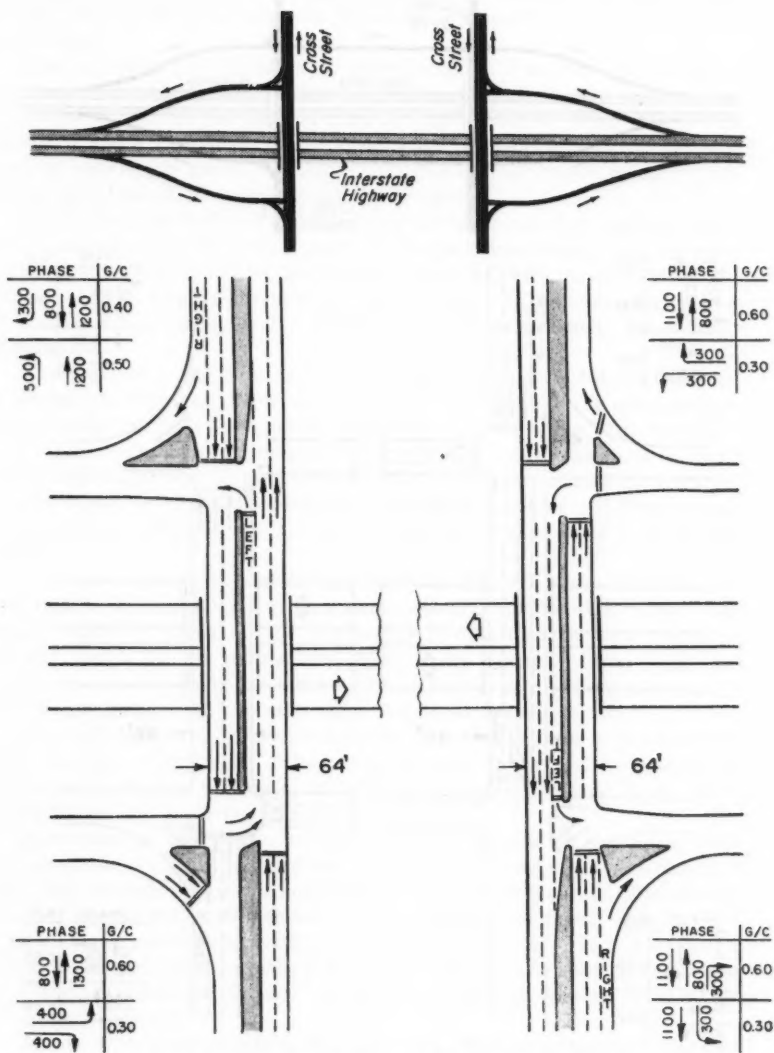


FIG. 6.—SOLUTION OF PROBLEM NO. 1 BY SPLIT DIAMOND

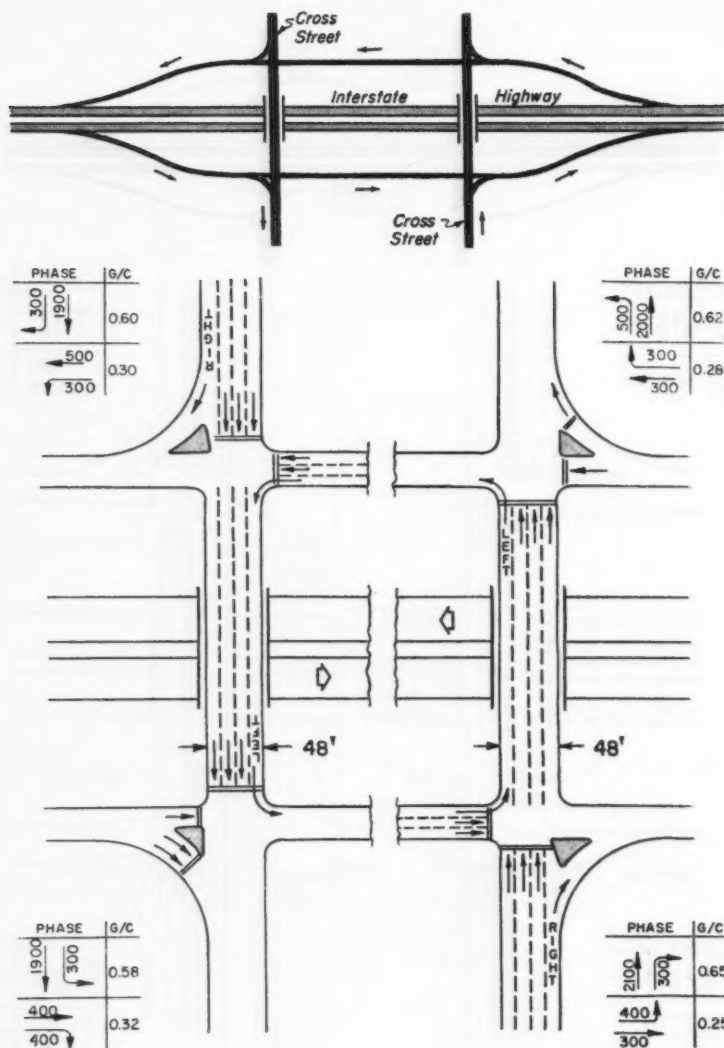


FIG. 7 — SOLUTION OF PROBLEM NO. 1 BY SPLIT DIAMOND WITH ONE-WAY CROSS STREETS

have been reduced and the operational efficiency considerably increased by the use of a two-phase, approximately 60-sec cycle instead of the longer, three-phase signal.

The split diamond with one-way operation (Fig. 7) requires no increase in the number of lanes on the two existing streets. A total of eight lanes is used, as compared with eleven and ten lanes in Figs. 5 and 6. With all one-way operation and a two-phase, 60-sec cycle signal, high-operational efficiency is realized, resulting in greater capacity and higher over-all speeds, made possible by the use of an effective progressive signal system.

Wherever a conventional diamond does not have sufficient capacity and a split diamond is not feasible, a parclo-A (4-quad) interchange may be used. For heavy traffic conditions, particularly large, left-exit movements on the cross street, this form of interchange is appropriate. It provides a high degree of operational efficiency and a potential to handle unusually large traffic volumes.

The example in Fig. 8(b), using rather high but realistic turning volumes, is designed to show the effectiveness of parclo-A (4-quad). To accommodate the indicated traffic, a conventional diamond, as shown in Fig. 8(a), requires a total of ten lanes, or a curb-to-curb width of 124 ft. Such design, involving a widening in each direction from a normal width of three lanes on the approaches to five lanes through the interchange, including a double left-turn lane, is awkward and inefficient. It normally would not be considered a practicable design.

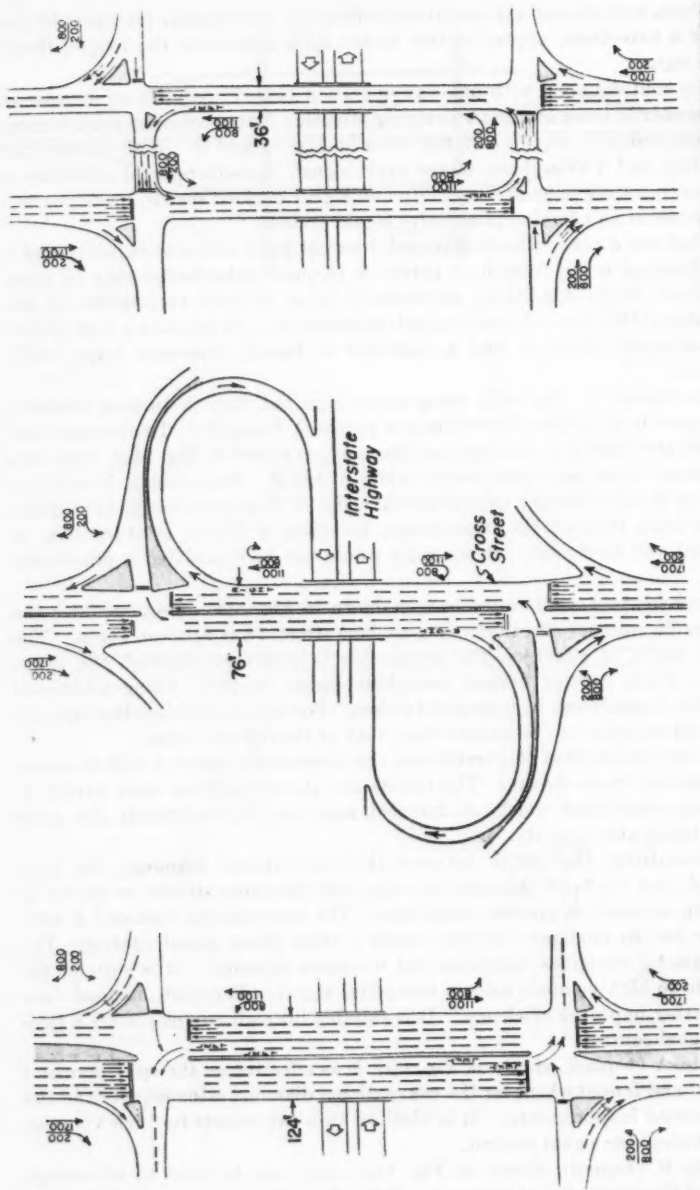
A parclo-A (4-quad) interchange, shown in Fig. 8(b), accommodates the same traffic volumes effectively on a six-lane street, 76 ft between curbs. The normal width of street on the approaches is continued through the interchange, which utilizes normal two-phase signal control. Using additional width the capacity can be increased further. For some conditions the capacity of this interchange can be greater than that of the full cloverleaf.

Fig. 8(c) shows that this traffic also can be provided for on a split diamond with one-way cross streets. The results are almost identical with parclo-A, producing equivalent widths of traveled ways and approximately the same signal timing and capacity.

Summarizing, the choice between the conventional diamond, the split diamond, and the split diamond one-way with the cross streets, as shown in Fig. 1(b), depends on specific conditions. The conventional diamond is suitable for low to moderate volumes using a three-phase signal control. The split diamond simplifies operation and increases capacity. It is suitable for moderate to high volumes using a two-phase signal. The split diamond (one way) further improves efficiency. It is suitable for high volumes using a two-phase signal control.

Parclo-A (4-quad), shown in Fig. 1(c), is as effective as the split diamond one-way) and is used whenever the conventional diamond is inadequate and the split diamond inappropriate. It is ideal on two-way streets for high volumes using a two-phase signal control.

Parclo-B (4-quad), shown in Fig. 1(c), may also be used to advantage instead of the conventional diamond. It is not as efficient as parclo-A because



(a) CONVENTIONAL DIAMOND
 (b) PARCLO-A (4-QUAD)
 (c) SPLIT DIAMOND - ONE-WAY STREETS
 FIG. 8.—ADAPTABILITY OF PARCLO-A (4-QUAD) INTERCHANGE TO MAJOR STREETS AND ITS COMPARISON WITH DIAMOND INTERCHANGES

the two direct left turns are made off rather than onto the cross street. It may be utilized wherever right-of-way restrictions or other physical controls preclude the development of the more desirable interchange type. Parclo-B (4-quadrant) is suitable for moderate to high volumes, utilizes two-phase signal control, but requires more street width than parclo-A as a result of left-turn lanes.

The full cloverleaf generally is not justified or fitting to the environment of a major street in built-up districts. However, primary highways running into or through cities as major streets may justify, in some parts of the urban area, the use of cloverleaf interchanges.

INTERCHANGES WITH PRIMARY HIGHWAYS—RURAL AND SUBURBAN

Interchanges between interstate highways and primary roads in rural areas and in suburban areas generally should be patterned to provide continuous movements. An appropriate form of interchange in such cases is the cloverleaf. However, other forms, which do not provide continuous operation, may be used under some circumstances. This depends on the character of the primary highway and the volume of traffic to be accommodated. These interchanges are primarily of the four-quadrant, parclo type. In special cases a diamond may be used in suburban areas. Previous statements regarding the diamond and parclo interchanges in urban areas pertain also to such interchanges in conjunction with primary highways in rural and suburban areas.

A basic feature of the cloverleaf is that it must have divided roadways through the interchange. Although the cloverleaf provides continuous movements, it does so at the expense of weaving maneuvers between the left-turning movements on adjacent loop ramps. This characteristic is not considered objectionable even for relatively heavy volumes on the primary highway. However, it is undesirable on an interstate highway unless design speed is low and traffic is light.

Interchange design should be tested for capacity in selection of type, and again in establishing the design details to assure a proper and adequate arrangement. Before this is done, the designer should have some concept of what the capacity potential of the cloverleaf may be under various traffic patterns and volume conditions. This is diagrammed in Fig. 9 and Fig. 10 for both rural and urban conditions, including variations with collector-distributor roads. All volumes are given in vehicles per hour. In each case two sets of volumes are shown, one with and the other without parentheses.

Three traffic patterns are used to illustrate a complete range of conditions of traffic loading, each producing design or practical capacity conditions as follows: (1) Highest equal volumes occurring simultaneously on adjacent loops; (2) highest volume occurring on the exit loop; and (3) highest volume occurring on the entrance loop. As a control, the first exit of the interchange involving the right-turn movement is taken as a range from zero to a volume equivalent to design capacity of the exit. Predicated on these conditions, the traveled way of approach and exit ends of the interchange are loaded then to or near practical capacity. Using this as a basis, the traffic-carrying capacity of the cloverleaf over an entire range of conditions is revealed. Also, direct compari-

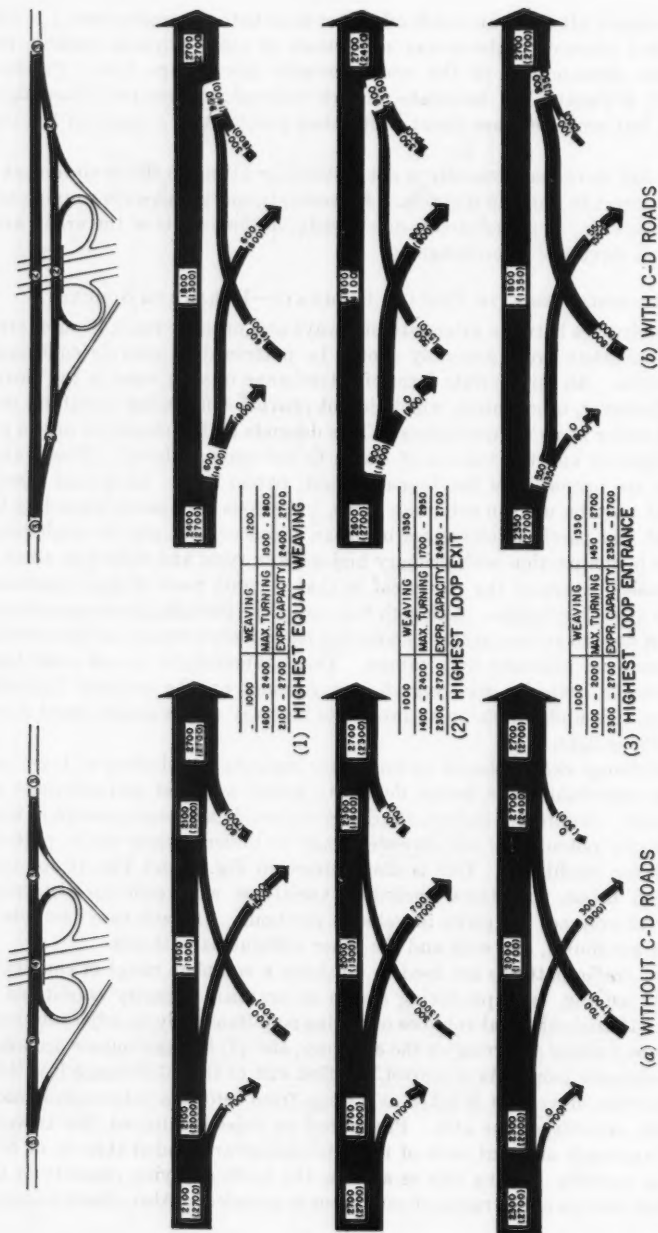
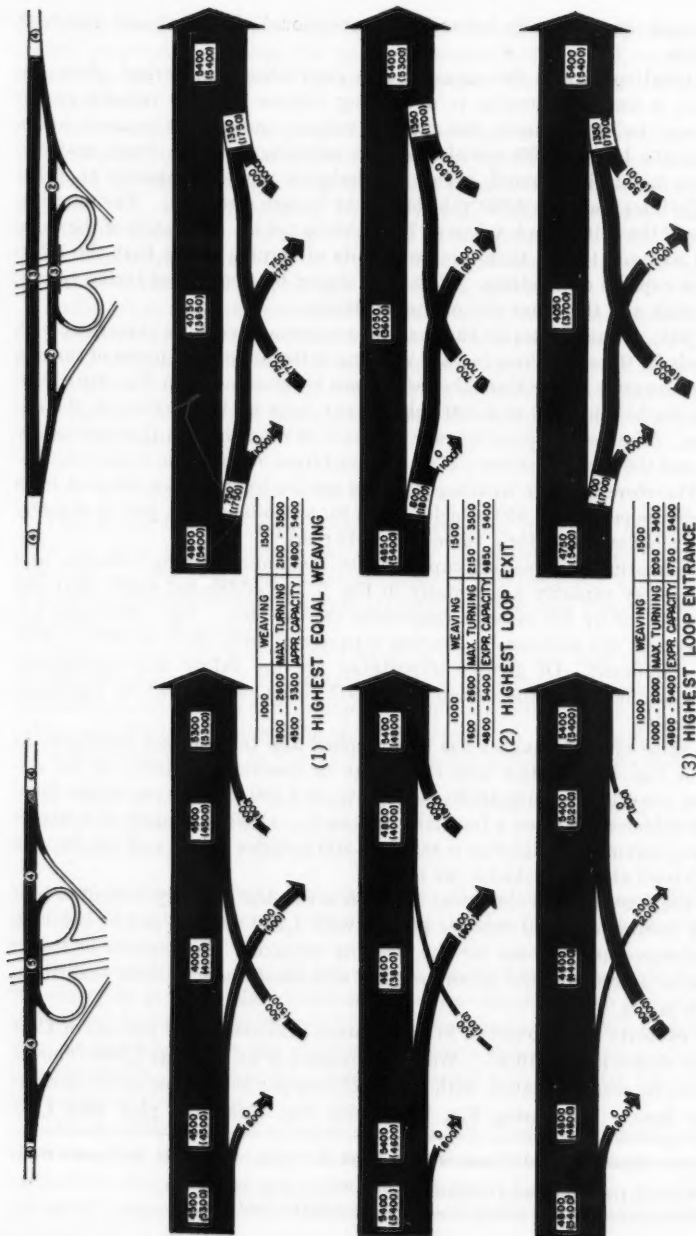


FIG. 9.—CAPACITY POTENTIAL OF RURAL CLOVERLEAF INTERCHANGES



(a) WITHOUT C-D ROADS
 (b) WITH C-D ROADS
 FIG. 10.—CAPACITY POTENTIAL OF URBAN CLOVERLEAF INTERCHANGES

son for each case is made between a conventional cloverleaf and one with C-D roads.

For rural conditions the capacity of a conventional cloverleaf, shown in Fig. 9(a), is limited generally to a weaving volume of 1,000 vehicles per hr (the sum of two movements, the entering volume and exiting volume), and a lane-capacity base of 900 vehicles per hr, allowing for 10% truck traffic.^{2,3} A six-lane facility is assumed, so that the design or practical capacity on either end of the interchange is 2,700 vehicles per hr in each direction. The practical capacity of the exit ramp is taken as 700 vehicles per hr. For each of the three cases of weaving traffic, there are two limits of turning traffic that the interchange is capable of handling. These are shown by two sets of traffic values, one set with and the other without parentheses.

Fig. 9(b) shows the traffic that can be accommodated by a cloverleaf with C-D roads for the same three cases of weaving patterns and two limits of turning traffic. Capacity of the through-traffic lanes is the same as in Fig. 9(a)—900 vehicles per hr per lane, or 2,700 vehicles per hr in each direction on the approaches. The design speed is lower on the C-D road than on the expressway proper, and the weaving is completely removed from other traffic on the expressway. Therefore, greater weaving volumes can be tolerated—a total of from 1,200 vehicles per hr to 1,350 vehicles per hr for a two-lane road, and to as many as 1,500 vehicles per hr for a three-lane C-D road.⁴

By comparing the weaving capacity, the maximum turning volumes, and the expressway capacity horizontally in Fig. 9, the additional traffic that can be provided for by the latter arrangement can be seen. The differences are not great, but the increase in weaving capacity of from 20% to 35% is considered significant. Of greater importance are the safety and operational advantages offered by the design with C-D roads, which will be examined subsequently.

The same type of analysis has been applied also to an urban condition, as shown in Fig. 10. In this case the design or practical capacity on the approaches, considering truck traffic to be 10%, is 1,350 vehicles per hr per lane, or 5,400 vehicles per hr on a four-lane approach. Design capacity of a single-lane ramp leaving the highway is taken at 800 vehicles per hr and one leaving the C-D road at 1,000 vehicles per hr.

For the conventional cloverleaf in urban areas, the capacity is limited to a weaving volume of 1,000 vehicles per hr, with 1,200 vehicles per hr per lane as the design-capacity base for the weaving section.⁴ The volume of traffic that can be accommodated by an ordinary cloverleaf under various conditions is shown in Fig. 10(a).

The capacity of a cloverleaf in urban areas is increased by the use of C-D roads, as shown in Fig. 10(b). Weaving volumes of as much as 1,500 vehicles per hr can be accommodated, with 1,200 vehicles per hr per lane as the design-capacity base.⁴ Comparing Fig. 10(a) with Fig. 10(b), the plan with C-D

² "Highway Capacity Manual," Bureau of Public Roads, U. S. Dept. of Commerce, Washington, D. C., 1950, p. 115.

³ "A Policy on Geometric Design of Rural Highways," A.A.S.H.O., 1954, p. 101.

⁴ "A Policy on Arterial Highways in Urban Areas," A.A.S.H.O., 1957, p. 490.

roads can handle 50% more weaving traffic. Considering total interchanging traffic, greater volumes also can be accommodated—from 17% to 35% more in the first case, 35% more in the second case, and from 70% to 100% more in the third case.

Interchanges adaptable to primary highways are summarized as follows: In rural areas the cloverleaf generally should be considered as most acceptable. Parclo-A (4-quad) on the less important primary highways also may be suitable. On the high-speed, relatively high-volume primary highways, directional types of interchanges may be appropriate (Fig. 1(e)). All other forms that require troublesome or hazardous maneuvers created by direct left turns on the highway generally should be avoided.

In suburban areas the cloverleaf is desirable. Wherever speeds are nominal and wherever occasional at-grade intersections are present on the highway, a parclo-A (4-quad) interchange usually is appropriate. Although less desirable, parclo-B (4-quad) may be used when it is not feasible to develop a parclo-A interchange. A diamond interchange may be considered, but the crossroad should be properly divided.

INTERCHANGES WITH EXPRESSWAYS AND FREEWAYS

Directional interchanges are used wherever the interstate highway intersects or joins an expressway or another interstate highway. Cloverleafs normally are not adaptable at interchanges of two freeways, except possibly in rural areas where turning volumes are relatively low, and then only when the design includes C-D roads.

There are numerous types of directional interchanges that can be utilized on interstate highways. The suitability of any type at a particular site depends primarily on the pattern and volumes of traffic, and site controls. The classification of directional interchanges, with respect to three basic operational characteristics, is shown in Fig. 11. Directional interchanges are classified as:

- a. With or without loops (latter referred to as all-directional);
- b. With or without weaving; and
- c. With one or two exits per approach.

Whether the design is with or without loop ramps is usually not important, provided the major turning movements are handled on direct or semidirect connections.

It is recommended that all weaving be removed from interstate highways in rural areas in which high sustained speeds are attained. No major weaving section should be allowed on such highways in urban areas. Weaving sections may be precluded by proper ramp arrangements and additional grade-separation structures. Weaving may also be removed from the main line of traffic by the use of C-D roads.

The characteristics of one-exit and two-exit directional interchanges are shown in Fig. 12. An approach to a directional interchange involving two exits, one on the right and one on the left, is shown in Fig. 12(a). An approaching driver preparing to leave the freeway must make two decisions: (1) That

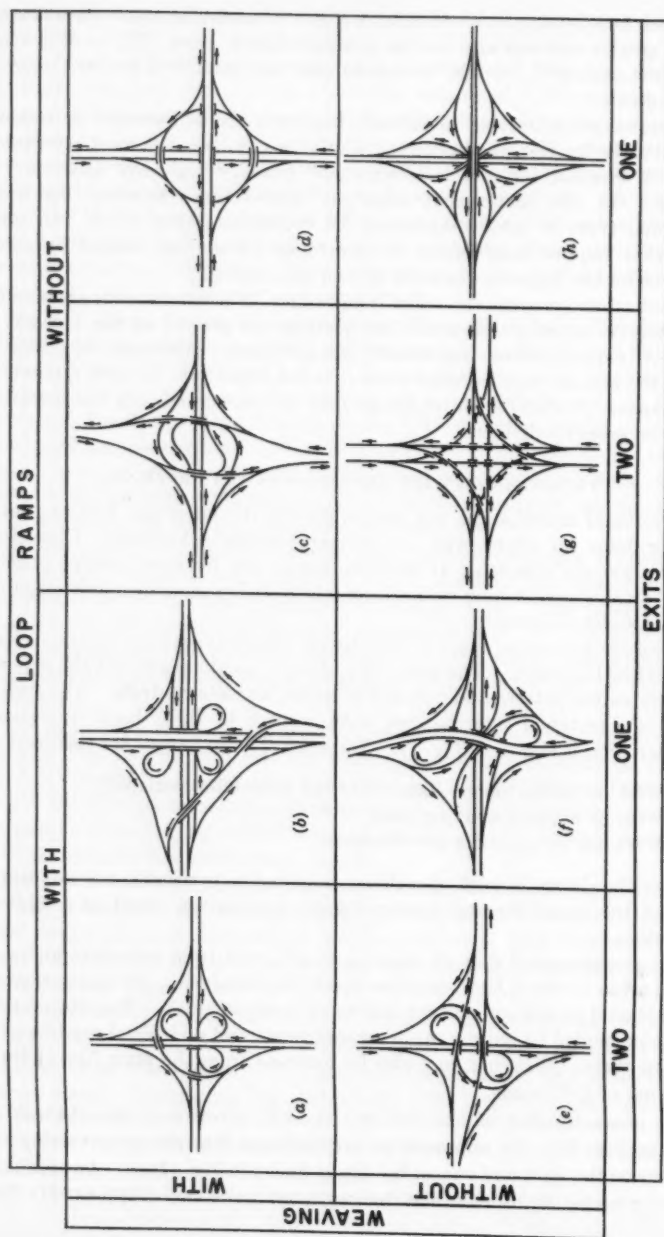


FIG. 11.—CLASSIFICATION OF DIRECTIONAL INTERCHANGES

the interchange ahead is or is not the one he is seeking; and (2) whether he must bear to the right or to the left, depending on his destination. The latter decision is made while traveling on the freeway along with traffic proceeding through the interchange.

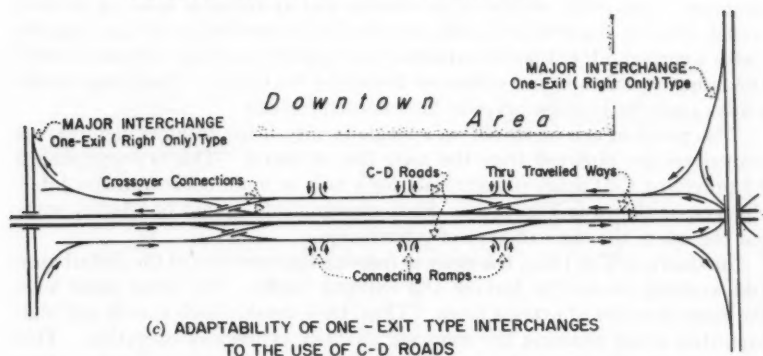
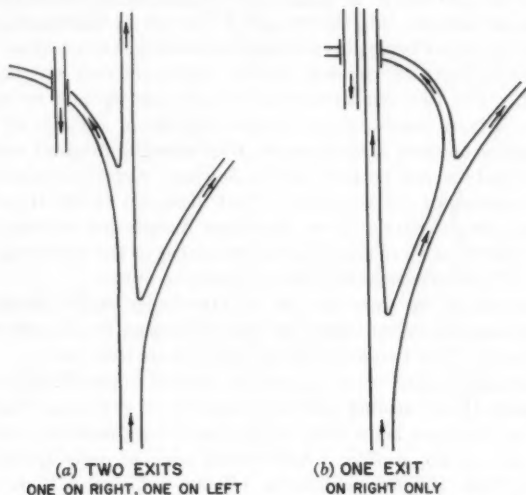


FIG. 12.—CHARACTERISTICS OF ONE-EXIT AND TWO-EXIT DIRECTIONAL INTERCHANGES

An approach to a directional interchange involving one exit, on the right only, is illustrated in Fig. 12(b). In this case the approaching driver makes only one decision—whether or not the intersecting highway ahead is the one he wishes to enter. The second decision, whether he should proceed to the right or left, is made while traveling at a reduced speed along the exit ramp, removed from high-speed through traffic. The directional sign is simplified

and more direct than in the two-exit arrangement, thus providing for safer operation.⁵

In the two-exit design, drivers bear left to turn left, and bear right to turn right. This may be considered an advantage because such maneuvers are natural. They are natural on at-grade intersections where the driver becomes aware of and turns directly onto the crossroad, but not on high-speed, expansive layouts, where the driver begins his turn without seeing the crossroad. Drivers are accustomed to leave the freeway on the right and may not be prepared for a left exit. The two-exit arrangements also are subject to more lane-changing when drivers maneuver for proper position in advance of the exits, than in the case of one-exit arrangements, thus creating internal weaving and friction. This problem can be alleviated somewhat by proper design of maneuver areas and spacing of the two exits. Exit distances of 600 ft or more are required by the design criteria of the American Association of State Highway Officials, and 1,000 ft or more according to standards of the California Division of Highways. These distances are often difficult to obtain.

Another feature of the one-exit type of interchange, which makes it most adaptable within metropolitan areas, is that the design fits a pattern of continuous C-D roads. The two-exit type of interchange does not.

Freeways situated adjacent to or near the central business district in large cities, particularly those forming part of an inner loop or circumferential highway, usually call for more lanes than can be reasonably used to accommodate future traffic on a single facility. Anticipated average daily traffic volumes in the range of from 100,000 vehicles to 150,000 vehicles in these areas are common. Unwieldy widths of pavements and unworkable weaving sections would often be required to handle such traffic at practical or design capacity (with a normal rather than an extended peak period condition) and still provide the frequency of exits and entrances demanded by traffic. These large traffic loads cannot be handled properly on a normal freeway.

The problem can be solved on a single facility if the troublesome weaving maneuvers are removed from the main line of travel. This is accomplished by providing C-D roads continuously for a mile or more between major interchanges, as shown in Fig. 12(c). Such arrangements cannot be effected without the use of the one-exit type of interchange.

As shown in Fig. 12(c), the inner or freeway lanes are free of the disturbance and weaving created by leaving and entering traffic. The inner lanes have the characteristics of express lanes. Thus, they develop high speeds and high capacities while retaining the intended qualities of freeway operation. This arrangement will permit the use of a total of twelve to sixteen lanes on four traveled ways on some sections of the circumferential route. The only other solution is the provision of parallel but independent freeways. This may be more difficult to attain in built-up areas.

In many instances the C-D roads need not be constructed at once. They can be delayed until some future date if the principal interchanges are designed to be one-exit types and sufficient right of way is provided initially. Fig. 13

⁵ "Correlation of Geometric Design and Directional Signing," by George M. Webb, *Proceedings Paper 1627*, ASCE, May, 1958.

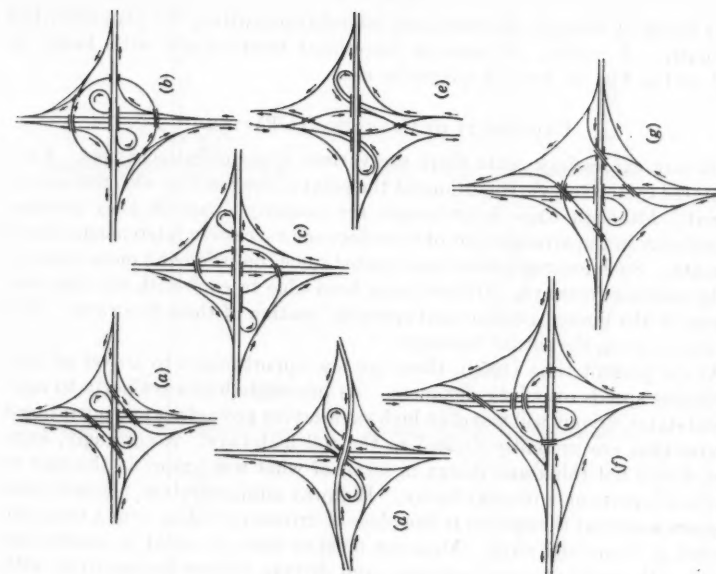


FIG. 13.—ALL-DIRECTIONAL INTERCHANGES HAVING ONE-EXIT ARRANGEMENTS

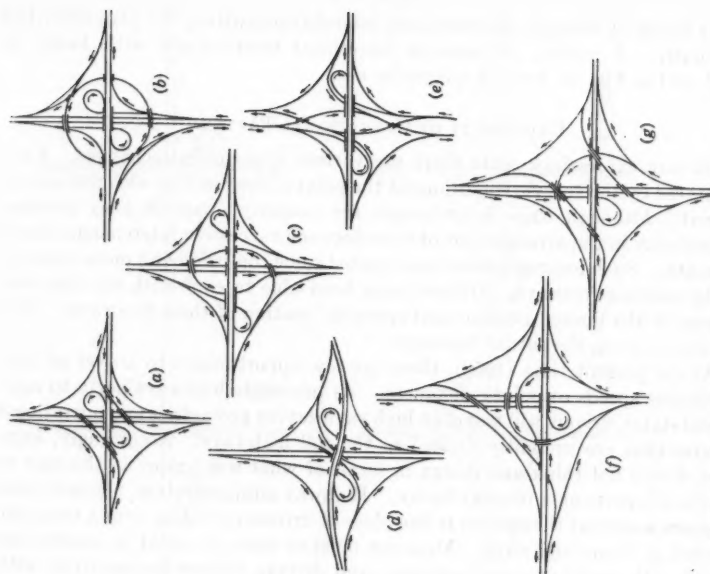


FIG. 14.—DIRECTIONAL INTERCHANGES HAVING ONE-EXIT ARRANGEMENTS WITH LOOP RAMPS

shows forms of one-exit all-directional interchanges, fitting the plan described previously. A variety of one-exit directional interchanges with loops, as developed in Fig. 14, may be adaptable also.

UNIFORMITY OF OPERATIONAL PATTERN

On any expressway route there are various types of interchanges. Each is dictated by the specific conditions at the point of intersection with the surface arterial. Although these interchanges are properly adapted, they produce dissimilarity in the arrangement of exits between successive interchanges along the route. Such inconsistencies have caused some confusion and inconvenience on the existing freeways. Drivers have been able to cope with the situation because of the limited number and sporadic location of these freeways. This will not be so on the future freeways.

At the present time (1959), there are few opportunities to travel at high continuous speeds over long distances. As interstate highways begin to span several states, drivers will travel on highways having geometrics and operational features that are presently limited to the toll highways. Accordingly, engineers should not think and design in terms of what was proper in the past or what is adequate on a freeway today. Highway administrators, planners, and designers must put themselves in the place of drivers operating over a complete network of future highways. Measures must be taken to avoid inconsistencies in design that will produce indecision and driving actions incompatible with the character and speed of operation.

Fig. 15(a) shows the dissimilarity in the arrangement of exits between successive interchanges that may occur with the normal use of basic forms of interchanges. The driver cannot be certain where the exit will be situated with respect to the crossroad—that is, in advance of or beyond the structure. Moreover, there may be one or two exits to the same crossroad. For example, in Fig. 15(a) at interchange A the driver leaves at a single ramp in advance of the structure. At interchange B he makes his exit beyond the crossroad. At interchange C to proceed south on the crossroad, the driver must use the exit in advance of the structure, but to go north he must travel beyond the crossroad and leave by means of the second exit. At interchange D he reverts to a single exit, and at interchange E he is confronted again with a choice between two exits. The cloverleaf design not only requires a realization on the part of the driver that there are two exits, but an immediate decision while on the freeway as to whether his destination is to the north or to the south of the interstate highway. A further complication arises when he finds that he has to weave with traffic entering the freeway using a ramp he has just passed. This confusion takes place amidst high-speed through-traffic along a facility that is supposed to be designed for a safe speed of 70 miles per hr.

The typical driver leaving the interstate highway generally has no concept of the form of interchange at which he is to make his exit. He relies completely on directional signs. He usually knows the name of the locality at or near his destination and the name of the crossroad or its route number. It is not likely that he knows whether his destination is to the north or to the south of the

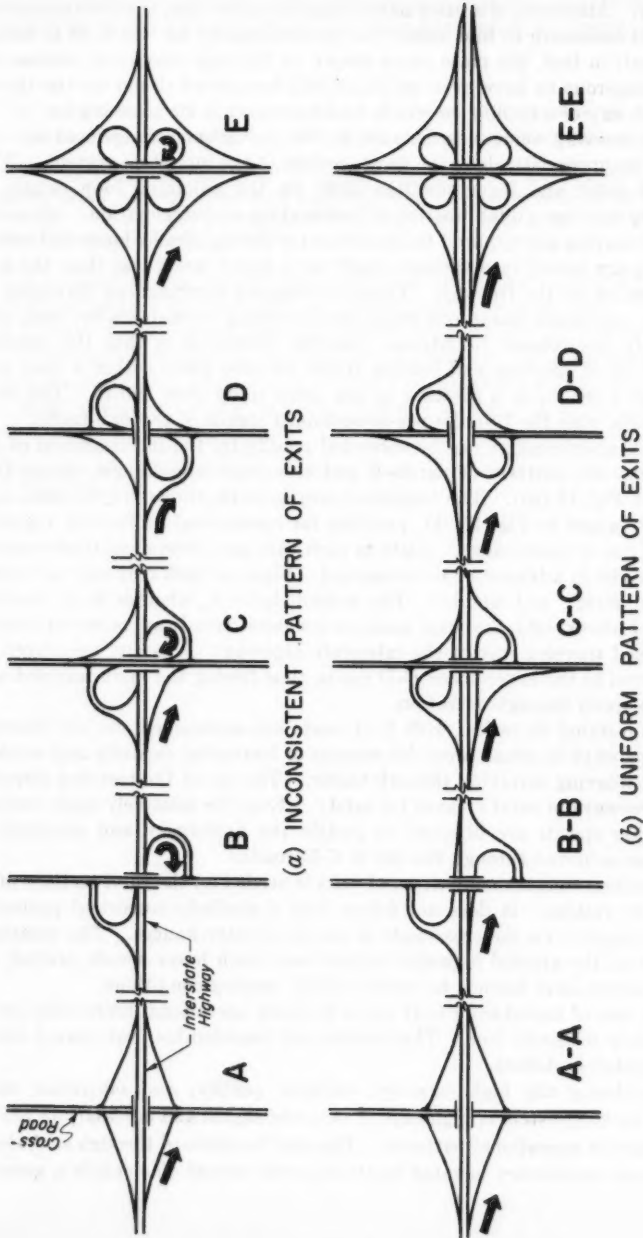


FIG. 15.—EXIT ARRANGEMENTS BETWEEN SUCCESSIVE INTERCHANGES

freeway. Moreover, if a place name is given on the sign, the information may be of no assistance to him unless the specific locality for which he is destined is named; in fact, the place name shown on the sign may even confuse him. It is dangerous to have even an occasional bewildered driver on the through traveled way of a facility on which vehicles travel at 70 miles per hr.

The weaving maneuvers created by the cloverleaf arrangement are completely inappropriate along the rural sections of the interstate system. Where vehicles enter and leave simultaneously on the adjoining loop ramps, the auxiliary lane has a dual function of deceleration and acceleration. As a result vehicles leaving are required to decelerate on through traffic lanes and vehicles entering are forced into through traffic at a speed much less than the speed of operation on the freeway. These overlapping merging and diverging maneuvers can create hazardous situations involving through traffic, even under relatively low-volume conditions. Another drawback is that the combined maneuvers of entering and leaving traffic all take place within a time space of about 5 sec, or in a distance of not much more than 500 ft. This is not compatible with the 70-miles-per-hr-sustained speeds of through traffic.

These shortcomings can be corrected readily by the incorporation of C-D roads into the patterns of parclo-B and cloverleaf interchanges (types B, C, and E in Fig. 15 (a)). The consistent arrangement, shown for the same series of interchanges in Fig. 15 (b), provides for operational uniformity regardless of the type of interchange. Exits in each case are always identical—one exit on the right in advance of the crossroad. Signs at each exit are consistently uniform, direct, and simple.⁵ The second decision, whether to go north or south, or left or right, is always made on a separate roadway, removed from the high-speed traveled way of the interstate highway. Weaving maneuvers are transferred to the lower-speed C-D roads, thus freeing the main traveled ways for high-speed through-operation.

The restyled cloverleaf with C-D roads has superseded the old cloverleaf along freeways in urban areas for reasons of increasing capacity and avoiding difficult weaving involving through traffic. The use of the restyled cloverleaf along freeways in rural areas is for safety. Even for relatively light volumes, the higher speeds are believed to justify the uniformity and simplicity of operation achieved through the use of C-D roads.

A uniform operational pattern of exits is needed on the rural sections of the interstate system. It does not follow that a similarly consistent pattern of exits is required on the crossroads at the same interchanges. The crossroads are part of the arterial highway network on which lower speeds prevail, and where drivers have learned to expect widely varying conditions.

The cost of introducing C-D roads to effect operational uniformity on the freeways is relatively low. The benefits are considerable, but cannot always be computed in dollars.

Considering the high capacity, superior quality, and maximum safety desired for this system of highways, it becomes logical and necessary to provide uniformity in operational patterns. This can be attained through such design features as consistency in ramp locations, even though this entails a generous

use of C-D roads. Therefore, it is recommended that this feature be incorporated immediately in the design of the interstate system of highways.

CONCLUSIONS

The objective in the development of a system of highways is indicated clearly in the American Association of State Highway Officials standards:⁶

*** In determination of all geometric features *** a generous factor of safety shall be employed and unquestioned adequacy should be the criterion.*** All known features of safety and utility should be incorporated in each design ***."

The selection of the proper type of interchange at intersections with thousands of highways is the first and perhaps the most important step. In urban areas the interchange should provide adequate capacity and efficient operation, and be sufficiently flexible to permit future expansion. In rural areas interchanges should fit the character of intersecting highways and be compatible with traffic operation on the interstate highway at the high sustained speeds experienced on turnpike facilities.

⁶ "Geometric Design Standards for the National System of Interstate and Defense Highways," A.A.S.H.O., 1956.

DISCUSSION

GERALD D. LOVE,⁷ J. M. ASCE.—Much basic interchange design information that should prove to be useful to engineers in the highway field has been presented.

Mr. Leisch has indicated the advantage of the diamond form of interchange. However, he considers that the diamond is inappropriate at minor rural crossroads because it is conducive to wrong-way movements. The terminal design of the diamond ramp-minor road intersection is more conducive to wrong-way maneuvers than the so-called parclo-B interchange design. On minor rural roads the traffic stream consists of predominantly local traffic. As a result motorists are familiar with the immediate local road, interstate highway intersections, and the directional flow of traffic on the interstate highway. It is unlikely that motorists who use a facility at frequent intervals are prone to make wrong-way movements, notwithstanding the fact that the design of ramp-crossroad intersections of diamonds may invite possible wrong-way maneuvers. Therefore, when traffic is primarily local in nature, as is the case on minor rural roads, the advantages Mr. Leisch presents against the use of a diamond design seem to be minimized and are more than offset by the benefits associated with this type of design. Some of the advantages of the diamond interchanges are as follows:

1. As a general rule, they require less right of way and are less expensive to construct than loop designs.
2. They provide a more direct connection and shorter travel distances.
3. They can be adapted to existing terrain features with minimum effort.

Although standard interchange designs are desirable as guides, they should not be utilized as the sole basis for design. All interchanges should be considered as individual problems, with due consideration given to all types of interchange designs and to all factors that must be evaluated before a good design can be developed. When standard designs are used, there is a tendency to apply them indiscriminately, resulting in stereotyped plans that do not reflect professional engineering quality.

JACK E. LEISCH,⁸ A. M. ASCE.—Mr. Love has cited several important advantages of diamond-type interchanges at minor rural roads. He has emphasized also that local drivers would be familiar with the intersections along any minor road that connected with as important a facility as an interstate highway. Therefore, motorists who use an interchange frequently are not likely to make wrong-way movements.

Occasionally there will be confused drivers on a local road, although it is less common than on a primary highway. Confusion may be caused by fatigue, liquor, fog, or snow, as well as by lack of familiarity with the locale. The problem cannot be ignored.

⁷ Highway Design Engr., Bureau of Public Roads, U. S. Dept. of Commerce, Albany, N. Y.

⁸ Chf. Highway Engr., De Leuw, Cather & Co., Chicago, Ill.

The local rural road under discussion is typically situated in a sparsely settled area. In mid-western or western states it is typified by the lightly traveled section-line roads. Such roads are used normally for interchange locations only because there are no primary highways in the vicinity.

By way of illustration, if primary highway crossings occur at intervals of approximately five miles in a rural area, the local road crossings in between are not provided with interchanges. On the other hand, where primary highway crossings are ten, twenty, or even fifty miles apart, some of the intermediate local roads should be provided with interchanges.

In some instances, the reason for interchanges at local roads is to provide a more flexible and useful system. A certain spacing of ingress and egress faci-

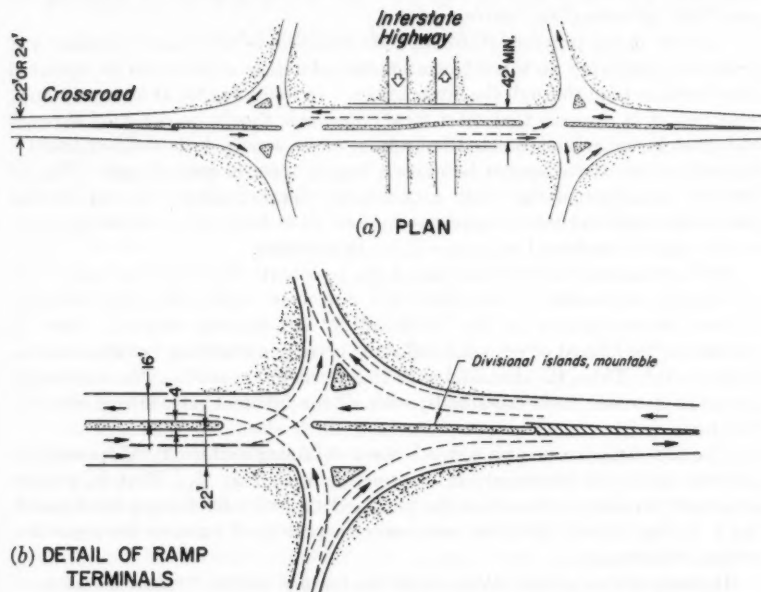


FIG. 16.—ADAPTABILITY OF DIAMOND INTERCHANGE TO MINOR RURAL CROSSROADS WITH DIVISIONAL ISLAND

ties is desirable and essential to the maintenance and operation of the highway. Reasonably close spacing of interchanges also adds to the convenience of traffic potential to an interstate highway. Facilities to provide such services as gasoline, automobile repairs, food, motels, and first aid will be situated on the crossroads at or near the interchanges.

Substantial volumes of traffic may result from service facilities at some of the interchanges with local roads. The problems thus created may be significant because this generation of traffic is not usually considered in design of interchanges at local roads. To comprehend what this traffic volume may be,

one need only observe the activity at service areas along modern turnpikes. A comparable situation may be created at many of these crossroads. In some cases it may be worse because traffic making left turns and weaving maneuvers to and from service areas will become intermixed with both crossroad and interchange traffic.

Thus, traffic using interchanges at local rural roads will involve the unfamiliar driver. In some instances use of the interchange will require turning movements far in excess of through traffic on these roads. Accordingly, the simple diamond interchange will be subject to wrong-way movements as discussed previously in conjunction with Fig. 2. If the local rural road is to be limited to a two-lane highway, the *parclo-B* type of interchange would be preferable because it greatly minimizes operational hazards by reducing the possibility of wrong-way movements.

In view of the previous statement, the question is raised as to whether any crossroad justifying an interchange on the interstate system can be operated as a two-lane road through the interchange. In designing for at least a twenty-year period, it appears that most local crossroads should be designed through the interchange with protected left turns, or even as a fully divided facility. In such a case the diamond becomes a logical form of interchange. Fig. 16 shows a minimum design with longitudinal channelization. A full divided section through the interchange having two 24-ft lanes and a 4-ft-wide divisional island is preferred wherever it can be justified.

By introducing the divisional island, the possibility of wrong-way maneuvers is virtually eliminated. The additional pavement width precludes blocking of through-movements on the crossroad by left-turning vehicles. Also, it minimizes the hazard of rear-end collisions involving standing vehicles waiting to turn left. Thus, the diamond with the divisional island may be considered desirable at minor rural crossroads, with all the inherent advantages cited by Mr. Love.

The use of the diamond is a step toward obtaining uniformity of operational pattern mentioned previously in conjunction with Fig. 15. That is, greater use of the diamond, rather than the *parclo-B* type of interchanges (sketches B and C in Fig. 15(a)), affords a more uniform pattern of exits on the interstate system of highways.

It is urged that all the states adopt the feature for the interstate system of highways, thus effecting uniformity in the operational pattern.

AMERICAN SOCIETY OF CIVIL ENGINEERS

Founded November 5, 1852

TRANSACTIONS

Paper No. 2995

DESIGN FEATURES OF THE DRESDEN NUCLEAR POWER STATION

BY JOSEPH E. LOVE,¹ A. M. ASCE, CHESTER S. DARROW,²
AND BURR H. RANDOLPH³

SYNOPSIS

Civil engineering design features of the Dresden Nuclear Power Station near Morris, Ill., are presented, and design considerations arising from the layout of nuclear power equipment within a vaportight sphere are examined. Civil engineering problems of a more conventional nature are reviewed and related to nuclear power plant design.

INTRODUCTION

This paper emphasizes the civil engineering aspects of the 180,000-kw Dresden Nuclear Power Station, near Morris, Ill., and approximately 50 miles southwest of Chicago at the confluence of the DesPlaines and the Kankakee Rivers. Primary emphasis is on the arrangement, coordination, and interrelation of plant components in a workable nuclear power plant design. The nuclear, mechanical, and electrical systems are covered briefly. A more detailed description of the Dresden Station may be found elsewhere.⁴ Financing is being provided by private industry at a cost of 45 million dollars.

Design of the Dresden Station began in April, 1956, and major construction was started early in 1957. It is scheduled to be completed in 1960. An artist's conception of the completed facility illustrating the compact nature of the arrangement is shown in Fig. 1. This view is taken looking north. The reactor vessel and its associated equipment are housed in the 190-ft-diameter steel sphere shown on the right. The large rectangular building to the left of the sphere contains conventional power plant components, such as the turbine generator, condenser, feedwater heaters, and control room. An administration

NOTE.—Published, essentially as printed here, in April, 1958, in the *Journal of the Power Division* as *Proceedings Paper 1800*. Positions and titles given are those in effect when the paper was approved for publication in *Transactions*.

¹ Atomic Power Equipment Dept., Gen. Electric Co., San Jose, Calif.

² Atomic Power Equipment Dept., Gen. Electric Co., San Jose, Calif.

³ Power Div., Bechtel Corp., San Francisco, Calif.

⁴ "A Design Description of the Dresden Nuclear Power Station," Gen. Electric publication GER-1301, ASME paper no. 56A169, November 28, 1956.

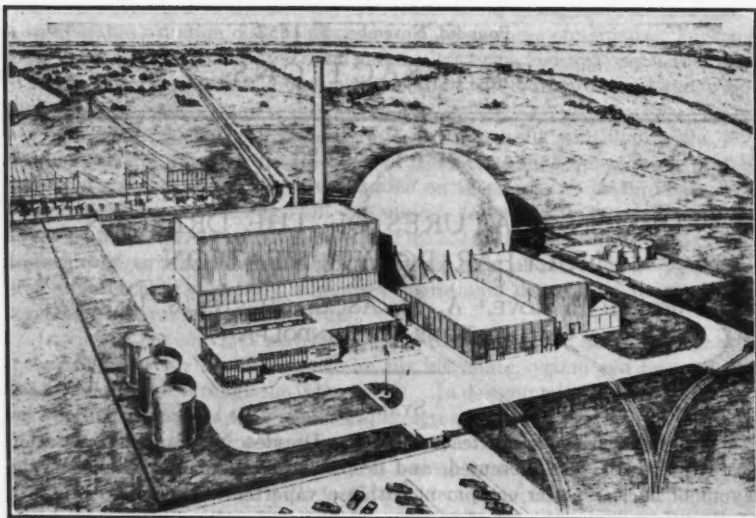


FIG. 1.—DRESDEN NUCLEAR POWER STATION

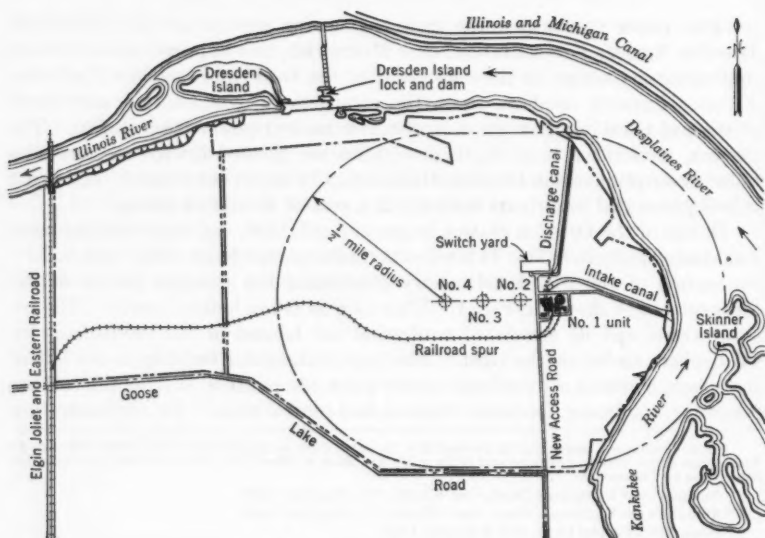


FIG. 2. POWER STATION SITE PLAN

building and an access control building are located in front of the turbine building. Shop-warehouse and fuel storage buildings are shown in front of the sphere, and a radioactive waste facility is seen on the extreme right. Circulating water to the main condenser in the turbine building enters by way of the canal on the right and is discharged by the canal on the upper left.

THE SITE

The site for the Dresden Station is approximately 1 mile wide by $1\frac{1}{2}$ miles long. As shown in Fig. 2 it is situated at the juncture of the DesPlaines and Kankakee Rivers where the Illinois River is formed. The plant itself is situated at least one-half mile from any off-site land as a safety feature. However, this necessitated long canals for circulating water (Fig. 2).

The ground surface is gently rolling and easily drained. However, bedrock underlies the general plant area within four ft of the ground surface, and construction requirements have necessitated the excavation of approximately 150,000 cu yd of rock.

The site is served by the Elgin, Joliet and Eastern Railroad. A spur has been built from the railroad at the western boundary to the plant area. Highway access is from the south, and the Illinois waterway will be used for barge access to the site.

UNIQUE FACTORS IN A NUCLEAR POWER PLANT

A modern, complex industrial plant presents problems of arrangement, structural type, and economy that are strongly influenced by the process for which the plant is built. This is certainly the case with a conventional fossil fuel fired power plant. The problems to be reviewed herein are those which have been superimposed on the power-plant design by virtue of its being a nuclear plant.

Radiation and Shielding.—The factors in a nuclear plant having the strongest influence on design and arrangement stem directly from the fact that the nuclear process produces ionizing particles and rays. Under certain conditions this radiation can be biologically harmful to man. Therefore, shielding protection from neutrons and gamma rays is required in certain areas.

The neutrons are generated in the core of the reactor and present a radiation problem in the immediate area around the reactor core. The thickness of the shielding concrete opposite the reactor core has been dictated by the neutron radiation from the core.

Water passing through the reactor is irradiated in the dense radiation flux in the core. The general result is that certain isotopes are created by fast neutron reactions in the water. Of those isotopes created, nitrogen 16 is generally most important in its effect on shielding design.

The 6 mev gamma rays originating from the decay of nitrogen 16 control the amount of shielding required for pipes and for equipment carrying reactor water and steam. In some locations, corrosion products or ruptured fuel particles will dominate, for example, in the demineralizers and cleanup equipment.

Fortunately, the nitrogen 16 has a short half-life so that equipment which may contain reactor water or steam will generally be accessible within a few

minutes after plant shut-down. However, radiation from corrosion products may still limit access in some areas.

Operation of the plant requires that the radiation be confined to the immediate vicinity of the equipment which is the radiation source. This is the reason for the relatively thick and massive concrete construction so characteristic of nuclear plants. Gamma radiation can be stopped or shielded most effectively by mass. Experience indicates that ordinary portland cement concrete is one of the most versatile and economical materials that can be used for shielding.

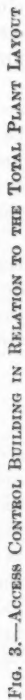
Heavy aggregate concrete, steel, and lead have been used in some nuclear plants for shielding where space was at a premium. One of the design objectives in the arrangement of the Dresden plant was to keep the use of such materials to the bare minimum for shielding. That the designers have succeeded in this objective is indicated by the fact that less than twenty cu yd of heavy aggregate concrete have been called for in the design.

Directly related to the problem of radiation and shielding is the fact that much of the plant system equipment is not accessible for adjustment or maintenance during operation. Instrumentation and control features will permit the station to operate with a degree of reliability and availability comparable to a modern conventional plant. Provisions for isolation of certain equipment, such as feedwater heaters, will permit direct maintenance without shutting the plant down.

Provision for Decay Heat.—When the fire is out in a conventional plant the boiler will cool down. It can then be physically inspected and repairs made directly as required. However, even after shutdown the nuclear reactor core continues to give off considerable heat. This decay heat comes from the gradual nuclear decay of the fission products formed in the reactor during operation. Because it is not economically desirable to remove all the fuel from the core at every shutdown, this heat must be dissipated. In the Dresden Station a shutdown heat-exchange system will remove the decay heat.

Radioactive Wastes.—The operation of the plant will not produce any fly ash but it will produce some waste products which must be disposed of. The ventilating air circulated through the process buildings will be discharged to the atmosphere through the 300-ft-high stack. There is a remote possibility that this air may on rare occasions pick up some contamination. Therefore, it will be routinely monitored before being discharged through the stack. Also, the air that passes the outside of the reactor vessel will be irradiated by those neutrons that escape the vessel. This air must be discharged at a safe location, in this case from the stack. The air ejectors in the condenser system will remove air in-leakage and gases formed in the reactor and turbine systems. These gases will be sent up the stack after suitable delay to permit decay of the nitrogen 16. As mentioned previously, all gases discharged from the stack will be monitored to insure environmental protection.

In general, liquid waste disposal will be to the Illinois River. A comprehensive, radioactive waste-disposal plant is provided for processing waste material that must leave the plant. Disposal will be constantly checked and controlled. Concentration and on-site storage of the more radioactive liquid waste is also provided for. Solid waste, whether it is broken glassware and



filter papers from the laboratories, or highly contaminated equipment no longer serviceable, will be disposed of in concrete underground vaults on the site. All waste disposal from the plant will be carefully regulated and held within the maximum permissible rates set by the regulatory groups.

Provision for Access Control.—One feature of this plant which has had an influence on total plant layout is the need to control the entry and exit of operations personnel in the areas which are potential radiation zones. It was recognized early in arrangement studies that this control over personnel was a feature which would have to be built into the plant rather than leaving it as an operational problem to be solved later. Therefore, the Dresden Station includes an access control building. Fig. 3 shows the relationship of the access control building to the total plant layout. The shaded areas are those which are subject to control from the access control building.

Operating personnel desiring to enter any of these areas must pass the control point in the building. At this point, the required authorizations will be checked and each man will acquire the necessary equipment for his own protection.

When a man returns from his duties in the controlled area he again passes the control point where he is cleared for access to the rest of the plant.

A central location close to the turbine building, the fuel handling building, the reactor enclosure, and the shop was chosen for this building. Access to all or parts of these buildings must be controlled, and, furthermore, no cross-connections could be permitted. That is, for example, the controlled area could not have uncontrolled corridors cutting across it.

NUCLEAR STEAM SUPPLY SYSTEM

Plant Cycle.—Fig. 4 shows the power cycle selected to fulfil the design requirements of the Dresden Station. Light water, serving both as coolant and moderator, passes through the reactor core of slightly enriched uranium dioxide and forms a steam-water mixture which is routed to a primary separating drum. The steam from this drum flows directly to the turbine at 965 lb per sq in. (gage) and 541° F. Water from the drum is returned to the reactor through four secondary steam generators. Feedwater to these generators removes additional energy from the recirculating water to form secondary steam for admission to the turbine at 500 lb per sq in. (gage) and 461° F. The term "dual cycle" is derived from the use of these two sources of steam.

Reactor Package.—The essential equipment of the nuclear steam supply system for the Dresden plant consists of the reactor vessel, primary steam drum, emergency condenser, secondary steam generator, recirculating pumps, and associated high-pressure piping system. The general arrangement is shown in Fig. 5.

This equipment is housed in a 190-ft-diameter steel sphere designed to contain fission products in the remote chance of a serious accident. Special feature such as escape locks and leak-tight openings for mechanical and electrical penetrations are provided in the design of the enclosure to satisfy the plant arrangements. The sphere extends 39 ft below grade, forming a suitable

base for the equipment and biological shielding associated with the nuclear steam supply system. Vertical space is provided directly below the reactor vessel for the removal of the bottom-mounted control rods. Surrounding this area are rooms for control-system piping and equipment, and for auxiliary equipment. The reactor vessel plus the refueling area above the reactor accounts for approximately 61 ft in height. The height of the steam drum above the exit elevation of the riser pipes is dictated by net positive suction head requirements on the recirculating pumps together with other hydraulic considerations. The emergency condenser, which forms an automatic heat sink for certain reactor shutdown conditions is located 23 ft above the centerline of the steam drum. The limits of the reactor package in a horizontal plane

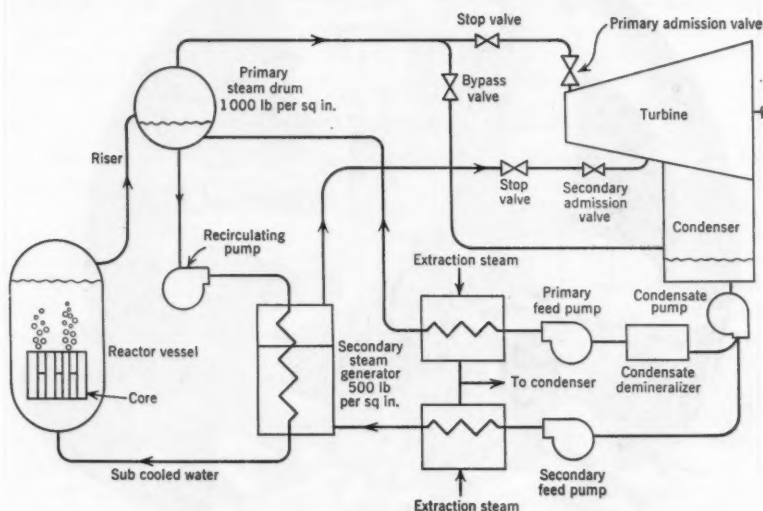


FIG. 4.—POWER CYCLE

are based on the space required for the secondary steam generators plus the shielding walls in one direction and the refueling area in the other.

Occupancy During Operation.—To achieve the necessary flexibility of operation during both normal plant operation and required down time, provision for access to key equipment has been incorporated in the arrangement of the plant. For example, the secondary steam generation equipment is divided into four separate loops contained in separate shielded compartments. Maintenance of equipment in any loop during plant operation is possible with the equipment shut down. Certain equipment is provided in duplicate with shielding walls arranged to permit access for maintenance during operation.

The over-all influence of providing habitable areas during operation requires that the arrangement of the package be spread and expanded beyond the minimum needs of shielding the equipment only. The access spaces are

shielded for radiation levels consistent with operational and maintenance requirements.

Reactor Vessel.—The reactor vessel, which is 12 ft 2 in. inside diameter, 41 ft high, with a 5½-in. wall, weighs approximately 580 tons in an operating condition and weighs 820 tons during the refueling cycle. The type of support for the reactor vessel was selected to best satisfy static loading, space limita-

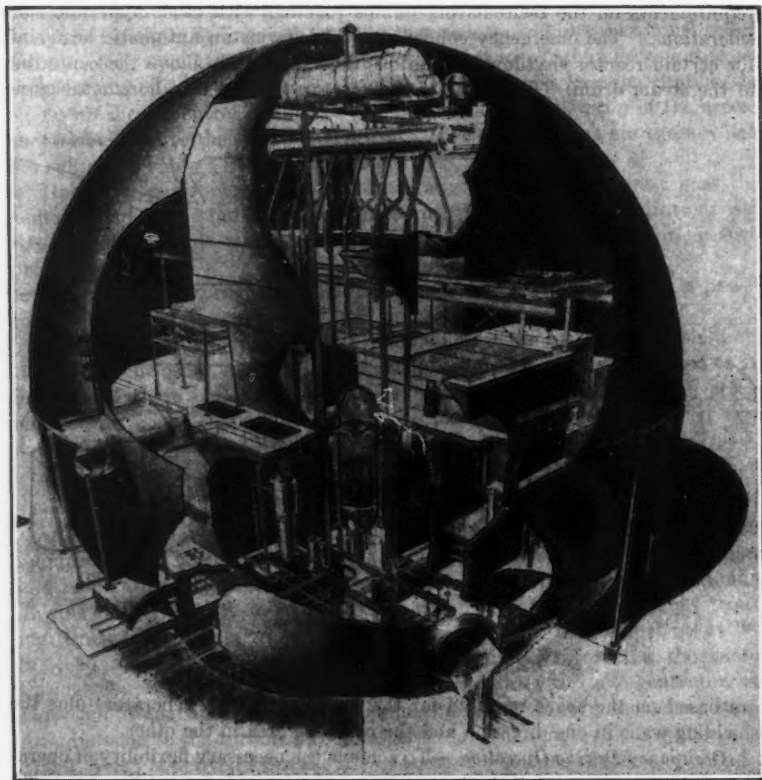


FIG. 5.—REACTOR ENCLOSURE

tions, and position in elevation for anchoring or being the "zero" point for the complex piping system connected to it. Twenty-four supporting brackets are built into the perimeter of the cylindrical part of the vessel and spaced as closely as possible to the 22-in. recirculating return nozzles. These brackets are supported on steel bases that transfer the vessel loads into the reinforced concrete foundation. Radial movement of the vessel from thermal expansion is taken on self-lubricating plates at the contact surfaces between the vessel brackets

and the ring girder. Four guides at the quarter points are provided 28 ft above the support plane in order to maintain vertical alinement when the vessel expands from thermal growth. These guides allow vertical and radial movement from thermal expansion while keeping the vessel in vertical alinement. A design load of .066 g based on the operating weight of the reactor vessel takes care of seismic loading.

The Dresden reactor uses bottom-entry vertical control rods that require a space approximately 15 ft in diameter and 36 ft deep for the rod mechanisms, their associated piping, and room for removal for maintenance. The auxiliary equipment for the control rods is in rooms adjacent to the control rod space.

The primary shield around the reactor vessel is comprised of 11 ft of ordinary reinforced concrete. Cooling coils within the primary shield are within the inner 2 ft of thickness and are used to keep concrete temperatures below 200° F. Where the primary shield is penetrated by large piping, space is provided for its installation and the opening closed with concrete block after erection and test. In areas requiring embedded sleeves, careful layout of the sleeves maintains the over-all shield integrity.

Primary Steam Drum.—The primary steam drum is located 83 ft above the riser piping of the reactor vessel. This drum is approximately 65 ft long and weighs 204 tons in an operating condition. Twelve 16-in. risers from the reactor vessel, together with ten 16-in. downcomer lines to the secondary steam generator piping loops are connected to the drum.

The steam drum is hung on twenty constant support hangers to minimize the length of piping to and from the drum, and to take care of the thermal expansion of the piping system without overstress. These hangers carry the weight of the drum and part of the piping load. Each hanger is designed for a travel of approximately 6 in. under load. Limit stops which are framed into the floor above and which are designed to prevent tipping along the longitudinal axis of the drum during operation are provided on each end of the drum. Horizontal ties with adjustment are provided to take care of lateral and possible seismic loads.

Emergency Condenser.—The emergency condenser is located with its centerline 23 ft above the centerline of the primary steam drum to provide the necessary elevation head to drain the condensate from the tube bundles. The tube bundles are located at each end of the tank shell. The entire weight of the unit is carried through support feet on the condenser tank shell.

Secondary Steam Generator Equipment.—The Dresden plant has four secondary steam generators, recirculation pumps and the necessary piping loops. The secondary steam generators are anchored in place with suitable provision for radial expansion of the shell. The recirculating pumps are supported by constant support hangers and float with the movement of the piping system. Provision is made for the complete removal of a recirculating pump and motor, minus the fixed bowl, by lifting the assembly through hatches above.

Auxiliary Facilities.—In addition to the equipment associated with the primary and secondary steam systems, space and shielding is provided for closely related auxiliary facilities. The shutdown heat exchangers and pumps used to dissipate residual heat during refueling are located as closely to the re-

actor vessel as possible and still provide access for maintenance during operation. The dual system of demineralization equipment is heavily shielded and space is provided for maintenance. Cooling water equipment, air conditioning units, and various shielded areas for special instrumentation are provided. The location and levels of piping penetrations for main piping as well as for service water of various kinds all are factors determined by the civil engineering aspects of the plant.

Personnel and Equipment Access.—Access to various operating levels within the sphere is still another civil engineering aspect of the work. Normal access into the sphere is provided by the personnel access lock located 12½ ft above established grade. An operating floor is provided all around the main shielded structure at this level. Stairways at each end of the structure lead upward to the other operating levels and down to work areas below grade. Supplementing the stairways, a personnel elevator is provided to certain key operating levels for use during refueling and shutdown periods. An emergency escape lock is located diametrically opposite the personnel lock and at the same elevation.

To provide for the replacement of certain large pieces of equipment during the life of the plant, a 16-ft-diameter, bolted-on cover is provided at an elevation approximately 12 ft above grade. This is located as closely as possible to the service of the 50-ton reactor crane.

An equipment removal lock with doors having a clear opening of 8 ft by 8 ft is provided at an elevation 48 ft above grade. The passage through this lock leads directly to the turbine building where equipment can be handled by the turbine building crane. Within the sphere, the elevation of the equipment lock coincides with the operating floor over the secondary steam generator cells. Therefore, equipment can be moved directly from these cells to the lock and out of the lock as necessary.

Refueling.—Water shielding is used in the Dresden plant to refuel the reactor. This means that the various functions of removing bolts, lifting heavy equipment, and the moving of fuel in and out of the vessel must be performed under water of various depths to give the necessary shielding for operating personnel. An open-top concrete pool or canal, 26 ft in height above the lip of the reactor vessel, is provided for this purpose. During normal operation, this canal is completely empty of water. When it is necessary to refuel, the following sequence is followed:

The canal is partially flooded and the reactor head is unbolted and stored in one end of the canal under water. Various removable fixtures within the vessel are also stored in the canal. With the proper depth of water in the canal the spent fuel is lifted out of the vessel, using special arms and grapples, and placed in a rack carrier near the vessel. This carrier moves the fuel to the south end where it is placed in a basket sized to fit a 42-in. vertical pipe. The basket is lowered through this pipe to a receiving carrier which maintains a water seal between the canal inside the sphere and the storage area outside the sphere. A tunnel connects to storage and work areas described subsequently.

To use this method of refueling, several items of interest are noted. One is the seal of the reactor vessel to concrete required because the canal and the

reactor vessel are flooded during refueling. This seal must provide for the expansion of the vessel both radially and vertically from the cold position to the hot operating condition. A large stainless-steel bellows seal integral with a metal skirt provides the seal and accommodates the movement. Another item of particular interest is the handling equipment which is provided for refueling. To assist in this operation, a 50-ton crane with auxiliary hook, a special moveable platform with hoist carriers, and an underwater rack carrier are provided.

Erection Sequence.—The steel containment structure was built first. This structure was completed and tested for leakage and structural requirements. During this phase of construction and testing the shell was entirely supported on steel columns.

At this stage a 24-ft-diameter construction opening was cut in the shell approximately at grade on the east side. Placement of foundation concrete inside and outside the sphere was carried on simultaneously to bring the work up to grade elevation. This involved placing approximately 3,000 cu yd of concrete outside the sphere and 11,000 cu yd inside the sphere. Another construction opening was now cut in the sphere at the north side. This opening was approximately 22 ft wide by 29 ft high and situated at grade elevation. In addition to serving as a construction access opening, it was large enough to permit entry of the reactor vessel.

The configuration of structures coupled with the size of the equipment is such that the support deck for the emergency condenser had to be erected as the first structural element above grade. The emergency condenser was shipped in sections of a size permitting field handling to its final elevation. After the emergency condenser was in place, the primary steam drum was hoisted in a horizontal position to its final location just below the emergency condenser deck and supported by its spring hangers. The large piping connecting to the drum was then brought in through the ends of the partially complete structure. The reactor vessel was brought into the sphere on special skids in a horizontal position. Sufficient structure was erected to lift the reactor vessel in place. Work can then proceed to finish the additional shielding structures and complete the piping assemblies. The total concrete work associated with the reactor enclosure is approximately 29,000 cu yd.

FUEL BUILDING

The fuel building, together with the storage areas for fuel, is the facility where the Dresden fuel is stored temporarily and made ready for off-site transportation. A vault for the new fuel is provided adjacent to the main structure as indicated in Fig. 6. The fuel building structure above grade is 61 ft by 95 ft by 46 ft high from grade to top of roof. This part above grade is of conventional design throughout. A 75-ton capacity crane, used for handling fuel casks, services the building. In addition, a special 1-ton capacity crane equipped with a telescoping grapple device is provided for moving fuel rod assemblies under water.

The fuel transfer tunnel, handling pool, and storage pool below grade are of special interest. The fuel handling tunnel has a cross section 7 ft 9 in. by

15 ft 6 in. in height with its invert 42 ft below grade. This tunnel extends 64 ft from the 42-in.-diameter discharge tube below the reactor enclosure to the open-topped fuel handling pool. The fuel carrier, mounted on tracks within the tunnel is used to convey the used fuel from the vertical discharge tube to the fuel building, or, conversely, to take new fuel to the discharge tube. During operation, this tunnel and associated pools are filled with water of high purity.

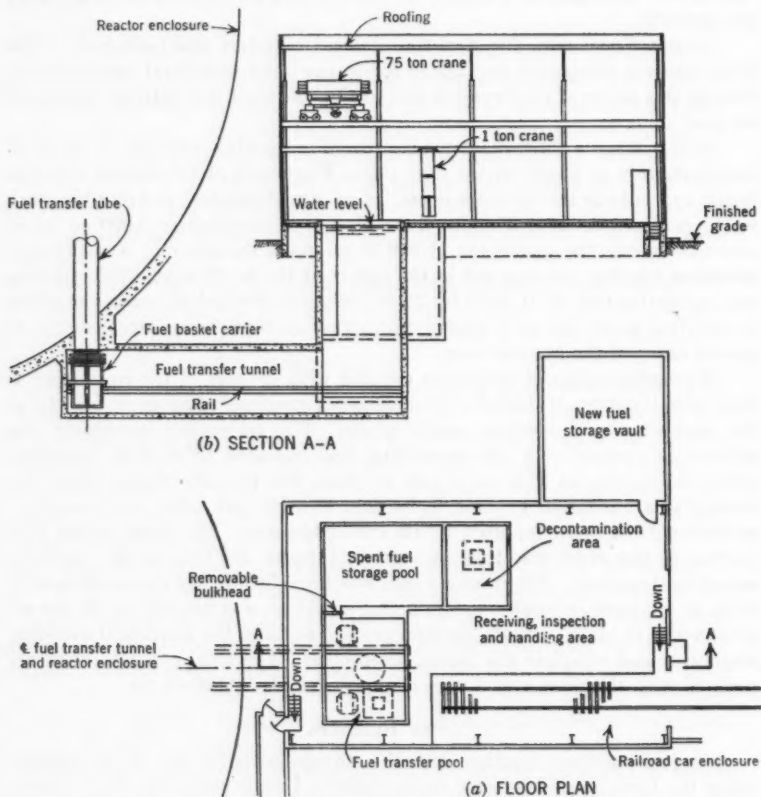


FIG. 6.—FUEL BUILDING AND STORAGE AREA

The outside surfaces are membrane waterproofed to prevent any possible leaks, either into the tunnel from ground water, or out from the tunnel or pools. Because part of the tunnel extends below the sphere, and as the rock excavation required extensive blasting, it was necessary to construct the structures below grade prior to erection of the sphere.

The fuel handling pool, 20 ft by 26 ft by 41 ft deep, provides a facility where the fuel can be removed from the carrier, inspected, and moved to other equip-

ment or areas. For temporary storage, a pool 20 ft by 29 ft by 25 ft 5 in. deep is used. Fuel is moved under water through a movable bulkhead by using the special crane and grapple mentioned previously. During normal operation, all the pools are flooded. By inserting the movable bulkhead between pools, it is possible to maintain the required depth of shielding water in the used fuel storage pit, and to dewater the tunnel and handling pool for maintenance and inspection.

Inside the fuel building and adjacent to these pools, a railroad well and siding are provided. Shipping casks for transporting used fuel from the plant site to reprocessing areas can be loaded on railroad cars.

TURBINE BUILDING

General Arrangement.—The turbine building houses the power-generating system and the heat-recovery system of this plant. In addition, the control room—the central control point for the plant—is located in the turbine building. The turbine floor is approximately 35 ft above grade. The turbine building has been so arranged that a logical separation of potentially contaminated and radiation source equipment is centrally grouped. This, as well, results in a functional arrangement for the major pieces of equipment. Grouped around this central area are areas containing equipment which are not radiation sources.

This division of equipment and the consequent division of the building into two general areas requires that there be access control. As has already been examined, an access control building is provided for separation and protection of employees.

The logical arrangement of the turbine building demanded that convenient access to the controlled part of the building be made. Corridors have been provided from which the radiation zones may be entered.

In general, the radiation levels in the access corridors are sufficiently low in order that continuous occupancy can be tolerated. However, operation of the plant will not require continuous occupancy of these corridors.

For operating convenience, access to the controlled corridors and to the controlled part of the building can be made at points other than the normal entrance through the access control building. When these additional entrances are used, a local control station can be set up to make certain that contamination is not spread from the controlled areas.

The centerline of the turbine-generator coincides with an extended diameter of the reactor enclosure. This arrangement was chosen because it offered maximum simplicity and symmetry of the main steam piping.

Turbine Generator.—The turbine generator is located approximately 35 ft above grade elevation. The turbine is an 1800-rpm, tandem-compound, dual-admission machine rated at 192,000 kw when operating at 2.5 in. mercury exhaust pressure and $\frac{1}{2}\%$ make-up. The generator is rated 245,000 kva with 30 lb per sq in. (gage) of hydrogen pressure and a 0.85 power factor.

The turbine will be operated on saturated steam with no superheat. The fact that steam generated directly in the reactor will be fed to the high-pressure section of the turbine will make the machine a radiation source during operation. Control of the turbine is arranged for remote operation.

Condenser.—The condenser is ideally located from a required shielding standpoint. The major source of radiation is nitrogen 16. It was found during plant arrangement studies that the condenser's location under the turbine and in practically the center of the building made it fairly simple to shield. The large volume of steam and condensate in the condenser will prevent access during operation. However, because of the short half-life of the nitrogen 16, the condenser should be accessible shortly after plant shutdown.

Circulating water for the condenser enters the turbine building from the intake structure through two 72-in. concrete lines approximately 10 ft below grade. The circulating water is discharged to the discharge canal through a 96-in. concrete pipe. The intake and discharge structures are described briefly in this paper.

The condenser is a horizontal, single-pass, divided water box type. Retubing of the condenser will be done from the north side. To provide for this necessity and at the same time to fulfil the shielding requirements, a concrete block wall will be erected opposite the condenser tube area. This wall can be taken down when retubing the condenser becomes necessary. Leaking condenser tubes can be plugged without removing this wall.

The three condensate pumps are under the generator just to the west of the condenser and the pumps are below the floor with only the drives projecting above the floor. It is anticipated that this area will be accessible during operation. A shielding wall is interposed between the condenser and the condensate pump room.

The gland seal condensers and the air ejectors are arranged along the north wall of the building in shielded rooms. This equipment is enclosed in two separate compartments, each containing a condenser and an ejector. This duplication will permit one set of equipment to be maintained while the other set carries the normal plant operation.

Additional equipment along the north wall includes the turbine lubricating oil reservoirs, pumps, and filter.

Feedwater Heaters.—To the south of the turbine are three compartments that contain the equipment for the five stages of feedwater heating. This equipment handles radioactive steam and condensate, and, consequently, shielding is required to protect the adjacent areas. In a conventional plant it is common practice to adjust and maintain this equipment during operation. In the Dresden plant operational adjustments to this equipment are made from an operating gallery just to the south of these feedwater heater cells. The gallery, of course, is shielded from the equipment.

The division of the equipment into three groups has been done to provide access for maintenance during operation. The equipment in any one cell can be completely isolated from the system and certain maintenance work can then be done.

The radiation levels, even after shutdown of the equipment, may be higher than in the uncontrolled areas. However, access will be strictly controlled to insure that personnel are protected at all times. This arrangement is an example of the problems posed by radiation and the manner in which they can be solved.

Feedwater Pumps.—The feedwater pumps are arranged in two groups of three each. The secondary feed pumps supply feedwater to the secondary steam generators and the primary feed pumps supply feedwater to the main steam drum. Inasmuch as the primary feedwater has been demineralized the radiation potential will be very low. This accounts for the difference in shielding around the secondary pumps as compared to the primary pumps.

Control Room.—The control room is at the west end of the turbine building under the turbine room floor. This room is the operating center of the plant—that is, the point from which the reactor, turbine, and generator will be controlled. In the extremely unlikely event of an accident to the nuclear section of the plant, it is essential that operating personnel be available. The location of the control room provides maximum shielding protection to operators at a minimum cost.

The remainder of the turbine building at the west end and on the south side houses conventional equipment which is not a source of radiation. These areas are completely accessible for operation and maintenance purposes.

SUPPORTING FACILITIES

Intake Structure.—An intake structure to the north of the turbine building is provided. Two 90,000 gal-per-min pumps will take chlorinated and screened river water and circulate it through the condenser. This water is discharged through a discharge structure. The intake structure also houses three vertical turbine pumps, each with a capacity of 4,300 gal per min, used for the service water system and for the fire system. An emergency diesel-powered fire pump is also housed in this structure.

Service Water.—The service water system removes heat from hydrogen and lubricating oil for the turbine-generator, air conditioning equipment, fuel storage pool, waste and drain tanks, the reactor during shutdown, and two separate closed-loop cooling water systems, one in the turbine building and one in the reactor enclosure. The service water is discharged through an underground pipe to the discharge canal.

Cooling Water System.—The two cooling water systems use demineralized well water with an anodic inhibitor added to minimize corrosion. The turbine building system removes heat from service and instrument air compressors, instrument air dryers, feed pump oil coolers, hydrogen seal oil cooler, and various samplers. The reactor enclosure system removes heat from recirculating pump motors, reactor coolant cleanup system, and reactor shielding concrete.

Two deep wells drilled on the site supply all well water requirements. In addition to make-up to the two cooling water systems, the well water furnishes make-up to the reactor circulating system.

Additional Facilities.—The service air systems and instrument air systems are similar to those in a conventional power plant.

In addition to the normal functions of protecting personnel, equipment, and parts of the structures from abnormal thermal and moisture conditions, the heating and ventilating systems of the Dresden station have the duty of keeping airborne radioactive contaminants within safe limits and preventing their spread to cleaner parts of the plant. To accomplish this, minimum face

velocities of air are provided across openings of cells containing possible contamination sources. Flow is always maintained from areas of little or no activity, and finally to the exhaust stack. Exit velocity at the top of the stack will be at least 3,000 ft per min. This will insure sufficient dispersion to the atmosphere to prevent harmful contamination.

Two oil-fired steam boilers will provide heat for the station. These are located in a bay on the north side of the turbine building at the east side.

CONCLUSIONS

Civil engineering has been described as the art and science of developing the great resources of nature for the benefit of man. Certainly, the development of systems for the generation of electrical power from the nuclear fission process is one of the most significant steps made by man. The civil engineer in company with his fellow engineers and scientists has been a partner in this development.

ACKNOWLEDGMENTS

The Dresden Nuclear Power Station was designed and is being built by the General Electric Company for the Nuclear Power Group. This group is composed of: American Electric Power Service Corporation, Bechtel Corporation, Central Illinois Light Company, Commonwealth Edison Company, Illinois Power Company, Kansas City Power and Light Company, Pacific Gas and Electric Company, and the Union Electric Company of Missouri. The Bechtel Corporation is the engineer-constructor for the plant under contract with the General Electric Company.

AMERICAN SOCIETY OF CIVIL ENGINEERS

Founded November 5, 1852

TRANSACTIONS

Paper No. 2996

ENGINEERING GEOLOGY OF THE MISSISSIPPI VALLEY

BY CHARLES R. KOLB,¹ AND WOODLAND G. SHOCKLEY,²
MEMBERS ASCE

WITH DISCUSSION BY MESSRS. SHU-T'UEN LI; AND CHARLES R. KOLB
AND WOODLAND G. SHOCKLEY

SYNOPSIS

The increasing importance of geologic information to the design of engineering structures in the lower Mississippi River valley is described herein. The various environments of alluvial deposition and the resulting soil formations relating to engineering problems are examined.

INTRODUCTION

It has been only since 1944 that the geology of the lower Mississippi River valley has contributed significantly to the problems besetting engineers working within this area. The basic outlines of the geology of the valley are known. A knowledge of its implications to foundation, flood control, bank stability, and other problems is mandatory for the practicing engineer working within the area.

The alluvial valley of the lower Mississippi River forms an elongated lowland extending from Cairo, Ill., to the Gulf of Mexico, and covers an area of approximately 50,000 sq miles. Its formation is closely associated with the last stages of glaciation and with the accompanying fall and the subsequent rise of sea level. The fall in sea level resulted in the scouring of an entrenched valley beneath the present flood-plain surface.

Rising sea level resulted in deposition of sands and gravels within the lower parts of this trench, followed by the deposition of a topstratum of finer-grained

NOTE.—Published, essentially as printed here, in July, 1957, in the Journal of the Soil Mechanics and Foundations Division, as *Proceedings Paper 1259*. Positions and titles given are those in effect when the paper or discussion was approved for publication in *Transactions*.

¹ Chief, Geology Branch, Soils Div., U. S. Army Engr. Waterways Experiment Station, Vicksburg, Miss.

² Chief, Embankment and Foundation Branch, Soils Div., U. S. Army Engr. Waterways Experiment Station, Vicksburg, Miss.

material. During an estimated interval of 25,000 yr as the sea level rose, the Mississippi River gradually changed from an overloaded, shallow stream with a braided regimen to its present deep, single-channel, meandering regimen. Details of this hypothetical sequence of geologic events are described by Harold N. Fisk.^{3,4}

Since 1944 this sequence of geologic events has been studied in detail by geologists working for the Corps of Engineers, United States Department of the Army. Studies were conducted of the processes of alluvial and deltaic sedimentation, the various environments of alluvial deposition, the resulting soil textures and stratum thicknesses and continuities, and of the physical properties of the soils deposited within the various environments. Thousands of borings made within the alluvial valley for engineering projects have been examined. Of immeasurable importance has been the gradual refinement of air-photo techniques of interpreting the various depositional environments. One of the more obvious purposes of these studies was the accurate prediction of engineering soil types without extensive and expensive boring programs.

The deposits that fill the entrenched valley of the Mississippi River and that make up its alluvial plain can be divided into two major groups—the sand and gravel substratum, and a finer-grained topstratum. As shown in Fig. 1, the topstratum can be further subdivided into four general types: (a) Ancient braided stream deposits of the Mississippi River and its tributaries; (b) meander belt deposits; (c) backswamp deposits; and (d) deltaic plain deposits.

The discussion which follows summarizes the method of deposition, the resulting soil sequence, the physical properties of each of these groups, and the engineering problems associated with each group.

THE SUBSTRATUM

The substratum consists of a wedge of coarse-grained material laid down during the earlier stages of the filling of the entrenched valley of the Mississippi River. It is composed predominantly of clean sand and gravel with the material normally becoming coarser with depth. Cobbles up to 4 in. in diameter are sometimes encountered near the base of the unit. Occasional lenses of clay, sandy silt, or silty sand are also found, but these are rare and discontinuous. Thicknesses of the substratum and of the depth to the top of the substratum generally increase in a down valley direction. The substratum is often encountered at depths as shallow as 10 ft and may average only 50 ft thick in the northern part of the valley. The depth to the substratum southwest of Baton Rouge, La., is as much as 100 ft, and the thickness of the substratum may be as much as 400 ft.

Although a shallow depth to firm substratum sands may be desirable from a foundation standpoint, the relatively high permeability of the substratum may often result in an expensive dewatering operation if deep excavations are involved. Pressure-relief wells are often installed to minimize undesirable uplift pressures in cases in which the bottom of the excavation is in clays overlying substratum sands at shallow depths. Where the excavation bottom is in the

³ "Geological Investigation of the Alluvial Valley of the Lower Mississippi River," by H. N. Fisk, Mississippi River Commission, Vicksburg, Miss., 1944.

⁴ "Mississippi River Valley Geology Relation to River Regime," by H. N. Fisk, *Transactions, ASCE*, Vol. 117, 1952.

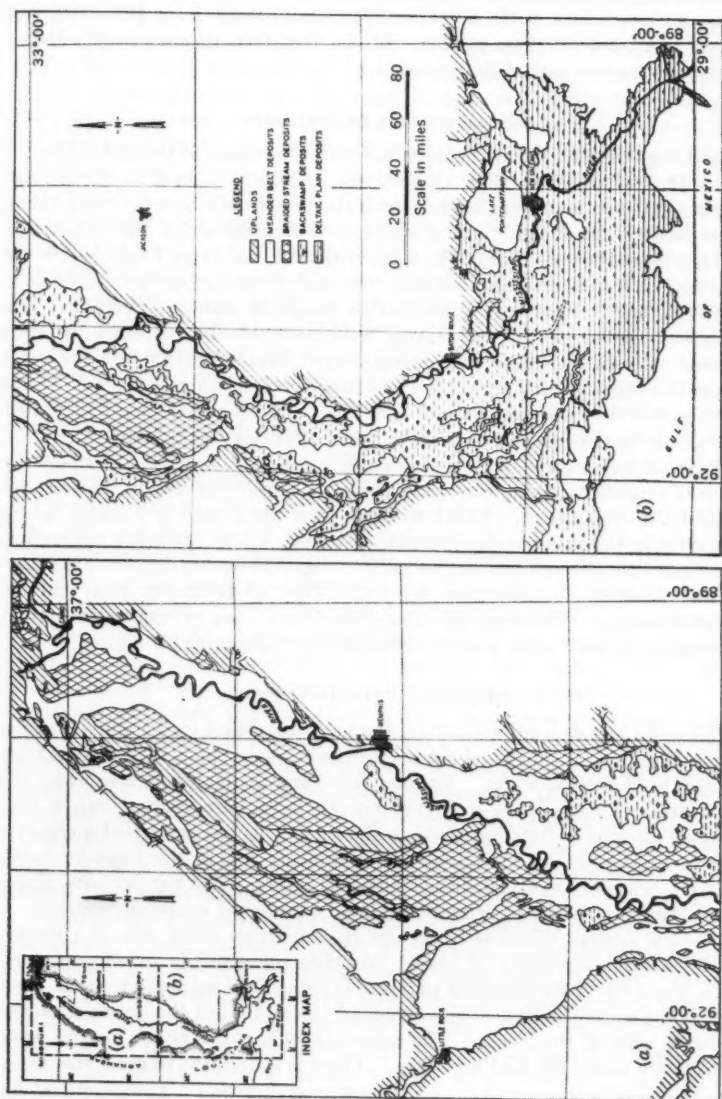


FIG. 1.—DISTRIBUTION OF DEPOSITIONAL TYPES IN THE LOWER MISSISSIPPI VALLEY

substratum, the problem of keeping the excavation free of water may be sizeable. Permeabilities of the substratum generally range from 400×10^{-4} cm per sec to $2,000 \times 10^{-4}$ cm per sec, with the larger values associated with the deeper and coarser part of the deposit.

BRAIDED STREAM DEPOSITS

Although braided stream deposits cover large sections of the alluvial valley of the Mississippi River (Fig. 1), they are usually so distant from the large streams that few major engineering projects have been concerned with them. Consequently, classification of various braided deposits and of their associated soils has lagged behind that of the other major alluvial types found within the flood plain. Braided stream deposits were laid down by overloaded, shallow, many-channeled rivers during the earlier stages of valley alluviation. The sands and gravels of the substratum were undoubtedly deposited by such streams. As sea level neared its present stand, braided channels in the lower part of the valley gradually changed into deep, single-channeled rivers. In the upper part of the valley, streams retained their braided character and deposited appreciable thicknesses of fine-grained braided topstratum deposits.

Braided topstratum deposits normally consist of complex, interfingering lentils of materials ranging from sand to clay. Most common soil textures are sandy silt and clay sand. Depth to clean substratum sand and gravel ranges from 40 ft in the lower parts of the valley to only a few feet below the surface in the extreme northern part of the valley. Braided stream deposits are generally the oldest of the topstratum deposits. They are relatively dense and low in water content. Their organic content is also low, and, except under unusual circumstances, they make good foundations for engineering structures.

MEANDER BELT DEPOSITS

Meander belt deposits are among the most important in the alluvial valley and are disposed up valley and down valley in elongate bands that average from 10 miles to 15 miles in width. Because they flank the major streams where the most intensive engineering-soils explorations have been carried out, a considerable amount of data have been collected. This has permitted a comprehensive breakdown of depositional environments within the meander belts. Four major types are distinguished—natural levees, point bar deposits, abandoned channel deposits of "clay plugs," and abandoned course deposits.

Natural Levees.—Natural levees are dikes built on either side of a stream by the natural deposition of coarse materials contained in overflow waters. These levees rise to elevations of 15 ft or more above the surrounding flood-plain level at the water's edge and slope gradually away toward the lowlands on the landward sides of the levees. The predominant textures of the natural levee deposits are sandy silt and silty clay. There is a decrease in grain size away from the crest of the levee and in a downstream direction. Fine sand and silt are commonly found in the northern part of the valley and clay in the southern part. Because of their elevated position the soils are well drained, water contents are usually low, and organic content is moderate to slight. They are normally too thin to be of consequence in the design of heavy structures but

provide excellent subgrades for highways and airfields or borrow material for fills.

Point Bar Deposits.—Point bar or accretion deposits are formed on the insides of river bends whenever the channel migrates. Sandy bar deposits or "ridges" are laid down during high stages of the river. As the water subsides, an arcuate depression or "swale" often flanks this bar on the landward side. The swale is modified by subsequent high-stage flow and is eventually isolated as the river continues to migrate. The depression is gradually filled with fine-grained material. An alternating series of sandy ridges and clayey swales results, thereby conforming to the curvature of the migrating channel. The ridges of point bar areas are characterized by sand at shallow depths. Sand within the ridges may reach the surface in the northern part of the valley.

In the southern parts, depths to sand range from 10 ft to 30 ft. The clayey swales of the point bar or accretion areas sometimes reach depths exceeding 60 ft but more often are on the order of 30 ft. The lower parts of swales consist almost entirely of clay. Water contents are high and organic content is moderate to high. The thin layer of soil covering both ridges and swales consists usually of relatively impermeable silty sands, clay silts, and silty clays. Other soil types make up less than one-quarter of these deposits. Organic materials are confined to infrequent lenticular pockets.

Because shallow sands are often desirable for engineering structure foundations, point bar deposits are ideally suited in such instances. However, subsurface conditions change laterally within short distances in these deposits and the clayey swales must be delineated with great care in selecting sites for structures. The spacing of alternately impermeable swales and permeable ridges beneath and adjacent to massive man-made levees along the Mississippi River results in occasionally severe underseepage conditions. These can be reliably predicted once the disposition of the alluvial deposits is known.

Abandoned Channel Deposits.—Abandoned channels are arcuate segments of the river left as oxbow lakes on the flood plain when the river shortens its course. These lakes are gradually filled with fine-grained deposits. The abandoned segment may consist of an entire meander loop when the river cuts directly across the narrow neck between two converging arms of the loop, or it may be a loop section cut off when the river chooses a larger swale during a flood and abandons the outer portion. The former is known as a "neck" cutoff, and the latter is known as a "chute" cutoff.

Deposits filling abandoned channels are predominantly clay and silty clay. Shortly after cutoff, a wedge of sand fills both arms of the abandoned channel at the point of cutoff and soon thereafter an oxbow lake is formed. The only material deposited within the oxbow lake is from periodic overbank flow from the river. As the channel migrates away from the point of cutoff only the finest materials find their way into the oxbow lake. Consequently, clays may fill these abandoned channels to the depth of the former active channel and clay deposits from 100 ft to 150 ft thick are not uncommon. Clays settling within deep oxbow lakes are characteristically high in water content. Because plants grow within the lake area only when it is filled or nearly filled with sediment, organic content is low except in the upper 10 ft of the clay body. Clay plugs or abandoned channel deposits are among the deepest clay bodies found in the

alluvial valley. They are relatively unconsolidated and tend to exhibit high compressibility and low strength. Special design and construction measures are usually necessary where levees cross abandoned channel deposits. Their distribution often vitally affects the location of engineering structures and drainage and navigation channels. In addition, these channel deposits have a significant effect on river migration. Wherever these deep clay bodies occur along the river they act as "hard" points which alter radically the normal rate and direction of stream migration and greatly influence revetment placement and levee location.

Abandoned Course Deposits.—Abandoned courses are the lengthy segments of the river that are left behind when the stream abandons a meander belt and chooses a new course within the flood plain. These courses mark the position of the last channel the river occupied in the abandoned meander belt. The

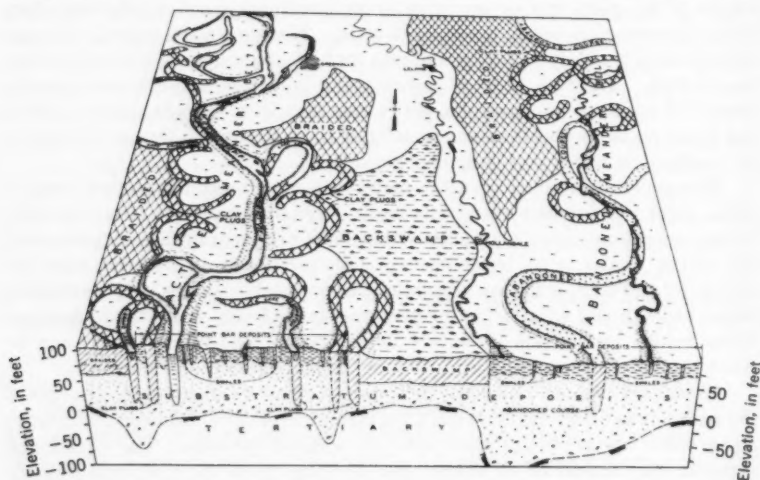


FIG. 2.—MAJOR ENVIRONMENTS OF DEPOSITION IN THE VICINITY OF GREENVILLE, MISS.

abandoned course is sometimes hundreds of miles in length. It gradually fills with sediment and is often occupied by a smaller stream. An abandoned meander belt with a centrally located abandoned course of the Mississippi River is shown in Fig. 2. On the subsurface profile, dots represent sand, slant lines denote clay, and dashed lines indicate silt. Little is known about the details of the filling of abandoned courses. Indications are that the old course fills with a wedge of sand that is thickest where the new course diverges from the old, and that gradually thins downstream. Subsequent stages involve the occupation of the abandoned course by smaller streams and gradual filling with fine-grained deposits. The fine-grained deposits within the abandoned course are normally clays or silty clays. Organic content is relatively low. Soil densities are normally low but vary directly with the age of the meander belt in which the course is located. Physical characteristics of the abandoned course

deposits are much the same as those of the abandoned channel. The most important difference is the normally shallower depth to sand within the abandoned course.

BACKSWAMP DEPOSITS

Backswamp deposits consist of sediment laid down in shallow ponded areas during overbank flow. The water may be trapped between high meander belt ridges or between a meander belt ridge and the valley wall. The coarser material from overbank flow is dropped near the stream to form natural levees. The finer material settles slowly in low-lying areas as the ponded water gradually drains off, seeps into the ground, or evaporates. Grasses, shrubs, and trees grow profusely in these areas and add to the organic content of the deposits. After each inundation of an individual area of backswamp deposition the clays may be desiccated. Thus, although backswamp deposits are generally finer than the clays of the abandoned channel, they are denser and water contents of the former are notably lower. Backswamp deposits are some of the most homogeneous deposits found within the flood plain. More than 80% of the deposits normally consist of clay. Thickness of the deposits increases in a down-valley direction and, where not underlain by meander belt deposits, the contact of the backswamp clays with the underlying sands and gravels is remarkably constant within any one area. Their normally high organic content make them occasionally undesirable as foundation material. Heavy engineering structures must often resort to pile foundations in underlying sands when located within areas of backswamp deposition. However, backswamp clays tend to be preconsolidated because they have been desiccated as a result of alternate wetting and drying, and settlements of structures resting directly on them are somewhat less than they would be if founded on abandoned channel deposits.

DELTAIC PLAIN DEPOSITS

Deltaic deposits are the result of the outbuilding of the land surfaces seaward by the various past deltas and the present delta of the Mississippi River. As soon as a delta of the Mississippi River is abandoned, the sea begins to work its way inland. This process is aided by subsidence of the whole of the deltaic plain, both tectonically and as a result of gradual consolidation of the soft deltaic plain sediments. However, the result of the struggle between the advancing deltas and the encroaching sea is an over-all increase in the size of the deltaic plain. Rapidly increasing development of the area during the past decade has resulted in intensified study of the deposits and the associated engineering problems. Highways and causeways, locks and waterways are part of an extensive transportation network. Levees and floodways have been built to protect the area from flooding.

In order to introduce the various environments characteristic of the deltaic plain, it is necessary to describe the much older and firmer materials which underlie them, often at shallow depths. These are the Pleistocene deposits—the ancient materials that flank and rise above the flood plain as terraces in the northern part of the valley, but that gradually slope beneath the surface of the flood plain farther south. Beneath New Orleans, La., these deposits lie at

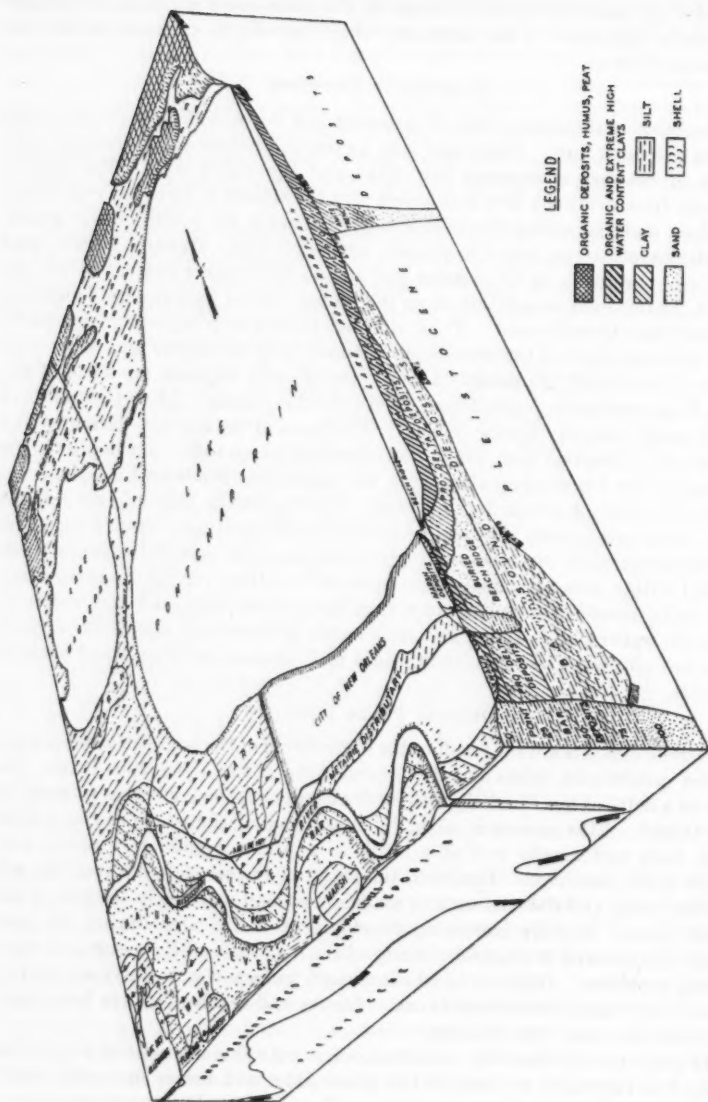


FIG. 3.—MAJOR ENVIRONMENTS OF DEPOSITION IN THE VICINITY OF NEW ORLEANS, LA.

depths as shallow as 50 ft, and, as shown in Fig. 3, slope gradually northward and emerge at the surface north of Lake Pontchartrain.

To properly visualize this surface, it must be imagined as a former flood plain of the Mississippi River before the advent of the last glaciers. As the glaciers grew, sea level dropped and the surface was subjected to erosion, desiccation, oxidation, and consolidation for tens of thousands of years. As the ice began to recede, the sea level rose and the former flood plain became covered by the sea. It is on this relatively firm surface that the considerably younger and less consolidated deltaic plain has been built.

A shallow depth to Pleistocene deposits is often the deciding factor in site selection for heavy structures. Densities of the Pleistocene deposits are high, the water contents are low, and organic deposits are compacted and fairly scarce. Soil textures range from clay to sand and gravel. Shear strengths of Pleistocene materials are normally 1,000 lb per sq ft or greater.

Overlying the Pleistocene deposits are the sediments of the deltaic plain. Since 1954 attempts have been made to arrive at a comprehensive classification of the important environments of deposition within the deltaic plain. Of particular importance was the development of a scheme of classification that had significance from the standpoint of engineering soils. The tentative classification devised is listed as follows:

Deltaic Environments of Deposition

Lacustrine environment
Bay-sound environment
Reef environment

Delta environments:
Pro-delta
Distributary bar fingers
Interdistributary troughs

Marsh environment

Swamp environment
Beach environments:
Sand beaches
Shell beaches
Stream environments:
Point bar
Natural levee
Abandoned course
Abandoned distributary
Tidal channel

Among the more important of the deltaic environments are those resulting in deposition of sands. These are found mainly in the sand beaches. Sand beaches higher than 15 ft are found today, particularly in areas just offshore of the ancient sand-depositing deltaic systems. The Chandeleur Islands, La., and The Grand Island, La., series of beaches northeast and west of the present delta are examples. Even more important from an engineering standpoint are ancient sand beaches now partly or completely buried by other deltaic deposits. Partly buried sand beaches are called cheniers, and are common along the coast of southwest Louisiana. Completely buried beaches are known to exist in a number of places within the deltaic plain. One, shown in Fig. 3, is directly beneath the city of New Orleans where it affords a relatively good foundation at fairly shallow depths.

Only slightly less important from the standpoint of foundations are the shell beaches and the shelly reef environments. Shell beaches consist largely of shell fragments intermixed with from 25% to 50% sand. They form relatively small, lenticular, discontinuous bodies completely or partly buried beneath less stable deltaic plain deposits similar to the sand beaches. However, reefs may be extensive, sometimes covering many square miles and reaching thicknesses

of 10 ft or more. The shells in the reef environment are usually entire rather than fragmented as in the case of the shell beaches. However, they may occur together with considerable amounts of clay and thus are normally less desirable as foundation material.

The swamp and marsh environments of deposition are comprised generally of fine-grained soils of varying organic content. Swamps are those areas characterized by growing trees, whereas marshes contain only occasional trees and extensive amounts of sedges and grasses. Organic content is highest within the marsh environment. Layers of peat and humus up to 25 ft thick are known to exist within some of these environments.

Organic soils associated with swamp and marsh environments are among the most treacherous within the deltaic plain. In almost every instance, organic materials must be removed prior to even lightweight construction. A costly phase in the replacement of U. S. Highway 51, which follows the narrow neck of land between Lake Maurepas, La., and Lake Pontchartrain (Fig. 3), has been the removal of an almost uninterrupted 10-ft layer of organic material. The old highway was built on fill placed directly on the swamp deposits. The many small bridges crossing drainage channels along the highway were placed on piles sunk to the shallow Pleistocene deposits. Over the years the roadway has subsided as much as 5 ft into the marsh, but the bridges have remained at essentially the same level at which they were built. As a result, travel over the old highway was roughly comparable to a ride on a roller coaster.

The gradual decay of organic materials beneath the deltaic plain results in the production of considerable quantities of marsh gases. The accumulation of gases in subsurface deposits often augments the water pressures that exist therein. These pressures sometimes can cause blow-ups in foundation excavations if adequate precautions are not taken. It has been noted in some cases that gases bleed up through open-grained timber piling penetrating gas-bearing strata. This can cause damage to freshly poured concrete around the pile caps unless preventive measures are taken. Gas has also been noted bleeding through construction joints in the base of lock structures in the southern Louisiana area. Some large buildings in New Orleans are provided with a sand filter blanket to bleed off excess marsh gases and thereby reduce uplift pressures.

The final type of deposit to be considered is the delta environment, the prime builder of the land surfaces. Nearly all of the inorganic deposits that make up the deltaic plain resulted from original deposition in an active delta or from subsequent reworking of these deposits by the sea. In addition to the present delta, five major deltas have been active in building the deltaic plain. These abandoned deltaic complexes swing in a 200-mile arc across the entire southern border of the plain. Recent work in the present Mississippi delta has gone far toward classifying the environments found there. Preceding each deltaic advance is a sequence of pro-delta clays and silty clays that gradually become coarser upward in the section. Above these are distributary bar fingers—finger-like wedges of fine sand that build seaward as the distributary advances. Between these fingers of sand are pockets of fine clays and silts, the interdistributary trough deposits. Intensified activity by oil interests in the shallow offshore areas of the Gulf of Mexico has resulted in comprehensive

TABLE 1.—TYPICAL PROPERTIES OF SELECTED ENVIRONMENTS OF DEPOSITION
WITHIN THE MISSISSIPPI ALLUVIAL VALLEY

Environment	Grain size and organic content ^{a,b}	Predominant soil texture ^c	Natural water content, in %	Liquid limit	Plasticity index	SHEAR STRENGTH ^d	
						Cohesion, in pounds per square foot	Angle of internal friction, in degrees
(1)	(2)	(3)	(4)	(5)	(6)	(7)	(8)
Braided stream ^a		Clay sands (SC) to silty clays (CL) Sands (SP)	25-40 ...	30-75 NP	10-55 NP	200-1,100 0	30 30-40
Natural levees ^c		Clays (CL) Silt (ML)	25-35 15-35	35-45 NP-35	15-25 NP-5	360-1,200 180-700	0 10-35
Point bar (ridges) ^c		Silt (ML) and silty sands (SM)	25-45	30-55	10-25	0-850	25-35
Abandoned channels ^c		Clays (CL & CH)	30-95	30-100	10-65	300-1,200	0
Backswamp ^a		Clays (CH)	25-70	40-115	25-100	400-2,500	0
Swamp ^c		Organic clay (OH)	110-265	135-300	100-165	Very low	Very low
Marsh ^c		Peat (Pt)	160-465	250-500	150-400	Very low	Very low
Pro-deltas ^c		Clay (CL & CH)	20-120	25-155	10-80	175-300	0
Lacustrine ^c		Clay (CH)	45-115	85-165	65-95	75-150	0
Beach ^c		Sand (SP)	Saturated	NP	NP	0	30
Bay-sound ^c		Clay silts and silty clays (CL & CH)	20-70	40-80	25-65	250-700	15-20
Substratum		Sand (SP)	Saturated	NP	NP	0	30-38
Pleistocene ^c		Clays and silty clays (CL & CH)	15-60	25-80	20-75	550-5,000	0

^aLegend: Gravel (>2.0 mm) Sand (2.0-0.06 mm) Silt (0.002-0.06 mm) Clay (<0.002 mm) Organic material

^bCharacteristic grain sizes for braided stream, natural levee, point bar, backswamp, and abandoned channel deposits based on "Fine-Grained Alluvial Deposits and Their Facies on the Mississippi River Valley," by H. H. Fisk, Mississippi River Commission, Vicksburg, Miss., 1947. Symbols based on unified soil classification system. The percentages of clay, silt, and sand are based on the following grain size distribution: 4.75 mm (No. 10) sieve, 100% sand; 75 microns (No. 200) sieve, 100% sand and silt; 4.75 microns (No. 40) sieve, 100% sand, silt, and clay.

^cShearing stresses of clay, based on data of D. C. Drayton, "Data on Shearing Stresses of Clay," U.S. Geological Survey, Washington, D.C., 1934.

^dGrain size based on approximately 25 borings in southern part of valley. ^eData other than grain size based on approximately 100 borings in valley south of Memphis, Tenn. ^fData other than grain size based on approximately 150 borings south of Natchez, Miss. ^gData other than grain size based on approximately 200 borings in New Orleans, La., area.

studies of the engineering characteristics of these sediments. Heavy, expensive drill rigs must be firmly anchored to the gulf bottom before successful drilling can begin. Changes in soil strength are due to (a) varying clay mineral types; (b) changes in strength brought about by flocculation of certain clay particles on contact with a saline environment; (c) the effect of disintegrating organic material on the strength of silts and clays; and (d) the correlation of sediment types with the environment in which they are deposited. The solutions of these problems will have direct and valued applications to the design of structures in shallow offshore areas.

SELECTED ENGINEERING APPLICATIONS

A knowledge of the various environments of deposition within the alluvial valley is a prerequisite for the prediction of soil types, and, in turn, of their effects on foundation conditions. Table 1 lists a group of these environmental types, the soil types normally associated with each environment, and gives representative ranges of physical properties having engineering significance. The importance of the various geologic deposits in the lower Mississippi valley with respect to engineering foundation problems has previously been mentioned briefly in this paper. Of equal importance are a number of related engineering problems that are also dependent on the geology of the lower Mississippi valley. Among these can be mentioned the location of aggregate sources, prediction of river stability, and the prediction of underseepage or dewatering conditions.

Aggregate Sources.—Aggregate sources are a particularly troublesome problem throughout the alluvial valley. A knowledge of the sequence of terrace alluviation is essential to locate the extensive sand and gravel deposits that occur toward the north and near the valley walls. Point bar deposits, particularly the active point bar deposits along the river, are the principal source of sand and gravel within the flood plain.

Aggregates are at a premium farther south. South of Baton Rouge river-deposited sands are too fine for use as aggregates and gravels are not to be found. Here another source, the shell beds of the shell beach and reef environments, assumes considerable importance. A knowledge of the disposition of the various former deltas of the Mississippi River eliminates search in large areas where such buried shell reefs are improbable. Careful study of limited borings and a knowledge of the growth characteristics of modern reefs permit fairly accurate guesses as to the extent of buried shell beds.

Of increasing importance in the southern part of the valley are lightweight aggregates produced by burning clays at high temperatures. Certain types of backswamp clays appear to be most desirable for use in such aggregates. Their grain size and clay mineral content, coupled with the proper amount of organic matter, make them ideally suited for use in what appears to be a fast-growing industry. The organic matter becomes gaseous during the burning process and expands the material to a light, durable brick-like aggregate that can be used satisfactorily in a variety of concrete structures.

River Migration and Channel Diversion.—Of considerable importance to engineers entrusted with site location on the banks of the Mississippi River is a valid prediction of the direction the river may migrate during the life of an

installation. Bridges, pipelines, overbank flow structures, docks, levees, and factories anxious to utilize cheap transportation facilities provided by the river are examples of the numerous installations that are affected by the stability of the river. Based on the mapped record of river migration during the past 200 yr, together with evidence from borings and airphotos, geologists have been able to delineate with remarkable success the position of the river during the past 3,000 yr. Refinements of these studies have enabled predictions to be made of future river migration based on a knowledge of rates of river meandering as controlled by the sediments along the river bed and banks. An example of an important application of such geologic studies has been recent work on the imminent diversion of the Mississippi River through its Atchafalaya distributary. To the geologist this impending diversion with its serious consequences is merely the latest in a series of similar occurrences in the normal sequence of flood-plain formation. Geologists working with engineers were able to establish the probability of such a diversion and to predict the time when it would become critical. Several large engineering works are now (1959) being planned and constructed by the Corps of Engineers to prevent such an occurrence.

Underseepage.—Seepage and sand boils landward of Mississippi River levees have been a problem during major high waters. One of the major contributory causes of this condition is the presence of the pervious sand substratum which is cut into by the river. Thus, nearly the full river head is transmitted in the form of hydrostatic pressures acting on the base of the relatively impervious topstratum. These high pressures have been found to exist for considerable distances away from the river. Where the topstratum is thin, as in point bar ridge deposits, the potential danger from underseepage is increased. There is usually little or no danger from underseepage where thick clays, such as back-swamp and abandoned channel deposits, are found. The configuration of point bar swales and abandoned channels with respect to the levees also has an important bearing on underseepage. The greatest concentration of seepage occurs along the riverward edges of swales and channels, and in instances where the long dimension of these features is parallel to or intersects the levee at a small angle and seepage is concentrated between them and the levee toe. Measures which have been or are being used to protect levees against excessive underseepage include sublevees, berms, and relief wells.

CONCLUSIONS

A knowledge of the mode of origin and of the depositional environments of sediments in the Mississippi River valley is essential to the engineer concerned with the location and design of structures in that area. The major types of depositional environments produce predictable sequences of soils, each having a fairly well defined range of engineering properties. Studies of past river migration and delta building processes permit an estimation of future behavior of the river. From such information the engineer is able to locate desirable sites for engineering structures, economize on soil boring and laboratory testing programs, and anticipate problems in structure design and construction.

DISCUSSION

SHU-T'EN LI,⁵ M. ASCE.—The authors have presented a valuable contribution toward clarifying the various environments of alluvial deposition and the resulting soil formations in relation to their associated engineering problems.

Between the valley walls and above the Pleistocene substratum or Pleistocene valley floor, the recent substratum and topstratum have been formed after the Mississippi River entrenched its valley system during the Later Wisconsin glacial stage, the last of the five Pleistocene glacial stages of the accepted worldwide Quaternary cycles. During each stage, as ice accumulated and melted, the sea level was lowered and later restored to near its present stand. Each entrenchment and later filling of the valley system was, in each event, an effort to adjust itself to the changed base level thereby imposed on it. The last valley filling began when the sea level started its rise with the melting of the Later Wisconsin glaciers some 25,000 to 30,000 yrs ago. The sea level reached its present stand some 5,000 yr ago.

Lower Region of the Lower Alluvial Valley.—Although the alluvial valley of the lower Mississippi River forms an elongate lowland extending from Cairo, Ill., to the Gulf of Mexico, the more complex and striking events have happened in the lower region of this alluvial valley. The lower region may be regarded as lying south of the latitude of Vicksburg, Miss. It is flanked on the east and west sides by Pleistocene uplands between which the Mississippi River has shifted its meandering⁶ courses over the previously filled valley systems.

Because the authors have treated the various environments of alluvial deposition, the resulting soil formations in the lower Mississippi alluvial valley and in the extreme lower-left region of the Lake Pontchartrain area, the writer's discussion will be confined to the more striking aspects of the lower-right region. This will include the area from Vicksburg down to the Gulf of Mexico, and from the former Teche Mississippi on the west to the Modern Mississippi River on the east. This lower-right region has been predominantly the shifting region of the lower meander belts.

Post-Pleistocene Epoch Events of the Lower-Right Region.—To comprehend the geological aspects of the lower-right region of the lower Mississippi alluvial valley, an account of the post-Pleistocene epoch events is necessary. The associated events may be conveniently treated and discussed under the following: (1) Recent substratum formation during the pre-meander-belt-shifting stage, (2) substratum and recent substratum, and (3) recent topstratum formation during meander-belt-shifting stages.

Recent Substratum Formation during the Pre-Meander-Belt-Shifting Stage.—Under the present substratum are the Pleistocene and older deposits in which the Mississippi River and its tributary streams entrenched their valley system during the Later Wisconsin glacial stage to as deep as 450 ft below the present

⁵ Chf. Technical Writer, Palmer and Baker, Inc., Cons. Engrs., Mobile, Ala.; formerly Deputy Pres., Yellow River Comm., Republic of China.

⁶ "Geological Investigations of the Alluvial Valley of the Lower Mississippi River," by H. N. Fisk, Mississippi River Comm., December, 1944.

sea level. The then exposed surface of this valley system experienced a weathered zone.

This deep valley system was later filled with the coarse basal fraction of the alluvial sequence, which consisted principally of sand and gravel in the lower substratum and of abundant sand in the upper substratum. Together, they formed the recent substratum. The coarser materials were deposited when the river had a steeper slope and was overloaded. The thickness of the substratum increases from north to south and decreases from the axis of the entrenched valley to virtually none near the Mississippi alluvial valley wall. Below the Upper Grand River in the Atchafalaya Basin⁷, the thickness of the substratum is approximately 300 ft or more and increases to as much as 400 ft further south. South of the latitude of Chicot Pass, La., gravel even of pea size is scarce above the elevation of about -160 ft M.G.L. (mean Gulf level).

After the former entrenched valley system had been filled by the coarser materials, the entire lower valley floor became a wide, more or less graded downward-sloping surface toward the Gulf. As the slope was still moderately steep and the river remained to be overloaded, a braided channel habit ensued. Materials reaching the Mississippi River were swept seaward by the numerous shallow channels of the braided stream and were deposited over wide areas as the aggrading valley surface developed. As slope decreased, the deposited material became finer toward the surface of the recent substratum and in the upstream direction. The generally coarse basal portion of the alluvium, called the recent substratum, accumulated in this manner and has a comparatively flat top surface.

This top surface, formed during the above braided stream stage, extends almost from the east valley wall to the west valley wall. This marks the top of the recent substratum over which the meander belts have shifted during the past 3,000 yr.

Substratum and Recent Substratum.—Under the heading, "Introduction," the authors ascribe the sand and gravel deposits to the substratum, and further under the heading, "The Substratum," state:

"The substratum consists of a wedge of coarse-grained material laid down during the earlier stages of the filling of the entrenched valley of the Mississippi River."

This latter statement confines the substratum to within the entrenched valley during the Later Wisconsin glacial stage. An examination of the substratum profile across the present Atchafalaya Basin from the present Mississippi River near Union, La., on the east to north of St. Martinville, La., near the former Teche Mississippi on the west, shows that an unbroken top surface of sand substratum exists throughout the entire trans-Atchafalaya line. The top surface of this sand substratum lies generally between -90 ft and -120 ft M.G.L. Only near the east side and west side Pleistocene uplands, it rises to -30 ft M.G.L. Because the last entrenched valley during the Later Wisconsin glacier stage could not be as wide as 64.4 miles from valley wall to valley wall, this

⁷ "Geological Investigation of the Atchafalaya Basin and the Problem of Mississippi River Diversion," by H. N. Fisk *et al.*, prepared for the President, Mississippi River Comm., by the U. S. Army Engr. Waterways Experiment Station, Corps of Engrs., Vicksburg, Miss.

unbroken sand substratum should have been laid down from time to time when the Mississippi River had the braided-stream character after the filling of the last entrenched valley. The authors confirm this view under the heading, "Braided Stream Deposits," by stating: "The sands and gravels of the substratum were undoubtedly deposited by such streams."

It appears more distinctive to term the "Pleistocene floor" here as the substratum and the "entrenched-valley filling" and the "braided stream deposits" as the recent substratum. It is on the top part of this recent substratum that most of the heavy constructions in the lower region of the lower Mississippi alluvial valley have been and will be founded.

The authors further state:

"Although braided stream deposits cover large sections of the alluvial valley of the Mississippi River, they are usually so distant from the large streams that few major engineering projects have been concerned with them."

This may be true from Cairo down to Natchez, Miss., but does not appear to be so from Natchez down to the Gulf. Systematically projected borings referred to previously indicate that the comparatively flat top of the recent substratum reaches on the west to the Teche ridge and on the east to the present Mississippi course. Furthermore, in this lower region of the alluvial valley, the ancient braided stream deposits are entirely buried underneath the meander belt deposits and backswamp deposits.

Of particular engineering significance for heavy construction is the existence or nonexistence of coarse sand and gravel in the recent substratum in the lower alluvial valley. It was reported in connection with the geological investigation of the Atchafalaya Basin made by the U. S. Army Engineer Waterways Experiment Station, that no such material was found in any of the bed material samples taken south of the Upper Grand River. This information indicates that the occurrence of gravel in the substratum south of the Upper Grand River is very rare, except at great depths. The log of a boring located nearly a mile south of Chicot Pass shows that pea gravel exists below -158 ft M.G.L.

Of equal engineering significance is the fact that the age determination of the samples taken from the Atchafalaya Basin indicates that a considerable amount of compaction, due to natural consolidation, of the sediments has taken place since deposition. It is reasonable to expect that the older deposits corresponding to the different ages and stages have become more compacted due to natural consolidation.

The Pleistocene substratum valley floor slopes rapidly upwards near the east side and the west side Pleistocene uplands. During the former Teche-Mississippi and the Modern-Mississippi meander belt formation stages, there were undoubtedly meander loops coming adjacent to the valley walls. Thus, point bar or accretion deposits of sand ridges were formed on the insides of river bends. Later meandering migrations turned away from the valley walls, leaving these sand bar deposits outside of natural levee formations or artificial levee building in the case of the present Mississippi. This explains why borings show that the recent substratum rises to -30 ft M.G.L. near the east side and west side Pleistocene uplands. It also confirms the statement under the head-

ing, "Point Bar Deposits," made by the authors: "In the southern parts, depths to sand range from 10 ft to 30 ft."

Though these sand deposits may be contiguous with the sand substratum, they were not left by the braided stream but were deposited during the meander-belt-shifting stages. An extreme case is shown by the projected boring L-57 made by the U. S. Army Engineer Waterways Experiment Station and located west of Donaldsonville, La. The log shows that brown clay with shell extends from the Lafourche ridge at +20 ft to -2 ft, then sand and gravel to -180 ft. The high elevation of sand and gravel deposits must have their origin from point bar deposits of the Lafourche stage.

Recent Topstratum Formation During Meander-Belt-Shifting Stages.—The recent topstratum was deposited over the recent substratum as the river gradually became graded to the stand in sea level. Ultimately, the graded condition extended up the main tributaries. As a result, sediments carried to the Mississippi River by tributaries became increasingly finer, the coarse fraction of the load diminished, and the tendency for the stream to be overloaded decreased. The larger portion of the sediments could be carried in suspension by the master stream and its braided channel was gradually replaced by a meandering one.

This brought about a concentration of flow into a single channel, resulting in deeper scouring action, period flooding, and systematic channel migration. The majority of the materials deposited, since the Mississippi became a meandering stream throughout the major portion of its lower valley, consists of clays, silts, and fine-grained sands that make up the recent topstratum.

The oldest meander belt of the Mississippi River that geologists have been able to detect authoritatively is the Maringonin-Mississippi. It began to develop approximately 3,000 yr ago, traversing longitudinally beneath the present Atchafalaya Basin. About 2,000 yr ago, the Mississippi abandoned the Maringonin meander course, leaving an alluvial ridge, and began to develop the Teche-Mississippi meander belt near the foot of the western Pleistocene uplands. The Mississippi later abandoned the Teche meander course approximately 1,600 yr ago, and began to develop the Lafourche meander belt to the east of the Maringonin-Mississippi alluvial ridge. The Modern Mississippi, forming the most easterly meander belt, was first occupied approximately 800 yr ago.

As pointed out by the authors, meander-belt deposits are among the most important in the alluvial valley. The foregoing account gives the ages during which the different meander-belt deposits were laid down over the recent substratum of the alluvial valley. These deposits comprise natural levee deposits, point bar deposits, abandoned channel deposits of "clay plugs," and abandoned course deposits—all of which have been well accounted for by the authors.

Geomorphologically, not all of the meander-belt ridges are now discernible. North of Donaldsonville and for some distance south the Modern-Mississippi meander belt overlies the next older Lafourche-Mississippi meander belt. It is known as the Modern Lafourche-Mississippi meander belt. The oldest meander belt, the Maringonin-Mississippi, has long been over-alluviated by the backswamp deposits of the Teche stage, the Lafourche stage, and the Atcha-

falaya stage. Though a few low arcuate features having the dimensions of the Red River and the Mississippi River meander loops are discernible from aerial photographs, they cannot be followed as uninterrupted ridges. These are remnants of the Maringonin alluvial ridge now largely buried beneath more recent deposits.

The Teche ridge on the west and the Modern Lafourche ridge on the east form the basin boundaries of the growing Atchafalaya stage. These boundary ridges were formed mainly of bar accretions laid down within the then Mississippi meander courses. They were capped by the broad natural levees of the Mississippi and have since been capped by narrow natural levees along minor streams that have flowed in the abandoned Mississippi channels.

Corresponding to the foregoing different ages, the backswamp deposits of the Maringonin stage were first laid down beyond its natural levees over the recent substratum in the alluvial valley. Those of the Teche stage were then similarly laid down between the west side Pleistocene uplands and the Maringonin ridge. Then those of the Lafourche stage were in like manner laid down between the Maringonin ridge and the east side Pleistocene uplands. Finally, the backswamp deposits of the Modern Mississippi stage were laid down between the east side Pleistocene uplands and the Lafourche ridge south of Donaldsonville and the older ridge north of it during its first 350 yr. After conditions for the formation of the Atchafalaya Distributary were established in about 1500 A.D.,⁷ the major part of the Atchafalaya Basin has become the backswamp of the Modern Mississippi on its west side.

Contemporary with the respective different stages, the different major deltaic deposits were formed seaward by the deltaic distributaries of each stage. The authors have ably contributed accounts for "Deltaic Plain Deposits" and "Deltaic Environments of Deposition."

During the Lafourche-Mississippi stage, in about 900 A.D., the Atchafalaya Basin was isolated by the coalescing of the Teche and Lafourche ridges in the area south of Houma, La. The southern part of the basin was marked by a small lake area. By 1400 A.D., when the Modern-Mississippi stage had established its new course, the ancient Grand Lake of the south Atchafalaya Basin lake area reached its maximum extent to as far north as the latitude of Baton Rouge. Since the formation of the Atchafalaya Distributary of the Mississippi in about 1500 A.D., the southern basin lake area has continually deteriorated as the Atchafalaya River delta growth has proceeded into the lake area.

In the northern part of the large ancestral Grand Lake, a blanket of deltaic deposits has been laid down in three layers. These consist of two bottom layers of ancient deltaic deposits and a top layer of modern Atchafalaya deltaic deposits. The lower bottom layer of red color deposits was derived from Red River sediments. The overlying brown and gray-brown deposits were mixed Red River and Mississippi River deposits.⁸ Overland deltaic deposits have been found to -21 ft below M.G.L. from a boring west of Chicot Pass of the Atchafalaya Distributary.

The main channel of the Atchafalaya River is leveed above Krotz Springs, La., below which, under natural conditions, the main channel separates into

⁷ "Fine-Grained Alluvial Deposits and their Effects on Mississippi River Activity," by H. N. Fisk, U. S. Army Engr. Waterways Experiment Station, Corps of Engrs., Vicksburg, Miss., 1947.

numerous small shallow streams that empty in a typical deltaic pattern into the Grand Lake. The northern boundary of the present Grand Lake has continually receded southward as a result of the filling of the ancient Grand Lake by the Atchafalaya deltaic deposits.

Composite Group of Deposits.—The authors mention some of the engineering problems associated with each single group of deposits. However, in general, except for foundations carrying rather light structures, a composite group of recent topstratum deposits of fine-grained materials to the recent substratum of fine, medium, and coarse sand will be encountered in the lower alluvial valley. In the region adjacent to the northern end of the present Grand Lake, for instance, the engineer may encounter a sequence of successive underlying layers consisting of:

- a. Overland deltaic deposits as the top layer;
- b. Backswamp deposits of comparatively recent origin;
- c. Buried ancient natural levee deposits of the Maringonin stage;
- d. Point bar deposits of the Maringonin stage; and
- e. Ancient braided stream deposits.

For heavy construction, although part of the top deltaic deposits may have to be excavated, the substructure will have to penetrate the first four groups and part of the fifth, and be founded on the denser part of the fifth group.

In the lower alluvial valley, such complex engineering problems involving a composite group of deposits are by far the more common for heavy construction than the single-group-deposit foundation materials treated by the authors.

The Situation of the Present Lower Mississippi River.—Under the heading, "River Migration and Channel Diversion," the authors state:

"Of considerable importance to engineers entrusted with site location on the banks of the Mississippi River is a valid prediction of the direction the river may migrate during the life of an installation."

The stability of a river regimen depends on the complex interaction of a number of separate factors such as valley slope, load, nature of the bed and bank materials, velocity, and volume of discharge, which in turn affect course migration. Within the meandering pattern of the Mississippi River (which has characterized its course since sea level became stationary), the orderly growth of beds, together with a knowledge of bed and bank materials and accurately mapped historic bank lines, makes it possible to predict future behavior.

Both straight reaches and bends may not be stable. A straight reach may be adversely affected by the gradual channel migration of upper and lower bends exposed to two contemporaneous actions of the river. These are bank caving on the outside of the bend, or concave bank, and bar building on the inside of the bend, or convex bank. As the bends enlarge themselves, the tail of the upper bend and the head of the lower bend will approach each other. The channel shoals between the pools of the bends constitute the crossing areas where velocities are highly variable and where the position of the thalweg changes constantly as bar deposits encroach from both ends. Aggradation and degradation do occur locally and, in fact, must occur whenever the stream

channel migrates. However, river channel migration can be controlled effectively by either indirect or direct measures or both, when encroaching signs have become noticeable. Well-planned groins and bank revetment are the familiar conventional measures for such control.

After careful study of engineering records and channel characteristics of the Mississippi River, Gerard H. Matthes,⁹ Hon. M. ASCE, concluded that the stream exhibits no over-all tendency either to aggrade or degrade its channel and for this reason he termed it "poised." However, a poised stream is in a condition of very sensitive equilibrium. If there is any change in the controlling factors, the equilibrium is shifted in a direction that tends to absorb the effect of the change. The resulting adjustments may rapidly propagate upstream or downstream, or both, from the location where such a change has taken place or been introduced. A major cutoff may be the cause of a minor change. An increase or decrease in discharge or load may be the cause of a major change. The threatened capture of the Mississippi River by the Atchafalaya Distributary has been thought to have accelerated due to downcutting of the Atchafalaya channel as the discharge increases, and silting of the Mississippi channel as its discharge decreases.

Be it poised as the present lower Mississippi River may seem, the increasing diversion of the Atchafalaya Distributary continues to threaten the over-all stability of its master stream. According to investigations made by the U. S. Army Engineer Waterways Experiment Station at Vicksburg, Miss., on the problem of Mississippi River Diversion,⁷ it has been shown conclusively that a conservative maximum estimate is placed at 40% diversion of the Mississippi flow in order to maintain the present course of the master stream below Old River junction (in La. opposite La.-Miss. border line). Both the trend established by the percentage of total annual flow diverted from the Mississippi River through the Old River and trends based on the establishment of a channel from the head of the Atchafalaya Distributary to its mouth, show that 40% of the Mississippi flow will be diverted by 1970. It is a threat that will affect the present course of the lower Mississippi not only as a drainage channel but also as an artery of water-borne commerce.

The Geophysical Dynamic Complexity of the Atchafalaya Distributary.—The Atchafalaya Basin is situated entirely within the boundary walls of the lower Mississippi alluvial valley, between the former Teche-Mississippi and the Modern Lafourche-Mississippi. It lies over the buried ancient Maringonin-Mississippi ridge; the backswamps of the Maringonin, Teche, Lafourche, and Modern Mississippi stages; the overland deltaic deposits of Red River, of mixed Red River and Mississippi; and of the Atchafalaya Distributary. Not only is the Atchafalaya Basin the major part of the lower region of the lower Mississippi alluvial valley, but also the Atchafalaya Distributary constitutes the most dynamic geological force system in the lower alluvial valley during recent centuries with ever-increasing importance. The associated physical environments coupled with the ever-increasing discharge through this distributary (already up to 30% of the total annual flow of the Mississippi past the latitude

⁹ "Basic Aspects of Stream Meanders," by Gerard H. Matthes, *Transactions, Am. Geophysical Union*, Pt. III, 1941.

of the Old River junction) certainly deserve their inclusion in the geological treatment of the lower Mississippi alluvial valley.

The geophysical dynamic force system of the Atchafalaya Distributary is of varying complexity from its head to the Grand Lake-Six Mile Lake region on the southern boundary of the basin.

Increasing Discharge.—The formation of the Atchafalaya Distributary was conditioned as far back as about 1500 A.D. A map¹⁰ dated 1578 A.D. drawn by Monk Ptolemy, who accompanied De Soto's expedition in 1542, shows conclusively that the Atchafalaya then, as now, served as an outlet for the Mississippi River. After the rafts¹¹ of logs had been entirely removed before 1855, the distributary has progressively increased its flow which has been diverted from the Mississippi. Since 1900, the discharge of the Mississippi through this distributary has increased from 5% to 25% of the total annual flow, and from 15% to 30% of the total annual flow past the latitude of the Old River. The estimated limiting condition of conservative maximum diversion of not more than 40% in order to keep the present course of the lower Mississippi is being approached.

This tendency of increasing discharge is further facilitated by the topographical advantage of the Atchafalaya Distributary. There is a much shorter distance and a much steeper slope from the Old River junction to the Gulf than the master stream to its present delta mouth.

Enlargement of Leveed Segment.—The increase in discharge through the Atchafalaya Distributary has resulted in a corresponding increase in channel width together with a gradual increase in depth through the years. North of Krotz Springs the Atchafalaya channel is leveed. In some reaches of this leveed segment, the channel width has doubled that of 50 yr ago. This trend of enlargement magnifies itself along many a reach of the river by caving of opposite banks. This condition is not observed on the Mississippi River where caving along an individual reach is usually confined to a single bank. This gradual enlargement of the cross-sectional areas of the leveed segment supplies material for natural levee formation in the unleveed segment below Krotz Springs.

Forming of Natural Levees.—Along the lower unleveed segment of the Atchafalaya, natural levees are forming at a rapid rate. It is conceivable that they will eventually become larger in areal extent than those along the artificially controlled upper reaches. Along the unleveed segment, the silty sand and fine sand carried in suspension during over-bank flow are deposited over the above-bank surface as the velocity slackens. This process of building up natural levees will continue to be pronounced as long as the cross-sectional areas of the leveed segment enlarge gradually to increase the load of the discharge.

Building Up of Overland Deltaic Deposits.—The southward retreating of the northern boundary of the Grand Lake has been accounted for in an earlier passage. From 1932 to 1950, the growth in thickness of deltaic deposits in the

¹⁰ "The Improvement of the Lower Mississippi River for Flood Control and Navigation," by D. O. Elliot, U. S. Army Engr. Waterways Experiment Station, Corps of Engrs., Vicksburg, Miss., May, 1932.

¹¹ "The Atchafalaya River Study," Report by the Mississippi River Comm., Vol. 2, May, 1951.

northern part of the ancient Grand Lake varied generally from below 3 ft to a maximum of about 10 ft.

Deepening of Unleveed Segment.—The Atchafalaya lower main channel has developed to a depth varying from 40 ft to 80 ft. This lower, unleveed segment of the Atchafalaya main channel consists principally of thick backswamp clays which offer comparatively more resistance to scour and consequent cross-sectional enlargement. Hence, the rate of increase in channel widths and depths in the unleveed segment of the main channel will be much slower than in the upper leveed segment. However, as natural levees are built up, and as volume of discharge continues to increase, higher velocities and consequent heavier scour will result in the channel. Except for minor channel migration, which might be initiated by local high substratum sand areas, the Atchafalaya main channel south of the leveed segment should develop a deep, narrow, nearly straight channel, comparable to the present Mississippi south of Donaldsonville.

Single or Multiple Channels.—In the unleveed segment, during flood and high-water stages, considerable volumes of water are carried along subsidiary channels, notably the Bayou L'Embarras-Lake Rond channel which has carried as much as 60% of the total discharge during recent floods. Hence, the question arises in the probable location of the future main channel, whether by enlargement of the present main channel on the east, or the L'Embarras-Lake Rond channel on the west, or the coexistence of multiple channels.

Repeating of Department of Characteristic Caving.—The department of characteristic caving of opposite banks of the upper segment of the Atchafalaya Distributary may be repeated in the future, though most probably to a lesser extent, in the unleveed segment of the main channel, when the latter has attained enough capacity and before it reaches a state of equilibrium.

Developing Pattern of Capturing the Master Stream.—The Atchafalaya Distributary is following a developmental pattern so characteristic of former Mississippi River diversions each of which captured the entire flow of the master stream within an estimated period of 100 yr or more. Now that a channel capable of carrying low-water flow has been established and enlargement has begun, no natural processes are known that might prevent enlargement and eventual diversion of the entire Mississippi flow, until the Corps of Engineers have completed their positive artificial control. Even after the completion of such large engineering control works, there is no guarantee that a major breach would not happen, should untenable conditions due to climatic abnormalities occur, because the control works are in an alluvial plain.

Past Foundation Lessons in the Lower Alluvial Valley.—The authors have cited some past foundation lessons in the lower-left region of the lower alluvial valley. The following are some past foundation case lessons that have occurred in the lower-right region.^{7,11}

Shifting of Thalweg.—The abandoned bridge structure of the Texas and Pacific Railroad over the Old River at Torras, La., has pier foundations down to -10.08 ft near the south bank and down to -101.92 ft near the center of the river. The mean-low-water elevation (M.L.W. El.) and mean-high-water elevation (M.H.W. El.) are, respectively, at 8.2 ft and 49.6 ft. Though it had carried no traffic after abandonment, the north span and approach collapsed in 1948. This indicated that foundations were not built to sufficient depths to

meet the possible shifting of the thalweg. At this crossing the thalweg had shifted itself for a distance of more than 900 ft from south to north between 1917 and 1951. Had the bridge not been abandoned, groins of proper location, direction, and dimensions should have been built as soon as signs of shifting had been noticed, to keep the thalweg unchanged.

Provisions for Thalweg Shifting.—The bridge for U. S. Highway Nos. 190 and 71 over the Atchafalaya Distributary at Krotz Springs has all its four river piers founded to the same depth of -139.95 ft. The M.L.W. El. at this crossing is at 6.1 ft, while the M.H.W. El. is at 33.0 ft. The founding of all the river piers to the same depth shows resourcefulness that will permit whatever shifting of the thalweg that may happen.

Deepening of Channel.—On the Kansas City Southern Railroad and the Louisiana State Highway No. 30, there is a combined bridge over the Atchafalaya Distributary at Simmesport, La. It was a wise precaution to build the main river piers down to -180 ft for both the old structure of 1928 and the modification of the structure in 1938. Here, the elevations of M.L.W. and M.H.W. are at 7.3 ft and 46.4 ft, respectively. The channel between piers No. 2 and No. 3 had a maximum increase in depth of 44 ft from 1888 to 1928.

Provisions for Channel Deepening.—The Missouri-Pacific Railroad has a bridge over the Atchafalaya Distributary at Krotz Springs, with its old structure piers built to depths from -67.01 ft to -89.43 ft. The Atchafalaya River has considerably deepened its channel in this segment. Consequently, the 1941 modification of the structure has river piers founded to -140.0 ft. This constitutes an additional provision of more than 50 ft for channel deepening as compared with the older piers.

Consequence of Shallow Bridge Foundation.—The Missouri, Louisiana, and Texas Railroad Bridge over the Atchafalaya Distributary at Atchafalaya, La., had its river piers founded only to -83.6 ft and -84.08 ft. The M.L.W. El. is at 5.8 ft, while the M.H.W. El. reaches 20 ft. higher. The pivot pier of the swing span was overturned in June, 1928. All spans were removed in November, 1929, and the east rest pier was destroyed in 1935. Such was the consequence of inadequate pier foundation depths in the deepening channel of the distributary in the lower alluvial valley.

CHARLES R. KOLB¹⁰ AND WOODLAND G. SHOCKLEY,¹¹ M. ASCE.—The remarks made by Mr. Li are much appreciated, and his account of geologic conditions in the Atchafalaya Basin is a valuable supplement to the writers' presentation of Mississippi Valley geology and its significance to engineers. Mr. Kolb was fortunate to have played a considerable part in the project entitled "Geological Investigation of the Atchafalaya Basin and the Problem of Mississippi River Diversion." Hence, he feels qualified to endorse fully Mr. Li's summary of geologic events that shaped the basin and that affect the diversion process.

However, one point should be examined further. Mr. Li states under the heading, "The Developing Pattern of Capturing The Master Stream:"

¹⁰ Chief, Geology Branch, Soils Div., U. S. Army Engr. Waterways Experiment Station, Vicksburg, Miss.

¹¹ Chief, Embankment and Foundation Branch, Soils Div., U. S. Army Engr. Waterways Experiment Station, Vicksburg, Miss.

"Even after the completion of such large engineering control works, there is no guarantee that a major breach would not happen—should untenable conditions due to climatic abnormalities occur—because the control works are in an alluvial plain."

Although no guarantee is possible, there is evidence to indicate that past diversions of the Mississippi River have occurred only when certain specific and unusual conditions have been met. Early stages of past diversions appear to have been gradual and unspectacular, with potential diversions often sealing themselves. It is only when the diversion channel takes low-water flow that it is capable of continued enlargement, and only when it has developed to the point where it takes approximately 40% of the flow of the master stream that the process accelerates. Available evidence indicates that this critical stage (40% diversion) takes as long as 50 yr. Sudden changes in the course of the Mississippi River are an extremely remote possibility. Normal diversionary development is so slow that engineering works can be constructed in ample time to prevent total diversion. Moreover, the size and cost of such structures can be reduced significantly when the geologic criteria that indicate and control diversion are understood and recognized at an early stage.

AMERICAN SOCIETY OF CIVIL ENGINEERS

Founded November 5, 1852

TRANSACTIONS

Paper No. 2997

GROUND TRANSPORTATION AT NEW YORK INTERNATIONAL AIRPORT

BY RICHARD I. STRICKLAND¹

SYNOPSIS

A new concept in airport terminals resulting in a 655-acre "Terminal City" includes ten passenger terminal buildings, 10 miles of two-lane roads, and multiple parking facilities. Basic planning data are presented herein, together with a study of the design of the roadway system and parking facilities.

NEW CONCEPT IN AIRPORT TERMINALS

In December, 1957 a new 655-acre "Terminal City" opened at New York (N.Y.) International Airport. The development includes 10 miles of two-lane roads, five parking areas with more than 6,000 spaces, a 220-acre International Park, and twelve separate major buildings.

Early plans for a passenger terminal to replace the temporary terminal, which was opened in 1948, visualized a large central building. However, as future airport activity was considered, it became obvious that the number of required airplane positions could not be placed functionally around a single building. The logical solution was to establish multiple terminal buildings. The plan was welcomed by the airlines operating from New York International Airport. (There are now 15 United States flag airlines and 22 foreign flag airlines operating at the airport.) The larger United States airlines will have their own separate terminals, and the foreign flag airlines are now provided with separate and ample ticket offices and lounges.

The largest structure is the combined International Arrival Building (IAB) and Airline Wing Buildings, which were opened on Dec. 6, 1957. The IAB is U-shaped and situated centrally. It provides facilities for all arriving airplanes from overseas points that require federal government inspection services. Incoming passengers use the ground floor of the two arcades, or fingers, and move directly to federal health, immigration, and customs inspection services. Then they exit to the street and ground transportation, using only the ground

NOTE.—Published, essentially as printed here, in May, 1958, in the Journal of the Highway Division, *as Proceedings Paper 1623*. Positions and titles given are those in effect when the paper was approved for publication in *Transactions*.

¹ Asst. Chief, Traffic Eng. Div., The Port of New York Authority, New York, N. Y.

floor of the building. The long fingers on each side of the IAB are the Airline Wing Buildings, containing the ticket counters, lounges, and offices of the foreign flag airlines. Outgoing overseas passengers arrive at the ticket offices in the Airline Wing Buildings directly from the street. Then they proceed on the second-floor level to the aircraft loading gates. The combined length of the IAB and Airline Wing Buildings is approximately 2,300 ft long.

The remaining terminal buildings around the central roadway system will be unit terminals, operated by various United States airlines. Construction of several of the buildings was begun in 1957, with completion of the first two scheduled for August and September, 1959. Upon completion of the other unit terminals, it will be possible to provide 140 aircraft loading positions.

To indicate the function of New York International Airport in serving the New York City area, Fig. 1 shows the regional airport system for northern

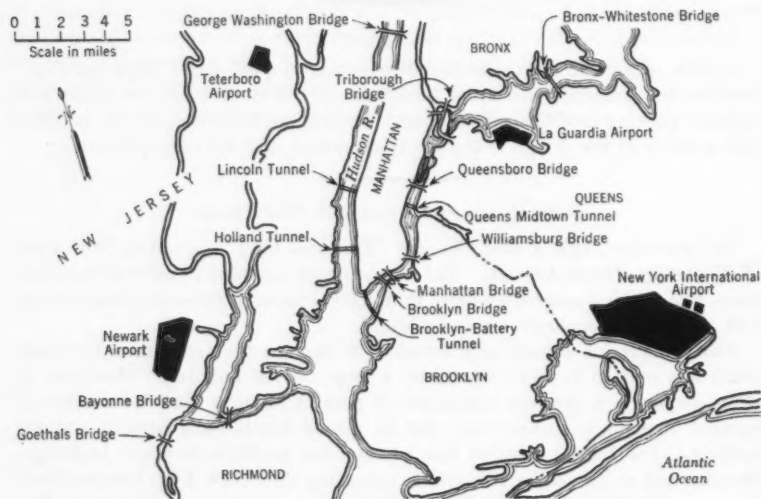


FIG. 1.—NORTHERN NEW JERSEY-NEW YORK REGIONAL AIRPORTS

New Jersey and New York. As the agency of both states, the Port of New York Authority finances, develops, and operates the four major airports shown in Fig. 1. This region, which is the principal airport traffic center of the United States and the air crossroads of the world, handled more than 13,500,000 passengers in 1958, including nearly 2,100,000 overseas air travelers. In the system, New York International Airport deals with all overseas air traffic as well as much of the domestic traffic. La Guardia (N.Y.) Airport and Newark (N.J.) Airport manage domestic flights only. It is anticipated that Teterboro (N.J.) Airport will continue to be the primary center of the increasingly important volume of business aircraft as well as training and private flights.

Fig. 2 shows the important features of New York International Airport. The area is almost 5,000 acres, which is nine times the size of La Guardia Air-

port, and is equivalent to all of Manhattan Island from 42nd Street to the Battery. The major artery into the airport is Van Wyck Expressway, which has a complete interchange with the Southern Parkway on the northern side of the airport and extends northward to the Kew Gardens (Queens, N.Y.) interchange with Grand Central Parkway and the Interboro Parkway. The limited-access nature of Van Wyck Expressway is continued into the airport. Taxiway and roadway underpasses bring it into the central terminal area. The other principal access is 150th Street, which is used predominantly by employees, and by cargo and service vehicles. Future highway plans envision a "Nassau Expressway" along the northern boundary of the Airport, with connections to the Southern Parkway and Van Wyck Expressway. A unique feature of the airport is a subway station of the New York City Transit System along its western boundary. At present (1959) thirteen hangars have

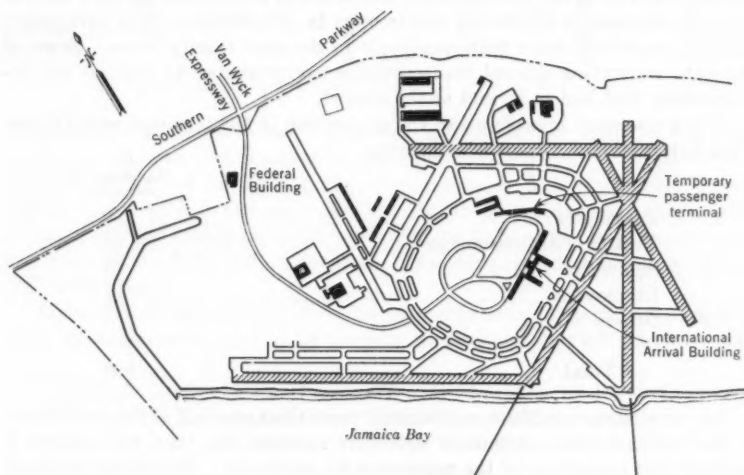


FIG. 2.—SIMPLIFIED DRAWING OF THE NEW YORK (N.Y.) INTERNATIONAL AIRPORT

been built, four are under construction, and several more are in the planning stage.

Four cargo buildings, providing direct transfer of cargo from airplane to truck, were completed in 1956 to meet the demands of the rapidly growing volume of air cargo. The buildings are leased in sections, so that each airline has its own airplane apron, truck apron, and employee parking space. There is a fifth structure in the center of the development that is a cargo service building, providing temporary warehousing and shipping.

When considering the scope of the development at New York International Airport, the complex nature of the planning required can be appreciated. The Traffic Engineering Division was just one of the many groups participating in the planning of the central terminal area. Under the supervision of the Authority commissioners and of the executive director, the Aviation Departmen

has over-all responsibility for the development. The Planning Division of this department employed airline experts and architectural and engineering consultants, as well as several other Port Authority departments. The final plan is the result of much effort and coordination and many conferences.

GROUND-TRANSPORTATION PLANNING DATA

A basic step in planning new facilities for New York International Airport was to collect and analyze airport operating data and to predict future requirements. The analyses of the Forecast and Analysis Division of the Aviation Department ranged from complex studies, such as predicting the United States domestic air-passenger market from the present to 1975, to detailed studies of the parking and traffic needs of the airport. It is of interest to note the forecasted growth of air-passenger volume. Compared with 38,700,000 domestic originating trips in the United States as of 1955, it is expected that in 1965 this sum will increase to 90,000,000 and in 1975 to 167,000,000. It is anticipated that air travel will more than quadruple in the next twenty years. Some of the data concerning ground transportation are presented to indicate the requirements that had to be met at the airport.

The percentage breakdown of the population in the terminal area at New York International Airport is as follows:

Type	Population, in percentage
Passengers.....	56
Visitors with passengers.....	23
Sightseers.....	5
Employees.....	11
Others.....	5
Total.....	100

Air passengers constitute only slightly more than one-half of the individuals in the terminal area. Although sightseers average 5%, they will present a much greater percentage of the population on weekends. The degree to which consumer services are supplied at airports can affect the population. At Newark Airport 12% of the vehicles using the parking lot belong to diners. Approximately 10% of the terminal-area population are employees, and an equal number of employees are situated outside the area.

As to the type of transportation used by the foregoing, the following is pertinent:

Employee mode of ground transportation	Percentage
Driving own automobile.....	71.8
Arriving in another employee's automobile.....	13.4
Deposited by nonemployee automobile.....	1.3
Using public bus.....	11.2
Arriving in company car.....	1.0
Other.....	1.3
Total.....	100.0

It is noteworthy that those driving their own automobiles or riding in someone else's form approximately 88% of the total. The ratio of employees per car is approximately 1.2, indicating a minimum usage of car pools. Although employee population is probably less than 20% of the total, it must be considered in highway capacity as shift changes cause heavy peak flows.

With reference to air passengers, Table 1 summarizes the mode of transportation used by outbound domestic air passengers at the three major Port Authority airports in the period from November, 1955, through October, 1956.

TABLE 1.—MODE OF GROUND TRANSPORTATION TO AIRPORTS,
EXCLUDING TRANSFERS, IN PERCENTAGE

Airport (1)	Automobile (2)	Taxi (3)	Airport coach (4)	Public bus (5)
New York International.....	42	26	31	1
La Guardia.....	37	41	20	2
Newark.....	46	12	38	4

These data were taken from an extensive in-flight survey made by the Port Authority with the cooperation of the commercial airlines. Domestic passengers are defined as those having destinations in the continental United States, in Mexico, or in Canada. Not included are transfer passengers who enter on one flight and transfer to a different outgoing flight at the same airport or at any other in the New York City area. Transfer passengers represent almost 20% of the total.

Ground transportation at New York International Airport is an approximate median between that at La Guardia Airport and Newark Airport. The

TABLE 2.—MODE OF GROUND TRANSPORTATION TO NEW YORK
INTERNATIONAL AIRPORT FROM METROPOLITAN AREA,
EXCLUDING TRANSFER PASSENGERS,
IN PERCENTAGE

	Automobile (1)	Taxi (2)	Airport coach (3)	Public bus (4)
Residents.....	58	20	21	1
Nonresidents.....	25	32	42	1
Total.....	42	26	31	1

different usage rates at the various airports are a result of several factors, such as location, type of flight, proximity to Manhattan, and type of travel. For example, La Guardia Airport is closest to Manhattan and is utilized most by business travelers, resulting in a heavy use of taxis to reach the airport. Coaches are used most at Newark Airport because this terminal is farther from the center of population concentration, and taxi service is relatively more expensive. The negligible use of public bus transportation by air passengers is notable. The importance of passenger automobiles in transporting air travelers

is indicated by the total automobile and taxi use, which varies from 58% to 78% at the three airports.

Table 2 provides a further insight into the variation in the use of ground transportation to airports. The usage rates are broken down by resident and nonresident users. The metropolitan area includes counties in New Jersey, Long Island, N.Y., and north of New York City, as well as the five boroughs of the city. With nonresidents the use of private automobiles is less than one-half of that by residents, and taxis and airport coaches are utilized to a greater degree to reach the airport.

The following indicates the various uses of private automobiles for different types of flights at New York International Airport:

Type of flight	Parking lot, vehicles per flight
Domestic coach.....	5
Domestic first class.....	6
Average.....	6
Overseas tourist.....	8
Overseas first class.....	10
Average.....	9

More vehicles must be accommodated in the parking lots for overseas flights. This is even more apparent from the domestic-flight figures for La Guardia Airport. At this terminal domestic coach flights resulted in six parked vehicles, and domestic first class flights generated only three parked vehicles, compared with the average of nine vehicles for overseas flights at New York International Airport.

In designing the roadway system to serve an airport terminal development, it is important to know the manner in which motorists wish to use the terminal and parking facilities. Table 3 summarizes observations made at the terminal areas of the three major airports during 1955 and 1956.

TABLE 3.—VEHICLE DISTRIBUTION ENTERING AND LEAVING TERMINALS

(a) Entering	Design, in percentage	Range, in percentage	(b) Exiting	Design, in percentage	Range, in percentage
To parking facility directly.....	65	60 to 75	Exit directly.....	90	75 to 95
To terminal, then to parking facility.....	10	5 to 15	Stop at terminal....	10	5 to 25
To terminal, then to exit.....	25	15 to 35			

It was found that most of the vehicles approaching a terminal area go directly to a parking facility, and only 10% stop at the terminal before parking. Therefore, providing direct access to parking facilities would relieve frontage roadways of most of the traffic that would otherwise pass the terminal. On leaving the parking lot, motorists again predominantly did not stop at the terminal, and 90% exited directly from the airport.

The parking habits of airport motorists are important also. Table 4 shows the average daily use of the three New York airport parking lots by purpose of

visit. Those parking while dining were excluded to provide a better basis for comparison. However, this category should not be disregarded because, as mentioned previously, diner parking might represent more than 10% of parking-lot users.

The bulk of parking-lot usage is generated by the transportation of airport passengers and ranges from 65% to 75% of the volume. Sightseeing constitutes

TABLE 4.—COMPOSITION OF PARKING-LOT VOLUMES
ON AN AVERAGE DAY

Purpose of visit	DISTRIBUTION, IN PERCENTAGE		
	La Guardia Airport	New York International Airport	Newark Airport
All purposes	100	100	100
To transport air passengers:	75	70	66
To airport	30	28	32
From airport	30	38	20
Duration parking	15	4	14
To transport sightseers	10	18	16
To transport others	15	12	18

approximately 15% of the parking volume on an average day. On a weekend the sightseeing volume rises sharply. Studies at Newark Airport showed a rise of more than 20% on Saturday and of more than 25% on Sunday. It should be noted especially that approximately 15% of parking-lot users at La Guardia Airport and Newark Airport parked for the duration of their air trips. Table 5 summarizes the duration of parking for various visit purposes

TABLE 5.—AVERAGE DAILY PARKING DURATION FOR
VARIOUS VISIT PURPOSES*

Purpose of visit	DURATION, IN HOURS		
	La Guardia Airport	New York International Airport	Newark Airport
All purposes	1.5	1.6	1.7
To transport air passengers:	1.2	1.6	1.2
To airport	1.2	1.4	1.2
From airport	1.2	1.7	1.1
Duration parking	(1.8) ^b	(4.8) ^b	(2.0) ^b
To transport sightseers	1.4	1.3	1.0
To transport diners	1.7
To transport others	2.1	1.9	3.6

* Average duration of parking is computed only for cars parked less than one day. ^b In days.

at the three major airports. It is important to note that the average shown for all purposes does not include the duration parking mentioned previously.

Although parking for most purposes averaged between 1 hr and 1.7 hr, duration parking averaged between 1.8 days and 4.8 days. The average duration parker at New York International Airport requires the same space hours in the parking lot as seventy-two parkers transporting passengers to or from

the airport. The duration parker at La Guardia Airport averaged only 1.8 days. This still represents the parking-lot space required by thirty-six vehicles transporting air passengers to or from the airport. The effect of duration parking on parking-lot congestion was demonstrated forcibly when a 3:00 a.m. check at Newark Airport revealed 500 parked automobiles in a lot with a capacity for 640.

ROADWAY SYSTEM

An airport roadway system must serve several functions, the most important of which is to provide direct access to the passenger terminal area. As mentioned previously, the Van Wyck Expressway approach into the New York International Airport is of limited access, with grade separations at taxiways and intersecting roadways. To provide for increased future activity, 150th Street is also being developed to serve as a limited-access route to Terminal City. It will be dualized and an overpass will be provided to connect it directly to the Terminal City loop. Underpasses are planned for the taxiways presently crossed at grade.

A second function of the roadway system is to provide satisfactory access to all areas of the airport. To allow access to hangars and service facilities along Van Wyck Expressway, it was necessary to build 24-ft-wide, two-way service roads on each side of the expressway. These roads are connected by a loop overpassing Van Wyck Expressway at one end and a traffic circle at the other. Entrance from the service roads is possible only at these extremities, more than a mile apart. An intermediate exit is provided from Van Wyck Expressway to the northern service road.

A similar design for service roads was found necessary for the future development of 150th Street. Service facilities along this road, such as those for air cargo, in-flight meal preparation, and airport coach maintenance, will generate peak traffic volumes that will eliminate grade intersections and warrant service roads with a connecting overpass.

The roadway system should allow truck traffic destined to airport service areas to be separated from passenger terminal traffic. Air-cargo trucks to New York International Airport are presently diverted from Van Wyck Expressway at the airport entrance and reach the cargo development by way of 150th Street.

The service roads of the Southern Parkway, North Conduit Boulevard, and South Conduit Boulevard connect conveniently between Van Wyck Expressway and 150th Street. It is planned also to provide a separate access route to serve an industrial area being developed in the northwestern section of the airport. Thus, Van Wyck Expressway will not be required to carry all the traffic generated by the industrial area. A special problem at New York International Airport has been the flow of ramp service vehicles, such as fuel trucks, food trucks, and baggage carts, to and from the airplane aprons of the various terminals. An entirely separate roadway presently accommodates these vehicles completely circling the Terminal City development. The peripheral service road accommodates two-way traffic and provides direct and convenient service to all apron areas. Connections to Van Wyck Expressway and 150th Street are controlled to prohibit their use by the public.

Within Terminal City the roadway system must allow convenient access to each terminal building as well as to the parking areas serving them. Fig. 3 shows Terminal City, with the roadway system developed to provide the necessary access. Terminal City includes four principal public parking lots, each associated with a group of terminals. Entering the terminal area from Van Wyck Expressway (in the lower right-hand corner of Fig. 3), a separate route reaches each of the four areas. For example, traffic to the lot 1 area exits first to the terminal loop. Traffic to lot 2, which serves the IAB, exits just beyond the service station. Vehicles destined for lot 3 turn off left of the two terminals depicted at the bottom of the illustration. The remaining traffic is routed to the lot 4 area. When exiting from the parking lots or from the terminals, it is possible to use similar separate routes to reach Van Wyck

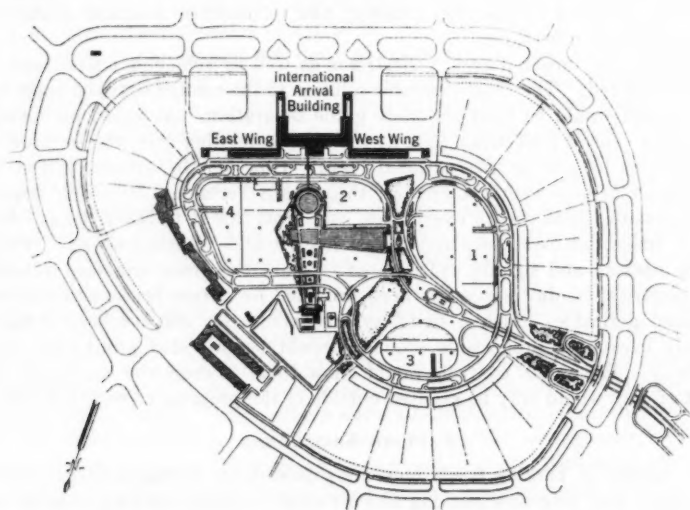


FIG. 3.—TERMINAL CITY, NEW YORK INTERNATIONAL AIRPORT

Expressway. Thus, the mixing of traffic to and from the various terminal areas is minimized within Terminal City.

Design standards for the roadway system are much the same as in current practice. With the exception of the inner service roadways at the terminal buildings, all the roadways have two lanes and are 24 ft wide. Mountable curbs and 8-ft stabilized shoulders are provided. All roadways transport one-way traffic and no direct crossing of traffic streams is permitted. Intersecting traffic is guided to merge and diverge in order to perform the turns required to reach terminal and parking areas. The center mall between the one-way loop roadways is 100 ft wide, so that the principal turnarounds have a 50-ft inner radius.

One of the most difficult design specifications to maintain was the provision of a 300-ft weaving distance between a major entrance and exit of the terminal loop. For example, a motorist leaving one of the parking lots and seeking to reach a terminal building across the mall must merge with the loop roadway and then crossweave in a distance of 300 ft in order to reach a turnaround roadway to the terminal-site entrance. Because of the quantity of terminals and the access connections that had to be provided to each, in several cases it was necessary to accept somewhat less than 300 ft of weaving distance.

An associated problem to which study is being given is the design of the roadway connections to the unit terminals from the terminal loop. Terminal City planning originally visualized a single inner service road at ground level at each unit terminal. However, several airlines have submitted building plans requiring roadways at two levels. Careful design will be necessary to maintain weaving distances on the loop roadway and to minimize roadway grades for unit-terminal connections.

Within the terminal area, pedestrians as well as vehicular traffic must be accommodated. The most desirable solution to the conflict between these two movements would be their complete grade separation. As noted previously, there is a central pedestrian walk at the IAB, extending from the terminal to the parking lot and to International Plaza. However, to separate pedestrian and vehicular movements completely throughout Terminal City would require approximately fifteen such overpasses, each from 200 ft to 300 ft long. As a result, pedestrian overpasses may be restricted to high volume crossings. Pavement marking and signing will be used to mark the grade crossings initially, and electrical-conduit space has been provided for future traffic signalization if found desirable. Such a signal system would not delay vehicular traffic unduly because a progressive sequence could be provided around the loop roadway. Pedestrian controls would allow them to cross the roadways, but right of way would only be granted outside of the progressive vehicle band.

PARKING FACILITIES

A variety of parking needs must be provided for Terminal City. Public short-time and long-time parking and terminal-employee parking must be accommodated. Special facilities are required for airport coaches, taxicabs, rented automobiles, airline business agents, and dignitaries.

Short-time parking is accomplished in the metered parking areas in the mall between turnaround roadways. In general, these areas are immediately in front of each building and allow 30-min parking. At present, right-angle parking is being replaced by 75 degree parking to encourage one-way movement. The entrance to the lots is at the far end as approached on the one-way loop roadway. Thus, an ample merging and crossweaving area is provided, eliminating direct crossing of traffic entering the metered areas with traffic using the turnaround roadways. Parking meters are being placed 3 ft from the curb at the center of the stall, and walks are being provided on the terminal side of the metered lots for the convenience of pedestrians. Double markings are placed between stalls, so that automobiles are guided into the center of the parking spaces.

Public parking lots were situated across the mall from the terminals within the terminal roadway loop. Conventional right-angle design parking was used with 8½-ft-by-18-ft spaces and 24-ft aisles. The latter are generally at right angles to the terminal buildings, thereby providing more convenient routes for pedestrians and eliminating long, speed-encouraging vehicular aisles with dangerous four-way right-angle intersections. Curbed islands were placed at each end of the parking rows to control parking and to create a site for necessary parking-lot section-number signs and traffic-control signs. Without such islands motorists park in the main aisles, and signs must be replaced constantly.

A new feature in the parking lots is the automatic equipment used at the entrances. This apparatus is a treadle-operated ticket dispenser. Similar types are presently being used by other concerns, although in the airport adaptation only a single vehicle gate is used. The sequence of operation is as follows: On approaching the ticket dispenser the vehicle crosses a treadle, which causes a single, time-stamped ticket to be extended from the dispenser. A flashing arrow and an audible bell draw attention to the dispenser. When the parking patron takes the ticket the parking gate ahead is actuated, and the vehicle is allowed to pass into the lot. A second treadle is crossed, which lowers the gate. In all equipment, operating-time requirements have been reduced to a minimum, and the design of the automatic gate allows it to reverse without lowering completely. Two outstanding advantages result from these automatically controlled entrances: (a) The cost of manning the parking lots is reduced, and (b) it is possible to use multiple entrances to serve parking patrons more conveniently. All traffic exiting from the parking lot must use the central exit.

Special attention was given to several features of the parking lots. Storage was provided on entrance and exit, based on the established rate of 240 vehicles per hour per attendant and on the expected peak rate of arrival and departure. Peak rates were derived by increasing average rates on the basis of the Poisson random-arrival theory. The parking aisles adjacent to the main entrance and exit were "dead-ended" to avoid congestion at the "T" intersection with the main parking-lot aisle. In anticipation of overflow public parking at times of special events at Terminal City, stand-by entrances were constructed into the employee parking lot directly in line with the main entrance and exit. Message "blank-out" signs were provided at the automatic entrances, so that if an entrance is closed traffic can be directed to the following one.

The public parking lots are situated nearer to the terminals, with employee parking to the rear. The employee areas have separate entrances and exits, generally situated away from the public parking entrances and exits and connecting more directly with Van Wyck Expressway. Thus, the mingling of employee and public parking is minimized. Automatic gates operated by special cards control the use of the employee areas. The cards are used instead of a key or similar device because of the flexibility of control required. Employee-parking permits generally are purchased on a monthly basis, and the gate control must allow the use of several different cards to permit grace periods on the monthly tickets and to admit other parkers.

Fig. 3 shows the roadway system and parking areas in front of the IAB, indicating provisions for special parking. Approximately 25% of the air passengers use taxicabs to and from the airport. Taxis will discharge along the full length of the terminal frontage. A six-cab taxi stand will be established for loading passengers at the western end of the IAB. Taxis will be fed to this cab stand as required from a taxi storage area in the center mall to the west of the stand. Airport coaches are used by approximately 30% of the air passengers, and also will be allowed to unload the full length of the terminal curb. A loading area will be established for airport coaches at the eastern end of the IAB. Airport coaches will be stored at a remote area on 150th Street and will be called as required, probably by radio. Rental vehicles will be treated similarly, with a few parking spaces convenient to the terminal, but with storage at a remote site. Special parking for business agents of the airlines and for important officials is convenient to the IAB and Airline Wing Buildings. In the mall two metered parking areas were extended for business-agent parking. Space for important officials is situated off the main entrance to parking lot 2, with a separate exit to the loop roadway.

A 33-ft, three-lane roadway was built in front of the IAB and Airline Wing Buildings. A three-lane road is recommended for terminal frontages because of the frequent double parking that would block a two-lane road completely. Even if there is ample curb space within 100 ft of the terminal doors, motorists frequently double park to discharge passengers immediately in front of the doors.

TRAFFIC SIGNING

Traffic signing at New York International Airport must be mentioned because of its importance in the efficient direction of ground transportation. Three interesting features were incorporated in the signing for Terminal City: (1) The use of color in the directional signs, (2) a progressive signing technique similar to that used by a commercial product, and (3) the coordinated design of light poles and signs so that signs could be light-pole mounted, with a pleasing architectural result.

The use of color and the progressive technique provide the best means devised to channel traffic destined to the various buildings. The challenge presented by the new development was to direct vehicular traffic, without confusion, to one of ten buildings. (Formerly, it had been necessary merely to direct air passengers to a single terminal, where, on foot, they sought out the individual airline.) Four sign colors were selected, one for directional signs pertaining to each parking lot in the terminal. The progressive concept was used to list the many terminal destinations in such a manner that they can be read at highway speeds.

AMERICAN SOCIETY OF CIVIL ENGINEERS

Founded November 5, 1852

TRANSACTIONS

Paper No. 2998

BEHAVIOR OF REINFORCED CONCRETE SHEAR WALLS

BY JACK R. BENJAMIN,¹ A. M. ASCE, AND
HARRY A. WILLIAMS,² M. ASCE

WITH DISCUSSION BY MESSRS. DEFOREST A. MATTESON, JR.;
AND JACK R. BENJAMIN AND HARRY A. WILLIAMS

SYNOPSIS

Comparative studies are presented of one-story, plain and reinforced concrete shear walls subjected to shear forces applied in the plane of the wall. Panel and column proportions and reinforcing were investigated. Some approximate relationships are suggested for predicting the load-deflection curves for these walls.

INTRODUCTION

The material presented herein is based on an investigation of the strength and behavior of shear walls that was conducted at Stanford University, Stanford, Calif., during the period from 1951 to 1956. The purpose of the investigation was to develop data that could be used in the design of atomic-blast-resistant structures. The advantages of shear walls as primary lateral-load resisting elements for such structures were recognized in 1948 during the initial development of design methods by the Office of the Chief of Engineers, Corps of Engineers, United States Department of the Army. Full-scale tests of shear-wall structures were conducted in 1951 at "Operation Greenhouse" in the Pacific Proving Ground for atomic weapons. Laboratory tests were initiated in 1949 by the Chief of Engineers at the Massachusetts Institute of Technology, Cambridge, Mass.³ These studies were continued at Stanford University.

NOTE.—Published, essentially as printed here, in May, 1957, in the Journal of the Structural Division, as *Proceedings Paper 1254*. Positions and titles given are those in effect when the paper or discussion was approved for publication in *Transactions*.

¹ Prof. of Civ. Eng., Civ. Eng. Dept., Stanford Univ., Stanford, Calif.

² Prof. of Civ. Eng., Civ. Eng. Dept., Stanford Univ., Stanford, Calif.

³ "Behavior of Structural Elements Under Impulsive Loads," Pts. I & II, reports to New England Div., Corps of Engrs., U. S. Dept. of the Army, Boston, Mass., 1958.

Although shear walls were used in earthquake design for many years, little was known of their ultimate strength or behavior in the cracked region. Some studies^{4,5} of shear walls for earthquake resistance have been made by Japanese investigators.

GENERAL DESCRIPTION

The behavior of one-story reinforced-concrete shear walls without openings (Fig. 1) is examined herein. The wall is loaded through a distributing member (either a beam or floor diaphragm) at the top of the wall. Both tension and compression columns are provided, and the wall is supported on an essentially rigid foundation. The tension and compression columns may have the same thickness as the panel but are provided with special steel in any case. Face walls may act as the bounding columns.

The important variables are (a) loading; (b) materials; (c) panel design (thickness, proportions, and reinforcing); (d) tension-column design; (e) compression-column design; and (f) method of construction.

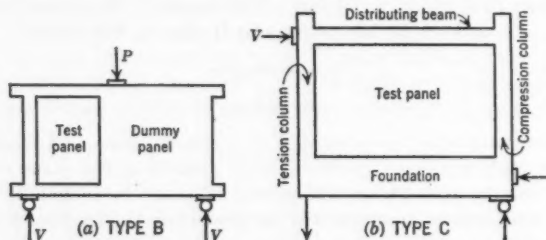


FIG. 1.—TYPE SPECIMENS B AND C AND METHODS OF LOADING

Shear walls can be subjected to three different loadings. The shear load from lateral forces acting in the plane of the wall is the primary condition that was studied. The wall can be used also as a bearing wall, and it can be subjected to loads perpendicular to its face. Under dynamic loading conditions from blast or earthquake, the combinations of loadings become complex because of the time relationships that can exist between the three types of loads.

The shear wall itself is subject to many variables. The construction materials (both concrete and steel) can vary considerably. Variations in panel proportions, length, height, thickness, and reinforcing influence the wall behavior. Similarly, variations in tension and compression-column design are important. Finally, the details of construction, such as pour joints, doweling, keying, and curing, must be considered.

The general problem is studied best from the standpoint of a typical load-deflection curve and the influence of the variables on this curve. The typical wall is shown by the type C specimen in Fig. 1(b); typical load-deflection curves are shown in Fig. 2. The problem is considered to be solved if the following

⁴ "Study of Vibration Resistant Walls," by T. Taniguchi, *Transactions, Architectural Inst. of Japan*, Tokyo, No. 41, 1953, p. 62.

⁵ "Stress Analysis of Walls with Rectangular Holes," by K. Otsuki, *ibid.*, p. 72.

factors are known:

1. The load at break in the load-deflection curve, V_e ;
2. The deflection at break in the load-deflection curve, δ_e ;
3. The ultimate load, V_u ;
4. The deflection, δ_u , at the ultimate load;
5. The post-ultimate general behavior; and
6. The mode of failure, failure characteristics, and extent of damage at particular load points.

Reinforced concrete is a statistical material. Considerable variation in experimental results always occurs. The method of prediction of shear-wall be-

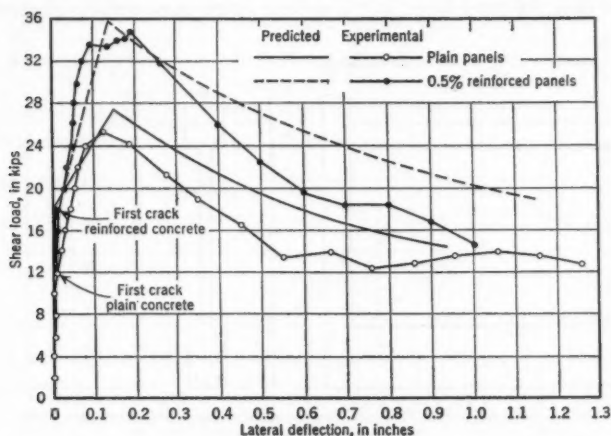


FIG. 2.—TYPICAL EXPERIMENTAL AND THEORETICAL CURVES FOR PLAIN AND REINFORCED PANELS

havior must fit the observed mode of failure and must agree generally with the observed load-deflection curve.

MATHEMATICAL INVESTIGATIONS

Extensive mathematical and experimental studies were made during the program. The mathematical studies were based on a simplification of the lattice analogy.^{6,7} These studies were invaluable in acquiring a basic understanding of shear-wall behavior. However, the complex procedures did not produce more accurate results than ordinary strength of materials in the prediction of general shear-wall behavior because the behavior of reinforced concrete is so variable.

⁶ "Solutions of Problems of Elasticity by the Framework Method," by A. Hrennikoff, *Journal of Applied Mechanics*, Vol. 8, December, 1941, pp. A-169 to A-175.

⁷ "A Lattice Analogy for the Solution of Stress Problems," by Douglas McHenry, *Journal, Inst. C. E.*, Vol. 21, No. 2, December, 1943, pp. 59-82.

Although it is not elastic in behavior, the load-deflection curve is essentially linear as far as some point close to the formation of the first crack. The cracked behavior can be approximated by lattice-analogy solutions if crack locations are assumed. Mounted on the wall panels were SR-4 rosettes, and SR-4 A-7 gages were mounted on the column steel of several model walls. The results neither proved nor disproved mathematical studies. The difficulty is that the panel concrete cracks at a very low stress, and as soon as the panel is cracked the rosette gages have little value. The strains to be measured before cracking are small. Three or four points on a load-strain curve are obtained before the wall cracks, and the probable error in any single reading is of the same order of magnitude as the difference in strains between the load points. Gages mounted on the column steel were of value only after extensive cracking had taken place provided that the bond failed in the vicinity of the gage without rupturing the

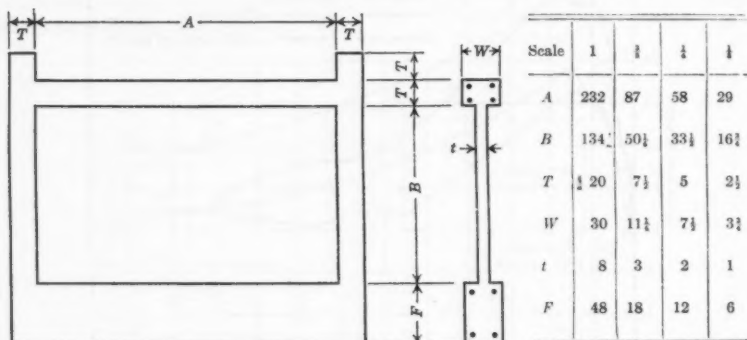


FIG. 3.—SCALE-EFFECT MODELS. REINFORCING USED IN SPECIMENS WITH REINFORCED PANELS-0.5%

leads. Therefore, intensive mathematical studies were instructive but inconclusive.

SCALE EFFECT

The first problem in any study using models is to determine if a scale effect is involved because areas scale differently from moments of inertia. Will a quarter-scale model yield results that are consistent with the prototype? A series of reinforced concrete walls, ranging from a scale of from one-eighth to three-eighths, was tested. Full scale was assumed as an 8-ft-high-by-12-ft-long wall with an 8-in.-thick panel. All walls were proportioned on a purely geometric basis. The testing-machine capacity limited the largest specimen to a three-eighths scale.

No scale effect was observed from these tests. If such an effect was present it was hidden by the general scatter of results. The model details are shown in Fig. 3, and load-deflection curves transformed to full-scale values are indicated in Fig. 4. The one-eighth-scale models were cracked before testing began as a result of shrinkage stresses in the thin panels.

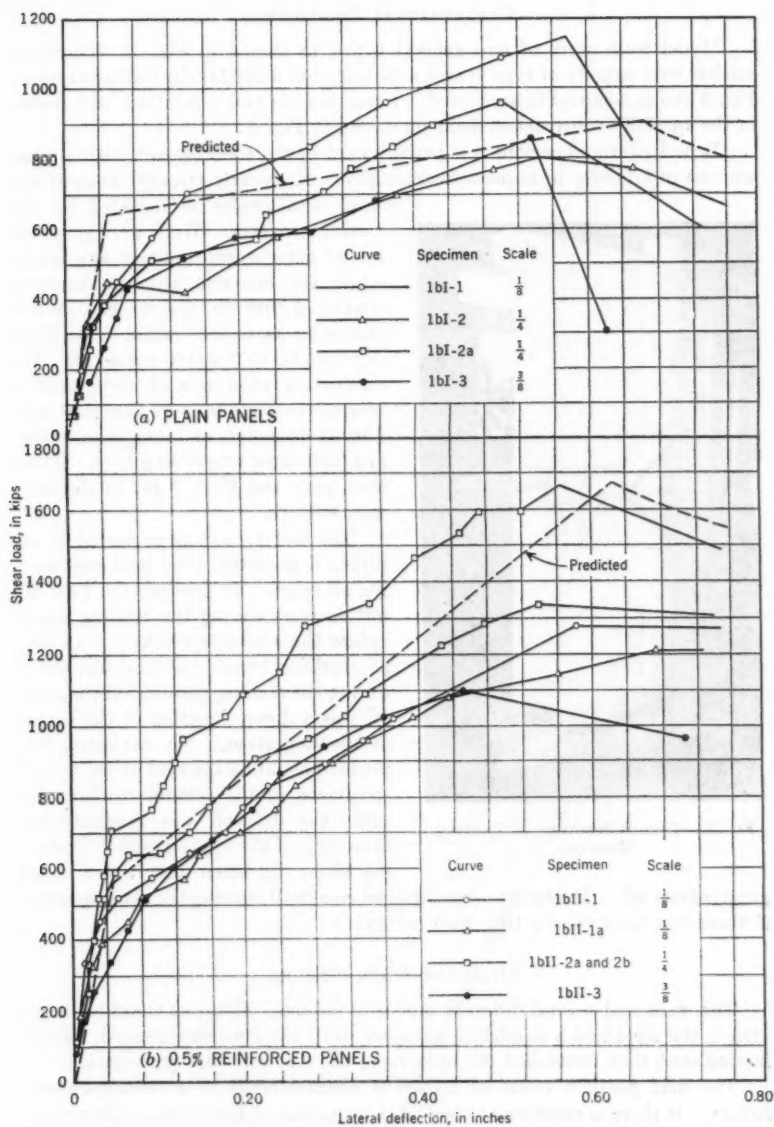


FIG. 4.—LOAD-DEFLECTION CURVES FOR PROTOTYPE

EXPERIMENTAL PROCEDURES

Model walls were of two general types, as shown in Fig. 1. The small models were usually of type B and were tested in a 200,000-lb testing machine. Fig. 5 shows a model being tested. Large models and assemblies were tested in the specially constructed shear jig shown in Fig. 6.

Type I portland cement was usually used in the concrete mix with a small amount of additive to improve workability. High-early-strength cement was

used occasionally as dictated by the testing program. Walls were generally tested after approximately two weeks when the concrete strength approximated 3,000 lb per sq in. Actual strengths as tested varied from 2,300 lb per sq in. to 3,800 lb per sq in. The reinforcing steel was of structural or intermediate grade. All bars that were $\frac{3}{8}$ in. in diameter, or more, were standard, deformed reinforcing bars. Those that were less than $\frac{3}{8}$ in. in diameter were smooth.

The test procedure consisted of applying a predetermined load and reading all gages. In general, the load did not decrease during the reading period before the concrete cracked. As soon as cracking began the load decreased during the reading period, and the drop-off was a direct function of the degree of disintegration. No attempt was made to maintain the load on the type B specimens in the testing machine because the drop-off was generally less than 10% of the applied load. Tests in the shear jig often involved a much

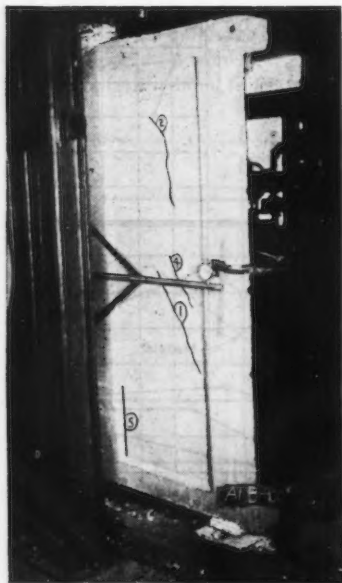


FIG. 5.—TYPE B SPECIMEN IN TESTING MACHINE

greater drop-off. The load was maintained essentially during the reading period if there was more than a 10% load reduction.

MODES OF WALL FAILURE

The walls had several different modes of failure. As far as could be determined, the steel had a negligible influence until the concrete cracked. Reinforcing steel then controlled the opening of the crack and its propagation.

The first possible mode of failure is characterized as a tension-column failure. If there is insufficient steel at the junction of the tension column and the foundation to take up the load when the concrete cracks, the crack opens and rapidly runs along the junction of the panel and the foundation to the compression column, as shown for specimens C-3 and 3A2-4 in Figs. 7 and 8.

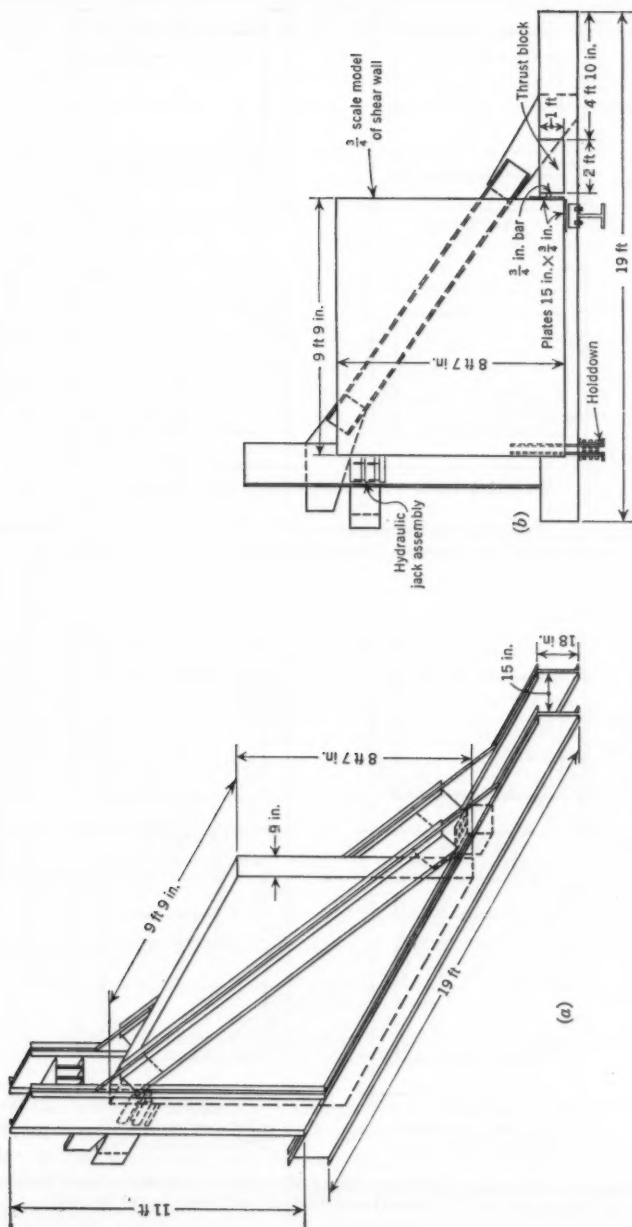


FIG. 6.—TYPE C SPECIMEN IN 300-KIP SHEAR JIG

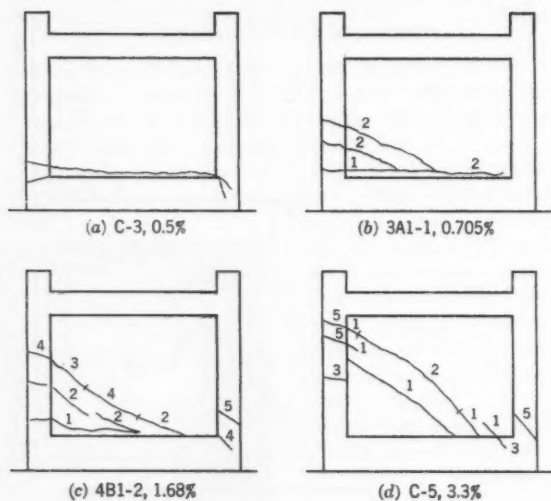


FIG. 7.—CRACKING PATTERNS FOR UNREINFORCED WALL PANELS WITH VARIED PERCENTAGES OF STEEL IN THE COLUMNS (LOAD APPLIED AT UPPER LEFT CORNER)

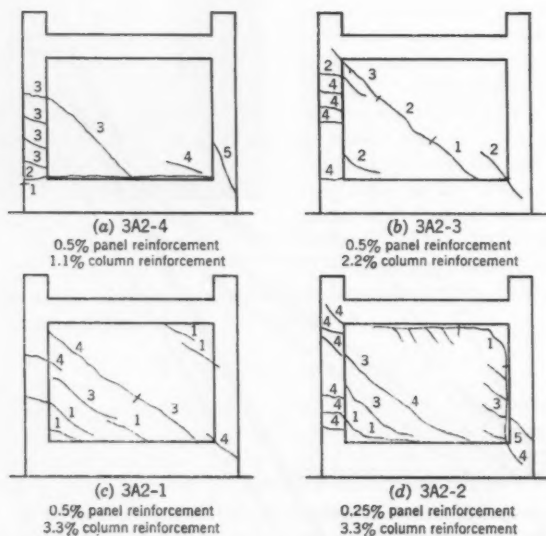


FIG. 8.—CRACKING PATTERNS FOR REINFORCED WALL PANELS WITH VARIED PERCENTAGES OF STEEL IN THE COLUMNS (LOAD APPLIED AT UPPER LEFT CORNER)

If first cracking in the tension column does not stress the tensile-column steel to the yield point, this crack may occur, but it does not open up and is difficult to see by visual inspection.

The second possible mode of failure involves the panel cracking diagonally in the tensile-stress region. If the panel is unreinforced or lightly reinforced,

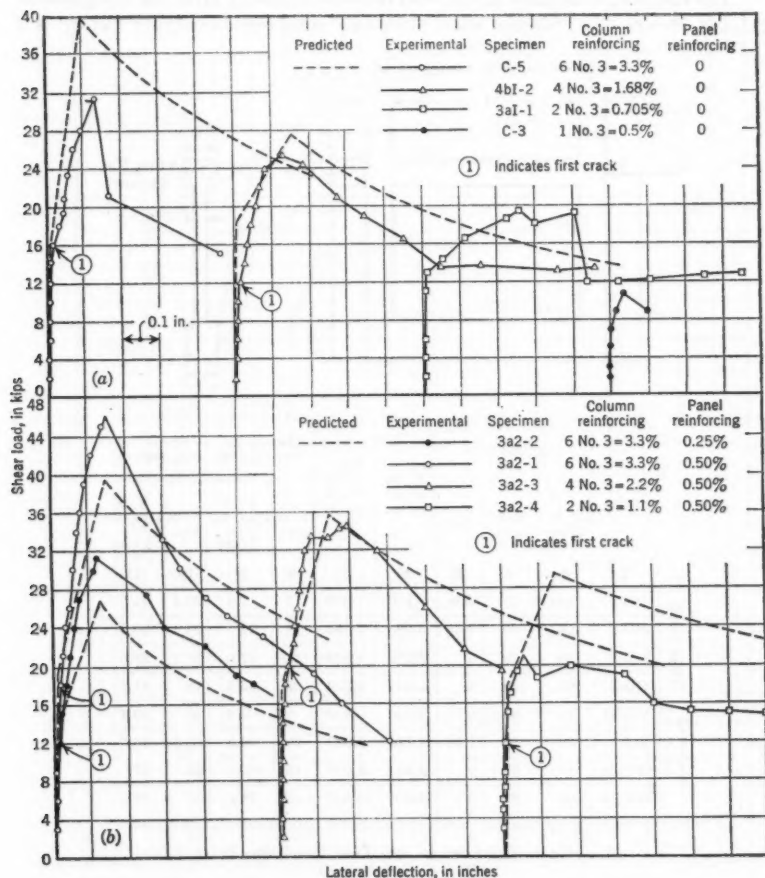
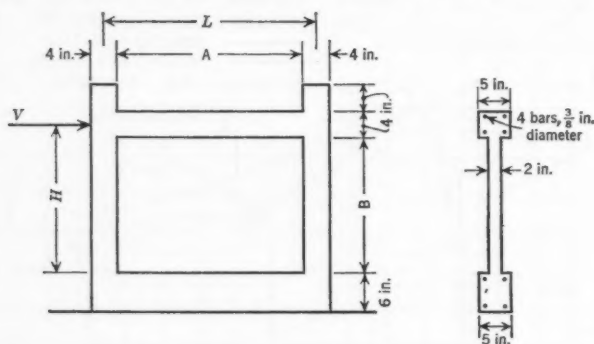


FIG. 9.—EFFECT OF COLUMN-STEEL VARIATION ON LOAD-DEFLECTION CURVES—
COLUMN AREA HELD CONSTANT, TYPE B SPECIMENS

the cracking follows the patterns shown in Fig. 7 and depends on the quantity of column steel. With unreinforced panels the first panel crack spreads rapidly to the foundation and tension column. An additional increase in shear load then produces cracks along the foundation to the compression col-

umn and along the tension column to the beam. The first break in the load-deflection curve occurs approximately at this load (Fig. 9). The shear load will increase further with more and more panel cracking until the compression column cracks at the foundation and finally shears off. Ultimate load occurs at this stage.

The shearing resistance of the wall decreases rapidly after the compression column shears off. Studies show that this compression-column failure is a



	Specimen	PROPORTIONS			f'_c , in lb per sq in.	Ratio V/Δ below cracking	SHEAR AT 1ST CRACK		SHEAR AT ULTIMATE	
		A, in inches	B, in inches	L/H			V , in kips	V , in kips, for $f'_c = 3,000$	V , in kips	V , in kips, for $f'_c = 3,000$
Plain panel	4BI-1	16	20	0.9	2,850	650	7	7.4	20.4	21.5
	4BI-2	28	20	1.45	3,290	2,080	12	11	25.3	23.2
	4BI-3	40	20	2	3,260	3,800	19.2	17.6	31.2	28.6
	4BI-4	62	20	3	3,500	4,200	39	33.5	48	41.2
Reinforced panel	4BII-1	16	20	0.9	2,920	590	9	9.3	20	20.4
	3A2-3	28	20	1.45	3,120	2,000	20	19.2	34.8	33.5
	4BII-3	40	20	2	2,830	2,000	15	15.9	45.3	47
	4BII-4	62	20	3	3,830	2,600	45	35.2	66	51.6

FIG. 10.—MODEL DIMENSIONS AND TEST RESULTS—WALL PANEL PROPORTION SERIES

function of the steel area, the concrete strength, and the panel proportions. The concrete area is unimportant as long as the bars are covered adequately. The failure mechanism apparently involves a cracking of the concrete at such an angle that friction is unimportant. Actual failure then occurs when the concrete around the bars is crushed at the crack line and the bars bend.

If the panel is moderately reinforced ($p \geq 0.0025$, in which p is the steel-to-concrete ratio) the failure mode is modified as a function of the amount of panel

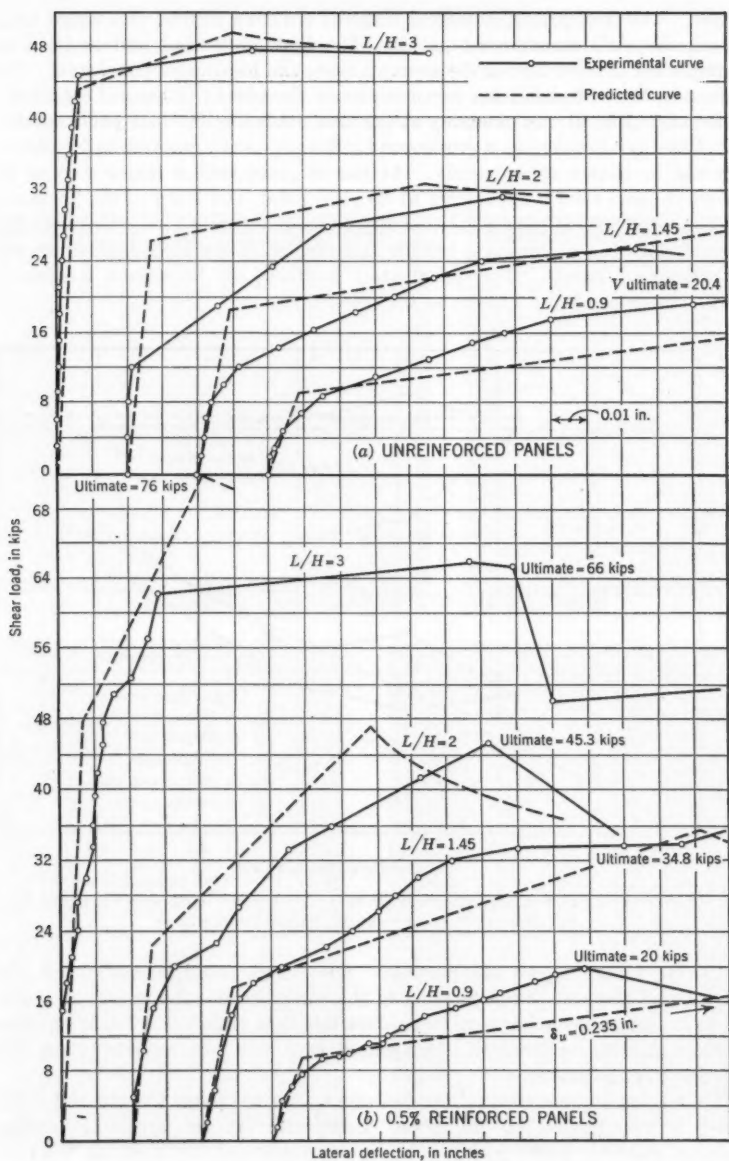


FIG. 11.—LOAD-DEFLECTION COMPARISONS—WALL PANEL PROPORTION SERIES

steel. The steel produces general diagonal cracking instead of a single major crack, as with unreinforced panels. The first crack load and location are completely independent of the amount, type, and location of panel steel. The break in the load-deflection curve occurs at the advent of general cracking in the panel (Fig. 9), not generally at the load producing the first panel crack.

Panel reinforcing has a pronounced influence on the cracked-wall behavior, as will be shown subsequently. At the ultimate load a major part of the vertical panel steel is apparently at its yield point, and a few of the horizontal bars are in the post-yield condition approaching actual failure. Ultimate load occurs with the compression column shearing off in the same manner as with unreinforced panels. The panel steel produces an important increase in ultimate strength and rigidity in the cracked region.

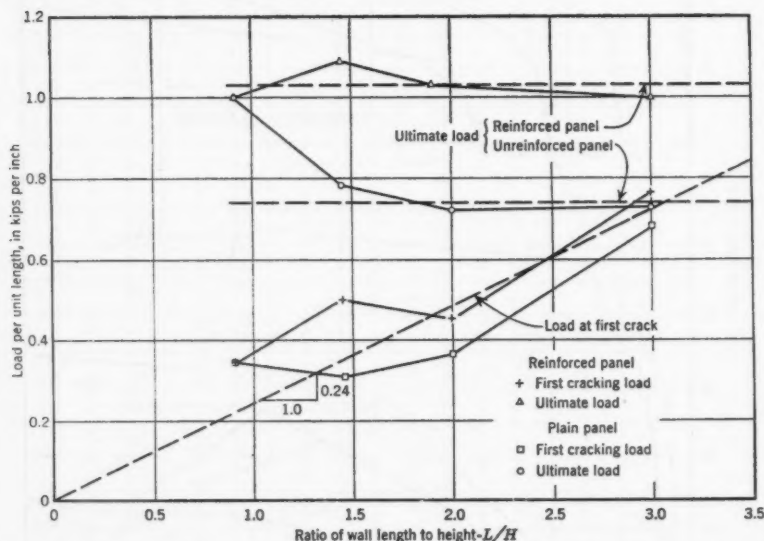


FIG. 12.—SHEAR LOAD PER UNIT LENGTH OF WALL AT FIRST CRACK AND ULTIMATE LOAD FOR SPECIMENS WITH VARYING PANEL PROPORTIONS

Other failure modes are possible. The failure could be associated with high panel cracking and a bending of the compression column. Some variations in panel reinforcing tend to produce this type of failure. No appreciable change in ultimate strength is associated with this failure mode unless it is carried to an extreme.

A tension-column steel failure can occur after the panel has cracked if this steel is overstressed at any time. Composite failures involving tension-column yielding, panel cracking, and compression-column shearing were observed in a few isolated cases. The tension-column influence was apparently small in the composite failures noted.

INFLUENCE OF PANEL VARIATIONS

The panel proportions (length, L , height, H , and thickness, t) and the panel reinforcing directly influence the cracking load of the shear walls. The rigidity is influenced indirectly because it is dependent on the moment of inertia of the section. The panel thickness is only of importance with uncracked panels.

The length-to-height ratio (L/H) has a direct and pronounced influence. This problem was studied using unreinforced and reinforced walls. The test

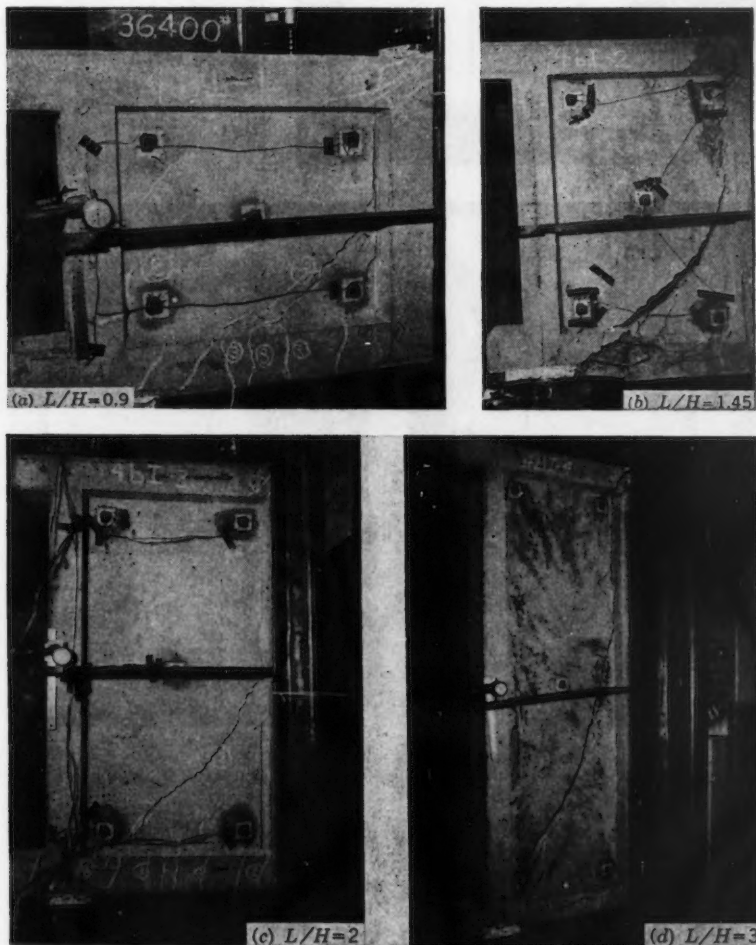


FIG. 13.—EFFECT OF LENGTH-TO-HEIGHT RATIO ON SHEAR WALLS; CRACKS NUMBERED IN ORDER OF OCCURRENCE—PLAIN PANELS

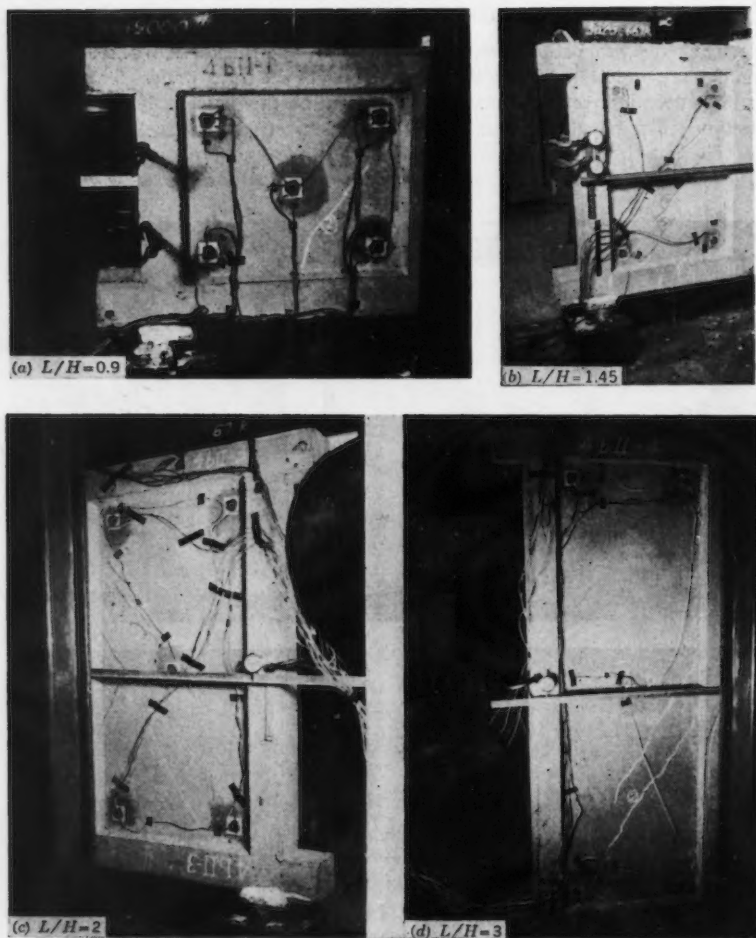


FIG. 14.—EFFECT OF LENGTH-TO-HEIGHT RATIO ON SHEAR WALLS; CRACKS NUMBERED IN ORDER OF OCCURRENCE—PANEL REINFORCING, 0.5%

results are given in Figs. 10 to 12, inclusive, and photographs are shown in Figs. 13 and 14.

A study of the load-deflection curves discloses that as L/H increases, the load at first crack, or the load at a major break in the load-deflection curve, approaches the ultimate load. For the tested specimens the two loads agree approximately at an (L/H) -ratio of 3 with unreinforced panels, and they agree approximately at 4 for the reinforced walls. The crack pattern changes

as the (L/H) -ratio increases. The cracks become progressively higher in the wall, finally approaching a pure diagonal crack.

The quantity and placement of panel reinforcing can be varied. In one series the steel ratio, p , was varied from 0 to 0.015, both horizontally and vertically. Results are shown by the load-deflection curves in Fig. 15 and in the photographs in Fig. 16. All walls have essentially the same behavior before cracking. Panel reinforcing is effective only after cracking begins. As the panel reinforcing increases, the number of cracks before the ultimate load increases and the individual width of each crack decreases.

Variations in panel-steel placement were studied in order to obtain the most efficient reinforcement system. Once again complex mathematical studies were completely ineffective. The first investigation was made with diagonal reinforcing as contrasted with the conventional type that is parallel to the sides of the panel. The diagonal reinforcing was varied from that which was dis-

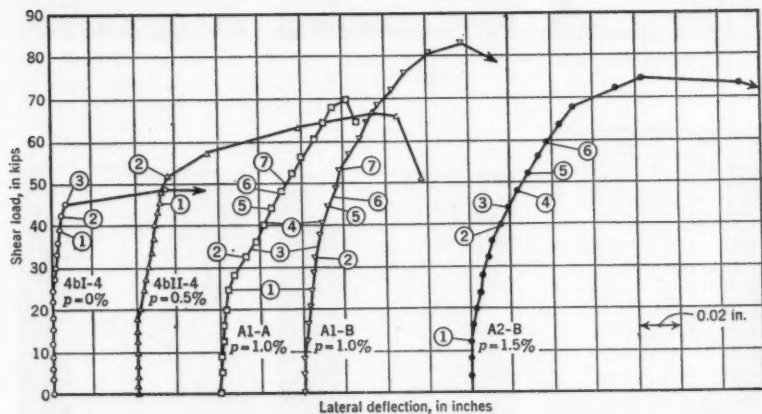


FIG. 15.—LOAD-DEFLECTION CURVES FOR WALLS WITH VARYING STEEL RATIOS

tributed uniformly to bands concentrated at the diagonals. Also, steel was concentrated at the diagonals, and special corner reinforcing was added in regions of highest stress. Specimen details are given in Fig. 17, and load-deflection curves are indicated in Fig. 18. The total quantity of steel in the panel was kept as nearly constant as possible. In every case the diagonal reinforcing was less effective than rectangular reinforcing. Special corner steel was ineffective in improving wall characteristics. Heavy concentrations of steel on the panel diagonals produced large shrinkage cracks along the panel diagonals and decreased the wall rigidity.

The possibility of adding special steel to a conventional rectangular pattern was investigated next. The four tested specimens are shown in Fig. 19. Specimens VR-1 and VR-4 doubled normal steel in the regions of highest stress. Specimens VR-2 and VR-5 were reinforced to control the crack pattern by

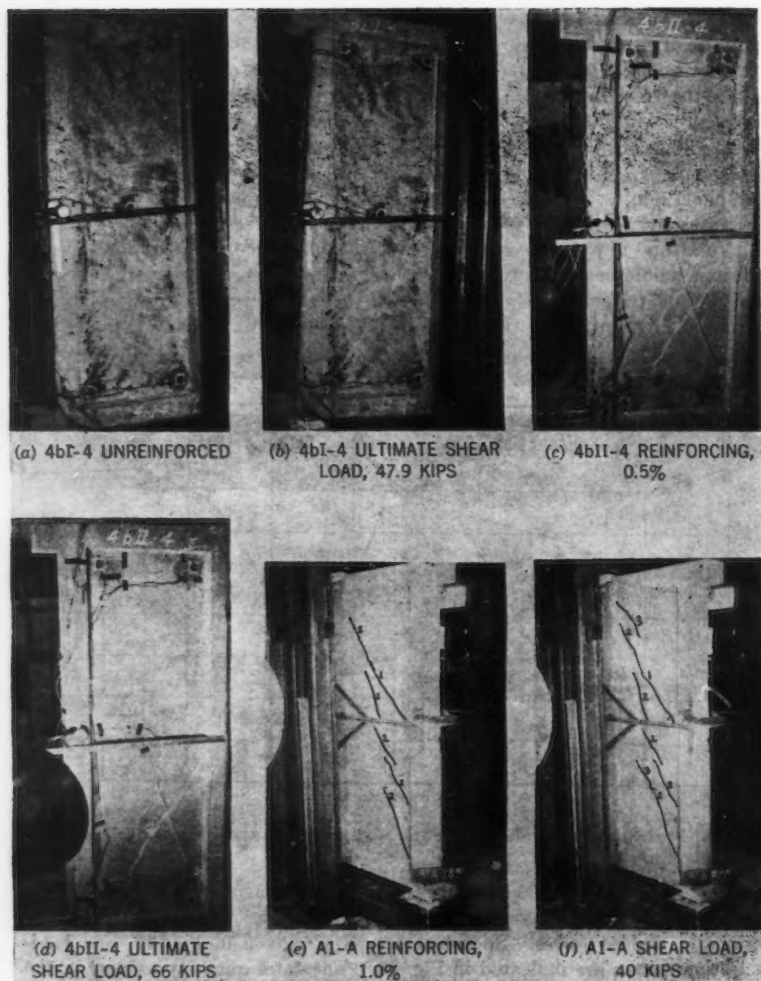


FIG. 16.—WALLS USED TO STUDY THE EFFECT OF VARYING THE PANEL REINFORCING

doubling the steel in the central section of the panel, thereby tending to force the cracks low in the panel. However, the progressive crack patterns were different in only a minor way, and the final patterns and load-deflection curves were essentially identical.

Conventional rectangular bar patterns have the same bar spacing and size horizontally and vertically. Three specimens were tested to determine the

relative effectiveness of horizontal and vertical reinforcing. The bar arrangements are shown in Fig. 20. The load-deflection curves are shown in Fig. 21, and the crack-pattern development is shown in Figs. 22 to 25, inclusive (VRR-1

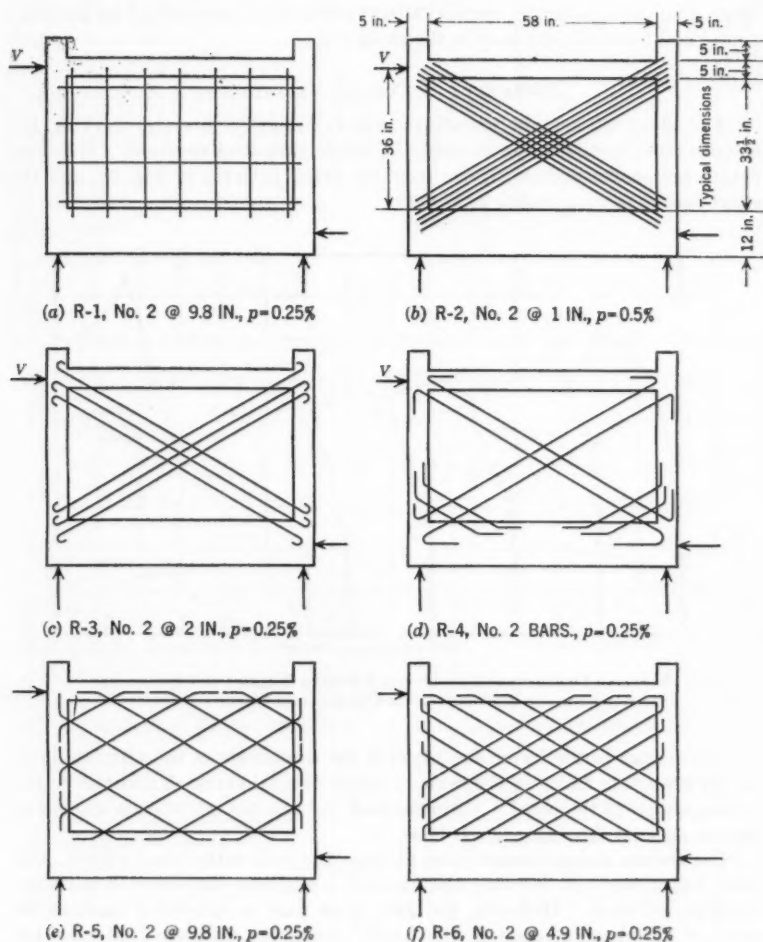


FIG. 17.—DETAILS OF R-SERIES WALLS

was a control panel with two-way reinforcing). The tests demonstrate that the vertical steel is much more effective than the horizontal steel. In fact, vertical steel by itself is fully as effective as vertical steel plus horizontal steel. Specimen VRR-7 (Fig. 26) was tested as a possible practical application of this

study. Horizontal steel was widely spaced in the upper three-fourths of the wall. Some horizontal steel is desirable to control the cracking of the concrete. The test results (Fig. 21) show that this wall has the same characteristics as one with conventional rectangular reinforcing. If a comparison with beam-shear reinforcing is made, vertical stirrups in a beam correspond to the horizontal and least efficient bars in the shear wall.

INFLUENCE OF COLUMN VARIATIONS

The effect of column variations was investigated first by varying the column cross section while keeping the reinforcing steel constant. Specimen details are shown in Fig. 27, the resulting crack patterns in Fig. 28, and the shear load-deflection curves in Fig. 29.

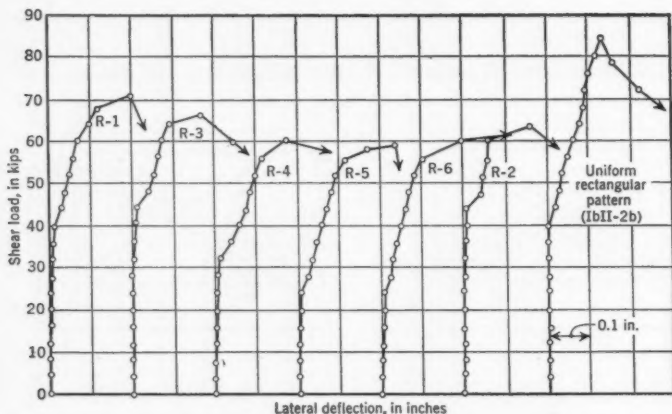


FIG. 18.—LOAD-DEFLECTION CURVES FOR R-SERIES WALLS AND COMPARABLE RECTANGULARLY REINFORCED WALLS

The change in the frame size affected the magnitude of the ultimate load, but all specimens failed in the same manner. Initial cracking occurred in the tension corner of the panel. Ultimate load was reached when the compression column sheared through near its base.

The results appear inconsistent because the wall with 5-in.-by-7½-in. columns had higher first cracking and ultimate loads than the one with the 5-in.-by-12-in. columns. However, the first crack load is somewhat random because of shrinkage stresses in the panel. Also, the ultimate load may not increase with column size because of a tendency for the wall to punch through the wider member. This fact was shown to be correct when columns were replaced with face walls. The shear panel punched through the compression-face wall. Hence, it is quite possible that there is an optimum column width for ultimate load although these tests are not sufficiently comprehensive to prove it.

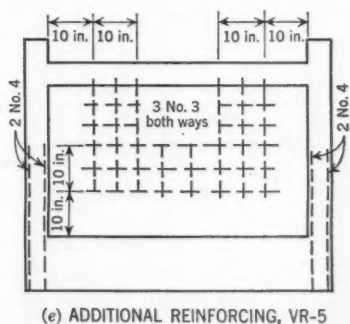
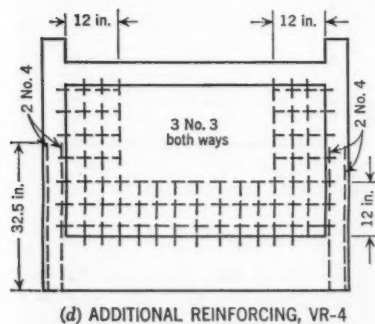
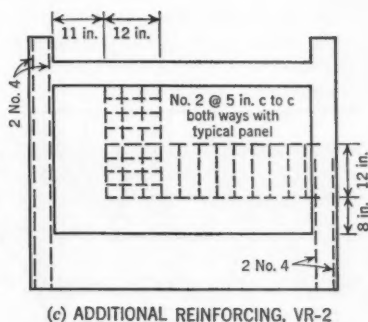
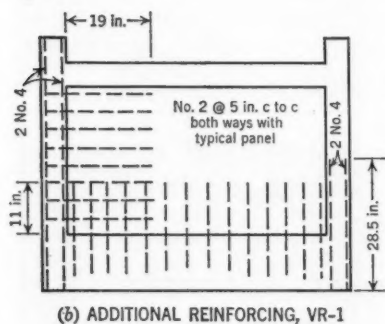
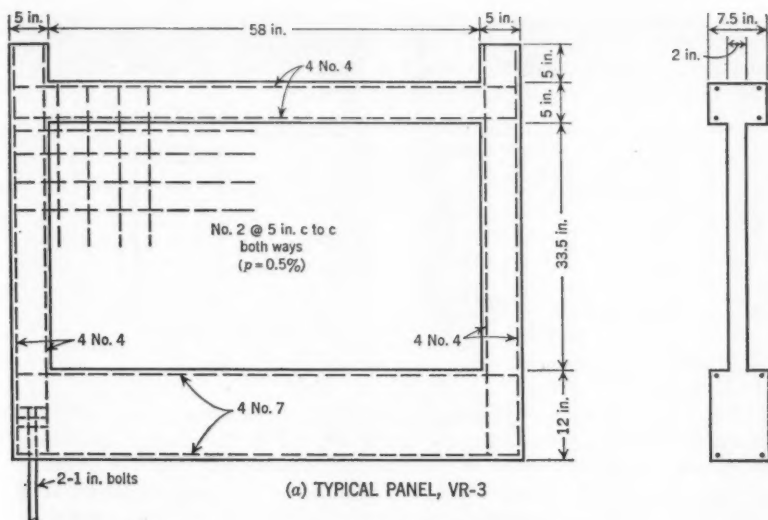


FIG. 19.—DETAILS OF VR-SERIES WALLS

A second investigation varied the frame reinforcing while the concrete cross section remained constant. The specimens had 4-in.-by-5-in. columns and 20-in.-by-28-in. panels that were 2 in. thick. The panel had no reinforcing for one series and nominal reinforcing for the other.

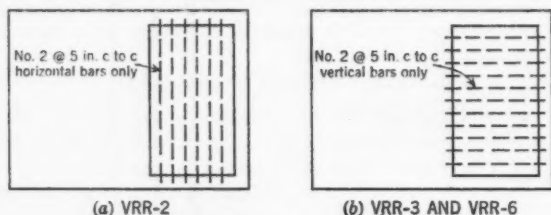


FIG. 20.—DETAILS OF VRR-SERIES WALLS

The results are shown by the curves in Fig. 9 and are summarized in Fig. 30. Crack patterns are given in Figs. 7 and 8 and in Fig. 31. It is evident that additional column steel is quite effective in increasing not only the ultimate strength, but also the energy-absorption capacity of the specimen as indicated by the area under the complete load-deflection curve. It has been noted that brick-walled bents also can be effective in this respect if the frame is strong.

Fig. 30 shows that added column steel has a nominal effect only on the first-crack load.

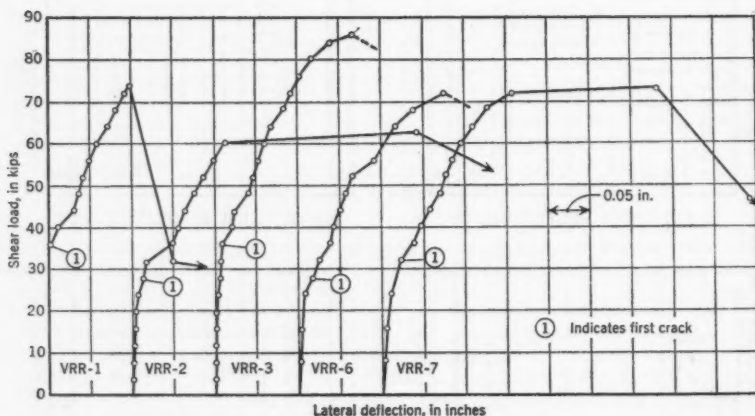


FIG. 21.—LOAD-DEFLECTION CURVES FOR VRR-SERIES WALLS

PREDICTION OF WALL BEHAVIOR

Notation.—The letter symbols adopted for use in this paper are defined where they first appear and are arranged alphabetically for convenience of reference in the Appendix.



FIG. 22.—CRACK FORMATION OF SPECIMEN VRR-1

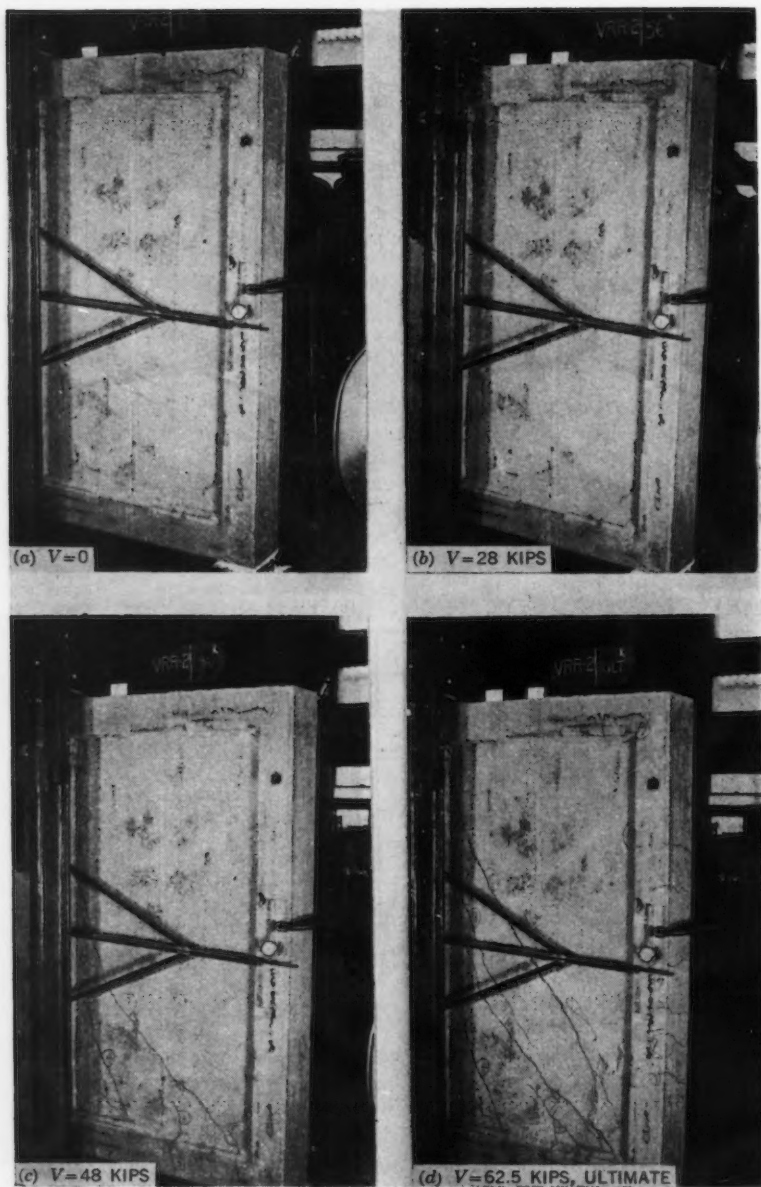


FIG. 23.—CRACK FORMATION OF SPECIMEN VRR-2

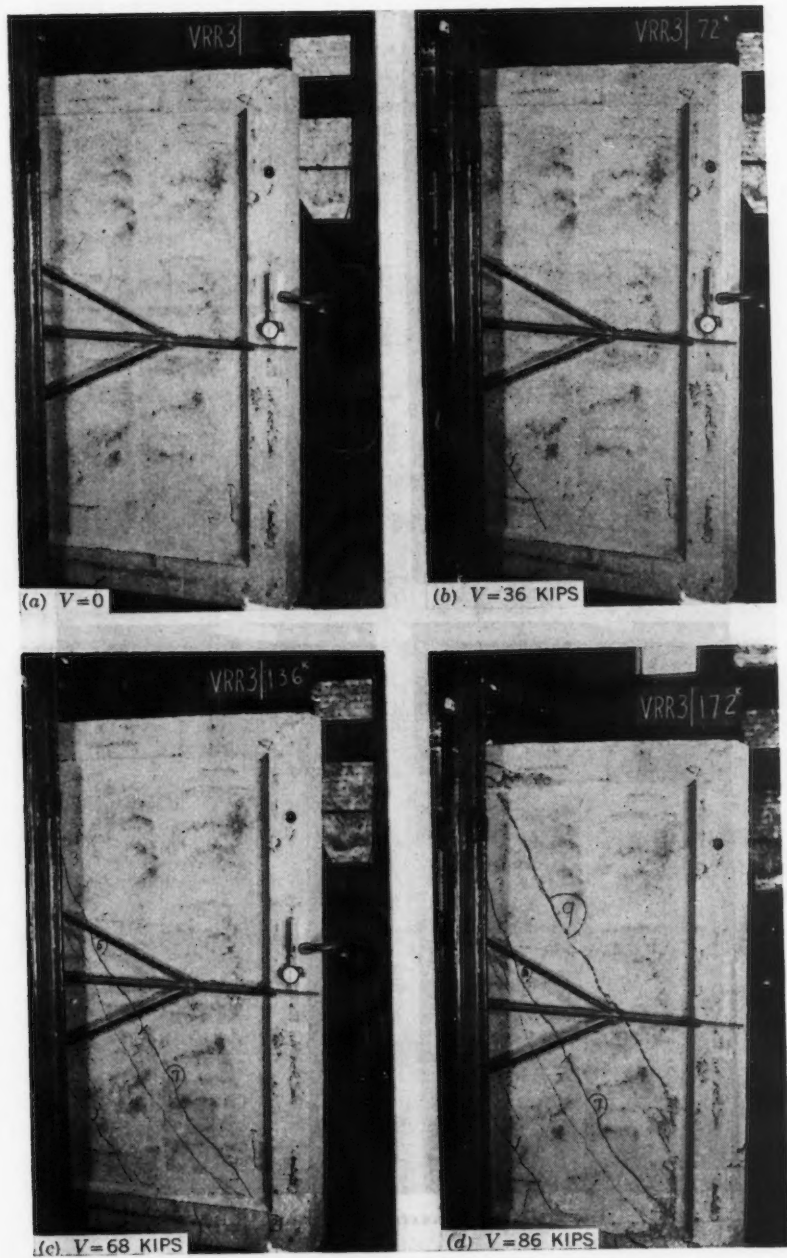


FIG. 24.—CRACK FORMATION OF SPECIMEN VRR-3

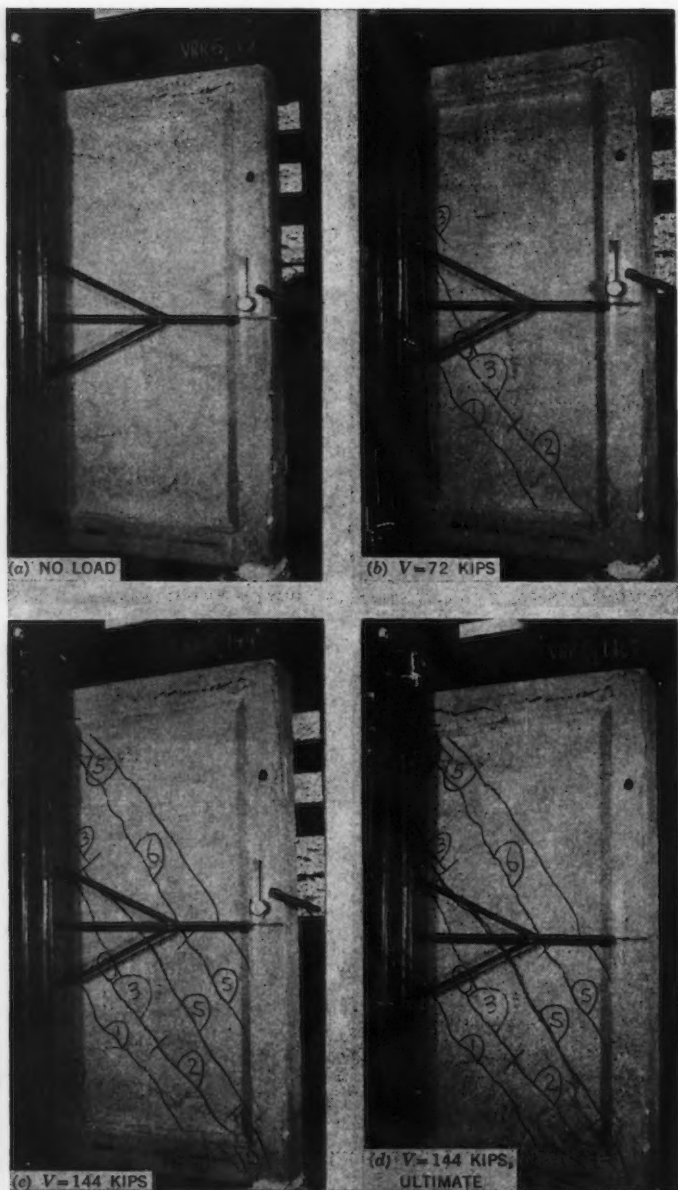


FIG. 25.—CRACK FORMATION OF SPECIMEN VRR-6

General.—Shear-wall deflections are proportional to the applied load until the panel cracks. This deflection is not necessarily elastic because of plastic flow and minor shrinkage cracking. The linear relationship cannot be predicted with any certainty. Although numerous studies were made involving exact mathematical procedures, the results were no better or more reliable than the most elementary procedures of strength of materials.

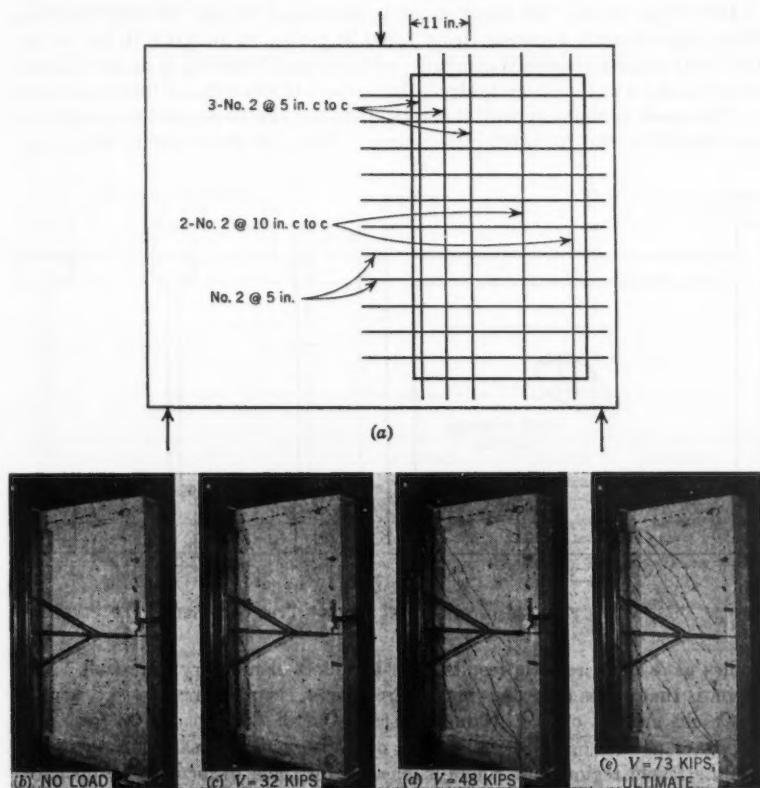


FIG. 26.—REINFORCING DETAILS AND CRACK FORMATION OF SPECIMEN VRR-7

The following formula is recommended:

$$\delta = V \left(\frac{H}{AG} + \frac{H^3}{3EI} \right) \dots \dots \dots (1)$$

in which δ is the wall deflection; V represents wall shear; H indicates the wall height from the foundation to the center of the loading beams; A denotes the

area of the wall-panel cross section, neglecting steel and columns; I is the moment of inertia of the entire cross section, including columns but neglecting steel; $G = E/2.2$; and E is equal to from 2,000,000 lb per sq in. to 2,600,000 lb per sq in. for concrete strengths of between 2,000 lb per sq in. and 4,000 lb per sq in.

The linear part of the load-deflection curve is a function of concrete strength beyond that reflected in the modulus of elasticity. With low-strength concrete (2,000 lb per sq in.) the linear range is shortened because of early cracking. With high-strength concrete (from 3,500 lb per sq in. to 4,000 lb per sq in.) the linear range is increased generally, with the wall behaving in an increasingly brittle manner as the concrete strength increases to more than 3,000 lb per sq in.

The most complex type of theoretical studies can be applied to predict the first break in the load-deflection curve. None of these highly theoretical

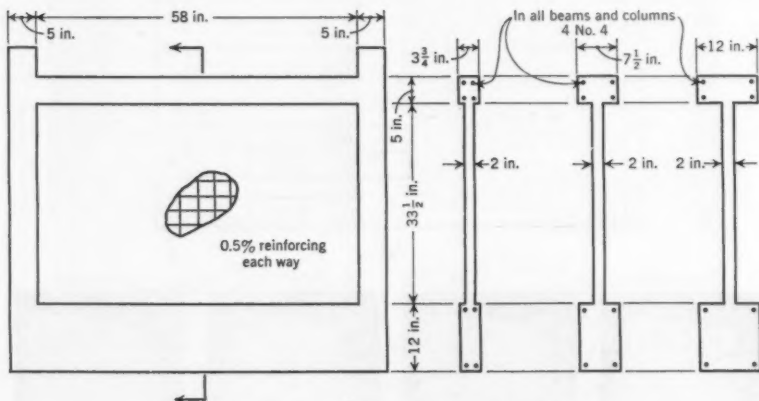


FIG. 27.—FRAME VARIATIONS SERIES—TYPE C MODELS

studies gave more reliable results than the most elementary approach. The reason is that stress only does not control the crack pattern.

Cracks are not only a product of stress but of the capacity to form and propagate as well. Thus, cracks are not observed necessarily in the most highly stressed regions but where it is easier for them to form and propagate. The average shear stress is recommended as an index of the first break in the load-deflection curve. Thus,

$$V_e = 0.1 f'_c A \dots \dots \dots (2)$$

in which V_e is the load at first break in the load-deflection curve; $0.1 f'_c$ represents the approximate tensile strength of the concrete; and A denotes the area of the panel section, neglecting steel and columns.

With certain specimens, other approaches have proved to be more valid. The probable prediction error is so great that only the simplest formulas are

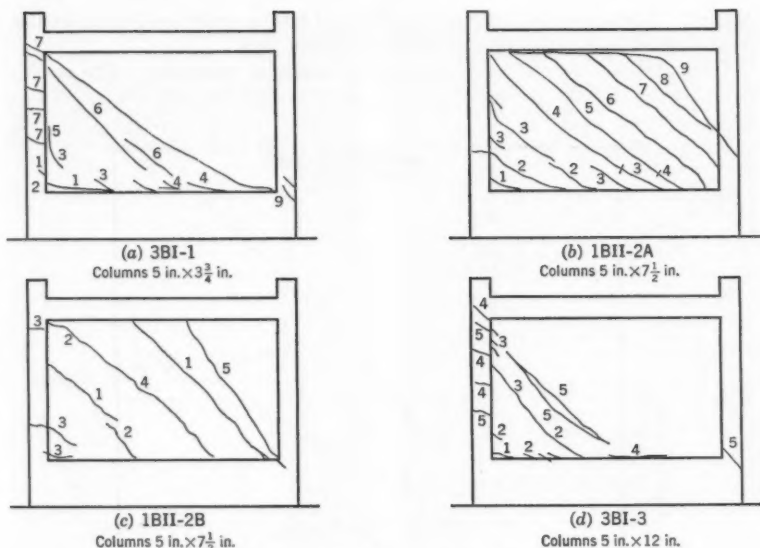


FIG. 28.—CRACK PATTERNS FOR SPECIMENS WITH VARIED COLUMN SIZE

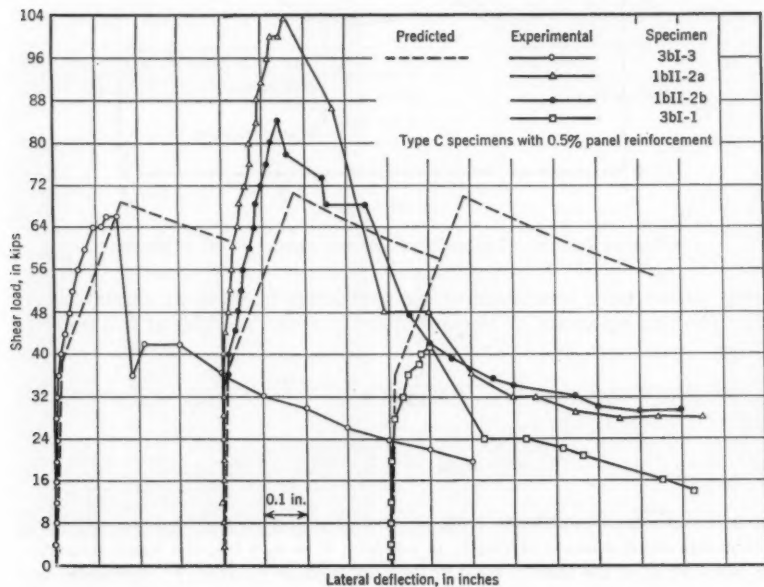


FIG. 29.—EFFECT OF VARIED COLUMN SIZE ON LOAD-DEFLECTION CURVES

justified. These approximations yield the best results under conditions similar to those most commonly used in building construction.

Ultimate load and deflection are highly statistical quantities. The results are influenced by the particular testing machine and test procedure. Num-

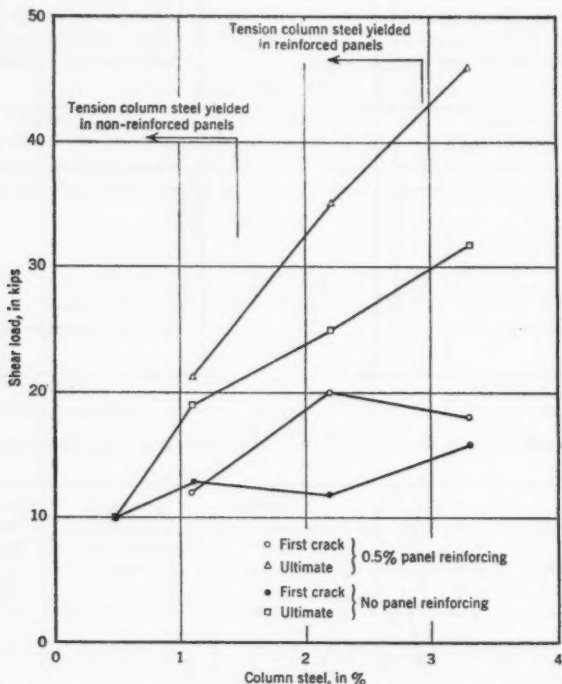


FIG. 30.—RESULTS—COLUMN STEEL EFFECT SERIES—TYPE B MODELS

erous studies have been made of the parameters involved at ultimate load. The following equations are the best approximations available at this time:

$$V_u = \frac{0.1}{P/C + 0.1} C + 2.2 P \dots \dots \dots (3)$$

and

$$\delta_u = 24 \left(\frac{H}{L} \right)^2 \delta_c \dots \dots \dots (4)$$

in which V_u is the ultimate load, in pounds; $C = A_s f_c' [15 + 1.9 (L/H)^2]$, the compression-column strength, in pounds; $P = \sigma_v p t L$, the panel strength, in pounds; A_s is the area of steel in the compression column; f_c' represents the concrete compression strength; L is the wall length, center to center of the

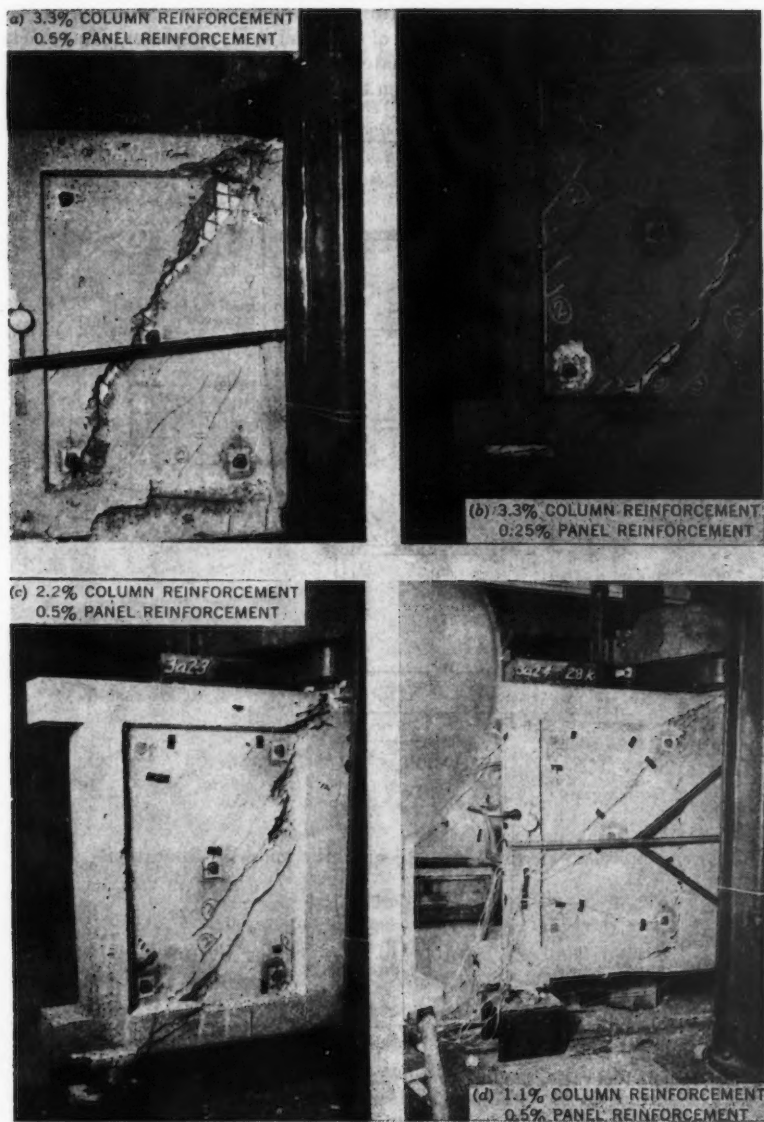


FIG. 31.—FRAME-EFFECT SERIES WITH VARIED COLUMN REINFORCEMENT

columns; H denotes the wall height, from the foundation to the center of the distributing beam; σ_y is the yield point of the panel steel; p represents the panel-steel ratio; δ_u is the deflection at ultimate load; and δ_c denotes the deflection at break in the load-deflection curve when the wall shear equals V_c .

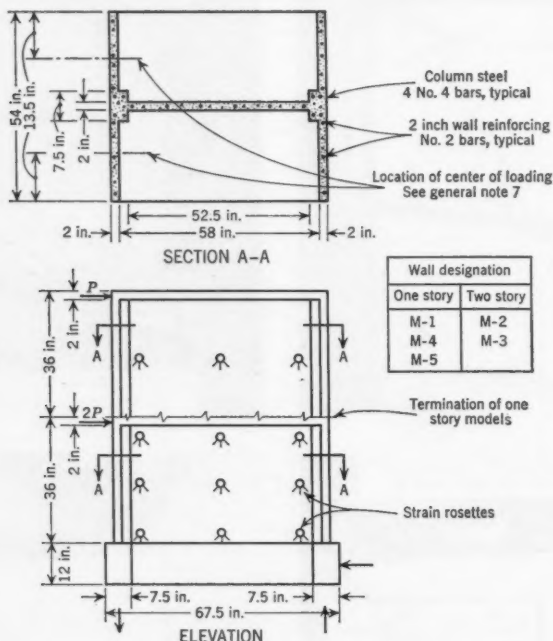


FIG. 32.—DETAILS OF M-SERIES WALLS

These empirical equations are subject to the following limitations:

1. Column steel—from 1% to 3.3%;
2. Column steel—adequately encased in concrete;
3. Concrete strength—from 2,000 lb per sq in. to 4,000 per sq in.;
4. Length-to-height ratio, L/H —0.9 to 3.0;
5. Ratio, P/C —0 to 3.26;
6. Yield point of the panel steel, σ_y —from 42 kips per sq in. to 52 kips per sq in.; and
7. Panel-steel ratio, p —0% to 1.5%.

The post-ultimate curves shown in the figures were simply sketched in to provide a curve similar to that found experimentally. The post ultimate curve is influenced both by the testing machine and rate of loading. Strengths increase with the increase in the loading rate.

OTHER INVESTIGATIONS

The influence of possible bearing loads on wall behavior was studied. It was found that if the total bearing load was equal to or less than the total shear force, its influence on the load-deflection curve was negligible. Substantial bearing loads are necessary to change the load-deflection curves appreciably.

Five confirmatory tests were made on simple shear-wall assemblies, consisting of a shear wall, face walls, and a loading diaphragm. Wall details are

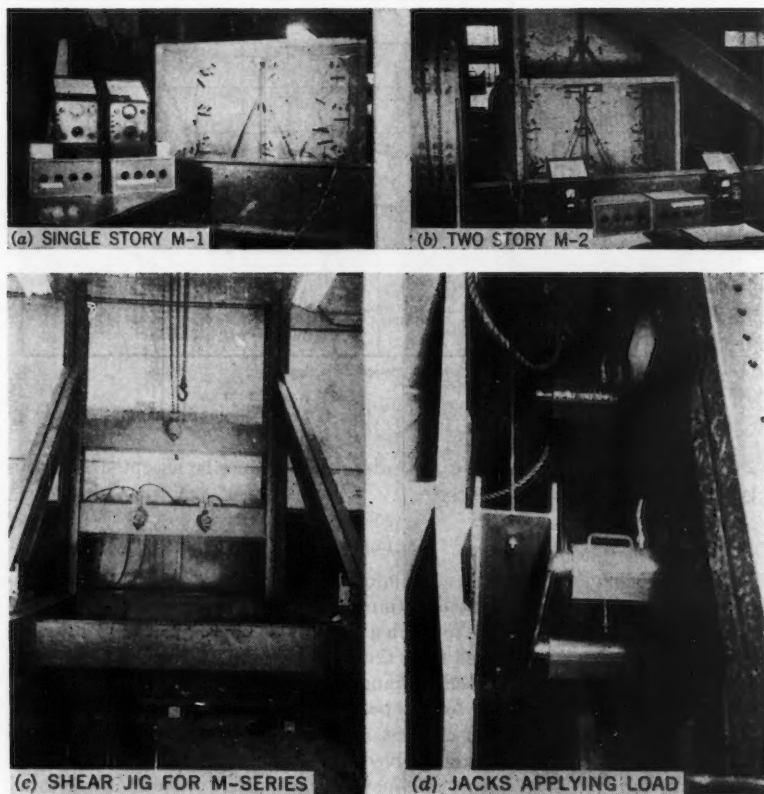


FIG. 33.—EXPERIMENTAL SET-UP FOR M-SERIES WALLS

given in Fig. 32. The shear jig was modified to test the specimens, as shown in Fig. 33. Three one-story assemblies were tested together with 2 two-story assemblies. The models were constructed as close to conventional practice as possible. They were constructed in several pours with successive pours doweled together. Shear keys were also used in specimen M-5. Loads were

applied to the diaphragm, with the first-to-second story loads being in the ratio of 2 to 1.

The load-deflection curves are given in Fig. 34, and typical cracking is seen in Fig. 35. In order to check stress distributions, SR-4 rosettes were mounted on the wall panels. However, the results were inconclusive.

The recommended formulas are influenced largely by these tests, and the futility of complex mathematical studies in such work was again demonstrated

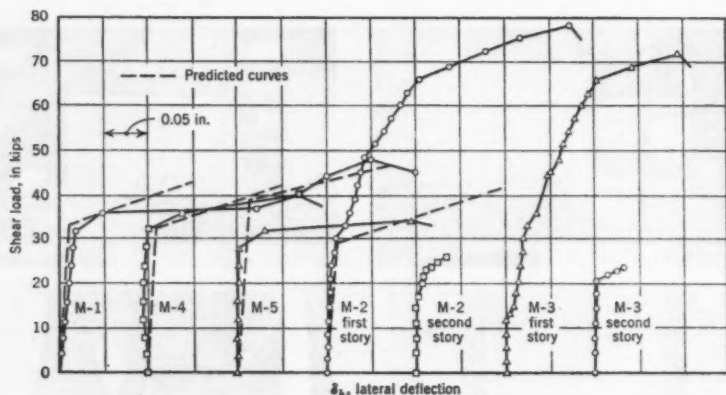


FIG. 34.—LOAD-DEFLECTION CURVES FOR M-SERIES WALLS

amply. Prediction errors of on the order of 20% must be accepted with this type of work in reinforced concrete.

CONCLUSIONS

1. The behavior of plain and reinforced concrete shear walls for single-story buildings can be predicted within acceptable design limitations. The predicted load-deflection curve for such a wall can be approximated to a reasonable degree by one straight line from the origin for the uncracked range, by a second straight line for the cracked range up to the ultimate load, and by a third somewhat indefinite line for the post-ultimate range.

2. Simple expressions from elementary strength of materials are adequate for the uncracked range. More involved methods of analysis are not justified because of the statistical nature of concrete, particularly when it is subjected to tensile stresses.

3. The prediction of the ultimate strength of a wall and the corresponding deflection appears possible only by use of empirical relationships. The suggested expressions have been revised several times during the investigations as more experimental evidence became available. Although the writers believe that the approach will give results of reasonable value in most conventional cases, future investigations may offer further improvement.

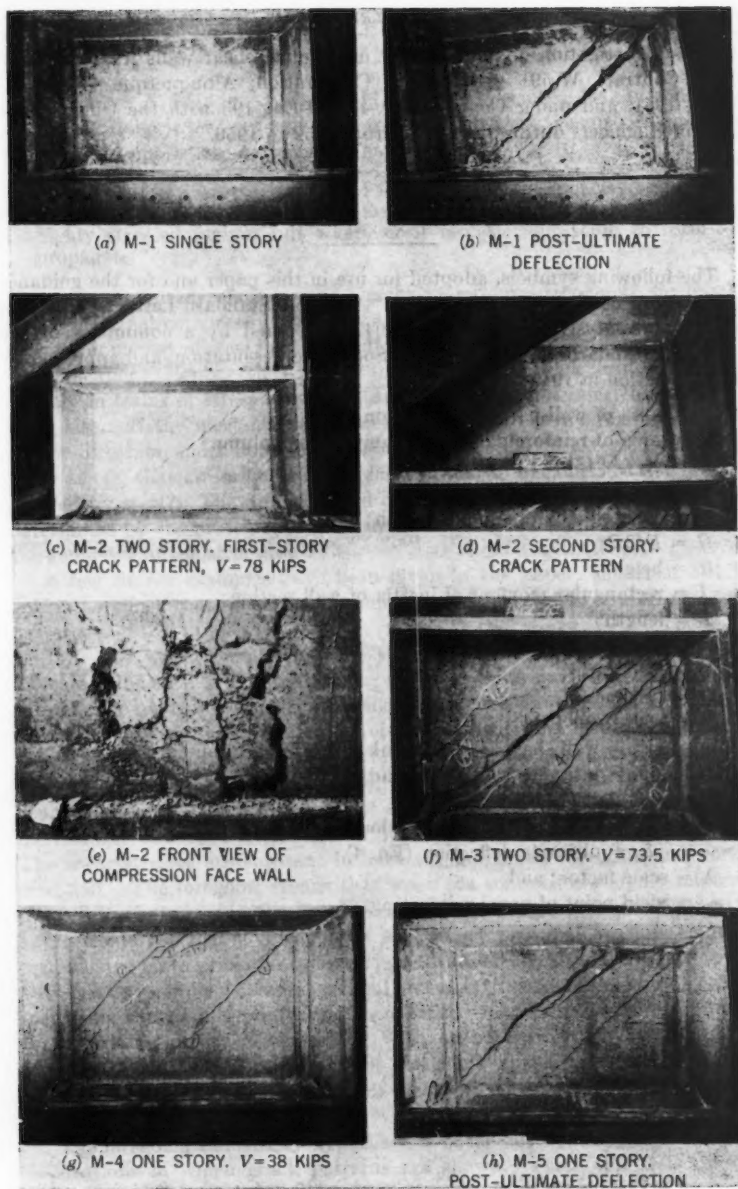


FIG. 35.—CRACK PATTERNS FOR M-SERIES WALLS

ACKNOWLEDGMENTS

This investigation of the behavior of concrete shear walls was conducted under Contract W-591 with Sandia Corporation, Albuquerque (N. Mex.) during 1951, and under Contract DA-49-129-Eng-193 with the Office of the Chief of Engineers during the period from 1952 to 1956.

APPENDIX. NOTATION

The following symbols, adopted for use in this paper and for the guidance of discussers, conform essentially with "American Standard Letter Symbols for Structural Analysis" (ASA Z10.8—1949), prepared by a committee of the American Standards Association with Society representation, and approved by the Association in 1949:

- A = area of wall-panel cross section;
- A_s = area of reinforcing steel in compression column;
- $C = A_s f_c' [15 + 1.9 (L/H)^2]$;
- E = modulus of elasticity;
- f_c' = concrete compression strength;
- $G = E/2.2$;
- H = height;
- I = rectangular moment of inertia of wall section;
- L = length;
- P = panel strength, $\sigma_y p t L$;
- p = steel ratio;
- t = thickness;
- V = wall shear load:
 - V_c = wall shear load at break in load-deflection curve;
 - V_u = ultimate wall shear load;
- δ = wall deflection:
 - δ_c = deflection at break in load-deflection curve;
 - δ_u = ultimate deflection (Eq. 4);
- λ = scale factor; and
- σ_y = yield point of panel reinforcing.

DISCUSSION

DEFOREST A. MATTESON, JR.,^{*} A.M. ASCE.—Despite a lack of conclusive strain-gage data, it seems worth while to try to interpret the authors' results in terms of principal-stress patterns. They state:

"Cracks are not only a product of stress but of the capacity to form and propagate as well. Thus, cracks are not observed necessarily in the most highly stressed regions but wherever it is easier for them to form and propagate."

This assertion needs clarification: Cracks in reinforced concrete lie parallel to the principal compressive stresses, and they occur where there is an insufficient component of steel in the direction of the principal tensile stress to prevent cracking. Hence, "the capacity to form and propagate" can be described entirely in terms of stress resistance, and one should not infer that it is anything else. If the most highly stressed regions are heavily reinforced in the proper direction, must not the first cracks then occur in a region carrying a lower stress, that stress being the highest principal tensile stress not properly resisted by steel? The direction and order of occurrence of these cracks are determined by the principal tensile stresses, the arrangement of the steel, and the geometry of the structure.

A few simple examples have been given in the paper, the most obvious being the effect that variation in column reinforcement exerts on the crack pattern.

It is the writer's understanding that as the column reinforcement was increased, the steel in the distributing beam also was increased. Because the columns are made increasingly stiff, the bending resistance of the web tends to become relatively negligible. Therefore, a theoretical condition must be approached in which shear stresses are constant across the web, including the shear stress at the juncture of the web and column. Also, as the distributing beam is stiffened, the distribution of shear between it and the web becomes increasingly uniform over its length. The limit is a web panel in pure shear. The shear stresses are constant in both the horizontal direction and vertical direction. The foregoing means that when the columns are highly reinforced the principal stresses in the panel lie at about 45° to the boundaries and are approximately constant throughout the panel, principal tension being numerically equal to principal compression. As a result, although the specimens with lightly reinforced columns will fail first near the base of the tension column, increasing the column reinforcing theoretically increases the tendency for the first crack to appear in the web. With heavily reinforced columns and a large (L/h)-ratio, the probability of the crack appearing in any particular part of the web decreases—all parts of the web tend to become indiscriminately susceptible.

The foregoing elementary hypothesis is borne out by many of the authors' illustrations in which crack patterns are shown. From this it is reasoned

^{*} Engr., Douglas Fir Plywood Assn., Tacoma, Wash.

further that web reinforcing is of little value if the columns are not heavily reinforced, but that it becomes progressively more desirable as the column reinforcing is increased. It appears also that because the principal stresses tend to lie diagonal to the web, it would be best to apply diagonal reinforcing wherever the columns are well reinforced. However, the authors found that diagonal reinforcing was less effective than rectangular reinforcing.

A possible explanation is suggested as follows: When principal stresses are equal but of opposite sign and lie at 45° (an idealized situation), all bars in a rectangular-reinforcement pattern act as components in resisting diagonal tension and cracking. If the bars remain at 90° to each other, but the grid is turned so that the bars lie at 45° to the boundary members only half of them act in resisting cracking. If the angle between these bars is gradually changed from 90° to 0° in such a fashion as to reduce the angle that all the bars make with the horizontal, the component of tension resistance in the vertical direction approaches the tensile strength of plain concrete. Similarly, the authors' diagonal reinforcement is stronger horizontally than vertically. It would seem that such an unbalanced pattern must certainly be more susceptible to diagonal-tension cracking than either the 45° pattern or the rectangular one. If specimen R-5 were to have its web reinforcement rotated further toward the horizontal, its p -value would approach that of specimen VRR-2. The fact that the two specimens have approximately the same ultimate load and load at first crack may be significant in this respect.

Panel VRR-2 probably had a little less resistance to bending than panel VRR-3 or panel VRR-6, but it appears to have been tenacious, absorbing much mechanical work before failure. Specimen VRR-3 probably was stiffer and stronger against bending than specimen VRR-2, but its failure was more sudden, and the authors do not indicate that its resistance to shear was clearly superior. Specimen VRR-6 had approximately the same ultimate load as specimen R-1 (but perhaps greater stiffness after first crack). Specimen R-1 was more lightly reinforced vertically but also had horizontal bars. These observations suggest that direction of panel reinforcing influences stiffness and suddenness of failure.

Little mention was made of energy-absorption capacity, although this factor is probably a criterion for design of reinforced-concrete shear walls under seismic loading. The greater the ability of the wall to continue carrying overload when badly deformed and the less brittle its mode of failure, the more valuable the wall will often be during an earthquake. To attain this state, the authors' results indicate that heavy column reinforcing is helped by adding panel reinforcement parallel to the load.

In specimens having heavy column steel, there was a tendency for the column to crack (subsequent to the first crack) at sections of low bending stress rather than at those of maximum bending stress. Frequently, these cracks do not seem to have been perpendicular to the steel, as were those at the bases of the lightly reinforced columns, but at a slight slope (Fig. 8). This fact seems reasonable because in areas in which shear stress predominates over bending stress, the principal tensile stress lies at some angle to the load other than perpendicular. Because the column steel was not bent at this angle also,

the specimen was reinforced incompletely against the principal tensile stress in this area, and it was merely necessary to increase the load to a certain magnitude for this principal tension to crack the concrete, although the base of this column (at which point bending stresses predominate) may not yet have cracked.

In the formula for linear deflection it is not clear why I does not include the column steel because this steel will have an effect on the deflection in the linear range. Furthermore, it would seem reasonable to omit the web cross section in computing the value of I because the expression VH/AG may be derived by assuming the shear to be constant over the width of the web, which implies an assumed absence of bending resistance in the web.

The elementary procedures to compute deflection will be reassuring to the designer who is concerned with the probable seismic deflection of a shear wall under design load. Using more involved methods to gain precision for such a purpose might be wasted because shear-wall deflection is increased by the rotation and slip at the base. Such rotation and slip depend on the design and construction of the anchorage of the wall to its foundation and on other possible factors. All these factors involve assumptions and approximations conducive to conservative design but not necessarily to exactness.

JACK R. BENJAMIN,⁹ A. M. ASCE, AND HARRY A. WILLIAMS,¹⁰ M. ASCE.—The writers stated that studies based on the lattice-analogy method of analysis were made for several models. Principal stress patterns were determined and contours were plotted for several cases. An example is shown in Fig. 36. (The results of a simplified approach are shown in Fig. 37 for comparison.) In this case, specimens C-1 and C-5 were identical, having 3.3% column steel and no panel reinforcing. However, the compressive concrete strength of specimen C-1 was 1.57 times that of specimen C-5.

An initial crack occurred near the edge of the most highly stressed region, where it was free to propagate rather than in the most highly stressed corner (Fig. 36). It is probable that the other branches of crack No. 1 shown in Fig. 3S and Fig. 7 formed after the initial crack as a result of stress redistribution in the panel. General failure occurred along crack No. 2, which was a continuation of the small branches of crack No. 1. The cracks that began in the corner did not progress because of resistance from the column and foundation. The increased thickness seems to have been sufficient for specimen C-5, and the column steel had the necessary retarding effect for specimen C-1.

A study of all the reinforced-concrete walls shows no relationship between panel reinforcing and the location of first crack. Local strengthening and weakening as well as many other variations were studied. The reinforcing is only effective after cracking begins and not before. This statement is correct with respect to the columns as well as the panel. Changes in the column reinforcing did not alter the mode of panel cracking, provided that tensile column failure could not occur. The tests indicate that the tensile column-foundation junction tends to fail first. If sufficient column steel is provided to carry the

⁹ Prof. of Civ. Eng., Civ. Eng. Dept., Stanford Univ., Stanford, Calif.

¹⁰ Prof. of Civ. Eng., Civ. Eng. Dept., Stanford Univ., Stanford, Calif.

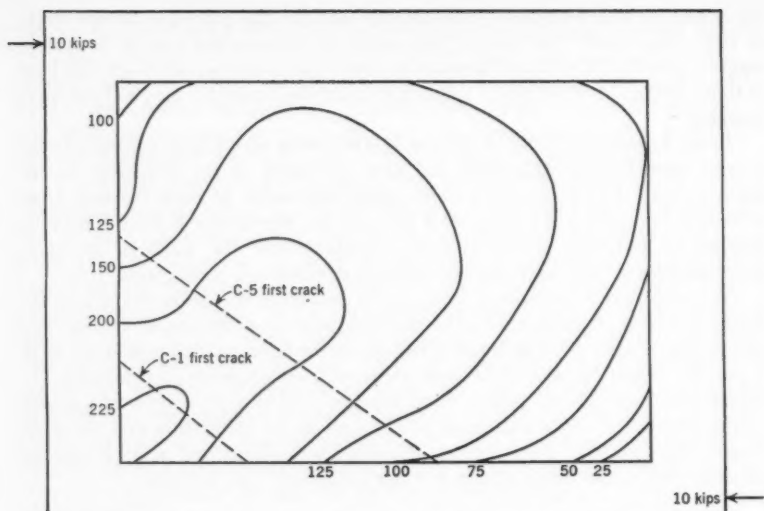


FIG. 36.—PRINCIPAL TENSILE-STRESS CONTOURS FOR WALLS C-1 AND C-5; SOLUTION BY LATTICE ANALOGY—STRESSES IN POUNDS PER SQUARE INCH

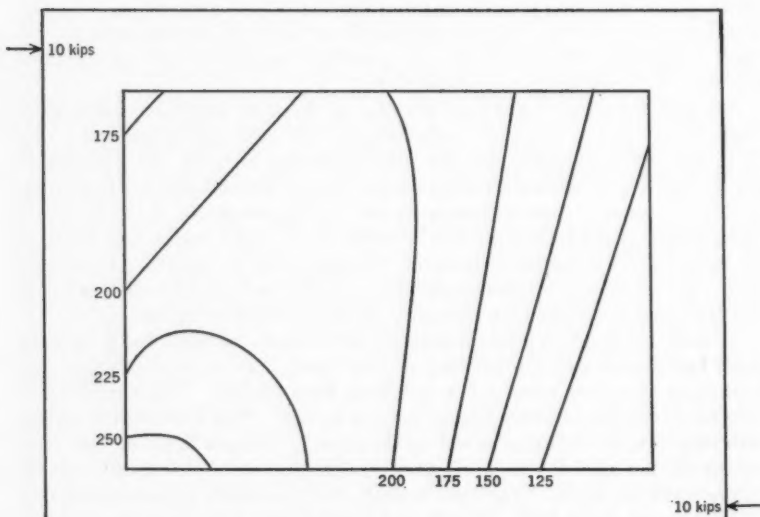


FIG. 37.—PRINCIPAL TENSILE-STRESS CONTOURS FOR WALLS C-1 AND C-5; SOLUTION BY ELEMENTARY BEAM THEORY—STRESSES IN POUNDS PER SQUARE INCH

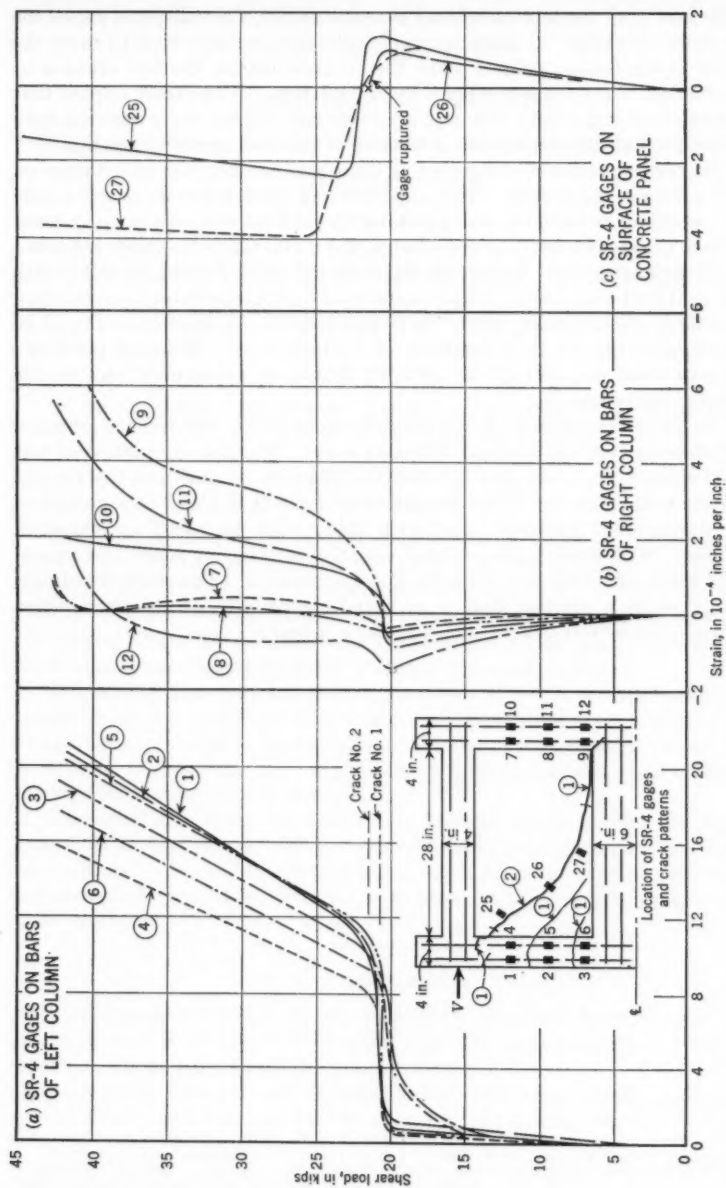


FIG. 38. REINFORCING STEEL AND CONCRETE STRAINS FOR SPECIMEN C-1

tensile load after the tension-column concrete cracks, the wall panel shows the first visual cracking. If there is insufficient tensile-column steel to carry the tension in the tension column when the concrete cracks, the first crack is at the junction of the tension column and foundation. This factor implies that the tension column cracks first with all specimens, but the crack does not open sufficiently that one can observe it because of the steel across the section.

The bending stiffness of the loading beam and columns has no influence on first cracking in shear walls. The larger the wall areas, the more closely a pure shear condition exists in the wall panel, which has been observed in many tests.

From the standpoint of seismic design, the useful range for design is limited to a damage criterion. In general, the walls are cracked so badly at the ultimate load that they are no longer useful even for blast-resistant construction where large cracks are expected. It is questionable if seismic loads should be allowed much beyond the appearance of the first crack. Although the structure may stand and actually be perfectly usable, its appearance may require extensive costly repairs.

The linear-deflection range was studied extensively to discover the influence of reinforcing steel on the load-deflection curve. Careful comparison of test results showed no correlation between the quantity of steel and the rigidity until the wall cracked. Thus, the deflection formula is based on a section of pure unreinforced concrete. Any such study must be based on statistical methods. With shear walls a normal variation in behavior makes the separation of small influences most difficult, if not impossible. Therefore, if a simple formula yields a solution that is as sound statistically as a more complex approach, the writers believe such a formula is best.

AMERICAN SOCIETY OF CIVIL ENGINEERS

Founded November 5, 1852

TRANSACTIONS

Paper No. 2999

REVIEW OF THE THEORIES FOR SAND DRAINS

BY F. E. RICHART, JR., M. ASCE¹

WITH DISCUSSION BY MESSRS. YOSHICHIKA NISHIDA; S. J. JOHNSON;
AND F. E. RICHART, JR.

SYNOPSIS

The existing theories for vertical consolidation of clays by vertical flow of water and by radial flow to a drain well are satisfactory within the limits of the assumptions. The effect of considering void ratio as a variable did not significantly change the consolidation-time characteristics of vertical consolidation by vertical flow. Thus, including the effects of variable void ratio does not contribute toward the explanation of secondary consolidation.

It has been demonstrated that a drain well having a smeared zone at its periphery can be considered as an equivalent "ideal" well of reduced diameter. Diagrams are included for quantitative evaluation of this relation. An example is included to show the effectiveness of even a small diameter ideal well in reducing the time for consolidation.

Numerical procedures were found to be versatile aids for solving the classical consolidation problems as well as for considering consolidation under a variety of conditions. Variable rates of loading, variable soil properties, and layered systems can be readily included in the treatment of consolidation problems by these methods.

INTRODUCTION

The purpose of a drain well is to provide an easier path for the excess water to follow as it is squeezed out of a soil layer during consolidation. Thus, an effective well will accelerate the process of consolidation.

In practice, however, such installations of drain wells, usually composed of sand columns and hence called "sand drains," have met with varied success

NOTE.—Published, essentially as printed here, in July, 1957, in the *Journal of the Soil Mechanics and Foundations Division*, as *Proceedings Paper 1301*. Positions and titles given are those in effect when the paper or discussion was approved for publication in *Transactions*.

¹ Div. of Eng. and Applied Physics, Harvard Univ., Cambridge, Mass.

In order to study the causes of the successes or failures of various installations, it is instructive to review the factors involved in the performance of a drain well, and, if possible, to evaluate the importance of each parameter. The following pages contain a review of the analytical approaches to the problem and a brief discussion of the effects of the more important variables involved.

Notation.—The letter symbols adopted for use in this paper are defined where they first appear and are arranged alphabetically, for convenience of reference, in Appendix II.

THEORY OF CONSOLIDATION

Because the sand drain is merely an auxiliary device to expedite the process of consolidation, it is evident that the consolidation of a soil layer is the fundamental subject to be considered. The theory of consolidation presented by Karl Terzaghi,^{2,3,4} Hon. M. ASCE forms the basis of conventional procedures for predicting the time rate of thickness decrease of clay layers under load. The assumptions made in establishing the theory are:

1. The voids in a soil are completely filled with an incompressible fluid, which is water.
2. The solid components of the soil are incompressible.
3. Darcy's law is valid.
4. The coefficient of permeability, k , is a constant.
5. The time lag of consolidation is due entirely to the low permeability of the soil.

Additional assumptions usually adopted unless it is specifically stated otherwise, are that the soil is laterally confined, and that the coefficient of compressibility, a_v , is a constant for the range of pressure considered. The assumption of lateral confinement restricts application of the theoretical solutions to conditions in which the lateral deformations in the consolidating material are small with respect to the vertical deformations. The assumptions for the consolidation theory are discussed more completely elsewhere.⁴

Utilizing the given assumptions, as well as the further assumptions that variations in the void ratio, e , are limited to small values so that $(1 + e)$ may be treated as a constant, and the conditions of equilibrium of flow of water through an elemental volume of soil, Mr. Terzaghi established the differential equation of one-dimensional consolidation as

$$\frac{\partial u}{\partial t} = \frac{k(1+e)}{a_v \gamma_w} \frac{\partial^2 u}{\partial z^2} = c_v \frac{\partial^2 u}{\partial z^2} \dots \dots \dots (1)$$

In Eq. 1, the excess pore water pressure, u , is expressed as a function of its vertical position in space, z , and time, t . The coefficient of consolidation, c_v , is a constant, because the unit weight of water, γ_w , is a constant and the other terms, k , a_v , and $(1 + e)$ have been assumed to be constants.

² "Erdbaumechanik auf Bodenphysikalischer Grundlage," by K. Terzaghi, Vienna, F. Deuticke, 1925.

³ "Theorie der Setzung von Tonschichten," by K. Terzaghi and O. K. Fröhlich, Vienna, F. Deuticke, 1936.

⁴ "Theoretical Soil Mechanics," by K. Terzaghi, John Wiley & Sons, Inc., New York, N. Y., 1943.

Eq. 1 defines the vertical consolidation of a loaded clay layer due to a vertical flow of water. By a procedure similar to that used to derive Eq. 1, the equations for vertical consolidation due to a two-dimensional and three-dimensional flow can be expressed in cartesian or cylindrical coordinates. When both radial and vertical flow of water exist so that the resultant flow path is inclined, the consolidation equation can be written in terms of cylindrical coordinates as

$$\frac{\partial u}{\partial t} = c_{vr} \left(\frac{\partial^2 u}{\partial r^2} + \frac{1}{r} \frac{\partial u}{\partial r} \right) + c_v \frac{\partial^2 u}{\partial z^2} \dots \dots \dots (2)$$

in which the coefficient of vertical consolidation due to radial flow (c_{vr}) has been assumed to be different from the coefficient of vertical consolidation due to vertical flow of water (c_v).

Consolidation Equation Considering Void Ratio as a Variable.—If the change of void ratio, e , is appreciable, such that it is no longer satisfactory to treat $(1 + e)$ as a constant, a one-dimensional equation of consolidation may be derived taking this into account. The expression, derived in Appendix I, is

$$\frac{\partial u}{\partial t} = \frac{k}{a_v \gamma_w} \frac{1}{(1 + e)} \frac{\partial^2 u}{\partial h^2} - \frac{k}{\gamma_w (1 + e)^2} \left(\frac{\partial u}{\partial h} \right)^2 \dots \dots \dots (3)$$

In which e , u , t , and h are variables, and k , a_v , and γ_w are considered to be constants.

The distance increment, h , is based on the equivalent height of the volume of solids in a given volume of soil. That is, for a soil element of unit area and height dz , the corresponding height of the volume of solids is dh . The relation between these distance elements, shown in Fig. 13, is

$$(1 + e) dh = dz \dots \dots \dots (4)$$

CONSOLIDATION BY VERTICAL FLOW OF WATER ONLY

For a horizontal clay layer of thickness $2H$, the top of the layer may be designated as the origin of the coordinate, z , which is measured positive downward.

The excess pore water pressure, u , existing in this layer as a result of an applied vertical load is determined by Eq. 1 or Eq. 3. Since Eq. 1 is simpler, in that it defines u as a function of position, z , and time, t , only, it will be considered first. The manner in which u varies with z and t depends upon the boundary conditions.

For the condition of free drainage at the upper and lower boundaries of the clay layer (that is, at $z = 0$ and $z = 2H$) the value of excess pore water pressure at these boundaries will be zero at any time. At the plane of symmetry, $z = H$, no water will flow in a vertical direction. At an infinite time the excess pore water pressure will be zero throughout the entire soil layer. Expressed in terms of symbols, these boundary conditions are

$$u = 0 \quad \text{at} \quad z = 0 \quad \text{and} \quad z = 2H \quad \text{for} \quad 0 \leq t \leq \infty \dots \dots \dots (5a)$$

$$\frac{\partial u}{\partial z} = 0 \quad \text{at} \quad z = H \quad \quad \quad \text{for} \quad 0 \leq t \leq \infty \dots \dots \dots (5b)$$

and

$$u = 0 \quad \text{at} \quad 0 \leq z \leq 2H \quad \text{for} \quad t = \infty \quad (5c)$$

In addition, there is a boundary condition defined by the initial excess pressure throughout the layer, which is entirely carried by the pore water. For the case of equal initial excess pore water pressure throughout the soil layer it has the value u_0 . This defines a further boundary condition of

$$u = u_0 \quad \text{at} \quad 0 \leq z \leq 2H \quad \text{for} \quad t = 0 \quad (6)$$

If the assumption is satisfied that the total settlement is small compared to the thickness of the clay layer, $((1 + e) \approx \text{constant})$ then utilizing the prior boundary conditions, the solution of Eq. 1 may be obtained by means of a Fourier series.

$$u = \frac{4}{\pi} u_0 \sum_{N=0}^{\infty} \frac{1}{2N+1} \sin \left[\frac{(2N+1)\pi z}{2H} \right] \epsilon^{-(2N+1)^2 \frac{\pi^2}{4} T_v} \quad (7)$$

in which $\epsilon = 2.718 \dots$ and

$$T_v = \frac{c_v}{H^2} t \quad (8)$$

The term T_v represents an independent dimensionless variable called the time factor. It is customarily used as the abscissa, with the ratio u/u_0 as ordinate to describe graphically the consolidation-time relationship established by Eq. 7.

Solutions of Eq. 1 for a number of different boundary conditions are given elsewhere.³

Effect of Variable Void Ratio.—An exact analytical solution for Eq. 3, satisfying the boundary conditions corresponding to Eq. 5 and Eq. 6, would be complicated. However, it was found possible to obtain an approximate solution for several examples through the use of the difference equation procedure. Eq. 3 is expressed in Appendix II in terms of finite differences and the method of solution is indicated.

Three examples were studied for which the initial void ratio, e_0 , and the final void ratio, e_2 , had the values of (a) $e_0 = 0.65$, $e_2 = 0.55$, (b) $e_0 = 1.00$, $e_2 = 0.80$, and (c) $e_0 = 0.90$, $e_2 = 0.40$. For cases (a), (b), and (c) the final thicknesses of the clay layers were 94%, 90%, and 74%, respectively, of the original thicknesses of these layers.

The consolidation-time curves for the three cases considering void ratio as a variable are shown on Fig. 1. Also shown are two curves obtained by the Terzaghi theory. Curve 1 is obtained using Eq. 7 and curve 2 is obtained by difference equations in which the same space interval ($0.25H$) was used as for the solution of the variable void ratio problems.

The general shape of the curves including the variable void ratio is similar to that of the curves obtained by the Terzaghi theory. The most significant effect of taking void ratio changes into consideration is exhibited by the position of these curves below and to the left of the usual curves. This indicates a

slightly greater degree of consolidation at any particular value of time. This might be expected since the term $(1 + e)$ appears in the denominator of the right side of Eq. 3. Thus, the Terzaghi theory gives a conservative estimate of the time required to reach a given degree of consolidation.

Because the difference in consolidation-time relationships by these two methods is unimportant when compared to the errors involved in establishing the soil constants, it is not necessary to introduce the added complication of variations in void ratio even for moderate changes in thickness of the clay layer.

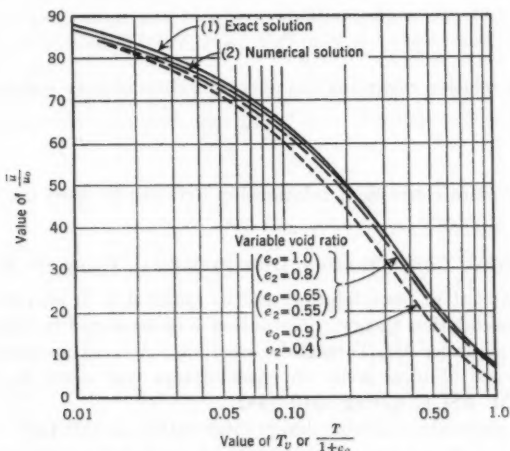


FIG. 1.—PORE WATER PRESSURE VERSUS TIME CURVES FOR VERTICAL WATER FLOW

The curves of Fig. 1 and the discussion included in Appendix I indicate that taking the variable void ratio into account does not contribute to the explanation of secondary consolidation.

SIMPLIFICATION OF ANALYSIS FOR CONSOLIDATION BY TWO OR THREE DIMENSIONAL FLOW

Consolidation by vertical flow alone involves only two variables, time, and depth, z . For consolidation by two-dimensional flow, the variables are x , z , and time, while for three-dimensional flow they are x , y , z , and time. Thus, the general solution for consolidation by three-dimensional flow for a given set of boundary conditions may become mathematically involved.

The method of separation of variables can be applied to this problem, as demonstrated by A. B. Newman⁵ and later by N. Carrillo.⁶ By use of this procedure, the expression for the resultant excess pore water pressure can be

⁵ "The Drying of Porous Solids," by A. B. Newman, *Transactions, Am. Inst. Chem. Eng.*, Vol. 27, 1931, p. 310.

⁶ "Simple Two- and Three-Dimensional Cases in the Theory of Consolidation of Soils," by N. Carrillo, *Journal of Mathematics and Physics*, Vol. 21, No. 1, March, 1942.

evaluated in terms of component solutions, which may be combined at the final step in the analysis. For example, in consolidation by two-dimensional flow the solution containing the variables x , z , and t can be determined by first evaluating u_x (which is a function of x and t), then evaluating u_z (which is a function of z and t), and combining these for a particular point in space at a particular time. The relation to be satisfied in the combining procedure is

$$\frac{u}{u_o} = \frac{u_x}{u_o} \frac{u_z}{u_o} \dots \dots \dots (9a)$$

OR

$$u = \frac{u_x u_z}{u_o} \dots \dots \dots (9b)$$

A similar relation regarding the average values of pore water pressure is

$$\bar{u} = \frac{\bar{u}_x \cdot \bar{u}_z}{\bar{u}_o} \dots \dots \dots (10)$$

which is the more convenient relationship and can be used for homogeneous layers.

VERTICAL CONSOLIDATION DUE TO RADIAL FLOW OF WATER

The treatment of consolidation due to radial flow is an extension of the Terzaghi consolidation theory. A solution was presented in 1935 by L. Reudulic,⁷ working under Mr. Terzaghi's direction. A more comprehensive study of the influence of ideal wells on consolidation was made by Reginald A. Barron,⁸ A. M. ASCE, during 1940-1942.

The first generally available design information on this topic was given by Mr. Terzaghi⁴ and was later supplemented by a paper which he published in 1945.⁹ In 1948, Mr. Barron¹⁰ presented a complete summary of the theory of sand drains, including new theories taking into account deviations from the ideal well conditions.

The two papers by Mr. Barron^{8,10} constitute the principal analytical studies available at present (1959) of radial flow toward a drain well and the resulting consolidation of the clay. He considered two types of vertical strain which might occur in the clay layer, (1) "free vertical strain" resulting from a uniform distribution of surface load, and (2) "equal vertical strains" resulting from imposing the same vertical deformation at all points on the surface. For both strain conditions he included an analysis of the effect of "smear" of the soil near the well boundary, and the effect of resistance to flow through the well itself.

"Smear" is the term used to define the wiping action provided by the casing or hollow mandrel used to form the well as it is driven down into the soil, and

⁷ "Der hydrodynamische Spannungsangleich in zentral entwässerten Tonzylindern," by L. Reudulic, *Wasserwirtsch. u. Technik*, Vol. 2, 1935, pp. 250-253, 269-273.

⁸ "The Influence of Drain Wells on the Consolidation of Fine Grained Soils," by R. A. Barron, Providence (R. I.) District, U. S. Engrs. Office, 1944.

⁹ "Drainage of Clay Strata by Filter Wells," by K. Terzaghi, *Civil Engineering*, October, 1945, pp. 463-464.

¹⁰ "Consolidation of Fine-Grained Soils by Drain Wells," by R. A. Barron, *Transactions, ASCE*, Vol. 113 1948, p. 718.

then pulled out after it has been filled with sand. This action tends to smear the soil at the well periphery. For a soil originally having a greater permeability in the horizontal than in the vertical direction, the smeared zone forms a barrier to the horizontal flow of water, thereby slowing down considerably the process of consolidation.

"Free Strain" Consolidation with No Smear and No Well Resistance.—A regular pattern of vertical drain wells, as shown in Fig. 2, will permit a radial as well as a vertical flow of water from the clay layer if it is subjected to an increase in pressure. Since in a previous section it was shown that the effects due to vertical flow and radial flow can be evaluated separately, and then combined to give the final consolidation behavior, only the radial flow consolidation is considered here.

As indicated on Fig. 2, for a triangular spacing of drain wells, a zone of influence exists having a hexagonal plan form. By approximating the hexagon

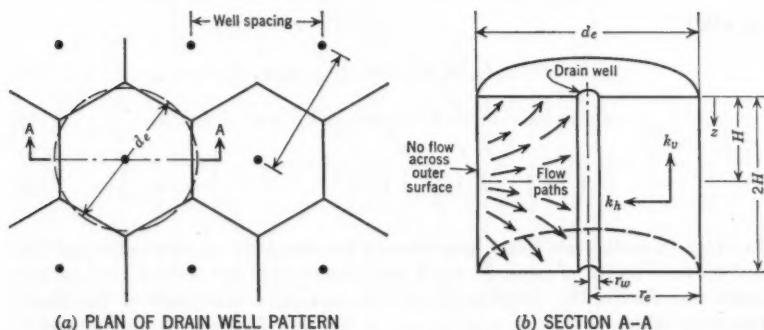


FIG. 2.—DRAIN WELLS AND FLOW WITHIN ZONE OF INFLUENCE OF EACH WELL

by a circle of equivalent diameter, d_e , this can be used as the outer limit of the zone of influence of each drain well. Thus it becomes sufficient to consider the radial flow and resulting consolidation of a soil volume of unit thickness contained between the distances d_e (diameter of well influence) and d_w (diameter of the drain well).

By eliminating the consideration of vertical flow, Eq. 2 becomes

$$\frac{\partial u}{\partial t} = c_{vr} \left(\frac{\partial^2 u}{\partial r^2} + \frac{1}{r} \frac{\partial u}{\partial r} \right) \dots \dots \dots (11)$$

which is the equation for consolidation expressed in terms of radial coordinates. The boundary conditions that must be satisfied are:

1. The initial pore water pressure, u_0 , is uniform throughout the soil mass when $t = 0$.
2. The excess pore water pressure at the drain well surface (r_w) is zero when $t > 0$.

3. The external radius, r_e , is considered impervious because of symmetry.

Thus, $\frac{\partial u}{\partial r} = 0$ when $r = r_e$

The solution of Eq. 11, subject to the boundary conditions indicated above, leads to the following expressions for u_r (the pore water pressure at any location, r , at any time, t , existing as a result of radial flow only) and \bar{u}_r (the average value of u_r throughout the soil mass at any time, t):

$$u_r = u_o \sum_{\alpha_1, \alpha_2, \alpha_3, \dots}^{\alpha=\infty} \frac{-2 U_1(\alpha) \cdot U_o \left(\frac{\alpha r}{r_w} \right)}{\alpha [n^2 U_o^2(\alpha n) - U_1^2(\alpha)]} e^{-4\alpha^2 n^2 T_h} \dots (12)$$

and

$$\bar{u}_r = u_o \sum_{\alpha_1, \alpha_2, \alpha_3, \dots}^{\alpha=\infty} \frac{4 U_1^2(\alpha)}{\alpha^2 (n^2 - 1) [n^2 U_o^2(\alpha n) - U_1^2(\alpha)]} e^{-4\alpha^2 n^2 T_h} \dots (13)$$

in which

$$U_1(\alpha) = J_1(\alpha) Y_o(\alpha) - Y_1(\alpha) J_o(\alpha) \dots (14a)$$

$$U_o(\alpha n) = J_o(\alpha n) Y_o(\alpha) - Y_o(\alpha n) J_o(\alpha) \dots (14b)$$

$$U_o \left(\frac{\alpha r}{r_w} \right) = J_o \left(\frac{\alpha r}{r_w} \right) Y_o(\alpha) - Y_o \left(\frac{\alpha r}{r_w} \right) J_o(\alpha) \dots (14c)$$

in which J_o and J_1 are Bessel functions of the first kind, of zero order and first order, respectively; Y_o and Y_1 are Bessel functions of the second kind, of zero order and first order, respectively; α_1, α_2 , and $\alpha_3 \dots$ are roots of the Bessel functions which satisfy $J_1(\alpha n) Y_o(\alpha) - Y_1(\alpha n) J_o(\alpha) = 0$; and n = ratio equal to $\frac{r_e}{r_w} = \frac{d_e}{d_w}$. The time factor for consolidation by radial flow, T_h = $\frac{k_h (1 + e) t}{a_v \gamma_w d_e^2}$, in which k_h is the coefficient of permeability in the horizontal direction.

Solutions similar to Eqs. 12 and 13 were derived by R. E. Glover¹¹ for the analogous heat flow problem.

Equal Strain Consolidation with No Smear and No Well Resistance.—Under the condition of free strain it was implied that the settlements at the surface did not change the distribution of the load to the soil. However, in an actual installation, the fact that consolidation proceeds faster near the drain well, thereby causing a greater surface settlement in that region, could very well cause a redistribution of the surface loading. This would be especially true if the loading material had any tendency to arch across such depressions. As an extreme case the arching action could redistribute the loads to the surface in such a fashion that the surface settlement is the same at all points. This is the

¹¹ "Temperature Movements in Concrete and other Materials, with Special Reference to Conditions at Boulder Dam," by R. E. Glover, Technical Memorandum No. 158, Bureau of Reclamation, U. S. Dept. of the Interior, Denver, Colo., 1930.

condition of equal vertical strains for which Mr. Barron has also developed an analytical solution,

$$u_r = \frac{4 \bar{u}}{d_v^2 f(n)} \left[r^2 \log_e \left(\frac{r}{r_w} \right) - \frac{r^2 - r_w^2}{2} \right] \quad (15)$$

in which

$$\bar{u} = u_o e^\lambda \quad (16)$$

$$\lambda = \frac{-8 T_h}{f(n)} \quad (17)$$

and

$$f(n) = \frac{n^2}{n^2 - 1} \log_e (n) - \frac{3 n^2 - 1}{4 n^2} \quad (18)$$

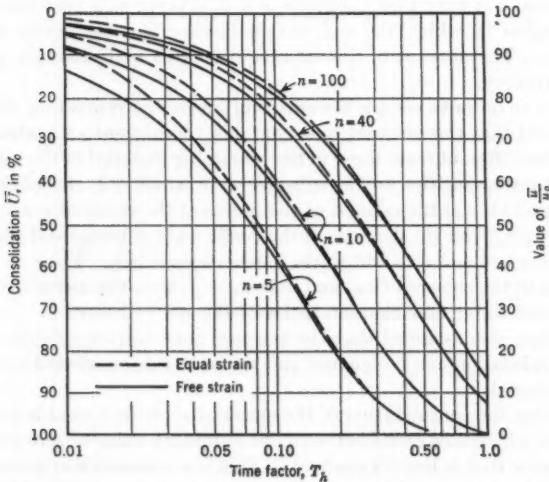


FIG. 3.—CONSOLIDATION VERSUS TIME FACTOR

The initial distribution of hydrostatic excess pressure is not uniform, but may be computed from Eq. 15 for $T_h = \lambda = 0$. Curves showing the relation between the average pore water pressure, \bar{u} , and the time factor, T_h , can also be obtained from Eq. 16. Such curves for $n = 5, 10, 40$, and 100 are shown on Fig. 3, together with the corresponding curves determined by the free strain case.

Comparison of Free Strain and Equal Strain Solutions.—The difference between the results obtained by the two extreme considerations of the process of consolidation is small, particularly for the curves representing values of n greater than approximately 10. For $n = 5$ the discrepancy is somewhat greater for the first part of consolidation, but above approximately 50% consolidation, the curves are almost identical.

Since the results are nearly identical, but the time needed to evaluate Eq. 13 is of the order of ten to fifteen times that needed to evaluate Eq. 16, the equal strain solution is preferable. Both Mr. Barron¹⁰ and W. Kjellman¹² recommended use of the equal strain solution.

Fig. 3 indicates that the curves representing the equal strain solutions for different values of n have the same shape, but are displaced horizontally. The location of the consolidation-time curve for any particular value of n depends upon the value of λ as determined from Eq. 17.

Effect of Peripheral Smear.—The remolded or smeared zone at the periphery of the drain well creates an additional resistance that must be overcome by the excess water being expelled. This additional resistance retards the consolidation process.

The smeared zone will not be uniform or homogeneous with regard to the soil properties. It very likely consists of a thin layer of actual smear plus an adjacent region in which the soil has undergone a considerable amount of disturbance. The amount of disturbance decreases with distance away from the well periphery.

However, in order to include the effects of smear and remolding, Mr. Barron⁸ has considered that the smeared zone contains a homogeneous material having soil properties different from those in the remaining material in the soil cylinder. The important quantities to be considered in analyzing the effects of this smeared region are (a) the ratio, s , of the radius of the smeared zone to the well radius ($s = r_s/r_w$) and (b) the ratio of the coefficients of horizontal permeability in the undisturbed soil (k_h) and in the smeared zone (k_s). For $s = 1$, there is no thickness to the smeared ring, and if $k_h/k_s = 1$, then the disturbed zone does not change the water flow characteristics of the soil cylinder.

Mr. Barron also assumed that the smeared zone will consolidate very fast, thus its consolidation can be ignored and the zone can be treated as an incompressible material.

By ignoring the consolidation of the smeared zone, he was able to treat this region as one where flow exists between one boundary value of zero and another boundary value that is time dependent. This is a reasonable approximation of the actual behavior, since the excess pore water pressure within the smeared region would quickly dissipate into this steady flow condition. For an extreme case in which $n = 5$, $s = 2$, and $k_h/k_s = 2$, and consolidation of the smeared zone was considered, the steady flow condition was reached at approximately $T_h = 0.025$.

Equal Strain with Smear.—Mr. Barron's solution for the excess pore water pressure in a soil cylinder undergoing equal vertical strains and containing a smeared region around the drain well is

$$u_r = \bar{u}_r \frac{\left[\log_e \left(\frac{r}{r_s} \right) - \frac{r^2 - r_s^2}{2 r_s^2} + \frac{k_h}{k_s} \left(\frac{n^2 - s^2}{n^2} \right) \log_e (s) \right]}{\nu} \dots \dots (19)$$

¹² Discussion by W. Kjellman of "Consolidation of Fine-Grained Soils by Drain Wells," by R. A. Barron, *Transactions, ASCE*, Vol. 113, 1948.

value of n . For a given radius of influence, a larger value of n determines the radius of an equivalent ideal well which is smaller than the radius of the actual well surrounded by a zone of smear. The effect on consolidation of the soil cylinder caused by the introduction of a smeared zone at the well periphery is identical to the effect caused by reducing the size of the ideal well.

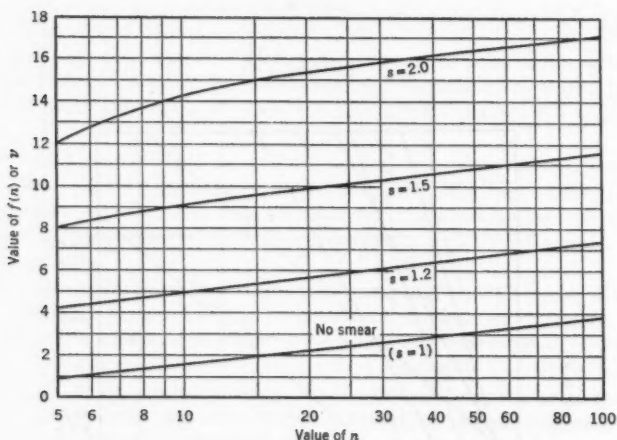


FIG. 5.—RELATIONSHIP BETWEEN n AND $f(n)$ OR v FOR $\frac{k_h}{k_s} = 20$

Fig. 4 shows the combinations of n , s , and k_h/k_s that may be used to give the same value of v . This figure, obtained by evaluating Eq. 20, uses the value of v as ordinate and the ratio k_h/k_s as abscissa. Families of lines for each selected value of n show the influence of variations in s . Only the lines for $n = 5$ and

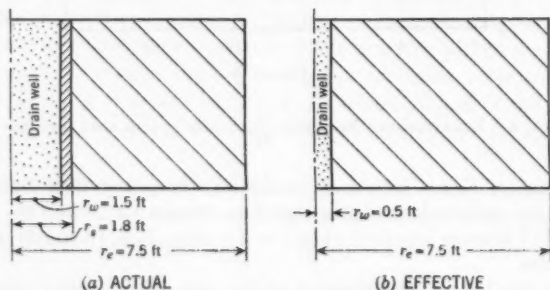


FIG. 6.—ACTUAL AND EQUIVALENT WELL INSTALLATIONS

$n = 15$ are shown on Fig. 4. However, by the use of Fig. 5, diagrams similar to Fig. 4 can be established for a wide range of values of n .

Fig. 6(a) is an example of the use of Fig. 4, considering a drain well for which $n = 5$, $s = 1.2$, and $k_h/k_s = 7$. The value of v determined from Fig. 4 is 1.97

for Fig. 6(a). This corresponds to $f(n) = 1.97$ (Fig. 5) for a well having no smear ($s = 1$), or it determines $n = 15$ for the equivalent ideal well in Fig. 6(b). Evaluating this in numbers indicates that if the original diameter of well influence was 15 ft, the diameter of the drain well was 3 ft (from $n = 5$), and the outer diameter of the smeared region was 3.6 ft ($s = 1.2$). The effect of the smeared region is to reduce the consolidation-time behavior to one identical to that of a 1 ft diameter well ($n_{eff.} = 15$) for which no smear is present.

Effect of Well Resistance.—The foregoing analyses have considered that there is unrestricted flow of the water through the drain well. Actually, head losses will occur due to the resistance to flow of the well backfill material. The magnitude of the head losses will depend upon the rate of flow, the size of the well, and the permeability of the material filling the well.

Mr. Barron has developed a solution for the case of equal vertical strain, with or without smear, for a material in which no vertical flow exists due to lack of permeability in the vertical direction, but $\frac{\partial u}{\partial z} \neq 0$.

However, for practical drain well installations for which n is approximately 7 to 15 and for $d_e/H \leq 1.0$, the effect on the consolidation behavior due to resistance of the drain wells should not be significant.

EXAMPLE CONSIDERING IDEAL WELLS

To illustrate the value of this information in selecting the size and spacing of drain wells for a particular installation, the following values were chosen: $a_v = 13 \times 10^{-8}$ cm per gm; $e = 1.50$; $H = 10$ ft; $k_v = 5 \times 10^{-8}$ cm per sec; $k_h = 25 \times 10^{-8}$ cm per sec; and $\Delta e = 0.125$; in which k_v is the coefficient of permeability in the vertical direction.

These values determine $c_v = 9.62 \times 10^{-4}$ cm² per sec, which is of the same order of magnitude as the test results given by K. Terzaghi and R. B. Peck,¹² M. ASCE. The clay layer is considered 20 ft thick if drainage occurs at both top and bottom surfaces, or 10 ft thick if drainage occurs at the top surface only. The horizontal permeability is five times that in the vertical direction.

For the initial conditions, assume that there is no smeared zone and no well resistance, so that the consolidation behavior depends only on the size and spacing of the drain wells.

Constant Well Diameter.—To compare the effects of well spacing a well diameter of 12 in., $\frac{k_h}{k_v} = 5$, and $c_v = 9.6 \times 10^{-4}$ cm² per sec were chosen. The consolidation percentage versus time curves are shown on Fig. 7. Fig. 7(a) shows the consolidation-time curves for radial or vertical drainage only. Fig. 7(b) shows the effect of a one-ft diameter well with a diameter of influence of ten ft when it is introduced into each of the clay layers. The time for consolidation is reduced to a fraction of the time for vertical drainage. The use of closer spacing of drain wells would further reduce this time, as would be demonstrated by using the curve for $d_e = 5$ ft in Fig. 7(b) instead of that for $d_e = 10$ ft.

¹² "Soil Mechanics in Engineering Practice," by K. Terzaghi and R. B. Peck, John Wiley & Sons, Inc., New York, N. Y., 1948, Fig. 29, p. 77.

It should be noted from Fig. 7(b), that the consolidation-time behavior due to combined radial and vertical drainage is nearly identical to that due to radial drainage alone, for $d_e = 10$ ft. This is influenced to a considerable extent by the conditions of $k_h = 5 k_v$. If $k_h = k_v$, it would be necessary to consider a smaller well spacing, or smaller ratio d_e/H , for the radial flow behavior to dominate the consolidation-time behavior of the clay layer due to combined vertical and radial flow.

Constant Well Spacing.—The consolidation versus time curves shown on Fig. 8 are for the conditions involving a constant spacing of the wells, but allowing the diameter of the wells to vary. The chosen well spacing was 10 ft which is the same as the thickness of the clay layer, $k_h/k_v = 5$ and $c_v = 9.6 \times 10^{-4}$ cm² per sec.

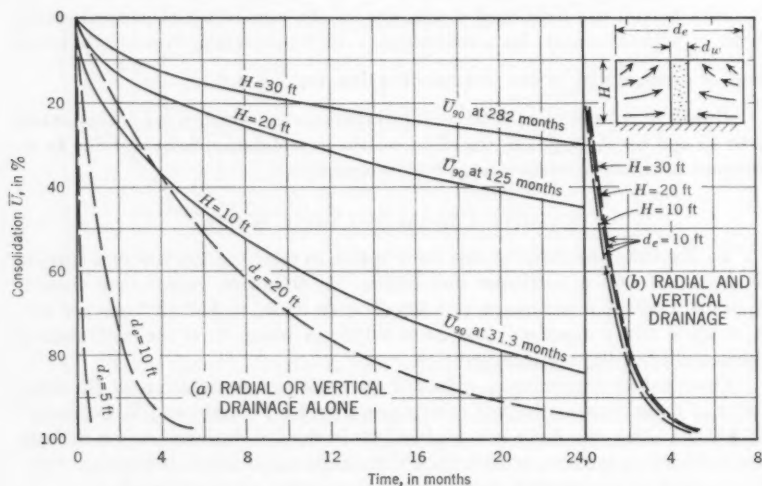


FIG. 7.—EFFECT OF DRAIN WELL ON TIME FOR CONSOLIDATION FOR VARIOUS THICKNESSES OF CLAY LAYER

Fig. 8(a) shows the consolidation versus time curves for the radial or vertical flow when they act independently. Fig. 8(b) shows the effect on consolidation due to combined flow. For 90% consolidation the time amounts to (a) 6.0 months (19.2% of time for vertical only) for $d_w = 1.2$ in.; (b) 3.9 months (12.5% of time for vertical only) for $d_w = 6$ in.; and (c) 1.7 months (5.4% of time for vertical only) for $d_w = 24$ in. Thus, even the 1.2-in. diameter well in a 10-ft soil cylinder cuts the consolidation time to approximately one-fifth of the time required for 90% consolidation by vertical drainage only.

It is of importance to note that doubling of the diameter of well influence (d_e), or essentially the well spacing, causes an increase in the time for 90% consolidation by roughly a factor of 6 (Fig. 7(a)). In Fig. 8(a) it is seen that by reducing the diameter of drain well by a factor of 20 only increases the time for

90% consolidation by a factor of approximately 4. Consequently, the effectiveness of a given drain well installation is considerably more dependent on the choice of well spacing than it is on the well diameter.

Effect of Horizontal Permeability.—To convert the nondimensional time factor, T_h , into terms of t_h in months, it is necessary to use the equation,

$$t_h = \frac{T_h \cdot \gamma_w \cdot a_v \cdot d_e^2}{k_h (1 + e)} \dots \dots \dots (23)$$

From Eq. 23 it is evident that the time for any given degree of consolidation is inversely proportional to the coefficient of permeability in the horizontal direction.

Fig. 9 illustrates the effect of k_h/k_v on t_{90} , the time required to obtain 90% consolidation by combined vertical and radial flow. Two well systems are used: (a) $d_e = 10$ ft, $d_w = 1.2$ in., $n = 100$; and (b) $d_e = 10$ ft, $d_w = 12$ in.,

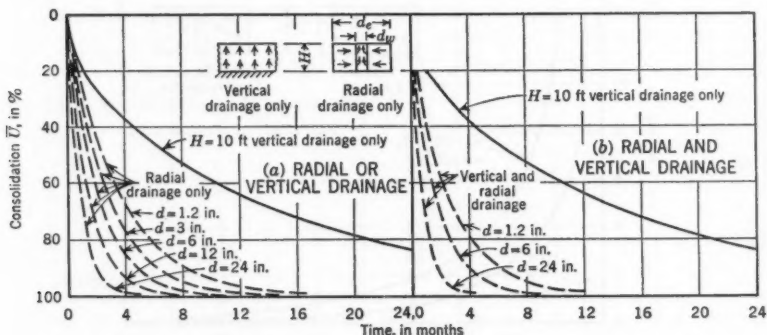


FIG. 8.—EFFECT OF SIZE OF DRAIN WELL ON TIME FOR CONSOLIDATION

and $n = 10$. For both systems, $c_v = 9.6 \times 10^{-4}$ cm² per sec. Fig. 9 demonstrates the pronounced effect of the ratio k_h/k_v for the two well systems. Even for the case of $k_h/k_v = 1.0$, the time for 90% consolidation is reduced to less than 55% of the time required when no wells are present. The 55% time corresponds to the well system made up of 1.2-in. diameter wells spaced every 10 ft.

Discussion of Example.—The 1.2-in. diameter well considered previously is an "ideal well" for which there is no smear and no well resistance. The significant point is that such a small well can be so effective. If the well spacing was reduced to three or four ft, the effectiveness of such a 1.2-in. diameter well would be increased many times. Thus, the basic idea of the cardboard wicks spaced at approximately 4 ft, as described by W. Kjellman¹² is based on sound theoretical considerations.

In order to design a system of drain wells, some numerical information is required about the well resistance, the extent or radius of the smear zone, and

the permeability of material in the smear zone. Then, using the desired diameter of the ideal well, for a given well spacing, Fig. 4 or Fig. 5 can be used to determine the actual size of well needed. That is, the actual size of well to be constructed is reduced in effectiveness by the smear and well resistance until it behaves similarly to an ideal well of smaller diameter. Then the behavior of the equivalent ideal well may be studied thoroughly with the aid of the many diagrams already prepared by Mr. Barron.^{8,10}

SOLUTION OF THE CONSOLIDATION PROBLEM BY NUMERICAL METHODS

Because the exact solutions for the consolidation problem become unwieldy for rather modest departures from the simplified case, such as when smear is

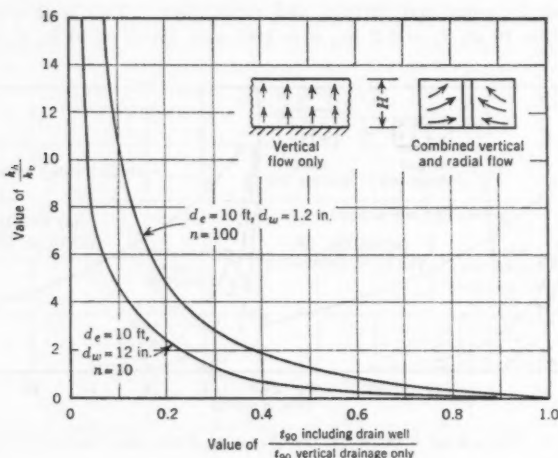


FIG. 9.—INFLUENCE OF PERMEABILITY RATIO ON TIME FOR 90% CONSOLIDATION

introduced into the problem of consolidation by radial flow, it is desirable to investigate methods that lead to approximate results. In recent years, an appreciable amount of work has been directed toward application of the difference-equation procedure to the problem of transient flow of heat in solids.^{14,15,16,17} The results of these studies may be used directly in analogous problems such as consolidation of clays.

¹⁴ "The Numerical Solution of Heat Conduction Problems," by H. W. Emmons, *Transactions, A.S.M.E.*, Vol. 65, 1943, pp. 607-615.

¹⁵ "A Practical Method for Numerical Evaluation of Solutions of Partial Differential Equations of the Heat-Conduction Type," by J. Crank and P. Nicolson, *Proceedings, Cambridge Phil. Soc.*, Vol. 43, 1947, pp. 50-67.

¹⁶ "Numerical Analysis of Heat Flow," by G. M. Dusenberre, McGraw-Hill Book Co., Inc., New York, N. Y., 1949.

¹⁷ "A Study of the Numerical Solution of Partial Differential Equations," by G. G. O'Brien, M. A. Hyman, and S. Kaplan, *Journal of Math. and Physics*, Vol. 29, 1950, pp. 223-251.

Explicit Expressions.—One procedure used extensively for numerical solutions of both the heat flow and consolidation^{18,19} equations permits a solution for the value of the dependent variable at a given point in space and time by considering only values of this variable at points in space at a previous time. The solution thus amounts to a step-by-step determination of these values at points in space as they vary along the time coordinate.

The expression resulting from replacing Eq. 1, for example, by its differences equivalent, is

$$\frac{u_{o,t+\Delta t} - u_{o,t}}{\Delta t} = c_v \left[\frac{u_{2,t} - 2u_{o,t} + u_{4,t}}{(\Delta z)^2} \right] \dots \dots \dots (24)$$

In Eq. 24 the first subscript for the u -terms denotes the position in space of the point under consideration (also shown on Fig. 11) and the second subscript denotes the time, with Δt equal to the time interval and Δz representing the interval of z .

Eq. 24 is usually rearranged, for convenience in computation, as

$$u_{o,t+\Delta t} = u_{o,t} + A \{u_{2,t} - 2u_{o,t} + u_{4,t}\} \dots \dots \dots (25)$$

in which the constant, A , represents

$$A = \frac{c_v \Delta t}{\Delta z^2} \dots \dots \dots (26a)$$

or

$$A = \frac{\Delta T}{(\Delta \zeta)^2} \dots \dots \dots (26b)$$

if ζ is defined as

$$\zeta = \frac{z}{H} \dots \dots \dots (27a)$$

and

$$\Delta z = H (\Delta \zeta) \dots \dots \dots (27b)$$

Previous studies¹⁷ of the heat flow equation have determined that if $A > 0.5$, the values of u determined by Eq. 25 diverge, and for $A \leq 0.5$, they converge. Also, Eq. 26 establishes a definite relation between the increments of time and space for a particular choice of A . Thus, even for a rather crude space network, such as $\Delta \zeta = \frac{1}{4}$, the maximum allowable time increment is $\Delta T_v = 0.03125$, with the result that numerous steps in time are required in the solution. Since this is a step-by-step procedure, in order to determine the excess pore water distribution at a particular time, it is necessary to work up to that time by using equal sized time intervals, starting from $T_v = t = 0$.

Implicit Expressions.—The size of the time interval dictated by the stability consideration of the explicit scheme is often inconveniently small, therefore a method permitting larger time increments is desirable. This has been accom-

¹⁸ "Numerical Solution of Some Problems in the Consolidation of Clay," by R. E. Gibson and P. Lumb. *Proceedings Inst. of Civil Engineers*, London, Vol. 2, Part I, 1953, pp. 182-198.

¹⁹ "Numerical Analysis of Consolidation Problems," by R. F. Scott, thesis presented to Massachusetts Inst. of Technology, at Cambridge, in 1953, in partial fulfillment of the requirements for the degree of Master of Science.

plished by turning around the difference equation, resulting in the form (corresponding to Eq. 1)

$$\frac{u_{o,t+\Delta t} - u_{o,t}}{\Delta t} = c_v \left[\frac{u_{2,t+\Delta t} - 2u_{o,t+\Delta t} + u_{4,t+\Delta t}}{(\Delta z)^2} \right] \dots \dots (28)$$

The form of Eq. 28 used for computation¹⁷ considers the average value of the space relations over the time interval as:

$$\frac{u_{o,t+\Delta t} - u_{o,t}}{\Delta t} = \frac{c_v}{2} \left\{ \frac{u_{2,t+\Delta t} - 2u_{o,t+\Delta t} + u_{4,t+\Delta t}}{(\Delta z)^2} + \frac{u_{2,t} - 2u_{o,t} + u_{4,t}}{(\Delta z)^2} \right\} \dots (29)$$

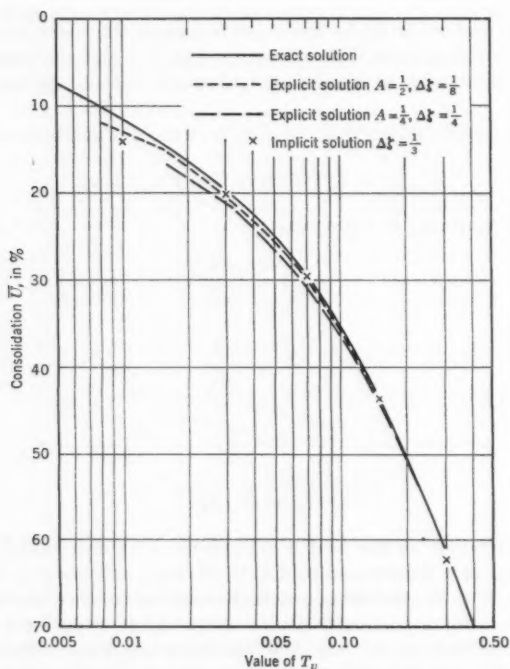
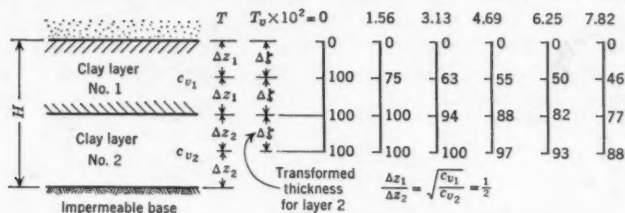


FIG. 10.—CONSOLIDATION VERSUS TIME CURVES FOR VERTICAL FLOW
COMPUTED BY EXACT AND NUMERICAL METHODS

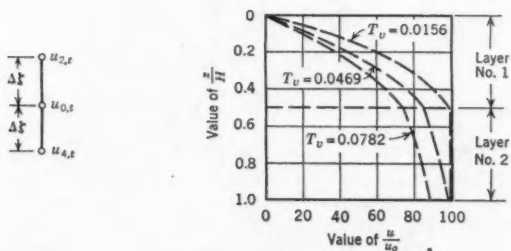
Eq. 28 is an implicit relation for the values of excess pore water pressure at the time $t + \Delta t$. That is, these unknowns occur simultaneously in the equations. This requires the solution of a set of simultaneous equations for each time interval adopted, but the size of the time interval is arbitrary and may be changed during the solution of a problem. The equations are stable and place no restriction on the size of the space or time increments. However, if a small space interval is required in order to gain accuracy, this increases the number

of simultaneous equations. For such cases, the use of digital computing machinery is nearly always required.

Although the implicit scheme does not place restrictions on the size of the time or space increments as a criterion of stability, the fact that the finite differences must be reasonable approximations to the corresponding differentials does prohibit large increments, particularly in time. The size of the allowable time increment depends on the rate of change of pore water pressure within that increment. Criteria for this and for related procedures have been given by T. P. Tung and N. M. Newmark, M. ASCE.²⁰



(a) PARTIAL SOLUTION FOR VARIATIONS IN $\frac{u}{u_0}$



(b) ISOCHRONES FOR LAYERED SYSTEM

FIG. 11.—NUMERICAL PROCEDURES FOR CONSOLIDATION OF A TWO-LAYER SYSTEM DUE TO VERTICAL FLOW

Numerical Solutions of Vertical Consolidation by Vertical Flow.—Eq. 24 was evaluated for two cases, $A = 1/4$, $\zeta = 1/4$ and $A = 1/2$, $\zeta = 1/8$, for which the resulting time intervals were $\Delta T = 0.015625$ and 0.0078125 , respectively. The curves thus obtained are shown on Fig. 10 as well as the curve corresponding to the exact solution. The agreement is good, particularly for values of $T_v > 0.10$.

Eq. 29 was also evaluated for comparison. Using $\zeta = 1/3$ and time increments which doubled in size at each time step, starting with $T_v = 0.010$ (that

²⁰ "A Method of Numerical Integration for Transient Problems of Heat Conduction," by T. P. Tung and N. M. Newmark, Structural Research Series No. 95, Civil Engineering Studies, Univ. of Illinois, Urbana, Ill., March, 1955.

is, $\Delta T_{v_1} = 0.010$, $\Delta T_{v_2} = 0.020$, $\Delta T_{v_3} = 0.040$) a curve was obtained that agreed more closely with the exact solution than did those computed by the explicit method.

Since the explicit method permits the use of a fine space mesh with little increase in computational effort above that for a coarse mesh, it appears desirable to use this scheme for small values of time for which u is changing rapidly. Then, for larger values of time, it would be convenient to switch to a coarse time mesh and use the implicit scheme.

Vertical Consolidation by Vertical Flow for Layered Systems.—A clay stratum, made up of two or more horizontal layers, may also be treated by numerical procedures. At the interface between any two layers the conditions of equilibrium require that the velocity of flow leaving one layer must be equal to the velocity of flow entering the other. Thus, for two materials having permeability coefficients of k_{v_1} and k_{v_2} , this condition at the interface requires that

$$k_{v_1} \left(\frac{\partial u}{\partial z_1} \right) = k_{v_2} \left(\frac{\partial u}{\partial z_2} \right) \dots \dots \dots (30)$$

The two layers also have different coefficients of consolidation, c_v , which are dependent upon a_v as well as k_v . In order to simplify the numerical procedure, it is convenient to adjust the size of the space intervals so that the term A remains the same in both layers for the same Δt . Thus,

$$A = \frac{c_{v_1} \Delta t}{(\Delta z_1)^2} = \frac{c_{v_2} \Delta t}{(\Delta z_2)^2} \dots \dots \dots (31)$$

or

$$\frac{\Delta z_1}{\Delta z_2} = \sqrt{\frac{c_{v_1}}{c_{v_2}}} \dots \dots \dots (32)$$

Fig. 11 illustrates the numerical solution for a two-layered system, consisting of a top layer, 1, resting on a second layer, 2, of equal thickness. Fig. 11(a) shows the partial solution for variations in u/u_o with time and depth and $\Delta \zeta$ is the transformed thickness for layer 2. For the two layers, $c_{v_2} = 4 c_{v_1}$, which determines for a choice of $\Delta \zeta = 0.25$ that the space increments are $0.25 H$ in layer 1 and $0.50 H$ in layer 2. In Fig. 11(b), the isochrones show a definite change in slope at the interface, which should correspond to Eq. 30.

Numerical Solution of Consolidation by Radial Flow.—Expressing Eq. 11 in terms of finite differences leads to

$$\frac{u_{o,t+\Delta t} - u_{o,t}}{\Delta t} = \frac{c_v}{\Delta r^2} \left[\left(1 + \frac{\Delta r}{2 r_o} \right) u_{1,t} + \left(1 - \frac{\Delta r}{2 r_o} \right) u_{3,t} - 2 u_{o,t} \right] \dots (33)$$

or

$$u_{o,t+\Delta t} = \frac{c_v \Delta t}{\Delta r^2} \left[\left(1 + \frac{\Delta r}{2 r_o} \right) u_{1,t} + \left(1 - \frac{\Delta r}{2 r_o} \right) u_{3,t} - 2 u_{o,t} \right] + u_{o,t} \dots (34a)$$

The network points used in Eq. 34 are spaced to the right and to the left of the point, o_r , for which the value of the excess pore water pressure is being determined.

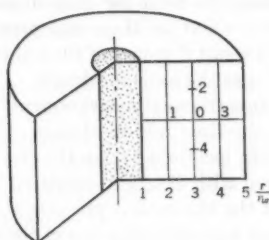
From Eq. 34(a) it is evident that a different equation must be used for each point under consideration, due to the specific value of r at each location. This slows the computations but does not otherwise complicate the solution. Fig. 12 illustrates the procedure for solution of a problem for radial flow in a homogeneous soil cylinder for the case of $n = 5$. As used in Fig. 12,

$$u_{o,t+\Delta t} = u_{o,t} + \frac{4r_o^2 \Delta T}{\Delta r^2} \left[\left(1 + \frac{\Delta r}{2r}\right) u_{3,t} + \left(1 - \frac{\Delta r}{2r}\right) u_{1,t} - 2u_{o,t} \right] \dots (34b)$$

in which $\Delta r = r_w$, $r_o = 5 r_w$, and $\Delta T_h = \frac{0.5 (\Delta r)^2}{4 r_o}$. By taking the average value of the excess pressure at any time, a curve of \bar{u}_r versus T_h can be constructed that corresponds to within a few percent of the values obtained by Mr. Barron's¹⁰ procedure.

Additional Variables Which Can be Treated by the Numerical Procedure.—

Because the numerical procedure involves the building up of a solution throughout a series of time intervals, it is ideally suited for consideration of quantities



$\frac{r}{r_w}$	1	2	3	4	5	$T_h \times 10^2$
0	100	100	100	100	100	0
0	62.5	100	100	100	100	0.5
0	62.5	84.4	100	100	100	1.0
0	52.7	84.4	93.2	100	100	1.5
0	52.7	76.3	93.2	93.2	100	2.0
0	43.8	64.3	78.9	78.9	100	4.0
0	26.4	38.8	47.7	47.7	100	10.0
0	11.5	16.9	20.7	20.7	100	20.0

FIG. 12.—NUMERICAL PROCEDURE FOR CONSOLIDATION BY RADIAL FLOW

that vary with time. For cases in which the surface load is varied during consolidation, this can be introduced into the problem simply as an over-all increase (or decrease) of the excess pore water pressure at a particular time. A gradually increasing load can be approximated by using a staircase variation of load with time.

Variations of fundamental soil properties, such as the coefficients of consolidation or swelling, can be included as they vary both with time and space. That is, the intergranular pressure changes affect the soil properties, which may be adjusted accordingly during the period of consolidation. The soil properties are considered to be constant during an interval of time, Δt , in accordance with the assumptions of the theory of consolidation, but the value of these constants may be changed in successive time intervals. The soil constants may also have different initial values at the various space locations of the network points under consideration.

The flexibility of the numerical procedures also permits studies of two and three-dimensional consolidation to be made without excessive effort. For example, R. E. Gibson and P. Lumb¹⁸ have obtained approximate solutions

for the time rate of settlement of circular pervious and impervious footings, resulting from consolidation of the underlying clay.

USE OF THEORIES FOR DESIGN OR ANALYSIS OF SAND DRAIN INSTALLATIONS

Limitations.—The theories for consolidation of clay layers including the effects of sand drains can be expected to give reasonable results only when the clay is comparable to the ideal material assumed as a basis for the theory. This requires the clay layer to be homogeneous if the analytical theories are to be used, or at least homogeneous in horizontal planes, and the variations in soil properties known in vertical direction, if the numerical procedures are to be used.

In addition, it is necessary that the values of the soil properties be established with a reasonable degree of accuracy. The coefficients of consolidation due to vertical and to horizontal flow of water, and the coefficients of permeability in the vertical and horizontal directions as well as for remolded samples, must all be determined from a large enough number of samples that a reliable average value of each is established. Because the need for sand drains and their effectiveness, if installed, is directly dependent on these soil properties, it is evident that serious miscalculations could result if values of the soil properties are inaccurately determined and then used as the basis for design.

Use of Point Pore Pressures.—In addition to settlement measurements which can be compared to theoretical predictions, the time rate of change of excess pore water pressure may be measured at specific locations within the clay layer. These pressure measurements can be compared with diagrams prepared by use of Eq. 7 and Eq. 12 or Eq. 15 which predict the theoretical pressure-time behavior during consolidation. However, unless a good evaluation of the radius of the smeared zone at the well periphery and the coefficient of permeability within this smeared region were obtained, it is likely that a considerable difference may occur between the geometrical value of $n \left(= \frac{d_s}{d_w} \right)$ and the effective value of n which includes the effect of well smear. This will lead to appreciable variation in the predicted excess pore pressure versus time relations.

Difficulties also arise in comparison of theoretical and field results. This is due partially to the fact that the piezometer readings define the behavior of the clay at a point, or at least within a small volume, while the theoretical predictions are based, at best, on representative values of the soil properties. It would be expected that better agreement between actual consolidation behavior and that predicted from theory would be obtained by increasing the number of piezometer installations, thereby minimizing the effects of local variations in soil properties.

CONCLUSIONS

In the preceding pages the available theories for vertical consolidation due to vertical flow and due to radial flow of water to a drain well have been reviewed. These theories are entirely satisfactory for the analysis of any situation conforming to the assumptions on which these theories are based.

Including void ratio as a variable did not significantly change the consolidation-time characteristics of vertical consolidations by vertical flow. Thus, a consideration of variable void ratio does not contribute to the explanation of secondary consolidation.

For vertical consolidation due to radial flow toward a drain well, the equal strain solutions given by Mr. Barron are much more convenient to use than are the free strain solutions. Using Mr. Barron's equal strain solutions for ideal wells and for smeared wells, it was shown that the consolidation behavior of the latter is identical to that of an equivalent ideal well of reduced diameter. Diagrams are given for quantitative evaluation of this relation between behavior of smeared and equivalent ideal wells. By interpreting the consolidation behavior due to an actual well in terms of that of an equivalent ideal well, the figures prepared by Mr. Barron for ideal wells can be used directly for design or analysis. An example shows the effectiveness of even a small diameter ideal well.

The numerical procedures for solving consolidation problems were found to be versatile aids for both checking the classical solutions and for evaluating new problems. Variable rates of loading, variable soil properties, and layered systems, can be readily included into the solution of consolidation problems by these methods.

ACKNOWLEDGMENTS

This review of the theories of sand drains was prepared for Moran, Proctor, Mueser, and Rutledge, Consulting Engineers, as a part of their research project for the Bureau of Yards and Docks, Department of the Navy, on the study and evaluation of sand drain installations. The author is grateful to the Bureau of Yards and Docks for their permission to publish the results of this section of the study.

The author wishes to acknowledge particularly the valuable advice and suggestions given by P. C. Rutledge, M. ASCE, and S. J. Johnson, M. ASCE. R. L. Schiffman, J. M. ASCE, checked the derivations of Barron's equations under the writer's supervision.

APPENDIX I. DERIVATION OF CONSOLIDATION EQUATIONS INCLUDING VOID RATIO AS A VARIABLE

For a soil element of area A and height dz (Fig. 13) the volume of solids can be represented by a height dh which does not change during the consolidation process. The total height of the element may always be determined by the relation $dz = (1 + e) dh$. The change of volume of a soil element is dependent on the change of the volume of voids which is $V_v = A e dh$. Thus, the change of volume with time is

$$\frac{\partial V}{\partial t} = - A dh \cdot \frac{\partial e}{\partial t} \dots \dots \dots (35)$$

Next, considering the upward vertical flow of water through this elemental volume, an amount equal to $-\frac{k}{\gamma_w} \frac{\partial u}{\partial z} A$ flows through the bottom face, and

an amount equal to $\frac{kA}{\gamma_w} \left(-\frac{\partial u}{\partial t} - \frac{\partial^2 u}{\partial z^2} dz \right)$ flows through the top face. The difference between flow at these two surfaces determines the rate of loss of water from the soil element as

$$\Delta Q = -\frac{k}{\gamma_w} \frac{\partial^2 u}{\partial z^2} A dz \dots \dots \dots (36)$$

Since it was assumed that the soil was completely saturated, and that both water and the solid soil particles are incompressible, the rate of water loss (Eq. 36) must equal the rate of volume change of the soil element (Eq. 35) or,

$$-A dh \frac{\partial e}{\partial t} = -\frac{k}{\gamma_w} \frac{\partial^2 u}{\partial z^2} A dz \dots \dots \dots (37)$$

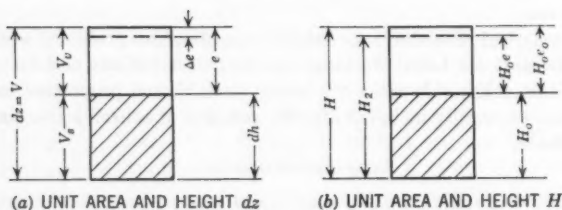


FIG. 13.—COMPONENTS OF A VOLUME OF SOIL

In order to convert Eq. 37 into terms involving h , the following relations may be used.

$$\frac{\partial u}{\partial z} = \frac{\partial u}{\partial h} \frac{\partial h}{\partial z} = \frac{\partial u}{\partial h} \frac{1}{1+e} \dots \dots \dots (38)$$

$$\frac{\partial^2 u}{\partial z^2} = \frac{\partial h}{\partial z} \frac{\partial}{\partial h} \left(\frac{\partial u}{\partial h} \frac{1}{1+e} \right) = \frac{1}{(1+e)^2} \left[\frac{\partial^2 u}{\partial h^2} - \frac{1}{(1+e)} \frac{\partial u}{\partial h} \frac{\partial e}{\partial h} \right] \dots \dots \dots (39)$$

$$\frac{\partial \bar{\sigma}}{\partial t} = -\frac{1}{a_v} \frac{\partial e}{\partial t} = -\frac{\partial u}{\partial t} \dots \dots \dots (40)$$

and

$$\frac{\partial \bar{\sigma}}{\partial h} = -\frac{1}{a_v} \frac{\partial e}{\partial h} = -\frac{\partial u}{\partial h} \dots \dots \dots (41)$$

in which $\bar{\sigma}$ is the effective, or intergranular pressure at any point in the soil layer.

By substituting Eqs. 38, 39, 40, and 41 into Eq. 37 the expression is,

$$\frac{\partial u}{\partial t} = \frac{k}{a_v \gamma_w} \frac{1}{(1+e)} \left[\frac{\partial^2 u}{\partial h^2} - \frac{a_v}{1+e} \left(\frac{\partial u}{\partial h} \right)^2 \right] \dots \dots \dots (42)$$

which is the general equation for consolidation with void ratio considered as a variable.

For a solution of Eq. 42 by the explicit numerical scheme, it was found convenient to substitute terms for void ratio in place of those for u , according to Eqs. 40 and 41. The resulting difference equation is

$$e_{o,t+\Delta t} = e_{o,t} + \frac{k \Delta t}{a_v \gamma_w (\Delta h)^2} \left[\frac{e_{2,t} - 2e_{o,t} + e_{4,t}}{1 + e_{o,t}} - \frac{(e_{2,t} - e_{4,t})^2}{4(1 + e_{o,t})^2} \right] \dots (43)$$

Let

$$T = \frac{k \cdot t}{a_v \gamma_w (H_o)^2} \dots (44a)$$

or

$$\Delta T = \frac{k \Delta t}{a_v \gamma_w (H_o)^2} \dots (44b)$$

which is similar to T_v (Eq. 8) in appearance and is related by $T = T_v (1 + e_o)$ since $H = H_o (1 + e_o)$ as shown on Fig. 13.

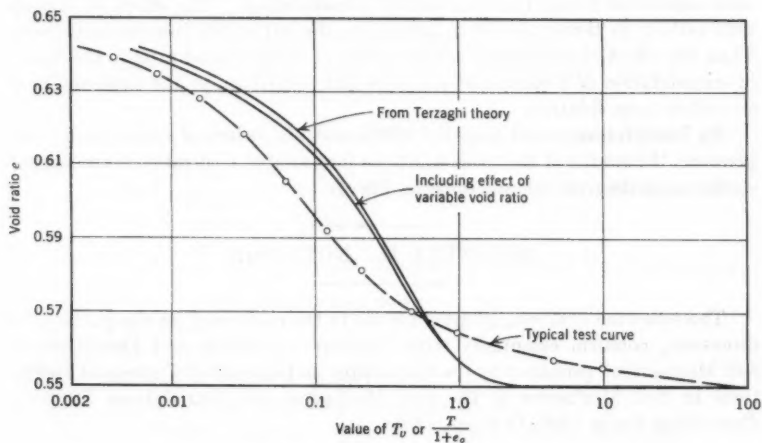


FIG. 14.—VOID RATIO VERSUS TIME FACTOR

Again

$$\zeta = \frac{h}{H_o} = \frac{h(1 + e_o)}{H(1 + e_o)} = \frac{z}{H} \dots (45a)$$

or

$$\Delta h = \Delta \zeta \cdot H_o \dots (45b)$$

and

$$\frac{k \Delta t}{a_v \gamma_w (\Delta h)^2} = \frac{\Delta T}{(\Delta \zeta)^2} = B \dots (46)$$

The curves shown on Fig. 1 were obtained by use of Eq. 43.

During consolidation, the void ratio changes with time from an initial value of e_o to a final value of e_2 which is reached at an infinite time. Thus, e_o and e_2

are taken as the boundary values, and Eq. 43 determines the manner in which the void ratio changes with time.

The void ratio versus the time factor curve that results from using the boundary values of $e_o = 0.65$, and $e_z = 0.55$ with Eq. 43 is shown as the solid line on Fig. 14, which is designated as including effect of variable void ratio. The other curve on Fig. 14 drawn as a solid line represents the results obtained from the Terzaghi theory if e_o and e_z are considered to represent 0% and 100% consolidation, respectively. The dashed curve represents a typical consolidation test, converted into terms of e and T_v , which exhibits the region of "secondary" consolidation.

Secondary consolidation is characterized by a nearly linear relation between decrease in void ratio and logarithm of time, over a considerable period of time during the final part of the test.

From Fig. 14 it is evident that the modification of the Terzaghi theory to include the consideration of variable void ratio does not appreciably change the void ratio-time factor relations during consolidation. The effect of variable void ratio is to throw the curve slightly to the left of the conventional curve. Thus, the effect of including a consideration of variable void ratio in the theory of consolidation of a saturated soil does not contribute to the explanation of secondary consolidation.

By interpreting e_o and e_z as the 100% and 0% values of excess pore water pressure, the results of the three solutions for variable void ratio can be plotted on the same diagram, as was done on Fig. 1.

APPENDIX II. NOTATION

The following symbols, adopted for use in the paper and for the guidance of discussers, conform essentially with "Glossary of Terms and Definitions in Soil Mechanics," prepared by the Committee on Glossary of Terms and Definitions in Soil Mechanics of the Soil Mechanics and Foundations Division, *Proceedings Paper 1826*, October, 1958:

$$A = \text{area, or } A = \frac{c_v \Delta t}{\Delta z^2} = \frac{k(1+e)\Delta t}{a_v \gamma_w (\Delta z)^2};$$

a_v = coefficient of compressibility;

$B = \frac{k \Delta t}{a_v \gamma_w (\Delta h)^2}$ = constant in numerical solution including variable void ratio;

c_v = coefficient of consolidation;

c_{vr} = coefficient of consolidation due to radial water flow;

d_e = diameter of well influence;

d_w = diameter of drain well;

e = void ratio at any point in the soil layer;

\bar{e} = average value of the void ratio in the soil layer;

$f(n)$ = function of n for equal strain solution (Eq. 18);

H = thickness of clay layer which is drained from one surface only, or half thickness of clay layer drained from top and bottom surfaces;

H_o = equivalent thickness of layer of solids in a clay layer of over-all thickness, H (Fig. 13);

h = measure of distance;

$J_o()$ = Bessel function of the first kind, zero order;

$J_1()$ = Bessel function of the first kind, first order;

k = coefficient of permeability (LT^{-1}):

k_h = coefficient of permeability in the horizontal direction;

k_v = coefficient of permeability in the vertical direction;

k_s = coefficient of permeability in the smeared zone;

$n = \frac{r_e}{r_w} = \frac{d_e}{d_w}$ = ratio of diameter of well influence to diameter of drain well;

$p = \bar{\sigma} + u$ = total pressure at any point in the soil layer;

r = radius:

r_s = radius of influence of drain well;

r_e = radius defining boundary of smeared zone;

r_w = radius of drain well;

$s = \frac{r_e}{r_w}$ = ratio of radius of smeared zone to radius of drain well;

$T_h = \frac{k_h (1 + e) t}{\gamma_w a_v d_e^2}$ = dimensionless time factor for consolidation by radial water flow;

$T_v = \frac{k_v (1 + e) t}{\gamma_w a_v H^2}$ = dimensionless time factor for consolidation by vertical water flow;

t = time;

Δt = time interval;

t_{90} = time for 90% consolidation;

\bar{U} = average percentage of consolidation;

u = excess pore water pressure at a point in the clay layer;

\bar{u} = average value of pore water pressure in the clay layer;

u_r = excess pore water pressure at a point in the clay layer as a result of radial flow of water;

u_x = excess pore water pressure at a point in the clay layer as a result of water flow in the x -direction;

u_z = excess pore water pressure at a point in the clay layer as a result of vertical flow of water;

$u_{o,t}$ = excess pore water pressure at point o , at time t ;

$u_{2,t+\Delta t}$ = excess pore water pressure at point 2, at time $t + \Delta t$;

V_v = volume of voids;

$Y_o()$ = Bessel function of the second kind, zero order;

$Y_1()$ = Bessel function of the second kind, first order;

z = distance below the top surface of a clay layer;

Δz = interval of z ;

$\alpha_1, \alpha_2, \alpha_3, \dots$ = roots of the Bessel function;

γ_w = density of water;

e = base of natural logarithms = 2.718...;

$\lambda = \frac{-8 T_h}{f(n)}$ = exponent for the "equal strain" solution;

$\xi = \frac{8 T_h}{v}$ = exponent in solution for equal strain with smear;

v = factor in the solution for equal strain with smear (Eq. 20);

$\zeta = \frac{z}{H}$ = ratio of depth to a point to the thickness of the clay layer; and

$\bar{\sigma}$ = effective, or intergranular pressure at any point in the soil layer.

DISCUSSION

YOSHICHIKA NISHIDA²¹.—The author has presented a review that is useful for performing computations on sand drains. Mr. Richart has stated that including the effects of variable void ratio did not contribute to the explanation of secondary consolidation, and this is agreed with by the writer. The secondary consolidation appears to be due mainly to the creep or the flow of clay, and it occupies, in some cases, more than 50% of the consolidation. Mr. Richart checked the influences of well spacing, and his conclusion, that the radial flow dominated the consolidation-time behavior, is easily understood. The fact that doubling of the diameter of well influence, or the well spacing, causes an increase in the time for 90% consolidation by roughly a factor of 6 agrees with the value of 5.65 obtained from studies made in Japan. These studies showed that the time for consolidation is proportional to the 2.5 power of the well spacing. The writer wishes to know the most suitable spacing from the practical point of view, because a spacing that is too small brings the influence of remolding and smearing to the clay.

S. J. JOHNSON,²² M. ASCE.—A singularly penetrating analysis of the influence of the various factors affecting the theoretical aspects of the design of sand drains has been presented by the author. The review of numerical methods of solution of consolidation phenomena and the means of taking into account variable loading and soil characteristics can be applied to problems of consolidation due to vertical flow and radial flow—of general interest beyond the particular field of sand drains. The effect of the diameter of sand drains pointedly illustrates how easy it would be to over-assess the importance of large diameters. However, the very small diameters referred to are presumably used only for illustration by the author. The writer interprets this presentation as not meaning to imply that such small diameters would be practicable for sand drains installed by methods currently used.

It is necessary for some purposes to know the theoretical excess pore water pressures at specific locations when piezometers are used for field control purposes and for evaluation of the coefficient of consolidation. These can be simply prepared from the property that, for the equal strain theory, the plot of $\log u/u_0$ versus the time factor is a straight line, as illustrated on Fig. 15(a). Also, the same is true for average excess pore water pressures as plotted on Fig. 15(b). This is not true for average consolidation due to vertical flow, which is plotted in a similar manner in Fig. 15(c). Fig. 15(a) shows the plots of curves for hydrostatic excess pressure versus time factor T_h and drain spacing, n , at the outer boundary, $r = 1.0 r_e$ and r_e being equal to the effective radius of influence of the sand drain. The curves in Fig. 15(b) are plotted for the average hydrostatic excess pressure versus time factor, T_h , and average consolidation, $\frac{\bar{u}}{u_0}$, for a varying drain spacing, $n = d_e/d_w$. The curve in Fig. 15(c) was

²¹ Lecturer, Kanazawa Univ., Ueno-hon-machi, Kanazawa-shi, Japan.

²² Associate, Moran, Proctor, Mueser & Rutledge, New York, N. Y.

plotted for the average hydrostatic excess pressure versus the time factor T_v and average consolidation, $\frac{u}{u_o}$ for consolidation resulting only from vertical drainage, Figs 15(a) and 15(b) are obtained as follows:

Eq. 15 and Eq. 16 can be written, for any specific sand drain installation and any point, r , from the drain, as:

$$\frac{u_r}{u_o} = \frac{4 \epsilon^\lambda}{d_e^2 f(n)} \left[r_e^2 \log_e \frac{r}{r_w} - \frac{r^2 - r_w^2}{2} \right] \\ = \text{constant} \times \epsilon^\lambda = \text{constant} \times \left\{ - \left[\frac{8 T_h}{f(n)} \right] \right\} \dots (47)$$

Therefore,

$$\log_e \frac{u_r}{u_o} = C_1 + C_2 T_h \dots (48)$$

in which

$$C_1 = \log_e \left\{ \frac{4}{d_e^2 f(n)} \left[r_e^2 \log_e \frac{r}{r_w} - \frac{r^2 - r_w^2}{2} \right] \right\} \dots (49)$$

and

$$C_2 = - \frac{8}{f(n)} \dots (50)$$

This is the equation of a straight line when u_r/u_o is plotted to a log scale and T_h is plotted to an arithmetic scale. Fig. 15(a) is this relationship at the external boundary where $r = d_e/2$.

The relationship between the average excess pore water pressure from $r = r_w$ to $r = r_e$, and the time factor T_h is given by:

$$\frac{\bar{u}}{u_o} = \epsilon^\lambda = \epsilon^{-8 T_h / f(n)} \dots (51)$$

from which:

$$\log \frac{\bar{u}}{u_o} = - \frac{8}{f(n)} T_h \dots (52)$$

This is also the equation of a family of straight lines, as plotted on Fig. 15(b). Plots of this type shown on Fig. 15(a) and Fig. 15(b) are readily constructed and are useful in analysis of field observations as well as in initial design.

F. E. RICHART, Jr.,²³ M. ASCE.—The writer wishes to thank Mr. Nishida and Mr. Johnson for their interest in the paper and for their generous comments.

Mr. Nishida notes that a study made in Japan found that the time for consolidation is proportional to the 2.5 power of the well spacing. By use of Eq. 16 the time required for a particular degree of consolidation is proportional

²³ Div. of Eng. and Applied Physics, Harvard Univ., Cambridge, Mass.

to the 2.76 power and the 2.38 power of the well spacings when comparing times for 5 ft and 10 ft spacings, and 20 ft and 40 ft spacings, respectively. Thus, the use of the 2.5 power of the well spacing agrees quite well with results obtained from Barron's equal strain condition of consolidation.

With regard to Mr. Nishida's request for information on the most suitable well spacing from the practical point of view, this would necessarily depend on local soil and construction conditions. The terms "suitable" and "practical" imply that the spacings must be feasible and economical in both time and money. From a recent study of existing sand drain installations^{24,25} the well spacings most frequently used in 83 installations were 8 ft to 10 ft.

Mr. Johnson is correct in his interpretation of the effectiveness of small diameter ideal wells. The writer was not proposing the use of actual sand drains of 1 in. or 2 in. in diameter. The discussion was intended to point out that even if the smeared zone around a 10 in. or 12 in. diameter actual drain well restricted drainage until the time for consolidation was comparable to that for a 1 in. or 2 in. diameter ideal well, the drain well would still be effective in reducing the time for consolidation.

Fig. 15 showing pore pressure on a log scale versus time factor on an arithmetic scale is most convenient. Values may be readily obtained from the figure, and there is little chance of drafting errors in constructing the diagrams. The writer thanks Mr. Johnson for pointing out this effective method of plotting consolidation-time information.

²⁴ "Study of Deep Soil Stabilization by Vertical Sand Drains," *Report No. 1*, by Moran, Proctor, Mueser, and Rutledge, Cons. Engrs., New York, N. Y., prepared for the Dept. of the Navy, Bureau of Yards and Docks, June, 1956.

²⁵ "Review of Uses of Vertical Sand Drains," by P. C. Rutledge and S. J. Johnson, presented at the 36th Annual Meeting of the Highway Research Board, Washington, D. C., January, 1957. *See 173*

AMERICAN SOCIETY OF CIVIL ENGINEERS

Founded November 5, 1852

TRANSACTIONS

Paper No. 3000

FIXED-WHEEL GATES FOR PENSTOCK INTAKES

BY SYLVAN J. SKINNER¹

WITH DISCUSSION BY MESSRS. JOSEPH R. BOWMAN;
AND SYLVAN J. SKINNER

SYNOPSIS

The paper covers the major design problems and the present design treatment by the Bureau of Reclamation, United States Department of the Interior, of high-head flat structural steel fixed-wheel gates used for emergency closure of penstock or other conduit intakes.

INTRODUCTION

In general, the designations "fixed-wheel gate" or "coaster gate" refer to fabricated flat structural steel gates used for high-head emergency applications, whereas radial gates, drum gates, and roller gates are usually considered as surface-regulating gates. The proportions and designs of fixed-wheel gates and coaster gates are determined primarily by their application for regulating flow in spillways or for emergency closure of the intake of penstocks, outlets, tunnels, or in surge tanks. The intended function, operating facilities, and equipment to be provided for handling during installation and for later servicing also have an important part in the design. Their use is restricted usually to cases in which emergency closure may be required to cut off the flow of water through penstocks or conduits in order to protect other equipment in the system. In addition to this emergency feature, their normal function is to close the conduit intake under balanced pressure conditions (no flow) so that the conduit may be unwatered for inspection or for the inspection and servicing of turbines, valves, and other equipment. They are usually raised (opened) under balanced pressures.

Design principles and general construction of fixed-wheel gates and coaster gates are similar, the main variation being in the mountings. Coaster gates

NOTE.—Published, essentially as printed here, in October, 1957, in the *Journal of the Power Division*, as *Proceedings Paper 1420*. Positions and titles given are those in effect when the paper or discussion was approved for publication in *Transactions*.

¹ Mech. Engr., Mech. Branch, Bureau of Reclamation, U. S. Dept. of the Interior, Denver, Colo.

are mounted on roller trains instead of wheels. They can be operated under higher heads because the roller mountings offer much less frictional resistance to movement than do bushed wheels. Coaster gates are more suitable for regulating purposes under high heads because they are less susceptible to vibration when operating for extended periods (at partial opening) with high-velocity flow. A more even distribution of load to the embedded gate frames and concrete structures is obtained with the coaster gate. Their main disadvantages are higher initial and maintenance costs resulting from the multiplicity of moving parts, and the accuracy of fit required for proper functioning. Therefore, the more rugged fixed-wheel gates are used whenever possible.

The gates are normally held in the open (stored) position, directly above the conduit intake, by hydraulic hoists located at the top of the dam or gate shaft. This position reduces the time required for emergency closure to a minimum. The hoists are connected to the gates by alloy steel or monel stems. The gates are lowered to the closed position under their own weight by releasing the supporting oil from the hoist cylinder, no downward force being exerted by the hoist. The design features of the fixed-wheel gate and its supporting frame,

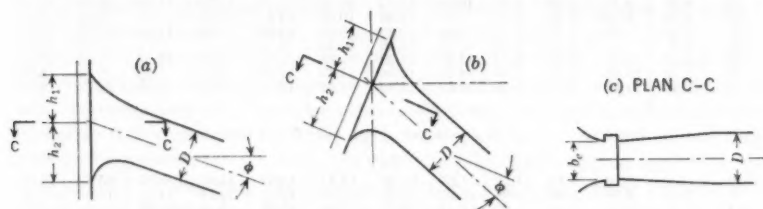


FIG. 1.—INTAKE PROPORTIONS FOR GATE SIZES

guides and anchorage for penstock intakes, as currently treated by the Bureau of Reclamation (USBR), United States Department of the Interior, are presented herein.

Notation.—The letter symbols adopted for use in this paper are defined where they first appear and are arranged alphabetically, for convenience of reference, in Appendix I.

GENERAL FEATURES AFFECTING DESIGN

As in any structure, the principal considerations in the design of a fixed-wheel gate are the magnitude of loading, the size of the gate, and the adequacy of its supports. The width and height of the gate are determined by the size of the penstock or conduit, and by the shape and slope of the intake which the gate is to close (seal off from the flow of water). The proportions of the trashrack and the penstock intake structures are determined by flow characteristics necessary to obtain Q , the required flow in cu ft per sec for operating the hydroelectric equipment at the power plant. The design of the trashrack and intake structures is beyond the scope of the paper. However, the nominal size of the gate required to close the intake is determined by the proportions of the rectangular entrance of the transition to the circular penstock. The face of the

rectangular transition entrance is usually coincident with the face of the dam and with the downstream face of the gate slot. Fig 1(a) shows an intake with a vertical face and in Fig. 1(b) the intake has a sloping face. The same nominal gate size will apply to an intake with either a vertical or a sloping face for the same size penstock, provided that the angle, θ , between the centerline of the penstock and the plane normal to the intake face, has the same magnitude.

TABLE 1.—PRELIMINARY ESTIMATION OF PENSTOCK INTAKE PROPORTIONS

Angle θ , in degrees	h_1	h_2	b_e	h_1	h_2	b_e	h_1	h_2	b_e	h_1	h_2	b_e
(1)	(2)	(3)	(4)	(5)	(6)	(7)	(8)	(9)	(10)	(11)	(12)	(13)
	(a) $D=10$ feet			(d) $D=13$ feet			(g) $D=16$ feet			(j) $D=19$ feet		
0	7.91	7.91	8.28	10.28	10.28	10.76	12.65	12.65	13.25	15.03	15.03	15.74
5	7.12	8.01	8.69	9.25	10.42	11.28	11.38	12.82	13.92	13.52	15.22	16.52
10	6.63	8.17	8.96	8.63	10.62	11.66	10.62	13.06	14.36	12.51	15.52	17.13
15	6.37	8.40	9.18	8.28	10.93	11.93	10.18	13.45	14.70	12.10	15.96	17.46
20	6.28	8.70	9.30	8.17	11.31	12.06	10.05	13.93	14.85	11.95	16.53	17.65
25	6.30	9.09	9.39	8.19	11.83	12.20	10.07	14.55	15.03	11.96	17.28	17.86
30	6.41	9.57	9.48	8.33	12.44	12.30	10.25	15.30	15.15	12.17	18.17	18.00
35	6.64	10.19	9.49	8.64	13.26	12.33	10.64	16.32	15.16	12.63	19.36	18.04
40	6.99	10.98	9.52	9.09	14.28	12.36	11.19	17.57	15.23	13.29	20.87	18.09
45	7.44	11.97	9.54	9.68	15.57	12.40	11.92	19.16	15.26	14.15	22.75	18.13
	(b) $D=11$ feet			(e) $D=14$ feet			(h) $D=17$ feet			(k) $D=20$ feet		
0	8.70	8.70	9.10	11.07	11.07	11.52	13.44	13.44	14.07	15.82	15.82	16.56
5	7.83	8.80	9.62	9.96	11.22	12.16	12.10	13.62	14.78	14.23	16.02	17.38
10	7.30	8.98	9.88	9.29	11.44	12.57	11.28	13.88	15.26	13.27	16.33	17.97
15	7.01	9.24	10.10	8.92	11.76	12.86	10.83	14.28	15.62	12.74	16.80	18.36
20	6.92	9.57	10.22	8.80	12.17	13.01	10.68	14.79	15.80	12.57	17.40	18.60
25	6.93	10.01	10.33	8.82	12.74	13.13	10.72	15.46	15.97	12.60	18.19	18.77
30	7.05	10.53	10.42	8.97	13.39	13.25	10.89	16.26	16.10	12.82	19.13	18.94
35	7.32	11.22	10.43	9.30	14.27	13.28	11.30	17.34	16.13	13.29	20.38	18.97
40	7.69	12.08	10.46	9.79	15.38	13.33	11.89	18.67	16.16	13.99	21.95	19.04
45	8.18	13.17	10.48	10.43	16.76	13.35	12.66	20.35	16.20	14.89	23.95	19.07
	(c) $D=12$ feet			(f) $D=15$ feet			(i) $D=18$ feet					
0	9.49	9.49	9.93	11.86	11.86	12.42	14.23	14.23	14.93			
5	8.54	9.61	10.43	10.67	12.02	13.04	12.80	14.42	15.64			
10	7.97	9.80	10.78	9.95	12.24	13.50	11.95	14.69	16.16			
15	7.64	10.08	11.02	9.55	12.60	13.76	11.46	15.13	16.47			
20	7.54	10.44	11.14	9.43	13.05	13.94	11.32	15.66	16.72			
25	7.57	10.92	11.26	9.45	13.64	14.10	11.34	16.37	16.89			
30	7.69	11.48	11.36	9.61	14.35	14.20	11.54	17.22	17.04			
35	7.98	12.24	11.37	9.97	15.30	14.23	11.96	18.35	17.06			
40	8.39	13.18	11.41	10.49	16.47	14.26	12.59	19.76	17.12			
45	8.93	14.37	11.44	11.16	17.96	14.31	13.40	21.55	17.16			

Table 1 lists intake proportions from which preliminary gate sizes may be obtained with sufficient accuracy for basing gate design stress computations and proportioning the various parts of the gate and its supporting frame. Table 1 is used in conjunction with Fig. 1 and is based on the following:

$$h_1 = \left(\sqrt{1.21 \tan^2 \theta + .0847} + \frac{1}{2 \cos \theta} - 1.10 \tan \theta \right) D \dots \dots (1)$$

and

$$h_2 = \left(\frac{0.791}{\cos \theta} + .077 \tan \theta \right) D \dots \dots \dots (2)$$

The opening area = $\frac{\text{penstock area}}{0.6 \cos \theta}$; $b_e = \frac{\text{opening area}}{h_1 + h_2}$; D denotes the nominal diameter of the penstock in feet; and h_1 , h_2 , and b_e are the transition face dimensions in feet. The nominal size of the gate is b_e feet wide by $(h_1 + h_2)$ feet high.

At an early stage in the proportioning of the intake structure and its emergency gate the operating requirements of the gate should be evaluated. This requires a determination of whether the gate can be closed by its own weight under free-flow emergency conditions. Free-flow emergency conditions are assumed to be equivalent to the flow from a burst penstock, if exposed, or to a runaway turbine with its wicket gates and protecting valve open and inoperative at the power plant. This evaluation is a compilation or summary of vertical forces existing during the closing and opening cycle of the gate. In so far as operation of the gate is concerned, the closing cycle is the more important because it determines whether closing can be accomplished by the weight of the gate alone. It determines also whether a normal fixed-wheel gate installation will be adequate or whether special considerations may be required, such as using retractable seals which practically eliminate seal friction, installing a coaster gate, or providing a hoist with supported stems capable of exerting sufficient downward force to close the gate. Each of these special features adds considerably to the cost. In such a summary the gate weight (submerged weight when downstream skinplate and seals are used) is the downward (positive) force, P_p . The sum of the forces resisting downward movement is considered the negative force, P_n . This negative force essentially comprises the wheel bearing friction, F_b , the wheel rolling friction on track, F_r , and the seal friction on the embedded seal seats, F_s . Of these, the wheel bearing friction, F_b , and the seal friction, F_s , are the most critical as they usually account for approximately 97% of the total negative force.

$$P_n = F_b + F_r + F_s \dots \dots \dots (3)$$

Experience demonstrates that a minimum wheel diameter to pin diameter (wheel-pin) ratio of approximately 5 to 1 is normally required to obtain a sufficiently low amount of wheel bearing friction for gates operating under high heads. Seal friction is greatly reduced by bonding a comparatively thin brass nosing over the bulb of the seal as indicated in Fig. 9 (to be shown and examined subsequently). The wheel rolling friction, F_r , being a very small percentage of the total negative force, is occasionally neglected in the preliminary summary of forces. Guide shoe friction is a negligible quantity because it can be no greater than a fraction of the guide shoe spring capacity. This spring capacity is seldom greater than 200 lb at maximum operating deflection.

The excess downward force available for closing the gate by its own weight is P_e .

$$P_p - P_n = P_e \dots \dots \dots (4)$$

An allowable minimum value of 25% of the total negative forces, P_n , is used for P_e . This is a safety factor to compensate for variations from assumed values of friction coefficients and unevaluated contingencies,

$$P_e = .25 P_n \dots \dots \dots (5)$$

in which P_e is the minimum allowable excess force. The wheel bearing friction is

$$F_b = \frac{W u_1}{5} \dots \dots \dots (6)$$

in which W represents the unbalanced hydrostatic load on the closed gate, in pounds; u_1 denotes the coefficient of friction for wheel bearings, assumed as 0.10

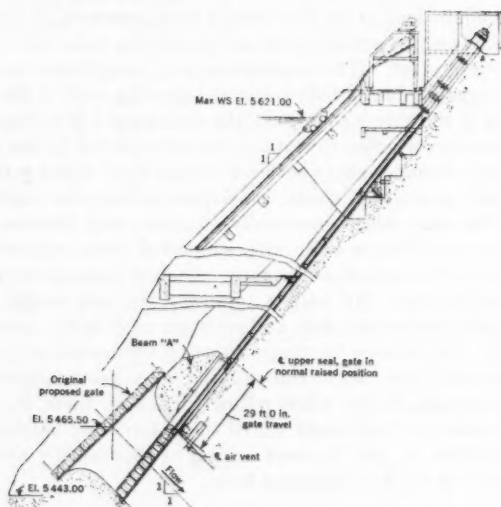


FIG. 2.—PENSTOCK SLOPING FACE INTAKE

for self-lubricating graphite-insert type bushings; and the wheel-pin ratio assumed for preliminary summary of forces is 5. The wheel rolling friction is

$$F_r = \frac{W u_2}{R_2} \dots \dots \dots (7)$$

in which u_2 is the coefficient of rolling friction assumed as 0.01 for steel on steel and R_2 represents the radius of wheels. The seal friction,

$$F_s = .217 H_a u_3 l = .091 H_a l \dots \dots \dots (8)$$

in which H_a denotes the average hydrostatic head at the horizontal centerline of gate; u_3 is the coefficient of friction for rubber-brass seals assumed as 0.42; and l denotes the total length in inches of rubber-brass seal on gate.

For a vertical or nearly vertical face of structure there is usually no particular difficulty in obtaining a sufficiently adequate excess downward force, P_e . A thorough analysis of the summary of forces is particularly important on installations where the face of the structure is on a comparatively flat slope. The fixed-wheel gate installations for the outlet and power tunnel intakes at the Palisades Dam on the South Fork of the Snake River near Idaho Falls, Idaho, are examples in which special treatment was required to reduce the gate size and resulting hydraulic hoist capacity requirements. The original plans

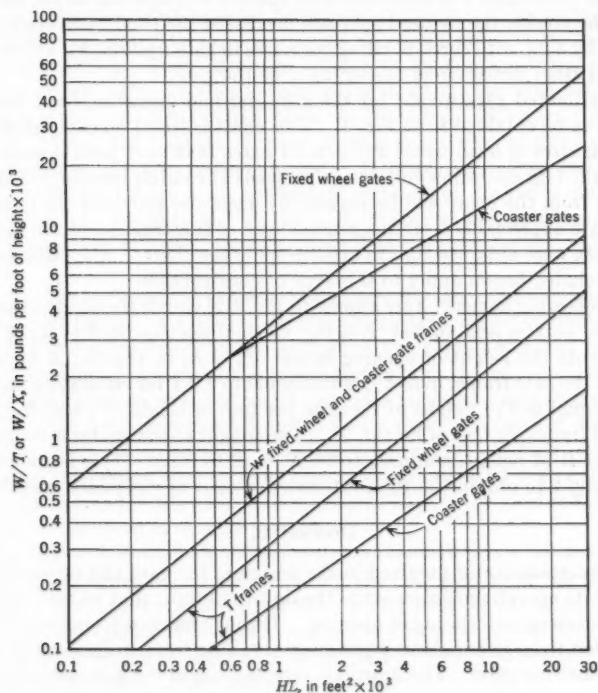


FIG. 3.—WEIGHT OF COASTER AND FIXED-WHEEL GATES

proposed the use of a normal face type gate installation as seen at the face of the intake in Fig. 2. This required 19.25-ft-by-46-ft fixed-wheel gates with an estimated weight of 442,000 lb each, and embedded gate frame and guides estimated at 200,000 lb for each gate. The sum of the submerged gate weight component and the hydrostatic load on the gate produced wheel and seal friction resistance to gate-closing movement that required an hydraulic hoist of extremely high capacity and a supported stem capable of exerting a heavy downward thrust on the gate. Design studies and hydraulic laboratory model tests indicated that the arrangement and proportions shown in Fig. 2 would be the

most satisfactory installation. The concrete beam, A, serves two major purposes. It permits retention of required intake proportions for desirable flow characteristics and relocates the gate slot a sufficient distance downstream from the face of the intake structure to materially reduce the gate size to 19.67 ft by 28.03 ft. This change in size reduced the weight of each gate to 280,000 lb, a decrease of 162,000 lb or nearly 36% of the estimated gate weight for the original plan. The weight of the frame and guides was reduced to 102,500 lb for each gate, nearly a 50% decrease. Although the maximum head at the centerline of the gate was increased from 155.5 ft to 168 ft due to the lower location in the intake, the reduced gate size decreased the total hydrostatic load on the gate by 33% with corresponding decreases in gate friction, F_n , and hydraulic hoist and stem thrust effort needed to close the gate.

An estimated gate weight for the gate size and operating head being considered can be obtained from Fig. 3. This chart is based on computed weights of various sizes of fixed-wheel and coaster gates that have been designed, built and installed for operation under varying heads at conduit intakes. The weight obtained from the chart will be reasonably accurate, provided the design does not deviate appreciably from the general type of construction of the gates from which data were obtained for use in developing the chart. The features of gate design included herein apply to this type of construction.

The following nomenclature applies to Fig. 3: H equals the head to the centerline of the bottom seal, in feet; L is the width of opening, in feet (b_c in Fig. 1); T represents the height of opening in feet ($h_1 + h_2$ in Fig. 1); X denotes the height of the gate frame, in feet (assume equal to $2.3 T$ for estimating purposes); W/T is equal to the weight of the gate per foot of height, T ; and W/X is the weight of frame per foot of height, X . The weight of the guides is estimated at 100 lb per ft of height, assumed to be $X + (2 \text{ to } 5 \text{ ft})$. This is added to the frame weight to obtain the total estimated weight of embedded metalwork.

DOWNPULL

An important factor involved in the design of the gate and especially in the design of its operating equipment is the downpull force that might be obtained during an emergency closing or opening. During emergency operation the gate is subjected to large unbalanced pressures resulting from an increase in velocity of flow under the gate. The upstream face and top of the gate are subjected to nearly constant pressures, while there is a decrease in pressure on the downstream face and bottom of the gate. The decrease in pressure on the bottom of the gate produces an unbalance of vertical pressures resulting in a downward force on the gate, generally referred to as downpull. The pressure variations on the bottom of the gate are functions of several factors: The shape of the intake; the velocity of flow under the gate; the angle at which the flow approaches the opening under the gate; the proportions of the gate bottom; the hydraulic conditions downstream from the gate; the amount of gate opening; the relative positions of the top and bottom seals; and the proportions of the recess in the face of the structure just above the conduit entrance. These factors all influence the flow pattern and the velocity distribution under the gate.

Because the pressure reduction at any point is controlled by the velocity distribution and is equal to the velocity head at that point, the downpull force is dependent on the summation of these velocity heads. There are no known available data that give sufficient information to determine accurate estimates of downpull values for various types of gates at any gate opening. Laboratory hydraulic model tests and studies, based on proportions of the proposed gate design, are at present the most satisfactory methods of determining a reasonably accurate estimate of the downpull force that can be expected for any particular installation.

Model tests conducted thus far have been confined to those installations in which it was necessary to solve a difficult downpull problem particular to a specific installation. Such tests are invaluable for similar installations, yet they serve at best only as guides for estimating downpull for other installations. Assumptions are necessary to adapt the tests generally. However, there are no means of proving the validity of such assumptions unless or until additional model or prototype tests are conducted. Although prototype tests are not usually made, they have been conducted occasionally to verify some of the special laboratory model tests. In one such prototype test, uplift forces on the gate were observed at certain gate openings that were not covered in the model tests.²

The physical proportions of the gate are generally large and require comparatively little additional construction to accommodate increased loads and stresses induced by downpull forces on the bottom of the gate and on the gate-lifting stem connections. In view of the uncertainties involved in the determination of the downpull forces, as noted previously, it is assumed reasonable to apply a full hydrostatic head pressure differential and design the bottom of the gate and the lifting stem connections on the gate accordingly. Because such forces result from emergency closures that occur infrequently and are of short duration, an increase in the allowable unit stresses to 75% of the yield of the material for the parts involved is usually permitted.

The effect of downpull on the operating equipment would be most severe if it should be necessary to completely open (raise) the gate under full unbalanced pressures. The maximum downpull force would then be added to all friction forces and the weight of the gate and hoist stems to obtain the necessary capacity for the hydraulic hoist. This condition should not occur because the gate is normally raised under balance pressures.

Provisions are usually made for obtaining balanced pressures after an unwatering of the penstock by installation of bypass lines and control valves for filling the empty penstock to reservoir head before raising the gate. An occasional installation may require the gate to be opened a slight amount to accomplish the backfilling, but only where installation of bypass lines and valves is unfeasible.

An air vent is provided immediately downstream of the gate in the top of the intake transition as shown in Fig. 4. It supplies air needed to reduce the

² "Model-Prototype Comparison of the Hydraulic Forces Acting on the Outlet Coaster Gate—Shasta Dam—Central Valley Project," by D. M. Lancaster *Hydraulic Laboratory Report No. Hyd.-233*, Research and Geology Div., Bureau of Reclamation, U. S. Dept. of the Interior, Denver, Colo., October 25, 1948.

tendency toward formation of negative pressures and vibration during emergency gate closure or when the conduit is drained after the gate has been closed under normal balanced pressures. It permits the release of air while the conduit is being filled with the gate closed or nearly closed. The air vent also relieves the tendency toward formation of partial vacuums in the conduit during normal flow conditions. Because the air vent relieves the tendency toward producing negative pressures on the downstream face of the gate, the maximum hydrostatic head on the gate is increased by 15 ft to obtain a design head which allows a safety factor for a possible partial vacuum on the moving gate. The minimum

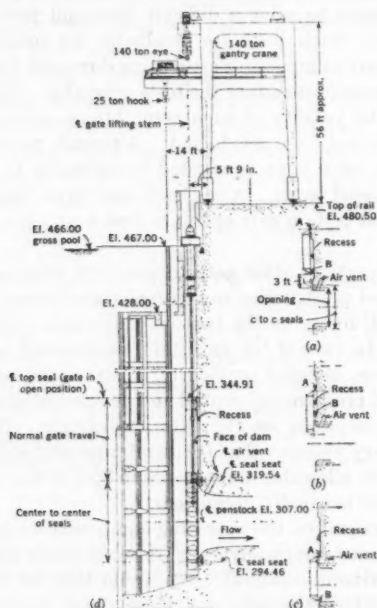


FIG. 4.—PENSTOCK VERTICAL FACE INTAKE

size of the air vent should be sufficient to admit air at the rate the turbine is discharging water during emergency closing of the gate, assuming headwater at the centerline of the transition and one-half atmosphere pressure on the downstream side of the gate.

A recess is built in the face of the concrete structure just above the intake and behind the gate in its normal raised position as indicated in Fig. 4. This recess serves the following purposes and should be properly proportioned to serve each to the best advantage.

1. With the gate in its normal raised (open) position, the recess serves to dampen gate vibration. This is accomplished by establishing the control of

flow, between the gate and the concrete structure, at the orifice formed by the top seal on the gate and the concrete structure—that is, orifice A must be smaller than orifice B (Fig. 4(a)). Under flow conditions this produces a reduced pressure on the downstream face of the gate between the gate and the recess, thus loading the gate and preventing vibration or flutter of the gate resulting from effects of the intake flow pattern.

2. The seal assembly on the gate projects a minimum of $2\frac{1}{2}$ in. beyond the face of the skinplate, and without a recess the top seal assembly will be subjected to unbalanced pressures when the gate is partly closed. This would be due to full reservoir pressure on the top side of the assembly and lower pressure on the under side. This unbalance of pressures on the top seal assembly contributes materially to the downpull force on the gate. The maximum downpull force usually occurs between gate openings of 20% to 80%. Tests³ have shown that a recess with a depth several times greater than the seal assembly projection is effective in reducing downpull by balancing the pressures on the top seal assembly. The effectiveness of the recess in balancing pressures is directly proportional to its depth. A recess with a depth equal to 3 or 4 times the projection of the seal assembly is usually built in the concrete structure and proportioned to be effective approximately through the 20% to 80% gate opening range, except in cases in which results of special model tests indicate other requirements. The recess is effective for this purpose through the gate travel in which orifice A is greater than orifice B as seen in Fig. 4(b).

3. As a closing gate approaches the closed position the spring point of flow jumps from the lip on the bottom of the gate to the bottom seal assembly. This shift of the spring point produces an unbalance of pressures on the bottom seal assembly similar to those that would occur on the top seal assembly with the gate open and no recess. Because the hydrostatic head is effective on the lower side of the bottom seal assembly and a reduced pressure (near atmospheric as air is supplied through the air vent) exists on the upper side, an uplift force on the projection of the bottom seal assembly results. The uplift can be sufficient to offset the otherwise net excess downward force, P_u , and stall the gate before it is completely closed. The effect of the recess in balancing the pressures on the top seal assembly is again taken advantage of to counteract this uplift force. Because the pressure-balancing effect of the recess on the top seal is directly proportional to its depth, the depth can be reduced near the end of the closing cycle. This produces a downward force on the top seal assembly counteracting the uplift on the bottom seal assembly, and, therefore, orifice A is less than orifice B as indicated in Fig. 4(c).

The foregoing functions of the recess are the major factors in determining the normal raised position of the gate. For obtaining the shortest distance of travel for closing and the resulting minimum size for the hydraulic hoist, the preferred position for the raised gate would be determined by locating the tangent point, or spring point of flow, on the gate to coincide with the vertex of an ellipse which is identical to the ellipse forming the top of the penstock intake.

³ "Coaster Gate and Handling Equipment for River Outlet Conduits in Shasta Dam," by J. E. Warnock and H. J. Pound *Hydraulic Laboratory Report No. Hyd-188*, Bureau of Reclamation, U. S. Dept. of the Interior, Denver, Colo., Nov. 26, 1945.

The tangent point, or spring point of flow, can be either at the upstream face of the gate or on the low edge of the skinplate. The position of the ellipse at the spring point of flow on the gate is determined by moving the vertex of the penstock ellipse along a line parallel to the centerline of the penstock until it is tangent to a vertical line drawn through the spring point of flow on the gate. The major axes of the ellipses remain horizontal at all locations. If these conditions cannot be met, the gate should be raised to a location approximately 3 ft higher than the preferred position described previously so that it will not effect materially the flow pattern through the penstock intake. In all installations in which a recess is required for dampening of gate vibration it will be necessary to raise the gate to the higher open position, because of the requirement that orifice A must be less than orifice B in Fig. 4(a).

TABLE 2.—ALLOWABLE UNIT STRESSES

Type of stress	MEMBERS EMBEDDED IN CONCRETE	GATE MEMBERS
	Stress, in pounds per square inch	
(a) Axial tension		
Net section	18,000	15,000
Power-driven rivets		5,000
Anchor bolts	15,000	...
(b) Tension in extreme fibers (bending)	18,000	15,000
(c) Compression ^a in extreme fibers (bending)	16,500	14,000
(d) Combined stress	24,000	20,000
(e) Shear		
Gross area webs	11,000	9,500
Power-driven rivets, fitted bolts, pins	13,500	11,500
Ribbed bolts ^b	18,000	15,000
Turned bolts	11,000	9,500
Tangential in wheels	...	90,000
(f) Bearing		
Pins	24,000	20,000
Power-driven rivets, ribbed bolts, tight-fit dowels and bolts, milled stiff	27,000	23,000
Turned bolts	20,000	17,000
Self-lubricating bushings 10 ft per min surface speed	...	4,000
Static	...	7,000
Concrete in blockouts under track bases	1/2 of ultimate strength	...

^a l/b less than 15; l = length of unsupported flange between connections in inches; b = flange width, in inches. ^b 70,000 lb per sq in. minimum ultimate tensile stress.

UNIT STRESSES

Allowable working stresses for the gate leaf are proportioned to compensate for corrosion. Previously, stresses were computed for sections from which $\frac{3}{8}$ in. had been deducted for exposed surfaces, a procedure requiring a special moment of inertia computation of standard rolled structural sections for the corrosion allowance. From comparisons of stresses on previous designs, before

and after the $\frac{1}{2}$ -in. deductions, allowable unit stresses, including corrosion allowances wherever applicable, were adopted. These allowable unit stresses are listed in Table 2. The maximum allowable axial tensile stress for power-driven rivets is 5,000 lb per sq in., or is determined⁴ from Eq. 9, whichever is the lesser.

$$S_r = \left(4,630 \frac{T_r}{V_r} - 8,000 d_r + 11,500 \right) 0.8 \dots \dots \dots (9)$$

in which S_r is the permissible tensile stress on the rivet, in pounds per square inch of rivet before driving; T_r denotes the total tension on rivet, in pounds; V_r represents the total shear on rivet, in pounds; and d_r is equal to the diameter of rivet before driving, in inches.

GATE LEAF

A fixed-wheel gate leaf is essentially a bulkhead gate mounted on wheels. It consists of a skinplate supported by horizontal beams connected to vertical

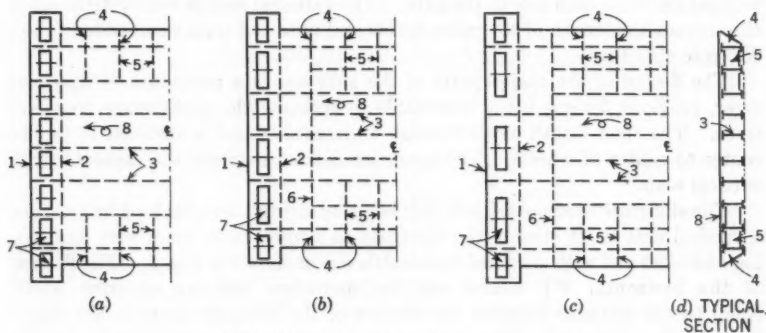


FIG. 5.—PENSTOCK FIXED-WHEEL GATES

end beams usually referred to as vertical girders. The wheels are mounted between two vertical girders at each end of the gate. Eccentric pins are used for mounting the wheels, with the eccentric being arranged to provide adjustment of wheel alinement so that the tread contact surface of all wheels on the gate can be alined to a common plane for bearing on the embedded track.

Three basic arrangements of the horizontal beams, vertical girders, and wheels are used. These are shown in Fig. 5 in which the numerals 1 through 8 represent: 1, the outside vertical girder; 2, the inside vertical girder; 3, the horizontal beams; 4, cantilever brackets; 5, the diaphragms; 6, the distributing beams; 7, the wheels; and 8, the skinplate. In Fig. 5(a) all of the horizontal beams extend through to the outside vertical girders, thus placing a wheel between each pair of horizontal beams. This arrangement is suitable for low

⁴"Rivets in Combined Tension, Shear and Flexure," by C. R. Young and W. B. Dunbar, reprinted by A. I. S. C. from *The Canadian Engineer*, Toronto, February 5, 1929.

operating heads where the wheel loads are comparatively light and no particular difficulty is encountered in obtaining a sufficiently large wheel-pin ratio to keep the wheel bearing friction, F_b , within usable limits. The use of load-distributing beams, or diaphragms, in Fig. 5(b) and Fig. 5(c) provides additional space for the use of larger wheels which are needed for higher heads. They permit the retention of close horizontal beam spacing which reduces the thickness of the skinplate. Their use also obviates the need for development of complicated connections at the eccentric pin nuts, pin bearing plates, and end connections for the horizontal beams. This is a condition that would exist if the horizontal beams extended to the inside vertical girder. The large wheel chamber provided in the arrangement of Fig. 5(c) adds flexibility to the location of the wheel. In some cases this is a distinct advantage in that it provides a simple means of redistributing the wheel loads by utilizing the effect of wheel spacing on the distribution of the vertical girder loads to the wheels. The arrangements can be used in combinations to suit the size of the gate and the design head.

The roller trains on coaster gates are located over the centerline of a single vertical girder at each side of the gate. The gate-leaf load is evenly distributed throughout the length of the roller trains and onto the tracks embedded in the concrete structure.

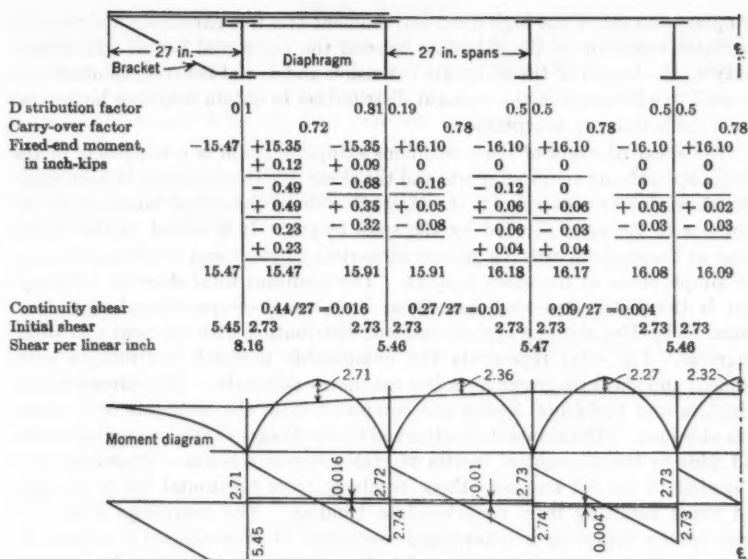
The design of the major parts of the gate leaf is a procedure of trial and error, previous designs being invaluable in choosing the preliminary trial sections. The span length of all through-horizontal beams is assumed to be the center to center of wheels. The spans are loaded between the centers of the vertical seals.

The skinplate moments, loads, and bending stresses are obtained by treating a vertical unit width strip of the skinplate as a continuous beam with reinforcing haunches and with modified end cantilevers as shown in Fig. 5. The flanges of the horizontal WF beams are the haunches with an effective width equal to the distance between the centers of the extreme rivets in the flange plus one rivet diameter. The parts of the skinplate that extend above the top beam and below the bottom beam are cantilevers, and are supported laterally at frequent intervals by brackets connected to the horizontal beams. These cantilever sections of the skinplate are analyzed as a series of rectangular plates, each simply supported on two opposite edges at a bracket, the third edge fixed (built in) at the horizontal beam, and the fourth edge free.⁵ Initial end moments for the continuous skinplate haunched beam and the resisting moments at the center of the fixed edges of the top and bottom rectangular plate cantilever are computed. These moments are used to obtain the actual moments at the supports by the method of moment distribution.⁶

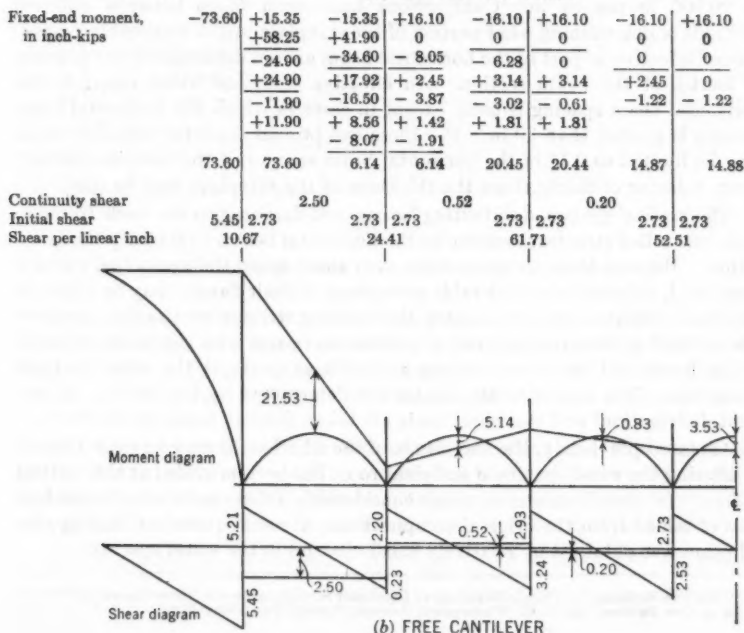
By combining these actual moments with the simple moments of the spans, the moment at any point on the continuous skinplate beam may be obtained. Relatively close spacing of the brackets under the cantilever sections of the

⁵"Theory of Plates and Shells," by S. Timoshenko, McGraw-Hill Book Co., Inc., New York, N. Y., 1st Ed., 1940.

⁶"Automatic Design of Continuous Frames," by Linton E. Grinter, The Macmillan Co., New York, N. Y., 1939, Chapters 3 and 5.



(a) MODIFIED CANTILEVER



(b) FREE CANTILEVER

FIG. 6.—TYPICAL MOMENT DISTRIBUTION

skinplate eliminates the high fixed-end moment of a free cantilever and permits a greater extension of the skinplate beyond the horizontal beam. This flexibility in the length of the skinplate extension and initial resisting moment can be used to advantage in the moment distribution to obtain resulting horizontal beam loads that are acceptable.

The shear diagram of the continuous skinplate beam is a composite of the simple span shears at the supports and the shear due to continuity in each span. The shear due to continuity is the algebraic sum of the actual moments at the supports of the span divided by the span length. It is added to the simple shear at the support with the greater numerical moment and is subtracted from the simple shear at the other support. The resultant total shear at each support is the distributed load, per linear inch, on the supporting longitudinal beam. Fig. 6(a) shows a typical moment distribution with moment and shear diagrams. Fig. 6(b) represents the comparable moment distribution with moment and shear diagrams for a free cantilever skinplate. The stresses in the skinplate and horizontal beams are computed from the moments and shears thus obtained. The skinplate is attached to the flanges of the horizontal beams and adds to the moment of inertia of each composite beam. Therefore, it is subjected to biaxial stresses—those resulting from horizontal beam bending and those resulting from the skinplate bending. The maximum combined stress in the skinplate is determined according to Westergaard's⁷ criteria of failure for ductile materials subjected to two-dimensional stress and is limited to 20,000 lb per sq in. Comparisons have been made between different methods of determining what portion of the skinplate might reasonably be considered effective as part of the horizontal beam area in determining the moment of inertia of the beam section. An effective skinplate width equal to the horizontal beam spacing is used, except in cases in which the horizontal beam spacing is greater than 30 in. For these exceptional cases the effective width may be limited to 0.11 of the horizontal beam span or, if the span is relatively short, a factor of thirty times the thickness of the skinplate may be used.

The vertical girders, distributing beams, and diaphragms are made from the same size rolled structural section as the horizontal beams to simplify the fabrication. Because these members have very short spans their principal stress is shear, and, although a considerable percentage of their flanges may be removed for wheel clearances or access holes, the bending stresses are usually very low. The vertical girders are analyzed as continuous beams with concentrated loads at the horizontal beam connections and with supports at the wheel and pin assemblies. The moments and shears are determined by the method of moment distribution⁶ and the wheel loads are taken directly from the results.

As stated previously, the magnitude of the wheel loads may be redistributed by altering the wheel spacing if sufficient room has been provided at the vertical girders. In some instances in which considerable difference in wheel loads had been obtained from the original computations, a more equivalent loading distribution was obtained by relatively small changes in the wheel spacing.

⁷ "On The Resistance of Ductile Materials to Combined Stresses in Two or Three Directions Perpendicular to One Another," by H. M. Westergaard, *Journal, Franklin Inst.*, May 1920.

WHEEL ASSEMBLY

The wheels are made of wrought steel, ASTM Specifications A57, with minimum rim hardness of 255 Brinell hardness number (BHN). The stress in the wheel tread is the controlling factor in the wheel design. The diameter of the wheel is usually determined by practical limits and by the available wheel space. The required projected area of the wheel tread (product of wheel diameter and tread width), is determined by a formula developed from tests on rollers.⁸ Eq. 10 gives a conservative critical stress in pounds per square inch for the design of wheels:

$$\text{Critical Stress} = (\text{BHN}) \times 24.5 - 2,200 \dots \dots \dots (10)$$

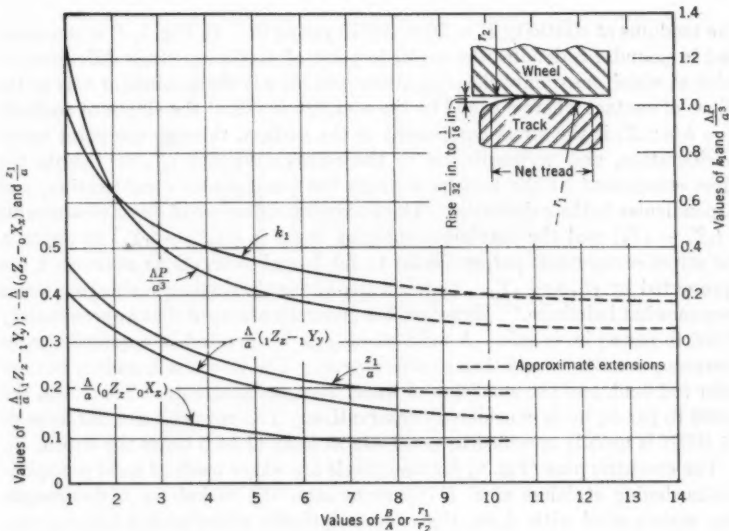


FIG. 7.—ANALYSIS OF STRESSES—WHEEL AND TRACK

A safety factor of 2 on the critical stress is assumed adequate for an overload condition in which any one wheel on a side of the gate may not bear on the track for a short distance of travel, thus causing an overload on the adjacent wheels. A safety factor of 3 on the critical stress is used for the normal wheel load.

The larger projected area, as determined by these two conditions, is used for the design of the wheels. The stresses are analyzed in accordance with a method derived⁹ for crossed cylinders, from which Fig. 7 was taken. The curves in Fig. 7 were derived for a Poisson's ratio (μ) of 0.25 and are not ap-

⁸ "Tests on Rollers," N. G. Noonan and W. H. Strange, *Technical Memorandum No. 399*, Bureau of Reclamation, U. S. Dept. of the Interior, Denver, Colo., Sept. 26, 1934.

⁹ "Stresses Due to the Pressure of One Elastic Solid Upon Another," H. R. Thomas and V. A. Hoersch, *Bulletin No. 212*, Eng. Experiment Station, Univ. of Illinois, Urbana, Ill., July 15, 1930.

plicable for values greater than $r_1/r_2 = 8$. The track radius is r_1 and r_2 is the wheel radius, each measured in inches. The mean of reciprocals of radii in the X-direction (A) is equal to $\frac{1}{2} r_1$ and the mean of reciprocals of radii in the Y-direction (B) is equal to $\frac{1}{2} r_2$.

$$B + A = \frac{1}{2} \left(\frac{1}{r_1} + \frac{1}{r_2} \right) \dots \dots \dots (11)$$

The evaluation of elastic properties and shape properties may be expressed as

$$\Lambda = \frac{2(1 - \mu^2)}{E(A + B)} \dots \dots \dots (12)$$

The modulus of elasticity $E = 30 \times 10^6$ lb per sq in. In Fig. 7, P is the wheel load in pounds; z_1 denotes the depth to point of maximum stress difference, or point at which maximum shearing stress occurs; a is the semimajor axis of the ellipse of contact where b would be the semiminor axis of the ellipse of contact; $k_1 = b/a$; ${}_0Z_z$ is the stress component at the surface, through the point under consideration, and perpendicular to the z -direction; and ${}_0X_z$ represents the stress component at the surface through the point under consideration, and perpendicular to the x -direction. The maximum difference of stress components is $({}_1Z_z - {}_1Y_y)$ and the maximum shearing stress is $\frac{1}{2}({}_1Z_z - {}_1Y_y)$ at depth z . The stress components perpendicular to the z - and y -directions at depth z , are represented by ${}_1Z_z$ and ${}_1Y_y$. Data on the allowable maximum shearing stress are somewhat indefinite.⁹ However, it is generally assumed that approximately 90,000 lb per sq in. is safe. A fixed-wheel gate is operated infrequently under emergency conditions and then at slow speeds. The wheels will seldom be used under full load, and the condition of wheel overload is remote. Therefore, the 90,000 lb per sq in. is considered conservative. The required rim hardness of 255 BHN is usually specified to penetrate at least $1\frac{1}{2}$ to 2 times the depth, Z_1 .

The eccentric pins (Fig. 8) for the wheels are either made of solid precipitation-hardening stainless steel (17% chromium, 7% nickel) or high-strength alloy carbon steel with $\frac{1}{32}$ -in. thick electrolytically nickel-plated bearing surfaces. During the years when the use of nickel was restricted pins were made of heat-treated solid stainless steel (12% chromium) and the alternate alloy carbon-steel pins were chrome-plated, 0.005-in.-to-0.010-in. thick. However, the chrome-nickel stainless pins or nickel-plated pins are used if obtainable because they are less susceptible to corrosion and electrochemical action when used with graphite-insert self-lubricating bushings in constantly submerged installations.

These pin materials are specified to have minimum physical properties in the ranges of 110,000 lb per sq in. to 120,000 lb per sq in. ultimate tensile strength, and 75,000 lb per sq in. to 90,000 lb per sq in. yield point in tension. An allowable bending fiber stress of 33,000 lb per sq in. is used for the pins, which are designed as partly uniformly loaded simple beams. The maximum deflection of the fully loaded pin must be less than the coarse-running fit clearance between the bushing and the pin. The bushings are made of high-strength manganese bronze with self-lubricating graphite inserts. The graphite inserts are pressed into drilled recesses in the bushing wall. The recesses do not ex-

tend through the wall, thus providing a solid backing for the lubricant and a stronger bushing. They are designed with an allowable average bearing stress of 3,500 lb per sq in. to 4,000 lb per sq in. on the projected area and are specified to have a minimum static load capacity of 7,000 lb per sq in. They are made as two-piece split bushings and are press-fitted into the wheels.

Disk springs are also included as a part of the wheel assembly (Fig. 8). Their function is to center the wheel on its pin when it is unloaded and free to move laterally. A wheel that is centered with adequate clearance on each side of the hub just prior to closing the gate under emergency conditions is free to float sidewise, a movement that may result from any slight misalignment in pin bores or in the track. Once a wheel has been loaded it is impossible to change

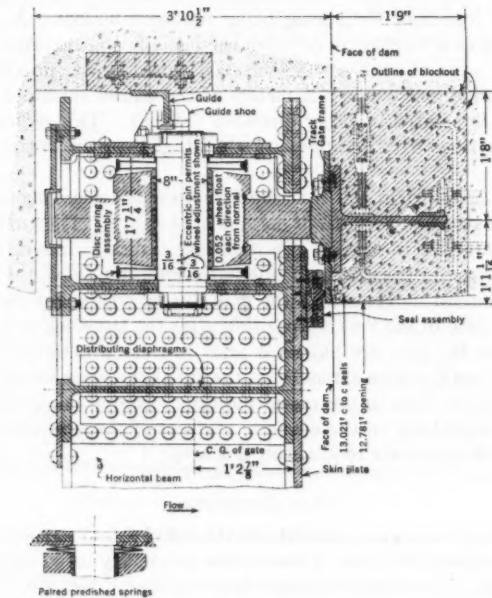


FIG. 8.—WHEEL ASSEMBLY

its lateral course because of the high friction between the tread and the track. The wheel float avoids a build-up of friction between the wheel hub and the vertical girder (which would tend to stall gate movement) by preventing contact of these parts while the gate is moving under load.

Initially flat uniform section disk springs are provided for each wheel Fig. 8. The springs are made of $\frac{3}{4}$ -hard, 18% chromium—8% nickel, or precipitation-hardening 17% chromium and 7% nickel stainless-steel sheet or strip. They are designed for installation with an initial preload deflection sufficient to produce a minimum load equal to the force required to slide $1\frac{1}{2}$ times the combined wheel and bushing weight on the pin. This holds true, assuming a sliding

friction coefficient of 0.10 between the bushing and pin. Stress in the springs, at a maximum deflection equal to one-half of the assumed wheel float, is limited to 125% of the yield point in tension of the spring material. The procedure of spring design otherwise follows that developed by Almen and Laszlo.¹⁰

Initially flat springs are used instead of the predished or initially coned type because they are simpler to manufacture and, as a group, are more consistent in their load capacities. This is due probably to elimination of the preforming operation required in the coned type. Also, the assembly of flat springs maintains a compact closed unit when released of load, making it less susceptible to accumulation of sediment. The initially coned type produces a higher initial load under very little deflection, a desirable characteristic. However, some installations of this type have encountered difficulty with the cone snapping-through under load and the spring being rendered useless. A combination, using a flat disk as a diaphragm between the initially coned springs would keep them effective, even though a snap-through should occur, provided all outer edges at the inside and outside diameters of the paired springs are supported when the cone is pointed in either direction (Fig. 8). This requires designing both types of springs with no apparent advantage over the initially flat spring assembly.

Guides are installed in the concrete structure and engaging spring-backed guide shoes are attached to the four corners of the gate. The guides and shoes serve a similar function to the gate as a whole as the disk springs do to the wheels (Fig. 8). They center the unloaded gate in the gate slot above the intake opening and allow lateral movement of the gate during emergency closure. They also center the gate in the lowered position after the penstock is backfilled and the pressures on the gate are balanced prior to raising it to the normal open position. The metal guides extend from the sill at the intake to approximately 5 ft above the gate when in the raised position. Above this point the gate is guided by shoes rubbing on the concrete surfaces of the gate slots because no close guiding tolerances are required in this area.

SEAL ASSEMBLY

For recent high head gate installations the double-stem seal assembly shown in Fig. 9 has replaced all types of assemblies previously using single-stem J or music-note seals. The solid bulb music-note seal is now used almost exclusively for bulkhead gate installations. The double-stem seal is attached to the seal base with clamp bars over the stems. All parts are proportioned to provide adequate clearances around the seal to permit flexing action of the stems and extension of the seal bulb to contact the embedded seal seats. Reservoir pressure is admitted to the chamber behind the seal through slots or grooves milled in the seal base. Because half of the seal bulb is under balanced pressure (reservoir head), the seal load on the seal seat is one-half of the total reservoir pressure on the unbalanced side of the bulb, assuming the clamp bar as taking its part of the total unbalanced load from the seal acting as a beam.

The brass nosing is bonded on the bulb and serves to reduce friction during an emergency closure of the gate. It also prevents distortion and displacement

¹⁰ "The Uniform Section Disk Spring," by J. O. Almen and A. Laszlo, *RP-58-10*, A.S.M.E., May 1936.

of the top seals and bottom seals when they make contact with the horizontal seats while extended under such closures. To effectively guard against leakage, rubber O-ring seals are used for all fastenings on the unbalanced pressure side of the seal and a cold water sheet packing gasket is provided between the seal base and the gate leaf. Field reports from project installations indicate that this type of seal and assembly is performing very efficiently.

Some emergency gate installations require the seals to be unloaded (sometimes referred to as retracted seals) until the gate is fully closed, to reduce the seal-to-seal seat friction to a minimum. This is accomplished by using a hydraulically-actuated seal controlled by a small regulating valve. This is a three-way type of valve with one port leading to the seal chamber, another leading to the low-pressure side of the gate, and the third to the high-pressure side, or reservoir side. A short overtravel of the hoist and gate stem actuates the valve. When the gate is fully supported by the stem, the high-pressure port is closed and the low-pressure port is open, thus preventing hydrostatic

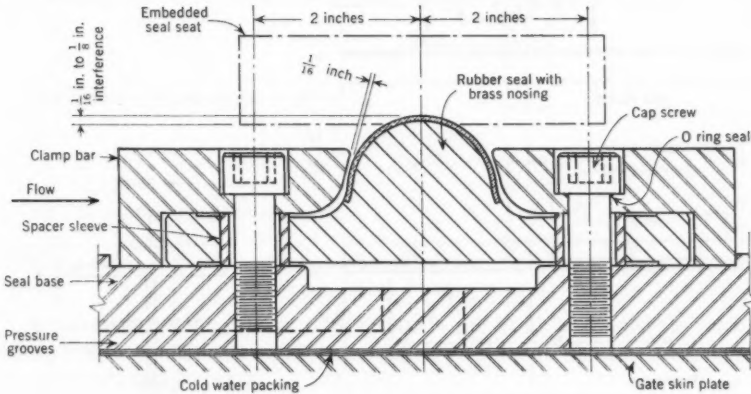


FIG. 9.—TYPICAL SEAL ASSEMBLY

pressure build-up on the seal. As a result, little or no seal friction exists. When the closing gate comes to rest on the gate stops, the short overtravel of the stem reverses the action of the valve ports and reservoir pressure is admitted to the seal chamber, effectively forcing the seal into contact with the seal seat. However, the installation increases the cost of the gate and hoist controls and is used only when deemed necessary.

GATE FRAMES

Gate frames consist of tracks, track bases, seal seats and bases, and the guides. Frames for penstock gates usually have the tracks and the vertical seal seats mounted on a common base. Anchor bolts are set in the first-stage concrete and project into blockouts provided in the first-stage concrete for the track bases, the seal seats, and the guides. After the frames are aligned accurately by means of the anchor bolts, the blockouts are filled with concrete.

The wheel loads are transmitted to the concrete structure through the tracks and the track bases. The deflection of the horizontal beams from bending due to the load on the gate will tend to rotate the vertical girders at the ends of the gate. The wheels will be rotated with the vertical girders. In order to prevent overstressing of the edges of the wheel treads and tracks, the track surface is finished with a transverse crown to compensate for the lateral rotation. The radius of the track crown is made sufficiently short to produce a rise of from $\frac{1}{8}$ in. to $\frac{1}{4}$ in., depending on the width of the track and the amount of deflection and rotation anticipated. The crown is made on the track instead of on the wheel tread so that there will be no tendency for the wheels to travel as a cone

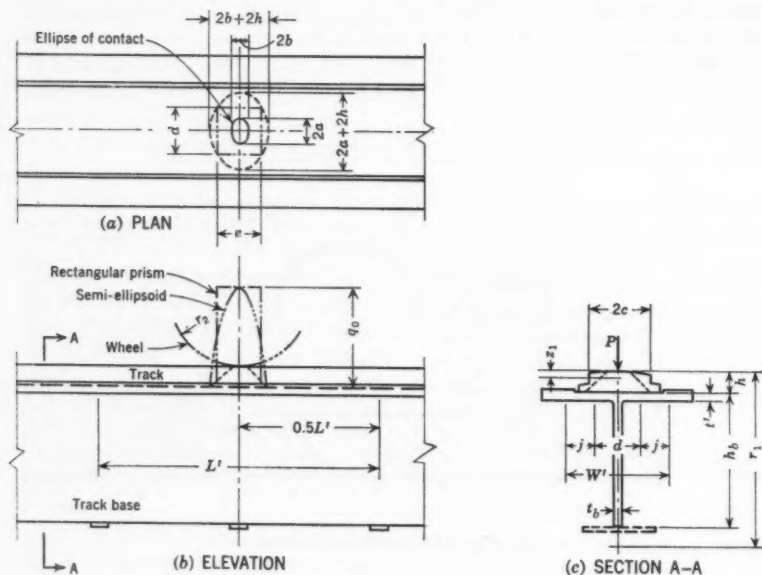


FIG. 10.—TRACK AND TRACK BASE

on the track, a condition which would make them travel on the flat track toward the center of the gate. As the wheels on opposite sides of the gate tend to travel toward each other, heavy opposing sliding friction would result between the wheel treads and the track face or (from side thrust) between the wheel hubs and vertical girders, contributing to stalling forces acting on the closing gate.

Tracks are usually inaccessible after installation and are therefore made with a BHN of 50 points or more higher than the BHN specified for the wheel treads. This tends to confine the wear to the wheels, which are more readily accessible for repair or replacement. Stainless steel (12% chromium) heat treated to a minimum ultimate tensile strength of 120,000 lb per sq in. and a

minimum yield point in tension of 90,000 lb per sq in. with a BHN 302 minimum is used for the tracks.

Only the maximum wheel load is considered for the design of the track and its base because both have constant cross sections for their loaded length. The track is assumed to act as an infinite beam on a two-dimensional foundation (the track base). The maximum bending moment¹¹ is

$$M_{\max} = 0.385 P \left(\frac{E I_t}{E c} \right)^{\frac{1}{2}} \dots \dots \dots (13)$$

which reduces to

$$M_{\max} = 0.212 P h \dots \dots \dots (14)$$

for a track and track base having the same modulus of elasticity and for a rectangular track having a height, h , and a width, $2c$, as indicated in Fig. 10. The term P is the maximum wheel load in pounds, and I_t represents the moment of inertia of the track.

The section modulus of the rectangular track can be computed from

$$S_t = (2c) \frac{h^2}{6} \dots \dots \dots (15)$$

The track bending stress is given by

$$f_t = \frac{M}{S_t} = \frac{(0.212 P h) 6}{(2c) h^2} \dots \dots \dots (16)$$

Eq. 16 can be rewritten as

$$(2c) h = \frac{1.27 P}{f_t} \dots \dots \dots (17)$$

A maximum bending stress, f_t , of 25,000 lb per sq in. is allowed for track material with a minimum 90,000 lb per sq in. yield point, and the track area required in square inches is

$$A_t = (2c) h = 5.08 (10^{-5}) P \dots \dots \dots (18)$$

The area of contact between the wheel and the track is an ellipse with major axis $2a$ and minor axis $2b$. Values of $\Lambda P/a^3$, z_1/a , and k_1 are taken from Fig. 7, and the axes of the ellipse are

$$2a = 2 \sqrt[3]{\frac{1.250 (10^{-7}) r_1 r_2 P}{C_1 (r_1 + r_2)}} \dots \dots \dots (19)$$

in which

$$C_1 = \frac{\Lambda P}{a^3} \dots \dots \dots (20)$$

and

$$2b = 2 k_1 a = k_1 (2a) \dots \dots \dots (21)$$

¹¹ "Bending of an Infinite Beam on an Elastic Foundation," by M. A. Biot, *Journal of Applied Mechanics*, March, 1937.

It is assumed that the cross section of the track is proportional to the major axis of the ellipse of contact and the depth of maximum shear stress, z_1 . Using a safety factor of 4 for the track depth, then

$$\frac{2c}{h} = \frac{2a}{4z_1} \dots \dots \dots (22)$$

in which

$$h = \frac{A_t}{2c} \dots \dots \dots (23)$$

Combining Eq. 22 and Eq. 23, the resulting track width is

$$2c = \sqrt{\frac{2aA_t}{4z_1}} \dots \dots \dots (24)$$

and the track height is

$$h = \sqrt{\frac{4z_1A_t}{2a}} \dots \dots \dots (25)$$

The wheel load is assumed to be transferred through the track onto the track base by the frustrum of an ellipsoid, the small base of which is the ellipse of contact between the wheel and track. The large base at the bottom of the track is a 45° projection of the periphery of the ellipse of contact, the altitude of the frustrum being the track height. The pressure on the ellipse at the bottom of the track is equal to the wheel load. It is maximum at the center and diminishes to zero at the edges, forming a semi-ellipsoid of pressure distribution. The maximum intensity of pressure, q_0 , at the center is $1\frac{1}{2}$ times the average pressure on the bottom ellipse¹² with major axis $(2a + 2h)$ and minor axis $(2b + 2h)$ (see Fig. 10(a)).

$$q_0 = \frac{3}{2\pi} \frac{P}{(a+h)(b+h)} \dots \dots \dots (26)$$

For the design of the track base, a rectangular prism with a base area of A_r is substituted for the semi-ellipsoid, and the pressure, q_0 , is assumed to be uniformly distributed over the base of the prism. The total load is equal to the wheel load

$$A_r q_0 = P \dots \dots \dots (27)$$

Substituting for q_0 in Eq. 26 and rearranging terms results in

$$A_r = \frac{3}{2} \pi (a+h)(b+h)$$

The sides of the prism base, d , and e , are proportional to the axes of the base of the semi-ellipsoid:

$$\frac{d}{e} = \frac{2a+2h}{2b+2h} \dots \dots \dots (28)$$

¹² "Theory of Elasticity," by S. Timoshenko, McGraw-Hill Book Co., Inc., New York, N. Y., 1st Ed., 1934.

or

$$d = \left(\frac{2a + 2h}{2b + 2h} \right) e \dots \dots \dots (29)$$

and

$$e = \sqrt{A_r / \frac{2a + 2h}{2b + 2h}} \dots \dots \dots (30)$$

If the previously determined track width, $2c$, is less than d , it must be increased to a minimum width of d to obtain adequate distribution of the wheel load to the track base.

The "tee section" track base design procedure is similar to the procedure used in column base plate design¹³ for distributing a column load over a sufficient area to satisfy the foundation-bearing pressure limitation. Although the column base is a flat plate free on all sides, the tee-track base flange is free on two sides but is restrained on the other two sides by the stem. The bending stresses of the net flange alone, about the longitudinal axis, determine the effective width, W' in inches of the flange,

$$W' = d + 2j \dots \dots \dots (31)$$

in which j is the effective cantilever projection of the flange loaded to the permissible concrete bearing stress, $P' = 1,125$ lb per sq in. (for the 3,000-lb ultimate strength concrete generally used). The net finished thickness of a tee-section flange is t' .

$$(t')^2 = P' \frac{(j)^2}{6,000} \dots \dots \dots (32)$$

and

$$j = 2.31 t' \dots \dots \dots (33)$$

The required effective length of the tee base, L' , measured in inches, is determined by the minimum concrete bearing area requirements:

$$L' = \frac{P}{1,125} W' \dots \dots \dots (34)$$

The track is not infinitely rigid along the longitudinal axis compared to the track base and the dimension, e , of the rectangular prism pressure base is small compared to the required effective length, L' , of the tee base. Therefore, the cantilever projection of the tee-track base on the longitudinal axis is taken as $0.5 L'$. With an allowable bending stress of 18,000 lb per sq in. the required section modulus of the track base about the transverse axis is:

$$S = \frac{M}{18,000} = P' (0.5 L')^2 \frac{W'}{36,000} = 0.00782 (L')^2 W' \dots \dots \dots (35)$$

In order to avoid overlapping the effect of adjacent wheel loads on the track base and foundation stresses, the length, L' , is not allowed to exceed the mini-

¹³ "Steel Construction Manual," A. I. S. C., New York, N. Y.

mum wheel spacing. This is accomplished by selecting a tee section with a thick flange, thereby obtaining a wide effective W' and a minimum length L' .

Using Mr. M. Hetenyi's¹⁴ work as a basis, the shear stress in the track base is determined. The load is assumed distributed uniformly along the length, e , of the prism base, and the load per unit length is $q' = P/e$. The maximum shear, V , occurs equally at the ends of the loaded length, e ,

$$V = \frac{q'}{4\lambda} (1 - C'_{\lambda e}) \dots \dots \dots (36)$$

in which $C'_{\lambda e}$ is determined from Table 3, and λ is the function of constant factors affecting deflection and is equal to

$$\lambda = \sqrt[4]{\frac{k}{4 E I_b}} \dots \dots \dots (37)$$

in which I_b is the moment of inertia of the track base.

TABLE 3.—FUNCTIONS OF λe AND $C'_{\lambda e}$

λe (1)	$C'_{\lambda e}$ (2)	λe (3)	$C'_{\lambda e}$ (4)	λe (5)	$C'_{\lambda e}$ (6)
0.25	0.5619	0.35	0.4204	0.45	0.2968
0.26	0.5469	0.36	0.4072	0.46	0.2853
0.27	0.5321	0.37	0.3943	0.47	0.2742
0.28	0.5175	0.38	0.3815	0.48	0.2632
0.29	0.5030	0.39	0.3688	0.49	0.2522
0.30	0.4888	0.40	0.3564	0.50	0.2414
0.31	0.4748	0.41	0.3441	0.51	0.2307
0.32	0.4609	0.42	0.3320	0.52	0.2204
0.33	0.4472	0.43	0.3201	0.53	0.2103
0.34	0.4337	0.44	0.3084	0.54	0.2002

The average shear stress is

$$v = \frac{V}{h_b t_b} \dots \dots \dots (38)$$

with the allowable shear stress for embedded materials equal to 11,000 lb per sq in. The net height of the tee is represented by h_b , and t_b denotes the tee web thickness.

The longitudinal shear, V_L , in the track base web is maximum at the neutral axis,

$$V_L = \frac{V M_s}{I_b t_b} \dots \dots \dots (39)$$

in which the maximum allowable longitudinal shear stress is 11,000 lb per sq in. and M_s is the statical moment of the track base.

The foundation modulus, k , is determined¹¹ from

$$k = 1.29 \left[\frac{1}{C'' (1 - u^2)} \frac{E_c \left(\frac{W'}{2} \right)^4}{E I_b} \right]^{0.11} \frac{E_c}{C'' (1 - u^2)} \dots \dots \dots (40)$$

¹⁴ "Beams on Elastic Foundation," by M. Hetenyi, *Scientific Series*, University of Michigan Studies, Vol. XVI, The Univ. of Michigan Press, Ann Arbor, Mich.

The modulus of elasticity for concrete $E_c = 3 \times 10^6$, C'' is a factor based on pressure distribution across the track base and is equal to 1 for assumed uniform distribution and the Poisson's ratio for the foundation, $\mu = 0.20$, for concrete. Substituting for the constants in Eq. 40 results in

$$k = 2.32 (10^6) \left[\frac{(W')^4}{I_b} \right]^{0.11} \dots \dots \dots (41)$$

The transverse bending stress in the track base is checked from the maximum moment occurring under the load¹⁴ $M = P/4 \lambda$ from which the stress $f_b = M/S$. The section modulus of the track base is S .

The track and the track base are designed as independent units. However, at any loaded point they deflect an equal amount, and the deflection¹⁴

$$y_0 = \frac{P \lambda}{2 k} \dots \dots \dots (42)$$

in which λ and k are functions of the combined moment of inertia, I , of the track and track base. As the I of the track is small compared to the I of the track base, the values of λ and k for the track base alone are sufficiently accurate to determine the deflection.

From the common deflection, y_0 , a value of λ for the track is obtained by expressing k in terms of λ in Eq. 42. Transposing Eq. 37,

$$k = (\lambda^4) 4 EI_t \dots \dots \dots (43)$$

and substituting for k in Eq. 42, yields

$$y_0 = P/8 \lambda^3 EI_t \dots \dots \dots (44)$$

then,

$$\lambda_t = \sqrt[3]{\frac{P}{8 y_0 EI_t}} \dots \dots \dots (45)$$

The maximum moment in the track is

$$M_t = P/4 \lambda_t \dots \dots \dots (46)$$

from which the stress in the track is checked:

$$f_t = \frac{M_t}{S_t} \dots \dots \dots (47)$$

If the stresses resulting from bending due to deflection of the track exceed the allowable, then the track or track base is stiffened.

The tracks, seal seats, and guides are submerged and are not readily accessible for maintenance or replacement. The plates and bars or angles of these members that have exposed surfaces subjected to rolling or sliding contact with the wheels and seals or guide shoes on the gate, are made of corrosion-resisting material (usually stainless steel) to reduce corrosion of the contact surfaces.

The screws, dowels, and bolts used for fastening these parts to their bases are specified to be made of comparable material to diminish galvanic corrosion tendencies. Other parts are made of ordinary structural grade carbon steel.

CONCLUSIONS

The design of gates is complicated, whether for use in controlling water flow for regulating purposes, emergency service or as a simple bulkhead. It requires coordination of the various functions and units into a composite structure whether used submerged under high hydrostatic head or near the surface. It is therefore necessary that the interests of the civil, structural, electrical, and mechanical engineering departments be carefully evaluated and coordinated to obtain an efficient and adequate installation.

ACKNOWLEDGMENTS

The writer is indebted to past and present colleagues at the Bureau of Reclamation who contributed to the development of the designs and data presented in this paper. The writer also wishes to express sincere appreciation to Messrs. Frank B. Cook, M. ASCE, James K. Richardson and William G. Weber, A. M. ASCE, for their encouragement in the preparation of the paper.

APPENDIX I. NOTATION

The following symbols, adopted for use in the paper and for the guidance of discussers, conform essentially with "American Standard Letter Symbols for Structural Analysis" (ASA Z10.8-1949), prepared by a committee of the American Standards Association with Society representation, and approved by the Association in 1949:

- A = mean of reciprocals of radii in x -direction;
- A_r = base area of a rectangular prism;
- A_t = track area, in square inches;
- a = semimajor axis of the ellipse of contact;
- B = mean of reciprocals of radii in Y -direction;
- b = semiminor axis of the ellipse of contact;
- b_e = transition face dimension, in feet (see Fig. 1);
- $C_1 = A P/a^3$;
- C' = function of $\lambda \epsilon$ (see Table 3);
- C'' = factor based on pressure distribution across track base = 1 for assumed uniform distribution;
- c = one-half the track width, in inches;
- D = nominal diameter of the penstock, in feet;
- d = side of prism (see Fig. 10(a));
- d_r = diameter of rivet before driving, in inches;
- E = modulus of elasticity of steel = 30×10^6 ;
- E_c = modulus of elasticity of concrete = 3×10^6 ;

- e = side of prism (see Fig. 10(a));
 F_b = wheel bearing friction;
 F_r = wheel rolling friction;
 F_s = seal friction;
 f_b = transverse bending stress;
 f_t = track bending stress;
 H = head to the centerline of the bottom seal, in feet;
 H_a = average hydrostatic head at the horizontal centerline of gate;
 h = track height, in inches;
 h_b = net height of tee;
 h_1 = transition face dimension, in feet (see Fig. 1);
 h_2 = transition face dimension, in feet (see Fig. 1);
 I = moment of inertia of the track and track base combined;
 I_b = moment of inertia of track base;
 I_t = moment of inertia of the track;
 j = effective cantilever projection of the flange (Fig. 10(c));
 k = foundation modulus;
 k_1 = ratio b/a ;
 L = width of the opening, in feet (b , in Fig. 1);
 L' = required effective length of the tee base (Fig. 10(b));
 l = total length of rubber-brass seal on gate, in inches;
 M = moment (Eq. 35);
 M_s = statical moment of track base;
 M_{\max} = maximum bending moment of track and track base;
 M_t = maximum moment in the track;
 P = maximum wheel load, in pounds;
 P' = permissible concrete bearing stress;
 P_e = excess downward force available for closing the gate by its own weight;
 P_p = positive forces (gate weight);
 P_n = summation of negative forces;
 Q = flow, in cubic feet per second;
 q_0 = maximum intensity of pressure;
 q' = load per unit length;
 r_1 = track radius, in inches;
 r_2 = wheel radius, in inches;
 S = required section modulus of the track base about the transverse axis (Eq. 35);
 S_r = permissible tensile stress on the rivet, in pounds per square inch;
 S_t = section modulus of the rectangular track;
 T = height of the opening, in feet ($h_1 + h_2$ in Fig. 1);
 T_r = total tension on rivet, in pounds;
 t_b = tee web thickness;
 t' = net finished thickness of a trial tee section flange (Fig. 10(c));
 u_1 = coefficient of friction for wheel bearings;

- u_2 = coefficient of rolling friction;
 u_3 = coefficient of friction for rubber-brass seals,
 V = maximum shear;
 V_L = longitudinal shear in the track base;
 V_r = total shear on rivet, in pounds;
 v = average shear;
 W = unbalanced hydrostatic load on the closed gate, in pounds;
 W/T = weight of gate per foot of height, T ;
 W/X = weight of frame per foot of height, X ;
 W' = effective width of the flange (Fig. 10(c));
 X = height of the gate frame, in feet;
 ${}_0X_x$ = stress component at the surface and perpendicular to the x direction;
 y_0 = deflection of track and track base;
 ${}_1Y_y$ = stress component perpendicular to the y direction, at depth z_1 ;
 z_1 = depth to point of maximum stress difference or point at which maximum shearing stress occurs (Fig. 10(c));
 ${}_0Z_z$ = stress component at the surface and perpendicular to the z direction;
 ${}_1Z_z$ = stress component perpendicular to the z direction, at depth z_1 ;
 μ = Poisson's ratio;
 Λ = evaluation of elastic properties and shape properties (Eq. 12);
 θ = angle between the centerline of the penstock and the plane normal to the intake face;
 λ = function of constant factors affecting deflection; and
 $\lambda_t = \lambda$ for the track.

DISCUSSION

JOSEPH R. BOWMAN,¹⁵ A. M. ASCE.—The author is to be complimented on a most comprehensive coverage of the design of high-head, fixed-wheel gates. The USBR has shown conclusively that the fixed-wheel gate is well suited to a large part of the field formerly dominated by the caterpillar gate. The term "caterpillar," as used herein, is intended to include tractor, coaster, and other continuous roller-train gate subtypes.

The relative merits of fixed-wheel gates and caterpillar gates are concisely summarized. However, one important advantage of the fixed-wheel gate has not been mentioned. This is that the deflection of the gate leaf is not as critical as in the caterpillar type. Deflection produces end rotation which in turn tilts the load-bearing assemblies of the gate. In the case of a fixed-wheel gate, a wheel bearing on a crowned track can be tilted an appreciable amount without materially changing its loading characteristics. Hence, a relatively large amount of gate leaf deflection can be tolerated. On the other hand, tilting the roller assemblies of a caterpillar gate results in loading the rollers eccentrically, inasmuch as they are cylinders bearing on flat track plates.

In order to limit the loads at the heavily loaded ends of the rollers to safe values, it is usually necessary to limit the deflection of the gate leaf by reducing its working stresses. This characteristic tends to limit the caterpillar gate to lesser widths than the fixed-wheel gate at certain heads. A number of schemes have been devised to compensate for eccentric roller loading without penalizing gate leaf design, but they leave much to be desired.

The caterpillar gate is not nearly as frictionless as some laboratory tests might indicate. Several gates of this type have failed to operate properly as the result of the assumption of too low a coefficient of friction. Values indicated by tests on single rollers or on models are almost impossible to attain in prototype. The clearances and tolerances among the roller-train components which are necessary to assure free movement tend to throw many of the rollers slightly askew. Their consequent "crabbing" motion introduces some sliding friction in addition to rolling friction. Thus, the over-all coefficient of "rolling" friction may be as great as two or three times the values ascribed to pure rolling motion. The writer notes that both he and the author agree on a "rolling" friction coefficient of 0.10.

The tabulation of conduit entrance proportions shown in Table I is a welcome addition to the gate designer's store of preliminary shortcuts.

The writer is in full accord with the author in that decisions as to the intended function and operation of a gate should be reached well before the selection of gate type is finalized. Moreover, the gate and its operating equipment should be treated as an integral unit. If the gate and hoist are considered independently, an incompatible combination may result.

Estimating Data.—The parameters used in the weight curves of Fig. 3 differ widely from those that have been developed for fixed-wheel gates at

¹⁵ Civ. Engr., Erik Floor and Associates, Inc., Chicago, Ill.

lower heads.¹⁶ At the higher heads the hydrostatic pressure is distributed nearly uniformly over the gate and the horizontal girders can be uniformly spaced. For this reason, the weight parameters need not be dependent on the gate height. On the other hand, at lower heads the hydrostatic pressure varies considerably over the height of the gate, and the spacing of the horizontal girders is varied so that they assume equal shares of hydrostatic load. As a result, the weight of the gate is not uniform throughout its height, and the weight parameters necessarily include the gate height.

The writer has found that the ratio of head on gate sill to gate height is a useful parameter for distinguishing between high-head and low-head submerged gates. When the ratio does not exceed six, low-head weight parameters and design procedures should be utilized. Conversely, if the ratio exceeds seven, high-head criteria should govern. A parameter of this nature will result in a few cases in which there will be no clear line of demarcation, and wherein the final classification will be resolved as a matter of preference. However, this head-to-height ratio can have considerable value in preparing quick preliminary estimates.

Design Details.—The writer observes that the Bureau of Reclamation now uses the self-lubricating type of wheel bushing exclusively on its fixed-wheel gates. In most high-head applications, this type is superior to grease-lubricated, anti-friction bearings. Prevailing water temperatures at deep intakes are so low that the grease in the housing of an anti-friction bearing tends to harden, producing locked-wheel conditions. Furthermore, a bearing seal that must perform the dual function of retaining the grease while keeping out water under high heads, and which must do so without introducing excessive friction on the axle against which it seals, is scarcely a minor item.

The USBR gates apparently make use of riveted connections to the exclusion of welding. Field assembly by riveting is often preferred to field welding because the distortion that may arise from welding is thereby eliminated. However, in view of the advanced welding techniques currently available, the writer fails to understand why shop-welded fabrication has not been utilized more extensively by the USBR. A good many gate designers have felt that riveting skin plates to their supporting frameworks became obsolete as more reliable welding techniques were developed. Moreover, it has long been recognized that rivet heads are focal points for corrosion of a skin plate.

Standardized Designs.—In contrast to the relationship between the private engineer and his client, the engineering staff of the USBR is in the enviable position of being its own client. As such, the staff can plan its requirements well into the future. This situation promotes a high degree of standardization in design criteria and in procedures. It also encourages development of standard-type designs that can be re-used many times with relatively little modification. The prospect of frequent re-use of a basic design economically justifies refinements in design procedure that many private engineers would not consider worthwhile.

In his dealings with a number of different clients, the private engineer as a rule must tailor his designs to conform to widely divergent client preferences as

¹⁶ "Estimating Data for Reservoir Gates," by F. L. Boissonault, *Transactions, ASCE*, Vol. 113, p. 992, 1948.

to design criteria, operational requirements, and numerous other governing factors. Consequently, opportunities for development of refined standardized designs are few and far between. By and large, however, gate designers in private practice have been inspired to many noteworthy achievements by the bold and successful venture into the field of high-head, fixed-wheel gates by the USSR.

SYLVAN J. SKINNER¹⁷.—The writer appreciates the views presented by Mr. Bowman, and the points he raises are worthy of further consideration. However, some of the points discussed need some clarification.

The additional data on the comparative merits of coaster (caterpillar) versus fixed-wheel gates are well presented by Mr. Bowman. The problem of eccentric loading of rollers due to deflection and end rotation of the gate leaf is evident. However, a successful and fairly simple method of correcting this condition consists of supporting the roller tracks (those on the gate leaf and on the embedded track base) on confined, hard rubber mats. The mats act as hydraulic supports and distribute the roller loads laterally and vertically, thus eliminating the high roller end-load condition cited. This construction will also tend to remove the need for restricting the gate-leaf width, which may have been considered necessary with high end-loaded rollers.

It is possible that failure of some coaster (caterpillar) gates to operate properly results from assuming too low a coefficient of friction, as stated in the discussion. However, a major part of the trouble is probably caused by an excessive accumulation of debris and deposits on the links and rollers, after having been submerged for an extended period of time. Frequent inspection and servicing of such installations is needed.

Estimating Data.—Mr. Bowman's comments regarding parameter requirements of weight curves for estimating purposes are correct when considering all types of gates and the full range of operating heads. The writer, however, presented data applicable to penstock intake high-head fixed-wheel gates for which the parameters of Fig. 3 are applicable. For other types of installations or installations at lower heads, other applicable weight curve charts are necessary. The magnitude of covering all installation variations would extend the scope beyond the intent of the present paper.

Design Details.—The writer's fixed-wheel gate designs incorporate completely welded, riveted or bolted structures, or combinations of these methods of construction. Completely welded gates requiring very heavy weld deposits for large, maximum stressed gate members are avoided. Distortion due to shop welding, even when using the submerged arc-welding process with twin electrodes (considered the least objectionable from a distortion standpoint), is difficult to control to the degree necessary for maintaining the required accuracy for alignment of members. Stress relieving is a definite requirement for such structures and can produce distortion or intensify that which already exists from the welding process. The large, heavy, multiple-unit gates are therefore usually specified to be fabricated using high-strength ribbed bolts with self-locking nuts. This method has proved to be quite satisfactory.

¹⁷ Mech. Engr., Mech. Branch, Bureau of Reclamation, U. S. Dept. of the Interior, Denver, Colo.

AMERICAN SOCIETY OF CIVIL ENGINEERS

Founded November 5, 1852

TRANSACTIONS

Paper No. 3001

DISCHARGE CHARACTERISTICS OF RECTANGULAR THIN-PLATE WEIRS

BY CARL E. KINDSVATER,¹ M. ASCE, AND
ROLLAND W. CARTER,² A. M. ASCE

WITH DISCUSSION BY MESSRS. TURGUT SARPKAYA; STEPONAS KOLUPAILA;
RALPH W. POWELL; JOHN W. PAULL; IWAO OKI; MARION R. CARSTENS;
AND CARL E. KINDSVATER AND ROLLAND W. CARTER

SYNOPSIS

A comprehensive solution is proposed for the discharge characteristics of rectangular, thin-plate weirs. The solution is based on a simple equation of discharge and experimentally derived coefficients which account for the influence of the fluid properties and the physical characteristics of the weir and the weir channel. The effects of viscosity and surface tension are related to an increase in the effective head and an increase or decrease in the effective notch width. Thus, the combined effects of the fluid properties are accounted for with adjustment coefficients which are applied to measured values of the head and width. Consequently, the coefficient of discharge is defined as a function of geometric ratios which describe the weir and the weir channel.

Values of the coefficients required to describe the discharge of water over rectangular, thin-plate weirs are determined from original tests covering a wide range of the significant ratios. Additional data needed to confirm the proposed method of analysis are obtained from the published results of experiments performed by other investigators. The proposed discharge equation is compared with some of the most widely used formulas.

NOTE.—Published, essentially as printed here, in December, 1957, in the Journal of the Hydraulics Division, as *Proceedings Paper 1453*. Positions and titles given are those in effect when the paper or discussion was approved for publication in *Transactions*.

¹ Regents Prof., School of Civ. Eng., Georgia Inst. of Technology, Atlanta, Ga.; and Consultant, Geological Survey, U. S. Dept. of the Interior, Washington, D. C.

² Chief, Research Section, Surface Water Branch, Water Resources Div., Geological Survey, U. S. Dept. of the Interior, Washington, D. C.

INTRODUCTION

The rectangular, thin-plate weir is defined herein as a basic weir form which includes rectangular-notch weirs as well as full-width or "suppressed" weirs. A typical rectangular-notch weir in a rectangular channel is shown in Fig. 1.

For many years investigators have sought a comprehensive equation that would describe the discharge characteristics of rectangular weirs for a full range of fluid, flow, and geometric variables. Because weir discharge involves free, curvilinear flow and the combined influences of several fluid properties, it is not subject to complete mathematical description. Most investigators have resolved their difficulties by restricting their research to the flow of water over full-width weirs of considerable height and width. Unfortunately, different workers continue to disagree regarding the physical limitations as well as the discharge characteristics of even this so-called standard measuring weir. There

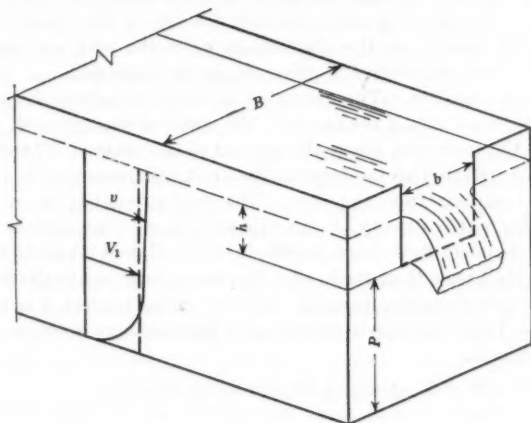


FIG. 1.—BASIC THIN-PLATE NOTCH WEIR

still exists a variety of weir formulas, each based on a different set of experimental data, which disagree so much that the weir is questioned as an accurate measuring device.

Most weir formulas are related to a quasi-rational analysis in which the weir is described as a limiting example of the two-dimensional orifice. The traditional form of the basic equation of discharge is obtained by integrating an approximate velocity equation over an approximate area. The result is a complex equation which must be modified to make it practical and adjusted to make it agree with a particular set of experimental data. The fact that a large number of different empirical formulas have been evolved by this procedure is evidence that the "theoretical" equation is inadequate. The obvious reason for the inadequacy is the fact that the basic assumptions are inaccurate.

Because the flow pattern for the weir is not yet subject to mathematical description, the most direct solution for the discharge function involves a

combination of dimensional analysis and experiment. Such an approach to the problem is used herein.

ANALYSIS OF THE DISCHARGE FUNCTION

Description of the Weir.—Fig. 1 shows a typical example of the basic weir form which is the subject of this investigation—a symmetrical, sharp-edge, horizontal-crest, rectangular notch in a smooth, vertical, thin plate located in a smooth, horizontal, rectangular channel. The nappe is fully ventilated and unsubmerged. The channel upstream from the weir, described hereafter as the approach channel, is assumed to be of sufficient length to develop the normal velocity distribution for all discharges. This ideal condition is seldom realized in practice. In fact, the use of short channels with various arrangements of baffles to control the velocity distribution is a major cause of disagreements in the results of experiments made by different investigators.

Notation.—The letter symbols adopted for use in this paper are defined where they first appear, in the illustrations or in the text, and are arranged alphabetically, for convenience of reference, in the Appendix.

Dimensional Analysis.—The geometry of the flow pattern shown in Fig. 1 is described by the width of the notch, b , the width of the approach channel, B , the height of the weir crest above the bottom of the channel, P , and the piezometric head, h , referred to the level of the crest and measured in the uniform flow section upstream from the weir. The fluid properties involved are the specific weight, γ , the density, ρ , the viscosity, μ , and the surface tension, σ . Only one independent flow characteristic is involved, and it can be represented by either the discharge, Q , or the head. However, because h is already involved as an independent geometric variable, Q is conveniently selected as the dependent variable. Thus, a complete statement of the discharge function will include both h and Q , as in

$$Q = f_1(b, B, P, h, \gamma, \rho, \mu, \sigma) \dots \dots \dots (1)$$

From Eq. 1, nondimensional ratios which describe the discharge function can be formed, as

$$\frac{Q}{b h \sqrt{g h}} = f_2 \left(\frac{b}{B}, \frac{b}{h}, \frac{h}{P}, R, W \right) \dots \dots \dots (2)$$

in which $g = \gamma/\rho$, the acceleration due to gravity. The dependent ratio in Eq. 2 is a coefficient of discharge. The first three independent ratios describe the geometry of the flow boundaries, and the last two symbols represent the Reynolds and Weber numbers.

In engineering practice in the United States, the acceleration due to gravity is commonly included in the definition of the coefficient of discharge. Thus, for practical purposes, a convenient definition of the coefficient, C , is

$$C = \frac{Q}{b h^1} = f_3 \left(\frac{b}{B}, \frac{b}{h}, \frac{h}{P}, R, W \right) \dots \dots \dots (3)$$

from which

$$Q = C_b^1 h^1 \dots \dots \dots (4)$$

The dimensions of C in Eqs. 3 and 4 are the dimensions of \sqrt{g} . Because of its obvious simplicity, and despite its lack of dimensional purity, Eq. 4 is used as the basic discharge equation herein.

The discharge function represented by Eq. 3 cannot be evaluated by analytical procedures. Accordingly, the relative influence of each of the independent ratios must be evaluated by experiment.

Significance of the Geometric Ratios in Eq. 3.—One of the most significant ratios in Eq. 3 is b/B . This ratio is a measure of the channel width-contraction characteristic of the weir. In combination with h/P , it is also an area-contraction ratio. The influence of b/B is similar to that of the diameter ratio which is used to describe thin-plate orifices. A better analogy is the width ratio which is used to describe open-channel constrictions.³ Strangely, in view of the extensive research on weirs, the relative influence of b/B has received little attention. The weir which has been investigated most extensively in the laboratory is the full-width weir, for which $b/B = 1.0$.

The (b/h) -ratio is a measure of the shape of the discharging liquid stream in the plane of the weir. The influence of this ratio is believed to be negligible over the full practical range of the other variables. An earlier investigation⁴ at the Georgia Institute of Technology, Atlanta, Ga., supports this conclusion. The fact that most of the published results of research on full-width weirs ignore the (b/h) -ratio indicates either that it was not recognized as an independent ratio or that its influence was not evident from the experimental data. A few recorded efforts to incorporate the (b/h) -ratio in discharge formulas are believed to be based on misinterpretations of influences related separately to the magnitudes of b and h .

The (h/P) -ratio is a measure of the depth-contraction characteristic of the weir. It is complementary to b/B as an area-contraction ratio. Because velocities in the channel upstream from the weir are proportional to the head, the (h/P) -ratio (in combination with b/B) is also a measure of the relative magnitude of the velocity in the approach channel. For this reason its influence is represented by a velocity-head term in some published formulas. It has also been described as a Froude number for the flow in the approach channel. Actually, for the boundary conditions specified, the flow in the approach channel is always tranquil, and flow with minimum specific energy always occurs in the vicinity of the weir crest. That is, the Froude number is not a significant independent ratio. (The Froude number would be significant if, for example, the approach channel were sloped or if the weir were located at the foot of a spillway or sluice.) Thus, to describe the (h/P) -ratio as anything but a geometric parameter is to disguise its fundamental significance in the discharge function.

Significance of R and W in Eq. 3.—Very little is known about the separate influences of viscosity and surface tension which are represented by R and W in Eq. 3. It is known, however, that the relative influence of the two fluid properties increases as the head on the weir and the size of the weir decrease.

³ "Tranquil Flow Through Open-Channel Constrictions," by Carl E. Kindavater and Rolland W. Carter, *Transactions, ASCE*, Vol. 120, 1955, p. 969.

⁴ "Discharge Characteristics of Rectangular Notch Weirs in Rectangular Channels," by James Robert Wells, thesis presented to the Georgia Institute of Technology, Atlanta, Ga., in 1954, in partial fulfillment of the requirements for the degree of Master of Science in Civil Engineering.

The Reynolds number is a measure of the relative influence of viscosity. It is usually expressed as

$$R = \frac{V L \rho}{\mu} = \frac{V L}{\nu} \dots \dots \dots (5)$$

in which V is a typical velocity, L is a conveniently evaluated and physically significant length, and ν is the kinematic viscosity of the fluid. For large, full-width weirs the most significant length is the head. For small, narrow weirs, however, the width (and possibly the height) of the weir, as well as the head, are independently significant. In general, therefore, the Reynolds number must be related to both the head and the width of the weir. Thus, there are at least two forms of R . Furthermore, because velocities in the vicinity of the weir crest are proportional to the square root of the head, \sqrt{h} can be substituted for V in Eq. 5, whence $\sqrt{h} (h)/\nu$ and $\sqrt{h} (b)/\nu$ are independent ratios which have the significance of Reynolds numbers. Thus, for a given fluid (ν constant), the total influence of viscosity on a given weir can be expressed in terms of the absolute magnitudes of h and b , or h alone.

The Weber number is a measure of the relative influence of surface tension. It is usually expressed as

$$W = \frac{V \sqrt{L}}{\sqrt{\sigma/\rho}} \dots \dots \dots (6)$$

in which the surface tension, σ , and the density, ρ , are essentially constant for a given liquid. Because V is proportional to \sqrt{h} , and because either h or b , or both, can be significant lengths, L , the ratios $\sqrt{h} (\sqrt{h})/\sqrt{\sigma/\rho}$ and $\sqrt{h} (\sqrt{b})/\sqrt{\sigma/\rho}$ are independent ratios which have the significance of Weber numbers. Thus, there are at least two independent forms of the Weber number as well as the Reynolds number. Furthermore, the effects of both viscosity and surface tension for a given weir and liquid are related to the absolute magnitudes of h and b . Consequently, it is impossible to distinguish the separate effects of the two fluid properties from experiments with a single liquid.

Because the Reynolds number for any flow pattern is inversely proportional to a typical viscous-shear force, the relative influence of viscosity decreases as R increases. Similarly, because the Weber number is inversely proportional to a typical surface-tension force, the relative influence of surface tension decreases as W increases. It follows from the foregoing definitions of R and W in terms of h and b that the relative influence of the combined fluid properties diminishes as either h or b becomes larger. Thus, for large heads on large weirs, the influence of viscosity and surface tension is negligible. This conclusion is substantiated, for example, by the observation that the coefficient of discharge for large weirs is essentially constant for all heads above a certain minimum. That is, C is independent of the fluid-property parameters for large values of h and b . Here the distinction between "small" and "large" must be based on systematic experimental investigations of the independent relationships between C and h and between C and b . Many investigators have attempted to determine the relationship between the absolute head and the dis-

charge coefficient for full-width weirs. The writers know of no systematic effort to evaluate the independent effects related to the absolute width of the weir.

If attention is henceforth restricted to water at ordinary temperatures, it follows from the foregoing that the quantities h and b can be used effectively to replace both R and W in Eq. 3. Furthermore, if the (b/h) -ratio is discarded on the basis of experimental evidence that it is insignificant, the discharge function represented by Eq. 3 can be changed to

$$C = f_4 \left(\frac{b}{B}, \frac{h}{P}, h, b \right) \dots \dots \dots (7)$$

which must be evaluated by experiment.

Evaluation of Eq. 7.—The function represented by Eq. 7 involves four independent variables, a condition which precludes the presentation of experimental data in simple graphical form. However, if the relatively minor effects represented by h and b are described by an approximate, independent, empirical equation, the coefficient of discharge, C , can be expressed as a function of b/B and h/P alone. That is, if the parameters representing the influence of viscosity and surface tension are effectively "removed" from Eq. 7, the relationship between the coefficient of discharge and the principal geometric ratios can be shown by a family of plane curves.

The effects of viscosity and surface tension cannot be described by exact physical equations. Nevertheless, any procedure whereby these effects are eliminated from the discharge function must be based on a general understanding of the manner in which the fluid properties influence the flow pattern.

The Influence of Viscosity.—A flow pattern which is determined by boundary conditions alone is described as a potential-motion pattern. The influence of viscosity in a real fluid motion can be illustrated by comparison with its potential-motion counterpart.

One of the effects of viscosity which can be ignored in many accelerated fluid motions is the energy loss which results from internal shear. The total loss of energy between the section of head measurement and the crest of a weir, for example, is generally insignificant. Therefore, the principal effects of viscosity on weir flow are those which are associated with flow-pattern modifications caused by boundary resistance and separation.

A separation zone occupied by a large eddy occurs in the corner between the weir plate and the bottom of the approach channel, as shown in Fig. 2(b). The effect of this occurrence on a low weir, in comparison with the potential pattern for the same weir, is similar to the effect of sloping the weir plate downstream. That is, compared with its potential-motion counterpart, the vertical trajectory of the nappe is lower and the coefficient of discharge, being virtually a coefficient of contraction, is larger. The comparable effect on the discharge, therefore, is the same as an increase in head.

A separation zone similar to that shown in Fig. 2(b) also occurs in the corner between the sides of a notch-weir plate and the walls of the approach channel. The effect of this occurrence, in comparison with potential motion, is to reduce

the width contraction of the weir nappe. Its influence on the discharge, therefore, is the same as an increase in the width of the notch.

Viscous shear causes the flow to be retarded in the vicinity of the boundaries. This condition can be described with respect to potential motion by means of the discharge-displacement, boundary-layer thickness, δ^* , shown schematically in Fig. 2. The cross-hatched areas in Fig. 2 represent the virtual displacement of the potential motion due to boundary resistance. On the surface of the weir plate, near the vertical edges of the notch as well as the horizontal crest (Fig. 2(a)), the effect of the boundary layer is similar to the effect of rounding the upstream corners of the notch. Compared with potential flow through a sharp-edged notch, therefore, the coefficient of contraction for the real fluid motion is larger. The effect on the discharge, on the other hand, is similar to the effect of increasing both h and b .

A boundary layer is also formed on the bottom and side walls of the approach channel. The effect of this occurrence is particularly significant for large values of h/P and b/B . For example, the flow through full-width weirs ($b/B = 1.0$)

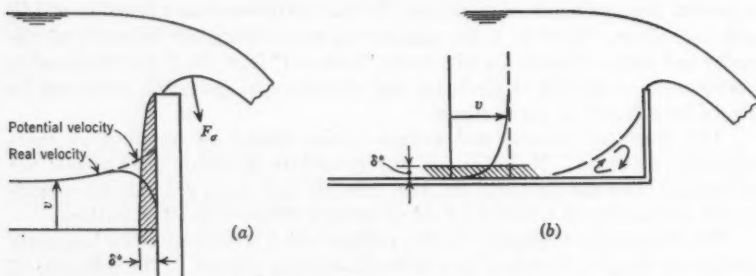


FIG. 2.—SCHEMATIC REPRESENTATION OF THE INFLUENCE OF VISCOSITY AND SURFACE TENSION

is characterized by boundary layers on both sides of the channel at the weir section. The effect of this occurrence on the discharge is similar to the effect of a reduction in the width of the weir. For values of b/B less than 1.0 the effect of the side-wall boundary layers is to increase the effective value of b/B by decreasing the effective channel width. Similarly, the influence of the boundary layer on the bottom of the approach channel resembles the influence of a decrease in P . The effect of this occurrence on the discharge function, therefore, is similar to the effect of an increase in h/P .

The influence of viscosity has been associated with the occurrence of boundary layers and separation zones. It should be emphasized, however, that the thickness of the boundary layers and the size of the separation zones are not directly proportional to the magnitude of the head or the size of the weir. (For this reason, the effects of viscosity are often described as "scale" effects.) Thus, for example, considering the small absolute magnitude of δ^* , the relative effect of each of the several boundary layers depends on the absolute magnitudes of h , b , and P . This observation is consistent with the previous conclusion that

the relative effects of viscosity diminish as the size of the weir and the head on the weir increase.

The Influence of Surface Tension.—Erik Lindquist, M. ASCE, in discussing⁵ the influence of surface tension on thin-plate, full-width weirs, described two significant phenomena. He observed, first, that the nappe clings to the top edge of the crest as shown in Fig. 2. Thus, compared with its potential-motion counterpart, a real fluid flow is characterized by a lower trajectory and a larger coefficient of contraction because of this surface-tension phenomenon. The effect of the occurrence is similar to the effect of rounding the upstream edge of the plate. Therefore, the effect on the discharge is the same as an increase in head.

The second phenomenon described by Lindquist is the result of surface tension in both the upper and lower nappe surfaces. The effect of this occurrence is a resultant force, F_s , shown schematically in Fig. 2(a), which acts in the direction of the center of curvature of the nappe. Because the radii of curvature of the nappe surfaces decrease with decreasing head, and because the surface-tension force varies inversely with the radius of curvature, the resultant force F_s increases as the head decreases. Furthermore, because the resultant surface-tension force has a dominant downward component, it has the same effect on the discharge as an increase in head.

The surface-tension phenomena described for full-width weirs are equally effective on notch weirs. In addition, similar phenomena occur at the vertical sides of the notch as well as the crest. Thus, the total influence of surface tension on the discharge through rectangular-notch, thin-plate weirs can be compared with an increase in the width of the notch as well as an increase in the head on the crest. It should be emphasized, however, that the relative influence of surface tension depends on the absolute magnitudes of h and b . Therefore, like the influence of viscosity, the influence of surface tension diminishes as the size of the weir and the head increase.

A Comprehensive Discharge Equation.—By comparing the flow of a real fluid with the potential flow for the same boundary conditions, the influence of the fluid properties has been related to an increase in the effective head, an increase or decrease in the effective width of the weir, and a decrease in the effective height of the weir. It has been suggested also that the coefficient of discharge can be expressed in terms of the principal geometric variables alone if the effects of the fluid properties are described by approximate, empirical equations. It is proposed, therefore, that the effective values of head and width be defined as

$$h_e = h + k_h \dots \dots \dots (8)$$

and

$$b_e = b + k_b \dots \dots \dots (9)$$

in which the quantities k_h and k_b represent the combined effects of the several phenomena attributed to viscosity and surface tension. It is also proposed that a coefficient of discharge which is independent of the size of the weir or the

⁵ Discussion by Erik Lindquist of "Precise Weir Measurements," by Ernest W. Schoder and Kenneth B. Turner, *Transactions, ASCE*, Vol. 93, 1929, p. 1168.

magnitude of the head be defined as

$$C_s = \frac{Q}{b_s h_s^{3/2}} = f_s \left(\frac{b}{B}, \frac{h}{P} \right) \dots \dots \dots (10)$$

It is assumed that k_A and k_b as well as C_s can be defined by experiment. Thus, from Eq. 10, the equation

$$Q = C_s b_s h_s^{3/2} \dots \dots \dots (11)$$

is proposed as a comprehensive equation of discharge for all rectangular, thin-plate weirs. The adequacy of this equation, and, in fact, the adequacy of the effective-head and effective-width concepts, must be examined in the light of experimental data.

SOURCES OF VERIFICATION DATA

Experiments of Bazin.—The classic experiments of Henri Bazin^{6,7} on full-width, thin-plate weirs were made in 1886 and 1887 in a flume located on the bank of the Canal de Bourgogne, near Dijon, France. Bazin's setup included a sluice-controlled forebay and a concrete flume 6.56 ft wide and approximately 700 ft long. The weirs consisted of a crest plate mounted on a timber bulkhead. The nappes were fully ventilated on the downstream side. The crest pieces were described as being iron, carefully straightened, 0.276 in. thick, sharp-edged, and with top surface perpendicular to the plane of the weir. Several different weirs were actually used in making the tests, but they were described as being "perfectly comparable with each other." All of the weirs were of the full-width type ($b/B = 1.0$). In order to cover a full range of values of h/P , Bazin made ten series of tests. The scope of his work is shown in Table 1(a).

Series 1, 2, and 3 of the Bazin experiments were described as reference tests, because they alone involved volumetric measurements of discharge. For all other tests the weirs were calibrated by comparison with the reference weirs. Head measurements were made with hook gages in stilling wells connected to large orifices in the walls of the flume 16.4 ft upstream from the weirs.

In general, Bazin's instrumentation was good and his technique was meticulous. His results differ considerably from those of most other investigators, however, and this has been attributed to the conclusion that, for different reasons, the crest pieces were not effectively thin and sharp-edged.⁸

Experiments of Schoder and Turner.—One of the most extensive investigations of full-width weirs reported in the literature is that performed under the direction of Ernest W. Schoder, M. ASCE, and Kenneth B. Turner at Cornell University, Ithaca, N. Y., from 1911 to 1920.⁹ Nearly 2,500 tests were made

⁶ "Expériences nouvelles sur l'écoulement en déversoir," by H. Bazin, *Annales des Ponts et Chaussées*, October, 1888, p. 393.

⁷ "Recent Experiments on the Flow of Water Over Weirs," by H. Bazin; English translation by Arthur Marichal and John C. Trautwine, Jr., *Proceedings, Engineers Club of Philadelphia*, Vol. VII, 1889, pp. 259-310.

⁸ Discussion by Ernest W. Schoder of "Precise Weir Measurements," by Ernest W. Schoder and Kenneth B. Turner, *Transactions, ASCE*, Vol. 93, 1929, p. 1189.

⁹ "Precise Weir Measurements," by Ernest W. Schoder and Kenneth B. Turner, *Transactions, ASCE*, Vol. 93, 1929, pp. 999-1110.

in this investigation, but many of these involved velocity distributions which were not uniform and crest plates which were not sharp-edged. The two series of tests which have been selected for use in this report are believed to have been made with "normal" velocity distributions. The scope of the tests used (series E and F) is shown in Table 1(b).

TABLE 1.—SCOPE OF VERIFICATION DATA

Series	Height, P , in feet	Notch width, b , in feet	Head, h , in feet	Contraction ratio, b/B
(1)	(2)	(3)	(4)	(5)
(a) Bazin Experiments				
1	3.72	6.56	0.19 to 1.01	} 1.0
2	3.72	3.28	0.19 to 1.34	
3	3.30	1.64	0.19 to 1.78	
4	2.47	6.54	0.48 to 1.28	
5	2.47	6.55	0.49 to 1.44	
6	1.64	6.54	0.31 to 1.22	
7	1.64	6.55	0.34 to 1.40	
8	1.16	6.53	0.29 to 0.94	
9	1.14	6.55	0.30 to 1.34	
10	0.79	6.55	0.30 to 1.34	
(b) Schoder-Turner Test Series E and F				
E	0.50	4.22	0.029 to 1.41	} 1.0
F	1.00	4.22	0.029 to 2.21	
(c) USBR Experiments				
1	5.00	2.007	0.14 to 1.26	} 1.0
2	4.60	2.007	0.46 to 1.25	
3	3.50	2.007	0.14 to 1.22	
4	2.50	2.007	0.14 to 1.25	
5	2.00	2.007	0.24 to 1.19	
6	1.50	2.007	0.28 to 1.20	
7	1.01	2.007	0.25 to 1.18	
8	0.57 to 0.65	2.007	0.44 to 1.11	
9	0.32 to 0.41	2.007	0.40 to 1.04	
10	0.13 to 0.14	2.007	0.35 to 0.89	
11	0.08 to 0.09	2.007	0.34 to 0.71	
(d) Georgia Tech Experiments				
	1.44	2.68	0.16 to 0.53	1.00
	1.44	1.80	0.14 to 0.58	0.90, 0.80, 0.60, 0.40, 0.20
	0.56	2.68	0.10 to 0.66	1.00
	0.56	1.80	0.10 to 0.72	0.90, 0.80, 0.60, 0.40, 0.20
	0.30	2.68	0.17 to 0.68	1.00
	0.30	1.80	0.10 to 0.76	0.90, 0.80, 0.60, 0.40, 0.20
	0.30	1.20	0.11 to 0.66	0.13
	0.30	0.577	0.28 to 0.71	0.06
	0.30	0.281	0.27 to 0.64	0.03
	0.30	0.118	0.08 to 0.65	0.01
	0.30	0.400	0.15 to 0.72	1.00, 0.80, 0.50
	0.30	0.200	0.10 to 0.62	1.00, 0.80, 0.50
	0.30	0.100	0.10 to 0.60	1.00, 0.80, 0.50

The Cornell tests described in Table 1(b) were made in a wooden flume 4.22 ft wide and approximately 30 ft long. Because of the short length of the flume, baffles were provided at the inlet to control the velocity distribution. A movable bottom was used to obtain different weir heights. Discharges were

measured volumetrically. The crest piece for this group of tests was made of rolled brass, $\frac{1}{4}$ -in. thick. It was described as having a straight, square, and sharp upstream top corner, with a machined $\frac{3}{32}$ -in. wide top surface and a beveled downstream face. The crest piece was mounted on a timber bulkhead. Head measurements were made with a float gage connected to piezometers 11.74 ft upstream from the weir.⁹

Experiments of the USBR.—Experiments on full-width weirs were performed by the Bureau of Reclamation, United States Department of the Interior (USBR), in connection with hydraulic investigations for the Boulder Canyon Project.¹⁰ A distinctive feature of the equipment used for the tests was a knife-edge, stainless-steel crest piece. The purpose of this innovation was to prevent the clinging-nappe phenomenon described previously. The crest piece was mounted on a steel plate located in a sheet-metal-lined wooden flume 2 ft wide and effectively 18 ft long. A movable floor was used to obtain different values of weir height. Baffles located at the upstream end were used to produce a uniform velocity distribution in the flume. Discharges were measured with Venturi meters in the supply line. Heads were measured with a hook gage in a stilling well connected to a piezometer in the movable floor 9.9 ft upstream from the weir. The scope of the USBR tests is shown in Table 1(c).

New Data on Rectangular Weirs.—Original experiments on rectangular weirs were performed in 1955 in the Hydraulics Laboratory of the Georgia Institute of Technology (Georgia Tech). For the Georgia Tech tests the weirs were located at the downstream end of a steel flume (30 in. deep, 10 ft wide, and 25 ft long). The floor of the flume was level and smooth. Its width was varied by means of movable walls faced with $\frac{1}{4}$ -in.-thick aluminum plates. For tests on full-width weirs the wall plates were made to project through the notch and past the crest a distance of 6 in. Baffles in the forebay and curved guide walls at the upstream ends of the movable walls were adjusted to produce a uniform velocity distribution. Surface floats were used at the entrance to damp waves in the flume.

The basic weir bulkhead was made of $\frac{3}{8}$ -in.-thick aluminum plate. The width and height of the weir notch was varied by means of lap-joined plate sections made of the same material. The notch edges, including the crest piece, were made of $\frac{1}{2}$ -in.-thick stainless-steel plates which were fastened to the aluminum plates with the upstream surfaces flush. The edge pieces were machined on a flat-bed planer to be smooth and flat on the upstream side and beveled on the downstream side. The top surface of the notch edges was $\frac{1}{16}$ in. wide and perpendicular to the upstream face of the weir. The upstream corners of the edge pieces were sharp.

Water was supplied to the flume from a constant-head system. Discharges were measured in an electrically operated weighing tank at the upstream end of the flume. Heads were measured with a hook gage in a stilling well which was connected to piezometers located in both movable walls 2 in. above the floor and 5 ft upstream from the weir.

The purpose of the Georgia Tech tests was to obtain the additional experimental data necessary to describe the discharge function over the full, practical

¹⁰ "Studies of Crests for Overfall Dams," *Bulletin 3*, Boulder Canyon Project, Final Reports, Bureau of Reclamation, U. S. Dept. of the Interior, Denver, Colo., 1948.

range of the variables shown in Eq. 7. The scope of the 249 tests which were made at Georgia Tech is shown in Table 1(d).

VERIFICATION OF THE PROPOSED SOLUTION

Recapitulation.—The coefficient, C_e , in the proposed discharge equation (Eq. 11) is defined in Eq. 10 in terms of the effective head, h_e , and the effective

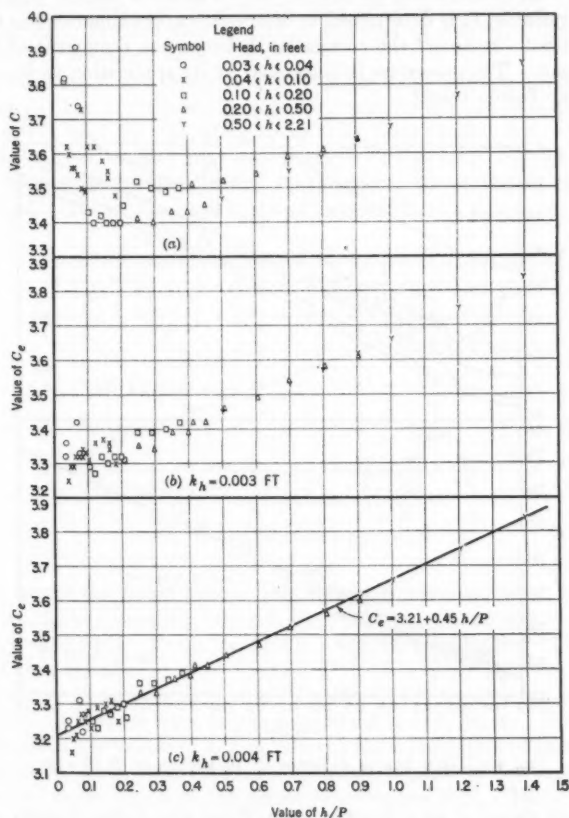


FIG. 3.—SCHODER AND TURNER SERIES E AND F ($b/B=1.0$)

notch width, b_e . It is also defined as a function of the geometric ratios, h/P and b/B . Unlike C (Eqs. 4 and 7), therefore, C_e is expected to be independent of the fluid-property effects represented by the magnitudes of h and b in Eq. 7.

It is assumed that C_e can be determined from laboratory data if the measured values of h and b are adjusted as indicated in Eqs. 8 and 9. In Eq. 8 the effective head is defined as the measured head plus a quantity, k_h . Similarly, in

Eq. 9 the effective width is defined as the measured width plus a quantity, k_b . It is reasonable to conclude that the proposed discharge equation will be practicable and convenient to use only if k_h and k_b are constants or functions of not more than one independent variable. Thus, verification of the proposed solution is critically related to the experimental evaluation of the k -quantities.

Evaluation of k_h .—The quantities k_h and k_b are evaluated from experimental data by a trial computation procedure. For a series of tests in which h is the principal variable, k_h is determined by successive approximations as the quantity which will "remove" the correlation between the coefficient of discharge and the head. The procedure is illustrated by its application to the results of the Schoder-Turner tests.⁹

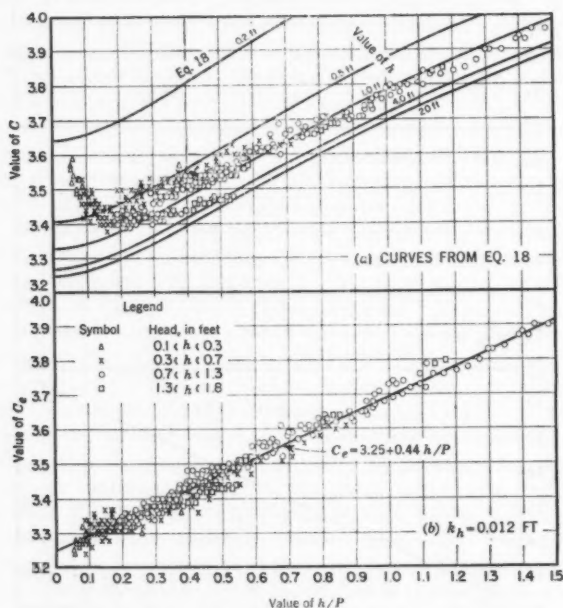


FIG. 4.—BAZIN SERIES 1 THROUGH 10 INCLUSIVE ($b/B = 1.0$)

Fig. 3(a) shows C as a function of h/P for two series of tests made by Schoder and Turner on full-width weirs (Table 1(b)). The scatter in values of C , which is most apparent at lower values of h/P , is systematically related to the magnitude of h . If a small quantity, k_h , is added to h , the value of the coefficient is reduced by an amount which is inversely related to the value of h . Values of the adjusted coefficient, C_e , from a trial computation, using $k_h = 0.003$ ft, are shown in Fig. 3(b). A second trial, with $k_h = 0.004$ ft, is shown in Fig. 3(c). From Figs. 3(a) and 3(c) it is apparent that a constant value of $k_h = 0.004$ ft effectively eliminates the correlation between the coefficient of

discharge and the head for series E and F in the Schoder and Turner tests. In Fig. 3(c), furthermore, C_s is conveniently related to h/P by a straight-line equation.

The Schoder and Turner series E and F were selected for two reasons. First, they included some tests with very low values of h . For these tests, therefore, the effects of viscosity and surface tension which are related to the magnitude of h are relatively large. Second, the width of the weir used for the tests was large enough (4.22 ft) that the influence of k_b on C_s could be assumed to be negligible. Proof of this conclusion is based on results of Georgia Tech tests which are described subsequently.

Fig. 4(a) shows C as a function of h/P for the Bazin tests on full-width weirs (Table 1(a)). Fig. 4(b) shows the same data in a plot of C_s as a function of h/P . The value of k_b used for computing C_s for these tests was 0.012 ft. This value was selected on the basis of trial computations as the value required to eliminate the correlation (evident in Fig. 4(a)) between the coefficient of discharge and the head. The effect of the width-adjustment factor, k_b , was assumed to be

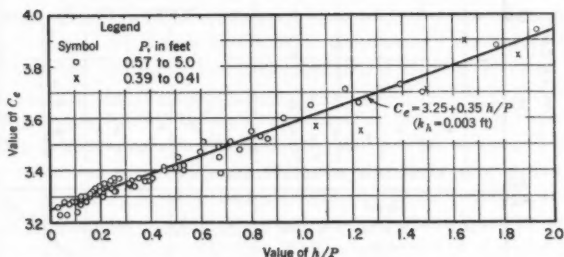


FIG. 5.—USBR TESTS ($b/B = 1.0$)

negligible for all the Bazin tests. This assumption is believed to have had a small effect on the computed values of C_s for only one group of tests, series 3, for which b was 1.64 ft. From Fig. 4(b) it is apparent, again, that C_s is a simple, linear function of h/P .

Fig. 5 shows C_s as a function of h/P for the USBR tests on full-width weirs (Table 1(c)). For these tests, k_b was determined to be 0.003 ft. The scatter in the points for larger values of h/P is believed to be indicative of experimental errors resulting from observational difficulties related to low values of P . Symbols are used in Fig. 5 to distinguish lower values of P . The width of the flume was approximately 2 ft. The effect of k_b was assumed to be negligible.

Only full-width weirs ($b/B = 1.0$) were involved in the tests made by Schoder and Turner, Bazin, and the USBR. Therefore, one of the principal purposes of the Georgia Tech tests (Table 1(d)) was to determine the validity of the proposed solution as applied to notch weirs. Tests made specifically to evaluate k_b included a complete series for each of the following values of b/B : 0.20, 0.40, 0.60, 0.80, 0.90, and 1.00. For the tests on notch weirs, the width was 1.80 ft. For the tests on full-width weirs, b was 2.68 ft. Thus, for all of

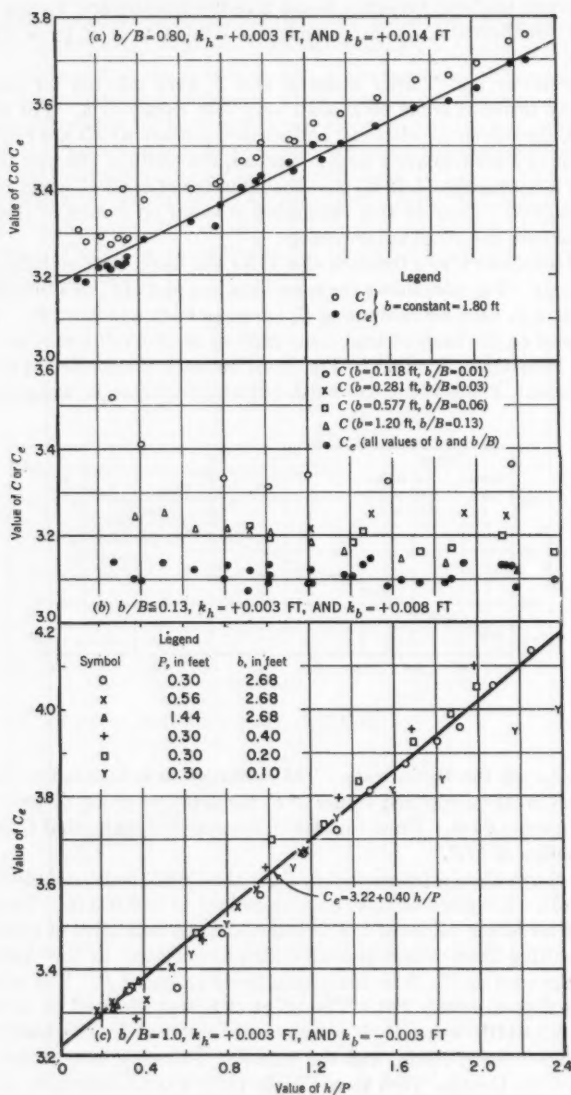


FIG. 6.—GEORGIA TECH TESTS

the k_h -tests the relative influence of effects related to b were negligible. Both h and P were varied in each series of tests in order to cover a full range of values of h/P . Values of h varied from 0.10 ft to 0.76 ft, and values of P varied from 0.30 ft to 1.44 ft. Sufficient tests were made to define the coefficient of discharge from $(h/P) = 0$ to $(h/P) = 2.4$. Fig. 6(a) shows the results of a typical series ($b/B = 0.80$).

The successive-approximations procedure was used to evaluate k_h for each series of tests. Remarkably, the value of k_h required to satisfy the effective-head criteria was the same for all values of b/B and all values of h/P included in the Georgia Tech tests. That is, for a full, practical range of the significant variables a constant value of k_h (0.003 ft) was adequate to compensate for the fluid-property effects related to the head. This conclusion was subsequently verified by successfully applying the same value of k_h to additional tests covering values of b/B from 0.01 to 1.00 and values of b as small as 0.10 ft. Thus, the effective-head concept is substantiated as an important part of the proposed solution.

Differences in values of k_h and in the C_e -curves determined from Schoder and Turner, Bazin, USBR, and Georgia Tech tests on full-width weirs are believed to have been caused by differences in test equipment. The larger value of k_h which characterizes the Bazin tests, for example, is believed to be an indication that Bazin's weir plate was not effectively thin. The results of the USBR tests are doubtless influenced by the fact that the crest piece of the weir was knife-edged. The Schoder and Turner tests may have been influenced by the fact that their flume was very short and entrance conditions were apparently poor for large values of P . Most of Bazin's tests, on the other hand, were made in flumes long enough to develop a normal, open-channel velocity distribution. Thus, the results of each investigation are characterized by the equipment used in making the experiments.

A constant value of k_h was found to be adequate for all weirs tested in the Georgia Tech investigation. Different values of k_h were determined for full-width weirs tested by other investigators. Therefore, although it is indicated that the same value of k_h can be used for all values of b/B , the value of k_h to be used is also dependent on the physical characteristics of the weir and weir channel.

Evaluation of k_b .—The weirs investigated by Bazin, Schoder and Turner, and the USBR were too wide to reveal the fluid-property effects related to small values of b . Therefore, the results of these tests could not be used to evaluate k_b . Some tests on weirs of relatively small width were included in the Georgia Tech experiments. It was the purpose of these tests to evaluate k_b and to investigate the validity of the effective-width concept.

In Fig. 6(a) the total displacement of values of C_e with respect to corresponding values of C is a measure of the combined effects of k_h and k_b . However, only a few points at low values of h/P represent heads so small that the adjustment caused by k_h was appreciable. The nearly uniform displacement at higher values of h/P therefore, is the result of using a value of $k_b = 0.014$ ft in the computation of C_e . This value was determined from trial computations as the

value of k_b which would eliminate the correlation between b and C_e in the results from a special series of tests with $(b/B) = 0.80$ (not shown in Fig. 6).

Fig. 6(b) shows the results of special tests made to evaluate k_b for another value of b/B . Actually, several values of b/B are represented on Fig. 6(b), but the results of the tests indicated that k_b is essentially constant for values of b/B less than 0.2. In Fig. 6(b) the effect of the k_b -adjustment is shown by the displacement of values of C_e with respect to corresponding values of C . The value of k_b used in computing C_e for this example was 0.008 ft.

Fig. 7 shows the results of all tests made to evaluate k_b . Fig. 7 indicates that k_b is a function of b/B , that it increases with increasing values of b/B until it reaches a maximum positive value of 0.014 ft at $(b/B) = 0.80$, and that it decreases rapidly thereafter, reaching a minimum value of -0.003 ft at $(b/B) = 1.0$. The writers acknowledge some uncertainty regarding the generality of the curve in Fig. 7. It is believed that the value of k_b obtained from the Georgia Tech tests may have been influenced, to an unknown extent, by the physical characteristics of the equipment used. Tests made especially to

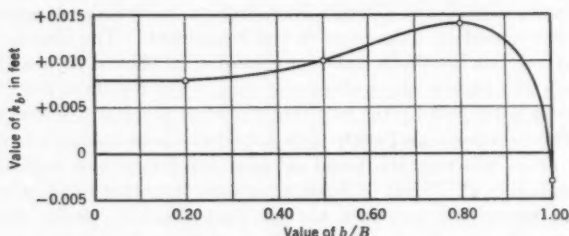


FIG. 7.—VALUE OF WIDTH-ADJUSTMENT FACTOR FROM GEORGIA TECH TESTS

evaluate k_b involved very small values of b and correspondingly small values of B and Q . Thus, unavoidable errors of measurement may account for comparatively large relative errors in the computed results. Nevertheless, the adequacy of the effective-width concept was demonstrated by the successful elimination of b as an independent variable in the experimentally determined relationship between C_e , h/P , and b/B .

A remarkable example of the experimental evidence which substantiates both the effective-head and the effective-width concepts is shown in Fig. 6(c). In Fig. 6(c) a single, straight line satisfactorily represents the relationships between C_e and h/P for full-width weirs involving values of b from 0.10 ft to 2.68 ft and values of h from 0.10 ft to 0.72 ft.

Evaluation of C_e .—The results of the tests from all sources indicate that C_e , the "effective" coefficient of discharge, is a function of b/B and h/P alone. Thus, in confirmation of Eq. 10, C_e is independent of the influences of viscosity and surface tension. Furthermore, the results show that the relationship between C_e and h/P for all values of b/B is conveniently defined by a family of straight lines.

Fig. 8 shows a summary of the results of the Georgia Tech tests. The information in Fig. 8, in combination with values of k_h and k_b (Fig. 7) determined from the same tests, is the information needed to evaluate the proposed discharge equation. Thus, Eq. 11, complemented by the effective-head and effective-width concepts, is confirmed as a comprehensive equation of discharge for all rectangular, thin-plate weirs.

SUMMARY

Experimental Results.—The proposed discharge equation (Eq. 11) and the concepts of effective head and effective width (Eqs. 8 and 9) have been sub-

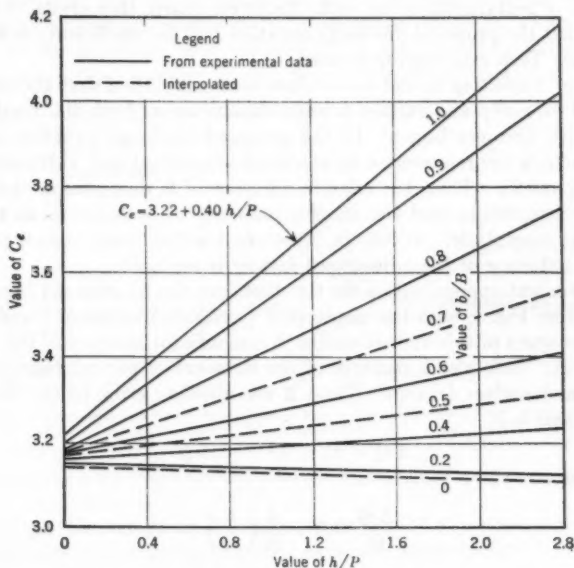


FIG. 8.—VALUE OF DISCHARGE COEFFICIENTS FOR ALL VALUES OF THE CONTRACTION RATIO FROM GEORGIA TECH TESTS

stantiated by experiments from various sources covering a wide range of test conditions. It has been demonstrated that C_e is a linear function of h/P for each value of b/B , that k_h is a constant for all values of b/B and h/P , and that k_b is a function of b/B .

From the results of tests made at Georgia Tech, values of C_e , k_h , and k_b have been determined for water at ordinary temperatures. Fig. 8 shows C_e for a full range of values of b/B , with h/P ranging from 0 to 2.0. From the information contained in Fig. 8, simple equations for C_e can be written if desired. The constant value of k_h determined from the Georgia Tech tests is 0.003 ft. Values of k_b are shown in Fig. 7.

Comparisons of values of C_e and k_h obtained from tests made by different investigators of full-width weirs confirm the general conclusion that weir discharge is critically influenced by the physical characteristics of the experimental equipment. Especially critical are the weir-notch edges and the channel properties which control the velocity distribution and turbulence upstream from the weir.

Neither superior equipment nor superior technique is claimed for the Georgia Tech tests. However, it is believed that the over-all quality of these data is as good as that of any other data available. Furthermore, this is the only investigation known to cover a full, practical range of the significant variables. Therefore, as a reasonably accurate solution for the comprehensive discharge characteristics of rectangular weirs with effectively sharp, thin crests, it is recommended that the proposed discharge equation and the coefficients derived from the Georgia Tech experiments be used.

Effect of Neglecting k_h and k_b .—It has been established that the relative influence of viscosity and surface tension diminishes as both the head and the notch width becomes larger. In the proposed discharge equation the fluid-property effects are represented by the head-adjustment and width-adjustment factors, k_h and k_b . Thus, the relative influence of k_h decreases as the head increases in magnitude, and the relative influence of k_b decreases as the width increases in magnitude. It follows, therefore, that for "large" heads on "large" weirs the influence of the adjustment factors is negligible.

A convenient approximation for the discharge can be obtained from Eq. 11, using C_e from Fig. 8, with the unadjusted (measured) values of h and b . The relative accuracy of this approximation is a significant measure of the influence of k_h and k_b . It is also a measure of the influence of the combined effects of viscosity and surface tension. Thus, if the absolute error (ΔQ) due to neglecting k_h and k_b is

$$\Delta Q = C_e b_e h_e^{\frac{3}{2}} - C_e b h^{\frac{3}{2}} \dots \dots \dots (12)$$

the relative error is

$$\frac{\Delta Q}{Q} = 1 - \frac{b}{b_e} \left(\frac{h}{h_e} \right)^{\frac{3}{2}} \dots \dots \dots (13)$$

The influence of k_h alone can be demonstrated by assuming that the notch width is very large, whence $b \approx b_e$ in Eq. 13. Then, from Eqs. 8 and 13,

$$\frac{\Delta Q}{Q} = 1 - \left(\frac{h}{h + k_h} \right)^{\frac{3}{2}} \dots \dots \dots (14a)$$

which is shown in Fig. 9(a) for $k_h = 0.003$ ft. Similarly, the separate influence of k_b can be demonstrated by assuming that $h \approx h_e$. Thus, from Eqs. 9 and 13,

$$\frac{\Delta Q}{Q} = 1 - \left(\frac{b}{b + k_b} \right) \dots \dots \dots (14b)$$

which is shown in Fig. 9(b) for several values of k_b . Figs. 9(a) and (b) are recommended for use in connection with Eq. 11 as a means of determining when (depending on the accuracy desired) the influence of the fluid properties may be neglected.

Upper Limit of h/P .—Paul Böss has shown¹¹ that critical depth will occur in the uniform flow upstream from a weir with h/P greater than about 5 and $b/B = 1.0$. For values of h/P greater than 5, therefore, the weir is not a control, and the ordinary weir-discharge equations are not applicable. Practical limitations on h/P are related to the observation that head-measurement difficulties and errors result from surges and waves which occur in the approach channel at larger values of h/P (in combination with larger values of b/B). For full-width weirs ($b/B = 1.0$), the recommended maximum value of h/P is 2.0. Limitations on h/P corresponding to smaller values of b/B have not been established, but it is assumed that the maximum permissible value of h/P increases as b/B decreases.

Influence of Weir Height.—The weir height, P , was acknowledged as a possible third significant length parameter in the discharge function. There is disagreement in the literature, however, regarding experimental evidence of a systematic correlation between P and the coefficient of discharge. Bazin

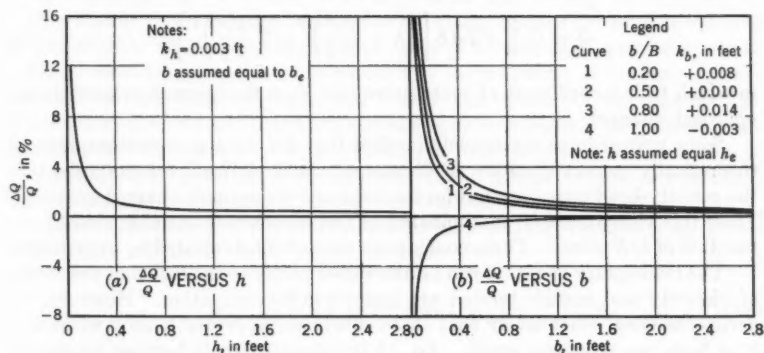


FIG. 9.—EFFECT OF VISCOSITY AND SURFACE TENSION RELATED TO h AND b

warned¹² against the use of his discharge formulas for a "very low weir * * * which should always be avoided." Th. Rehbock acknowledged¹³

" * * * some disturbance, which is not yet clearly understood, [and because of which] the coefficient C is not exactly the same for any two sharp-crested weirs of different absolute heights, P , even if the ratios, h/P , are identical."

Weirs as low as 0.08 ft were used in the USBR tests in order to achieve the higher values of h/P . The results of these tests show a definite correlation between C_e and P for values of h/P greater than 2 (not included in Fig. 5). The Georgia Tech tests, however, failed to show a similar correlation for values of P as low as 0.30 ft and values of h/P as high as 2.4.

¹¹ "Berechnung der Abflussmengen und der Wasserspiegellage bei Abstürzen und Schwellen unter besonderer Berücksichtigung der dabei auftretenden Zusatzspannungen," by Paul Böss, *Wasserkraft und Wasserversorgung*, Vol. 22, 1929, pp. 13-33.

¹² "Recent Experiments on the Flow of Water Over Weirs," by H. Bazin, English translation by Arthur Marichal and John C. Trautwine, Jr., *Proceedings, Engineers Club of Philadelphia*, Vol. VII, 1889, p. 309.

¹³ Discussion by Th. Rehbock of "Precise Weir Measurements," by Ernest W. Schoder and Kenneth B. Turner, *Transactions, ASCE*, Vol. 93, 1929, p. 1148.

It is generally acknowledged that observational difficulties and errors in measurement may account for appreciable errors in the results of experiments involving small values of P and large values of h/P . For this reason alone, weirs lower than 0.3 ft are not recommended for precise measurement of discharge. Nevertheless, although questions regarding the influence of weir heights less than 0.3 ft may be academic, additional experiments are needed to resolve the contradictions to be found in the literature.

COMPARISON WITH OTHER EXPERIMENTS AND FORMULAS

Some Classic Formulas.—One equation is frequently described as the basic equation of discharge for all weirs. It is founded on an assumed analogy between the weir and the two-dimensional orifice. In its derivation an approximate velocity equation is integrated over the approximate area limits of the nappe in the plane of the weir. The effects of viscosity and surface tension are ignored. The result, in the form usually ascribed to J. Weisbach, is

$$Q = C_c \frac{2}{3} \sqrt{2g} b \left[\left(h + \frac{V_1^2}{2g} \right)^{\frac{3}{2}} - \left(\frac{V_1^2}{2g} \right)^{\frac{3}{2}} \right] \dots \dots \dots (15)$$

in which C_c is a coefficient of contraction and V_1 is the average velocity in the approach channel.

Some writers have erroneously implied that Eq. 15 is a comprehensive and theoretically correct equation of discharge. It is claimed, for example, that the velocity-head terms account for the influence of approach-channel geometry. From this viewpoint h/P is eliminated as an independent variable, and C_c is a function of b/B alone. These conclusions are not substantiated by experiment.

The inadequacy of Eq. 15 can be attributed partly to the fact that the effects of viscosity and surface tension are ignored in its derivation. However, experiments show conclusively that these effects are appreciable only when h or b , or both, are relatively small. Eq. 15 is deficient largely because its derivation was based on several erroneous assumptions.

Unjustifiable alterations of Eq. 15 have been made for the purpose of improving agreement between the equation and experimental data. It is quite common to omit the second velocity-head term in the brackets, and, subsequently, to attribute great significance to the "total head" term which remains. The result is an equation such as that proposed¹⁴ by Hamilton Smith, Jr., in 1884:

$$Q = C_s \frac{2}{3} \sqrt{2g} b \left[h + k_1 \left(\frac{V_1^2}{2g} \right)^{\frac{1}{2}} \right] \dots \dots \dots (16)$$

in which both C_s and k_1 are coefficients determined from experiment. Smith described the coefficient k_1 as a number which represents "the portion of the kinetic energy [which] produces a useful effect at the opening of discharge." He recognized that k_1 is a variable which depends on the velocity distribution in the approach channel. Nevertheless, he recommended a constant value of 1.33 for all full-width weirs and 1.40 for all "fully contracted" weirs. He de-

¹⁴ "Hydraulics," by Hamilton Smith, Jr., John Wiley & Sons, Inc., New York, 1884.

scribed C_s as a discharge coefficient, and he concluded that it was a function of the head, the notch width, and the width-contraction ratio (b/B). Actually, both k_1 and C_s are functions also of the ratio h/P , and they are critically dependent on the physical characteristics of the weir and the approach channel. Therefore, Eq. 16 is little more than a basis for the experimental definition of the discharge function. It is obviously not the most convenient formula for this purpose, nor is it the comprehensive solution which is needed.

Smith's exhaustive study and detailed exposition of the influence of the velocity of approach was subsequently ignored or misinterpreted by others. Some writers have inferred that his k_1 -coefficient can be associated with the kinetic energy coefficient, (α_1). Accordingly, they have perpetuated the misconception that the coefficient of discharge is a constant when the quantity within the brackets in Eq. 16 is evaluated as the true total energy head in the approach channel $\left[h + \alpha_1 \left(\frac{V_1^2}{2g} \right) \right]$.

The coefficient, α , is defined as the ratio of the true average velocity head in a cross section to the velocity head computed on the basis of the average velocity in the section. It is a dimensionless measure of the degree of nonuniformity of velocity, but it does not account specifically for the shape of the velocity-distribution curve. Smith, Schoder and Turner, and others who have studied the influence of the velocity distribution in the approach channel have shown conclusively that the pattern of nonuniformity is more critical than the degree of nonuniformity. Thus, experiments performed in a large variety of weir channels have failed to reveal a satisfactory correlation between α_1 and k_1 .

Most of the defects of Eq. 16 are common also to a large number of equations in the form suggested¹⁵ by Weisbach in 1844,

$$Q = C_w \frac{2}{3} \sqrt{2g} \left[k_2 + k_3 \left(\frac{h}{P+h} \right)^2 \right] b h^{3/2} \dots \dots \dots (17)$$

in which C_w , k_2 , and k_3 are experimentally determined coefficients which account for the influence of the fluid properties, the velocity distribution, and the physical characteristics of the weir and approach channel. The principal advantage of Eq. 17 is that the velocity-head term in Eq. 16 is replaced by a term which involves the (h/P)-ratio. The effect of this modification is to avoid a successive-approximations solution for discharge. Equations of this general variety include some of the most widely used formulas for full-width weirs ($b/B = 1.0$). Among these are the Bazin formula,⁷

$$Q = \left(3.25 + \frac{0.079}{h} \right) \left[1 + 0.55 \left(\frac{h}{P+h} \right)^2 \right] b h^{3/2} \dots \dots \dots (18)$$

the Rehbock formula of 1912,¹⁶

$$Q = \left(3.24 + 0.43 \frac{h}{P} + \frac{0.018}{h} \right) b h^{3/2} \dots \dots \dots (19)$$

¹⁵ "History of Hydraulics," by Hunter Rouse and Simon Ince, Iowa Institute of Hydraulic Research, State University of Iowa, Iowa City, Iowa, 1957, p. 163.

¹⁶ Discussion by Th. Rehbock of "Precise Weir Measurements," by Ernest W. Schoder and Kenneth B. Turner, *Transactions, ASCE*, Vol. 93, 1929, p. 1147.

and the S.I.A. (Swiss Society of Engineers and Architects) formula,¹⁷

$$Q = \left(3.29 + \frac{0.011}{h + 0.005} \right) \left[1 + 0.5 \left(\frac{h}{P + h} \right)^2 \right] b h^{\frac{3}{2}} \dots \dots (20)$$

The complex expressions which are the coefficients of the quantity $b h^{\frac{3}{2}}$ in each of these equations are equivalent to C in the simple equation of discharge (Eq. 4). The numerical quantities are experimentally derived coefficients which account for the influence of the fluid properties as well as the weir and channel characteristics. Specifically, a term involving and having the dimensions of h is now recognized as a means of compensating for the combined effects of viscosity and surface tension. Because it is a dimensional quantity, the h term restricts the application of Eqs. 18, 19, and 20 to the fluid used for the experiments (water at ordinary temperatures). However, it is apparent that the influence of the head term is negligible except when h is relatively small.

An alternate formula for full-width weirs was proposed by Rehbock in 1929:¹⁸

$$Q = \left(3.22 + 0.44 \frac{h}{P} \right) b h_e^{\frac{3}{2}} \dots \dots \dots (21)$$

This was the first formula known to involve the effective head ($h_e = h + 0.004$ ft). The quantity 0.004 ft, corresponding to k_h in Eq. 8, was apparently derived by Rehbock from an analysis of his own experiments.

Rehbock did not associate the h term in Eq. 19 or the effective-head term in Eq. 21 with the influence of the fluid properties. He described both terms as a means of accounting for a disturbance related to the magnitude of P . He hesitated to endorse L. Prandtl's suggestion that they were related to the effect of capillarity.¹³

Various restrictions were placed on Eqs. 18, 19, 20, and 21 by their authors. Bazin¹² specified that "the arrangement of our standard weir [must be] exactly reproduced." Rehbock¹⁸ required that the head be large enough to ensure a free nappe, but he claimed a high degree of accuracy for both of his formulas (Eqs. 19 and 21) when applied to full-width weirs of all sizes. The S.I.A. restricts¹⁷ the application of Eq. 20 to values of P not less than 1 ft, values of h between 0.08 ft and 2.6 ft, and values of h/P not greater than 1.0.

One of the few formulas developed for rectangular-notch weirs ($b/B < 1.0$) is that proposed by the S.I.A.:¹⁷

$$Q = \left[3.09 + 0.20 \left(\frac{b}{B} \right)^2 + \frac{0.063 - 0.053 \left(\frac{b}{B} \right)^2}{h + 0.005} \right] \times \left[1 + 0.5 \left(\frac{b}{B} \right)^4 \left(\frac{h}{P + h} \right)^2 \right] b h^{\frac{3}{2}} \dots (22)$$

¹⁷ Normen für Wassermessungen, Normen des Schweizerischen Ingenieur- und Architekten-Vereins, Swiss Society of Engineers and Architects, No. 109, 1924.

¹⁸ Discussion by Th. Rehbock of "Precise Weir Measurements," by Ernest W. Schoder and Kenneth B. Turner, *Transactions*, ASCE, Vol. 93, 1929, p. 1149.

The application of Eq. 22 is restricted to values of P not less than 1 ft, values of h between $0.08 (B/b)$ and 2.6 ft, values of h/P not greater than 1.0, and values of b/B not less than 0.3. Eq. 22 is widely quoted in European technical literature, but correspondence and library research failed to reveal the source of the data on which it was based. The formula is virtually unknown in the United States.

In engineering practice in the United States, approximate formulas for notch weirs are adapted from formulas for full-width weirs by means of the contracted-width equation ascribed to James B. Francis:^{19,20}

$$b_c = b - 0.2 h \dots \dots \dots (23)$$

in which b_c is the width of the contracted stream and the quantity 0.2 is a coefficient recommended by Francis for "fully contracted" rectangular-notch weirs. Thus, from Eqs. 4 and 23, the Francis discharge formula for notch weirs is

$$Q = C_1 (b - 0.2 h) h^{3/2} \dots \dots \dots (24)$$

in which C_1 is the coefficient of discharge in any of the formulas for full-width weirs ($b/B = 1.0$).

Smith, after reviewing the experiments of Francis, A. Fteley and F. P. Stearns,²¹ and others, described the requirements for "full contraction" as follows:²⁰ The weir height should be not less than twice the head or not less than 1 ft; the width from the side of the approach channel to the end of the notch should be not less than twice the head or twice the width of the notch. Thus, Smith's recommendations included the requirement that h/P be not greater than 0.5 and that b/B be not greater than 0.2. Francis²⁰ added the requirement that b/h be not less than 3.0. It is recognized now that the concept of "full contraction" is inconsistent with the true significance of b/B as an independent variable.

Comparison of Experiments and Formulas for Full-Width Weirs.—The experiments of Schoder and Turner, Bazin, and the USBR, as well as the Georgia Tech experiments, were used to confirm the method of analysis and the discharge equation proposed herein. Consequently, values of C_e and k_b were determined, and these values can be used to compare the results of the tests made by the different investigators. Comparable values of k_b could not be determined because only the Georgia Tech experiments included tests on weirs narrow enough to reveal the fluid-property effects associated with small values of b .

From the results of the Georgia Tech tests on full-width weirs, $k_b = 0.003$ ft, $k_b = -0.003$ ft, and C_e is given by,

$$C_e = 3.22 + 0.40 \frac{h}{P} \dots \dots \dots (25)$$

¹⁹ *Lovell Hydraulic Experiments*, by James B. Francis, D. Van Nostrand, New York, fourth ed., 1883.

²⁰ "Weir Experiments, Coefficients, and Formulas," by Robert E. Horton, *Water-Supply Paper 200* Geological Survey, U. S. Dept. of the Interior, 1907.

²¹ "Description of Some Experiments on the Flow of Water Made During the Construction of Works for Conveying the Water of Sudbury River to Boston," by A. Fteley and F. P. Stearns, *Transactions, ASCE* Vol. 12, 1883, pp. 1-118.

From the Schoder and Turner tests (series E and F) in Fig. 3(c), $k_h = 0.004$ ft, and

$$C_e = 3.21 + 0.45 \frac{h}{P} \dots \dots \dots (26)$$

The results of the Bazin tests on full-width weirs are shown in Fig. 4. The value of k_h required for the Bazin tests is considerably larger than that determined from the other experiments. From Fig. 4(b), $k_h = 0.012$ ft, and

$$C_e = 3.25 + 0.445 \frac{h}{P} \dots \dots \dots (27)$$

The results of the USBR tests (Fig. 5), in comparison with the others, are characterized by smaller values of C_e at the larger values of h/P . For the USBR tests, $k_h = 0.003$ ft, and

$$C_e = 3.25 + 0.35 \frac{h}{P} \dots \dots \dots (28)$$

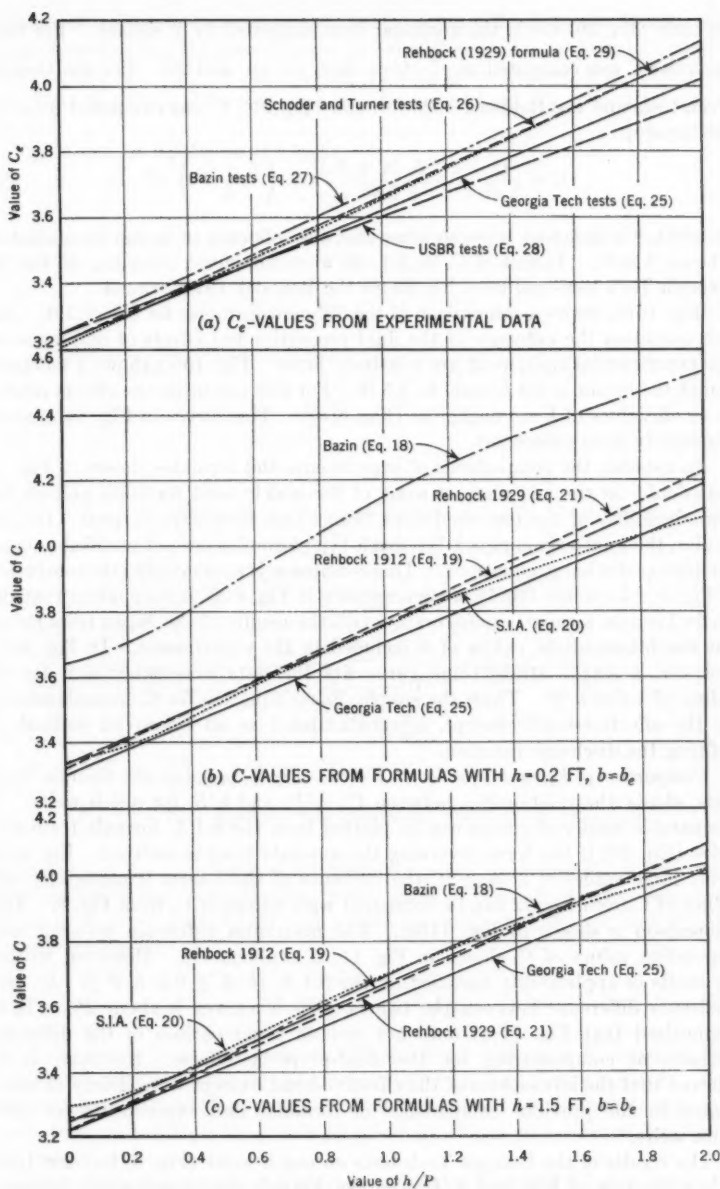
Rehbock's 1929 formula (Eq. 21) is also based on the effective-head concept. Furthermore, his equation for C_e is in the linear form of Eqs. 25 to 28, inclusive. Thus, for comparison with those equations, Rehbock's 1929 formula gives

$$C_e = 3.22 + 0.44 \frac{h}{P} \dots \dots \dots (29)$$

with $k_h = 0.004$ ft. Rehbock did not recognize the existence of k_b , although some writers have indicated that his experiments were made in a very narrow flume. Therefore, it is possible that Eq. 29 would be modified if k_b were taken into account. This conclusion could not be verified because Rehbock's experimental data were not available.

Eqs. 25 to 29, inclusive, are compared in Fig. 10(a). The Schoder and Turner, Bazin, and Rehbock curves agree reasonably well. The curve determined from the Georgia Tech tests lies below these curves and above the USBR curve. It was suggested previously that the differences in the results of the experiments shown in Fig. 10(a) were caused by differences in the test equipment. Thus, the distinctive character of the C_e -curve from the USBR tests can be associated with the fact that the crest piece for these tests was knifedged. Similarly, the larger value of k_h determined from Bazin's tests can be related to the conclusion that his crest was not truly thin and sharp. Such details as these, frequently unknown or uncontrollable, are believed to be the cause of the variance shown in Fig. 10(a). Nevertheless, it is noteworthy that the equations for C_e derived from various sources are all simple, linear functions of the (h/P) -ratio.

Fig. 10(b) and (c) shows a comparison of the results of the Georgia Tech tests with some of the most widely used formulas for full-width weirs. The comparison is made for two values of h and a full range of values of h/P . The Bazin formula (Eq. 18), the Rehbock 1912 formula (Eq. 19), and the S.I.A.

FIG. 10.—COMPARISON OF DATA AND FORMULAS ($b/B=1.0$)

formula (Eq. 20) are in the nonlinear form suggested by Weisbach. For these formulas C was computed as $\frac{Q}{b h^{3/2}}$ from Eqs. 18, 19, and 20. For the Georgia Tech tests and the Rehbock 1929 formula (Eq. 21), C was computed from the relationship

$$C = \frac{Q}{b h^{3/2}} = \frac{C_e b_e (h + k_h)^{3/2}}{b h^{3/2}} \approx \left(\frac{h + k_h}{h} \right)^{3/2} C_e \dots \dots \dots (30)$$

in which b is assumed to be so large that the influence of k_h can be neglected, whence $b \approx b_e$. Values of C_e in Eq. 30 were computed from Eq. 25 for the Georgia Tech tests and from Eq. 29 for the Rehbock 1929 formula.

Fig. 10(b) shows a comparison of the different formulas for $h = 0.2$ ft. For this condition the influence of the fluid properties and effects of differences in the experimental equipment are relatively large. Fig. 10(c) shows a comparison of the formulas for h equal to 1.5 ft. For this condition the effects related to small values of h are negligible (Fig. 9(a)). The curves in Fig. 10(c) show reasonably good agreement.

In general, the comparisons of experiments and formulas shown in Fig. 10 cast doubt on the adequacy of some of the widely used formulas and on the reproducibility of the test conditions from which they were derived. In particular, the relatively complex Weisbach-type formulas are not justified as comprehensive discharge equations. This conclusion is emphatically demonstrated in Fig. 4. From the family of curves shown in Fig. 4(a), it is apparent that the Bazin formula compares unfavorably with the results of the Bazin tests for all but the intermediate values of h included in the experiments. In Fig. 4(b), however, a single, straight-line curve fits the data reasonably well for all values of h and h/P . Thus, the simple, linear equation for C_e , complemented by the effective-head concept, is substantiated as an improved method of defining the discharge function.

Comparison of Formulas for Notch Weirs.—Fig. 8, based on the Georgia Tech tests, shows the relationship between C_e , h/P , and b/B , for notch weirs. A comparable family of curves can be plotted from the S.I.A. formula for notch weirs (Eq. 22) if the term involving the absolute head is omitted. For relatively large values of h (and b), the influence of the h -term is negligible, and values of C from Eq. 22 can be compared with values of C_e from Fig. 8. The comparison is shown in Fig. 11(a). The maximum difference between corresponding values of C_e shown in Fig. 11(a) is about 4%. However, within the limits of applicability specified by the S.I.A. ($b/B \geq 0.3$, $h/P \leq 1.0$), the maximum difference between the two families of curves is about 2%. It is emphasized that Fig. 11(a) does not include a comparison of the different methods of compensating for the fluid-property effects. However, it is believed that the advantages of the effective-head concept were clearly demonstrated in the previous comparisons of formulas and experiments for full-width weirs.

The results of the Georgia Tech tests on notch weirs (Fig. 8) indicate that C_e is a function of b/B and h/P . In the Francis contracted-width formula (Eq. 23), however, a correction for "end contractions" is assumed to be a

function of h alone. Because of this fundamental difference, the Francis discharge formula (Eq. 24) cannot be compared with the Georgia Tech tests or the S.I.A. formula on a graph such as Fig. 11(a). Nevertheless, it is possible to show that the Francis formula is not substantiated by the curves shown in Fig. 8.

Eq. 23 can be written in the form

$$b_e = b - K h \dots \dots \dots (31)$$

in which, according to Francis, K is a constant equal to 0.2 for "fully contracted" rectangular-notch weirs. From Eqs. 11, 24, and 31,

$$Q = C_e b_e h_e^{3/2} = C_{e1} (b - K h) h^{3/2} \dots \dots \dots (32)$$

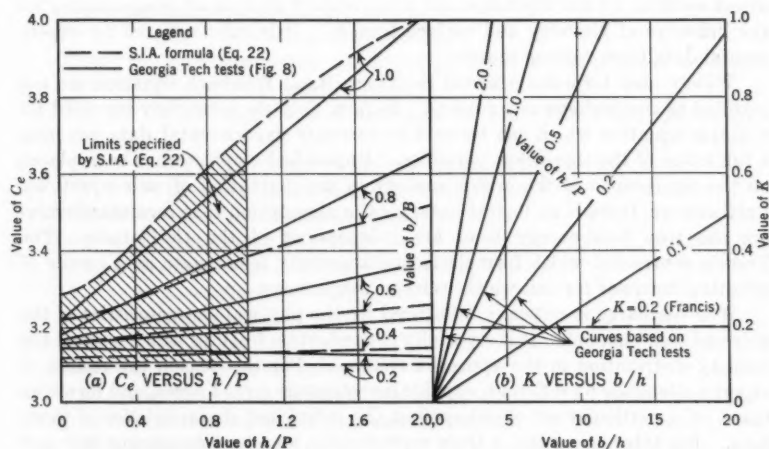


FIG. 11.—TEST RESULTS COMPARED WITH NOTCH-WEIR FORMULAS

in which C_e is the coefficient of discharge for notch weirs and C_{e1} is the corresponding coefficient for full-width weirs ($b/B = 1.0$). If the fluid-property effects related to small heads and widths are neglected, $h \approx h_e$ and $b \approx b_e$. Thus, from Eq. 32,

$$K = \left(\frac{C_{e1} - C_e}{C_{e1}} \right) \frac{b}{h} \dots \dots \dots (33)$$

Fig. 11(b) shows K as a function of h/P and b/h . Values of K shown in Fig. 11(b) were computed from Eq. 33, using values of C_e and C_{e1} from Fig. 8. It is apparent that the constant value of K recommended by Francis is not substantiated, even within the limits specified by Smith and Francis for "fully contracted" weirs.

The comparison shown in Fig. 11(a) indicates that the S.I.A. formula for notch weirs agrees reasonably well with the results of the Georgia Tech tests.

However, the complexity of the formula is a deterrent to its use, and the limits of applicability specified by the S.I.A. prevent its being a comprehensive solution for a full, practical variety of notch weirs. Furthermore, the effective-head and effective-width concepts that are complementary to the simple C_d equations derived from the Georgia Tech tests are believed to be superior to any other method for accounting for the influence of viscosity and surface tension.

CONCLUSIONS

The flow pattern for rectangular, thin-plate weirs is not subject to complete mathematical analysis. Consequently, an analytical solution for the discharge characteristics has not been developed. A comprehensive solution based on dimensional analysis and experiment has been presented. It provides a simple, direct solution for the discharge and a convenient method of compensating for the influence of viscosity and surface tension. It is substantiated by experimental data from various sources.

Widely used formulas adapted from the classic Weisbach equation are not justified as comprehensive solutions. In fact, they do not satisfy the need for a simple equation which can be used to correlate experimental data covering a full range of the significant variables. Unjustified emphasis has been placed on the significance of the orifice analogy in the derivation of weir equations. Furthermore, there is no logical basis for the assumption that formulas involving the true total-energy head are independent of the (h/P) -ratio. The Francis contracted-width formula is fundamentally inadequate as a means of adapting formulas for full-width weirs to notch weirs.

Weir discharge is critically influenced by the physical characteristics of the weir and weir channel. It is especially dependent on features which control the velocity distribution in the approach channel. For this reason the results of experiments made by different, capable investigators do not agree, and formulas based on a particular set of data reflect the individual characteristics of those data. For this reason, too, a truly reproducible, standard measuring weir and a precise, universal discharge formula are impractical.

ACKNOWLEDGMENTS

The investigation on which this paper is based is part of a comprehensive study of the discharge characteristics of weirs and spillways which is being undertaken (as of 1959) by the Water Resources Division (Surface Water Branch) of the Geological Survey, United States Department of the Interior (USGS). Original experimental data on notch weirs were obtained from a thesis investigation²² conducted at the Georgia Institute of Technology. The thesis was originally undertaken to substantiate the analysis proposed by the senior author in unpublished reports prepared for the USGS. Engineer personnel of the Research Section, USGS, at Atlanta, Ga., participated in the computations and in the preparation of this report.

²² "A Comprehensive Discharge Equation for Rectangular-Notch Weirs," by Rolland W. Carter, thesis presented to the Georgia Institute of Technology, Atlanta, Ga., 1956, in partial fulfillment of the requirements for the degree of Master of Science in Civil Engineering.

APPENDIX. NOTATION

The following symbols, adopted for use in the paper and for the guidance of discussers, conform essentially with "American Standard Letter Symbols for Hydraulics" (ASA Y10.2-1958), prepared by a committee of the American Standards Association with Society representation, and approved by the Association in 1958:

- B = width of approach channel;
 b = width of weir notch;
 b_s = width of the contracted stream;
 b_e = effective notch width;
 C = coefficient of discharge:
 C_c = coefficient of contraction;
 C_d = coefficient of discharge that is independent of fluid-property effects;
 C_{d1} = coefficient of discharge for full-width weirs, used in Eq. 32;
 C_s = discharge coefficient used in Eq. 16;
 C_w = discharge coefficient used in Eq. 17;
 F = resultant surface-tension force;
 g = acceleration due to gravity;
 h = piezometric head referred to crest of weir:
 h_e = effective head;
 K = constant in Eq. 31;
 k_b = width-adjustment factor;
 k_h = head-adjustment factor;
 k_1 = experimental coefficient used in Eq. 16;
 k_2, k_3 = experimental coefficients used in Eq. 17;
 L = a length;
 P = height of weir crest above bottom of channel;
 Q = discharge;
 R = Reynolds number;
 V = average velocity:
 V_1 = average velocity in approach channel;
 W = Weber number;
 α = kinetic-energy coefficient:
 α_1 = kinetic-energy coefficient for the approach section;
 γ = specific weight;
 μ = absolute viscosity;
 ν = kinematic viscosity;
 ρ = density; and
 σ = surface tension.

DISCUSSION

TURGUT SARPKAYA,²² A. M. ASCE.—The study of the characteristics of flow over a weir has become a basic and challenging problem for research workers in fluid mechanics, quite apart from the interest it holds for its purely practical engineering applications. Therefore, any engineer who is concerned with the measurement of discharge by the use of a thin-plate rectangular weir, together with a true understanding of the limitations of various approximate formulas, should welcome this most noteworthy addition of experimental data. The precision of the measurements, the wide variation of the parameters involved (excluding the fluid properties), and the qualitative physical explanations of the observed characteristic curves of discharge coefficients are outstanding features of the paper.

The authors associate the influence of viscosity and surface tension with a fictitious increase in head, h , and in width, b , in order to obtain a discharge coefficient independent of the size of the weir and of the magnitude of the head. They also embody the combined effects of the several phenomena attributed to viscosity and surface tension in the quantities k_h and k_b without fully acknowledging the limitations that these quantities imposed on the proposed formula. It is not implied, however, that formulas developed by the adjustments of head and width, or by any other method, are not valuable as long as they satisfy the experimental results within the range for which they are developed. However, it is hoped that the development of empirical formulas will be related closely with the natural variations of the parameters involved and will be interpreted in that manner wherever possible. At all times it should be kept in mind that an empirical equation derived by fitting a curve to a certain range of data can scarcely be expected to be generally or physically sound.

The standard form of flow formula is based on the Bernoulli proposition of equality of the sum of pressure and kinetic energies in the two sections concerned. Changes of energy due to fluid friction are allowed for only in their effect on the discharge coefficient, which is a value that is determined experimentally. In addition to the fluid friction, the discharge coefficient is influenced by, and allows for, other departures from ideal conditions, such as the nonuniformity of velocity distribution, the contraction of jet, and the mean curvature of the stream lines. The velocity distribution is determined by initial accelerations, fluid and boundary friction, and the geometrical characteristics of the weir. The increasing viscosity shown by the lower Reynolds numbers influences the coefficient of discharge as follows:

1. Internal fluid and boundary friction is increased, leading to greater resistance to shear in the acceleration through the notch, and, hence, a lowering of the discharge coefficient.
2. The velocity distribution of flow approaching the weir notch is changed in a direction that increases the central velocity in relation to the mean. This results in a greater total kinetic energy in the approach flow and a lower re-

²² Associate Prof., Dept. of Eng. Mechanics, Univ. of Nebraska, Lincoln, Nebr.

quirement of pressure energy to accelerate through the notch, thus raising the discharge coefficient.

3. Increased wall friction on the upstream face of the weir plate causes a retardation of the layers close to the surface that form, by their momentum, the lower and side boundaries of the nappe. This results in an enlargement of the latter quantities in comparison with the ones in potential flow—hence, an increased coefficient.

The foregoing reasoning is in close conformity with the one given by the authors. However, they failed to set forward the limitations of their reasoning. Is it true that the discharge coefficient will always increase with viscosity and surface tension? If this is correct then highly viscous fluids, such as glucose, honey, and molasses, would flow faster than water for a given head. What then is the answer to the apparent reversal of the foregoing reasoning? The

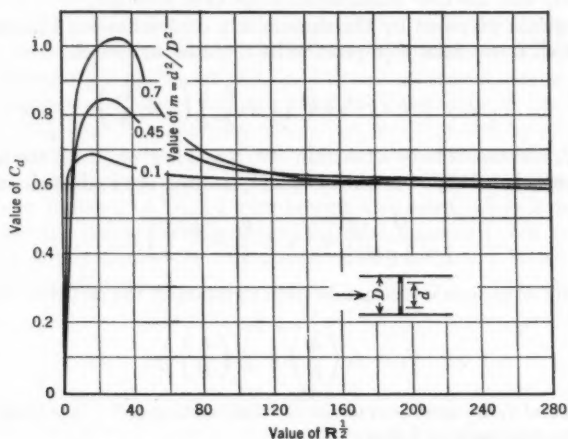


FIG. 12.—DISCHARGE-COEFFICIENT CURVES FOR SQUARE-EDGED ORIFICES

only explanation is that for values of the Reynolds number lower than a certain value, the discharge coefficient decreases rapidly. This is already a well-known phenomenon for flow in orifices, nozzles, and Venturi tubes. The humped shape of the orifice-coefficient curves in Fig. 12 is quite comparable with rectangular notch-weir discharge-coefficient curves. Obviously, the predominance of the foregoing influences 2 and 3 over a limited flow phase for Reynolds numbers greater than R_{cr} creates the hump on the coefficient curve. For values of R smaller than R_{cr} , the first influence is predominant. In the case of a low ratio of area with practically zero approach velocity, the hump is due to influence 3 only. Because the flow over the weir is a free surface flow, the surface tension has an additional effect on the foregoing influences and makes the analysis of the problem even more complicated. However, because the viscosity seems to play a more important role for lower values of the

Reynolds number, the coefficient of discharge will decrease instead of increase, which would be expected.

Therefore, the authors' explanations of the influences of viscosity and surface tension should be confined to a flow range in which the Reynolds number is greater than a certain critical value. Moreover, for certain values of the Reynolds number, some irregularities can be expected in the discharge coefficient, due to the transitional instability of the flow in the approach channel at the transition between turbulent and viscous flows. The proof for the existence of a critical Weber number and its experimental verification is rather difficult because for the liquids commonly used the one with a higher viscosity has a lower surface tension at a given temperature. Second, for a given liquid the increase of surface tension with a decrease in temperature is much slower than the increase of viscosity. Therefore, the viscosity always becomes predominant and makes it difficult to obtain a wide range of Weber numbers when the viscosity and the flow characteristics are kept constant.

The formula proposed by the authors as a comprehensive equation of discharge for all rectangular thin-plate weirs could be written as

$$Q = \frac{2}{3} \sqrt{2g} C_o b h^{\frac{3}{2}} \left(1 + \frac{k_b}{b}\right) \left(1 + \frac{k_h}{h}\right)^{\frac{1}{2}} \dots \dots \dots (34)$$

in which C_o is assumed to be a function of b/B and h/P only. If the last parenthesis is opened and higher orders of small quantities are neglected, one obtains

$$\frac{Q}{\frac{2}{3} \sqrt{2g} b h^{\frac{3}{2}}} = \left(1 + \frac{k_b}{b} + \frac{k_h}{h} \frac{3}{2}\right) C_o \dots \dots \dots (35)$$

Experiments of various investigators seem to establish the fact that C_o could be written as

$$C_o = f_6 \left(\frac{b}{B}\right) + f_7 \left(\frac{b}{B}\right) \frac{h}{P} \dots \dots \dots (36)$$

in which f_6 and f_7 are used as symbols of "the function of." It is proposed that f_6 and f_7 be expressed as follows:

$$f_6 \left(\frac{b}{B}\right) = \alpha + \beta \left(\frac{b}{B}\right)^m \dots \dots \dots (37a)$$

and

$$f_7 \left(\frac{b}{B}\right) = \gamma + \delta \left(\frac{b}{B}\right)^n \dots \dots \dots (37b)$$

in which α , β , γ , δ , m , and n are assumed to be constants, independent of the characteristics of the weir and of the properties of fluid. Hence, the coefficient of discharge becomes

$$C_d = \frac{Q}{\frac{2}{3} \sqrt{2g} b h^{\frac{3}{2}}} = \left\{ \left[\alpha + \beta \left(\frac{b}{B}\right)^m \right] + \left[\gamma + \delta \left(\frac{b}{B}\right)^n \right] \frac{h}{P} \right\} \times \left(1 + \frac{k_b}{b} + \frac{3}{2} \frac{k_h}{h}\right) \dots (38)$$

and the mean velocity at the section of weir notch is given by

$$V = \frac{2}{3} C_d \sqrt{2gh} \dots \dots \dots (39)$$

The derivation of a general equation that should be applicable to any liquid flowing over a rectangular notch weir is aided by a dimensional analysis of the problem. Although Eq. 38 is empirical, it should remove some of the objections to its use for liquids other than those actually tested if it is expressed in terms of the Reynolds number and the Weber number and verified by subsequent experiments. The coefficient of discharge, C_d , which is defined herein as independent of the acceleration of gravity is

$$C_d = \frac{Q}{\frac{2}{3} b h \sqrt{2gh}} = F\left(\frac{b}{B}, \frac{b}{h}, \frac{h}{P}, R, W\right) \dots \dots \dots (40)$$

The influence of the ratio, b/h , will be neglected in view of the experimental results mentioned by the authors. The definitions of the Reynolds number and Weber number for this particular problem is somewhat crucial because both the Reynolds number and Weber number must be related to both the head and the width of the weir. In addition, one cannot predict which length is physically more significant for each number. In each, velocity can be replaced by a dimensional equivalent, \sqrt{gh} . However, it should be remembered that if the particular function of Eq. 39 were known, this substitution would not be entirely correct. However, because the particular function is not known, the replacement is impossible. In this discussion Reynolds and Weber numbers will be defined as follows:

$$R = \frac{h^3}{\nu} \dots \dots \dots (41a)$$

and

$$W = \frac{\sqrt{b h}}{\sqrt{\frac{\sigma}{\rho}}} \dots \dots \dots (41b)$$

If b/B is replaced by Π_1 , h/P by Π_2 , $1/R$ by Π_3 , and $1/W$ by Π_4 , the following results:

$$C_d = F(\Pi_1, \Pi_2, \Pi_3, \Pi_4) \dots \dots \dots (42)$$

Dimensional analysis states that the general solution of the problem is

$$P_1 (\Pi_1)^{r_1} (\Pi_2)^{s_1} (\Pi_3)^{t_1} (\Pi_4)^{q_1} + P_2 (\Pi_1)^{r_2} (\Pi_2)^{s_2} (\Pi_3)^{t_2} (\Pi_4)^{q_2} + \dots = 0 \dots (43)$$

in which P , r , s , t , and $q \dots$ are constants to be determined. Letting α be the value of C_d as Π_1 , Π_2 , Π_3 , and Π_4 approach zero results in

$$C_d = \alpha + \frac{M_1 (b/B)^{r_1} (h/P)^{s_1}}{R^{t_1} W^{q_1}} + \frac{M_2 (b/B)^{r_2} (h/P)^{s_2}}{R^{t_2} W^{q_2}} \dots \dots \dots (44)$$

If Eq. 44 is compared with Eq. 38,

$$C_d = \left\{ \left[\alpha + \beta \left(\frac{b}{B} \right)^m \right] + \left[\gamma + \delta \left(\frac{b}{B} \right)^n \right] \frac{h}{P} \right\} \left(1 + \frac{N_1}{R^1} + \frac{N_2}{R^{-1} W^2} \right) \quad (45)$$

is obtained, in which

$$N_1 = \frac{3 k_h}{2 \nu^1} \dots \dots \dots (46a)$$

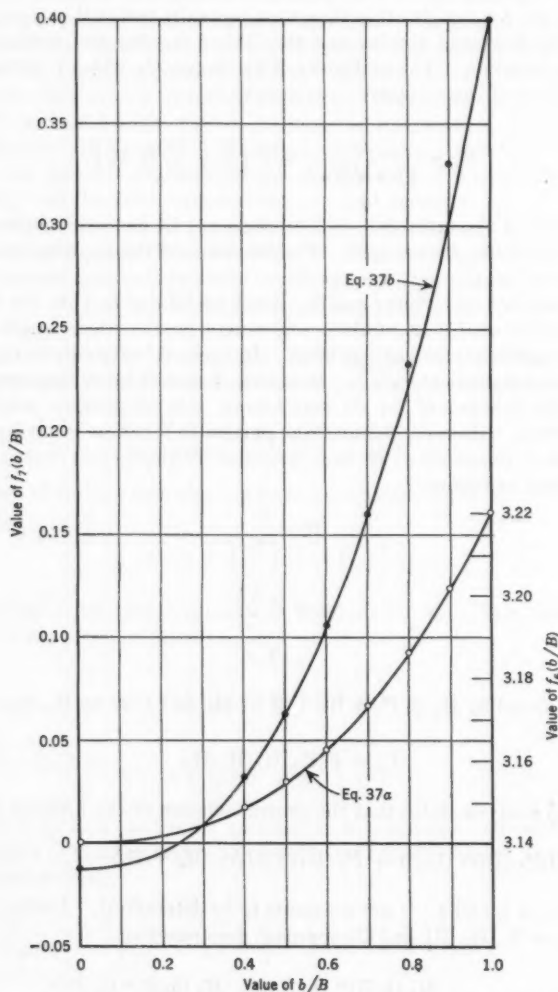


FIG. 13.—DETERMINATION OF THE CONSTANTS IN EQS. 37

and

$$N_2 = \frac{k_b \nu^{\frac{1}{2}}}{\frac{\sigma}{\rho}} \dots \dots \dots (46b)$$

The constants in Eqs. 37 are obtained by plotting the values of $f_6(b/B)$ and $f_7(b/B)$ versus b/B , as derived from Fig. 8. A logarithmic plot of these values yields a perfect straight line. However, the plots in Fig. 13 have been made on normal coordinate axes. The values obtained are $\alpha = 0.587$, $\beta = 0.015$, $\gamma = -0.0023$, $\delta = 0.0773$, $m = 2.43$, and $n = 2.43$.

Substituting $\nu = 11 \times 10^{-6}$ ft² per sec, $k_h = 0.003$ ft, $\sigma = 0.005$ lb per ft, and $\rho = 1.94$ slugs per ft³ Eq. 45 takes the following final form:

$$C_d = \left\{ \left[0.587 + 0.015 \left(\frac{b}{B} \right)^{2.43} \right] + \left[-0.0023 + 0.773 \left(\frac{b}{B} \right)^{2.43} \right] \frac{h}{P} \right\} \times \left(1 + \frac{9.11}{R^{\frac{1}{2}}} + \frac{0.1915 k_b}{R^{-\frac{1}{2}} W^2} \right) \dots (47)$$

Eq. 47 is satisfactory for all values of b/B and h/P except for $b/B = 0.9$. For the latter value experimental results yield C_d -values that are approximately 1% greater. In Eq. 47 the value of $\alpha = 0.587$ deserves more attention. The theoretical value of α for slots, orifices, sluice gates, and rectangular weirs is 0.611.

With the definitions accepted for the Reynolds number and Weber number, the variation of k_h and k_b with the fluid properties can be obtained from

$$k_{hx} = k_{hw} \left(\frac{\nu_x}{\nu_w} \right)^{\frac{1}{2}} \dots \dots \dots (48a)$$

and

$$k_{bx} = k_{bw} \left(\frac{\nu_w}{\nu_x} \right)^{\frac{1}{2}} \frac{(\sigma/\rho)_x}{(\sigma/\rho)_w} \dots \dots \dots (48b)$$

in which subscripts x and w indicate for any liquid and for water, respectively. It would be interesting to determine experimentally the variation of k_h and k_b with viscosity and surface tension. If Eqs. 48 hold for various liquids tested, Eq. 47 could be used for all liquids. Then Fig. 9 would have a true and broader meaning. Moreover, the usage of highly viscous fluids will remove the uncertainties existing in k_h and k_b , particularly, in k_b . The foregoing is correct because, according to Eq. 48a, the value of k_{hx} for a liquid that is eight times more viscous than water would be 0.012 ft, which is a value sufficiently great to determine more accurately by experiments. It should be recognized that, after the demonstration of the use of R and W as suitable parameters, the treatment is purely empirical. It is conceivable that several different functions might exist that would satisfy the experimental data equally well. Extrapolation of these functions outside the experimental range is unwarranted and should be used with caution or not at all.

STEPONAS KOLUPAILA²⁴.—The investigation of weirs is one of the most popular experiments in hydraulic laboratories. In the first 122 volumes of *ASCE Transactions*, there are no less than 100 valuable papers and important discussions on water flow over the weirs. Perhaps the best contribution was the paper⁹ by Schoder and Turner. Since that time new experiments have been made, more empirical formulas published, contradictions discussed, and sources of errors investigated. It was found that triangular, circular, parabolic, and hyperbolic notches proved to be more accurate and reliable for small water rates. However, the rectangular weir remains unconquerable for larger discharges. The majority of known formulas assure $\pm 2\%$ accuracy under conditions of adequate arrangement. A search for higher precision was the purpose of new investigation. A series of 249 new tests was performed, and some previous results were reviewed and collated. It was hoped that there would result a modern dimensionless formula correct to $\pm 0.5\%$. Regretfully, the authors conclude that a truly reproducible, standard measuring weir and a precise, universal discharge formula are impractical.

The writer cannot agree with this pessimistic view and with some other statements by the authors. For example, the opinion that the flow pattern for rectangular weirs is not subject to complete mathematical analysis is not entirely true. The flow over the weir must be studied as

$$Q = \int_A v \cos \phi \, dA \dots \dots \dots (49)$$

in which ϕ is the variable angle of stream lines with the normal to the cross section, A . A certain law of stream lines is to be established, or an approximation assumed, before the integration can be done. Finally, small correction factors may be introduced to account for secondary influences such as wall roughness, edge character, surface tension, and viscosity. Gustav Kirchhoff applied this method (1883) to a two-dimensional slot in the bottom of a container and derived²⁵ the theoretical value of

$$C_d = \frac{\pi}{\pi + 2} = 0.611 \dots \dots \dots (50)$$

Work by Kirchhoff was continued²⁶ by Fritz Kötter in 1887. Ludwig A. Ott tried²⁷ to use an approximate pattern, assuming concentric circles as equipotential lines, for orifices, sluices, and weirs. He derived for a weir, as a first approximation, the value,

$$C_d = \frac{2}{\pi} = 0.637 \dots \dots \dots (51)$$

²⁴ Prof. of Civ. Eng., Univ. of Notre Dame, Notre Dame, Ind.

²⁵ "Vorlesungen über mathematische Physik, I. Mechanik," by G. Kirchhoff, Leipzig, 3d Ed., 1883, p. 297.

²⁶ "Ueber die Contractio venae bei spaltförmigen und kreisförmigen Oeffnungen," by F. Kötter, *Grunert's Archiv der Mathematik und Physik*, Leipzig, Vol. 5, 2 ser., 1887, pp. 392-417.

²⁷ "Ausfluss, Durchfluss und Überfall," by Ludwig A. Ott, *Wasserkraft und Wasserwirtschaft*, Munich, Vol. 27, No. 18, 1932, pp. 205-210.

Velocity distribution over the crest of the weir was investigated, as the most important factor, by Christian Keutner in his thesis and in several papers.²⁹ He used projections of $v \cos \phi$ and derived a set of formulas, taking into account the velocity laws.

The authors term it a misinterpretation to associate the coefficient k_1 with the kinetic energy (Coriolis) coefficient, α . Their opinion is based on usually assumed values of α of approximately 1, whereas k_1 in the Bazin derivation is taken as 2. Actually, the velocity distribution approaching the weir is very irregular and α can be much greater than 2. Harold Lauffer computed³⁴ values for several velocity diagrams in the Schoder and Turner work and obtained values of 1.64, 1.85, and 1.99. Values as high as 3.87 and even 7.4 before a turbine are mentioned in the literature.³⁵ Little is known about the Coriolis coefficient, and for this reason the writer presented³⁶ the methods of determination of this important factor.

Engineers who use the metric system would probably be more satisfied if data could be made dimensionless by dividing c_e by $\sqrt{2g}$. This could simplify the comparison with many European tests.

The most comprehensive paper on the weir with lateral contractions was presented by Erhard Zschiedrich in 1939 as a thesis³⁷ at the Technical University of Dresden.

Results of high quality were gained³⁸ by Otto Kirschmer and Bernhard Esterer in the Walchensee hydraulic laboratory in 1929. The writer compared these with Georgia Tech tests and found some difference. Surprisingly, the conclusions from the Walchensee tests were dismissed as being unfavorable by the authors.

RALPH W. POWELL,³⁹ M. ASCE.—The formulas proposed are refreshingly simple and seem to be satisfactory for water at ordinary temperatures. A complete treatment, including the effect of viscosity and surface tension, such

²⁸ "Neues Berechnungsverfahren für den Abfluss an Wehren aus der Geschwindigkeitsverteilung des Wassers über der Wehrkrone," by Ch. Keutner, *Die Bautechnik*, Vol. 7, No. 37, Berlin, 1929, pp. 575-582.

²⁹ "Entstehung und Wasserabführungsvermögen verschiedener Strahlformen an scharfkantigen Wehren," by Ch. Keutner, *ibid.* Vol. 9, No. 50, 1931, pp. 714-716.

³⁰ "Abfluss-Untersuchungen und Berechnungen für Überfälle an scharfkantigen Wehren," by Ch. Keutner, *Mitteilungen aus dem Gebiete des Wasserbaues und der Baugrundforschung*, Berlin, No. 4, 1931.

³¹ "Wassermengenmessung an Wehren mit zwei- und dreiseitiger (Ponceletüberfall) Einschnürung," by Ch. Keutner, *Der Bauingenieur*, Berlin, Vol. 13, No. 31/32, 1932, pp. 399-405.

³² "Der Einfluss der Krümmung der Wasserfäden auf die Energiebilanz und das Wasserabführungsvermögen von abgerundeten und scharfkantigen Wehrkörpern," by Ch. Keutner, *Wasserkraft und Wasserwirtschaft*, Munich, Vol. 28, No. 3, 1933, pp. 25-29; No. 4, pp. 43-47.

³³ "Strömungsvorgänge an breiten Wehrkörpern und an Einlaufbauwerken," by Ch. Keutner, *Der Bauingenieur*, Berlin, Vol. 15, Nos. 37-38, 1934, pp. 366-371; Nos. 39-40, pp. 389-392.

³⁴ "Wasserspiegellage und Fließzustand bei Berücksichtigung der Geschwindigkeitsverteilung," by H. Lauffer, *Der Bauingenieur*, Berlin, Vol. 16, No. 33/34, 1935, pp. 353-356.

³⁵ "Gidrometriia gidrotekhnicheskikh sooruzhenii i gidromashin," by N. M. Shechapov, Gosenergoizdat, Moscow, 1957.

³⁶ "Methods of Determination of the Kinetic Energy Factor," by S. Kolupaila, *The Port Engineer*, Calcutta, India, Vol. 5, No. 1, 1956, pp. 12-18.

³⁷ "Neue Untersuchungen an Überfällen mit Seiteneinschnürung," by E. Zschiedrich, *Mitteilungen aus dem Flussbau-laboratorium der Technischen Hochschule Dresden*, Leipzig, 1939.

³⁸ "Die Genauigkeit einiger Wassermessverfahren," by O. Kirschmer and B. Esterer, *Zeitschrift des Vereins deutscher Ingenieure*, Berlin, Vol. 74, No. 44, 1930, pp. 1499-1504.

³⁹ Prof. Emeritus, Engineering Mechanics, Ohio State Univ., Columbus, Ohio.

as given by Arno T. Lenz,⁴⁰ M. ASCE, for the V-notch, must await experiments on the flow of other liquids.

Putting $h_e = h + 0.003$ in Eq. 11, expanding by the binominal theorem, and dropping terms that are insignificant yields

$$Q = C_e \left(1 + \frac{0.0045}{h} \right) b_e h^{1.5} \dots \dots \dots (52)$$

Substituting Eq. 29 into Eq. 52 leads to

$$Q = \left(3.22 + 0.44 \frac{h}{P} + \frac{0.0145}{h} + \frac{0.0020}{P} \right) b_e h^{1.5} \dots \dots \dots (53)$$

which is similar to Rehbock's 1912 formula. In fact, if K_h is taken as 0.0037 instead of 0.003, P is taken as 0.5 ft, and b_e as $b(1 - 0.003)$, then

$$Q = \left(3.23 + 0.44 \frac{h}{P} + \frac{0.0178}{h} \right) b h^{1.5} \dots \dots \dots (54)$$

which is almost identical with Eq. 19.

Treating the full-width weir as the limiting case of the rectangular notch is novel but seems to be justified in view of the data presented. The use of a crest only 0.30 ft above the floor for some of the tests is unusual. Because the authors wished to find the proper coefficient of the (h/P) -term, it was wise to make the term large by making P small. However, as one can never be sure that one has found the best value of this coefficient, it is believed that P should ordinarily be made at least 2 ft. Messrs. Kindsvater and Carter found that their experiments yielded the value of the coefficient of h/P to be 0.40, and that the USBR tests yielded only 0.30. However, because the Bazin tests and Rehbock's 1929 formula yield a value of 0.44 and the careful and extensive tests of Schoder and Turner give at least that much, the value of 0.44 is used herein.

Although the height of the weir should not be too small, C. G. Cline⁴¹ demonstrated that it is unnecessary to make weir boxes as deep as had been thought necessary. In fact, there seems to be a definite disadvantage (other than expense) in making the weir box much deeper than the approach channel, or, if it is supplied by a pipe, in having the weir more than 3 ft high. The reason is that it is difficult to distribute the velocity of approach in a stable manner. Regions of high velocity tend to form and move about in a deep weir box. When these areas are along the bottom, the water approaching the weir has an upward velocity, which raises the lower nappe and decreases the discharge. When the higher velocity is along the surface, the contraction is decreased and the discharge increased, although the head on the weir remains exactly the same.

⁴⁰ "Viscosity and Surface Tension Effects on V-Notch Weir Coefficients," by Arno T. Lenz, *Transactions, ASCE*, Vol. 108, 1943, p. 759.

⁴¹ "Discharge Formulas and Tables for Sharp-Crested Suppressed Weirs," by C. G. Cline, *Transactions, ASCE*, Vol. 100, 1935, p. 396.

The authors have emphasized the importance of the velocity distribution in the weir box, but they have given no quantitative information as to the error resulting from having a distribution other than "normal." The writer has been faced with this problem and wishes to suggest a solution. The particular problem was to compute flows over a full-width weir 8 ft long, with $P = 5.5$ ft, at the end of a weir box 45 ft long. The water entered from a semi-circular flume 6 ft in diameter, with its bottom approximately 3 ft above the bottom of the weir box. When the water was turned on, a current flowed along the floor of the weir box that tended to persist even after the box was filled to a depth of 6.5 ft and water flowed over the weir with a head of 1 ft. The foregoing occurred despite the baffle that had been placed near the upstream end.

It was first thought that all that was necessary was to make a velocity traverse at the section where the head was being measured (14 ft upstream from the weir), and to use Schoder and Turner's formula,⁹

$$Q = 3.33 B \left[\left(h + \frac{V_a^2}{2g} \right)^{1.5} + \frac{h}{3.33} \times \frac{V_b^2}{2g} \right] \dots \dots \dots (55)$$

in which V_a is the mean velocity of approach in the part of the cross section above the level of the weir crest, and V_b is the mean velocity of approach in the part below the level of the weir crest. However, it was noted that Eq. 55 always made Q more than $3.33 B h^{1.5}$, although the data on which it was based showed four cases in which the observed Q -value was less than $3.33 B h^{1.5}$ and many others in which it was less than shown by Eq. 55. These runs tended to occur in cases in which $V_b > V_a$, and, as this was true in the case under consideration, it was thought best to make a new study of the original data. The first result was not satisfactory,⁴² and since reading the authors' paper, a second study has been made.

It was assumed that

$$C_e = 3.22 + 0.44 \frac{h}{P} + \phi(r) \dots \dots \dots (56)$$

in which $r = V_a/V_b$ and $\phi(r)$ is an unknown function to be determined. Then seventy-two of the Schoder and Turner runs⁹ for which the velocity distribution had been measured were selected. These included all of the thirty-six runs in which the velocity distribution had been changed by "fences" and an equal number of runs without fences. They included runs from series D through O. Assuming that

$$b_e = b - 0.003 \dots \dots \dots (57a)$$

and

$$h_e = h + 0.003 \dots \dots \dots (57b)$$

C_e was computed for each of these runs and $\phi(r)$ was computed as

$$\phi(r) = C_e - 3.22 - 0.44 \frac{h}{P} \dots \dots \dots (58)$$

⁴² "Tests of the Flow of Water in a Smooth V-Shaped Flume," by R. W. Powell and C. J. Posey, Report No. 21, Rocky Mountain Hydr. Lab., Allenspark, Colo., June, 1957, p. 6.

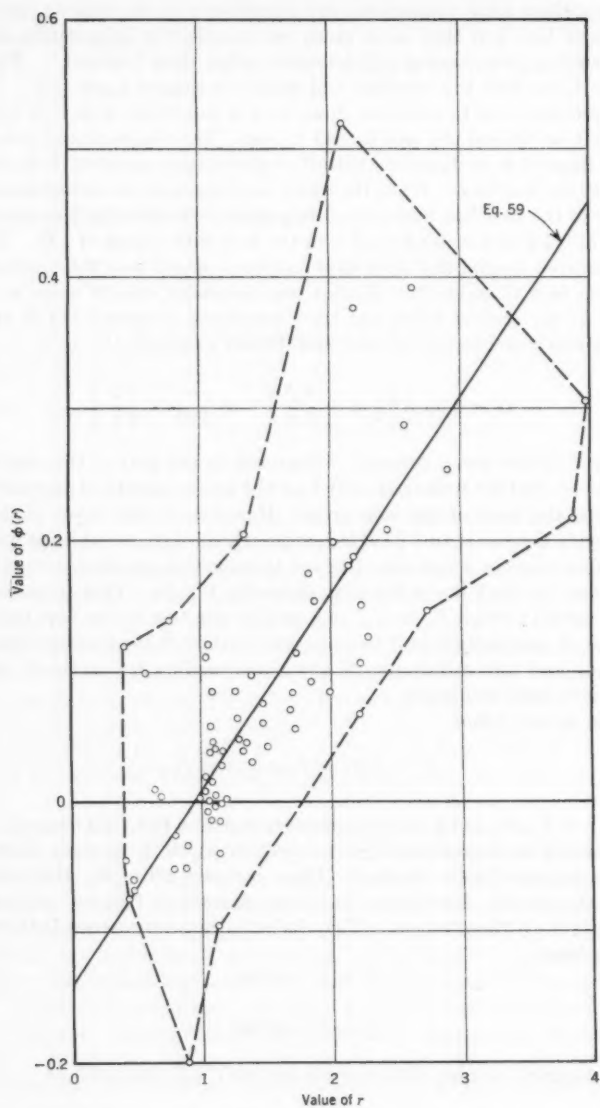


FIG. 14.—RELATIONSHIP BETWEEN EQ. 58 AND THE VELOCITY RATIO

These values were plotted against r in Fig. 14. Because this small residual includes all the experimental errors, there was a great deal of "scatter," but a line drawn through the points by eye had the equation,

$$\phi(r) = 0.15r - 0.14 \dots \dots \dots (59)$$

which leads to

$$C_e = 3.08 + 0.44 \frac{h}{P} + 0.15r \dots \dots \dots (60)$$

Values of C_e computed from Eq. 60 were compared with the values of C_e derived from the observed data for each of the seventy-two runs. The average discrepancy was 1.41%, as compared with 1.09% for the same seventy-two runs computed from Eq. 55. However, the algebraic sum of the seventy-two discrepancies was 17.56% by Eq. 55 and only 7.37% by Eq. 60. If one studies only the fourteen runs in which $V_b > V_a$, Eq. 60 gives a mean discrepancy of 1.70% and a total algebraic discrepancy of 10.47%. On the other hand, Eq. 55 gives a mean discrepancy of 2.15% and a total algebraic discrepancy of 22.8%. If one includes only the eight of these runs in which P was 2.0 ft or more, Eq. 60 gives a mean discrepancy of 0.47% and a total algebraic discrepancy of 0.33%, whereas Eq. 55 gives a mean discrepancy of 1.22% and a total algebraic discrepancy of 5.51%. Therefore, it is felt that Eq. 60 is a more satisfactory empirical formula than Eq. 55, especially because it is simpler to compute.

In these runs, the r -value varied from approximately 0.4 to approximately 4.0, making C_e vary from $(3.14 + 0.44 h/P)$ to $(3.68 + 0.44 h/P)$, or 17.2%, resulting from changes in the velocity distribution only. In series C the actual individual runs vary even more than this, for it is stated⁴³:

"For the same head, an extreme difference of 26% in discharge was produced by variations in the velocity distribution * * * No doubt careful inspection of the appearance of the flow in the channel of approach would enable cases of extremely high surface or bottom velocities to be noticed by an experienced engineer. It seems certain, however, that no visual inspection could distinguish between discharges that differ as much as 4 or 5% at the same head due solely to different distributions of velocities in the channel of approach."

Although Schoder and Turner referred to Eq. 55 as "perhaps the best tentative formula (which they) found" and admitted that there were still fairly large discrepancies, it has been regarded as an accurate formula, not used simply because of the difficulty of measuring V_a and V_b . In this connection it may be mentioned that Francis M. Dawson, M. ASCE, who did a great deal of work for Schoder and Turner,⁹ has noted (to the writer) that it is a misconception that V_a and V_b must be measured for each run. If the approach arrangement remains unchanged, a few gagings for various heads will determine curves yielding V_a and V_b as functions of h that will be accurate enough to use in Eq. 55. The same applies even more to Eq. 60 because in this case only one curve, V_a/V_b as a function of h , is required. In the writer's problem, after additional baffles had been installed near the upstream end of the weir

⁴³ "Precise Weir Measurements," by Ernest W. Schoder and Kenneth B. Turner, *Transactions, ASCE*, Vol. 93, 1929, p. 1065.

box to improve the velocity distribution, it was found that

$$\frac{V_a}{V_b} = 0.435 h + 0.870 \dots \dots \dots (61)$$

which, with $P = 5.5$ ft, reduces Eq. 60 to

$$C_e = 3.210 + 0.145 h \dots \dots \dots (62)$$

or

$$Q = (3.210 + 0.145 h) (b - 0.003) (h + 0.003)^{1.5} \dots \dots \dots (63)$$

However, it is obvious, that the problem has been oversimplified. For a high weir the same value of V_b may represent quite different distributions, some with a maximum velocity near the bottom and some with the maximum velocity near the top. This is probably the principal reason for the large scatter of the points in Fig. 14. It is probable that the ratio of the velocity at 0.1 depth to that at 0.9 depth would be a much better criterion on which to base the "distribution of velocity of approach" correction. This would require an entirely new series of experiments. In the meantime, errors of 1% or more can be expected from weir measurements. Rehbock's statement¹⁸ that the mean discrepancy should not exceed 0.2% or 0.3% seems too optimistic except for exactly the same entrance conditions to exactly the same weir box and weir as he used.

JOHN W. PAULL⁴⁴.—Dimensional analysis has been used to obtain a fundamental solution to a fluid-flow problem for which only empirical formulas were available before.

The discharge equation selected by the authors (Eq. 11) is very simple. As the C_e -term takes into account what has been termed "the velocity of approach," and k_b and k_h take into account the effects of viscosity and surface tension, a very simple way has been devised for eliminating complexities. It would be valuable to know, however, what accuracies can be expected under a variety of conditions.

IWAO OKI⁴⁵.—The proposed comprehensive solution for the discharge characteristics of rectangular, thin-plate weirs is very adequate and engineers in this field will benefit from this achievement.

In 1929, the writer presented a paper on the discharge characteristics of rectangular weirs,⁴⁶ the object of which was to establish an empirical formula which had a wider range of applicability and which could be conveniently used in practice.

From several formulas known at that time, the writer selected two typical ones. The first was the Francis formula,

$$Q = 3.33 (b - 0.2 h) [(h + h')^1 - h'^1] \dots \dots \dots (64)$$

in which h' is the head due to the velocity of approach.

⁴⁴ Lecturer, Civ. Eng. Dept., Univ. of New South Wales, Sydney, Australia; formerly Lecturer, Hydr. Eng., Dept. of Civ. and Aeronautical Eng., Royal Melbourne Technical College, Melbourne, Australia.

⁴⁵ Emeritus Prof., Waseda Univ., Tokyo, Japan; Member of the Japan Academy.

⁴⁶ "An Empirical Formula for Discharge over Rectangular Weirs with Complete or Slightly Incomplete Contractions," by Iwao Oki, *Proceedings*, No. 224, World Eng. Cong., Tokyo, Japan, 1929.

The second was the Barnes formula,

$$Q = 3.324 h^{1.49} b^{1.11} (b + 2h)^{-0.11} \dots \dots \dots (65)$$

in which h is the observed head + $(1/70) u^2$, and u is the mean velocity in the approach channel.

When these formulas were rewritten in the form

$$Q = C \frac{2}{3} \sqrt{2g} b h^1 \dots \dots \dots (66)$$

the ratio h/b seemed to be a predominant parameter in the coefficient, C . By comparison with the results of many experiments, including several on models in Japan, the writer suggested the following expression for the coefficient, C :

$$C = 0.6224 \left(1 + \frac{0.004}{h} \right) \left[1 - \frac{\sqrt{m}}{10} \left(1 - \frac{m}{3p} \right) \right] \left[1 + \frac{1}{2} \left(\frac{bh}{B(p+h)} \right)^2 \right] \dots (67)$$

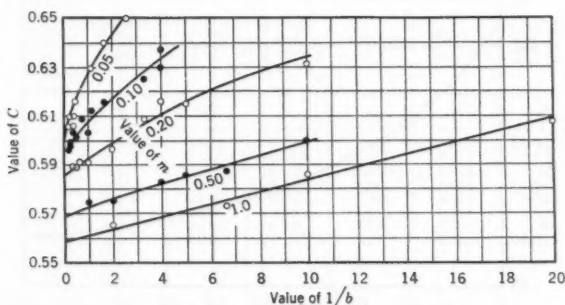


FIG. 15.—RELATIONSHIP BETWEEN THE DISCHARGE COEFFICIENT AND WEIR-NOTCH WIDTH

in which m is the ratio, h/b , and P denotes the height, in feet, of the weir crest above the bottom, and B is the width of the channel. Adopting 0.623 instead of the constant, 0.6224, this formula has been in wide use in Japan.

In 1935, the writer prepared a paper⁴⁷ on a method of studying further the coefficient, C , for discharge. The values of the coefficient are affected by so many factors that they have not yet been exactly determined, notwithstanding the elaborate experiments by many authors. The writer thought the first thing to be done was to determine the coefficients of discharge for weirs with absolutely complete contractions.

From the most reliable results of experiments on rectangular weirs with two side contractions, including those in the Hydraulic Laboratory of Waseda University, Tokyo, Japan, the writer chose those cases in which it was considered that the flows were entirely free from bottom and side wall effects. The coefficients of discharge thus selected were arranged in groups for the same values of m against $1/b$, the reciprocal of the width of the weir notch.

⁴⁷ "A Method of Studying the Coefficients of Discharge for Rectangular Weirs with Two Side-Contractions," by Iwao Oki, *Transaction, Soc. of Mech. Engrs., Japan*, Vol. 1, No. 4, October, 1935.

The curves in Fig. 15, drawn through the points for each group, were extended until they intersected the axis of the ordinate, where b is infinite. The values of the coefficients at the intersections were denoted by C_∞ , which represented those for absolutely complete contractions, because in those cases the influences by all the factors except the ratio, m , upon the values of discharge coefficients, become negligibly small. The coefficients C_∞ were plotted against the ratio m (Fig. 16). To fit these values of C_∞ , the writer deduced in 1954 a new formula,⁴⁸

$$C_\infty = 0.612 \left(1 - \frac{\sqrt{m}}{10 + 1.8 m^2} \right) \dots \dots \dots (68)$$

for rectangular weirs with absolutely complete contractions. For $m = 1$, $C_\infty = 0.560$, and when $m = 1.36$, $C_\infty = 0.558$, a minimum value. When $m = 0$, $C_\infty = 0.612$. If the potential-flow theory in two dimensions holds in these cases, the constant 0.612 would be replaced by 0.611.

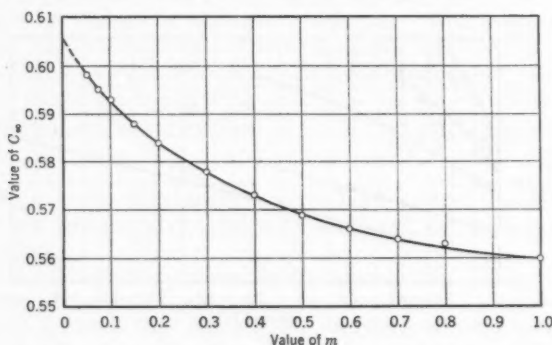


FIG. 16.—THE VARIATION OF C_∞ WITH m

When C denotes the discharge coefficient of a rectangular weir and C_∞ represents the discharge coefficient expressed by Eq. 68, then $C - C_\infty$ or $\frac{C}{C_\infty}$ will be a function of several factors, which could be solved by applying the authors' propositions.

The writer hopes that the propositions stated will contribute to the development of an equation that covers the discharge over rectangular, thin-plate weirs of all sizes and proportions.

MARION R. CARSTENS,⁴⁹ A. M. ASCE.—An attempt has been made by the authors to eliminate the effects of viscosity and surface tension from experimentally determined values of the discharge coefficient of a thin-plate weir by the simple expedient of an effective head and width. The successful elimination of these two effects should result in the coefficient of discharge of potential

⁴⁸ "The latest Trend of our Researches on the Discharge Coefficients for Rectangular Weirs," by Iwao Oki, *Transaction, Soc. of Mech. Engrs., Japan*, Vol. 20, No. 89, 1954 (in Japanese).

⁴⁹ Prof., Dept. of Civ. Eng., Georgia Inst. of Technology, Atlanta, Ga.

(irrotational) flow without surface tension. Thus, the equations for the coefficient of discharge for the full-width weir, Eqs. 25 through 29, should be identical for these five series of tests. The small differences in these equations could be attributed to the following causes:

1. The use of the effective head does not completely eliminate the effect of viscosity and surface tension, and the differences in the equations represent the remaining differences between the five series of experiments in this regard;

2. The geometry in each of the five experiments was sufficiently different to account for the small differences; and

3. The differences are merely an indication of the order of accuracy with which the coefficient of discharge can be experimentally determined.

TABLE 2.—VALUES OF C_d FOR A FULL-WIDTH WEIR

Value of b/P	Coefficient of discharge for a two-dimensional orifice	Theoretical discharge coefficient	Georgia Tech., Eq. 25	Schoder and Turner, Eq. 26	Bazin, Eq. 27	USBR, Eq. 28	Rehbach (1929), Eq. 29	Kandaswamy and Rouse
(1)	(2)	(3)	(4)	(5)	(6)	(7)	(8)	(9)
0	0.611	0.611	0.602	0.600	0.608	0.608	0.602	0.61
0.111	0.612	0.614	0.610	0.610	0.617	0.616	0.611	0.62
0.250	0.616	0.623	0.621	0.621	0.626	0.625	0.623	0.63
0.429	0.622	0.637	0.634	0.636	0.644	0.636	0.638	0.64
0.667	0.631	0.658	0.653	0.656	0.662	0.651	0.656	0.66
1.000	0.644	0.687	0.677	0.684	0.690	0.674	0.684	0.69
1.500	0.662	0.733	0.714	0.727	0.731	0.706	0.726	0.73
2.333	0.687	0.800	0.776	0.762	0.795	0.80
3.200	0.708	0.86	0.87
4.000	0.722	0.91	0.93
5.000	0.741	0.97	1.01
6.000	0.757	1.03	1.08
7.000	0.767	1.07	1.14
8.000	0.775	1.11	1.17
9.000	0.781	1.14	1.18
10.000	0.786	1.17	1.18

Because the maximum deviation of the data from each experiment (Figs. 3, 4, 5, and 6(c)) is greater than the deviations between the equations, it is believed that item 3 is the explanation for the small differences in Eqs. 25 through 29. Therefore, the writer would have combined all the data (reduced to potential flow) shown in Figs. 3, 4, 5, and 6(c).

Despite the tenuous derivation of Eq. 15 the solution for the coefficient of discharge is amazingly good. Eq. 15 can be placed in the usual form of the discharge equation by factoring the quantity, $h^{\frac{1}{2}}$, from the parentheses to result in

$$Q = C_c \frac{2}{3} \sqrt{2g} b \left\{ \left[1 + \frac{V_1^2}{2gh} \right]^{\frac{1}{2}} - \left[\frac{V_1^2}{2g} \right]^{\frac{1}{2}} \right\} h^{\frac{1}{2}} \dots \dots \dots (69)$$

The quantity, $V_1^2/(2gh)$, can be transformed as follows:

$$Q = V_1 b (h + P) \dots \dots \dots (70a)$$

and

$$Q = C_d \frac{2}{3} \sqrt{2g} b h^{\frac{3}{2}} \dots \dots \dots (70b)$$

from which

$$\frac{V_1^2}{2g h} = \frac{4}{9} C_d^2 \left(\frac{h/P}{h/P + 1} \right)^2 \dots \dots \dots (71)$$

Substitution into Eq. 69 leads to

$$C_d = C_c \left\{ \left[\frac{4}{9} C_d^2 \left(\frac{h/P}{h/P + 1} \right)^2 + 1 \right]^{\frac{1}{2}} - \left[\frac{4}{9} C_d^2 \left(\frac{h/P}{h/P + 1} \right)^2 \right]^{\frac{1}{2}} \right\} \dots (72)$$

If the theoretical values of C_c for a two-dimensional orifice are utilized in Eq. 72, the equation can be solved by successive approximation for C_d as a function of h/P . In Table 2 the theoretical values of C_d are tabulated for comparison purposes with the best available experimentally determined values—that is, Eqs. 25 through 29. In addition, the experimentally determined⁵⁰ values of Pattanam K. Kandaswamy, A. M. ASCE, and Hunter Rouse, M. ASCE, are tabulated in order to compare the theoretical solution with an experimental solution obtained at larger values of h/P .

The theoretical solution for the coefficient of discharge is within a few percent of the various experimental solutions throughout the entire range of the weir—that is, $0 < h/P < 10$. The writer cannot agree with the authors' statement, in the "Introduction:"

"The result is a complex equation which must be modified to make it practical and adjusted to make it agree with a particular set of experimental data. The fact that a large number of different empirical formulas have been evolved by this procedure is evidence that the "theoretical" equation is inadequate. The obvious reason for the inadequacy is the fact that the basic assumptions are inaccurate."

Rather it appears to the writer that too many people write empirical equations.

CARL E. KINDSVATER,⁵¹ M. ASCE, AND ROLLAND W. CARTER,⁵² A.M. ASCE.
—Few subjects in the literature of hydraulics are more revealing of the personalities of its students. It is indeed remarkable that a comparatively simple physical phenomenon has inspired such an astounding number of printed words, formulas, laboratory investigations, and disagreements. Over a period of 250 yr, nearly every name in the history of hydraulics is identified with contributions to the great store of weir literature. It is not amazing, therefore, that the most common ingredient in this inheritance is repetition.

Much more discouraging than the repetition which characterizes weir literature is the fact that some of the best thought on the subject is buried in the

⁵⁰ "Characteristics of Flow Over Terminal Weirs and Sills," by P. K. Kandaswamy and Hunter Rouse, *Proceedings Paper 1345*, ASCE, August, 1957.

⁵¹ Regents Prof., School of Civ. Eng., Georgia Inst. of Technology, Atlanta, Ga; and Consultant, Geological Survey, U. S. Dept. of the Interior, Washington, D. C.

⁵² Chief, Research Section, Surface Water Branch, Water Resources Div., Geological Survey, U. S. Dept. of the Interior, Washington, D. C.

avalanche of printed words. On the other hand, the substantial area of ignorance regarding weirs which still exists is often dismissed with the casual implication that the solution to the problem is contained in a given formula—which is then quoted without reference to the qualifications which were prescribed by its author.

Pride and prejudice seem to have played a large part in the history of the simple weir. Counterclaims of accuracy and scientific truth have been hurled across battle lines drawn up behind purely empirical formulas based on limited, often questionable experimental data. The futility of one such argument is revealed in Fig. 4(a). Here it is clearly demonstrated that, regardless of the quality of Bazin's data, the form of discharge equation used by Bazin and others is fundamentally inadequate.

The writers share with Mr. Sarpkaya his concern with the practical limitations of empirical equations. They are aware of the dangers of extrapolating empirical relationships beyond the range of conditions represented by the experiments from which they were derived. Persons who publish empirical equations are obliged to state very clearly the purpose and limitations of their work. It is the reader's obligation to observe these limitations in the application of the results.

It was made quite clear in the paper that the writers were concerned with the weir as a discharge-measuring device, and that, for practical reasons, the verification of the proposed formula was limited to "water at ordinary temperatures." Furthermore, the range of values of each variable involved in the experimental verification is explicit in the paper. The writers are inclined to observe that, apart from the acknowledged limitations in their study of the fluid-property variables, their work covers a broader range of geometric conditions than any other single work known. They, along with Mr. Sarpkaya, hope that others will extend its boundaries.

It should be quite clear from the paper that values of k_h and k_b are dimensional quantities derived from experiments with a single liquid and a practical range of geometric conditions. The general relationships between k_h , k_b , R , and W are carefully detailed. One accustomed to using the Reynolds and Weber numbers to describe the relative influence of viscosity and surface tension, respectively, would not expect "glucose, honey and molasses" to exhibit unique characteristics as long as they behave as true fluids.

Mr. Sarpkaya's Eq. 36 is a general statement of the slope-intercept form of the C_s -curves (Fig. 8), which describe the interrelationship of the principal geometric variables. On the other hand, Eq. 35 involves a nondimensional representation of the fluid-property adjustment factors, k_h and k_b . It is not clear why he presumes that an additional fluid-property adjustment should be made to the relationship between the geometric ratios. Indeed, Eq. 38 appears to hold little promise of simplification or clarification. And, while it is considerably more complex than Eq. 11, it is certainly no less empirical. Subsequent algebraic steps and the unlikely assumption that k_h is independent of surface tension do not seem to lend credence to Eq. 38.

Mr. Kolupaila incorrectly attributes certain objectives to the investigation (for example, "A search for higher precision [than $\pm 2\%$] was the purpose of

the new investigation"). He is also incorrect in stating that the writers "assumed values of α of approximately 1," and "the conclusions from the Walchensee tests were dismissed as being incorrect."

The writers agree with Mr. Kolupaila that the flow pattern for rectangular weirs might be subject to complete mathematical analysis if "A certain law of stream lines" were known. Unfortunately, the solution is hardly forthcoming in view of his subsequent qualification that such a law remains to be "established or an approximation assumed" along with other "small correction factors." Mr. Kolupaila's remarks concerning k_1 and α are somewhat contradictory, but, in general, they appear to substantiate the writers' conclusions regarding the tenuous relationship between these two coefficients.

Mr. Kolupaila makes reference to many foreign publications on weirs. Failure to refer to certain of these publications in the original paper is evidence that they were not considered of particular value. It is not clear why Mr. Kolupaila refers to the foreign publications without identifying and supporting his own preference among the diverse opinions and formulas proposed therein. A casual review of recent European reference works indicates that few of the papers referred to have been recognized as substantial contributions in their own native lands. Finally, an examination of the paper which describes the Walchensee tests will show that Mr. Kolupaila, not the writers, must have misinterpreted the conclusions drawn by O. Kirschmer and B. Esterer. The following free translation of their conclusions clearly supports the conclusions stated by the writers:

"The results of the weir measurements substantiate the criticism of this method which has been expressed by others. Indeed, general reliance upon one of the rational formulae has not yet been satisfactorily proven."

Mr. Powell emphasized the unreliability of coefficients derived from experiments on physically small values of P . This uncertainty, as well as the uncertainty of results of tests made with very small values of b and h , was acknowledged in the paper. Mr. Powell's suggested method of correcting for the distribution of velocity in the approach channel is a worthwhile and practical contribution. The results which he obtained from an analysis of the Schoder and Turner data⁹ are encouraging. It is hoped that additional tests made to define the r -function will refine the method. Thus, the weir which is unavoidably located in a channel which produces a nonuniform velocity distribution might still be salvaged as a satisfactory meter. As pointed out by Mr. Powell, the r -value is essentially a characteristic of the installation which, like the dimensions of the weir, need be determined only once. It follows that his method of adjusting the coefficient of discharge is completely practical. It seems reasonable to assume that r is a function of h alone. Mr. Powell's willingness to settle for "errors of the order of 1%" is quite realistic if not optimistic.

It is regretted that Mr. Paull cannot be given dependable information regarding the inaccuracies to be expected under a full variety of applications. Disregarding such very real problems as variations in velocity distribution and "nonstandard" geometric conditions, the order of magnitude of the errors to be

expected are suggested by the scatter of the plotted points in Figs. 3 through 6.

Mr. Oki has presented experimental data and formulas previously unknown to the writers. In Fig. 15 Mr. Oki proposes to demonstrate a relationship between C and h/b . Under the heading "Analysis of the Discharge Function: Significance of the Geometric Ratios in Eq. 3" it was stated:

"The independent influence of this ratio $[b/h]$ is believed to be negligible over the full practical range of the other variables. An earlier investigation⁴ supports this conclusion. * * * A few recorded efforts to incorporate the (b/h) -ratio in discharge formulas are believed to be based on misinterpretations of influences related separately to the magnitudes of b and h ."

This statement is actually supported by Fig. 15. Indeed, closer study will reveal that the slope of the curves in Fig. 15 shows the effect of b , whereas the vertical distance between the curves shows the effect of h . In fact, all of the data on Fig. 15 can be replotted to show a relationship between C_d and h for various constant values of b . However, if this is done, Mr. Oki's data appear to show a considerably larger influence due to both h and b than has been reported by the writers and others.

The writers are especially puzzled by some of the very low values of C_d shown in Fig. 15. All values of C_d for h/b greater than 0.5, for example, are less than the "theoretical" minimum, 0.611. This trend is believed to be unique in the literature. It is implied, of course, that the decrease in C_d is related to the increase in h/b . It can only be repeated that the (h/b) -ratio is not believed to be significant. In support of this conclusion the writers submit the observation that the data presented cover a range of values of h/b from 0.03 to 6.0.

Mr. Carstens lists several reasons for the difference in the results obtained by applying the writers method of analysis to the experimental data obtained by different investigators. His general diagnosis is agreed with, but the writers fail to see the logic in the conclusion that the maximum experimental error in one set of data is an explanation of the difference between curves which were drawn to represent mean values for different sets of data. Such an unusual conclusion ignores, for example, the systematic variation with velocity distribution, weir crest condition, etc., shown by Schoder and Turner² and others. It is felt that Mr. Carstens' item 2, namely, the "geometry of the experiments," is the major cause of the difference between the results of different experiments. A large part of the tremendous store of weir literature is evidence to support this conclusion.

Mr. Carstens' light dismissal of the "small differences" between various formulas ignores the purpose of most of the work done in this field since the original derivation of Eq. 15 by Weisbach. His comparison of the "theoretical" and measured values of C_d is a classic demonstration of circumstantial evidence rather than theoretical proof of the merit of the orifice analogy. The writers are pleased to endorse the conclusion that too many people write empirical equations (or equations that are too empirical!), but they fail to see the relationship between this thesis and the statement quoted from the original paper

which preceded his pronouncement. Also, that the weir which is the subject of Mr. Carstens' attention, $(b/B) = 1.0$, is only a limiting case of the problem under investigation, that values of h/P greater than 2.0 are impractical for reasonably accurate flow measurement, and that the fluid-property effects associated with small values of h and b cannot be ignored for all practical purposes.

In general, the discussers did not challenge the writers' candid disrespect for the traditional "theoretical" equation and the orifice analogy. However, most of them appeared to favor the use of a coefficient C_d which is equal to the writers' C divided by a quantity $(\frac{2}{3} \sqrt{2g})$ derived from the orifice analogy. The principal advantage attributed to C_d is that it is nondimensional.

The writers are staunch proponents of nondimensional ratios. In the present instance, however, they question the logic of straining to make the coefficient of discharge nondimensional when the equation of discharge contains other terms which are dimensional. In the writers' equation (Eq. 11) for example, evaluation of the discharge depends on knowledge of k_a and k_b , quantities which are absolute measures of the combined influences of viscosity and surface tension for a particular liquid. Similarly, in Eqs. 18 (Bazin), 19 (Rehbock), and 20 (S. I. A.), dimensional terms which are related to the magnitude of h restrict the application of those equations to water at ordinary temperatures.

It has been observed that the quantity $\frac{2}{3} \sqrt{2g}$ is obtained from the derivation based on the orifice analogy. Bazin and others have at one time proposed equations in which $\frac{2}{3} \sqrt{2g}$ was replaced by $\sqrt{2g}$ or \sqrt{g} . In these alternate forms of the discharge equation the coefficient is quite nondimensional but the writers are loath to use them because of the almost exclusive division of preference between C (widely preferred by engineers in practice) and C_d (preferred by some researchers) as defined herein. While they find it difficult to be concerned about the choice, the writers decided to use C primarily because it concedes to the practicing engineer the margin of convenience.

The writers freely admit the advantage of C_c rather than C_d (Eq. 15) for certain purposes. A reason seldom mentioned, for example, is that C_c is remarkably similar for different shapes of notch weirs. Thus, the researcher finds it convenient to use C_c to correlate meagre data from different sources. However, this reason does not justify the preservation of the C_c -form of the discharge equation for practical use.

AMERICAN SOCIETY OF CIVIL ENGINEERS

Founded November 5, 1852

TRANSACTIONS

Paper No. 3002

SEWAGE DISPOSAL IN SANTA MONICA BAY

BY CHARLES G. GUNNERSON,¹ A. M. ASCE

WITH DISCUSSION BY MESSRS. CHARLES H. LAWRENCE AND DAVID R. MILLER; DAVID I. H. BARR; AND CHARLES G. GUNNERSON

SYNOPSIS

The expansion of the Hyperion Treatment Plant of Los Angeles, Calif., has required studies of the physical, chemical, biological, and bacteriological factors that operate in the receiving waters of Santa Monica Bay. The findings of these studies are summarized, and factors of significance in the reduction of coliform bacteria in surface waters are evaluated for different effluents.

INTRODUCTION

The proposed works for the Hyperion Treatment Plant in Los Angeles, Calif., included modification of plant processes as well as construction of two ocean outfalls to be located on a shelf bounded by submarine canyons. They will discharge the plant effluent and digested sludge at 5 miles and 7 miles offshore, respectively. The existing high-rate activated sludge effluent is discharged 1 mile offshore. In general, these studies were directed toward determining the degree of treatment required for effluents discharged at varying distances from shore. The general area of oceanographic investigation in Santa Monica Bay, Calif., is shown in Fig. 1. The contours show depth in fathoms and were adapted from chart No. 5101 of the Coast and Geodetic Survey, United States Department of Commerce.

The location, depth, and diffuser details of an ocean outfall establish the initial dilution of the sewage as it rises. Essentially, it rises vertically, either to the surface where the mixture appears as a visible "boil" or to some intermediate depth at which it is in general equilibrium with the surrounding waters. This phenomenon was first investigated by A. M. Rawn, Hon. M. ASCE, and

NOTE.—Published, essentially as printed here, in February, 1958, in the Journal of the Sanitary Engineering Division, as *Proceedings Paper 1534*. Positions and titles given are those in effect when the paper or discussion was approved for publication in *Transactions*.

¹ Civ. Engr., Bureau of Sanitation, Dept. of Public Works, Los Angeles, Calif.

Harold K. Palmer,² M. ASCE, and more recently was re-evaluated by Rawn, Francis R. Bowerman, A. M. ASCE and Norman H. Brooks,³ A. M. ASCE. It has also been reviewed by Erman A. Pearson,⁴ A. M. ASCE.

The initial diffusion represents the point at which control exercised by engineering works ends. This study is concerned with those factors operating subsequently in the marine environment which may be expected to indicate the degree of treatment required of the plant on shore.

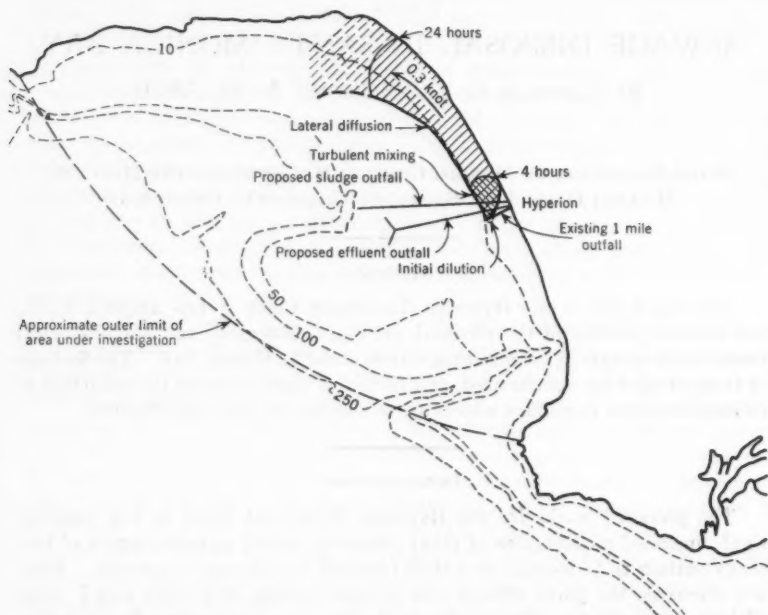


FIG. 1.—GENERAL AREA AND DILUTION PROCESSES AT EXISTING HYPERION OUTFALL

A treatment plant effluent will necessarily undergo various changes in characteristics after discharge into the receiving waters, and this implies consequent changes within the waters themselves. The factors that produce these changes may be classified as physical, chemical, biological, and bacteriological. However, it must be recognized that the various factors are interrelated and that, while an arbitrary separation permits a reasonable analysis of their effects, such a separation is, in fact, artificial.

² "Pre-determining the Extent of a Sewage Field in Sea Water," by A. M. Rawn and H. K. Palmer, *Transactions, ASCE*, Vol. 94, 1930, pp. 1036-1060.

³ "The Diffusion of Sewage in Sea Water," by A. M. Rawn, F. R. Bowerman, and N. H. Brooks, 1956. Prepublication manuscript reviewed by Pearson (reference 4), pp. 60-61.

⁴ "An Investigation of the Efficacy of Submarine Outfall Disposal of Sewage and Sludge," by E. A. Pearson, *Publication No. 14*, California State Water Pollution Control Board, Sacramento, Calif., 1956.

PHYSICAL AND CHEMICAL FACTORS

The physical dilution of an effluent discharged into marine waters is ultimately limited by the amount of new water being brought into the area. The determination of the circulation pattern and of the variations of the currents contributing to this pattern is therefore essential. A study of the currents and circulation of Santa Monica Bay, Calif., based on data obtained from current meters, drift cards, current crosses at both the surface and at depth, and observations of the areal extent and location of the various water masses, indicated the average currents, variations from the average, and generalized circulation of the waters in the bay.^{5,6}

In general, current observations in the upper 10 ft of water indicate that effluent discharged 5 miles offshore which reaches the surface immediately will require approximately 20 hr to reach the surf zone during those periods when onshore currents prevail, and that significantly lower current velocities prevail in waters at depth.

TABLE 1.—OPERATION OF THE EXISTING OUTFALL

Time from boil, in hours	Phenomenon	APPROXIMATE AVERAGE DILUTION FACTOR	
		Parts new sea water per part influent	Net dilution parts sea water per part sewage
(1)	(2)	(3)	(4)
0	Initial dilution	20	20
0-4	Turbulent mixing	4	104
4-24	Lateral diffusion (estimated)	2	314

The operation of the diffuser system, indicated by the dilution at the boil, will determine the efficiency with which the effluent will be initially diluted by the waters coming into the area. It should be noted, however, that the initial dilution will result in a mixture that will normally spread out at an intermediate depth.

Subsequent dilution of the mixture will occur, and may be tentatively divided into two separate phenomena: (1) Turbulent mixing due to density variations in the initial mixture which may continue for some 3 or 4 hr downstream from the boil, and (2) lateral mixing due to eddy diffusion which is effective thereafter.

Turbulent mixing is assumed herein to be due to the initial mixture at the top of the rising column not being completely homogeneous. Therefore, there are significant variations in solids, bacteria, salinity, temperature, density, and other characteristics among successive samples taken from the boil as well as from closely-spaced locations within the sewage field immediately downstream.

⁵ "Summary Report, Oceanographic Investigation of Santa Monica Bay," Bureau of Sanitation, Los Angeles, Calif., 1956.

⁶ "The Oceanography of Santa Monica Bay, California," by R. E. Stevenson, R. B. Tibby, and D. S. Gorsline, Allan Hancock Foundation, Univ. of Southern California, Los Angeles, Calif., 1956.

A significant amount of energy, represented by variations in density, is available for turbulent mixing, both vertical and horizontal.

Lateral mixing that occurs after the first 3 or 4 hr of flow from the boil is evidenced by the progressive widening of the field as it travels with the current. This is assumed to be due to eddy diffusion defined⁴ as "the inter-

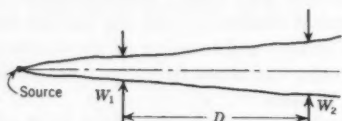


FIG. 2.—LOCATION OF W_1 AND W_2

change or translation of molecules or suspended colloidal matter by the random velocities or turbulence in turbulent flow." Only the lateral or horizontal eddy diffusion is here considered to be important, because the stable stratification in the upper layers of the ocean indicates that the vertical eddy diffusion is reduced to a relatively small amount.⁷

Several observations^{8,9} of the operation of the existing outfall are summarized in Table 1. Fig. 1 shows a typical configuration of the sewage field with a northerly current of approximately 0.3 knot. The dilution factors in

TABLE 2.—OBSERVED LATERAL DILUTION

Observation	Date	W_1 , in feet	W_2 , in feet	D , in feet	ΔT , in minutes	k		Scale, L , in centimeters	ΔT , in seconds
						Feet ² per minute	Centimeter ² per second		
(1)	(2)	(3)	(4)	(5)	(6)	(7)	(8)	(9)	(10)
1	5/24/55	150	225	1020	28	31.4	487	5.7×10^3	1.7×10^4
2*	5/24/55	225	600	2100	90	107.4	1665	1.3×10^4	5.4×10^4
3	12/30/55	60	120	1500	30	11.2	174	2.7×10^3	1.8×10^4
4	12/30/55	67	233	3000	60	25.9	402	4.6×10^3	3.6×10^4
5	12/30/55	150	475	6750	135	47.0	729	9.5×10^3	8.1×10^4
6	12/30/55	150	500	7500	150	47.4	735	9.9×10^3	9.0×10^4

* Near convergence.

parts new sea water per part of plant discharge or subsequent mixture influent to the particular phenomenon are approximately 20, 4, and 2 for initial dilution, turbulent mixing, and lateral dilution, respectively. The resulting net dilutions in parts sea water per part of plant effluent are approximately 20:1 for

¹ "The Oceans," by H. U. Sverdrup, M. W. Johnson, and R. H. Fleming, Prentice-Hall, 1946.

² "Oceanographic Investigation of Santa Monica Bay," Progress Report No. 3, Bureau of Sanitation, Dept. of Public Works, Los Angeles, Calif., 1955.

³ "Studies on Coliform Bacteria Discharged from the Hyperion Outfall, Final Bacteriological Report," by S. C. Rittenberg, Allan Hancock Foundation, Univ. of Southern California, Los Angeles, Calif., 1956.

initial dilution, 100:1 after some 4 hr of turbulent mixing and 300:1 after an additional 20 hr of lateral dilution.

Lateral dilution has also been evaluated by means of fluorescein dye streams released in 180 ft of water from anchored skiffs located 5 miles offshore. The dye streams were subsequently observed from both the surface and the air. The results of these studies are summarized in Table 2. The location of W_1 , W_2 , and the distance, D , is shown in Fig. 2. From an investigation conducted by Pearson⁴ it can be shown that

$$k = \frac{\sigma_2^2 - \sigma_1^2}{2(t_2 - t_1)} \dots \dots \dots (1)$$

Assume:

$$\sigma_1 = \frac{W_1}{4} \dots \dots \dots (2)$$

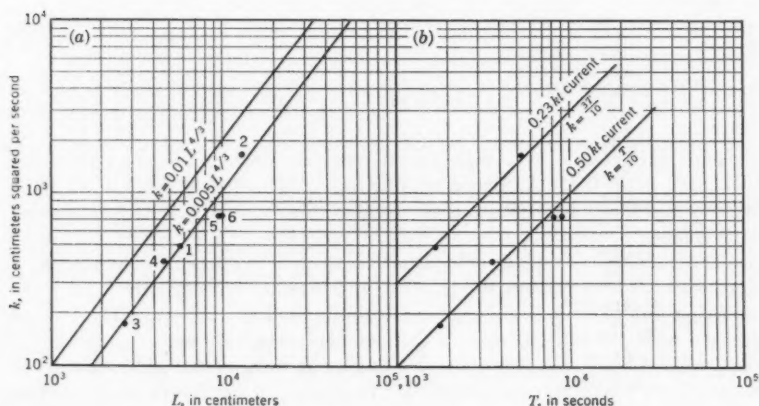


FIG. 3.—EDDY DIFFUSIVITY k VERSUS SCALE L AND TIME T

and

$$\sigma_2 = \frac{W_2}{4} \dots \dots \dots (3)$$

therefore

$$k = \frac{W_2^2 - W_1^2}{32 \Delta T} \dots \dots \dots (4)$$

Fig. 3(a) shows, in c.g.s. units, the eddy diffusivity constant as a function of the scale of the phenomena, L , where the scale is taken as the average width of the dye stream.

$$L = \frac{W_1 + W_2}{2} \dots \dots \dots (5)$$

The function $k = 0.01 L^{4/3}$ is taken from Pearson⁴ for comparison, while the best-fit curve $k = 0.005 L^{4/3}$ is based on the observed data. Figure 3(b) shows

TABLE 3.—EFFECT OF EXISTING HYPERION

Faunal zone	BENTHOS		
	Distance from outfall, in miles	Number of species	Number of individuals
(1)	(2)	(3)	(4)
Limited pollution (generally nonreproductive stages)	0- $\frac{1}{2}$	Minimum	
Pollution tolerant (limited number of species maturing and reproducing)	$\frac{1}{2}$ -2	Increasing ↓	Increasing ↓
Limited enriched	2-4		Maximum
Unlimited diminished	4-6		Decreasing ↓
Normal	>6		

* While indicator species are not exclusively restricted to the faunal zone shown, they form a significant

the eddy diffusivity constant as a function of time in which the effect of current velocity is indicated. A further examination of the effect of dilution upon the density of coliform bacteria in ocean waters will be found in a subsequent section of this paper.

The discharge of a plant effluent into sea water has been observed to affect markedly the temperature and salinity, and thus the density, structure of the receiving waters, as well as its general turbidity and appearance. This is most marked near the outfall where a distinct field may be seen. In addition, a fairly well-defined inshore water mass having an areal extent of 20 sq miles in Santa Monica Bay may be identified. In general, it has intermediate characteristics between those of the distinct field and of the offshore waters. This water mass is characteristically outlined by alternating streaks of smooth and rough water, foam lines consisting essentially of marine organisms, and color changes at the surface.

Other discharges contributing to the inshore water mass include the cooling waters from two nearby steam power plants. Calculations of the heat budget of the Santa Monica Bay have shown⁵ that the contributions of sensible heat from the two major sources, Hyperion effluent and the cooling waters, are nearly equal. The greater effect of the salinity difference of the fresh water effluent indicates that the inshore mass is almost entirely due to Hyperion operations.

The chemical changes in the receiving waters near Hyperion include generally a minor reduction in dissolved oxygen and a significant increase in the nutrient elements, nitrogen, and phosphorous, near the outfall.¹⁰ Present ana-

¹⁰ "Plankton and Associated Nutrients Surrounding Three Outfalls in Southern California," by R. E. Stevenson and J. R. Grady, Allan Hancock Foundation, Univ. of Southern California, Los Angeles, Calif., 1956.

DISCHARGE UPON BENTHOS AND BOTTOM FISH

BENTHOS			Average number of bottom fish (flatfish) from trawling
Bio-index number species/ number individuals column 3/column 4 (5)	Number of detritus feeders (6)	Typical indicator species ^a (7)	
Decreasing ↓ Minimum ↑ Increasing	Maximum	<i>Capitella capitata</i> <i>Diopatra ornata</i>	12.5
	Decreasing ↓	<i>Nereis procera</i> <i>Nothria elegans</i>	16.0
		<i>Amphipolis squamata</i> <i>Astropecten californicus</i>	21.9
		<i>Onuphis nebulosa</i>	12.4

portion of the bottom forms present.

lytical techniques are such that changes in concentrations of these elements can be measured with assurance only in the area near the outfall.

BIOLOGICAL FACTORS

Sewage plant effluents which are of necessity rich in both nutrient elements and food for saprophytes and are discharged into marine waters may be expected to have varying effects upon the plankton (floating or weakly swimming forms, both plant and animal), nekton (swimming animals), and benthos (attached, burrowing, or creeping organisms found on the bottom). General considerations of the role of nutrients in marine life cycles are given by H. U. Sverdrup, Martin W. Johnson, and Richard H. Fleming,⁷ and by H. W. Harvey.¹¹

The discharge of significant quantities of nutrients may reasonably be assumed to result in increased growths of plants (phytoplankton) in the area affected, and possibly an increase in the number of grazing animals (zoöplankton) as well. An increase in plankton populations in the vicinity of various ocean outfalls in the Los Angeles area has been noted during the investigations referred to herein.^{8,10,12} However, there is no evidence that the increased nutrient concentrations will, in themselves, cause the intense blooms which are occasionally noted. In this regard, Robert E. Stevenson has stated¹⁰ that once a bloom is initiated, "the nutrients contributed by the effluent markedly increase the reproductive rate, and thus the numbers of plankton."

The California Department of Fish and Game has made a limited study of bottom fish in Santa Monica Bay indicating that the Hyperion discharge has

¹¹ "The Chemistry and Fertility of Sea Waters," by H. W. Harvey, Cambridge Univ. Press, Cambridge, England, 1955.

¹² "Plankton in the Summer Months of 1956 Around the Orange County Sewer Outfall," by R. E. Stevenson and J. M. Resig, Allan Hancock Foundation, Univ. of Southern California, Los Angeles, Calif., 1956.

had no significant effects upon the fish population.¹³ A qualitative confirmation of these results is gained from the observation of sardine and bait boats occasionally operating in the general area of the outfall.

As might be expected, however, the effects of Hyperion sewage upon the benthos is more marked. Olga Hartman^{14,15} has examined these effects, and has, on the basis of the types and numbers of worms, starfish, and crustaceans, defined bottom areas in the vicinity of the existing ocean outfall into various faunal zones. This study is summarized in Table 3. The relationships shown in Table 3 are generalized from data obtained from locations on the shelf in order to permit an evaluation of pollution. Variations in individual samples may be expected due to the depth, type of sediment, temperature, currents, and biological associations. The effect of the existing discharge on the benthos is reflected in the numbers of bottom-dwelling fish (flounders and soles) caught per 10 minute drag with an otter trawl by the State Department of Fish and Game.¹³ It may be assumed that these fish, having a certain freedom of movement, will be found in greatest numbers where their food is most abundant—in this case, over the limited-enriched faunal zone.

Because of the general nature of the bottom and its normally associated organisms, the existing Hyperion discharge has had no noticeable economic effect upon commercial or sport fishing. However, the Department of Fish and Game has made observations indicating that abalone have been significantly affected by sewage discharged into their normal habitat.¹³ Similar effects on such other shellfish as oysters and clams have long been noted and reported.⁴ Thus, the effects of sewage treatment plant effluents must be evaluated in terms of a particular area of discharge, and can be applied to other areas only with considerable caution.

BACTERIOLOGICAL FACTORS

Studies of the viability of enteric organisms in sea water have been conducted for many years, and reviews of the literature have been reported by B. Moore,¹⁶ Pearson,⁴ A. E. Greenberg,¹⁷ Gerald T. Orlob,¹⁸ J. M. ASCE, and Richard D. Terry.¹⁹ The various studies have been directed primarily toward determining the ultimate survival of bacteria in sea water. The results of such studies are somewhat difficult to apply to an operating ocean outfall as they necessarily involved certain artificial conditions. However, the reported times of survival and rates of reduction are significant in terms of the different conditions they represent.

¹³ "Sewage in Santa Monica Bay: A Critical Review of the Oceanographic Studies," Marine Advisers, La Jolla, Calif., 1956.

¹⁴ "Results on Investigations of Pollution and Its Effects on Benthonic Populations in Santa Monica Bay, California," by Olga Hartman, Allan Hancock Foundation, Univ. of Southern California, Los Angeles, Calif., 1956.

¹⁵ "Contributions to a Biological Survey of Santa Monica Bay, California," by Olga Hartman, Allan Hancock Foundation, Univ. of Southern California, Los Angeles, Calif., 1956.

¹⁶ "Sewage Contamination of Coastal Bathing Waters," by B. Moore, *Bulletin of Hygiene*, Vol. 29, No. 7, 1954, pp. 689-704.

¹⁷ "Survival of Enteric Organisms in Sea Water," by A. E. Greenberg, *Public Health Reports*, Vol. 71, No. 1, 1956, pp. 77-86.

¹⁸ "Viability of Sewage Bacteria in Sea Water," by G. T. Orlob, *Sewage and Industrial Wastes*, Vol. 28, No. 9, 1956, pp. 1147-1167.

¹⁹ "An Annotated Bibliography on Bacteriology, Oceanography, and Marine Geology as They Relate to the Disposal of Waste Material into the Sea," by R. D. Terry, Allan Hancock Foundation, Univ. of Southern California, Los Angeles, Calif., 1956.

A study was made by Pearson⁴ of the persistence or survival of pathogenic and coliform bacteria respectively, in sea waters from various locations and subjected to different treatments and methods of analysis. From this study there is considerable evidence that, under some conditions, both pathogens and coliforms may survive for significant periods of time. That these conditions do not exist in nature is apparent from the reported details of the test procedures. Nevertheless, it is indicated that raw sea water provides a more hostile environment to enteric organisms than does filtered or sterilized sea water.

Evidence that coliforms are viable for longer periods than *E. typhosa* is reported by Paul J. Beard and Neil F. Meadowcroft,²⁰ M. ASCE. They found that coliforms survived for more than 35 days while *E. typhosa* survived for from 12 to 28 days. While these results are not necessarily valid for all pathogens, they indicate that the use of coliform bacteria determinations as indices of pollution is reasonable and, considering other available information, is probably a conservative method.

The various factors which have been suggested as being important in reducing bacterial populations may be divided into two general classifications:

1. Bacteriological factors inherently present in the marine environment, including competition for available food, predation by protozoa or zoöplankton, salinity, sunlight, temperature, pressure, bacteriophage, and heat-labile bactericidal substances. It is assumed herein that these factors operate universally in marine waters, and that they may be combined into a single factor, namely, mortality. Included is the effect of breaking up by waves or surf of flocs or clumps of bacteria which might superficially indicate an increase in bacterial population, although the actual numbers present would remain constant.¹³ This is due to the nature of the most probable number technique (MPN), where either a single organism or a group of organisms could cause a positive tube reading.

2. Factors which are dependent on the sewage, the type of sewage treatment and, thus, the previous history of the bacteria, and the initial dilution of the plant effluent as well as subsequent dilution of the mixture as it travels with the ocean currents. Of particular importance are the settling characteristics of the suspended solids in the effluent, within or upon which the bacteria are found.

EVALUATION OF BACTERIOLOGICAL FACTORS IN SANTA MONICA BAY

Early in the investigation, it became apparent that the available information had to be supplemented to permit a reasonable analysis of the persistence of coliform bacteria from the proposed effluent in ocean waters. Thus, studies were made^{5,8,9} in the receiving waters surrounding the outfalls from the Hyperion plant, the Los Angeles County Sanitation Districts' plant, the Orange County Sanitation Districts' plant, and the City of Los Angeles Terminal Island Treatment Plant.

Areas within the particular sewage field were tagged by fluorescein dye, current crosses, or other suitable means. Samples were taken at regular inter-

²⁰ "Survival and Rate of Death of Intestinal Bacteria in Sea Water," by P. J. Beard and N. F. Meadowcroft, *American Journal of Public Health*, Vol. 25, No. 10, 1935, pp. 1023-1026.

vals for as much as 26 hr during which time the tagged area moved away from the outfall. Determinations of the most probable number (MPN) of coliform densities were made in accordance with Standard Methods²¹ for lactose-broth presumptive tests using 2 tubes in each of 3 decimal dilutions and brilliant green bile confirmations.

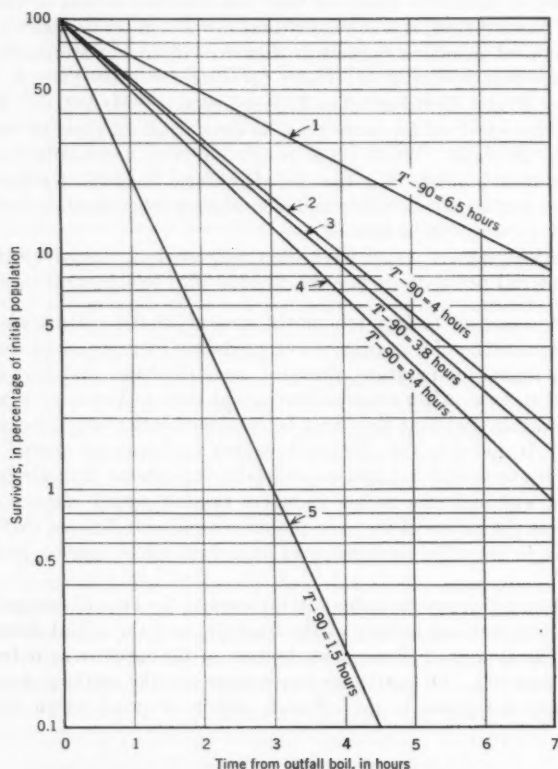


FIG. 4.—PERSISTENCE OF COLIFORM BACTERIA IN OCEAN SURFACE WATERS

These studies were directed primarily toward determination of the over-all rate of disappearance of coliforms in order that the effects of effluents discharged offshore could be evaluated. However, additional observations to determine the net dilution of the effluent were also made. Dilutions have been studied by means of a radioactive tracer⁹ which permitted calculations of dilutions of as high as 10,000 parts of sea water to 1 of effluent, and by determinations of salinity which may be used to calculate dilutions of up to approximately 300

²¹ "Standard Methods for the Examination of Water, Sewage, and Industrial Wastes," H. A. Faber, W. D. Hatfield, M. H. McCrady, and E. K. Kline, Editors, 10th Ed., American Public Health Assn., 1955.

to 1. The results of these studies^{5,9} are indicated on Fig. 4. The curves in Fig. 4 compare the average reductions of coliform densities in the ocean surface waters for various effluents in the Los Angeles area. Curve 1 indicates the Hyperion secondary effluent, $T_{-90} = 6.5$ hr; curve 2 represents the Los Angeles County Sanitation Districts and the City Terminal Island Plant primary effluents, $T_{-90} = 4$ hr; curve 3 indicates the Hyperion primary effluent, chlorinated, $T_{-90} = 3.8$ hr; curve 4 is the Hyperion primary effluent, $T_{-90} = 3.4$ hr; and curve 5 denotes the Orange County Sanitation Districts primary effluent, $T_{-90} = 1.5$ hr.

A considerable variation in the persistence of coliform bacteria from the several outfalls is thus indicated. It should be noted that the studies at Hyperion were conducted for periods of up to 26 hr, while those at other outfalls were for periods of approximately 8 hr. However, there was no significant variation in the over-all rates of reduction at Hyperion over the entire period, so that results obtained at the other locations are assumed to have essentially the same validity.

The persistence of coliform bacteria in sea water may be formulated in accordance with the following:^{4,22}

$$\frac{N_t}{N_0} = 10^{-\frac{t}{T_{-90}}} \dots \dots \dots (6)$$

in which N_t is the number of survivors after t hours, N_0 represents initial population at $t = 0$, and T_{-90} denotes the time for a 90% reduction in bacterial density.

The over-all reduction is assumed to follow the relationship

$$\frac{1}{T_{-90_{o/a}}} = \frac{1}{T_{-90_m}} + \frac{1}{T_{-90_d}} + \frac{1}{T_{-90_s}} \dots \dots \dots (7)$$

in which $T_{-90_{o/a}}$ is the observed time for a 90% reduction, T_{-90_m} denotes time for a 90% reduction due to mortality as defined above, T_{-90_d} represents time for a 90% reduction due to dilution of the field as it moves down-current, and T_{-90_s} is the time for a 90% reduction due to sedimentation.

It is possible to make approximations of the various T_{-90} 's in Santa Monica Bay. As stated earlier, the over-all T_{-90} is essentially constant for the period of approximately one day. This is of significance at Hyperion because of the general currents and circulation of the bay. Thus, in order to evaluate the relative effects of the various factors that serve to reduce coliform densities in the surface waters, it is assumed that these factors are essentially constant for the one-day period.

The considerable difference between the over-all rates of coliform reduction for primary and secondary effluent at Hyperion suggested that sedimentation of the suspended solids was a major cause of disappearance of coliforms from the surface waters. This has been confirmed by the observations of Sydney C. Rittenberg,⁹ which showed a progressive sinking of the zone of maximum

²² "Investigation of the Laws of Disinfection," by H. Chick, *Journal of Hygiene*, Vol. 10, No. 3, 1910, p. 237.

coliform densities and maximum turbidities as the field moved downstream. The observations also demonstrated extensive fields of coliforms in the upper layer of the bottom sediments near the several outfalls studied. These are in accordance with observations on the importance of sedimentation made over a number of years in studies of shellfish pollution as well as water pollution.^{4,23}

The greater persistence of coliform bacteria in surf waters has been noted in Santa Monica Bay and other nearby locations where ocean outfalls are in

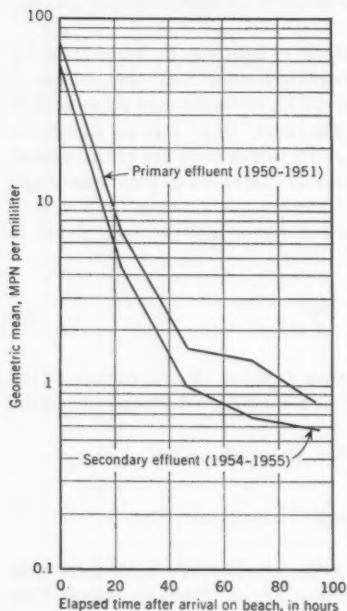


FIG. 5.—PERSISTENCE OF COLIFORM BACTERIA IN SURF ZONE

operation. The results of one study of this phenomenon, based upon 50 cases of each type of effluent with no chlorination when high counts occurred on the beach, is presented in Fig. 5. As indicated, after the bacteria arrive in the surf zone, the reduction in coliform concentrations continues at a gradually decreasing rate. Thus, the first 24 hr in the surf zone shows a reduction of some 90%, the second 24 hr shows approximately an 80% additional reduction, and so on. These observations were made during previous winter months when the effluent was not being chlorinated.

A similar analysis of beach pollution occurring after short periods of no chlorination in 1955 and in 1956 is summarized in Fig. 6. The numbers in parentheses indicate the number of cases from which the geometric mean was derived. The average travel time to the surf zone was 15 hr and the period of time during which determinations were made of over-all reductions of bacterial density in offshore waters was 1 day. The curve plotted in Fig. 6 includes both the primary and secondary effluent. The unchlorinated slug was sampled at sea and followed to the surf zone. A more accurate estimate of the travel time from the outfall is therefore possible. It may be noted that the rates from the two sets of data indicated on Fig. 5 and Fig. 6 are in very close agreement. No significant difference between the rates of reduction of coliforms from unchlorinated primary and secondary effluents has been observed in the surf zone. Therefore, the past history of the organisms does not here appear to be significant. It is indicated in Fig. 4 that the remaining coliforms in chlorinated effluents show a greater persistence, due presumably to a selective action by the chlorine.

It is reasonable to assume that within the surf zone sedimentation is no longer effective in removing coliforms from the surface waters. Similarly, it

²³ "Marine Microbiology," by Claude E. ZoBell, *Chronica Botanica*, 1946.

is reasonable to assume that dilution is of minor significance since no upwelling was taking place during the observations and there was no significant net movement of the polluted zone along the beach. Therefore, what dilution occurred was probably negligible compared with the dilution which obtained offshore.

Elimination of the sedimentation and dilution factors leaves only mortality. It is probable that the various contributing factors that cause mortality vary

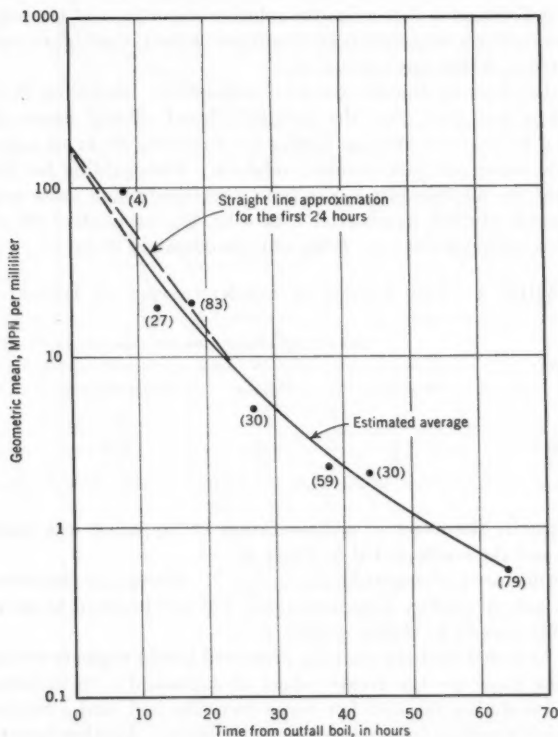


FIG. 6.—PERSISTENCE OF COLIFORM BACTERIA IN SURF ZONE FOLLOWING A SHORT PERIOD OF NO CHLORINATION

among themselves, but the combined effect seems to be fairly uniform. With this in mind, the curve shown on Fig. 6 has been extrapolated backward in order to obtain a reasonable approximation of the mortality T_{90} for the first 24-hr period referred to earlier. Thus, T_{90}_m is indicated to be approximately 17.8 hr. This figure necessarily includes any effect of breaking up of clumps of coliforms by wave or surf action which might result in a superficial increase in the MPN. Such a phenomenon, while it has not been evaluated for the

Hyperion discharge, would imply a higher true coliform density at the boil than the observed values. Thus, assuming that the disintegration of clumps is progressive as the sewage field moves downstream, a lower value for the $T-90_m$ would result since the true coliform density would approach the observed density with the passage of time. As an extreme example, a ten-fold apparent increase in MPN due to the complete breaking up of clumps within the first 24 hr would result in a 50% reduction in $T-90_m$. However, since several other unknown variables are involved, and since the primary purpose of estimating the value of $T-90_m$ is to determine the relative importance of the major factors that reduce coliform concentrations in surface waters, the higher value of 17.8 hr is adopted as a first approximation.

Next, the effect of dilution must be considered. Referring to Fig. 1 and Table 1, it is seen that after the initially diluted effluent leaves the boil, it undergoes a subsequent dilution during the following 24 hr of approximately 14 parts sea water per part of initial mixture. Disregarding for the moment the fact that the dilution rate varies from a relatively high value near the boil to a comparatively low figure after 3 to 4 hr, the cumulative effect over the 1-day period is equivalent to a $T-90_d$ of approximately 20 hr.

TABLE 4.—THE EFFECT OF SEDIMENTATION AT HYPERION

Effluent	TIME FOR 90% REDUCTION IN COLIFORMS, IN HOURS			
	Mortality	Dilution	Sedimentation	Over-all
(1)	(2)	(3)	(4)	(5)
Secondary	17.8	20	21.0	6.5
Primary	17.8	20	5.3	3.4

Using Eq. 7, the effect of sedimentation at Hyperion was computed by difference, and the results listed in Table 4.

These results are shown graphically in Fig. 7. Except for the over-all reductions, they are, of course, approximations, but are believed to be reasonable and probably correct to within $\pm 50\%$.

It may be noted that the analysis presented herein neglects several factors. Chief among these are the greater effect of dilution due to turbulent mixing which obtains during the first few hours from the boil, and a reduced rate of sedimentation resulting from the greater turbulence. Another factor not taken into account is the partial isolation and, thus, a possible protection of bacteria from the various bactericidal factors in sea water by virtue of clumping and a lower net dilution. The available data do not permit a complete evaluation of these variables. They do, however, indicate that their net effect is essentially constant in so far as the over-all reduction of coliforms is concerned.

An evaluation of the relative effects of the various factors is now possible. It is seen that with secondary effluent, mortality, dilution, and sedimentation are of essentially the same importance in the disappearance of coliform bacteria from surface waters. However, with primary effluent, sedimentation is by far the most important factor. A similar analysis of the data from the Orange

County Sanitation District Outfall⁹ also indicates that sedimentation is the predominating factor.

Because sedimentation is shown to be a significant factor in the disappearance of coliforms from surface waters, it follows that resuspension of the settled particles might cause pollution of overlying waters. Another possibility that might be considered is the behavior of grease slicks or surface films that, being wind-driven, could carry concentrations of bacteria to the surf zone in relatively

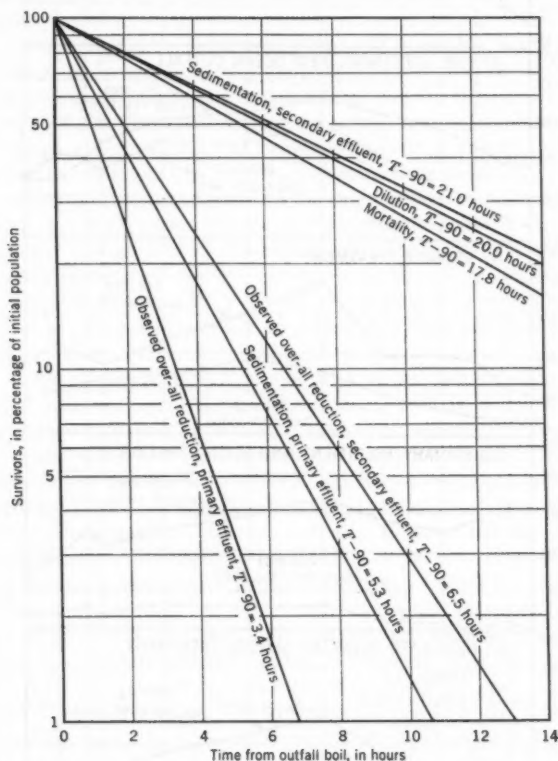


FIG. 7.—FACTORS AFFECTING PERSISTENCE OF COLIFORM BACTERIA FROM HYPERION PRIMARY AND SECONDARY EFFLUENTS

short periods of time.¹³ These factors can be discounted in Santa Monica Bay since it has been possible to account for the location and intensity of observed coliform densities in the surf waters entirely from the movements of the sewage field in the water itself.

The possibility that greater amounts of suspended matter present in the receiving waters during plankton blooms could affect the survival of coliform

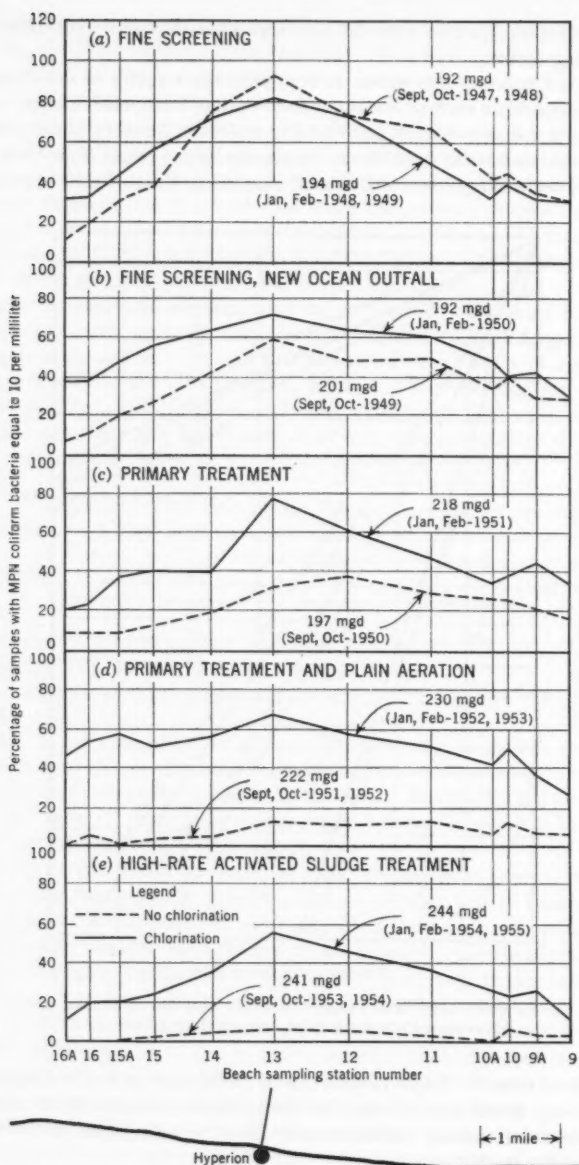


FIG. 8.—EFFECT OF CHLORINATION OF EFFLUENTS FROM HYPERION TREATMENT PLANT

bacteria in the surface waters has been investigated by Stevenson and Resig.¹² They conclude that the persistence of coliforms is not related to the numbers of plankton present.

REQUIREMENTS FOR SEWAGE TREATMENT AND DISPOSAL WORKS

The significance of the bacteriological factors that operate in marine waters upon a sewage plant effluent being discharged through a submarine outfall may be summarized in terms of the outfall requirements and the treatment requirements.

Where the oceanographic conditions permit, it is possible to utilize a lesser degree of treatment on shore and rely upon the ocean to provide the final treatment of the sewage. Oceanographic conditions include currents, the circulation pattern, and the distance to which an outfall can be constructed before reaching unreasonable depths. Suitable conditions are indicated for the Hyperion Treatment Plant where primary treatment is proposed.

A higher degree of treatment such as the existing high-rate activated sludge process now in use at Hyperion will result in an effluent having a lower bacterial density but that appears to be less amenable to final bacteriological reduction in the receiving waters.

More complete treatment by either standard-rate activated sludge or trickling filter processes will produce an effluent that can be further treated or chlorinated so that no bacterial pollution of the receiving waters can result.

Fig. 8 demonstrates the effect of chlorination on various effluents at Hyperion and compares the beach conditions during periods of chlorination and nonchlorination. It is seen in Fig. 8(a) that chlorination of screened sewage discharged through the old ocean outfall having inshore leaks of some 5% to 10% of the flow had no significant effect. Utilization of the present (Fig. 8(b)) outfall which provided an average contact time of 30 minutes resulted in a slight reduction of coliform densities near the outfall. However the chlorination was less effective at greater distances. Chlorination of primary effluent (Fig. 8(c)) showed significant reductions of coliforms, but the California State bathing water standards of an MPN of 10 per milliliter which may not be exceeded more than 20% of the time were not met at surf stations near Hyperion. Chlorination of secondary effluent resulted in reducing coliform concentrations to permissible levels. It may be noted that the 18 to 20 tons per day of chlorine used in 1947-1948 was reduced to 6 to 8 tons per day in 1955.

A comparison from Fig. 8(d) and (e) of the effects of unchlorinated effluents from primary and high-rate activated sludge indicates that approximately a 35% reduction in beach pollution was obtained with the latter. The discrepancy between experience on the beach and the data obtained from reproducible experiments in the water has not been entirely resolved. However, it should be noted that the periods of nonchlorination were during winter (wet weather) months and that the effect of runoff must be considered. It is unreasonable to assume that aeration of primary effluent would lower its bacteriological quality as indicated by the beach pollution data shown on Fig. 8(d). Thus, the effect of runoff was probably a major contributing factor.

A quantitative evaluation of beach pollution from runoff is not possible from data presently available. Qualitatively, however, it can be stated that such pollution is determined by the frequency, intensity, and duration of rains, and that major drains, such as the one discharging near Station 10) (Fig. 8), show a pronounced effect upon beach pollution.

Other factors which are significantly variable during the winter months are oceanographic which result in regional variations in current direction indicated by beach pollution data obtained daily⁸ since March, 1946. Meteorological conditions under which winds are strongly directed offshore are also of considerable importance in the surface currents of the bay⁶ during these months.

The final selection of treatment facilities necessarily rests upon the determination of the most economical method which will result in satisfactory receiving water conditions. This has resulted in the choice of primary treatment and disposal of the effluent through a five-mile outfall at Hyperion. The effluent outfall is to be provided with diffusers which will result in an estimated initial dilution of a minimum of 60:1 and an average of approximately 200:1.

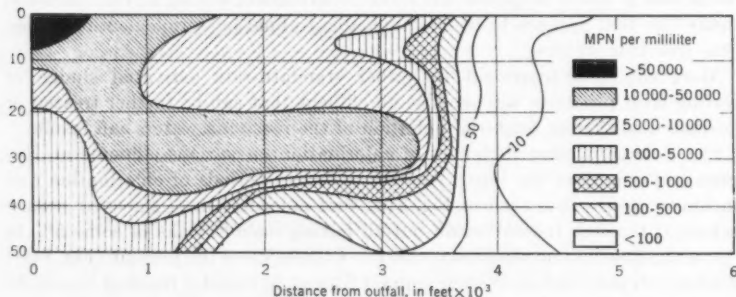


FIG. 9.—VERTICAL DISTRIBUTION OF COLIFORMS INDEPENDENT OF DIRECTION

A prediction of the bacterial densities in the surf waters can now be made. If it is assumed that the average coliform density in the effluent is 500,000 ml, the average initial dilution is 100:1, and the travel time to shore (based on surface observations) is 20 hr, the indicated bacterial concentration in the surf zone will be less than 0.01 ml. The worst condition may be similarly evaluated, assuming an effluent coliform density of 1,000,000 ml, an initial dilution of 60:1, and a travel time of 13 hr (a current of this sort has never been observed, and may be roughly estimated from the available data to occur significantly less than 1.0% of the time). Even these conditions would result in a mean bacterial concentration within the particular surf zone area affected of approximately 2.5 ml. This has been found to be equivalent to the California State bathing water standard.^{24,25}

In the application of the basic plan of primary treatment at Hyperion, the existing aeration and effluent chlorination facilities have been retained in order

²⁴ Annual Report for 1952-1953, Bureau of Sanitation, Dept. of Public Works, Los Angeles, Calif.

²⁵ "Bacteriological Standards for Bathing Waters," by W. F. Garber, *Sewage and Industrial Wastes*, Vol. 28, No. 6, 1956, pp. 795-808.

to provide maximum flexibility in the operation of the enlarged plant.²⁶ Thus, at the ultimate design flow of an average 420 million gal per day, up to 120 million gal per day of the total flow can receive standard-rate activated sludge treatment, up to 245 million gal per day can receive high-rate activated sludge treatment, or up to the hydraulic capacity of approximately 315 million gal per day can receive a modified secondary treatment. The remainder of the flow will receive primary treatment. In addition, various combinations of flows through the existing 1-mile outfall and the proposed 5-mile outfall can be effected while any portion of the flow receiving standard-rate treatment may, when practicable, be reclaimed as industrial or ground-recharging water.

CONCLUSIONS

Studies conducted over a period of two years in marine receiving waters surrounding various sewer outfalls in the vicinity of Los Angeles have indicated the following general findings:

1. After the sewage undergoes an initial dilution as measured at the top of the rising column, additional dilution will derive from turbulent mixing which, at Hyperion, is effective for some 4 hr and from lateral diffusion thereafter.

2. Sewage discharged into relatively near-shore waters will result in a distinct field of a comparatively small size as well as a larger inshore water mass with characteristics generally between those of the distinct field and the normal coastal waters.

3. The various constituents of the effluent have a measurable effect on the normal ecological pattern of the receiving waters and the underlying ocean floor. Since there are considerable variations of these patterns in nature, the biological effects of any waste discharge must be evaluated for the specific area under consideration.

4. The factors of primary significance in the reduction of coliform bacteria in marine waters include dilution, sedimentation, and "mortality." Mortality includes the effects of competition for available food, predation, salinity, sunlight, temperature, pressure, phage, and other characteristics inherently present in the receiving waters. The combined effect of the above factors is such as to result in over-all rates of 90% reduction in coliform densities in surface waters of from 1.5 hr to 6.5 hr for the various effluents studied. It follows that with the present state of knowledge, evaluation of the sanitary significance of either existing or proposed works must be made for the specific discharge under consideration.

5. The feasibility of providing primary treatment followed by discharge through a 5-mile ocean outfall at Hyperion is indicated by the following findings:

- (a) It is possible to construct an outfall in the 190-ft depths which obtain at that distance.

²⁶ "Enlarged Sewage Disposal Facilities for Los Angeles," by Robert J. Theroux, *Sewage and Industrial Wastes*, Vol. 29, No. 2, 1957, pp. 124-133.

(b) The current pattern in Santa Monica Bay is such that, during that portion of the time that onshore currents prevail, sewage discharged offshore which reaches the surface immediately (an unlikely event) will generally not arrive at the surf zone until after approximately 20 hr.

(c) Reduction of coliform density in surface waters is due in about equal part to dilution, sedimentation and mortality for the existing high-rate activated sludge effluent where the time for 90% reduction is indicated to be 6.5 hr.

(d) Reduction of coliform density for primary effluent is due largely to sedimentation, where the time for 90% reduction is indicated to be 3.4 hr.

(e) Prediction of coliform densities in surf waters of Santa Monica Bay indicate that the bacteriological standards for bathing waters can easily be met.

(f) While the existing discharge has altered the biological pattern of the bottom-dwelling organisms, no significant effect on fish has been observed.

ACKNOWLEDGMENTS

The participation, assistance, and suggestions of many individuals throughout the period of investigation have made this study possible. Appreciation is expressed to Warren A. Schneider, A. M. ASCE, Norman B. Hume, M. ASCE, G. A. Parkes, Robert D. Bargman, M. ASCE, William F. Garber, A. M. ASCE, and B. L. Jones of the Bureau of Sanitation. The writer is indebted to K. O. Emery, S. C. Rittenberg, R. E. Stevenson, R. B. Tibby, and Olga Hartman of the Allan Hancock Foundation of the University of Southern California; to Norman H. Brooks, A. M. ASCE, of the California Institute of Technology, and to C. E. ZoBell, D. L. Inman, and J. D. Frautschy of the Scripps Institution of Oceanography. The writer is also indebted to David L. Narver, Jr., M. ASCE, Reuben R. Alvy, M. ASCE, David R. Miller, A. M. ASCE, and Charles H. Lawrance, A. M. ASCE, of Hyperion Engineers.

DISCUSSION

CHARLES H. LAWRANCE²⁷ AND DAVID R. MILLER,²⁸ ASSOCIATE MEMBERS, ASCE.—The paper represents a good condensation of the most important phases of the extensive offshore oceanographic and biological investigations accomplished by the City of Los Angeles. Particularly important is the demonstration of the cardinal importance of *T-90*, the rate of coliform decline in sea water, and what wide variations may be experienced from one discharge condition to another with corresponding wide variations in over-all coliform decline. Because of the dearth of field data regarding the operation of existing ocean outfalls, many of the factors considered by the author were not fully appreciated until only very recently. The City of Los Angeles is to be commended for its whole-hearted efforts to solve its difficult sewage problem in the best interests of all concerned. The City's oceanographic program is an example of this endeavor.

The sewerage problems of Los Angeles are perhaps unique. Few cities have grown at such a rate in the post-war period and none has grown in population as has Los Angeles. Its sewerage system now serves an estimated 2,500,000 persons. Furthermore, the Santa Monica Bay area, which is bordered full length by extensive and extremely valuable bathing beaches has been and continues to be the logical disposal site, both from an economic standpoint and from other considerations, for large volumes of treatment plant effluent. The burgeoning population of the Los Angeles metropolitan area increases the use of these beaches and of the offshore water. With the passage of time, increasingly higher standards for these receiving waters are being demanded by the public and required by state authorities. The completion of the existing plant in 1951 removed the unsatisfactory disposal conditions that had prevailed for many years and restored the bathing beaches to acceptable conditions. However, with the rapid development of the area, overflow conditions were experienced in the Los Angeles sewage collection system and the treatment plant approached its capacity sooner than had been expected. By the time a Citizens Committee had received and reviewed engineering reports on the possible courses of action for the City and had made its recommendation, the sewerage conditions had reached an emergency state. The City foresaw that its own staff would be unable to complete soon enough the bulk of the major design required for relief of the situation, involving collection, treatment, and disposal facilities. The City therefore engaged a joint venture of private Los Angeles engineering firms to perform this design work with the stipulation that the resulting design would meet all state and local requirements. The works designed by the engineers in connection with this program are as follows:

²⁷ Sr. San. Engr., Koebig and Koebig, Cons. Engrs., Los Angeles, Calif.; formerly, San. Engr., Hyperion Engrs., Los Angeles, Calif.

²⁸ Project Mgr., Daniel, Mann, Johnson, & Mendenhall, Cons. Engrs., Los Angeles, Calif.; formerly, Project Engr., Hyperion Engrs., Los Angeles, Calif.

1. The North Central Outfall consisting of 8 miles of 112-in.-diameter trunk sewers constructed for the most part in tunnels;
2. The expansion of the Hyperion Treatment Plant to 420 million gal daily average flow capacity and the construction of modifications;
3. A 22-in.-diameter steel sludge outfall running 7 miles to sea;
4. An ocean outfall for effluent disposal consisting of a 144-in.-diameter concrete outfall running 5 miles to sea and terminating in a major diffuser; and
5. An effluent pumping station having a 720 million gal daily capacity.

The basic premise used in this program was that the ocean would be used as a means of secondary treatment as well as disposal and that the treatment would consist of coarse bar screens, aerated grit removal, and primary sedimentation before disposal to the effluent outfall.

This effluent outfall was of unprecedented magnitude, and the timetable permitted and required thorough investigations before design was finalized. Therefore, the engineers undertook an exhaustive research and investigation program dealing with the problems incident to the disposal of primary effluent into the ocean. The oceanographic studies described by the author were one of the phases of this program. In order to insure that all of the aspects of the program were thoroughly explored, a one-year study of the oceanographic and biologic conditions existing in Santa Monica Bay was undertaken. In addition, a program was initiated to study the performance of existing outfalls, and other research programs were authorized. This material was correlated with the studies described by the author and then the two outfalls were designed.

The following paragraphs will offer comments on certain sections of the author's paper, and are made in the light of the other studies previously described.

The point made by the author that the physical dilution of an effluent discharged into marine waters is ultimately limited by the amount of new water brought into the area should be emphasized particularly in the case of large quantities of effluent discharged in regions where the natural currents tend to be sluggish. However, the difference in density of effluent compared to sea water will, in itself, generate minor currents. The minimum dilution that could be expected even under quiescent conditions would be 1 in 60 for the proposed effluent diffuser. However, in the design of an ocean outfall there is no substitute for a comprehensive study of long-term current and temperature conditions in the vicinity of the outfall in order to be able to predict with reasonable assurance the action of a large scale diffuser.

In regard to the coefficient of eddy diffusion, it should be remembered that the bacteriological factors far overshadow the physical factors, following initial discharge and particularly as time increases.

In Eq. 6 the use of N_t = number of survivors after t hours makes it difficult to apply the formula without having current studies. Knowledge of the currents cannot be emphasized too much in studies of this kind. Also, coliform

²² "A Final Report submitted to Hyperion Engineers," the Allan Hancock Foundation, Univ. of Southern California, Los Angeles, 1956.

bacteria are not the most reliable indicator of sewage pollution, and certainly further research in this field is needed. Coliform bacteria tests should be used with caution. It is essential that statistical methods be used in the interpretation of test results.

The thought that the waves or surf breaking up clumps of coliforms might alter the apparent MPN could be misleading. The coliform test procedure calls for a vigorous shaking of the sample bottle and if followed would be expected to simulate the effect of the more common waves or surf. Admittedly, large breakers would produce a greater turbulence than bottle-shaking.

The author states in his summary that the reduction of coliform density for primary effluent ($T-90$) is 3.4 hr. The engineers did not use this value in the design of the effluent outfall. Rather, they used a figure of 8 hr as a matter of conservative practice.

The conclusion of the author that a higher degree of treatment results in an effluent less amenable to ocean disposal sounds paradoxical, but the results of studies that were undertaken would support this conclusion.

Separation of the major factors that combine to produce a reduction of chemical and bacterial pollutants following injection of sewage effluent into sea water is of particular concern for a specific discharge condition under study and is valuable from the standpoint of basic knowledge. This analysis has been handled very adeptly by the author in his studies in Santa Monica Bay. He has shown that for high-rate activated sludge effluent the elements of sedimentation, physical dilution, and mortality were approximately equal for reduction of coliform densities. The writers found it possible to approximate the separate effects of certain factors responsible for coliform decline in some of the data analyzed in their studies using somewhat different methods.

For example, in the data for the Deer Island Outfall in Boston Harbor³⁰ where coarse-screened sewage was discharged through a small diffuser with average port submergence of 43 ft at mean low water, the physical dilution was computed from recorded chemical data and also by a formula developed by Norman H. Brooks, J.M. ASCE.³¹ The respective results were in fair agreement. The eddy diffusivity employed in the formula was $K = 0.01 L^{3/4}$ cm² per sec as compared to the value of $0.005 L^{3/4}$ which the author determined for the mildly turbulent Santa Monica Bay. The average current was taken as 0.97 ft per sec and the average initial dilution was 23 parts of diluted effluent per volume of undiluted effluent. The original measurements were made from surface samples taken at intervals from the approximate center of the sewage field near current floats, as the field moved away from the diffuser from distance and time up to approximately 16,500 ft and 4.7 hrs. Although the data were somewhat erratic, physical dilution of the sewage effluent beyond the outlets did generally increase and was, for example, approximately 140 after 13,000 ft and 3.7 hr of travel. From data such as this it was determined that the decline

³⁰ "Report of the Special Commission on the Investigation of the Discharge of Sewage into Boston Harbor," House No. 1600, Mass. Dept. of Public Health, Boston, Mass., December, 1936.

³¹ "Appendix A, Methods of Analysis of the Performance of Ocean Outfall Diffusers With Application of the Proposed Hyperion Outfall, April 3, 1956," by Norman H. Brooks, in "Hyperion Engineers Report Relating to Length of Outfall and Types of Diffusers for the Ocean Outfall for Effluent Disposal, April 6, 1956," Hyperion Engineers, A Joint Venture, Los Angeles, Calif.

rate of sewage bacteria attributable to all causes except turbulent diffusion was approximately 4.4 hr for 90% decline. The over-all decline rate of sewage bacteria including the dilution effect was determined graphically from the bacterial data as about 2 hr for 90% decline. Thus the nondilution effects were responsible for approximately 55% of the over-all bacterial decline, since

$$\frac{1}{2} = \frac{1}{4.4} + \frac{1}{3.66}$$

and

$$\frac{1}{3.66} \times \frac{1}{(1/2)} = 55\%$$

or dilution effects and nondilution effects following initial discharge were approximately equivalent in causing bacterial decline.

For Deer Island Outfall, Moon Island Outfall, and Nut Island Outfalls in Boston Harbor, a substantial portion of the dissipation of the field was vertically downward by the sedimentation of the heavier particles of suspended solids, accompanied by many bacteria associated with particulate matter. This is attested both by the results of subsurface water sampling carried on in some of the studies and by the high bacterial concentrations found in the bottom muds of the harbor.

A fairly striking example of the effects of sedimentation appeared in recent offshore studies²² made over the Orange County Sanitation Districts Outfall. This is a 78-in.-diameter pipe extending approximately 7,000 ft into the Pacific Ocean and terminating at a bottom depth of about 55 ft in a small diffuser yielding an initial dilution of about 26. Observations of coliform densities were taken in depth in the vicinity of the outfall on four separate cruises in the autumn of 1955. It was noted that as one moved away from the outfall outlets, the surface coliform densities declined but that beneath the surface a zone of higher coliform density developed and extended outward like a "tongue" before diminishing. Chlorinities and temperatures were also determined and showed that the sewage-sea water mixture remained near the surface above this subsurface tongue which was entirely within water characteristic of the normal sea water in the area.

The generalized pattern of these observations is shown in the bacterial profile of Fig. 9. The general configuration of the coliform contours showed a coliform density in profile which subsided roughly at a slope of 10 ft vertical depth per 600 ft or 700 ft horizontal distance or, at an average current of 1000 ft per hr, at a rate of approximately 13 ft per hr. The over-all decline rate of coliform organisms at the surface may be approximated by noting the distance from the outlets required per magnitude (90%) reduction in coliform density and applying the average current of 1000 ft per hr. When this is done it can be seen that values of *T*-90, after an initial value of about 2.0 hr, tend to average 1.3 hr or 1.4 hr. This is close to the 1.5 hr over-all average depicted in the author's Fig. 4.

²² "The Distribution of Coliform Bacteria in the Waters Surrounding the Orange County Sewer Outfall," The Allan Hancock Foundation, Univ. of Southern California, Los Angeles, Calif., March 2, 1956.

The subsurface coliform decline rate, slanting downward from the surface above the outlets and following the subsurface tongue, proceeds much slower than the surface rate. Initially it is in the order of 3.3 hr per magnitude, speeding up appreciably after about 3.3 hr have elapsed. Because the physical and chemical characteristics of these subsurface waters were nonsewage in nature, it could be inferred that a substantial portion of the coliform population present was associated with particulate matter that settled out of the surface layer of diluted sewage.

The profiles represented in Fig. 9 were run generally parallel to the coastline, and, hence, sedimentation of particulate matter and bacteria was not ultimately impeded by surf conditions as in the generalized case described by the author for Santa Monica Bay. The data of Fig. 9 and those of individual cruises characteristically showed coliform sedimentation. It is of interest to note that the primary effluent discharged from this outfall originates at two treatment plants where the primary sedimentation overflow rate was in the order of 800 and 2200 gal per day per sq ft, respectively, or 1500 gal per day per sq ft on the average corresponding to 8.3 ft per hr settling rate in fresh water. It might appear that the settling rate of the particulate matter in the primary effluent in the sea water after initial dilution was approximately 13 ft per hr, corresponding to the general slope of those coliform contours closest to the outfall as previously mentioned. However, the factors of dilution and mortality both tend to obscure the true settling rate of the bacteria measured by the concentration of the bacteria themselves. Also of importance in regard to this are these factors: (1) The horizontal currents tend to vary both in magnitude and even in direction as one moves from the surface towards the bottom. Usually the current magnitude decreases with depth and subsurface currents at depth may sometimes be at an appreciable angle to those at the surface. For this reason, the path of a settling particle would probably curve downwards and perhaps even laterally as opposed to the two-dimensional slanting line of a settling particle in an "ideal" settling tank. (2) The settling particles are heterogeneous and there is probably a distribution of settling rates among the various particles. For these reasons it is impossible to isolate the separate elements of sedimentation, dilution, and mortality without resorting to certain generalizations and speculations. The following illustration uses such a premise.

The maximum depth of the sewage field was found by chlorinity measurements to be approximately ten ft. Often the field was much shallower. The physical dilution in this surface water was computed both by chlorinity measurements and Brooks' formula,³¹ and the two methods gave fair agreement. The physical dilutions, S_t , were found to be approximately 1.5 times S_0 (initial dilution) after 1 hr, 2.0 times S_0 after 2 hr, 2.5 times S_0 after 3 hr, 3.5 times S_0 after 4 hr, and 6.0 times S_0 after 6 hr. The chlorinity measurements were from surface samples taken within the sewage field "tagged" by sea-marker dye as it moved away from the outlets. These "dye patch" experiments were made on five separate days, covering a total of 34 samples, and covered intervals of 1 hr, 2 hr, 3 hr, 4 hr, and 6 hr away from the "boil" above the outlets. Coliform determinations were also made and were the basis of the value of the $T-90$ of

1.5 hr referred to by the author. Table 5 summarizes some of these dye patch experiment results as analyzed by the writers.

The values of N_o/N_i in Table 5 expressing over-all effects of coliform reduction measured by coliforms represent geometric means of the individual determinations. Among the values listed, those for 2 hr and 4 hr time have the greatest number of samples and are presumably the most reliable while those for 3 hr and 6 hr have the fewest samples and are probably the least reliable. A statistically significant difference among the $T-90$ values of a given category for differing times would be hard to establish. However, except for the 6th hr the patterns for all categories are quite consistent and show a more rapid reduction of coliform organisms in the first hr by dilution effects, nondilution effects, and over-all causes, than for subsequent hours, particularly the 3 and 4 hr. Therefore, at least a portion of this effect is caused by the phenomenon of sedimentation of the bacteria, the bulk of which would be expected to occur fairly early in the life of the sewage field. It follows that

TABLE 5.—DYE PATCH EXPERIMENTAL DATA,
ORANGE COUNTY, CALIFORNIA

Time, in hours	OVER-ALL EFFECTS BY COLIFORMS			PHYSICAL DILUTION		NONPHYSICAL DILUTION EFFECTS	
	Number of samples	N_o/N_i	$T-90$	S_i/S_o	$T-90_d$	N_o/N_i	$T-90$
(1)	(2)	(3)	(4)	(5)	(6)	(7)	(8)
1	6	5.16	1.40	1.5	5.69	3.44	1.86
2	10	22.0	1.49	2.0	6.67	11.0	1.92
3	4	54.7	1.73	2.5	7.54	21.9	2.24
4	10	187	1.76	3.5	7.36	53.5	2.32
6	4	13,800	1.45	6.0	7.70	2300	1.78

the nonphysical dilution effects for the later hours of life of the field, typically 3 hr and 4 hr (assuming that the 6-hr condition is for some reason nonrepresentative) would represent mortality alone, or $T-90_m$ would be perhaps 2.3 hr.

During the first hr bacteria which have settled out of the stratified sewage field at the median rate will generally have been reduced in volumetric concentration only by the action of dilution and mortality. First-hr dilution accounts for a dilution ratio of 1.5, and this would apparently hold true no matter how fast the bacteria settled, provided they dropped out of the surface field in the first hr, for which there is indication. The assumed mortality rate of 2.3 hr per magnitude corresponds to an "apparent" dilution ratio of 2.7, resulting in an over-all dilution ratio.

$$\frac{N_o}{N_i} = 1.5 \times 2.7 = 4.05$$

This value would represent the concentration of typically settling coliforms after 1 hr as compared to their initial value in the "boil." The surface con-

centration after 1 hr, on the other hand, has received an over-all "apparent" dilution of 5.16 times over the "boil" concentration. Under these approximations and suppositions therefore, first-hr sedimentation would have accounted for

$$\frac{(5.16 - 4.05)}{4.05} = 27.5\%$$

or between 25% and 30% of the over-all first-hr coliform decline.

After the first hr or actual time required for the average settling bacteria to drop out of the sewage field the effect of dilution would be curtailed because of decreasing turbulence. Also, the over-all decline rate would be proportionately slowed down, hence the tendency for the subsurface "tongue" of Fig. 9 to persist.

One point not stressed by the author yet tacitly contained within the presentation is the great effort and expense required to obtain significant sampling data, especially offshore data. The surf sampling program alone has involved thousands of samples each year with concurrent field, laboratory, and statistical work. Offshore sampling requires an oceanographic vessel with navigational and laboratory equipment. Operation of such a vessel is in itself expensive and when the ever-changing waters of the ocean are to be studied to any significant degree, the requirements for time and money are magnified.

A further difficulty in the quest for the all-important data regarding bacterial decline in sea water for areas such as Santa Monica Bay is the inability to perform measurements except under very limited circumstances. This is because the ever-rising standards for water quality for Santa Monica Bay generally preclude the cessation of chlorination of plant effluent for bacterial reduction. As recently as early 1955, the standards in force did not require that the beaches and offshore waters receive full protection during the winter months, and, therefore, chlorination was not practiced during these months except when warm weather was forecast and many bathers were expected. This condition no longer holds and chlorination is practiced continually on a year-round basis with the obvious consequence of preventing plant-scale experiments in decline of unchlorinated effluent in the ocean. During the design of the proposed 5-mile Hyperion Outfall for effluent disposal there were only four occasions for which the chlorination at Hyperion was intentionally interrupted. These intentional interruptions ranged from 10 to 24 hr in duration. One of these occasions was the radioactive tracer experiment of May 22-23, 1956. The radioactive tracer SC-46 was discharged with the effluent and subsequently measured in the sewage field and receiving waters. Special advance permission had to be obtained from state authorities before this experiment could be performed.

The extensive surf sampling experience for Santa Monica Bay augmented the more limited offshore studies in Santa Monica in the vicinity of the Hyperion outfall. These were supplemented by the offshore studies off Whites Point and Orange County in the vicinity of the Los Angeles County Sanitation Districts outfalls and the Orange County Sanitation Districts outfall, alluded to by the author.

DAVID I. H. BARR,²² A. M. ASCE.—In considering the hydraulics of dilution of sewage effluent released offshore, the author divides dilution subsequent to that caused by diffusers into two separate phenomena—turbulent mixing due to density variations, and lateral mixing due to eddy diffusion. Both the terminology and the tentative assumption seem to require further consideration.

Since the term eddy diffusion is intended to describe the process analogous to diffusion due to turbulent mixing, in which separation between the vertical and lateral coefficient of diffusivity has been noted as being largely due to density stratification,⁷ it is not obvious why turbulent mixing and lateral mixing are separated in the paper.

Regarding the dilution process, it would seem more correct to say that dilution is caused by the two phenomena, density currents and turbulent mixing. Considering the details given of dilution at the existing Hyperion outfall, local horizontal variations in density would give rise to irregular mass-transferring density currents superimposed on the general bay current and causing turbulence over and above the general turbulence. The level of turbulence would appear to affect the dilution and thus the depth of the density layer, whether on the surface or at intermediate depth, rather than its extent. Subsequent to the disappearance of local density differences, density difference would appear to have a continuing effect on the spread of the contaminated zone. The average ratio of spread on one side of the test dye streams to the travel length is approximately 1 to 30 and for the isolated maximum the ratio is approximately 1 to 11.

However in Fig. 1, when one side of the sewage effluent zone is bounded by the shore, the ratio of spread to travel length of the other side is approximately 1 to 6. If the density of the sewage effluent approximates that of fresh water, as compared with sea water, the dilution of 1 part per 314 parts sea water, given as typical after 24 hr, would cause a density difference of approximately 0.00009 g per ml. Although small, this could cause a spread of several thousand ft in 24 hr starting from stratified area of a few feet in depth. Precise figures of densities and details of local conditions are not available to the writer, but the author's comments on this hypothesis would be of interest. The mechanics of lateral spread of nonhomogeneous water with a slight density difference for both the case where a nonhomogeneous stream is moving with the main body of water and for the case where it is moving through the main body of water do not appear to be fully investigated.

CHARLES G. GUNNERSON,²⁴ A.M. ASCE.—Messrs. Lawrance and Miller point out that the rate of reduction of coliforms is lower in subsurface waters. This is reasonable because some of the factors in the mortality of the bacteria, particularly sunlight, are more effective at the surface. The decreasing rate of reduction (or increasing persistence) continues after the solids have been deposited on the bottom where dilution and sedimentation are no longer operative, and mortality is significantly different. Rittenberg et al.,²⁵ have pointed

²² Research Student, Royal College of Science and Technology, Glasgow, Scotland.

²⁴ Civ. Eng. Bureau of Sanitation, Dept. of Public Works, Los Angeles, Calif.

²⁵ "Coliform Bacteria in Sediments around Three Marine Sewage Outfalls," by S. C. Rittenberg, Tod Mittler, and Daniel Ivler, *Limnology and Oceanography*, Vol. 3, No. 1, 1958, pp. 101-108.

out that the coliform populations per unit area on the bottom are greater than those contained in the overlying water at any one time, and that

"the coliforms must survive for a sufficiently long period of time in the sediments to allow large populations to be built up by deposition"

As a result, bottom populations measured in tens of thousands per square centimeter may be found near the Orange County outfall where the overlying waters contain less than 10 coliforms per ml.

It is possible to make a first approximation of the survival time in the sediments by considering the total daily discharge of coliforms and that part that settles with the solids, the rate of solids accretion assuming general similarity with the Hyperion sludge studies made by Brooks³⁶, the general ocean current pattern, and the steady-state requirements for maintaining the observed bottom coliform populations assuming, as did Rittenberg, no multiplication in the sediments. Such an analysis suggests a *T*-90 in the sediments around the Orange County outfall measured in months.

Mr. Barr suggests that further work on the mechanics of effluent dilution in sea water is desirable. The need for such additional experimental and analytical study is apparent to anyone who is concerned with waste discharges into any body of water. It is recognized that the terminology employed to describe dilution processes at Hyperion is imperfect—it simply calls attention to the observed dilutions in time and space which seem to require more than one diffusion phenomenon. Additional field work will undoubtedly refine the data presented earlier and may ultimately permit a rigorous analysis.

In any event, the major objective in studying dilution of Hyperion effluent is to evaluate the bacterial decline rates, and the effect of dilution has been computed. Variation of the computed dilution effect within any reasonable limits will not change the primary conclusion that sedimentation is always important, and may be the predominating factor in reduction of coliform populations in surface waters.

The available data do not permit a complete analysis of the effect of sea state on dilution. The observations on which the bacteriological studies were based required suspension of effluent chlorination. Such interruptions were of necessity held to an absolute minimum for public health reasons. However, the sea state varied from calm to a heavy chop for the various series of tests, and no significant difference in the behavior of the effluent field was found. This is in good agreement with observations of the chlorinated effluent field which have been made weekly since July, 1956. These indicate that the prevailing current controls the configuration of the field, and that variations in surface wave conditions have a negligible effect.

³⁶ "Prediction of Sedimentation and Dilution of Digested Sludge in Santa Monica Bay," Report to Hyperion Engineers, August, 1956.

AMERICAN SOCIETY OF CIVIL ENGINEERS

Founded November 5, 1852

TRANSACTIONS

Paper No. 3003

WAVE RUN-UP ON ROUGHENED AND PERMEABLE SLOPES

BY RUDOLPH P. SAVAGE¹

SYNOPSIS

Laboratory tests determining run-up on various beach slopes as a result of wave action are described. Curves relating the run-up to wave steepness, beach slope, slope roughness, and slope permeability are presented.

INTRODUCTION

Wave run-up is defined as the vertical height of the limit of uprush reached by a wave breaking on a slope, using the still-water level as a reference. Run-up is important because it determines the height to which certain structures must be built in order to prevent overtopping from waves and thus eliminate flooding landward of the structures. Artificial sand fills are used extensively for shore protection and beach restoration, and wave run-up is of significance in determining the design berm elevation of these sand fills.

Until recently, few run-up data were available for design purposes. In 1953, Kenneth N. Grantham² published data on run-up on smooth and permeable slopes of 15°, 30°, and 45°. In 1958 Thorndike Saville, Jr.,³ A. M. ASCE, presented data on run-up on a wide range of smooth continuous slopes and smooth composite slopes, and data on run-up on a 1-on-1½ riprap-faced slope. However, only a few of the foregoing data deal with the effect of slope roughness on wave run-up, and the data on the effect of slope permeability are confined to a narrow range of slopes. Presented herein are the results of wave run-up tests made on smooth, roughened, and permeable slopes ranging from a relatively gentle 1-on-30 slope to a vertical wall.

NOTE.—Published, essentially as printed here, in May, 1958, in the *Journal of the Waterways and Harbors Division*, as *Proceedings Paper 1640*. Positions and titles given are those in effect when the paper was approved for publication in *Transactions*.

¹ Hydr. Engr., Research Div., Beach Erosion Board, Corps of Engrs., U. S. Dept. of the Army, Washington, D. C.

² "Wave Run-up on Sloping Structures," by Kenneth N. Grantham, *Transactions, Am. Geophysical Union*, Vol. 34, No. 5, 1953, pp. 720-724.

³ "Wave Run-up On Shore Structures," by Thorndike Saville, Jr., *Transactions, ASCE*, Vol. 123, 1958, pp. 139-150.

TEST FACILITIES

Notation.—The letter symbols adopted for use in this paper are defined where they first appear, in the illustrations or in the text, and are arranged alphabetically, for convenience of reference, in the Appendix.

General.—The experimental apparatus used in the tests is shown in Fig. 1. The vertical height of wave run-up above the still-water level is represented by R , in feet; along the face of the slope, the distance that the waves surged up is

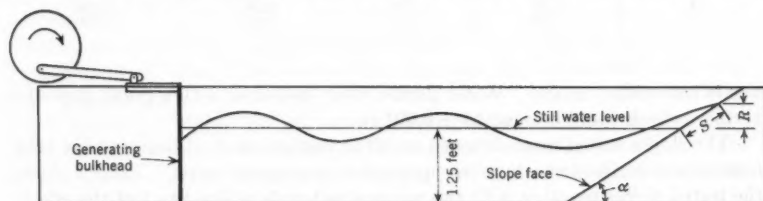


FIG. 1.—APPARATUS FOR WAVE RUN-UP TESTS

indicated by S , in feet; and α is the angle, between the face of the slope and the horizontal, in degrees. The wave tank shown is 96 ft long, 2 ft deep, and $1\frac{1}{2}$ ft wide. The wave generator is a vertical-bulkhead, push-pull type of generator, attached eccentrically by a connecting arm to a driving disk 2 ft in diameter. The disk is driven through a varidrive unit by a $2\frac{1}{2}$ -hp electric motor. The wave period was changed by varying the gear ratio of the varidrive unit, enabling the generation of a continuous range of wave periods of from 0.5 sec to 5 sec. The wave height was changed by varying the eccentricity of the connect-

TABLE 1.—SLOPES AND MATERIALS TESTED ^a

Beach-material size, in milli- meters	ROUGHENED SLOPES								PERMEABLE SLOPES									
	1 on 30	1 on 10	1 on 6	1 on 4	1 on 2½	1 on 1½	1 on 1	1 on ½	Vertical	1 on 30 ^b	1 on 10	1 on 6	1 on 4	1 on 2½	1 on 1½	1 on 1	1 on ½	Vertical
Smooth	x	x	x	x	x	x	x	x	x	x	x	x	x	x	x	x	x	x
0.2	x	x	x	x	x	x	x	x	x	x	x	x	x	x	x	x	x	x
1.0	x	x	x	x	x	x	x	x	x	x	x	x	x	x	x	x	x	x
2.0	x	x	x	x	x	x	x	x	x	x	x	x	x	x	x	x	x	x
3.5	x	x	x	x	x	x	x	x	x	x	x	x	x	x	x	x	x	x
10.0	x	x	x	x	x	x	x	x	x	x	x	x	x	x	x	x	x	x

^a Slopes tested indicated by x. ^b 5-in. layer of beach material (except 0.2 mm and 10.0 mm).

ing arm on the driven disk. Thus, a continuous range of wave heights could be generated, varying from small heights (of on the order of 0.001 ft) to the greatest stable height for any particular water depth and wave period. The wave periods and heights actually used in these tests are shown in Table 3.

Wave heights were measured with parallel-wire resistance wave gages⁴ and were recorded on an oscillograph. The accuracy of individual height measure-

⁴ "Measurement of Heights by Resistance Elements," by J. R. Morrison, Technical Report HE-166-313, Univ. of California, Berkeley, Calif., June, 1950.

TABLE 2.—CHARACTERISTICS OF MATERIALS USED FOR ROUGHNESS AND PERMEABILITY

Curve (1)	<i>d</i> , in mm (2)	<i>C_s</i> (3)	<i>C_k</i> (4)	<i>k</i> , in square feet ×10 ⁻³ (5)
1	0.22	1.14	1.06	0.033
2	0.97	1.06	0.99	0.420
3	1.96	1.03	0.99	1.380
4	3.53	1.52	0.94	1.490
5	9.90	1.33	0.93	14.100

ments was within $\pm 5\%$. Water depths were measured with a point gage and vernier, which could be read to ± 0.001 ft.

The slopes tested ranged from 1 on 30 to vertical, and all began at the tank bottom and inclined continuously upward on a constant slope. Table 1 shows the tested slopes together with the various materials utilized to test the effects of roughness and permeability. The smooth slopes used were constructed of plywood except for the 1-on-10 slope and 1-on-30 slope, which were constructed with a base of fine sand covered with a $\frac{1}{2}$ -in. smooth-concrete layer. The effect of roughness was tested by gluing a single layer of material to the smooth slopes. The effect of permeability was tested on slopes composed entirely of the material to be tested.

Table 2 indicates the characteristics of the materials, including the coefficient of sorting, C_s , and the coefficient of skewness,⁵ C_k , as determined from standard

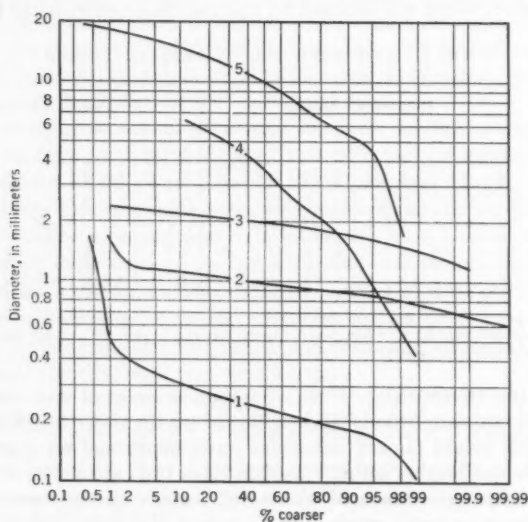


FIG. 2.—DIAMETER VERSUS PERCENTAGE COARSER

sieve analyses and permeability tests.⁶ The permeability, k , is in square feet (a darcy = 1.0624×10^{-11} sq ft) and d represents the median diameter, in mm. The curves in Fig. 2 show the diameter versus percentage coarser. The 0.2-mm sand (curve 1) was a typical fine beach sand. The 1.0-mm and 2.0-mm sands (curves 2 and 3) were well-sorted sands obtained by sieving out the particles finer or coarser than those near the median diameter. The 3.5-mm material (curve 4) was a poorly sorted, well-rounded pea gravel, and the 10.0-mm material (curve 5) was a typical crushed stone commonly used as an aggregate in concrete.

TEST PROCEDURE

In general, the procedure involved placing a test slope in the end of the wave tank opposite the generator and propagating waves of known characteristics against the slope. The first few waves were ignored, and the run-up for the next six to fifteen waves was measured by reading the run-up visually for each wave on a scale marked on the face of the slope in hundredths of a foot of verti-

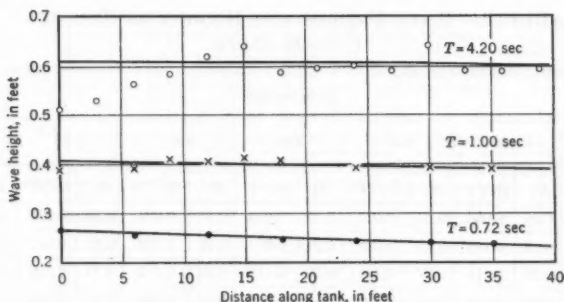


FIG. 3.—WAVE HEIGHT VERSUS DISTANCE ALONG TANK

cal elevation. Run-up measurements were stopped before reflections from the beach could travel to the generator and back to the beach. The average of the individual run-up readings was taken as representative of that run.

A constant water depth of 1.25 ft was used in all the tests. Saville³ showed that varying the water depth at the toe of the structure has a negligible effect on the relative wave run-up when the water depth at the toe of the structure is on the order of three times the deepwater wave height or greater.

The wave characteristics were determined by calibrating the wave generator for the 1.25-ft water depth. The wave generator was calibrated by placing a wave absorber in the beach end of the tank and by producing a wave train with known and reproducible settings on the generator eccentric and varidrive. The average height of the generated wave train was measured with a parallel-wire gate at 6-ft intervals along the tank beginning near the generator. This procedure was repeated for each combination of wave heights and periods used. The heights then were plotted (Fig. 3), versus the distance along the tank and

³ "Sedimentary Rocks," by F. J. Pettyjohn, Harper & Brothers, New York, N. Y., 1940, pp. 22-25.

⁶ "Symposium on Permeability of Soils," *Special Technical Publication No. 163*, A.S.T.M., April, 1955.

a smooth curve was drawn through these points. The wave period is represented by T , in seconds. The wave-height value obtained from the smooth curve at a distance coinciding with the toe of the test slope then was used as the value for that particular generator setting and test slope. In this manner, wave heights were determined for all wave and test-slope conditions. The wave heights at the toe of the 1-on-30 slope for each of the seven wave periods are shown in Table 3. The wave heights for the steeper slopes are slightly smaller than those shown in Fig. 3 because the steeper slopes were shorter. Thus, a longer decay distance was provided before the waves reached the toe of the slope. With the known wave heights, water depth, and wave periods, the other needed wave characteristics were computed, using shallow-water theory.

After the wave characteristics had been determined, the slope to be tested was constructed in the beach end of the wave tank. The smooth surface was tested with the wave conditions generated by the previously calibrated settings on the wave generator. Then the surface of the slope was roughened by being

TABLE 3.—WAVE PERIODS AND HEIGHTS AT TOE OF
1-ON-30 SLOPE

<i>T</i> , in seconds													
0.72		1.00		1.55		1.82		2.63		3.65		4.70	
<i>H</i> '	<i>H</i> '/ <i>T</i> ²	<i>H</i> '	<i>H</i> '/ <i>T</i> ²	<i>H</i> '	<i>H</i> '/ <i>T</i> ²	<i>H</i> '	<i>H</i> '/ <i>T</i> ²	<i>H</i> '	<i>H</i> '/ <i>T</i> ²	<i>H</i> '	<i>H</i> '/ <i>T</i> ²	<i>H</i> '	<i>H</i> '/ <i>T</i> ²
0.07	0.14	0.05	0.054	0.03	0.013	0.05	0.015	0.03	0.004	0.10	0.006	0.08	0.0026
0.17	0.33	0.10	0.108	0.13	0.058	0.21	0.064	0.07	0.009	0.21	0.013	0.18	0.0057
0.21	0.41	0.20	0.215	0.27	0.121	0.39	0.118	0.24	0.032	0.33	0.020	0.30	0.0097
0.26	0.51	0.30	0.322	0.42	0.188	0.46	0.139	0.44	0.058	0.46	0.028	0.45	0.016
		0.40	0.410	0.56	0.250	0.59	0.178	0.61	0.081	0.60	0.036	0.60	0.019

painted with a water-resistant glue, which was spread with a roughness material. After the glue was dry the excess roughness material was swept away, leaving a single layer approximately one diameter deep over the face of the slope. This roughened surface was tested with the same wave conditions that were used on the smooth slope. The first roughness material was removed, and another was applied and tested until each slope had been tested with different materials as shown in Table 1.

The permeable slopes were tested similarly and were composed entirely of the material to be tested except for the 1.0-mm, 2.0-mm and 3.5-mm material on the 1-on-30 slope. Enough of these materials was not available to construct a 1-on-30 slope, and, consequently, only a 5-in. layer was used over the surface of the 1-on-30 smooth slope. It was felt that this would have essentially the same effect on the wave run-up as a 1-on-30 slope constructed entirely of these materials. In order to check the foregoing, the 10.0-mm material was tested, using both a 5-in. layer of permeable material over the smooth 1-on-30 slope and a 1-on-30 slope constructed entirely of the 10.0-mm material. The results of

the tests are shown in Fig. 4. The relative run-up, R/H_0' , is plotted against a function of the deep water wave steepness, H_0'/T^2 , for both a 5-in. layer of the 10.0-mm material and the slope composed entirely of the 10.0-mm material. The deepwater wave height is shown by H_0' , in feet. Although the difference in results is small, it is significant. However, because the 10.0-mm material is approximately ten times as permeable as the 3.5-mm material (14×10^{-8} sq ft compared with 1.5×10^{-8} sq ft), it is believed that the results of the tests with 5-in. layer of the smaller materials did not vary significantly from what they would have been, had a complete slope of these materials been tested.

Essentially the same problem arose with the steep permeable slopes. That is, what length of permeable structure would be required in front of the back wall of the wave tank for a 1-on- $\frac{1}{2}$ slope or vertical permeable wall to assure that the wave run-up would not be a function of the length of the permeable structure as well as the other parameters involved. Several check tests were made, and it was found that for the material having the greatest permeability

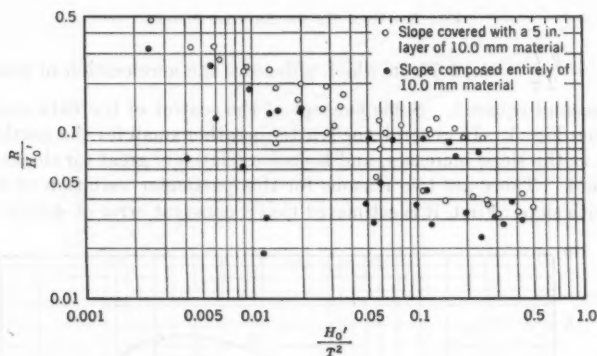


FIG. 4.—RELATIVE WAVE RUN-UP

(the 10.0-mm material), a 3-ft structure length behaved as a structure of infinite length. Therefore, all the permeable slopes steeper than 1 on 6 contained enough material to fill the first 3 ft immediately in front of the rear tank wall. The test slope slanted downward from a point 3 ft in front of the rear tank wall.

The materials in some of the permeability tests would not stand on the steep angle required for the steeper slopes, especially under the agitating wave action. This difficulty was overcome by holding the face of the test slope in place with a wire screen having a mesh slightly smaller than the diameter of the material.

EXPERIMENTAL RESULTS

The data from the smooth-slope tests were plotted as shown in Fig. 5. This form is a dimensionless plot of R/H_0' versus H_0'/T^2 . Actually, $H_0'/T^2 = 5.12 H_0'/\lambda$ (the deepwater wave steepness) because the deepwater wave length,

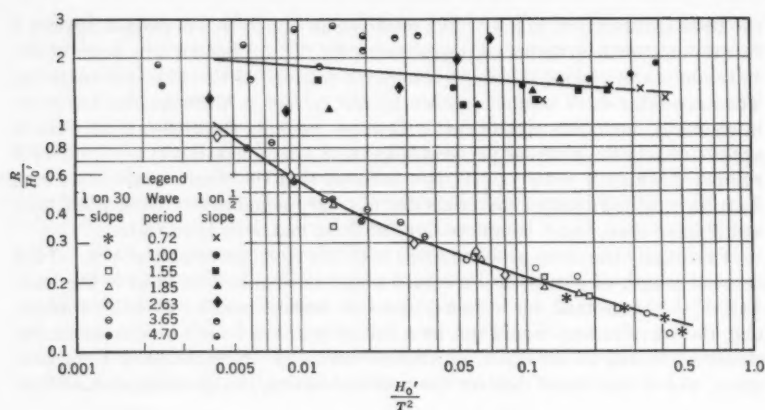
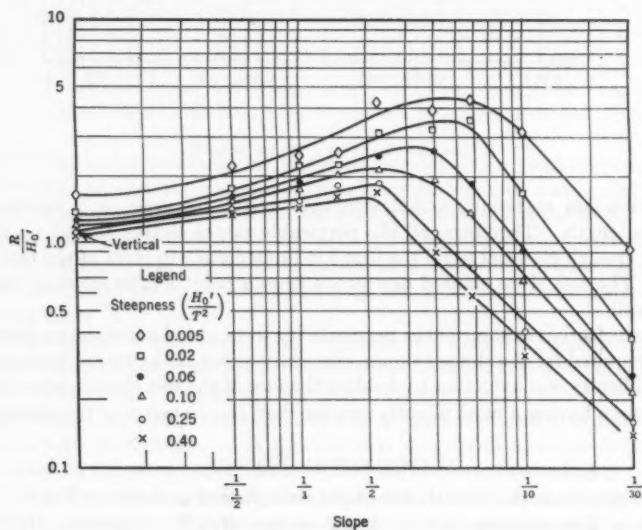


FIG. 5.—RUN-UP ON SMOOTH SLOPES

in feet, $\lambda = \frac{g T^2}{2\pi} = 5.12 T^2$, in which g denotes the acceleration of gravity, in feet per second squared. Some concept of the scatter of the data can be obtained from Fig. 5. In general, the scatter is rather small for the gentle slopes, increases as the slope increases, and becomes relatively great for slopes steeper than 1 on 4. There are two reasons for this particular variation of the data scatter with slope: First, it is estimated that a constant error of ± 0.05 ft could

FIG. 6.— R/H_0' VERSUS SLOPE

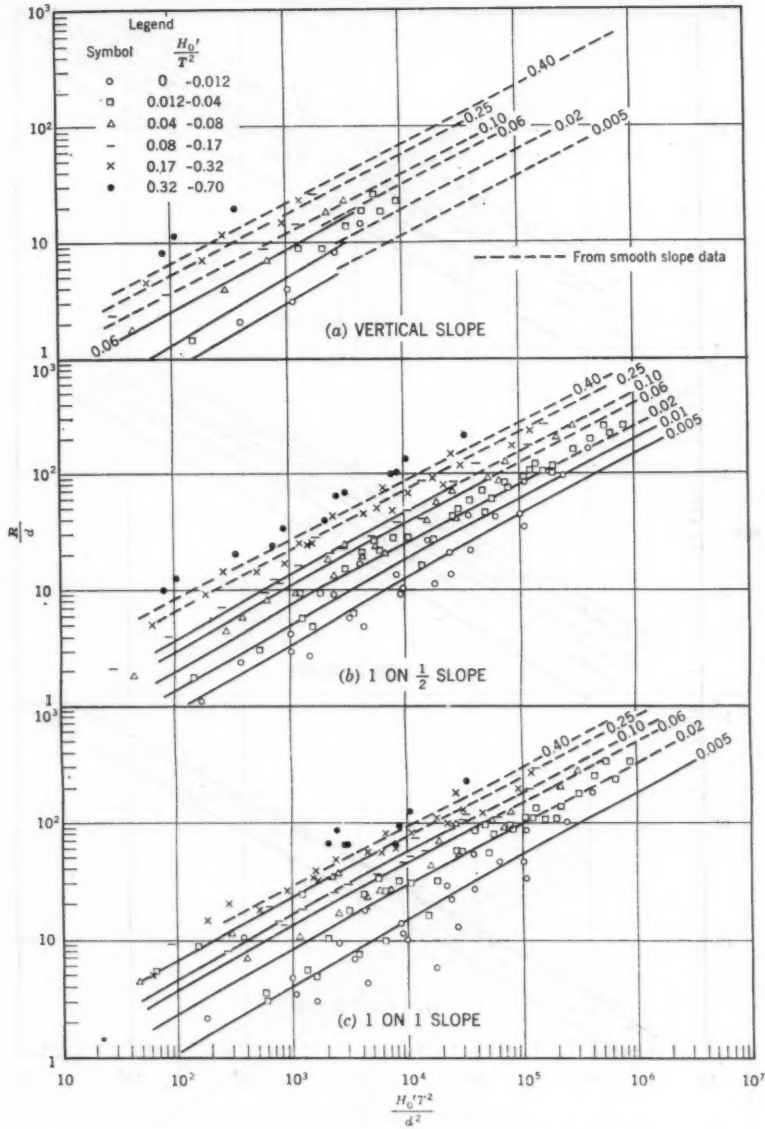


FIG. 7.—WAVE RUN-UP ON SLOPES ROUGHENED WITH A LAYER OF SAND OR GRAVEL

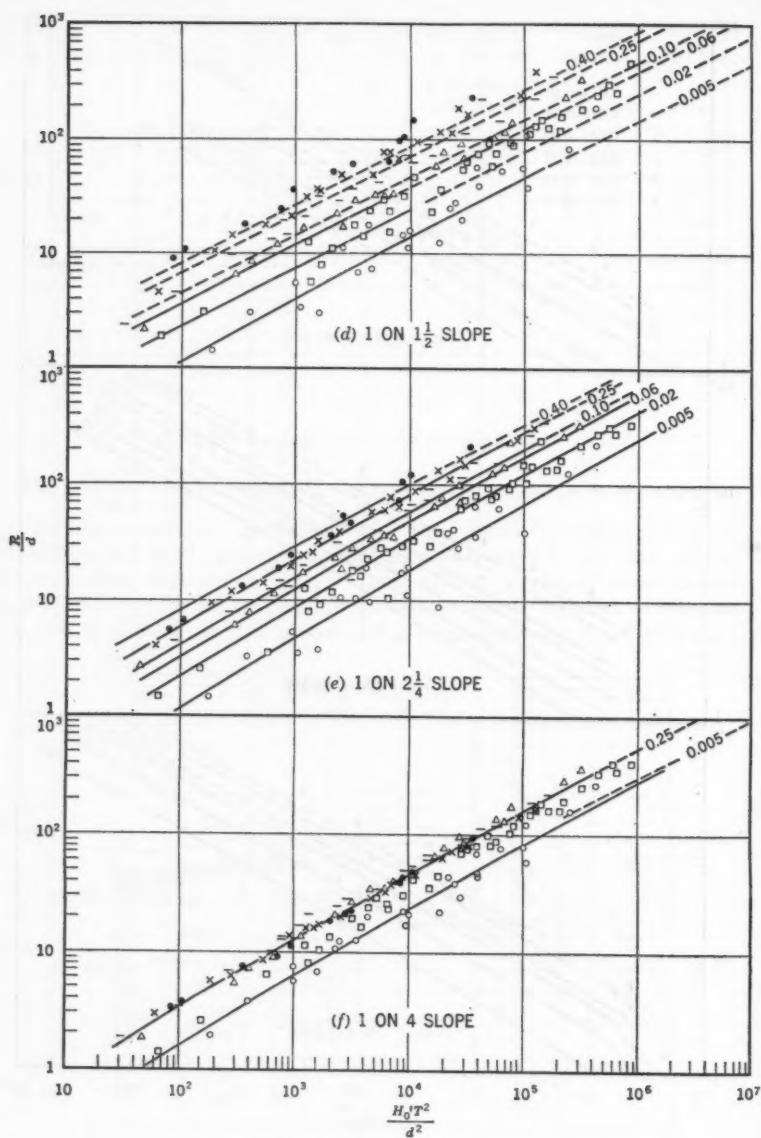


FIG. 7.—Cont.

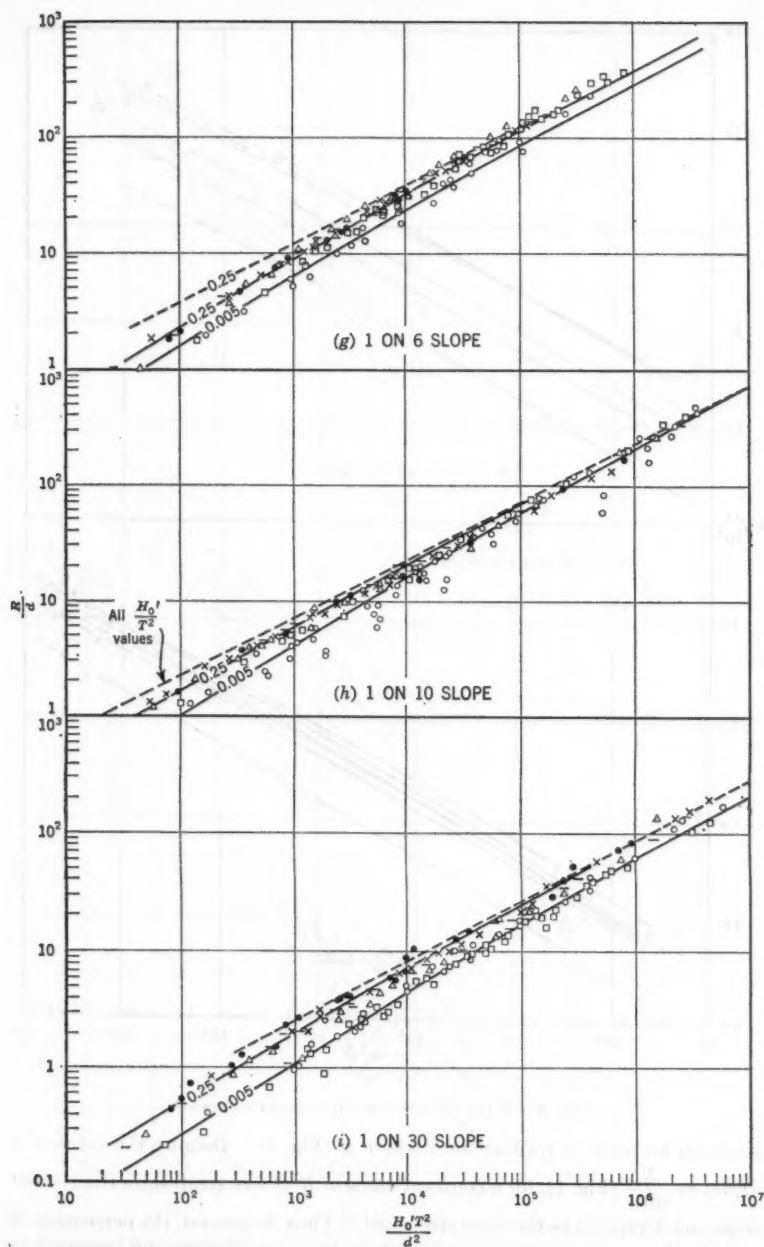


FIG. 7.—Cont.

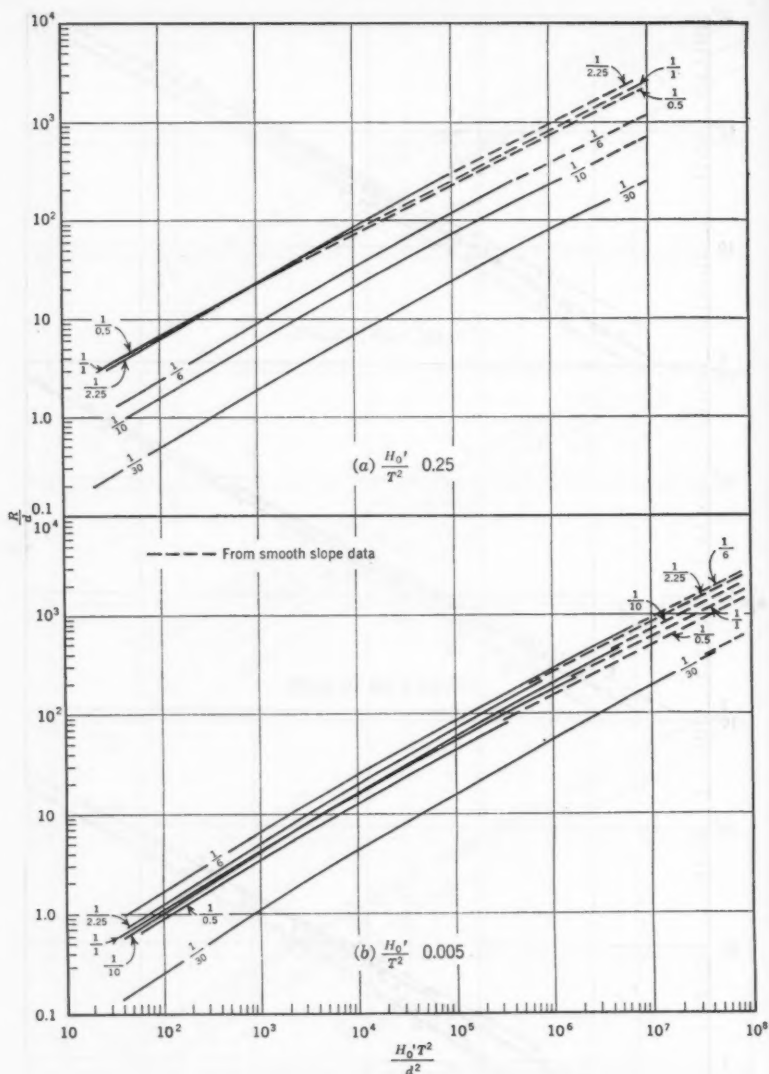


FIG. 8.—WAVE RUN-UP ON ROUGHENED SLOPES

probably be made in reading the value of S (Fig. 1). Because the value of S varies as $\frac{R}{\sin \alpha}$ (Fig. 1), for a constant value of R , S was greatest on the 1-on-30 slope and decreased as the slope steepened. Thus, in general, the percentage of error in the run-up readings was lowest for the 1-on-30 slope and increased as

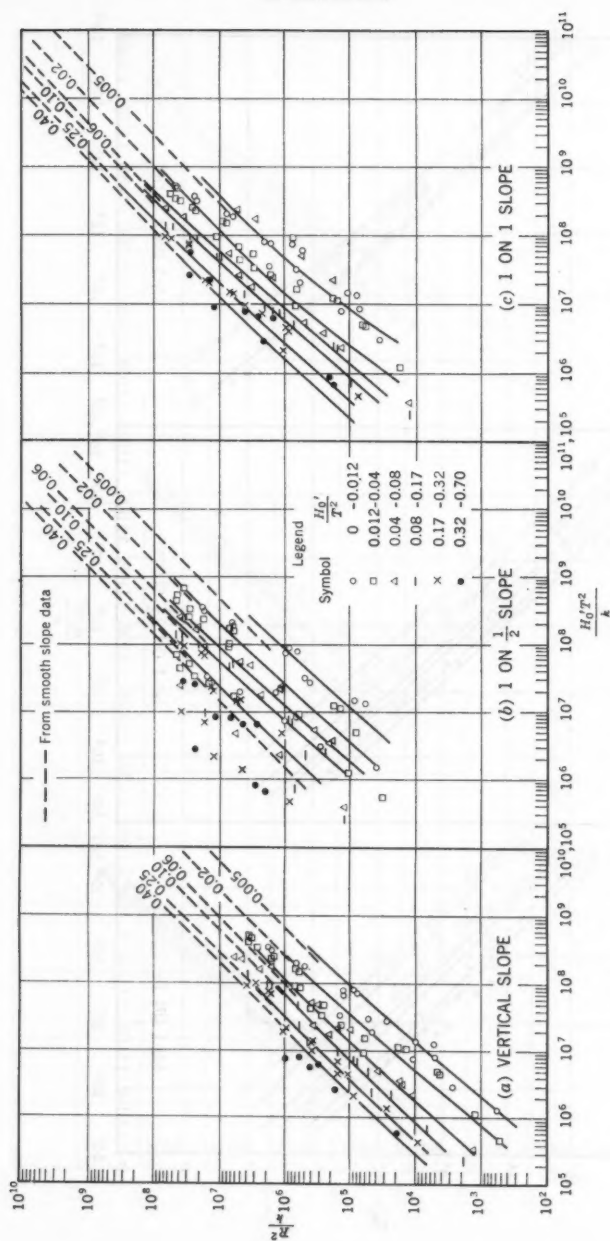


FIG. 9.—EFFECT OF SLOPE PERMEABILITY ON WAVE RUN-UP FOR VARIOUS SLOPES

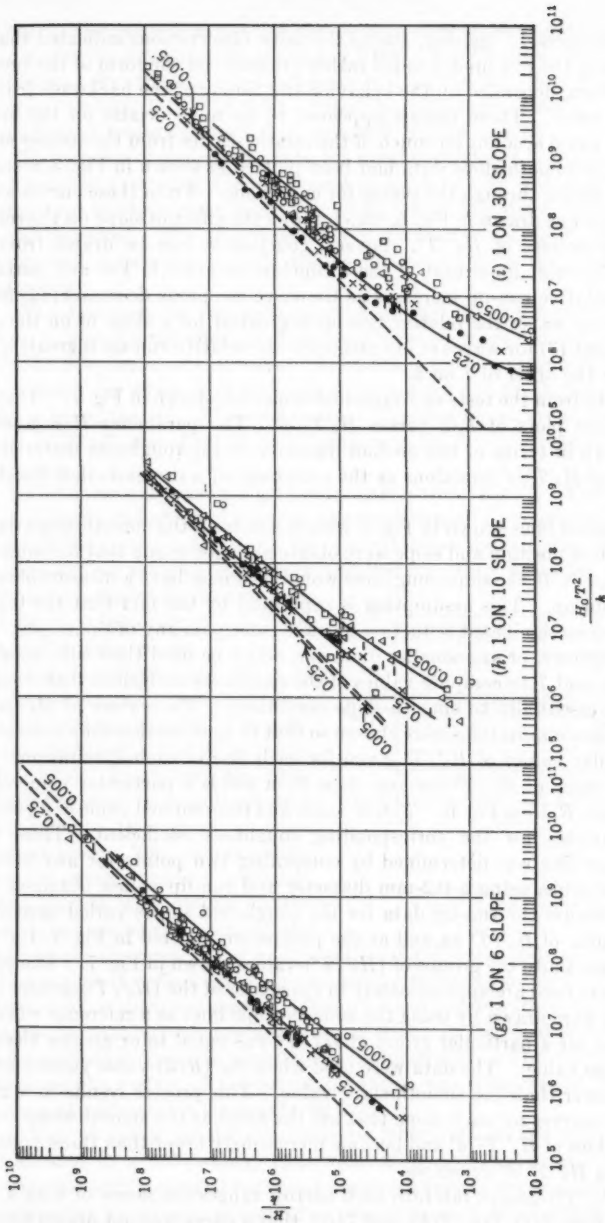


FIG. 9.—Cont.

the slope steepened. Second, during the tests, observations indicated that the magnitude of the run-up depended rather critically on the form of the breaker, which, in turn, depended on the behavior and timing of the backwash from the preceding wave. These factors appeared to be more erratic on the steeper slopes and could account for much of the erratic scatter from the steeper slopes.

After the smooth-slope data had been plotted as shown in Fig. 5, a smooth curve was drawn through the points for each slope. From these curves a composite graph was drawn in Fig. 6, which shows the effect of slope on the relative run-up for isolines of H_o'/T^2 . Several conclusions can be drawn from this graph. The most important of these conclusions are: (1) For any particular slope the relative run-up increases as the wave steepness decreases; (2) for extremely steep waves the relative run-up is greatest for a slope of on the order of 1 on 2; and (3) for waves of low steepness the relative run-up is greatest for a slope of on the order of 1 on 5.

The data from the tests on roughened slopes are shown in Fig. 7. These are dimensionless plots of R/d versus $H_o'T^2/d^2$. The parameter R/d gives the wave run-up in terms of the median diameter of the roughness material, and the value of $H_o'T^2/d^2$ functions as the reciprocal of a dimensionless roughness coefficient.

The dashed lines shown in Fig. 7 were taken from the smooth-slope data in Fig. 6. Their position and slope were obtained by assuming that for some high value of $H_o'T^2/d^2$, the slope roughness would no longer have a measurable effect on wave run-up. This assumption is supported by the fact that the 0.2-mm sand caused no significant reduction in wave run-up on any of the slopes. The 0.2-mm diameter, or any smaller diameter, could be used then with combinations of H_o' and T to compute values of the roughness coefficient that would be equivalent essentially to smooth-slope conditions. The values of H_o' and T used in these computations were chosen so that in combination they represented the particular values of H_o'/T^2 given for each line in each illustration. The particular value of H_o'/T^2 for any slope then yields a particular value of the smooth slope, R , from Fig. 6. This R -value and the assumed value of d yield the (R/d) -parameter for the corresponding roughness coefficient. Thus, each smooth-slope line was determined by computing two points for any value of H_o'/T^2 and slope, using a 0.2-mm diameter and run-up values obtained from Fig. 6. Because the run-up data for the roughened slopes varied apparently with the value of H_o'/T^2 as well as the parameters plotted in Fig. 7, the data were separated into the groups of (H_o'/T^2) -values shown in Fig. 7. The values for the curves used are approximately in the center of the (H_o'/T^2) -groups used. The curves were drawn by using the smooth-slope lines as a reference when the (R/d) -value for a particular group of H_o'/T^2 was equal to or greater than the smooth-slope value. The data were used when the (R/d) -value yielded by the data was lower than the smooth-slope value. This process results in a group of (H_o'/T^2) -curves for each slope that are the same as the smooth-slope curves for high values of $H_o'T^2/d^2$ and become increasingly lower than those values as the value of $H_o'T^2/d^2$ decreases.

The (H_o'/T^2) -groups fall into such narrow ranges for slopes of 1 on 4, and shallower (Figs. 7(f), 7(g), 7(h), and 7(i)), that a curve was not drawn for each

group. The plotted points are shown according to their group, but only the curves for the 0.25 (H_0'/T)-group and 0.005 (H_0'/T^2)-group are indicated. It is believed that the 0.25-curve adequately describes the effect of high-steepness waves, in which $H_0'/T^2 \geq 0.02$. Also, the 0.005-curve satisfactorily describes the effect of low-steepness waves, in which $H_0'/T^2 < 0.02$.

The scatter of the run-up data for roughened slopes is subject to the same factors cited previously for the smooth-slope data. In addition, the run-up on roughened slopes became more difficult to read as the size of the roughness material increased. For this reason the data scatter should be greater for the roughened slopes, particularly the conditions utilizing the greater roughness materials.

The data from the run-up tests on roughened slopes shown in Fig. 7 indicate that, in general, the effect of slope roughness on wave run-up increases as the ($H_0'T^2/d^2$)-parameter decreases. In addition, for a constant value of $H_0'T^2/d^2$ and slope, the effect of slope roughness on wave run-up increases as the wave steepness or the (H_0'/T^2)-value decreases. Also, for values of constant H_0'/T^2 and $H_0'T^2/d^2$, the effect of slope roughness on run-up decreases as the slope steepens.

The curves shown in Fig. 8 were taken from Fig. 7. They demonstrate more clearly the effect of slope on the wave run-up on roughened slopes. The dashed lines were taken from the smooth-slope data in Fig. 6. Again it is apparent that the greatest run-up occurred on a slope of on the order of 1 on 6 for low-steepness waves and on a slope of on the order of 1 on 2 for high-steepness waves.

Fig. 9 indicates the effect of slope permeability on wave run-up for the various slopes. These are dimensionless plots of R^2/k versus $H_0'T^2/k$. In general, the plots have the same form as those used to indicate the effect of slope roughness. The smooth-slope curves were obtained similarly. The curves were drawn in the same fashion and, in general, the results are the same. The most significant difference between the two sets of data is that the effect of slope permeability on wave run-up is more pronounced than that of slope roughness. This is logical because the data for the effect of slope permeability on wave run-up, as shown in Fig. 9, demonstrate both the effect of slope roughness and slope permeability. The foregoing is correct because the surface of the permeable slopes was composed of the same roughness materials used in the roughness tests.

Fig. 10 compares the smooth-slope laboratory results with run-up values measured in a 635-ft-long, 15-ft-wide, 20-ft-deep wave tank. The latter is equipped with a vertical-bulkhead push-pull type of wave generator capable of generating waves with periods of as long as 16 sec and heights of as much as 6 ft.

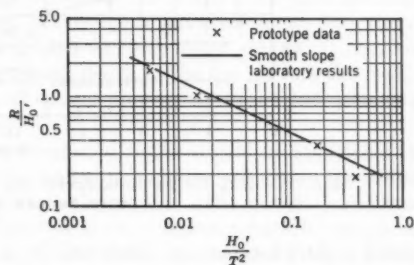


FIG. 10.—PROTOTYPE DATA COMPARED WITH LABORATORY RESULTS

The prototype run-up data shown in Fig. 10 were obtained from an experimental program on the equilibrium profile of beaches conducted in the tank. In the equilibrium-profile tests a wave train of constant period and height was allowed to impinge on an initially constant 1-on-15 sand slope (the 0.2-mm sand described in Fig. 2) until the slope profile had attained its equilibrium shape for that wave train. The run-up measurements were taken at the beginning of each of four tests and represent wave periods ranging from 3.75 sec to 16 sec and heights ranging from 2.0 ft to 5.3 ft. As the lowest $(H_o' T^2/d^2)$ -value for these runs would be approximately 10^7 and the lowest $(H_o' T^2/k)$ -value would be approximately 10^4 , it appears from the results shown in Figs. 8(a), 8(b), 9(h), and 9(i) that the roughness or permeability effects would be negligible. Therefore, the data are compared with the smooth 1-on-15-slope data taken from Fig. 6 and represented in Fig. 10 by the smooth curve. The prototype data indi-

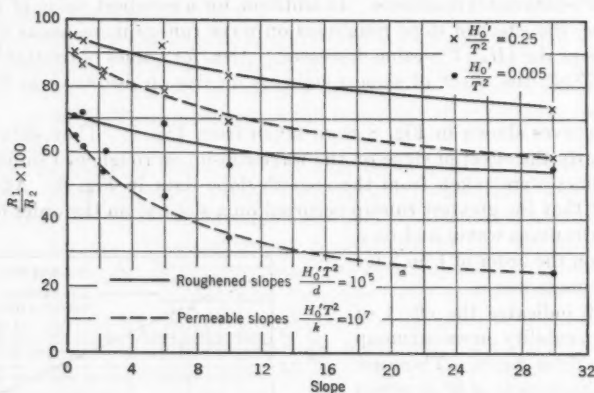


FIG. 11.—RUN-UP ON ROUGHENED AND PERMEABLE SLOPES COMPARED WITH SMOOTH SLOPES

cated slightly less run-up. However, in general, they agree with the smooth-slope laboratory data.

Fig. 11 compares the wave run-up on roughened and permeable slopes, R_1 , with the run-up on smooth slopes, R_2 for comparable slope and (H_o'/T^2) -values. Because the effect of roughness and permeability varies with the values of $H_o' T^2/d^2$ and $H_o' T^2/k$, constant values of $H_o' T^2/d^2 = 10^5$ and $H_o' T^2/k = 10^7$ were chosen for the comparison. The curves in Fig. 11 show that the percentage of reduction in wave run-up varies with the (H_o'/T^2) -value and the slope, decreasing as the (H_o'/T^2) -value increases and the slope steepens.

CONCLUSIONS

The results of the laboratory experiments on smooth structures of constant slope show that the relative wave run-up is a function of the deepwater wave steepness and the structure slope. Also, for a constant structure slope the greatest relative run-up for steep waves occurs on a slope of on the order of 1

on 2, and the greatest relative run-up for low-steepness waves occurs on a slope of on the order of 1 on 5.

The results of the experiments on roughened and permeable structures demonstrate that the run-up is a function of the deepwater wave steepness, the structure slope, and the median diameter of the roughness material for roughened slopes, or of the permeability of the slope material for permeable slopes. For the roughened slopes the run-up, divided by the median diameter of the roughness material, is related to an inverted roughness coefficient of $H_o' T^2/d^2$ for isolines of H_o'/T^2 . For the permeable slopes the run-up squared is related to an inverted permeability coefficient of $H_o' T^2/k$ for isolines of H_o'/T^2 . In both the roughness tests and permeability tests, the effect of the slope roughness or permeability on wave run-up increases as the values of $H_o' T^2/d^2$ or $H_o' T^2/k$ decrease and as the slope flattens.

The data scatter about the various curves is extensive for the steeper smooth slopes and relatively smooth slopes and for all conditions involving the use of the great roughness and permeability materials. However, it is believed that the methods utilized in correlating the run-up with the various parameters are promising. In the future, the accuracy of the data should be increased by testing larger waves with longer periods. Meanwhile, the user should consider the data scatter in the vicinity of the curves used when the results of these tests are applied.

The results are not valid when the water depth at the toe of the slope is less than approximately three wave heights because the relative run-up is affected by the depth at the toe.³ In general, as this depth decreases to less than three wave heights, the relative run-up increases to a maximum value that may be twice the relative run-up for a great water depth at the toe. From the maximum value the relative run-up decreases as the depth at the toe decreases further.

The test results on smooth and roughened slopes should be applicable to prototype conditions when the dimensionless parameters are within the range of the dimensionless parameters shown in the graphs. The possible exception would be conditions in which the diameter of the roughness material equals or exceeds the impinging wave heights. Under these circumstances, the validity of the curves would be doubtful because this range of wave heights compared with material diameters was not tested. However, the curves should be applicable in many cases involving riprap-slope protection wherever only one or two layers of riprap are used.

The test results on permeable slopes should apply to prototype conditions in the same dimensionless-parameter range. The latter should include all natural beach materials, and the test results should be valid for designing artificial beach fills. In order to use the test results to include the effect of the permeability or porosity of rubble-mound jetties or sea walls, it should be realized that the term "permeability," as used to describe these test results, becomes difficult to obtain quantitatively when the median diameter of the permeable material is greater than the 10.0-mm material used. Also, such structures rarely are thick enough, front to back, to eliminate the effect of structure thickness on run-up.

APPENDIX. NOTATION

The following symbols, adopted for use in this paper, conform essentially with "American Standard Letter Symbols for Hydraulics" (ASA Y10.2—1958), prepared by a committee of the American Standards Association with Society representation, and approved by the Association in 1958:

C_k = coefficient of skewness;

C_s = coefficient of sorting;

d = median diameter of roughness material, in feet;

g = acceleration of gravity, in feet per second squared;

H_o' = deepwater wave height, in feet:

H_o'/λ = deepwater wave steepness;

$H_o'/T^2 = 5.12 H_o'/\lambda$, functional deepwater wave steepness;

$H_o' T^2/d^2$ = inverted roughness coefficient;

$H_o' T^2/k$ = inverted permeability coefficient;

k = permeability of permeable materials, in square feet;

R = vertical height of wave run-up above still-water level, in feet:

R_1 = wave run-up on roughened and permeable slopes in Fig. 11 only;

R_2 = wave run-up on smooth slopes in Fig. 11 only;

R/H_o' = relative run-up;

S = distance along the face of the slope up which the waves surged;

T = wave period, in seconds;

α = angle between the face of the slope and the horizontal, in degrees; and

λ = deepwater wave length, in feet.

AMERICAN SOCIETY OF CIVIL ENGINEERS

Founded November 5, 1852

TRANSACTIONS

Paper No. 3004

VORTEX FLOW THROUGH HORIZONTAL ORIFICES

BY JOHN C. STEVENS,¹ M. ASCE, AND RICHARD C. KOLF,²
J. M. ASCE

WITH DISCUSSION BY MESSRS. JOHN W. CUNNINGHAM; CHESLEY J. POSEY;
AND JOHN C. STEVENS AND RICHARD C. KOLF

SYNOPSIS

The paper presents (a) the theory of vortex flow through horizontal orifices, (b) the results of laboratory experiments, and (c) some practical applications of the principles and data derived from the paper.

INTRODUCTION

Practical use of vortex flow has been made in connection with the diversion of sewage from combined sewers. By causing the sewage to approach a horizontal orifice tangentially, a vortex was established.

Vortex flow through such orifices is given by the formula $Q = C A \sqrt{2 g H}$. However, for a vigorous vortex from a storm head in the sewer, the coefficient is not the usual 60% but may drop to as little as 10%, with the result that only a small amount of storm water can pass into the interceptor.

However, at low stages the entire sanitary flow is diverted. This device becomes an effective control without moving parts for the diversion of sewage from combined sewers into interceptors. Facilities for research had to be confined to a few model experiments. However, these were amply sufficient to prove the efficacy of the vortex diversion.

NOTE.—Published, essentially as printed here, in December, 1957, in the Journal of the Sanitary Engineering Division as *Proceedings Paper 1461*. Positions and titles given are those in effect when the paper or discussion was approved for publication in *Transactions*.

¹ Cons. Hydr. Engr., Stevens & Thompson and Leupold & Stevens Instruments, Inc., Portland, Ore.

² Asst. Prof. of Fluid Mechanics, Marquette Univ., Milwaukee, Wis.

THEORY OF VORTEX FLOW

The differential equation that gives the pressure change normal to a streamline for flow in a curved path is

$$dp = \rho \frac{u^2}{r} dr \dots \dots \dots (1)$$

Because no torque is applied to the fluid mass in the case of the irrotational free vortex, Newton's second law gives $\frac{d}{dt} (r u) = 0$ and

$$u = \frac{K}{r} \dots \dots \dots (2)$$

in which K is a numerical constant and shows the degree of the "vorticity." The vorticity can also be described by a characteristic, Γ , designating the velocity of rotation in the vortex as

$$\Gamma = 2 \pi r u \dots \dots \dots (3)$$

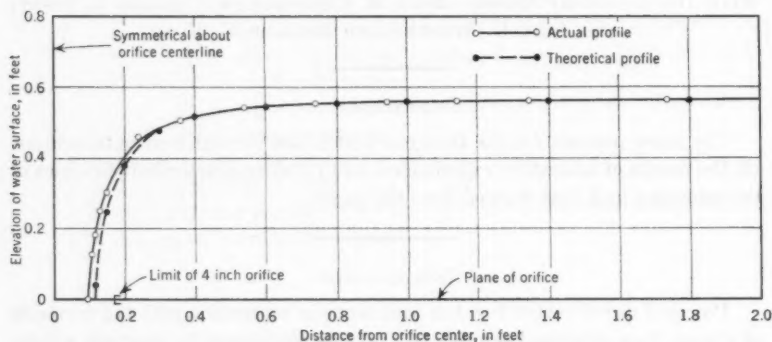


FIG. 1.—COMPARISON OF THEORETICAL AND ACTUAL WATER SURFACE PROFILES

Eq. 2 can be combined with Eq. 3 to obtain

$$\Gamma = 2 \pi K \dots \dots \dots (4)$$

Eq. 4 gives the relationship between the factors Γ and K , both of which are related to the degree of vorticity. Assuming superposition of radial flow on this ideal vortex flow, and applying the equation of continuity to the radial flow will result in

$$Q = 2 \pi r Y v \dots \dots \dots (5)$$

in which Y is the vertical distance between the flow boundaries and will be considered constant. Thus,

$$v = \frac{K_1}{r} \dots \dots \dots (6)$$

The velocity at any point is the vector sum of the tangential and radial velocities, u and v , each of which has the same inverse relation to the radius. Thus, the streamlines are equiangular and are theoretical logarithmic spirals.

Using Eqs. 1, 2, and 6, and the Bernoulli theorem results in

$$\frac{p_1 - p_2}{w} = \left(\frac{K^2}{2g} + \frac{K_1^2}{2g} \right) \left(\frac{1}{r_2^2} - \frac{1}{r_1^2} \right) = \frac{K_2^2}{2g} \left(\frac{1}{r_2^2} - \frac{1}{r_1^2} \right) \dots \dots \dots (7)$$

showing that the radial-pressure variation is hyperbolic for the idealized spiral motion between two parallel boundaries. It is to be expected that for free vortex motion through a horizontal orifice, Eq. 7 will be altered because of two factors. First, if the upper boundary is the free surface of the liquid, the distance, Y , in Eq. 5 is not a constant. The depth of flow will be nearly constant, except in the region near the axis of rotation. Because of the reduction in flow area caused by the drop in the liquid surface, the velocities near the axis tend to be greater than predicted from the hyperbolic $V = K/R$. However, this is in contradiction to the effect of viscosity. As the velocity becomes higher in the region near the orifice, the viscous resistance becomes appreciable, thereby reducing the velocities to values less than those predicted in the theoretical equation. Actual measurements show that the surface profile is above the theoretical hyperbola, as shown in Fig. 1. It must be concluded that in this region the viscous forces predominate and overwhelm completely the effects resulting from a theoretical free-surface boundary.

Application of the π -Theorem.—It can be assumed that the variables describing free spiral vortex flow through horizontal orifices are

$$f(D, B, \rho, \mu, V, \Gamma, p) = 0 \dots \dots \dots (8)$$

The boundary conditions are characterized by the variables, D and B ; ρ and μ represent the fluid properties; V and Γ denote the kinematic conditions and the surface force producing motion. According to the π -theorem^{3,4} there will be four dimensionless π -groupings or

$$\phi(\pi_1, \pi_2, \pi_3, \pi_4) = 0 \dots \dots \dots (9)$$

It is assumed that D , ρ , and V are the repeating terms so that

$$\pi_1 = D^{x_1} V^{y_1} \rho^{z_1} B^{-1} \dots \dots \dots (10)$$

$$\pi_2 = D^{x_2} V^{y_2} \rho^{z_2} \mu^{-1} \dots \dots \dots (11)$$

$$\pi_3 = D^{x_3} V^{y_3} \rho^{z_3} \Gamma^{-1} \dots \dots \dots (12)$$

and

$$\pi_4 = D^{x_4} V^{y_4} \rho^{z_4} p^{-1} \dots \dots \dots (13)$$

It can be shown that

$$\pi_1 = \frac{D}{B} \dots \dots \dots (14)$$

³ "Dimensional Analysis," by P. W. Bridgeman, Yale University Press, New Haven, Conn., 1931, p. 36.

⁴ "On Physical Similar Systems," by E. Buckingham, *Phys. Review* No. 4, 1914, p. 545.

$$\pi_2 = \frac{\rho V D}{\mu} \dots \dots \dots (15)$$

$$\pi_3 = \frac{V D}{\Gamma} \dots \dots \dots (16)$$

and

$$\pi_4 = \frac{\rho V^2}{p} \dots \dots \dots (17)$$

In the foregoing, π_1 describes the boundary proximity, π_2 is the Reynolds number, π_3 is a new ratio defined here as the reciprocal of the Kolf vortex number, and π_4 is the Euler number.

Eq. 9 becomes

$$\phi \left(\frac{D}{B} \mathbf{R} \mathbf{K} \mathbf{E} \right) = 0 \dots \dots \dots (18)$$

in which \mathbf{K} is the Kolf vortex number. Choosing the Euler number as the dependent term leads to

$$\frac{V^2 \rho}{p} = f_1 \left(\frac{D}{B} \mathbf{R} \mathbf{K} \right) \dots \dots \dots (19)$$

or

$$V = f_2 \left(\frac{D}{B} \mathbf{R} \mathbf{K} \right) \sqrt{2 g H} \dots \dots \dots (20)$$

utilizing

$$Q = A V = C A \sqrt{2 g H} \dots \dots \dots (21)$$

Substituting for V , and canceling the common terms results in

$$C = f_2 \left(\frac{D}{B} \mathbf{R} \mathbf{K} \right) \dots \dots \dots (22)$$

Eq. 22 shows that the discharge coefficient should in some way be related to the shape and character of the boundaries, the effects of viscous shear, and the effects of vorticity. It should be noted that Eq. 21 is the formula used for the flow through standard orifices.

Dynamic Similarity.—Considering the centrifugal force acting on a fluid element flowing in a curved path of radius, r , and tangential velocity, u ,

$$F_c = \rho dr dA \frac{u^2}{r} = \rho dr dA \frac{\mathbf{K}^2}{r^3} \dots \dots \dots (23)$$

The total inertia force will be

$$F_1 = \rho dr dA \frac{dV}{dt} = \rho dr dA \frac{d(V)^2}{ds} \dots \dots \dots (24)$$

and

$$\frac{F_c}{F_1} = \frac{\mathbf{K}^2 ds}{r^3 V dV} \dots \dots \dots (25)$$

which becomes dimensionally

$$\frac{F_c}{F_i} = \frac{K^2}{L^2 V^2} \dots \dots \dots (26)$$

showing that the Kolf vortex number,

$$K = \frac{V}{D} \dots \dots \dots (27)$$

is proportional to the square root of the ratio of the centrifugal force to the total inertia force. It is the criterion for dynamic similarity for all cases in which the inertial and centrifugal forces predominate.

LABORATORY EXPERIMENTAL WORK

In 1929, studies⁵ of the Thoma counterflow brake were completed at the Technical University of Munich, in Germany. This device consists of a spiral vortex chamber with tangential and axial connections. Because of the tangential approach of the water and the resulting vortex, the apparatus had a great resistance to flow in one direction, whereas the flow in the opposite direction encountered far less resistance. The apparatus was considered as a type of pipe fitting that might replace the check valve in special cases. The changes in the fitting resistance factor for various designs in the two directions of flow were studied.

Studies of free vortex flow through orifices were completed⁶ just prior to 1950 at the State University of Iowa at Iowa City. Tests were made on a 4-in. sharp edge circular orifice in the center of the bottom of a 6-ft-diameter tank. Tangential flow was directed into the tank trough containing four 1-in. pipes equally spaced about the circumference and radial flow was guided in through a false bottom directly below these jets. A constant head of 1.63 ft was maintained with the variables being the tangential and radial approach velocities. Attempts were made to show the normal-orifice discharge coefficient as a function of the ratio of the average tangential velocity component to the average radial velocity component.

During this same period studies were made⁷ at the University of Wisconsin at Madison, of the flow in centrifugal pressure nozzles to be used as atomizers. The atomization is caused largely by a vortex motion imparted to the liquid as it passes through the nozzle. A common method of imparting this vortex motion to the liquid is to provide a chamber within the nozzle with a tangential inlet. The characteristics that were studied in this investigation were the nozzle spray cone angle and the discharge coefficient for various nozzle designs.

The objectives of an experimental program begun by Mr. Kolf were to extend the fundamental and practical knowledge of the spiral vortex and, in particular, to find the head-discharge relations for a series of orifices with a variety of boundary conditions.

⁵ "An Investigation of the Thoma Counterflow Brake," by Richard Heim, *Transactions, Munich, Hydraulic Inst., A.S.M.E.*, 1953.

⁶ "How the Vortex Affects Discharge," by C. J. Posey and H. C. Hau, *Engineering News-Record*, March 9, 1950.

⁷ "Fluid Flow in Centrifugal Pressure Nozzles," by W. R. Marshall and W. H. Darnell, *Bulletin, Eng. Experiment Station, Univ. of Wisconsin, Madison, Wis.*

This experimental work consisted of tests made in two different tanks. The initial tests were made in a 12-ft-diameter tank with sheet metal sides, 2 ft high. Orifices were cut in 2-ft-diameter, 14-in. gage sheet metal plates and were placed in the center of the bottom of the tank. Water was admitted to the tank at four points around its periphery and allowed to approach the orifice uniformly after passing through a rock baffle ring. The discharge was measured by the direct-volumetric method. Static head was measured at the third point of the periphery by three point gages situated in from the rock baffle ring approximately 3 in. Vortex-profile measurements were taken with a moving point gage on a 6-in. structural aluminum I-beam 12 ft long. An angle mount was fastened to the center of the beam to support a special inside caliper that could be lowered into the vortex air core to measure its diameter.

Using uniform approach conditions the vortices that formed during this stage of testing were small and unstable. The direction of rotation would change from clockwise to counterclockwise with no definite pattern and the air core would form only momentarily. These vortices were found to have no noticeable effect on the standard-orifice coefficients.

In order to induce greater degrees of vorticity a 4.5-ft-diameter ring using 19 guide vanes was constructed concentric with the orifice opening. The vanes were 1 ft wide and 1.5 ft high and were spaced evenly around the circumference of the ring. They were arranged so that each could be pivoted about its center or bolted shut to the adjacent vanes. With the aid of these vanes the water could be directed toward the orifice opening with any desired approach angle.

When the water was allowed to pass through the vanes with a velocity component tangential to the orifice a stable vortex formed and centered itself above the orifice opening. Tests were made using combinations of vane openings from all vanes open tangential to the orifice opening, to one vane open and all the others closed. The type of entrance did not appear to have any effect on the stability or the geometry of the vortex as long as the entrance velocity had a tangential component.

A second series of tests were made in a 6-ft-diameter steel tank, 3 ft high, in order to extend the data with respect to head and boundary proximity. The orifices were cut into 18-in.-diameter, 14-gage sheet-metal plates and were fastened to the tank in the geometric center. Two inner boundary rings were used in this tank. Each was constructed of 16-gage sheet metal with two diametrically opposite vanes which could be pivoted to any desired entrance angle. The larger boundary ring was 4.5 ft in diameter and 2.5 ft high whereas the smaller ring was 2 ft in diameter and 3 ft high.

No baffles were provided for the initial tests on this apparatus. The water was allowed to approach the inner boundary ring with an initial-vortex motion imparted to the water admitted through six 2-in. pipes. On centers welded into the tank tangentially at each of two diametrically opposite points 6-in. pipes were used. At the higher flow rates large eddies were formed behind the entrance vanes, which greatly disturbed the surface both inside and outside the boundary ring. As a result, deflector vanes 6 in. wide and 3 ft high were

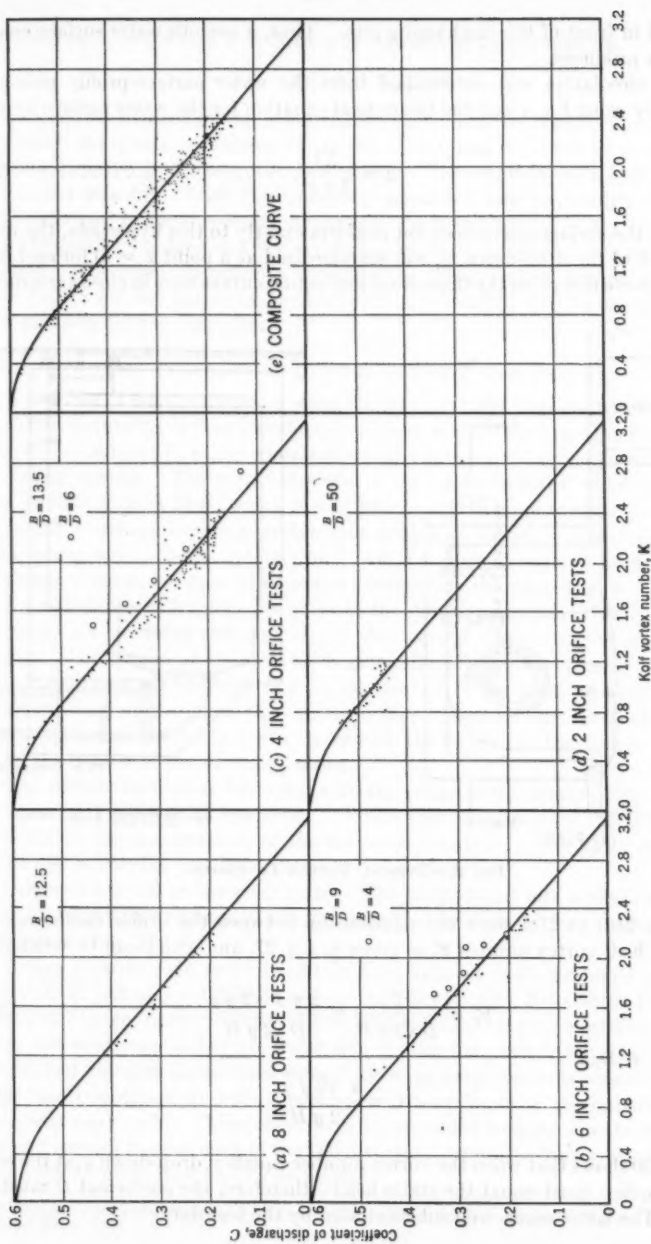


FIG. 2.—COEFFICIENT OF DISCHARGE VERSUS KOLF VORTEX NUMBER

fastened in front of the discharging jets. Thus, a smooth water surface condition was produced.

The circulation was determined from the water surface-profile measurements, by using Eq. 4 and the theoretical equation for the water surface hyperbola.

$$y = \frac{K^2}{2g x^2} \dots \dots \dots (28)$$

Because the surface curve does not conform exactly to this hyperbola, the measurement of the drop-down, y , was standardized at a point $x = D$ for each test run. Above this point the theoretical and actual curves were in close agreement.

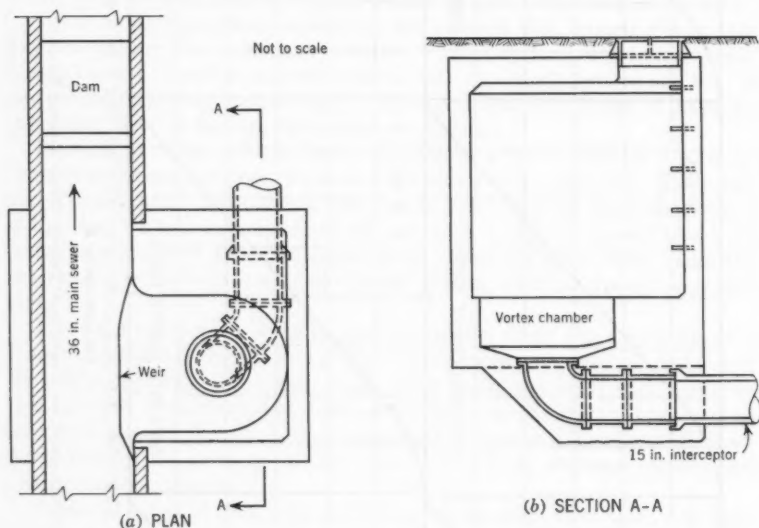


FIG. 3.—TYPICAL VORTEX DIVERSION

Figs. 2(a) to 2(e) show the relationship between the orifice coefficient, C , and the Kolf vortex number K as given in Eq. 27, and which can be written as

$$K = \frac{\Gamma}{D \sqrt{2gH}} = \frac{2\pi x \sqrt{2gy}}{D \sqrt{2gH}} \dots \dots \dots (29)$$

When $x = D/2$

$$K = \frac{\pi \sqrt{2gy}}{\sqrt{2gH}} \dots \dots \dots (30)$$

Eq. 30 shows that when the vortex number equals π , drop-down y , at the edge of the orifice must equal the static head—therefore, the coefficient C must be zero. The latter seems well substantiated by the test data.

Between $V = 0.8$ and $V = 3.14 = \pi$, the straight-line equation,

$$C = 0.686 - 0.218 K \dots \dots \dots (31)$$

is proposed to determine the approximate coefficient for vortex flow through horizontal sharp-edged orifices. Between $V = 0$ and $V = 0.8$ the coefficient can be estimated from the curve (Fig. 2(e)). The smallest ratio of B/D that was tested was 4.0. With this boundary proximity the water-surface profile still conformed to the theoretical hyperbola above the point $x = D$. However, with the small boundary ring the asymptote of the water-surface curve was not reached. Therefore, in order to compute the circulation it was necessary to solve Eq. 28 for two points on the curve simultaneously, which amounts to an extrapolation for the static head, H .

THE PORTLAND (ORE.) INTERCEPTOR DIVERSIONS

A number of devices for controlling the flow diverted into interceptors from combined sewers³ have been developed. These devices have moving parts and, as such, are subject to heavy maintenance and occasional stoppage from solids carried by sewage. The most successful of such devices is the motor-operated gate, controlled by a float, which is only practicable in large sewers.

In the Portland sewerage system one such gate device was installed on a 96-in. sewer with a 54-in. interceptor. All the other diversions were effected by vortex control. A typical diversion structure is shown in Fig. 3.

A small dam was built in the sewer at the downstream side of the diversion manhole. It has faces of 1 on 2 slopes that permit the passage of grit downstream. The height of these dams is generally about 10% greater than the normal depth of the sanitary flow in the sewer. They must be high enough to divert all the sanitary flow through the orifice. Beyond this, local conditions, such as slope of the main sewer, governed the height of the dams. Fig. 4 shows the details of the diversion dams.

The vortex chamber is U-shaped with the orifice in the center of the arc and the open part tangent to the sewer. When the upper part of the sewer was removed for the construction of the diversion manhole, a low lip or weir was left to aid in keeping grit from entering the interceptor.

Orifices were cut in the steel plate. The latter fitted into a shallow recess made by brazing a ring around the flange of the cast iron entrance elbow of the interceptor (Fig. 3).

Design Criteria.—In order to obtain flow data for each combined sewer in Portland, 42 out of a total of 54 sewers that flowed into Willamette River, or Columbia Slough, in the vicinity of Portland were selected for continuous measurements of sewage and storm water flow during the years from 1941 to 1943. Certain criteria were ascertained from the sewage measurements concerning the residential population and the character and magnitude of the industrial development near each. These could then be expanded to approximate the sanitary and normal flows of each of the 160 diversion structures from various points on the interceptors that had to be made.

³ "Handbook of Applied Hydraulics," Edited by Calvin Davis, McGraw-Hill Book Co., Inc., New York, N. Y., 2d Ed., p. 1066.

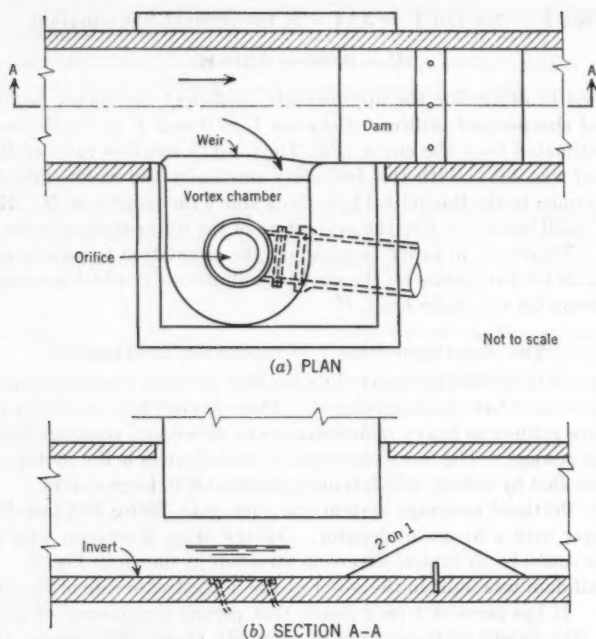


FIG. 4.—DIVERSION DAM DETAILS

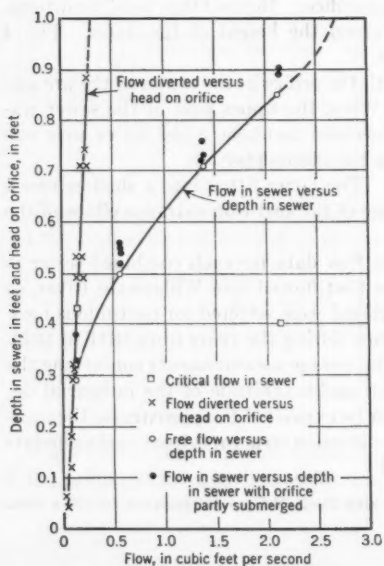


FIG. 5.—FLOW RELATIONSHIPS OF A VORTEX

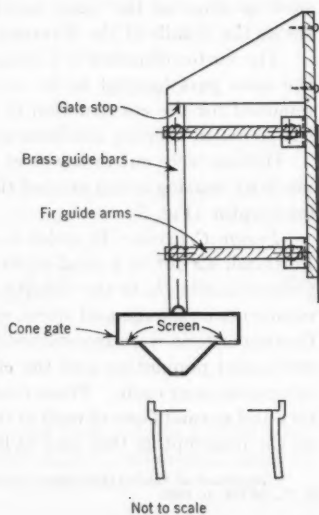


FIG. 6.—CONE GATE

Table 1 shows how the design criteria thus obtained were applied to a few sample diversion structures.

Model Studies of Diversion.—In addition to the laboratory experiments described previously, a model of a diversion-vortex chamber, in which the orifice sizes could be changed, was built and tested.

These experiments produced valuable data on the vortex flow through horizontal orifices ranging from 3 in. to 6 in. in diameter under both free flow and submerged conditions. Desirable sizes of the vortex chamber and the proportion of grit that could be kept out of the interceptor were also determined.

Data on grit were determined by introducing known weights of coarse sand and small gravel into the sewer and then weighing the quantity that passed through the orifice and down the sewer. For the 3-in. orifice 90% of the grit that was introduced passed over the dam and on down the sewer. For the 5-in.

TABLE 1.—DESIGN CRITERIA FOR TYPICAL DIVERSIONS

MAIN SEWER		DIVERSION		FLOW, IN CUBIC FEET PER SECOND		ORIFICE		SANITARY	VORTEX CHAMBER	DAM
Size, in inches	Slope	Symbol	Size, in inches	Design	Sanitary	Elevation, in feet	Diameter, in inches	Depth, in feet	Diameter, in feet	Height, in inches
(1)	(2)	(3)	(4)	(5)	(6)	(7)	(8)	(9)	(10)	(11)
18	.048	SJ 17	8	0.46	0.13	74.7	6	0.26	3.0	5
8	.072	SW 72	8	0.13	0.06	55.5	6	0.16	3.0	4
22	.013	SE 119	12	0.35	0.09	33.0	8	0.29	4.0	5
36	.002	SW 21	15	1.15	0.62	28.8	12	0.59	4.5	13
36×36	.069	NW 9	15	3.57	2.84	41.9	12	0.73	4.5	13
48	.031	CE 12	18	2.62	1.26	52.5	16	0.80	5.0	12
42	.024	SW 6	21	4.95	3.08	22.5	18	0.95	5.0	13
62	.020	EC 93	24	4.80	2.07	54.0	20	0.95	5.0	13
87	.0034	EC 127	27	7.44	3.14	159.8	24	1.09	5.0	13
48×72	.022	WC100	24	9.61	6.20	25.5	20	1.20	5.0	16
72×80	.009	WC 7	24	10.70	5.83	15.0	20	1.24	5.0	16
54×54	.022	NE 55	30	10.50	2.72	51.2	28	1.24	5.0	17
66×72	.014	EC 109	36	7.52	4.03	56.0	33	1.08	6.0	14

orifice 87% of that introduced continued on down the main sewer. The grit that passed through the orifices was of the smaller sizes, having been thrown into suspension upstream of the diversion. The coarser grit formed a blanket just upstream of the dam and was later carried above the dam during higher flows.

Coefficients of Flow.—For 1-ft heads under vortex flow the coefficient, C , in Eq. 21 was 0.49, 0.39, and 0.36 for 3-in., 4-in., and 5-in. orifices, respectively. These are not as low as those obtained under higher heads (Fig. 2(b) and 2(c)) and, of course, not as low as actually obtained under the higher heads during freshets.

The flow relationships of a vortex are shown in Fig. 5, for a model with a 4-in. orifice. The vortex is free—that is, there are no external forces applied and it is completely aerated through the orifice. Note that at a 1-ft head the flow in the sewer was 2.7 cu ft per sec whereas the flow passing through the orifice was only 0.3 cu ft per sec, or 11% of the sewer flow.

Automatic Shut-Offs.—Two devices were tested in the laboratory to shut off the interceptor entirely during heavy storms. This compensates for the increased flow to the treatment plant from sewers having only vortex control in the smaller diversions. Thus, the treatment plant is not overloaded. The device that appeared to be the most practical is known as the cone gate (Fig. 6).

The stem of the gate is supported on a pair of hinged bars or links so that the gate always moves parallel to itself. The cone, which is normally held well above the orifice, permits the passage of practically all the debris and does not interfere with the vortex. The cone is enclosed from the top and sides by brass plate. Between the cone and the sides is a horizontal screen forming a ring through which water can enter and fill the brass cone.

The cone stem is normally held against a stop by a small cable passing above overhead pulleys and counterweighted. When storm water appears and rises high enough to pour through the screen and fill the cone, the increased weight overcomes the counterweight and the cone seats itself in the orifice, shutting off the flow into the interceptor.

A hole in the bottom of the cone permits it to empty as the storm subsides, whereupon the cone is automatically raised against the stop by the counterweight. Any solids caught against the screen fall off.

ACKNOWLEDGMENTS

The experiments performed at the hydraulics laboratory of the University of Wisconsin by Richard C. Kolf were under the direction of James R. Villemonste, A. M. ASCE, and were supported by James G. Woodburn, M. ASCE, and Arno T. Lenz, of the civil engineering department. In Mr. Kolf's thesis the term "Kolf vortex number" used herein was referred to as the "vortex number." It is hoped that the term used in this paper will be used by others in this field of investigation so that Mr. Kolf's contributions will be properly recognized.

The writers express their appreciation to B. E. Hirsch, T. J. Kontos, and D. W. Hinderman, for their assistance in the construction of the apparatus and the collection of data.

Ben Stodgen Morrow, A. M. ASCE, gave valuable assistance for the vortex model studies during the design and construction stages of the Portland Sewerage Project.

APPENDIX. NOTATION

The following letter symbols, adopted for use in the paper and for the guidance of discussers, conform essentially with American Standard Letter Symbols for Hydraulics (ASA-Y10.2-1958), prepared by a committee of the American Standards Association with Society representation, and approved by the Association in 1958:

A = area of orifice;

B = diameter of boundary ring;

- C = discharge coefficient;
 D = diameter of orifice;
 E = Euler number;
 F = Froude number;
 F_c = centrifugal force;
 F_i = inertia force;
 g = acceleration due to gravity;
 H = static head on center of orifice;
 h = drop-down to the vortex surface for $x = D$;
 K = Kolf vortex number;
 K = a constant vorticity factor;
 K_1, K_2 = profile constants;
 p = pressure per unit area;
 Q = actual discharge = $C Q_t$;
 Q_t = theoretical discharge;
 q = theoretical discharge through 1-ft orifice;
 R = Reynolds number;
 r = radius of vortex profile from center of orifice;
 u = tangential velocity vector;
 V = velocity vector-resultant of u and v ;
 v = radial-velocity vector;
 w = specific weight;
 x, y = coordinates of a point on the vortex surface; x is also a subscript denoting a different diameter, discharge, and head coefficient;
 Y = vertical spacing of boundaries in two-dimensional flow;
 Γ = circulation;
 ρ = mass density;
 μ = dynamic viscosity; and
 Θ = the angle between the velocity vector and the radius.

DISCUSSION

JOHN W. CUNNINGHAM,⁹ M. ASCE.—An important practical application in the design of regulators for intercepting flow from combined sewers has been presented by the authors. The design utilizing the vortex principle proved very successful for the diversions of the Portland (Oregon) intercepting sewer system.

The Portland sewer system was predominantly one of "combined" sewers, which during the rainy season carried large volumes of storm water. It had sixty-one trunk sewer outfalls, of which fifty-seven were intercepted and brought to a single treatment plant. Because of the prevailing elevations and grades, it was in many cases necessary to make diversions from laterals that fed the trunk sewers, resulting in more than one-hundred and fifty separate points of diversion. Many of these diversions became flooded at high river stages, with the result that not only sanitary and storm flow but also backwater from the river might, in the absence of control, enter the interceptors. Altogether, the problem of diversion was complicated and difficult.

Consideration was given to all of the regulating devices that have been described in the literature, and considerable correspondence brought out additional ideas. Models were made for a number of devices and some of these were given small-scale operating tests, though not on a quantitative basis. Reliability under variable and adverse conditions was given prime consideration. The regulators had to operate with a minimum of maintenance in locations where access was difficult and where they probably would be neglected.

An orifice diversion of any kind, horizontal or vertical, is subject to the formula $q = Ca\sqrt{2gh}$. For a cylindrical pipe sewer, for flows up to two-thirds or more of the depth, the flow varies approximately as the square of the depth. Therefore an orifice, and particularly a horizontal orifice, diverting from a sewer constitutes an excellent regulator and has been widely used in different combinations, sometimes with a float-operated device to completely close the diversion when the sewage level reaches a given point.

Following the preliminary studies for the Portland system, which were made by the writer with the cooperation of Ray E. Koon, it was decided to use the horizontal orifice diversion in most cases, but for a few of the larger sewers to use a plug-valve type of closure that would completely interrupt the flow during major storms and offset the excess flow coming from the simpler type of diversion. One problem was related to the grit. It was feared that an orifice located at the sewer invert would pick up most of the bed load grit and carry it into the interceptor system, a very undesirable condition. Designs were at this stage when Mr. Koon retired from activity in the project, and Mr. Stevens, (the author) succeeded him.

Mr. Stevens decided to construct and test a model diversion quantitatively and primarily to observe the behavior of the bed load grit. The model was made from sheet metal, and the curved shape surrounding the orifice was for

⁹ Cons. Engr., John W. Cunningham & Associates, Portland, Ore.

convenience in fabrication. When tested, the very desirable vortex action was observed. This action was entirely fortuitous and unexpected, and was an added advantage for a device which would have been practical in the absence of vortex action. In the same experiments it was observed that the bed-load grit was largely carried past the orifice and over the dam. The vortex seemed to skim off the top sewage carrying less grit. The device was adopted for practically all of the Portland diversions.

The writer also designed a plug valve closure, somewhat like that shown in Fig. 11, but built of cast iron to meet the severe conditions of a sewer manhole. A modification of this, made of sheet metal and wood, was installed in the 13th Avenue diversion but due to the flimsy construction did not prove successful. The idea has possibilities if the construction is sound and permanent.

The later model studies conducted by Mr. Stevens and Mr. Kolf give further design data and coefficients that will permit engineers to plan horizontal orifices with assurance of the desired results. There may be other applications in addition to the one that has been demonstrated.

CHESLEY J. POSEY,¹⁰ M. ASCE.—For the case of purely radial inflow, the experimental results obtained by the authors corroborate the results of the Iowa tests.⁶ The authors state under the heading, "Laboratory Experimental Work" that

"Using uniform-approach conditions the vortexes that formed during this stage of testing were small and unstable. The direction of rotation would change from clockwise to counterclockwise with no definite pattern and the air core would form only momentarily. These vortexes were found to have no noticeable effect on the standard-orifice coefficients."

The corresponding conclusion from the Iowa tests was that "with purely radial inflow the vortex is small and transitory; its effect on discharge is negligible." It was further determined in the Iowa tests that if "the tangential component of inflow is shut off after the vortex has become stable, it will soon die out." The question of vortex formation when the inflow is purely radial would therefore seem to be fairly well settled, with the possible exception of the case of a tank so large and perfectly symmetrical that the earth's rotation would have a measurable effect.¹¹

In the Iowa investigation the values of C in the standard-orifice formula, Eq. 21, were computed for those tests in which the inflow was purely radial. They were found to range from 0.562 to 0.582, based on the depth as measured by piezometer holes 13 in. from the center of the 4 in. diameter sharp-edged orifice.¹² Fig. 2 indicates that the authors believed C should be 0.600 or slightly less. No values are given nor plotted points shown, however, for vortex numbers of less than 0.3.

¹⁰ Prof. and Head, Dept. of Civ. Eng., State Univ. of Iowa, Iowa City; Director, Rocky Mountain Hydr. Lab., Allenspark, Colo.

¹¹ "Earth's Rotation Has Little Effect on Vortex Motion," by C. J. Posey, *Civil Engineering*, December, 1953, p. 68.

¹² "Vortex Over Outlet," by Haieh-Ching Hsu, thesis presented to the State University of Iowa, Iowa City, Iowa, in 1947, in partial fulfillment of the requirements for the degree of Master of Science.

Comparison of the quantitative results of the two investigations for cases in which the inflow was partially tangential is made difficult or impossible by the authors' choice of variable. Apparently, it is necessary to determine the water-surface profile measurements and use the theoretical equation for the water-surface hyperbola to determine the "Kolf vortex number," in terms of which the results are summarized. The designer who wishes to use the authors' data to determine the effect of a vortex on the discharge through a certain outlet will find it difficult to estimate the value of the "Kolf number." The authors themselves give no estimation of its value for the sewerage vortex chambers described in the last part of the paper.

The variable used in summarizing the results of the Iowa tests, can be computed easily if the angularity of the approach flow is known. It is the ratio of the tangential component of the average velocity to its radial component, or the tangent of the angle θ between the resultant velocity and the radius from the center of the outlet. The radial component of the average velocity

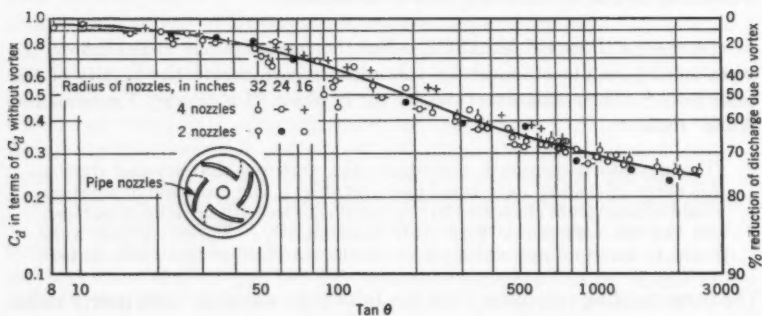


FIG. 7.—EFFECT OF ANGULARITY OF APPROACH VELOCITY ON DISCHARGE

at any point is the discharge divided by the surface area of a hypothetical cylinder through the point, concentric with the outlet. The tangential component of the velocity through the sides of this cylinder depends on the strength of the vortex, or circulation. The Iowa tests show that it can be computed as the sum of the product of (a) the discharge; (b) the tangential component of velocity; and (c) the radius, for each of the sources of inflow, divided by the product of the total discharge and the radius of the cylinder. The ratio of tangential to radial components of velocity, $\tan \theta$, is constant for any radial distance from the center of the orifice over which no appreciable tangential force or momentum is introduced. This corresponds to the authors' statement under the heading, "Theory of Vortex Flow," that " * * * the streamlines are equiangular and are theoretical logarithmic spirals." $\tan \theta$ can be shown to be equal to the ratio between the circulation and the discharge per unit depth and is just as dimensionless as is the authors' "Kolf number." ¹²

Fig. 7 summarizes the results of the Iowa tests and is reproduced for the benefit of designers who may wish to estimate the effect of a nonradial approach

on the discharge through a bottom outlet. The validity of $\tan \theta$ as a measure of the effect of the vortex is apparent especially when it is realized that in these tests both the radius and the velocity of the tangential inflow were varied over a wide range.

The following practical example illustrates the use of Fig. 7. A tank 10 ft in diameter has a 6-in., sharp-edged circular orifice in the center of its bottom, which is horizontal. Pipe connections to the tank introduce tangential discharges of 0.20 cu ft per sec and 0.15 cu ft per sec through two 3 in. pipes at distances of 4 ft and 5 ft, respectively, from the center. A 2 in. pipe introduces 0.05 cu ft per sec at the edge of the tank, which is inclined 45° with the radius, and opposes the rotation caused by the two 3 in. pipe inlets. An additional 0.6 cu ft per sec enters the tank radially. It is required to determine the depth of water at the outside edge of the tank.

For computational purposes, assume a hypothetical cylinder 4 ft in diameter and H ft high. The components of the average velocity through the sides of the cylinder are computed as follows:

$$Q_1 \times V_1 \times R_1 = 0.20 \times \frac{0.20}{.049} \times 4 = 3.27$$

$$Q_2 \times V_2 \times R_2 = 0.15 \times \frac{0.15}{.049} \times 5 = \frac{2.30}{5.57}$$

$$Q_3 \times V_3 \times R_3 = 0.05 \times \frac{0.05}{0.022} \times .707 \times 5 = \frac{.40}{5.17}$$

The tangential component = $\frac{\sum Q V R}{R \sum Q} = \frac{5.17}{2 \times 1} = 2.58$ and the radial component = $\frac{\sum Q}{H \pi D} = \frac{1.00}{12.6 H} = .079 \frac{1}{H}$. Hence, $\tan \theta = \frac{2.58}{0.079} H = 32.6 H$. Assuming that $H = 3.0$ ft, then $\tan \theta = 98$ and from Fig. 7 the ratio of the discharge to the vortex-free discharge is 0.65. If C for purely radial discharge is taken as 0.57 (the mean of the Iowa values) the value for the present example becomes $(0.65) \times (0.57) = 0.37$, from which $H = \frac{Q^3}{2 g C^2 A^2} = \frac{1.0}{2 g (.37)^2 (.196)^2}$

$= 2.94$ ft. Evidently the trial value of $H = 3.0$ was a little too high, and a slightly smaller value could be assumed. Then, $\tan \theta$ and H could be recomputed according to the correspondingly revised value from Fig. 7. However, such precision would not be justified and the required depth at the periphery of the tank can be taken as 2.95 ft or 3.0 ft. The use of Fig. 7 in this manner involves an extrapolation from the experimental results. Most of the uncertainty is whether the resistance torque in the tank of the example would be comparable to that used in the Iowa experiments.

Unfortunately, the pipes used in the Iowa experiments to introduce the tangential position of the inflow projected into the tank, thus impeding the circulation to some extent. Hence the results of Fig. 7 will indicate too much discharge for a tank that has less drag torque than the Iowa tank. Inasmuch as this effect might be appreciable, the writer hoped that the authors' tests would show its magnitude, but the authors' expression of their results in terms

of an esoteric variable, which can only be evaluated implicitly from laboratory measurements, prevents any direct quantitative comparison. Fig. 1 does give some indication that the friction drag is only appreciable near the center, so that conditions around the periphery may not be important.

While attempting to improve the theoretical analysis of the phenomena in order to find a basis for comparing the experimental results, the writer discovered that neither investigation included any consideration of what must be a sizable term in the equation—the angular momentum of the effluent. Any future investigation should include measurement of this quantity. Without it (or the more difficult measurement of the torque on the tank) there is no way to evaluate the friction drag.

JOHN C. STEVENS,¹³ M. ASCE AND RICHARD C. KOLF,¹⁴ J. M. ASCE.—The following pertains to certain features of the Portland vortex interceptor diversions. Table 1 gives a sampling of the design data to which no flow coefficients were applied. The orifices were made in standard sizes matching standard sewer pipe sizes. The orifice diameter is from 2 in. to 4 in. less than the diversion interceptor. The object was to insure a vortex through the orifice for all high flows. Other flows would pass through the orifice with or without appreciable vortices, due to the small dam in the sewer just below the orifice chamber.

The vortex flow for combined sewer diversions was so successful that Mr. Stevens tried a vortex for the separation of gas from mineral water.

A company operates plants in Oregon and Washington for the manufacture of dry ice and liquid CO₂. This gas is found in heavily charged water, and is obtained by pumping the water into a separator from drilled wells. The separator is merely a vertical concrete structure sealed at the top while the escaping effluent maintains a water seal at the bottom.

The pump discharge pipe passes through the separator wall approximately 8 ft above the bottom. The gas is recovered by spraying the pumped water onto the inside face of the structure wall. The gas is drawn off through a pipe sealed in the top and connected to the suction side of an air compressor in the distant plant. This maintains a vacuum of approximately 6 in. of mercury in the pipeline and the interior of the separator.

Fig. 8 shows a vortex chamber sealed into the top of the separator with the gas line sealed into its top. The effluent passed out of the bottom of the separator through a trap and a vacuum was maintained inside. Upon testing, a very vigorous vortex was formed, but the gas recovery was no more than had been previously obtained very cheaply with the old nozzle spray. To obtain more gas the separation chamber would have to be under a much greater vacuum and the water might require heating. Both methods were impracticable.

Mr. Cunningham suggests that there may be other practicable applications of vortex flow. Any type of solid in air, water, smoke, or any mixed fluids of different densities is susceptible to separation by vortices. Many similar examples are already in successful use.

¹³ Cons. Hydr. Engr., Stevens & Thompson and Leupold & Stevens Instruments, Inc., Portland, Ore.

¹⁴ Asst. Prof. of Fluid Mechanics, Marquette Univ., Milwaukee, Wis.

In Mr. Hsu's thesis¹² the "variable" used is the tangent of the angle of incidence to the vortex wherein values range between zero and infinity. The Kolf vortex number expressed in Eq. 27 and in subsequent equations in a finite dimensionless parameter whose value lies between zero and π .

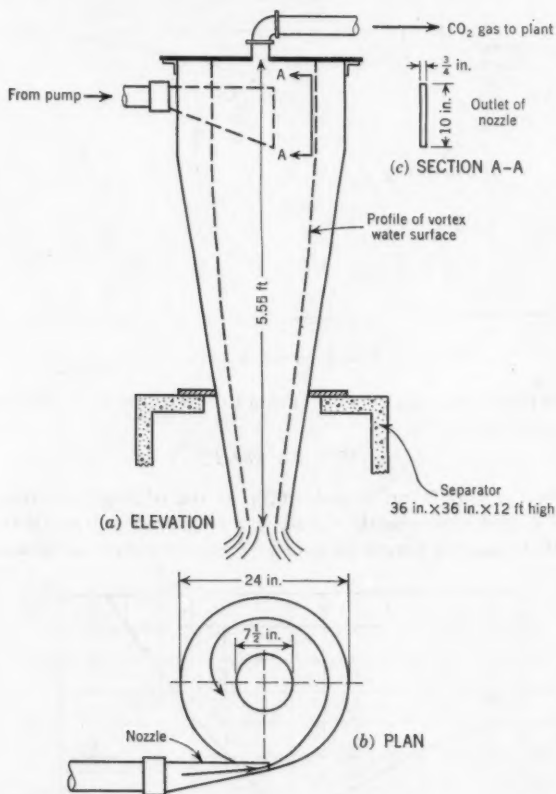


FIG. 8.—VORTEX CHAMBER

Mr. Posey states

"Apparently, it is necessary to determine the water surface-profile measurements and use the theoretical equation for the water-surface hyperbola to determine the Kolf vortex number * * *. The designer who wishes to use the authors' data * * * will find it difficult to estimate the value of the Kolf vortex number."

For every Wisconsin laboratory experiment two important quantities were observed: (a) H , the static head on the center of the orifice, and (b) the drop-

down of the water surface, y , at a point on the profile for $x = D$. Because of its importance and in order to avoid confusion, this value of y has been designated as h herein. The ratio h/H then becomes an important variable for any

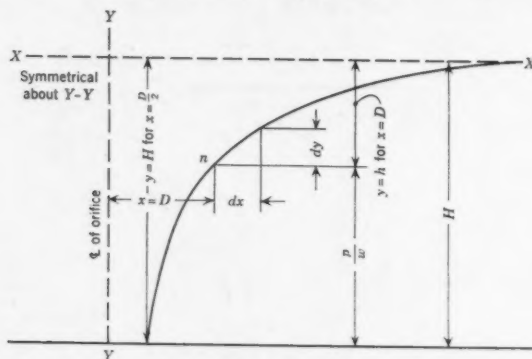


FIG. 9.—FREE VORTEX

symmetrical free-flow water vortex. From Eq. 29 it is obvious that for $x = D$, the Kolf vortex number is

$$K = 2\pi \sqrt{h/H} \dots \dots \dots (32)$$

Also, when $x = D/2$ the drop-down, y , at the edge of the orifice (Fig. 9) $= H$; $K = \pi$, and consequently C and $Q = 0$ —purely a hypothetical condition. Furthermore, the actual value of h/H cannot exceed .25 because $K = \pi$.

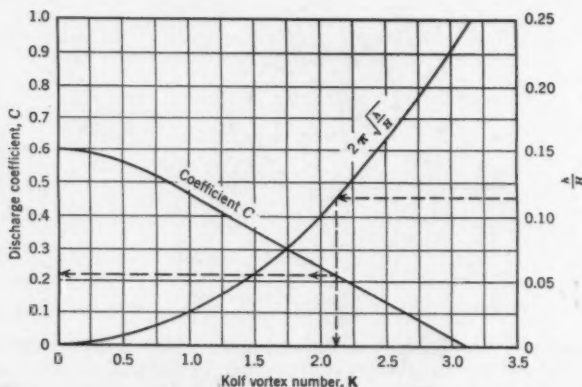


FIG. 10.—DETERMINATION OF THE KOLF VORTEX NUMBER AND DISCHARGE COEFFICIENT

Fig. 10 and Fig. 11 show the essential characteristics of a symmetrical free-flow water vortex. In Fig. 10 the ratio h/H is the independent variable from which the Kolf vortex number, K , is read on the lower scale and the discharge coefficient C on the left.

In Fig. 11, the theoretical flow, q , for an orifice 1 ft in diameter is given versus H , the static head on the center of the orifice for which the discharge coefficient is 1.00. The corresponding flow through any other diameter D_z is given by

$$Q_z = q (D_z)^2 \dots \dots \dots (33)$$

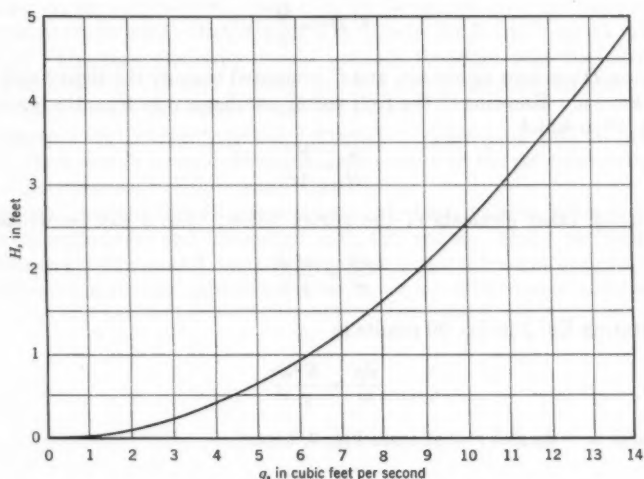


FIG. 11.—HEAD VERSUS FLOW THROUGH ORIFICE

for the same head and discharge coefficient. The flow for a different diameter and head is given by

$$Q_z' = q (D_z)^2 \sqrt{H_z/H} \dots \dots \dots (34)$$

A different diameter and head and discharge coefficient results in

$$Q_z'' = q (D_z)^2 C_z \sqrt{H_z/H} \dots \dots \dots (35)$$

Examples of the use of Fig. 10 and Fig. 11 are given in Table 2.

TABLE 2.—EXAMPLES OF THE USE OF FIG. 10 AND FIG. 11

Example (1)	h (2)	H (3)	h/H (4)	K (5)	C (6)	q (7)	C_q (8)	D_z (9)	C_z (10)	H_z (11)	Q_z (12)
1	.052	4.00	.130	2.25	.18	12.5	2.25	1.75	38.2
2	.040	2.50	.16	.80	.52	10.0	5.20	3.00	...	1.25	63.6
3	1.00	5.00	.200	2.81	.075	14.2	.99	.667	.10	4.20	.040

The theoretical flow through a 1-ft orifice as shown in Eq. 21 is

$$q = \frac{\pi}{4} \sqrt{2gH} \dots \dots \dots (36)$$

The actual flow for a different diameter becomes

$$Q = \frac{\pi}{4} D^2 C \sqrt{2 g H} \dots \dots \dots (37)$$

Combining Eq. 36 and Eq. 37 yields

$$C D^2 = \frac{Q}{g} \dots \dots \dots (38)$$

The term D can now be chosen, and C computed because the right-hand member is known. Knowing C , the Kolf vortex number is read from the lower scale of Fig. 10 in which

$$\frac{h}{H} = \frac{K^2}{4\pi^2} \dots \dots \dots (39)$$

from which other elements of the vortex follow. Eq. 1 can be written as:

$$\frac{dp}{w} = \frac{u^2 dr}{g r} \dots \dots \dots (40)$$

Substituting Eq. 2 in Eq. 40 results in

$$\frac{dp}{w} = \frac{K^2 dr}{g r^3} \dots \dots \dots (41)$$

but $dp/w = -dy$ and $r = x$, from Fig. 9, hence

$$-dy = \frac{K^2}{g x^3} dx \dots \dots \dots (42)$$

When Eq. 42 is integrated, Eq. 28 is obtained. Substituting $x = D$ and $y = h$ in Eq. 28 results in

$$K = D \sqrt{2 g h} \dots \dots \dots (43)$$

When the centrifugal effects govern the fluid motion and the Kolf vortex number, K , becomes the parameter governing dynamic similarity, it can be shown from Fig. 9 that at a distance, $x = D$,

$$v = \frac{Q}{\pi D (H - h)} \dots \dots \dots (44)$$

and

$$u = \sqrt{2 g h} \dots \dots \dots (45)$$

Combining Eq. 41 and Eq. 42 with Eq. 21 and Eq. 29 yields

$$K = \frac{C \pi D}{4 (H - h)} \tan \theta \dots \dots \dots (46)$$

The tangent of the angle that the velocity vector makes with the radius is

$$\tan \theta = \frac{u}{v} = \frac{4 V (H - h)}{C \pi D} \dots \dots \dots (47)$$

Because the value of C is determined by the dynamic similarity criteria, K , it is obvious that the value of $\tan \theta$ is dependent both on the depth of flow and the orifice diameter. Therefore, a set of curves similar to Fig. 7 could be drawn for each combination of these terms. In the Iowa tests⁶ a single 4-in. diameter orifice and a nearly constant head of about 2 ft were used.

However, the curves of K versus C in the Wisconsin tests are valid for the entire range of the tests—that is, from 2 in. to 8 in. for D and from 0.1 ft to 2.7 ft for H . Dynamic similarity would indicate therefore that the curves of Figs. 2(e) and Figs. 10 and 11 may be used for orifice diameters and heads considerably outside the values of the Iowa tests.

It appears that whether existing vortices or the design of vortices are considered, there should be no difficulty in determining all the essential characteristics of symmetrical free-flow water vortices.

It should be noted that all previous tests have been made in orifice chambers that were cylindrical and concentric with the orifice. Many problems will not fit these conditions and, therefore, the experimental tests at both Iowa and Wisconsin can give only approximate results for nonsymmetrical installations.

AMERICAN SOCIETY OF CIVIL ENGINEERS

Founded November 5, 1852

TRANSACTIONS

Paper No. 3005

THIXOTROPIC CHARACTERISTICS OF COMPACTED CLAYS

BY H. BOLTON SEED,¹ A. M. ASCE AND
CLARENCE K. CHAN,² J. M. ASCE

WITH DISCUSSION BY MESSRS. EDWARD S. BARBER; D. P. KRYNINE;
AND H. BOLTON SEED AND CLARENCE K. CHAN

SYNOPSIS

Previous investigations of thixotropic effects in saturated clays are summarized. The existence of thixotropic effects in compacted clays and their variation with soil composition is demonstrated. Test data indicating the magnitude of thixotropic-strength increases with time for compacted clays in normal compression tests and under repeated loading conditions are presented. The significant effects of thixotropy on the results of tests conducted using different rates of loading and different frequencies of repeated loading are described and illustrated.

INTRODUCTION

The detrimental effects of disturbance, or remolding, on the properties of natural deposits of saturated clay have long been recognized by soil engineers. For most natural deposits, remolding causes a pronounced reduction in strength even though the composition of the soil is unchanged. This characteristic of saturated clays is expressed by the ratio of the strength of undisturbed material to the strength of remolded material. This ratio is termed the sensitivity of a clay. The following descriptive terms have been used to classify clays with different sensitivities:

NOTE.—Published, essentially as printed here, in the *Journal of the Soil Mechanics and Foundations Division*, in November, 1957, as *Proceedings Paper 1427*. Positions and titles given are those in effect when the paper or discussion was approved for publication in *Transactions*.

¹ Associate Prof. of Civ. Eng., Univ. of California, Berkeley, Calif.

² Asst. Research Engr., Inst. of Transportation and Traffic Eng., Univ. of California, Berkeley, Calif.

Sensitivity	Type of Clay
0 to 1	Insensitive
1 to 2	Low sensitivity
2 to 4	Medium sensitivity
4 to 8	Sensitive
8 to 16	Extra sensitive
16	Quick

It has been observed that heavily preloaded clays are insensitive³ but the vast majority of natural clay deposits have sensitivities in the range from 2 to 8. However, extra-sensitive clays are not uncommon and a number of examples of quick clays, which become practically fluid on remolding, have been reported. The highest value determined (as of 1959) is approximately 150 for a deposit at St. Thuribe, Canada.⁴

For many years the loss of strength accompanying remolding was attributed mainly to a breakdown of a complex structure of the natural clay. However, more recent investigations have shown that for some materials a good proportion of the loss in strength is due to thixotropy and that the sensitivity of some moderately sensitive deposits possibly may be attributed entirely to thixotropy.

THIXOTROPY

As defined originally by H. Freundlich,⁵ thixotropy is an isothermal reversible sol-gel transformation. It has also been described⁶ as a process of softening caused by manipulation or working followed by a gradual return to the original

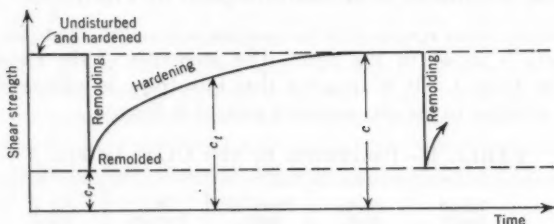


FIG. 1.—STRENGTH REGAINED IN A THIXOTROPIC MATERIAL

strength when the material is allowed to rest. Because the process of softening and stiffening is completely reversible in a thixotropic material, the phenomenon in soils excludes any changes in water content or chemical composition of the soil.

The properties of a purely thixotropic material have been illustrated by A. W. Skempton and R. D. Northey³ as shown in Fig. 1. In its undisturbed

³ "The Sensitivity of Clays," by A. W. Skempton and R. D. Northey, *Geotechnique*, Vol. III, No. 1, March, 1952.

⁴ "Studies of Soil Characteristics: The Earth Flows of St. Thuribe, Quebec," by R. B. Peck, H. O. Ireland, and T. S. Fry, *Soil Mechanics Series No. 1*, Univ. of Illinois, Urbana, Ill., 1951.

⁵ "Thixotropy," by H. Freundlich, Hermann et Cie, Paris, 1935.

⁶ "Report on the Principles of Rheological Nomenclature," by J. M. Burgers and G. W. Scott Blair, *Proceedings, Joint Committee on Rheology of the International Council of Scientific Unions, International Rheologic Congress, Amsterdam, 1948*.

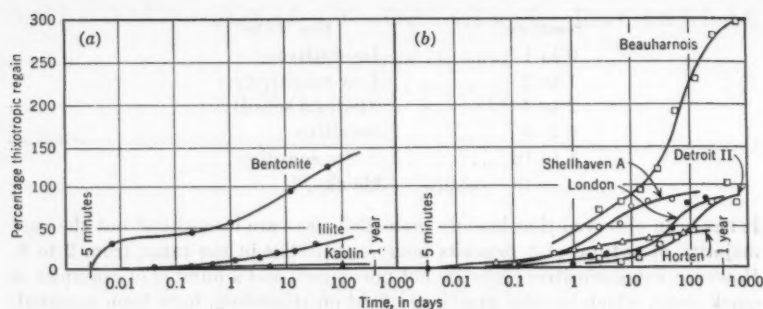


FIG. 2.—THIXOTROPIC REGAIN IN CLAYS

state the material has a shear strength of value c . When tested at the same rate of shear immediately after remolding the shear strength is reduced to a value of c_r . If the material is allowed to remain under constant external conditions, without any change in composition, the strength will gradually increase and after a sufficient length of time the original strength c will be regained.

Fig. 2(a) shows the thixotropic strength increase for three clay minerals as measured by Skempton and Northey, who report:

"Kaolin shows almost no thixotropy and illite shows only a small effect. In contrast, the bentonite shows a remarkable regain at very short time intervals and it is not possible to suggest an upper limit for this material since the strength continued to increase throughout the experiment."

A comparison of these results with the increase in strength due to thixotropy in natural clays is shown in Fig. 2(b). The properties of the clays in Fig. 2 are given in Table 1. It is apparent that thixotropy is influenced by other factors, in addition to the clay minerals present in the soil.

TABLE 1.—PROPERTIES OF THE CLAYS IN FIG. 2

Clay	Liquid limit,* in %	Plastic limit, in %	Plasticity index, in %	Clay fraction, in %	Col. 4 Col. 5	Base exchange capacity
(1)	(2)	(3)	(4)	(5)	(6)	(7)
Fig. 2(a)						
Bentonite	580	40	540	87	6.2	100
Illite clay	73	28	45	50	0.90	8.4
Kaolin	64	38	26	78	0.33	3.8
Fig. 2(b)						
Beauharnois	66	25	41	79	0.52	...
Shellhaven A	97	32	65	51	1.27	31
London	73	25	48	50	0.96	17
Detroit II	51	25	26	65	0.40	...
Horten	29	16	13	38	0.35	18

* Water content \approx liquid limit.

THIXOTROPY IN SATURATED CLAYS

Several investigations have been conducted to determine the extent to which the sensitivity of natural deposits of saturated clays may be attributed to thixotropy. Oreste Moretto,⁷ M. ASCE, conducted tests to measure the strength increases with time of four soils maintained at various constant water contents. Typical results of tests on a Laurentian clay showed that this material, when tested immediately after remolding at a water content approxi-

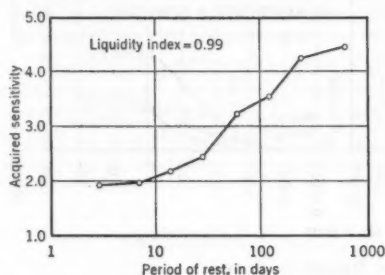


FIG. 3.—EFFECT OF PERIOD OF REST ON STRENGTH OF LAURENTIAN CLAY

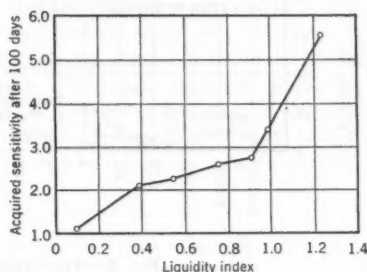


FIG. 4.—VARIATION OF SENSITIVITY WITH LIQUIDITY INDEX FOR LAURENTIAN CLAY

mately equal to its liquid limit, had a strength of only approximately 26 gm per sq cm, but the strength increased to about 114 gm per sq cm after 610 days, by which time it had acquired a sensitivity of about 4.4. The acquired sensitivity is defined as the ratio of strength of clay tested at time t after remolding to the strength of clay immediately after remolding. The rate of increase in acquired sensitivity for this material is shown in Fig. 3, from which it will be seen that further increases in sensitivity even after 610 days are likely to occur.

Similar results were obtained for the other three soils investigated but the strength increase for these materials was not as great as that for the Laurentian clay. Typical results are as follows:

Clay	Liquidity Index	Acquired Sensitivity at 60 days
Laurentian.....	0.99	3.2
Detroit I.....	0.98	2.0
Detroit II.....	0.94	1.6
Mexico City.....	1.03	1.4

The investigation also showed that the acquired sensitivity decreases with a decrease in water content of the clays. The water content of a soil may be conveniently expressed in relation to its liquid and plastic limits by the liquidity index:

$$I_L = \frac{w_n - P_w}{L_w - P_w} \quad (1)$$

⁷ "Effect of Natural Hardening on the Unconfined Compression Strength of Remolded Clays," by O. Moretto, *Proceedings*, 2d International Conference on Soil Mechanics, Vol. I, 1948.

in which I_L is the liquidity index; w_n denotes the natural water content; P_u is the plastic limit; and L_w represents the liquid limit. The acquired sensitivity after 100 days for samples of Laurentian clay at various values of the liquidity index are shown in Fig. 4. After this time a sample of the soil at a water content approaching the plastic limit appears to be practically insensitive.

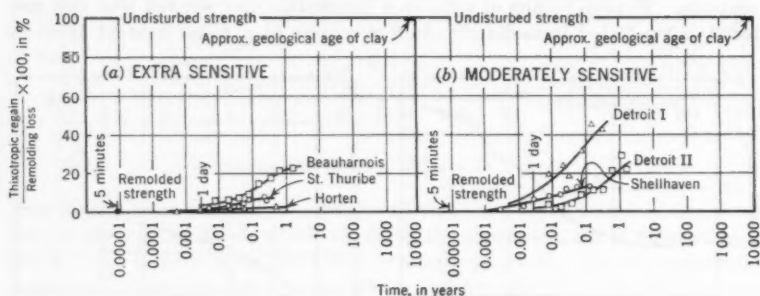


FIG. 5.—THIXOTROPIC REGAIN IN CLAYS

Further data on the thixotropic characteristics of a number of saturated clays were obtained by Skempton and Northey.³ Fig. 2(b) summarizes the rate of increase in acquired sensitivity for five clays at water contents approximating their liquid limits—these data include two of the clays tested by Moretto. In a period of approximately 1 yr three of the clays had acquired a sensitivity

of 2, whereas the Beauharnois clay had acquired a sensitivity of approximately 4. However, although these materials, especially the Beauharnois clay, acquired considerable strength as a result of thixotropy, the strength acquired in 1 yr was, for three of the clays, only a small proportion of the original strength loss which occurred upon remolding.

In comparing the natural sensitivity of a clay with that acquired due to thixotropy, it is necessary to consider the age of the undisturbed soil and the probable increase in thixotropic strength throughout the entire period since its deposition. Comparisons of the rate of

TABLE 2.—PROPERTIES OF CLAYS IN FIG. 5

Clay	Natural sensitivity	Liquidity index
Fig. 5(a)		
Beauharnois	14	1.3
Horten	19	1.2
St. Thuribe	150	1.9
Fig. 5(b)		
Detroit I	2.5	0.60
Detroit II	4.8	0.84
Shellhaven	7.6	0.63

strength increase due to thixotropy with the loss in strength caused by remolding were made for six soils by Skempton and Northey. The results are shown in Fig. 5. The properties for these clays are shown in Table 2.

The proportion of the original strength loss which has been regained at different times after remolding is shown in Fig. 5(a) for three clays of high sensitivity. The estimated age of these clays is about 5,000 yr to 10,000 yr.

It can be observed from the measured rate of strength increase that in this period of time it is unlikely that the clays would regain, due to thixotropy, the full strength loss which occurred on remolding. Although thixotropy can account for part of the original sensitivity, the greater part of the loss in strength that occurs on remolding would seem to be due to a change in structure.

Similar curves for three clays of moderate sensitivity and the same geological age are shown in Fig. 5(b). For these clays there appears to be a reasonable possibility that the entire strength loss on remolding might be recovered over a period of 5,000 yr as a result of thixotropy and the original sensitivity might be due entirely to this phenomenon.

This does not necessarily mean that thixotropy alone can account for the sensitivity of all moderately sensitive clays. Test data reported⁸ by Louis Berger, M. ASCE and John Gnaedinger, A. M. ASCE for two clays of medium sensitivity and the same geological age as those cited previously, show that it is improbable that their original sensitivity could be due entirely to thixotropy.

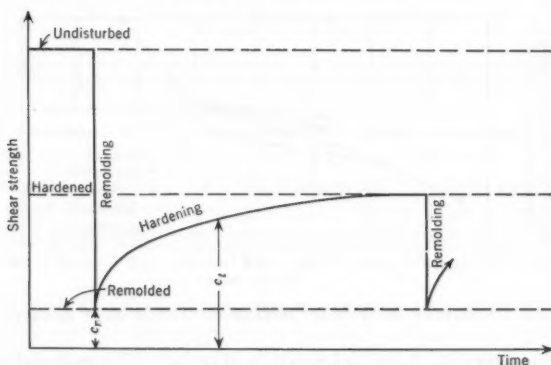


FIG. 6.—STRENGTH REGAIN IN A PARTLY THIXOTROPIC MATERIAL

Thus, most natural clays are not truly thixotropic materials and are likely to recover only part of their original strength loss on remolding due to thixotropy. The influence of remolding on the strength of these materials is thus represented in Fig. 6. However, even a partial recovery of the original loss in strength may, on occasions, have important practical applications.

The difference in thixotropic behavior of different clays might be attributed in part to differences in their liquidity indices. Both Moretto and Skempton and Northey observed that thixotropic-strength regain decreases with decreasing water content below the liquid limit. The ratio of the acquired sensitivity after 100 days at various water contents to the acquired sensitivity at the liquid limit is shown in Fig. 7 for five clays. It will be seen that the thixotropic regain decreases with decreasing water content below the liquid limit, and for the Beauharnois clay appears to approach zero at the plastic limit. The

⁸ "Strength Regain of Clays," by L. Berger and J. Gnaedinger, *Bulletin, A.S.T.M.*, September, 1949.

results presented in Fig. 7, together with the observation that heavily preconsolidated boulder clays are insensitive, led Skempton and Northey to the conclusion that

"heavily over-consolidated clays with water contents typically equal to about the plastic limit are insensitive probably for the following reasons:

- a. thixotropy is negligible at such water contents, and
- b. any meta-stable micro structure that may have existed in the clay at an earlier stage in its geological history, when still under comparatively low overburden pressures, will have been broken down by the intense loading and deformation to which the clay has been subjected."

THIXOTROPY IN PARTIALLY SATURATED AND COMPACTED CLAYS

Little data have been reported to show the influence of thixotropy in partially saturated or compacted clays. Kaziro B. Hirashima, M. ASCE has described⁹ difficulties in compacting a volcanic ash with an extremely high water content

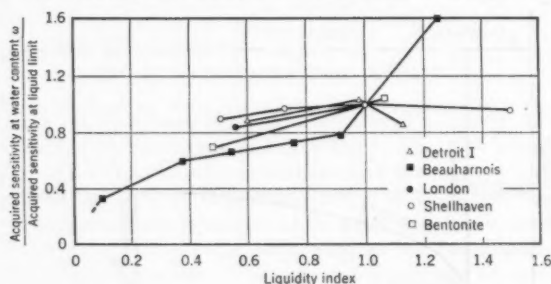


FIG. 7.—EFFECT OF WATER CONTENT ON THIXOTROPIC REGAIN

during the construction of embankments in Hawaii. This material apparently lost strength during compaction but regained strength during periods of rest.

Most clays are normally compacted at water contents nearer the plastic limit than the liquid limit and at these low water contents it would be expected, from the data presented in Fig. 7, that thixotropic effects would be quite small. Furthermore, tests¹⁰ conducted by G. A. Leonards on a compacted clay showed no tendency for this material to increase in strength over a period of approximately 1 yr. However, the analysis of test results during an investigation of soil deformation under repeated loading led to the belief that this is not always the case. As a result the following studies of thixotropic effects on compacted clays were conducted.

EFFECT OF REMOLDING ON DEFORMATION OF COMPACTED CLAY IN REPEATED LOADING TESTS

The first evidence of thixotropic effects in compacted clays was obtained during tests on samples of a silty clay (liquid limit = 37%, plastic limit = 23%)

⁹ "Highway Experience with Thixotropic Volcanic Clay," by K. B. Hirashima, *Proceedings, Highway Research Board, National Research Council, Washington, D. C., 1948.*

¹⁰ "Strength Characteristics of Compacted Clays," by Gerald A. Leonards, *Transactions, ASCE, Vol. 20, 1955.*

subjected to repeated applications of a constant axial stress. In these, and all the subsequent tests described, samples were compacted to a 1.4 in. diameter, and a height of approximately 3.5 in. using the Harvard miniature compactor.

After compaction each specimen was placed between a lucite cap and base and surrounded by two thin rubber membranes with a layer of grease between the membranes. The membranes were sealed against the lucite cap and base

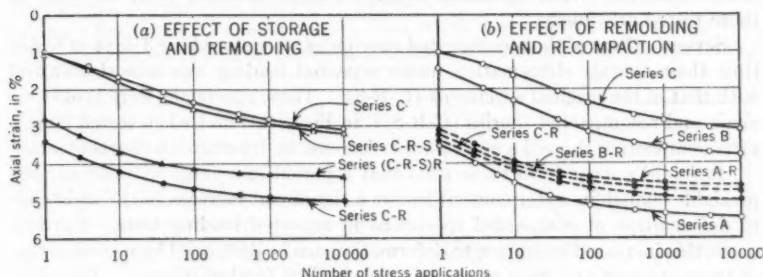


FIG. 8.—TWO SERIES OF TESTS TO DETERMINE THE EFFECT ON DEFORMATION OF SILTY CLAY UNDER REPEATED APPLICATIONS OF CONSTANT STRESS

by means of neoprene O-rings and the entire specimen was placed under water, either in the triaxial compression cell or in a lucite storage tank.

Figs. 8(a) and (b) show the results of two series of tests on specimens having a water content of 18%, a dry density of 112 lb per cu ft, and a degree of saturation of 95%. These specimens (data shown in Table 3) were placed in triaxial compression cells as for a normal type of unconsolidated-undrained test. A

TABLE 3.—DATA FOR SPECIMENS IN FIG 8*

Series	Description	Water content, in %	Degree of saturation, in %	Interval from compaction to test
A	...	18.2	93	22 min
A-R	Series A remolded and recompacted	17.9	96	20 min
B	...	18.5	93	1 day
B-R	Series B remolded and recompacted	17.8	96	20 min
C	...	18.1	93	3 days
C-R	Series C remolded and recompacted	18.0	96	20 min
C-R-S	Series C remolded and recompacted	18.0	96	3 days
(C-R-S)R	Series C-R remolded and recompacted	17.8	97	20 min

* For all specimens: Confining pressure = 1.0 kg per sq cm; repeated deviator stress = 0.8 kg per sq cm; duration of stress application = 0.2 sec and frequency of stress application = 20 per min.

confining pressure of 1 kg per sq cm was applied, but instead of gradually increasing the deviator stress to failure, a deviator stress of 0.8 kg per sq cm was repeatedly applied and removed, each application having a duration of 0.2 sec, with a frequency of 20 applications per min.

In the first series of tests, several specimens were tested 3 days after compaction. The average deformation of these specimens under various numbers

of stress applications is shown by the curve for Series C in Fig. 8(a). The specimens were then broken up and recompactd in the same manner as before. As a result of the slight drying during this operation, the recompactd specimens had slightly lower water contents and slightly higher densities. Several of these specimens were subjected to repeated loading 20 min after recompactd and their deformations are shown by the curve for Series C-R in Fig. 8(a). It can be seen that these specimens deformed approximately twice as much as those tested previously.

Several others of the recompactd specimens were stored for 3 days at which time their average deformation under repeated loading was almost identical with that of the original specimens (C-R-S). These specimens were broken up again and recompactd (Series (C-R-S)R in Fig. 8(a)) and when tested 20 min after compaction showed a considerable increase in deformation characteristics.

It would appear from these tests that a period of storage without any appreciable change in water content causes a significant increase in the resistance to deformation of compactd specimens in repeated loading tests. Furthermore, this increased resistance to deformation can be destroyed by recompactd of the specimens and then once again regained on further storage. The effect is therefore reversible and has the characteristics of thixotropy.

In the second series of tests compactd specimens were tested 20 min after compaction, 1 day after compaction, and 3 days after compaction, with a progressive decrease in the deformation occurring under the same series of repeated stress applications, as shown by the curves for Series A, B, and C in Fig. 8(b). In each case the specimens were broken up and recompactd after being subjected to 10,000 stress applications and then retested 20 min after compaction. The deformations of the recompactd specimens are shown by the dashed curves in Fig. 8(b).

Although the deformations of the original specimens were markedly different, the deformations of the recompactd specimens were almost identical. Therefore, it would appear, that remolding and recompactd can completely destroy the strength increases resulting from different periods of storage and result in specimens having similar deformation characteristics.

It is believed that these two series of tests provide clear evidence of the existence of thixotropic characteristics in compactd clays.

EFFECT OF WATER CONTENT ON THIXOTROPY

In the test series described previously, the specimens were compactd on the wet side of optimum to a degree of saturation of approximately 95%. In order to determine if the thixotropic effects observed were a result of the high degree of saturation of these specimens, a series of tests were conducted on samples of the same soil prepared at different water contents using the same compactive effort. The stress-strain relationships of these samples were determined by normal triaxial compression tests of the unconsolidated-undrained type using a lateral pressure of 1 kg per sq cm.

Samples were prepared at four different water contents. At any one water content four samples were compactd, two of which were tested immediately

after compaction and two tested after a 1-week period of storage. The water content and densities for all specimens are shown in Fig. 9. All the specimens lie essentially on the same compaction curve.

Typical stress-strain curves for samples having high and low degrees of saturation are shown in Fig. 10. In each case the specimens tested after a period of storage had a higher strength than those tested immediately after compaction, though the difference appears to be greater for the specimens having a high degree of saturation. This result is shown more clearly in Fig. 9(b) which shows the stress required to cause 10% strain for all the specimens

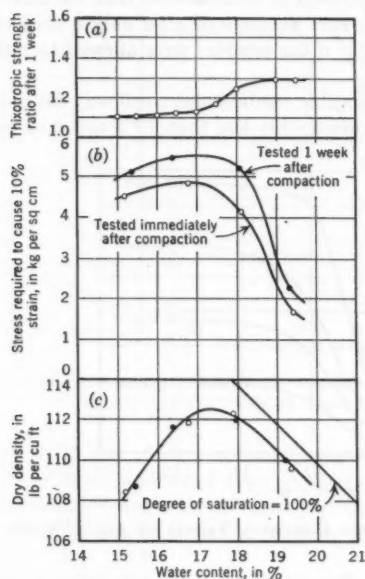


FIG. 9.—COMPOSITION, STRENGTHS, AND THIXOTROPIC-STRENGTH RATIOS FOR SPECIMENS OF SILTY CLAY

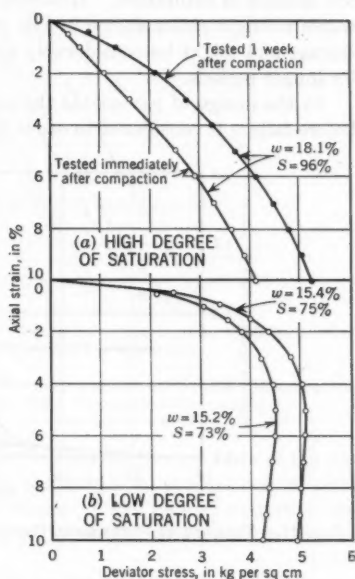


FIG. 10.—STRESS-DEFORMATION CURVES FOR SILTY CLAY (CONFINING PRESSURE = 1 KG PER CM; RATE OF DEFORMATION = 0.03 IN. PER MIN)

tested. It is apparent that a period of storage causes an increase in strength for specimens at all water contents.

In order to compare the magnitude of the thixotropic strength increase, the term "thixotropic-strength ratio" was introduced. This is defined as the ratio of the strength of a specimen tested after time t to the strength of an identical specimen tested immediately after compaction. This term for partially saturated specimens corresponds to the acquired sensitivity of saturated specimens. However, it is necessary to adopt this term because the strength of partially saturated soils is not independent of the confining pressure, and different values

of thixotropic strength ratio may be obtained depending on the magnitude of the lateral pressure used in the triaxial-compression tests.

For the foregoing tests, the thixotropic-strength ratios at different water contents can be determined by a comparison of the ordinates of the two strength-water content curves and the computed values are plotted in Fig. 9(a). There is a pronounced increase in thixotropic effects at a water content of approximately 17% which is close to the optimum water content for the compactive effort used. Therefore, it would appear, that thixotropy in compacted soils is of special significance at higher degrees of saturation and is relatively small at low degrees of saturation. However, it should be remembered that the thixotropic strength ratios shown in Fig. 9(a) were determined after only 1 week of storage and might be considerably greater if the samples were allowed to rest for longer periods.

In the design of pavements the permissible strain which a soil may develop before failure is considered to occur is considerably less than 10% and may be

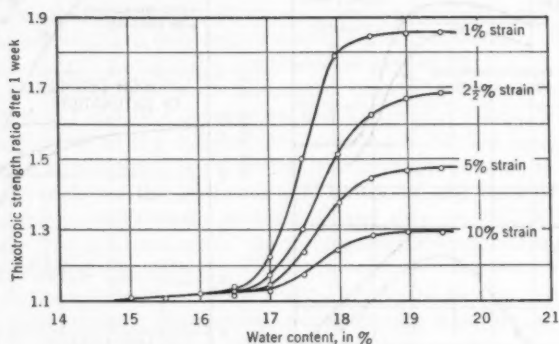


FIG. 11.—THIXOTROPIC-STRENGTH RATIOS FOR DIFFERENT VALUES OF AXIAL STRAIN

more on the order of as much as 5%. The thixotropic strength ratios when failure is defined as the stress required to cause 5% strain are shown in Fig. 11—they are appreciably greater than those determined for higher strains and also become more significant at lower values of water content.

A summary of thixotropic strength-ratios determined at different values of axial strain is shown in Fig. 11. It can be seen that thixotropic effects (a) become increasingly significant at smaller strains; (b) are relatively small for samples compacted on the dry side of optimum for the compactive effort being used; and (c) may be quite appreciable for samples compacted on the wet side of optimum even after 1 week.

INCREASE IN THIXOTROPIC EFFECTS WITH TIME IN NORMAL STRENGTH TESTS

The increase in thixotropic strength with time for compacted samples of the same silty clay soil is shown by the data presented in Fig. 12. The stress-strain

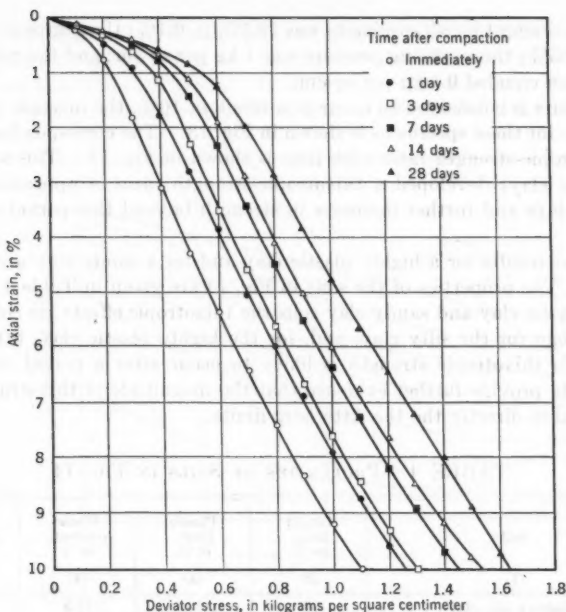


FIG. 12.—EFFECT OF STORAGE AT CONSTANT WATER CONTENT ON STRESS-DEFORMATION RELATIONSHIPS FOR SILTY CLAY WITH HIGH DEGREE OF SATURATION

curves in Fig. 12 were obtained by normal triaxial compression tests of the unconsolidated-undrained type on specimens compacted on the wet side of optimum and tested after different periods of storage. The general pattern of the curves is somewhat similar to that obtained for saturated clays. In Fig. 12

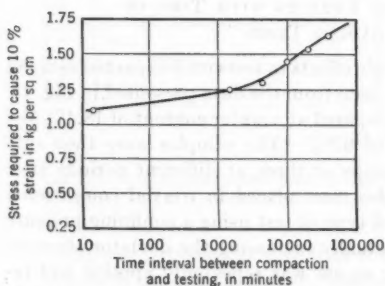


FIG. 13.—EFFECT OF STORAGE AT CONSTANT WATER CONTENT ON STRENGTH OF SILTY CLAY

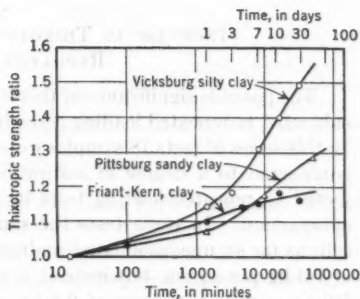


FIG. 14.—INCREASE IN THIXOTROPIC STRENGTH WITH TIME FOR THREE COMPACTED CLAYS

the water content for all specimens was $19.5\% \pm 0.1\%$; the degree of saturation equaled 95%; the confining pressure was 1 kg per sq cm; and the rate of stress application equaled 0.1 kg per sq cm.

If failure is considered to occur at a strain of 10%, the increase in strength with time for these specimens is shown in Fig. 13. The corresponding increase of thixotropic-strength ratio with time is shown in Fig. 14. This soil (Vicksburg silty clay) developed a thixotropic-strength ratio of approximately 1.5 after 28 days and further increases in strength beyond this period are like to occur.

Similar results for a highly plastic clay and for a sandy clay are shown in Fig. 14. The properties of the soils in Fig. 14 are given in Table 4. For the highly plastic clay and sandy clay soils the thixotropic effects are considerably smaller than for the silty clay, and, for the highly plastic clay, little further increase in thixotropic strength is likely to occur after a period of 28 days. These data provide further evidence that the magnitude of thixotropic effects is not related directly the the Atterberg limits.

TABLE 4.—PROPERTIES OF SOILS IN FIG. 14

Soil	Liquid limit, in %	Plastic limit, in %	Water content, in %	Degree of saturation, in %
(1)	(2)	(3)	(4)	(5)
Vicksburg silty clay	37	23	19.5	95
Pittsburg sandy clay	35	20	17.4	96
Friant Kern clay	59	35	22	95

Consideration has been given to the fact that the observed increase in strength with time might possibly be due to a redistribution of water in the specimens resulting from the method of storage. However, a careful study of the water content at the outside and inside sections of specimens has failed to reveal any measurable difference.

INCREASE IN THIXOTROPIC EFFECTS WITH TIME IN REPEATED LOADING TESTS

The possible significance of thixotropic effects in tests on compacted samples subjected to repeated loading is readily seen from the data presented in Fig. 15. In this series of tests 18 samples were prepared at a water content of 18.4% and compacted to a degree of saturation of 92%. The samples were then subjected to repeated-loading tests in groups of three at different periods after compaction. In these tests the samples were placed in triaxial compression cells as for an unconsolidated-undrained type of test using a confining pressure of 1.0 kg per sq cm, but instead of gradually increasing the deviator stress to failure, a deviator stress of 0.8 kg per sq cm was repeatedly applied and removed, each application having a duration of 0.2 sec, with a frequency of 20 applications per min. The tests were continued until 10,000 stress applications had been applied to each specimen.

The deformations of the samples resulting from different numbers of stress applications are shown in Fig. 15—the curves represent the averages for the three specimens tested in each group. It will be seen that a 3-day period of storage prior to testing caused a reduction of almost 50% in the deformations of the

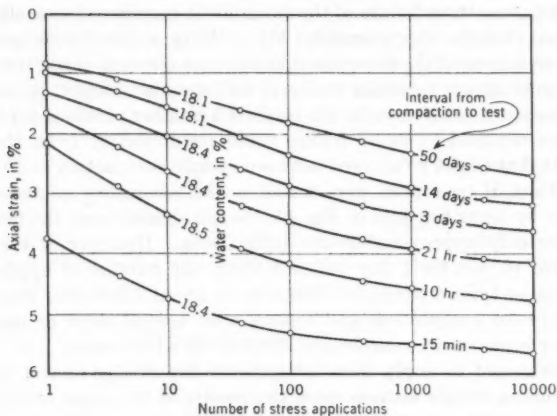


FIG. 15.—EFFECT OF STORAGE AT CONSTANT WATER CONTENT ON DEFORMATION OF SILTY CLAY UNDER REPEATED APPLICATIONS OF CONSTANT STRESS

specimens and that further reductions resulted from longer periods of storage. The large increase in resistance to deformation occurring during the first 3 or 4 days after compaction is shown clearly in Fig. 16(a), and the probability of further stiffening even after 50 days of storage is shown in Fig. 16(b).

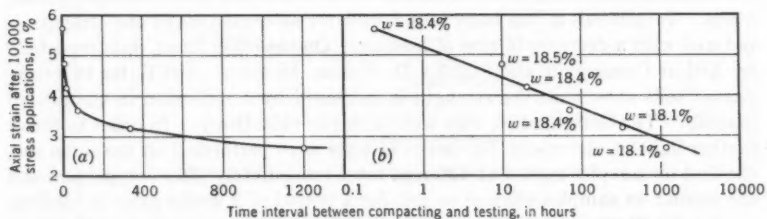


FIG. 16.—DECREASE IN DEFORMATION OF SILTY CLAY UNDER REPEATED LOADING RESULTING FROM STORAGE AT CONSTANT WATER CONTENT

It is interesting to note that thixotropic stiffening appears to have greater effects in these tests than in the normal type of strength tests. After 3 days the same soil had a thixotropic strength ratio of only 1.2 in a normal strength test, yet its deformation in repeated loading tests was reduced approximately 50%. This discrepancy is not surprising, however, in view of the fact that

thixotropic effects become increasingly significant at smaller strains and the deformation in the repeated load tests did not exceed approximately 6%.

The change in deformation characteristics which may result from a period of rest after compaction is indicative of the great difficulty encountered in predicting the probable life of pavements from laboratory tests. In some pavement-design procedures failure of the subgrade is considered to occur when the deformation exceeds approximately 5%. Using a triaxial-compression-test procedure to represent the stress conditions on an element of soil under a pavement and postulating vehicular traffic of uniform size, weight, speed, and frequency, enormous differences in the predicted number of wheel loads or stress applications required to cause failure could result simply from the different rest periods that might be allowed between sample compaction and the start of testing. Thus, if specimens were tested in the laboratory immediately after compaction by using the data in Fig. 15, the soil should reach the failure strain of 5% after only approximately 20 applications. However, if the specimen were allowed to rest for 1 day before testing, the number of applications required to cause failure would be increased to about 1,000,000, whereas if the interval between compaction and testing were several days or more, failure might never occur under conceivable numbers of wheel loads.

It is not meant to imply that the probable life of a pavement can be predicted in such a simple fashion from the results of this type of test, but the general nature of the effect and its possible significance are illustrated by these comparisons. The possible error in the predicted life of a pavement that might result from computations based on tests conducted soon after sample compaction is also apparent.

EFFECT OF RATE OF LOADING ON THE STRENGTH OF COMPACTED CLAY

The thixotropic characteristics of a compacted clay may have important effects in investigations of the influence of rate of loading on the strength of such a soil. In general, it has been found that for saturated clays the strength is reduced with a decrease in rate of loading. On the other hand, data reported¹¹ by Arthur Casagrande and Stanley D. Wilson, Members, ASCE, for two compacted soils show that the strength is increased by a reduction in the rate of loading. The latter finding may well be due to thixotropy. In order to throw further light on the result, two series of tests were performed on the same soil, the first on samples loaded at different rates immediately after compaction and the second on samples allowed to rest for a period of 2 weeks prior to loading.

A total of twenty samples were compacted at a water content of 18.5% \pm 0.2% to a dry density of 112 lb per cu ft \pm 0.2 lb per cu ft, corresponding to a degree of saturation of 96%. Five pairs of these samples were subjected to unconsolidated-undrained triaxial compression tests, using a confining pressure of 1 kg per sq cm immediately after compaction (curve labeled "Immediately" in Fig. 17(a)) using the following rates of loading: (a) 2-kg load increments at 30-sec intervals; (b) 2-kg load increments at 1-min intervals; (c) 2-kg load incre-

¹¹ "Effect of Rate of Loading on Strength of Clays and Shales at Constant Water Content," by A. Casagrande and S. D. Wilson, *Geotechnique*, Vol. II, No. 3, June, 1951.

ments at 10-min intervals; (d) 2-kg load increments at 1-hr intervals; and (e) 2-kg load increments at 1-day intervals. The other ten specimens were stored in rubber membranes under water for 18 days and then tested in pairs using the same test procedure and essentially the same rates of loading.

Thus, Fig. 17(a) shows the average strength of the pairs of specimens (determined at the stress required to cause 10% strain) plotted against the time of loading, that is the time required for the specimens to reach 10% strain.

For the specimens tested immediately after compaction, there was a slight but gradual decrease in strength for times of loading between 5 min and 100 min, but a progressive increase in strength for times of loading greater than 100

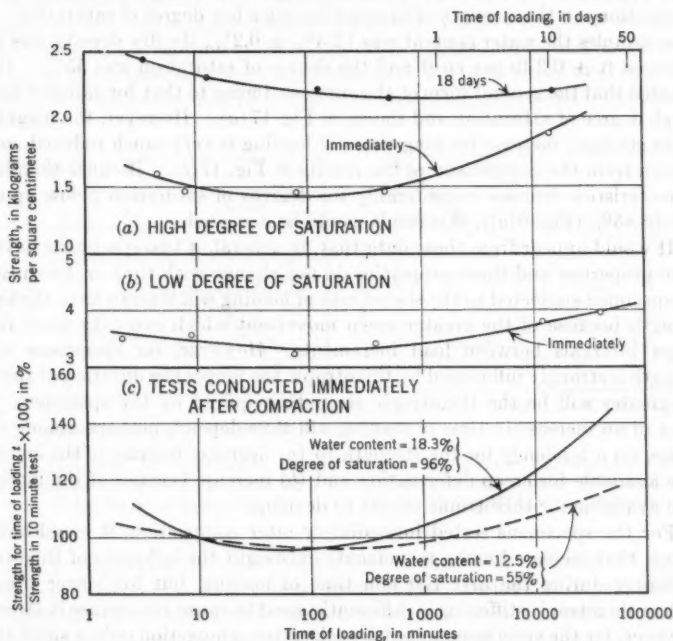


FIG. 17.—EFFECT OF RATE OF LOADING ON STRENGTH OF SILTY CLAY

min. For a test lasting 10 days the strength was about 30% greater than that measured in a standard 10-min test.

For the specimens tested 18 days after compaction increases in time of loading up to 1 day caused a small decrease in strength, and there was only a very slight increase in strength when the time of loading was increased to 10 days. However, the strength of a specimen in a test lasting for 10 days was about 4% less than that in a test lasting 10 min.

These results would seem to indicate that the pronounced increase in strength at long times of loading for specimens tested immediately after compaction is

due primarily to the normal thixotropic increase in strength with time of the specimens. For the specimens tested after being stored for 18 days the greater part of the thixotropic strength increase had occurred before the tests were begun and the relatively small thixotropic effects during the following 10 days for which the longest test was conducted had only a slight influence on the results.

Further evidence that the influence of rate of loading on the strength of compacted samples tested immediately after compaction depends largely on the thixotropic characteristics of the samples is provided by the results presented in Fig. 17(b). These data were obtained in tests on samples of the same silty clay soil and show the effect of rate of loading, for tests begun immediately after compaction, on the strength of samples having a low degree of saturation. For these samples the water content was $12.5\% \pm 0.2\%$, the dry density was 104.8 lb per cu ft \pm 0.3 lb per cu ft and the degree of saturation was 55%. It will be noted that the general form of the curve is similar to that for samples having a high degree of saturation and shown in Fig. 17(a). However, the magnitude of the strength increase for long times of loading is very much reduced, as will be seen from the comparison of the results in Fig. 17(c). Because thixotropic characteristics decrease considerably for degrees of saturation below approximately 85% (Fig. 9(a)), this result would be expected.

It would appear from these data that, in general, if two specimens have the same properties and these properties do not change with time or deformation, the specimen subjected to the slower rate of loading will tend to have the lowest strength because of the greater creep movement which can take place in the longer intervals between load increments. However, for specimens whose strength is strongly influenced by thixotropy, the longer the duration of the test, the greater will be the thixotropic strength acquired by the specimen. The effect of an increase in time of loading will thus depend, perhaps among other things, on a tendency for the strength to (a) decrease because of the increased time available for creep deformation and (b) increase because of the increased time available for thixotropic effects to develop.

For the specimens tested immediately after compaction, it could thus be argued that increased creep movements outweigh the influence of thixotropic hardening during the first 100 min time of loading, but for longer times of loading thixotropic stiffening is sufficiently great to cause an increase in strength. However, for the specimens tested 2 weeks after compaction only a small thixotropic strength increase is likely to occur in the interval from 14 days to 24 days, during which the longest test was being conducted (Fig. 14). Thus, the increased creep movement will tend to control the result leading to the observed decreases in strength with increased time of loading.

Although this simple concept of the phenomenon would seem to be adequate to explain the observed results, the other factors are also likely to influence the behavior of specimens in long time test under slow rates of loading. For a material having no structural sensitivity, but some sensitivity due to thixotropy, tests on undisturbed samples might give results similar to those on newly compacted clay, even though the material exhibits no further increase in

thixotropic strength with time. Deformations of such a soil will cause some disturbance and a loss of thixotropic strength. If the total time of the test is insufficient for the thixotropic strength to be recovered, the strength will decrease with an increase in time of loading. However, if the rate of loading is so slow that the soil can regain some strength between load increments, the strength might begin to increase with increased time of loading. Thus, the relationship between strength and time of loading might be similar to the curves in Fig. 17(c), although the upward trend in the curve would be expected to occur at a longer time of loading than those shown.

That a soil may gain strength in the intervals between stress applications is shown by the test data in Figs. 18 and 19. Fig. 18 shows the results of triaxial compression test on samples of silty clay compacted to a degree of saturation of 96% at a water content of $19.1\% \pm 0.1\%$. Each curve in Fig. 18 is the average of three tests on identical specimens. The first group (curve labeled "28 days") of specimens was tested 28 days after compaction and loaded slowly

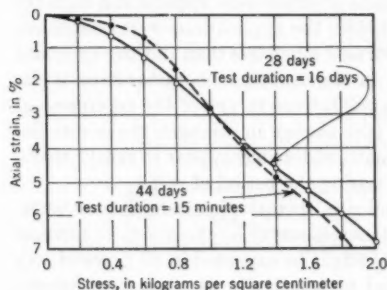


FIG. 18.—INCREASE IN RESISTANCE TO DEFORMATION OF SILTY CLAY DUE TO SLOW RATE OF LOADING

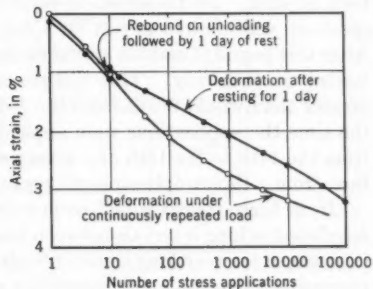


FIG. 19.—EFFECT OF PERIOD OF REST ON DEFORMATION OF SILTY CLAY UNDER REPEATED LOADING

(0.15 kg per sq cm per day) over a period of 16 days with intervals of 1 day between load increments. The second group (curve labeled "44 days") of specimens was tested 44 days after compaction (that is, when the tests on the first group were completed) and loaded to failure in a period of 15 min with only a 1-min interval between load increments. It will be seen that because these specimens were tested at a longer time after compaction, they were initially stiffer than the first group. However, as the deformation increased they became weaker than the first group, despite the fact that they were being loaded at a later date. This would seem to indicate that the specimens subjected to a slow rate of loading possessed some source of strength not available to those subjected to a rapid rate of loading. The source of this strength could not be due to the normal increase in thixotropic strength with time as they were tested at an earlier date than the others. Furthermore, the long interval between load increments permits more creep to occur and would be expected to cause a

greater strain under any given applied stress. Therefore, it seems reasonable to conclude that the source of this strength stems primarily from the fact that long time intervals between stress applications enable the specimens to regain some of the thixotropic strength which is lost when they are first deformed by the application of a stress increment. On the other hand, with a high rate of loading there is no time between stress increments for such a strength regain to occur and as a result, specimens which are initially stronger (Fig. 17(c)) lose a greater proportion of their thixotropic strength. At higher strains they may have lower strengths than specimen subjected to very slow rates of loading.

The strength regain of a compacted soil specimen following deformation is also illustrated by the data in Fig. 19. Two identical specimens ($w = 19.0\%$) were subjected to repetitions of the same deviator stress (repeated stress = 0.7) kg per sq cm, duration of stress application = 0.2 sec, and confining pressure = 1.0 kg per sq cm) at a frequency of 20 applications per min. On one specimen the applications were continuous until about 10,000 repetitions had been applied. On the other, 10 repetitions of stress were applied and then the specimen was allowed to rest for 1 day before the applications were continued. After this period of rest the specimen deformed much less than did the specimen loaded continuously. This difference in deformation characteristics is far greater than would result from the 1-day difference in age of the specimens at the time the applications were applied (the change in strength characteristics from the 14th to the 15th day is very small) and would appear to result, therefore, from a thixotropic-strength regain during the period of rest.

If, as these results would seem to indicate, thixotropic strength may be redeveloped in long intervals between load increments or applications, an increase in strength for very long times of loading might be expected in all types of soils possessing thixotropic characteristics and no sensitivity as a result of natural structure. This would be expected to apply to saturated clays as well as compacted clays. The work³ of Skempton and Northey has indicated that the sensitivity of some natural deposits of saturated clay may be due entirely to thixotropy. For such materials it would be expected that the effect of rate of loading on strength would be similar to the upper curve in Fig. 17(a). However, if a soil has considerable sensitivity as the result of natural structure the upward trend in the curve for long times of loading is unlikely to occur. Strength loss due to structural disturbance on loading is likely to exceed any strength regain by thixotropy between load increments, with the result that the strength will decrease progressively with an increase in time of loading. Such results for sensitive clays have been reported¹¹ by Casagrande and Wilson.

The foregoing material does not take into account the sudden loss of strength which occurs in some soils at high strains, or possible strength changes resulting from changes in void ratio or grain arrangement that may occur during loading. Whereas these factors might also affect the results, it would appear that thixotropic influences and structural disturbances are likely to be the dominating influence and might reasonably account for the observed effects of rate of loading on the strength of most soils.

EFFECTS OF FREQUENCY OF STRESS APPLICATION ON SOIL DEFORMATION UNDER REPEATED LOADING

Because the data in Fig. 17(c) indicate that there may be a significant strength regain during periods of rest following deformation of a compacted clay possessing appreciable thixotropic characteristics, it would seem logical to expect some influence of frequency of stress application on the deformation of soils possessing thixotropic strength when they are subjected to repeated loading. A comparison of the deformations of samples of silty clay subjected to repeated applications of a constant stress of the same magnitude and duration, but with frequencies of application of 20 per min and 1 per 2 min is shown in Fig. 20. The tests were started 1 month after compaction of the specimens.

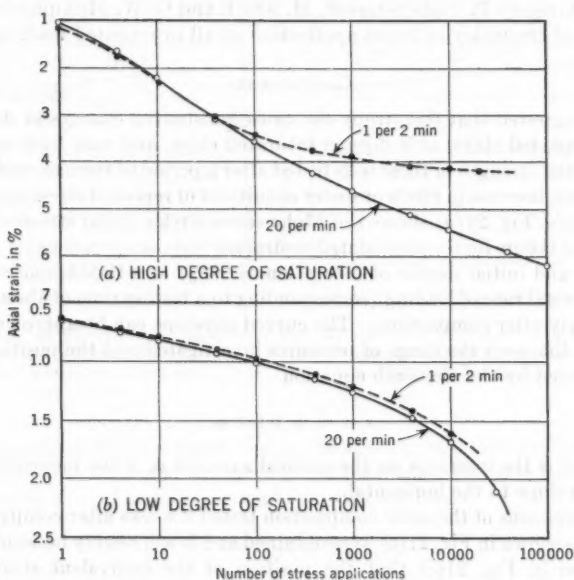


FIG. 20.—EFFECT OF FREQUENCY OF REPEATED STRESS APPLICATION ON DEFORMATION OF SILTY CLAY

In Fig. 20(a) data is shown for samples having a high degree of saturation ($w = 18.5\% \pm 0.15\%$ and degree of saturation = 95%) and, thus, 1 month after compaction possessing appreciable thixotropic strength. In these tests the axial stress was 0.75 kg per sq cm and the duration of the stress application was 0.33 sec. There is considerably more deformation of the specimens for the higher frequency of stress application than for the lower frequency of application. Apparently this is due to the greater thixotropic regain between stress applications for the lower frequency. It should be noted that this effect is due to a regain of the thixotropic strength lost during the deformation occurring

under the first few load increments and not to the normal increase in thixotropic strength of the specimens with time. The magnitude of the latter effect after 30 days of storage is negligible compared with that observed in the tests.

It would be expected, from the data previously presented, that for soils in which thixotropic effects are small the influence of frequency of stress application on the deformation occurring under repeated loading would also be small. This is shown by the data in Fig. 20(b) for samples of the same silty clay compacted to a low degree of saturation ($w = 14.0\% \pm 0.1\%$ and the degree of saturation = 70%). In these tests the axial stress was 3.0 kg per sq cm and the duration of the stress application was 0.33 sec. Thixotropic effects in these samples are small and, as shown in Fig. 20(b), variations in frequency have only slight effects in repeated loading tests. It is interesting to note in this connection that Gregory P. Tschebotarioff, M. ASCE and G. W. McAlpine found¹² no influence of frequency of stress application at all in repeated loading tests on sands.

CONCLUSIONS

It is suggested that thixotropy can cause substantial changes in strength in some compacted clays, as it does in saturated clays, and may have significant effects on the strength of these soils tested after a period of storage, under conditions of slow increase in stress or under conditions of repeated stress application. For example, Fig. 21(a) shows the Mohr stress circles (total stresses) and the envelope of failure for unconsolidated-undrained tests on specimens ($w = 18.9\% \pm 0.15\%$ and initial degree of saturation = 96%) of a thixotropic soil tested using a normal rate of loading (corresponding to a testing time of about 10 min) immediately after compaction. The curved envelope can be approximated by a straight line over the range of pressures investigated and the position of this line expressed by the Coulomb equation

$$s = c_e + p \tan \phi_e \dots \dots \dots (2)$$

in which c_e is the intercept on the vertical axis and ϕ_e is the inclination of the failure envelope to the horizontal.

For specimens of the same composition tested 2 weeks after compaction the test results shown in Fig. 21(b) were obtained and it will readily be seen from the comparison in Fig. 21(c) that the position of the equivalent straight-line-strength envelope is significantly changed. However, the slope of the line is essentially the same and the change is confined simply to the intercept on the shear-stress axis. It would be expected from the nature of thixotropy that a change in strength resulting from a period of storage would be independent of the confining pressure and would be reflected by the intercept on the vertical axis of the Mohr diagram. However, because the deformation occurring during these tests will destroy some of the original thixotropic strength gain, it would appear that in the standard type of strength test having a duration of about 10 min, samples having the same initial composition are likely to lose the same proportion of their original thixotropic strength. However, the latter would

¹² "The Effect of Vibratory and Slow Repetitional Forces on the Bearing Properties of Soils," by G. P. Tschebotarioff and G. W. McAlpine, *Technical Development Report No. 57*, C.A.A., October, 1947.

not be true, for samples tested at the same age with different rates of loading. In this case specimens tested with a slower rate of loading have a greater thixotropic regain following deformation and ultimately exhibit a higher strength than those tested with a faster rate of loading. This is shown by the data in Fig. 22, which compares the envelopes of failure for similar specimens tested at the same age but with widely different rates of loading. Again it is apparent that the effect of rate of loading is confined to a vertical displacement of the envelope of failure and is independent of the confining pressure.

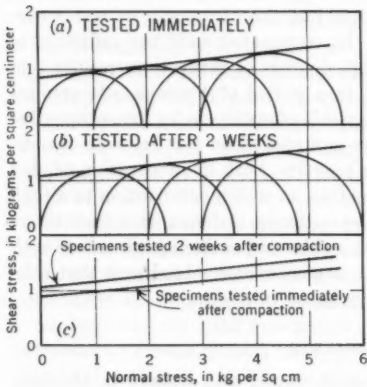


FIG. 21.—EFFECT OF STORAGE AT CONSTANT WATER CONTENT ON ENVELOPE OF FAILURE FOR UNDRAINED TESTS ON SILTY CLAY

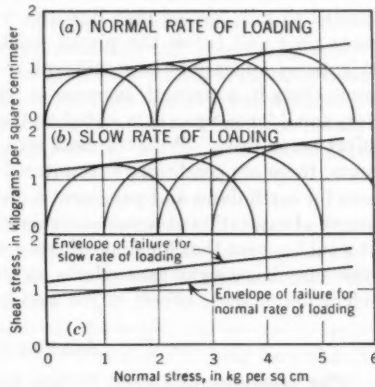


FIG. 22.—EFFECT OF RATE OF LOADING ON ENVELOPE OF FAILURE FOR UNDRAINED TESTS ON SILTY CLAY

Thus, it appears that the value of c_e in the approximate Coulomb equation is a function of both the age of the specimen at the start of the tests (t_a) and the time of loading (t_e). Therefore, it might be expressed as

$$c_e = c f(t_a) \phi(t_e) \dots \dots \dots (3)$$

in which c denotes the value of the intercept resulting from causes other than thixotropy, and $f(t_a)$ and $\phi(t_e)$ are functions of the age of specimens and time of loading, respectively.

It is recognized that the foregoing result was obtained from a comparison of strength envelopes for total stresses in triaxial compression tests and that a more conclusive determination of the effects of thixotropy could have been made if the envelopes for effective stresses had been used. Also, the effects of changes in rate of loading on soil strength may be due to other factors in addition to thixotropy. Nevertheless, the result is apparently applicable to unconsolidated-undrained tests and there would seem to be sufficient evidence that somewhat similar effects might be obtained for envelopes of failure based on effective stresses.

Furthermore, the results would be expected to apply to all types of soil possessing thixotropic strength, but no sensitivity due to natural structure. These would include remolded saturated clays after they had developed thixotropic strength following a period of rest and apparently to some natural clays whose sensitivity may be due entirely to thixotropy. A study of the influence of thixotropy on the results of tests conducted at widely different rates of loading might well serve to clarify the meaning of the terms "true cohesion" and "true angle of internal friction" for saturated clays.

It would also appear from the results that thixotropic changes are not limited to soils having high liquidity indices but can also occur at water contents near and below the plastic limit. In compacted soils the influence of thixotropy appears to be significant at high degrees of saturation, resulting in some cases in a strength increase of 50% in a period of 4 weeks. It appears very small for samples compacted on the dry side of optimum for the compactive effort being used. Whereas most soils are compacted on the dry side of optimum, there are conditions encountered in practice, both in compaction of clay soils for earth dams and pavement construction, in which compaction to a high degree of saturation at water contents above optimum is desirable or inevitable. It would appear that for some of these soils a thixotropic strength increase with time may have significant effects on their behavior under load and that consideration of these effects might well be included in design.

ACKNOWLEDGMENTS

The assistance of Lowell Shifley, Gerald L. Baker and Robert L. McNeill, Junior Members, ASCE, in performing many of the tests described in this paper, and of George T. Dierking, A. M. ASCE, who prepared the original drawings, is gratefully acknowledged.

DISCUSSION

EDWARD S. BARBER,¹³ A. M. ASCE.—It should be noted that the authors measured thixotropy on samples molded by a kneading type of compaction, whereas Leonards reported¹⁰ a constant strength with time for samples molded by static compaction. Some thixotropy is caused by redistribution of non-uniformly distributed moisture to make a more uniform, and therefore stronger, material.

The tabulation under the heading, "Thixotropy in Saturated Clays," shows no thixotropy for good mixing and static molding, but shows appreciable thixotropy due to redistribution of moisture after poor mixing and after kneading compaction, which produces nonuniform moisture across shear surfaces.

The equalization of moisture after shearing is a factor that must be considered in studying the thixotropy exhibited by undisturbed clays after remolding.

D. P. KRYNINE,¹⁴ M. ASCE.—The laboratory investigation into the rheology of compacted clays has been excellently executed and clearly presented. Although the measurements were made with instruments of high precision, the conclusions are only qualitative in character.

Definitions.—In 1935 Freundlich described⁵ the isothermal reversible transformation of a true sol to a true gel and vice versa as a "limiting case of thixotropy." According to Freundlich "thixotropy also includes some related phenomena." Pastes of clay including bentonite, for example, "may show an extremely pronounced thixotropic behavior." In a dissertation by H. L. Roeder it is stated¹⁶ that the concept of thixotropy was "gradually extended to all those systems which are liable to a temporary change of consistency upon mechanical deformation." This is practically the same point of view that prevails at the present time (1958). Thus, the concept of thixotropy presented⁶ by J. M. Burgers and G. W. Scott Blair does not advance anything different from Freundlich's widened concept. It is to the credit of Messrs. Seed and Chan that their paraphrase of the definition of thixotropy is clearer and more acceptable to the engineer than the original version. The definition given³ by Skempton and Northey is brief and clear, but leaves unexplained the term "bonding forces." The thixotropic process consists of two steps—a destructive one and a constructive one. The definition covers only the constructive step.

Rheologists distinguish thixotropy of shape (or volume), and thixotropy of rheological properties. Soil strength should be considered as a rheological property of the soil. The rheologists use the terms "recovery" and "restoration" for the constructive step of these two types of thixotropy. Skempton and Northey and the authors use the term "regain." The writer believes that these three terms may be used interchangeably.

¹³ Univ. of Maryland, College Park, Md.

¹⁴ Cons. Engr., Berkeley, Calif.

¹⁶ "Rheology of Suspensions: a Study of Dilatancy and Thixotropy," by H. L. Roeder, H. J. Paris, Amsterdam, 1939.

Since Freundlich's work, little was done on thixotropy during the period from 1935 to 1948. Some work was done, however, by Henry Green and R. N. Weltmann¹⁶ and Ernst Ackermann.¹⁷

Stirred State of Compacted Clays.—A substance that at proper occasions shows thixotropic effects, is termed a "thixotropic substance" by the rheologists. As stated, clays have been found to be thixotropic substances by Freundlich. Also, Skempton and Northey found thixotropy with basic clay minerals. A thixotropic substance (that is, clay) if subjected to a deformation process¹⁸ "exhibits a change in rheological properties," particularly partial loss of strength and occasionally change in shape or even volume. Rheologically, it is then in the so-called stirred state¹⁹ which is not a state of equilibrium, however, and the substance in this state is always subject to a gradual change, particularly thixotropy. Compacted clays may be in this stirred state just by virtue of compaction. Hence, rheological effects (particularly thixotropy) may be expected in them.

Clay Structure and Structure-Building Factors.—Clay strength is controlled predominantly by its microstructure. Macrofeatures (such as inclusions or fissures) may have only a local influence on the strength of the clay mass.

Clay particles are tiny crystals, mostly platy, that are composed of exceedingly thin atomic sheets. When dry, a clay mass is electrically neutral and does not show attractive properties. However, when placed in water, individual clay platelets become negatively charged and individual atoms constituting the clay material are either positively or negatively charged—these are cations and anions, respectively.

The negative charge of the clay particles in water is the reason for what is termed clay activity. The manifestations of the clay activity are (a) the clay particle may attract cations of aluminum, iron, sodium, potassium, and other elements that may constitute clay and are swarming in the clay suspension around the clay particles; (b) the clay particle may attract water from the ambient suspension; and (c) the clay particle may exchange the attracted cations against those swarming around especially if some electrolyte solution is added to the suspension. This is the so-called base exchange or, more appropriately, the cation exchange.

So far as attraction of water by the clay particles is concerned it should be remembered that the water molecules are dipoles and may be visualized as exceedingly short flexible strings carrying a positive charge at one end and a negative charge at the other. Thus, a water molecule may be attached by its positive end to a clay particle and by its negative end to a cation or another water molecule. It is understandable that in a row of molecules attached to each other, starting at the surface of a particle, the attraction force gradually decreases. It is at a maximum just close to the clay particle where it is heavily reinforced by the attractive van der Waals-London forces (the latter being

¹⁶ "Thixotropy," by Henry Green and R. N. Weltmann, *Colloid Chemistry*, Vol. 6, 1946, pp. 328-347.

¹⁷ "Thixotropie und Fließeigenschaften feinkörniger Boeden," by Ernst Ackermann, *Geologische Rundschau*, Vol. 36, 1948, pp. 10-29.

¹⁸ "Report on the Principles of Rheological Nomenclature," by J. M. Burgers and G. W. Scott Blair, *Proceedings, Joint Committee on Rheology of the International Council of Scientific Unions, International Rheologic Congress, Amsterdam, 1948*, pp. 41-42.

¹⁹ *Ibid.*, p. 43.

operative in all kinds of matter). At a short distance from the clay particle these forces practically vanish.

Thus, in a saturated clay a portion of its water is strongly attached to the clay particles, representing an exceedingly thin but highly rigid framework of the clay mass. Inside of this framework there are clay particles, and outside of it, there is (a) a not-so-strongly-attracted but nevertheless immobilized layer of water and (b) around this layer, free water. A clay mass with a high degree of saturation (most of the experimental clay examined herein) is, in reality, a clay suspension and may be treated as such.

Clay particles, anions, cations, water in different states of attraction, and the electrical forces constitute the structure of compacted clay. The fruitful idea of considering the electrical forces as a component of any clay structure belongs to T. William Lambe.^{20,21} The explanation of thixotropic processes then becomes relatively simple.

Residual and sedimentary clays are built in two different ways. A residual clay deposit is formed essentially by physical and chemical destruction of the parent rock, and is subject to thixotropic changes if compacted. The thixotropic process will be intensified if the compacted clay is loaded or otherwise stirred (to use the rheological term).

A sedimentary clay is built by the process of sedimentation which occurs when clay particles settle and are accommodated in their places by gravity and mutual attraction. Flocculation is a particular case of the sedimentary clay building process in which the repulsing forces acting on the particles charged with electricity of the same sign are overcome by the van der Waals-London forces. Flocculation is generally accompanied by the base exchange. Besides gravity and mutual particle attraction there are many other structure-building factors in a sedimentary clay, such as the nature of the attracted cations, water-sorption characteristics, particle orientation and spacing, capillary tensions (especially in the partly saturated soils), and similar items.^{22,23}

When compacted clay is mechanically disturbed (for example, by loading), some structure-building factors may decrease in intensity or completely vanish whereas some other factors may even increase in intensity. The two clay structure-building factors that always survive a mechanical disturbance are gravity and attraction forces (or more broadly, clay activity). Thus, these two factors are responsible, fully or partly, for recovery and restoration processes. Attraction forces in clay may be operative only if there is enough water around the particles. All writers on thixotropy emphasize this requirement. Freundlich, for example, states²⁴ that "thixotropy implies that the systems of particles enclose a fairly large amount of liquid, i.e., they must be loosely packed." In reality, a loose structure is not a cause of thixotropy, but a contributing

²⁰ "The Structure of Compacted Clay," by T. William Lambe, *Proceedings Paper 1654*, ASCE, May, 1958.

²¹ "The Engineering Behavior of Compacted Clay," by T. William Lambe, *Proceedings Paper 1655*, ASCE, May, 1958.

²² "The Structure of Inorganic Soil," by T. William Lambe, *Proceedings-Separate 315*, ASCE, October 1953.

²³ Discussion by James K. Mitchell of "Strength Characteristics of Compacted Clays," by Gerald A. Leonards, *Transactions*, ASCE, Vol. 120, 1955, p. 1465.

²⁴ "Thixotropy," by H. Freundlich, Hermann et C^{ie}, Paris, 1935, p. 16.

factor. Thus, one of the reasons why the montmorillonites show more thixotropy than the kaolinites is that the loose packing of their atomic sheets permits water to enter a particle. Thixotropic effects also take place in the case of low water content, as demonstrated in the paper.

Thixotropic and Partially Thixotropic Clays.—Thixotropy is not an intrinsic property of a clay. Clay may be more or less thixotropic according to the degree of clay activity in the presence of water, and efficiency of other structure-building factors in operation. As far as compacted clays are concerned they are all potentially thixotropic. From this point of view a subdivision of clay materials does not appear justified. In fact, Fig. 1 if applied to clays is a particular case of Fig. 6. The level marked "hardened" in Fig. 6 may coincide with the level marked undisturbed or even may be higher. The latter case corresponds to the building up of a completely new clay structure by the structure-building forces. A well-known example is pile driving into clay of low sensitivity with considerable increase in shearing strength of the material around the pile—in strict terms, this is no longer thixotropy.

Thixotropic-Strength Ratio.—In Fig. 9(a) the thixotropic-strength ratio may not be sensitive enough. Also, it may be misleading as in the following example:

(a) Consider samples at 19% and 16% of molding water content, one on the wet side and the other on the dry side of optimum. Whereas the respective thixotropic-strength ratios are 1.3 and slightly more than 1, the increase in the value of the stress causing a 10% strain is the same in both cases, namely 0.6 kg per sq cm as measured in Fig. 9.

(b) Take samples at 18% and 19% of molding water content, both samples being on the wet side of optimum. The increases in strength are 1.1 kg per sq cm and 0.6 kg per sq cm respectively, whereas the respective values of the thixotropic-strength ratios are 1.25 and 1.3. From an engineering point of view, the effect of thixotropy on the 18% water-content sample is more pronounced than on the 19% water-content sample, whereas the thixotropic-strength ratios inform the engineer otherwise.

Increase in Thixotropic Effects in Normal Strength Tests.—The correctness of Fig. 12 may be proved by a rheological analogy, which is also based on laboratory tests. The figures prepared by Burgers and Scott Blair⁶ are reproduced in Figs. 23.

If a stirred thixotropic substance is acted on by a constant shearing stress and the resulting deformations γ are plotted against time t , the γ - t curve "will be concave upwards (accelerated flow), and will probably finally approximate * * * a straight line." This is curve *a* in Fig. 23. Furthermore, "if the experiment is interrupted * * * and if after a very short interval the same stress is applied again, flow will appear again with, from the start, practically the same high value of velocity as was obtained at the end of the first experiment." This is depicted by curve *b* in Fig. 23.

If the experiments shown in Fig. 12 were performed successively on one sample in each series shown in the figure, the horizontal axis could be considered as the time axis and the vertical one as the deformation axis. Hypothetical deformations γ and actual strains plotted on the vertical axis in Fig. 12, will

be assumed to be proportional. Therefore, the experiments should give six curves qualitatively similar to those shown in Fig. 12, but located in the reverse order. That is, the curves at the extreme left and the extreme right of the series now corresponding to 0 and 28 days of storage, will correspond to 28 and 0 days, respectively. A time scale cannot be properly selected in this case because of the uncertainty of numerical characteristics of the experimental material. The curves in Fig. 12 are fairly straight and parallel where they should be. The slope of these lines may differ from that of Fig. 12 according to the time scale chosen.

Retardation.—It is convenient to introduce the concept of retardation at this point in the discussion. When the load causing deformation in clay is gradually relieved, a portion of the deformation is recovered. The rate of such recovery is not constant, but gradually increases toward the end of the relieving

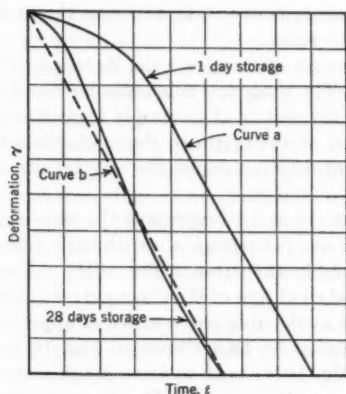


FIG. 23.—DEFORMATION-TIME CURVES FOR A THIXOTROPIC SUBSTANCE ACTED ON BY A CONSTANT SHEARING STRESS

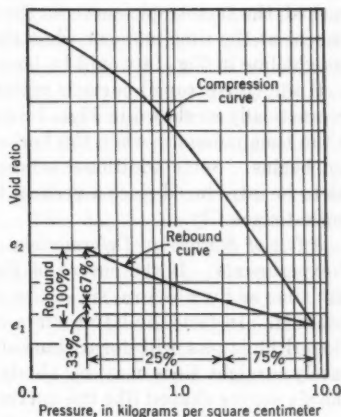


FIG. 24.—VOLUME RECOVERY AFTER CONSOLIDATION TEST

process—that is, the recovery is retarded. A well-known case of retardation is depicted by the rebound curve in the unloading stage of the familiar consolidation test. The curve is generally concave, often with increasing curvature toward the end. Fig. 24 is an example of such a curve obtained in an actual test on silty clay. The pressure on the sample was relieved by a certain amount (for example, 100%). When 75% of that amount was relieved, the deformation decreased 33% only as shown in Fig. 24.

It is probable that in such cases the cause of recovery is partly elasticity and partly thixotropy. In fact, upon application of the load on the sample its microstructure changes, as do the electric forces. Particularly, water is torn off the particles, becomes free, and is squeezed out by being acted on by the gradient developed. However, the clay is still active, and as soon as water is readmitted back to the sample, the recovery process begins. Strictly speaking, this is a case of volume recovery, but retardation took place also in the Skemp-

ton and Northey's observation of thixotropic-strength regain in five clays. Rheologists are familiar with the recovery retardation in thixotropy. It would appear that soil mechanics investigators should pay more attention to this phenomenon.

Figs. 13 and 14.—As one can conclude from Figs. 13 and 14, an idealized thixotropic curve on a logarithmic scale is concave, degenerating into a practically straight line. This is a theoretical case of an infinitely long thixotropic recovery. The curves for Vicksburg silty clay and Pittsburg sandy clay fit this pattern. The curve in Fig. 13 would also perfectly fit this pattern if a reading at 100 min were taken in the laboratory. The curve for Friant-Kern clay has not been considered by the writer because it is constructed from erratic data. Not only does the curve in Fig. 13 show that the thixotropic recovery is still going on as the authors state, but this is also the case of all curves in Fig. 14. In fact, in order to show that the process of thixotropic recovery is finished, the thixotropic curve on the logarithmic plot should have a horizontal tangent at the time moment when the recovery is over. In this case the final straight line in Fig. 14 would be bent to the right.

If the (thixotropic) curve is replotted on an arithmetic scale, its shape will be practically as shown in Figs. 1 and 6. The tangency point will correspond to the time moments when the horizontal tangent to the curve in logarithmic plot begins. Some additional arrangement at the origin to show retardation has to be introduced since a vertical tangent does not depict the original situation satisfactorily.

Effect of Storage on Deformations.—Figs. 15 and 16 represent the same set of experiments. If the curves of Fig. 15 are plotted on an arithmetic scale with time as the abscissa, six curves shaped like the curve in Fig. 16(a) will be obtained. In fact, the latter curve is a detail of one of those six curves. On a logarithmic plot with logarithms of time as the abscissa, a series of approximately straight lines may be obtained similar to that shown in Fig. 16(b). The six curves shaped like the curves in Fig. 16(a) tend to have a horizontal tangent as the time between compaction and testing grows. That is, under the given laboratory conditions after a considerable time following compaction, to each number of standard stress applications a definite maximum strain corresponds. This may be approximately true for sandy and silty clays, but probably not of the more plastic materials.

As to the difficulty of predicting the probable life of pavements from the laboratory tests of this kind the writer agrees with the authors' opinion.

Effect of Rate of Loading.—It may be well to clarify the authors' use of the term "creep." In the geotechnical literature this term is sometimes used to describe the slow translational deformations of an unloaded ground surface. The authors use the term in the sense attributed to it by Casagrande and Wilson,¹¹ and possibly elsewhere.

From several cases of strength decrease with time given in the paper, the writer noted the decrease in strength of compacted clays for a certain rather short time after loading. Qualitatively similar results for a short time of loading were obtained by Casagrande and Wilson and by the authors (Fig. 17). This means that under a long-term loading the clay strength first decreases and after a certain time increases to the preloading value, after which it continues

increasing thixotropically. The authors explain this fact by creep deformations. However, the writer believes that at the time of loading the compacted clay (which is already in a disturbed condition and ready to have its strength increased thixotropically) is additionally disturbed and needs a certain time to have its preloading strength restored. This additional disturbance caused by loading may consist in the damage of the bonds and the small displacements of particles. It is evident in the writer's opinion that this restoration to the preloading condition is done by the clay structure-building forces—that is, by thixotropy.

It is pertinent to state at this point that the possibility of the regain of rheological properties of a material during the intervals between the "stirring" experiments is known to rheologists.

The Authors' Conclusions.—Under the heading, "Conclusions," the authors in Fig. 21 show that thixotropic processes practically do not change the angle of shearing resistance of clay but influence the intercepts on the vertical axis of the diagram expressing the Coulomb equation (Fig. 21(c)). This result is quite natural as thixotropy does not alter the material, but essentially increases and reinforces the bonds. The writer believes, however, that the problem of the true cohesion and true angle of internal friction in saturated clays will not be definitely solved unless more efficient research tools are used, particularly physical chemistry and allied sciences.

The Writer's Conclusions.—Atterberg was probably the first man who observed thixotropy in the field intelligently. This was during the construction of a railroad in northern Sweden, when a stratum of clay with a high-water content showed a semifluid behavior. His observation was published in 1908 in an agricultural journal;²⁵ and in the same year Atterberg's paper on his "limits" appeared. This work was done only 8 yr after he had begun pioneering in soil investigations as a middle-aged chemist and agriculturist. His work is a good example of a desirable combination of laboratory soil work and field observations.

At the present time (1958) there are still papers on soil mechanics in which laboratory and field data are harmoniously combined.²⁶ However, it is becoming a rather widespread tendency to try to solve problems of soil mechanics without going to the field at all. It is convenient to recall here a statement²⁷ by Karl Terzaghi, Hon. M. ASCE as follows:

"Soil mechanics as taught and practised at present is likely to create a dangerous illusion that the processes in the natural soil strata are always, or at least usually, as clear and simple as those in the cylindrical specimens subject to investigation in the laboratory."

Although a number of years have passed since these lines were written and many improvements have been made in sampling and testing, the statement is still fundamentally true and the writer shares its sentiment wholeheartedly.

²⁵ "Studien auf dem Gebiete der Bodenkunde," by A. M. Atterberg, *Die Landwirtschaftlichen Versuchsanstalten*, Vol. 69, 1908, Berlin, p. 134.

²⁶ "The Action of Soft Clay Along Friction Piles," by H. Bolton Seed and Lymon C. Reese, *Transactions*, ASCE, Vol. 122, 1957, p. 731.

²⁷ Discussion by Karl Terzaghi of "Geology in Highway Engineering," by Marshall T. Hunting, *Transactions*, ASCE, Vol. 110, 1945, p. 324.

H. BOLTON SEED,²⁶ A.M. ASCE AND CLARENCE K. CHAN,²⁷ J.M. ASCE.—In his discussion Mr. Barber points out that "Some thixotropy is caused by redistribution of nonuniformly distributed moisture to make a more uniform, and therefore stronger, material." The writers would not consider such a strength increase as thixotropy although moisture redistribution after compaction may well be a factor promoting strength increase in cases in which the water and soil were poorly mixed initially. However, this is not believed to be a significant factor in the tests reported in the paper, for which the soil and water were well mixed and subsequently cured for 1 day to allow further moisture redistribution before compaction.

Furthermore, in contrast to the data presented by Mr. Barber, studies indicate that samples prepared by static compaction may exhibit appreciable thixotropic properties. Although the thixotropic strength increases for samples prepared by static compaction appear to be proportionately less than for samples prepared by kneading compaction, it is believed that this might well be due to the initially higher strength of samples prepared by static compaction. Mr. Barber's tests were conducted on samples prepared "near optimum moisture and maximum density." In the writers' experience, samples compacted to such a condition can show marked differences in strength due to minor changes in density and water content and, in the absence of this information, it is difficult to determine what proportion of the strength change reported by Mr. Barber may be due to composition changes and what proportion is due to other factors including thixotropy. Near optimum water content one would expect a relatively small thixotropic strength increase.

The writers welcome the historical background provided by Mr. Krynine and his discussion of the need for an adequate amount of water in a soil before thixotropic properties can develop. It was, in fact, one of the objects of the paper to demonstrate that compacted clays contain sufficient water to produce thixotropic properties in spite of the suggestion by two previous investigations that this would not be the case and the apparent confirmation of this suggestion by tests conducted by G. A. Leonards.

The writers also agree with Mr. Krynine's remarks concerning the misleading conclusions which may sometimes be indicated by the use of the term "thixotropic strength ratio." While this may be a useful term in some cases, it does not necessarily reflect the actual thixotropic strength increase of a soil.

The writers cannot agree, however, with some of the other comments in Mr. Krynine's discussion. First, the writers do not consider that with the consideration of electrical forces as a component of clay structure, "explanation of thixotropic processes becomes relatively simple." It would hardly seem adequate to simply attribute thixotropy to "structure building forces" without investigating further the mechanism of these forces. In fact the writers believe that a comprehensive investigation of the cause of thixotropy would be a major contribution to fundamental knowledge of soil behavior.

Secondly, the authors do not believe that the stress-strain curves in Fig. 15 can be compared with the deformation-time curves in Fig. A or that

²⁶ Associate Prof. of Civ. Eng., Univ. of California, Berkeley, Calif.

²⁷ Asst. Research Engr., Inst. of Transportation and Traffic Eng., Univ. of California, Berkeley, Calif.

an idealized curve, on a semi-logarithmic plot, of strength increase with time "is concave degenerating into a practically straight line." This is not the form of any of the curves in Fig. 5. Further, any resemblance between Figs. 18 and 19(a) would seem to be merely one of shape and not of actual data.

Finally, in concluding his discussion, Mr. Krynine gives a warning concerning the care required in translating the results of laboratory tests to field problems. The writers would be the first to agree with this. However, it is often necessary to study phenomena under carefully controlled conditions in the laboratory to establish the qualitative nature of their effects before field studies can be intelligently planned. It is to such an end that the present paper was prepared. While recognizing the need for an appropriately careful approach, the writers believe that thixotropic effects measured in the laboratory may have an important influence in a variety of engineering problems.

AMERICAN SOCIETY OF CIVIL ENGINEERS

Founded November 5, 1852

TRANSACTIONS

Paper No. 3006

TURBULENCE CHARACTERISTICS OF THE HYDRAULIC JUMP

BY HUNTER ROUSE,¹ M. ASCE, TIEN TO SIAO,² AND
S. NAGARATNAM³

WITH DISCUSSION BY MESSRS. EDWARD SILBERMAN; ALVIN J. PETERKA AND
JOSEPH N. BRADLEY; JAMES M. ROBERTSON; DONALD R. F. HARLEMAN;
PHILIP G. HUBBARD; AND HUNTER ROUSE, TIEN TO SIAO,
AND S. NAGARATNAM

SYNOPSIS

Because the fluid discontinuities produced by entrapped air interfere with the measurement of turbulence in the hydraulic jump itself, the flow pattern of the jump has been simulated in an air duct and the hot-wire anemometer used to determine the corresponding pattern of turbulence for Froude numbers of 2, 4, and 6. In the analytical section of the paper the modeling method is justified and the differential and integral forms of the pertinent momentum and energy equations are explained. The experimental apparatus and techniques are described next, and the basic data are presented in diagrams. The measured characteristics of the mean flow and of the turbulence are then correlated in accordance with the momentum and energy equations, and the process of energy conversion from the mean flow through turbulence to heat is followed in detail. Various aspects of the hydraulic jump, long subject to conjecture or misunderstanding, are thereby clarified.

INTRODUCTION

Three sorts of information pertinent to the present investigation of the hydraulic jump are contained in discussions of an earlier paper⁴ by Boris A.

NOTE.—Published, essentially as printed here, in February, 1958, in the Journal of the Hydraulics Division, as *Proceedings Paper 1628*. Positions and titles given are those in effect when the paper or discussion was approved for publication in *Transactions*.

¹ Director, Iowa Inst. of Hydr. Research, State Univ. of Iowa, Iowa City, Iowa.

² Hydr. Engr., Inst. of Hydr. Research, Academia Sinica, Peking, China.

³ Engr., Harza Eng. Co., Chicago, Ill.

⁴ "The Hydraulic Jump in Terms of Dynamic Similarity," by Boris A. Bakhmeteff and Arthur E. Matzke, *Transactions, ASCE*, Vol. 101, 1936.

Bakhmeteff and Arthur E. Matzke, A. M. ASCE: First, a well-annotated account of the gradual development of knowledge on this subject; second, a somewhat contradictory mixture of factual matter, hypothesis, and error; third, and by inference only, a guide to further research. In 1936, when the paper and discussions were published, the tools for such research had only recently come into use in other fields, and it is hardly to be expected that they would already have been applied in hydraulics. In fact, the investigation herein described had the purpose of demonstrating the efficacy of the new approach as well as providing greater insight into the phenomenon under consideration.

As was evident from the aforementioned paper and its discussions, past advancements had been concerned with the vertical elements (that is, depths and heads) of the mean-flow pattern as correlated by the one-dimensional forms of the continuity, momentum, and energy relationships. Some attention had been given to the empirical evaluation of the longitudinal elements as well, and to the expression of the functional relationships in terms of what is now called the Froude number. However, concern with the accompanying pattern of turbulence was almost entirely speculative. For lack of even an approximate evaluation of the turbulence characteristics, their importance to the phenomenon was both overestimated and underestimated. For example, the senior writer claimed that the computed loss in head at the jump represented merely a transfer of energy from the mean motion to the turbulence, and, hence, that the total head would be found to remain practically constant through the jump if the kinetic energy of the turbulence could be measured and included as velocity head. Others, on the contrary, did not sense the importance of eddy generation along the surface of discontinuity between the secondary flow of the roller and the primary flow beneath, some even going so far as to claim that the roller played no essential part in the phenomenon.

The difficulty lay, as is now apparent, in the general lack of clarity that prevailed in nearly all matters involving fluid turbulence. Not only did existing turbulence theories seem to have little connection with hydraulic reality, but the only practicable means of measuring turbulence—the hot-wire anemometer—was restricted to use in air. During the intervening years, progress has been made in the interpretation, if not in the quantitative prediction, of the transformation from energy of the mean motion through energy of turbulence to that of heat, and the hot-wire technique itself has been extended to use in water. Means would therefore seem to be at hand for the measurement of the primary and secondary patterns of flow in the hydraulic jump, and at least the evaluation of the various energy forms at representative sections. Unfortunately, the jump will probably be one of the last hydraulic phenomena to prove susceptible to exploration with the hot-wire instrument, because of the presence of countless fluid discontinuities (bubbles of entrained air) in the region of greatest interest.

To overcome this rather formidable obstacle (yet without having recourse to the extremely tedious process of statistically analyzing motion pictures of suspended particles), it was resolved at the Iowa Institute of Hydraulic Research, at Iowa City, Iowa, to simulate the flow pattern of the hydraulic jump in an air duct, and then use the hot-wire anemometer for turbulence surveys,

just as in previous Institute studies of other diffusion phenomena. The analog will seem, at first glance, a rather artificial one, to say the least. However, it must be realized that few model flows portray perfect dynamic similarity with their prototypes, and that, for all practical purposes, only the pertinent part of the phenomenon need be closely approximated. In the present instance it is not the gravitational action that is to be evaluated but the viscous action. If the mean-flow patterns are geometrically similar, and if the changes in energy are comparable, then it would seem safe to assume that the patterns of turbulence are also similar, and it is specifically these with which the present investigation is concerned.

ANALYTICAL BASES OF EXPERIMENTATION

Notation.—The letter symbols adopted for use in this paper are defined where they first appear, in the illustrations or in the text, and are assembled, for convenience of reference, in the Appendix.

Air-Water Correlation.—Application of the simplified continuity, momentum, and energy relationships for one-dimensional flow to the conditions shown in Fig. 1 leads to the following well-known equations for the hydraulic jump in

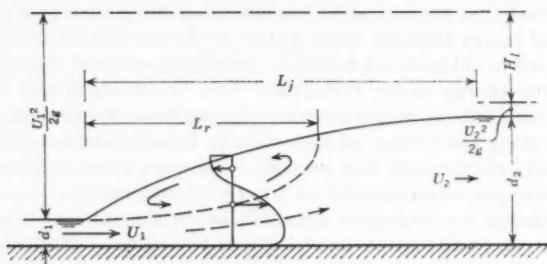


FIG. 1.—DEFINITION SKETCH OF HYDRAULIC JUMP

homogeneous liquid flowing through a horizontal, resistance-free channel of rectangular cross section:

$$\frac{d_2}{d_1} = \frac{1}{2} \left(\sqrt{1 + 8 \frac{U_1^2}{g d_1}} - 1 \right) \dots \dots \dots (1)$$

and

$$\frac{H_l}{d_1} = \frac{1}{2} \frac{U_1^2}{g d_1} \left(1 - \frac{d_1^3}{d_2^3} \right) - \frac{d_2}{d_1} + 1 \dots \dots \dots (2)$$

in which d is the depth of flow; U denotes the average across a vertical section of the instantaneous longitudinal component of velocity at a point (u); g is the acceleration of gravity; and H_l represents the head loss in the jump. In Fig. 1, L_j is the length of the jump, and L_r denotes the length of the roller. Both the depth ratio, d_2/d_1 , and the relative loss of total head, H_l/d_1 , are explicit functions of the Froude number, F_1 , of the approaching flow,

$$F_1 = \frac{U_1}{\sqrt{g d_1}} \dots \dots \dots (3)$$

as are also such longitudinal characteristics as the relative length of the jump, L_j/d_1 , and the shape of the flow profile.

It is not too difficult to visualize the application to the flow of an upper boundary having the same profile as the mean free surface. Like the spillway profile that is shaped according to the lower surface of the corresponding weir nappe, the presence of the solid boundary may be expected to have some effect on the flow. In the case of the spillway the predominant effect is the addition of shear. In the case of the jump it is rather the elimination of both the freedom of the surface to fluctuate and the presence of entrained air. However, measurements of the pressure head along the floor of a flume under a jump yield values that differ from the local depths by no more than the experimental error, indicating at once that the pressure distribution can be assumed to be hydrostatic and that the quantity of air in suspension is actually insufficient to change appreciably either the density or the specific weight. As for the surface fluctuations, measurement of the resulting wave amplitudes just downstream and approximation therefrom of the resulting wave energy have shown this to be less than 1% of the energy of the flow itself. It would thus seem reasonable to assume that the presence of the upper boundary would have, at most, only a secondary effect on the flow pattern.

If the foregoing premise is accepted, then it must also be granted (in accordance with the general mechanics of confined flow) that the same pattern would obtain between the upper and lower boundaries at other rates of flow, if only the Reynolds numbers did not differ greatly. However, no longer would the mean pressure intensity along the upper boundary be atmospheric at all points, for it must change in accordance with the Bernoulli equation. On the other hand, if the linear quantities in Eqs. 1 and 2 are considered to be the piezometric heads, h (that is, the sum of pressure head and elevation, which is presumably constant over any vertical section), the following relationships must continue to prevail between the enclosed model and its free-surface prototype:

$$\frac{h_2 - h_1}{\frac{U_1^2}{2g}} = \frac{d_2 - d_1}{\frac{U_1^2}{2g}} \dots \dots \dots (4)$$

and

$$1 - \frac{h_2 - h_1}{\frac{U_1^2}{2g}} - \frac{d_1^2}{d_2^2} = \frac{H_1}{\frac{U_1^2}{2g}} \dots \dots \dots (5)$$

Again in accordance with the principles of fluid mechanics, it makes no difference whether the fluid is a liquid or a gas as long as the Reynolds numbers are still comparable and the velocities of the gas are not so high (that is, 200 or 300 ft per sec) as to cause compressibility effects. Hence, the same patterns of mean flow and turbulence should be obtainable through use of air of density ρ as the experimental fluid. Moreover, since the elevation term then could be neglected in the Bernoulli and related equations, the foregoing model-prototype expressions would reduce to the following pressure forms:

$$\frac{p_2 - p_1}{\frac{\rho U_1^2}{2}} = \frac{d_2 - d_1}{\frac{U_1^2}{2g}} \dots \dots \dots (6)$$

and

$$1 - \frac{p_2 - p_1}{\frac{\rho}{2} U_1^2} - \frac{d_1^2}{d_2^2} = \frac{H_1}{\frac{U_1^2}{2g}} \dots \dots \dots (7)$$

in which p is the pressure intensity.

Although the Froude number cannot be expressed by replacing d_1 with either h_1 or p_1/γ (the term γ is the specific weight of the fluid), since the pressure load on the system is no longer determined by free-surface conditions, it will be seen that the right-hand sides of Eqs. 4 and 6 still are governed completely by the prototype magnitude of F_1 , as are hence the left-hand sides. Moreover, for any Froude number the pressure-distribution terms $(p - p_1)/(p_2 - p_1)$ and $(h - h_1)/(h_2 - h_1)$ should be numerically equal to the profile dimension $(d - d_1)/(d_2 - d_1)$ at homologous sections. To the extent that these equalities are actually realized in prototype and model, the flow patterns themselves may be considered comparable.

Momentum Relationship.—To obtain a more precise form of the momentum equation than that customarily used in one-dimensional hydraulics, recourse must be had to the differential equations of motion as adapted to turbulent flow by Osborne Reynolds from the form derived for laminar flow by G. G. Stokes, and as presented in standard texts on hydrodynamics.⁵ Space limitations prevent the inclusion in full of the derivations outlined herewith. However, they are readily available in the literature, and they can probably be checked by those with advanced training even without reference to the papers cited. What is important is the implicit demonstration that (a) the customary jump relationships are one-dimensional approximations, (b) a more refined analysis of the role of turbulence must stem from the basic equations of motion, (c) the derived expressions must in turn be simplified, but only in accordance with experimental evidence, and (d) the final results are broadly significant.) Reynolds' adaptation involved, in brief, the replacement of every instantaneous velocity magnitude by the sum of its mean value and its deviation therefrom, and then the retention of only those terms having a temporal average other than zero. Thus, in general, the local vector magnitude of the velocity, V , is considered to have the mean velocity components, \bar{u} , \bar{v} , and \bar{w} , in the directions x , y , and z , respectively, with the corresponding instantaneous deviations, u' , v' , and w' . For the direction x , the Reynolds equation has the typical form (bars denoting temporal means):

$$\begin{aligned} \bar{u} \frac{\partial \bar{u}}{\partial x} + \bar{v} \frac{\partial \bar{u}}{\partial y} + \bar{w} \frac{\partial \bar{u}}{\partial z} + \overline{u' \frac{\partial u'}{\partial x}} + \overline{v' \frac{\partial u'}{\partial y}} + \overline{w' \frac{\partial u'}{\partial z}} \\ = -\frac{1}{\rho} \frac{\partial \bar{p}}{\partial x} + X + \frac{\mu}{\rho} \left(\frac{\partial^2 \bar{u}}{\partial x^2} + \frac{\partial^2 \bar{u}}{\partial y^2} + \frac{\partial^2 \bar{u}}{\partial z^2} \right) \dots \dots \dots (8) \end{aligned}$$

in which μ is the dynamic viscosity and X the x -component of the body force (such as the attraction of gravity) per unit mass.

Eq. 8 is fundamentally an equation of acceleration, for the terms to the left of the equality sign represent the rates of change of the velocity components

⁵ "Hydrodynamics," by H. Lamb, Dover Publications, New York, N. Y., 6th Ed., 1946.

of the mean motion and of the turbulence, and the terms to the right of the equality sign represent the pressure, body, and viscous forces per unit mass by which the velocity changes are produced. Through introduction of the two equations of continuity,

$$\frac{\partial \bar{u}}{\partial x} + \frac{\partial \bar{v}}{\partial y} + \frac{\partial \bar{w}}{\partial z} = 0 \dots \dots \dots (9)$$

and

$$\frac{\partial u'}{\partial x} + \frac{\partial v'}{\partial y} + \frac{\partial w'}{\partial z} = 0 \dots \dots \dots (10)$$

the acceleration terms can be written in the alternative form,

$$\frac{\partial(\bar{u}^2)}{\partial x} + \frac{\partial(\bar{u} \bar{v})}{\partial y} + \frac{\partial(\bar{u} \bar{w})}{\partial z} + \frac{\partial \bar{u}^2}{\partial x} + \frac{\partial \bar{u}' v'}{\partial y} + \frac{\partial \bar{u}' w'}{\partial z}$$

which will be used in a subsequent derivation.

Because there is an equation of acceleration for each of the three coordinate directions, a considerable saving in space, without sacrifice of clarity, is gained by the use of tensor notation, in which the quantities u , v , and w are represented by u_i or u_{ij} , and x , y , and z by x_i or x_j . In shorthand form the indices i and j denote, in turn, each of the three coordinate directions. Thus, Eq. 8 and its counterparts for the other two directions are represented at one and the same time by

$$\frac{\partial(\bar{u}_i \bar{u}_j)}{\partial x_i} + \frac{\partial \bar{u}_i' u_j'}{\partial x_i} = -\frac{1}{\rho} \frac{\partial p}{\partial x_i} + X_i + \mu \frac{\partial^2 \bar{u}_i}{\partial x_i \partial x_j} \dots \dots \dots (11)$$

in which the tensor subscript i refers to the direction characterizing each equation, and j denotes the direction of each independent term within it. Therefore, repetition of indices represents a summation of terms.

Any equation of acceleration (like the Newtonian equation itself) may also be regarded as an equation of momentum. It will be noted that multiplication of both sides of Eq. 11 by the mass density will give each term the dimension of rate of change of momentum per unit volume or impulse per unit volume per unit time. The physical significance of the resulting expression becomes greater as it is integrated over a given space through which the fluid moves. By the Gaussian rule of the calculus relating volume integrals and surface integrals,

$$\int_V \frac{\partial(-)}{\partial x_i} dV = \int_S (-) \frac{\partial x_j}{\partial n} dS \dots \dots \dots (12)$$

the result can be put in the following general form:

$$\begin{aligned} \int \rho \bar{u}_i \bar{u}_j \frac{\partial x_j}{\partial n} dS + \int \rho \bar{u}_i' u_j' \frac{\partial x_j}{\partial n} dS \\ = - \int_S \bar{p} \frac{\partial x_i}{\partial n} dS + \int_V \rho X_i dV + \int_S \mu \frac{\partial \bar{u}_i}{\partial x_j} \frac{\partial x_j}{\partial n} dS \dots (13) \end{aligned}$$

Herein S denotes the surface of the region over which the integration is performed, n the outward normal to the surface, and V the enclosed volume. The terms at the left of the equality sign (each representing nine different quantities) embody the net flux of momentum (three components in each of three directions) of the mean flow and of the turbulence out of the region in question—that is, the difference between the rates of efflux and influx. The first term at the right denotes the three components of the mean normal force exerted externally on the surface of the region; the second term, the three components of the weight of the fluid contained within the region; and the third term, the three components of the mean tangential force exerted on the surface.

For the case in which the hydraulic jump is formed on a horizontal bed of great width, the pertinent momentum equation is that for the direction x . If it is assumed that the turbulence is negligible at the initial section, that the pressure distribution is hydrostatic at any arbitrary section, and that both the viscous stress and the turbulent stress are negligible over the free surface, Eq. 13 reduces to

$$\int_0^d \rho \bar{u}^2 dy - \int_0^{d_1} \rho \bar{u}^2 dy + \int_0^d \rho \overline{u'^2} dy \\ = \frac{\gamma d_1^2}{2} - \frac{\gamma d^2}{2} - \int_0^x \mu \left(\frac{\partial \bar{u}}{\partial y} \right)_{y=0} dx \dots (14)$$

For the limiting case in which $x = L_j$ and $d = d_2$, Eq. 14 will be seen to differ in the following ways from the simpler version normally used in studying the jump. First, the change in the mean momentum flux, which is expressed as the difference between the first two integrals, perforce includes the effect of local departure from the average velocity over the vertical section. Second, the change in the momentum flux of the turbulence is represented by the next integral, which embodies the sole effect of turbulence in the force balance. Finally, the effect of variable bed shear,

$$\tau_0 = \mu \left(\frac{\partial \bar{u}}{\partial y} \right)_{y=0} \dots \dots \dots (15)$$

over the length of the jump is included in the integral to the right. Obviously, in applying Eq. 14 each integral must be determined from known distributions of the variables in question, an evident reason for the more customary use of the simplified relationship. However, only through the quantitative evaluation of the integral terms can the magnitude of the error arising from the neglect of the distribution details be appraised.

Equations of Energy.—An essential characteristic of the Reynolds equations of motion, and hence of the momentum equations derived from them, is the absence of all viscous stresses except those involving the mean velocities. However, although the viscous terms containing the velocity fluctuations are invariably eliminated by the averaging process, there remain certain inertial terms consisting of fluctuation products which can conveniently be considered to have the nature of a stress and hence to take their place. These are the

momentum-transport terms of the secondary motion, which may be combined with the terms for mean viscous stress to yield

$$\tau_{ij} = \mu \left(\frac{\partial \bar{u}_i}{\partial x_j} + \frac{\partial \bar{u}_j}{\partial x_i} \right) - \rho \overline{u_i' u_j'} \dots \dots \dots (16)$$

The momentum-transport terms are known as Reynolds stresses.

If, before averaging, each of the equations of motion is multiplied by the corresponding component of the instantaneous velocity, and the three equations are then added, there will result a differential equation of work and energy* of the form

$$\begin{aligned} \bar{u}_j \frac{\partial}{\partial x_j} \left(\frac{\rho \bar{V}^2}{2} + \frac{\rho \bar{V}'^2}{2} \right) + \overline{u_j' \frac{\partial (\rho V'^2/2)}{\partial x_j}} + \frac{\partial (\bar{u}_i \rho \overline{u_i' u_j'})}{\partial x_i} \\ = - \bar{u}_i \frac{\partial \bar{p}}{\partial x_i} - \overline{u_i' \frac{\partial p'}{\partial x_i}} + \rho \bar{u}_i X_i + \mu \bar{u}_i \frac{\partial^2 \bar{u}_i}{\partial x_j \partial x_j} + \mu \overline{u_i' \frac{\partial^2 u_i'}{\partial x_j \partial x_j}} \dots (17) \end{aligned}$$

Inspection of Eq. 17 will reveal not only that many of the fluctuating stresses which disappeared from the momentum equations during the averaging process are now retained, but also that there is a fairly consistent parallel between the terms for the mean flow and those for the turbulence. In fact, it is instructive to segregate the terms of the two categories in the following work-energy relationships for the mean flow and for the turbulence (which are also directly derivable by combining the pertinent equations and velocity components):

$$\bar{u}_j \frac{\partial (\rho \bar{V}^2/2)}{\partial x_j} + \rho \bar{u}_i \frac{\partial \overline{u_i' u_j'}}{\partial x_j} = - \bar{u}_i \frac{\partial \bar{p}}{\partial x_i} + \rho \bar{u}_i X_i + \mu \bar{u}_i \frac{\partial^2 \bar{u}_i}{\partial x_j \partial x_j} \dots (18)$$

and

$$\bar{u}_j \frac{\partial (\rho \bar{V}'^2/2)}{\partial x_j} + \overline{u_j' \frac{\partial (\rho V'^2/2)}{\partial x_j}} + \rho \overline{u_i' u_j'} \frac{\partial \bar{u}_i}{\partial x_j} = - \overline{u_i' \frac{\partial p'}{\partial x_i}} + \mu \overline{u_i' \frac{\partial^2 u_i'}{\partial x_j \partial x_j}} \dots (19)$$

As was done with the momentum form of the equations of motion, it is now in order to integrate the differential work-energy equations over a given region of space. After the appropriate volume integrals have been changed by the Gaussian rule to surface integrals, the work-energy equation for the mean flow assumes the form,

$$\begin{aligned} \int_S \frac{\rho \bar{V}^2}{2} \bar{u}_j \frac{\partial x_j}{\partial n} dS + \int_S \rho \overline{u_i' u_j'} \frac{\partial x_j}{\partial n} dS - \int_V \rho \overline{u_i' u_j'} \frac{\partial \bar{u}_i}{\partial x_j} dV \\ = - \int_S \bar{p} \bar{u}_i \frac{\partial x_i}{\partial n} dS + \int_V \rho X_i \bar{u}_i dV + \int_V \mu \left(\frac{\partial \bar{u}_i}{\partial x_j} + \frac{\partial \bar{u}_j}{\partial x_i} \right) \bar{u}_i \frac{\partial x_j}{\partial n} dS \\ - \int_V \mu \left(\frac{\partial \bar{u}_i}{\partial x_j} + \frac{\partial \bar{u}_j}{\partial x_i} \right) \frac{\partial \bar{u}_i}{\partial x_j} dV \dots (20) \end{aligned}$$

The successive terms have the following significance: The term at the extreme left represents the net flux of kinetic energy of the mean motion out of the

* "The Structure of Turbulent Shear Flow," by A. A. Townsend, Cambridge University Press, Cambridge, 1956.

region in question (that is, the rate of increase in kinetic energy as the fluid passes through the region). The second and third terms, while also representing energy transport, can best be explained as the rates at which work is done by the Reynolds stresses over the surface and throughout the interior of the region, respectively. The first and second terms on the right of the equality sign are the rates at which work is done by the external pressures and the body forces. The third and fourth terms are evidently the rates at which work is done by the viscous stresses of the mean flow over the surface and throughout the interior of the region, respectively.

Now the work done externally by the viscous stresses (the third term at the right) is wholly conservative (since, as is evident from the Gaussian transformation, it is derivable from a potential or space derivative), whereas that done internally (the last term) is wholly dissipative. Because of the analogy between the turbulent stresses and viscous stresses, one might seek a further parallel between the types of work done in each instance. In fact, whereas the second term at the left (like the third term at the right) is conservative, the third term at the left can be considered dissipative like the last at the right if one assumes that energy transferred from the mean flow to the turbulence can never be recovered. The third term at the left, in other words, represents the rate at which turbulence is produced at the expense of the mean flow. (The integral itself is inherently negative, so that the negative sign before it denotes a positive rate of production.)

The corresponding work-energy equation for the secondary motion is

$$\begin{aligned} \int_S \frac{\rho \bar{V}^2}{2} \bar{u}_i \frac{\partial x_j}{\partial n} dS + \int_S \frac{\rho \bar{V}^2}{2} u_i' \frac{\partial x_j}{\partial n} dS + \int_V \rho \overline{u_i' u_i'} \frac{\partial \bar{u}_i}{\partial x_j} dV \\ = - \int_S \overline{p' u_i'} \frac{\partial x_i}{\partial n} dS + \int_S \mu \left(\frac{\partial u_i'}{\partial x_j} + \frac{\partial u_j'}{\partial x_i} \right) u_i' \frac{\partial x_j}{\partial n} dS \\ - \int_V \mu \left(\frac{\partial u_i'}{\partial x_j} + \frac{\partial u_j'}{\partial x_i} \right) \frac{\partial u_i'}{\partial x_j} dV \dots (21) \end{aligned}$$

The first two terms at the left, by analogy to the first term in Eq. 20, represent the net flux of kinetic energy of turbulence out of the region by convection and diffusion (that is, by the mean flow and by the turbulence), respectively. The third term is again the rate of production of turbulence, now a negative quantity in so far as the work accomplished by the turbulence is concerned. The first term on the right of the equality sign is the rate at which work is done externally on the surface of the region by the fluctuating pressures. The last two terms represent the rates at which work is done by the viscous stresses of the turbulence over the surface of the region and throughout the interior, respectively, the former being conservative and the latter dissipative.

On the previous assumptions that the initial section is free from turbulence, that both the mean stresses and turbulent stresses can be neglected over the free surface, and that the pressure distribution is hydrostatic throughout, reduction of the work-energy equation for the mean motion to the case of the

hydraulic jump on a level bed of great width yields

$$\begin{aligned} & \int_0^d \frac{\bar{v}^2}{2g} \bar{u} dy - \int_0^{d_1} \frac{\bar{v}^2}{2g} dy + \int_0^d \frac{\bar{u} \bar{u}'^2 + \bar{v} \bar{u}' \bar{v}'}{g} dy \\ & - \int_0^d \int_0^x \left[\frac{\bar{u}' \bar{v}'}{g} \left(\frac{\partial \bar{u}}{\partial y} + \frac{\partial \bar{v}}{\partial x} \right) + \frac{\bar{u}'^2 - \bar{v}'^2}{g} \frac{\partial \bar{u}}{\partial x} \right] dy dx \\ & = q d_1 - q d + \int_0^d \frac{\mu}{\gamma} \left[2 \bar{u} \frac{\partial \bar{u}}{\partial x} + \bar{v} \left(\frac{\partial \bar{u}}{\partial y} + \frac{\partial \bar{v}}{\partial x} \right) \right] dy \\ & - \int_0^d \int_0^x \frac{\mu}{\gamma} \left[4 \left(\frac{\partial \bar{u}}{\partial x} \right)^2 + \left(\frac{\partial \bar{u}}{\partial y} + \frac{\partial \bar{v}}{\partial x} \right)^2 \right] dy dx \dots (22) \end{aligned}$$

For the limiting case that $x = L_i$ and $d = d_2$, the first two terms on each side of Eq. 22 correspond to those of the usual one-dimensional open-channel relationship, with due account being taken of the variation in velocity over the cross section. The third terms represent work done on the end section by the turbulent and viscous stresses. The last terms combine to form the quantity $H_1 g$, since they indicate the rate at which turbulence is produced by the mean motion and the rate at which energy is dissipated by the mean viscous stresses.

Reduction of the energy equation for the turbulent motion to the same conditions yields

$$\begin{aligned} & \int_0^d \frac{\bar{V}'^2}{2g} \bar{u} dy + \int_0^d \frac{\bar{V}'^2}{2g} \bar{u}' dy \\ & + \int_0^d \int_0^x \left[\frac{\bar{u}' \bar{v}'}{g} \left(\frac{\partial \bar{u}}{\partial y} + \frac{\partial \bar{v}}{\partial x} \right) + \frac{\bar{u}'^2 - \bar{v}'^2}{g} \frac{\partial \bar{u}}{\partial x} \right] dy dx \\ & = - \int_0^d \frac{\bar{p}'}{\gamma} \bar{u}' dy + \int_0^d \frac{\mu}{\gamma} \left[\frac{\partial}{\partial x} \left(\frac{\bar{V}'^2}{2} + \bar{u}'^2 \right) + \frac{\partial \bar{u}' \bar{v}'}{\partial y} \right] dy \\ & - \int_0^d \int_0^x K \frac{\mu}{\gamma} \left(\frac{\partial \bar{u}'}{\partial x} \right)^2 dy dx \dots (23) \end{aligned}$$

In Eq. 23 terms appear only for the arbitrary section, as it was assumed that no turbulence existed at the initial section. The proportionality factor, K , permits what are actually nine terms to be written as one. Its use is justified herein by the fact that (a) the dissipation is most intense in the smallest eddies, (b) the smallest eddies tend to be isotropic, and (c) in isotropic turbulence this factor has the constant magnitude⁷ of 15. Only if the cumulative production (the third term on the left in Eq. 23) and the cumulative dissipation (the third term on the right) are equal will the turbulence at the final section (that is, for $d = d_2$ at $x = L_i$) be negligible. The extent of the actual inequality of these terms evidently can be ascertained only through detailed measurement and analysis of the mean and fluctuating patterns of flow.

⁷ "Modern Developments in Fluid Dynamics," by S. Goldstein, Oxford University Press, 1938.

EXPERIMENTAL EQUIPMENT AND PROCEDURE

To simulate the mean and fluctuating patterns of the hydraulic jump in air, a special duct having a length of 9 ft, a width of 1 ft, and a maximum depth of 1 ft was built of plywood and plexiglass. Both the front wall and the curved surface were made transparent to simplify the visual setting of instruments, and, for added convenience in supporting them, the plane surface corresponding to the bed of the channel was placed on top (Fig. 2). The form of the curved surface was controlled by successive pairs of adjusting screws at 6-in. intervals over the entire length of the duct. Both the plane surface and the curved surface were provided with piezometer holes along the center line, and a grid with a 0.02-ft mesh was ruled on the rear wall as a guide in controlling the surface profile. At the downstream end the duct underwent a smooth

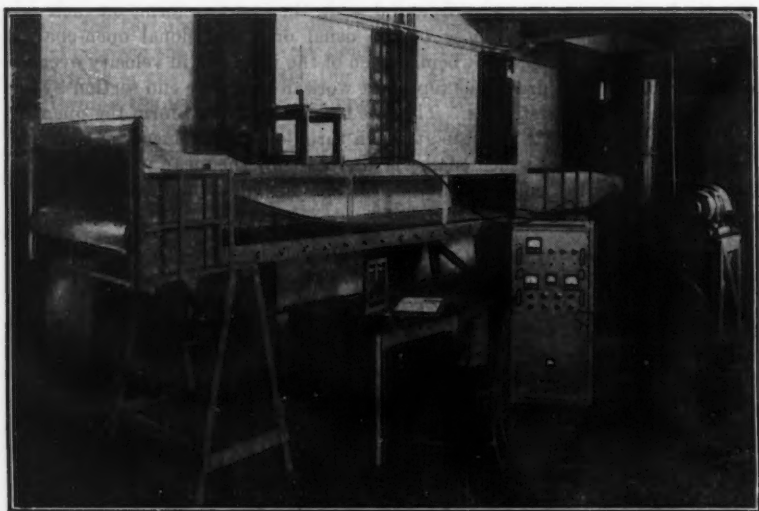


FIG. 2.—AIR-FLOW MODEL

transition to a 12-in.-diameter circular section connected to the intake of a 5-hp centrifugal blower, which discharged into the surrounding space through a baffled diffuser. The intake end was provided with a rectangular bell having carefully rounded sides. The bottom side of the bell was adjustable in position, and the curved surface of the test section was hinged to it after a 2.5-in. tangent.

Because the velocity of the flow varied greatly in magnitude and direction, even undergoing full reversal in the roller, it was considered desirable to utilize a single instrument that would respond in the same manner to flow in either direction. This precluded the ordinary type of pitot tube, but either a pitot cylinder with opposing holes or a simple hot-wire anemometer would have sufficed. The instrument actually used was a double pitot, symmetrical upstream and down, formed of two L's of 0.04-in. tubing placed back to back with

stagnation openings 0.6 in. apart. The tube was calibrated in an air stream for both magnitude and inclination of the velocity vector, differential pressures being indicated on a precision manometer reading to 0.001 in. of alcohol. In operation the tube was inserted through each of a series of center-line openings at 6-in. intervals in the plane top of the duct, and a velocity traverse was made with the tube in its normal position. On the assumption that the velocity indication corresponded to a zero inclination, the location of the streamlines for equal increments of the stream function, ψ , was evaluated from plots of the velocity distribution (Fig. 3) according to the relationship,

$$\psi = \int_0^y \bar{u} dy \dots \dots \dots (24)$$

With the approximate angularity thus indicated by the streamline pattern, the velocity readings were corrected by use of the angularity calibration, and the

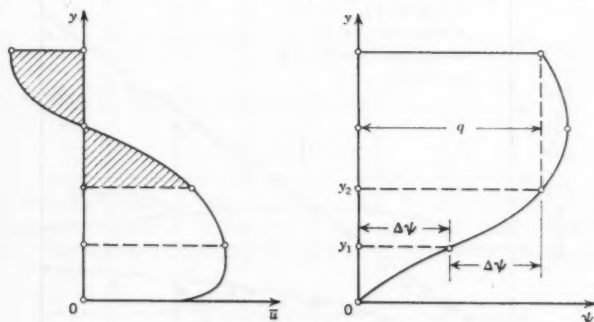


FIG. 3.—LOCATION OF STREAMLINES FROM VELOCITY DISTRIBUTION

determination of streamline location was repeated. A single correction of this nature usually proved sufficient.

Supplementary measurements for the determination of the local intensity of boundary shear were made with a 0.04-in. stagnation tube in contact with the plane boundary. The tube had been calibrated in connection with other boundary-layer measurements, and J. H. Preston's method of shear calculation⁸ was followed in both instances. The various characteristics of turbulence ($\sqrt{u'^2}$, $\sqrt{v'^2}$, $\sqrt{w'^2}$, $u'v'$, and $(\partial u'/\partial t)$) were measured with a constant-temperature hot-wire anemometer,⁹ the operation of which is also too specialized for further comment here. It should be remarked, however, that—although designed for a precision of $\pm 2\%$ under ideal conditions—the hot wire (like any method of turbulence measurement) must be expected to have a probable error ranging from $\pm 5\%$ to $\pm 10\%$ in practice and to as much as $\pm 20\%$ in zones of abnormally great intensity of fluctuation.

⁸ "The Determination of Turbulent Skin Friction by Means of Pitot Tubes," by J. H. Preston, *Journal of the Royal Aeronautical Society*, London, Vol. 58, 1954.

⁹ "Operating Manual for the IHHR Hot-Wire and Hot-Film Anemometers," by P. G. Hubbard *Bulletin 37, State Univ. of Iowa Studies in Eng.*, Iowa City, 1957.

Because the efficacy of the air-model method depends entirely on the degree of similarity between the model and its water prototype, rather extensive preliminary tests were conducted to determine both the mean-flow characteristics of the jump itself and the accuracy with which they could be simulated in the air duct. The jump was produced at various Froude numbers in the 1-ft glass-walled flume of the Institute at approximately the same scale as the air duct (that is, $d_2 = 1$ ft). The form of the free surface was determined by point gage, the pressure distribution on the bottom by water manometer, and the end of the roller by surface float. The several length ratios thus obtained are plotted in Fig. 4. For the Froude number $F_1 = 4$, the velocity distribution was also measured by the double pitot tube (using the technique of flushing before each reading to eliminate errors due to entrapped air). The streamlines are plotted in Fig. 5 at a distorted scale to exaggerate the vertical displacement

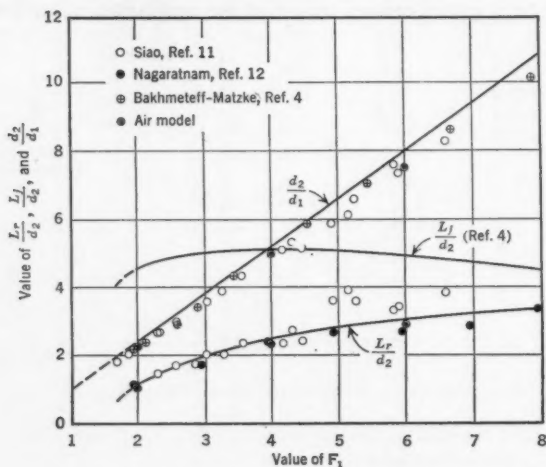


FIG. 4.—LINEAR CHARACTERISTICS OF THE JUMP

Superposed on Fig. 5 are the corresponding streamlines for flow in the air duct at a comparable depth ratio, surface profile, and Reynolds number, together with the pressure distribution on plane and curved surfaces. The agreement between the model and prototype results is seen to be quite satisfactory.

Fig. 4 shows the usual slight deviation of the measured depth ratio from that computed by means of the simplified momentum relationship of Eq. 1. The variation is attributable primarily to the neglect of boundary shear in the course of the derivation. In fact, it was the measured depth ratio rather than the computed ratio that had to be used in setting the duct profile. Moreover, in order to reduce wall shear (and, hence, its influence on the flow pattern) to a minimum, after introductory measurements the original duct was rebuilt to a width of 2.5 ft. All additional data presented herein were obtained with the wider flow section. However, even then, wall effects on the center-line flow

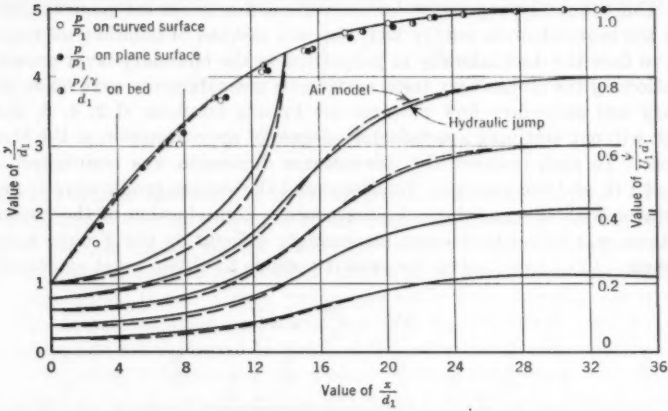


FIG. 5.—COMPARISON OF MEAN PATTERNS OF FLOW IN MODEL AND PROTOTYPE FOR $F_1 = 4$

were still noticeable, because the unit discharge,

$$q = \int \bar{u} dy \dots \dots \dots (25)$$

gradually increased with distance downstream. As a first-order correction for this variation, the local unit discharge rather than the initial unit discharge was used in computing the reference velocity. In no case did the change exceed

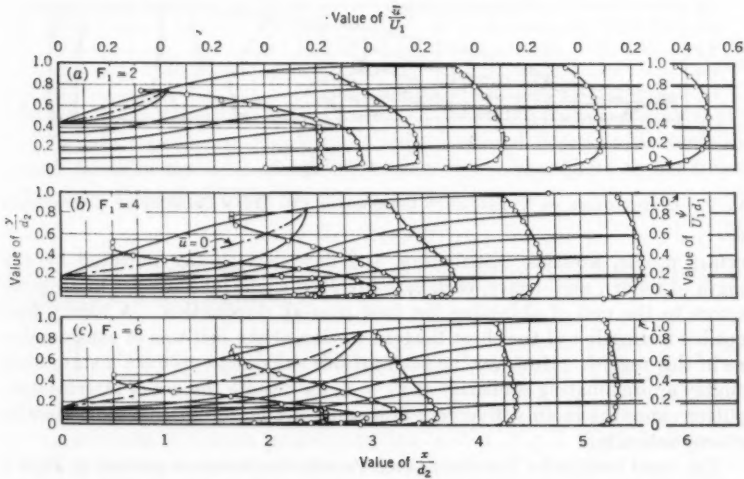


FIG. 6.—DISTRIBUTION OF MEAN LONGITUDINAL VELOCITY AND CORRESPONDING PATTERNS OF FLOW

6%. Unfortunately, correction for the volume flux is not the same as that for either the momentum or energy flux, the only method of handling all together being to flare the duct laterally in proportion to the boundary-layer growth.

Following the preliminary tests, systematic measurements were made of the primary and secondary flow patterns for Froude numbers of 2, 4, 6, and 8, though without attaining a satisfactory degree of approximation at the highest of these. In each instance the downstream dimension was maintained constant at 1 ft, and the upstream dimension and the surface profile were varied in accordance with the prototype requirements. Reproduction of the necessary conditions was found to become increasingly difficult as the Froude number increased. In no event, of course, was it possible to obtain exact agreement of

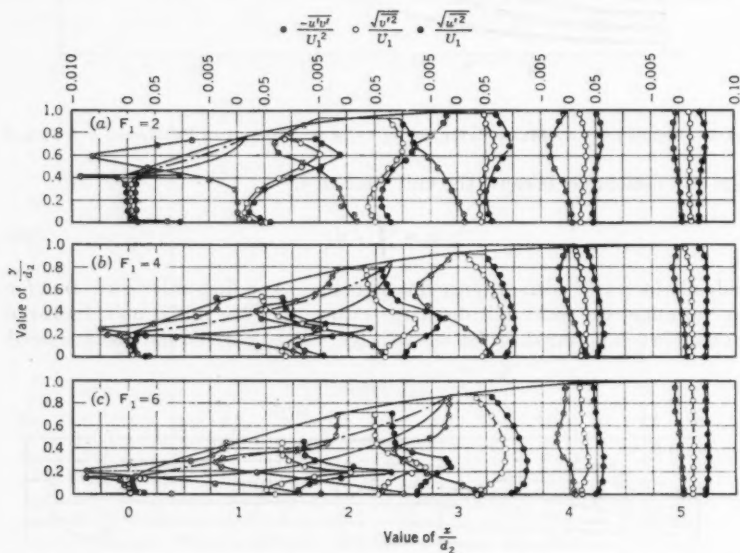


FIG. 7.—DISTRIBUTION OF TURBULENCE INTENSITIES AND MEAN PRODUCT OF COMPONENTS

surface profile, pressure distribution, and flow pattern (as indicated by the length of roller), and, hence, each case involved slight inaccuracies in all three factors to the end of obtaining the best over-all duplication. A barely perceptible inclination of the short tangent section of the bell was of considerable use in this regard. However, no such artifice sufficed to produce a state even roughly approximating similarity at $F_1 = 8$, for despite the use of intermediate splitter vanes the rapidly divergent flow could not be stabilized either laterally or longitudinally.

The basic results for the other three Froude numbers are plotted in Figs. 6 and 7. Fig. 6 embodies the mean-flow data and Fig. 7 the turbulence data. (For reasons of simplicity the w' -component of turbulence is not shown. It

did not differ greatly from v' , and, moreover, the measurements indicated that

$$\int_0^d \overline{u'^2} dy \approx \int_0^d (\overline{v'^2} + \overline{w'^2}) dy \dots \dots \dots (26)$$

that is,

$$\int_0^d \overline{V'^2} dy \approx 2 \int_0^d \overline{u'^2} dy \dots \dots \dots (27)$$

Values of the time derivative of u' will be introduced subsequently.) Whereas the initial depth is commonly used as the length parameter in dealing with the jump as such, in comparing the results for various Froude numbers it proved to be more convenient to use the final depth, as this maintains essentially the same longitudinal scale. Hence, purely geometric ratios are given in terms of d_2 . The Froude number necessarily involves d_1 , of course, and all other parameters also are expressed in terms of the initial depth and velocity.

Interpretation of Results.—Even without further manipulation of the data, Figs. 6 and 7 display trends of great significance in both the primary and the secondary aspects of the flow. First of all, the roller is seen to become progressively longer as the Froude number increases. From the curves of velocity distribution, three pertinent loci can readily be traced: (1) That of zero velocity, passing through the middle of the roller; (2) that of maximum velocity gradient near the roller edge; and (3) that of maximum velocity, essentially midway between the roller and the bed. Examination of the curves of turbulence intensity will show that this is a minimum where the velocity gradient is a minimum, and vice versa. The intensity of turbulent shear is likewise highest in zones of maximum velocity gradient, and the distribution curves of $-\overline{u'v'}$ are seen to undergo a change in sign with the velocity gradient much in accordance with the Boussinesq-Prandtl approximation,¹⁰

$$\overline{\tau} = -\rho \overline{u'v'} \approx \rho \epsilon \frac{\partial \bar{u}}{\partial y} \approx \rho l \left. \frac{\partial \bar{u}}{\partial y} \right| \dots \dots \dots (28)$$

in which ϵ is the Boussinesq mixing coefficient and l is the Prandtl mixing length.

The data presented in Figs. 6 and 7 may be utilized directly to evaluate the several terms in the momentum relationship of Eq. 14 reduced to nondimensional form through division by

$$\rho U_1^2 d_1 = \rho U_1 q \dots \dots \dots (29)$$

The relative magnitudes of the terms can be shown most conveniently by computing and plotting the sum

$$\frac{1}{U_1^2 d_1} \int_0^d \bar{u}^2 dy + \frac{1}{U_1^2 d_1} \int_0^d \overline{u'^2} dy + \frac{1}{2 F_1^2 d_1^2} + \frac{1}{R_1 U_1} \int_0^d \left(\frac{\partial \bar{u}}{\partial y} \right)_{y=0} dx \dots (30)$$

as a function of longitudinal distance, as shown in Fig. 8. In Eq. 30, the first term represents the mean momentum flux, and in Fig. 8 this is represented by MM; the second term is pressure, represented by P; the third term denotes

¹⁰ "Modern Conceptions of the Mechanics of Fluid Turbulence," by H. Rouse, *Transactions, ASCE*, Vol. 102, 1937.

turbulent momentum flux—TM in Fig. 8; and the fourth term is shear, denoted by S. Because the sum should be a constant at all successive sections, departure from its original value is a measure of the experimental error. Of principal significance in connection with these results is the fact that the contribution of the turbulence to the momentum flux, although it is of considerable importance at intermediate sections, is small at each final section. The contribution of the bed shear, although small also, necessarily increases with both

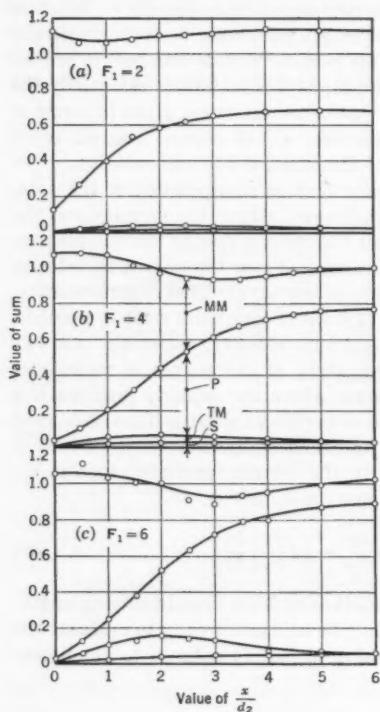


FIG. 8.—DIMENSIONLESS PLOTS OF MOMENTUM BALANCE

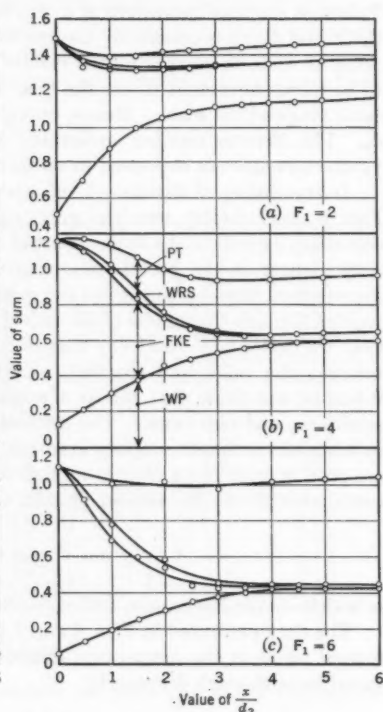


FIG. 9.—DIMENSIONLESS PLOTS OF MEAN-ENERGY BALANCE

distance and Froude number (and, it should be noted, with the viscous and roughness effects as well).

A comparable analysis of the energy relationship for the mean flow (Eq. 22) proceeds in much the same fashion. On the assumption (verified experimentally) that the terms involving the mean viscous stresses are of much smaller order than the others, and with

$$d_1 \frac{U_1^3}{2g} = q \frac{U_1^2}{2g} \dots \dots \dots (31)$$

as the common denominator, now it is the nondimensional sum

$$\frac{1}{U_1^3 d_1} \int_0^d \bar{v}^2 \bar{u} dy + \frac{2}{F_1^2 d_1} + \frac{2}{U_1^3 d_1} \int_0^d (\bar{u} \bar{u}'^2 + \bar{v} \bar{u}' \bar{v}') dy - \frac{2}{U_1^3 d_1} \int_0^d \int_0^x \left[\bar{u}' \bar{v}' \left(\frac{\partial \bar{u}}{\partial y} + \frac{\partial \bar{v}}{\partial x} \right) + (\bar{u}'^2 - \bar{v}'^2) \frac{\partial \bar{u}}{\partial x} \right] dy dx \quad (32)$$

that should be constant from section to section. In Eq. 32, the first term to the right of the equality sign represents the flux of kinetic energy and is represented by FKE in Fig. 9; the second term is the work done by pressure, and

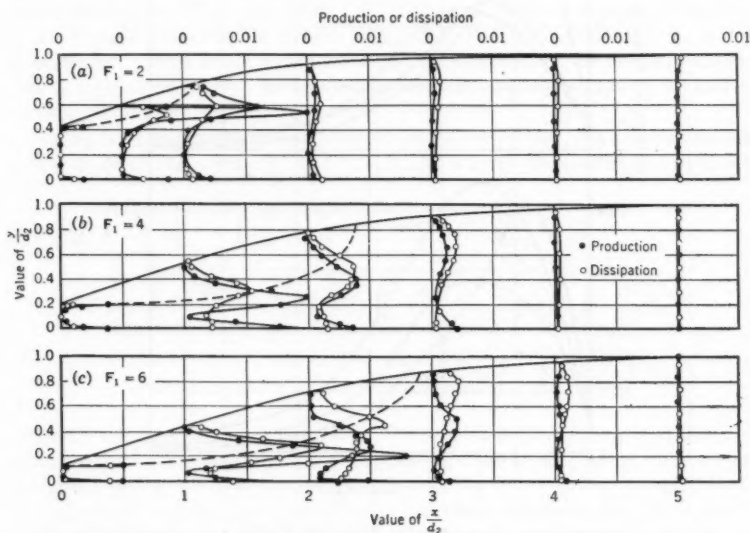


FIG. 10.—DISTRIBUTION OF TURBULENCE PRODUCTION AND DISSIPATION

WP is its symbol in Fig. 9; the third term denotes the work performed by Reynolds stresses—WRS in Fig. 9; and the last term is the production of turbulence and is denoted by PT. Calculation of the various quantities from the data presented in Figs. 6 and 7 yields the curves shown. The gradual change that characterized the corresponding sum in the momentum calculations is even more pronounced (particularly for $F_1 = 4$). No explanation is evident beyond experimental error, including the effect of wall retardation on the central flow.

Since it reappears in the energy equation of the turbulence, it is the turbulence-production term (the last member of Eq. 32) that remains of primary interest. In fact, its variation in comparison with that of the turbulence-dissipation term is particularly significant, not only from section to section but over each section as well. For this reason the nondimensional form of the

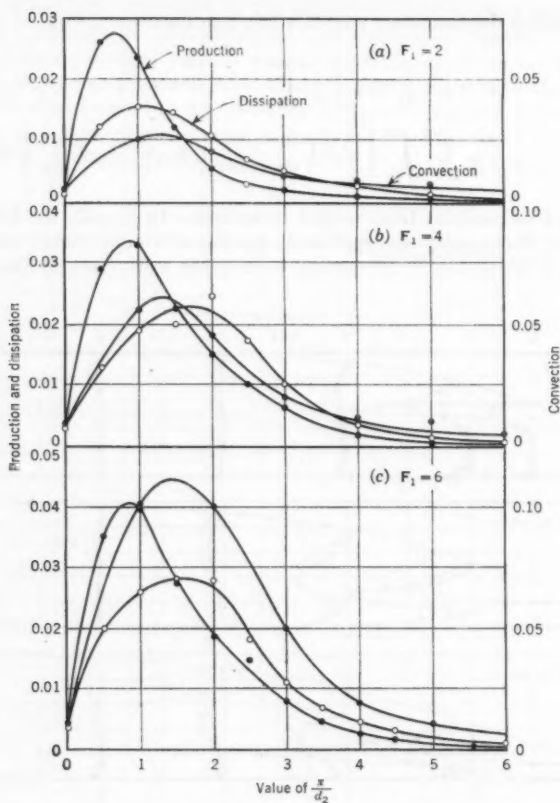


FIG. 11.—LONGITUDINAL VARIATION IN RATES OF PRODUCTION, CONVECTION, AND DISSIPATION OF TURBULENCE

local rate of production,

$$-2 \frac{d_1}{U_1^3} \left[\overline{u'v'} \left(\frac{\partial \bar{u}}{\partial y} + \frac{\partial \bar{\theta}}{\partial x} \right) + (\overline{u'^2} - \overline{v'^2}) \frac{\partial \bar{u}}{\partial x} \right] \dots \dots \dots (33)$$

(the double integral of which was used in preparing Fig. 9) is shown in detail in Fig. 10. Also shown in Fig. 10 is the corresponding distribution of the local rate of dissipation,

$$2 \frac{K}{R_1} \frac{d_1^2}{U_1^3} \left(\overline{\frac{\partial u'}{\partial x}} \right)^2 \dots \dots \dots (34)$$

The measured mean-square temporal gradient $\overline{(\partial u' / \partial t)^2}$ was used to approximate the required mean-square spatial gradient through division by \bar{u}^2 . The integrals of these distribution curves over the vertical sections are plotted

against longitudinal distance in Fig. 11, together with the corresponding integral for the rate at which the kinetic energy of the turbulence is convected past each section:

$$\frac{1}{U_1^3 d_1} \int_0^d \overline{V'^2} \bar{u} dy \dots \dots \dots (35)$$

Use of the isotropic value $K = 15$ would have yielded dissipation curves differing only slightly from those plotted. However, estimation of the remaining terms of Eq. 23 for the final section of the jump showed them to be so small that the cumulative production and dissipation of turbulence energy through the jump (the areas under the curves of Fig. 11) could be considered essentially equal. This permitted bulk values of K to be computed for each of the Froude numbers, the results being 12.2, 13.5, and 15.0 for 2, 4, and 6, respectively. How much significance can be attached to the trend in magnitude is a moot question. In any event, the curves plotted in Figs. 10 and 11 correspond to these values.

In studying the energy transformation of the turbulence, the nondimensional sum that should be constant (that is, essentially zero) from section to section is

$$\begin{aligned} & -\frac{2}{U_1^3 d_1} \int_0^d \int_0^x \left[\overline{u'v'} \left(\frac{\partial \bar{u}}{\partial y} + \frac{\partial \bar{v}}{\partial x} \right) + (\overline{u'^2} - \overline{v'^2}) \frac{\partial \bar{u}}{\partial x} \right] dy dx \\ & - \frac{1}{U_1^3 d_1} \int_0^d \overline{V'^2} \bar{u} dy - \frac{2}{\rho U_1^3 d_1} \int_0^d \overline{p' u'} dy - \frac{1}{U_1^3 d_1} \int_0^d \overline{V'^2} \bar{u'} dy \\ & - \frac{2K}{R_1 U_1^2} \int_0^d \int_0^x \overline{\left(\frac{\partial u'}{\partial x} \right)^2} dy dx \dots (36) \end{aligned}$$

in which the first term is production, the second is convection, and the fifth is dissipation. The corresponding diagrams for the three Froude numbers are presented in Fig. 12. Not included either in Eq. 36 or in Fig. 12 itself is the rate at which work is done externally by the viscous stresses, for calculation of this term (the fifth) in Eq. 23 showed it to be of much lower order than the others. On the other hand, it was impossible to evaluate either the rate at which work was done by the fluctuating pressures or the rate of diffusion of the turbulent energy, since neither the velocity-pressure correlation involved in the former nor the triple velocity correlation in the latter could be measured with available equipment. The small difference between the computed values of the other terms might hence be assumed to represent—except for experimental error—the sum of these two.

Several related characteristics of the turbulence should be noted in Figs. 10, 11, and 12. In Fig. 10, the locus of points of maximum production coincides closely with the border of the roller, whereas that for maximum dissipation lies appreciably higher, and the vertical spread of the dissipation curves is likewise greater. This emphasizes the fact that the turbulence is not wholly dissipated at its point of formation, but is convected by the mean motion (including the secondary flow of the eddy) and diffused by its own mixing action. Much

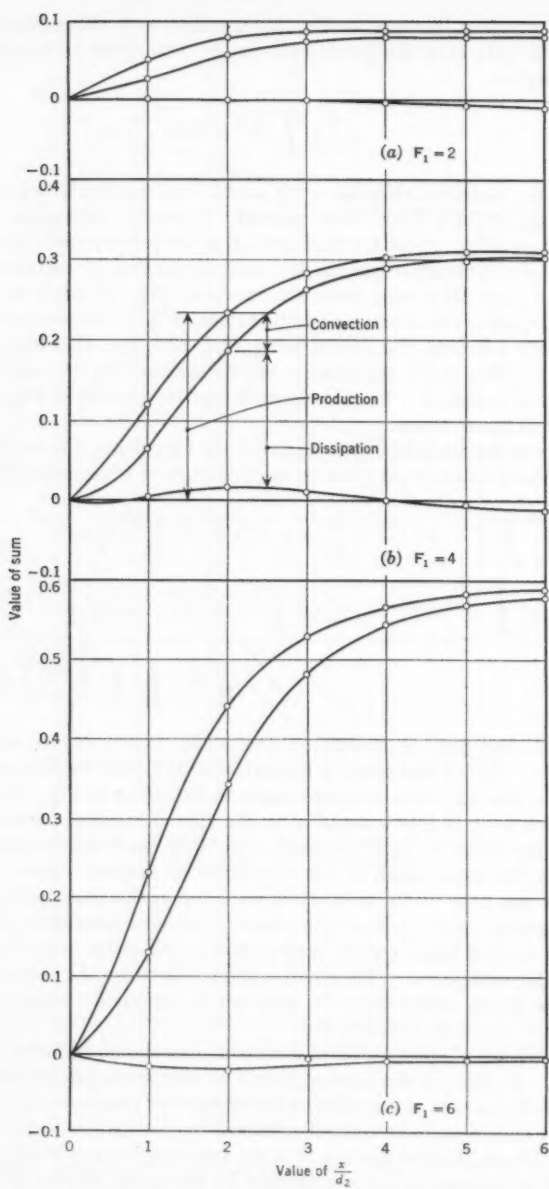


FIG. 12.—DIMENSIONLESS PLOTS OF TURBULENT-ENERGY BALANCE

the same situation is seen from Fig. 11. Even though the maximum rate of production per section occurs even ahead of the middle of each roller, the maximum rate of dissipation per section (as well as the maximum cross-sectional energy of the turbulence itself) occurs shortly before its end. As shown graphically by Fig. 12, the difference between the cumulative production rate and the cumulative dissipation rate up to a given section is represented with close approximation by the rate of convection of turbulence past that section.

The most essential of the foregoing results are summarized in the three geometric diagrams of Fig. 13. Whereas these correspond to the usual one-

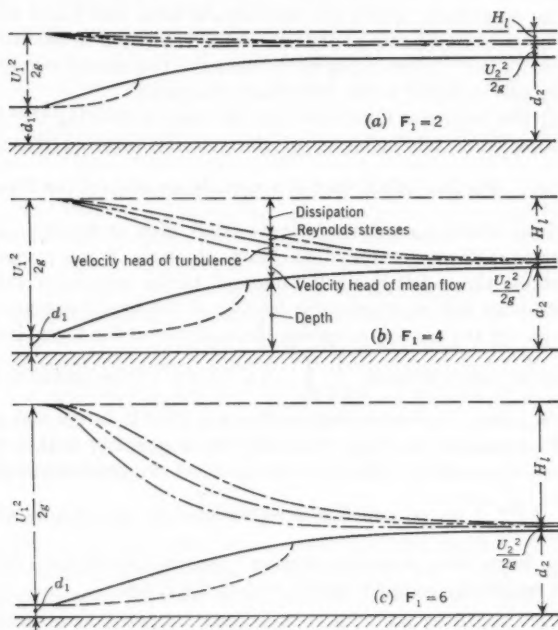


FIG. 13.—GENERALIZED DIAGRAMS OF ENERGY TRANSFORMATION THROUGH THE JUMP

dimensional representations of the jump, not only are they drawn to proper scale longitudinally as well as vertically, but they are quantitatively significant within the nonuniform zone of transition as well as in the uniform zones upstream and downstream. They are, to be sure, approximations rather than exact renditions of the phenomenon, because the least important of the variables have been ignored and the discrepancies evident in Figs. 9 and 12 have been distributed among the remaining terms. All in all, however, the inaccuracies are judged to be no greater than the variable effects of bed roughness and slope encountered in the field.

Lowermost among the curves plotted in Fig. 13 are those showing the variation of depth (that is, the profile of the free surface) for each of the Froude numbers. Next are those representing the addition of the velocity head of the mean flow, $\frac{1}{q} \int_0^d \frac{\bar{v}^2}{2g} \bar{u} dy$, to the depth, much as in the usual manner. However, although the correction factor

$$\alpha = \frac{1}{U^2 q} \int_0^d \bar{v}^2 \bar{u} dy \dots \dots \dots (37)$$

compensating for the use of the mean velocity $U = q/d$ is usually assumed to be unity, its magnitude within the nonuniform zone was found to rise to as high as 4; on the other hand, at the end of the transition it was within 5% of unity in every case. It should be noted that the two sets of curves just cited are the only two included in the customary diagrams.

Third in the sequence illustrated are the curves showing the increase in head resulting from the inclusion of the velocity head of the turbulence, $\frac{1}{q} \int_0^d \frac{\bar{v}^2}{2g} \bar{u} dy$. For the effect that the turbulence has on the flow the relative magnitude of this term is surprisingly small, even at the sections where it is a maximum; at the beginning of the jump, of course, it was purposely made insignificant; at the end it is small compared to the maximum value that it attained, although still an appreciable fraction of the final mean-velocity head. Next in order are the curves indicating the addition of the terms for the work done by the Reynolds stresses, $\frac{1}{g q} \int_0^d (\bar{u} u'^2 + \bar{v} v' v') dy$ —quantities that are very small in zones of normal turbulence but too great to be ignored completely in zones of pronounced mixing. The only other quantity with a magnitude comparable to those already plotted is the head lost through viscous dissipation, $\frac{K \nu}{g q} \int_0^d \int_0^x \left(\frac{\partial u'}{\partial x} \right)^2 dy dx$, and this is represented by the drop in the sum of all the other terms from section to section. As has already been emphasized, this drop is essentially complete at the end of the jump.

CONCLUSIONS

Through the analysis of turbulence measurements conducted in an air-flow model of the hydraulic jump under conditions simulating three representative Froude numbers, significant information has been obtained on the energy transformation associated with the phenomenon. In particular, the part played by the roller in producing the turbulence by which the transformation is effected has taken on new clarity. Although the measurements were necessarily lacking in both precision and completeness, their analysis proceeded in accordance with the basic equations of motion, and conclusions based thereon can be considered to have both qualitative and quantitative worth.

As in any other type of flow past a zone of discontinuity, at the juncture between the oncoming stream and the return flow or roller of the hydraulic

jump there is a pronounced velocity gradient, and the resulting shear gives rise to the rapid generation of turbulence. The effect of the turbulence, as usual, is twofold. On the one hand, the mixing process diffuses all characteristics of the flow—momentum, energy, and even the turbulence itself—both laterally and longitudinally. On the other hand, the increased viscous shear produces a rapid conversion of mechanical energy to heat. Were it not for the roller, the formation of the turbulence—and hence the dissipation of energy—would be minimal, as can be demonstrated in a closed duct so formed that the roller is eliminated. Except for Froude numbers well below 2, however, the hydraulic jump without a breaking front is physically impossible. The roller is thus an inseparable part of the phenomenon.

In view of the customary practice of considering the length of the jump to be the distance between the limiting sections of uniform flow, it should be noted that the roller extends about one-half this distance, and that one-half the energy of the turbulence is produced within the first half length of the roller. Because of both the convective effect of the mean flow and the diffusive effect of the turbulence itself, this energy is not wholly dissipated at the point that it is produced, but rather some distance away both vertically and longitudinally. In other words, there is a distinct lag between the loss of energy to the mean flow in the form of turbulence and its ultimate dissipation in the form of heat.

Of interest in this connection is the surprisingly small kinetic energy of the turbulence at any section, even in the zone of maximum production, convection, and dissipation at the midsection of the roller. At the final section of the jump, moreover, it is already small in comparison with the maximum value that it attained. Hence the belief that the energy lost to the mean flow persists for a considerable distance in the form of turbulence is definitely in error. In fact, the hydraulic jump is not only an effective means of reducing mean-flow energy but a very efficient mechanism for restoring conditions of uniformity to the flow.

ACKNOWLEDGMENTS

Development of the experimental technique and method of analysis, as well as the complete investigation for the intermediate Froude number in the original duct, formed the dissertation project¹¹ of the second writer and one of his assignments as Research Associate of the Iowa Institute. Measurement and evaluation of data for all three Froude numbers in the enlarged duct served as the thesis project¹² of the third writer and his sole assignment as Research Assistant. Both were frequently assisted by Philip G. Hubbard, A. M. ASCE, in the operation of the hot-wire anemometer. The senior writer conceived and directed the investigation and prepared the final manuscript. Partial support was received from the Office of Naval Research, Washington, D. C., under Contract N8onr-500(03) with the Iowa Institute.

¹¹ "Characteristics of Turbulence in an Air-Flow Model of the Hydraulic Jump," by T. T. Siao, thesis presented to the State University of Iowa, at Iowa City, in 1954, in partial fulfillment of the requirements for the degree of Doctor of Philosophy.

¹² "The Mechanism of Energy Dissipation in the Hydraulic Jump," by S. Nagaratnam, thesis presented to the State University of Iowa, at Iowa City, in 1957, in partial fulfillment of the requirements for the degree of Master of Science.

APPENDIX. NOTATION

The following symbols, adopted for use in the paper, conform essentially with "American Standard Letter Symbols for Hydraulics" (ASA Y10.2—1958), prepared by a committee of the American Standards Association with Society representation, and approved by the Association in 1958:

- d = depth of flow;
- F = Froude number;
- g = acceleration of gravity;
- H = total head (sum of velocity and piezometric heads);
- H_i = head lost in jump;
- h = piezometric head (sum of pressure head and elevation);
- i = tensor subscript, corresponding to coordinate direction of equation of motion;
- j = tensor subscript, corresponding to each coordinate direction in succession;
- K = dissipation coefficient;
- L_i = length of jump;
- L_r = length of roller;
- l = Prandtl mixing length;
- n = the outward normal to the surface;
- p = pressure intensity;
- q = rate of flow per unit width;
- R = Reynolds number;
- S = surface area;
- t = time;
- U = average of u across vertical section;
- u = instantaneous longitudinal component of velocity at a point;
- V = local magnitude of velocity vector;
- V = volume;
- v = instantaneous vertical component of velocity at a point;
- w = instantaneous lateral component of velocity at a point;
- X = longitudinal component of body force per unit mass;
- x = longitudinal coordinate;
- y = vertical coordinate;
- z = lateral coordinate;
- α = velocity-head coefficient for energy equation;
- γ = specific weight;
- ϵ = Boussinesq mixing coefficient;
- μ = dynamic viscosity;
- ν = kinematic viscosity;
- ρ = mass density;
- ψ = stream function; and
- τ = bed shear.

A bar ($\bar{}$) denotes the temporal mean value of the quantity beneath it, and a prime (\prime) denotes an instantaneous deviation from the temporal mean.

DISCUSSION

EDWARD SILBERMAN,¹³ A. M. ASCE.—It is surprising to note that no attention was paid to the abrupt separation of the boundary layer under the beginning of the jump due to the rapid decrease in velocity. The separation is identical with that occurring at transition from a parallel-sided flume to a diverging flume, for example, and is accompanied by a similar eddying motion under the jump. In fact, there are two rollers at the jump—one on the surface and one on the floor—and similar turbulence phenomena are associated with both.

To demonstrate separation under the jump a simple experiment can be performed. A 6-in.-wide, glass-sided, smooth-bottom flume is prepared by connecting a dye tube to the outside of a piezometer tap on the bottom of the channel. A jump is established in the channel in such a fashion as to move downstream, passing over the piezometer tap. Observation of a dye stream that is emitted slowly from the tap as the jump passes yields the following information:

- a. In the subcritical region, dye leaves the hole in a downstream direction, as would be expected in a normal boundary layer.
- b. As the end of the upper roller reaches the hole, the dye stream begins to waver. The general motion is still downstream, but wisps of dye are transported along the bottom to both sides.
- c. Further within the roller the dye has no characteristic direction, indicating that there is no boundary layer at all, and complete separation has occurred.
- d. From approximately one-half to one-third of the length of the surface roller forward to very near the beginning of the jump, the dye stream on the bottom actually moves upstream, indicating complete reversal of the boundary layer and the existence of a bottom roller.
- e. Just downstream of the beginning of the jump there is an abrupt change in direction of the dye from upstream to downstream again. A stagnation point and the beginning of the roller occur at this point.

The phenomenon described can be observed at Froude numbers of at least as low as 3, and for all higher numbers.

In this investigation the authors apparently did not note vertical velocity traverses through the jump. These traverses should have indicated the existence of the bottom roller. However, it is noted that the jump streamlines shown in Fig. 5 are displaced upward with respect to the air-flow streamlines. The displacement possibly is a consequence of the phenomenon under discussion. Separation on the bottom under the jump already had been referred to¹⁴ by Morrough P. O'Brien, M. ASCE.

¹³ Prof., St. Anthony Falls Hydr. Lab., Univ. of Minnesota, Minneapolis, Minn.

¹⁴ Discussion by Morrough P. O'Brien of "The Hydraulic Jump in Terms of Dynamic Similarity," by Boris A. Bakhmeteff and Arthur E. Matske. *Transactions, ASCE*, Vol. 101, 1936.

In view of the existence of this bottom roller, there is some question as to whether the turbulence characteristics of the jump have been modeled adequately by the subsonic air-flow model. It is suggested that the use of a sonic throat at entrance to the model, accompanied by a normal shock wave in the diverging section of the duct, would probably be a better model of the jump. Similar separation on a straight wall occurs behind a shock wave as occurs behind the hydraulic jump.

ALVIN J. PETERKA¹⁵ AND JOSEPH N. BRADLEY,¹⁶ MEMBERS, ASCE.—The authors have explained the workings of the hydraulic jump by means of its internal mechanics. Although the study is academic in nature, there are certain aspects of the results that help the practicing hydraulic engineer to rationalize the use of stilling basins shorter than the hydraulic-jump length.

It is common practice to make the stilling-basin floor (usually of concrete) shorter than the true length of the hydraulic jump. Hydraulic-model tests and prototype-verification tests have shown that, within limits, this is a desirable procedure because little is lost in the way of performance and because the cost of the stilling basin is reduced appreciably. In analyzing the action in the jump, it has been shown why it is possible to reduce the apron length to less than the jump length. Fig. 13 indicates that most of the losses occur upstream from the end of the roller and that the downstream end of the jump is relatively ineffective in accomplishing hydraulic losses. However, the velocity-distribution curves in Fig. 6 show that a redistribution of velocity occurs after the majority of the losses have occurred. For this reason it is not feasible to reduce the apron length as much as appears in Fig. 13. For example, in this figure, for $F_1 = 2$ it might be concluded that the apron need extend a distance of only approximately $3 d_2$ downstream from the beginning of the jump. However, for $F_1 = 2$, Fig. 6 shows that at a jump length of $3 d_2$ there is a major redistribution of velocity yet to be effected. If the apron were ended at this point the high bottom velocity might scour an unprotected riverbed. An end sill on the apron would help to redistribute the bottom velocity. According to Fig. 6, even at the end of the jump ($4.5 d_2$, as indicated in Fig. 4) a slight velocity redistribution still is to be expected.

In tests reported by the writers¹⁷ the jump was found to be imperfectly formed for a Froude number of 2 ($d_2 = 2.1 d_1$). The total energy loss was only approximately 7% in a jump $4.5 d_2$ long. Thus, the length of the jump was more useful to redistribute the velocities than to effect losses. Nevertheless, the apron length could not be reduced appreciably from the value of $4.5 d_2$ given as the jump length.

For a Froude number of 4 the writers found that the hydraulic jump had better form because $d_2 = 4.5 d_1$. The energy loss was approximately 40%, and the incoming jet showed some instability, tending to flutter from top to bottom of the jump. Surface waves downstream from the jump presented

¹⁵ Hydr. Engr., Bureau of Reclamation, U. S. Dept. of the Interior, Denver, Colo.

¹⁶ Hydr. Engr., Bureau of Public Roads, U. S. Dept. of Commerce, Washington, D. C.; formerly with Bureau of Reclamation, U. S. Dept. of the Interior, Denver, Colo.

¹⁷ "Hydraulic Design of Stilling Basins," by J. N. Bradley and A. J. Peterka, *Proceedings Papers* 1401-1406, ASCE, October, 1957.

more of a problem than scour tendencies. It was found that the apron length could be reduced considerably, however, without changing the jump action. With the addition of chute blocks and an end sill, the apron length was reduced to approximately $3.6 d_2$. For a Froude number of 4, Figs. 13 and 6 indicate that most of the losses have already occurred at $3.6 d_2$, and only a slight redistribution of bottom velocity will occur downstream from $3.6 d_2$.

For a Froude number of 6 the writers found the hydraulic jump to have the ideal form $d_2 = 8 d_1$, and the energy loss in the jump was approximately 55%. The apron length was reduced to $4 d_2$ when chute blocks and an end sill were added to the apron. Figs. 6 and 13 help to justify this length reduction.

It is unfortunate that the authors' tests for $F_1 = 8$ could not have been completed. These data probably would have shown that the roller occupied more than one-half the jump length, as stated in the section entitled "Conclusions." The writers' tests demonstrated that as the Froude number increased, the roller size increased until its length became the controlling factor in determining the jump length. The roller length approached the jump length for $F_1 = 8$, $d_2 = 10.7 d_1$, and the energy loss in the jump was approximately 65%. A discharge of 28 cu ft per sec in a 4-ft-wide flume produced a jump that was extremely turbulent and rough, and the jump itself surged because the bottom jet did not carry through at all times for the full length of the jump. Bottom-jet action was extremely erratic, sometimes penetrating the jump for the full length and at other times, for only a short distance. At intervals, the jet appeared to jerk horizontally and flutter vertically.

Also, the great difference in conjugate depths resulted in the jump having a steep profile. Slugs of water rolled intermittently down the steep face and fell into the high-velocity jet. A surface surge was created each time a slug made contact with the jet. This was strictly a gravitational effect that an air model may not duplicate. Actually, flow down the face is common to all jumps, but usually it is steady. These findings probably aid in explaining the difficulty experienced by the authors in adjusting their air model to obtain satisfactory data for $F_1 = 8$. Therefore, it is suggested that perhaps the agreement between the air model and the water model at $F_1 = 8$ was better than the authors surmised. The writers believe that with presently known equipment it would be impossible to make accurate measurements in a water jump of $F_1 = 8$ having appreciable physical size. In addition, if the air-model boundary were set to the jump length (Fig. 4), it is possible that the d_2 -test length was too short. In the writers' tests the jump length was considerably longer for the higher Froude numbers than shown in Fig. 4. It is not clear in the description of the water-model tests whether the length ratio, L_j/d_2 , was actually measured in the water model, or whether the Bakhmeteff-Matzke curve was accepted as the correct length of jump. In the air model the shape of the boundary (the jump profile in a water model) could influence greatly the action within the jump. The jump length given in Fig. 4 for $F_1 = 8$ is $4.2 d_2$. The writers' tests showed $6.1 d_2$. The difference is believed to be due primarily to the greater thickness of the incoming jet and to the width of the test flume used. Excessive friction in models that are too small can lead to erroneous results. The authors found it necessary to widen their air model to decrease the wall

effects noted in the 1-ft duct. This should serve as a warning to other experimenters who are tempted to use very narrow test facilities when wider sections could be used.

JAMES M. ROBERTSON,¹⁸ M. ASCE.—The study reported by the authors is of great interest because of the light which it sheds on the hydraulic jump and because it presents a thorough study of a separated flow that became re-attached. Many flow situations other than the jump occur with a separated zone of flow and with a roller-like action of the separated flow on the main stream.

The authors justify the suitability of air flow in the carefully formed diverging channel as a model of the hydraulic jump on the basis of expediency and verification of the mean-flow pattern. Although it is not intended to undervalue the significance of the study, it will be shown that certain aspects of the flow model could not have been similar to a jump. Two features of the flow model

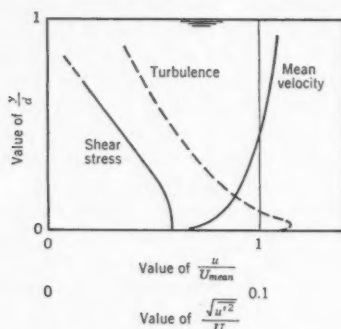


FIG. 14.—VELOCITY AND TURBULENCE VARIATION IN UNIFORM FLOW

differed from those of the hydraulic jump, one being inherent in the type of model chosen. The presence of a curved rigid boundary rather than the upper free surface of the jump certainly caused some modification in the nature of the flow. On the other hand, the initial mean and turbulence velocity conditions for the model jump differed from those normally expected in open-channel flow.

The flow conditions at the initial station of most hydraulic jumps should be those of fully developed, turbulent open-channel flow. The probable variations in mean velocity, turbulent shear stress, and turbulence intensity for this situation are shown in Fig. 14. By contrast, the initial conditions tested in the air-flow analogy involved relatively thin boundary layers at the upper surface and lower surface, with an intervening core of essentially shearless turbulence-free flow. In the case in which $F_1 = 2$, for example, the shear-stress curves of Fig. 7 indicate that the thickness of the boundary layer along the bottom was, at most, one-quarter of the initial flow "depth" even at relative distances, x/d_2 , of at least 2. Because the behavior of the turbulent boundary layer in

¹⁸ Prof. of Theoretical and Applied Mechanics, Univ. of Illinois, Urbana, Ill.

adverse pressure gradients is sensitive to initial flow conditions, the actual flow following this condition must have differed considerably from that in a proper hydraulic jump. In this respect the condition studied appears to conform closely to a jump following a sluice gate, a situation still of considerable interest.

Because the pressure increases as the flow proceeds in the x -direction (Fig. 5), one would expect to note separation along the "bed" of the channel. That no separation is in evidence might appear to be due to the existence of an abnormally thin boundary layer along this surface. Further consideration indicates that this explanation is not correct. The likely occurrence of turbulent boundary-layer separation has been shown¹⁹ to depend on the Reynolds number of the boundary layer at the beginning of the pressure gradient and also on the rate of pressure rise. The paper does not provide sufficient data to determine the initial conditions properly, but it appears that at the initial station the Reynolds number of the momentum thickness probably lay between 10^3 and 10^4 . If this is correct it is expected¹⁹ that the maximum mean-flow velocity could not be changed by a factor of less than from 0.76 to 0.69 for the test in which $F_1 = 2$ and from 0.78 to 0.67 for the test in which $F_1 = 6$. Actually the apparent reduction in maximum velocity is closer to 0.50 and 0.12 in the two cases. It is not clear why separation did not occur along the bed at $x/d_2 = 1.2$.

The second reservation with respect to the air model of the hydraulic jump concerns the upper, or free, surface of the jump and the roller. Because the streamline separating the roller from the main flow and the bed-pressure distributions are well verified, it appears that the model is adequate. This mean-flow similarity is certainly a necessary condition for similarity, but its character is essentially geometric. From a dynamic standpoint two other factors must be considered. The first factor is that a finite wall shear must have occurred in the air model due to the air motion past the rigid upper boundary. In the actual jump no such shear occurs, at least if air friction is neglected. The other divergence of the upper surface from the true hydraulic jump is less simply presented. In the true hydraulic jump the surface and its roller appear to be far from steady. Instantaneous views of the upper surface of the jump tend to give the appearance of a breaking wave falling backwards on the oncoming flow. The fluctuating nature of the free surface may have a significant effect on the flow at some distance below the surface even though none is apparent in the mean-flow characteristics.

In the upper boundary, or free surface, differences between the air model and the water prototype may be likened to the differences between the outer (distant from the wall) sections of boundary layer and pipe flows. Early analyses of the boundary layer assumed in the two cases that the velocity profiles (and, by implication, the turbulence pattern) were the same if the thickness of the boundary layer was equated to the pipe radius. More recently, careful studies have indicated significant divergences, both in mean velocity and turbulence characteristics, in the region away from the wall. G. B. Schubauer

¹⁹ "Prediction of Boundary-Layer Separation," by J. M. Robertson, *Journal of the Aeronautical Sciences*, Vol. 24, 1957, p. 631.

has shown²⁰ that this difference in turbulence is explained completely by the phenomenon of intermittency that occurs only at the outer, or free-stream, edge of turbulent flows. As shown in Fig. 15, the division between the turbulently flowing fluid and the liquid outside the boundary layer does not always occur at the same site, as in the case of laminar boundary layers. Instead, the interface, which occurs between turbulent flow and nonturbulent flow, fluctuates with time and is conceived of as waves or wrinkles that travel along the outer edge of the layer.

The fluctuation of the outer edge of a turbulent boundary layer differs vastly from the situation that exists at the center of a pipe, where the fluid is always turbulent. A velocity-indicating instrument with fast time response, when placed in the outer boundary-layer region, will note patches of turbulent and nonturbulent fluid in transit. This condition is termed "intermittency," and the fraction of time that the flow is turbulent is defined as the intermittency

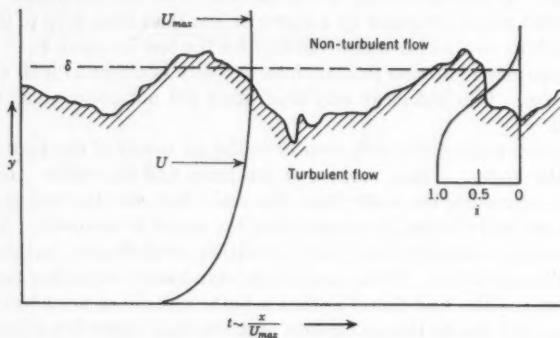


FIG. 15.—INTERMITTENCY AT OUTER EDGE OF TURBULENT BOUNDARY LAYER

factor, i . Schubauer demonstrated that if consideration is given to only the time when the flow is turbulent in the boundary layer, the turbulence in the outer region agrees satisfactorily with pipe measurements. It is probable that the differences in mean-velocity profile are also connected with intermittency.

Intermittency cannot be applied immediately to the hydraulic jump. Even in uniform open-channel flow, the free edge of flow is subject to a strong limitation, and the air-water interface must inhibit, if not eliminate, the occurrence of this phenomenon. In the case of the hydraulic jump it would appear that the unsteady roller may result in an intermittency type of behavior. Certainly the upper surface of the roller is rather intermittent in shape and position. The occurrence of air bubbles in this region should also lead to intermittency. As a further bit of suggestive evidence, it may be noted that in simple boundary-layer flows the wave or wrinkle length of the free boundary is of the order of two boundary-layer thicknesses. This is of the same order of magnitude as the relative length of the surface roller in the jump.

²⁰ "Turbulent Processes as Observed in Boundary Layer and Pipe," by G. B. Schubauer, *Journal of Applied Physics*, Vol. 25, 1954, p. 188.

Although one might question whether the authors have "modeled" the hydraulic jump adequately, it is agreed that some valuable data have been obtained pertinent to the flow behavior in the jump. Actual turbulence studies of a wet hydraulic jump will be needed to ascertain the extent to which the model studied was appropriate.

Other than its hydraulic-jump connotation, the study is an extremely valuable piece of basic research. Very few turbulence measurements have been

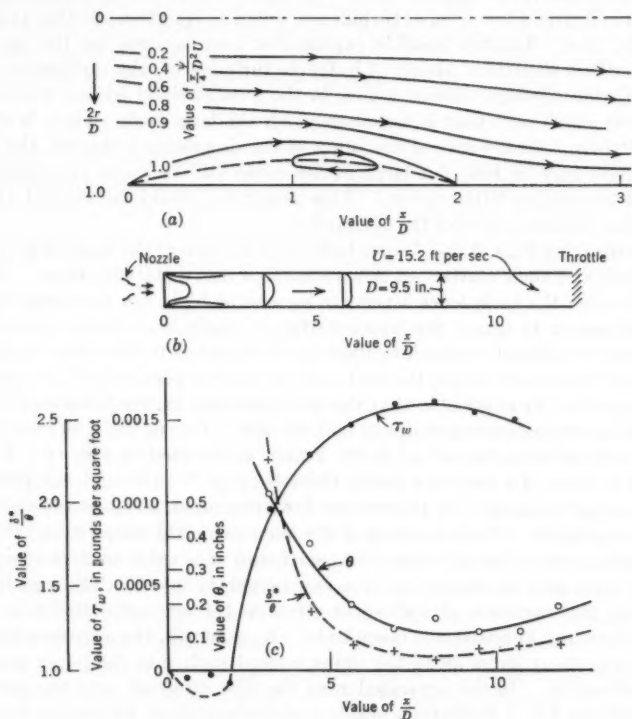


FIG. 16.—FLOW CHARACTERISTICS OF A REATTACHING FLOW IN A PIPE

made of separating and reattaching flows; yet these are quite common occurrences (for example in valves). The only comparable study with which the writer is familiar was conducted by Anton A. Kalinske,²¹ M. ASCE. In this project the sudden expansion and large angle diffusers involved separation and subsequent reattachment. The experimental techniques used were much cruder than those utilized in the present study, but somewhat similar conclu-

²¹ "Conversion of Kinetic to Potential Energy in Flow Expansions," by A. A. Kalinske, *Transactions, ASCE*, Vol. 111, 1946, p. 355.

sions were reached. Kalinske stated that "the maximum total turbulence energy is a small part of the total energy change taking place" and "the principal loss of energy occurs at the outside of the high velocity stream as it passes into the expansion due to the very high shear developed."

The authors note the relatively rapid disappearance of the extra turbulence energy generated in their expanding flow. Kalinske's sudden-expansion results indicate a decay that was almost as rapid. Because to the observer of the hydraulic jump it still appears quite "turbulent" at its downstream end, where Fig. 10 indicates a low level of turbulence, one may question whether to believe what he sees. Another possible explanation may account for this anomaly. In other flow situations (decay of isotropic turbulence), the turbulence energy is dissipated through viscous action in the smaller-sized eddies, whereas the relatively small part that is associated with the large-scale eddies, is affected only slightly. In the case of the jump at the downstream station, the turbulence level may be low, but large eddies could still be quite prominent even though containing little energy. This possibility could be verified through spectrum measurements of the turbulence.

By studying Figs. 6 and 7 some indication is given of the manner in which a separated and then reattached flow redevelops into a stable pattern. Following the roller the turbulence levels are seen to be high, but the mean-velocity profiles appear to ignore the upper surface. Analysis of mean-velocity data from other studies of reattaching flows have suggested to the writer that a new boundary layer forms along the wall more or less independently of any previous development. It is possible that the measurements in the jump case did not proceed far enough downstream to indicate this. One of the flow cases, which were analyzed with the aid of H. R. Fraser, is depicted in Fig. 16. This involved the flow of a jet into a partly throttled pipe.²² Although the pitot tube used was not calibrated for the reverse flows measured, a significant separation zone is apparent. The low values of the momentum thickness, θ , and the ratio of displacement to momentum thickness found at a value of x/D of approximately 8 suggest the beginning of a new boundary layer. Although it is inaccurate, the variation of wall shear stress in the separated region is of the proper sign and approximate magnitude. By contrast, the apparent behavior of the wall-shear stress along the upper curved surface in the paper seems incomprehensible. In the separated zone the flow direction near the surface is reversed; yet Fig. 7 indicates a negative wall-shear stress within the roller and following it.

To compute the turbulence dissipation the authors utilized the isotropic relationship (constant K -values across and along the flow). However, the value was adjusted in a bulk fashion for the several Froude-number models studied. Certainly the value of K must vary throughout the flow field as the turbulence is far from isotropic and because the sort or degree of isotropy can hardly be uniform. P. S. Klebanoff has measured²³ most of the terms appearing in the

²² "Mixing and Equilibrium in Pipe Flow," by W. H. Carrier and W. S. Misener, *Paper 53-5-44*, ASME, May, 1953.

²³ "Characteristics of Turbulence in a Boundary Layer with Zero Pressure Gradient," by P. S. Klebanoff, *Report 1247*, National Advisory Committee for Aeronautics, Washington, D. C., 1955.

turbulence-dissipation relationship for a boundary-layer flow. Some of the terms differed by a factor of 10 from the isotropic values. Based on plausible assumptions for the unmeasured terms, a transverse integral of the dissipation indicated more than twice the dissipation computed with the isotropic relationship. It is difficult to believe that the more involved pressure gradient and separation-flow case in the jump model would come out as closely. Therefore, the dissipation relationships of Fig. 11 must be considered as being of suggestive value rather than absolute value.

Even within the limitations that should be placed on the results, much valuable information has been presented. Perhaps more detailed data on the quantities measured could be made available in order that they may be studied independently of the hydraulic-jump framework within which the paper is cast.

DONALD R. F. HARLEMAN,²⁴ A. M. ASCE.—As a supplement to an otherwise comprehensive treatment, it may be of interest to determine the explicit equation for the exact depth ratio of the hydraulic jump. This will permit an investigation of the small but systematic deviation of the experimental depth ratio, d_2/d_1 , from that predicted by the elementary momentum analysis given by

$$\frac{d_2}{d_1} = \frac{1}{2} (\sqrt{1 + 8 F_1^2} - 1) \dots \dots \dots (38)$$

This variation is shown graphically in Fig. 4, in which the authors' hydraulic experiments,^{12,13} together with those of Bakhmeteff and Matzke,⁴ are compared with Eq. 38. At a Froude number of $F_1 = 6$, for example, the measured depth ratio is 5% lower than that given by the elementary theory.

Edward R. Van Driest²⁵ also presents the analytical expressions for the depth ratio of the hydraulic jump that take into account (a) the boundary shear, (b) the excess of mean momentum flux due to nonuniform velocity distributions at the beginning and end of the jump, and (c) the momentum flux due to turbulence. However, for the first time, the authors' paper permits these terms to be evaluated quantitatively from direct measurements.

The exact equation for the depth ratio, d_2/d_1 , can be obtained by evaluating the indefinite integrals of Eq. 14 at the end of the jump, where $d = d_2$ and $x = L_j$. Then Eq. 14 becomes

$$\int_0^{d_2} \rho \bar{u}_2^2 dy - \int_0^{d_1} \rho \bar{u}_1^2 dy + \int_0^{d_2} \rho (\overline{u_2'})^2 dy \\ = \frac{\gamma d_1^2}{2} - \frac{\gamma d_2^2}{2} - \int_0^{L_j} \mu \left(\frac{\partial \bar{u}}{\partial y} \right)_{y=0} dx \dots (39)$$

²⁴ Associate Prof. of Hydraulics, Hydrodynamics Lab., Massachusetts Inst. of Technology, Cambridge, Mass.

²⁵ "Steady Turbulent-Flow Equations of Continuity, Momentum and Energy for Finite Systems," by E. R. Van Driest, *Journal of Applied Mechanics*, ASME, Vol. 13, No. 3, September, 1946.

Then the following dimensionless coefficients are introduced:

$$\beta_1 = \frac{\int_0^{d_1} \bar{u}_1^2 dy}{U_1^2 d_1} \dots \dots \dots (40a)$$

$$\beta_2 = \frac{\int_0^{d_2} \bar{u}_2^2 dy}{U_2^2 d_2} \dots \dots \dots (40b)$$

and

$$I_2 = \frac{\int_0^{d_2} (\overline{u_2'})^2 dy}{U_2^2 d_2} \dots \dots \dots (41)$$

in which β_1 and β_2 are the momentum-flux correction terms for nonuniform velocity distribution, and I_2 is the downstream turbulence-flux correction term (I_1 assumed to be equal to zero). After dividing through by γ , Eq. 39 may be rewritten as

$$\beta_1 U_1^3 \frac{d_2}{g} - \beta_1 U_1^3 \frac{d_1}{g} + I_2 U_2^3 \frac{d_2}{g} = \frac{1}{2} (d_1^3 - d_2^3) - \frac{\mu}{\gamma} \int_0^{L_j} \left(\frac{\partial \bar{u}}{\partial y} \right)_{y=0} dx \dots (42)$$

By introducing the continuity equation ($U_1 d_1 = U_2 d_2$) and defining the Froude and Reynolds numbers as

$$F_1 = \frac{U_1}{\sqrt{g d_1}} \dots \dots \dots (43a)$$

and

$$R_1 = \frac{U_1 d_1}{\nu} \dots \dots \dots (43b)$$

Eq. 42 may be written as

$$F_1^3 = \frac{\frac{J}{2} [(J+1)(J-1) + S]}{\beta_1 J - (\beta_2 + I_2)} \dots \dots \dots (44)$$

in which $J = d_2/d_1$ and

$$S = \frac{2 F_1^2}{U_1 R_1} \int_0^{L_j} \left(\frac{\partial \bar{u}}{\partial y} \right)_{y=0} dx \dots \dots \dots (45)$$

Eq. 44 should reduce to the form of the elementary momentum solution of the hydraulic jump if $\beta_1 = \beta_2 = 1$ and $I_2 = 0$ and $R_1 = \infty$ (frictionless flow, $S = 0$). Under these conditions,

$$F_1^3 = \frac{J}{2} (J+1) \dots \dots \dots (46)$$

which is in agreement with Eq. 38.

The dimensionless quantities β_1 , β_2 , I_2 , and S can be evaluated from the authors' experimental data for each Froude number tested, and the corresponding values of the depth ratio, J , can be computed from Eq. 44.

Table 1 shows the quantities determined from Figs. 7 and 8. Each of the downstream quantities, β_2 , I_2 , S , were determined at the end of the jump ($x/d_2 = 5$).

Table 1 also cites the values of the depth ratio, $J = d_2/d_1$, from the exact analysis (Eq. 44) and the elementary analysis (Eq. 46). The exact depth ratio is systematically less than the elementary one.

TABLE 1.—MOMENTUM, TURBULENCE, AND SHEAR PARAMETERS

F_1	β_1	β_2	I_2	S	Exact J (Eq. 44)	Approximate J (Eq. 46)
2	1.01	1.02	0.01	0.16	2.31	2.37
4	1.01	1.05	0.06	1.05	5.02	5.18
6	1.01	1.02	0.15	3.60	7.70	8.00

A verification of the authors' measurements and the general validity of Eq. 44 can be demonstrated by comparing the three predicted (exact) values of the depth ratio with Fig. 4. The comparison is shown in Fig. 17, which indicates that the predicted values (shown by the dashed line) account for the

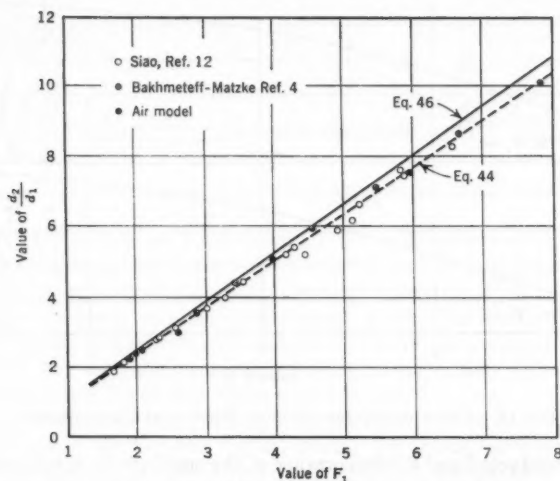


FIG. 17.—COMPARISON OF EXACT AND ELEMENTARY MOMENTUM EQUATIONS FOR JUMP-DEPTH RATIO

departure of the experimental depth ratios from the elementary momentum equation for both the hydraulic and air-model tests.

The bottom shear, S , is by far the most important corrective term in the exact equation for the depth ratio of the jump. In fact, it can be shown that the momentum-flux corrections and the turbulence-flux corrections tend to cancel each other. In this respect the effect of bottom shear in reducing the

downstream depth of a hydraulic jump is similar to the effect of baffle piers.²⁶ With the latter the distributed boundary-shear parameter, S , may be replaced by a term that is descriptive of the concentrated force exerted by the piers on the fluid.

PHILIP G. HUBBARD,²⁷ A. M. ASCE.—The analogy between the air-flow system and an actual hydraulic jump may seem to be rather artificial at first glance, so that further verification may be needed, or at least an evaluation of the applicability of the results. Because of the thoroughness with which the

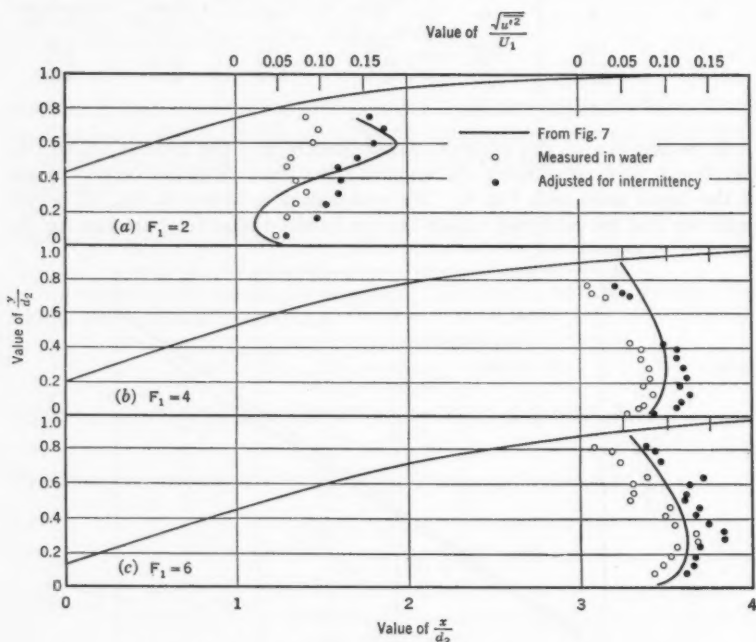


FIG. 18.—CHECK ON DISTRIBUTION OF TURBULENCE INTENSITIES

study was conducted and the importance of the conclusions, it seems desirable to take advantage of any technique that might supply additional evidence. The hot-film anemometer mentioned by the authors is such a technique, and some exploratory measurements with it are presented herein.

Fortunately, the flume used for the measurements in water is permanent equipment, so that it was possible to reproduce the conditions of the earlier experiments. In order to obtain representative results in a brief time, measurements were made at each Froude number for which results were reported, but

²⁶ "Effect of Baffle Piers on Stilling Basin Performance," by Donald R. F. Harleman, *Journal*, Boston Soc. of Civ. Engrs., April, 1955.

²⁷ Research Engr., Iowa Inst. of Hydr. Research, Iowa City, Iowa.

they were made only for one representative zone in the flow. The zone chosen was near the downstream end of the roller, where the longitudinal component of turbulence was measured along a vertical line. Although a complete comparison cannot be made on the basis of this one component, it is probably the most representative single parameter. As mentioned by the authors, the total turbulence intensity is nearly equal to twice the intensity of the longitudinal component—

$$\int_0^d \overline{V'^2} dy \approx 2 \int_0^d \overline{u'^2} dy \dots \dots \dots (47)$$

When the measuring instrument was placed in the chosen zone, two pertinent characteristics were immediately evident. The passage of innumerable air bubbles past the probe had scarcely any discernible effect on the velocity indications, so that some earlier misgivings were without basis. Also the fluctuations were so erratic that only a rough indication could be obtained of either the mean velocity or the root-mean-square deviation of the instantaneous velocity from that mean. Although this problem had been encountered to some extent in the air jump, it was greatly compounded in water. It had been

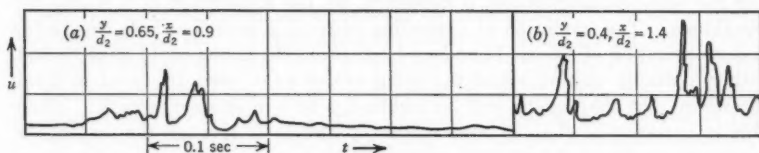


FIG. 19.—VELOCITIES IN AND IMMEDIATELY DOWNSTREAM FROM THE ROLLER

expected that the frequency spectrum of the turbulence would be shifted downward because of the lower velocities used in water, and this shift was expected to cause difficulty because the time constants of the turbulence-analyzing instruments were marginally small. Even when the probable error due to inadequate frequency range in the root-mean-square analyzer was taken into account, however, the measured intensities of turbulence shown in Fig. 18 were discouragingly lower than those shown in Fig. 7.

In order to examine more carefully the variation of the fluid velocity, the output voltage of the hot-film control circuit was connected directly to the deflection terminals of a cathode-ray oscillograph so that no error was introduced by coupling networks. Some typical records obtained in this fashion have been traced from photographs for reproduction in Fig. 19, and it is believed that they contain the key to the discrepancy noted already. It was observed that bursts of high-intensity turbulence were interspersed with periods of relatively tranquil flow. This intermittency existed not only near the upper edge of the boundary layer, but was quite pronounced inside the roller. If the data of Fig. 18 are modified by eliminating the periods of tranquil flow from the record, then the intensity of the remaining fluctuations is slightly greater than that indicated in Fig. 7.

Any evaluation based on the results reported herein can only be tentative pending a more complete investigation, but two conclusions can be made:

1. The diffusion characteristics of the hydraulic jump are probably represented quite well by the results of the paper, but those flow characteristics that depend on the smaller-scale components are probably distorted slightly by the higher indications of the intensity of fluctuation.

Techniques and possibly definitions will have to be developed, especially for flow conditions where intermittency may occur.

HUNTER ROUSE,²⁸ M. ASCE, TIEN TO SIAO,²⁹ AND S. NAGARATNAM³⁰.—Comments on the paper were of particular interest in that they reflected the views of investigators at five of the principal hydraulics laboratories engaged in research on turbulent flow. Significant points already considered during the preparation of the paper were emphasized, and others not considered, or at least not given their proper attention, were very pertinently noted. As is always the case, the net result is a marked improvement over the original contribution.

The writers recommend that everyone who has access to a glass-walled flume carry out the experiment described by Mr. Silberman—artificially varying the velocity distribution, if necessary, by the application of a coarse bed roughness. The formation of a standing eddy on a level floor is as convincing a demonstration of a basic boundary-layer principle as one could hope to find. Other hydraulic distortions of the jump proper have been discussed in detail elsewhere, but they might well be mentioned here in this connection: Those due to variation of channel cross section, particularly through the trapezoidal range; to variation of bed slope, as in a chute, bed curvature, as on a spillway bucket, or bed alignment, as at the end of an apron; and variation in wall alignment or curvature, as in flared or warped chute spillways. Each of these will have an influence upon the jump characteristics that is just as important in its way as that of bed roughness, but just as inessential to the basic jump phenomenon. In conducting the investigation the writers attempted to eliminate every possible extraneous factor, including initial velocity distribution, so that full attention could be given to the mechanism of turbulent expansion. Surely the introduction of a sonic throat and shock wave, as suggested by Mr. Silberman, would not have been an effective step in this direction.

Messrs. Peterka and Bradley introduced a welcome note into the literature in their immediate recognition of the usefulness of academic findings in clarifying the practical aspects of a related problem. The question of jump length has long been a matter of controversy, in part for lack of agreement on nomenclature, and in part because the jump actually never ends but only approaches asymptotically a state of depth, velocity, and turbulence equilibrium. Designation of an end thus is purely arbitrary. Messrs. Peterka and Bradley have realistically adopted a criterion based upon bed velocity; Bakhmeteff and Matzke logically based theirs on depth; the writers conveniently terminated

²⁸ Director, Iowa Inst. of Hydr. Research, State Univ. of Iowa, Iowa City, Iowa.

²⁹ Hydr. Engr., Inst. of Hydr. Research, Academia Sinica, Peking, China.

³⁰ Engr., Harza Eng. Co., Chicago, Ill.

their boundary curves where the effect of further curvature seemed to be inappreciable. Were residual turbulence (the academic choice) to determine the nominal end, its position would obviously depend on the percentage arbitrarily chosen for the permissible turbulence remainder. Since this remainder continues to be appreciable in comparison with that of the subsequent uniform flow for some distance downstream, such a definition would produce by far the greatest nominal length. The discussers are correct in their belief that length of roller and length of rapid expansion would approach equality as the Froude number became very large. If the residual turbulence were related to the over-all loss, all definitions would then agree at the (unfortunately, purely academic) limit.

Mr. Robertson, to select a minor comment from his discussion at this point, speaks of a normal or "proper" hydraulic jump as one which occurs in established open-channel flow. This recalls, of course, the discussion by Mr. Silberman. Messrs. Peterka and Bradley, on the other hand, may well think of a proper jump as one controlled by the baffle piers of a foreshortened apron. "Established" flow is actually no more definite than is the design of a pier and apron, for it can vary through wide limits with channel roughness and shape. For this reason Mr. Harleman's detailed momentum analysis of the jump, and his application of the resulting equation to the three conditions described in the paper, represent supplementary material of basic import. The writers fear, however, that readers will ignore the equation and assume the plotted curve to indicate a general solution. The fact should hence be emphasized that even in established flow there will be a different deviation from the elementary equation for every Reynolds number, relative roughness, and channel shape.

To return to Mr. Robertson's discussion, the writers can only report that there was no indication of bottom separation in either flume or duct for the condition of minimal boundary-layer growth that was sought experimentally. In so far as the upper-boundary effect was concerned, in the vicinity of the nonuniformity it was surely not one of shear. Whereas a more refined method of measurement would undoubtedly have revealed a positive shear above the roller, as correctly expected by Mr. Robertson, comparison of its probable magnitude with that in the region of high velocity gradient below would not lead one to anticipate much change from the conditions shown. The effect of the boundary upon large-scale fluctuations, on the other hand, was admittedly considerable, and some indication of its magnitude is undoubtedly to be found in Mr. Hubbard's measurements.

Free-turbulence literature now distinguishes between three different regions of the turbulence spectrum—the fine-scale region, in which the major part of the dissipation occurs; the normal-scale region, containing the eddies in which most of the energy of the turbulence is concentrated; and the large-scale region of intermittency described by Mr. Robertson. In this sense the large eddies which are so obvious a part of the true hydraulic jump represent neither an appreciable concentration of energy nor an important source of dissipation. They can, however, play a considerable role in the process of mixing. At the juncture between the roller and the main stream, the intermittent formation of these large eddies (often distinguishable in jump photographs) is much like

that observed at the edges of jets, wakes, and boundary layers. The free surface, which is the more noticeable zone of intermittent fluctuation and is that to which Mr. Robertson refers, has some of the same characteristics. However, as noted in the discussion, it also has two interrelated features which distinguish it: Abrupt discontinuity of the liquid medium itself, and the stabilizing or restoring action of gravity. The air model surely duplicated the essential freedom of motion in the lower zone of intermittency; to what extent the fluctuations in this zone are actually controlled by the free-surface fluctuations remains to be determined.

Mr. Robertson correctly implied that the plotted dissipation functions were of a partially assumed rather than a completely measured nature, in view of the representation of the nine velocity derivatives by a single one through the relationships of isotropy. Whether this assumption requires only a high Reynolds number to be closely valid, or the components even then would deviate to different degrees in different directions and different zones of flow, must also remain to future investigations for a conclusive answer. Surely the present measurements do not indicate the existence of much variation in validity from section to section; otherwise the production-convection-dissipation sum would have departed more radically than it did from a zero value. It should also be remarked in this regard that such indications of small-scale isotropy as exist to date have been found under conditions of free turbulence, whereas deviations therefrom have all been noted in the vicinity of solid boundaries.

Measurements of the type proposed implicitly by Mr. Robertson and explicitly by Mr. Hubbard must eventually be made, although the writers shudder to think of the painstaking labor involved in determining at many successive sections—under conditions in which even the depth itself is very hard to define—what, to date, has been measured only for representative sections of flows which are either uniform or similar from section to section. Mr. Hubbard apparently has at hand equipment that will accomplish some part of the measurements required—at least at a safe distance below the freely fluctuating surface—and he has demonstrated a knack of filling other needs as they arise. Still to be found are a group of expert laboratory technicians with considerable time at their disposal, and an unusually patient and sympathetic sponsor!

AMERICAN SOCIETY OF CIVIL ENGINEERS

Founded November 5, 1852

TRANSACTIONS

Paper No. 3007

PRESSURE LINES AND INELASTIC BUCKLING OF COLUMNS

BY FRANK BARON,¹ M. ASCE AND HAROLD S. DAVIS,²
A. M. ASCE

SYNOPSIS

The pressure-line concept developed for elastic arches and rigid frames, and for the inelastic deformations of structural elements, ds in length, is applicable to studies of the inelastic behavior of columns and of rigid frames. The concept is extended herein for the inelastic behavior of such structures and for eccentrically and laterally loaded columns. In the same way as for structural elements, ds in length, the inelastic behavior of such columns can be stated in terms of the elastic behavior modified to take into account the effects of plasticity.

INTRODUCTION

A pressure line is defined as a string polygon that shows the successive resultants of the reactions and loads acting on a structure. The concept had its origin in studies of masonry construction³ and in the development of graphical methods of analysis. It has been used in the study of walls, buttresses, chimneys, as well as structures that lie in a plane and consist of single closed circuits. Examples of such structures are arches and rigid frames. When applied to these structures, the concept has ordinarily been used for elastic behavior and for loads that lie in the planes of the structures.

The concept has been extended⁴ to structures that lie in a plane, are loaded normal to their plane, and are continuous between two supports. It was also extended⁴ to structures that are curved in space, are loaded in any direction, and are continuous between two supports. However, in each case, only elastic behavior was considered.

NOTE.—Published, essentially as printed here, in October, 1957, in the Journal of the Engineering Mechanics Division, as *Proceedings Paper 1484*. Positions and titles given are those in effect when the paper was approved for publication in *Transactions*.

¹ Prof. of Civ. Engr., Univ. of California, Berkeley, Calif.

² Sr. Structural Engr., Hanford Atomic Products Operation, General Electric Co., Richland, Wash.

³ "A Treatise on Masonry Construction," by Ira O. Baker, John Wiley & Sons, Inc., New York, N. Y., 1902, p. 463.

⁴ "Laterally Loaded Plane Structures and Structures Curved in Space," by Frank Baron and James P. Michalos, *Transactions*, ASCE, Vol. 117, 1952, p. 279.

A time-saving procedure based on the pressure-line concept was developed⁵ for estimating the effects of inelasticity on the behavior of structural elements, ds in length, subjected to axial and flexural loads. The procedure consists of obtaining an initial estimate by means of an elementary theory of mechanics and adjusting the estimate to fit the conditions of a theory of plasticity. In this way, the moment-angle change relationship can readily be obtained for all values of axial thrust and moment. The procedure was demonstrated pictorially. It can be used also in conducting algebraic studies, which will be demonstrated herein for several kinds of stress-strain curves.

The pressure-line concept can be used in studying the inelastic behavior of arches, rigid frames, and the inelastic buckling of eccentrically and laterally loaded columns. This is demonstrated herein in two ways—namely, pictorially for arches and frames, and algebraically for columns.

THE PRESSURE LINE FOR ARCHES AND FRAMES

The paper is restricted to arches and frames that lie in a plane and are loaded in their plane. It is assumed that (1) the loads are increased from zero to their final values; (2) the effects of shear and residual strains can be neglected; (3) the dimensions of the undeflected structure can be considered in determining the pressure line; (4) buckling will not occur; and (5) if failure develops, it is caused by a sufficient number of hinges being formed to produce a mechanism in the plane of the arch.

A. Winkler proposed^{3,6} a theorem concerning the position of the pressure line, or line of resistance, for single-span elastic arches. He stated,

"for an arch ring of constant cross section that line of resistance is approximately the true one which lies nearest to the axis of the arch ring, as determined by the method of least squares."

This theorem was drawn from conclusions based on studies of the voussoir masonry arch and is approximately correct for the elastic theory of solid arches.

The foregoing theorem was extended by the late Hardy Cross, Hon. M. ASCE, for loads lying in the plane of single-span elastic arches and closed rings.⁷ He restated the theorem in three forms as follows:

1. "The pressure line for a group of loads lying in the plane of an arch is that string polygon for the loads which most nearly fits or hugs the axis of the arch."

"Fit" in this statement is to be judged by eye.

2. "The pressure line for a group of loads is that string polygon which makes the moment areas balance or vanish."

For vertical loads, the moments in the arch are proportional to the vertical intercepts between the string polygon and the axis of the arch. For horizontal loads, the moments are proportional to horizontal intercepts. In general, the moment at any point in a loaded arch is equal to the force represented by the

⁵ "A Pressure-Line Concept for Inelastic Bending," by Frank Baron, *Transactions, ASCE*, Vol. 123, 1958.

⁶ "Zeitschrift des Architekten und Ingenieur Vereins zu Hannover," p. 199.

⁷ "Continuous Frames of Reinforced Concrete," by Hardy Cross and N. D. Morgan, John Wiley & Sons, Inc., New York, N. Y., 1932.

corresponding string of the pressure line times the perpendicular distance from the point to the string. "Balance" in this statement means that the total positive area of the moment diagram equals the total negative area and that the centroid of the total positive area coincides with the centroid of the total negative area. This statement is for fixed-end arches of constant cross section and can easily be modified for arches with hinges.

3. "The pressure line for a group of loads is that string polygon which makes the M/EI -diagram balance or vanish."

This statement is the same as statement 2 except that provisions are made for variations in I along the axis of the arch.

To obtain timesaving estimates of the affects of loads on an arch, statement 1 is the most useful of the previous statements. Statements 2 and 3 modify successively the definition of "fit" and lead to a greater precision in computed effects. Statement 3 fulfils the same requirements of statics and geometry as are observed in the column analogy, the hydrostatic analogy, the neutral point method, and other formalized statements of the theory of the elastic arch. Statics is satisfied by specifying that the pressure line for a group of loads is a string polygon for the loads. All statical relationships in the arch, such as shears, thrusts, and moments can be read directly from the string polygon. A force polygon for the loads is not needed in constructing the string polygon nor in obtaining the scale of moments in the arch. For example, the diagram of moments in an arch for a group of vertical loads on the arch is drawn to the same scale as that of the moments in a cantilevered beam or of the moments in a simple beam supporting the same loads and having the same span length as the arch. Also, the intercept (parallel to a load and at a unit perpendicular distance away from the load) measured between the two rays of a string polygon intersecting at the load is proportional to the load and to the moment of the load about an axis at the intercept. This is particularly useful in obtaining all shears and thrusts in a loaded arch.

The requirements of geometry for fixed-end arches loaded in the elastic range are fulfilled in statement 3 by specifying that the (M/EI) -diagram must balance. The requirements, stated in a more formal way, are as follows:

$$\int_0^L \left(\frac{M}{EI} \right) ds = 0 \dots\dots\dots (1a)$$

$$\int_0^L x \left(\frac{M}{EI} \right) ds = 0 \dots\dots\dots (1b)$$

and

$$\int_0^L y \left(\frac{M}{EI} \right) ds = 0 \dots\dots\dots (1c)$$

For the inelastic behavior of arches and rigid frames, statement 3 needs to be modified slightly to take into account the effects of nonlinear stress-strain characteristics of materials. The modification is as follows:

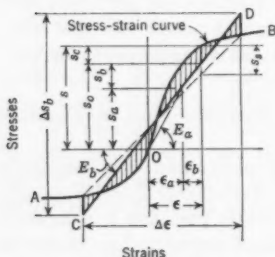
4. The pressure line for a group of loads on an arch is that string polygon for the loads which makes the $(M/E_b I)$ -diagram balance or vanish. In this

statement, E_b is a modified modulus of elasticity, and, for an element one unit in length, E_b is a measure of stiffness to relative rotation of the adjacent cross sections. The value of E_b at a section depends on the shape of the cross section, the stress-strain relationship, the history of loading, and the magnitudes of the

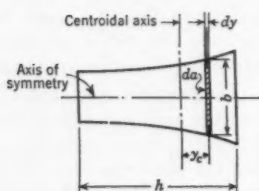
thrust and moment. For ultimate loads provisions can be made for the development of "plastic hinges."

For a specific case, the values of E_b can be obtained by means of the pressure-line concept developed for the inelastic bending of structural elements.⁵ This is shown in Fig. 1 for a rectangular cross section subjected to given values of load P and moment M . In accordance with the usual theory of plasticity,^{5,8} the distribution of strains across the section is assumed to be planar. It is also assumed that the history of loading used in the paper is statical, and that the strain in each fiber is increased from zero to its final tensile or compressive value. Other histories of deformations are possible and are examined elsewhere.^{5,9} In this paper, the stress-strain relationships for the fibers of a member subjected to a simultaneous, axial and flexural load are assumed to be the same as those obtained from simple tension and compression tests. In Fig. 1(a) the stress-strain relationship of the material is represented by curve AOB and is assumed to be the same for each longitudinal fiber. As previously stated, the effects of a shear, (Poisson's ratio), residual strains, and local instability of projecting elements of the cross section are neglected herein. In addition, the effects of lateral-torsional instability are not considered.

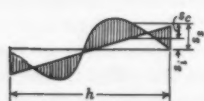
In Fig. 1 the stress, as given by the usual theory of plasticity, is interpreted to be equal to the stress computed by the elementary



(a) VALUES OF STRESSES AND STRAINS



(b) PROPERTIES OF CROSS SECTION



(c) CORRECTION STRESSES TO THE ELEMENTARY THEORY

FIG. 1.—THE ELEMENTARY THEORY OF MECHANICS COMPARED WITH A THEORY OF PLASTICITY

theory of mechanics plus a correction stress to account for the nonlinear stress-strain characteristics of the material. That is,

$$s = s_o + s_c \dots \dots \dots (2)$$

and

$$s_o = s_a + s_b \dots \dots \dots (3)$$

⁵ "Plasticity," by A. Nadai, McGraw-Hill Book Co., Inc., New York, N. Y., 1931.

⁸ "Theory of Elasticity," by S. Timoshenko, McGraw-Hill Book Co., Inc., New York, N. Y., 1936, p. 156.

in which $s_a = P/A$ and $s_b = M y_c/I$. The area of the cross section is designated by $A = \Sigma da$, and the moment of inertia about the centroidal axis by $I = \Sigma y_c^2 da$. The ordinates bounded by the stress-strain curve AOB are in accordance with the theory of plasticity whereas those bounded by the straight line CD are in accordance with the elementary theory. The shaded diagrams of Fig. 1(a) and Fig. 1(c) represent the correction stresses as defined in Eq. 2. The correction stresses that are indicated in Fig. 1 must satisfy the following conditions:

$$\Sigma s_c da = 0 \dots \dots \dots (4)$$

and

$$\Sigma s_c y_c da = 0 \dots \dots \dots (5)$$

The correction stresses must balance or vanish. "Balance" in this case means that (1) the sum of the positive correction forces must equal the sum of the negative correction forces, and (2) the centroid of the positive correction forces must coincide with the centroid of those that are negative. A correction force is equal to a correction stress times its corresponding differential area. A pictorial procedure for effecting such balance has been presented elsewhere⁵ and will not be described herein. The procedure is similar to that used in sketching the pressure line for fixed-end beams.

Two modified moduli of elasticity are represented in Fig. 1—namely,

$$E_a = s_a/\epsilon_a \dots \dots \dots (6a)$$

and

$$E_b = \Delta s_b/\Delta \epsilon \dots \dots \dots (6b)$$

in which $s_a = P/A$, $\Delta s_b = M h/I$, ϵ_a is the strain of the fibers along the centroidal axis, and $\Delta \epsilon$ is the difference in the strains of the extreme fibers. The values of E_a and E_b are represented in Fig. 1 as slopes of corresponding straight lines and may be interpreted as reduced moduli of elasticity. For example, the value of E_b in this case is the slope of line CD shown in Fig. 1(a). The values of E_a and E_b may also be interpreted as measures of stiffness to the relative translation and to the relative rotation of adjacent cross sections, respectively. The relative translation is associated with the strain, ϵ_a , and the relative rotation with the strain, ϵ_b . Consequently, the strain in any fiber can be written as

$$\epsilon = \epsilon_a + \epsilon_b \dots \dots \dots (7)$$

By definition of the preceding terms, the angle change per unit of length can be written as

$$\Delta \phi = \frac{\Delta \epsilon}{h} = \frac{\Delta s_b}{E_b h} = \frac{M}{E_b I} \dots \dots \dots (8)$$

The revised statement of the pressure line (statement 4), when used jointly with the prior procedure for obtaining values of E_b , is useful for quickly estimating the inelastic behavior of structures such as arches and rigid frames. The suggested procedure for making these estimates consists of the following steps:

1. Draw a string polygon for a given set of loads which you think is the best "fit" to the axis of the given arch. Obtain scale on the magnitudes of the moments as interpreted through the string polygon.

2. Check "fit" by inspecting whether the moment diagram balances. Revise the string polygon if necessary to obtain a more satisfactory balance.

3. Draw the (M/EI) -diagram and check the balance of this diagram. Revise the string polygon until a satisfactory balance of the (M/EI) -diagram is obtained. The revision is aided by noting that a section with a small value of I tends to draw the pressure line toward itself, whereas a section with a large I -value tends to push the pressure line away. Thus, a section with a small value of I tends to attract less moment whereas a section with a large I -value tends to attract more moment. By means of the string polygon, obtain all shears, thrusts, and moments in the arch. The results at this stage are in accordance with the elastic theory based on the original dimensions of the structure.

4. For the distributions of moments and corresponding thrusts previously obtained, estimate the values of E_s . (If convenient, draw diagrams relating moments with angle changes for different values of thrust. See Fig. 6(a) shown subsequently).

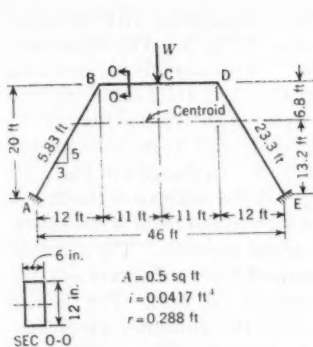
5. Draw the $(M/E_s I)$ -diagram and check the possible unbalance. If necessary, revise the string polygon and the values of E_s until the $(M/E_s I)$ -diagram is considered sufficiently balanced. (The revision is aided by noting that a section with a reduced modulus of elasticity tends to draw the pressure line toward itself.) By means of the string polygon interpret all shears, thrusts, and moments.

Step 3 is not necessary in studies restricted to inelastic behavior. However, it is useful in developing judgement as to the final position of the pressure line. It is useful also in comparing the results of the elastic theory with those of the inelastic theory. This in itself suggests that interaction diagrams, as for columns with axial and flexural loads, can be developed for the elastic and inelastic behavior of arches and rigid frames.

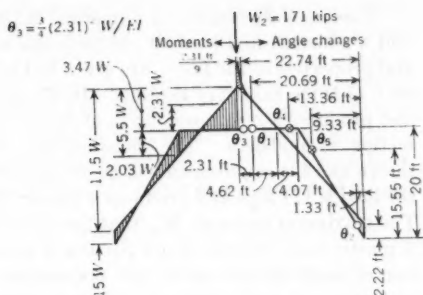
In the previous procedure, the distributions of angle changes per unit of length are assumed to be known for both theories. Consequently, estimates can be made of the corresponding deflections. If desired, the procedure can be extended to the theory of the flexible arch. The pressure line in that case must fit the axis of the deflected arch. For these studies, larger scales usually are required for the sketches of the arch and more accuracy in the computations of fit. The latter computations, however, become sensitive to changes in the modified moduli of elasticity which result from changes in moments and deflections of the arch. This is particularly true when total yielding is approached. For these cases, the sketching procedure becomes inadequate and a numerical procedure of successive approximations, similar to that of L. Vianello,^{10,11} is usually required.

¹⁰ "Theory of Elastic Stability," by S. Timoshenko, McGraw-Hill Book Co., Inc., New York, N. Y., 1936, p. 84.

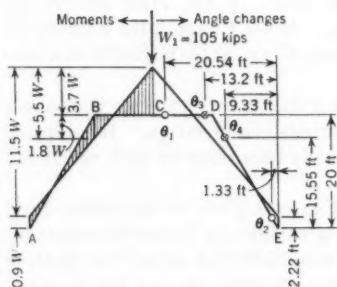
¹¹ "Numerical Procedure For Computing Deflections, Moments, and Buckling Loads," by N. M. Newmark, *Transactions, ASCE*, Vol. 108, 1943, p. 1161.



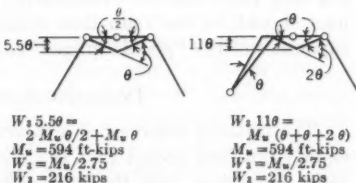
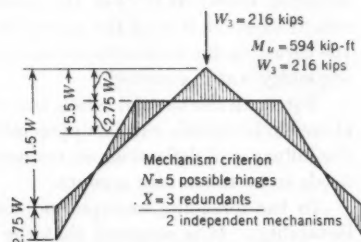
(a) Properties and Dimensions



(c) Range 2



(b) Range 1



(d) Range 3

(e) Comparison

$$W_2/W_1 = 2.06; W_3/W_1 = 1.26;$$

$$W_2/W_1 = 1.63; \Delta c_2/\Delta c_1 = 2.05$$

FIG. 2.—NUMERICAL EXAMPLE OF A LOADED RIGID FRAME FIXED AT ITS ENDS

Numerical Example.—A numerical example of a rigid frame with fixed ends and a concentrated load, W , at midspan is shown in Fig. 2. The dimensions and properties of the frame are given in Fig. 2(a). A pressure line is drawn for each of three ranges of loading. In Range 1 of Fig. 2(b), the load is 105 kips and produces a maximum stress of 33 kips per sq in. in an extreme fiber of the section at midspan. The distributions of moments and angle changes are shown and the requirements of geometry are checked. In Range 2 of Fig. 2(c), the load is 171 kips and produces a plastic "hinge" at the midspan of the frame. The maximum moment, M_u , that the given cross section can resist is 594 kip-ft. A plastic zone extends over a portion of the horizontal member. The distribution of angle changes along this portion was obtained from a diagram relating moments and angle changes as shown subsequently in Fig. 6(a). For the rise to span ratio considered, the influence of the thrust on the moment-angle change relationship is negligible and, consequently, is neglected. The requirements of geometry for Range 2 are checked as for Range 1 except that provisions now are made for the effects of plasticity. By comparing the pressure line for Range 2 with that for Range 1 it is observed that the plastic zone attracts the pressure line toward itself whereas the sections at the abutments and the knees push the pressure line away.

In Range 3 of Fig. 2(d), the load is 216 kips and produces yielding at a sufficient number of sections to cause collapse. This load was obtained by means of the pressure line as well as by means of the "mechanism" criterion obtained elsewhere.¹² For the pressure line drawn in Fig. 2(d), observe the extent to which it hugs the axis of the frame. As for Range 2, the influence of the thrust on the maximum moment that a section can take is negligible and consequently was discounted.

For small rise to span ratios, the influence of the thrust on the moment-angle change relationship can be appreciable and merits consideration. In addition, the influence of deflections on moments is usually important for such ratios and needs to be taken into account.

In the foregoing example, no consideration was given to lateral-torsional instability. It is assumed that the frame is sufficiently braced for such instability not to occur. Obviously, if such instability can occur, the limiting load should be less than that obtained in the example because the moment capacities of the "plastic hinges" could not be developed.

INELASTIC BUCKLING OF COLUMNS

The inelastic behavior of a column can be studied in the same way as previously outlined except that the pressure line for a group of loads must now be in agreement with the final deflections of the column. In addition, the curvatures of the column, proportional to $\Delta\phi = M/E_s I$, must be in agreement with the values of E_s and with the deflections of the column. As indicated in Fig. 1, the value of E_s at a section depends on the shape of the cross section, the stress-strain relationship, and on the magnitudes of the thrust and moment. The value of E_s also depends on the history of loading. The history of loading

¹² "Simple Plastic Theory," by B. Thurlimann, *Proceedings, A.I.S.C. National Engineering Conference, Lehigh University, Bethlehem, Pa., 1956*, p. 13.

and the mode of failure are of such importance in column theory that certain assumptions which are made in the preceding discussion are herein repeated. The strain in each fiber is assumed to gradually increase from zero to its final tensile or compressive value. Other histories of deformations are possible, including residual strains, and are discussed elsewhere.^{5,9} Local instability and lateral-torsional instability are not considered. The latter type of instability can be important and is frequently obtained in laboratory tests.¹³ In such tests, no resistance is frequently offered to a twist at the ends or to a yaw and a twist at the mid-portion of a column.

In actual practice, such resistance is frequently offered by end connections and by walls or bracing along the length of the column. The succeeding examination is based on the assumption that the failure of a column is due to excessive bending about the axes of moments. The use of the pressure-line concept for such columns will be illustrated. The development is analytical rather than pictorial or numerical.

Fig. 3 shows typical pressure lines (curves of moments) for various conditions of loading on columns. It is assumed for the present that the loads are less than the critical loads at which instability occurs. In each diagram, curve *e* represents the deflected position of the column as if the behavior of the column was completely elastic. A generalized statement concerning the behavior of such columns was given by H. M. Westergaard.¹⁴ The statement was given in the form of a Fourier series and considerable liberty has been taken by restating it as follows: The elastic behavior (lateral deflection and moments) of a structural member subjected to axial and lateral loads is equal to its behavior as a laterally loaded member multiplied by a magnification factor. The magnification factor depends on the ratio of the axial load to the Euler load for an idealized straight column.

In Fig. 3, a comparison also is shown between the elastic and the inelastic behavior of each column. Curve *i* in each diagram represents the deflections

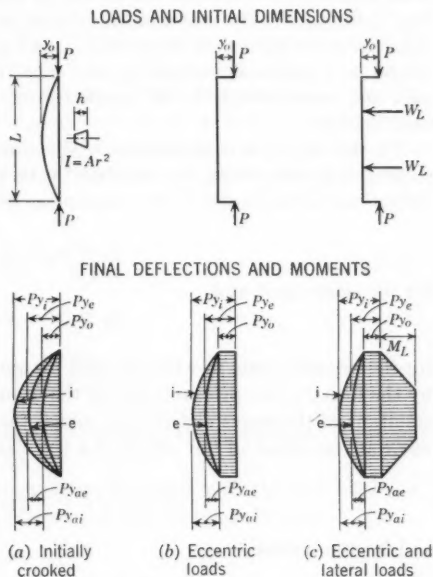


FIG. 3.—ECCENTRICALLY AND LATERALLY LOADED COLUMNS

¹³ "Steel Columns of Rolled Wide Flange Section," by B. G. Johnston and L. Cheney, *Progress Report No. 2*, A.I.S.C., November, 1942.

¹⁴ "Buckling of Elastic Structures," by H. M. Westergaard, *Transactions, ASCE*, Vol. 85, 1922, p. 576.

of the column in accordance with a theory of inelasticity. The inelastic behavior of the column can be stated in the same way as the elastic behavior modified to take into account the effects of plasticity.¹⁸ This is illustrated for the case of a column as shown in Fig. 3(c). The column is assumed to have a symmetrical distribution of lateral loads along its length and to have a load P of equal eccentricity at each end. The initial eccentricity is designated by y_o . It is assumed that the column has a symmetrical curve of deflections, that bending occurs about axes normal to the plane of the bent column, and that the cross section of the column has an axis of symmetry lying in this plane. The final deflections at the center of the column for conditions of elastic and inelastic behavior respectively are designated y_e and y_i . The effects of residual strains, lateral and torsional instability, and local buckling are not considered. In addition, uncertainties in the properties of materials are not a part of this examination.

In the subsequent examination, the elastic and inelastic behavior of the column will respectively be associated with the subscripts e and i . The final deflections at the center of the column are defined by

$$y_e = y_o + y_{ae} \dots \dots \dots (9a)$$

for the elastic case and

$$y_i = y_o + y_{ai} \dots \dots \dots (9b)$$

for the inelastic case, in which y_{ae} and y_{ai} are the additional deflections caused by the loads. The pressure line for the group of loads must coincide with the resultant of the stress distribution across the section. By definition, the moment at the center of the column for the elastic case is given by

$$M_e = M_L + P (y_o + y_{ae}) \dots \dots \dots (10a)$$

and for the inelastic case

$$M_i = M_L + P (y_o + y_{ai}) \dots \dots \dots (10b)$$

in which M_L is the moment due to the lateral loads. Eq. 10a can be rewritten as

$$M_e = M_{om} + M_{ae} \dots \dots \dots (11a)$$

and Eq 10b as

$$M_i = M_{om} + M_{ai} \dots \dots \dots (11b)$$

in which

$$M_{ae} = P y_{ae} \dots \dots \dots (12a)$$

$$M_{ai} = P y_{ai} \dots \dots \dots (12b)$$

and

$$M_{om} = [1 + (M_L/M_o)] M_o \dots \dots \dots (12c)$$

¹⁸ "The Elastic and Inelastic Behavior of Columns," by Harold S. Davis, thesis presented to Northwestern University, Evanston, Ill., in 1949, in partial fulfillment of the requirements for the degree of Doctor of Philosophy.

For elastic and inelastic behavior $M_o = P y_o$. It is observed that M_{om} is the moment at the center of the column with respect to the original dimensions of the column and is a constant for a given case of loading.

The additional deflections caused by the loads can be written as follows:

$$y_{ae} = \frac{1}{k_e} \Delta \phi_e L^2 \dots \dots \dots (13a)$$

for the elastic case and

$$y_{ai} = \frac{1}{k_i} \Delta \phi_i L^2 \dots \dots \dots (13b)$$

for the inelastic case, in which k_e and k_i are coefficients depending on the distributions of the angle changes (or curvatures) along the length of the column and $\Delta \phi_e$ and $\Delta \phi_i$ are the angle changes per unit of length at the center of the column. The angle changes per unit of length are related to the moments as defined for the elastic case by

$$\Delta \phi_e = \frac{M_e}{E I} \dots \dots \dots (14a)$$

and for the inelastic case by

$$\Delta \phi_i = \frac{M_i}{E_s I} \dots \dots \dots (14b)$$

In Eqs. 14 E is the tangent modulus at the origin of the stress-strain curve and E_s is a reduced modulus of elasticity.

By means of Eq. 14a and Eq. 14b and the definition of the Euler load, $P_E = \pi^2 E I / L^2$, the deflections at the center of the column are as follows:

$$y_{ae} = \left[\frac{1}{c_e \frac{P_E}{P} - 1} \right] y_{om} \dots \dots \dots (15a)$$

and

$$y_e = y_o + \left[\frac{1}{c_e \frac{P_E}{P} - 1} \right] y_{om} \dots \dots \dots (15b)$$

For the elastic case, and for the inelastic case

$$y_{ai} = \left[\frac{1}{c_i \frac{P_E}{P} - 1} \right] y_{om} \dots \dots \dots (15c)$$

and

$$y_i = y_o + \left[\frac{1}{c_i \frac{P_E}{P} - 1} \right] y_{om} \dots \dots \dots (15d)$$

in which

$$c_e = \frac{k_e E}{\pi^2 E} \dots \dots \dots (16a)$$

$$c_i = \frac{k_i E_b}{\pi^2 E} \dots \dots \dots (16b)$$

and

$$y_{om} = [1 + (M_L/M_o)] y_o \dots \dots \dots (16c)$$

Thus,

$$M_{om} = P y_{om} \dots \dots \dots (17)$$

In the same way as for deflections, the moments at the center of the column for the elastic case are given by

$$M_{ae} = \left[\frac{1}{c_e \frac{P_E}{P} - 1} \right] M_{om} \dots \dots \dots (18a)$$

and

$$M_e = \left[\frac{c_e \frac{P_E}{P}}{c_e \frac{P_E}{P} - 1} \right] M_{om} \dots \dots \dots (18b)$$

and the inelastic case are given by

$$M_{ai} = \left[\frac{1}{c_i \frac{P_E}{P} - 1} \right] M_{om} \dots \dots \dots (18c)$$

and

$$M_i = \left[\frac{c_i \frac{P_E}{P}}{c_i \frac{P_E}{P} - 1} \right] M_{om} \dots \dots \dots (18d)$$

In Eq. 15 and Eq. 18 the terms in the brackets can be interpreted as modification factors of y_{om} and M_{om} , respectively. A comparison of the moments defined by Eq. 18a and Eq. 18b yields

$$\frac{M_e}{M_{ae}} = c_e \frac{P_E}{P} \dots \dots \dots (19a)$$

and similarly a comparison of Eq. 18c and Eq. 18d yields

$$\frac{M_i}{M_{ai}} = c_i \frac{P_E}{P} \dots \dots \dots (19b)$$

It is of interest to note that the form of Eqs. 9 to 19 are the same for elastic and inelastic behavior except for the values of c_e and c_i . A further comparison

of the moments defined by Eqs. 19a and 19b yields the following relationship:

$$\frac{M_i}{M_{ai}} / \frac{M_e}{M_{ae}} = \left[\frac{c_i}{c_e} \right] = \left[\frac{k_i E_b}{k_e E'} \right] \dots \dots \dots (20)$$

Thus, in a general way the inelastic behavior is the elastic behavior modified by the terms in the brackets of Eq. 20.

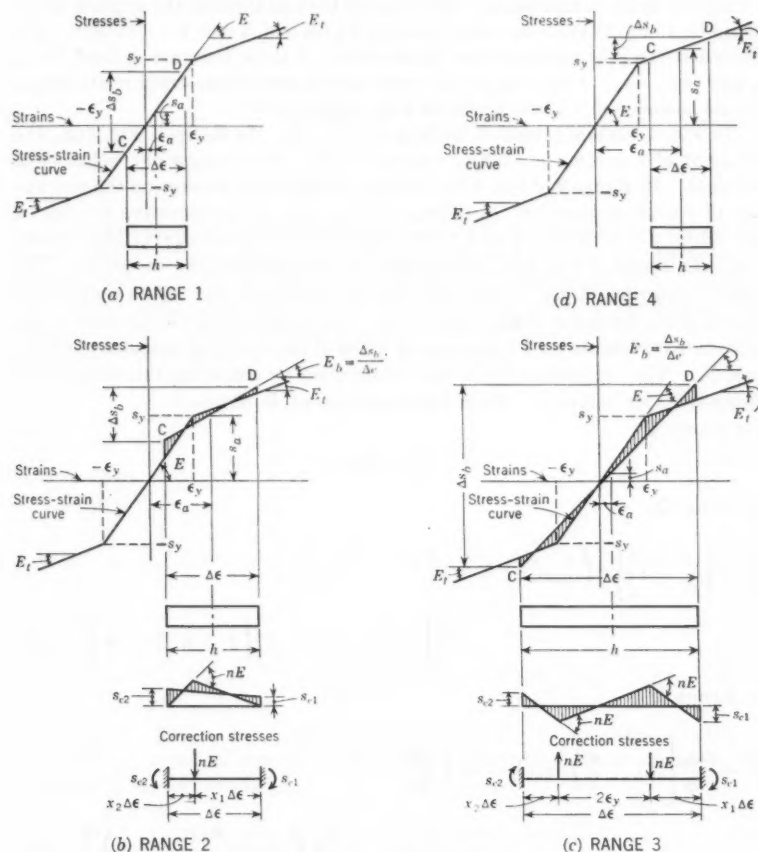


FIG. 4.—RELATIONSHIPS FOR GENERALIZED STRESS-STRAIN CURVE

Values of c_e for elastic columns have been reported by Westgaard¹⁴ for various conditions of axial and lateral loads. For a symmetrical condition of load, the value of c_e is not sensitive to the type of loading and is approximately equal to 1.0; that is, $k_e \cong \pi^2$. The values of x_i in the previous equations de-

pend on the deflected shape of the column and on the P - M - $\Delta\phi$ relationships for a given cross section and stress-strain characteristics of the column.

The values of E_b/E in the expression for c_i can be obtained by means of the pressure-line concept developed for the inelastic deformations of structural elements. For example, consider an element with a rectangular cross section and an idealized stress-strain curve as shown in Fig. 4. The stress-strain curve consists of three straight lines defining material properties which are the same for tension as for compression. The slope of the line through the origin is designated by E and that of the other lines by E_t (in which $n = 1 - (E_t/E)$). For reference, the coordinates of the intersections of these lines are defined by s_y , ϵ_y and $-s_y$, $-\epsilon_y$. Other shapes of cross sections and stress-strain relationships can be considered. These are dealt with elsewhere.¹⁵

In Fig. 4, several ranges of loading are defined. In Range 1 Fig. 4(a), the behavior of a column is elastic, whereas in the other ranges the behavior is inelastic. In Range 2 of Fig. 4(b), only the compressive stresses on the concave side of a column exceed s_y . In Range 3 Fig. 4(c), the compressive stresses on the concave side exceed s_y and the tensile stresses on the convex side exceed $-s_y$. In Range 4 Fig. 4(d), all stresses are compressive and exceed s_y . The shaded diagrams in Fig. 4 represent the correction stresses to the elementary theory of mechanics as defined by Eq. 2. The slope of line CD for each range of loading represents the corresponding value of the modified modulus of elasticity, E_b . The expressions for E_b can be obtained by observing that the shaded diagrams must balance.⁵ From this requirement, is obtained:

For Range 1,

$$\frac{E_b}{E} = 1.0 \dots \dots \dots (21)$$

for Range 2,

$$\frac{E_b}{E} = \left[\frac{2}{n} - 1 \right] \left[4 \left(\frac{1}{n} - 1 \right) + 3a \right] - \frac{2}{n} \left[4 \left(\frac{1}{n} - 1 \right) + a \right] \left[1 - n(1-a) \right]^{\frac{1}{2}} \dots (22)$$

for Range 3,

$$\frac{E_b}{E} = \frac{\Delta\phi_y}{\Delta\phi} \left[\left(1 + \frac{n}{2} \right) + (1-n) \left(\frac{\Delta\phi}{\Delta\phi_y} - 1 \right) - \frac{n}{2 \left(\Delta\phi / \Delta\phi_y \right)^2} - \frac{3}{2} n \left(\frac{P/P_y}{\frac{\Delta\phi}{\Delta\phi_y} (1-n) + n} \right)^2 \right] \dots (23)$$

and for Range 4

$$\frac{E_b}{E_t} = 1.0 \dots \dots \dots (24)$$

in which

$$n = 1 - \frac{E_t}{E} \dots \dots \dots (25a)$$

$$a = \frac{1 - (P/P_y)}{\Delta\phi/\Delta\phi_y} \dots \dots \dots (25b)$$

$$P_y = A s_y \dots \dots \dots (25c)$$

$$\Delta\phi = \frac{M}{E_b I} \dots \dots \dots (25d)$$

$$\Delta\phi_y = \frac{M_y}{E I} \dots \dots \dots (25e)$$

and

$$M_y = 2 s_y I/h \dots \dots \dots (25f)$$

The expressions for E_b can also be obtained by observing that the correction stresses at the extreme fibers of the cross section are numerically the same as the fixed-end moments of a fictitious beam having a span length of $\Delta\epsilon$ and having concentrated loads equal to $E - E_t$ at the corresponding positions of the abrupt changes in the stress-strain curve. This is illustrated in Fig. 4. The correction stresses in the extreme fibers, 1 and 2, are

$$s_{c1} = x_1 (1 - x_1)^2 n E \Delta\epsilon \dots \dots \dots (26a)$$

and

$$s_{c2} = x_1^2 (1 - x_1) n E \Delta\epsilon \dots \dots \dots (26b)$$

for Range 2, and

$$s_{c1} = \left[x_1 \left(x_2 + \frac{1}{\Delta\phi/\Delta\phi_y} \right)^2 - x_2^2 \left(x_1 + \frac{1}{\Delta\phi/\Delta\phi_y} \right) \right] n E \Delta\epsilon \dots \dots (27a)$$

and

$$s_{c2} = \left[x_1^2 \left(x_2 + \frac{1}{\Delta\phi/\Delta\phi_y} \right) - x_2 \left(x_1 + \frac{1}{\Delta\phi/\Delta\phi_y} \right)^2 \right] n E \Delta\epsilon \dots \dots (27b)$$

for Range 3. The x_1 and x_2 terms in Eq. 26 and Eq. 27 are defined in Fig. 4. From the geometry of the stress-strain curve and definition of s_a and s_b , the following Eqs. are obtained:

$$s_a + s_b = s_{c1} + s_y + x_1 \Delta\epsilon (1 - n) E \dots \dots \dots (28a)$$

and

$$s_a - s_b = s_{c2} + s_y - (1 - x_1) \Delta\epsilon E \dots \dots \dots (28b)$$

for Range 2, and

$$s_a + s_b = s_{c1} + s_y + x_1 \Delta\epsilon (1 - n) E \dots \dots \dots (29a)$$

and

$$s_a - s_b = s_{c2} - s_y - x_2 \Delta \epsilon (1 - n) E \dots \dots \dots (29b)$$

for Range 3. Eq. 22 and Eq. 23 can be verified by means of Eqs. 26 through 29 and the relationship $E_b = \Delta s_b / \Delta \epsilon$.

For future reference, it is convenient to summarize for each range of loading the rate at which the internal moment changes due to a small increase in the angle change $\Delta \phi$. The following expressions can be obtained by performing the necessary differentiations of Eq. 25d and Eqs. 21 through 24:

For Range 1,

$$\left[\frac{d(M)}{d(\Delta \phi)} \right]_{int} = E I \dots \dots \dots (30)$$

for Range 2,

$$\left[\frac{d(M)}{d(\Delta \phi)} \right]_{int} = E I \left\{ 4 \left(\frac{2}{n} - 1 \right) \left(\frac{1}{n} - 1 \right) + \frac{\left[4 \left(\frac{1}{n} - 1 \right) + a \right] a}{[1 - n(1 - a)]^{\frac{1}{2}}} - \frac{8 \left(\frac{1}{n} - 1 \right) [1 - n(1 - a)]^{\frac{1}{2}}}{\dots} \right\} \dots (31)$$

for Range 3,

$$\left[\frac{d(M)}{d(\Delta \phi)} \right]_{int} = E I \left\{ (1 - n) \left\{ 1 + \frac{3n(P/P_y)^2}{\left[\frac{\Delta \phi}{\Delta \phi_y} (1 - n) + n \right]^3} \right\} + \frac{n}{(\Delta \phi / \Delta \phi_y)^3} \right\} \dots (32)$$

and for Range 4,

$$\left[\frac{d(M)}{d(\Delta \phi)} \right]_{int} = E I \dots \dots \dots (33)$$

In the subsequent examination, particular consideration will be given to a material having a well defined yield point—that is, $n = 1 - (E_t/E) = 1$ or $E_t = 0$. The stress-strain curve that is being considered is shown in Fig. 5. When $n = 1$, the equations for E_b/E and $\Delta \phi / \Delta \phi_y$ are as follows:

For Range 2,

$$\frac{E_b}{E} = \frac{1 - (P/P_y)}{\Delta \phi / \Delta \phi_y} \left[3 - 2 \sqrt{\frac{1 - (P/P_y)}{\Delta \phi / \Delta \phi_y}} \right] \dots \dots \dots (34a)$$

$$\frac{E_b}{E} = \frac{M}{M_y} \frac{\{3[1 - (P/P_y)] - (M/M_y)\}^2}{4[1 - (P/P_y)]^3} \dots \dots \dots (34b)$$

and

$$\frac{\Delta \phi}{\Delta \phi_y} = \frac{4[1 - (P/P_y)]^3}{\{3[1 - (P/P_y)] - (M/M_y)\}^2} \dots \dots \dots (34c)$$

For Range 3,

$$\frac{E_b}{E} = \frac{1}{2 \Delta\phi / \Delta\phi_y} \left\{ 3 [1 - (P/P_y)^2] - \frac{1}{(\Delta\phi / \Delta\phi_y)^2} \right\} \dots \dots \dots (34d)$$

$$\frac{E_b}{E} = \frac{M}{M_y} \{ 3 [1 - (P/P_y)^2] - 2 M/M_y \}^{1/2} \dots \dots \dots (34e)$$

and

$$\frac{\Delta\phi}{\Delta\phi_y} = \{ 3 [1 - (P/P_y)^2] - 2 M/M_y \}^{-1/2} \dots \dots \dots (34f)$$

in which the subscripts i previously associated with $\Delta\phi_i$ and M_i have been dropped for convenience in writing. Families of curves,¹⁵ based upon the relationships defined by Eq. 34 are shown in Fig. 6 for $n = 1.0$ and for a rectangular cross sections.

In Fig. 6(d) curves also are given which relate the maximum values of M/M_y for WF sections when the values of P/P_y are kept constant. More complete curves and corresponding expressions for P - M - $\Delta\phi$ relationships of WF and other rolled sections are given elsewhere.^{15,16,17} In Fig. 7 curves are given¹⁵ which relate P/P_y , M/M_y , and $\Delta\phi/\Delta\phi_y$ for rectangular cross sections when $E_i/E = 0.1$ and $n = 9$. The influence of the stress-strain characteristics of a material on the resulting P - M - $\Delta\phi$ relationships can be seen by comparing Fig. 6(a) with Fig. 7(b).

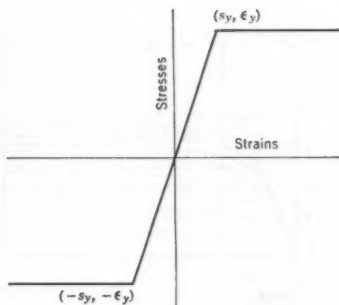


FIG. 5.—STRESS-STRAIN CURVE WITH A DEFINED YIELD POINT

Critical Loads.—Mirko Ros,¹⁸ M. ASCE defined a critical load to be obtained when the external moment at any section of a column increases at a rate equal to the rate of increase of the internal resisting moment offered at the same section. This criterion stated in the form of an equation is as follows:

$$\left[\frac{d(M)}{d(\Delta\phi)} \right]_{ext} = \left[\frac{d(M)}{d(\Delta\phi)} \right]_{int} \dots \dots \dots (35)$$

It is used herein^{15,17} to develop significant expressions associated with critical loads. Because the external moment (Fig. 3) at a section can be written as

$$M_{ext} = M_L + P (y_o + y_{ai}) \dots \dots \dots (36)$$

¹⁴ "Plastic Deformation of Wide-Flange Beam-Columns," by Robert L. Ketter, Edmund L. Kaminisky, and Lynn S. Beedle, *Proceedings-Separate No. 330*, ASCE, October, 1953.

¹⁷ "Stability of Beam Columns Above the Elastic Limit," by Robert L. Ketter, *Proceedings-Separate No. 692*, ASCE, May, 1955.

¹⁸ "Die Knicksicherheit von an beiden Enden gelenkig gelagerten Stäben aus Konstruktionsstahl," by M. Ros, *Proceedings*, 2d International Cong. of Applied Mechanics, Zurich, 1926, p. 368.

its rate of increase becomes

$$\left[\frac{d(M)}{d(\Delta\phi)} \right]_{\text{int}} = \frac{d(P y_{ai})}{d(\Delta\phi)} = \frac{d(P y_{ai})}{d\left(\frac{k_i}{L^2} y_{ai}\right)} = P \frac{L^2}{k_i} \dots \dots \dots (37)$$

This assumes that k_i is a constant during the increase. The critical load then becomes

$$P_{cr} = \frac{k_i}{L^2} \left[\frac{d(M)}{d(\Delta\phi)} \right]_{\text{int}(cr)} = P_E \frac{k_i}{\pi^2 E I} \left[\frac{d(M)}{d(\Delta\phi)} \right]_{\text{int}(cr)} \dots \dots \dots (38)$$

This permits a more direct means for determining critical values of slope along P - M - $\Delta\phi$ curves than semigraphical methods used in the past.

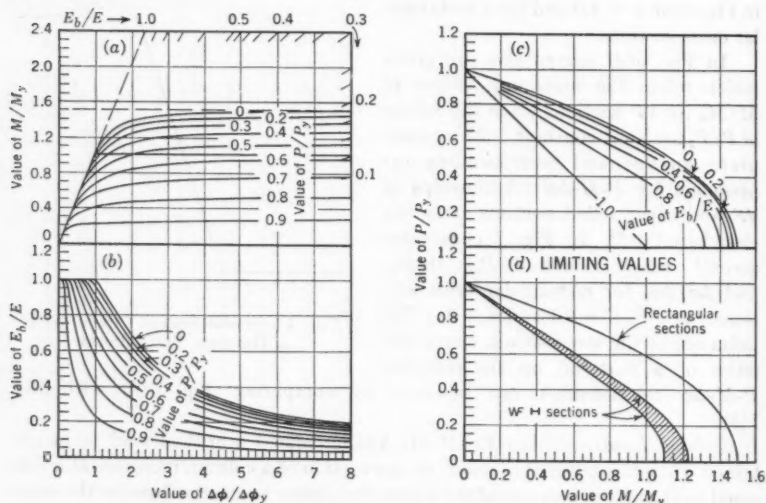


FIG. 6.—RELATIONSHIPS BETWEEN P , M , $\Delta\phi$, AND E_b WHEN $n = 1.0$

Proceeding as previously, we obtain by means of Eq. 34, the following for $[d(M)/d(\Delta\phi)]_{\text{int}}$ —
 For Range 2,

$$\left[\frac{d(M)}{d(\Delta\phi)} \right]_{\text{int}} = E I \left[\frac{1 - (P/P_y)}{\Delta\phi/\Delta\phi_y} \right]^2 \dots \dots \dots (39a)$$

and

$$\left[\frac{d(M)}{d(\Delta\phi)} \right]_{\text{int}} = E I \left\{ \frac{3 [1 - (P/P_y)] - M/M_y}{2 [1 - (P/P_y)]} \right\}^2 \dots \dots \dots (39b)$$

For Range 3,

$$\left[\frac{d(M)}{d(\Delta\phi)} \right]_{int} = E I \left(\frac{1}{\Delta\phi/\Delta\phi_y} \right)^3 \dots\dots\dots (39c)$$

and

$$\left[\frac{d(M)}{d(\Delta\phi)} \right]_{int} = E I \{ 3 [1 - (P/P_y)^2] - 2 M/M_y \}^{\frac{1}{3}} \dots\dots\dots (39d)$$

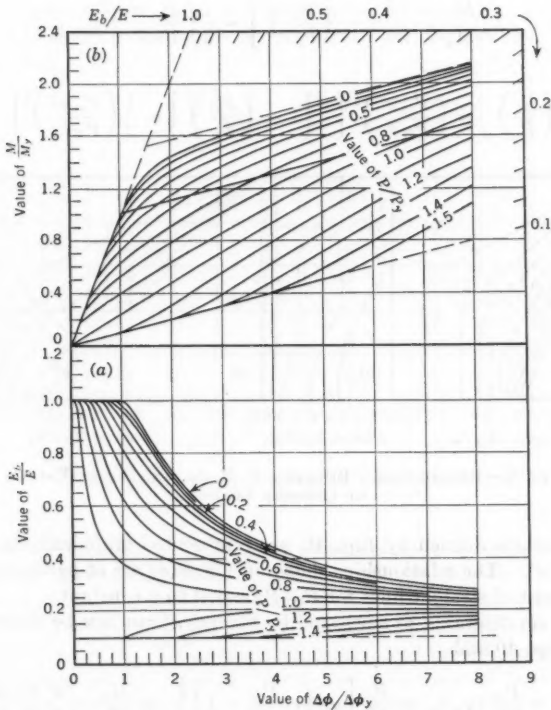


FIG. 7.—RELATIONSHIPS BETWEEN P , M , $\Delta\phi$, AND E_b WHEN $n = 0.9$

Substituting Eqs. 39 into Eq. 38 and noting that $\frac{\Delta\phi}{\Delta\phi_y} = \frac{E}{E_b} \times \frac{M}{M_y}$, the follow-

ing relationships associated with critical loads are obtained:

For Range 2

$$\frac{\Delta\phi_{cr}}{\Delta\phi_y} = \left(1 - \frac{P_{cr}}{P_y} \right) \left(\frac{P_E k_i}{P_{cr} \pi^2} \right)^{\frac{1}{3}} \dots\dots\dots (40a)$$

$$\frac{M_{cr}}{M_y} = \left(1 - \frac{P_{cr}}{P_y} \right) \left[3 - 2 \left(\frac{P_{cr} \pi^2}{P_E k_i} \right)^{\frac{1}{3}} \right] \dots\dots\dots (40b)$$

and

$$\left(\frac{E_b}{E}\right)_{cr} = \frac{P_{cr} \pi^2}{P_E k_i} \left[3 \left(\frac{P_E k_i}{P_{cr} \pi^2} \right)^{\frac{1}{2}} - 2 \right] \dots \dots \dots (40c)$$

for Range 3,

$$\frac{\Delta \phi_{cr}}{\Delta \phi_y} = \left(\frac{P_E k_i}{P_{cr} \pi^2} \right)^{\frac{1}{2}} \dots \dots \dots (40d)$$

$$\frac{M_{cr}}{M_y} = \frac{3}{2} \left[1 - \left(\frac{P_{cr}}{P_y} \right)^2 \right] - \frac{1}{2} \left(\frac{P_{cr} \pi^2}{P_E k_i} \right)^{\frac{1}{2}} \dots \dots \dots (40e)$$

and

$$\left(\frac{E_b}{E}\right)_{cr} = \left(\frac{P_{cr} \pi^2}{P_E k_i}\right)^{\frac{1}{2}} \left\{ \frac{3}{2} \left[1 - \left(\frac{P_{cr}}{P_y} \right)^2 \right] - \frac{1}{2} \left(\frac{P_{cr} \pi^2}{P_E k_i} \right)^{\frac{1}{2}} \right\} \dots \dots \dots (40f)$$

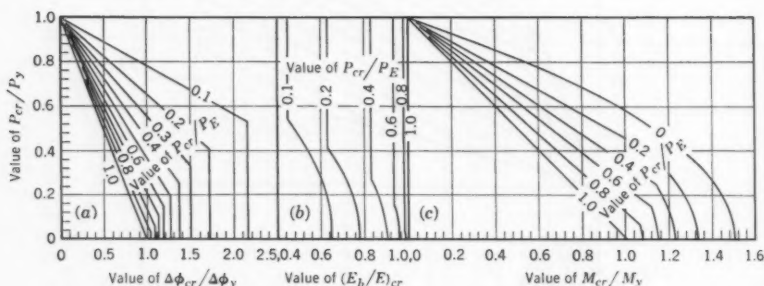


FIG. 8.—RELATIONSHIPS BETWEEN P , M , $\Delta\phi$, AND P_E AT VALUES OF CRITICAL LOADS

The relationships defined by Eqs. 40, are represented graphically in Fig. 8 in which $k_i = \pi^2$. The relationships shown in Fig. 8(a) are of particular interest as they consist of straight lines for P_{cr}/P_E equal to a constant.

Interaction diagrams, as suggested by Shanley,¹⁹ can now be determined by means of Eqs. 40 and

$$\left(\frac{M_{om}}{M_y}\right)_{cr} = \frac{P_{cr}}{M_y} (y_{om})_{cr} = \frac{P_{cr}}{M_y} \left[y_{ai} \left(c_i \frac{P_E}{P} - 1 \right) \right]_{cr} = \frac{M_{cr}}{M_y} - \frac{\pi^2 P_{cr} \Delta \phi_{cr}}{k_i P_E \Delta \phi_y} \dots (41)$$

Substitution into Eq. 41 the relationships defined by Eqs. 13, Eqs. 40a, c, d, and f yields the following results:

For Range 2,

$$\left(\frac{M_{om}}{M_y}\right)_{cr} = 3 \left(1 - \frac{P_{cr}}{P_y} \right) \left[1 - \left(\frac{\pi^2 P_{cr}}{k_i P_E} \right)^{\frac{1}{2}} \right] \dots \dots \dots (42a)$$

for Range 3,

$$\left(\frac{M_{om}}{M_y}\right)_{cr} = \frac{3}{2} \left[1 - \left(\frac{P_{cr}}{P_y} \right)^2 - \left(\frac{\pi^2 P_{cr}}{k_i P_E} \right)^{\frac{1}{2}} \right] \dots \dots \dots (42b)$$

¹⁹ "Applied Column Theory," by F. R. Shanley, *Transactions, ASCE*, Vol. 115, 1950, p. 698.

Eqs. 42 can be rewritten in terms of L/r , because

$$\frac{\pi^2 P_{cr}}{k_i P_E} = \frac{s_y}{k_i E} \frac{P_{cr}}{P_y} \left(\frac{L}{r} \right)^2 \quad (43)$$

for each range of loading. The resulting expressions define interaction diagrams as shown in Fig. 9. Values of $k_i = \pi^2$ and $s_y/E = 33/30,000$ were assumed in plotting this figure.

The eccentricity ratio, $y_{om}h/2r^2$, associated with the value of a critical axial load on a laterally loaded column can readily be determined in Fig. 9 by observing that

$$\frac{y_{om} h}{2 r^2} = \frac{M_{om}}{M_y} \frac{P}{P_y} \quad (44)$$

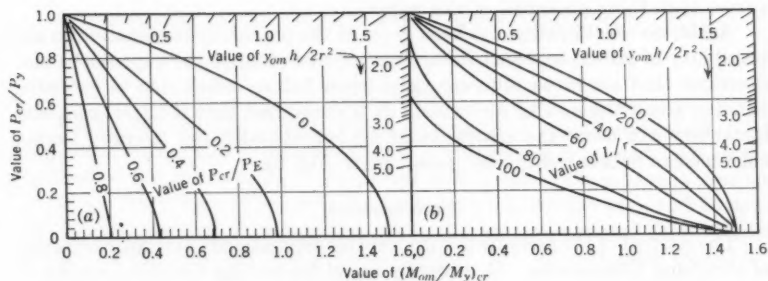


FIG. 9.—INTERACTION DIAGRAMS FOR ECCENTRICALLY AND LATERALLY LOADED COLUMNS

Thus, the inverse value of the slope of a line drawn from the origin in Fig. 9 is equal to the eccentricity ratio associated with the corresponding values of P_{cr}/P_y and M_{om}/M_y . The intersection of such a line in Fig. 9 with a curve for L/r equal to a constant defines the corresponding values of P_{cr}/P_y and M_{om}/M_y of the loaded column. This same concept has been used in constructing interaction diagrams for the flexural stresses and deflections of flexible arch ribs²⁰ and of the stiffening girders of suspension bridges.²¹ Similar constructions can be made in Fig. 6, Fig. 7, and Fig. 8, as shown in Fig. 6(a), in which

$$\frac{E_b}{E} = \frac{M}{M_y} \frac{\Delta\phi}{\Delta\phi_y} \quad (45)$$

The values of k_i in the preceding equations are not sensitive to reasonable assumptions concerning the distributions of angle changes along a column.^{15,17} This is particularly true for straight columns loaded eccentrically at their ends

²⁰ "Design of Flexible Steel Arches by Interaction Diagrams," by O. J. Sotillo, thesis presented to Rensselaer Polytechnic Institute, in 1956, in partial fulfillment of the requirements for the degree of Doctor of Philosophy.

²¹ "Bending Interaction in Suspension Bridges," by Haaren A. Miklofsky, *Proceedings-Separate 652*, ASCE, March, 1955.

and for columns resisting axial and lateral loads. The values of k_i for triangular, parabolic, sinesoidal, and rectangular distributions of angle changes along a pin-ended column respectively are 12, 9.6, 9.87, and 8. For a straight column loaded eccentrically at its ends, the value of k_i is usually between 8 and π^2 . However, for rectangular columns which are initially bent, studies reported elsewhere¹⁵ show that the values of k_i may vary from approximately π^2 to 16. For these cases, values of k_i equal to π^2 , 12 and 16 correspond to columns having slenderness ratios of about 100, 40 and 15, respectively.

For k_i equal to π^2 , Eqs. 42 yield the same results as those interpreted by means of the equations developed by K. Jezek.²² The equations cited herein, however, are more general and permit allowances to be made for variations in k_i . It also is observed that the methods and concepts presented herein are general and can be used to determine P - M - $\Delta\phi$ relationships and interaction diagrams for columns having other shapes of cross sections and stress-strain curves than those presented in this paper.

Again, no consideration has been given in the preceding examination to the possibility of lateral-torsional instability. Consequently, the expressions and diagrams that are given are only valid when failure occurs due to excessive bending about the axes of moments. It is recognized that if lateral-torsional instability can occur the critical loads for eccentrically and laterally loaded columns can be less than those given herein (Fig. 9).

CONCLUSIONS

The concept of the pressure line is useful for estimating the inelastic behavior of structural frameworks. It is equally useful for making analytical studies of the inelastic behavior of columns.

In addition, the inelastic behavior of columns for the cases studied can be stated in terms of the elastic behavior modified to take into account the effects of plasticity.

²² "Die Festigkeit von Druckstaben aus Stahl," by K. Jezek, Julius Springer, Wien, 1937.

AMERICAN SOCIETY OF CIVIL ENGINEERS

Founded November 5, 1852

TRANSACTIONS

Paper No. 3008

HAAS HYDROELECTRIC POWER PROJECT

BY J. BARRY COOKE,¹ M. ASCE

WITH DISCUSSION BY MESSRS. F. L. LAWTON; AND J. BARRY COOKE

SYNOPSIS

Engineering considerations, design criteria, and construction data for a high-head hydroelectric project located in granite are presented. Of special interest is the powerhouse, constructed underground for economic reasons.

Major features in addition to the underground plant are (a) a rockfill dam, (b) an underground free-discharge valve, (c) an underground power-tunnel intake valve, (d) an unlined pressure tunnel, (e) a storage sand trap, (f) a surge chamber, (g) two impulse turbines, and (h) a high-head penstock.

INTRODUCTION

The Haas Power Project is on the North Fork of the Kings River, Calif.^{2,3} At this site a static head of 2,444 ft and a flow of 760 cu ft per sec develops 128,000 kw in a two-unit underground plant. This project was the first large underground hydroelectric plant to be constructed in the United States^{4,5} and it went into operation in December, 1958.

The outstanding characteristics of the Haas Power Project are the extent of the underground construction and the use of rock from the massive granite formation of the Sierra Nevada Mountains in California. Granite was used in the rockfill dam and crushed granite from the powerhouse excavation was used as concrete aggregate.

NOTE.—Published, essentially as printed here, in February, 1958, in the Journal of the Power Division, as *Proceedings Paper 1529*. Positions and titles given are those in effect when the paper or discussion was approved for publication in *Transactions*.

¹Superv. Civ. Engr., Pacific Gas and Electric Co., San Francisco, Calif.

²"Kings River Will Be Big Addition to California Hydro," *Electrical West*, Vol. 115, December, 1955, pp. 62-64.

³"Hydroelectric Development on the North Fork of the Kings River," by W. R. Johnson, D. P. Dinapoli, and J. B. Cooke, *Electrical Engineering*, Vol. 75, October, 1956, pp. 900-905.

⁴"Bibliography: Underground Hydroelectric Power Plants," by J. Barry Cooke and A. G. Strassburger, *Proceedings Paper 1560*, ASCE, August, 1957.

⁵"California Hydro Project to Have First Big Underground Plant in U. S.," *Engineering News-Record*, Vol. 157, October, 1956, pp. 26-27.

The Kings River Development, Fig. 1, utilizes all of the 5,650 ft of static head between the maximum water-surface elevation at Wishon Reservoir and the Pine Flat Reservoir.³ In planning the Haas Power Project both ends were fixed by the Wishon Dam and by the Balch Diversion Dam. Five alternate plans to develop the 2,444-ft head were studied. Two used a single powerhouse and three used two powerhouses. The annual cost of power was a minimum for the adopted alinement using one plant having a conventional surface pen-

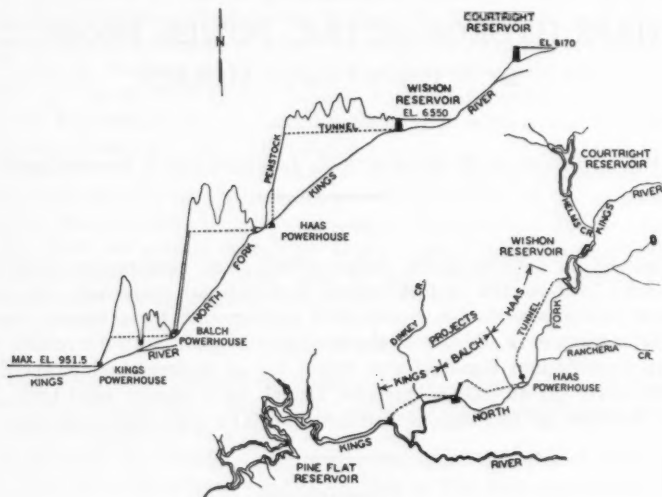


FIG. 1.—KINGS RIVER DEVELOPMENT

stock and powerhouse arrangement. The ultimate arrangement, however, proved to be even more economical.

DAM AND CONDUIT DESIGN

The rockfill dam and unlined tunnel is similar to the Bear River Project on the Bear River, near Stockton, Calif., completed in 1952.⁶ Different conditions and greater experience resulted in simpler details and different appurtenant structures for the dam and tunnel at the Haas Power Project.

Concrete-Face Rockfill Dam.—Courtright Dam on Helms Creek and Wishon Dam on the North Fork of the Kings River, near Stockton, Calif., both supply stored water to the three downstream power projects with the Wishon Dam, Fig. 2, being the diversion dam to the Haas Power Project. However, the design and specifications were essentially the same for both dams.⁷

⁶ "Design Features of Bear River Hydroelectric Project," by J. Barry Cooke, *Proceedings-Separate 636*, ASCE, March, 1955.

⁷ "Rockfill Dams: Wishon and Courtright Concrete Face Dams," by J. Barry Cooke, *Proceedings Paper 1746*, ASCE, August, 1958.

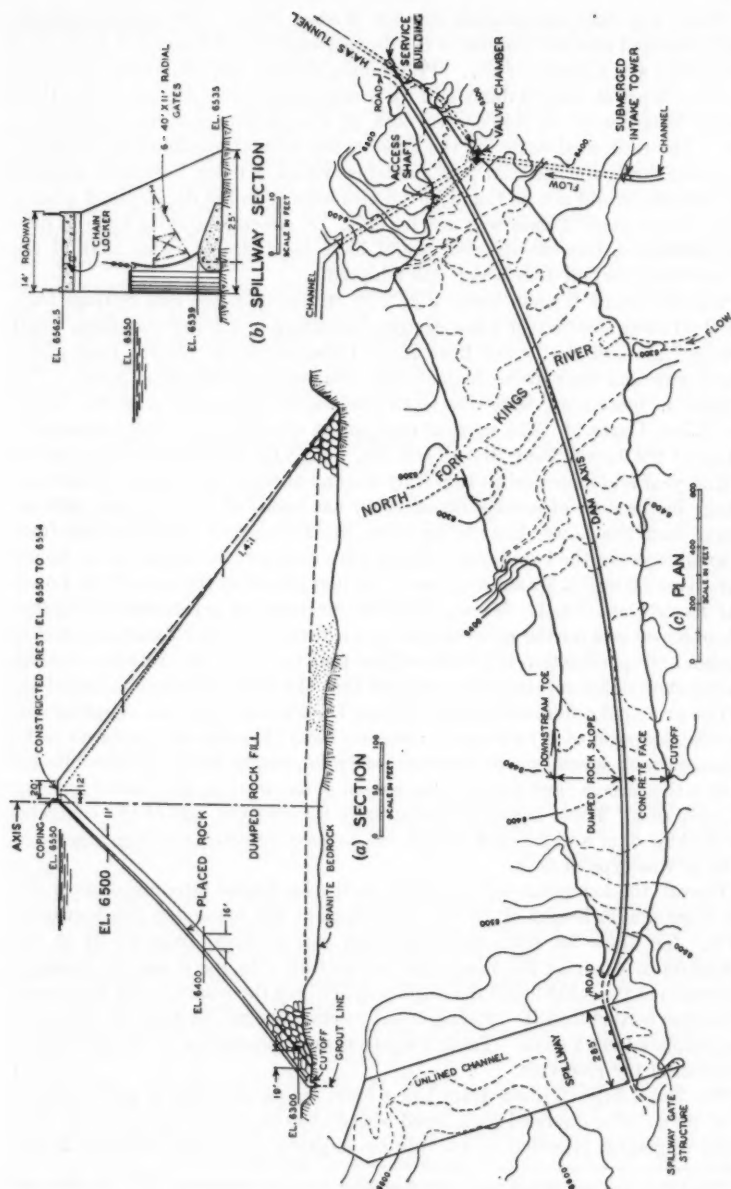


FIG. 2.—WISHON DAM PLAN, SECTION AND SPILLWAY SECTION

There was only one possible site for Wishon Dam. An exposed granite ridge projected into the canyon at the downstream end of a meadow to provide both a dam and a reservoir site. Preliminary designs and estimates were made for three types of rockfill dams and for a concrete-gravity section. The three rockfill designs were (a) thin central core, (b) thin sloping core, and (c) concrete face. The estimated costs for the three types were approximately the same, assuming that core material was available within 5 miles. Because suitable core material could not be found in the meadows or in the decomposed granite zones, a core rockfill dam was not feasible. A concrete-gravity type of dam was eliminated because its cost would have been nearly twice that of the concrete-face rockfill dam which was adopted.

The section of Wishon Dam, Fig. 2(a), differs from the Salt Springs Dam and the Lower Bear River Dam designs,⁷ resulting in a lower-cost dam. Salt Springs Dam and the Lower Bear River Dams are on the North Fork of the Mokelumne and Bear River, respectively, and both near Stockton, Calif. The changes, in most part, were due to the successful experience with the Lower Bear River Dams.^{6,8} The vertical component of settlement at the maximum section of the Lower Bear River Dam No. 1 (245 ft) was 1.12 ft at the end of the first year and increased to 1.30 ft by the end of the fourth year. Maximum leakage in the 4 yr of service (as of 1959) has been 3.0 cu ft per sec with no leakage from the Lower Bear River Dam No. 2 and most of the leakage from the knoll between the two dams. There have been no face cracks in the Lower Bear River Dam No. 2 and only two of limited extent in the face of the Lower Bear River Dam No. 1. These favorable measures of performance, together with observations during construction and a review of other dams, resulted in a design and specification for Wishon Dam that made the concrete-face rockfill dam construction competitive in cost with that of a thin-earth-core rockfill dam.

The principal differences in the Wishon Dam design from the other designs were the adoption of (a) a steeper upstream face; (b) more thinly-placed rock; (c) placed-rock specifications that are easier to comply with; (d) face lifts for construction access; and (e) the elimination of keyways in the placed rock for the joint ribs. These changes substantially lowered the cost of the concrete-face rockfill dam and are not considered to have affected the high degree of safety of this type of dam.

Though the low point in foundation in the excavated streambed gives the dam a maximum height of 296 ft, the height of the maximum full section is 255 ft. To allow for settlement the crest was crowned from 0.5 ft at the abutments to 4.0 ft at the maximum full section. In the 6 months between completion of the rockfill and the beginning of filling the reservoir the maximum full section settled 0.24 ft. Filling of the reservoir began on May 13, 1958 and was completed in 13 days. Table 1 shows the settlement due to the first year's operation of the reservoir.

The 296-ft-high Wishon Dam has a crest length of 3,330 ft and contains 3.7×10^6 cu yd of quarried rock, faced with 80,000 cu yd of reinforced concrete. It was originally intended to provide an ungated open-crest spillway in the

⁸ "Rockfill Dams: Salt Springs and Lower Bear River Concrete Face Dams," by I. C. Steele and J. Barry Cooke, *Proceedings Paper 1737*, ASCE, August, 1958.

left-abutment quarry for this high-elevation unattended dam. The ungated crest spillway would have required a 5-ft higher dam than would a gated-crest spillway. The cost of 5 ft of additional height for this dam was \$500,000, as compared to \$100,000 for the radial-gate spillway that was adopted. The height of the six gates is small (11½ ft wide by 40 ft in length) in order to use the wide quarry-spillway excavation and to have a minimum quantity of water subject to gate control. The gates are blocked open in the winter and an attendant is necessary to "top the reservoir off" in the spring.

Diversion Tunnel.—The diversion tunnel was designed with a 15-ft-horse-shoe cross section to permit storage of 80,000 acre-ft between the second and third construction seasons when there would be no spillway. Between the first and second construction seasons any one of three floods that occurred during the 36 yr of record prior to construction would have raised the water level to the top of, and over, the first year's rockfill level. The rockfill would have been 90 ft high with placed rock on the upstream face, but with no con-

TABLE 1.—VERTICAL CREST-SETTLEMENT—WISHON DAM

Date of reading and reservoir operation	Days	MAIN SECTION Ht. 255 Ft Sta. 22 + 20		WING SECTION Ht. 150 Ft Sta. 7 + 80	
		Ft	% Ht.	Ft	% Ht.
(1)	(2)	(3)	(4)	(5)	(6)
5-13-58.....	0				
Filling + 9 days full.....	22	1.31	0.52	0.40	0.27
6-4-58.....	22	1.31	0.52	0.40	0.27
Reservoir full.....	54	0.37	0.14	0.12	0.08
7-28-58.....	76	1.68	0.66	0.52	0.34
Reservoir full.....	141	0.05	0.02	0.04	0.02
12-16-58.....	217	1.73	0.68	0.56	0.37
Res. 6550 to 6502.....	121	-0.01	...	-0.01	...
4-15-59.....	277	1.72	0.67	0.55	0.37

crete slab. Flood water would have percolated through the placed rock and approximately 1,000 cu ft per sec would have overtopped the fill. Unfortunately, for rockfill-dam experience, the 1956-1957 runoff was less than in an average year.

Dam Outlet: Intake Tower.—The intake tower, Fig. 3(b), is at the upstream end of the diversion tunnel and serves as the permanent outlet for the dam and also as the intake to the Haas Powerhouse power tunnel. The 15-ft square tower is capped by a 30-ft-high, square, galvanized-steel trash rack with a 2-in. clear bar spacing. The gross trash rack area of 2,000 sq ft gives an average velocity of approximately 0.4 ft per sec for the power-tunnel flow of 760 cu ft per sec, and 1.7 ft per sec for the outlet flow of 3,500 cu ft per sec. The clear bar spacing of 2 in. is about the same as the minimum dimension of the nozzle opening. The flow of 760 cu ft per sec will pass through twelve small nozzles having a donut-shaped opening of 7.4 in. outside diameter, and is approximately 2 ⅞ in. thick. The bar spacing should, perhaps, be less than 2 in., but it has been found that pine needles can thoroughly plug trash racks with smaller spacing. No trouble has been experienced on similar installations with impulse-

wheel nozzles in which the clear rack-bar spacing is approximately the dimension of the annular opening at the nozzle ring.

The top of the concrete tower is set at an elevation to give a pool of 1,200 acre-ft or less when the tunnel is unwatered for inspection or maintenance. Two 4-ft-by-5-ft oil-cylinder-operated slide gates, normally closed, make it possible to draw water below the top of the concrete tower at a flow of 760 cu ft per sec. Closing these gates permits inspection of the unlined tunnel between the tower and the butterfly valves. The cylinders are above the top of the concrete tower to allow for maintenance. The stroke of the operating cylinder is the gate height plus several inches, and the cylinder is grouted in place with the gate properly seated and the piston against the end of the cylinder to prevent jamming of the gate.

Dam Outlet Valve Chamber.—A capacity of 3,500 cu ft per sec was required in the 1957–1958 runoff period to permit storage of 80,000 acre-ft in the partly-

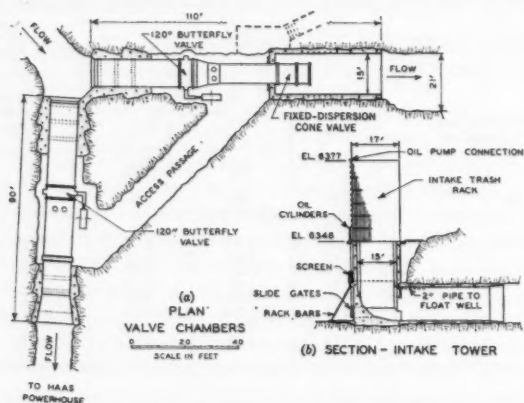


FIG. 3.—HAAS POWERHOUSE INTAKE WORKS

completed dam with no spillway. The capacity of 80,000 acre-ft will store any high-peak winter floods of record because they are of short duration for the high-elevation drainage area. The snowmelt provides the sustained flow and on three of the thirty-six years of record, with the outlet fully open, the 80,000 acre-ft would have been stored and approximately 1,000 cu ft per sec would have gone through the rock fill. The 3,500-cu-ft-per-sec discharge will be more than necessary for future use and will permit flood regulation. Discharge in advance of spilling can appreciably reduce the peak flood flow and such has been done with the 5,000 cu-ft-per-sec outlet works at Salt Springs Dam on the North Fork of the Mokelumne River, near Stockton, Calif.

An underground discharge chamber for a fixed-dispersion cone valve has been used at Watauga Dam on the Watauga River, near Elizabethton, Tenn., and at Fontana Dam on the Little Tennessee River near Robbinsville, N. C.⁹

⁹ "Characteristics of Fixed-Dispersion Cone Valves," by Rex A. Elder and Gale B. Dougherty, *Transactions, ASCE*, Vol. 118, 1953, p. 907.

It is a coincidence that the head and discharge requirements are the same at Wishon Dam as at Fontana Dam and that the size of the valves is the same (84 in.). The Wishon Dam discharge chamber is patterned after the Fontana Dam installation and Fig. 3(a) shows this arrangement. A 6-ft-by-6-ft shaft inclined at 45° and that is 210 ft long, serves as access and as air vent. The 10-ft-diameter butterfly shut-off valve is operated by an oil cylinder. The trunnion-mounted cylinder is preferred to a fixed cylinder with crosshead on the basis of being lower in cost, more easily set up, and best from the standpoint of simplicity of operation and maintenance. The piston rod is in the oil cylinder when the valve is in its normal position. Oil pressure is provided by a water-motor oil pump (300 lb per sq in.) or a gravity tank (100 lb per sq in.) in the service house on the crest of the dam. The pressure of 100 lb per sq in. can be boosted to 300 lb per sq in. by a hand pump if necessary. It is considered desirable to be able to close both 120-in. butterfly valves from the service house in the event of operating difficulties in the underground valve chamber. The fixed-dispersion cone valve is water-motor operated. When the discharge valve is open, an ejector is operated to keep the valve chamber drained. The fixed-dispersion cone valve demands considerable air, and because of the freezing conditions at Wishon Dam, precautions were taken to prevent freezing of any of the pipes in the valve chamber.

The unlined discharge tunnel is in excellent massive granite and is considered suitable for the turbulent flow as it leaves the discharge chamber. The original plan was for a 108-in.-diameter pipe to be on piers from the plug to an outdoor valve house. The diversion tunnel was already driven when the underground discharge plan was adopted, and it was necessary to enlarge the 15-ft tunnel section to assure free flow in the tunnel. The underground discharge arrangement is lower in cost, eliminates maintenance and possible vibration of the high-velocity discharge pipe, and eliminates freezing problems.

Power Tunnel Intake.—The intake tower and the unlined tunnel to the wye serve both the permanent dam outlet works and the power tunnel. The power tunnel intake, Fig. 3(a), consists of a 10-ft-diameter butterfly valve in a dry chamber. Pipes with 10-ft. diameters are embedded in concrete plugs on each side of the valve. The valve is identical to the outlet shut-off valve. Both valves are designed to open or close under free-discharge conditions. Access is from the outlet valve chamber. The butterfly valve is exceptionally reliable and the single valve controlling flow from the large storage reservoir is considered satisfactory. The operating company has ninety five butterfly valves in sizes ranging from 3 ft to 13 ft in diameter and all have given trouble-free service (as of 1959).

A dresser coupling is used between the plugs to eliminate longitudinal stresses that would be caused by temperature changes and by the application of Poisson's ratio to the hoop stress. A draft-tube taper is used on the discharge end to minimize head loss. Both the 120-in. butterfly valves can, in emergency, be closed from the service building on the crest of the dam. The air valves release air when the tunnel is being filled by the partly-opened butterfly valve and admit air when the valve closes under flow conditions.

Reservoir Level Indicator.—To allocate irrigation water on a basis of daily natural flow it is necessary to know the water level of Wishon Reservoir to 0.01 ft. The reservoir site is subject to severe freezing and heavy snow, and is inaccessible for approximately five months each winter. A 4-in. drill hole 270 ft deep from service house to tunnel is used as a well for a water-surface detector. The detector actuates both a recorder and a radio that transmits the water level to the control room at Balch Powerhouse. It was planned to grout and redrill the 4-in. well to give a well that should not corrode, leak, or ravel, but perfect cores made it unnecessary to grout.

Power Tunnel.—The power tunnel is a 13-ft unlined horseshoe section, 6½ miles long. The rails and ties used during construction were removed, but no mucking of the invert was required. There is one adit having a 7-ft square sliding door in the plug for future access. Upstream from the surge chamber is a large storage sand trap, and downstream is a steel liner to the portal. Where support was required, a concrete horseshoe or circle was used. Soft seams that would wash and later create rock falls were mined 6 in. deep and plugged by gunite.

Alinement and Exploration.—Because of the high head, 240 ft to 330 ft, resulting from the storage reservoir and the long length of tunnel, core holes were drilled at points that would control alinement. At four creeks holes were drilled from El. 6550, the maximum static gradient elevation for the tunnel, to tunnel grade. It was considered that if these holes showed good rock the tunnel alinement would be such that a minimum depth of cover equal to the static head would be used. The upper section of the holes showed hard granite with seams and some extensive zones of soft-grained granite. At tunnel grade the rock was sound and the alinement of total cover equal to static head was accepted but lateral cover at these creeks is three times the static head. An exception to the criteria was made at a deep draw near Wishon Dam where the surface granite was so sound that no drill holes were put down and cover of 180 ft was used where head was 280 ft to save tunnel length. To line with concrete the length of tunnel with less than criteria cover would have cost less than the additional length of unlined tunnel necessary to obtain criteria cover. However, after inspection of the excellent granite of the driven tunnel the length having less than criteria cover was left unlined.

Unlined Section.—It is the operating company's practice to use unlined tunnels where rock conditions permit because of the savings involved and because of a long period of successful experience with unlined tunnels. Rock falls in early tunnels were due to not plugging soft seams so that water would wash out the seams and cause large blocks of rock to fall in the tunnel. No rock falls have occurred in tunnels constructed since 1947 where proper "dental work" has been done during construction. An unsupported tunnel lined with concrete costs approximately 50% more than an unlined tunnel of equal head loss. This conclusion is based on $n = 0.014$ for concrete and $n = 0.030$ on design area for the unlined section; unlined horseshoe sizes from 11 ft to 26 ft; and on bid prices; the term n being the coefficient in the Manning formula. The value of n for new concrete may be 0.012, but if the water acts on the mortar it may reach 0.015 in time. The additional excavation for the larger unlined

tunnel was at a low incremental cost as compared to the cost per cubic yard for the smaller lined tunnel. Because the unlined tunnel costs less for a section of equal head loss, the economic size is larger with less of a head loss, therefore, in addition to the economy in using an unlined tunnel, more effective head is economically developed.

Unlined Invert.—None of the operating company's unlined tunnels have a concrete-lined invert because the cost cannot be justified. The lined invert would save the cost of a large storage or sluiced sand trap and would earn power benefits due to improved hydraulics, but not enough to justify its cost. The smooth maintenance-roadway provided by a lined invert is given no monetary value as an unlined tunnel with proper work on seams should require no maintenance. Also the unmucked and unlined invert of a low velocity pressure tunnel provides a waterbound macadam surface that can be traveled upon. A large access door in the adits is essential for maintenance, should it ever be necessary. A lined invert only slightly improves the hydraulics because the muck on the invert is the smoothest part of the unlined tunnel. The weighted effect of the relative roughnesses is considered to be proportional to the square of n . A design value of $n = 0.030$ on design area is based on head-loss measurements in a number of tunnels and on design area is possibly a composite n of unlined walls and waterbound macadam invert with possibly $n = 0.032$ on walls and 0.024 for the invert. For concrete-lined inverts n may be assumed to be 0.015. The 0.015-value for screeded invert concrete includes increased roughness due to erosion and to rock spalls that will collect on the invert. On the basis of the foregoing values, a comparative composite value of n for a lined invert is computed to be 0.028. Using this value of n , and allowing for reduced area due to a 6-in. invert, the reduction in head loss for the lined invert is 10%.

An estimate of the net saving in not lining the invert of the Haas Powerhouse tunnel is as follows:

Invert lining (31,270 ft @ \$18).....	\$563,000
Sand trap (bid price less cost of equivalent length of tunnel).....	66,000
Direct Saving of Capital Cost.....	<u>\$497,000</u>
Appropriation saving ($1.15 \times$ direct saving).....	574,000
Penalty for head loss is 0.10×60 ft \times \$14,000 in which \$14,000 is the capital value of 1 ft of head after the increased cost of the power plant has been paid for.....	<u>84,000</u>
Net Capital Saving.....	<u>\$490,000</u>

Hydraulics.—Before driving an unlined tunnel the hydraulics are based on the design area as the amount of overbreak is not known. The contractor drills several inches outside the design line to avoid the cost of removal of rock points at the lesser cost of a slightly increased volume of mucking. This results in an average overbreak of approximately 6 in. to 9 in., or an overbreak area of some 10% to 25% of the design area. Tests on unlined tunnels have given values of n to be 0.029 to 0.035 on measured areas and of 0.024 to 0.029

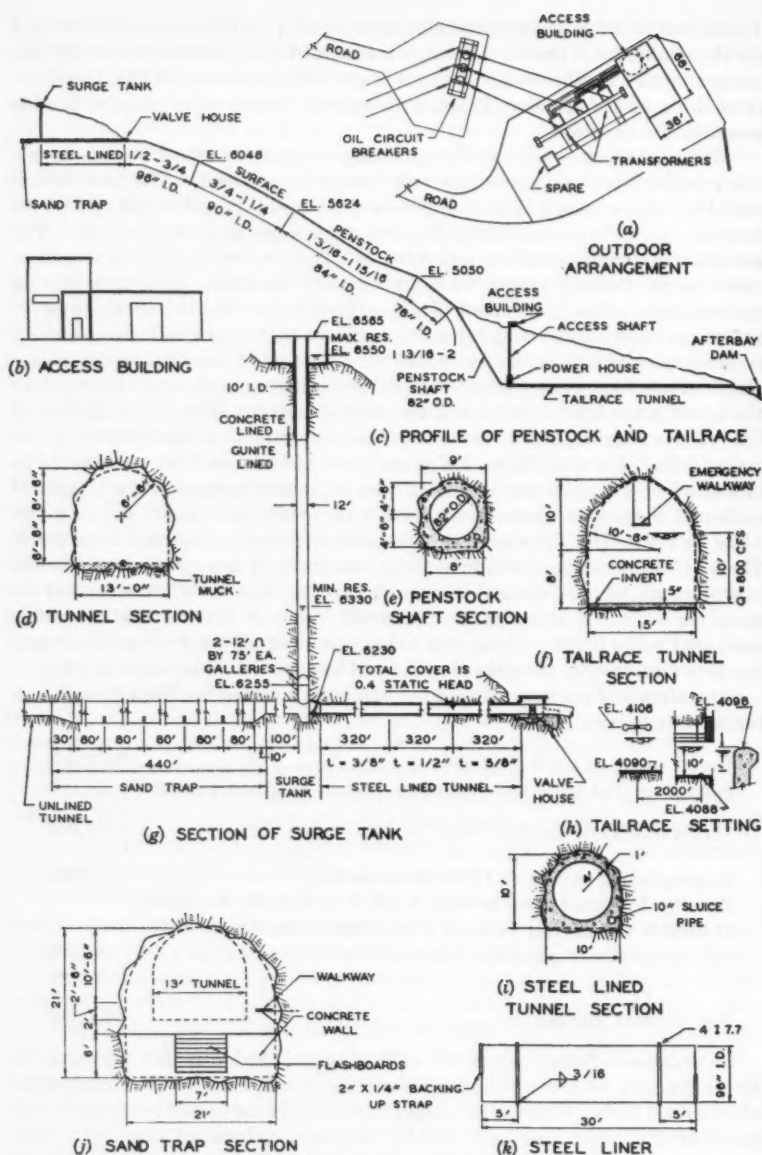


FIG. 4.—HAAS PROFILE AND SECTIONS FROM SAND TRAP TO AFTERBAY

on design areas. The smaller values on the design area are due to the over-break area. A value of 0.030 on the design area was used for economic studies and for determining the plant capacity for the Haas Powerhouse. For setting tunnel grade and for computing surge chamber load-on, a conservative value of $n = 0.035$ on design area was used so that greater than design flow can be safely carried.

Storage Sand Trap.—A large storage sand trap, without sluice, was used to collect the sand and gravel that will travel down the tunnel from the unmucked and unlined invert. The trap, shown in Fig. 4, will store 2,600 cu yd of material which is equivalent to a 2.2-in. depth of muck on a 12-ft width of invert 31,270 ft long. The trap was divided into five sections to be certain of effective storage. The tunnel velocity of 5 ft per sec on the design area is reduced to 2.8 ft per sec over the dividing walls. The trap is not expected to fill but if it does, a 12-in. sluice from the downstream section will indicate the presence of sand or gravel in the downstream section. Fine material from the downstream sections can be pumped out through this 12-in. line on a scheduled shutdown.

The large storage trap was adopted in preference to a small trap with a sluice on the basis of lowest capital and operating cost, and better performance. Much of the drainage channel from the tunnel portal is in erodable decomposed granite and regular sluicing would have caused severe erosion or required approximately $1\frac{1}{2}$ miles of pipe. Also, sluicing from a pressure conduit does not move much material each time, is not always satisfactory, and requires operation and maintenance. It has been found that surface muck with a dimension of as much as 2 in. travels down the tunnel invert during the first year of operation. The larger-sized muck then retains the remaining small material and little material moves after the first year.

Steel Liner.—A 96-in-diameter by 960-ft-long steel liner was used from the surge chamber, where the cover equals the static head of 330 ft, to the portal. The economic penstock diameter at the portal is 96 in. Actually, the theoretical economic diameter of a steel-lined tunnel is less than 96 in., but it is not considered reasonable or practical to construct one any smaller. The tunnel is driven to a 10-ft section rather than the 13-ft horseshoe unlined section. The liner is designed for full head to a point where cover is 40% of static head with a stress of 12,500 lb per sq in., 25% of the strength of A285B plate. The $\frac{5}{8}$ -in. plate thickness is decreased to $\frac{1}{2}$ in. and $\frac{3}{8}$ in., which results in free pipe stresses of 15,500 lb per sq in. and 20,800 lb per sq in. for increased cover. If supports had been required, the $\frac{3}{8}$ -in. or $\frac{1}{2}$ -in. plate pipe would have been backed up by reinforcing steel hoops as the plate was on order before the tunnel was driven. Only 160 ft from the portal required timber support and no reinforcing hoops were used. The $\frac{5}{8}$ -in.-plate pipe sections were radiographed and stress relieved, and the $\frac{1}{2}$ -in. and $\frac{3}{8}$ -in. thick pipe sections were not. I-stiffeners of 4 in. were used at 20-ft spacing to stiffen the pipe during shipping and erection, and to localize buckling that may occur due to outside water pressure. The crown concrete-to-rock contact and any hollows between the liner and concrete were grouted to minimize the danger from external water pressure. Field joints were single butt welded from the inside with backing-up strips. Sections

were limited to 30-ft lengths because of the mountain road to the portal. The interior received a shop-spun coating of hot coal-tar enamel and an exterior spray coat of whitewash to protect the shop enamel from excessive heat of the sun during shipping.

Surge Chamber.—The Haas power plant is a system-governing plant designed for load-on or load-off in 1 min. This time would not be rapid enough for governing local load or a small system, but for a large integrated system, a 1-min plant is suitable and does not require a premium to be paid in penstock waterhammer. A 10% value is used as a minimum. In dropping load at a rate faster than full load in 1 min, the jet deflector operates in 2 sec and a 1-min needle closure keeps pressure rise below 10% and minimizes loss of water.

Two 300-ft-deep diamond drill holes indicated that the formation would be fractured and of poor quality for the upper half of the surge tank. It was therefore planned to line the upper 50 ft of the surge shaft with concrete and reinforce for full head. Concrete with nominal reinforcing or gunite lining, as determined by rock conditions, was planned for the remaining 250 ft. A drill hole in a creek 2,400 ft upstream indicated ideal massive granite and an unlined surge chamber at that location was studied. However, cost for this upstream location, due to increased waterhammer and the lower tunnel portal, exceeded the cost of full concrete lining for a surge chamber near the portal.

The surge chamber type might be described as a gallery-simple-differential design (Fig. 4(g)). The unusual design is occasioned by the 220-ft operating range of the storage and diversion reservoir, by the very high-head plant (2,444 ft), and the cost of 1 ft of head on the long (4,600 ft) penstock. An important criteria in load-on design, in addition to that of minimum cost, was to keep the downstream tunnel portal as high as possible, and consequently minimize the head on the unlined tunnel. To accomplish this, galleries were used to give minimum draw-down for load-on, and load-on design was from a Wishon Reservoir level of El. 6366 rather than from the minimum storage level of El. 6330. Operation is restricted on the very infrequent occasions when large storage reservoir is operated below El. 6366. For rejection from maximum reservoir level the tank acts as a differential tank with most of the water spilling over the riser. The diameter of the rejection tank is such that the sum of tank cost plus the incremental liner and penstock cost is minimal. The surge above static head is only 15 ft for the $6\frac{1}{4}$ -mile tunnel and 1-min rejection. The ports are small as they are not necessary for load-on and this gives an efficient differential design for rejection. The surge chamber is located so that the large rejection tank is in an open cut to avoid the higher cost of underground excavation. The steep hillside slope did not make possible a open-cut basin still lower in cost. For intermediate reservoir levels the galleries or tank will not always come into action, and surges in the simple shaft may be as great as 110 ft for a 1-min load change. Economy in the small-diameter shaft is possible because of the high-head plant, and such large surges should not interfere with the governing process as they are a small percentage of the effective head.

Penstock Valve.—It was decided to use a butterfly valve at the top of the penstock because there is only one valve at the tunnel intake and it is inaccessi-

ble for 5 months of the year. The penstock valve is operated by an oil-pressure, trunnion-mounted cylinder and closes automatically on 10% excess flow. Four 12-in.-diameter air valves are used downstream from the valve. The air valves are cast steel with bronze seats and stainless steel stem.¹⁰ Oil is provided from a 300-lb-per-sq-in. accumulator set. The valve house has concrete block walls with a flat concrete roof supported on steel beams.

Surface Penstock.—The operating company's penstock practice¹⁰ was used in the design of the Haas powerhouse penstock. Three changes from earlier practice, made for this project and also for the Balch project, were (a) the increase to a working stress of 17,500 lb per sq in., (b) the use of 20% minimum efficiency riveted joints, and (c) the painting of an exterior aluminum coating in the shop. A thorough study of stresses, occasioned by the 7,000 tons of penstock required at the two projects, resulted in increasing the working stress above that used on previous jobs. The adoption of joints with 20% efficiency permitted the use of two rows of rivets, rather than three or four, in connecting the heavy walled pipe. With the use of an expansion joint between anchors the longitudinal stress was limited to the friction on piers, dead-end pressure on the expansion joint, and bending moment. Although the joints are located at points of zero moment the joint is designed for the moment over the support to give a measure of resistance to moment in addition to the other forces. The joint is designed for the foregoing loads, or 20% minimum efficiency, and the 20% holds true for the heavier walled penstock. Changes in diameter are made in bends to eliminate longitudinal stresses and to minimize the head loss and cost.

The interior shop-spun coal-tar coating is very important from the standpoint of hydraulic economy because the head loss is 40% less than for a hand-daubed coal tar ($n = 0.010$ as compared to $n = 0.013$). At the Haas Power Project the use of spun coal tar provides \$400,000 more net capitalized power value (28 ft at \$14,000) than a hand-daubed coating and costs less. (Net value refers to the value after the units and powerhouse have been enlarged to produce the power). The shop-spun coating, including sand blasting and priming, is approximately \$0.30 per sq ft as compared to approximately \$0.60 per sq ft for a field hand-daubed job. For the Haas Power Project the cost difference was approximately \$30,000, which is important but not as great as the hydraulic saving. During shipment the pipe was subjected to very warm weather in the San Joaquin Valley of California, and to minimize the possibility of heat damage to the enamel, the penstock was given a shop coat of aluminum over the shop sand-blasted and red-lead primed pipe. Again, the shop exterior painting is much lower in cost than field painting, and damage in shipping is nominal.

Underground Penstock.—The underground penstock (Fig. 5) consists of 760 ft of 82-in. (outside-diameter) pipe embedded in concrete in a shaft inclined at 65° to the horizontal, a 76.5-in.-by-52-in.-by-52-in. symmetrical wye at the base of the shaft, and two 52-in.-diameter, 60-ft. long branch lines to the units. The heads at the top and bottom of the shaft are 1,500 ft and 2,444 ft, respectively. This high-head pipe in a rock cover of nominal depth but excellent

¹⁰ "Penstock Experience and Design Practice," by G. V. Richards, *Proceedings Paper 1397*, ASCE, October, 1957.

quality is not a normal problem of concrete back-filled steel liner or penstock design. It was decided not to share load with the excellent granite but to use somewhat higher free-pipe working stresses. The embedded pipe is not subject to being hit by rocks, to high temperature changes, or to such high secondary stresses as a surface line, and the granite will, certainly, take some stress.

The criteria used for determining design stresses in the embedded penstock are arbitrary. Table 2 shows the stresses for a free pipe and also for an embedded pipe. The embedded stresses are based on equal radial movement of the shell and the rock. The properties of the A242 steel for this penstock are a yield stress of 47,000 lb per sq in. and an ultimate strength of 67,000 lb per sq in. Conventional surface penstock stresses were used through the decomposed and weathered surface granite and from the wye to the units. After entering sound seamless granite, thicknesses were decreased $\frac{1}{2}$ in. per 40-ft section until the safety factor of free pipe was 2.6 on the ultimate stress, which, for A242 steel, is 1.8 on the yield stress. By keeping a uniform thickness of

TABLE 2.—PENSTOCK STRESSES

Location in Fig. 5	Thickness of plate, in inches	FREE PIPE			EMBEDDED PIPE			
		Stress, in pounds per square inch	Factor of safety based on yield stress	Factor of safety based on ultimate stress	Stress, in pounds per square inch	Factor of safety based on yield stress	Factor of safety based on ultimate stress	Percentage of load taken by rock
(1)	(2)	(3)	(4)	(5)	(6)	(7)	(8)	(9)
1	2 $\frac{1}{2}$	17,500	2.7	3.9	0
2	1 $\frac{1}{2}$	21,450	2.2	3.1	14,430	3.3	4.6	33
3	1 $\frac{1}{2}$	23,550	2.0	2.9	15,630	3.0	4.3	34
4	1 $\frac{1}{2}$	26,000	1.8	2.6	16,640	2.8	4.0	36
5	1 $\frac{1}{2}$	29,300	1.6	2.3	19,200	2.5	3.5	34
6	1 $\frac{1}{2}$	27,300	1.7	2.5	18,500	2.6	3.6	32
7	1 $\frac{1}{2}$	25,600	1.8	2.6	17,800	2.7	3.8	30
8	2	22,600	2.1	3.0	16,200	2.9	4.1	28
9	2 $\frac{1}{2}$	20,200	2.3	3.3	15,100	3.1	3.5	25
10	2 $\frac{1}{2}$	17,500	2.7	3.9	0
11	1 $\frac{1}{2}$	17,500	2.7	3.9	0

1 $\frac{1}{2}$ in. to point 5 in Fig. 5(b), the stresses were increased as rock cover increased, to 2.3 on ultimate stress, which is 1.6 on yield stress for a free pipe. Between point 5 and the wye, the stresses were decreased because of proximity to the chamber, and as a transition to normal stresses at the wye. With 25% to 35% of the load absorbed by rock the minimum safety factor is computed to be 3.5 on ultimate stress and 2.5 on yield stress. The design is perhaps conservative, but it is observed that this section of penstock is subject to very high head and not a great deal of rock cover. The saving in plate for the adopted design over a free pipe line with surface-penstock design stress of 25% of the ultimate is 210 tons, or \$150,000.

Welded field joints were adopted for the embedded 82-in. line in the shaft. The riveted field joints of 20% efficiency, as used on the surface line, would be weak links due to the longitudinal stresses caused by Poisson's ratio applied to the hoop stress, temperature contraction, and concrete setting. A riveted joint with 50% or greater efficiency would require 4 rows or 5 rows of 1 $\frac{1}{2}$ in.

rivets for the thick $1\frac{1}{2}$ in. to $2\frac{1}{4}$ in. pipe. Use of the riveted joint in the steep shaft was difficult and inadvisably expensive, both in the joint cost and in the concrete backfill for a larger bell hole. The welded joint was selected on the basis of being most suitable from the standpoint of its giving a high roundabout joint efficiency and lowest cost. Due to the excessive thickness required for A285 steel and the undesirability of the non-stress-relieved field weld on thick A212 plate, these steels were eliminated. A review of possible steels resulted in selection of A242 steel with a chemical composition favoring the physical properties of ductility and weldability.

Double-butt field welds, Fig. 5(d), were chosen in preference to single-butt welds. Although a single-butt weld from the inside would be more easily accomplished and would eliminate the bell-hole cost, the double-butt weld would provide a weld more suitable to radiographing and more acceptable as a non-stress-relieved weld. Preheat of 250°F to 300°F by electric pads was specified and may have had some stress-relieving effect. The shop-spun coal tar was stopped 2 ft back from the joint to permit preheat and welding.

The wye field joints and the joints in the 52-in. branch pipes were field riveted for several reasons. The wye and branches are adjacent to the powerhouse chamber and all factors in design and installation had to be conservative. It was considered undesirable to field weld to the very rigid and heavy wye. The pipe is horizontal, excavation gives several feet of working room for other reasons, and the butt strap fitting up and riveting may be done conveniently and at reasonable cost. The 50%-efficiency riveted penstock joints between the wye and turbine are preferred and are convenient.

The 82-in. pipe was specified to an outside diameter so that erection skids, drainline, and all installation clearance could work to the line of the outside of the pipe. Shop fabrication was in 40-ft sections, the heaviest being 32 tons. All welds were double-butt welds and radiographed. The completed sections were stress-relieved.

The wye is of A242 plate with shell thickness of $2\frac{1}{4}$ in. and ring and clamp plate thickness of 4 in., which is the maximum for A242 plate. The cylindrical and cone-butt welds were radiographed and fillet welds were magnafluxed. The pressure test was conducted at 1,530 lb per sq in., 150% of the design stress. Guide plates were used in the crotch of the wye to minimize wye head loss. In making the Balch Power Project wye one crack developed in the middle of the 5-in. plate ring clamp as the last cone section was welded. The procedure was to weld the large-diameter section to the ring clamp, then weld one cone leg to the ring and C-clamp, and then to weld the last cone leg. Carbon-arc gouging of the crack, stress relieving, rewelding, stress relieving, and pressure testing completed the job. At the Haas Power Project the schedule was very tight and all pieces were welded at the same time. Several cycles of gouging and stress-relieving were required. Cracks several feet long and several inches deep occurred in the 4-in. plate adjacent to the weld. Both a spherical and a pantleg wye were bid on. All bidders submitted lower prices for the pantleg wye, prices 60% to 70% of the lower-weight spherical wye.

A 6-in. drain (Fig. 5(c)) placed alongside of the penstock was not actually required as the thick-walled 82-in. pipe was in no danger of collapsing. A

drain, that would discharge visibly in the powerhouse, was needed to warn of any penstock leak which might be a hazard to the powerhouse chamber. The 6-in. size was chosen to minimize the possibility of plugging and was to be located in a part of the excavation where there was room for it. The top was to be accessible so that the drain could be cleaned and tested.

The penstock backfill concrete was 2,000-lb-per-sq-in. concrete with low-heat cement. The mix was designed to minimize shrinkage. Two tapped and threaded 1½-in. holes, opposite each other at 10-ft spacing, were provided for grouting between steel and concrete and between concrete and rock. The tapped holes were plugged and seal-welded after grouting. The drain holes were then diamond drilled through 1½-in. tapped holes in the shell and into the 6-in. drain, and on until it was 1 ft into rock.

The design size of the shaft gives 13 in. of clear distance from pipe to rock. Bell holes at field joints were required for welding and radiographing. A horseshoe shape provided room for the rail skids, the drain line, and a manway for access to joints and for vibrating concrete during construction. Minimum thickness of concrete was desirable both from the standpoint of cost and shrinkage.

UNDERGROUND PLANT DESIGN

General.—The underground powerhouse is approximately 500 ft vertically below the surface and 2,000 ft from the river. The general arrangement of the powerhouse is shown in Fig. 6. The penstock is in a 760-ft shaft leading to the powerhouse chamber. The chamber, which houses valves, units, auxiliaries, and control room, is 173 ft by 56 ft in plan and 100 ft high. An 18-ft-diameter access shaft leads to the surface and contains generator leads, elevator, stairway, piping, and control leads, and serves as the exhaust ventilating duct. The 2,000-ft-long, 17.5-ft-by-15-ft unlined tailrace tunnel serves as construction and future access for heavy loads, as well as an emergency personnel access and ventilating duct.

The Haas Power Plant was originally laid out as a surface plan and on essentially the same alinement as the adopted underground plan. The surface layout was the most economical of five alternate plans, but the high cost and head loss of the heavy walled penstock (2-in. to 3-in. thickness) on the flat profile at the lower end was discouraging. A study of an underground layout was made and this indicated that the underground layout was substantially lower in cost and developed 30 ft more effective head. Even if the chamber excavation were to cost several times the estimate, it was still economical to go underground. With such a margin for contingencies, and with nominal exploration, it was decided to go underground for the purpose of effecting capital savings and increasing power values. Additional inherent benefits were the development of maximum effective head, the conservation of 2,500 tons of steel, a safer and more permanent installation, and minimum maintenance.

Exploration.—As part of the initial exploration it was decided to put down a 500-ft-deep core hole at each end of the proposed chamber. The first hole provided all 10-ft cores of ideal granite. The second, 200 ft away, was a perfect hole until the elevation of the chamber was reached, where some 50 ft of close cleavage planes and soft seams in a plane 20° to the horizontal were encountered.

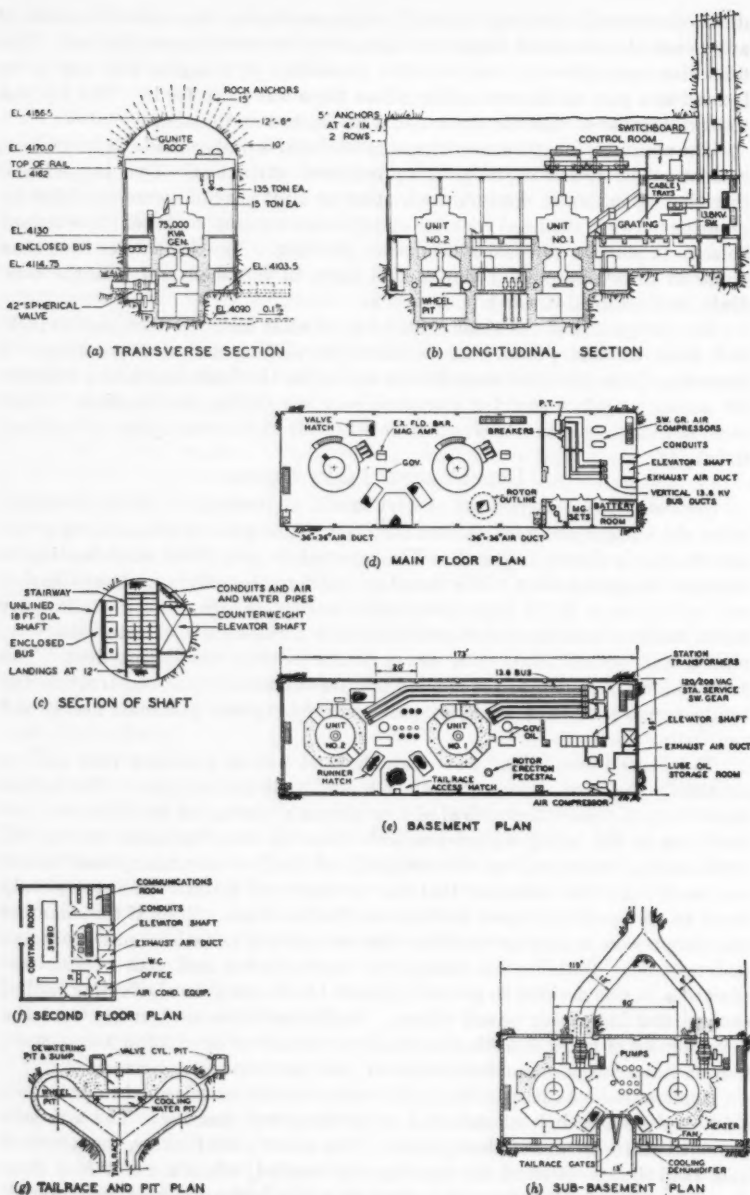


FIG. 6.—Haas Powerhouse Sections and Plans

This second hole was away from the ridge and toward a nearby creek which may have been in a faulted zone. A third hole was started a distance equal to the chamber length, 170 ft, from the first and was essentially a perfect hole of the same grain structure granite as the first. With an excellent core at each end of the then relocated chamber, it was decided to go underground and do no more drilling.

Economics.—In deciding to go underground, a capitalized saving of \$1,600,000 was estimated. After all contracts had been let and all excavations had been completed it was found that the actual saving over a surface scheme was \$900,000. This difference is the result, primarily, of excavation costs that were higher than estimated.

The capital and power value benefits in going underground are in the conduit from the point where it enters the penstock shaft to the afterbay. The 3,100 tons of penstock required for this part of the surface penstock, at \$900 per ton (installed), would have cost approximately \$2,800,000. The installed cost of the underground penstock (\$1,050,000) plus the tailrace tunnel (\$600,000) is \$1,650,000, which gives a conduit saving of \$1,150,000. The underground power plant, consisting of powerhouse, access shaft, service building, and switchyard, cost approximately \$700,000 more than the comparable installation for the surface plan. The net direct capital saving is thus approximately \$450,000. In addition to the capital saving the capitalized value of the increased power output due to 30 ft more of head is \$450,000. The net saving in being underground is therefore on the order of \$900,000.

Optimum Location and Alinement.—It has been demonstrated that the higher cost of the underground powerhouse and access shaft was more than paid for by the savings in the flat section of penstock of 2-in. to 3-in. shell thickness. The top of the penstock shaft is at the bottom of a steep surface-penstock slope. Any further shortening of the surface penstock (by moving the powerhouse further into the mountain), would not decrease penstock length very much and the penstock saved would be of thinner plate. The cost of the increased length of penstock in shaft and of the longer access shaft, would have exceeded the savings in surface penstock. The optimum location was therefore rather closely defined by the topography.

As is customary, the surface penstock was located on a ridge to keep the quantity of steel at a minimum. For the initial underground layout the penstock dropped off the ridge steeply to the top of the penstock shaft. The relocation of the powerhouse directly under the basic ridge, as dictated by the diamond drill holes, required a somewhat longer penstock shaft, access shaft, and tailrace tunnel. The optimum design location was thus changed slightly by the exploration.

Having located the powerhouse and tailrace tunnel, the penstock shaft alinement was then determined. The point of intersection of the wye and the horizontal penstock adjacent to the powerhouse chamber was arbitrarily located 70 ft upstream from the powerhouse wall in order that the wye and branch excavations would not undermine the high chamber wall. This left a substantial block of rock to support the wall during construction. Later the penstock was backfilled with concrete to the wall of the powerhouse chamber. The economic slope of the penstock shaft was determined to be 65° to the

horizontal. Even using higher stresses for the penstock in the shaft the cost of shaft and concrete backfill made it apparent that a minimum length of penstock should be underground. Alternate studies showed that the annual costs were approximately the same within the accuracy of the estimates between 90° and 65° to the horizontal. The 65° slope was selected in preference to the 90° slope because at the same annual cost it gave slightly more power. A 50° slope, which might be very appropriate if the penstock were already underground, was not economical in this case.

Basic Decisions.—It was recognized that the cost and possible contingency in the excavations was a major factor of uncertainty in an underground power plant. The main criterion in selecting a layout was to have minimum excavation.

The most significant decision in the basic layout was to use the tailrace tunnel for construction and for permanent access, with a minimum-size vertical shaft. The use of the tailrace tunnel for permanent heavy maintenance access makes it possible to accommodate all other access requirements in a small-diameter vertical shaft. The cost of a high-capacity crane at the top of a large-diameter shaft or a separate access tunnel was thus avoided. This multiple use of the tailrace tunnel requires that the plant be shut down when loads greater than 2½ tons (shaft-elevator capacity) are handled, and that flood flow be such that it is possible to enter the tunnel. Access for heavy loads is seldom required and two large upstream storage reservoirs provide substantial control of the river. The capital cost saving in using the tailrace tunnel as the access tunnel greatly outweighs the possible, but improbable, impairment of operation. The large size and growth of the operator's system is such that reasonable operating risks are increasingly more acceptable than the expenditure of capital.

A brief study showed conclusively that the transformers should be above ground. The 500 ft of isolated bus in the shaft is expensive but is appreciably lower in cost than the underground alternative which requires underground excavation and a high-voltage cable.

Two independent means of personnel access were considered necessary. The access shaft with elevator and stairs is the primary access. A small 45° stairway shaft at the opposite end of the chamber was considered, but was abandoned in favor of a walkway in a Gothic-arch tailrace tunnel. The 2,000-ft hanging walkway, Fig. 4(f), was estimated to cost less, including the incremental cost of the larger tailrace tunnel. The additional space is useful in plant ventilation and assures free-flow conditions. The emergency walkway will be awash but still usable during flood conditions.

The underground estimate, used in comparison with the surface layout, included a concrete-arch ceiling in the powerhouse, a concrete-block curtain wall in event of dampness, and other items that were not intended to be used unless essential, but were included to allow for contingency. Fortunately, the very favorable dry and safe rock conditions have permitted economies that have helped to offset the higher-than-estimated excavation costs.

POWER PLANT EQUIPMENT

Turbines.—The selection of two 92,000-hp, vertical-shaft, multi-nozzle, impulse turbines was uncomplicated. The criteria for number of units for the

large integrated system is the largest economical and practicable size. Machines having six nozzles and operating at 400 rpm with integral cast runners were used. The turbines operate with a static head range of from 2,444 ft to 2,224 ft. The design horsepower is for a flow of 792 cu ft per sec and a static head of 2,444 ft (effective head of 2,324 ft). The dependable capacity is for minimum level and for the same nozzle stroke which delivers 760 cu ft per sec. The vertical-shaft and multi-nozzle turbine was selected over a horizontal-shaft unit because (a) it had a higher efficiency, (b) it required fewer units, (c) the nozzles may be set closer to the tailwater, (d) it had a higher speed and therefore required a smaller turbine and generator, (e) of greater effective energy dissipation into wheel pit walls, (f) there was less hazard due to wheel or bucket failure, and (g) less water-hammer hazard to the penstock from a single faulty nozzle operation because each nozzle controls a small part of the flow. The turbine distributor casing was tested to 150% of working pressure both in the shop and in place, and concrete was poured with no pressure in the casing.

Turbine Valve.—The turbine valve is of the straight-flow, spherical type. The economic diameters of the penstock leading to the valve, the valve, and the distributor casing entrance are 52 in., 42 in., and 46½ in., respectively. Bid prices on valves of 42 in. and 46½ in. sizes indicated that the 42-in. valve was economically appropriate. The valve is double-seated with normal closure of the downstream seats and upstream closure to permit maintenance and adjustment of the downstream seat. A flexible coupling is located between the valve and distributor casing to control longitudinal pipe stresses and permit disassembly.

Generator.—Two 75,000-kva, 0.9 power factor, 400-rpm, 60-cycle, 3-phase generators were furnished. An overhead-thrust bearing supports the rotating parts and the generator and turbine guide bearings are capable of carrying the maximum side thrust caused by the hydraulic unbalance of any combination of nozzles. Generator cooling water is pumped from the tailrace.

Governor.—The governors are of the actuator type and control the needles and jet deflectors. The needles are operated by individual servomotors and the rate of closing and opening is set for 1 min. The needle servomotors are provided with external springs to automatically close the needle nozzles in the event of the loss of governor oil pressure. In the event of sudden load rejection, deflectors will deflect the jets in approximately 2 sec from the runner buckets to the energy absorbers in the walls of the wheel pit. Thus, speed rise will be held to a low value.

Low-Voltage Leads.—The six enclosed bus generator leads are connected to a metal-clad, air-blast switchgear in the powerhouse. From the switchgear, three enclosed bus leads carry the power up the shaft to the transformers. Air is admitted into the enclosed bus ducts in the powerhouse and released at the access building. Low-voltage cables for this installation might have cost a little less but at approximately equal cost, the enclosed bus was preferred.

High-Voltage Equipment.—Single phase 13,800/220,000 kv-37,500/50,000 kva transformers have been furnished. Their 50-ton shipping weight is under the 60-ton hauling limit for the Haas Project site whereas two 3-phase transformers of some 80 tons each could not have been transported. Because the full plant capacity is dependent on any one of the single-phase transformers and the plant can be snowed in, a spare is provided. At the Balch Project, where

access is better, 3-phase transformers of 68 tons shipping weight could be transported and no spare was provided. Oil-blast circuit breakers connect the circuit to a single circuit 220-kv transmission line.

UNDERGROUND POWERHOUSE

A basic design criterion was to put all facilities, valves, units, control room, and tailrace gates in one excavation. It was considered that this would give the lowest cost plant and the safest excavation. The height, crane rail to the top of stator, for installation of rotor was carefully determined to be a minimum. Factors that make this dimension a minimum are the (a) use of two bridge cranes with equalizing beam, (b) connection of hooks to the equalizing beam to permit the top of the beam to raise to the bottom of the crane bridge, (c) lifting thrust ring on shaft to be as far down on shaft as possible, (d) flange between generator shaft and turbine shaft to be as close to rotor as possible, and (e) lift the shaft flange only enough to clear top of stator. At the Haas Project only 6 in. clear over stator coil was allowed after all dimensions were determined. An excavation width of 56 ft was governed by the need for passing the low-voltage leads along the upstream side of Unit No. 1 and space for runner and tailrace access hatch downstream from the unit. Space for the turbine valves and needle removal did not govern but it was just adequate without special blockouts in the walls. Crane access to turbine valves was not considered a requirement in determining the powerhouse width, as it seldom, if ever, is necessary after installation. At the Haas Powerhouse it was conveniently provided to the Unit No. 2 valve because of the space required for the enclosed bus. Unit No. 1 valve can be raised to the basement floor by lowering the crane cable between bus bars and skidding it to the runner hatch for removal to the main floor. The length of the excavation is based on the minimum passage needed past Unit No. 2, the Unit No. 2 turbine foundation block, 15-ft clearance between nozzle servomotors of Units No. 1 and 2 to permit access between them during construction, Unit No. 1 turbine block, and minimum rotor assembly space. All remaining facilities are crowded in four stories at the access shaft end of the chamber.

Arrangement.—Fig. 6 illustrates the general arrangement. An unusual feature is the discharge and tailrace gate arrangement. The runner hatches are as close as physically possible to the units. The runner is lowered by a portable hydraulic device onto a small rail car. The car is bolted to the runner and both are lifted through hatches of minimum size to clear the runner and car when they are hanging on edge. There is no room for a lift tailrace gate. Hydraulically-operated hinged gates, which also serve to improve tailrace hydraulics, are used. Powerhouse compressed air, at 125 lb per sq in., is used to operate the gates.

Rock Anchor and Gunite Arch.—It was considered that no actual support would be required other than for a few rock anchors. However, spalling in the arch could be expected and it was decided, arbitrarily, to secure the ceiling for safety of both personnel and equipment. A rock-anchored and gunited arch was estimated to cost one-half as much as a concrete arch and to have other advantages. It was accomplished with minimum delay and cost to the exca-

vation and the rough surface was accoustically desirable. The anchor-gunite arch required a shorter span excavation and less volume of excavation. The rock anchors are 1-in.-diameter reinforcing bars, 10 ft, 12.5 ft, and 15 ft. long, and at 3½ ft spacing both ways. The anchors and gunite in effect provide a reinforced or sewn rock arch, from which a loosened rock cannot fall. The method used for overhead grouting of the rock anchors was developed in Sweden. Two half-round perforated tubes of sheet metal for the full length of hole are filled with a stiff sand cement grout and then wired together. This is inserted in the hole and the reinforcing rod is driven in by an air hammer. The volume of grout is such that a slight amount is extruded as the rod is driven to the end of the hole. Gunite mesh is formed to cover the rock with 1½ in. minimum clearance over rock. Two No. 4 by 2-ft reinforcing rods were welded to the anchor at 90° to each other, parallel to the rock face. These bars supplement the mesh and anchor the gunite to the rock. Gunite of 4 in. thickness, and 1½ in. minimum cover over mesh and rock points was applied to the shape of the rock.

Formation Drainage.—Damp areas were drained and not grouted. Diamond-drill drain holes (3-in.) approximately 50 ft long and sloping upward were drilled into wet or damp zones in the powerhouse chamber walls. Cores were supplied to obtain knowledge of the rock near the chamber walls.

Cranes.—Two 135-ton bridge cranes that require no alterations were taken from the Rock Creek powerhouse on the North Fork of the Feather River near Oroville, Calif. One of the two 110-ton cranes from the nearby Cresta powerhouse on the Feather River near Oroville, Calif., was moved to Rock Creek.

The rotor lift is very seldom made after erection. If major maintenance of the generator ever becomes necessary, it can be done in place or the rotor can be jacked up using the equalizing beam supported on cribs outside the stator. If cranes were to have been purchased for the Haas Project, two rather than one would have been used. The cost of two cranes is greater than the cost of a single larger crane, but when structural steel and additional height of building is taken into account the over-all cost of two as against one is approximately the same. Installation of the cranes is made very early and the construction advantage of two cranes is valuable. Two cranes give minimum height and excavation for the underground powerhouse. The use of an equalizing beam to permit the top of the shaft to extend up and between the cranes, and the reduction of the distance above the crane rail necessary to accommodate the smaller trolleys reduces the powerhouse height. Another example of economy in cranes is the use of a temporary construction crane for rotor installation and a permanent 25-ton gantry for the outdoor Feather River plants.

Structural Steel.—The structural-steel crane columns and girders were installed immediately after the excavation was completed in order to make the cranes available for construction. Footings for the steel crane columns were all on rock to permit the early installation. The column webs are parallel to the crane girders as they can be given lateral support by rock anchors, and the columns can deflect readily with movement of the rock walls. The webs of the 14WF136 columns are tied to a 1½-in. diameter rock bolt every 14 ft for support. The 36WF194 girders are centered on the columns and the upper flange was

rock-bolted to the walls to take lateral loads. The steel was sand blasted and coated with red lead in the shop. The walls remain as exposed rock. The multistory construction above the main floor for control room, low-voltage switching, and power-plant auxiliary services is a structural-steel frame with reinforced concrete floor, concrete block walls, and metal decking roof. This structural steel also goes down to rock so that it can be erected with the crane steel. It thus permitted early installation, use of the elevator and stairs, and provided early floor space for construction use.

Concrete.—For the powerhouse and machine foundations 3,000-lb-per-sq-in. concrete having 1½-in. maximum size aggregate was specified. Construction joints were arranged to give three basic pours. The first pour included all possible concrete that could be poured before installing the turbines. This included wheel pits, subbasement floor, and all the concrete at the service end of the powerhouse. The main floor was poured up to Unit No. 1. This first pour provided early construction space and access from the shaft and elevator. The second pour was the turbine generator blocks along with the adjacent basement and main floors except for most of the area between units, which was essential for access of several trucks under the cranes. The third pour was between units and was made as late as possible because it limited tailrace access to one vehicle under the tailrace hatch and under the powerhouse cranes.

Ventilation.—Air is drawn from each side of the tailrace into two independent and identical systems. Each can handle 15,000 cu ft per min and consists of a cooler-dehumidifier, blower, and heater in the subbasement. Cooling and dehumidifying coils use the cold tailrace water as the cooling media and heating is done by electricity (160 kw total). Cool air is delivered by 36-in.-by-36-in. ducts to the crane rail level at each corner of the powerhouse where it is sprayed into the chamber over each unit. The only other release is a small 2,000 cu ft per sec release to each end of the subbasement. Between the dehumidifier and the blower is a return air damper which is automatically adjusted with the fresh-air damper when heat is required. The bottom of the access shaft is air-sealed from the powerhouse and air-tight elevator doors are used in the powerhouse.

Outgoing air is admitted from the basement and main floors to the shaft, or upon temperature rise at the top of the chamber, directly to the access shaft through a motor-controlled damper. The outgoing air goes up the unlined rock shaft and not in a duct. It is beneficial in keeping the shaft dry and minimizes blower requirements and cost of ducts. A 22,000-cu-ft-per-min blower is mounted at the top of the access shaft to aid in exhausting air from the powerhouse. Two separate small systems are also provided. One is a quality air-conditioning unit for the control room and for adjacent second-story rooms. The other is two 8,000-cu-ft-per-min blowers to the bus ducts which discharge at the roof of the access building and control temperature rise in the ducts. Either blower may be the preferred unit with the other as a standby. Battery-room air is exhausted through a transite pipe to the shaft.

Lighting.—Machine-hall lighting is by fixtures suspended from the arched ceiling with supplementary light from wall-bracket fixtures mounted on the crane columns. The vertical panel lights near the main floor level on each

crane column increase intensity and reduce shadows near the floor level. The rest of the plant, except for the control room, has incandescent fixtures. The quality lighting is in the control room where a uniform level of illumination on the vertical surface of the switchboard and high wall reflectance is desired. Large square modul-type fixtures were used with a plastic instead of a glass bottom and with rapid-start lamps for higher lumen output and lower power consumption. A two-section, hollow square pattern is used to accommodate air vent diffusers, maintain distance from switchboard, and proximity to walls.

POWERHOUSE ACCESS

Access Shaft.—The access shaft, Fig. 6(c), is 389 ft long and 18 ft in diameter. The location of the shaft at the centerline of the service and control end of the powerhouse chamber gives minimum length of shaft, minimum length of 13.8-kv bus, and elevator access to all floor levels. One of the exploratory drill holes was at the shaft, and, except for the upper 20 ft, the cores were perfect. The circular shape rather than a more efficient square shaft was used to simplify excavation and to give the most favorable shape for an unlined shaft. The shaft contains the 13.8-kv bus, the 2.5-ton elevator, stairway, control leads, air and water pipes, and serves as the exhaust air duct. Platforms of 8 I 18.4 members every 60 ft are securely anchored to rock. Intermediate platforms at 12-ft spacing are supported by hangers and then rock doweled and welded to give lateral rigidity. The method of hangers was adopted to speed erection. All metal in the shaft is galvanized.

Elevator.—The 2.5-ton capacity for the elevator was governed primarily by construction requirements rather than by operating requirements. The car is 12 ft high by 5 ft 10 in. by 4 ft 6 in. in plan. It can handle the generator pole pieces. Specifications called for a geared-traction, 300-ft-per-min, automatic, self-leveling elevator. Landings are at basement, main, and second floor levels in the powerhouse and at 60-ft intervals in the shaft. The elevator was installed soon after the structural steel in order to be available during construction.

Access Building.—A concrete-block building with steel beams and metal decking roof is located on top of the shaft. The second story houses elevator equipment, communications room, and storage. Communication-room equipment includes a radio to receive daily water-level readings from the unattended Courtright and Wishon storage reservoirs. The elevator hoist is mounted on a rigid structural-steel frame. Beneath the second story is the elevator lobby, change room, and tool room. The single-story part of the building is a service and garage area, 42 ft by 36 ft in plan. An overhead 2½-ton monorail crane can unload trucks to the elevator dolly. There can be several feet of snow at this site and therefore some covered space for working, garage, and warehouse is necessary.

Tailrace Tunnel.—The tailrace tunnel, Fig. 4(f), is slightly larger in width and height than the economic size for hydraulics, in order to provide the additional services of main construction access, heavy maintenance access, emergency personnel access, and ventilation. The tunnel grade and the unit

setting¹¹ were lowered to take advantage of the hydraulics of the wider tunnel and concrete lined invert. The grade is only 1 ft in 1,000 ft.

TAILRACE SETTING AND AFTERBAY

For a Francis turbine, a setting involving no loss of head between plants is possible, but for the impulse turbine some head is lost. The design setting shown in Fig. 4(h) loses very little head. For full load operation and reservoir level at El. 4097, the water surface at the upstream end of the tailrace tunnel will be at El. 4100, 6 ft below the nozzle centerline. In the wheelpits, the surface of the aerated water may be approximately 4 ft below nozzle centerline. The units should operate normally with 2 ft or 3 ft of overpour at the dam. Greater overpour would be infrequent due to the upstream storage reservoirs and to the sluice capacity through the Balch Diversion Dam. The setting is practically the same as if the afterbay were at a controlled level. The surge in the tailrace tunnel from the 1-min load-on time does not control the setting. Provisions have been made to test the operation of both the Haas and Balch vertical-shaft impulse turbines with compressed air in the wheelpit when tail-water is high. It will be of particular value to establish how much air is required and whether such operation is practicable.

The Balch Diversion Dam is a concrete arch dam with an overpour crest for the full 400-ft crest length. It will pass the design flood with a depth of 10 ft which would submerge the runner. The sluice capacity is 1,700 cu ft per sec and is provided to limit overpour that would restrict operation of the Haas Project, and to sluice silt from the reservoir. Crest gates on the dam were considered but not used because of their high cost as compared to the adopted design. Excellent abutment granite permits the overpour crest from abutment to abutment. Some rock anchors and abutment paving was required.

The Balch Diversion Dam, Fig. 7 (to be shown subsequently), was constructed to its initial height in 1927 and has been raised to the ultimate height in 1957 and 1958.¹¹ Two construction seasons were scheduled for several reasons. In 1957, a 60-in.-diameter sluice was installed and the existing dam thickened. This gave the new concrete time to reach equilibrium temperature with the old concrete before raising the dam in the late summer and fall of 1958. The low-flow construction season is only 3 months. The thickening was done with the reservoir empty and all work on Balch Project that requires shutdown of the small existing plant was done in 1957. The existing unit was not shut down in 1958. Completion of the dam will be at approximately the same time as the powerhouse so that a cofferdam for the Haas tailrace tunnel portal is not necessary.

PROJECT CONSTRUCTION

The Haas Project work was awarded on the basis of competitive bidding in six contracts. The contracts were: (a) Wishon Dam, (b) Wishon Reservoir clearing, (c) tunnel, (d) penstock, (e) powerhouse excavation, (f) powerhouse civil work, and (g) powerhouse electrical-mechanical work. Contracts (d) and (f) included the same work for the Balch Project. The six contracts were decided on due to the practical matter of scheduling the engineering, construc-

¹¹ "Thickening and Raising the Balch Concrete Arch Dam," by J. B. Cooke and J. E. Schumann, *Paper R. 187*, Sixth International Congress on Large Dams, September, 1958.

tion and expenditures, rather than a preference for smaller contracts. The main contracts, except for the Wishon clearing and Haas Powerhouse excavation, were completed at the same time although they varied in length from 1 yr to 4 yr. This, of course, is normal practice to keep interest during construction to a minimum. The closeness of the schedule in the last months of construction presented many crises.

Major equipment such as penstocks, valves, structural steel, turbines, generators, and transformers were ordered and purchased by the owner and furnished to the contractor for installation. All such items were usually on order in advance of awarding the construction contracts. Smaller items, where delivery was not a problem, were furnished and installed by the contractor. Purchasing and administration of contracts was done by the owner's purchasing

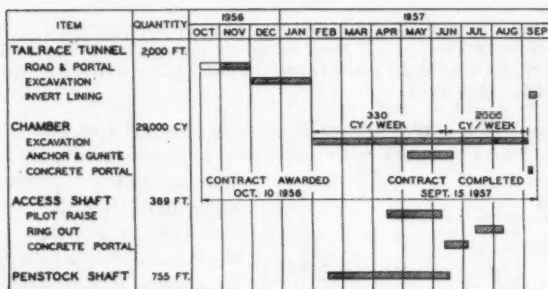


FIG. 7.—HAAS POWER PLANT, EXCAVATION PROGRESS

department, and supervision and inspection of the work was done by the owner's construction department.

DAM AND CONDUIT CONSTRUCTION

Details of construction methods and equipment are well covered and illustrated in the engineering and construction literature^{7,12,13,14,15,16,17} and will only be summarized and supplemented herein. Fig. 8 shows a phase of rockfill-dam construction for Courtright Dam, construction being the same as for Wishon Dam. Power tunnel¹⁵ and surface penstock construction will be reviewed briefly.

Wishon Dam: Quarrying.—Approximately 2,500,000 cu yd of solid rock to provide 3,700,000 cu yd of rockfill were required for the Wishon Dam. The dam is surrounded by exposed massive granite. The specifications required that the spillway be one quarry, and that one or more other (not closer than 200 ft to the dam cutoff) be located to suit the contractor. The spillway floor was made

¹² "Kings River Project—Two Rock-Filled Dams Under Construction in California Sierras," *Pacific Road Building and Eng. Review*, Vol. 84, September, 1956, pp. 8-10.

¹³ "Two Rockfill Dams on Kings River," *Southwest Builder and Contractor*, October, 1956, pp. 16-24.

¹⁴ "Builders Save Millions on Two Faced-Rockfill Dams," by L. L. Wise, *Engineering News-Record*, Vol. 159, August, 1957, pp. 38-44.

¹⁵ "Kings River Construction; Haas Power House, Tunnel—Wishon, Courtright Dams," *The Em-Kayan J10*, August, 1957.

¹⁶ "Efficient Rock Placing Speeds High Dams and Crews Hollow Mountain to Build Underground Power House," *Construction Methods and Equipment*, Vol. 39, September, 1957, pp. 158-162, 166-175.

¹⁷ "The Kings River Project; Latest Methods for Rockfill Dams—Building a Power House Underground," *Western Construction*, Vol. 32, No. 11, November, 1957, pp. 25-37.

essentially level and wide in order that it be a satisfactory quarry. No payment was made for spillway excavation, except as rockfill in the dam. Rockfill was paid for by a specified price of \$0.50 per cu yd (solid) in the quarry plus a bid price per cubic yard in the dam. This price was not intended to fully cover quarry costs. The pricing method was such that both the contractor and owner lost money when material was wasted, which reduced the risk to the contractor and reduced the contingency money in his bid. The specified spillway quarry was permitted to be enlarged on the side away from the dam to suit the contractor. An enlarged spillway quarry on the left abutment and a major quarry near the right abutment were used. The right abutment quarry was developed in two main benches, each 50 ft high.

Dumped Rockfill.—The rockfill is sound, hard, and durable granite. The specifications require

At least 50% by weight of all the rock in the entire dam shall range from $\frac{1}{2}$ to 10 tons and over . . . rock handling equipment shall be of ample capacity and strength to load, transport, and place individual rock to at least 15 tons in weight.

The objective was to strive toward clean large quarried rock and to be able to handle it. Quarry-run rock with essentially no waste was used. Main lifts

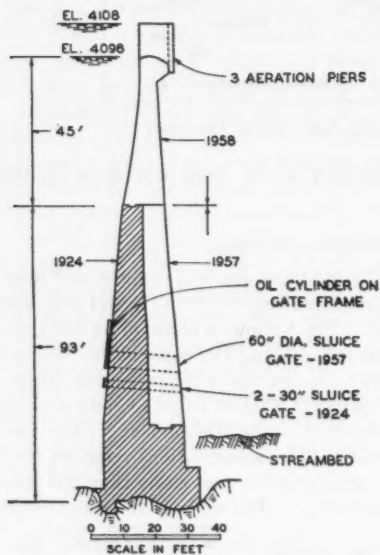


FIG. 8.—BALCH DIVERSION DAM

were higher than the specified 60-ft minimum. Sluicing was specified to be at not less than three times the volume of rock being placed and by nozzles of 2-in. minimum size. The pumping system design was based on a minimum pressure of 100 lb per sq in. at the nozzles, but a minimum pressure of 70 lb per sq in. was permitted. Peak production was at a rate of 16,000 cu yd per day to 18,000 cu yd per day.

Placed Rock.—The design and specifications, and the contractor's well-planned production operation, combined to increase the speed and lower the cost of the placed rock.^{14,15,16,17} Peak production of the Lower Bear River Dam averaged 45 cu yd per crane shift for one month of 670 crane shifts. At Wishon Dam the rate peaks at approximately 200 cu yd per crane shift and averages 135 cu yd.

Design changes following construction of the Bear River Dam were (a) use of face lifts, (b) elimination of keyways, and (c) placed-rock specifications that are easier to comply with. Face lifts were small lifts approximately 30 ft high with a 40-ft road width on top.

The upstream face of the main lifts was kept back approximately 40 ft to leave space for the face lifts that provided access to the placed rock and concrete. The placed rock is of large size, 5 tons to 15 tons, on both dams, as shown in Fig. 9.

Concrete Face.—The concrete face was placed by buckets handled from a crane on the face lift. A slip form pulled itself up the face by electrically-operated winches on the slip form. It was moved by cranes operating on the face lift. The face lift and slip form combination made a straightforward job. Aggregate was produced from pit-run material located in the reservoir site. The presence of many cobbles and little $\frac{1}{4}$ in. to $1\frac{1}{2}$ in. material made crushing



FIG. 9.—COURTRIGHT DAM: PLACED ROCK, JOINT RIBS, AND CONCRETE FACE SLABS

necessary. Because of the friable nature of the aggregate, it was furnished in four sizes rather than in three sizes, and was rescreened at the batch plant to assure grading that would result in a dense frost-resistant concrete. The 3,000-lb-per-sq-in., air-entrained concrete contained a water reducing agent, pozzolan and type II cement.

Power Tunnel.—The 32,850-ft long tunnel was driven from one adit on two headings: 19,560 ft upstream, and 12,830 ft downstream. The first 2,800 ft in each direction from the adit was driven by alternate headings at an average rate of 90 ft per day, for one crew on each of three shifts, until daily progress dropped to the required minimum schedule of 1000 ft per month (40 ft per day) in the long upstream heading. The overall average rate of driving was 57 ft

per day, including the slower alternate heading driving. Maximum single heading progress was 70 to 75 ft per day and monthly averages in the latter half of the job were 65 to 70 ft per day. The average overbreak was 21.9% which is equivalent to an overbreak of 0.71 ft all around the 13-ft horseshoe design section. The tunnel is 97% unlined with 14 short pieces of concrete or gunite lining of 10 to 150-ft length totaling 1,020 ft in faulted, soft seam and fractured zones that required support. Concrete lining was used in supported zones of soft and fractured material. Gunite was used wherever considered suitable since the larger cross-section is associated with smaller transition losses. Also, gunite was used on occasional seams that might otherwise erode and cause rockfalls. An accurate leakage test on the completed $6\frac{1}{4}$ mile tunnel indicated a loss of 0.6 cu ft per sec.

Surge Chamber.—The 300-ft-long by 12-ft-diameter shaft was excavated from the top and bottom. Drill holes indicated that the upper 150 ft was in poor granite and it was considered safer to excavate down rather than up. It was in fractured and soft-grained granite and was concrete-lined. The procedure was to excavate 10 ft and then line it. The bottom 150 ft was driven as a raise from a steel cage suspended from a cable in a 6-in. drill hole. A 4-in. gunite lining with 4-in.-by-4-in.-by-6-by-6 mesh was used. The galleries at the base of the surge shaft, Fig. 4(g), were unlined.

Surface Penstock.—Approximately one-third of the way up the penstock, a road crosses the penstock. An old gantry was set across the road to transfer the 40-ft-long, 12-ton-to-40-ton sections from truck to the tram cars. Two separate cars with saddles, and connected by cable, made it possible to negotiate the vertical and horizontal curves. Below the road the tramway was on the penstock centerline and installation proceeded from the bottom of the shaft to the road. Above the road the tram paralleled the penstock, sections were rolled and skidded over to the penstock line, and erection began at several anchors. The expansion joint travel was made such that the expansion joint below an anchor could be rolled in place and expanded into the line as a closure section. The first pours of piers and anchors were made in advance of pipe erection. In several zones of several hundred feet each, the foundation material was undisturbed, decomposed granite. It was good foundation material but subject to weathering and erosion. In such areas, the penstock trench and 4 ft up each side was protected by 2-in. gunite with 4-in.-by-4-in.-by-8-by-8 mesh, applied to the irregular excavated surface without trimming. Drainage was taken away from the penstock as frequently as the topography and penstock cuts permitted.

UNDERGROUND PLANT EXCAVATION

General.—The power plant excavation contract, Fig. 9, included tailrace tunnel, powerhouse chamber, access shaft, and penstock shaft. The contract was completed on Sept. 15, 1957, and work on the civil contract began on the same day, which left 1 yr and 2 months for powerplant construction. All the excavation was uneventful in that practically no support was required and no water was encountered. Fig. 7 is a record of the excavation progress, and

Fig. 10 illustrates the excavation methods. Details of the excavation have been covered elsewhere^{15,16,17,18,19} and will only be summarized and supplemented herein.

The excavation contract included some concrete work considered essential to turn the job over to the next contractor in safe condition and with unrestricted access. A concrete collar with an 18-ft inside diameter was installed at the top of the access shaft to a depth of 20 ft to cover the surface zone of fractured and weathered rock. A 10-ft long portal, of tailrace tunnel inside dimensions, at the wall of the powerhouse was installed as its later forming would interfere with access. The pouring of the tailrace tunnel invert was also included.

The first step in the excavation contract was to complete the tailrace tunnel in order to gain access to the powerhouse and to the shaft excavations. A small chamber was excavated, from which work was begun simultaneously on the penstock tunnel and shaft, two 8-ft-by-8-ft raises to the crown of the chamber, and a 5-ft-by-10-ft, 51° raise to the base of the access shaft, Fig. 10. As indicated by Fig. 7, the excavations proceeded together with the chamber excavation determining the completion date.

Tailrace Tunnel.—Excavation.—The 2,000-ft long, 15-ft-by-18-ft tailrace tunnel was driven in fifty-eight working days at an average rate of 34 ft per working day, which includes one and two-shift days. For three-shift driving, the average was 47-ft with maximum days of 55 ft to 60 ft per day. Excavation was by rubber-tired diesel equipment.^{18,19} Four 40-ft long passing areas were constructed, each giving a total width of 20 ft for passing instead of the tunnel's 15-ft width. No support was required and no water was encountered.

Invert lining.—Upon completion of the chamber excavation, it was necessary to pour the 2,000-ft length of invert rapidly to give the powerhouse contractor access to the job. The pour was made in 40 hours. The muck was removed down to rock points by equipment. A profile was taken and a grade established to give a 5-in. minimum slab that was at a variable slope between horizontal and design grade. This departure from design grade gave maximum hydraulic section and minimum concrete. The invert concrete is a plain slab with no gutters or curbs, Fig. 4(f).

Powerhouse Chamber.—The size of the initial working chamber, 25 ft by 70 ft in plan and 23 ft high, was governed by the wheel pit and sump area being at tailrace grade and by the top of the penstock tunnel, Figs. 6 and 10. Two 8-ft-by-8-ft raises were driven to the crown and an 8-ft-by-20-ft crown drift was driven the full 173-ft length of the powerhouse. In order not to interfere with the access-shaft excavation, the excavation of the arch, rock anchoring, and guniting (construction steps 3, 4, and 5 of Fig. 10) were started at the opposite end. The rock anchor and gunite work, step 5, was carried out from pipe scaffolding on floor El. 4164.5. Scaffolding was moved as work progressed toward the access-shaft end of the powerhouse. The work was well organized and the 2,000 anchors and 13,000 sq ft of gunite were completed in six weeks

¹⁵ "Haas Underground Powerhouse," *Pacific Road Builder and Eng. Review*, Vol. 88, June, 1957, pp. 25-33.

¹⁹ "P. G. and E. Goes Underground for Power," by L. L. Wise, *Engineering News-Record*, Vol. 159, September, 1957, p. 51.

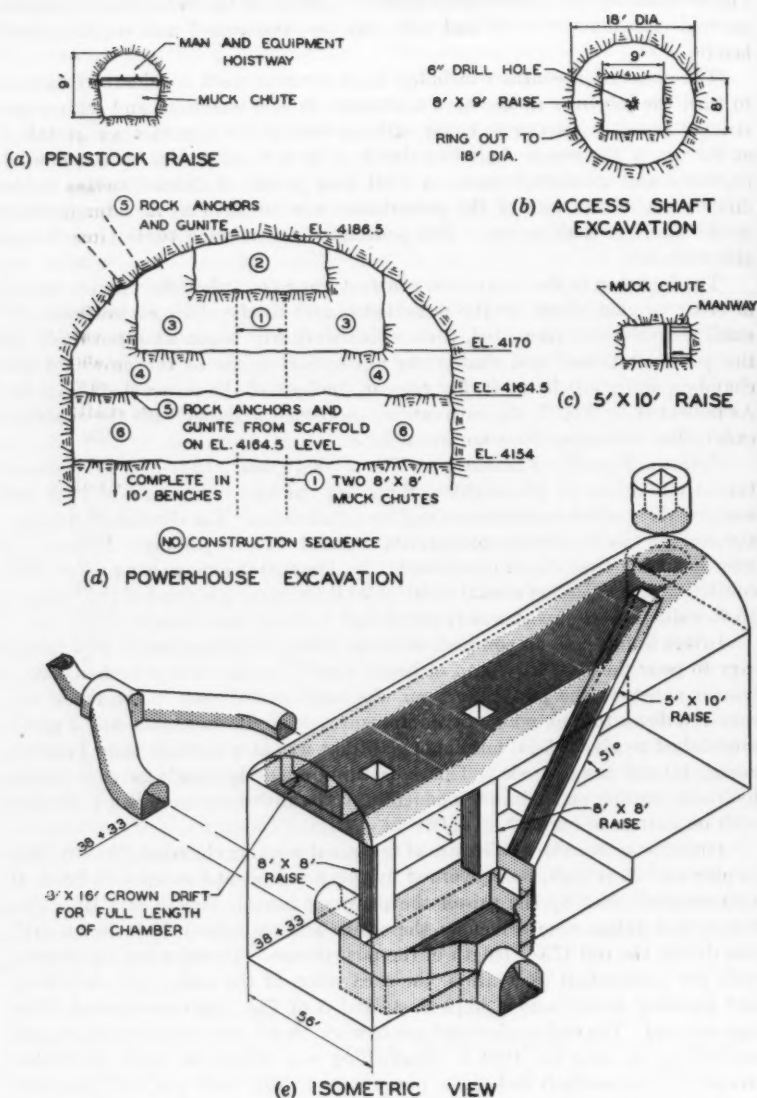


FIG. 10.—HAAS POWERHOUSE EXCAVATION

along with some remaining step 3 and 5 excavation (Fig. 10). After the arch was completed, the excavation proceeded rapidly, Fig. 7, at an average of 2,000 cu yd per six-day week with daily production varying between 200 cu yd per day and 1,100 cu yd per day. The main excavation was carried out in irregular benches approximately 10 ft or more in height. Muck was brought to the chutes by a slusher, which is a "bucket" operated by cables between a



FIG. 11.—HAAS POWERHOUSE EXCAVATION COMPLETED

dead-man anchor and a compressed air hoist. The excavation between the two 8-ft square chutes was completed first in order not to interfere with the access-shaft excavation. Only a few rock anchors were used other than the pattern arbitrarily established for the roof.

No water was encountered but there were several damp spots on one wall and at each end. The moist seams were drilled to drain them and minimize dampness, but no curtain walls were used. The rock temperature was a very

favorable 58° F when the tailrace tunnel reached the chamber in Feb., 1957. It has increased about 0.5° per month due to the warm ventilating air, and in Sept., 1957, it was 62° F. Fig. 11 shows the chamber with structural steel and cranes installed. The powerhouse walls remained unlined and there has been no incident of a spalling rock in the first two years of service.

Access Shaft.—The access-shaft excavation, Fig. 10, began with a 6-in.-diameter hole. An 8-ft-by-9-ft raise was driven using a cable-supported steel cage. The cage was pulled under the chamber arch and the cable was raised in the 6-in. hole when a round was to be shot. The 18-ft diameter was then ringed out from the top down. The top 20 ft of the shaft was in weathered rock and was excavated from the surface bench and concreted before ringing out the 18-ft unlined shaft, which is in excellent and dry rock. The concreted rock carried water and the formation was grouted. All the rest of the shaft remained unlined.

The 389 ft of 8-ft-by-9 ft raise was driven in twenty-five working days at 16 ft per day. Progress increased from 8 ft to 15 ft initially, to 20 ft to 25 ft per day near completion. Ringing out took twenty-three days at an average of 17 ft per day.

Penstock Shaft.—After 635 ft of the 760-ft shaft was raised, fractures and then soft-grained granite was encountered. The remaining 125 ft was driven from the surface bench downward and required timber support for safety. The poor rock extended lower than anticipated and the penstock design was changed to begin the increase in free pipe stresses where seamless granite began (Fig. 5).

Men and supplies were brought to the raise heading by a small car in the manway (Fig. 10). The car was pulled by a tugger hoist located in the 9-ft penstock-branch excavation. The muck was moved by rail through the 12-ft branch excavation and dumped into the chamber. The branch pipes are only 4 ft 7½ in. outside diameter, but the 12-ft size tunnel is necessary to install the two 82-in. diameter bend pipes and the wye.

The raise was driven in 113 days at an average rate of 7 ft per day with days varying from 5 ft to 10 ft depending on whether one or two rounds were pulled.

CONCLUSIONS

An appreciable economy in the use of rockfill dams and unlined tunnels has been obtained in a number of previous projects. In the Haas Project, the rockfill dam design has used experience to provide a more simple and lower cost dam without changing its high degree of safety. The underground intake valve, gallery-simple-differential surge chamber, and storage rock trap combine with the unlined tunnel to provide a simple and economical conduit. It is believed that the combined work of designers and contractors can further reduce the cost of concrete-faced rockfill dams. In the case of unlined tunnels, further economies largely rest with the contractors.

The Haas Powerhouse is the largest of three underground hydroelectric powerhouses in the United States.⁴ The other two are Snoqualmie Falls on the Snoqualmie River near Seattle, Washington (1899) and Spaulding No. 1, on

the South Fork of the Yuba River near Sacramento, Calif. (1917). The combination of very high head, flat penstock profile near the river, and excellent rock provided the conditions that made the Haas Project underground layout attractive. Because the major contingency item, excavation, was completed without delay or mishap the underground scheme at Haas is, in fact, substantially more economical than the surface scheme.

ACKNOWLEDGMENTS

The owner and operator of the Haas Power Project is the Pacific Gas and Electric Company of San Francisco, Calif.

Engineering was under the direction of Walter Dreyer, M. ASCE, Henry V. Lutge, M. ASCE, and William R. Johnson. I. Cleveland Steele, M. ASCE, was consulting engineer on the dams.

The writer is indebted to J. E. Schumann, Arthur G. Strassburger, J. M. ASCE, and others who have been engaged in the engineering studies and design for the Kings Development.

Construction was under the direction of Arthur J. Swank, vice president in charge of general construction, and H. W. Haberkorn, manager of hydroelectric construction. Joe Pirtz, A. M. ASCE, is project superintendent and George Thacher, A. M. ASCE, project engineer.

The major civil engineering contracts of dam, tunnel, and power house excavation are sponsored by Morrison-Knudsen Company, represented by Jim Wells. Burt L. Perkins, Whitey Lee, and Carl Larsen are project managers, and John F. Erdle, A. M. ASCE, is project engineer.

DISCUSSION

F. L. LAWTON,²⁰ M. ASCE.—A most comprehensive and interesting study has been presented of the first large underground hydroelectric plant in the United States and the associated elements of the development—notably the Wishon Dam, the outlet, and power intake.

It is noted that the steel trash rack at the intake tower is galvanized. This appears to be somewhat unusual in North American practice and it would be useful to know the relative life as compared with ordinary steel provided with more customary forms of underwater corrosion protection. Also of interest would be the pH-value of the water from the Wishon reservoir.

It is noted that the intake tower provides for the oil cylinders that operate the two 4-ft-by-5-ft slide gates to be located approximately 30 ft below the full reservoir level. Has such an arrangement proved to be free from trouble due to corrosion?

The comprehensive experience of the operator with unlined tunnels, where rock conditions permit, adds significance to the statement under the heading, "Dam and Conduit Design: Power Tunnel: Unlined Section,"

"Rock falls in early tunnels were due to not plugging soft seams so that water would wash out the seams and cause large blocks of rock to fall in the tunnel. No rock falls have occurred in tunnels constructed since 1947 where proper 'dental work' has been done during construction."

The reference to proper "dental work" is a recognition of the fact that relatively unsuitable rock can be fully utilized, in short sections, without the necessity of costly lining if it is correctly treated. A full knowledge of rock mechanics is essential to secure the best results from structures involved in underground power developments, not only including pressure tunnels.

Mr. Cooke's statement of the operator's experience and evaluation of the significance of an unlined invert is particularly valuable. This indicates the importance which should be attached to a proper evaluation of the economic significance of lining, whether the invert only or the entire periphery of the tunnel. It would be of interest to know of determinations of n -values for unlined tunnels with and without a paved invert.

Apparently, the author has found under the heading "Dam and Conduit Design: Power Tunnel: Storage Sand Trap," that

"* * * surface muck, with a dimension of as much as 2 in. travels down the tunnel invert during the first year of operation. The larger-sized muck then retains the remaining small material reducing the content of sand or gravel after the first year."

Is this material only that arising from the scouring action of a 5-ft-per-sec tunnel velocity on the material left in the invert?

It was noted (under the heading "Dam and Conduit Design: Underground Penstock") that "Cracks several feet long and several inches deep occurred in

²⁰ Chf. Engr., Power Dept., Aluminium Labs., Ltd., Montreal, Canada.

the 4-in. plate adjacent to the weld" in the Haas wye and, by implication, inferred that this was due to a very tight schedule and the actual welding program. It is suggested that a sketch or other illustration indicating the location of the cracks be included by Mr. Cooke as it appears that cracks of one type or another have occurred in many large wyes fabricated in North America.

The thorough-going nature of the economic studies that led to the decision to construct the Haas Power Project as an underground scheme is thoroughly demonstrated by the realistic statements concerning economics. The generally excellent granite formation obviously played a substantial part in the net direct capital saving of \$400,000 shown for the underground scheme. In this connection the observation (under the heading "Underground Plant Design: Basic Decisions") that

"* * * the cost and possible contingency in the excavations was a major factor of uncertainty in an underground power plant. The main criterion in selecting a layout was to have minimum excavation"

is particularly significant. It should be repeated every time this type of plant is under consideration. Further, excavation in such a manner as to minimize damage to rock intended to serve a structural purpose can result in material savings, in eliminating "dental work" otherwise necessary.

The rock-bolted and gunited arch for the powerhouse is in line with a practice adopted in some cases in Sweden. The rather elaborate method of applying the rock anchors would appear more expensive than the use of the split rock anchor and wedge where the friction developed between the split end and the rock periphery of the hole is depended on to develop the strength of the anchor.

J. BARRY COOKE,²¹ M. ASCE.—A number of important features have been emphasized by Mr. Lawton and some questions have been raised.

Galvanizing has been used extensively for ladders, transmission towers, and other structures exposed to the weather. The life of the coating is of long and indefinite length. However, the use of galvanizing underwater is satisfactory in some watersheds and not in others. On the Mokelumne River in California, galvanized steel installed on various structures in 1931 is now (1959) badly corroded underwater and in perfect condition where only exposed to the weather. On the Kings River, a galvanized trash rack installed in 1927 is now only partly tuberculated and it was decided to galvanize the new underwater trash racks on that river. Unless there was experience to show underwater galvanizing to be satisfactory, it would seem wise to use some other protective coating.

A number of submerged oil cylinder gate operators have been used by the operating company in the past 10 yrs. The piston shaft is, of course, of stainless steel, and there have been no corrosion problems to date. Where the cylinder may not be used for many years, the packing-gland end of the cylinder and the stainless steel shaft have been packed in grease and wrapped with burlap.

It is felt that comparisons of n -values between tunnels with and without lined inverts cannot reasonably be made on the basis of measured head losses

²¹ Superv. Civ. Engr., Pacific Gas and Electric Co., San Francisco, Calif.

of different tunnels, because of the variation in overbreak and roughness of the rock. It is believed that a theoretical analysis, such as made for the Haas Power Project, is necessary even though head losses for unlined tunnels with and without lined inverts are available.

The capacity of the storage sand trap is based on an estimate that the 5-ft-per-sec velocity on the design area will not move more than the top 2.2 in. of the 12-in.-to-15-in. depth of muck. The largest material moved is estimated to be less than 2 in. and close to 1½ in. in dimension. The difference in size and amount of material moved from an unmucked invert varies greatly between velocities of 4.0 ft per sec to 6.5 ft per sec.

Cracks similar to those which occurred at the wye-branch have also occurred on the C-clamps of many other wye-branches. The cracks on the Haas wye were more extensive due to the welding sequence required by the delivery schedule. Where the pant-leg is welded to the side of the C-clamp, tension due to shrinkage from the welding occurs across the C-clamp plate. The tensile strength across the thick C-clamp plate is sometimes inadequate to resist the stresses, and cracks in the plane of the laminations of the rolled C-clamp plate occur. One method of avoiding this is to make the intersection of C-clamp and pant-legs without welding the pant-legs to the side of the C-clamp, but to a forged round member. This would avoid the poor detail of taking stresses across the plane of rolling the C-clamp plate at the cost of more welding.

The method used for the roof bolting was adopted on the basis of its being a very satisfactory and minimum cost method of obtaining a fully grouted overhead anchor. It costs a little more than an ungrouted split-wedge rock anchor, but definitely less than grouted overhead split-wedge rock anchors, and grouting was considered to be required to prevent corrosion and assure permanence. The rock was of such quality that tensioning of the anchors was not necessary. The method is adaptable to simple production work and the anchors went in very rapidly.

AMERICAN SOCIETY OF CIVIL ENGINEERS

Founded November 5, 1852

TRANSACTIONS

Paper No. 3009

FLOW EQUATIONS FOR NATURAL GAS PIPELINES

BY RICHARD F. BUKACEK¹

WITH DISCUSSION BY MESSRS. JAMES H. DOROUGH; WILLIAM T. IVEY;
JOHN F. SCHOMAKER; AND RICHARD F. BUKACEK

SYNOPSIS

The flow equations used by the natural gas transmission industry are examined in relation to their application. The factors determining resistance to flow are related to the operating conditions of natural gas pipelines to show the limitations inherent in any practical flow equation.

INTRODUCTION

To obtain a proper perspective on the flow equations for the natural gas transmission industry it is necessary to distinguish among their three principal applications: (a) Design of pipelines for capacity; (b) pipeline operations study; and (c) pipeline capacity testing.

PRINCIPAL APPLICATIONS

Design of Pipelines for Capacity.—The problem of designing pipelines for capacity involves a multitude of economic factors. However, this examination is limited to the question of the equations which relate operating conditions and pipeline dimensions to capacity. In combination with other factors, a flow equation is used to determine the diameter and wall thickness of pipe, and the spacing and horsepower requirements of compressor stations. The capacity basis for design is an estimate of future requirements. This uncertainty in design basis makes the absolute accuracy of the flow equation used less significant. In general it would be desirable that the flow equation yield conservative results so that a margin of safety in operation would be obtained.

NOTE.—Published, essentially as printed here, in the Journal of the Pipeline Division, in June, 1958, as *Proceedings Paper 1667*. Positions and titles given are those in effect when the paper or discussion was approved for publication in *Transactions*.

¹ Instructor, Chem. Eng. Dept., Illinois Inst. of Technology, Chicago, Ill.

The practice in the design of pipelines has been to make use of one of the various equations and then correct its prediction at given operating conditions with an experience factor, generally called pipeline efficiency. The numerical value of the pipeline efficiency chosen as a design base thus depends on three factors: (a) The particular flow equation chosen; (b) the terms included in the equation (for example, the compressibility factor is often omitted); and (c) experience in applying the equation to past operations. For large diameter lines (20-in. diameter and larger) under design conditions of high throughput, experience among pipeline designers has been rather consistent. The three flow equations most widely used for design purposes are:

The Weymouth,

$$Q_b = 433.5 \left(\frac{T_b}{P_b} \right) D^{8/3} \left(\frac{P_1^2 - P_2^2}{G T L} \right)^{0.5} \dots \dots \dots (1)$$

the Panhandle A,

$$Q_b = 435.7 \left(\frac{T_b}{P_b} \right)^{1.0788} D^{2.6182} \left(\frac{P_1^2 - P_2^2}{G^{0.8539} T L} \right)^{0.5392} \dots \dots \dots (2)$$

and the New Panhandle

$$Q_b = 737 \left(\frac{T_b}{P_b} \right)^{1.02} D^{2.53} \left(\frac{P_1^2 - P_2^2}{G^{0.961} T L Z} \right)^{0.51} \dots \dots \dots (3)$$

in which Q_b is the gas flow rate in million standard cu ft per day; T represents the average temperature of the gas in the pipeline section, in degrees Rankine, and T_b denotes the base temperature in degrees Rankine which defines the standard conditions. P_1 and P_2 are the pressures in pounds per square inch absolute at the upstream and downstream ends of the pipeline section; and P_b is the base pressure in pounds per square inch absolute which defines the standard conditions. The term D is the pipe section internal diameter, in inches; G represents the specific gravity of the gas relative to air; L is the pipeline section length, in miles; and Z denotes the average supercompressibility factor of the gas in the pipeline section. The design efficiencies for these equations are usually assigned the following values; for the Weymouth, 110%; for the Panhandle, 92%; for the New Panhandle, 90%. Note that Eq. 1 and Eq. 2 do not include the compressibility factor Z .

For purposes of design Eqs. 1, 2, and 3 yield similar results, at least for certain ranges of flow rate and pipe size. In Fig. 1 the flow rates given by the Panhandle A and New Panhandle equations are shown relative to those given by the Weymouth equation. A compressibility factor of 0.9 was used with the New Panhandle equation.

Fig. 1 indicates that the Weymouth and New Panhandle equations are in agreement for pipeline sizes whose diameters are more than 20 in., but do not agree closely for smaller diameters. The Panhandle A equation is in close agreement only over the range of flows which corresponds to ordinary design

conditions. In general, the three flow equations with the design bases given agree within $\pm 4\%$ over the range of ordinary design flow rates for the pipe sizes larger than 20 in. Because design flow rates are usually estimates of future requirements, there is little basis for distinguishing among the equations at higher rates of flow for the larger sizes of pipe.

Pipeline Operations Study.—Pipeline flow equations are used also to study the behavior of a pipeline system under various operating conditions. Whenever interruptible customers are spaced along the pipeline it is desirable to determine the most economical way of curtailing these customers, given the conditions that determine pipeline drawoff by noninterruptible customers. Another example is the determination of the system capacity given the compressor station outage or similar contingency. Eqs. 1, 2, and 3 are equally

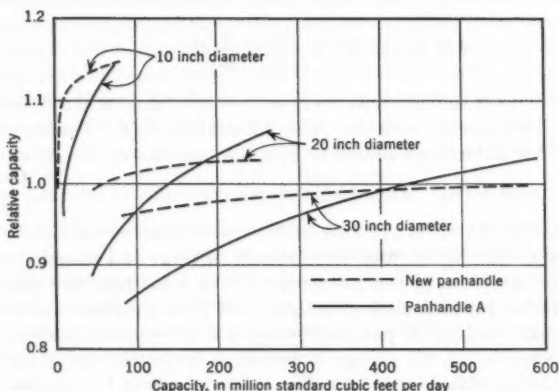


FIG. 1.—COMPARISON OF NEW PANHANDLE AND PANHANDLE A WITH WEYMOUTH DESIGN BASIS

useful for studies of this type, which are necessarily based on estimated system loads.

Pipeline Capacity Testing.—Fig. 1 indicates that the equation selected for use in pipeline capacity testing has a more significant bearing on the results than it does in the case of design for capacity. This is true because pipeline throughput is not maintained at the design capacity but varies depending on the character of the system's sales. Fig. 1 shows that the agreement among the equations is not uniform throughout the range of flow rates common to pipeline operation. For example, Fig. 1 shows exact agreement for a 30-in.-diameter pipe between the Panhandle A and Weymouth predictions of flow rate at 425 million standard cu ft per day (MMcfd), but 7.5% difference in prediction at 200 MMcfd. Assuming the Weymouth efficiency to be correct throughout the range, the Panhandle A equation would show an efficiency at 200 MMcfd of approximately 100% rather than the 92% used as a basis for design. In practice the significance of efficiency test results depends on the

flow equation used, and a change in efficiency may be due to the flow equation used rather than a change in pipe conditions.

Fig. 1 also shows that the different equations are inconsistent with regard to the effect of pipeline diameter. In particular, the agreement among the equations is much less marked for small diameter lines than for larger sizes. Thus the meaning of efficiency test results is dependent on pipe diameter as well as the flow rate and the equation used.

RESISTANCE COEFFICIENT

The Flow Equations and the Resistance Coefficient.—To clarify the differences between flow equations, it is necessary to remember that they arise from consideration of the balance of energy across a pipeline section operating at a steady-state condition. This balance may be written in differential form:

$$dE + d(PV) + \frac{dv^2}{2g_c} + \frac{g}{g_c} dh = q - W_s \dots \dots \dots (4)$$

in which E denotes the internal energy per pound of fluid and PV is the product of pressure and specific volume. The differential of (PV) represents the net work involved in forcing a pound of fluid into and out of the incremental pipeline section considered. The kinetic energy per pound of fluid is $\frac{V^2}{2g_c}$; g denotes the acceleration of gravity; g_c represents a dimensional conversion factor for the engineering system which uses both pounds of force and pounds of mass; h is equal to the elevation of the gas stream above some reference plane; q is the heat transferred per unit mass of the gas; and W_s is the shaft work done by the gas on the surroundings in passing through the incremental section considered.

The change in kinetic energy is negligible under the operating conditions of natural gas pipelines. Additionally, it is convenient to consider W_s and dh to be zero. Thus, the pipeline is assumed to be horizontal—no shaft work is done on or by the gas in passing through the section. The resulting equation,

$$dE + d(PV) = q \dots \dots \dots (5)$$

is correct within the limitations imposed. However, Eq. 5 yields no information about the effect of line length or pipe diameter on pressure drop. To obtain this relationship it is necessary to introduce the additional concepts of friction and resistance coefficient. If friction is considered a form of energy transformation corresponding to the nonideal behavior of the system, one can conveniently write

$$dE = q - P dV + F \dots \dots \dots (6)$$

in which F is a term representing an energy transformation not accounted for in the heat transfer or $P dV$ term. Combining Eq. 5 and Eq. 6 results in

$$V dP + F = 0 \dots \dots \dots (7)$$

Having introduced the concept of friction, its correlation with the variables of line length and diameter must be considered. This is conventionally ac-

complished through the resistance coefficient, f , as follows:

$$F = 4f \left(\frac{V^2}{2g_c} \right) \frac{dL}{D} \dots \dots \dots (8)$$

This form is the simplest way to introduce the variables of flow rate, length, L , and diameter, D , in a dimensionally consistent way. Combining Eq. 7 and Eq. 8 results in an equation, which when integrated is the basic flow equation.

$$Q_b = K \frac{T_b}{P_b} D^{2.5} \left(\frac{P_1^2 - P_2^2}{G T L Z f} \right)^{0.5} \dots \dots \dots (9)$$

The problem of determining the values to be assigned to the resistance coefficient remains to be resolved.

From the definition there is no obvious way to determine the behavior of the resistance coefficient except by the analysis of experimental data. Dimensional analysis shows that the Reynolds number may be a correlating parameter, but does not tell what relationship exists between the resistance coefficient and the Reynolds number. Similarly, if it is supposed that conduit surface characteristics may be important, the dimensionless group, k/D , may be a correlating parameter in which k is the effective height of surface irregularities. However, there is no substitute for an experimental study of the resistance coefficient.

Experimentally three stable types of behavior for the resistance coefficient have been found as well as two regions of transition that lie between the patterns for stable behavior. At small values of the Reynolds number, R (below approximately 2,000), a type of flow called streamline is found in which $f = 16/R$. As Reynolds numbers increase beyond 2,000, a transition region is encountered which is followed by a stable regime where resistance coefficients can be approximated by the form $f = a R^b$. This is the region where turbulent conditions exist in the vicinity of the center of the pipeline but a condition of streamline flow persists near the conduit walls. In this region the flow pattern is equivalent to that in perfectly smooth pipes. The thickness of this boundary layer in streamline flow decreases as the Reynolds number increases until turbulence introduced at the irregularities on the conduit surface render impossible its further existence. At the state of complete turbulence the resistance coefficient no longer depends on the Reynolds number.

The transition between smooth pipe behavior and complete turbulence depends on conduit surface roughness in a complex way. The beginning of the transition occurs when appreciable turbulence is induced in the boundary layer at the largest roughness elements on the conduit wall. The development of additional turbulence depends on the size, shape, and placement of the surface roughness elements. It follows that this transition region will not be the same for different conduit surfaces, and no two commercial pipes can be expected to have the same transition behavior. This is demonstrated in Fig. 2, taken from the report of R. V. Smith et al.² In Fig. 2, k is the effective height of surface roughness elements and r is the radius of the pipe.

² "Flow of Natural Gas Through Experimental Pipe Lines and Transmission Lines," by R. V. Smith, J. S. Miller, and J. W. Ferguson, *Monograph 9*, Bureau of Mines, U. S. Dept. of the Interior, Washington, D. C., 1956.

These types of resistance-coefficient behavior have been established by the work of many investigators. Outstanding among them is J. Nikuradse³ whose experimental work on pipes coated with uniformly sized sand grains was the first to demonstrate convincingly the existence of the region controlled by surface conditions. Nikuradse's work has been confirmed by Smith² whose experimental data on commercial pipe has extended the range of Reynolds numbers investigated to 11×10^6 . The experiments were done with pipes, the diameters of which ranged from 2 in. to 8 in. Investigations covering large diameter natural gas pipelines⁴ by the Institute of Gas Technology, confirm also the basic pattern of resistance-coefficient behavior outlined above.

Natural Gas Pipelines and the Resistance Coefficient.—Given the previous description of resistance-coefficient behavior, it is necessary to arrange these facts in the perspective of natural gas pipeline problems. The first important

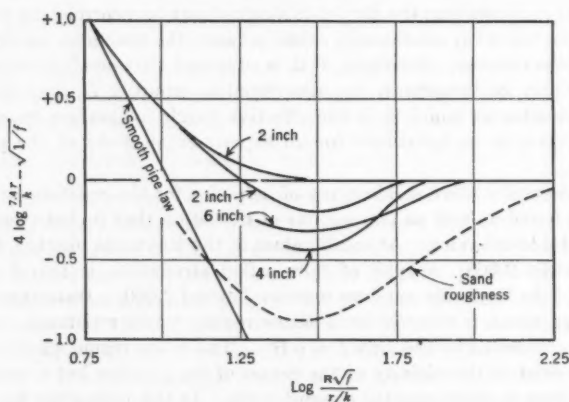


FIG. 2.—TRANSITION REGION

observation is that the viscosity of natural gases is small. Therefore, the Reynolds numbers characteristic of natural gas pipeline operation are very large. It is unlikely that there will be a practical natural gas pipeline operation where streamline flow might be involved. The Reynolds numbers are so large, in fact, that for high-pressure pipelines with diameters greater than 10 in., only the extremely small flow rates even approach the region in which the resistance coefficients depend greatly on Reynolds number. For example, in order to achieve a Reynolds number of 10^6 in a 12-in. line, the flow rate must be 10 MMcfd. This is a low rate for this size line in high-pressure natural gas service. For a 30-in. line, the flow rate to achieve a Reynolds number of 10^6 is 26 MMcfd, which is small for this size of line. Therefore, flow equations based on an expression for a resistance coefficient showing little or no de-

³ "Stromungsgesetze in Rauhen Röhren," by J. Nikuradse, *Forschungsheft, Verein Deutscher Ingenieure*, No. 361, 1933.

⁴ Soon to be published.

pendence on Reynolds number correspond to the operating conditions for large diameter high-pressure natural gas pipelines.

The coefficient used in the Weymouth equation (Eq. 1) is $f = 0.008/D^5$. Because this expression shows no dependence on Reynolds number it agrees with the findings of Nikuradse and Smith for the range of high Reynolds numbers. The Panhandle A equation (Eq. 2) is based on a friction factor of the form $f = a R^b$. Reference to Fig. 1 shows that this leads to substantial deviations from the realities of pipeline operation. The new Panhandle equation (Eq. 3) is also based on the form $f = a R^b$, and inspection of Fig. 1 indicates that the dependence of f on the Reynolds number for the larger sizes of pipe is small in the ordinary range of flow rates. To rephrase the foregoing observations: It would be expected that pipeline efficiencies based on the Weymouth or New Panhandle equations would depend to a small extent on the rate of flow chosen for the test, whereas efficiencies determined from the Panhandle A Equation would decrease with increasing flow rate. Again, considering the range of flow rates corresponding to commercial operation of large diameter high-pressure pipelines, the use of the Weymouth or New Panhandle equations will be more consistent with the known behavior of pipelines than will the use of the Panhandle A equation.

Another consideration is the fact that in the range of flow rates common to large diameter high-pressure pipelines, the resistance coefficient is controlled by conduit surface conditions. Pipeline interior surfaces are not uniform and depend on the extent of corrosion, the method of pipe manufacture, and the accumulation of foreign materials (both solid and liquid) on the surfaces. Thus, it is clear that the resistance coefficient which characterizes a section of pipeline can change with time. Immediately following construction, pipe surface condition will depend on such factors as the length of pipe storage time above the ditch and the extent to which construction dirt has been removed. Once in operation the surface condition will be modified by factors such as the water and hydrocarbon wetness of the gas, and the possibility of processing fluids and solids being dumped into the gas. Consequently, each pipeline section has its own peculiar surface condition determined by its past history. It is not reasonably possible for a flow equation to be devised so as to contain the variables necessary to describe the effect on resistance coefficient of pipe section past history. What can be devised is, at best, a flow equation that will (1) take into account the fact of surface control over resistance coefficient, and (2) contain an experience factor or efficiency which does not depend on pipe diameter or flow rate.

Fortunately, the internal surfaces of natural gas pipelines are not as variable as they might be. Current pipe manufacturing methods do not result in grossly different base metal surfaces. Pipe cleaning practices following construction are fairly standard, and practices in connection with gas conditioning are rather uniform. Once the pipe is in the ground interior corrosion is generally not a problem. The net result is that in practice pipe wall conditions vary only narrowly, except where the possibilities of accidental dumping of processing fluids and solids are frequent. Thus, there is a practical upper limit to the degree of smoothness possible in a pipeline. Also, there is an effective

roughness that characterizes the general run of pipelines but is not too greatly different from the practical extremes of commercial smoothness and roughness. This is shown by Smith's data,² who recommended that for the range of high

Reynolds numbers the Nikuradse Rough Pipe Law $\left(\sqrt{1/f} = 4 \log \frac{3.7 D}{k}\right)$, with the value $k = 0.0007$, could represent the average pipeline surface condition. It is also confirmed by the data of Ivey and Dorough.⁵ Therefore, it should be possible to devise an equation characterizing the commercially smoothest pipe to which an efficiency (or experience factor) with a value approaching unity can be applied for particular pipelines, or for design purposes.

CONCLUSIONS

In some applications, the data required for use in the flow equations are so inexact that there is no real basis for distinguishing among the usual flow equations on the basis of their accuracy. This is not the case for pipeline capacity test data. Because the different equations do not agree on the effect of flow rate or pipe diameter on pressure drop, the equations are not equally good. Consideration of the available data on resistance coefficients, and the conditions of natural gas pipeline operations leads to the conclusion that an equation of the Weymouth type is most satisfactory for large diameter lines. Because resistance coefficients for pipeline operating conditions are fixed by the internal surface of the pipe, no two pipe sections will be exactly the same, although it is to be expected that in natural gas service they will not vary too widely. Although it may be possible to develop a flow equation with somewhat better properties than those currently available, it will always be necessary to use an efficiency or experience factor to account for the unpredictability of pipe surface condition.

⁵ "Flow of Natural Gas in Pipelines," by William T. Ivey, and James H. Dorough, *Transactions, ASCE*, Vol. 124, 1959.

DISCUSSION

JAMES H. DOROUGH.⁶—The paper is an excellent presentation of the flow formulas that have found widespread use within the gas transmission industry. The comparison of the computed results as to expected capacity is valuable, especially with the appraisal of the Weymouth equation used as a basis for comparison.

The writer does not concur fully with the views expressed by the author in subordinating the significance of absolute accuracy in the first and second applications. These applications as stated in the paper are: (a) Design of pipelines for capacity, and (b) pipeline operations study.

The point was made that in these applications the designer is working with estimated loads usually subject to sizable errors. Although it is true that the estimate for future requirements is subject to error, once these estimates are made they become fixed quantities in the design or determination of capacity

TABLE 1.—FLOW TESTS

Test Number	Pipe Diameter, in inches	Flow Rate, in million stand- ard cubic feet per day	Reynolds Number $\times 10^{-4}$	Transmission Factor	Absolute Roughness from Colebrook Equation* $\times 10^4$
(1)	(2)	(3)	(4)	(5)	(6)
179	16	126.993	7.728	19.745	.478
171	16	120.668	7.232	19.585	.531
174	16	97.780	6.054	19.574	.498
175	16	71.539	4.440	19.309	.538
178	16	57.159	3.565	18.945	.668
180	18	142.800	7.721	20.024	.425
172	18	125.740	6.737	19.972	.414
173	18	101.610	5.498	19.909	.385
176	18	76.768	4.249	19.611	.432
177	18	57.653	3.199	18.709	.880

* "Flow of Natural Gas Through Experimental Pipelines and Transmission Lines," by R. V. Smith, J. S. Miller, and J. W. Ferguson, Monograph 9, Bureau of Mines, page 40.

available for sale through existing facilities. The design engineer makes definite statements as to the expenditures required for given increases in capacity, or sales available from existing facilities. It is necessary to be able to support his conclusions.

Based on these statements the capacity available is usually written as firm commitments in sales contracts. Therefore, it is advantageous for the design engineer to select an equation, which will result in the best possible accuracy regardless of the specific application.

The paper is characteristic of the present thinking within the high-pressure transmission companies. They are seeking a solution to their particular problems and are forgetting the distribution companies whose flow rates are not as great for given pipe diameters operating at lower pressures. Lower rates of flow give corresponding lower Reynolds numbers.

⁶ Planning Engr., Southern Natural Gas Co., Birmingham, Ala.

Investigation of flow tests⁵ indicate that the Reynolds number does have a slight influence on flow characteristics even in the range of 3×10^6 to 7×10^6 for 16-in. and 18-in. pipe diameters.

Attention is called to test numbers 171 through 180 in Table 1. These tests⁵ were performed on the same sections of 16-in. and 18-in. pipe for varying flow conditions.

The 18-in. pipe was installed seven yr after the 16-in. pipe, which is apparent from the slight increase in absolute roughness. The transmission factor also increases with the increase in flow rates.

Test No. 178 and No. 177 are obviously not in good agreement. A possible explanation for this variance could be explained by the fact that the flow rate had been reduced to such an extent that the pressure drop was only 8.5 lb per sq in. for test number 177. The pressures were taken with dead weight gages reading to the nearest 1/10 of a pound and possible error of as much as 2/10 would make a significant difference. The test section was approximately 16.56 miles in length.

Although there is only a slight change in transmission factors for flow rates usually encountered in natural gas transmission companies, research efforts should strive to give consideration to this change. A general equation considering this change in transmission factor for various rates of flow would be applicable for use by both distribution and transmission companies.

With the present trend toward the use of high-speed computers in design of pipelines, it is no longer desirable to sacrifice accuracy for simplicity.

Considering the possible refinements to the flow equation, it is conceivable that once the absolute roughness of a section of pipe is determined by flow test this section can be used for main-line measurement in day-to-day dispatching, and for efficiency checks of the entire gas transmission system.

WILLIAM T. IVEY,⁷ M. ASCE.—The author indicates that at the state of complete turbulence, the resistance coefficient no longer depends on Reynolds number, and that it is virtually impossible to imagine a practical natural gas pipeline operation in which streamline flow might be involved. The mass of evidence of actual tests on commercial pipelines supports this conclusion. The writer has personally examined over two hundred tests on commercial pipelines under varied operating conditions that support this conclusion.⁵ Since the author's paper was presented, Ellington, Bukacek and Staats⁸ have presented information supporting the same premise. Under the heading, "Natural Gas Pipelines and the Resistance Coefficient," it is stated " * * * in the range of flow rates common to large diameter high-pressure pipelines, the resistance coefficient is controlled by conduit surface conditions," and under the heading, "Conclusions," "an equation of the Weymouth type is most satisfactory for large diameter lines."

It is evident also that the roughness of the internal surface of the pipe has a major influence on the flow characteristics. This is evidenced by the countless pipe cleaning programs of major pipeline companies and the standardiza-

⁵ These tests in Table I with test numbers 171 through 180 are selected tests from Paper 1194, Journal of the Pipeline Division Proceedings of the American Society of Civil Engineers.

⁷ Chf. Statistician and Planning Engr., Southern Natural Gas Co., Birmingham, Ala.

⁸ "Flow Phenomena in Large Diameter Natural Gas Transmission Lines," by R. T. Ellington, R. F. Bukacek, and W. R. Staats, *Project NB-13*, Extension for the Pipeline Research Comm., American Gas Assn., 1958.

tion of pipelines design to include facilities for the introduction of pipe cleaning devices. The author quotes Smith et al² as recommending the Nikuradse Rough Pipe Law, with a value of $k = 0.0007$ to represent average pipe surface conditions. Variation from such averages, or norms might be evaluated as pipeline efficiency.

Designers are ready for a standard flow equation for use in the turbulent flow area in which all large commercial pipelines operate. This equation would disregard Reynolds number, recognize the Nikuradse Law, assume a standard k -factor for maximum commercial smoothness, and evaluate pipeline efficiencies against this standard formula. The absolute characteristic of absolute roughness, k , was determined by Nikuradse as being the diameter of a sand grain glued to the internal surface of the pipe to produce a ratio r/k , a roughness factor. Such a standard flow equation should include a correction factor for deviation, which might be a direct adjustment of the pressure factor.

JOHN F. SCHOMAKER.³—The application of theory to natural gas pipelines still leaves one area in which the accuracy of any of the flow formulas, now in use or proposed, is poorly defined. The smooth flow region has been verified by tests conducted² by the Bureau of Mines, United States Department of the Interior, with small diameter pipe. Similarly, the fully turbulent region seems to have been firmly substantiated by test information on large diameter pipelines. However, the transition region between these two modes of flow is only defined approximately. The Bureau of Mines' results on 2-in. to 8-in.-diameter pipe indicate that the transition region is a relatively wide range, and their correlations would predict that the Reynolds numbers are rather high for the transition region for large diameter pipe. The majority of natural gas pipeline operations would seem to fall in this transition region.

The use of fully turbulent theory for the transition region is probably a satisfactory solution. Perhaps some compromise with theory may provide a better practical answer. In any event, the accuracy of mathematical prediction of flows in the transition region leaves something to be desired.

RICHARD F. BUKACEK¹¹.—The question of the transition region raised by Mr. Schomaker is one which admits of several points of view. Examination of the Bureau of Mines¹² results indicates the following:

1. There is no single behavior pattern in the transition range. The curves in the report that show a particular transition behavior for all pipe sizes were drawn arbitrarily.
2. The only consistent feature of the different data sets covering the transition region is the fact that deviations from the limiting curves (the curve for fully developed turbulent flow in smooth pipes, and the respective curves for flow in rough pipes) are almost as small as the experimental errors involved.

The writer's position in the matter is that for commercial large diameter pipes the transition behavior is probably unique for each pipe section and the assumption that rough pipe behavior is followed back to the junction with the smooth pipe law is probably as accurate as any. Considerably more experimental work in the transition region would be necessary to justify any other position.

³ Sr. Research Engr., Panhandle Eastern Pipe Line Co., Kansas City, Mo.

¹¹ Instructor, Chem. Eng. Dept., Illinois Inst. of Technology, Chicago, Ill.

AMERICAN SOCIETY OF CIVIL ENGINEERS

Founded November 5, 1852

TRANSACTIONS

Paper No. 3010

CURRENT CHALLENGES IN CIVIL ENGINEERING

ANNUAL ADDRESS AT THE CONVENTION
CLEVELAND, OHIO, MAY 5, 1959

BY FRANCIS S. FRIEL,¹ PRESIDENT, ASCE

INTRODUCTION

Perhaps the most important new activity of the American Society of Civil Engineers in the year 1958-1959 has been fund raising for the United Engineering Center. Fund raising for causes of interest and value to us is an American way of life. From the cradle to the grave, whatever our walk of life, our profession, our religion, we are almost continuously involved in the process of soliciting, collecting, distributing (or less often, receiving) money in the name of some worthy cause. So when money was needed we knew how and where to get it.

A sort of military command was set up, consisting of "generals," "captains," "lieutenants," and so on down to the "privates," or "workers." As in any army, the generals planned the strategy and gave the commands. The privates were out on the firing line doing the "hand-to-hand" fighting—that is, they put out their hands, and didn't pull them back until they got money from another hand. Privates run certain risks and frequently suffer discomfort. They seldom become eligible for the Purple Heart but they are frequently victims of battle fatigue.

For the ASCE organization of zones, districts and sections there was little difficulty in arranging the chain of command for the campaign.

Once the goals and quotas are set and the workers enlisted, it is obligatory to have a "kick-off". This amounts to a formal declaration of war, and no campaign can be conducted without one. We had ours, a fine kick-off, and we had Herbert Hoover, Hon. M. ASCE, to initiate the attack. We were indeed honored that the most distinguished living American engineer was willing to state for us our need, so clearly and forcefully. It is well, now, to remind ourselves again of his words:

¹ Pres., Albright & Friel, Inc., Philadelphia, Pa.

Today marks the launching of a drive by the United Engineering Societies for the funds to erect a new building. We need the support of all our members. And especially we need support from Industry. The activities of these Societies are of vital importance to the American people, to the engineers, and to the industries.

We have about 250,000 engineer members in these Societies, and the membership is constantly increasing. We are overcrowded in our present headquarters. It has become clear that we must have more room if we are to effectively conduct what has become one of the nation's greatest educational centers.

The effort to raise money from the membership for the engineering center has taught many lessons which are vital to the welfare of the Society. It has pointed up both our strength, as a group, and our weakness. It has revealed a reassuring degree of unity with our brother societies, but it has also disclosed some disquieting, although not yet critical, conflicts with other groups.

The statistics of the campaign have been well publicized. Industry was asked to contribute \$5,000,000. Member giving was set at \$3,000,000 for the members in the five Founder Societies. Quotas were equitably apportioned among the participating engineering organizations, that for ASCE was \$800,000. Society quotas, in turn, were assigned by zones and sections.

CAMPAIGNS CALL FOR STOCK-TAKING

As we explain, study, and consider the need for which we are trying to meet with this money-raising effort we cannot avoid analyzing the purpose of our Society, re-examining our work, taking stock to see in what respects we measure up to our stated purpose, and in which we fail. This, to me, is one of the most valuable by-products of a campaign.

The campaign has also disclosed that it is easy to lose focus in trying to transmit the ideas and enthusiasms of UEC and ASCE leaders to the rank and file. Why is this true? Perhaps we do not know enough about the art and techniques of communication. There is perhaps another reason. Not all local sections have strong national interests.

Standards of Practice.—One reason for founding ASCE, perhaps the first reason, was to establish a Code of Ethics, to set standards for conditions of practice. This has been an essential service, and certainly one of the most valuable of the accomplishments and services of our group. If a society of engineers did nothing else, its work in the field of ethics would be reason enough for the establishment of the society. So much has been accomplished, and we take so much for granted, that we sometimes forget how important this function is. A campaign which forces us to justify our activities reminds us of the value of this function. We have agreed on standards, and our Society is responsible for control and enforcement. Here we have been truly successful.

Yet, at this time of stocktaking, it might be a good idea to ask ourselves if the emphasis is not too much on the negative, rather than the positive. With more than 42,000 members, instances of punitive action for violations of our Code of Ethics are relatively few. We don't (quoting from the Canons of Ethics for Engineers) " * * * accept compensation, financial or otherwise, from more than one interested party for the same service, or for services pertaining to the same work, without the consent of all interested parties." Nor are we

often tempted to " * * * accept commissions or allowances, directly or indirectly, from contractors or other parties dealing with his client or employer in connection with work for which he is responsible."

The ASCE Committee on Conditions of Practice sees to it that standards are reasonable in the light of the times; that they are up to date; that they are realistic; and that they take care of current problems. This is fine. But is it enough? Are we guilty, as Mark Twain put it, of being "good men in the worst sense of the word?" Are we content simply to do no wrong? Do we sometimes fail, for instance, to protest against unnecessary construction? More important, do we fail to take the initiative where we are highly qualified, in suggesting, for example, good city and regional planning, and taking part in the drudgery and hard work in civic committees to promote such plans?

We as engineers must see to it that our great cities do not suffer from their growing pains. We must see that our water supplies remain adequate and we must be sure that we maintain adequate standards of sanitation. We must control floods. While we have made progress in flood control, floods continue to destroy and kill, as they did only recently in Ohio. The works of engineers are right now preventing such disasters in many areas of the nation, notably along the great Mississippi River. The engineer in these matters has more of a responsibility than merely designing projects at the will or request of others. Better than anyone else, he is equipped to handle the long-range planning as cities grow. His training is such that he is well aware of the problems that always seem to accompany growth and development—yes, even prosperity.

It behooves us to weigh the ethical implications of any failure on our part to do everything we can to take and keep the initiative in solving some of the problems I have just noted.

Professional Status for Young Engineers.—What about our work with young engineers? One of the essential services of ASCE is to help young engineering graduates attain professional status. This we conscientiously have done and do. But in our determination to maintain standards are we sometimes guilty of failing to develop leadership? Do we encourage our younger members to take real responsibility in our Society while they are still young? In this respect I feel that our re-classification of member grades is a step in the right direction. Also, the section "The Younger Viewpoint" in *Civil Engineering* encourages young members to express their ideas. Fund raising is an excellent means of developing leadership and discovering leadership potentials. The more active young members are in this important effort, the more they will learn about ASCE, the more they will gain from the Society, and the more quickly will they advance in Society affairs. Fund raising is a means to more than one end, and we would do well to remember it. As stated previously, when we talk about fund raising we talk about every aspect of our work!

Publications, Meetings, and Conferences.—Publications, meetings, and conferences are, of course, the essence of the ASCE program. This fund raising, successfully completed, will enable us to do a much more effective job along these lines than has been possible heretofore. The facilities, equipment, and space available in the new Engineering Center will make a tremendous difference in our meetings; in the efficiency, size, and service of our library; in the effectiveness of our operations; and in the quality of our publications.

The Society has always been strong in the technical field, and it must retain its dominance, for the technical phase of our operations is the heartbeat of our organization. The work of our Technical Divisions has attained nationwide—and indeed international—prominence for its proficiency and effectiveness. We now have fourteen Technical Divisions, and, as a measure of accomplishment during the past year, there were 95 technical sessions during the three national conventions, and approximately 400 papers were presented. This does not include the papers and discussions which were presented at Technical Division Conferences; and at the Local Section Conferences. Last year we published 403 papers.

Research.—We have continued to encourage research among our members by the presentation of prizes to those who have done outstanding work each year on various research projects. In 1958 we established a Research Fellowship in civil engineering. The grant, which will aid in the creation of new knowledge “* * * for the benefit and advancement of the science and profession of civil engineering,” is to be made from current society income, in the amount of \$5,000 annually.

As Martin Mason, M. ASCE (Dean of the School of Engineering, George Washington University, Washington, D. C.), has pointed out²

“Not only as a profession, but also as individuals, we must press forward the frontiers of knowledge. We must encourage that most ephemeral and elusive of all human qualities—original creative thought. As a profession we should be, as many individuals are, constantly dissatisfied with what we know because of the much wider knowledge we lack. As a profession we should take the lead in searching out the new knowledge lying all around us, only awaiting discovery.”

Mason also reminded us of two serious weaknesses which I feel we should make every possible effort to overcome. It is my hope that the new Engineering Center will help us to conquer these shortcomings. He said,

“This odd spectacle of a profession mute on matters about which it is presumed to be expert is serious. It not only contributes to the assumption that the engineering profession is not competent, but it also creates an atmosphere in which anyone who chooses can assume the status of expert . . .

“In our society the individual engineer or scientist is almost powerless to act alone. He doesn't know how to gain the support he needs; he can't or won't speak a language that millions of non-engineers can understand; he believes his economic situation as an employee is precarious. In short, he decided to store his ideas in the confines of his own mind at the slightest sign of opposition.”

These criticisms are more than justified. It seems to me that we must acknowledge that at these two points our performance is inadequate. We are not doing enough basic research; we do not make our proper contribution to the advancement of knowledge. We can try to correct this weakness by providing greater incentive to research, as we have already started to do; by providing improved facilities for research as the new Engineering Center will help to do; by urging more pure science requirements in engineering education;

² “Our Professional Responsibility—Development of New Knowledge,” by Martin A. Mason, *Civil Engineering*, Vol. 28, No. 6, 1958, p. 38.

by supporting those institutions of higher learning in which such research can be conducted; and by making provision in industry, and indeed in our own firms, for research.

We must, in the second place, share the expert knowledge we have and we must use the results of the research we have done. Suppose, for instance, that as civil engineers we have engaged in a piece of basic research which has resulted in the discovery of a new and better method of sewage treatment, or a better system of safe highway construction. It is not enough to sit back and wait to be asked to build such a sewerage system, or such a highway. We may need to get the public to demand such an installation. We may have to form a committee and put on an educational campaign to make that research "pay off." It may be necessary to join with our neighbors to raise a little money for community betterment. Now it is not necessarily meant to imply that the same engineer who conducted the research should form the committee and raise the money, but among our membership these jobs should be done.

It is time, I think, for us as members of the ASCE to consider our responsibilities in relation to recent developments in science and research. The great new discoveries, the astonishing progress in science of the last decade has imposed relentless demands on all men, everywhere. To live in this new world much is required of us. We need more knowledge than we used to have, and more courage, more wisdom, better judgement, more imagination. Mankind's most urgent need right now is not bigger and better laboratories where faster and more powerful rockets can be built, but laboratories conducting research to discover how man can live in an environment which has suddenly expanded to include not one planet but many. Our mind's eye must be trained to focus on these ever-retreating horizons. By judicious study we can learn what we don't know, and what we need to know, of the new knowledge discovered by science and research. By concerted effort we can help others learn. By deliberating and acting together we can maintain the balance we need if mankind is to survive in his new environment, if mankind is to survive as man.

STRENGTH AND WEAKNESS

You see, we keep coming back to fund raising. Through fund raising and its results we have seen how we can strengthen our work, develop leadership, and expand our services. Specifically, what has this intensive fund-raising effort shown us about the structure of the ASCE, its strengths, and weaknesses? We have learned, for one thing, the rather obvious fact that the Society is only as strong as the leadership of the local sections. The problems of local sections mirror the larger problems of the Society.

Unity.—Unity, which is one of our most urgent needs and important policies, has been demonstrated throughout the year, in practice, as we worked with the other Founder Societies on this joint endeavor. It has been proved that problems can be met on a day-to-day basis. Task forces have worked together in a friendly way. I believe that we have already achieved a greater degree of unity than most of the membership realizes. Perhaps the time has come to accentuate the positive. Individual members have had a chance during the fund drive to appraise the Society for themselves in relation to their own personal interests, and also in relation to the other Societies.

Communications.—The campaign has also disclosed the fact that it is easy to lose focus in trying to transmit the ideas and enthusiasms of Society officers and committees to the rank and file. We need to help local groups achieve a stronger sense of relationship with the national structure—and vice versa. Much has been done to accomplish just this. The introduction of a different style of *Annual Report* has been effective. The section of personal notes in *Civil Engineering*, and the expansion of visiting schedules will strengthen the ties between local and national aspects of the Society. Yet more needs to be done to give the individual engineer in the local section a sense of professional identification and pride not only with his local unit but with all that goes on nationally. This is a two-way street.

Communications narrow down to two basic problems: First, the art of saying something; second, the genius of having something to say. The best techniques will fail if we have nothing to say in the first place. Our structure of a national board of directors, local zones and districts is a sound and efficient one, and the headquarters staff and the work it does is necessary to the life of the Society. Within this network of organization we do have something to say to each other and we are component parts of a whole. On the other hand, membership will be meaningless to the individual if there is no national structure to provide the essential services of the Society, the meetings, the publications, and the library. We need all the parts of the whole, and we must learn to communicate effectively in order to realize the full value of the organization.

In all complex problems—and the art of effective communication is extremely complex—it is impossible to get away from some homely virtues in their solution. These virtues must be exercised by those who attack the problems: Patience, persistence, and flexibility. The mere fact that we have scientific and technological advances at our command does not in itself alter the nature of man. We are dealing with human problems and human nature is what it always was. Perhaps we can learn something from history and philosophy that will let us use our new powers of science and technology more effectively in order to understand each other better.

Public Relations.—The problem of adequate communications includes not only the internal exchange of ideas, but the external expression of our beliefs, the announcements of our achievements, and the explanation of our opinions. All these external communications add up to a public-relations program. A sound public-relations program is crucial for us as a society and as individual engineers. We need to acquaint local sections with some of the "How to do it Yourself" principles of a public-relations program. The first step in this direction has already been made with the publication of the ASCE Public Relations Guide. There are many aspects of public relations. There are large issues and there are minute techniques. All need to be blended and used together.

For one thing we ought to take proper credit for some of the accomplishments of the Society. There is a tendency to stress technical and private issues rather than public ones when the Society speaks to the general public. Not only is the Society not understood, it is not saying what the public is interested in hearing.

We must try to find some graceful way out of the uncomfortable position we find ourselves in when it is necessary to advocate essential public expendi-

tures on projects on which we must be employed. On the other hand we need to take credit for those instances in which we recommend public action which adversely affect our private interest. We must learn the art of recognizing and confessing our mistakes. We are not infallible. To point up our errors and show what we have learned from them is good public relations, too.

Do we ourselves have clearly in our own minds a picture of what we think a civil engineer should be? We can't hope to convince others of the high attributes of civil engineering if we don't know what they are ourselves. As we work with each other and for each other, we will incidentally be talking about what civil engineers do and what we are, and what we should be, both as individuals and as a group. As was suggested earlier, it is not enough merely to be honest, proficient, and blameless. We must be much more. Now is the time, now in this age when engineering has come into its own, to set our sights high, and to let the public know about our accomplishments and our ambitions.

We live in an age of wonders, in a time of great discovery, infinite daring, and unpredictable danger. It is no longer enough for us as civil engineers to use our talents to conceive and build as others dictate. We must use our skill and imagination to determine how best our local, regional, and national—indeed international—problems can be solved. We have not only the right but the moral obligation to express our opinions and make ourselves heard.

In his work of construction, the civil engineer must consider effects other than those of simple physical stress and strain on his materials. It is no longer enough to know how to construct a dam which will hold water, and let it go at that. We must also learn to think of the social and political implications of all our works. The civil engineer may some day be required to work on problems of construction in locations where the law of gravity does not exist. But before we engage in that activity we must be sure that we are ready for such advances. Before we can build bridges on the moon, we must necessarily build bridges of understanding among men. We are now beginning to understand the forces of nature, and we are harnessing nuclear and solar power. But isn't the first requisite that we learn to measure and harness our own emotions? We are now sending powerful missiles into space, and should we not learn to make them truly guided missiles? We must know where we are going and why—to know how is just not enough.

What is the picture of the engineer we would each like to be?

What are the qualities which today's civil engineer must have? Initiative, ingenuity, independence, individualism, the willingness to work hard, to work with his hands if that's helpful; humility; diplomacy; common sense; all of which adds up to another quality—maturity. A man who thinks for himself, stands on his own feet, is not dependent for his happiness on a false security from some father-figure or on conformity, and is strong but still humble is a mature man—a man we badly need today. This is the space age, when it's necessary to think big. Our minds must stretch to visualize these vast spaces, to see those infinitely distant horizons. This is a time for maturity, for big men. The organization man is all right in his place. We like him, we need him, we can and will work with him. But our place of world leadership as a nation must not be allowed to become a vacuum, which it will if America is

populated by organization men only. It's time for some good old-fashioned rugged individualists to step out. Let us not now shirk our responsibility for this world we have made.

We are products of our education and our education is something we can never see completed because it goes on as long as we live. But we can see some results. The results of our educational efforts should show each of us not only a well-educated engineer, but a well-educated man. A man expert at his job, a man who is on top of this job, not work-driven, but in control of his means of earning a living. A man who, because he has a profound knowledge of his own subject, has also some understanding and appreciation of other disciplines. A man able and willing, because of his education, to take his part in the civic and cultural affairs of his country and that larger community which transportation and communication advances now make possible—a world community.

RESULTS OF CAMPAIGN

A powerful symbol of unity in the engineering profession is available to us in the new Engineering Center which will stand on the United Nations Plaza. This spectacular building will focus the attention of the peoples of the nation and of the world on the position that engineers hold in the affairs of the American people. This is not just office space for the people who are employed by our societies or meeting facilities for those members who serve our profession. It is much more—a spectacular and lasting symbol to the public of the importance of engineering and the engineer in our way of life—for the benefit of mankind.

This is the age of science and engineering. Mankind looks to us for leadership. We must not fail that trust. Yet we, as engineers, have been notoriously inarticulate. We are willing and able to build dams for flood control, to build irrigation systems that the desert may bloom, but we wait until someone else has pointed out the need for these things, and labored with Congress to obtain the necessary appropriations—then we follow orders. We can no longer afford to sit back and wait till someone hires us to build a dam. The country, yes, the world, needs our advice, our suggestions, our planning, in short our leadership. We need to plan, to persuade, and to educate, as well as to build.

We can do this on a national scale through committees of ASCE. We must arrange a system of committees to do basic national planning, so that we can go to our government, and to the people, and say as experts we recommend this sort of national highway system for these reasons. A major part of our work as a society should, in my opinion, be devoted to this kind of thinking and to this kind of work. This fund-raising campaign has helped us to develop the kind of leadership which is being demanded of us. I believe that the fund-raising experience has helped us to set our sights high, to think big.

How can we influence our universities to provide the sort of engineering education we think best? By saying that the young engineering graduates they turn out these days are poorly prepared and lazy? Complaints alone will not be heard. But if we serve on the Alumni Giving Program and on the College Capital Funds Drive, then when we speak, we speak with a voice which

is heard. We may even speak eventually, as a member of the board of Trustees. Many of you have earned your right to be heard in this way. You have found the work rewarding and satisfying. But more of us have not bothered to go out and try to raise money for the causes we believe in. Look at the lists of committee members of almost any civic enterprise. Whose names appear? Educators, doctors, lawyers, businessmen. But where are the engineers? We must do our share. We must take out part.

One thing it has done more effectively than any questionnaire could have done. It has brought an awareness of the Society to every member, no matter how remote from New York City. It has forced him to appraise the value of the Society in cold hard cash—its value to his professional life and his career. By the very act of deciding how much or how little to contribute, he has told his fellow engineers, without inhibition, how much the Society means to him, and the Society's planners can reach realistic conclusions from the analysis. The results are at once heartening and disheartening; and remoteness from Society headquarters gives the planner no clue as to the reasons for one or the other.

It has demonstrated conclusively a fact which was suspected for a long time; namely, that the Society is as healthy as the sum total of its working members in local sections. Dues can buy services. They can buy administrative staff to implement the orders of the secretariat. They can support a top-notch executive secretary, to convert Board orders into action. But when offered passively, like a tax dutifully paid, they cannot buy lasting achievement. That membership organization, supported by passive members who pay dues in exchange for such services as they each can get in return, is headed for oblivion. The health and vigor of a professional Society—like the health and vigor of a professional man—is measured directly by the things it does for itself, through volunteer individual and enthusiastic effort.

I am proud of this ability of ours. Our fund-raising campaigns, frequently (and understandably) the object of complaints and the butt of jokes, are nevertheless fundamental to our way of life, they are so numerous and so much a part of our lives that we take them for granted. We fail to recognize them for the tools they are, we don't realize the far-reaching impact of these drives on us as individuals and as a nation.

Our drive to raise money for our Engineering Center has helped us to examine our strengths and weaknesses as a Society, it has given us an opportunity to work with the other Founder Societies demonstrating a degree of unity which is most gratifying, it has developed leadership within our ranks, and it has measurably improved our public relations. Finally, and most important, it focuses our attention on the part we should play as citizens.

So as we approach the last lap of our activities for this year and our campaign for the engineering center, we may be battle-scarred and weary, but we are, I am convinced, a stronger organization and better men for having made this effort.

Let us not forget the lessons of this campaign. Whatever we would achieve, whatever we would be, it is up to us. It is up to every single one of us.

MEMOIRS OF DECEASED MEMBERS

ABSTRACTS

Past-President

Wesley Winans Horner	1049
----------------------------	------

Honorary Members

Gerard Hendrik Matthes.....	1050
Wilbur M. Wilson.....	1051

Other Members

Robert Edmund Andrews.....	1053
Guy Mannering Bassel.....	1054
Ulysses Grant Brown.....	1054
Leon Everett Chase.....	1055
Ben Taylor Collier.....	1056
Ernest Elwood East.....	1057
Nelson Andrew Eckart.....	1057
William Gilbert Fargo.....	1058
John Dayton Faylor.....	1059
Edwin Morrell Grime.....	1059
Eugene Grove Haines.....	1060
Thaddeus Leon Euclid Haug.....	1061
Christopher Frank Heiselman.....	1062
Harry Hemmings.....	1062
Charles Stephen Hill.....	1063
Howard Howie.....	1064
Charles Jensen.....	1065
Andre Laurent Jorissen.....	1065
Arthur Dale Kidder.....	1066
Jack Adelbert Killalee.....	1067
Frederick Laurence Klein.....	1068
Hans Kramer.....	1068
Kenneth Winans Lefever.....	1069
Andrew Cavitt Love.....	1070

Leon Waddell Mashburn.....	1071
Frank Duff McEnteer.....	1071
Thurmond Armour Munson.....	1072
Charles Fernald Niles.....	1073
Robert Preston Parker.....	1073
James Lindsay Paton.....	1074
John Charles Rathbun.....	1075
Donald Joseph Sadar.....	1076
Thomas Duncan Samuel, Jr.....	1076
Robert Radcliffe Shoemaker.....	1077
Frederick Josiah Spry.....	1078
Thomas Johnson Strickler.....	1078
Richard Randolph Tipton.....	1079
Harry Bruce Walker.....	1080
Robert Patterson Woods.....	1081
George Dunton Youngclaus.....	1081

WESLEY WINANS HORNER, PAST-PRESIDENT, ASCE¹

DIED SEPTEMBER 22, 1958

Wesley Winans Horner, the son of William A. and Minnie (Winans) Horner, was born on September 22, 1883, in Columbia, Mo. He was graduated with the degrees of Bachelor of Science in civil engineering (1905), Civil Engineer (1909), and Doctor of Engineering (1952) from Washington University in St. Louis, Mo.

From 1905 until he entered private consulting practice with the firm of Horner & Shifrin, St. Louis, in 1933, he was employed by the City of St. Louis in varying capacities in the Water and Sewer Departments. He assumed positions of major responsibility for the St. Louis Department of Sewers and Paving, in which he conceived and executed the design of the large and important River des Peres drainage project. He served as consulting engineer on a national board of review of the Public Works Administration; member of the National Resources Planning Commission; member of the Board of Consultants on Flood Control for the Department of Agriculture; chairman of the Engineers' Joint Council, Committee on National Water Policy; and chairman of the Committee on Flood Control of the Hoover Commission Task Force on Water Resources and Power. Other important engineering achievements included collaboration in the planning and drainage for the Idlewild and Washington National Airports; water supply planning for Houston (Tex.), New York (N. Y.), and St. Louis; design of sewerage projects and pumping stations in East St. Louis and St. Louis; hydrologic studies of internal drainage and sewer design for flood-protection projects in St. Louis and Kansas City (Mo.); airport planning at St. Louis, Milwaukee (Wis.), and Detroit (Mich.); and extensive airport design at St. Louis and the Blytheville Air Force Base in Arkansas. From 1937 to 1942 he was professor of engineering at Washington University.

Mr. Horner originated the method of sewer design usually referred to as the rational method. He was the recipient of the Rudolph Herring Medal of the Society in 1937, the Gold Achievement Award Medal of the Engineers' Club of St. Louis in 1955, and the Award Medal for Distinguished Service in Engineering by the University of Missouri, Columbia in 1958. He wrote many papers on engineering subjects, and was the author of the section on "Hydrology" of the recently published American Civil Engineering Practice Manual.²

He was a member of the American Institute of Consulting Engineers, American Water Works Association, Federation of Sewage and Industrial Waste Associations, American Society for Testing Materials, and the American Geophysical Union. He was also a member of Tau Beta Pi and Sigma Xi. He

¹ Abstract of memoir prepared by Erwin E. Bloss, and Vance C. Lischer, Members, ASCE.

² "American Civil Engineering Practice," edited by Robert W. Abbett, John Wiley & Sons, Inc., New York, N. Y.

served as past-president of the American Public Works Association and The Engineers' Club of St. Louis. In 1946 he served as President of the Society.

Mr. Horner was married to Elinor Hall on June 16, 1908 in St. Louis. He is survived by his widow; four sons, Frederic W., John L., Richard W., and David A.; and fifteen grandchildren.

He was elected a Junior of the Society on September 1, 1908, an Associate Member on April 4, 1911, and a Member on September 11, 1917. He became a Life Member in 1946.

GERARD HENDRIK MATTHES, HON. M. ASCE¹

DIED APRIL 8, 1959

Gerard Hendrik Matthes, the son of Willem Ernst and Johanna (Van der Does de Bijde) Matthes, was born in Amsterdam, Holland, on March 16, 1874. He received the degree of Bachelor of Science in civil engineering from the Massachusetts Institute of Technology, Cambridge, in 1895.

Early in his career, Mr. Matthes spent five years performing hydrologic and reclamation surveys for the Water Resources Branch, United States Geological Survey. In 1907 he became an engineer for the Colorado Power Company. Mr. Matthes organized the aerial photographing of the Tennessee River Valley for the War Department in 1923.

From 1924 to 1928 he was a consulting engineer in New York, N. Y., dealing mainly with aerial surveys and maps. At this time he was retained by Fairchild Aerial Surveys, Inc., New York, as a consulting engineer on the development of commercial aerial surveys. He also assisted the consulting engineering firm of Daniel W. Mead and F. W. Scheidenhelm, N. Y., with foundation investigations for the hydroelectric development on New River, near Radford, W. Va. From 1929 to 1932 he served the War Department as senior hydraulic engineer and principal engineer in charge of comprehensive studies relating to water power, flood control, and navigation improvement in the southeastern United States. From 1932 to 1945 Mr. Matthes acted as principal engineer, head engineer, and consultant to the president of the Mississippi River Commission.

Throughout his professional career he served as a consultant to various engineering firms. He was a member of the Advisory Council to the Federal Board of Surveys and Maps in connection with aerial photographic mapping (1923-1932); consultant to the National Resources Committee, Washington, D. C., for reports dealing with the lower Mississippi Valley (1934-1936); and a member of the consulting board, Corps of Engineers, United States Department of the Army, on the design and construction of Conchas Dam on the South Canadian River, N. Mex. (1935-1937).

¹ Abstract prepared by Mrs. Gerard H. Matthes.

Mr. Matthes also served as a consultant in connection with various flood-control projects, some of which included: Tennessee Valley Authority; flood control for Buffalo Bayou floods, Houston, Tex. (1936); a project for by-passing the Red River above Denison Dam, Denison, Tex. (1943); consultant, Azucarera Colombiana, Medellin, Columbia, S. A., for a 25,000-acre irrigation and drainage project in the Cauca River Valley (1946-1947); and Ministry of Hydraulic Resources, Mexico, for improvement of the Papaloapan River, Vera Cruz State (1947-1949). He served as an expert witness on various federal and state court cases involving claims for flood damages.

Mr. Matthes was active in Society affairs. He served as Chairman of Committees on Flood-Protection Data (1934-1935); Contact Member on a special committee to report on flood-control methods with special reference to their physical and economic limitations (1937-1939); and Chairman of several committees on floods and flood control (1935-1945). He received the Society's Norman Medal in 1949 for a paper dealing with Mississippi River Cutoffs.¹ In 1945 he received the medal for Exceptional Civilian Service with Citation, for his work on the Mississippi River and at the Waterways Experiment Station, Vicksburg, Miss., during World War II.

He was the author of numerous technical articles and reports on river hydraulics, flood control, and aerial photographic map making. His latest contribution was a section in a comprehensive textbook on civil engineering practice² which has been widely accepted throughout the world.

He had been a member of the American Geophysical Union; American Institute of Mining and Metallurgical Engineers; Society of American Military Engineers; the Engineers' Club of Vicksburg, Miss., and Dayton, Ohio; the National Research Council; and the Explorers Club.

On March 3, 1904, he was married to Mary Bewick at Lawton, Okla. He is survived by his widow; a daughter, Mrs. Florence Stephens; three grandchildren; and nine great-grandchildren.

He was elected an Associate Member of the Society on April 6, 1900; a Member on January 31, 1905; and an Honorary Member on October 11, 1943. He became a Life Member in 1935.

WILBUR M. WILSON, HON. M. ASCE³

DIED NOVEMBER 28, 1958

Wilbur M. Wilson, the son of Mathias and Ruth (Mosher) Wilson, was born near West Liberty, Iowa, on July 6, 1881. He was graduated with the degrees of

¹ "Mississippi River Cutoffs," by Gerard H. Matthes, *Transactions, ASCE*, Vol. 113, 1948.

² "American Civil Engineering Practice," edited by Robert W. Abbett, John Wiley & Sons, Inc., New York, N. Y., Vol. II.

³ Abstract of memoir prepared by Edward E. Bauer, M. ASCE.

Bachelor of mechanical engineering from Iowa State College, Ames, in 1900 and Master of mechanical engineering from Cornell University, Ithaca, N. Y., in 1904. In 1942 he received the honorary degree of Doctor of engineering from Iowa State College.

He served as an instructor in mechanical engineering at Iowa State College from 1901 to 1903, and as an assistant professor and associate professor in mechanical engineering from 1904 to 1907. From 1907 to 1913 he practiced structural engineering in Chicago with the Illinois Steel Company and the Strauss Bascul Bridge Company. In 1913 he became an assistant professor at the University of Illinois, Urbana, and was on the staff continuously except for the period from 1917 to 1919 when he served with the Corps of Engineers of the United States Army. He became an associate professor in 1919 and research professor of structural engineering in 1921.

From 1919 until his retirement in 1949 his experimental work on the strength and behavior of structures and structural elements has been widely acclaimed throughout the world. He conducted investigations and studies of arch bridges, rigid-frame bridges, and many other types of structures, materials and connections, the results of which have played an important role in the field of structural engineering. His interest in the behavior of rollers led him to design equipment for repeated load tests of structures and structural members. A major part of his time in the 1930's and early 1940's was devoted to the determination of the fatigue strength of structural members subjected to repetitions of load. The fatigue-testing machines which he designed and constructed are still used in the Arthur Newell Talbot Laboratory at the University of Illinois, and have been copied in laboratories throughout the United States and in the world.

In the ten years immediately preceding his retirement he became interested in more efficient means of fastening structural members and developed modern procedures for the use of high-strength bolts. He was responsible for the establishment of the Research Council on Riveted and Bolted Structural Joints of the Engineering Foundation and through that organization carried on much of his research work in this field. His early research, supported by the later work of his successors, has made the use of high-strength bolts one of the most striking recent developments in structural engineering.

Mr. Wilson was the recipient of the Chanute Medal of the Western Society of Engineers (1915, 1937); the Wason Medal, the American Concrete Institute (1939); and the Marston Medal, Iowa State College (1949). He received the J. James R. Croes Medal from the Society in 1936. In 1956 he received a bronze plaque from the Research Council on Riveted and Bolted Structural Joints which is permanently mounted in the Arthur Newell Talbot Laboratory. He was presented with the Army-Navy certificate of appreciation in connection with determining the causes of fractures in ship plates in 1949.

Mr. Wilson was active in the American Railway Engineering Association on committee 15 (iron and steel structures) and committee 30 (impact and bridge stresses). He was a member of many organizations, including: American Society for Testing Materials; American Society for Engineering Education; American Welding Society; American Concrete Institute; American Association for the

Advancement of Science; Illinois Society of Professional Engineers; Tau Beta Pi; Sigma Xi; and Theta Tau.

He served as Director of the Society from 1944 to 1947, and represented the Society as one of the nonparticipating science observers in the atomic bomb tests at Bikini in 1946.

Mr. Wilson was married to Teresa May Stewart of Iowa City, Iowa in 1905. He is survived by a son, Matt; a daughter, Grace; and five grandchildren.

Mr. Wilson was elected a Member of the Society on August 28, 1922 and an Honorary Member on October 31, 1949. He became a Life Member in 1952.

ROBERT EDMUND ANDREWS, M. ASCE¹

DIED JULY 29, 1958

Robert Edmond Andrews, the son of George Emery and Mary Alice (Spease) Andrews, was born on October 9, 1880, in Rochester, N. Y. He received the degrees of Bachelor of Arts in 1903 and Bachelor of Science in civil engineering from the University of Michigan (Ann Arbor) in 1905.

He served as assistant engineer, Board of Water Commissioners, Detroit, Mich. (1905-1911), and in various capacities as engineer or in supervisory positions with the National Board of Fire Underwriters, mainly in San Francisco, Calif. (1911-1947). From 1917 to 1919 he worked for the United States government as supervisor of fire protection during the construction of Camp Sherman, Chillicothe, Ohio; advisory fire protection engineer with the Bureau of Yards and Docks, United States Department of the Navy; and in June, 1918, served in the latter capacity for the United States Housing Corporation, Washington, D. C., until January, 1919. At that time he returned to the National Board of Fire Underwriters as chief of field party. From 1921 until his retirement in 1947, he served as assistant chief engineer, reviewing the water supply facilities of many large western cities and the Territory of Hawaii. During World II he acted as a consultant regarding fire protection of Army and Navy establishments on the Pacific Coast. His numerous papers on fire protection were presented to many technical societies.

Mr. Andrews was a member of the Seismological Society of America and served as Director (1917-1947) and President (1939-1941). He attended the Baptist Church, and belonged to many professional, civic, and social organizations. Following his retirement he practiced his hobbies of photography and classical music. His biography of Gasparo Bertolotti Da Salo was published in 1953.

On June 26, 1907, he was married to Sarah Eleanor Thomas.

Mr. Andrews was elected an Associate Member of the Society on January 2, 1912, and a Member on June 24, 1916. He became a Life Member in 1947.

¹ Abstract of memoir prepared by Carl A. Weers, A.M. ASCE.

GUY MANNERING BASSEL, M. ASCE¹

DIED JULY 19, 1958

Guy Mannering Bassel, the son of Daniel and Louisa (Burr) Bassel, was born at Lost Creek, Harrison County, W. Va., on July 21, 1867. He was graduated from the University of Nashville, Tenn., in 1888, with the degree of Bachelor of Arts.

From 1888 to 1903 he was associated with the Arrowhead Construction Co., San Bernardino, Calif., as draftsman and surveyor. He was office engineer for the Coal & Coke Railway of Weston, W. Va. (1904-1906); resident engineer for the construction of the Carolina, Clinchfield & Ohio Railroad between Erwin, Tenn., and Marion, N. C. (1906-1908); and in 1909 entered private engineering practice in Clarksburg, W. Va. From 1911 to 1928 he was planning and construction engineer for the Aluminum Company of America in Alcoa, Tenn. In 1928 he returned to private engineering practice in Maryville, Tenn. From 1929 to 1940 he served as city engineer in Maryville and was also engaged in private practice. He designed and supervised the construction of Maryville's first sewage disposal plant, as well as the Laurel Lake Dam near Townsend, Tenn. Thereafter, he practiced privately until his death.

Mr. Bassel was an active member of the First Baptist Church of Maryville, and a member of the A.F. & A.M. His many hobbies included bear hunting, fishing, and a fine garden.

Mr. Bassel was married to Maude Estelle Swisher on October 25, 1900, at Rockford, W. Va. He is survived by his widow; two daughters, Elizabeth B. (Mrs. Robert L. Belt) and Dorothy (Mrs. Benton McKeehan); and a son, John Burr.

He was elected an Associate Member of the Society on February 6, 1907, and a Member on November 27, 1917. He became a Life Member in 1938.

ULYSSES GRANT BROWN, A.M. ASCE²

DIED MARCH 23, 1954

Ulysses Grant Brown, the son of Archie and Mary (Ford) Brown, was born on April 7, 1882, in Butler County, Pa. He was graduated from the New Mexico College of Agriculture and Mechanical Arts at Mesilla Park (N. Mex.) with the degree of Bachelor of Science in mechanical engineering in 1906.

Upon graduation he entered the special apprentice training course of the Santa Fe Railroad at La Junta, Colo. He was employed as mechanical drafts-

¹ Abstract of memoir prepared by Benton McKeehan and Robert H. Nagel, A.M. ASCE.

² Abstract of memoir prepared by George D. Hack.

man by the Southern Pacific Company (1907), mechanical draftsman for George Fouts, (1908-1909), and civil engineering draftsman for the city engineer of San Francisco, Calif. (1909-1913). He was assistant superintendent for the Panama Pacific International Exposition Company until April, 1915. He returned to the San Francisco city engineer's office as concrete designer until February, 1917. At that time he was employed by the California and Hawaiian Sugar Refining Corporation as chief designer of structures in their modernization of the Crockett (Calif.) plant. After the completion of this extensive program, he worked on several construction projects, and in September, 1931, he returned to the corporation as structural engineer until his retirement in 1947. Thereafter, he was consulted on various industrial and civic projects.

Mr. Brown was a member of the Presbyterian Church.

On July 5, 1913, he was married to Merle Anna Blinn at Burbank, Calif. He is survived by his widow; a daughter, Virginia Elizabeth; a son, Robert Blinn; and three grandchildren.

Mr. Brown was elected an Associate Member of the Society on October 11, 1920. He became a Life Member in 1953.

LEON EVERETT CHASE, M. ASCE¹

DIED APRIL 26, 1958

Leon Everett Chase, the son of Charles W. and Mary (Roberts) Chase, was born near Viroqua, Wis., on October 3, 1899. He was graduated from the University of Wisconsin (Madison) with the degree of Bachelor of Science in civil engineering, in 1922.

Mr. Chase served in various engineering capacities in midwestern and western cities from 1922 to 1930. In addition to contracting and private work, he served with the Corps of Engineers, United States Department of the Army, St. Paul, Minn., and on projects with the Emergency Construction Works (Vernon and Richland Counties, Wis.), and the Civil Works Administration. He was resident engineer for the Public Work Administration at Oshkosh, Wis., and Sheboygan, Wis., on sewage projects (1935-1940); construction engineer for the Public Buildings Administration at Columbus, Ga., and Burlington, Iowa; and engineer and inspector (1942-1943) at Baraboo, Wis.

From 1943 to 1953 he was responsible for the installation of many projects for the United States Army and the United States Navy. In 1953 he returned to Viroqua in the capacity of city engineer. In January, 1957, he became associated with the firm of Alvord, Burdick, and Howson, Chicago, Ill., as resident engineer in Racine, Wis., while he continued his work in Viroqua as part-time engineer.

¹ Abstract of memoir prepared by Martha Chase.

Mr. Chase was a member of the Methodist Church as well as many civic and professional organizations.

On June 14, 1936, Mr. Chase was married to Marjorie Ann Buchanan of Viroqua. He is survived by his widow; four daughters, Kathryn, Martha, Roberta, and Cynthia; a brother; and a sister.

Mr. Chase was elected an Associate Member of the Society on June 4, 1928, and a Member on January 6, 1958.

BEN TAYLOR COLLIER, M. ASCE¹

DIED JULY 21, 1957

Ben Taylor Collier, the son of Edward and Annie (Taylor) Collier, was born on May 29, 1891, in Decatur, Ala. He was graduated from the Alabama Polytechnic Institute (Auburn), with the degree of Bachelor of Science in civil engineering in 1910.

After preliminary experience in Decatur, Mr. Collier was employed as assistant city engineer (Clarksdale, Miss.) from 1912 to 1915. From 1915 to 1917 he was sales engineer for the Chattanooga Sewer Pipe Company. In 1918 Mr. Collier became a partner with the firm of Bobo and Collier at Clarksdale until 1942, when he was named county engineer for Coahoma County (Miss.), pioneering in low-cost road construction. In May, 1950, he was appointed first state aid road engineer for Mississippi, a position he held until his death.

Mr. Collier was president of the State Board of Registration for Professional Engineers; the Road Builders Association (County Division); and a member of numerous professional and honorary societies. He was President of the Jackson (Miss.) branch of the Society, and Director of its Mid-South Section. He also received many formal citations for outstanding work in his field. Mr. Collier was active in the Galloway Methodist Church (Jackson), various civil enterprises, and was a musician, an able speaker, and an entertainer.

On May 11, 1917, he was married to Gladys Whiting at Humber, Miss. He is survived by his widow; three daughters, Mrs. Carolyn Bates, Mrs. Gladys Ratliff, and Mrs. Perian Conerly; three sisters; and his father.

Mr. Collier was elected a Member of the Society on October 4, 1950.

¹ Abstract of memoir prepared by Sydney W. Chandler, M. ASCE.

ERNEST ELWOOD EAST, A.M. ASCE¹

DIED NOVEMBER 7, 1957

Ernest Elwood East, the son of Thomas and Barbara (Bronnenberg) East, was born in March 22, 1880, in Anderson, Ind. He was graduated from Purdue University (Lafayette, Ind.), in 1908, with a degree in civil engineering.

From 1908 to 1912, Mr. East was associated with steam and electric railroads. In 1912 he became one of the first engineers employed by the California Highway Commission. During World War I he held the rank of captain in the Engineering Corps, United States Army.

In 1920 he became chief engineer of the Automobile Club of Southern California and was in charge of two expeditions to explore possible routes for the International Pacific Highway through Mexico and Central America. In 1937 Mr. East proposed the building of a system of freeways to serve the Los Angeles (Calif.) metropolitan district. The proposal is considered to be the first for freeways in the United States.

During World War II he was a member of the Los Angeles County Civilian Protection Corps. Mr. East was very active in professional and civic groups, amongst which were the Los Angeles Traffic Advisory Board; the California State Chamber of Commerce; and the Commonwealth Club of California. Besides his active participation in the foregoing, he pursued his hobbies of gardening and tennis.

On July 6, 1916, he was married to Gertrude Rieke Coffy. He is survived by his widow; a daughter, Barbara; and a stepson, Joe Coffy.

Mr. East was elected an Associate Member of the Society on August 31, 1925. He became a Life Member in 1951.

NELSON ANDREW ECKART, M. ASCE²

DIED JANUARY 13, 1958

Nelson Andrew Eckart, the son of William Roberts and Harriet Louise (Gorman) Eckart, was born on December 8, 1878, in Virginia City, Nev. He was graduated from the University of California (Berkeley) in 1899, with the degree of Bachelor of Science in mechanical and electrical engineering.

He served as apprentice (1899-1900), Union Iron Works, San Francisco, Calif.; resident engineer (1900-1903) on the Mokelumne River development, Mokelumne Hill, Calif.; junior electrical engineer (1903-1904) for Westinghouse Electric and Manufacturing Company, Pittsburgh, Pa.; resident engineer,

¹ Abstract of memoir prepared by Harold F. Holley, M. ASCE.

² Abstract of memoir prepared by Leslie W. Stocker, M. ASCE.

and later deputy state engineer, (1904-1908) for the California State Board of Prison Directors. He was resident engineer (1908-1912) for the Snow Mountain Power Company at Potter Valley, Calif.; assistant engineer (1912) to consulting engineers C. E. Grunsky and John R. Freeman for the city of San Francisco; and chief field engineer (1912-1913) of the Oro Development Company on the Feather River in California. He served San Francisco as assistant city engineer (1913-1920); chief assistant city engineer (1920-1930); and general manager and chief engineer (1930-1949) of the water department. In 1949 he retired and entered private engineering practice.

Mr. Eckart was a member of civic and social organizations as well as President of the San Francisco Section of the Society in 1927.

He was married to Grace Knowlton on December 26, 1913, in San Francisco. He is survived by his widow; a son, William Nelson; two daughters, Mrs. Eleanor Matteson and Elizabeth; a brother; and four grandchildren.

Mr. Eckart was elected an Associate Member of the Society on November 1, 1905, and a Member on January 3, 1911. He became a Life Member in 1940.

WILLIAM GILBERT FARGO, M. ASCE¹

DIED FEBRUARY 2, 1957

William G. Fargo, the son of William H. and Nellie (Gilbert) Fargo, was born in Jackson, Mich., on December 6, 1867. He received his elementary and high school education in Jackson, and acquired his engineering education mostly by home study and correspondence courses.

Mr. Fargo did general surveying and mapping privately (1888-1892) and was employed by the Consumer's Power Company of Jackson as consulting engineer (1895-1925). He made appraisals and reports and designed and supervised the construction of many projects for N. W. Harris, Chicago, Ill.; Graham & Company, Philadelphia, Pa.; and supervised the hydroelectric work of the Indiana-Michigan Electric Company, South Bend, Ind. (1915-1925). From 1913 to 1925 he was a partner in the Fargo Engineering Company (Jackson). During those years sixty-one hydroelectric developments and nine major steam plants were designed and constructed as well as structural designs for high-tension transmission lines, special towers, substations, and office and factory buildings.

Mr. Fargo was very active in the civic affairs of Jackson, including many phases of zoning and city development. His lifelong study of mineralogy and geology was fully realized when he became curator of birds for the Michigan Museum of Zoology, Ann Arbor, Mich., in 1927, and honorary curator of

¹ Abstract of memoir prepared by James S. Bowman, M. ASCE.

paleozoology in 1943. He contributed more than thirteen thousand bird specimens, skins, and skeletal material from North and South America to the museum.

Mr. Fargo was elected a Member of the Society on April 1, 1908. He became a Life Member in 1938.

JOHN DAYTON FAYLOR, A.M. ASCE¹

DIED MARCH 19, 1958

John Dayton Faylor, the son of Ernest and Helen (Cressman) Faylor, was born on February 14, 1915, in Quakertown, Pa. He was graduated from Lafayette College (Easton, Pa.), in 1936, with the degree of Bachelor of Science in civil engineering.

Immediately following graduation, he was employed by Armeo Drainage & Metal Products, Inc., as a trainee in their mills in Middletown, Ohio. During the succeeding years he advanced to various positions within that organization. In 1937 he was transferred to the Ingot Iron Railway Products branch as a construction supervisor, later becoming district manager of the construction division. In March, 1946, he was appointed division sales engineer of the Iowa-Nebraska division of Armeo, and in 1953 he became its division sales manager. At the time of consolidation (1956) of the Iowa-Nebraska and the Missouri-Kansas divisions of Armeo, Mr. Faylor was division sales manager for the four-state group, a position he held until his death.

Mr. Faylor was a member of the Iowa Engineering Society, Phi Beta Kappa, Topeka Engineers' Club, Kansas Engineering Society, and the Masonic Lodge.

On March 21, 1939, in Middletown, Ohio, he was married to Ruth Bauer. He is survived by his widow.

Mr. Faylor was elected an Associate Member of the Society on April 12, 1948.

EDWIN MORRELL GRIME, M. ASCE²

DIED FEBRUARY 7, 1959

Edwin Morrell Grime, the son of John and Emma (Morrell) Grime, was born on July 1, 1876 in Minneapolis, Minn. He was graduated with the degree of Bachelor of Science in civil engineering from the University of Minnesota, Minneapolis, in 1900.

¹ Abstract of memoir prepared by Harvey B. Leaver, A.M. ASCE.

² Abstract of memoir prepared by Harold R. Peterson and Carl E. Ekberg, Members, ASCE.

From 1900 to 1907 he served the Chicago Great Western Railway in various capacities and attained the rank of division engineer. From 1907 to 1946 he was employed by the Northern Pacific Railway, becoming bridge and building supervisor on April 1, 1909. For six months he worked on a special committee that surveyed water resources and requirements for the railway. Thereafter, he was transferred to St. Paul, Minn., in 1925 to become the Northern Pacific Railway's first engineer of water service, a position he held until his retirement on December 31, 1946.

Mr. Grime pioneered in the field of railroad water for steam locomotives and power plants on the Northern Pacific Railway. The results of his accomplishments permitted extension of locomotive runs and important reductions in the cost of locomotive operation.

Mr. Grime was a member of many professional and civic groups including the American Railway Engineering Association, American Water Works Association, Engineers' Society of St. Paul, Minnesota Geological Society, and the A. F. & A. M. He was senior warden and a member of the vestry of St. Clement's Episcopal Church. He was President of the Northwestern Section of the Society from 1946 to 1947.

In September, 1908 he was married to Grace C. Horton at Seattle, Wash. He is survived by a daughter, Elsie, and a sister.

He was elected a Member of the Society on June 10, 1940.

EUGENE GROVE HAINES, M. ASCE¹

DIED JANUARY 11, 1959

Eugene Grove Haines, the son of William and Caroline (Fanning) Haines, was born on April 22, 1874 in Catskill, N. Y. He studied engineering through a correspondence course with the Colliery Engineering Company of Scranton, Pa.

He was a surveyor for Evans Brothers in Jamaica, N. Y. (1891), transitman and draftsman with the Long Island Railroad (1892-1899), and resident engineer for the following railroads: West Virginia Short Line Railroad (1899-1901), Western Maryland Railroad during 1902, and the Long Island Railroad (1902-1904). In October, 1904 he served as assistant engineer on subway and tunnel construction for the Rapid Transit Railroad Commission of the City of New York, which in 1907 came under the jurisdiction of the Public Service Commission and, later, the Board of Transportation. Except for a short period in 1909 when he worked on the Catskill Aqueduct at New Paltz, N. Y., for the Board of Water Supply he was engaged in subway and tunnel construction in Manhattan, Brooklyn, and Queens, and was also in charge of various subway and tunnel projects.

¹ Abstract of memoir prepared by Aksel H. Jorgensen and Arthur I. Heim, Members, ASCE.

During the latter part of his career serving New York City, he was in charge of arbitration of contractors' claims for extra work in connection with subway and tunnel construction. He worked for the Federal Emergency Administration of Public Works after his retirement in 1933 and resumed his retirement in May, 1934 to live at Roxbury, Conn.

On September 6, 1916, he was married to Anna J. Heim in Richmond Hill, N. Y. His first wife, Betsy Tuthill Saxton, died in July, 1915. He is survived by his widow; a daughter, Dora (Mrs. Edward Grace); a granddaughter; and two great-grandsons.

Mr. Haines was elected an Associate Member of the Society on May 1, 1901 and a Member on April 5, 1910. He became a Life Member in 1936.

THADDEUS LEON EUCLID HAUG, M. ASCE¹

DIED OCTOBER 22, 1957

Thaddeus Leon Euclid Haug, the son of John and Ida (Lowe) Haug, was born in Philadelphia, Pa., on October 31, 1885. He was graduated from the University of Pennsylvania at Philadelphia, with the degree of Bachelor of Science in mechanical engineering, in 1907.

After gaining experience as an apprentice machinist with the Pennsylvania Railroad at Altoona, Pa. (1905-1906) and various engineering services for the Union Iron Works and C. C. Moore and Company, both in San Francisco, Calif. (1907-1912), he spent four years designing and developing Diesel engines (1912-1916) for John Haug, Consulting Engineer, San Francisco. Following a period as industrial engineer with A. Schilling and Company, San Francisco, principally on salt works (1916), he became assistant marine superintendent with the Bethlehem Shipbuilding Corporation, Ltd., Alameda, Calif. (1916-1921). Records were established during World War I for launching ships (twenty-three days from laying the keel to launching) largely due to Mr. Haug's methods of expediting and lining up the ship for machine installations.

With diminution of shipbuilding, after serving as automobile design engineer with Doble Steam Motors, San Francisco, (1922-1923) and structural designer with Pacific Portland Cement Company (1923-1924), he served with the East Bay Municipal Utility District, Oakland, Calif., at which time he designed the Pardee Dam and Inlet Tower (1924-1929). Following an interim period with Verde River Irrigation and Power District, Phoenix, Ariz., on similar structures (1930-1931) and various engineering projects in 1932 and 1933, he returned to the East Bay Municipal Utility District in 1934 to become senior designing engineer. He served in this capacity until his retirement in 1950. It was during the latter period that the design for flexible steel supports for long-

¹ Abstract of memoir prepared by Robert C. Kennedy, M. ASCE.

span pipelines, as used on the second Mokelumne Aqueduct, and proposed for the larger new third aqueduct, was developed. He obtained patents on this as well as on other inventions.

On November 11, 1918, he was married to Marie C. Sidle at San Jose, Calif. He is survived by his widow; two daughters, Audrey B. (Mrs. Edward E. Anderson, Jr.) and Roxanne Marie; a brother; and four grandchildren.

Mr. Haug was elected a Member of the Society on November 15, 1926. He became a Life Member in 1956.

CHRISTOPHER FRANK HEISELMAN, A.M. ASCE¹

DIED DECEMBER 22, 1957

Christopher Frank Heiselman, the son of John and Anna (Neebe) Heiselman, was born on March 2, 1906, in Kingston, N. Y.

From September, 1929, to May, 1932, Mr. Heiselman was employed by the New York State Department of Public Works on highway projects, and served the city of Kingston from May, 1938, to November, 1938, as Superintendent of the Board of Public Works.

On November 15, 1938, he joined the staff of the Board of Water Supply (New York, N. Y.) as an engineering inspector and rose to the rank of civil engineer in that department. Mr. Heiselman's work was in the field of soil mechanics. He was active in that field during the planning and construction of the following: Merriman Dam (Rondout Creek), Neversink Dam (Neversink River), and Downsville Dam (east branch of the Delaware River), all in New York State. At the time of his death he was engaged in investigations for a proposed dam on the west branch of the Delaware River.

On December 24, 1930, Mr. Heiselman was married to Gertrude Welanetz at Cornwall, N.Y. He is survived by his widow; a son, Kurt; and two daughters, Anna Christine and Isobel.

Mr. Heiselman was elected an Associate Member of the Society on November 10, 1941.

HARRY HEMMINGS, A.M. ASCE²

DIED SEPTEMBER 27, 1958

Harry Hemmings, the son of Harry and Agnes Louise (Scannevin) Hemmings, was born on March 6, 1896 in Fredericksburg, Va. He was graduated from Cornell University, Ithaca, N. Y., with the degree of Civil Engineer in 1917.

¹ Abstract of memoir prepared by Thomas W. Fluhr, M. ASCE.

² Abstract of memoir prepared by Nathan Chernlack, M. ASCE.

He was employed as an assistant engineer, Curtiss Engineering Corp., New York, N. Y. (1917-1919); served with the United States Navy Bureau of Construction and Repair, Washington, D.C. (1919-1920); and was a member of the staff that drew up the Regional Plan and Its Environs (New York, N. Y.) between 1922 and 1926. He held the positions of designer, Louisville Bridge & Iron Company, Ky. (1927-1928); designer of dams and evaluation engineer, International Paper Company, New York (1928-1929); and traffic engineer, Robinson & Steinman, New York (1929-1930). In 1930 he became associated with the Metropolitan Life Insurance Company as an evaluation engineer and assistant to the vice-president on city mortgages. He was also adjunct professor of traffic engineering and city planning at Brooklyn Polytechnic Institute, N. Y. (1940-1958).

He was member of the Institute of Traffic Engineers as well as being its founder.

On January 27, 1924 he was married to Esther Turk at Geneva, N. Y. He is survived by his widow; five sons, Robert S., John S., Nicholas J., Anthony T., Richard B.; and a daughter, Pamela.

Mr. Hemmings was elected an Associate Member of the Society on February 25, 1924.

CHARLES STEPHEN HILL, M. ASCE¹

DIED JUNE 13, 1957

Charles Stephen Hill, the son of Benjamin F. and Mary L. (Rimmer) Hill, was born in Canton (Miss.) on August 1, 1905. He was graduated from Mississippi Agricultural and Mechanical College (Starkville, Miss.), with the degree of Bachelor of Science in civil engineering in 1925.

Immediately after graduation, Mr. Hill taught summer school mathematics in the Canton public schools. Thereafter his career was spent on various phases of bridge building. He was employed as a draftsman (1925) in the bridge section of the Mississippi State Highway Department in Jackson (Miss.); assistant state bridge engineer (1927-1929); assistant project engineer for the construction of the Biloxi Bridge, Miss. (1929-1930); assistant district engineer at Hattiesburg, Miss. (1931-1934); and served as chief bridge engineer for the Mississippi State Highway Department (1934-1951). He was employed by the firm of Hazelet and Erdal, Consulting Engineers, Louisville, Ky. (1951); and was resident engineer on the Mississippi Gulf Coast (1951-1954), where he was in charge of the construction of the Bay Saint Louis Bridge and Pascagoula River Bridge on U. S. 90. He did private consulting work in Jackson (1955), was a bridge engineer for the State Air Road Division, and held the position of assistant bridge engineer with the firm of Michael Baker, Jr., Inc., in Jackson.

¹ Abstract of memoir prepared by Edwin E. Ware, J.M. ASCE.

Mr. Hill was a member of the A.F. & A.M., and attended the First Baptist Church as well as belonging to many professional organizations. He was the recipient of numerous awards for outstanding work in his field.

On September 28, 1935, he was married to Helen Francis Bolton at Jackson. He is survived by his widow; a daughter, Janice; and three brothers.

Mr. Hill was elected a Member of the Society on September 1, 1950.

HOWARD HOWIE, M. ASCE¹

DIED MARCH 20, 1958

Howard Howie was born on July 22, 1879, at Cheboygan, Mich. He worked his way through the University of Michigan (Ann Arbor) by doing diving and salvage operations around the Great Lakes, and in 1905 received Bachelor of Science degrees in both Civil Engineering and Marine Engineering. He was fullback on Michigan's famous "Point-a-Minute" football team.

In Chattanooga, Tenn., Mr. Howie served as assistant city engineer (1906-1913), and as an appraisal estimator for the ICC (1914-1915). He was later connected with metal companies in Tennessee, Virginia, and Ontario, including the Roane Iron Company at Rockwood, Tenn. (1918-1932), where he rose from chief engineer to general manager. He was employed by the TVA (1934-1943), becoming in 1940 the chief of the Chemical Engineering Design Division. He was president of Knoxville Iron Company (1943-1944), employed in the Special Design Division of Fulton Sylphon Company (1944-1948), and for his last ten years he was engineer statistician for the Knoxville Utilities Board.

During the 1932-1933 period he was known as a "great white father" for his many kind deeds and aid when people were hungry. He is said to have greatly helped families who were bereaved because of mine explosions.

Mr. Howie married Ruth Naomi Hill, a native of Indiana. He is survived by his widow and one son, Howard Richmond Howie.

He was a member of The Technical Society of Knoxville, the American Society of Mechanical Engineers, and the American Institute of Mining and Metallurgical Engineers.

He was elected a Junior of the Society on March 6, 1906; an Associate Member on December 6, 1910; and a Member on June 4, 1913. He became a Life Member in 1945.

¹ Abstract of memoir prepared by Robert Forbes, A.M. ASCE.

CHARLES JENSEN, A. M. ASCE¹

DIED OCTOBER 24, 1958

Charles Jensen, the son of Frands Peder and Maren Christine (Jensen) Jensen, was born in Aarhus, Denmark, on September 8, 1895.

In 1919 he was employed by the Price-Evans Foundry Corporation in Chattanooga, Tenn., as a draftsman. In 1921 he entered the Georgia Institute of Technology, and was graduated with the degree of Bachelor of Science in mechanical engineering in 1925. After graduation he worked as draftsman, designer, and office engineer for J. B. McCrary, consulting engineer of Atlanta, Ga., until June, 1932. Mr. Jensen was employed by the Tennessee Valley Authority in November, 1933, as a computer in the highway and railroad division, now a part of the civil design branch of the Authority. He retired in September, 1957, with the title of civil engineer, after twenty-four years of service. During that time he had an active and responsible part in the location and design of many major highway and railroad projects. In later years, he was responsible for the design of site grading, storm drainage, railroad yards, and related work for the Kingston Steam Plant, near Kingston, Tenn. During his retirement Mr. Jensen became affiliated with the firm of Sullivan and Hoebel, consulting engineers of Chattanooga, as a civil engineer, a position he held until his death.

Mr. Jensen was a member of the A.F. & A. M., the Lutheran Church, and the American Legion. He was active in the Tennessee Valley Section of the Society. During World War I he served as sergeant in the United States Army. In 1919 he was awarded American citizenship on the basis of his military record.

He was married on November 26, 1921, in Chattanooga, to Beatrice Baldwin. He is survived by his widow; two daughters, Aline (Mrs. William T. Smith) and Barbara (Mrs. Ray E. Watson); and a granddaughter.

Mr. Jensen was elected an Associate Member of the Society on December 16, 1946.

ANDRE LAURENT JORISSEN, M. ASCE²

DIED FEBRUARY 27, 1958

Andre Laurent Jorissen, the son of Jacques and Marguerite (Daubecourt) Jorissen, was born on January 17, 1913, in Liege, Belgium. He was graduated from the University of Liege with the degree of Bachelor of Science in civil

¹ Abstract of memoir prepared by Robert H. Nagel, A.M. ASCE.

² Abstract of memoir prepared by Paul G. Mayer, A.M. ASCE.

engineering in 1935, and in 1936 was awarded the degree of Master of Science in civil engineering from the Massachusetts Institute of Technology (Cambridge), where he was a Fellow of the Belgian-American Educational Foundation. In 1949 he received the degree of Doctor of Science from the University of Liege.

He was an associate of the Belgium National Fund for Scientific Research (1943-1949), an Advanced Fellow of the Belgium-American Educational Foundation (1946), and a scientific advisor (1947) to the Laboratoire Central d'Hydraulique at Paris.

In 1949 he joined the teaching and research staff of the Pennsylvania State University (University Park) as a professor of civil engineering. In 1951 he was awarded a Hooker Fellowship from Cornell University (Ithaca) and, subsequently, became the head of the department of hydraulics and hydraulic engineering in its school of civil engineering.

Throughout his lifetime, Mr. Jorissen wrote many papers dealing with fluid metering devices. He was interested in Napoleonic and United States history as well as being an ardent stamp collector and traveler. He was a member of numerous American and foreign engineering societies as well as many honorary societies.

On October 6, 1937, he was married to Lucy Moulinasse at Brussels, Belgium. He is survived by his widow and a daughter, Anne.

Mr. Jorissen was elected an Associate Member of the Society on November 7, 1949, and a Member on April 29, 1955.

ARTHUR DALE KIDDER, M. ASCE¹

DIED JUNE 13, 1958

Arthur Dale Kidder, the son of Willard and Louise (Kendall) Kidder, was born in Terre Haute, Ind., on March 26, 1876. He received the degrees of Civil Engineer from Rose Polytechnic Institute at Terre Haute, Master of Science from George Washington University, Washington, D. C., in 1901, and an honorary degree of Doctor in Engineering from Rose Polytechnic Institute in 1949.

In 1899 he became superintendent of the Blue Bell Mining Company at Webb City, Mo. In 1901 Mr. Kidder was surveyor at the General Land Office, United States Department of the Interior, at Washington, D. C. He held the following positions with the United States Department of the Interior: Surveyor (1901-1911), supervisor of surveys (1911-1918), associate supervisor of surveys (1918-1940), and district cadastral engineer (1940-1947). In 1947 he became a senior member of Kidder and Thoma, Cadastral Engineers.

From 1910 to 1947 he prepared astronomical annuals to meet the needs of

¹ Abstract of memoir prepared by Joseph C. Thoma, M. ASCE.

the General Land Office and was editor for the Manual of Surveying Instructions for surveying public lands. He acted as surveyor in the opening of the Kiowa and Comanche Indian reservation in Oklahoma, and was appointed by the United States Supreme Court as one of the two boundary commissioners to locate and mark the Texas and Oklahoma boundary along Red River, as well as the New Mexico and Colorado boundary. Another phase of his work included improvements in the adjustments of the solar transit.

He was a member of many scientific associations including the American Congress on Surveying and Mapping, and the Wisconsin Society of Land Surveyors.

He was married to Fidelia Royse in 1904 at Terre Haute, Ind. He is survived by a son, Arthur Royse; a sister; a brother; and two grandchildren.

Mr. Kidder was elected a Member of the Society on July 6, 1925. He became a Life Member in 1950.

JACK ADELBERT KILLALEE, A.M. ASCE¹

DIED NOVEMBER 17, 1957

Jack Adelbert Killalee, the son of John Joseph and Ethel Charlotte (Frederick) Killalee, was born in San Francisco, Calif., on July 17, 1889. During World War I, he served in the 157th Ambulance Corps and attained the rank of sergeant. He was graduated from the University of California, Berkeley, in 1925, with the degree of Bachelor of Science in civil engineering.

In 1925 he was employed as junior highway engineer by the Bureau of Public Roads, United States Department of Commerce (BPR), and served on various assignments in survey and construction on national forest and national park highways in California and Arizona. In 1935 he was transferred to the land planning section. He served with the BPR in Alaska on the construction of the Alcan Highway, Alaska-Canada (1943); assistant division engineer in Turkey for the Aid to Greece and Turkey Program (1947-1950); and highway planning engineer (1950-1955) in San Francisco. He retired in March, 1955. In April, 1955, he became a consultant for Tippetts-Abbett-McCarthy-Stratton, and served as advisor to the Lebanon Ministry of Public Works on the construction of Lebanon's first divided highway and on the survey of the Damascus-Beirut Highway (1955-1957).

Mr. Killalee was a member of the A.F.&A.M., the Highway Research Board, and Argonaut Lodge 461.

He was married on April 6, 1927, to Gladys Emilie Thompson in San Francisco. He is survived by his widow, and a daughter, Nancy May.

Mr. Killalee was elected an Associate Member of the Society on September 8, 1947.

¹ Abstract of memoir prepared by Henry Raymond Angwin, M. ASCE.

FREDERICK LAURENCE KLEIN, M. ASCE¹

DIED FEBRUARY 16, 1958

Frederick Laurence Klein, the son of Laurence and Lucy (Arthur) Klein, was born in New Haven (Conn.), on October 6, 1889. He completed the civil engineering course at the Sheffield Scientific School of Yale University (New Haven) and was graduated with the degree of Bachelor of Philosophy in 1912.

After graduation he worked successively for the American Bridge Company, the city of Philadelphia, and the bridge department of the Oregon Highway Department. In November, 1922, he was appointed highway bridge engineer by the Bureau of Public Roads, United States Department of Commerce, at Phoenix (Ariz.), where he served as district bridge engineer until July, 1925. At that time he was transferred to the regional office (later designated western headquarters of the United States Department of Commerce). In December, 1928, he became chief designer and first assistant to the chief, in which capacity he served until his death. During this period he supervised the designing of more than 1,200 bridges for federal projects in national forests and parks in eleven western states, Hawaii, and Alaska.

Mr. Klein was a member of Pacific Lodge No. 50, A.F.&A.M. of Salem (Ore.), Yale Alumni Association, and the First Presbyterian Church of Berkeley (Calif.).

He was married to Ida Josephine Osborne on January 1, 1915, in Philadelphia, Pa. He is survived by his widow; a daughter, Isabel (Mrs. O. Kusick); and two brothers.

Mr. Klein was elected a Member of the Society on March 3, 1952.

HANS KRAMER, M. ASCE²

DIED FEBRUARY 16, 1957

Hans Kramer, the son of Adolph and Toni Kramer, was born at Magdeburg, Germany, on December 12, 1894. He was a student at the University of Michigan from 1912 to 1913, and was graduated from the United States Military Academy at West Point, N.Y., in 1918. He was graduated from the civil engineer course of the Army Engineer School at Fort Belvoir, Va., in 1927; received the degree of Master of Science from the University of Pennsylvania, Philadelphia, in 1928; and was graduated from the company officers' course of the Army Engineer School, in 1929.

¹ Abstract of memoir prepared by Henry Raymond Angwin, M. ASCE.

² Abstract of memoir prepared by Dwight F. Johns, M. ASCE.

In 1930 he was awarded the John R. Freeman traveling scholarship from the Society, and received the degree of Doctor of Engineering from the Technical University of Dresden, Germany, in 1932.

Mr. Kramer participated actively throughout his military career in the civil and military activities of the Corps of Engineers (United States Department of the Army). He served as professor of Military Science and Tactics at the California Institute of Technology at Pasadena (1920-1924); area engineer and chief of operations in Memphis, Tenn. (1932-1935); district engineer for the Conchas Dam Project in New Mexico (1936-1939); and assistant supervising engineer, and supervising engineer of the Panama Canal (1939-1942). He attained the rank of brigadier general in 1942. In that year he was transferred to Hawaii where he became, in succession, department engineer of the Hawaiian department (September, 1942), and theater engineer of the Central Pacific Theater (June, 1943). After his retirement in 1945 he was a consultant on many hydroelectric projects.

Mr. Kramer was a member of numerous professional, civic, and honorary organizations, as well as a registered civil engineer in California.

On May 20, 1939, he was married to Alice Elizabeth Harvey in Washington, D. C. He is survived by his widow and a son, Hans Harvey.

He was elected a Junior of the Society on November 25, 1919, an Associate Member on December 15, 1924, and a Member on May 28, 1934.

KENNETH WINANS LEFEVER, M. ASCE¹

DIED FEBRUARY 21, 1957

Kenneth Winans Lefever, the son of Henry Donaldson and Grace (Winans) Lefever, was born on May 17, 1897, in Jackson, Miss. He received his education in Little Rock, Ark.

His first engineering assignment was with the firm of Lund & Hill (Little Rock) in 1916 in the capacity of rodman. In 1917 he became associated with the firm of Ford & McRae as instrument man and in 1944 became a partner of McRae, Bair, and Lefever, all of Little Rock. In 1945 he established his own firm of Kenneth W. Lefever, Consulting Engineer. Mr. Lefever worked on various projects, including the Hot Springs Waterworks and Dam, Searing Water Plant, Little Rock Airport Construction, and several government housing projects in Little Rock. He was employed also by the city of Little Rock as consulting engineer on the Maumelle Water Project, at which time he was associated with the firm of Lefever, Mehlburger & Pirnie.

In 1943 he became president of the Arkansas Society of Professional Engineers (Little Rock), and in 1956 became President of the Mid-South Section of the Society. He was president of the Arkansas Engineers Club (1956), and a

¹ Abstract of memoir prepared by Max A. Mehlburger, M. ASCE, and Barney B. Brown.

member of the Little Rock Engineers Club, the chamber of commerce, and St. Paul's Methodist Church. His various hobbies included stamp collecting and woodworking.

On January 8, 1922, Mr. Lefever was married to Alice Hopkins at Alexandria, La. He is survived by his widow; a son, Kenneth, Jr.; two sisters; and a grandchild.

Mr. Lefever was elected a Junior of the Society on September 11, 1917, an Associate Member on November 12, 1928, and a Member on March 10, 1941.

ANDREW CAVITT LOVE, M. ASCE¹

DIED SEPTEMBER 5, 1958

Andrew Cavitt Love, the son of Benjamin F. and Amelia M. (West) Love was born on April 1, 1876, near Calvert, Tex. He was graduated from the Agricultural and Mechanical College of Texas at College Station with the degrees of Bachelor of Science in civil engineering in 1899, and Civil Engineer in 1917.

He was assistant professor of drawing at the Agricultural and Mechanical College of Texas (1899-1903); field engineer for the Santa Fe Railroad (1903-1904); resident engineer for the Southern Pacific Railroad (1904-1908); general superintendent, Beaumont Irrigation Company, Beaumont, Tex. (1908-1912); and in 1912 established and organized the Love Abstract Company, Franklin, Tex. with his brother Ben C. Love. In 1913 he became associate professor of civil engineering and superintendent of buildings and grounds at the Agricultural and Mechanical College of Texas where he remained until 1920. At that time Mr. Love became district engineer with the Texas State Highway Department. He held many positions, both for the state and for Jefferson and Liberty Counties, including that of state highway engineer until his retirement in 1947.

After his retirement he visited various Indian tribes in Oklahoma, New Mexico, and Arizona, in order to teach the Boy Scout dance teams tribal dances and ceremonies. He maintained an active interest in his Alma Mater, serving as president of the Former Students Association from 1911 to 1912, and was a member of the A.F. & A.M., the Baptist Church, and the Rotary Club of Beaumont.

On June 20, 1899 he was married to Laurel Sronce at Houston, Tex. He is survived by his widow; a daughter, Jeane Love Bonner; and a son, Alan C.

He was elected an Associate Member of the Society on February 6, 1907 and a Member on September 3, 1912. He became a Life Member in 1947.

¹ Abstract of memoir prepared by Carl E. Sandstedt, M. ASCE.

LEON WADDELL MASHBURN, M. ASCE¹

DIED JUNE 15, 1958

Leon Waddell Mashburn, the son of James Edward and Eliza Jane (Carter) Mashburn, was born in Bolivar, Tenn., on September 5, 1881. He studied civil engineering at the University of Tennessee, Knoxville.

He was drainage engineer with the Corps of Engineers, United States Department of the Army, along the Wabash River, Ind.; served on the original Mississippi River Levee System (1910-1915); location engineer for various railroads in Alabama; and organized and operated the Southern Engineering Company of Clarksdale, Miss., in the design and supervising of road construction and drainage projects throughout the Mississippi Delta. Mr. Mashburn was instrumental in the development of the Mississippi Delta Area from a swampland into a fertile farm territory by the construction of drainage canals, levees, and roadways. In 1932 Mr. Mashburn became drainage and irrigation project appraiser for the Reconstruction Finance Corporation working throughout the United States, a position he held until his retirement in 1950. From that time until his death he managed his farm properties in Mississippi and Arkansas.

Mr. Mashburn was a member of the A.F. & A.M., the Elks, and was a Shriner and a Rotarian. He was an active member of the Presbyterian Church.

He was married on May 7, 1906 to Pearl Roach of Collierville, Tenn. He is survived by a son, Leon, Jr.; two daughters, Anne (Mrs. Graves Sproles) and Janie; and five grandchildren.

He was elected an Associate Member of the Society on May 6, 1914 and a Member on April 21, 1920. He became a Life Member in 1949.

FRANK DUFF McENTEER, M. ASCE²

DIED SEPTEMBER 4, 1957

Frank Duff McEnteer, the son of Michael J. and Carrie (Andrews) McEnteer, was born in Reynoldsville, Pa., on May 23, 1882. He received the degree of Bachelor of Arts from Harvard University, Cambridge, Mass., in 1905.

From 1905 to 1912 he worked in the capacities of draftsman, designer, and construction engineer for various steel companies. From 1912 to 1932 he was president and general manager of the Concrete Steel Bridge Company, Clarksburg, W. Va. Mr. McEnteer was responsible for the first reinforced-concrete building to be built in Clarksburg. He was associated with the State Road

¹ Abstract of memoir prepared by Francis Marion Brewer, M. ASCE.

² Abstract of memoir prepared by Roland P. Davis.

Commission of West Virginia as a district engineer (1932-1938), and later as a construction engineer (1938-1940).

In 1942 he accepted a position with Johnson, Drake and Piper, Inc., as project engineer in Tel Aviv and in 1943 became an assistant foreign manager in the construction of an army base and hospital in Palestine. In 1944 he was chief engineer, construction division, United States Army Forces, Middle East (USAFIME) in Cairo, Egypt, in connection with the construction of airports. In 1944 he set up a consulting office in Clarksburg which he maintained until his death.

Mr. McEnteer held executive positions in many professional and civic organizations and was a member of various fraternal organizations. He was President of the West Virginia Section of the Society in 1950.

On April 6, 1910, he was married to Jessie Louise Horner of Dubois, Pa. He is survived by his widow; two daughters, Caroline (Mrs. Merlin H. Aylesworth) and Mary Louise (Mrs. John R. Horner); a sister; and two grandchildren.

Mr. McEnteer was elected a Member of the Society on November 21, 1931, and became a Life Member in 1953.

THURMOND ARMOUR MUNSON, M. ASCE¹

DIED OCTOBER 6, 1958

Thurmond Armour Munson, the son of Joseph W. and Mary C. (West) Munson, was born on June 15, 1889, at Columbus, Tex. He was graduated from the Agricultural and Mechanical College of Texas at College Station with the degree of Bachelor of Science in civil engineering in 1910. He received the degrees of Civil Engineer from the Iowa State College at Ames, Iowa, in 1924, and Master of Science in civil engineering in 1925.

He was employed as assistant engineer, Fort Bend County, Tex. (1910-1911), and sanitary engineer, Tolman Engineering Company, Houston, Tex. (1911-1912). From 1913 to 1921 he established a general consulting practice dealing with drainage projects, flood control, highway surveys, land surveys, and subdivisions. He became an associate professor (1920) and a professor (1926) of hydraulic engineering at the Agricultural and Mechanical College of Texas. In 1946 he accepted the position of chief civil engineer for the Dow Chemical Company at Freeport, Tex., and continued in that position until his retirement in 1955. During his professional career Mr. Munson made surveys and reports on highway and public utility locations. He was also well known as a hydraulic engineer and an expert on land boundary suits. Mr. Munson was Lieutenant Colonel of the Inspector General Department during World War II.

He was a member of the City Council of College Station (1940-1942); acted as city engineer (1946); was a member of Tau Beta Pi; and a registered Professional Engineer of the State of Texas.

¹ Abstract of memoir prepared by Carl E. Sandstedt, M. ASCE.

On December 21, 1929 he was married to Mary Harwick at Stephenville, Tex. He is survived by his widow; a son, Thurmond A. Munson, Jr.; a daughter, Mary Jane Hirsch; a sister; and four grandchildren.

Mr. Munson was elected an Associate Member of the Society on May 28, 1923 and a Member on December 13, 1944. He became a Life Member in 1958.

CHARLES FERNALD NILES, M. ASCE¹

DIED DECEMBER 1, 1956

Charles Fernald Niles, the son of Laverna and Carrie (Fernald) Niles was born on July 3, 1895, in South Levant, Maine. He was graduated from the University of Maine (Orono) with the degrees of Bachelor of Science in civil engineering in June, 1919, and Civil Engineer in June, 1925.

His early experience consisted of various positions with the Delaware Highway Department, Dover (1919-1921). He was draftsman and resident engineer, North Carolina Highway Department (1921-1927); junior engineer, United States Engineers, Myrtle Beach, S. C. (1927-1928); resident engineer, Tennessee Highway Commission (1928-1931); inspector, draftsman, and resident engineer, Maine Highway Department (1932-1933); assistant engineer, Cherokee National Forest, Tenn. (1933-1938); and forest engineer, Kisatchie National Forest, La. (1938-1940). In November, 1940, he was transferred to the Ozark National Forest at Russellville, Ark., as forest engineer, a position he held until his death.

Mr. Niles was a veteran of World War I and a member of the American Legion. He held memberships in the Methodist Church; Tau Beta Pi; the American Military Engineers; the F. & A. M.; and other fraternal organizations.

On December 30, 1919 he was married to Olive Gladys Cook at Rumford, Maine. He is survived by his widow; a son, Charles, Jr.; a daughter, Mrs. Travis O. Morgan; four brothers; a sister; and eight grandchildren.

Mr. Niles was elected an Associate Member of the Society on August 16, 1948, and a Member on June 19, 1956.

ROBERT PRESTON PARKER, A.M. ASCE²

DIED JANUARY 18, 1957

Robert Preston Parker, the son of John Henry and Mildred Ellen (Lacy) Parker, was born in Richmond, Va., on May 6, 1868. He received the degree

¹ Abstract of memoir prepared by Henry C. Sellers, A.M. ASCE.

² Abstract of memoir prepared by Earl C. Meserve, M. ASCE.

of Bachelor of Science in civil engineering from Lehigh University (Bethlehem, Pa.) in 1892.

Mr. Parker's career covered a wide field of civil engineering, including land surveying and design and construction of railroads, highways, streets, sewers, water supply, and water distribution. From 1892 to 1927 he was employed as chief engineer of maintenance and construction for many national railway systems.

Mr. Parker worked from time to time with Coverdale and Colpitts (New York, N. Y.) from 1904 to 1920 as construction engineer. During World War II he assisted in the construction of Camp Polk (Leedville, La.) and in the maintenance of Longhorn Ordnance (Marshall, Tex.) and Pine Bluff Arsenal (Pine Bluff, Ark.). From 1945 to 1954 Mr. Parker, as city engineer, designed and supervised the construction of the water and sewerage systems in Star City (Ark.), and in 1953, designed and supervised an extension to its sewerage system.

Another highlight of Mr. Parker's colorful career was the four years he spent in Alaska during the gold rush of 1898-1902.

He was married to Blanche Porter in Jackson, Tenn., in 1919. He is survived by his widow; a daughter, Anne (Mrs. M. E. Nobles); and a son, Robert Porter.

Mr. Parker was elected an Associate Member of the Society on August 31, 1915, and became a Life Member in 1940.

JAMES LINDSAY PATON, M. ASCE¹

DIED MARCH 29, 1959

James Lindsay Paton, the son of John and Maud (Mathias) Paton, was born on January 23, 1910 in West Terre Haute, Ind. He was graduated from the Rose Polytechnic Institute, Terre Haute, with the degree of Bachelor of Science in civil engineering in 1933.

He held the positions of assistant project engineer (1933-1935); chief of survey party (1935-1936); and topographer (1936-1938) with the State Highway Commission of Indiana; and was engineer-inspector, Federal Works Agency at Indianapolis, Ind. (1938-1941). From April, 1941 to July, 1947 he served in the Corps of Engineers, United States Department of the Army, as chief in the Training Publication Section, The Engineer School, Fort Belvoir, Va.; assistant corps engineer (1942-1945); and engineer unit commander (1945-1947). He rose from the rank of first lieutenant to colonel. From 1947 until 1959 he was employed by Whitman, Requardt and Associates during which time he served on the Engineer Board of the Corps of Engineers.

Mr. Paton was a member of the National Society of Professional Engineers,

¹ Abstract of memoir prepared by A. Russell Vollmer, M. ASCE.

the Maryland Society of Professional Engineers, the Maryland-Delaware Water and Sewage Association, and the Society of American Military Engineers.

He was married to Bunetta F. Bixby. He is survived by his widow; two sons, John and James Lowell; and two daughters, Ellen and Jean.

Mr. Paton was elected a Member of the Society on May 6, 1957.

JOHN CHARLES RATHBUN, M. ASCE¹

DIED NOVEMBER 12, 1958

J. Charles Rathbun, the son of John Chauncey and Elizabeth (Goldenberg) Rathbun, was born in Mondovi, Wis., on March 14, 1882. He was graduated with the degrees of Bachelor of Arts (1903); Master of Arts (1904); Bachelor of Science in civil engineering (1908); and Civil Engineer (1909) from the University of Washington, Seattle. In 1934 he received the degree of Doctor of Philosophy in civil engineering from Columbia University, New York, N. Y.

He taught in Amoy, China (1904-1906); served with the Bureau of Public Works in the Philippine Islands, as designing engineer for the consulting architect (1912-1915); and was superintendent of bridge construction for the City of Seattle, Wash. (1915-1918). He became assistant professor at the University of Washington (1919-1925); head of the Department of Civil Engineering, South Dakota State School of Mines, Rapid City, S. Dak. (1925-1929); professor, and head of Department, Antioch College, Yellow Springs, Ohio (1929-1931); and associate professor of civil engineering, The College of the City of New York (1931-1941); and professor (1941-1949). He retired as Emeritus Professor on February 1, 1949. Mr. Rathbun was a licensed Professional Engineer in South Dakota and New York. He was a member of the American Society of Engineering Education; the International Association of Bridge and Structural Engineers; the A.F. & A.M.; Shriners; and the Circumnavigation Club, N. Y. He was also a member of Phi Beta Kappa, Sigma Xi, and Tau Beta Pi.

On June 29, 1910 he was married to Dora Frances Breece in Seattle. He is survived by his widow; a daughter, Mary Charlotte (Mrs. Walter L. Dillinger); and four grandchildren.

He was elected a Junior of the Society on October 6, 1908; an Associate Member on May 6, 1914; and a Member on September 12, 1921. He became a Life Member in 1949.

¹ Abstract of memoir prepared by Sydney Willmot, M. ASCE.

DONALD JOSEPH SADAR, J.M. ASCE¹

DIED OCTOBER 13, 1956

Donald Joseph Sadar, the son of Joseph and Carmen (Bashor) Sadar, was born on September 20, 1931, at Denver, Colo. He was graduated from the Colorado State University (Fort Collins, Colo.) with the degrees of Bachelor of Science in civil engineering in June, 1952, and Master of Science in irrigation engineering in 1955.

During the summers of 1951 and 1952 he worked for the Bureau of Reclamation, United States Department of the Interior, and in the summer of 1953, he was employed by the Universal Engineering Company of Denver. From July, 1954, to November, 1954, he was employed by the Agricultural Research Service, United States Department of Agriculture, as an irrigation engineer. In 1954 he was issued a leave of absence for military service.

In February, 1955, he began his tour of active duty at the United States Army Engineer Waterways Experiment Station. Because of his academic training and experience, Mr. Sadar was assigned to the special investigations section of the hydraulics division, where he became a project engineer engaged in investigating hydraulic problems connected with the effects of atomic weapons.

Mr. Sadar was a member of Sigma Xi, Phi Kappa Phi, Sigma Tau, Chi Epsilon, Kappa Mu Epsilon, and Lancer. He was also an active member of the Methodist Church.

On September 6, 1953, he was married to Edith L. Stanton at Johnson, Kans. He is survived by his widow and his parents.

Mr. Sadar was elected a Junior Member of the Society on October 14, 1952.

THOMAS DUNCAN SAMUEL, JR., M. ASCE²

DIED MARCH 27, 1958

Thomas Duncan Samuel, Jr., the son of Thomas D. and Elizabeth (Naismith) Samuel, was born in Kansas City, Mo., on July 15, 1883. He attended the University of Kansas (Lawrence) and the University of Missouri School of Mines and Metallurgy at Rolla.

From 1906 to 1907 Mr. Samuel was employed as a draftsman by the Bell Telephone Company and by the engineering firm of Tuttle and Pike from 1907 to 1908 (both in Kansas City). From 1908 until his retirement in 1940, he was employed by the Kansas City, Missouri Water Department as a draftsman

¹ Abstract of memoir prepared by William J. Flathau, J.M. ASCE.

² Abstract of memoir prepared by Thomas D. Samuel III, M. ASCE.

(1908-1917); assistant engineer in charge of construction of the old Quindaro pumping station near Kansas City, Kans. (1917-1919); and chief draftsman (1919-1924), first assistant engineer (1924-1925), and chief engineer and superintendent (1925-1940).

Mr. Samuel was a member of numerous civic and technical groups. He was formerly President of the Kansas City Section of the Society (1937) and a life member of the Kansas City Engineers' Club (1957). He was also a member of the A.F.&A.M.; a Shriner; a member of the Westport Scottish Rite Lodge (Kansas City, Mo.), and a member of Beta Theta Pi, the Milburn Golf and Country Club, and the Presbyterian Church.

On May 9, 1905, Mr. Samuel was married to Alma Matilda Strobach in Rolla. He is survived by his widow; two sons, Charles F. and Thomas D. III; a sister; and three grandchildren.

Mr. Samuel was elected an Associate Member of the Society on March 15, 1926, and a Member on July 14, 1930. He became a Life Member in 1954.

ROBERT RADCLIFFE SHOEMAKER, M. ASCE¹

DIED JANUARY 26, 1958

Robert Radcliffe Shoemaker, the son of William C. and Mabel O. (Stein) Shoemaker, was born on July 17, 1897, in Lima, Ohio. He was graduated from Purdue University, Lafayette, Ind., in 1920 with the degree of Bachelor of Science in civil engineering. During World War I he served as an Army lieutenant.

From 1920 to 1939 he served at the Port of Los Angeles, Calif., in the capacities of structural engineer and civil engineer. He became chief harbor engineer at the Port of Long Beach, Calif. on January 1, 1940, and remained in that capacity until his death. He was largely responsible for the growth of the Port into one of the major facilities of its kind in the world.

Mr. Shoemaker was a member of Triangle, Tau Beta, and Sigma Xi. He was a member and served as president of the American Association of Engineers (in 1929 and 1941); the Los Angeles Engineering Council of Founder Societies (1953); and was a member of the Board of Directors of the Los Angeles Section of the Society and President (1950). Mr. Shoemaker was also a member of the Structural Engineers Association of California; the American Concrete Institute; the American and Pacific Coast Associations of Port Authorities; and chairman of the Port Construction and Development Committee from 1954 to 1957. He was affiliated with the Rotary Club, University Club, and Virginia Country Club, all of Long Beach.

On September 19, 1926 he was married to Roberta Allen in Long Beach. He is survived by his widow.

Mr. Shoemaker was elected a Member of the Society on May 18, 1943.

¹ Abstract of memoir prepared by Bob N. Hoffmaster, A.M. ASCE.

FREDERICK JOSIAH SPRY, A.M. ASCE¹

DIED DECEMBER 17, 1958

Frederick Josiah Spry, the son of Josiah and Elizabeth (Joel) Spry, was born in Plymouth, Pa., on October 18, 1888. He received the degrees of Bachelor of Science in civil engineering from Lafayette University, Easton, Pa. in 1914, and Master of Science in civil engineering from Cornell University, Ithaca, N. Y., in 1928.

From 1915 to 1922, except for a short term of military service, Mr. Spry worked as a maintenance-of-way engineer for the Lehigh Valley Railroad at Easton and Sayre, Pa., and in Auburn, N. Y. In 1922 he was assistant city engineer in Auburn. He became an instructor in the School of Civil Engineering at Cornell University in October, 1923, and in 1944 was appointed assistant professor. From 1944 to 1945 he taught geodetic surveying in the Navy V-12 program at Swarthmore College, Swarthmore, Pa. on a leave of absence. In 1949 he was appointed associate professor of civil engineering. He was secretary of the faculty of the School of Civil Engineering from 1950 until his retirement as an Emeritus Professor in June, 1956.

Mr. Spry was active in the Civil Engineering Surveying Camps of various universities in New York State. He was a member of numerous professional societies, and served as president (1955) of the Central New York Section of the American Society of Photogrammetry. He was a Charter Member of the Ithaca Section of the Society. He was active in the First Presbyterian Church, and in the Boy Scouts of America.

On August 27, 1919, he was married to Mary Williams in Plymouth, Pa. He is survived by his widow; a son, Frederick J.; and a granddaughter.

Mr. Spry was elected an Associate Member of the Society on February 25, 1924.

THOMAS JOHNSON STRICKLER, M. ASCE²

DIED NOVEMBER 20, 1958

Thomas Johnson Strickler, the son of Jacob Nissley and Mary (Johnson) Strickler, was born on May 21, 1883, in Topeka, Kans. He was graduated from Wentworth Military Academy, Lexington, Mo., in 1900, and completed graduate study in 1901. He received the degree of Bachelor of Science in civil engineering from the University of Kansas, Lawrence, in 1906. He also attended night classes at Washburn Law School in Topeka.

¹ Abstracts of memoir prepared by Arthur J. McNair, John E. Perry, Members, ASCE, and George E. Lyon, A.M. ASCE.

² Abstract of memoir prepared by Arlow V. Ferry, M. ASCE.

Mr. Strickler served with the United States Bureau of Reclamation in various engineering capacities from 1902 to 1910. He was assistant manager and engineer of the Federal Structural Steel Co., Cherryvale, Kans. (1910-1911); and assistant engineer (1911-1913) and chief engineer (1913-1920) of the Kansas Public Utilities Commission. He was admitted to the Kansas Bar in 1917, and the United States Supreme Court Bar in 1947. He served in the capacity of consulting engineer with the following companies: Empire Gas & Fuel Co. at Bartlesville, Okla. (1920-1922); Henry L. Doherty & Co., N. Y. (1922-1925); and the Gas Service Company, Kansas City, Mo. (1925-1927). Mr. Strickler was vice-president and general manager, Kansas City Gas Company (1927-1947). He also served in many executive positions with the Gas Service Company (1926-1956).

Mr. Strickler was extremely active in Kansas City community affairs, directing many fund-raising campaigns, and acting in an executive capacity for music and art institutions. He was a member of many professional, fraternal, and honorary societies.

On August 8, 1929, he was married to Margaret Jane Armstrong in Chicago, Ill.

Mr. Strickler was elected an Associate Member of the Society on May 3, 1910, and a Member on November 28, 1916. He became a Life Member in 1945.

RICHARD RANDOLPH TIPTON, M. ASCE¹

DIED OCTOBER 4, 1955

Richard Randolph Tipton, the son of Carl Grant and Elizabeth Marie (Dwyer) Tipton, was born on November 11, 1894, in Cheyenne, Wyo. He was graduated from the University of Washington in Seattle with the degree of Bachelor of Science in civil engineering in 1918.

For fourteen years he was engaged in professional work in Washington and Oregon and thereafter did two years of bridge contracting in California. In 1934 he began his twenty-one-year association with the Bureau of Public Roads, United States Department of Commerce, as associate bridge engineer (1934-1938); senior bridge engineer (1939-1941); senior structural engineer in the design and construction of bridges on the Alcan Highway, Alaska and Canada (1942-1943); and supervising engineer in charge of bridge and structural work in Iowa, Kansas, Missouri, and Nebraska (1946-1955). He retired in 1955 and entered private practice as a consulting engineer in Berkeley, Calif.

Mr. Tipton was a second lieutenant, United States Army, during World War I. He was a member of the Engineers' Club of Kansas City, Kans., Theta Xi, the A.F. & A.M., and the American Legion. He was active in Society

¹ Abstract of memoir prepared by George D. Whittle, M. ASCE.

affairs as Program Chairman (1950), Director (1951-1953), and President of the Kansas City Section (1954).

On August 11, 1922, he was married to Roberta Ann Heavens in Portland, Ore. He is survived by two sons, Richard Carl and Robert Randolph, and a granddaughter.

Mr. Tipton was elected an Associate Member of the Society on December 21, 1943, and a Member on November 7, 1949.

HARRY BRUCE WALKER, M. ASCE¹

DIED JULY 27, 1957

Harry Bruce Walker, the son of Henry Boyd and Margaret Alcinda (Yeast) Walker, was born near Macomb, Ill., on April 13, 1884. He received the degree of Bachelor of Science in civil engineering in 1910, and the degree of Civil Engineer in 1920 from Iowa State College (Ames). He completed additional graduate work at Kansas State College of Agriculture (Manhattan) in 1925.

After preliminary experience as a topographer for the Chicago, Burlington & Quincy railroad (1906), he served as drainage engineer for Humboldt County, Iowa (1909-1910); drainage and irrigation engineer, and extension engineer at Kansas State College of Agriculture (1910-1917); state irrigation engineer of Kansas (1913-1917); professor of agricultural engineering at Kansas State College of Agriculture (1921-1928); and professor of agricultural engineering and agricultural engineer (emeritus) in the experiment station at the University of California at Davis (1928-1950). During 1927-1928 he directed a survey for the United States Department of Agriculture, and in 1929, the President of the United States appointed him a delegate to the World Engineering Congress in Tokyo, Japan.

Mr. Walker was a member of numerous civic, professional, and honorary societies, and was active in the Community Church in Davis, Calif. He was active in the American Society of Agricultural Engineers and served as president for two terms (1924-1925, 1942-1943).

He was married to Coralie Harris, in 1912 at Bardolpa, Ill. He is survived by his widow; a daughter, Mary Margaret (Mrs. Alan Laidlaw); and a son, Boyd Wallace.

Mr. Walker was elected an Associate Member of the Society on June 24, 1914, and a Member on July 11, 1921. He became a Life Member in 1949.

¹ Abstract of memoir prepared by Jerald E. Christiansen, A.M. ASCE, Roy Balner, and Frank J. Veihmeyer.

ROBERT PATTERSON WOODS, M. ASCE¹

DIED MAY 20, 1958

Robert Patterson Woods, the son of Thomas Hamilton and Margaret Jane (Patterson) Woods, was born in Buffalo, N. Y., on March 4, 1870. He gained his engineering education through practical experience and home study.

Mr. Woods was assistant engineer to Henry L. Lyon, civil engineer (1888-1891); city engineer of Wabash, Ind. (1891-1901); chief engineer in the construction of various railway lines (1901-1908) in the Indianapolis vicinity; chief engineer of irrigation projects in New Mexico (1910-1911); and engineered the building of the old Kansas City, Mo., Clay County and St. Joseph, Mo., electric railroad and the Kansas City, Missouri-Excelsior Springs, electric railroad (1912-1913). Between 1914 and 1920 Mr. Woods was a member of the old Kansas City Railway Company Board of Control, resigning to become general manager and president of the Kansas City-St. Joseph line from 1921 to 1930. From 1930 to 1936 he was receiver of the line of the Electric Urban Railroad Company. From 1938 until his retirement on March 4, 1958, Mr. Woods was street railways commissioner for Kansas City and director of the Kansas City Public Service Company.

Mr. Woods was active in various civic affairs in Kansas City, as well as a member of numerous professional societies. He received the Collingwood Prize for Juniors for a paper in *Transactions*² in 1900 and was President of the Kansas City Section of the Society in 1936.

On October 10, 1894, he was married to Bertha Dicken in Wabash, Ind. He is survived by two daughters, Helen (Mrs. Ansel N. Mitchell) and Dorothy (Mrs. Lester D. Castle); six grandchildren; and eight great-grandchildren.

Mr. Woods was elected a Junior of the Society on February 2, 1897, an Associate Member on March 7, 1900, and a Member on April 1, 1903. He became a Life Member in 1935.

GEORGE DUNTON YOUNGCLAUS, A.M. ASCE³

DIED JULY 25, 1958

George Dunton Youngclaus, the son of Percy M. and Randa (Stout) Youngclaus, was born in Denver, Colo., on December 12, 1920. He was graduated with the degree of Bachelor of Science in architectural engineering from the University of Colorado at Boulder, in 1948. During the years 1942 to 1945

¹ Abstract of memoir prepared by Arlow V. Ferry, M. ASCE.

² "Street Grades and Cross-Sections in Asphalt and Cement," by Robert P. Woods, *Transactions*, ASCE, Vol. XLII, 1899, p. 1.

³ Abstract of memoir prepared by Samuel Hobbs, A.M. ASCE.

he served in the Army Air Force as a first lieutenant and navigator, receiving numerous service decorations.

Before resuming university work in 1946 and after graduation in 1948, he was employed by architectural and engineering offices in Denver. He was field engineer from 1949 to 1956 with the Portland Cement Association at the Los Angeles District Office. From 1956 to 1958 he was vice-president of Western Concrete Structures Co., Inc., Gardena, Calif. He worked in close association with the Prestressed Concrete Institute and served as president of the Fire Prevention Research Institute, where he was instrumental in the planning of fire tests to develop information on prestressed concrete. Throughout his career he exhibited a strong interest in concrete engineering. In 1953 he became a registered Civil Engineer in California.

Mr. Youngclaus held membership in the American Concrete Institute, the Structural Engineers Association of Southern California, Chi Epsilon, and was a charter member of Chi Epsilon's Los Angeles Alumni Chapter. He was also active in the Boy Scouts of America, the Hillcrest Congregational Church in Whittier, Calif., and was a volunteer worker for the downtown Y.M.C.A. in Los Angeles.

He was married to Marjorie Ingersoll on November 16, 1943 at Fairbury, Nebr. He is survived by his widow; a son, David; a daughter, Linda; his mother; and two brothers.

Mr. Youngclaus was elected a Junior of the Society on August 16, 1948 and an Associate Member on May 12, 1952.

TRANSACTIONS
OF THE
AMERICAN SOCIETY OF CIVIL ENGINEERS

INDEX
VOLUME 124
1959

SUBJECT INDEX, PAGE 1084
AUTHOR INDEX, PAGE 1113

Titles of papers are in quotation marks when given with the
author's name.

VOLUME 124

SUBJECT INDEX

ACCELERATION

See VELOCITY... (cross references thereunder); *see also* VIBRATION

ACCOUNTS AND ACCOUNTING

See COMPUTATION AND COMPUTERS; COSTS...; VALUATION; *also* subheading Financing under relative subject

ADDRESSES

See AMERICAN SOCIETY OF CIVIL ENGINEERS—Addresses; *see also* under subject of address

AERIAL...

See AIR...

AGGREGATES AND AGGREGATION

Aggregate sources as a problem in alluvial deposits of Mississippi River valley, 644.

AGRICULTURE

See DRAINAGE; FLOOD...; IRRIGATION; RUNOFF; SOIL...

AIRCRAFT

See BUCKLING

AIR DEMAND

See CONDUITS

AIR ENTRAINMENT

See WATER, FLOW OF...

AIRFIELDS

See AIRPORTS

AIR FLOW

"Turbulence Characteristics of the Hydraulic Jump," Hunter Rouse, Tien To Siao and S. Nagaratnam (with discussion), 926.

AIRPORTS (structures and localities)

See also PAVEMENT AND PAVING...

"Ground Transportation at New York International Airport," Richard I. Strickland, 657.

Northern New Jersey-New York regional airports and nearby tunnel and bridge structure locations, 658, 659, 665.

AIR TERMINALS

See AIRPORTS

AIR TRANSPORT

See AIR TERMINALS (cross reference thereunder); TRANSPORTATION

ALLUVIATION

See BARS (alluvia); EROSION...; VALLEYS

AMERICAN SOCIETY OF CIVIL ENGINEERS (General)

Concise statement of the Society's policies, performance and projected program, 1038.

Addresses

1959—Annual Address at the Convention, Cleveland, Ohio, May 5, 1959, Francis S. Friel, 1038.

Memoirs of Members. *See* name of member in Author Index. (*See also* p. 1047)

ANALOG COMPUTERS

See ELECTRONIC INSTRUMENTS; *see also* under relative subject

ANALOGS AND ANALOGIES

See under relative subject

ANALYSIS, DESIGN

See under relative subject, e.g., VIBRATION; WELLS

ANALYSIS OF DATA

See EQUATIONS; MATHEMATICS; STRUCTURES, THEORY OF; *also* under relative subject, e.g., WAVES

ANALYSIS, STRUCTURAL

See EQUATIONS; STRESS AND STRAIN; STRUCTURES, THEORY OF

APPARATUS

See under relative subject; *also* INSTRUMENTS (cross references thereunder); *also* under general types of apparatus, e.g., VIBRATION RECORDING APPARATUS

APPARATUS, DEFLECTION RECORDING

See DEFLECTION RECORDING APPARATUS

APPRAISAL*See* VALUATION**ARCH BRIDGES***See* BRIDGES, ARCH**ARCHES***See also* BRIDGES; BRIDGES, ARCH; STRESS AND STRAIN—Arches; TRUSSES, ARCH

"Design of Flexible Steel Arches by Interaction Diagrams," Haaren A. Miklofsky and Omar J. Sotillo, 1. Discussion: Reinaldo Garcia-Iturbe; and Haaren A. Miklofsky and Omar J. Sotillo, 30.

ARCHITECTS AND ARCHITECTURE*See* type of structure or structural part, BRIDGES; BUILDINGS**ARCH TRUSSES***See* TRUSSES, ARCH**ASSOCIATIONS***See* AMERICAN SOCIETY OF CIVIL ENGINEERS**ATMOSPHERIC PRESSURE**

"Design of Masonry Walls for Blast Loading," Keith E. McKee and Eugene Sevin, 457.

ATOMIC BLAST

"Behavior of Reinforced Concrete Shear Walls," Jack R. Benjamin and Harry A. Williams (with discussion), 669.

"Design of Masonry Walls for Blast Loading," Keith E. McKee and Eugene Sevin, 457.

AUTOMOBILE...*See also* MOTOR...; TRAFFIC...**AUTOMOBILE PARKING***See also* COSTS, AUTOMOBILE PARKING

"Ground Transportation at New York International Airport," Richard I. Strickland, 657.

BACTERIA

"Sewage Disposal in Santa Monica Bay," Charles G. Gunnerson (with discussion), 823.

BANKS AND BANK PROTECTION, RIVER*See* RIVER BANKS AND BANK PROTECTION (cross references thereunder)**BARS (alluvia)**

"Engineering Geology of the Mississippi Valley," Charles R. Kolb and Woodland G. Shockley (with discussion), 633.

BASE SLABS*See* SLABS**BASINS (depression in earth's surface)***See* DRAINAGE; RESERVOIRS ...; RUNOFF; VALLEYS**BASINS, STILLING***See* WATER, FLOW OF, IN OPEN CHANNELS**BEACHES***See* EROSION, BEACH; SHORES AND SHORE PROTECTION**BEACH SLOPES***See* SHORES AND SHORE PROTECTION**BEAMS (General)**

See also BUCKLING; FAILURES, BEAM; STRESS AND STRAIN—Beams; STRUCTURES, THEORY OF—Beams and Girders (General); TORSION; WHEEL LOADS; *also* under structure or structural part, e.g., BRIDGES...

"Strength of Very Slender Beams," Ernest F. Masur, 63.

BEAMS, CONTINUOUS*See* STRUCTURES, THEORY OF—Beams and Girders, Continuous; WHEEL LOADS**BEARING CAPACITY (foundations, rocks, soils)**

For more general interpretation *see* cross references under LOAD

"Compacting Earth Dams with Heavy Tamping Rollers," Jack W. Hilf, 409. Discussion: Jack D. Hodgson; C. Y. Li; and Jack W. Hilf, 436.

Origin and use of USBR rollers (including sheepfoot rollers), 410.

Tamping roller specifications (1959) and sheepfoot roller compaction test results on 44 dams with various type soils in United States, 411, 438.

"Thixotropic Characteristics of Compacted Clays," H. Bolton Seed and Clarence K. Chan (with discussion), 894.

Bibliography

Compacting earth dams with tamping rollers, 434.

BEARINGS

"Fixed-Wheel Gates for Penstock Intakes," Sylvan J. Skinner (with discussion), 740.

BENDING

See BUCKLING; MOMENTS; STRESS AND STRAIN; *also* under relative structure, structural part or material, e.g., BEAMS

BIBLIOGRAPHY

See subheading Bibliography under relative subject. (Comprehensive bibliographical footnotes existing in individual papers in which books and other material are cited)

BIOGRAPHIES OF DECEASED MEMBERS

See cross reference under MEMOIRS OF DECEASED MEMBERS. (*See also* p. 1047)

BLAST, ATOMIC

See ATOMIC BLAST

BLASTING

"Design of Masonry Walls for Blast Loading," Keith E. McKee and Eugene Sevin, 457.

Effective usage of air bubble screen to prevent shock pressure wave damage in underwater blasting, 455.

BOUNDARY LAYER, THEORY OF (fluid flow)

See WATER, FLOW OF...

BRACING

See TRUSSES (cross reference thereunder)

BREAKWATERS

See also SHORES AND SHORE PROTECTION; WAVES

"Offshore Breakwaters," Richard Silvester, 356.

BRIDGES (General)

See also BEAMS...; IMPACT; PILES AND PILE DRIVING (cross references thereunder); STRESS AND STRAIN—Bridges; STRUCTURES, THEORY OF—Bridges...; TRAFFIC, BRIDGE; TRUSSES...; VIBRATION; WATER, FLOW OF, IN OPEN CHANNELS; WHEEL LOADS

BRIDGES, ARCH

See also ARCHES

Design of the two hinged Rainbow Bridge at Niagara gorge of Niagara River, 15.

BRIDGES, GIRDER

See STRESS AND STRAIN—Bridges, Girder; STRUCTURES, THEORY OF—Bridges, Girder; VIBRATION

BRIDGES, MOVABLE (TRANSFER)

"Characteristics of New-Type Cargo Ships," Douglas C. MacMillan, 179.

BRIDGE TRAFFIC

See TRAFFIC, BRIDGE

BUBBLES

See VISCOSITY

BUCKLING

"Plate Buckling in the Strain-Hardening Range," Geerhard Haaijer, 117.

"Pressure Lines and Inelastic Buckling of Columns," Frank Baron and Harold S. Davis, 967.

"Prestressed Truss-Beams," Ralph L. Barnett, 472.

"Strength of Very Slender Beams," Ernest F. Masur, 63.

BUILDING (process)

See CONSTRUCTION (cross references thereunder)

BUILDING MATERIALS

See MATERIALS OF CONSTRUCTION (cross references thereunder)

See also FAILURES, BUILDING...; STRESS AND STRAIN...; STRUCTURES...; VIBRATION; *also* under type of building, e.g., AIRPORTS

"Behavior of Reinforced Concrete Shear Walls," Jack R. Benjamin and Harry A. Williams, 669. *Discussion:* DeForest A. Matteson, Jr.; and Jack R. Benjamin and Harry A. Williams, 703.

"Design of Masonry Walls for Blast Loading," Keith E. McKee and Eugene Sevin, 457.

BULKHEADS

See SHORES AND SHORE PROTECTION; WAVES

CALCULATION AND CALCULATORS

See COMPUTATION AND COMPUTERS

CANALS (General)

See also CHANNELS (cross references thereunder); LOCK-GATES; LOCKS; TOLLS; TRAFFIC, CANAL; WATER, FLOW OF, IN OPEN CHANNELS; WATER TRANSPORTATION; WATERWAYS (cross references thereunder); WAVES

CANALS (Geographical)**Welland Ship Canal**

History of first, second, third and fourth Welland Ship Canals, with chronological data, 443.

CANALS (Geographical) (Continued)

"The Welland Canal," William A. O'Neil, 443.

CARGO SHIPS

See SHIPS AND SHIPPING (cross reference thereunder)

CARRIERS

See COSTS...; MOTOR...; TRANSPORTATION; WATER TRANSPORTATION

CARS

See AUTOMOBILE...; MOTOR...; TRAFFIC...; WHEEL LOADS

CAR WHEELS

See WHEEL LOADS

CATERPILLAR GATES

See INTAKE GATES (cross reference thereunder)

CAVITATION

Damage during prototype testing with possible prevention procedures indicated, 505.

CEMENT

See AGGREGATES AND AGGREGATION; CLAY; also under structure

CEMENT PAVEMENT AND PAVING

See PAVEMENT AND PAVING, CEMENT

CHANNEL BANKS AND BANK PROTECTION

See WATER, FLOW OF, IN OPEN CHANNELS; WAVES

CHANNELIZATION

See TRAFFIC, HIGHWAY AND ROAD

CHANNEL RECTIFICATION

See BARS (alluvia); WATER, FLOW OF, IN OPEN CHANNELS

CHANNELS (waterways)

See HYDRAULIC JUMP; RIVERS; WATER, FLOW OF, IN OPEN CHANNELS

CHARTS

See under relative subject

CHEMISTRY

See under relative technical subject, e.g., CORROSION AND PROTECTION OF METALS

CHLORINATORS AND CHLORINATION

"Sewage Disposal in Santa Monica Bay," Charles G. Gunnerson (with discussion), 823.

CITIES

See AIRPORTS; AUTOMOBILE PARKING; BUILDINGS; COSTS...; EMPLOYEES AND EMPLOYMENT; EXPRESSWAYS (cross reference thereunder); FIRE... (cross reference thereunder); FREIGHT; GAS AND GASWORKS; GOVERNMENT (cross references thereunder); INDUSTRIAL...; PUBLIC UTILITIES; SEWAGE...; SEWERS; STREETS; TERMINALS (cross references thereunder); TRAFFIC, STREET; WATER SUPPLY; also geographical subheadings under relative subject, e.g., HARBORS—Madras, India

CIVIL ENGINEERS AND ENGINEERING

See AMERICAN SOCIETY OF CIVIL ENGINEERS; ENGINEERS AND ENGINEERING

CLASSIFICATION OF SOILS

See SOILS—Classification

CLAY

See also SHEAR; SOIL...

"Review of the Theories for Sand Drains," F. E. Richart, Jr. (with discussion), 709.

"Thixotropic Characteristics of Compacted Clays," H. Bolton Seed and Clarence K. Chan, 894. Discussion: Edward S. Barber; D. P. Krynine; and H. Bolton Seed and Clarence K. Chan, 917.

COAST

See SEACOAST (cross references thereunder)

COASTER GATES

See INTAKE GATES (cross reference thereunder)

COATINGS, PROTECTIVE

See CORROSION AND PROTECTION OF METALS

CODES (law codes)

See LAW (cross reference thereunder)

COLUMNS

See BUCKLING; FAILURES, COLUMN; STRESS AND STRAIN—Columns

COMMERCE

See AIRPORTS; AIR TRANSPORT (cross references thereunder); CANALS; CHANNELS (cross references thereunder); CITIES (cross references thereunder); FREIGHT; HARBORS; HIGHWAYS AND ROADS; RIVERS; TERMINALS (cross references thereunder); TRANSPORTATION; WATER TRANSPORTATION; WATERWAYS (cross references thereunder); and other relative subject headings

COMPACTION

See BEARING CAPACITY; IMPACT; SOILS

COMPRESSION

See STRESS AND STRAIN

COMPRESSION MEMBERS

See COLUMNS

COMPRESSION TESTS, SOILS

See SOILS—Tests and Testing

COMPRESSORS AND COMPRESSION

See under relative type

COMPUTATION AND COMPUTERS

See ELECTRONIC INSTRUMENTS

"Electronic Computers in Surveying," Arthur J. McNair, 252.

Numerical procedures as aids in solving soil consolidation problems, 709, 737.

Reservoir Control Center (Omaha, Nebraska), operations applying electronic computers for analyses procedure solutions, 390.

COMPUTERS, DIGITAL

See ELECTRONIC INSTRUMENTS

COMPUTERS, ELECTRONIC

See COMPUTATION AND COMPUTERS; ELECTRONIC INSTRUMENTS; *see also* under relative subject

CONCRETE (General)

See also AGGREGATES AND AGGREGATION; CEMENT (cross references thereunder); GRAVEL; PAVEMENT AND PAVING, CONCRETE; SAND; SEEPAGE; SLABS; STRESS AND STRAIN—Concrete (General); *also* under special structure or structural part, e.g., WALLS (cross references thereunder)

Cracks and Cracking

"Behavior of Reinforced Concrete Shear Walls," Jack R. Benjamin and Harry A. Williams (with discussion), 669.

Tests and Testing

"Inelastic Behavior of Impulsively Loaded Beams," Melvin J. Greaves and Frederic T. Mavis, 395.

CONCRETE-METAL

See cross reference under REINFORCED CONCRETE

CONCRETE PAVEMENT AND PAVING

See PAVEMENT AND PAVING, CONCRETE

CONCRETE, REINFORCED

See CONCRETE...

CONDUITS

See also PENSTOCKS; PIPE LINES; TUNNELS...

"Field Investigations of Spillways and Outlet Works," Benson Guyton, 491.

"Fixed-Wheel Gates for Penstock Intakes," Sylvan J. Skinner (with discussion), 740.

CONSOLIDATION TESTS, SOIL

See SOILS—Tests and Testing

CONSTRUCTION

See WATER, FLOW OF...

CONSTRUCTION

See BUILDINGS; COSTS...; EXCAVATION...; FAILURES...; MATERIALS OF CONSTRUCTION (cross references thereunder); STRESS AND STRAIN...; STRUCTURES, THEORY OF...; *also* under type of construction, e.g., POWER PLANTS

CONSTRUCTION MATERIALS

See MATERIALS OF CONSTRUCTION (cross references thereunder)

CONTAINERSHIPS

See SHIPS AND SHIPPING (cross reference thereunder)

CONTINUOUS BEAMS

See BEAMS, CONTINUOUS (cross references thereunder)

CONTINUOUS FRAMES

See STRESS AND STRAIN—Frames, Continuous; *see also* BEAMS...; COLUMNS (cross references thereunder)

CONTINUOUS STRUCTURES

See STRUCTURES, THEORY OF...

CONTRACTION

See under relative subject

CONTROL AND CONTROLLERS

See WATER, FLOW OF, THROUGH ORIFICES

CONVENTIONS (American Society of Civil Engineers)

See AMERICAN SOCIETY OF CIVIL ENGINEERS—Addresses

CORROSION AND PROTECTION OF METALS

Steel galvanizing for underwater usage, 1024, 1025.

COSTS (General)

See also subheading Financing under relative subject

COSTS (of work)

See COSTS...

COSTS, AUTOMOBILE PARKING

Airport entrance automatic equipment in parking lots as related to costs, 667.

COSTS, CRANE, DERRICK AND POWER SHOVEL

Crane usage economy, 1011.

COSTS, DAM

Rock fill dam types compared as to costs, 992, 1022.

COSTS, DREDGING

Economical dredging for littoral drift deposit removal, 535.

COSTS, FREIGHT SERVICE

Prepacked container shipments in relation to cost, 179, 180, 181, 188, 190, 191.

COSTS, HIGHWAY AND ROAD

Partial cloverleaf versus diamond interchanges in relation to cost and operational safety, 592.

Typical highway program planning cost percentage breakdowns, 156.

COSTS, HYDRAULIC WORK

Purpose of field tests in relation to costs, 491.

COSTS, INSURANCE

"Technical Problems of Flood Insurance," H. Alden Foster (with discussion), 366.

COSTS, INTAKE GATE

Fixed wheel and coaster gate costs compared, 741, 743, 759.

COSTS, POWER PLANT

"Haas Hydroelectric Power Project," J. Barry Cooke (with discussion), 989.

COSTS, SOIL TESTING

Compacting various soil types by tamping rollers (including earth dam water barrier sections), 434, 439, 441.

COSTS, UNDERGROUND STRUCTURE

Powerhouse constructed underground for economic reasons, 989, 990, 1005, 1023.

COSTS, WATER SUPPLY

Water costs in California, 229, 230, 231, 234.

COURT DECISIONS

See under relative subject (under the subject LAW heading)

CRACKS AND CRACKING

See under relative subject, e.g., CONCRETE—Cracks and Cracking

CRANES, DERRICKS AND POWER SHOVELS

See also COSTS, CRANE, DERRICK AND POWER SHOVEL

Crane requirements for newer type cargo ship usage, 192.

CREEP

See STRESS AND STRAIN

CRIPPLING

See FAILURES

CROSS SECTIONS

See under relative subject

CULVERTS

"The Welland Canal," William A. McNeil, 443.

CURRENTS

See ELECTRIC POWER (cross reference thereunder); OCEAN CURRENTS; RIVERS; WATER DIVERSION; WAVES

CURVES (design curves)

See relative subject of design, e.g., BEARING CAPACITY

CURVES (elastic curves)

See STRUCTURES, THEORY OF

CURVES, FREQUENCY

See under topic, e.g., FLOODS

CURVES, WAVE RUN UP

"Wave Run-Up on Roughened and Permeable Slopes," Rudolph P. Savage, 852.

CUTOFFS, TRANSPORTATION

See HIGHWAYS AND ROADS

DAMPING

See STRESS AND STRAIN; STRUCTURES, THEORY OF; VISCOSITY

DAMS (General)

See also COSTS, DAM; LOCKS; MODELS, HYDRAULIC; RESERVOIRS; SPILLWAYS; VALVES; WATER DIVERSION; WATER, FLOW OF, OVER DAMS AND WEIRS; WATER PRESSURE

"Haas Hydroelectric Power Project," J. Barry Cooke (with discussion), 989.

DAMS, EARTH

See also SEEPAGE; WAVES

"Compacting Earth Dams with Heavy Tamping Rollers," Jack W. Hilf (with discussion), 409.

Bibliography

Compacting with heavy tamping rollers for various soil types, 434.

DAMS, FIXED

See DAMS, EARTH; DAMS, ROCK-FILL

DAMS, MASONRY AND CONCRETE

See SEEPAGE; UPLIFT, HYDROSTATIC (cross reference thereunder); WATER PRESSURE

DAMS, ROCK-FILL

"Haas Hydroelectric Power Project," J. Barry Cooke (with discussion), 989.

DEFINITIONS

See TERMINOLOGY

DEFLECTION RECORDING APPARATUS

Deflectometers used in testing dynamic deflections in girder bridges, 299.

DEFLECTIONS

See DEFORMATION (cross references thereunder); MOMENTS; STRESS AND STRAIN; STRUCTURES, THEORY OF; VIBRATION; *also* under relative structure or structural part, e.g., BEAMS; BUILDINGS

DEFORMATION

See FAILURES...; STRESS AND STRAIN; STRUCTURES, THEORY OF; *also* under specific type of stress, e.g., TORSION; *also* under type of material, e.g., CLAY; *also* under type of structure, e.g., BUILDINGS

DELTAS

See RIVER DELTAS

DEPRECIATION

See VALUATION

DESIGN

See under relative subject, e.g., ARCHES; BRIDGES, MOVABLE; *see also* STRUCTURES, THEORY OF

DESIGN ANALYSIS

See under relative subject, e.g., VIBRATION; WELLS

DESIGN CURVES

See CURVES (design curves) (cross reference thereunder)

DIAGRAMS

See under relative subject, e.g., ARCHES; WELLS

DIGITAL COMPUTERS

See ELECTRONIC INSTRUMENTS; *see also* under relative subject

DIKES

See RIVER BANKS AND BANK PROTECTION (cross references thereunder)

DISCHARGE

See PUMPS AND PUMPING; SLUICES; WATER, FLOW OF ...

DISCHARGE COEFFICIENTS

See under relative subject, e.g., WATER, FLOW OF...

DISINTEGRATION OF MATERIALS

See CORROSION AND PROTECTION OF METALS

DISTORTION

See STRESS AND STRAIN; TORSION

DIVERSION

See WATER DIVERSION

DIVERSION DAMS

See DAMS

DOCKS AND WHARVES

See BULKHEADS (cross references thereunder); HARBORS; PILES AND PILE DRIVING (cross references thereunder); WATER TERMINALS

DRAINAGE

See also RUNOFF; SEWERS; VALLEYS; WELLS

White River Basin, Indiana as a typical humid region area, 285.

DRAINAGE BASINS

See DRAINAGE

DRAIN WELLS

See WELLS

DRAWINGS

See under relative subject

DREDGES AND DREDGING

See also COSTS, DREDGING; EXCAVATION, HYDRAULIC

"Littoral-Drift Problem at Shore-Line Harbors," Joe W. Johnson (with discussion), 525.

DRIFT, LITTORAL

See SHORES AND SHORE PROTECTION

DROP-DOWN

See also SPILLWAYS; WATER, FLOW OF, IN OPEN CHANNELS

"Model Studies of Remedial Works for Niagara Falls," Andrew P. Rollins, Jr. and George B. Fenwick, 236.

DROP STRUCTURES

See DAMS

DYNAMICS OF FLUIDS

See HYDRODYNAMICS

DYNAMICS OF STRUCTURES

See STRUCTURAL DYNAMICS

EARTH...

See also GROUND...; SOIL...

EARTH DAMS

See DAMS, EARTH

EARTH PRESSURE

"Compacting Earth Dams with Heavy Tamping Rollers," Jack W. Hilf (with discussion), 409.

EARTHQUAKES

See VIBRATION...

EARTHS

See SOILS

EARTHWORK

See DAMS, EARTH; EXCAVATIONS; FOUNDATIONS...; LEVEES; SOILS

ECONOMICS

See COSTS...; VALUATION; *also* under relative subject, subheading Financing

EDDIES

See WATER, FLOW OF, IN OPEN CHANNELS; WATER, FLOW OF, THROUGH ORIFICES

EDUCATION

Electronic computers in teaching surveying, 255.

EFFLUENTS, SEWAGE

See SEWAGE DISPOSAL

ELASTIC CURVES

See CURVES (elastic curves) (cross reference thereunder)

ELASTICITY

See also PLASTICITY; STRESS AND STRAIN

"Behavior of Reinforced Concrete Shear Walls," Jack R. Benjamin and Harry A. Williams (with discussion), 669.

"Design of Masonry Walls for Blast Loading," Keith E. McKee and Eugene Sevin, 457.

"Prestressed Truss-Beams," Ralph L. Barnett, 472.

"Strength of Very Slender Beams," Ernest F. Masur, 63.

ELECTRIC GENERATORS

"Generating Station on the Niagara River," Frank Dobson, 32.

ELECTRIC POWER (General)

See POWER...; PUBLIC UTILITIES

ELECTRIC POWER PLANTS

See POWER PLANTS

ELECTRONIC COMPUTERS

See COMPUTATION AND COMPUTERS; ELECTRONIC INSTRUMENTS; *see also* under relative subject

ELECTRONIC INSTRUMENTS

See also COMPUTATION AND COMPUTERS...; SURVEYS AND SURVEYING

Digital computers used to simplify rapid gas flow formula application, 341.

"Vibration of Simple-Span Highway Bridges," John M. Biggs, Herbert S. Suer and Jacobus M. Louw, 291.

EMBANKMENTS

See DAMS, EARTH; LEVEES; ROCK; SOILS

EMPLOYEES AND EMPLOYMENT

Mode of ground transportation for employees at New York International Airport, 660.

ENERGY

See ELECTRIC POWER (cross references thereunder); HYDRODYNAMICS; KINETIC ENERGY (cross references thereunder); POWER; STRUCTURAL DYNAMICS; STRUCTURES, THEORY OF; WATER, FLOW OF...; WATER POWER; WIND

ENERGY, KINETIC

See DYNAMICS... (cross references thereunder); IMPACT

ENERGY, LOSS OF

See FRICTION...; HYDRAULIC JUMP; WATER, FLOW OF; WATER HAMMER

ENGINEERING

See ENGINEERS AND ENGINEERING

ENGINEERING BIBLIOGRAPHY

See BIBLIOGRAPHY (cross references thereunder)

ENGINEERING EDUCATION

See EDUCATION

ENGINEERING GLOSSARIES

See TERMINOLOGY

ENGINEERING HISTORY

See AMERICAN SOCIETY OF CIVIL ENGINEERS; *also* under relative subject, e.g., CANALS; PIPE LINES

ENGINEERING SOCIETIES

See AMERICAN SOCIETY OF CIVIL ENGINEERS

ENGINEERS AND ENGINEERING (General)

See also AMERICAN SOCIETY OF CIVIL ENGINEERS. (For memoirs of deceased members, *see* name of member in Author Index.) (*See also* p. 1047); EDUCATION; RESEARCH; TERMINOLOGY

United Engineering Center fund raising campaign reviewed as engineering activity stimulus, 1038.

ENGINES, STEAM

See TURBINES, STEAM

ENTRAINMENT, AIR

See WATER, FLOW OF...

EQUATIONS

See also under relative subject, e.g., WATER, FLOW OF...

"Design of Masonry Walls for Blast Loading," Keith E. McKee and Eugene Sevin, 457.

Empirical equations discounted, 818, 821.

Simultaneous equations solved rapidly by electronic computers, 252.

ERECTION

See CONSTRUCTION (cross references thereunder)

EROSION, BEACH

"Offshore Breakwaters," Richard Silvester, 356.

EROSION, TAIL WATER

"Hydraulic Jump at an Abrupt Drop," Walter L. Moore and Carl W. Morgan (with discussion), 507.

ESTIMATES

See COSTS

EVALUATION

See VALUATION

EXCAVATION (General)

See also EARTHWORK (cross references thereunder); FOUNDATIONS...

"Haas Hydroelectric Power Project," J. Barry Cooke (with discussion), 989.

EXCAVATION, HYDRAULIC

See also DREDGES AND DREDGING

Methods used for Welland Ship Canal, 454, 456.

EXPERIMENTS AND EXPERIMENTATION

See MODELS...; TESTS AND TESTING (cross references thereunder); *also* under material, structure or structural part tested; *also* under relative subject

EXPLOSION

See BLASTING

EXPLOSION, ATOMIC

See ATOMIC BLAST

EXPLOSIVES

See BLASTING

EXPRESSWAYS

See HIGHWAYS AND ROADS

FABRICATION

See under relative subject, e.g., BRIDGES, ARCH; *see also* CONSTRUCTION (cross references thereunder)

FACT FINDING

See RESEARCH

FACTOR, ROUGHNESS

See cross reference under ROUGHNESS FACTOR

FAILURES (General)

See also STRENGTH OF MATERIALS; STRESS AND STRAIN; STRUCTURES, THEORY OF; *also* under relative subject, e.g., BUILDINGS

FAILURES, BEAM

"Prestressed Truss-Beams," Ralph L. Barnett, 472.

FAILURES, BUILDING WALL

"Behavior of Reinforced Concrete Shear Walls," Jack R. Benjamin and Harry A. Williams (with discussion), 669.

"Design of Masonry Walls for Blast Loading," Keith E. McKee and Eugene Sevin, 457.

FAILURES, COLUMN

"Behavior of Reinforced Concrete Shear Walls," Jack R. Benjamin and Harry A. Williams (with discussion), 669.

FAILURES, CONCRETE

"Behavior of Reinforced Concrete Shear Walls," Jack R. Benjamin and Harry A. Williams (with discussion), 669.

FAILURES, FOUNDATION

"Tests to Evaluate Concrete Pavement Subbases," Lawrence D. Childs, Bert E. Colley, and Joe W. Kapernick, 556.

FAILURES, PAVEMENT AND PAVING

Pavement design procedures in relation to cause of failures, 908.

FAILURES, PILE

"Ocean-Wave Forces on Circular Cylindrical Piles," Robert L. Wiegel, Kenneth E. Beebe, and James Moon (with discussion), 89.

FAILURES, STEEL

"Behavior of Reinforced Concrete Shear Walls," Jack R. Benjamin and Harry A. Williams (with discussion), 669.

FATIGUE

See under relative subject; see also FAILURES

FINANCE

See COSTS...; VALUATION; see also subheading Financing under relative subject, e.g., HIGHWAYS AND ROADS—Financing

FIRE PROTECTION

See WATER SUPPLY

FISH INDUSTRY

See under relative technical subject, e.g., RESERVOIRS; WATER POLLUTION

FIXED DISPERSION CONES

See VALVES

FIXED WHEEL GATES

See INTAKE GATES (cross reference thereunder)

FLANGES

See STRESS AND STRAIN—Flanges

FLEXURE

See STRESS AND STRAIN

FLOOD CONTROL

See FLOOD ROUTING; RESERVOIRS, FLOOD CONTROL

FLOOD FORECASTING

See FLOODS

FLOOD LAW

Development of 1928 Mississippi River control plan and its relation to Flood Control Act of 1928 (and 1936 and 1941 and other amendments), 215, 216, 217.

FLOOD ROUTING

"Evolution of Mississippi Valley Flood-Control Plan," John R. Hardin, 207.

Flood control methods grouped in six major categories, 212.

FLOODS (General)

See also INSURANCE; LEVEES; RUNOFF; VALUATION

Statistical methods in estimating flood frequencies, 367.

FLOW

See AIR FLOW; FLOODS; RUN-OFF; SEWERS; TURBULENCE; WATER, FLOW OF...

FLOW, LAMINAR

See WATER, FLOW OF, IN OPEN CHANNELS

FLOW METERS

See WEIRS (cross reference thereunder)

FLOW OF FLUIDS

See GAS...; WATER, FLOW OF...

FLOW OF WATER

See WATER, FLOW OF...

FLOW, SEPARATION OF

See WATER, FLOW OF, IN OPEN CHANNELS

FLUID DYNAMICS

See HYDRODYNAMICS

FLUID FRICTION COEFFICIENTS

See FRICTION COEFFICIENTS, FLUID

FLUID MECHANICS

See WATER, FLOW OF...

FLUIDS, DYNAMICS OF

See HYDRODYNAMICS

FLUIDS, FLOW OF

See GAS...; WATER, FLOW OF...

FLUMES

See also WATER, FLOW OF, IN OPEN CHANNELS

Measurement errors in Parshall flume discharge, 322, 327, 337.

Venturi flume advantages, 337, 340.

FORMULAS

See under relative subject, e.g., FLOW OF FLUIDS (cross references thereunder)

FOUNDATIONS (General)

See also FAILURES, FOUNDATION; PILES AND PILE DRIVING (cross reference thereunder); STRESS AND STRAIN—Foundations

FOUNDATIONS, UNDERWATER

"Engineering Geology of the Mississippi Valley," Charles R. Kolb and Woodland G. Shockley (with discussion), 633.

FRAMES (General)

See STRESS AND STRAIN—Frames

FRAMES, CONTINUOUS

See STRESS AND STRAIN—Frames, Continuous; *see also* BEAMS ...

FRAMES, RIGID

See STRESS AND STRAIN—Frames, Rigid

FREEWAYS

See HIGHWAYS AND ROADS—Location

FREIGHT

See also COSTS, FREIGHT SERVICE; MOTOR TRUCKS (cross reference thereunder)

"Characteristics of New-Type Cargo Ships," Douglas C. MacMillan, 179.

FREQUENCY CURVES

See under topic, e.g., FLOODS

FRICTION

"Errors in Measurement of Irrigation Water," Charles W. Thomas (with discussion), 319.

"Field Investigations of Spillways and Outlet Works," Benson Guyton, 491.

"Flow Equations for Natural Gas Pipelines," Richard F. Bukacek (with discussion), 1027.

"Wave Run-Up on Roughened and Permeable Slopes," Rudolph P. Savage, 852.

FRICTION COEFFICIENTS

"Fixed-Wheel Gates for Penstock Intakes," Sylvan J. Skinner (with discussion), 740.

FRICTION COEFFICIENTS, FLUID

"Flow of Natural Gas in Pipelines," William T. Ivey and James H. Dorough, 341.

GAGES, PRESSURE

"Field Investigations of Spillways and Outlet Works," Benson Guyton, 491.

GAGES, STRAIN

"Ocean-Wave Forces on Circular Cylindrical Piles," Robert L. Wiegel, Kenneth E. Beebe, and James Moon (with discussion), 89.

"Vibration of Simple-Span Highway Bridges," John M. Biggs, Herbert S. Suer and Jacobus M. Louw, 291.

GAGES, STREAM

See also WATER LEVEL RECORDING AND INDICATING INSTRUMENTS

"Errors in Measurement of Irrigation Water," Charles W. Thomas (with discussion), 319.

GAGING

See WATER, FLOW OF, IN OPEN CHANNELS

GAS AND GASWORKS

See also PIPE LINES

Design flow equations most widely used, 1028.

"Flow Equations for Natural Gas Pipelines," Richard F. Bukacek (with discussion), 1027.

GAS DISTRIBUTION

See GAS AND GASWORKS

GATES

See under type of gate, e.g., LOCK-GATES; WATER GATES...

GENERATORS

See ELECTRIC GENERATORS

GEOLOGY

"Engineering Geology of the Mississippi Valley," Charles R. Kolb and Woodland G. Shockley, 633. *Discussion:* Shu-T'ien Li; Charles R. Kolb and Woodland G. Shockley, 646.

GEOMETRY

See under relative subject, e.g., WATER, FLOW OF, OVER DAMS AND WEIRS

GIRDER BRIDGES

See BRIDGES, GIRDER (cross references thereunder)

GIRDERS (General)

See STRESS AND STRAIN;
STRUCTURES, THEORY OF

GIRDERS, CONTINUOUS

See STRUCTURES, THEORY OF

GLOSSARIES

See TERMINOLOGY

GOVERNMENT

See PUBLIC...; see also LAW sub-
ject heading under related topic, e.g.,
HIGHWAY AND ROAD LAW

GRAVEL

See also SOILS

"Engineering Geology of the Missis-
sippi Valley," Charles R. Kolb and
Woodland G. Shockley (with discus-
sion), 633.

GROUND...

See also EARTH...; SOIL...

GROUND WATER

See also WATER SUPPLY

"Salt Balance in Ground-Water Reser-
voirs," David B. Willets and Charles
A. McCullough (with discussion),
224.

HARBOR POLLUTION

See WATER POLLUTION

HARBORS (General)

See also SHORES AND SHORE
PROTECTION

HARBORS (Geographical)**California**

Littoral drift problems, 525.

Madras, India

Littoral drift problems, 529, 536, 545,
546, 552.

HEAD, LOSS OF

See FRICTION; WATER, FLOW
OF...

HIGHWAY AND ROAD LAW

"Highway Planning in the Past, Pres-
ent, and Future," Edward H. Holmes
and John T. Lynch, 149.

HIGHWAY BRIDGES

See BRIDGES (cross reference there-
under)

**HIGHWAYS AND ROADS (Gen-
eral)**

See also BRIDGE...; COSTS,
HIGHWAY AND ROAD; FOUN-
DATIONS, HIGHWAY AND
ROAD; MOTOR...; PAVE-
MENT AND PAVING...; TRAF-
FIC, HIGHWAY AND ROAD;
VEHICLES (cross reference there-
under)

Costs. See COSTS, HIGHWAY AND
ROAD

Financing

State highway planning surveys initiated
through federal aid financing, 151.

Location

"Adaptability of Interchanges to Inter-
state Highways," Jack E. Leisch
(with discussion), 588.

Planning and Design

"Adaptability of Interchanges to Inter-
state Highways," Jack E. Leisch,
588. Discussion: Gerald D. Love;
and Jack E. Leisch, 614.

"Highway Planning in the Past, Pres-
ent, and Future," Edward H. Holmes
and John T. Lynch, 149.

Research

"Highway Planning in the Past, Pres-
ent, and Future," Edward H. Holmes
and John T. Lynch, 149.

Traffic. See TRAFFIC, HIGHWAY
AND ROAD

Transportation. See HIGHWAY
TRANSPORTATION

New Jersey

"Ground Transportation at New York
International Airport," Richard I.
Strickland, 657.

New York

"Ground Transportation at New York
International Airport," Richard I.
Strickland, 657.

United States

"Highway Planning in the Past, Pres-
ent, and Future," Edward H. Holmes
and John T. Lynch, 149.

National wide through route numbering
system adopted, 150.

HIGHWAY TRAFFIC

See TRAFFIC, HIGHWAY AND
ROAD

HIGHWAY TRANSPORTATION

"Highway Planning in the Past, Pres-
ent, and Future," Edward H. Holmes
and John T. Lynch, 149.

HISTORY, ENGINEERING

See under relative subject, e.g., CA-
NALS; PIPE LINES

HOISTING MACHINERY

See under specific type of machines,
e.g., CRANES, DERRICKS AND
POWER SHOVELS

HURRICANES

See WIND...

HYDRAULIC EXCAVATION

See EXCAVATION, HYDRAULIC

HYDRAULIC JUMP

"Hydraulic Jump at an Abrupt Drop," Walter L. Moore and Carl W. Morgan, 507. *Discussion:* Murray B. McPherson, John W. Forster, and Walter L. Moore and Carl W. Morgan, 517.

"Turbulence Characteristics of the Hydraulic Jump," Hunter Rouse, Tien To Siao and S. Nagaratnam, 926. *Discussion:* Edward Silberman; Alvin J. Peterka and Joseph N. Bradley; James M. Robertson; Donald R. F. Harleman; Philip G. Hubbard; and Hunter Rouse, Tien To Siao and S. Nagaratnam, 951.

Bibliography

Exhaustive bibliographic information cited on hydraulic jump under various channel and flow conditions, 516.

HYDRAULIC LABORATORIES

See MODELS, HYDRAULIC

HYDRAULIC MODELS

See MODELS, HYDRAULIC

HYDRAULICS

See BREAKWATERS; CHANNELS (cross references thereunder); COSTS...; DRAINAGE; DROP-DOWN; EROSION...; FAILURES...; FLOOD...; FLOW... (cross references thereunder); FLUID... (cross references thereunder); FLUMES; FRICTION...; GAGES...; GROUND WATER; HYDRO...; IRRIGATION; LEVEES; MODELS, HYDRAULIC; PILES AND PILE DRIVING (cross references thereunder); PIPE...; POWER...; PUMPS AND PUMPING; RESERVOIRS...; RIVER...; RUNOFF; SEA... (cross references thereunder); SEWERS; STRESS AND STRAIN...; TERMINOLOGY; VALLEYS; VALUATION; VISCOSITY; WATER...; WAVES

HYDRAULIC STRUCTURES

See also under type of structure, e.g., DAMS; SPILLWAYS

"Field Investigations of Spillways and Outlet Works," Benson Guyton, 491.

HYDRAULIC TURBINES

See TURBINES, WATER

HYDRODYNAMICS

"Attenuation of Solitary Waves on a Smooth Bed," Yoshiaki Iwasa, 193.

"Discharge Characteristics of Rectangular Thin-Plate Weirs," Carl E. Kindsvater and Rolland W. Carter (with discussion), 772.

"Hydraulic Jump at an Abrupt Drop," Walter L. Moore and Carl W. Morgan (with discussion), 507.

"Ocean-Wave Forces on Circular Cylindrical Piles," Robert L. Wiegel, Kenneth E. Beebe, and James Moon (with discussion), 89.

"Predicting Surge Pressures in Oil Pipelines," Robert D. Kersten and Edwin J. Waller (with discussion), 258.

"Turbulence Characteristics of the Hydraulic Jump," Hunter Rouse, Tien To Siao and S. Nagaratnam (with discussion), 926.

HYDROELECTRIC GENERATORS

See ELECTRIC GENERATORS

HYDROELECTRIC PLANTS

See POWER PLANTS

HYDROELECTRIC POWER

See WATER POWER

HYDROELECTRIC POWER PLANTS

See POWER PLANTS

HYDROLOGY

See DRAINAGE; FLOOD...; RIVERS; RUNOFF; WATER...

HYDROMETRY

See WATER DIVERSION; WATER, FLOW OF...

HYDROSTATIC PRESSURE

See HYDROSTATIC UPLIFT (cross reference thereunder)

HYDROSTATICS

See WATER PRESSURE

HYDROSTATIC UPLIFT

See WATER PRESSURE

IMPACT

See also VIBRATION; WHEEL LOADS

"Design of Masonry Walls for Blast Loading," Keith E. McKee and Eugene Sevin, 457.

"Inelastic Behavior of Impulsively Loaded Beams," Melvin J. Greaves and Frederic T. Mavis, 395.

IMPULSE

See STRUCTURAL DYNAMICS

INDUSTRIAL PLANTS

See specific type of plant, e.g., POWER PLANTS

INDUSTRIAL WASTE

Radioactive waste products of a nuclear power station, 620.

INDUSTRIAL WATER SUPPLY

See IRRIGATION; RESERVOIRS ...; WATER SUPPLY

INDUSTRY

See under type of industry or industrial plant, e.g., FISH INDUSTRY (cross reference thereunder); GAS AND GASWORKS; POWER PLANTS

INFILTRATION

See GROUND WATER

INFLUENCE LINES

See MOMENTS

INSTRUMENTS

See GAGES; also under general types of instruments, e.g., ELECTRONIC INSTRUMENTS; see also cross references under APPARATUS; see also under usage

INSURANCE

See also COSTS, INSURANCE

Flood damage losses classified, 370.

"Technical Problems of Flood Insurance," H. Alden Foster, 366. Discussion: Geoffrey N. Alexander; Steponas Kolupaila; and H. Alden Foster, 376.

INTAKE GATES

See INTAKES

INTAKES

See also STRESS AND STRAIN—Intakes

Coaster caterpillar gate characteristics, 769.

"Fixed-Wheel Gates for Penstock Intakes," Sylvan J. Skinner, 740. Discussion: Joseph R. Bowman; and Sylvan J. Skinner, 769.

"Haas Hydroelectric Power Project," J. Barry Cooke (with discussion), 989.

IRRIGATION (General)

See also RESERVOIRS, IRRIGATION; WATER SUPPLY

"Errors in Measurement of Irrigation Water," Charles W. Thomas (with discussion), 319.

"Water Supply Versus Irrigation in Humid Areas," Marion C. Boyer, 280.

JETS

See WATER, FLOW OF, THROUGH ORIFICES

JUMP, HYDRAULIC

See HYDRAULIC JUMP

KINETIC ENERGY

See DYNAMICS... (cross references thereunder); IMPACT

LABORATORIES

See under specific type of laboratory, e.g., HYDRAULIC LABORATORIES (cross reference thereunder); also under relative subject; also under MODELS...; TESTS AND TESTING (cross references thereunder); also under material, structure, or structural part tested

LAMINAR FLOW

See WATER, FLOW OF, IN OPEN CHANNELS

LAND

See EARTH...; GROUND...; SOIL...

LAW

See LAW subject heading under relative subject, e.g., FLOOD LAW; HIGHWAY AND ROAD LAW

LEAST WORK, PRINCIPLE OF

See STRUCTURES, THEORY OF

LEGISLATION

See under relative subject (under the subject LAW heading, e.g., HIGHWAY AND ROAD LAW)

LEVEES

"Engineering Geology of the Mississippi Valley," Charles R. Kolb and Woodland G. Shockley (with discussion), 633.

"Evolution of Mississippi Valley Flood-Control Plan," John R. Hardin, 207.

LIQUIDS, FLOW OF

See WATER, FLOW OF...

LIQUIDS, FLOW OF, OVER WEIRS

See WATER, FLOW OF, OVER DAMS AND WEIRS

LIQUIDS, FLOW OF, THROUGH ORIFICES

See WATER, FLOW OF, THROUGH ORIFICES

LITTORAL DRIFT

See SHORES AND SHORE PROTECTION

LOAD

See ATOMIC BLAST; BEARING CAPACITY; BUCKLING; IMPACT; STRESS AND STRAIN; STRUCTURES, THEORY OF; WHEEL LOADS; also under structure, structural member or part, e.g., BEAMS

LOAD, SUSPENDED

See SILT AND SILTING

LOCK-GATES

"The Welland Canal," William A. O'Neil, 443.

LOCKS

"The Welland Canal," William A. O'Neil, 443.

LOSS OF ENERGY

See WATER, FLOW OF

LOSS OF HEAD

See FRICTION; WATER, FLOW OF...

MANOMETERS

See GAGES, PRESSURE

MARINE

See SEA...

MASONRY

See WALLS (cross references thereunder)

MASONRY DAMS

See DAMS, MASONRY AND CONCRETE (cross references thereunder)

MATERIALS OF CONSTRUCTION

See CLAY; FAILURES...; ROCK; SOILS; STEEL... (cross references thereunder); STRESS AND STRAIN...; STRUCTURES, THEORY OF...

MATERIALS, PERMEABILITY OF

See PERMEABILITY OF MATERIALS (cross references thereunder)

MATERIALS, STRENGTH OF

See STRENGTH OF MATERIALS

MATHEMATICS

See also COMPUTATION AND COMPUTERS; EQUATIONS; see also under relative subject

Continuous beam analysis by infinite trigonometric series (Fourier Series) and redundant reactions determined by Castigliano's theorem, 164.

MEANDERS AND MEANDERING

See RIVERS

MECHANICS, FLUID

See WATER, FLOW OF...

MEMBERS (ASCE)

See AMERICAN SOCIETY OF CIVIL ENGINEERS. (For memoirs of deceased members, see name of member in Author Index.) (See also p. 1047)

MEMBERS, STRUCTURAL

See BEAMS...; STRUCTURES, THEORY OF

MEMOIRS OF DECEASED MEMBERS

See name of member in Author Index. (See also p. 1047)

METAL PROTECTION

See CORROSION AND PROTECTION OF METALS

METALS

See CORROSION AND PROTECTION OF METALS

MINERALS

See under relative technical subject, e.g., GROUND WATER

MODELS, HYDRAULIC

Air flow model and procedure for determining mean flow patterns of the hydraulic jump, 936, 948, 952, 953, 954, 955, 957, 966.

"Model Studies of Remedial Works for Niagara Falls," Andrew P. Rollins, Jr. and George B. Fenwick, 236.

"Offshore Breakwaters," Richard Silvester, 356.

United States Army Corps of Engineers prototype testing advantages as opposed to model testing, 491.

"Vortex Flow Through Horizontal Orifices," John C. Stevens and Richard C. Kolf (with discussion), 871.

MODELS, STRUCTURAL

"Behavior of Reinforced Concrete Shear Walls," Jack R. Benjamin and Harry A. Williams (with discussion), 669.

"Inelastic Behavior of Impulsively Loaded Beams," Melvin J. Greaves and Frederic T. Mavis, 395.

"Vibration of Simple-Span Highway Bridges," John M. Biggs, Herbert S. Suer and Jacobus M. Louw, 291.

MOMENT DISTRIBUTION

See MOMENTS

MOMENTS

See also STRESS AND STRAIN; STRUCTURES, THEORY OF; also under specific type of stress, e.g., BUCKLING; TORSION

MOMENTS (Continued)

"Analysis of Continuous Beams by Fourier Series," Seng-Lip Lee (with discussion), 164.

Influence line expressions derived by infinite trigonometric series, 170.

"Prestressed Truss-Beams," Ralph L. Barnett, 472.

MOMENTUM

See HYDRODYNAMICS; WATER, FLOW OF...

MOTOR TRUCKS

See TRAFFIC...; WHEEL LOADS

MOTOR VEHICLES

"Vibration of Simple-Span Highway Bridges," John M. Biggs, Herbert S. Suer and Jacobus M. Louw, 291.

MOTORWAYS

See HIGHWAYS AND ROADS

MOVABLE BRIDGES

See BRIDGES; MOVABLE

MOVABLE WATER GATES

See WATER GATES; MOVABLE

MULTI-PURPOSE RESERVOIRS

See RESERVOIRS, MULTI-PURPOSE

MUNICIPALITIES

See CITIES (cross references thereunder)

NAVIGATION

See BRIDGES; CANALS; FLOODS; RIVERS; WATER TRANSPORTATION

NAVIGATION LOCKS

See LOCKS

NETWORKS

See HIGHWAYS AND ROADS

NIAGARA GORGE

See RIVERS (Geographical)—Niagara River

NOMENCLATURE

See TERMINOLOGY

NONUNIFORM FLOW

See WATER, FLOW OF...

NOZZLES

See WATER, FLOW OF, THROUGH ORIFICES

NUCLEAR POWER PLANTS

See POWER PLANTS

OBITUARIES OF MEMBERS

See name of member in Author Index. (See also p. 1047)

OCEAN...

See also SEA...; WAVES

OCEAN BEACHES

See EROSION, BEACH; SHORES AND SHORE PROTECTION

OCEAN CURRENTS

See also EROSION, BEACH; WAVES

"Sewage Disposal in Santa Monica Bay," Charles G. Gunnerson (with discussion), 823.

OCEAN WAVES

See WAVES

OIL, FLOW OF

See PIPE LINES

OPEN CHANNELS

See WATER, FLOW OF, IN OPEN CHANNELS

ORGANIZATIONS

See AMERICAN SOCIETY OF CIVIL ENGINEERS

ORIFICES

See WATER, FLOW OF, THROUGH ORIFICES

OSCILLATION

See VIBRATION

OSCILLOGRAPHS

See VIBRATION RECORDING APPARATUS

PALLETS

See SHIPS AND SHIPPING (cross reference thereunder)

PARKING REGULATIONS

See AUTOMOBILE PARKING

PARSHALL FLUMES

See FLUMES

PAVEMENT AND PAVING (General)

See also STRESS AND STRAIN—Pavement and Paving

Bibliography

Concrete pavement testing, 585.

PAVEMENT AND PAVING, CEMENT

Predicting life of pavement in its relation to interval existing between compaction and testing, 908.

PAVEMENT AND PAVING, CONCRETE

"Tests to Evaluate Concrete Pavement Subbases," Lawrence D. Childs, Bert E. Colley, and Joe W. Kapernick, 556.

PENSTOCKS

"Fixed-Wheel Gates for Penstock Intakes," Sylvan J. Skinner (with discussion), 740.

"Haas Hydroelectric Power Project," J. Barry Cooke (with discussion), 989.

PERCOLATION

See SOILS

PERMEABILITY OF MATERIALS

See SEEPAGE; also under type of material, e.g., SOILS

PIEZOMETERS

See GAGES, PRESSURE

PILES AND PILE DRIVING

See FAILURES, PILE; STRESS AND STRAIN—Piles

PIPE LINES

See also PUMPS AND PUMPING; WATER HAMMER

Basic design formula proposed for natural gas flow, 351.

"Flow Equations for Natural Gas Pipelines," Richard F. Bukacek, 1027.

Discussion: James H. Dorrough; William T. Ivey; John F. Schomaker; and Richard F. Bukacek, 1035.

"Flow of Natural Gas in Pipelines," William T. Ivey and James H. Dorrough, 341.

History of development of gas flow formulas in pipelines, 341.

"Predicting Surge Pressures in Oil Pipelines," Robert D. Kersten and Edwin J. Waller (with discussion), 258.

PIPES AND PIPING (fluid conveyance)

See PIPE LINES; SEWERS; WATER HAMMER

PLANNING

See under relative subject, e.g., FLOOD ROUTING; HIGHWAYS AND ROADS—Planning and Design

PLANTS (industrial buildings and equipment)

See under type of plant, e.g., POWER PLANTS

PLASTICITY

See also ELASTICITY; STRESS AND STRAIN

"Inelastic Behavior of Impulsively Loaded Beams," Melvin J. Greaves and Frederic T. Mavis, 395.

"Plate Buckling in the Strain-Hardening Range," Geerhard Haaijer, 117.

PLASTIC THEORY

See PLASTICITY

PLATES

See STRESS AND STRAIN—Plates

POLLUTION, STREAM

See WATER POLLUTION

POPULATION

United States population rapid growth trends, with reasons specified, 283.

PORE WATER PRESSURE

See WATER PRESSURE

POROSITY

See SEEPAGE

POWER (General)

See also ELECTRIC POWER (cross reference thereunder); PUMPS AND PUMPING; WATER POWER

POWER (Geographical)**North Central States**

Power generation in Missouri River main-stem reservoir system power plants, years 1952-1956, 394.

POWER GENERATION

See POWER

POWER HOUSES

See POWER PLANTS

POWER PLANTS (General)

See also COSTS, POWER PLANT

Financing

Dresden Nuclear Power Station, near Morris, Illinois and its financing by private industry, 617.

POWER PLANTS (Geographical)**California**

First large underground hydroelectric plant in the United States, 989, 1022.

"Haas Hydroelectric Power Project," J. Barry Cooke, 989. Discussion: F. L. Lawton; and J. Barry Cooke, 1024.

Canada

"Generating Station on the Niagara River," Frank Dobson, 32.

Illinois

"Design Features of the Dresden Nuclear Power Station," Joseph E. Love, Chester S. Darrow, and Burr H. Randolph, 617.

POWER STATIONS

See POWER PLANTS

PRESIDENTIAL ADDRESSES

(American Society of Civil Engineers)

See AMERICAN SOCIETY OF CIVIL ENGINEERS—Addresses

PRESSURE

See ATMOSPHERIC PRESSURE; EARTH PRESSURE; IMPACT; PUMPS AND PUMPING; WATER HAMMER; WATER PRESSURE; WAVES

PRESSURE GAGES

See GAGES, PRESSURE

PRESSURE TUNNELS

See TUNNELS, WATER

PRINCIPLE OF LEAST WORK

See STRUCTURES, THEORY OF

PRINCIPLE OF SUPERPOSITION

See STRUCTURES, THEORY OF

PRINCIPLE OF VIRTUAL WORK

See VIRTUAL WORK, PRINCIPLE OF

PROPERTY (landed property)

See INSURANCE; VALUATION

PROTECTIVE COATINGS

See CORROSION AND PROTECTION OF METALS

PROTOTYPES AND MODELS

See MODELS

PUBLIC HEALTH

See WATER SUPPLY

PUBLIC UTILITIES

See also POWER; POWER PLANTS; WATER POWER

United States electric utility system capacity and production, years 1920–2000, by decades, 284.

PUBLIC WORKS

See under type of structure or project

PUMPS AND PUMPING

"Generating Station on the Niagara River," Frank Dobson, 32.

"Predicting Surge Pressures in Oil Pipelines," Robert D. Kersten and Edwin J. Waller (with discussion), 258.

RADIOACTIVE TRACERS

Effluent dilutions studied by usage of radioactive tracers, 832.

RADIOACTIVE WASTE

See INDUSTRIAL WASTE

RADIOACTIVITY

"Design Features of the Dresden Nuclear Power Station," Joseph E. Love, Chester S. Darrow, and Burr H. Randolph, 617.

RECORDING APPARATUS

See under relative subject; *also* under general types of apparatus, e.g., DEFLECTION RECORDING APPARATUS; VIBRATION RECORDING APPARATUS

RECORDING INSTRUMENTS

See under relative subject; *also* under general types of instruments; e.g., WATER LEVEL RECORDING AND INDICATING INSTRUMENTS

RECREATIONAL FACILITIES

See RESERVOIRS

REDUNDANCE, STRUCTURAL

See STRUCTURES, THEORY OF

REINFORCED CONCRETE

See CONCRETE...

RESEARCH

See also LABORATORIES (cross references thereunder); *see also* under relative subject, e.g., HIGHWAYS AND ROADS—Research; WAVES

Hydraulic jump turbulence presented as a possible guide to needed future research, 927, 957, 964.

RESERVOIRS (General)

Work of Reservoir Control Center, Omaha, Nebraska, representing nine Missouri River states and seven federal agencies, 381, 389.

RESERVOIRS, FLOOD CONTROL

"Operation of Missouri River Main-Stem Reservoirs," Robert J. Pafford, Jr., 381.

RESERVOIRS, IRRIGATION

See also RESERVOIRS, WATER STORAGE

"Operation of Missouri River Main-Stem Reservoirs," Robert J. Pafford, Jr., 381.

RESERVOIRS, MULTI-PURPOSE

"Operation of Missouri River Main-Stem Reservoirs," Robert J. Pafford, Jr., 381.

RESERVOIRS, WATER STORAGE

"Salt Balance in Ground-Water Reservoirs," David B. Willets and Charles A. McCullough, 224. *Discussion:* Robert O. Thomas; and David B. Willets and Charles A. McCullough, 232.

- RIGHT OF WAY** (vehicle passage)
See TRAFFIC...
- RIGID FRAMES**
See STRESS AND STRAIN—
 Frames, Rigid
- RIVER BANKS AND BANK PROTECTION**
See FLOODS; LEVEES
- RIVER BASINS**
See DRAINAGE; RESERVOIRS
 ...; RUNOFF; VALLEYS
- RIVER DELTAS**
 "Engineering Geology of the Mississippi Valley," Charles R. Kolb and Woodland G. Shockley (with discussion), 633.
- RIVER MEANDERING**
See RIVERS
- RIVER REGULATION**
See FLOOD ROUTING; WATER, FLOW OF, IN OPEN CHANNELS
- RIVERS (General)**
See also BRIDGES...; DRAINAGE; FLOOD ROUTING; FLOODS; LEVEES; RESERVOIRS...; RUNOFF; VALLEYS; WATER...; WAVES
- RIVERS (Geographical)**
Kings River
 "Haas Hydroelectric Power Project," J. Barry Cooke (with discussion), 989.
- Mississippi River**
 Meander belt deposits and their geological importance, 636, 646, 647, 648, 649, 651.
- Missouri River**
 "Operation of Missouri River Main-Stem Reservoirs," Robert J. Pafford, Jr., 381.
- Niagara River**
 "Generating Station on the Niagara River," Frank Dobson, 32.
 "Model Studies of Remedial Works for Niagara Falls," Andrew P. Rollins, Jr. and George B. Fenwick, 236.
- RIVER VALLEYS**
See VALLEYS
- ROADS**
See HIGHWAYS AND ROADS
- ROCK**
 "Haas Hydroelectric Power Project," J. Barry Cooke (with discussion), 989.
- ROCK-FILL DAMS**
See DAMS, ROCK-FILL
- RODS, TIE**
See STRESS AND STRAIN—Tie Rods
- ROLLED-FILL DAMS**
See DAMS, EARTH
- ROLLERS, TAMPING**
See SOILS—Compaction (cross reference thereunder)
- ROUGHNESS**
See FRICTION
- ROUGHNESS FACTOR**
See FRICTION COEFFICIENTS...
- ROUTING, FLOOD**
See FLOOD ROUTING
- RUNOFF (Geographical)**
Missouri River Basin
 Annual runoff above Sioux City, Iowa during 1898-1956 record period, 385.
- SALT**
 Californian salt balance in ground water reservoirs, and salt balance problems, 224.
 Salt sources, 225.
- SAMPLING**
See under relative subject, e.g., FLOODS
- SAND**
See also SEEPAGE; SILT AND SILTING
 "Engineering Geology of the Mississippi Valley," Charles R. Kolb and Woodland G. Shockley (with discussion), 633.
- SAND BARS**
See BARS (alluvia)
- SAND DRAINS**
See WELLS
- SAND TRAPS**
See WATER, FLOW OF, IN OPEN CHANNELS
- SANITATION**
See SEWAGE DISPOSAL; SEWERS
- SCIENTIFIC SOCIETIES**
See AMERICAN SOCIETY OF CIVIL ENGINEERS
- SCOUR**
See EROSION, BEACH
- SEA...**
See also MARINE; OCEAN...; WATER...; WAVES

SEACOAST

See SHORES AND SHORE PROTECTION; WAVES

SEASHORE

See SHORES AND SHORE PROTECTION

SEATRAINS

See SHIPS AND SHIPPING (cross reference thereunder)

SEA WATER

"Sewage Disposal in Santa Monica Bay," Charles G. Gunnerson (with discussion), 823.

SEAWAYS

See WATERWAYS (cross references thereunder)

SEDIMENT AND SEDIMENTATION

See SILT AND SILTING

SEEPAGE

"Compacting Earth Dams with Heavy Tamping Rollers," Jack W. Hilf (with discussion), 409.

"Review of the Theories for Sand Drains," F. E. Richart, Jr. (with discussion), 709.

"Wave Run-Up on Roughened and Permeable Slopes," Rudolph P. Savage, 852.

SEWAGE DISPOSAL (Geographical)

Los Angeles, Calif.

"Sewage Disposal in Santa Monica Bay," Charles G. Gunnerson (with discussion), 823.

Santa Monica Bay, Calif.

"Sewage Disposal in Santa Monica Bay," Charles G. Gunnerson, 823.
Discussion: Charles H. Lawrance and David R. Miller; David I. H. Barr; and Charles G. Gunnerson, 843.

SEWAGE EFFLUENTS

See SEWAGE DISPOSAL

SEWAGE SLUDGE

See SEWAGE DISPOSAL

SEWAGE TREATMENT

See SEWAGE DISPOSAL

SEWAGE WORKS

See SEWAGE DISPOSAL

SEWERAGE

See SEWERS

SEWERS (General)

"Vortex Flow Through Horizontal Orifices," John C. Stevens and Richard C. Kolf (with discussion), 871.

"Water Supply Versus Irrigation in Humid Areas," Marion C. Boyer, 280.

SEWERS (Geographical)

Portland, Ore.

Flow diversions into interceptors from combined sewers, 879, 884, 888.

SHAFTS

"Haas Hydroelectric Power Project," J. Barry Cooke (with discussion), 989.

SHEAR

"Behavior of Reinforced Concrete Shear Walls," Jack R. Benjamin and Harry A. Williams (with discussion), 669.

"Compacting Earth Dams with Heavy Tamping Rollers," Jack W. Hilf (with discussion), 409.

"Hydraulic Jump at an Abrupt Drop," Walter L. Moore and Carl W. Morgan (with discussion), 507.

"Ocean-Wave Forces on Circular Cylindrical Piles," Robert L. Wiegel, Kenneth E. Beebe, and James Moon (with discussion), 89.

"Prestressed Truss-Beams," Ralph L. Barnett, 472.

"Thixotropic Characteristics of Compacted Clays," H. Bolton Seed and Clarence K. Chan (with discussion), 894.

"Turbulence Characteristics of the Hydraulic Jump," Hunter Rouse, Tien To Siao and S. Nagaratnam (with discussion), 926.

SHEARING STRESS

See SHEAR

SHEEPSFOOT ROLLERS

See SOILS—Compaction (cross reference thereunder)

SHIP CANALS

See CANALS

SHIPS AND SHIPPING

See WATER TRANSPORTATION

SHOCK

See ATOMIC BLAST; BLASTING

SHORES AND SHORE PROTECTION (lands adjacent to lake, ocean or sea water)

See also BREAKWATERS; EROSION, BEACH; WAVES; also cross references under RIVER BANKS AND BANK PROTECTION

SHORES AND SHORE PROTECTION (*Continued*)

"Littoral-Drift Problem at Shore-Line Harbors," Joe W. Johnson, 525.
Discussion: Richard Silvester; and Joe W. Johnson, 547.

"Wave Run-Up on Roughened and Permeable Slopes," Rudolph P. Savage, 852.

SILT AND SILTING (*General*)

"Littoral-Drift Problem at Shore-Line Harbors," Joe W. Johnson (with discussion), 525.

"Sewage Disposal in Santa Monica Bay," Charles G. Gunnerson (with discussion), 823.

Three main methods by which silt is moved alongshore, 547.

SLABS

"Tests to Evaluate Concrete Pavement Subbases," Lawrence D. Childs, Bert E. Colley, and Joe W. Kapernick, 556.

SLOPE PROTECTION

See WAVES

SLOPES, BEACH

See SHORES AND SHORE PROTECTION

SLUICES

"Field Investigations of Spillways and Outlet Works," Benson Guyton, 491.

SOCIETIES, TECHNICAL

See AMERICAN SOCIETY OF CIVIL ENGINEERS

SOIL...

See also EARTH...; GROUND...

SOIL MECHANICS

See SOILS

SOIL PRESSURE

See EARTH PRESSURE

SOILS (*General*)

See also STRESS AND STRAIN—Soils

Bibliography

Tamping roller usage for compressing various soil types, 434.

Classification

"Compacting Earth Dams with Heavy Tamping Rollers," Jack W. Hilf (with discussion), 409.

Mississippi River alluvial valley soils and their characteristics, 633, 643, 651.

Compaction. *See* BEARING CAPACITY

Tests and Testing. *See also* COSTS, SOIL TESTING

"Compacting Earth Dams with Heavy Tamping Rollers," Jack W. Hilf (with discussion), 409.

"Review of the Theories for Sand Drains," F. E. Richart, Jr. (with discussion), 709.

"Thixotropic Characteristics of Compacted Clays," H. Bolton Seed and Clarence K. Chan (with discussion), 894.

SOIL TRANSPORTATION

See SILT AND SILTING...

SOLITARY WAVES

See WAVES

SPEED

See TRAFFIC...; VELOCITY (cross reference thereunder)

SPILLWAYS (*Geographical*)

Vicksburg, Miss.

"Field Investigations of Spillways and Outlet Works," Benson Guyton, 491.

STATICALLY INDETERMINATE STRUCTURES

See STRUCTURES, TRUSSED (cross reference thereunder)

STATIONS

See under relative subject, e.g., POWER PLANTS; *see also* cross reference under TERMINALS

STATISTICS

See under relative subject; *see also* COMPUTATION AND COMPUTERS

STEAM TURBINES

See TURBINES, STEAM

STEEL (*General*)

See CORROSION AND PROTECTION OF METALS; FAILURES, STEEL; STRENGTH OF MATERIALS; *also* under special structure or structural part, e.g., ARCHES

STEEL PLATES

See PLATES (cross, reference thereunder)

STIFFENING TRUSSES

See TRUSSES, STIFFENING

STIFFNESS

"Design of Flexible Steel Arches by Interaction Diagrams," Haaren A. Miklofsky and Omar J. Sotillo (with discussion), 1.

STILLING BASINS

See WATER, FLOW OF, IN OPEN CHANNELS

STORAGE

See RESERVOIRS...

STORMS

See WAVES; WIND

STORM WATER

See SEWERS

STRAIN

See STRESS AND STRAIN

STRAIN GAGES

See GAGES, STRAIN

STREAM CONTAMINATION

See WATER POLLUTION

STREAM FLOW

See WATER, FLOW OF, IN OPEN CHANNELS and cross references thereunder

STREAM GAGES

See GAGES, STREAM

STREAMS

See RIVERS and cross references thereunder

STREETS (General)

See also TRAFFIC, STREET

Planning and Design

"Adaptability of Interchanges to Interstate Highways," Jack E. Leisch (with discussion), 588.

STRENGTH OF MATERIALS

See also FAILURES...; STRESS AND STRAIN; also under specific material (see list under MATERIALS OF CONSTRUCTION); also under fabricated structure or structural part, e.g., BEAMS

"Inelastic Behavior of Impulsively Loaded Beams," Melvin J. Greaves and Frederic T. Mavis, 395.

STRESS AND STRAIN (General)

See also ELASTICITY; FAILURES; GAGES, STRAIN; MOMENTS; PLASTICITY; STIFFNESS; STRUCTURES, THEORY OF; VIBRATION; WAVES; WHEEL LOADS; WIND; also under specific type of stress, e.g., BUCKLING; SHEAR; TORSION

Arches

"Design of Flexible Steel Arches by Interaction Diagrams," Haaren A. Miklofsky and Omar J. Sotillo (with discussion), 1.

"Pressure Lines and Inelastic Buckling of Columns," Frank Baron and Harold S. Davis, 967.

Beams (General)

"Design of Flexible Steel Arches by Interaction Diagrams," Haaren A. Miklofsky and Omar J. Sotillo (with discussion), 1.

"Inelastic Behavior of Impulsively Loaded Beams," Melvin J. Greaves and Frederic T. Mavis, 395.

"Prestressed Truss-Beams," Ralph L. Barnett, 472.

Bridges, Girder

"Vibration of Simple-Span Highway Bridges," John M. Biggs, Herbert S. Suer and Jacobus M. Louw, 291.

Clay. See SHEAR**Columns**

"Pressure Lines and Inelastic Buckling of Columns," Frank Baron and Harold S. Davis, 967.

Concrete (General)

"Behavior of Reinforced Concrete Shear Walls," Jack R. Benjamin and Harry A. Williams (with discussion), 669.

"Tests to Evaluate Concrete Pavement Subbases," Lawrence D. Childs, Bert E. Colley, and Joe W. Kapernick, 556.

Flanges

"Plate Buckling in the Strain-Hardening Range," Geerhard Haaijer, 117.

"Prestressed Truss-Beams," Ralph L. Barnett, 472.

Foundations

"Tests to Evaluate Concrete Pavement Subbases," Lawrence D. Childs, Bert E. Colley, and Joe W. Kapernick, 556.

Frames, Continuous

Plate buckling in continuous frames based on ultimate strength design, 145.

Frames, Rigid

"Pressure Lines and Inelastic Buckling of Columns," Frank Baron and Harold S. Davis, 967.

Intakes

"Fixed-Wheel Gates for Penstock Intakes," Sylvan J. Skinner (with discussion), 740.

Pavement and Paving

"Tests to Evaluate Concrete Pavement Subbases," Lawrence D. Childs, Bert E. Colley, and Joe W. Kapernick, 556.

STRESS AND STRAIN (General)

(Continued)

Piles

"Ocean-Wave Forces on Circular Cylindrical Piles," Robert L. Wiegel, Kenneth E. Beebe, and James Moon, 89.
Discussion: Thomas E. Stelson; and Robert L. Wiegel, Kenneth E. Beebe, and James Moon, 114.

Plates

"Plate Buckling in the Strain-Hardening Range," Geerhard Haaijer, 117.

Reinforced Concrete.

See Concrete (hereunder)

Soils

"Thixotropic Characteristics of Compacted Clays," H. Bolton Seed and Clarence K. Chan (with discussion), 894.

Structures (General)

"Pressure Lines and Inelastic Buckling of Columns," Frank Baron and Harold S. Davis, 967.

Trusses and Trussed Structures

"Prestressed Truss-Beams," Ralph L. Barnett, 472.

STRESS, SHEARING

See SHEAR

STRINGERS

See BEAMS

STRUCTURAL ANALYSIS

See EQUATIONS; STRESS AND STRAIN; STRUCTURES, THEORY OF

STRUCTURAL DYNAMICS

See also VIBRATION

"Design of Masonry Walls for Blast Loading," Keith E. McKee and Eugene Sevin, 457.

"Inelastic Behavior of Impulsively Loaded Beams," Melvin J. Greaves and Frederic T. Mavis, 395.

STRUCTURAL MATERIALS

See MATERIALS OF CONSTRUCTION (cross references thereunder)

STRUCTURAL MEMBERS

See MEMBERS, STRUCTURAL (cross reference thereunder)

STRUCTURAL MODELS

See MODELS, STRUCTURAL

STRUCTURAL REDUNDANCE

See STRUCTURES, THEORY OF

STRUCTURES (General)

See also BUILDINGS; CONSTRUCTION (cross references thereunder); MATERIALS OF CONSTRUCTION (cross references thereunder); MODELS, STRUCTURAL;

STRESS AND STRAIN; STRUCTURES, THEORY OF; VIBRATION; *see also* under specific type of structure, or related subject

"Engineering Geology of the Mississippi Valley," Charles R. Kolb and Woodland G. Shockley (with discussion), 633.

"Hurricane Design-Wave Practices," Charles L. Bretschneider, 39.

"Wave Run-Up on Roughened and Permeable Slopes," Rudolph P. Savage, 852.

STRUCTURES, HYDRAULIC

See HYDRAULIC STRUCTURES

STRUCTURES, THEORY OF

See also STRESS AND STRAIN; *also* under type of structure, or structural part

Beams and Girders (General)

"Design of Masonry Walls for Blast Loading," 457.

Linear theory to which principle of superposition is applied, 81.

Principle of least work and its extension into the nonlinear range, 70.

"Strength of Very Slender Beams," Ernest F. Masur, 63.

Beams and Girders, Continuous

"Analysis of Continuous Beams by Fourier Series," Seng-Lip Lee, 164.
Discussion: Stefan J. Medwadowski, and Seng-Lip Lee, 175.

Bridges, Girder

"Vibration of Simple-Span Highway Bridges," John M. Biggs, Herbert S. Suer and Jacobus M. Louw, 291.

Walls

"Design of Masonry Walls for Blast Loading," Keith E. McKee and Eugene Sevin, 457.

STRUCTURES, TRUSSED

See TRUSSES...

STRUCTURES, UNDERGROUND

See UNDERGROUND STRUCTURES (cross reference thereunder)

SUBGRADES

See PAVEMENT AND PAVING, CONCRETE

SUPERPOSITION, PRINCIPLE OF

See STRUCTURES, THEORY OF

SURFACE PROFILES

See WATER SURFACE PROFILES (cross reference thereunder)

SURFACE RUNOFF

See RUNOFF

SURGES (water surface)

See WATER HAMMER; WAVES

SURGE TANKS

See TANKS, SURGE

SURVEYING

See SURVEYS AND SURVEYING

SURVEYS (research data)

See under relative subject, e.g., HIGHWAYS AND ROADS—Research; see also RESEARCH (cross references thereunder)

SURVEYS AND SURVEYING (General)

Electronic computer usage in teaching of surveying, and in surveying problems, 252, 255.

SUSPENDED LOAD

See SILT AND SILTING

TAIL WATER EROSION

See EROSION, TAIL WATER

TAMPING ROLLERS

See SOILS—Compaction (cross reference thereunder)

TANKS, SURGE

"Haas Hydroelectric Power Project," J. Barry Cooke (with discussion), 989.

TANKS, WATER

"Vortex Flow Through Horizontal Orifices," John C. Stevens and Richard C. Kolf (with discussion), 871.

TAXATION

See under relative subject, subheading Financing

TECHNICAL SOCIETIES

See AMERICAN SOCIETY OF CIVIL ENGINEERS

TENSILE STRESS

See STRESS AND STRAIN

TENSION

See STRESS AND STRAIN

TERMINALS (structures and localities)

See AIR TERMINALS (cross reference thereunder); WATER TERMINALS; see also cross references under STATIONS

TERMINOLOGY (Arranged hereunder by specific or comprehensive subject word when possible)

Beams. (Dynamic strength of a beam), 399.

Civil engineering defined, 632.

Clay sensitivity in soil terminology, 894.

Flood frequency. (Statistical method terms used), 368, 378.

Friction coefficient redefined, 342, 343.

Gas. (Critical temperature and critical pressure defined in relation to pure gas), 350.

Harbors. (Shore line harbor defined), 525, 526.

Highways and Roads. (Interchange terms), 589, 590.

Littoral drift. (Saltation in littoral drift process), 548, 554.

Load. (Critical load explained), 983.

Materials of construction. (Thixotropy as originally and later defined), 895, 917, 919, 920.

Pressure line defined and usage of concept extended, 967.

Rivers. (Natural levees, bar deposits, abandoned channels, and similar terms), 633.

Salt balance and effective salinity, simply defined and also amplified, 225, 228.

Sand drains. (Smear as used in relation to drain wells), 714.

Strength of materials. (Thixotropic strength ratio as a term), 903, 924.

Turbulence. (Intermittency as a term relating to fluid in transit), 956.

Water flow. (Eddy diffusion in sewage disposal), 826.

Wave run up defined, 852.

Waves. (Diffraction of ocean waves defined), 364.

Waves. (Solitary waves and incoming coastal surf wave differentiated), 193.

TESTS AND TESTING

See BUCKLING; ELASTICITY; FAILURES...; LABORATORIES... (cross references thereunder); MODELS...; SHEAR; STRESS AND STRAIN; STRUCTURES, THEORY OF; TORSION; WATER, FLOW OF...; also under material, structure or structural part tested, e.g., PAVEMENT AND PAVING, CONCRETE; PIPE LINES

THEORIES

See cross references hereunder and under ANALYSIS OF DATA; see also STRUCTURES, THEORY OF; see also under relative subject or its relative science, e.g., MATHEMATICS; WELLS

THEORY OF BOUNDARY LAYER
(fluid flow)

See BOUNDARY LAYER, THEORY OF (cross reference thereunder)

THEORY OF PLASTICITY

See PLASTICITY

THEORY OF STRUCTURES

See STRUCTURES, THEORY OF

THEORY, PLASTIC

See PLASTICITY

THIXOTROPY

See CLAY

THRUST

See under relative structure, structural part or material, e.g., ARCHES

TIE RODS

See STRESS AND STRAIN—Tie Rods

TOLLS (General)

Toll system on the Welland Ship Canal, 453.

TORSION

"Strength of Very Slender Beams," Ernest F. Masur, 63.

TRACERS, RADIOACTIVE

See RADIOACTIVE TRACERS

TRAFFIC, BRIDGE

"Vibration of Simple-Span Highway Bridges," John M. Biggs, Herbert S. Suer and Jacobus M. Louw, 291.

TRAFFIC, CANAL

Tonnage passing through the Welland Ship Canals, 452.

TRAFFIC, HIGHWAY AND ROAD

"Adaptability of Interchanges to Interstate Highways," Jack E. Leisch (with discussion), 588.

"Highway Planning in the Past, Present, and Future," Edward H. Holmes and John T. Lynch, 149.

TRAFFIC, STREET

"Adaptability of Interchanges to Interstate Highways," Jack E. Leisch (with discussion), 588.

TRAILERSHIPS

See SHIPS AND SHIPPING (cross reference thereunder)

TRAINSHIPS

See SHIPS AND SHIPPING (cross reference thereunder)

TRANSFER BRIDGES

See BRIDGES, MOVABLE (TRANSFER)

TRANSLATORY WAVES

See WAVES

TRANSPORTATION

See also FREIGHT; HIGHWAY TRANSPORTATION; PIPE LINES; RIVERS; SOIL TRANSPORTATION (cross reference thereunder); TERMINALS (cross references thereunder); TRAFFIC ...; WATER TRANSPORTATION

Modes of ground transportation to and from large airports, 657.

TRAVELING CRANES

See CRANES, DERRICKS AND POWER SHOVELS

TRIGONOMETRY

See under relative subject

TRIAxIAL SHEAR

See SHEAR

TRUCKS

See MOTOR TRUCKS (cross reference thereunder)

TRUSSED STRUCTURES

See TRUSSES...

TRUSSES (General)

See also STRESS AND STRAIN—Trusses and Trussed Structures

Weight saving possibility of a variation of the Queen Port truss with a pretensioned tie rod, 472, 480.

TRUSSES, ARCH

"Design of Flexible Steel Arches by Interaction Diagrams," Haaren A. Miklofsky and Omar J. Sotillo (with discussion), 1.

TRUSSES, STIFFENING

"Design of Flexible Steel Arches by Interaction Diagrams," Haaren A. Miklofsky and Omar J. Sotillo (with discussion), 1.

TUNNELS, PRESSURE

See TUNNELS, WATER

TUNNELS, WATER

"Haas Hydroelectric Power Project," J. Barry Cooke (with discussion), 989.

TURBINES, STEAM

"Design Features of the Dresden Nuclear Power Station," Joseph E. Love, Chester S. Darrow, and Burr H. Randolph, 617.

TURBINES, WATER

"Haas Hydroelectric Power Project," J. Barry Cooke (with discussion), 989.

TURBULENCE (water agitation)

See also EDDIES (cross references thereunder); FRICTION...; WATER, FLOW OF...

"Field Investigations of Spillways and Outlet Works," Benson Guyton, 491.

"Flow Equations for Natural Gas Pipelines," Richard F. Bukacek (with discussion), 1027.

Recognition of three different regions of the turbulence spectrum, 965.

"Sewage Disposal in Santa Monica Bay," Charles G. Gunnerson (with discussion), 823.

"Turbulence Characteristics of the Hydraulic Jump," Hunter Rouse, Tien To Siao and S. Nagaratnam (with discussion), 926.

TURNPIKES

See HIGHWAYS AND ROADS

TWISTING

See TORSION; see also under relative material, structure or structural part, e.g., BEAMS

UNDERGROUND STRUCTURES

See under type of structure, e.g., POWER PLANTS

UNDERGROUND WATER

See GROUND WATER

UNDERWATER FOUNDATIONS

See FOUNDATIONS, UNDERWATER

UPLIFT, HYDROSTATIC

See WATER PRESSURE

URBAN...

See CITIES (cross references thereunder)

UTILITIES

See PUBLIC UTILITIES

VALLEYS (Geographical)**Mississippi River Valley**

Alluvial valley of the lower Mississippi River, 209.

"Engineering Geology of the Mississippi Valley," Charles R. Kolb and Woodland G. Shockley (with discussion), 633.

"Evolution of Mississippi Valley Flood-Control Plan," John R. Hardin, 207.

VALUATION

See also COSTS...

"Technical Problems of Flood Insurance," H. Alden Foster (with discussion), 366.

VALVES

"Haas Hydroelectric Power Project," J. Barry Cooke (with discussion), 989.

VEHICLES

See under general types of vehicles, e.g., MOTOR VEHICLES; also under specific type of vehicle, e.g., AUTOMOBILE...

VEHICLE SHIPS

See SHIPS AND SHIPPING (cross reference thereunder)

VEHICULAR TRAFFIC

See TRAFFIC...

VELOCITY

See VIBRATION; WATER, FLOW OF...; WIND

VELOCITY DISTRIBUTION

See WATER, FLOW OF...

VENTURI FLUMES

See FLUMES

VIBRATION

"Behavior of Reinforced Concrete Shear Walls," Jack R. Benjamin and Harry A. Williams (with discussion), 669.

"Field Investigations of Spillways and Outlet Works," Benson Guyton, 491.

"Ocean-Wave Forces on Circular Cylindrical Piles," Robert L. Wiegel, Kenneth E. Beebe, and James Moon (with discussion), 89.

"Vibration of Simple-Span Highway Bridges," John M. Biggs, Herbert S. Suer and Jacobus M. Louw, 291.

VIBRATION RECORDING APPARATUS

"Ocean-Wave Forces on Circular Cylindrical Piles," Robert L. Wiegel, Kenneth E. Beebe, and James Moon (with discussion), 89.

Two lane girder bridge model test apparatus, 295.

VIRTUAL WORK, PRINCIPLE OF

Usage of principle in design procedure for prestressed truss beams, 478.

VISCOSITY

"Attenuation of Solitary Waves on a Smooth Bed," Yoshiaki Iwasa, 193.

"Discharge Characteristics of Rectangular Thin-Plate Weirs," Carl E. Kindsvater and Rolland W. Carter (with discussion), 772.

VISCOSITY (*Continued*)

"Flow of Natural Gas in Pipelines," William T. Ivey and James H. Dorrough, 341.

"Turbulence Characteristics of the Hydraulic Jump," Hunter Rouse, Tien To Siao and S. Nagaratnam (with discussion), 926.

VOID RATIO

See SOILS

VORTEXES

See VORTICES (cross reference thereunder)

VORTEX FLOW

See WATER, FLOW OF, THROUGH ORIFICES

VORTICES

See EDDIES (cross references thereunder)

WALLS

See under relative structure or type of wall, e.g., BUILDINGS; see also STRUCTURES, THEORY OF—Walls

WASTE DISPOSAL

See SEWERS

WATER...

See also COSTS...; DRAINAGE; DROP-DOWN; EROSION...; FLOODS; FLUMES; GROUND WATER; HYDRAULIC... (cross references thereunder); HYDRO...; IRRIGATION; MODELS, HYDRAULIC; OCEAN (cross references thereunder); PIPE LINES; RESERVOIRS; RUNOFF; SEWERS; TERMINOLOGY; TURBULENCE; WAVES

WATER, CONSUMPTION OF (consumer usage)

"Water Supply Versus Irrigation in Humid Areas," Marion C. Boyer, 280.

WATER DIVERSION

See also FLOOD ROUTING

"Model Studies of Remedial Works for Niagara Falls," Andrew P. Rollins, Jr. and George B. Fenwick, 236.

"Vortex Flow Through Horizontal Orifices," John C. Stevens and Richard C. Kolf (with discussion), 871.

WATER, FLOW OF (General)

See also TURBULENCE; VISCOSITY

Head losses due to resistance to flow in drain wells, 721.

"Review of the Theories for Sand Drains," F. E. Richart, Jr. (with discussion), 709.

WATER, FLOW OF, IN OPEN CHANNELS

See also DROP-DOWN; FLOODS; RUNOFF; WAVES

Abrupt separation of boundary layer under the beginning of the hydraulic jump and its cause, 951, 955.

"Attenuation of Solitary Waves on a Smooth Bed," Yoshiaki Iwasa, 193.

"Discharge Characteristics of Rectangular Thin-Plate Weirs," Carl E. Kindsvater and Rolland W. Carter (with discussion), 772.

Eddy motion violence in upper levels of downstream channel flow, 512.

"Errors in Measurement of Irrigation Water," Charles W. Thomas, 319. *Discussion:* Odon Starosolszky; Steponas Kolupaila; Armando Balloffet; and Charles W. Thomas, 333.

"Fixed-Wheel Gates for Penstock Intakes," Sylvan J. Skinner (with discussion), 740.

"Hydraulic Jump at an Abrupt Drop," Walter L. Moore and Carl W. Morgan (with discussion), 507.

Sand trap type used at Haas Power Project on Kings River, California, 999, 1026.

Submerged weir usage in water diversion on the Niagara River, 236, 251.

"Turbulence Characteristics of the Hydraulic Jump," Hunter Rouse, Tien To Siao and S. Nagaratnam (with discussion), 926.

WATER, FLOW OF, IN PIPES

See PIPE LINES; PUMPS AND PUMPING; SEWERS

WATER, FLOW OF, OVER DAMS AND WEIRS

Complete mathematical analysis of flow patterns for rectangular weirs versus dimensional analysis and experiment, 773, 808, 814, 820.

"Discharge Characteristics of Rectangular Thin-Plate Weirs," Carl E. Kindsvater and Rolland W. Carter, 772. *Discussion:* Turgut Sarpkaya; Steponas Kolupaila; Ralph W. Powell; John W. Paull; Iwao Oki; Marion R. Carstens; and Carl E. Kindsvater and Rolland W. Carter, 802.

WATER, FLOW OF, OVER DAMS AND WEIRS (*Continued*)

Exceptional range of geometric conditions existing in the analysis of flow over rectangular thin plate weirs, 817, 819, 820, 821.

Extensive tests of full width weirs, 'years 1911-1920, 780.

"Field Investigations of Spillways and Outlet Works," Benson Guyton, 491.

WATER, FLOW OF, THROUGH ORIFICES

"Vortex Flow Through Horizontal Orifices," John C. Stevens and Richard C. Kolf, 871. *Discussion:* John W. Cunningham; Chesley J. Posey; and John C. Stevens and Richard C. Kolf, 884.

WATER GATES, MOVABLE

"Field Investigations of Spillways and Outlet Works," Benson Guyton, 491.

WATER, GROUND

See GROUND WATER

WATER HAMMER

"Predicting Surge Pressures in Oil Pipelines," Robert D. Kersten and Edwin J. Waller, 258. *Discussion:* Henry M. Paynter; and Robert D. Kersten and Edwin J. Waller, 273.

WATER INSTRUMENTS

See under types of instruments, e.g., GAGES...

WATER LEVEL RECORDING AND INDICATING INSTRUMENTS

"Errors in Measurement of Irrigation Water," Charles W. Thomas (with discussion), 319.

WATER POLLUTION**Sewage pollution**

Fish life off the California coast, 828, 829, 834, 842.

WATER POWER (Geographical)**Niagara River**

"Model Studies of Remedial Works for Niagara Falls," Andrew P. Rollins, Jr. and George B. Fenwick, 236.

WATER PRESSURE

"Field Investigations of Spillways and Outlet Works," Benson Guyton, 491.

"Fixed-Wheel Gates for Penstock Intakes," Sylvan J. Skinner (with discussion), 740.

"Hydraulic Jump at an Abrupt Drop," Walter L. Moore and Carl W. Morgan (with discussion), 507.

"Review of the Theories for Sand Drains," F. E. Richart, Jr. (with discussion), 709.

USBR pore water pressure theory tested, 431.

WATER, SEA

See SEA WATER

WATERSHEDS

See DRAINAGE; RUNOFF

WATER STORAGE

See RESERVOIRS...

WATER, STORM

See SEWERS

WATER SUPPLY (General)

See also COSTS, WATER SUPPLY; FLOOD...; GAGES...; GROUND WATER; IRRIGATION; RESERVOIRS...; WATER... (related subject headings thereunder)

Irrigation water quality classified, 228.

"Water Supply Versus Irrigation in Humid Areas," Marion C. Boyer, 280.

WATER SUPPLY (Geographical)**California**

"Salt Balance in Ground-Water Reservoirs," David B. Willets and Charles A. McCullough (with discussion), 224.

Indianapolis, Ind.

Water requirements, with statistics, for Indianapolis and vicinity, 288, 290.

WATER SURFACE PROFILES

See WATER, FLOW OF, THROUGH ORIFICES

WATER SURFACE SURGES

See WAVES

WATER TANKS

See TANKS, WATER

WATER TERMINALS (structures and localities)

"Characteristics of New-Type Cargo Ships," Douglas C. MacMillan, 179.

WATER TRANSPORTATION

See also FREIGHT; RIVERS; WATER TERMINALS

Cargo ship types and their characteristics tabulated, 183.

"Characteristics of New-Type Cargo Ships," Douglas C. MacMillan, 179.

WATER TUNNELS

See TUNNELS, WATER

WATER TURBINES*See* TURBINES, WATER**WATER WAVES***See* WAVES**WATERWAYS (General)**

See CANALS; CHANNELS (cross references thereunder); FREIGHT; OCEAN... (cross references thereunder); RIVERS; SEA... (cross references thereunder); WATER DIVERSION; WATER TRANSPORTATION

WAVES

See also CURVES, WAVE RUN UP; SHORES AND SHORE PROTECTION; WATER PRESSURE

Apparatus for wave run up tests, 853.

"Attenuation of Solitary Waves on a Smooth Bed," Yoshiaki Iwasa, 193.

"Hurricane Design-Wave Practices," Charles L. Bretschneider, 39.

Linear wave theory disadvantages, 109, 112.

Maximum expected ocean wave steepness for various periods and depths of water, 358.

"Ocean-Wave Forces on Circular Cylindrical Piles," Robert L. Wiegel, Kenneth E. Beebe, and James Moon (with discussion), 89.

"Offshore Breakwaters," Richard Silvester, 356.

Shallow water wind wave forecasting techniques and computing procedures, 55, 61.

"Wave Run-Up on Roughened and Permeable Slopes," Rudolph P. Savage, 852.

WEATHER*See* FLOODS; WIND**WEB BUCKLING***See* BUCKLING**WEBS***See* BEAMS**WEIRS (General)**

See WATER, FLOW OF, IN OPEN CHANNELS; WATER, FLOW OF, OVER DAMS AND WEIRS

WELLS

"Review of the Theories for Sand Drains," F. E. Richart, Jr., 709.
Discussion: Yoshichika Nishida; S. J. Johnson; and F. E. Richart, Jr., 737.

WHEEL GATES, FIXED

See INTAKE GATES (cross reference thereunder)

WHEEL LOADS

"Vibration of Simple-Span Highway Bridges," John M. Biggs, Herbert S. Suer and Jacobus M. Louw, 291.

WHIRLPOOLS

See EDDIES (cross references thereunder)

WILDLIFE

See under relative technical subject, e.g., RESERVOIRS

WIND (General)

"Hurricane Design-Wave Practices," Charles L. Bretschneider, 39.

Tide and wave "energy indexes" as used in classifying hurricanes and their frequency, 48, 60.

WORKS (industrial buildings and equipment)

See under specific type of works, e.g., GAS AND GASWORKS; SEWAGE WORKS (cross reference thereunder)

AUTHOR INDEX

(including Memoirs of deceased members)

-
- ALEXANDER, GEOFFREY N.**
Flood insurance, 376.
- ANDREWS, ROBERT EDMUND**
Memoir of, 1053.
- BALLOFFET, ARMANDO**
Irrigation water measurement errors, 336.
- BARBER, EDWARD S.**
Compacted clays, 917.
- BARNETT, RALPH L.**
"Prestressed Truss-Beams," 472.
- BARON, FRANK**
"Pressure Lines and Inelastic Buckling of Columns," 967.
- BARR, DAVID I. H.**
Sewage disposal, 850.
- BASSEL, GUY MANNERING**
Memoir of, 1054.
- BEEBE, KENNETH E.**
"Ocean-Wave Forces on Circular Cylindrical Piles," 89.
- BENJAMIN, JACK R.**
"Behavior of Reinforced Concrete Shear Walls," 669.
- BIGGS, JOHN M.**
"Vibration of Simple-Span Highway Bridges," 291.
- BOWMAN, JOSEPH R.**
Gates, 769.
- BOYER, MARION C.**
"Water Supply Versus Irrigation in Humid Areas," 280.
- BRADLEY, JOSEPH N.**
Hydraulic jump, 952.
- BRETSCHNEIDER, CHARLES L.**
"Hurricane Design-Wave Practices," 39.
- BROWN, ULYSSES GRANT**
Memoir of, 1054.
- BUKACEK, RICHARD F.**
"Flow Equations for Natural Gas Pipelines," 1027.
- CARSTENS, MARION R.**
Thin plate weirs, 816.
- CARTER, ROLLAND W.**
"Discharge Characteristics of Rectangular Thin-Plate Weirs," 772.
- CHAN, CLARENCE K.**
"Thixotropic Characteristics of Compacted Clays," 894.
- CHASE, LEON EVERETT**
Memoir of, 1055.
- CHILDS, LAURENCE D.**
"Tests to Evaluate Concrete Pavement Subbases," 556.
- COLLEY, BERT E.**
"Tests to Evaluate Concrete Pavement Subbases," 556.
- COLLIER, BEN TAYLOR**
Memoir of, 1056.
- COOKE, J. BARRY**
"Haas Hydroelectric Power Project," 989.
- CUNNINGHAM, JOHN W.**
Vortex flow, 884.
- DARROW, CHESTER S.**
"Design Features of the Dresden Nuclear Power Station," 617.
- DAVIS, HAROLD S.**
"Pressure Lines and Inelastic Buckling of Columns," 967.
- DOBSON, FRANK**
"Generating Station on the Niagara River," 32.
- DOROUGH, JAMES H.**
Flow equations, 1035.
"Flow of Natural Gas in Pipelines," 341.
- EAST, ERNEST ELWOOD**
Memoir of, 1057.
- ECKART, NELSON ANDREW**
Memoir of, 1057.
- FARGO, WILLIAM GILBERT**
Memoir of, 1058.
- FAYLOR, JOHN DAYTON**
Memoir of, 1059.
- FENWICK, GEORGE B.**
"Model Studies of Remedial Works for Niagara Falls," 236.

- FORSTER, JOHN W.**
Hydraulic jump, 519.
- FOSTER, H. ALDEN**
"Technical Problems of Flood Insurance," 366.
- FRIEL, FRANCIS S.**
"Current Challenges in Civil Engineering": Annual Address at the Convention, Cleveland, Ohio, May 5, 1959, 1038.
- GARCIA-ITURBE, REINALDO**
Interaction diagrams, 30.
- GREAVES, MELVIN J.**
"Inelastic Behavior of Impulsively Loaded Beams," 395.
- GRIME, EDWIN MORRELL**
Memoir of, 1059.
- GUNNERSON, CHARLES G.**
"Sewage Disposal in Santa Monica Bay," 823.
- GUYTON, BENSON**
"Field Investigations of Spillways and Outlet Works," 491.
- HAAIJER, GEERHARD**
"Plate Buckling in the Strain-Hardening Range," 117.
- HAINES, EUGENE GROVE**
Memoir of, 1060.
- HARDIN, JOHN R.**
"Evolution of Mississippi Valley Flood-Control Plan," 207.
- HARLEMAN, DONALD R. F.**
Hydraulic jump, 959.
- HAUG, THADDEUS LEON EUCLID**
Memoir of, 1061.
- HEISELMAN, CHRISTOPHER FRANK**
Memoir of, 1062.
- HEMMINGS, HARRY**
Memoir of, 1062.
- HILF, JACK W.**
"Compacting Earth Dams with Heavy Tamping Rollers," 409.
- HILL, CHARLES STEPHEN**
Memoir of, 1063.
- HODGSON, JACK D.**
Tamping rollers, 436.
- HOLMES, EDWARD H.**
"Highway Planning in the Past, Present, and Future," 149.
- HORNER, WESLEY WINANS**
Memoir of, 1049.
- HOWIE, HOWARD**
Memoir of, 1064.
- HUBBARD, PHILIP G.**
Hydraulic jump, 962.
- IVEY, WILLIAM T.**
Flow equations, 1036.
"Flow of Natural Gas in Pipelines," 341.
- IWASA, YOSHIAKI**
"Attenuation of Solitary Waves on a Smooth Bed," 193.
- JENSEN, CHARLES**
Memoir of, 1065.
- JOHNSON, JOE W.**
"Littoral-Drift Problems at Shore-Line Harbors," 525.
- JOHNSON, S. J.**
Sand drains, 737.
- JORISSEN, ANDRE LAURENT**
Memoir of, 1065.
- KAPERNICK, JOE W.**
"Tests to Evaluate Concrete Pavement Subbases," 556.
- KERSTEN, ROBERT D.**
"Predicting Surge Pressures in Oil Pipelines," 258.
- KIDDER, ARTHUR DALE**
Memoir of, 1066.
- KILLALEE, JACK ADELBERT**
Memoir of, 1067.
- KINDSVATER, CARL E.**
"Discharge Characteristics of Rectangular Thin-Plate Weirs," 772.
- KLEIN, FREDERICK LAURENCE**
Memoir of, 1067.
- KOLB, CHARLES R.**
"Engineering Geology of the Mississippi Valley," 633.
- KOLF, RICHARD C.**
"Vortex Flow Through Horizontal Orifices," 871.
- KOLUPAILA, STEPONAS**
Flood insurance, 379.
Irrigation water measurement errors, 336.
Thin plate weirs, 808.
- KRAMER, HANS**
Memoir of, 1068.
- KRYNINE, D. P.**
Compacted clays, 917.
- LAWRANCE, CHARLES H.**
Sewage disposal, 843.

- LAWTON, F. L.**
Haas hydroelectric power project, 1024.
- LEE, SENG-LIP**
"Analysis of Continuous Beams by Fourier Series," 164.
- LEFEVER, KENNETH WINANS**
Memoir of, 1069.
- LEISCH, JACK E.**
"Adaptability of Interchanges to Interstate Highways," 588.
- LI, C. Y.**
Tamping rollers, 438.
- LI, SHU-T'IEH**
Geology, 646.
- LOUW, JACOBUS M.**
"Vibration of Simple-Span Highway Bridges," 291.
- LOVE, ANDREW CAVITT**
Memoir of, 1070.
- LOVE, GERALD D.**
Highway interchanges, 614.
- LOVE, JOSEPH E.**
"Design Features of the Dresden Nuclear Power Station," 617.
- LYNCH, JOHN T.**
"Highway Planning in the Past, Present, and Future," 149.
- MacMILLAN, DOUGLAS C.**
"Characteristics of New-Type Cargo Ships," 179.
- MASHBURN, LEON WADDELL**
Memoir of, 1071.
- MASUR, ERNEST F.**
"Strength of Very Slender Beams," 63.
- MATTESON, DeFOREST A., JR.**
Shear walls, 703.
- MATTHES, GERARD HENDRIK**
Memoir of, 1050.
- MAVIS, FREDERIC T.**
"Inelastic Behavior of Impulsively Loaded Beams," 395.
- McCULLOUGH, CHARLES A.**
"Salt Balance in Ground-Water Reservoirs," 224.
- McENTEER, FRANK DUFF**
Memoir of, 1071.
- McKEE, KEITH E.**
"Design of Masonry Walls for Blast Loading," 457.
- McNAIR, ARTHUR J.**
"Electronic Computers in Surveying," 252.
- McPHERSON, MURRAY B.**
Hydraulic jump, 517.
- MEDWADOWSKI, STEFAN J.**
Continuous beams, 175.
- MIKLOFSKY, HAAREN A.**
"Design of Flexible Steel Arches by Interaction Diagrams," 1.
- MILLER, DAVID R.**
Sewage disposal, 843.
- MOON, JAMES**
"Ocean-Wave Forces on Circular Cylindrical Piles," 89.
- MOORE, WALTER L.**
"Hydraulic Jump at an Abrupt Drop," 507.
- MORGAN, CARL W.**
"Hydraulic Jump at an Abrupt Drop," 507.
- MUNSON, THURMOND ARMOUR**
Memoir of, 1072.
- NAGARATNAM, S.**
"Turbulence Characteristics of the Hydraulic Jump," 926.
- NILES, CHARLES FERNALD**
Memoir of, 1073.
- NISHIDA, YOSHICHIKA**
Sand drains, 737.
- OKI, IWAO**
Thin plate weirs, 814.
- O'NEIL, WILLIAM A.**
"The Welland Canal," 443.
- PAFFORD, ROBERT J., JR.**
"Operation of Missouri River Main-Stem Reservoirs," 381.
- PARKER, ROBERT PRESTON**
Memoir of, 1073.
- PATON, JAMES LINDSAY**
Memoir of, 1074.
- PAULL, JOHN W.**
Thin plate weirs, 814.
- PAYNTER, HENRY M.**
Surge pressures, 273.
- PETERKA, ALVIN J.**
Hydraulic jump, 952.
- POSEY, CHESLEY J.**
Vortex flow, 885.
- POWELL, RALPH W.**
Thin plate weirs, 809.
- RANDOLPH, BURR H.**
"Design Features of the Dresden Nuclear Power Station," 617.

- RATHBUN, JOHN CHARLES**
Memoir of, 1075.
- RICHART, F. E., JR.**
"Review of the Theories for Sand Drains," 709.
- ROBERTSON, JAMES M.**
Hydraulic jump, 954.
- ROLLINS, ANDREW P., JR.**
"Model Studies of Remedial Works for Niagara Falls," 236.
- ROUSE, HUNTER**
"Turbulence Characteristics of the Hydraulic Jump," 926.
- SADAR, DONALD JOSEPH**
Memoir of, 1076.
- SAMUEL, THOMAS DUNCAN, JR.**
Memoir of, 1076.
- SARPKAYA, TURGUT**
Thin plate weirs, 802.
- SAVAGE, RUDOLPH P.**
"Wave Run-Up on Roughened and Permeable Slopes," 852.
- SCHOMAKER, JOHN F.**
Flow equations, 1037.
- SEED, H. BOLTON**
"Thixotropic Characteristics of Compacted Clays," 894.
- SEVIN, EUGENE**
"Design of Masonry Walls for Blast Loading," 457.
- SHOCKLEY, WOODLAND G.**
"Engineering Geology of the Mississippi Valley," 633.
- SHOEMAKER, ROBERT RADCLIFFE**
Memoir of, 1077.
- SIAO, TIEN TO**
"Turbulence Characteristics of the Hydraulic Jump," 926.
- SILBERMAN, EDWARD**
Hydraulic jump, 951.
- SILVESTER, RICHARD**
Littoral drift, 547.
"Offshore Breakwaters," 356.
- SKINNER, SYLVAN J.**
"Fixed-Wheel Gates for Penstock Intakes," 740.
- SOTILLO, OMAR J.**
"Design of Flexible Steel Arches by Interaction Diagrams," 1.
- SPRY, FREDERICK JOSIAH**
Memoir of, 1078.
- STAROSOLSZKY, ODON**
Irrigation water measurement errors, 333.
- STELSON, THOMAS E.**
Wave forces, 114.
- STEVENS, JOHN C.**
"Vortex Flow Through Horizontal Orifices," 871.
- STRICKLAND, RICHARD I.**
"Ground Transportation at New York International Airport," 657.
- STRICKLER, THOMAS JOHNSON**
Memoir of, 1078.
- SUER, HERBERT S.**
"Vibration of Simple-Span Highway Bridges," 291.
- THOMAS, CHARLES W.**
"Errors in Measurement of Irrigation Water," 319.
- THOMAS, ROBERT O.**
Salt balance, 232.
- TIPTON, RICHARD RANDOLPH**
Memoir of, 1079.
- WALKER, HARRY BRUCE**
Memoir of, 1080.
- WALLER, EDWIN J.**
"Predicting Surge Pressures in Oil Pipelines," 258.
- WIEGEL, ROBERT L.**
"Ocean-Wave Forces on Circular Cylindrical Piles," 89.
- WILLETS, DAVID B.**
"Salt Balance in Ground-Water Reservoirs," 224.
- WILLIAMS, HARRY A.**
"Behavior of Reinforced Concrete Shear Walls," 669.
- WILSON, WILBUR M.**
Memoir of, 1051.
- WOODS, ROBERT PATTERSON**
Memoir of, 1081.
- YOUNGCLAUS, GEORGE DUNTON**
Memoir of, 1081.

